

LBL-11650  
UC-13 c.2 Rpl.

# Energy & Environment Division

RECEIVED  
LAWRENCE  
BERKELEY LABORATORY

OCT 24 1983

LIBRARY AND  
DOCUMENTS SECTION

## Annual Report 1979

October, 1980

### TWO-WEEK LOAN COPY

*This is a Library Circulating Copy  
which may be borrowed for two weeks.  
For a personal retention copy, call  
Tech. Info. Division, Ext. 6782.*



Energy & Environment Division

Lawrence Berkeley Laboratory

University of California, Berkeley

LBL-11650 c.2  
repl.

**LEGAL NOTICE**

This book was prepared as an account of work sponsored by an agency of the United States Government. Neither the United States Government nor any agency thereof, nor any of their employees, makes any warranty, express or implied

N  
U  
S  
S  
P

**Lawrence Berkeley Laboratory Library**  
University of California, Berkeley

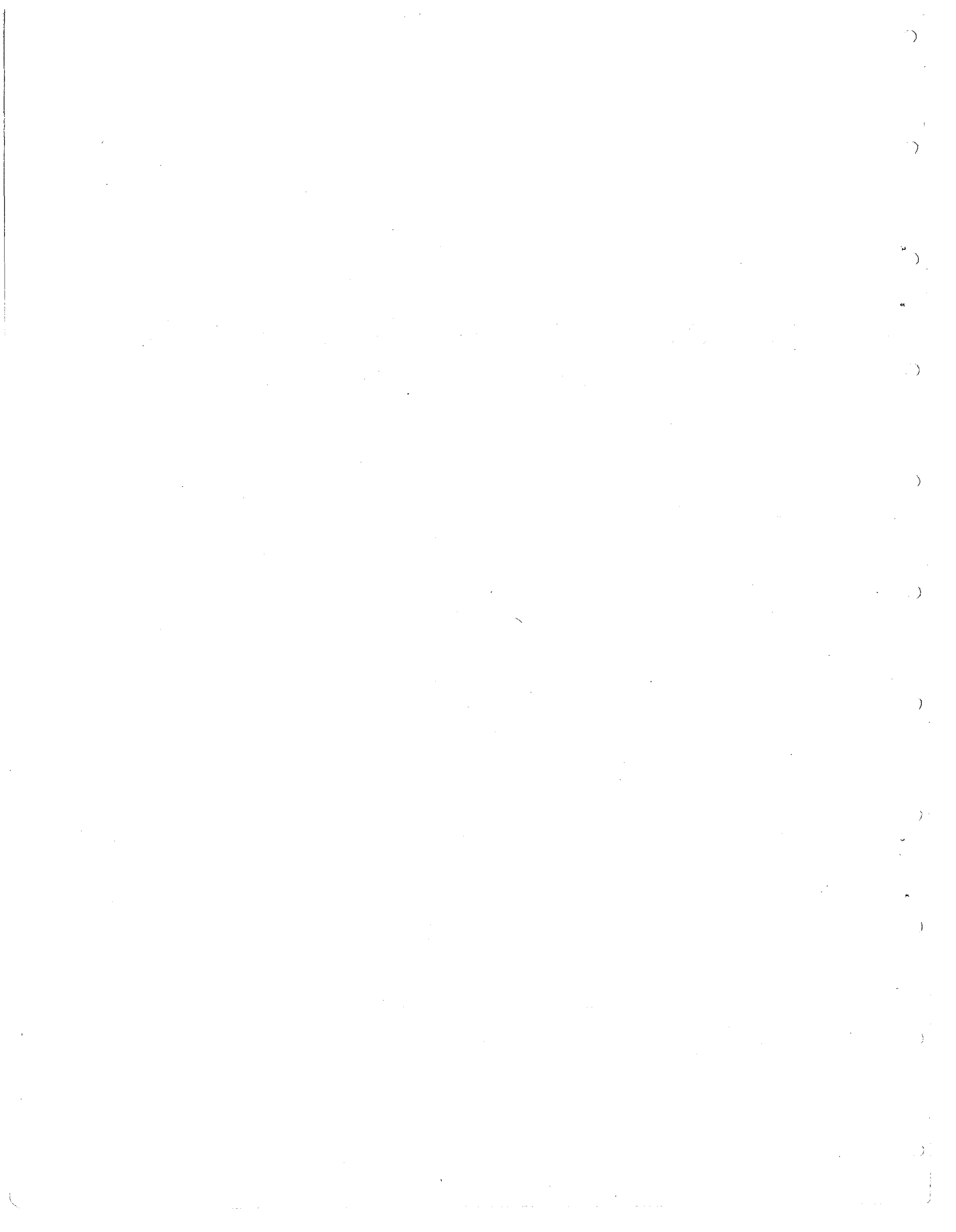
**ENERGY & ENVIRONMENT DIVISION  
ANNUAL REPORT  
1979**

Elton J. Cairns  
*Head, Energy & Environment Division*  
*and*  
*Associate Director, LBL*

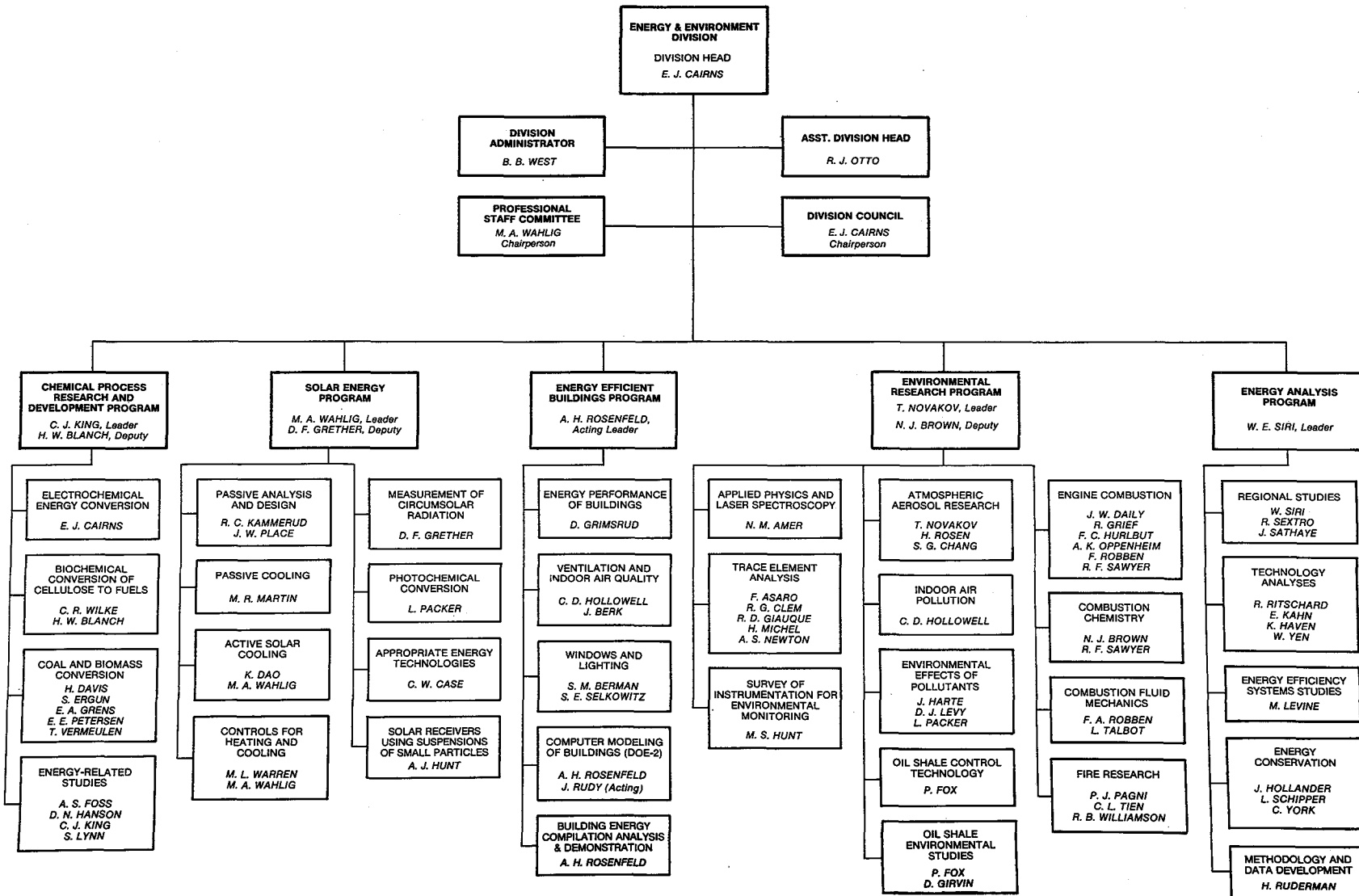
*Report Editors*  
Jeffrey Kessel  
Maya Osowitt

Energy & Environment Division  
Lawrence Berkeley Laboratory  
University of California  
Berkeley, California 94720

This work was supported by the U.S. Department of  
Energy under Contract No. W-7405-ENG-48



LAWRENCE BERKELEY LABORATORY  
UNIVERSITY OF CALIFORNIA  
ENERGY & ENVIRONMENT DIVISION



111



## ENERGY & ENVIRONMENT DIVISION

### Personnel Listing

Helen Adamson	Hannah Clark	William Hall
James Adams	Peter Cleary	Anthony Hansen
Jess Albino	Robert Clear	Donald Hanson
James Allen	Ray Clem	John Harte
Nabil Amer	Sidney Cohen	Mary Hart
Claire Amkraut	Patrick Coico	Kendall Haven
Robert Antonoplis	Paul Condon	Ronald Haynes
David Anderson	Craig Conner	Kathryn Hendricks
Brandt Andersson	Raymond Coover	Mark Henriquez
Douglas Anthon	Eric Courtney	Charles Henry
Michael Apte	Greg Cremer	Horace Herring
Keith Archer	Richard Creswick	James Hirsch
Haldun Arin	Enrique Cuellar-Ferrera	David Hirvo
Frank Asaro	Margaret Curtis	Alfred Hodgson
Cynthia Ashley	Pavel Curtis	Craig Hollowell
Myra Baker	John Daily	Kenneth Hom
Ridgway Banks	Francis D'Amato	Jonathan Huebner
Fred Bauman	Lynn Danielson	Joseph Humphrey
Jo Beck	Linda Davis	Arlon Hunt
Richard Beerman	Thomas Delfino	Mary Hunt
Richard Beier	Robert Demyanovich	Franklin Hurbut
Peter Benenson	Richard Diamond	Daniel Iacofano
William Benner	Dennis DiBartolomeo	John Ingersoll
Paul Berdahl	Darryl Dickerhoff	Bruce Ingraham
Vincent Berg	John Dickinson	Warren Jackson
Neil Bergstrom	Raymond Dod	Linda Jenks
James Berk	George Dove	Ralph Johnson
Samuel Berman	Michael Dudzik	Richard Johnson
Jacqueline Bernier	Harry Dwyer	Bonnie Jones
Rakefet Bitton	Mohamed El-Gasseir	Laura Joseph
Harvey Blanch	Jon Elliott	William Judd
Carl Blumstein	Kathleen Ellington	Edward Kahn
Mary Boegel	Margaret Endersby	Ronald Kammerud
Pipon Boonchanta	Sabri Ergun	Stephen Kanzler
Dale Bowyer	David Evans	Cihan Karatas
Dorothy Bottini	Arnold Falick	Mahmut Karayel
Denise Boudreau	Maryleah Fanning	Joshua Kay
Kathleen Boyer	Robert Feinbaum	Michael Kennedy
Gabriella Brazil	Jean Ferrari	Jeffrey Kessel
David Brink	Carlos Figueroa	Andrea Ketoff
Richard Brodzinsky	Alice Filmer	Sean Killeen
Patricia Bronnenberg	Richard Fish	C. Judson King III
Burnet Brown	William Fisk	Mathilde Kland
Nancy Brown	Steven Fong	Joseph Klems
Stephen Brown	Alan Foss	Craig Kletzing
Walter Buhl	Phyllis Fox	Stanley Kohn
Charla Burgraff	Nina Freidman	Thomas Kokoska
Garth Burns	Raymond Freitas	James Koonce, Jr.
Elton Cairns	Peter Fuller	Douglas Kosty
Clifford Cannon	Ashok Gadgil	David Krinkel
Jeremy Cantor	Kristin Geisling	Mark Kruskopf
Jade Carroll	Robert Gerlach	John LaFond
William Carroll	Andre Ghirardi	Alan Laird
Charles Case	Robert Giauque	Gregg Langlois
Eduardo Ceballos	Gloria Gill	Amev Lee
Shih-Ger Chang	John Girman	Siu Chun Lee
Peter Chan	Donald Girvin	Susan Lepman
Timothy Chapman	Ronald Glas	Mark Levine
Michael Charney	Richard Goodman	Donald Levy
Daih-Yeou Chen	James Gray	Janet Linse
Robert Cheng	Ralph Grief	Metin Lokmanhekim
Jennifer Cherniss	Edward Grens	Billy Long
Kirk Chi	Donald Grether	Frank Lucarelli
Stephen Choi	David Grimsrud	Donald Lucas
Mark Christensen	Lara Gundel	Scott Lynn

John MacGlashan  
 Patricia Mackenzie  
 John Maguire  
 Samuel Markowitz  
 Marlo Martin  
 James Mass  
 Jeana McCreary  
 Michael McKinney  
 Frank McLarnon  
 Ralph McLaughlin  
 James McMahan  
 Janet McQuillan  
 Brian Maiorella  
 Rolf Mehlhorn  
 Alan Meier  
 Moya Melody  
 Atila Mertol  
 John Metcalf  
 Carl Meyer  
 Steven Meyers  
 Helen Michel  
 Robert Miksch  
 Harry Miller  
 Matthew Milukas  
 Sandra Mocco  
 Mark Modera  
 Donald Mohr  
 Fred Mowrer  
 Kevin Murphy  
 Eli Naor  
 Mojtaba Navvab  
 David Nawrocki  
 William Nazaroff  
 Anthony Nero, Jr.  
 John Neuhaus  
 Amos Newton  
 James Nichols  
 Tihomir Novakov  
 Steven Oblath  
 Francis Offermann  
 Marjorie Olmstead  
 Karen Olson  
 Antoni Oppenheim  
 Brian O'Regan  
 Maya Osowitt  
 Maria Ossa  
 William Oswald  
 Roland Otto  
 Lester Packer  
 Monica Padilla  
 Patrick Pagni  
 Rebecca Palmer  
 Gary Parsons  
 Michael Pedersen  
 John Pennucci  
 James Pepper  
 Javier Perez  
 Peter Persoff

Richard Petersen  
 Nils Peterson  
 Wayne Place  
 Cindy Polansky  
 Martin Pollard  
 Thomas Powell  
 Carmen Privat  
 Alexandre Quintanilha  
 Suzan Rainey  
 John Randolph  
 Ola Rashed  
 Lisa Rau  
 John Rees  
 Kenneth Revzan  
 Robert Risebrough  
 Ronald Ritschard  
 Franklin Robben  
 Alan Robb  
 Stephen Roberts  
 Gary Roseme  
 Steven Rosenberg  
 Arthur Rosenfeld  
 Hal Rosen  
 Michael Rubin  
 Francis Rubinstein  
 Henry Ruderman  
 Christopher Ruhm  
 William Ryan  
 Ellen Saegbarth  
 Richard Sakaji  
 Michael Salo  
 Laurie Sampietro  
 Jayant Sathaye  
 Robert Sawyer  
 Larry Schaleger  
 Robert Schefer  
 Steven Schiller  
 Leon Schipper  
 Emily Schmidt  
 Heidi Schmidt  
 Richard Schmidt  
 Nancy Schorn  
 Richard Schneider  
 Aldo Sciamanna  
 Stephen Selkowitz  
 Robert Selleck  
 Steve Selvin  
 Richard Sextro  
 Brenda Soares  
 Elizabeth Sherman  
 Max Sherman  
 Gautam Shiralkar  
 Barbara Shohl  
 Linda Sindelar  
 William Siri  
 Renee Slonek  
 Brian Smith  
 Michael Smith

Angela Smothers  
 Aram Sogomonian  
 Robert Sonderegger  
 Irene Stachura  
 Charlotte Standish  
 Carol Stoker  
 Philip Strong  
 Paul Stuart  
 Mark Sutton  
 Lawrence Talbot  
 S. Krishen Tangnu  
 Miles Tashima  
 Seyed Tavana  
 Jerome Thomas  
 John Thornton  
 Chang-Lin Tien  
 Timothy Tong  
 Gregory Traynor  
 Hai Lung Tsai  
 Karen Tsao  
 Isaac Turiel  
 Dorothy Turner  
 Robert Twiss, Jr.  
 Anthony Usibelli  
 Linda Veneziano  
 Rudolph Verderber  
 Theodore Vermuelen  
 Gleb Verzhbinsky  
 Bruce VickRoy  
 Hector Villareal  
 Steven Vosen  
 Thomas Wagner  
 Michael Wahlig  
 Douglas Wake  
 Ezzat Wali  
 James Walter  
 Mashuri Warren  
 Barbara West  
 Dale Wiley  
 Charles Wilke  
 Robert Williamson  
 Frederick Winkleman  
 Warren Winkelstein  
 Gloria Winston  
 Dora Wolosin  
 Harry Wong  
 James Wrathall  
 Linda Wroth  
 Nasser Yaghoubzadeh  
 Joseph Yang  
 Zafer Yasa  
 Winifred Yen  
 Carl York  
 Rodger Young  
 Karen Yu  
 Suen-Man Yu  
 Geordie Zapalac  
 Sharran Zeleke

# CONTENTS

## ENERGY ANALYSIS PROGRAM

Introduction: The Case for Energy Analysis. . . . .	1-1
Economic Impacts of Two Energy Projections J. Sathaye, H. Ruderman, P. Chan, and H. Estrada. . . . .	1-2
Assessments of Regional Issues and Impacts Associated with National Energy Scenarios R. Sextro, P. Chan, P. Deibler, M. El-Gassier, P. Gleick, K. Haven, M. Henriquez, J. Holdren, Y. Ladson, M. Messenger, R. Ritschard, H. Ruderman, J. Sathaye, W. Siri, S. Smith, K. Tsao, and T. Usibelli. . . . .	1-5
Evaluating Air Quality Associated with Future Energy Projections R. Sextro and M. Messenger. . . . .	1-9
Institutional and Political Issues in Power Siting in the State of California Y. Ladson . . . . .	1-13
Integrated Assessment for Energy-Related Environmental Standards J. Holdren. . . . .	1-15
Energy Water Issues M. El-Gassier . . . . .	1-18
The Development of Numerical Methods for Characterization of Aquatic Systems Dissolved Oxygen Profiles M. Henriquez. . . . .	1-22
Regional Energy Issues: Summary of a Workshop Held at Lawrence Berkeley Laboratory R. Ritschard and K. Haven . . . . .	1-24
National/Regional Energy-Environment Modeling Concepts: Summary of a Workshop R. Ritschard, K. Haven, H. Ruderman, and J. Sathaye . . . . .	1-27
Critique of Energy Information Administration Energy Scenarios for Region 9 J. Sathaye and A. Usibelli. . . . .	1-28
Energy Analysis by Means of Computer Generated Interactive Graphics M. Henriquez . . . . .	1-30
The Hawaii Integrated Energy Assessment J. Weingart, A. Ghirardi, K. Haven, M. Merriam, R. Ritschard, H. Ruderman, J. Sathaye, L. Schipper, and W. Siri . . . . .	1-32

<b>Assessment of Solar Energy Within a Community: Synopsis of Three Community-Level Studies</b>	
R. Ritschard . . . . .	1-37
<b>Utility Solar Finance: Economic and Institutional Analysis</b>	
E. Kahn . . . . .	1-40
<b>Local Population Impacts of Geothermal Energy Development in the Geysers-Calistoga KGRA</b>	
K. Haven, V. Berg, and Y. Ladson . . . . .	1-41
<b>Conservation Strategies for Community Colleges</b>	
B. Krieg and C. York . . . . .	1-44
<b>International Residential Energy Conservation</b>	
L. Schipper . . . . .	1-46
<b>Overcoming Social and Institutional Barriers to Energy Conservation</b>	
C. Blumstein, B. Krieg, L. Schipper, and C. York . . . . .	1-48
<b>Energy Policy Decisions and Consumer Decision Making: Application to Residential Energy Conservation</b>	
J. Corfee, M. Levine, and G. Pruitt . . . . .	1-49
<b>The Use of DOE-2 to Evaluate Advanced Energy Conservation Options for Single-Family Residences</b>	
D. Goldstein, J. Mass, and M. Levine . . . . .	1-53
<b>Application of the ORNL Residential Energy Demand Model to the Evaluation of Residential Energy Performance Standards</b>	
J. McMahon and M. Levine . . . . .	1-54
<b>Energy Information Validation</b>	
M. Horovitz . . . . .	1-55
<b>Evaluation of Building Energy Performance Standards for Residential Buildings</b>	
M. Levine, D. Goldstein, M. Lokmanhekim, J. Mass, and A. Rosenfeld . . . . .	1-56 (note)
<b>Energy Efficient Standards for Residential Appliances Including Heating and Cooling Equipment</b>	
M. Levine, S. French, J. McMahon, R. Pollack, and I. Turiel . . . . .	1-56 (note)
<b>The Impact of Energy Performance Standards on the Demand for Peak Electrical Energy</b>	
M. Levine, J. McMahon, S. French, and R. Pollack . . . . .	1-56 (note)

## ENERGY EFFICIENT BUILDINGS PROGRAM

## Introduction

A. Rosenfeld, C. Hollowell, S. Berman, and T. Edlin . . . . . 2-1

## Building Envelopes Program

R. Sonderegger, R. Beerman, A. Blomsterberg,  
W. Carroll, J. Casey, P. Condon, R. Diamond,  
D. Grimsrud, D. Krinkel, C. Ma, M. Modera,  
A. Rosenfeld, M. Sherman, and B. Smith . . . . . 2-2

## Building Ventilation and Indoor Air Quality Program. . . . . 2-7

## Introduction

C. Hollowell. . . . . 2-7

## Gas Stove Emissions

G. Traynor. . . . . 2-10

## Organic Contaminants

R. Miksch, D. Anthon, M. Barnes, L. Fanning,  
J. Glanville, H. Schmidt, and M. Tashima. . . . . 2-13

## Radon Measurements and Emanation Studies

J. Berk, M. Boegel, J. Ingersoll, W. Nazaroff,  
B. Stitt, and G. Zaplac . . . . . 2-18

## Indoor Radon Health Risks

A. Nero . . . . . 2-23

## Field Monitoring of Indoor Air Quality

J. Berk, T. Boyan, S. Brown, I. Ko, J. Koonce,  
B. Loo, J. Pepper, A. Robb, P. Strong, I. Turiel  
and R. Young. . . . . 2-24

Mechanical Ventilation Systems Using Air-to-Air Heat  
Exchangers

G. Roseme . . . . . 2-35

## Subcontract Activities

I. Turiel . . . . . 2-37

## Ventilation-Indoor Air Quality Data Base

R. Langenberg . . . . . 2-39

## DOE-2 Computer Program for Building Energy Analysis

W. Buhl, R. Curtis, S. Gates, J. Hirsch,  
S. Jaeger, M. Lokmanhekim, A. Rosenfeld,  
J. Rudy, and F. Winkelman . . . . . 2-42

## Hospitals Program

R. Pollack and I. Turiel. . . . . 2-46

<b>Energy Efficient Windows Program</b>	
S. Berman, R. Johnson, J. Klems, M. Rubin, S. Selkowitz, and R. Verderber. . . . .	2-51
<b>Energy Efficient Lighting Program</b>	
S. Berman, R. Clear, J. Klems, F. Rubinstein, S. Selkowitz, and R. Verderber. . . . .	2-59
<b>Conservation Potentials: Compilation, Publication, and Demonstration</b>	
A. Rosenfeld, H. Arin, M. Maulhard, A. Meier, J. Poling, L. Schipper, L. Wall, and J. Wright. . . . .	2-63
<b>Summary and Discussion of Potential Savings in the Buildings Sector</b>	
A. Rosenfeld. . . . .	2-68
<b>Evaluation of Building Energy Performance Standards for Residential Buildings</b>	
M. Levine, D. Goldstein, M. Lokmanhekim, J. Mass, and A. Rosenfeld. . . . .	2-70
<b>Energy Efficient Standards for Residential Appliances Including Heating and Cooling Equipment</b>	
M. Levine, S. French, J. McMahon, R. Pollack, and I. Turiel . . . . .	2-80
<b>The Impact of Energy Performance Standards on the Demand for Peak Electrical Energy</b>	
M. Levine, J. McMahon, S. French, and R. Pollack. . . . .	2-82
<b>SOLAR ENERGY PROGRAM</b>	
<b>Introduction . . . . .</b>	3-1
<b>Ultrafine Particle Suspensions for Solar Energy Collection</b>	
A. Hunt . . . . .	3-2
<b>Sensible Heat Storage for a Solar Thermal Power Plant</b>	
T. Baldwin, S. Lynn, and A. Foss. . . . .	3-5
<b>Passive Systems Analysis and Design</b>	
R. Kammerud, H. Akbari, B. Andersson, F. Bauman, C. Conner, M. B. Curtis, M. Daneshyar, A. Gadgil, A. Mertol, J. W. Place, T. Webster, K. Whitley, and T. Borgers . . . . .	3-6
<b>Nitinol Engine Development</b>	
R. Banks, W. Hubert, R. Kopa, M. H. Mohamed, and M. Wahlig . . . . .	3-9
<b>Appropriate Energy Technology</b>	
C. Case, H. Clark, J. Kay, R. Lucarelli, J. Morris, J. Rees, and S. Rizer . . . . .	3-13

<b>Energy Conversion by Halobacteria</b>	
L. Packer, R. Mehlhorn, A. Quintanilha, C. Carmeli, P. Scherrer, N. Kamo, P. Sullivan, S. Tristram, J. Herz, T. Racanelli, I. Probst, and A. Pfeiffhofer . . . . .	3-15
<b>Solar Heated Gas Turbine Process Using Sulfur Oxides for Power Production and Energy Storage</b>	
G. Tyson, S. Lynn, and A. Foss. . . . .	3-20
<b>Experimental and Theoretical Evaluation of Control Strategies for Active Solar Energy Systems</b>	
M. Warren, S. Schiller, M. Martin, M. Wahlig, and G. Sadler . . . . .	3-21
<b>Development of Solar Driven Absorption Air Conditioners</b>	
K. Dao, M. Wahlig, and E. Wali. . . . .	3-27
<b>Passive Cooling</b>	
M. Martin, P. Berdahl, F. Sakkal, and M. Wahlig . . . . .	3-30
<b>LBL Solar Demonstration Project</b>	
T. Webster. . . . .	3-34
<b>Support for Commercial Solar Demonstration Program</b>	
S. Peters, F. Salter, and T. Webster. . . . .	3-36
<b>Measurement and Analysis of Circumsolar Radiation</b>	
D. Evans, D. Grether, A. Hunt, and M. Wahlig. . . . .	3-37
<b>Instrumentation and Data Processing Modifications in the PG&amp;E/LBL Solar Data Network</b>	
D. Anson. . . . .	3-41
<b>Support Activities for DOE Solar Heating and Cooling Research and Development Program</b>	
M. Wahlig, M. Martin, R. Kammerud, W. Place, B. Boyce, M. Warren, and A. Heitz . . . . .	3-42
<b>CHEMICAL PROCESS RESEARCH AND DEVELOPMENT PROGRAM</b>	
<b>Introduction . . . . .</b>	4-1
<b>Process Development Studies on the Bioconversion of Cellulose and Production of Alcohol</b>	
C. Wilke, H. Blanch, S. Rosenberg, S. Tangnu, A. Sciamanna, and R. Freitas. . . . .	4-2
<b>Low-Cost, Low-Energy Flash Ethanol Fermentation</b>	
B. Maiorella, H. Blanch, and C. Wilke . . . . .	4-9
<b>Studies on the Physiology and Enzymology of Lignin Degradation</b>	
S. Rosenberg and C. Wilke . . . . .	4-14
<b>Status of the Biomass Liquefaction at Lawrence Berkeley Laboratory</b>	
S. Ergun. . . . .	4-18

<b>Pretreatment of Biomass Prior to Liquefaction</b>	
L. Schaalenger, N. Yaghoubzadeh, and S. Ergun. . . . .	4-19
<b>Catalytic Liquefaction of Biomass</b>	
M. Seth, R. Djafar, G. Yu, S. Ergun, and T. Vermeulen . . . . .	4-21
<b>Monitoring the Biomass Liquefaction Process Development</b>	
Unit at Albany, Oregon	
S. Ergun, C. Figueroa, and C. Karatas . . . . .	4-24
<b>LBL Continuous Biomass Liquefaction Process Engineering</b>	
Unit (PEU)	
S. Ergun, C. Figureroa, C. Karatas, and J. Wrathall . . . . .	4-26
<b>Selective Hydrogenation of Coal</b>	
E. Grens, T. Vermeulen, J. Edwards, F. Hershowitz, P. Joyce, J. Mainenschein, C. Onu, J. Shin, and G. Zieminski. . . . .	4-27
<b>Coal Desulfurization</b>	
S. Ergun, S. Lynn, E. E. Petersen, T. Vermeulen, J. A. Wrathall, L. Clary, G. Cremer, J. Mesher, D. A. Dixon, and M. C. Smith. . . . .	4-32
<b>Processing of Condensate Waters from Solid-Fuel Conversion</b>	
C. King, S. Lynn, D. Hanson, D. Greminger, G. Burns, D. Mohr, J. Hill, and N. Bell . . . . .	4-34
<b>Applied Battery and Electrochemical Research Program</b>	
E. Cairns and F. McLarnon . . . . .	4-37
<b>Battery Electrode Studies</b>	
E. Cairns and F. McLarnon . . . . .	4-38
<b>ENVIRONMENTAL RESEARCH PROGRAM</b>	
<b>OIL SHALE RESEARCH</b>	
Introduction . . . . .	5-1
<u>Characterization Studies</u>	
<b>Trace Contaminants in Oil Shale Retort Water</b>	
M. J. Kland, A. S. Newton, and H. L. Eaton . . . . .	5-3
<b>Speciation of Inorganic and Organic Arsenic Compounds</b>	
in Oil Shale Process Waters	
R. H. Fish, J. P. Fox, F. E. Brinckman, and K. L. Jewett . . . . .	5-7
<b>Use of Capillary Column Gas Chromatography-Mass</b>	
Spectrometry to Identify Organic Ligands of Metals	
in Oil Shale Process Waters	
R. H. Fish, A. S. Newton, A. M. Bowles, and P. C. Babbitt. . . . .	5-11

Characterization of Two Core Holes from the Naval Oil Shale Reserve No. 1 R. D. Giaque, J. P. Fox, J. W. Smith, and W. A. Robb . . . . .	5-15
<u>Ecological Studies</u>	
The Effects of Oil Shale Retort Water on Some Benthic Freshwater Organisms P. P. Russell, A. J. Horne, J. F. Thomas, and V. H. Resh . . . . .	5-18
<u>Trace Element Studies</u>	
Mass Balance and Partitioning Studies of Simulated In-Situ Retorts J. P. Fox. . . . .	5-22
Partitioning of As, Cd, Hg, and Se during Simulated In-Situ Oil Shale Retorting A. T. Hodgson, D. C. Girvin, G. Winston, and S. Doyle. . . . .	5-26
On-Line Measurement of Trace Elements in Oil Shale Offgases by Zeeman Atomic Absorption Spectroscopy D. C. Girvin, A. T. Hodgson, and S. Doyle. . . . .	5-29
<u>Retort Abandonment</u>	
Control Strategies for Abandoned In-Situ Oil Shale Retorts P. Persoff and J. P. Fox . . . . .	5-34
Hydraulic Cement Production from Lurgi Spent Shale P. K. Mehta and P. Persoff. . . . .	5-38
Water Quality Effects of Leachates from an In-Situ Oil Shale Industry J. P. Fox. . . . .	5-43
A Mathematical Model for Leaching of Organic Carbon from In-Situ Retorted Oil Shale W. G. Hall, R. E. Selleck, and J. F. Thomas . . . . .	5-49
Penetration of Non-Newtonian Grouts through Rubble P. Persoff . . . . .	5-52
<u>Wastewater Treatment Studies</u>	
Treatment of Wastewater from In-Situ Retorting of Oil Shale R. H. Sakaji, J. P. Fox, R. E. Selleck, D. Jenkins, and C. G. Daughton . . . . .	5-54
The Analysis of Oil and Grease in Oil Shale Retort Waters R. H. Sakaji, S. Onysko, J. P. Fox, C. G. Daughton, D. Jenkins, and R. E. Selleck. . . . .	5-59

Spent Shale as a Control Technology for Oil Shale Retort Water J. P. Fox, D. E. Jackson, and R. H. Sakaji. . . . .	5-62
<b>COMBUSTION RESEARCH</b>	
Introduction . . . . .	6-1
<u>Engine Combustion and Ignition Studies</u>	
Advanced Optical Measurements in Automobile Engines J. Daily, D. Pechter, and J. Metcalf . . . . .	6-2
Heat Transfer with Combustion R. Greif, H. Heperkan, J. Naccache, D. Huang, and W. Leung . . . . .	6-2
Experimental Facility for Engine Combustion Studies R. Sawyer, A. Oppenheim, and H. Stewart. . . . .	6-4
Ignition Studies A. Oppenheim, F. Hurlbut, and F. Robben. . . . .	6-5
Numerical Analysis of a Hypothetical Explosion J. Kurylo and A. Oppenheim . . . . .	6-12
<u>Combustion Chemistry and Pollutant Formation</u>	
Comparative Studies of Combustion Inhibition R. Schefer and N. Brown . . . . .	6-14
Measurements of Nitrogenous Pollutants in Combustion Environments N. Brown, E. Cuellar, T. Eitzen, A. Newton, R. Schefer, and T. Hadeishi. . . . .	6-16
The Selective Reduction of NO by NH <sub>3</sub> N. Brown, T. Eitzen, and R. Sawyer . . . . .	6-17
Unimolecular Dissociation and Recombination Reactions N. Brown and A. Abdel-Hafez. . . . .	6-19
Combustion Characteristics of Coal and Coal Related Fuels R. Sawyer and W. Chin . . . . .	6-20
Optical Measurement of Combustion Products by Zeeman Atomic Absorption Spectroscopy E. Cuellar and T. Hadeishi . . . . .	6-21
Combustion Sources of Nitrogenous Compounds R. Matthews and R. Sawyer. . . . .	6-24
Parametric Study of Submicron Particulates from Pulverized Coal Combustion J. Pennucci, R. Greif, F. Robben, and P. Sherman . . . . .	6-25

Surface Catalyzed Combustion	
R. Schefer and F. Robben. . . . .	6-26
Combustion Characteristics of Spouted Beds	
R. Sawyer, H. Arbib, and F. Weinberg . . . . .	6-28
<u>Combustion Fluid Mechanics</u>	
Flame Propagation in Grid Induced Turbulence	
R. Bill, I. Namer, R. Cheng, F. Robben, and L. Talbot. . . . .	6-29
Combustion in a Turbulent Boundary Layer	
R. Cheng, R. Bill, T. Ng, F. Robben, and L. Talbot . . . . .	6-30
Chemically Reacting Turbulent Free Shear Layers	
J. Daily, J. Keller, and R. Pitz . . . . .	6-33
Laser Induced Fluorescence Studies of Turbulent Reacting Flows	
J. Daily, N. Al-Shamma, C. Chan, and M. Azzazy . . . . .	6-35
Two-Line Laser Fluorescence Temperature Measurements in Turbulent Flows	
J. Daily and R. Joklik . . . . .	6-35
Combustion in a Vortex Dominated Two Dimensional Flow	
A. Ganji, R. Sawyer, and L. Parker . . . . .	6-36
Numerical Modeling of Turbulent Combustion	
A. Ghoniem, A. Chorin, and A. Oppenheim. . . . .	6-38
Interaction of a Flame with a Kármán Vortex Street	
I. Namer, R. Bill, F. Robben, and L. Talbot. . . . .	6-41
Thermophoresis of Particles in a Heated Boundary Layer	
L. Talbot, R. Cheng, R. Schefer, and F. Robben . . . . .	6-43
<u>Fire Research</u>	
Polymer Combustion	
W. Pitz, R. Sawyer, and N. Brown . . . . .	6-44
Particulate Volume Fractions in Diffusion Flames	
P. Pagni and S. Bard . . . . .	6-45
Laminar Wake Flame Heights	
C. Kinoshita and P. Pagni. . . . .	6-47
Flame Radiation	
C. Tien and S. Lee . . . . .	6-50
Fire Growth Experiments - Toward a Standard Room Fire Test	
R. Williamson and F. Fisher. . . . .	6-51
Tests and Criteria for Fire Protection of Cable Penetrations	
R. Williamson and F. Fisher. . . . .	6-55

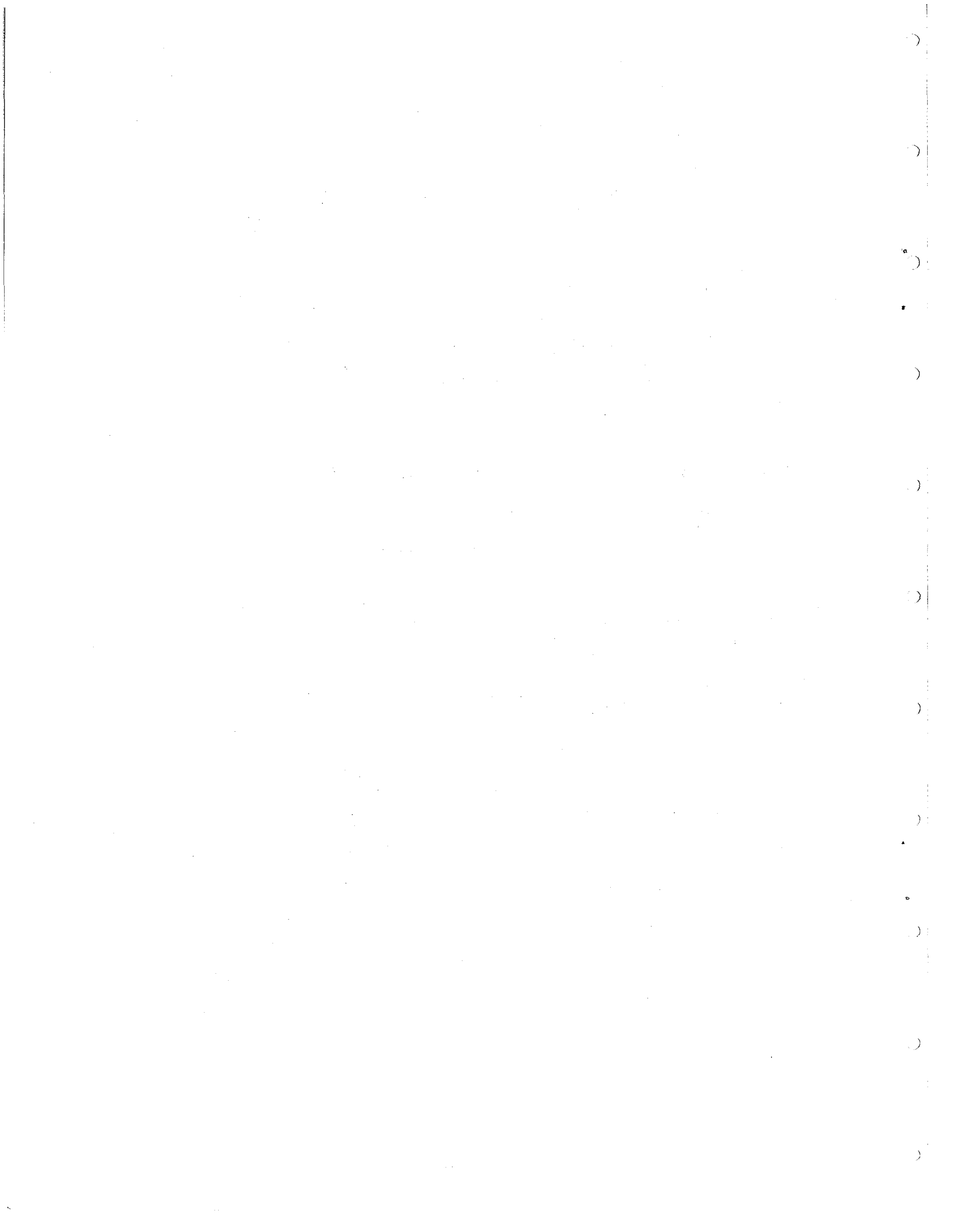
## EFFECTS OF POLLUTANTS ON BIOLOGICAL SYSTEMS

Introduction . . . . .	7-1
<b>PAREP: Populations at Risk to Environmental Pollution</b>	
D. Merrill, B. Levine, S. Sacks, S. Selvin, and C. Hollowell . . . . .	7-2
<b>Membrane Oxidative Damage</b>	
L. Packer, A. Quintanilha, E. Kellogg III, R. Mehlhorn M. Nova, L. Cheng, and J. Maguire. . . . .	7-5
<b>Lake Ecotoxicology: Methods and Applications</b>	
J. Harte and D. Levy . . . . .	7-8
<b>Treatment Methods for Removal of Boron from Brines</b>	
W. Garrison and S. L. Phillips . . . . .	7-12
<b>Organic Compounds in Coal Slurry Pipeline Waters</b>	
A. S. Newton, J. P. Fox, and R. Raval. . . . .	7-13
<b>Protection of Geothermal Brine Piping Using Electrodeposited Organic Linings</b>	
S. L. Phillips, R. G. Clem, and S. G. Chang. . . . .	7-16

## ATMOSPHERIC AEROSOL RESEARCH

Introduction . . . . .	8-1
<b>Carbon Catalyzed Reactions in Aqueous Suspensions: Oxidation of SO<sub>2</sub> at Low Concentrations</b>	
R. Brodzinsky, et al.. . . . .	8-2
<b>Reduction of NO<sub>x</sub> by SO<sub>2</sub> in Aqueous Solution</b>	
S. Oblath, et al.. . . . .	8-4
<b>Sulfate Formation by Combustion Particles in a Laboratory Fog Chamber</b>	
W. Benner, et al.. . . . .	8-7
<b>Lifetime of Liquid Water Droplets: An Experimental Study of the Role of Surfactants</b>	
R. Toossi, et al.. . . . .	8-10
<b>A Photoacoustic Investigation of Urban Aerosol Particles</b>	
Z. Yasa, et al.. . . . .	8-14
<b>The Use of an Optical Attenuation Technique to Estimate the Carbonaceous Component of Urban Aerosols</b>	
A. Hansen, et al.. . . . .	8-16
<b>Identification of Soot in Urban Atmospheres by an Optical Absorption Technique</b>	
H. Rosen, et al. . . . .	8-22

<b>Application of Thermal Analysis to the Characterization of Nitrogenous Aerosol Species</b>	
R. Dod, et al. . . . .	8-25
<b>Application of Selective Solvent Extraction and Thermal Analysis to Ambient and Source-Enriched Aerosols</b>	
L. Gundel, et al. . . . .	8-27
<b>Determination of Carbon in Atmospheric Aerosols by Deuteron-Induced Nuclear Reactions</b>	
M. Clemenson, et al. . . . .	8-30
<b>Investigation of Sampling Artifacts in Filtration Collection of Carbonaceous Aerosol Particles</b>	
R. Dod, et al. . . . .	8-35
<b>Surface Characterization of Flyash</b>	
S. Cohen, et al. . . . .	8-37
<b>APPLIED RESEARCH IN LASER SPECTROSCOPY AND ANALYTICAL TECHNIQUES</b>	
<b>Applied Physics and Laser Spectroscopy Research</b>	
N. Amer, N. Bergstrom, J. Costello, R. Gerlach, W. Jackson, R. Johnson, S. Kohn, C. Rosenblatt, D. Wake, and Z. Yasa . . . . .	9-1
<b>Operation of a Gas Chromatograph/Mass Spectrometer for the Identification of Components in Fossil Energy and Environmental Samples</b>	
A. Newton and W. Walker. . . . .	9-15
<b>Development and Application of X-Ray Fluorescence Analytical Methods</b>	
R. Giaque . . . . .	9-17
<b>Survey of Instrumentation for Environmental Monitoring</b>	
M. Quinby-Hunt, Y. Agrawal, C. Chen, R. McLaughlin, G. Morton, D. Murphy, and A. Nero. . . . .	9-18
<b>Extraterrestrial Cause for Cretaceous-Tertiary Extinction: Experiment and Theory</b>	
L. Alvarez, W. Alvarez, F. Asaro, and H. Michel. . . . .	9-19
<b>Precise Analysis for Better Understanding of Guatemalan Obsidian</b>	
F. Stross, F. Asaro, and H. Michel . . . . .	9-23



# ENERGY ANALYSIS PROGRAM

## INTRODUCTION: THE CASE FOR ENERGY ANALYSIS

*W. Siri*

Is energy analysis basic research or even a discipline? As perceived by the practitioners of the established disciplines, perhaps not. As a struggling juvenile in the world of intellectual pursuits, it may appear only a somewhat capricious application to practical problems of bits and pieces from physics, chemistry, biology, economics, mathematics and a host of other fields. Energy analysis has not yet, in the short span of its life, acquired the trappings and body of sophisticated doctrine that gives identity and prestige to the mature disciplines. It has not even acquired a proper name.

In this context, however, one is reminded that physics, chemistry, biology, mathematics and economics had humble beginnings in theology and practical problems of agriculture and commerce. Their evolution is familiar and one need not dwell on the contribution of cannons to thermodynamics, or of a bed of flowers to biology, or the troubled intellectual histories of all disciplines to achieve maturity, originally also without names to identify them.

The assertion that all scientific disciplines--or at least most of them--had humble beginnings in mundane matters does not prove that energy analysis is destined for distinction as a recognized discipline with its own adult name. It says only that the path along which it stumbles to adulthood is well trod by others. It does, however, lead to another perspective; one that may seem presumptive, and for which we ask the reader's indulgence.

The established disciplines, with the possible exceptions of theology and pure mathematics, are ruled by the energetics of the system for which each discipline has established its territorial imperative. For the "hard" sciences, this would seem self evident. In essence they explain, in diverse tongues, how energy drives and structures their chosen segments of the universe, from quarks to galaxies. This would include biology, which implicitly, if not always explicitly, addresses the energetics of complex, integrated, reproducing systems; chemistry which treats the energetics of aggregates of atoms; and physics, the science of matter's elementary constituents and energy ground rules. One can, for example, argue that evolution is in essence an energy problem. Does "survival of the fittest" simply mean that a species produced by random gene mutation--itself an energy induced process--can survive only if it can acquire, transform, and use energy to sustain itself, however preposterous its form?

But what about the soft sciences? While economics, for example, speaks of goods, and rents, of transactions, and capital, and intricate movements of money and credit, is it possible these derive from more fundamental processes of energy flows and uses? Witness the close relation of GNP

to energy use, granted there are differences in energy efficiency among nations. One can add many of the other social sciences. Eskimo and Tahitian cultures differ in detail, but do the significant differences simply reflect the nature of their energy inputs? Both operated on solar energy, but coconuts and high solar insolation are bound to produce a different "system" from one functioning on blubber and low insolation. And neither culture could form appreciable capital and launch a technological culture. The needed energy was inaccessible, a situation that still represses much of the world's population today. But what of the oil-rich but underdeveloped nations? Until recently, their oil stores were to them only potential energy; others used it and grew prosperous.

Thus it can be argued, just short of tongue-in-cheek, that nearly all established research disciplines may be regarded as subdivisions of energy analysis, each tailored to the system, and more often, an aspect of the system it explores. Is there a gap in the spectrum of systems from quarks to galaxies not fully covered by an established discipline? The answer is the integrated analysis of energy in human society. The system, moreover, is unique. Human society is the only system that manipulates at will the flows, conversions and uses of energy, subject, of course, to physical law. This feature is not shared by the systems analyzed by physics, chemistry, biology, and astronomy in which energy flows unmodified by intervention of cognitive brain and opposable thumb.

Energy analysis in this context attempts to understand the volitional choices of energy use and supply available to human society, and the multi faceted consequences--the good and the bad--of choosing any one of them. To be more specific, it examines the purpose and manner of energy use--efficiency and conservation are now major intellectual attractions--as well as the sources, resources, and technology options to serve the chosen uses of energy. On the consequences side, this effort becomes more complex and diffuse. It must attempt to integrate the interacting elements of environmental, economic, social, institutional, legal, political and health impacts. To complete the field's scope, all this needs to be done spacially from the local to the global level, and temporally for a span of two decades or more, the minimum time for significant technological and institutional change.

Finally, having pleaded for a place in the sun for the juvenile field of energy analysis, how has Lawrence Berkeley Laboratory nurtured its growth? The answer lies imbedded in the short reports that follow. A substantial part of the analysis program focuses on the myriad impacts of energy technologies and fuels and the regional

implications of national energy policy. The means to mitigate constraints on deployment of technologies and implementation of policy that emerge from such studies particularly interest decision makers. On the supply side, individual technologies, but more importantly, integrated assemblies of fuel cycles must be devised and evaluated. As an example, a study of Hawaii's energy options to reduce dependence on imported oil holds special fascination. It is a well-defined study area with high potential for developing its rich renewable energy resources. It is an analyst's demonstration

piece with the promise that the analytical structure is applicable elsewhere.

Other studies analyze and develop criteria for building and appliance efficiency, and explore potentials for energy conservation. Still others concentrate on special environmental, economic, and technical issues. And all the studies in varying degrees advance the grasp of underlying concepts and the art of analysis. In all this activity, it may be noted, University of California (Berkeley) faculty members and graduate students play important roles.

## ECONOMIC IMPACTS OF TWO ENERGY PROJECTIONS

*J. Sathaye, H. Ruderman, P. Chan, and H. Estrada*

### INTRODUCTION

Over the past few decades the U.S. has enjoyed abundant and relatively inexpensive energy supplies --in some instances even with declining fuel prices. However, future energy supplies are likely to come from inhospitable domestic or insecure foreign environments. The price of oil and gas has risen several fold during the past few years, reflecting the impact of these two factors. The increased prices will provide some incentive to further exploration and extraction of oil and gas as well as other competitive substitutes from inhospitable domestic reserves. The marginal costs of extraction, production and conversion of all these fuels will be much higher because of more complicated and exotic technologies required to supply these fuels. The capital costs and labor requirements for energy industries will therefore assume more importance as a fraction of the total investment and employment in the economy. The capital requirements would also impose a larger burden on secondary support industries supplying materials and services for the construction of energy development facilities.

### MODELS AND DATA

In order to capture these economic impacts due to development of new energy supplies, two inter-linked models were used (Fig. 1). The first model, a modified version of the Energy Supply Planning Model (ESPM)<sup>1</sup>, is used to estimate the direct impacts. The ESPM takes the fuel supplies in the scenario and sets up an annual schedule of facility construction and operation needed to provide these supplies. Based on construction and operation data for each facility, the model calculates the annual requirements for 140 types of materials and manpower skills. The construction and operating data used in estimating the capital and manpower requirements relate to facilities as they would have been designed in 1974. The data are in constant 1978 dollars, with factors such as land costs and other owner's costs included along with the manpower, materials and equipment costs.

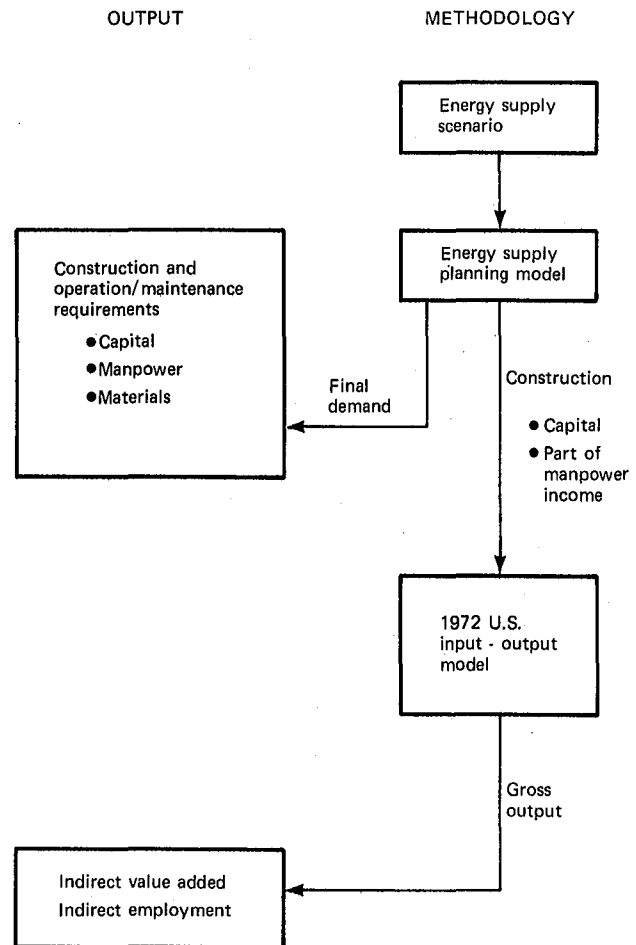


Fig. 1. Analytical methodology. (XBL 801-125)

The regional fuel demands and supplies for 1985, 1990 and 1995 are taken from the regionally

disaggregated C-high and C-low scenarios. Historical fuel and electricity consumption data for 1975 provide a baseline. The locations of announced power plants in 1975, 1985 and 1990 are based on the Generating Unit Reference File provided by ORNL. Energy demand for intermediate years is estimated by interpolation. Energy demand is also extrapolated to the year 2000 to include the construction requirements for facilities coming on line after 1995.

The estimates of expenditures on direct manpower and materials for construction are the starting point for calculating the indirect impacts. The calculation is performed using a 368 sector input-output (I-O) model of the U.S. economy for 1972. The results of the ESPM calculations are disaggregated to form incremental final demand vectors for the I-O model. The model calculates the change in gross output which, in turn, is used to calculate the change in income and employment.

#### DIRECT IMPACTS

Annual capital investment in the energy industries increases from roughly \$34 billion in 1975 to \$56 billion and \$52 billion in the C-high and C-low scenarios respectively. The cumulative requirements over the twenty year period from 1975 to 1995 are not very different for the two scenarios. For the C-low scenario the capital investment amounts to \$899 billion, whereas for the C-high scenario it amounts to \$990 billion, a difference of 10 percent. Almost 80 percent of this \$91 billion dollars of additional investment is required between 1980 and 1990 with \$33 billion required in the first five-year period and \$40 billion in the second five-year period. The additional investment occurs due to expanded development of coal supplies, conventional and shale oil and electricity generation facilities in the C-high scenario. At the same time, the high price of oil reduces the projected oil consumption and thus decreases the refining requirements in the C-high scenario.

In addition to the capital required for new construction, the energy facilities require substantial expenditures for operation and maintenance. Excluding fuel costs, the annual O&M expenditures grow steadily from \$84 billion in 1976-80 to \$131 billion in 1991-95 in the C-high scenario and to \$120 billion in the C-low scenario.

Manpower requirements follow the same temporal pattern exhibited by capital costs. Five year cumulative requirements are about the same for the first (1976-80) and the last (1990-95) periods for the two scenarios. In the first period they are 341 and 362 thousand man-years, while in the last period they are 428 and 442 thousand man-years for the C-low and C-high scenarios respectively (Table 1).

Requirements for the C-high scenario are 20 percent higher during the decade from 1981 to 1990. The majority of this increase is due to the increased requirements for constructing new coal facilities, with smaller increases due to increased shale oil production and electricity distribution and transmission activities.

Most of the demand for occupational skills increases at about the same rate as do total manpower requirements. However, demand for two specific skill categories, pipefitters and carpenters, almost doubles in the fifteen years from the first to the last period primarily due to construction of solar power plants and active solar heating units.

Manpower engaged in O&M of all facilities increases from 1.3 million to 1.9 and 1.8 million man-years respectively in the C-high and C-low scenarios.

#### INDIRECT IMPACTS

The indirect economic impacts of constructing energy facilities result from direct payments to construction labor and to the suppliers of materials and equipment. These payments are used to purchase goods and services from all sectors of the economy giving rise to additional employment and income.

The indirect or secondary impacts show generally the same trends as the direct impacts. For the C-low scenario they increase with time. Employment in industries stimulated by energy activities increases from 1.2 million to 1.35 million man-years between the first and last period (Table 1). In the C-high scenario secondary employment decreases more rapidly than does direct employment between the last two periods primarily due to decreased expenditure on equipment. Direct and indirect employment associated with C-high scenario is at its maximum in the last period. This 3.5 million man-years of employment represents 4 percent of the estimated 1978 employment (93.2 million).

There is no significant difference between the various time periods as regards the indirect employment per dollar of investment in both C-high and C-low scenarios. The ratio of indirect employment to direct employment does decrease slightly from 4.7 to 4.2 indicating a shift from capital intensive to more labor intensive energy construction activities.

The indirect employment per dollar of expenditure by labor (manpower) is higher than the expenditure on materials and equipment category. Therefore, a dollar spent on materials and equipment generates less indirect employment than a dollar spent by labor.

The estimates made of the secondary impacts are based on linear models and average values for coefficients; these impacts, however, are marginal. Since it is expected that marginal increases in employment and income are less than their average values, these results may overestimate the direct impacts. For example, construction workers in general have above average incomes and thus are likely to have a lower marginal propensity to consume. However, these employment coefficients have been corrected for increases in productivity as forecast by BLS. Overall, it is estimated that results could be 10-15 percent too high by 1990.

It should be pointed out that these indirect impacts may not represent a net increase in employment and income for the economy as a whole. If the

Table 1. Comparison of direct and indirect impacts, annual averages.

	1981-85		1986-90		1991-95	
	C-High	C-Low	C-High	C-Low	C-High	C-Low
<b>Capital Investment</b> (10 <sup>9</sup> 1978 \$)						
Manpower	12.7	11.0	15.0	13.1	14.3	13.7
Materials	8.6	7.6	9.7	8.3	9.3	8.4
Equipment	13.8	12.0	16.0	13.9	14.9	14.4
Other	15.2	13.1	17.7	15.2	17.2	15.6
Total	50.3	43.7	58.4	50.5	55.7	52.1
<b>Employment</b> (10 <sup>3</sup> man-years)						
Direct Construction	388.4	334.2	465.3	406.0	441.7	428.3
Direct Operation	1325.9	1305.0	1619.9	1517.6	1943.2	1770.8
Indirect <sup>a</sup>	1405.4	1211.2	1485.8	1293.3	1393.3	1346.1
Total	3119.7	2850.4	3571.0	3216.9	3778.2	3545.2
<b>Indirect Employment per Million Dollars of Capital Investment</b>						
Manpower	42.9	42.9	39.3	39.3	39.3	39.3
Materials, Equipment & Other	34.4	32.7	31.4	31.4	31.3	31.6
<b>Employment per Million Dollars of Capital Investment</b>						
Direct Construction	7.7	7.6	8.0	8.0	7.9	8.2
Indirect	36.5	33.6	33.4	33.4	33.4	33.6
Indirect/Direct	4.7	4.4	4.2	4.2	4.2	4.1

<sup>a</sup>Indirect employment includes the portion of direct operating required to satisfy the incremental construction requirements. The total employment therefore overestimates the actual impact by a small margin.

economy were at full employment, the energy sectors would have to compete against other industries for employees. Only if there were unemployment in the required skill categories would there be a net increase in employment. The results, therefore, should be interpreted as the amount of employment and income attributable to energy facility construction.

#### CONCLUSIONS

In conclusion, it should be noted that most of the larger impacts of the C-high scenario as compared to C-low scenario occur during the ten years between 1980 to 1990. These larger impacts stem from construction of more coal power plants, development of shale oil and increased electricity

transmission and distribution. Demand for occupational skills, except for pipefitters and carpenters which doubles, grows at the same rate as overall capital investment requirement.

Indirect impacts amount to roughly five times the direct impacts. Again the overall impacts are small although as much as ten percent of the employment in sectors such as metal products would be devoted to producing goods for energy facility construction.

#### REFERENCES

1. Bechtel Corporation, The Energy Supply Planning Model, Volumes I and II, NSF-C867, San Francisco (August 1975).

## ASSESSMENTS OF REGIONAL ISSUES AND IMPACTS ASSOCIATED WITH NATIONAL ENERGY SCENARIOS\*

*R. Sextro, P. Chan, P. Deibler,<sup>†</sup> M. El-Gasseir, P. Gleick,<sup>†</sup> K. Haven,  
M. Henriquez, J. Holdren,<sup>†</sup> Y. Ladson, M. Messenger, R. Ritschard,  
H. Ruderman, J. Sathaye, W. Siri, S. Smith,<sup>‡</sup> K. Tsao, and T. Usibelli*

### INTRODUCTION

This study is part of a continuing effort to evaluate the regional environmental and socioeconomic impacts of future energy development. The Regional Issue Identification and Assessment program is conducted by the Regional Assessments Division, Office of Technology Impacts for the Assistant Secretary for Environment, Department of Energy. This study is an analysis of one of a number of national energy scenarios developed by DOE.

### ACCOMPLISHMENTS DURING 1979

#### Scenario Discussion

As a basis for this study, the Series C energy scenario developed by the Energy Information Administration<sup>1</sup> was used for the projected energy development pattern for the nation and the region. It is a projection based upon the continuation of energy policies in effect at the beginning of 1978. The main assumptions are:

- constant world oil prices of \$15.32/bbl in 1978 dollars,
- increasing reliance on oil imports through 1990,
- continued decline in domestic natural gas production (lower forty-eight states),
- slight increase in domestic oil production due to Alaskan and OCS development, and
- continued growth in the use of coal and nuclear energy.

Energy supply and use projections based on this scenario are summarized in Table 1 for both the nation and for Region 9. The regional energy mix changes little over the next 15 years, with the largest changes occurring due to increased use of coal, nuclear and geothermal energy sources. Overall, the change to 1990 represents an annual growth rate of 1.8% per year, compared with a projected 2.9% per year for the nation as a whole. For electrical energy, the regional growth rate is 2% per year, contrasted with a 4.6% annual rate for the total nation. The resulting energy use, on a per capita basis, is shown in Fig. 1.

The issues and impacts discussed in this report are for the states in Federal Region 9, consisting of California, Arizona, Nevada and Hawaii. A detailed energy facility siting pattern was formulated, based upon the forecasted energy use by fuel type, and upon the present development plans of energy supply industries in the region. Figure 2 illustrates changes in electrical generating capacity by

state. Production and processing of fossil fuels is expected to take place at existing sites or installations, with the exception of an additional amount of OCS oil and gas activity off the California coast.

#### Regional Assessment Results

The assessment of impacts and issues arising from this national energy scenario was done for several study areas--air quality, water quality and availability, ecology, land use, solid waste, local socioeconomic, and institutional and political issues. This section summarizes the results by issue area. Air quality, water, regional economic and institutional and political issues are also discussed in individual reports elsewhere in this Annual Report.

#### Air Quality

Changes in air quality were estimated from long-range transport of particulates and sulfur oxides and from localized changes in emissions in each county. Based upon present and projected energy and process facilities, sulfur oxide concentrations are projected to increase by 1990 in the agricultural regions of California from emissions in the San Francisco Bay area, and in the South Coast Basin. Violations of the Prevention of Significant Deterioration (PSD) standards for sulfur oxides are possible for Class I areas in southern California due to emissions in the South Coast Air basin. Major emission sources in Nevada and Arizona, both power plants and process sources such as smelters, contribute to sulfur oxide problems in adjoining states of New Mexico and Utah.

Based upon the scenario projections of fuel use and new generating capacity requirements, emissions estimates from both stationary and mobile sources were used to predict changes in air quality for each Air Quality Control Region (AQCR). Continued violation of ambient air quality standards is expected for most of the urban basins in the region. In addition, siting in specific rural areas may be constrained by continued non-attainment problems for certain pollutants for which no local emissions offsets are available. Figure 3 shows the results of the local air quality calculations for each AQCR for oxides of nitrogen. Other pollutants show similar results.

#### Water Quality and Availability

Overall, regional water quality impacts do not appear to be significant as long as the present permitting processes and regulatory enforcement policies continue in the future. Point sources should not, therefore, constitute major sources of water pollutants; however, possible site specific concerns

Table 1. National and regional energy consumption based on the Series C scenario.

<u>National energy consumption</u>	<u>(10<sup>15</sup> BTU per year)</u>					
	<u>1975</u>		<u>1985</u>		<u>1990</u>	
		<u>imports*</u>		<u>imports*</u>		<u>imports*</u>
oil	32.8	.27	43.9	.38	48.5	.43
natural gas	20.0	.05	19.1	.10	19.3	.13
coal	12.8	(.14)	21.2	(.09)	25.4	(.08)
nuclear	1.8	0.0	6.2	0.0	10.3	0.0
hydro + geothermal	3.2	0.0	4.2	0.0	5.0	0.0
TOTAL	72.6		96.9		110.9	
<u>Regional energy consumption</u>	<u>(10<sup>12</sup> BTU per year)</u>					
oil	3665	.57	4263	.49	4554	.53
natural gas	2213	.85	1945	.79	2100	.78
coal	247	.36	397	.34	409	.34
nuclear	65	1.0	359	1.0	611	1.0
hydro + geothermal	510	0.0	773	0.0	822	0.0
TOTAL	6700		7738		8507	
<u>Consumption by end-use sector</u>						
	<u>National (10<sup>15</sup> BTU)</u>			<u>Regional (10<sup>12</sup> BTU)</u>		
	<u>1975</u>	<u>1985</u>	<u>1990</u>	<u>1975</u>	<u>1985</u>	<u>1990</u>
residential	10.0	12.1	12.8	928	805	816
commercial	7.3	7.8	8.2	671	600	611
industrial	18.1	26.9	32.3	1127	1610	1901
transportation	18.6	21.4	23.3	2382	2831	3063
TOTAL	54.0	68.2	76.6	5108	5846	6391

\* Fraction of fuel supplied by foreign or out-of-region imports (indicates net export fraction).

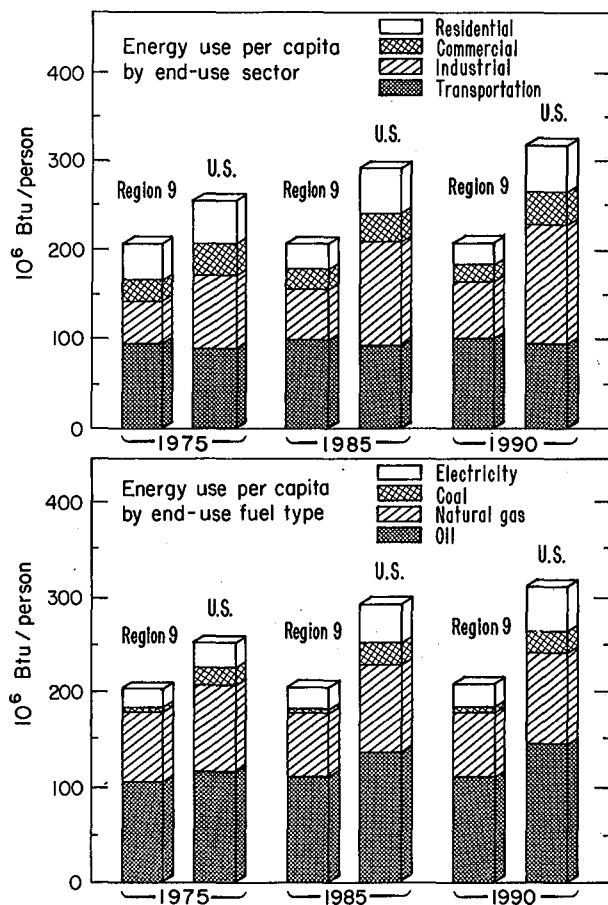


Fig. 1. A comparison of present and projected energy use per capita for Region 9 and the U.S. (XBL 797-2042)

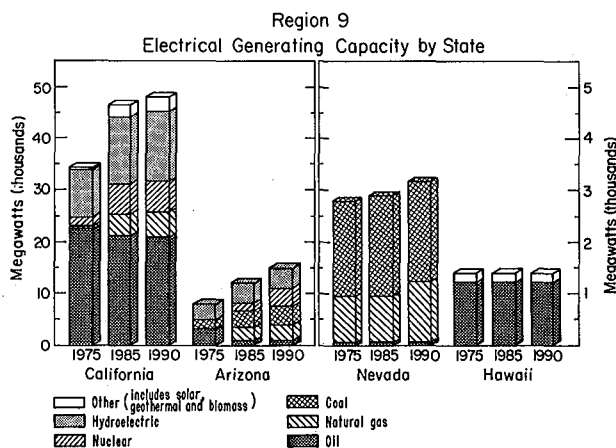


Fig. 2. Electrical generating capacity by state (Region 9). (XBL 797-2041)

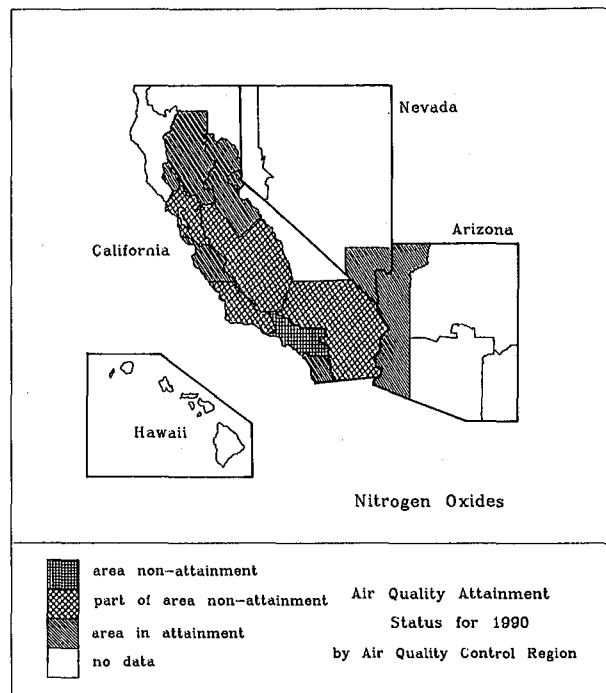


Fig. 3. Projected air quality status for 1990 by air quality control region (nitrogen oxides). (XBL 797-10564)

have been identified. Water quality impacts may result in areas with new or expanded geothermal energy development.

Water availability issues in this region focus primarily on the future uses of fresh water and the competition among many potential users. The lack of available water in certain parts of the region may constrain energy development in those areas unless sources of reusable water, such as municipal wastewater, are made available. The use of such water raises the secondary issue of the effect of cooling tower drift and blowdown on surrounding land uses.

Ecology

Although ecological impacts are generally site-specific, broader problems such as impacts upon sulfur-oxide sensitive crops will also be important if fuel burning increases as projected. Parts of California have large acreages of sulfur-oxide sensitive crops, as shown in Fig. 4, which total to nearly 2 billion dollars in value. Another important aspect of energy facility siting, especially in California, is the possible conflict with endangered species habitat. In Arizona, much of the land disturbed by strip mining has not been reclaimed, creating additional pressures upon rare and endangered species in that area.

Land Use

The major scenario-related land use issues in the region involve those projected facility sites

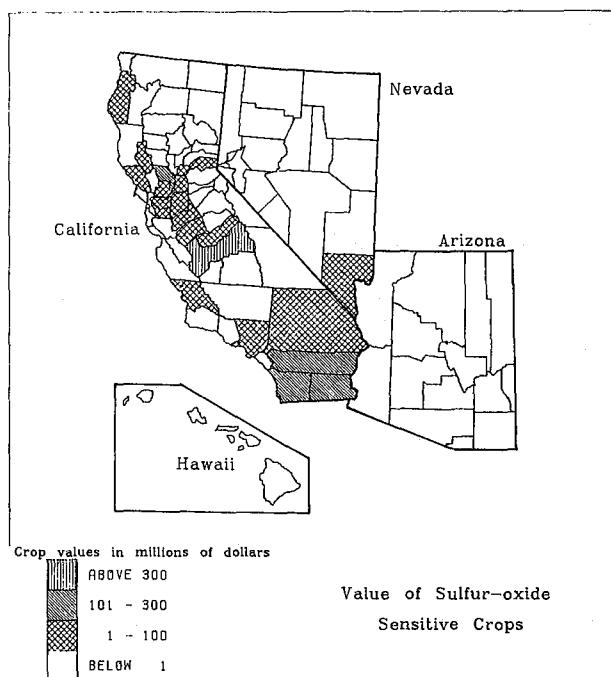


Fig. 4. Value of sulfur-oxide sensitive crops.  
(XBL 797-10571)

which conflict with other high-priority land uses, particularly in the coastal zone and in agricultural areas. Increases in refinery capacity, necessitated by the projected increase in the use of oil in the region, will conflict with, and in some cases be constrained by, existing coastal land use regulations and plans. Energy development in or near agricultural areas presents possible land use conflicts because of the increases in air emissions and conflicting demands for fresh water.

#### Solid Waste

Solid waste residuals resulting from increased energy activity in the region are not expected to be a serious regional problem, although this assessment presupposes that waste materials will be disposed of in a way that will not affect water quality.

#### Local Socioeconomics

At a regional level, the scenario presents no major socioeconomic issues. However, local issues will be very important, especially in those cases where the energy development is very site specific such as geothermal energy development. Local employment and population impacts appear to be small or moderate except in those rural coastal counties where new off-shore oil and gas production will induce on-shore development impacts. Other sociological factors may be important in those rural areas where increased energy development is expected.

Among the most important of these are potential conflicts with Indian tribal cultures in Arizona due to increased coal mining activity, and the potential changes in community infrastructures resulting from geothermal development activities in predominately rural areas in California.

#### Institutional and Political

While each state in the region has a unique set of institutions, there appear to be a number of issues common to all. Public awareness and debate over environmental and energy issues in the region have resulted in the establishment of local and statewide institutions charged with resolving these problems. These institutions, along with other political factors, may constrain certain types of energy development in the region. The use of natural gas in new power plants, as proposed by the scenario, appears to be infeasible due to federal and state regulatory actions that have given a low priority for such uses. Large portions of Nevada, Arizona, and parts of California are under direct federal control, and siting of facilities or transmission lines will require federal approvals.

Finally, the economics of various energy supply sources influence both private and public institutional decision making. Some of the provisions of the scenario appear economically less viable than alternatives such as conservation and improved end-use efficiencies, and as such, may not be implemented.

#### PLANNED ACTIVITIES FOR 1980

A second regional assessment study has been initiated, based upon the most recent National Energy Plan (NEP-2).<sup>2</sup> This plan incorporates a number of new DOE energy policies, and is based upon a more up-to-date set of energy resource prices and constraints. The analysis will extend to the year 2000, and will cover a broader range of energy supply technologies than the previous study.

#### FOOTNOTES AND REFERENCES

\* Condensed from Lawrence Berkeley Laboratory report LBL-9609.

† Energy and Resources Group, UC Berkeley  
‡ Present address: California Energy Commission, Sacramento, CA 95825

1. U.S. Department of Energy, Energy Information Administration, Annual Report to Congress; Vol. II, 1977, DOE/EIA-0036/2, April 1978, and Vol. II Appendix, DOE/EIA-0036/2 App. (Sept. 1978).
2. U.S. Department of Energy, "National Energy Plan II" (May 1979).

## EVALUATING AIR QUALITY ASSOCIATED WITH FUTURE ENERGY PROJECTIONS

*R. Sextro and M. Messenger*

### INTRODUCTION

Air quality considerations are a key issue in the assessment of future energy projections for both energy production and use. Given a set of assumptions regarding choices of sites and technologies, changes in air quality due to a given energy scenario can be tested against present and future air quality standards and emissions regulations as a way of examining possible constraints to energy development and use.

### ACCOMPLISHMENTS DURING 1979

As part of the analysis of regional impacts associated with the national energy scenario described in this Annual Report,<sup>1</sup> changes in air quality were estimated both as a result of local emission sources and effects due to long-range transport of pollutants. The resulting projections of air quality were compared with state and federal air quality standards and with regulations governing Prevention of Significant Deterioration (PSD) increments. Possible degradation of visibility in Class I air areas was also assessed.

### Analysis Procedure

The six national laboratories involved in the assessment project developed a common set of analytical procedures for the study. Local air quality projections were made using a roll-back technique which assumes that the ratio of future emissions and the resulting air quality remains the same as the ratio of present emissions to present air quality. The use of this technique implies a number of assumptions, among them are that meteorological conditions in the present or base year will remain the same in future years and the spatial distribution of emission sources will be approximately the same in the future as in the base year. In those areas where the emissions increments were large compared with existing sources, a separate procedure was used to estimate the contribution to local air quality from the large incremental sources. For Region 9 the detailed siting pattern based upon the scenario did not result in the siting of large emitting facilities in areas where existing sources are small.

In addition to the mesoscale effects estimated using the roll-back technique, long range transport of sulfur oxides and particulates was calculated. For the Western states, including Region 9, Pacific Northwest Laboratory (PNL) was responsible for these calculations (see Ref. 2 for model details), while Brookhaven National Laboratory (BNL) had a similar responsibility for the Eastern U.S. The resulting estimates of air concentrations for SO<sub>2</sub>, SO<sub>4</sub>, and particulates were compared with PSD Class I regulations. These estimates were also used as input

parameters to the Los Alamos Scientific Laboratory (LASL) visibility computations. This model<sup>3</sup> was used to evaluate visibility impairment for Class I air areas.

### Siting and Emissions Inventories

The siting of new energy consuming facilities such as industrial or utility boilers involves a number of complicated steps.<sup>3</sup> The first main element of the siting process is that the energy scenario, which specifies energy use by end use and by fuel type at the federal region level, is disaggregated into the state and Bureau of Economic Analysis (BEA) region level. The fuel use projections at the BEA level are then used for industrial fuel consumption patterns at the county level, based upon the 1974 geographic distribution of industrial facilities or major fuel burning installations (MFBI). No specific facilities were associated with these county-level projections of industrial fuel use; however, the existing (1974) MFBI combustor size distributions were used, along with information on State Implementation Plan (SIP) requirements for different facility sizes and fuels to derive emissions resulting from industrial fuel use.

Siting of present and proposed utility facilities was obtained from the FERC power plant site file maintained by ORNL and from individual utilities in the region. This information was used to site electrical generating facilities for future years. Additional "phantom" facilities were added in order to meet the fuel specific regional energy requirements of the scenario. The siting of these facilities was done at the county level.

Due to the importance of mobile sources of air pollution in this region, estimates were made for emissions from motor vehicles, based upon the region and sub-region disaggregation of gasoline use projections. These estimates include new car and fleet mileage standards, and the present and new mobile source emissions standards summarized in Table 1. As a consequence of the gasoline demand projections, the overall vehicle miles travelled are projected to increase dramatically. Because the emissions standards are based upon emissions per mile, the mobile source emissions are expected to increase in importance.

Emissions and air quality for the baseline year of 1975 were taken from a number of sources, including the NEDS emissions data base and the SAROAD air quality data base, both maintained by EPA. These were augmented by information from state and local air agencies. A major portion of California inventories was obtained from the California Air Resources Board.<sup>4</sup> The 1975 emissions inventories for selected California air basins are shown in Table 2.

Table 1. Federal and state emissions factors and standards for light duty vehicles.  
(grams/mile)

Year	Hydrocarbons		CO		NO <sub>x</sub>		SO <sub>x</sub>	Particulates
	CA	U.S.	CA	U.S.	CA	U.S.	U.S.	U.S.
1975	0.9	1.5	9	15	2.0	3.1	0.13	0.45
1976	0.9	1.5	9	15	2.0	3.1	↓ linear decrease ↓	↓
1977	0.41	1.5	9	15	1.5	2.0		
1978	0.41	1.5	9	15	1.5	2.0		
1979	0.41	1.5	9	15	1.5	2.0		
1980	0.41	1.5	9	15	1.5	2.0		
1981	0.41	0.41	9	7	1.0	2.0	0.07	0.25
1982	0.41	0.41	7	3.4	1.0	1.0	0.07	0.25
1983	0.41	0.41	7	3.4	0.4	1.0	0.07	0.25
1984	0.41	0.41	7	3.4	0.4	1.0	0.07	0.25
1985	0.41	0.41	7	3.4	0.4	1.0	0.07	0.25
1986	0.41	0.41	7	3.4	0.4	1.0	0.07	0.25
1987	0.41	0.41	7	3.4	0.4	1.0	0.07	0.25
1988	0.41	0.41	7	3.4	0.4	1.0	0.07	0.25
1989	0.41	0.41	7	3.4	0.4	1.0	0.07	0.25
1990	0.41	0.41	7	3.4	0.4	1.0	0.07	0.25

Table 2. Summary of air emissions for 1975 by air basin.  
(tons/day)

	South Coast			SF Bay			Southeast Desert			San Diego		
	TSP	SO <sub>2</sub>	NO <sub>x</sub>	TSP	SO <sub>2</sub>	NO <sub>x</sub>	TSP	SO <sub>2</sub>	NO <sub>x</sub>	TSP	SO <sub>2</sub>	NO <sub>x</sub>
Petroleum refining	3.5	47.0	38.	3.0	47.0	6.0	---	---	---	---	---	---
Power Plants	40.1	184	133	6.6	26.4	64.9	0.6	6.3	4.1	8.5	34.7	28.0
Industrial	8.4	14.1	75.4	6.1	15.3	102	1.4	0.3	29.4	0.6	1.9	2.7
Area Sources	97.8	0	15.3	20.2	0	2.8	81.2	0	6.0	90.5	0	0.7
Other	48.2	54.9	104.3	78.1	90.3	35.3	116.8	48.5	60.5	22.4	0	7.1
Total Stationary	198	300	366	114	197	211	200	55.1	100	122	36.6	38.5
Autos	58.4	21.8	418	28.5	5.1	204	2.7	0.8	20.1	8.9	3.3	63.6
Trucks (incl. diesels)	25.5	20.0	228	13.3	8.8	119	2.0	1.4	18.3	4.5	3.6	40.4
Other	26.1	46.0	171	13.8	26.6	71	4.4	5.2	32.4	6.6	10.2	32.0
Total Mobile	110	87.8	817	55.6	40.5	394	9.1	7.4	70.8	20.0	17.2	136
TOTAL	307	388	1180	169.6	219.5	605	209	62.5	171	142	53.8	174

Air Quality Results

Region 9 has 44 mandatory Class I air areas where Prevention of Significant Deterioration increments are  $2 \mu\text{g}/\text{m}^3$  for  $\text{SO}_2$  and  $5 \mu\text{g}/\text{m}^3$  for particulate matter. Figure 1 shows counties in the region with Class I areas where fuel burning in either utility or industrial facilities is expected to increase. The long range transport calculations for 1990, shown in the lower half of Fig. 1, indicate possible violations of the  $\text{SO}_2$  standards in the southern part of California. Visual air quality has been identified as an important value for all Class I air areas in this region. The visual range calculations by LASL, based upon the 1990 scenario conditions and resulting long-range transport of pollutants, show no change over the 1975 background conditions. However, plume blight due to light scattering could have a moderate effect on the Grand Canyon National Park because of increased coal-fired electrical capacity in nearby counties.

The results of the local air quality rollback calculations are summarized below by state. Basically, the present air quality picture in the region changes little by 1990. The major urban air basins, with the exception of Honolulu, generally continue to be non-attainment for one or more pollutants. Much of the improvement in the control of emissions from stationary sources is offset by increases in mobile source pollutant levels. The projected air quality status for 1990 is summarized in Figs. 2 and 3 for  $\text{SO}_2$  and particulates, respectively. Nitrogen oxide results are described in Ref. 1.

Presently 60 percent of the counties in California are non-attainment for particulates, 80 percent are non-attainment for oxidants, and 40 percent are non-attainment for carbon monoxide. This analysis of the 30 major fuel burning counties indicates that implementation of the scenario will exacerbate most air quality problems. Emissions of particulates from mobile sources increase dramatically which, when coupled with the 20 to 30 percent increase in emissions from process sources, leads to an overall increase in most counties of 50 to 200 percent. This overrides the 20 to 40 percent decrease expected in utility and industrial sources. The resulting changes in air quality are summarized in Table 3.

Sulfur oxide emissions increase somewhat in the fuel burning counties, with increased utility emissions replacing industrial sources. However, none of the counties presently in attainment are expected to change to non-attainment by 1990.

Hydrocarbon emissions in most counties do not change significantly by 1990 as increased emissions from process sources compensate for decreased emissions from mobile sources. While this pollutant is an important precursor of oxidant formation, increased hydrocarbon concentrations do not translate directly into higher oxidant concentrations since other chemical species also play a role in oxidant formation. The increased emission levels of carbon monoxide and oxides of nitrogen from mobile sources are the major cause of air quality degradation. CO levels increase substantially for all counties, with an average increase of nearly 80 percent for industrial counties. Emissions of

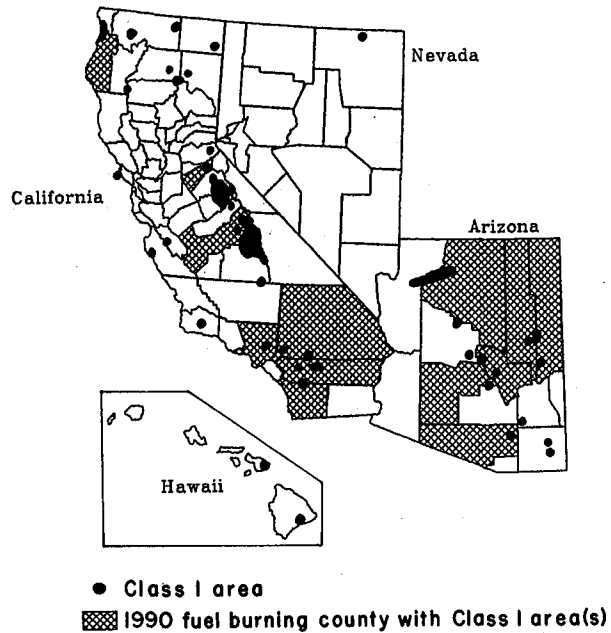


Fig. 1a. Counties in Region 9 with Class I areas. (XBL 797-10560)

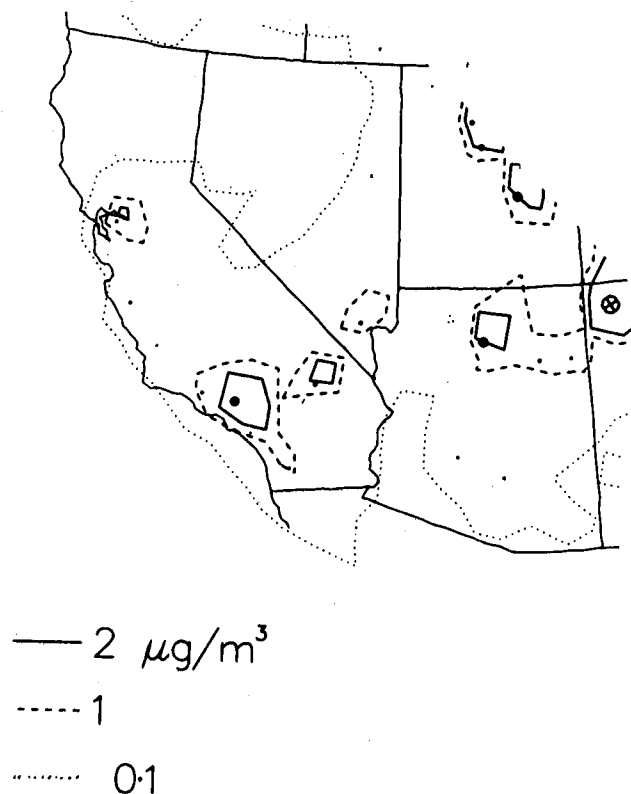


Fig. 1b. Projected  $\text{SO}_2$  concentrations for 1990 from industrial and utility sources. (XBL 797-10486A)

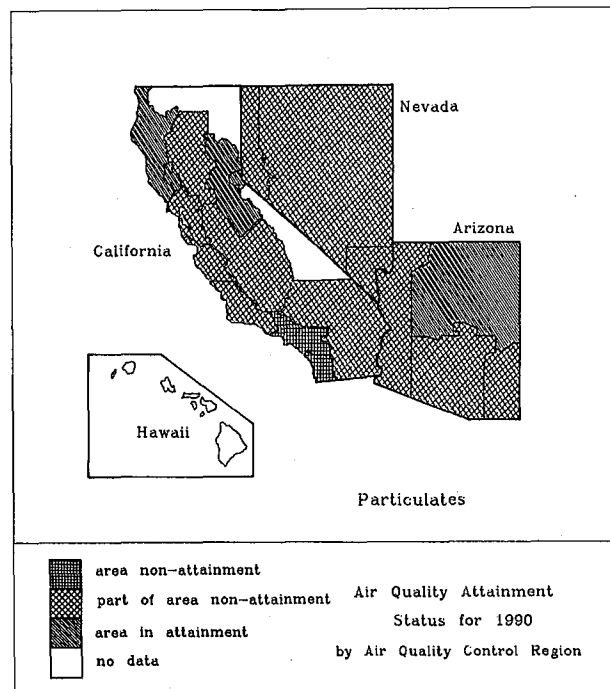
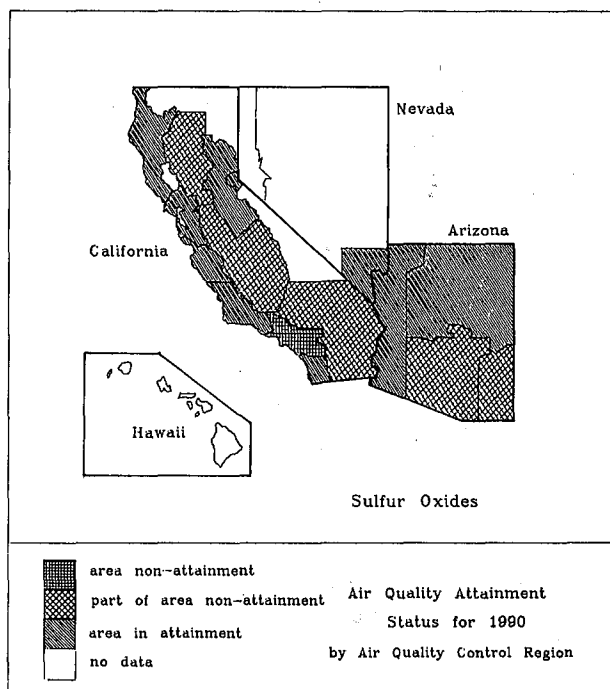


Fig. 2. Projected air quality status for 1990 by air quality control region (sulfur oxides). (XBL 797-10565)

Fig. 3. Projected air quality status for 1990 by air quality control region (particulates). (XBL 797-10563)

Table 3. Changes in federal primary pollutant attainment status for California fuel burning counties from 1975 to 1990.

	Remains in Attainment		From Attainment (1975) to Violation (1990)	Continued Non-Attainment
	Static <sup>a</sup> or Improved Air Quality	Degraded Air Quality		
<b>Industrial Counties (12)</b>				
Particulates	0	0	0	12
Sulfur Oxides	2	5	0	5
Hydrocarbons	0	0	0	12
Carbon Monoxide	0	2	3	7
Nitrogen Oxides	0	4	3	5
<b>Rural Counties (18)</b>				
Particulates	5	5	6	2
Sulfur Oxides	7	11	0	0
Hydrocarbons <sup>b</sup>	1	0	0	11
Carbon Monoxide	2	7	2	7
Nitrogen Oxides	5	10	3	0

<sup>a</sup>Static air quality is defined as total emissions within 10 percent of 1975 baseline.

<sup>b</sup>No ambient oxidant data are available for six of the 18 rural counties but they are assumed to be in attainment in 1975.

nitrogen oxides from stationary sources stay close to 1975 levels.

The two major urban areas of Nevada are presently non-attainment for particulates, hydrocarbons and carbon monoxide, primarily from mobile source emissions. The high rate of gasoline consumption projected by the scenario will aggravate these problems unless proposed emission standards for motor vehicles are enforced. Particulate emissions from process sources also contribute 50 to 70 percent of total emissions in four of the six fuel burning counties in Nevada. Sulfur dioxide emissions are not a major problem in Nevada at present, with the closing of the copper smelter in White Pine county. New sources will require better emission controls, and hence will not add substantially to SO<sub>2</sub> air quality problems.

At present, the metropolitan areas of Arizona are non-attainment for SO<sub>2</sub> and particulates, and based upon the scenario, no significant change is expected. The most serious problems are due to SO<sub>x</sub> emissions from copper smelters, and the clean-up of these emissions by 1990 is uncertain due to postponement of retrofit of control equipment.

All of the islands of Hawaii are air quality attainment areas, and the scenario projections are not expected to alter this status. The increased gasoline consumption projection raises the possibility of local violations of the CO standards in downtown Honolulu.

## PLANNED ACTIVITIES FOR 1980

A new set of air quality projections will be initiated based on the analysis of a new energy scenario. A more detailed analysis of emissions offset policies currently in place at local and state levels will be conducted. In addition, modeling for large point sources will be done for facilities projected on sites where existing emissions are small.

## REFERENCES

1. R. Sextro, et al., "Assessments of Regional Issues and Impacts Associated with National Energy Scenarios," the first article in this Annual Report.
2. W. F. Sandusky, et al., "Long Range Transport of Pollutants in the Western United States," Pacific Northwest Laboratory, Reports PNL-SA-7486, and PNL-RAP-26 (Jan. 1979).
3. U.S. Department of Energy, "Regional Issue Identification and Assessment: Study Methodology," Draft (September 1979).
4. California Air Resources Board, Air Resources Board Fact Sheet, Table 5-4, "New Vehicle Standards Summary", Sacramento, CA, (Jan. 1978).

## INSTITUTIONAL AND POLITICAL ISSUES IN POWER SITING IN THE STATE OF CALIFORNIA\*

Y. Ladson

### INTRODUCTION

This study was conducted as part of the Regional Issues and Identification Assessment (RIIA) Program. RIIA, developed to identify and assess the environmental, social, economic and institutional impacts of alternative scenarios defined at the regional level, is described in more detail in the second article of this Annual Report.

The analysis of institutional impacts performed for RIIA focused on major legislative, organizational, and political factors which could either inhibit or enhance energy development in each state within DOE Federal Region 9 (California, Nevada, Arizona, and Hawaii). The primary objectives of the task are threefold:

- to identify current legislation, statutes, and organizations affecting energy development;
- to ascertain major institutional factors constraining or promoting each type of energy development; and

- to assess the impacts of conflicts, barriers and promotional factors which arise from the national energy scenario.

A case study approach was selected as the vehicle to identify the relevant issues. The case studies chosen in each state allowed the analysis to focus on the actions associated with a single facility or decision. These studies should illuminate the major issues which will arise for most facilities.

### ACCOMPLISHMENTS DURING 1979

In California, the controversial Sundesert nuclear power plant proposal and the siting of an LNG terminal were selected as possible case studies for FY 1979 because they had drawn much attention state-wide and involved a wide range of agencies and interest groups. In the end, Sundesert was chosen as the issue for the first case study.

### The Case Study

The objective of the case study is twofold: 1) identification of major institutional structures, organizations and actors affecting energy development; and 2) illustration of institutional conflicts, constraining factors and the political nature of issues which arise in the decision-making process. The DOE energy development scenario was used as a basis for an assessment of issues arising from the Sundesert case study effort.

Any assessment of institutional impacts of power plant siting in California must start with a review of the legislative authority creating the state's siting permitting process and energy development program. Thus the first task was to examine the California Energy Resource Conservation and Development Act of 1974, the most comprehensive state energy legislation in the nation. The next phase of the study consisted of a review of the literature and publications concerning the Sundesert nuclear power plant proposal and related power plant siting and energy development program in the state of California. An examination of the major state "energy agencies" included agencies identified in the Regional Energy Data Book as having a major role in energy facility siting. A detailed critical review of the State's Energy Resources Conservation and Development Commission was conducted because of its role as the central, one-stop energy facility siting agency with exclusive state level authority to approve and certify power plants.

A review of public hearing records identified major actors who participated either as proponents or opponents to the siting of the nuclear power plant. These organizations were contacted for further information or for clarification of issues which developed during this controversy.

The final phase related identified issues which arose during the case study to the RIIA scenario. Issues which were identified included both scenario-specific and non-scenario-specific.

### The Issues

The analytical process described above identified several key institutional issues. In summary these include:

#### • Nuclear Development

The State's nuclear safety legislation prohibits any new nuclear facilities until an adequate federal nuclear waste program is developed. Further, since the Three Mile Island accident, concerns raised by state government officials and environmental groups have jeopardized the licensing and operation of plants presently under construction.

#### • Jurisdictional Disputes

Jurisdictional conflicts between the State Energy Act and other state and federal laws constrain the power plant siting process resulting in permit delays.

#### • Air Pollution Tradeoffs

Air pollution tradeoff policies must be addressed on a case-by-case basis. Inter-pollutant or inter-basin tradeoff questions must be resolved; this issue affects both utility and industrial siting decisions. Major fuel burning installations will require emission offsets in non-attainment areas.

#### • Alternative Technologies and Renewable Energy Sources

Geothermal, solar, coal gasification, wind, cogeneration and biomass are all seen as alternative energy sources. State government supports a diversified energy mix and is strongly pursuing the development of many of these options.

#### PLANNED ACTIVITIES FOR 1980

The institutional and political issues in power plant siting in California can be categorized into three areas: legislative and regulatory decision framework; intra-interagency jurisdictional questions; and local political traditions. Each of these areas will be studied in detail under RIIA II through the development of additional case studies.

#### FOOTNOTES

\* Condensed from Lawrence Berkeley Laboratory report, LBID-052.

# INTEGRATED ASSESSMENT FOR ENERGY-RELATED ENVIRONMENTAL STANDARDS

J. Holdren\*

## INTRODUCTION

The aim of this two and a half year project is to explore--and to suggest improvements in-- the assessment mechanisms available for use in the formulation of environmental standards applied to energy technologies. At the core of the work is the idea that rational standards should be based on integrated assessment. That is, the assessment should compare the environmental benefits sought by regulatory action not only to the direct economic costs and the transaction costs of the regulation but also to the regulations's consequences in displacing environmental effects from one energy source to another, one fuel-cycle step to another, one pollutant to another, one environmental medium to another, one class of victims to another, and so on.

## Background

Environmental impacts of energy technologies arise from many stages in the flow of an energy source from discovery to end-use (e.g., mining, processing, combustion), propagate via disruptions in many media (e.g., air, water, soil), and manifest themselves as many different undesirable effects (e.g., occupational disease, public disease, property damage, loss of service functions performed by ecosystems).<sup>1</sup> Attempts to control environmental impacts have evolved in a piecemeal fashion, focusing typically on one stage at a time, one medium at a time, one effect at a time. But the pieces are not independent, and the damages associated with each cannot be independently minimized. As the degree of control sought in different sectors has increased, the nature of the troublesome linkages has become clearer. Controlling air quality may impose additional burdens on water and soil; emissions restrictions at the combustion stage may push impacts back to the processing stage (as, e.g., in solvent refining or liquefaction of coal); and reductions in public disease may be bought at the expense of occupational health. The substantial inability to systematically and objectively determine whether any given "trade-off" of the kind just described leaves us better or worse off in the aggregate--that is, the lack of an integrated environmental assessment capability--is emerging as the central problem of contemporary environmental policy.<sup>2</sup>

## History of this Study

Following preliminary discussions with the projects's sponsors in the Office of Technology Impacts of the U.S. Department of Energy, work on this study began in June 1978. The effort consisted, in its initial phase, of the following two elements:

- (1) literature review and synthesis exploring the adequacy, for purposes of integrated assessment, of the tools and data presently available in environmental science and environmental economics;

- (2) case studies illuminating the extent to which available tools and data were actually used in the decision-making processes that led to major U.S. federal environmental standards relevant to energy technologies.

This work was carried out by the three senior investigators on the project: John P. Holdren, Principal Investigator and Professor of Energy and Resources, Anthony C. Fisher, Professor of Energy and Resources and of Economics, and John Harte, Senior Staff Scientist and Head of the Ecology Group, Energy and Environment Division, and four Graduate Student Research Assistants (Charles Blanchard, Veronica Kun, Michael Simpson, and Kathy Tonnessen). The results were described in six papers: two critical reviews surveyed economic valuation of environmental damages and status of major environmental data bases and integrated environmental economic models; and four case studies covered the Federal Water Pollution Control Act, the EPA's New Source Performance Standards for Fossil-Fuel Power Plants, the national emissions standards for mobile sources of air pollution, and the Surface Mining Control and Reclamation Act of 1977.<sup>3-8</sup>

The initial survey papers and case studies served to identify and characterize the obstacles that stand in the way of more systematic assessment of the benefits and costs of alternative environmental policies. With respect to the tools available in environmental science and environmental economics, these obstacles include problems of:

1. comprehensiveness/completeness (some links between contemplated actions and well-being do not get identified, and for some that are identified the information needed to characterize the link is missing);
2. quantification/accuracy (many effects that can be identified and characterized cannot be quantified, and much of what has been quantified is inaccurate or characterized by very large uncertainties);
3. comparability/valuation (even among effects that have been accurately quantified, the units of measurement are often incommensurable, which frustrates comparative valuation, and even where valuation is possible the capacity to weigh alternate distributions of costs and benefits among winners and losers is absent).

With respect to the application of available tools in actual standard-setting decisions, important additional obstacles revealed by the case studies (which employed interviews with parties to the decisions as well as use of documentary materials) include:

1. lack of awareness, on the part of decision makers and their staffs, of the full range of analytical tools that exist;
2. lack of confidence in available tools and data;
3. lack of time or money to apply tools and data to pending decisions;
4. agency structures and division of responsibilities that discourage or frustrate integration across media, fuel-cycle steps, energy sources, and so on;
5. the influence of political pressures on environmental decision makers.

(It must be noted that the last item is not necessarily an obstacle to systematic assessment, but can be a legitimate component of it.)

#### ACCOMPLISHMENTS DURING 1979

##### Workshop

The initial activity in FY 1979 was the "Workshop on Integrated Assessment for Energy-Related Environmental Standards", held at LBL November 2 and 3, 1978. A major purpose of the workshop was to expose the results of the FY 1978 effort--published in the papers described above--to the scrutiny of an array of individuals who either have studied these questions from other perspectives or who have been participants in the kinds of standard-setting processes under study. Accordingly, invited discussants included people with experience in the Congress and Executive Branch agencies with environmental responsibilities, as well as people from other national laboratories, universities, and industry. Following presentation and criticism of the six LBL papers, roundtable discussions explored possible characteristics of improved mechanisms for integrated environmental assessment, obstacles to implementing such mechanisms, and possible directions for the continuation of the LBL project. Proceedings of this workshop have been in preparation during FY 1979 and will be published in 1980.<sup>9</sup>

##### Approach for Continuing Work

The continuation of our investigation subsequent to the workshop has been aimed at clarifying the possibilities and pitfalls in integrated assessment relevant to standard setting for emerging energy options. One part of this work has involved the application of the analytical framework and insights derived in the earlier phase of the study to case studies of three such emerging options: photovoltaics, biofuels, and increased end-use efficiency in residential and commercial buildings. (The Graduate Student Research Assistants engaged in these case studies are Kent Anderson, Irving Mintzer, and Gregory Morris.) The case studies are investigating the technological characteristics of the relevant "fuel cycles" in sufficient detail to be able to identify and characterize the types of environmental effects likely to be most important. How the integrated-assessment issues identified earlier apply in the context of these environmental effects can then be explored. In parallel with--

and drawing on--the case studies, a set of issue papers is treating cross-cutting, integrated-assessment issues identified in the previous phase as being both important and difficult. These cross-cutting issues are:

1. degree to which environmental damages can be estimated using data generated by markets or simulated by market-like processes;
2. accounting for effects of stochasticity (of environmental insults and of the environmental systems and processes on which they are imposed) in assessment for standard setting;
3. distributional and equity effects of standards and of uncontrolled impacts, among different groups and over time.

Additional Graduate Student Research Assistants involved with issue (1) are Suzanne Scotchmer and Nobu Yagi.

##### Findings of 1979 Research

The findings of the 1979 continuation outlined above are treated in a set of seven papers submitted in draft form to the Office of Technology Impacts in October 1979.<sup>10-16</sup> These findings include the following.

1. There are many types of biomass resources, many technologies for transforming these resources into useful energy forms, and a very wide variety of environmental effects that may result. Potentially the most serious of these are damages to ecosystem function associated with biomass project land use, water use, fertilizer use, pesticide use, and other management practices. Alteration of pre-existing processes of soil building and conditioning, and erosion control, are particularly worrisome in some approaches. On the other hand, in cases where collected biomass materials otherwise would have posed a disposal problem, the use of such materials as an energy source provides an environmental benefit.
2. The most troublesome environmental problems potentially associated with large-scale use of photovoltaic cells are probably the health consequences of worker and public exposure to toxic substances mobilized in the production of the cells (silica dust in the case of silicon cells, cadmium in the case of cadmium sulfide cells, and arsenic in the case of gallium arsenide cells). Release of toxic cell constituents from rooftop collectors in the event of fire may be a significant pathway. Damage to desert ecosystems could be an important consequence of centralized deployment of photovoltaic technology.
3. Energy conservation is equivalent at the margin to new energy supply and should be treated as an energy source for purposes of comparison of environmental consequences per unit of energy "delivered". Use of

- simply models to predict the energy yield of conservation measures in residential and commercial buildings, combined with preliminary assessment of the environmental effects of these measures, suggests a more favorable ratio of environmental cost to economic benefit than other forms of energy supply, in most cases. The most important environmental problem in residential and commercial energy conservation is probably the effect of reduced infiltration or ventilation on concentrations of indoor air pollutants, both natural (radon) and anthropogenic (carbon monoxide, nitrogen oxides, tobacco smoke).
4. Developing quantitative measures of pollution-induced damage to economic goods and services (e.g., damages to crops and buildings) is worthwhile but laden with theoretical and empirical pitfalls. There is reason to believe that the net effect of these difficulties in most studies done to date is to understate damages.
  5. Study of pre-existing equilibrium relations between property values and environmental amenity cannot by itself predict new equilibrium property values following a change in environmental conditions, but it can yield accurate estimates of the economic benefit of small environmental improvements and a reasonable approximation of the benefit of large improvements. This approach errs on the side of overstatement of given damages (measured by the benefits of removing them).
  6. Attitude surveys and related schemes to determine the economic value of environmental damages tend to suffer from a variety of types of strategic behavior (i.e., consciously self-serving responses) by respondents.
  7. The cost of occupational hazards in energy production can be disaggregated into the cost of lost human capital and the cost of pain and suffering. The former cost in principle can be internalized through employer-paid insurance systems, but in actuality present Workmens' Compensation does not capture this cost entirely. Cost of pain and suffering can be internalized through wage differentials, wherein a premium is paid for riskier work. This mechanism is compromised by restricted mobility in labor markets, weak worker bargaining power, and worker misperception of risks.
  8. Stochasticity in the natural environment makes it difficult to predict stresses from insults, to predict effects from stresses, and to predict human consequences from effects. The rationality of standard setting could be appreciably improved by explicit incorporation into the assessment process of the effects of stochasticity.
  9. Both economic efficiency and distributional equity require that the full costs of energy use be borne by those who use the energy and choose the technologies with which it is provided. Achieving this desideratum requires that resistant externalities (those resisting internalization either because they are not monetizable or because there is no mechanism for gainers to compensate losers) either be small or be distributed naturally among users roughly in proportion to use. A number of decentralized renewable energy sources meet these conditions much better than do such conventional alternatives as coal, nuclear fission, and imported oil.

#### PLANNED ACTIVITIES DURING 1980

The work in FY 1980 will refine the case studies and issue papers developed in FY 1979, adding comparisons and contrasts among the case studies and exploring linkages between the issue papers and the case studies. At the same time, a synthesis will be undertaken to draw from the entire body of work in the project a set of guidelines, criteria, and suggestions for improvement of integrated assessment applied to energy-related standards. The last half of FY 1980 will be devoted largely to the preparation of a book-length final report describing the findings of the entire project.

#### FOOTNOTES AND REFERENCES

\*Professor in Energy and Resources, University of California, Berkeley, and Participating Guest, Energy and Environment Division.

1. R. J. Budnitz and J. P. Holdren, "Social and environmental costs of energy systems", Annual Review of Energy 1, 553 (1976).
2. Peter W. House, Trading Off Environment, Economics, and Energy (D.C. Heath and Co., Lexington, MA, 1977).
3. J. P. Holdren, J. Harte, and K. Tonnessen, "Environmental Data Bases and Integrated Models as Assessment Tools: A Critical Survey of Accomplishments, Potential, and Limitations", in Ref. 9.
4. A. C. Fisher, "Tools for Measuring Pollution Damage Costs: A Critical Review", in Ref. 9.
5. C. L. Blanchard, "Integrated Assessment: A Case Study of the Federal Water Pollution Control Act", in Ref. 9.
6. V. Kun, "A Review of EPA's Evaluation of the Environmental Impacts of New Source Performance Standards for Fossil-Fuel Power Plants", in Ref. 9.
7. M. M. Simpson, "Integrated Assessment of Environmental Impacts: A Case Study of Mobile Sources of Air Pollution", in Ref. 9.

8. K. Tonnessen, "Integrated Assessment of Environmental Impacts: A Regulatory Approach to the Problems of Reclamation of Strip-Mined Lands", in Ref. 9.
9. Proceedings of the Workshop on Integrated Assessment for Energy-Related Environmental Standards, Lawrence Berkeley Laboratory, 2-3 November 1978, LBL/U.S. Department of Energy, 1979 (in press).
10. N. Yagi and A. C. Fisher, "Cross-cutting issues in integrated environmental assessment of energy alternatives: The cost of occupational hazards", Energy and Resources Group Preprint, University of California, Berkeley, October 1979 (Draft).
11. S. Scotchmer and A. C. Fisher, "Cross-cutting issues in integrated environmental assessment of energy alternatives: Evaluation of external impacts, with referende to the case studies", Energy and Resources Group Preprint, University of California, Berkeley, October 1979 (Draft).
12. John Harte, "Cross-cutting issues in integrated environmental assessment of energy alternatives: Environmental stochasticity", Energy and Resources Group Preprint, University of California, Berkeley, October 1979 (Draft).
13. J. P. Holdren, "Cross-cutting issues in integrated environmental assessment of energy alternatives: Distribution of costs and benefits", Energy and Resources Group Preprint, University of California, Berkeley, October 1979 (Draft).
14. Irving Mintzer, "Integrated-assessment issues raised by the environmental effects of photovoltaic energy systems: A case study of centralized and decentralized options", Energy and Resources Group Preprint, University of California, Berkeley, Ocotober 1979 (Draft).
15. Gregory Morris, "Integrated-assessment issues raised by the environmental effects of biomass energy systems: A case study", Energy and Resources Group Preprint, University of California, Berkeley, Ocotober 1979 (Draft).
16. Kent B. Anderson, "Integrated-assessment issues raised by the environmental effects of energy conservations: A case study of space conditioning in residential buildings", Energy and Resources Group Preprint, University of California, Berkeley, Ocotober 1979 (Draft).

## ENERGY WATER ISSUES

*M. El-Gasseir*

### INTRODUCTION

This research is part of the Regional Issues Identification and Assessment (RIIA) project.<sup>1</sup> Specifically, we seek to identify and assess the water availability and quality issues resulting from the constraints and impacts of implementing certain energy plans, represented by a set of six Department of Energy (DOE) scenarios. Until the recent addition of Arizona, LBL's responsibility had been limited to a region including the states of California, Hawaii, and Nevada.

There are two long-term objectives to this research. The first is to identify and evaluate the water-related issues and impacts of each energy scenario. The second objective is to establish and update a water/energy information base, so that the RIIA process is improved as it progresses from one scenario to another. The lack of an adequate centralized information base and the very complex nature of the "energy/water interface" have necessitated the adoption of the second objective. The same two factors have also forced a selective approach in the analysis of the energy-water issues.

### ACCOMPLISHMENTS DURING 1979

In 1979 the energy/water research activities involved two areas. In the first, an analysis of

one scenario was carried out. The second area involved the preparation of a data base and an analytic framework for a more comprehensive assessment to be carried out in conjunction with a second scenario.

#### The First-Scenario Assessment

In the Southwest, an overriding concern is the maintenance of a delicate balance between the supply and demand for water. In the assessment of the first scenario (the DOE/EIA mid-mid scenario) a decision was made to concentrate efforts on the energy issues pertaining to water availability. Since electricity generating steam power plants are the major energy sector consumers of water, the study was further limited to this type of facility.

The methodology consisted of four steps. First, the new power plants were identified whose cooling-water requirements could not be specifically identified. This identification was accomplished by comparing the scenario with state and utility plans. The results are shown in Table 1. The scenario did not assign any new generating facilities in the State of Hawaii. Hence no futher analysis for Hawaii was carried out. In the second step, the cooling water requirements for each power plant type were established (see Table 2). In establishing these requirements allowance was made for technical

Table 1. Steam electric-generation capacities requiring new cooling-water sources, MWe

County	Plant Type and Year							
	Combined Cycle		Gas		Geothermal		Solar	
	1985	1990	1985	1990	1985	1990	1985	1990
<b>California:*</b>								
Contra Costa	0	0	0	320	0	0	0	90
Humboldt	0	0	0	52	0	0	0	0
Imperial	0	0	0	46	736	876	0	0
Lake	0	0	0	0	681	731	0	0
Los Angeles	81	81	0	285	0	0	0	0
San Bernardino	0	0	0	0	0	0	20	120
San Francisco	190	190	0	0	0	0	0	0
Sonoma	0	0	0	0	381	591	0	0
<b>Nevada:**</b>								
Clark	0	0	0	90	0	0	0	0
Lyon	0	0	0	105	0	0	0	0
Storey	0	0	0	110	0	0	0	0

\*The results for California were obtained by subtracting from the 1985 and 1990 capacities of Table 1, the 1975 capacities of the same table and the capacities of power plants recently completed or under construction. The latter data were obtained from Refs. 2-8.

\*\*The Nevada results were obtained in a similar manner to California. However, an update on recent electric-power capacity expansion activities were obtained through personal communications with Nevada Power Company officials.<sup>9</sup>

uncertainties (e.g., the method of cooling to be implemented). The third step involved the computation of each county's total future cooling-water requirements associated with the mid-mid scenario (Table 3). In the final step, the cooling requirements were compared with estimates of present and future water needs for each county's municipal and industrial, and agricultural sectors, and total use.

There are two major findings to this study:

1. For most of the Southwest Region, the proper identification and analysis of the water availability issues and impacts cannot be accomplished by comparing the new water requirements with the supply of water naturally available. Three factors prevent completion of this analysis. First, existing demand already exceeds supply with the excess being met by groundwater overdrafts. Thus new fresh water cooling needs will most probably be satisfied by diverting water from other users. Secondly, state policies exist which discourage the use of fresh water for cooling purposes.<sup>14</sup> A number of utilities have already started using reclaimed waste water as a coolant.<sup>15</sup> The competition over water and the economics of electric power generation will soon force a gradual phase out of freshwater use in evaporative cooling systems. Finally, in the Southwest there is a high degree of water regulation and (physical) integration. Lowflow analyses

would be useful over very large areas comprising one or more basins or an entire state and would have to cover the entire economies of these areas. The scenarios (particularly the low-growth mid-mid scenario) are not likely to affect the outcome of such lowflow analyses to a significant extent. For a localized assessment (i.e., at the county level) the best approach is to measure the new water requirements against present and projected water use rates.

2. In spite of being a low-growth scenario for electrical generation, problems of water availability are expected. This is especially true in California's Contra Costa and Imperial counties and Nevada's Clark, Lyon, and Storey counties. In these cases, the new requirements were found to be relatively large when compared with estimates of present and projected water use rates. It is unlikely that the additional cooling requirements will be met by diverting fresh water from other users. The problems of water availability can be ameliorated by considering the use of reclaimed waste water. Adequately treated municipal waste water could meet the requirements in Contra Costa and Clark counties; however, the public health implications of cooling-tower drift could be a source of further obstacles. In the remaining counties part or all of the cooling water needs can be satisfied through the use of reclaimed agricultural drainage water. Cost and

Table 2. Cooling-water requirements of steam electric-generating facilities, 10-3 MGD/1MW<sub>e</sub> a,b

Facility Type	Thermal Efficiency <sup>c</sup> (%)	Circulation <sup>d</sup>	Evaporation <sup>e</sup>	Blowdown <sup>f</sup>	Drift <sup>g</sup>	Makeup <sup>h</sup>	Consumption <sup>i</sup>
Combined Cycle	40.3	620	7.4	4.7	0.31	12	7.7-12
Gas	38	830	9.9	6.2	0.41	16	10-16
Geothermal:							
Geysers	15.5	1,400	46	9.1	0.70	47	0-47
Imperial	16.5-9.8	2,100/3,000	60/82	27/4.0	1.1/1.5	88/84	88/84
Solar:							
Central Tower	38.5/41	440/610	5.8/8.0	3.6/5.3	0.22/0.31	9.6/14	6.0-9.6/8.3-14
Solid Wastes	25/18	2,000/3,000	24/37	15/23	0.98/1.5	40/61	25-40/38-61

<sup>a</sup>The values given are for peak or full capacity conditions. To obtain annual averages apply a capacity factor of 70%.

<sup>b</sup>In all cases, the cooling system is assumed to be evaporative mechanical-draft towers.

<sup>c</sup>The efficiency values for the combined cycle, gas, and Geysers cases were borrowed from Ref. 10. The efficiencies for the Imperial, central-tower, and solid-wastes facilities were obtained from Refs. 11-13 respectively. In the Imperial case the lower and the upper values represent a binary-cycle system and a steam turbine design, respectively. The solar central-tower efficiencies represent a design similar to the planned facility at Barstow, California and a Martin Marietta design where the plant can operate 24 hours on certain days.

<sup>d</sup>Except for the Imperial facilities, all cases assume a 15°F condenser temperature rise. The Imperial designs assume condenser temperature rise of 23 and 29°F.<sup>11</sup>

<sup>e</sup>The evaporation rates for the combined cycle, gas, and Geysers plants are borrowed from Ref. 10. The Imperial values are from Ref. 11. The evaporation rates for the solar plants were calculated under the assumption that 90 and 85% of the heat discharged by the central-tower and solid-wastes facilities would be disposed of by evaporating water.

<sup>f</sup>With the exception of the Imperial plants, these rates were calculated on the basis that blowdown from the towers would contain 2.5 times the amount of total dissolved solids in the makeup water. The Imperial values are from Ref. 11.

<sup>g</sup>In all cases, drift rates are assumed to be 0.05% of the circulation rates.

<sup>h</sup>Except for the Geysers and Imperial steam facilities, the makeup is equal to the sum of the rates of evaporation, blowdown, and drift. In the Geysers and Imperial-steam designs the makeup is equal to the sum of the rates of evaporation and drift. The makeup rates represent the withdrawal rates.

<sup>i</sup>In all cases other than the geothermal types, the lower rates of consumption assume that the blowdowns are adequately treated before being returned to the original sources of water; these values are the sum of evaporation and drift losses. In the Geysers case, consumption is allowed to approach the zero value since the geothermal steam condensate is the cooling medium and since the reinjection of water at rates equal to the rates at which geothermal steam is withdrawn may not be considered necessary (to prevent land subsidence).

technical uncertainties cast some doubt over the effectiveness of this alternative in the near future.

#### Preparing for RIIA II

Efforts have been made to establish a data base and a methodology for making an integral assessment of the water availability and water quality implications for upcoming DOE scenarios. Because of the progress already made in the area of water availability the emphasis has been on water quality. The work accomplished covers both point and nonpoint sources of pollution. In the case of the point source pollution, data on steam electric power plant and petroleum refinery effluents have been obtained from the various regional water quality control boards and from the U.S. Environmental Protection Agency. These data will permit an estimation of the pollutant loading rates of both existing facilities and of future installations.

While efforts to control the pollution from point sources have been successful, the nonpoint sources remain largely unchecked,<sup>16</sup> and will soon be the major contributors of certain pollutants. Energy development could have profound effects on the course of this type of pollutant and on the

efforts to control it. A search is now being conducted to find ways for quantitatively linking certain types of nonpoint pollution with hypothesized energy activities such as those prescribed in a RIIA scenario. Because of the quality of available data and the importance of the problem itself, the contribution of transportation fuel-end use to urban runoff pollution has been selected for the initial efforts.

#### REFERENCES

1. Lawrence Berkeley Laboratory Energy and Environment Division, Annual Report, J. Kessel, Ed., Lawrence Berkeley Laboratory report, LBL-8619, July 1979.
2. California, Energy Resources Conservation and Development Commission, "California Energy Trends and Choices: Power Plant Siting (Vol. 7)," 1977 Biennial Report of the State Energy Commission.
3. California, Energy Resources Conservation and Development Commission, "Staff Proposed Electricity Forecasting and Planning Report, Vol. II," (October 1976).

Table 3. Cooling water requirements

State and County	Drift,* 1000G/D		Consumption,** MGD	
	1985	1990	1985	1990
<u>California</u>				
Contra Costa:				
Gas	0	130	0	3.3-5.3
Solar Solid Waste	0	88-140	0	2.3-5.5
Total	0	220-270	0	5.6-11
Humboldt:				
Gas	0	22	0	0.53-0.86
Imperial:				
Geothermal	790-1,100	940-1,300	62-65	73-77
Gas	0	19	0	0.47-0.76
Total	790-1,100	960-1,300	62-65	74-78
Lake:				
Geothermal	480	510	0-32	0-34
Los Angeles:				
Combined Cycle	25	25	0.63-1.0	0.63-1.0
Gas	0	120	0	2.9-4.7
Total	25	140	0.63-1.0	3.5-5.7
San Bernardino:				
Solar	4.4-6.1	26-37	0.12-0.27	0.72-1.6
San Francisco:				
Combined Cycle	59	59	1.5-2.4	1.5-2.4
Sonoma:				
Geothermal	270	420	0-18	0-28
<u>Nevada</u>				
Clark:				
Gas	0	37	0	0.92-1.5
Lyon:				
Gas	0	43	0	1.1-1.7
Storey:				
Gas	0	45	0	1.1-1.8

\*The concentration of total dissolved solids in the drift from the geothermal power plants is assumed to be 3 and 21 times that of the intake cooling water (Ref. 11). For the rest the concentration factor is 2.5. G/D is gallons per day.

\*\*The upper values represent the withdrawal rates. MGD is million gallons per day.

4. Southern California Edison Company, Energy Resources Conservation and Development Commission, "Supply Plans for Common Forecasting Methodology-II, submission of Southern California Edison Company," (March 1978).
5. San Diego Gas and Electric Co., "Response by San Diego Gas and Electric Co. to CEC Order on Supply Plan Forms and Summary of Loads and Resources," (March 1978).
6. Pacific Gas and Electric Co, "Pacific Gas and Electric Co. Electric Supply Plan Forms and Summary of Loads and Resources 1978-1998, Common Forecasting Methodology-II, Docket No. 77-EA-10," (March 1978).
7. California, Department of Water Resources, "Department of Water Resources Plan Forms and Summary of Loads and Resources, Common Forecasting Methodology-II, Docket No. 77-EA-10," (March 1978).
8. Sacramento Municipal Utility District, "Supply of Electricity for the CFM II Forecast 1978-1998," (May 1978).
9. Personal communication with Joe Fujimoto, Mechanical Engineer, Nevada Power Company, Las Vegas, on Jan. 29, 1979.
10. T. H. Pigford et al., "Fuel Cycles for Electric Power Generation," Teknekron, Inc., Energy and

- Environmental Engineering Division, Report No. EEED 101. P. M. Cukor, "Fuel Cycle for Combustion Turbine-Steam Turbine Combined Cycle Power Plant," Teknekron, Inc., Energy and Environmental Engineering Division, Report No. EEED 106, Berkeley, California (March 1975).
11. R. C. Robertson, "Waste heat rejection from geothermal power stations," Oak Ridge National Laboratory, ORNL/TM-6533 (December 1978).
  12. SANDIA Laboratories, "Energy report, Department of Energy large solar central power systems semiannual review," SAND 78-8511, UC-62 (November 1978).
  13. R. L. Ritschard et al. "Characterization of solid waste conversion and cogeneration systems," Final Draft Report (August 1978).
  14. California State Water Resources Control Board, "Water Quality Control Policy on the Use and Disposal of Inland Waters Used for Power Plant Cooling," (June 1975).
  15. J. D. Woodburn, "Use of reclaimed wastewater for power plant cooling tower make up," Unpublished paper, City of Burbank-Public Service Department, Burbank, California (January 1979).
  16. F. X. Browne and T. J. Grizzard, "Water pollution: Nonpoint sources," J. of Water Pollution Control Federation, 51, No. 6, (June 1979).

## THE DEVELOPMENT OF NUMERICAL METHODS FOR CHARACTERIZATION OF AQUATIC SYSTEMS DISSOLVED OXYGEN PROFILES

*M. Henriquez*

### INTRODUCTION

The recent passage of Public Law 92-500 has mandated strict water quality standards for much of the nation. As a result there has been increasing interest on the part of the water management community in methods which can simulate the impact that man made or natural actions will exert on aquatic systems. In the past, techniques for forecasting water quality phenomena have been based on predictive or deterministic methods. As a result of renewed interest in the field, there has been a realization that these methods, while adequate in the past, often fail to reflect complex synergistic relationships which increasingly characterize the nation's waterways. Simply put, the problem has often been the result of fitting linear models to essentially non-linear natural systems.

Many new approaches have been developed which take these factors into account. Often this new school of numerical analysis is characterized by a high degree of specificity in terms of the aquatic system to which the approach is applied. For example, recent efforts include one by Chandler<sup>1</sup> who developed a biological approach to water quality modeling by using a modified form of the standard diversity index calculation. Salis and Thomann<sup>2</sup> presented a simplified approximation of a three dimensional time variable system. This was based on reaction kinetics as described by non-linear theory. An important qualification of this approach is that it assumes steady state conditions in which a single nutrient is limiting. Hochman et al.<sup>3</sup> have developed a stochastic pollution model which was applied to dairy waste runoff into San Francisco Bay. It soon became clear that the wide range of approaches

and their concurrent underlying assumptions more often than not tended to limit the application of a given algorithm to a wide range of potential real world impacts. General methods, on the other hand, are useful for 'first cut' approximations but at the expense of reliability and precision.

### ACCOMPLISHMENTS DURING 1979

Clearly there is a need for numerical methods to possess sufficient incremental detail for application to a range of questions, while at the same time to provide reliable output in a form which allows intelligent decision making by those who may not be familiar with the intricacies of specific calculations. Such a model has been developed by the author during 1979. The purpose was to develop a quantitative methodology to assess the impacts of existing and proposed energy generating activity on adjacent water quality. It is based on the accepted role of dissolved oxygen (DO), and the biochemical oxygen demand (BOD) as basic quality indicators for natural systems. The algorithm is heuristic and reiterative. The results may be displayed as a two dimensional representation of a 3 variable interaction. This display option provides a useful and realistic picture of the interaction under study. At the same time it is compatible with newly developed techniques for energy analysis through matrix theory and interactive computer cartography.

The model assumes that in the base case natural system changes in dissolved oxygen are largely the result of photosynthetic oxygenation which is directly proportional to algal cell concentration

within the reach. The model is reiterative and utilizes the following procedure:

1. Calculation of maximum oxygen evolution rate in mg/l/hr,
2. Determine respiration coefficients,
3. Determine reaeration constants by means of the O'Connor-Dobbins formulation,
4. Use the results of steps 1 to 3 to determine net photosynthetic oxygenation, deoxygenation and the appropriate reaeration rates.

The results of step 4 are modified by inclusion of log based velocity terms which reflect specific reach flow characteristics. From this, one is able to determine an accurate expression for two dimensional dissolved oxygen levels. A rearrangement of terms provides an expression for the calculated maximum allowable BOD for which a given reach can self correct.

Having obtained this "first cut" result for oxygen parameters, it is desirable to elucidate the manner in which these levels change with respect to changes in the steady state. The second increment of the model involves solving a series of six sequential non-linear equations which provide an expression of DO levels in two hour steps. The terms of these equations may be altered to reflect conservative or non-conservative reach loadings. These might include thermal loading or chemical additives such as chlorine or alum. Using the values from the preceding steps in a modified version of the Streeter-Pheleps equation, an expression for reach specific aquatic productivity is obtained which reconciles the often observed difference between 5 day BOD levels and real world water quality for a particular reach.

Having completed these steps, the model provides an expression which relates the cost of treatment with respect to plant size and degree of pollutant removal. This expression is based in part on reach specific information provided as model outputs and on engineering data characteristic of the proposed treatment process. It allows examination of the variation in treatment cost corresponding with an alteration in ambient environmental quality.

The model was applied to the San Joaquin River. It was able to produce results to within 5% of measured values obtained from the STORET computerized environmental data base (see Fig. 1). This information was applied in an assessment of ambient water quality impacts resulting from the siting of a hypothetical conventional generating plant along a given reach. The resultant temperature profiles are shown on Fig. 2. A sensitivity analysis was carried out as part of the assessment procedure. Outputs from the model may be displayed as one variable in a three variable interaction (Fig. 3). As shown, a biomass removal factor is plotted against plant characteristics (capacity) and cost of treatment. From this interaction the impacts of alterations in aquatic environmental quality may be directly expressed in terms of the

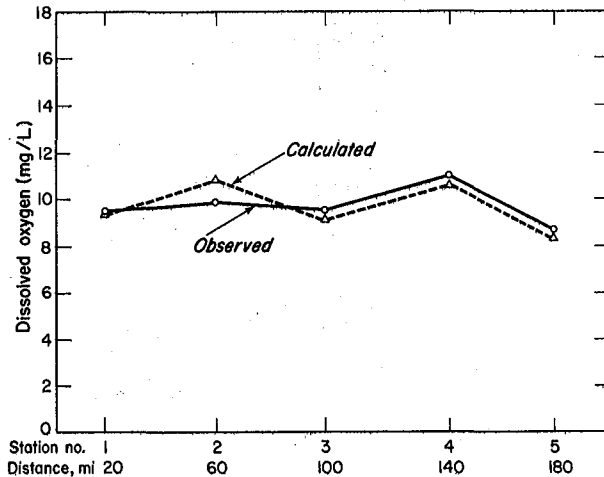


Fig. 1. Calculated vs observed DO levels in San Joaquin. (XBL 802-313)

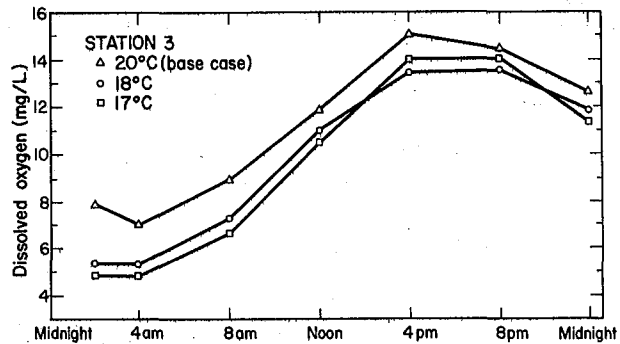


Fig. 2. Dissolved oxygen profile vs temp drop 5°C and alum coagulant addition. (XBL 802-314)

cost of compliance with existing or proposed water quality standards.

#### PLANNED ACTIVITY FOR 1980

The model developed here has the advantage of 'modular' construction. One is able to use parts of it to answer specific questions without neces-

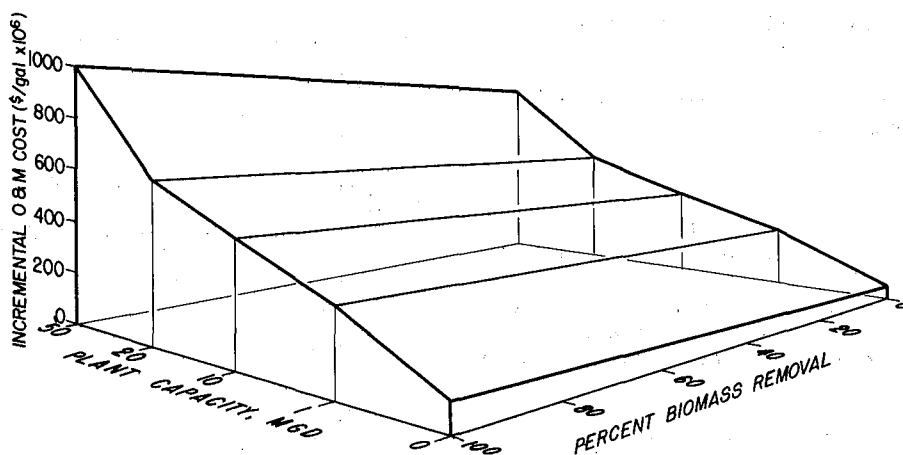


Fig. 3. Cost-treatment relations for photosynthetic oxygenation treatment processes where incremental cost to meet additional removal standards can be expressed  $1/r_1 - 1$ . (XBL 802-316)

sarily having to apply the entire model at once. The model is currently designed for application on fresh water aquatic systems.

The possibility of increasing model coverage even further by a more thorough treatment of the related engineering and economic factors is being studied. Additionally specific subroutines to address the flow and effects of pesticides are under study.

#### REFERENCES

1. R. J. Chandler, "A biological approach to water

quality management," Water Pollution Control Journal, 1970.

2. H. J. Salis and R. V. Thomann, "A steady state phytoplankton model of Chesapeake Bay," Journal Water Pollution Control Federation, December 1978.
3. E. Hochman, D. Zilberman, and R. Just, "Internalization in a stochastic pollution model," Water Resources Research, Vol. 13, No. 6, December 1977.

## REGIONAL ENERGY ISSUES: SUMMARY OF A WORKSHOP HELD AT LAWRENCE BERKELEY LABORATORY\*

*R. Ritschard and K. Haven*

#### INTRODUCTION

The Energy Analysis Program at Lawrence Berkeley Laboratory (LBL), under Department of Energy (DOE) sponsorship, convened a one-day workshop in Berkeley on January 19, 1979. The primary purpose of the workshop was to identify from various perspectives the important energy-related environmental issues relevant to California, Hawaii and Nevada. It was not intended that all energy-related issues nor all perspectives within the region would surface in so short a time, but rather that the issues foremost in the minds of the chosen participants would be identified and discussed. The participants represented the diverse views of state

energy offices and regulatory agencies, the public utilities commission, utility companies, local government, several public interest groups and DOE.

The workshop was divided into four sessions. The mid-range/mid-term energy supply scenario for 1985 and 1990 was used as a framework for the conference, since the discussion of issues required some point of departure. The energy projections of the "mid-mid" scenario are based upon the recent forecasts of domestic energy supply and demand by the Energy Information Administration within DOE. The projections were disaggregated at the county level for Federal Region 9, which included California, Hawaii and Nevada.

Following a brief presentation of the energy supply scenario, a brain-storming session was conducted to identify a list of energy-related environmental issues. This initial list was discussed by two working groups, each consisting of eight participants plus an LBL facilitator and recorder. The mini working groups provided a description and definition of each issue from the perspectives of the participants. Finally, the workshop reassembled in a closing session to integrate and formulate the regional perspectives in a free and open manner. During these discussions, no opportunity was presented for the participants to modify the original list of issues.

Eight general issues were identified at the Regional Workshop. Some of these issues have sub-issues either related to their geographic specificity or to the nature of the topic. The perspectives of the participants on each issue are summarized below. Finally, a series of multi-issue conclusions are presented.

#### ISSUES

##### Nuclear Power in California

- Diablo Canyon. Substantial environmental opposition to licensing and operation exists.
- San Onofre. Thermal discharge questions may delay licensing.

Several distinct perspectives were presented on both the licensing of the two planned nuclear expansions and on the more general issue of the use and expansion of nuclear power in California.

The consensus was that both nuclear stations currently under construction will be licensed. It is less certain that they will actually go on-line as substantial opposition still exists within California. In either event, no additional nuclear plants will be built in this region (California, Nevada and Hawaii) within the foreseeable future.

##### Geothermal Energy Development in California

- Imperial Valley. Environmental issues may arise as development expands.
- Expansion in Geysers Area. Substantial environmental and socio-economic opposition exists to current geothermal expansion paths into Lake and Mendocino counties.

Geothermal development in both the Imperial Valley and the Geysers region will most probably proceed at a cautious pace. All parties agree that extensive commercially viable resources exist in both areas. However, technical and political constraints will prevent widespread expansion over the near term.

##### Alternative Renewable Resource Technologies

- Less than one percent of the projected regional energy supply (1990) is attributed to renewable technologies.

Two distinct views were voiced concerning DOE support of renewable resource technologies. The first opinion was that DOE should greatly accelerate support of both development and commercialization of renewable technologies. The opposing view was that commercialization of any technology should be a function of the market place, not governmental policy. Neither view argues that solar technologies should not be developed. The issue is the rate of development and the respective roles of DOE and the private sector. It was agreed that the conversion of technologically feasible systems into "on-line" energy supplies is a major obstacle for solar technologies, and the federal government has little understanding of how to get a decentralized technology commercialized. Private and public sector cooperation will be required and it is unclear as to the role each should play in expediting the process.

##### Use of Natural Gas

- Increased reliance on natural gas is a reversal of past policies which shift from gas to oil and coal.

The discussion centered on the future need and source of California's natural gas. It was argued by some participants that the additional gas required to meet future needs would become available from fuel switching, conservation and increased domestic supplies resulting from price deregulation. On the other hand, some participants felt that increased use of natural gas will lead to increased imports requiring new pipelines and LNG terminals. Consensus was that an increased reliance on natural gas in this region could create substantial environmental problems if new sources and/or delivery systems are required. The primary issue is the siting of a LNG terminal especially related to who controls the siting decisions and where the facility is located.

##### Coal for Electricity Generation in California and Nevada

- Projections for coal use in California and Nevada were considered as unrealistic.

The major issue related to the use of coal in California and Nevada was that the mid-mid scenario did not reflect the current and future plans for electricity generation. In addition, there were several environmental areas perceived as possible impediments to future development of coal including air quality standards, transmission corridors and endangered species.

Energy Facilities Siting

- Conflicts exist between urban and rural siting of major energy facilities.
- Energy Imperialism. Local entities perceive a forced planning and siting of major energy facilities by federal governmental agencies.

No consensus was reached on these issues. The rural versus urban siting conflict is a major regional issue but does not directly involve DOE. The second issue includes important implications for federal energy planning. Local and Indian interest can influence the pattern of energy development in this region and therefore should be considered in federal energy planning and scenario development (bottom-up approach).

Conflict Between National Energy Plans and Regional, State and Local Environmental Goals

- Federal government does not always consider regional, state and local environmental goals, policies and regulations in planning national energy policy.

A theme that was expressed during the entire one day workshop was the need to incorporate regional, state and local information into the federal energy planning process. The "top down" planning process creates problems and antagonism at the state and local level with which the populace and governmental jurisdictions must live.

Institutional Issues

- Energy development is hindered by conflicts between regulations and regulators at local, state and federal levels.
- Energy development is delayed by the increasing amount of time required for a project to complete the regulatory process.

There was no consensus achieved on the resolution of these issues. It was agreed that additional effort by DOE to disseminate information to local public groups and potential intervenors and to increase involvement during the initial stages of energy planning (scenario development) will help. This type of involvement will bring the relevant parties, issues, and data into focus as soon as possible and thus minimize the potential for delays through last minute intervention.

## CONCLUSIONS

By definition, an issue is a matter in dispute. It was the purpose of this one day workshop to

identify the key issues confronting energy development in the region (California, Hawaii and Nevada). In addition to the issue-by-issue consensus reached by the participants, several general, multi-issue trends and conclusions were noted.

- There is a pervasive resentment of federal energy planning and intervention within this region. It was felt that the federal government has an obligation to support energy research and planning but this activity should be conducted at a state or local level. It is not appropriate for federal agencies to make decisions at a local level. They lack the site-specific data and perspectives required to produce effective, equitable decisions.
- There is a strong desire at the regional level to incorporate state and local planning into the federal planning process. However, there is a general lack of understanding of the mechanisms and contact points available to insert local concerns into the federal process.
- In general, the participants placed their emphasis on social and political solutions to issues rather than on technical ones.
- Significant intra-regional issues exist in addition to issues between regional and federal actors. Intra-regional issues are concentrated in the institutional and facilities siting areas.
- The general trends in regional energy development identified during the workshop are: 1) there is a high regional interest in solar/renewable technologies. Regional interest appears to be substantially higher than national in these technologies; 2) relative to other available fuels, e.g., fossil and nuclear, there are fewer major regional objections to expanded coal use; 3) no new nuclear facilities will be sited in this region in the foreseeable future; 4) expanded use of natural gas is desirable unless its use requires the development of new gas sources and delivery systems, e.g., LNG terminals, which can create substantial environmental impacts.

## FOOTNOTE

\* Condensed from Lawrence Berkeley Laboratory report, LBID-061 (June 1979).

## NATIONAL/REGIONAL ENERGY-ENVIRONMENT MODELING CONCEPTS: SUMMARY OF A WORKSHOP\*

*R. Ritschard, K. Haven, H. Ruderman, and J. Sathaye*

### INTRODUCTION

On May 30, 31 and June 1 Lawrence Berkeley Laboratory, under the sponsorship of the Office of Technology Impacts (OTI), U.S. Department of Energy (DOE), held a workshop at Reston, Virginia on national and regional modeling. The workshop entitled "National/Regional Modeling Concepts for Energy and Environmental Analysis" brought together 35 experts from a wide range of disciplines including energy and economic modeling and several aspects of regional sciences.

The purpose of the workshop was to identify and evaluate approaches to regional economic and energy supply/demand forecasting that are best suited to assisting DOE in the assessment of environmental impacts of national energy policies. Specifically, OTI uses models to assess the impacts of technology change, to analyze differential impacts of various energy policies, and to provide an early warning system of possible environmental constraints. Currently, OTI employs both a "top down" model system to analyze national scenarios and a "bottom up" assessment conducted from a regional perspective. A central theme of the workshop was addressing the problem of how OTI should integrate the so called "top down" and "bottom up" approaches. To aid in resolving that problem, the workshop was structured to examine the experience of many fields of regional analysis.

The format of the workshop provided a flexible structure emphasizing small working groups. The first day of the workshop consisted of a plenary session which began with presentations that described the DOE/OTI policy impact assessment program and its goals and problems. After a brief discussion period, several different perspectives on energy and economic modeling were presented. The aim of these presentations was to examine the modeling experience in several fields of regional analysis and to focus subsequent discussion by the subpanels. The organization for the remaining two days, including the composition of the working groups and their general topic area, evolved from the presentations and discussions on the first day.

During the second session the participants were divided into three subpanels which addressed specific topics related to the overall objective of the workshop. The topics of the subpanels were: measurement issues and approaches, structure of models, and the application of models to policy analysis. The working group members were responsible collectively for developing a list of recommendations on their assigned topic during a day-long discussion period.

The last day was a plenary session in which each working group presented the findings of its discussion on the previous day. An open discussion period followed each presentation and provided an

opportunity for further elaboration and refinement of the specific issues and recommendations produced by the workshop participants.

### SUMMARY OF WORKSHOP FINDINGS

The goal of the workshop was to identify approaches for integrating the top-down and bottom-up methodologies currently being used by DOE/OTI. Several major problems which would limit using such an approach in energy policy analysis, described on the first day of the workshop, were discussed on subsequent days by the separate working groups. The conclusions and recommendations of each group are presented in order to address the overall theme of the workshop.

A need was expressed for both top-down and bottom-up approaches so that all interactions in energy-economic-environmental modeling systems could be adequately represented. For the short-term, recommendations were suggested for improving the current OTI models, but most of the comments were directed toward the development of a new methodology. It was recommended that a core set of related models be developed that are modular, dynamic and consistent; that have inter-industry accounting framework; that have inter-regional linkages; and that have adequate documentation. Further, it was suggested that an advisory group be formed to establish the appropriate methodological framework of the model system.

With regard to data used in any policy analysis model, it was recommended that OTI develop and maintain an integrated system of economic, environmental and energy accounts which is coordinated with the statistical agencies that collect the data. It was further suggested that an independent group be established to oversee energy data collection, coordination and verification. OTI can play a major role in ensuring that the data it needs for policy analysis models is collected and compiled in a suitable way.

The basic discussion regarding the use of models in policy analysis centered on the need for state and regional involvement in the assessment process. It was suggested that the state act as the basic geographic unit. State involvement was encouraged for use in the siting and disaggregation processes as well as in the interpretation and evaluation of the impacts. Further, there were several recommendations presented to improve the design of the assessment program. These covered the areas of energy and economic scenarios, cost of environmental standards, and the appropriate time frame for conducting a given policy analysis. Finally, it was emphasized that a closer relationship should be established between the decision-maker, the model and the modeler in order to guard against misuse of the model results.

In conclusion, five major themes emerged from the individual working group recommendations. These overall concepts seemed to dominate the discussions and may serve as the main conclusions of the workshop. First, the top-down and bottom-up approaches to policy analysis are compatible and can be used in an integrated fashion. Second, the methodology suggested for the integration process should consist of a core set of linked basic models with other special purpose models for specific assessments. Third, the data and models used in this methodology require review, verification and validation by outside groups. Fourth, regional and state involvement

are necessary in any federal assessment process to enhance credibility and to increase accuracy. Finally, there is a need for a close relationship and communication between the decision-maker, the model and the modeler in order to maximize the proper use of the output.

#### FOOTNOTE

\* Condensed from Lawrence Berkeley Laboratory report, LBID-078, draft.

## CRITIQUE OF ENERGY INFORMATION ADMINISTRATION ENERGY SCENARIOS FOR REGION 9

*J. Sathaye and A. Usibelli*

### INTRODUCTION

Each year the Energy Information Administration (EIA) of the Department of Energy is required to present a detailed Report to Congress. A large portion of this report consists of energy supply/demand scenarios output by EIA's Midterm Energy Forecasting System (MEFS). These midterm scenarios, covering the period from 1985 to 1995, are designed to portray a range of possible energy futures based upon variations in energy production, consumption, price, and related parameters. Output from the system is presented both in the form of national level projections and as regional disaggregations.

### PROJECT OVERVIEW

The purpose of our study was to undertake a detailed examination of the MEFS output for Federal Region 9, (Arizona, California, Hawaii, and Nevada). The analysis is used by the Energy Information Administration as an aid in improving the quality of output from subsequent MEFS scenarios. LBID-133, "Region 9 Energy Supply Analysis", examined the supply component of MEFS in an effort to determine if the national forecasts for regional supply were in agreement with state and regional sources. Our analysis did not attempt to critique the models(s) used to derive the MEFS projections, but concentrated on the validity of the projections in view of regionally available information. Our work consisted chiefly of a search of energy supply literature published by agencies such as the California Energy Commission, the Hawaii Department of Planning and Economic Development, and a number of other public and private organizations. This material was supplemented by conversations with public officials and energy industry representatives.

Region 9 receives energy supply from a wide range of geographic sources both in and out of the region. Electricity is supplied from intraregional power plants and from imports from the Southwest and the Pacific Northwest. Oil is provided by indigenous California fields, Alaskan North Slope

supplies, and numerous foreign countries. Natural gas, although produced in small quantities in California, is transported via pipelines primarily from the Southwest and from Canada. Coal, mined in fields in Arizona and several Rocky Mountain states, supplies a small fraction of total energy demand. This diversity of supply sources will increase in the future. The analysis concentrated on six major energy conversion/energy supply areas: electricity, refinery operations, new energy technologies, coal, natural gas, and oil supply. As an example of the type of comparisons made between MEFS and regionally derived estimates, Table 1 presents the natural gas supply projections made by MEFS<sup>1</sup> and the California Energy Commission.<sup>2</sup>

### CONCLUSIONS

The Midterm Energy Forecasting System scenarios present a picture of increasing complexity in regional energy supply; however, our analysis found many of the specifics of MEFS scenarios in major disagreement with regional estimates. Some general conclusions of our report are:

- The MEFS supply projections for the region are overly optimistic. New electric generating facilities, refinery capacity additions, centralized new energy technologies (e.g. OTEC, STEC), crude oil from thermal enhanced recovery, and domestic natural gas supplies are from a few percent to many times greater than regional estimates.
- Price projections, especially for crude oil (a very significant parameter in the models) are underestimated by one-third or more.
- Regional supply projections are often based on outdated or erroneous information.
- Accurate supply (and demand) scenarios require much more careful consideration of regional level information.

Table 1. MEFS C-mid scenario projections (BCF/year)

Source	1985	1990	1995
Intrastate	238	275	304
NPC <sup>1</sup> 1N	245	245	332
NPC 1S	23	289	437
NPC 3	406	361	340
NPC 5	512	179	73
NPC 7	16	8	4
Other NPC 2, 2A, 4)	68	166	334
Canada	<u>418</u>	<u>418</u>	<u>25</u>
TOTAL	1,947	1,990	2,036

CEC<sup>2</sup> natural gas supply projections

Intrastate	117	73
El Paso (NPC 3, 5, and 7)	673	526
Transwestern (NPC 5 and 7)	106	107
Canada	348	73
Rocky Mts. (NPC 3)	37	62
PAC Interstate	<u>9</u>	<u>11</u>
Sub total	1,290	852
North Slope/LNG	220	365
Pan Alberta/Mexico	<u>77</u>	<u>131</u>
TOTAL <sup>3</sup>	1,587	1,348

<sup>1</sup>NPC = National Petroleum Council Regions

<sup>2</sup>CEC = California Energy Commission

<sup>3</sup>Total for California only. Supplies to Arizona and Nevada would increase regional projections by 10 to 15%.

## FOOTNOTE AND REFERENCES

\*Condensed from Lawrence Berkeley Laboratory report, LBID-133.

1. Energy Information Administration, Annual Report to Congress 1978, Volume 3.
2. California Energy Commission, Natural Gas Supply and Demand for California 1978-1990, p 180.

## ENERGY ANALYSIS BY MEANS OF COMPUTER GENERATED INTERACTIVE GRAPHICS\*

M. Henriquez

### INTRODUCTION

In an age where resolution of complex technical questions is characterized by the use of large data sets, informational display in the form of interactive computer graphics has become an increasingly valuable research tool. The advantages of cartographic output over alternatives such as a tabular format for selected applications have increasingly become clear.

The primary value of maps is their ability to display clearly a number of different variables and their distribution in a form which is accessible to those who are neither familiar with nor involved in the original research.

This is not to suggest that the use of maps has totally eclipsed tabular or graphical displays. On the contrary, for any hand manipulation of data or in other cases where absolute values are desired, tables are inherently superior to maps. However, by making use of both options, a more comprehensive picture can be presented than the use of either option alone would allow.

### GENERAL PROCESS DESCRIPTION

A collaborative effort by the Energy Analysis Program (EAP) and the Computer Science and Applied Mathematics Group (CSAM) at the Lawrence Berkeley Laboratory has resulted in a method for analyzing and displaying energy analyses. The software necessary for implementation has been undergoing various stages of development by CSAM over a period of years. The author, on behalf of EAP, has used the system extensively to accomplish his research objective.

The heart of the system is the Socio-Economic Environmental Demographic Information System, or SEEDIS, an integrated system of data manipulation and display similar to an earlier version stored at the laboratory's computer center. From an applications point of view, this approach has allowed runs to be made in a fraction of the time and cost that would have been incurred with conventional methods. As many as 23 separate maps of a federal region by county have been produced during an interactive session lasting about one hour.

It is helpful to examine the steps necessary to produce a color map by this new system. First, one enters the interactive SEEDIS monitor to select the area and geographic level desired. The result of this step is a geocode file, which is used in subsequent steps to extract the data automatically and interface the selected information with previously created base maps which reside in the system. Possible choices for areas include one or more federal regions, standard metropolitan statistical areas, census tract, counties or water quality control regions, among others. Population

limits on the desired area may be set at this time. It is possible to use either packaged data already installed on line as part of the SEEDIS monitor, or to insert original data to map onto the related geographic level. Examples of installed data bases include the Housing and Home Heating Characteristics data base developed by Brookhaven National Laboratory, the Federal Energy Regulatory Commission Electrical Generating Unit Reference File or the Populations at Risk to Air Pollution (PARAP) file. For example, data may be selected on the concentrations of specific airborne pollutants for the counties of California, along with information on death rates due to various forms of cancer for a given segment of the population. In some cases it is desirable to determine the ratio of two variables, and straightforward arithmetic subroutines are available for this purpose.

Having assembled the desired information, the user creates maps within SEEDIS, using the CARTE program developed by CSAM. The graphic files thus created are saved for additional processing, and are recorded on tape. The maps themselves are drawn by a Zeta plotter which is an output peripheral on the BKY system. Alternatively, the tape may be processed in such a way as to allow for cartographic output in the form of Dicomed transparencies. These transparencies are available in a variety of film formats and are characterized by intense color saturation and high resolution.

### PROCESS APPLICATIONS

This process has demonstrated its usefulness in applications where a number of variables interact in a complex or synergistic manner. One example is in the case of certain water quality treatment problems which are usually impacted by energy technologies. Previous work<sup>1,2</sup> has shown such interactions involving the degree to which a given waste stream can be treated, the cost of treatment, and the size of the treatment facility. For any given treatment system, there will be a specific number of plants which may be located in a county to meet a given level of treatment. In evaluating the applicability of a given treatment technology to a county, it is helpful to know the number of separate plants that such a county can support. Competing factors in the selection of plant sites include population trends, land use patterns, and ambient environmental quality. Cartographic displays are an ideal way to present these diverse information files.

The relationships of cost, degree of treatment, and size of plant may be displayed as a two-dimensional representation of the relationship between these three variables and would take the form of Fig. 1. If a three-dimensional matrix is superimposed on the design envelope shown in Fig. 1, it is possible to define equi-distant points within the matrix through or near which descriptive curves for any treatment system must pass. Each point may be identified by a code specific to its location in

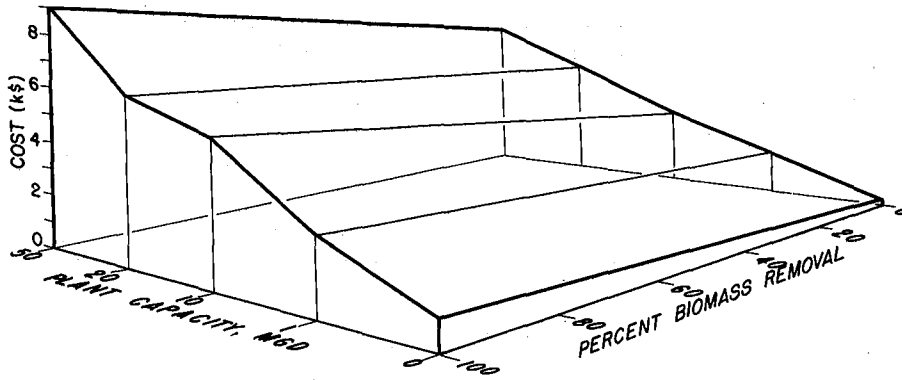
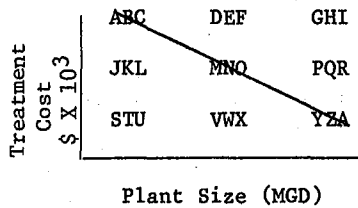


Fig. 1. Hypothetical relationship between cost, degree of treatment and size of plant for a photosynthetic secondary sewage treatment process. (XBL 802-315)

the matrix. Each location-specific code also identifies several frames of cartographic output which were constructed using data values valid for that point in the design space. By inputting two or more of the desired parameters (cost, degree of treatment, plant size) into a separate FORTRAN program, points in the matrix corresponding to points in the design curve are identified and the graphical information corresponding to the number of plants per county can be easily extrapolated.

For example, consider a specific treatment technology for which a linear relationship exists between the size of the plant and the cost of treatment over the interval of interest. Such a relationship may look like the curve pictured below and is shown in two dimensions for clarity.



By superimposing a variable matrix on the resulting design space, three points, namely ABC, MNO and, YZA, can be identified which are at or adjacent to the cost/size function. Location ABC may serve as the address for one or more frames of cartographic output; that is, it may define a unit of physical space on a data tape. This would show the number of treatment plants per county which may be sited if each of the plants operate within the extreme low range of plant size and the high range of treatment cost. The system described above may be expanded for three dimensions and would take the form shown in Fig. 2. This matrix is in the form for superposition over a design envelope.

This technique allows up to twenty separate frames to be stored per design point, or three variable addresses with the option of having each frame represent a multiple of the basic design space units. It is interesting to note that when the

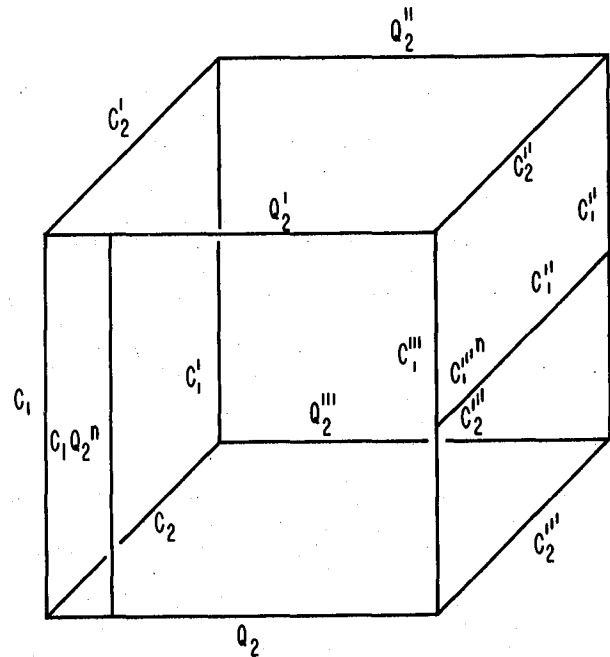


Fig. 2. Arrangement of individual addresses within a cartographic data storage matrix. (XBL 799-2867)

graphics data quantities are consistent with quantities derived from the characteristic engineering equations identified for a given system, proportionality between the engineering process and graphics data results. Because the maps themselves may be previously prepared, this system has applications in instances where users are lacking sophisticated computer skills. They need only identify system operation points to produce an array of the relevant cartographic data without actually constructing the maps.

PLANNED ACTIVITIES FOR 1980

Applications of the cartographic tools described in this paper are not restricted either

to water quality or energy related applications. Many fields can benefit from interactive graphics. Additional applications within the field of energy development impacts using the PARAP data base are anticipated for inclusion in FY 1980 regional assessment efforts.

#### FOOTNOTE AND REFERENCES

\*Presented at the 4th International Symposium on

Computer Assisted Cartography (Autocarte 4), Reston, Va, November 1979.

1. M. Henriquez, "The development of numerical methods for characterization of aquatic systems' dissolved oxygen profiles," unpublished draft (April 1979).
2. M. Henriquez, "Sewage and electronics," California Engineer, October 1977.

## THE HAWAII INTEGRATED ENERGY ASSESSMENT

*J. Weingart, A. Ghirardi, K. Haven, M. Merriam, R. Ritschard,  
H. Ruderman, J. Sathaye, L. Schipper, and W. Siri*

### INTRODUCTION

The Hawaii Integrated Energy Assessment is a joint research activity of the Energy and Environment Division's Energy Analysis Program and the Hawaii State Department of Planning and Economic Development (DPED). The overall objective of the project is to assess the opportunities for and impacts of displacement of imported petroleum by use of indigenous renewable and geothermal energy resources in Hawaii over the coming quarter century. DPED began its work on this activity in late 1978. LBL cooperative research began late July, 1979. This report covers work through the end of FY79 and outlines the work planned for FY80.

### BACKGROUND

Hawaii is dependent on imported petroleum for over 90 percent of its energy needs. The remainder comes primarily from the combustion of bagasse (sugar cane waste) in boilers for production of process steam and electricity. Total oil imports into Hawaii in 1977 were on the order of 40 million barrels or 8 GW(th), equivalent to roughly 1.5 percent of total U.S. oil imports (Table 1). Thirty-six percent of this is for jet fuel, which is not strictly considered a form of internal state energy consumption. The 1973 oil embargo was strongly felt in Hawaii and stimulated both public interest in and political commitment to development of Hawaii's seemingly abundant natural energy resources. A major element of Hawaii's energy policy

Table 1. Hawaii energy use, 1977.

	<u>10<sup>6</sup> bbl/y</u>	<u>GW(th)</u>
Jet fuel	14.3	2.88
Electricity	9.7	1.95
Other fuel	<u>15.6</u>	<u>3.12</u>
TOTAL	39.6	7.95

has been the goal of reduction of the state's extreme vulnerability to disruptions in oil imports.

The indigenous energy resources include abundant sunshine (average insolation of 250 watts per sq. meter over much of the state), the trade winds, biomass, ocean thermal energy gradients, and geothermal energy. Some advocates for the use of renewable energy systems in Hawaii have proposed twin goals of electrical energy self-sufficiency by the early 1990's, and complete energy self-sufficiency by the beginning of the next century.

It is widely agreed by analysts that the counties of Hawaii, Kauai and Maui (islands of Maui, Molokai and Lanai) could eventually become energy self-sufficient. However, 80 percent of the energy used in the state is consumed on Oahu, primarily in Honolulu. Energy independence for Honolulu, which in turn makes possible this goal for the entire state, will require a state-wide integrated energy system. This system would include inter-island transport of liquid fuels derived from biomass throughout the state, and possibly the electrical interconnection of some of the islands using undersea DC transmission cable. Existing cable technology would permit, for example, interconnection of wind energy "farms" on Molokai with Oahu; new technology would be required to permit use of Big Island geothermal systems as electrical sources for Oahu.

### Project Context

While the focus of our work is energy independence for the state of Hawaii, the context of this effort is both national and global. No industrialized region in the world yet derives a substantial fraction of its commercial energy needs from renewable energy sources. This is in contrast to the economies of the rural regions of the developing world, which are almost totally dependent on biomass fuels. Interestingly, the urban regions of the developing world are very similar to the urban regions of the industrialized nations in both their reliance on high quality chemical fuels and electricity, and in their overall power densities.

Hawaii could become the first industrial region to make the transition to major or even complete reliance on a mix of renewable and geothermal resources. If this occurs, Hawaii could serve as a prototype for other island regions with similar energy resources (e.g., Puerto Rico, Micronesia, the Indonesian archipelago, etc.). We regard Hawaii as a potential "pathfinder" for the large-scale use of renewable energy resources for commercial energy production in both industrialized and developing tropical regions of the Pacific Basin, the Caribbean and elsewhere.

The implications are also important for the United States. The eventual large-scale use of renewable energy technologies for production of chemical fuels and electricity in the U.S. will require integration of these technologies into large, interconnected electrical networks and fuel systems. Hawaii seems likely to play a major role as a showcase and proving ground for development and test of renewable energy technologies. The technologies appropriate for Hawaii include biomass fuel production, and systems for production of electricity from wind, OTEC, photovoltaics, solar thermal electric systems and geothermal energy. Solar and geothermal energy can also be used as sources of process heat. Domestic solar water heating is already a well-established commercial activity in Hawaii. In a few decades, solar thermochemical and/or electrolytic production of hydrogen, and subsequent production of carbonaceous liquid fuels, may be technically and economically practical. By this route, Hawaii could eventually produce sufficient liquid fuels for all its energy needs, including those of jet aircraft.

#### Project Objectives

The objective of this joint research is to examine dispassionately the potential opportunities and costs associated with a transition to major or full independence of imported petroleum for the entire state through the use of indigenous energy resources. In particular, we are attempting to describe the evolution of an integrated energy system for production of electricity and chemical fuels over the coming 25 years. Other possibilities include importation of coal and/or coal-derived liquid fuels from Australia, Alaska, and the U.S. mainland. However, these are not being considered in this study due to funding constraints. The specific project objectives include:

1. Development of several scenarios for demand for electricity and liquid fuels by county, for the period 1980-2005.
2. Development of a scenario(s) for the transition to major reliance on indigenous sources of liquid fuels and electricity.
3. Characterization of the technical, economic, environmental and other aspects of a number of energy supply technologies essential for such a transition, including
  - solar water heating
  - hot water heat pumps

- wind energy conversion for utility applications
- solar thermal electricity
- photovoltaics
- liquid fuels from biomass
- ocean thermal energy conversion
- geothermal electricity and process heat
- solar process heat
- deep (2000m) undersea DC transmission cables
- utility scale stationary battery systems

4. Calculation of the impacts of the supply scenario(s) on the labor sector, the environment and the state economy.

#### ACCOMPLISHMENTS DURING 1979

The initial efforts, carried out during the three month period of July-September, 1979 were aimed at developing a set of useful and Hawaii-specific technology characterizations for specific technologies, for creating a set of 25 years energy demand forecasts, and for a preliminary set of indigenous energy supply scenarios.

#### Technology Characterizations

Technology characterizations for solar water heating, wind energy systems, and biomass fuels in Hawaii have been completed and documented in a set of LBL reports now in press.<sup>1-5</sup> Additional characterizations for geothermal energy, OTEC, solar thermal electricity and photovoltaics are underway; technical reports on these will be completed in the first quarter of CY80. Additional technologies, including advanced stationary battery systems for utility applications and deep (2000 meter) undersea DC transmission cable technology, will be examined during CY80.

Some preliminary conclusions based on the technology characterizations completed to date are relevant. First, the potential role of solar water heating appears to be limited by competition from the hot water heat pump, which can displace similar amounts of electricity at a third or a quarter of the capital cost of domestic solar water heating systems (the latter costing over \$3,000 for single family applications, before tax credits are applied). In any case, the ultimate displacement of total energy by solar water heating and heat pumps combined is only a few percent of the state's energy demand.

Second, the only solar electric technology available to utilities in commercial form in the next few years is large scale (multi-MW) wind generators. At expected installed costs of \$1,000 per kW(e) or less, operation in a good wind regime (capacity factor of 0.3 to 0.5) permits displacement of oil for power generation. With a fixed charge rate of 0.15, the levelized busbar cost of electricity from wind generation would be equivalent to displacement of oil in the range of \$20 to \$35 per barrel. In the event that the installed costs of wind machines could, in mass production (several hundred identical units per year) be reduced to \$500 per kW(e), oil would be displaced

for an equivalent cost of \$10 to \$18 per barrel. Thus, in a utility system which is completely reliant on imported petroleum, partial displacement of oil by wind appears to be an economically and technically attractive option now, although the need to establish technical reliability and actual installed costs will inhibit massive installations of such systems for several years.

Third, any fuel-free technology capable of producing electricity from the sun at costs of under \$5,000 per average kW(e) must be considered a serious contender. Such technologies include photovoltaics, solar thermal electric plants, ocean thermal energy plants (OTEC) and certainly geothermal plants, perhaps even future advanced systems designed to harness the energy in magma.

Solar thermal electric systems are projected to have capital costs (in current dollars) ranging from \$1,000 to \$3,000 per kW(e) at a 0.5 load factor in ideal sunny areas. With a 0.15 fixed charge rate, this corresponds to displacement of oil in the range of \$20 to \$60 per barrel. Some capacity credit is also possible. However, the European and American prototype STEC facilities coming on line in the next two years will cost \$10,000 to \$20,000 per kW(e). Commercial production of affordable plants seems unlikely before the early 1990's, and there is much less certainty than in the case of wind that economically interesting plants can really be produced. Nonetheless, the option appears potentially interesting for Hawaii.

Photovoltaic systems have systems goals of \$1,000 per PEAK kW(e), equivalent to roughly \$4,000 per average kW(e) in Hawaii. This corresponds to displacement of oil at \$40 per barrel, and some capacity credit can also be assumed, depending on the extent of photovoltaic implementation. The cost goals are expected by those active in the photovoltaic field to be reached by the mid-80's. Again, we will not really know until the mid to late 80's what the commercial and technical characteristics of fully commercial photovoltaic power systems will be. As with STEC, the high conversion efficiency of the system makes photovoltaics an attractive option for a sunny, land-constrained region like Hawaii.

Geothermal energy is available primarily on the Big Island of Hawaii. The potential production rate is estimated to be in the range of 500 MW(e) to 2,000 MW(e). More exploration is required to determine this. Uncertainties in the lifetime for a plant built in the Big Island rift zone and the lack of large markets for electricity on the Big Island will constrain both the rate and scale of geothermal development. DC cabling to Oahu will require new cable technology which may be available late in this decade or early in the next.

#### Energy Demand Projections

An Energy Demand Forecasting Model was developed by DPED and subsequently modified through joint LBL/DPED efforts. This tool is an econometric-based simulation model designed to generate annual consumption forecasts of various fuel types for each of the four counties in Hawaii, through the

coming 25 years. The model comprises a set of equations that relate the demand for energy to price, income, and other endogenous economic and demographic variables. Using forecasted values of the endogenous variables, the model forecasts energy consumption under the assumption that the coefficients in the equations will not change over the forecast period. The projected demands are then modified to take into account conservation measures such as anticipated improvements in appliance efficiencies and automobile gas mileage.

The model operates on a data base of historical time series data on the consumption and price of electricity, utility gas and liquid fuels. The data base also contains historical and projected data on demographic and economic variables such as population and income, visitor arrivals, and consumer prices. Prices for gasoline and imported oil were taken from the Department of Energy's series C forecasts. Electricity rates are generated internally in the model.

Such a model has its greatest utility when the future is expected to be much like the past. However, the unprecedented rise in oil prices and the rapid emergence of concern for conservation and increased energy efficiency requires modification of the model output. We have conducted an initial inquiry into the potential impact of increased energy efficiency on projected demands for various fuels and for electricity, whether from imported petroleum or from harnessing indigenous energy sources, will be much more expensive than energy savings through increased efficiency. An integrated energy strategy for Hawaii requires intensive efforts at conservation and improved efficiency coupled with development of indigenous energy resources.

The econometric forecasts for electricity and gasoline consumption were modified to take into account anticipated improvements in gas mileage and appliance efficiencies. No improvements in airplane efficiencies were assumed, since the new generation of widebody jets coming into service in the 1980's (e.g. Boeing 757, 767) will not have the range to service Hawaii. Estimates of the national average automobile fleet fuel efficiencies were based on the Energy Policy and Conservation Act of 1975. The efficiency is assumed to increase from 13.1 mpg in 1978 to 21.1 mpg in 2005, a 61 percent improvement. The gasoline consumption for each year as forecasted by the model was modified by a savings factor derived from the mileage estimates to provide the total consumption. For electricity, demand was disaggregated and modest estimates for improved efficiencies (Table 2) were used to obtain total electrical sales for the coming 25 years.

Figure 1 shows the substantial reduction in projected electricity demand due to improved efficiencies. We expect that substantially greater savings are possible with a state-wide aggressive and cost-effective conservation program. Figure 2 demonstrates the enormous savings possible in gasoline with improved vehicle efficiencies. The possibility of reducing by roughly a factor of 2 the projected gasoline consumption at the end of the

Table 2. Honolulu County conservation factors.

	End Use Percentages	Reduction Factors for Projected Years		
		1985	1995	2005
<b>Residential Rates</b>	<b>100.0%</b>			
Lighting	8.0	90%	80%	80%
Heating and Cooling	(see misc.)			
Water Heating	40.0	80	50	25
Frost-free Refrigeration	16.0	87	71	57
Electric Cooking	15.0	90	80	80
Dryer	8.0	90	80	75
TV-Radio	5.0			
Dishwasher	3.0	90	80	75
Miscellaneous	5.0	95	90	90
<b>OTHER RATES</b>				
Lighting	29.7%	80%	75	70%
Miscellaneous	8.4	90	80	80
Pumping	5.2			
Cooling	31.7	80	75	70
Commercial Refrigeration	8.2			
Motors	5.8			
Water Heating	3.8	80	65	65
Frost-free Refrigeration	1.6	87	71	57
Cooking	1.4	90	80	80
Dryer	.8	90	80	75
Communication	2.5			
Radio and TV	.5			
Dishwasher	.3	90	80	75

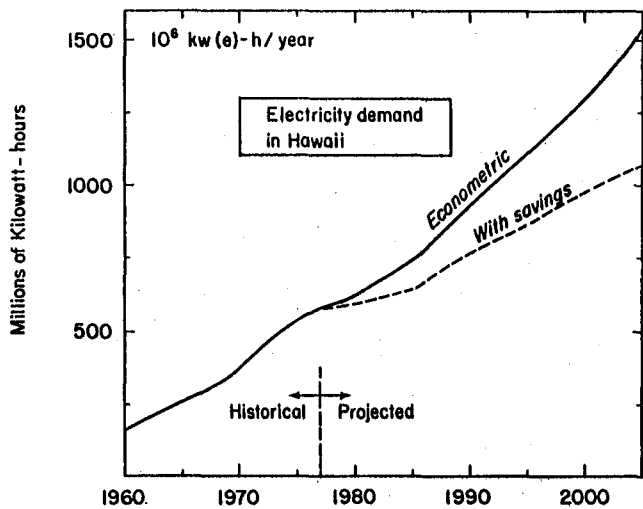


Fig. 1. Electricity demand in Hawaii. (XBL 7912-13144)

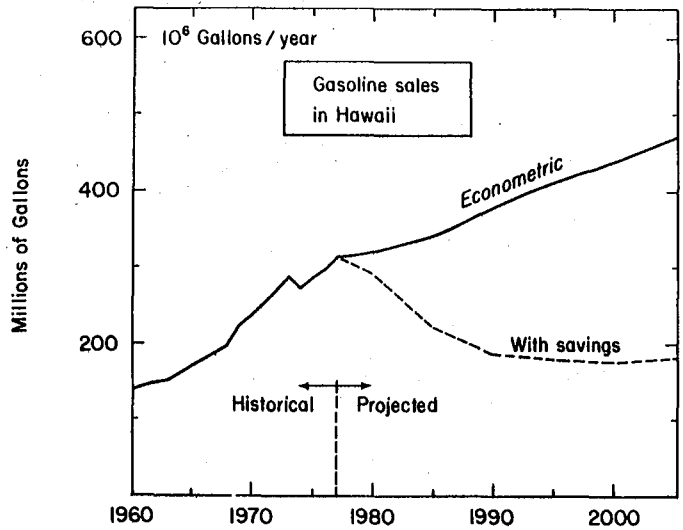


Fig. 2. Gasoline sales in Hawaii. (XBL 7912-13145)

centruy is significant. It permits, in principle, the entire fuel requirements for ground transport to be provided by a biomass fuels industry in Hawaii. The unrestricted growth in demand for gasoline leads to a demand level which cannot, due to limits of available land and overall efficiency in production of biomass fuels, be met by a local fuels industry. Thus, conservation and improved efficiency will change Hawaii's energy situation in a qualitatively significant manner. Figure 3 shows projected demand for jet fuel. There is no way in which a biomass fuels industry in Hawaii could supply a substantial fraction of this demand. In the absence of high efficiency fuel production techniques (e.g. solar thermochemical or electrolytic production of hydrogen and liquid fuels), the jet fuel or its precursors must come from outside the state.

#### PLANNED ACTIVITIES FOR 1980

A one year continuation of the work (through 1980) has been funded by DOE for \$170K, split equally between LBL and DPED. The major effort will be to develop a set of scenarios describing possible indigenous integrated energy systems which could be in place in Hawaii in 2005, and the paths for getting from here to there. Some preliminary assessment has been conducted during 1979. It is not possible to predict the future course of energy system evolution in Hawaii, availability of computer-based forecasting and other tools not withstanding. Our approach has been to identify to the extent possible the timetable for commercial development and the maximum rate of market penetration possible under various circumstances for the relevant energy technologies. In addition, we have compiled much of the available data on the extent and character of the various geophysical and biophysical resources in Hawaii. Preliminary scenarios have been developed for the maximum possible rate and scale of deployment of a number of technologies, including geothermal electricity

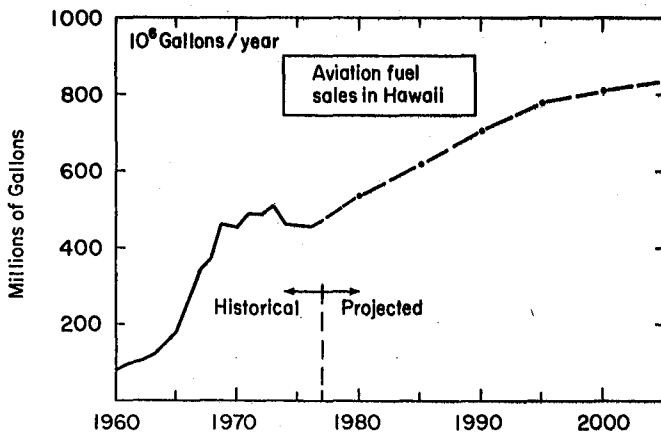


Fig. 3. Aviation fuel sales in Hawaii.  
(XBL 7912-13143)

on the Big Island, OTEC, wind energy systems, biomass fuels and solar water heating. Details appear in a forthcoming set of reports on the technologies<sup>1-5</sup> and on the project itself.<sup>6-7</sup> The scenarios are being developed through a series of workshops in which experts from industry, state and county agencies, the Hawaii Natural Energy Institute, the University of Hawaii, the utilities and elsewhere participate. Families of scenarios for the various technologies are emerging due to the dispersion in individual perspectives and assumptions. Our purpose in this process is not to attempt a forced convergence, but rather to display the range of possible futures over which informed individuals disagree. Making explicit this dispersion is an essential step in providing an informed basis for decision-making in Hawaii, and emphasizes the risk associated with premature foreclosure of options of large energy supply potential.

In addition, energy demand forecasts will be revised to take into account improved energy efficiency and conservation in a more detailed way than possible during the initial studies. Institutional issues associated with inhibition of stimulation of the large-scale use of indigenous energy resources in Hawaii will be examined, and the results of the entire research program presented to both specialists and the general public through an "outreach" program.

#### REFERENCES

1. M. Merriam, "Solar water heating in Hawaii," to be published (1980).
2. M. Merriam, "Wind energy studies for Hawaii - a concise review," to be published (1980).
3. M. Merriam, "Wind electric generation equipment - the present situation," to be published (1980).
4. M. Merriam, "Potential role of wind energy systems in Hawaii," to be published (1980).
5. A. Ghirardi and R. L. Ritschard, "Liquid fuels from biomass in Hawaii," Lawrence Berkeley Laboratory Report, LBL-10328 (1980).
6. J. Weingart et al, "The Hawaii integrated energy assessment - Phase I progress report," Energy and Environment Division, Lawrence Berkeley Laboratory, Berkeley, CA (1980).
7. J. Muller, "The Hawaii integrated energy assessment," Department of Planning and Economic Development, Honolulu (1980).

Note: References 1-4 will be published as LBL reports in conjunction with the Hawaii Integrated Energy Assessment. Additional technical reports will be published by members of the HIEA team during the course of 1980.

## ASSESSMENT OF SOLAR ENERGY WITHIN A COMMUNITY: SYNOPSIS OF THREE COMMUNITY-LEVEL STUDIES\*

*R. Ritschard*

### INTRODUCTION

The Office of the Assistant Secretary for Environment of the Department of Energy through its Division of Technology Assessments initiated a comprehensive project in mid FY 1978 relating to the extensive use of solar energy technologies. The project, entitled "Technology Assessment of Solar Energy Systems" (TASE), will determine the long-range environmental and socioeconomic impacts of solar energy systems. Since local or community impacts (e.g. land use, institutional requirements, etc.) may be greater than state, regional or national impacts with regard to solar technologies, a series of community level studies were initiated.

The overall purpose of the community level studies is to investigate the range of impacts of various solar-based energy systems on community environment, both physical and social. The studies also identify issues and constraints to local and regional deployment of decentralized solar technologies. The community level studies are divided into three task areas:

1. community impact analysis,
2. threshold impact analysis, and
3. solar city and state analysis.

The major findings of each study are presented in the subsequent sections followed by the general conclusions that emerge from the individual community-level studies.

### COMMUNITY IMPACT ANALYSIS<sup>1</sup>

This study examines potential impacts of decentralized solar technologies on the physical structure of a community, that is, on its physical, spatial and land use characteristics. Land use types representative of those found in most U.S. cities were analyzed for the residential, commercial and industrial sectors according to the high solar use scenario, 14.2 quads of energy in the year 2000. Six different solar energy supply systems were examined, including thermal collectors of today's design and output with both short-term and long-term storage, thermal collectors with a 33 percent increase in efficiency using reflectors for both short-term and long-term storage, and cogenerating photovoltaic arrays with short-term and long-term storage.

Specifically, the analysis examines:

- the maximum on-site collector area for each land use type in the residential, commercial and industrial sectors;
- the land-use impacts likely to occur when achieving the scenario goal;
- characteristics of the natural and man-made environment which would effect the ability

of the community to rely on decentralized solar energy technologies; and

- the percentage of each parcel's total on-site energy demand that could be provided by each solar technology.

The study team concluded that the high solar use scenario for the year 2000 is achievable without significant physical impacts. The decentralized technologies can, in many cases, produce substantially greater amounts of on-site energy supply than projected.

Only one land-use type, the commercial central business district, could not achieve solar goals on-site. The deficits, however, can be offset by the ability of other land-use types to supply increments of solar energy in excess of the levels projected. The team also concluded that low density single-family development (i.e., urban sprawl) is not required to meet the high solar scenario, but that industrial users in the central city would need to use cogeneration and biomass resources in addition to direct solar technologies to meet the high solar use projections.

The following activities were discussed as achieving a solar supply greater than that projected:

- use of long-term storage and cogenerating systems;
- use of shared energy systems including combined storage;
- transfer of surplus thermal and electrical energy to land-use types deficient in on-site solar potential;
- control of land development patterns eliminating characteristics that constrain on-site collecting; and
- the removal of 15 to 35 percent of the tree canopy in residential areas using on-site thermal collectors.

### THRESHOLD IMPACT ANALYSIS<sup>2</sup>

The second community study examines potential community-level institutional impediments to the implementation of the dispersed solar technologies by the year 2000. The SRI team formulated a prototypical city of 100,000 population and projected a high solar use scenario to meet residential, commercial and industrial solar heat and electrical loads for the city. The team identified the institutions most likely to be involved with solar installations (utilities, financial institutions, community planning groups, construction industries, environmental protection organizations, special consumer groups, and legal and insurance interests) and described the complex ways they must interrelate

to achieve the high solar use scenario by the year 2000. Also described was an array of institutional problems which can be expected to develop, in different degrees in different parts of the country, when solar technologies are implemented. This study provides background information from which national level policies can be formulated to achieve national solar energy goals.

Study findings are described in terms of two formats. The first uses three time frames to describe delays caused by the inherent difficulties a national energy policy would encounter in changing the ways in which community institutions respond to decentralized solar technologies. The second approach describes community-level difficulties associated with implementing each solar technology.

Three groups of institutional barriers were defined. Those barriers potentially causing 10 or more years delay concern:

- the rate of adoption of solar technologies by residential and commercial building industries;
- the rate of public and local government acceptance of new aesthetic standards;
- resolution of the legal issues of solar access easements, and the use of public funds for solar technology installations.

Other institutional barriers specified as more amenable to policy influence than those noted above, are in the 6 to 8 year impediment category and concern:

- financing;
- utility involvement with residential solar technology;
- cooperative neighborhood-scale installations; and
- the application of cogeneration technology.

Finally, in the 3 to 5 year delay category are barriers to solar technology development which are the most amenable to resolution including:

- performance warranties for complete solar installations;
- liability insurance for solar architects and engineers;
- solar technology standards;
- interfaces between solar technology owners and utilities;
- retrofit markets for homeowners;
- utility developments to accommodate solar owners for back-up service;
- small-scale distribution grids for cooperatives or neighborhoods;

- building performance applications as alternatives to building codes and specified insulation ratings;
- innovative planning at the community level;
- life style changes; and
- maintenance of a viable solar industry.

The second format describes the difficulties associated with the implementation of each solar technology. These include the complexity of installing approximately a million new solar space and hot water units and a million solar retrofits a year to reach the high solar use goal, and the extent to which utilities will be willing and permitted to participate in the installation, maintenance and control of solar equipment. The institutional impediments and problems of implementation for larger scale technologies such as wind energy conversion, biomass conversion, photovoltaics and solar thermal were also briefly described and are similar to those found for solar heating and cooling. Included are problems of financing, siting, environmental hazards, legal and regulatory issues, and gaining the cooperation of planning agencies and local utilities. The SRI study team used all of these findings to emphasize the need for a strong federal policy on energy and solar technology to implement a strong national energy plan.

#### END STATE ANALYSIS<sup>3</sup>

The third community study investigates the structure of a typical community as it would appear in the year 2025 under varying solar growth scenarios, and examines the potential impacts on the physical form, environmental quality, socioeconomic structure and quality of life.

The UCLA team analyzed a hypothetical city of 100,000 after a period of growth based on three different energy scenarios:

- Future 1 specifies that 6 percent of the city's energy needs are met by solar technologies;
- Future 2 is based on 25 percent of the city's energy being supplied by solar technologies, where the city is dependent upon imported electricity;
- Future 3 represents a hypothetical city that is built to maximize the use of solar energy technologies.

All three scenarios are identical in terms of population and land use, goods and services produced, and energy demand and consumption. The hypothetical city was designed to reflect the median characteristics of existing U.S. cities, including prototypical building types in the three sectors, residential, commercial and industrial. Transportation energy use was excluded from consideration. The energy supply scenarios identified the energy supplied by each solar technology and the end-use demand for each building type.

The study concluded the following:

- For all three solar futures, there would be potentially no significant increase in environmental impacts.
- The major noticeable aesthetic impact would be considerable increase in the amount of roof space covered with solar collectors.
- In Futures 1 and 2, all on-site energy requirements for the residential, commercial and industrial sectors could be met.
- In Future 3, the commercial sector would require the doubling of photovoltaic arrays and an additional 650 acres of land to be energy self-sufficient.
- In Future 3, the industrial sector could collect 18 percent of its energy needs on-site, but would require an additional 2800 acres of land to meet all of its energy needs.
- In Future 3, if the land area of the city were increased 34.5 percent, all three sectors of the hypothetical city could be energy self-sufficient. The resulting energy self-sufficient city of 13,450 acres would still be less than the median area (14,780 acres) of 23 existing U.S. cities of approximately the same populations.

## CONCLUSIONS

Several general conclusions emerge from the individual community-level studies. Even though each task area used a different study methodology and format, the results provide some generalized trends that should enrich the overall TASE analysis. The conclusions are related to the scenario and study assumptions and should be viewed as illustrations of potential opportunities and impacts and not as projections of a likely urban future.

### Land Use Impacts

The first general conclusion is that a community can meet the on-site energy demands assumed by the scenario in all but the most dense land-use sectors (e.g. central business district). In the residential sector, however, this may require removal of 15 to 35 percent of the tree canopy. Further, it may be required that greater than 80 percent of the total area in the industrial sector and about 50 percent of the available commercial parking area be covered with solar collectors.

### Community Expansion

Secondly, decentralized solar technologies can produce substantially greater amounts of on-site energy supply than was prescribed by the scenario. Greater solar development can be realized by using "shared neighborhood systems" and by employing passive design in all new buildings. As evidenced in the hypothetical "solar city" (Future 3), a community may become self-sufficient if the commercial sector is allowed to expand by 65 percent and the industrial sector by over 400 percent.

### Institutional Impacts

A third conclusion is that various institutional impediments produce time delays in achieving acceptance of solar technologies within the structure. Most important among those barriers are the acceptance and adoption of solar by residential and commercial building industries, the legal issues of solar access, easements and use of public lands for solar installations, and the aesthetic concerns of the public and planning agencies. In order to meet the levels of on-site solar collection that are prescribed in this study, these impediments must be removed.

### Building and Urban Design

A fourth general conclusion is that passively designed buildings in future residential, commercial and industrial sectors need not look different from existing versions that consume up to 25 times more energy. However, the overall appearance of a community with a high level of solar development resulting in large collector areas, tree removal, and community expansion may be quite different based on current urban design and aesthetic criteria.

### Community-Level Planning

There are great opportunities for implementing decentralized solar technologies within a community. This implementation will require the integration of urban and energy planning at the local level in order to avoid potential aesthetic, institutional and land use impacts.

### Federal-Level Planning

Although decentralized solar technologies can be implemented within a community with few environmental impacts, a new set of issues are created at the local level which federal policy makers are not accustomed to addressing. These issues may be quite different than those raised by the utilization of more conventional centralized types. Therefore DOE should recognize that different approaches may be necessary when dealing with decentralized and centralized energy systems.

### FOOTNOTE AND REFERENCES

\*Condensed from R. Ritschard, "Assessment of Solar Energy Within a Community: Summary of Three Community-Level Studies," US DOE, OTI, October 1979.

1. A synopsis of "Community level impacts of decentralized solar technologies," University of California, Berkeley, Robert Twiss, Principal Investigator (1979).
2. Synopsis of "Community impediments to implementation of solar energy," SRI, International, Marilyn Duffey-Armstrong and Joe Armstrong (1979).
3. Synopsis of "Three solar urban futures: Characterization of a future community under three energy supply scenarios," Urban Innovations Group, University of California, Los Angeles, Murray Milne, Marvin Adelson, and Ruthann Corwin (1979).

## UTILITY SOLAR FINANCE: ECONOMIC AND INSTITUTIONAL ANALYSIS

E. Kahn

### ACCOMPLISHMENTS DURING 1979

One generic approach to accelerating the widespread adoption of residential solar technology is the use of public utilities as financial intermediaries. Although substantial tax credits currently exist which might induce consumers to invest in solar technology, their effect has been limited. Tax credits have more value to upper income groups than to other classes of consumers as evidence shows that credits have been utilized to a greater extent by this group than by the population as a whole. Public utilities, on the other hand, offer a number of advantages as a vehicle for the widespread commercialization of solar technology in the residential sector. These include access to high-volume, long-term capital; an existing collection mechanism; an incentive to minimize long run marginal costs; and credibility in the energy marketplace.

Analysis of the role public utilities might play in the commercialization of solar technology has normative and positive aspects. The normative question is: should regulated utilities be allowed a role in the solar market? What are the dangers to society of such policies? The positive aspects center on the institutional arrangements and implementing mechanisms necessary to implant the desired utility role. The residential solar market does not exhibit the economies of scale that normally justify regulated monopoly. Moreover, there is the perception in some quarters that utilities would distort the solar market by their disproportionate influence. The anticipated dangers range from a tendency to over-price the technology to the opposite fear that they will subsidize it excessively from other operations.

Various regulatory arrangements are possible to limit the dangers of utility involvement in the solar market. Most of these dangers center around how the role of "ownership" for solar technology is different from that of central station power plants. Efficient use of residential solar technology depends on adaptation to localized, site-specific conditions. Utility investment in conventional plant and equipment benefits from standardization. Ordinary utility investment procedures may lead to inefficient solar installations. This kind of potential distortion can be remedied by limiting the utility role to financial mediation with a local solar contractor industry. Such a limitation also would tend to reduce unjustified cross-subsidization from other utility operations.

Constructing a solar finance program for a particular utility will require explicit consideration of local conditions. This can be seen most clearly when the question of utility subsidies for solar finance is considered. Because many residential solar applications are less expensive than their conventional alternatives, it is reasonable to allow some of these savings to be passed along

to the solar user. One widely accepted criterion that can be used to evaluate the appropriate size of utility subsidy is the marginal cost minus the average cost limit. This criterion will protect the interests of utility customers who do not participate in a solar finance program. Accepting this for the moment, it becomes clear that each utility will have a different situation with regard to marginal costs, average costs, and their difference. Other local conditions must also be considered. These include economic factors affecting solar costs (local wage rates, utility tax policies, etc.) and climatological factors affecting solar performance and the durability of equipment.

The regulatory specification of a utility solar finance program is further complicated by demographic mobility. Most solar systems require at least ten, and more commonly, twenty years amortization to be cost-effective. Yet the average family changes place of residence every five or ten years. How should a finance program be structured to account for this fact? This is not a problem under ordinary utility capitalization. The cost of the solar system would be part of the rate-base, to be paid for by all rate-payers, regardless of whether the occupant of a given dwelling with solar changed or not. If the new occupant did not want a solar system for some reason, he need not move in to such a dwelling. Accepting the solar system as part of the dwelling would impose no cost on the occupant other than what he already bears as a rate-payer. Since ordinary utility capitalization of residential solar systems may be excluded for normative reasons, we must consider how a financing program might deal with demographic mobility.

Conventional finance involves the specification of an interest rate and an amortization period. It might be possible in particular circumstances to justify a subsidy to utility sponsored loans that would reduce the amortization period to the average turnover time of housing occupancy. If this is not possible, some arrangement must be made to liquidate the loan at the time of turnover or to provide for the new occupant to assume the unpaid balance. Since the latter alternative would place significant barriers on the transfer of property, it is likely to be opposed by the real estate industry if not the market at large. A particularly imaginative solution to this problem is embodied in the residential weatherization program adopted by the Pacific Power & Light Co. (PP&L). This program provides zero-interest loans to single-family homeowners for weatherization investment. The carrying costs of this capital investment are borne by the rate-payers as a whole. This subsidy passes the marginal cost minus the average cost criterion. When such dwellings change hands, the original owner liquidates the loan, and that amount is removed from the utility company rate base.

The PP&L plan was designed for conservation investment. Since the economic advantages of solar

applications are typically less compelling, there is a question concerning the feasibility of such programs for utility solar finance. To investigate this question, a case study was made of the Pacific Gas and Electric Company. The results of that investigation showed that while solar hot water heating could be expected to be less expensive than the marginal cost of electric water heating, the appropriate subsidy criterion could not be met for a zero-interest loan program. By comparison, utility finance of weatherization for electrically heated houses passes the test easily. The result for solar hot water heating does not bar a utility finance program. One method for retaining the

features of a PP&L-type program is to average solar hot water in with conservation. Such a program meets the appropriate subsidy test.

#### PLANNED ACTIVITIES FOR 1980

Future work on utility solar finance will assess the impact of such programs on the financial position of participating utilities.

#### FOOTNOTE

\* Condensed from Lawrence Berkeley Laboratory Report LBL-9959

## LOCAL POPULATION IMPACTS OF GEOTHERMAL ENERGY DEVELOPMENT IN THE GEYSERS-CALISTOGA KGRA\*

*K. Haven, V. Berg, and Y. Ladson*

### REGIONAL BACKGROUND

The Geysers region is a subregion of northern California which contains large amounts of commercially attractive geothermal resource and the only vapor dominated geothermal field in the United States. The subregion includes the Geysers-Calistoga, Lovelady Ridge, Knoxville, Little Horse Mountain and Witter Springs KGRA's (Known Geothermal Resource Areas) and is located in portions of Colusa, Lake, Mendocino, Napa, Sonoma and Yolo counties about 75 miles north of San Francisco. The five KGRA's include roughly 420,000 acres with close to 380,000 in the Geysers-Calistoga KGRA alone. The bulk of the region lies in Lake County but most of the development to date has occurred in Sonoma County, including over 600 MWe in 13 units operated by the Pacific Gas and Electric Company.

### INTRODUCTION

A majority of the previous studies which have addressed geothermal development in the Geysers area have focused on the characteristics of the resource and its potential for generating electric power. A second series of studies (principally EIR/EIS's) have addressed in detail the environmental and socio-economic impacts of the construction and operation of a single plant. However, little effort has been put forth to assess the potential effects associated with enactment of a long term development scenario.

A major study program with this objective was developed by DOE. The program has been conducted through the regional DOE office (the San Francisco Regional Office) and through Lawrence Livermore Laboratory (LLL), the lead laboratory for geothermal energy assessments, and has included an initial overview program and a series of follow-on assessments.

An umbrella research plan for socio-economic impacts was developed by LLL to provide a compre-

hensive response to the issues identified by the overview program conducted during FY 78. This multi-year umbrella study plan identified research tasks in all areas of socioeconomic concern and is built on collaborative LLL/LBL efforts.

LBL undertook one element of this program during FY 79. The central goal was to assess county level population impacts resulting from probable future (1979-2000) geothermal energy development paths. LBL task efforts included the development of electric and non-electric geothermal scenarios, the evaluation of existing county population growth trends, and the estimation of geothermal impacts on those growth trends.

### GEOTHERMAL DEVELOPMENT SCENARIOS

#### Electrical Energy Production

The electrical scenarios developed for this study were conceived in a top down manner. Regional electrical production goals were forecasted based upon previous analyses and a set of scenario assumptions. Resulting totals were apportioned to counties as a function of KGRA potential,<sup>1,2</sup> and of existing development and drilling patterns.<sup>2</sup> Assumptions were made concerning the future split of steam flash hot water and binary hot water systems. Steam plants were limited to the existing steam field. System cost differentials were used to phase binary and flash systems into production as the steam field approached capacity. All scenarios recognized ongoing development activities and forecasted development as a function of a series of variables including energy price, water availability, activity in other geothermal areas, and ultimate capacity of the steam field, among others.

Two scenarios were selected for analysis: one describing a rapid geothermal growth rate, and one describing a slow growth rate. On line capacities for these scenarios are shown in Figs. 1 and 2. From the total capacities shown on these

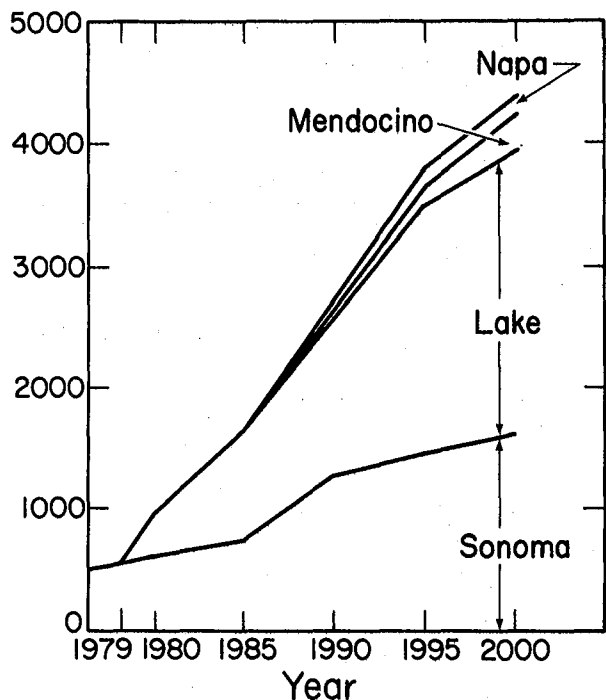


Fig. 1. County level capacity for the high growth scenario. (XBL 7911-13317)

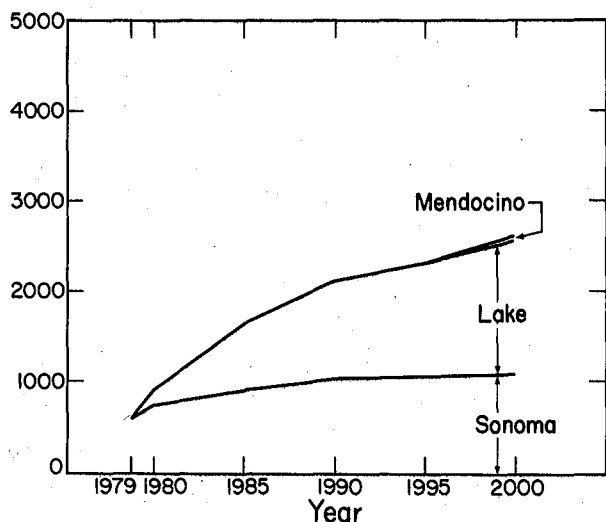


Fig. 2. County level capacity for the low growth scenario. (XBL 7911-13316)

figures, annual capacity additions, individual plant additions, and associated plant construction schedules and field development schedules were calculated. Data were obtained to describe industry employment patterns,<sup>3,4</sup> and total annual employment rates for the geothermal industry were calculated.

Sector multipliers calculated by PG&E for Lake County<sup>3</sup> were used to estimate indirect, or induced employment within the regional economy

associated with geothermal development. Total employment (direct plus induced) was calculated for the region (see Fig. 3) and for the individual counties. The number of new jobs available each year was calculated and the portion of these available for non-residents (in-migrants) was estimated. Thus annual in-migrant workers and total in-migration rates were calculated for each scenario for use in population impact assessment.

Non-Electric Energy Development

Direct (non-electrical) applications of geothermal energy were investigated for the Geysers region. Successful operations in other areas have shown some potential for creating new jobs in geothermal resource areas. Direct uses were investigated from the viewpoint of the demographic impacts which might result from new employment opportunities. Direct-heat applications of geothermal energy which have the greatest potential for use in the Geysers area, including geothermally-heated greenhouses, crop drying, refrigeration systems and space heating were investigated.

While the opportunities for extensive direct use of geothermal resources in the Geysers region exist, direct-use applications have several characteristics which may result in a slow rate of market penetration. The most important of these is the requirement that the user be located at or very near the geothermal well site. Transportation and market location thus become important issues for the relatively remote geothermal resource areas. Other barriers to direct uses include the high capital cost of the systems, the depth of the local geothermal reservoir, the hard volcanic rock in the Geysers region, and a need for technology transfer to potential users.

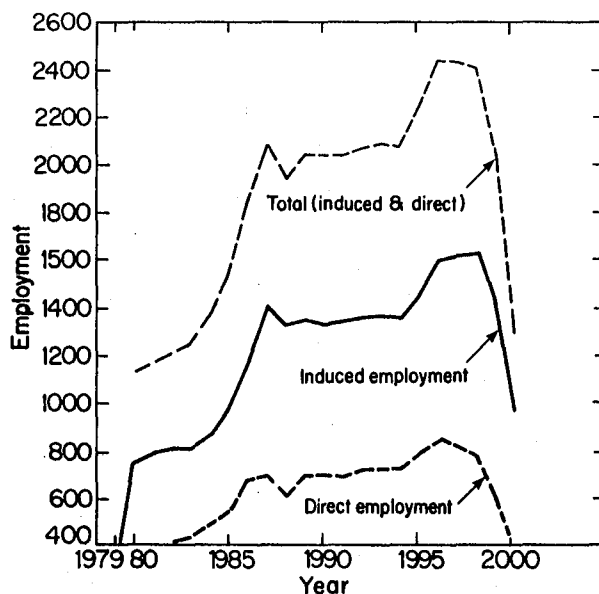


Fig. 3. Regional direct and induced employment for the high growth scenario. (XBL 7911-13315)

From the viewpoint of this study, an important characteristic of most direct uses is that they are capital-intensive and not labor-intensive. The result is that from 2 to 20 people may be employed for a few months to install the equipment, but very few, if any, permanent employees will be needed to operate and maintain the equipment.

In a probable development scenario, the first major uses of geo-heat in the Geysers region will be the retrofitting of existing public and private activities to use geothermal energy. In these cases, no additional (induced) jobs are likely to be created from the use of geothermal heat. A second stage of development will be the relocation of businesses into the Geysers region to take advantage of the geothermal resource. With the sole exception of greenhouse crop production, most businesses which could economically relocate to the rather remote geothermal area are small scale employers.

Under this scenario, both direct and induced employment opportunities created by direct use in the Geysers region are expected to be limited. A net increase in the order of 30 full-time employees in any one of the counties may be expected within the 1990-2000 time frame.

#### POPULATION IMPACTS

Net immigration figures (direct and indirect employment plus dependents) associated with the

high and low growth rate geothermal development scenarios are shown in Table 1. These immigration figures were added to forecasted county immigration rates for a "no geothermal activity" case and used to drive the State of California Department of Finance (DOF) population forecasting model.<sup>5</sup> This model is a county level cohort-survival model and is used for all state population projections.

Five runs were made on the DOF model for each county within the region: a "no geothermal" run, runs including only direct geothermally related immigration for both the high and low scenario, and runs including both direct and indirect immigration for both the high and low scenario.

The overriding general conclusion of the study is that geothermal energy development will not create major county level population impacts. Major specific conclusions of the study include:

- The course of geothermal development over the next five years appears to be relatively fixed and is not significantly affected by the major variables used in this study.
- The development of new employment opportunities within the geothermal industry occurs primarily when development first begins in a county. Subsequent capacity expansions tend to draw from the same labor pool with few expansions of the total in-county direct labor force.

Table 1. County level net immigration caused by projected geothermal development.

Year	Low Growth Scenario				High Growth Scenario			
	Lake	Sonoma	Mendocino	Napa	Lake	Sonoma	Mendocino	Napa
79	522	744	0	0	524	743	0	0
80	520	558	0	0	697	858	0	0
81	225	-111	0	0	337	-125	0	0
82	159	-44	0	0	230	-68	0	0
83	103	-41	0	0	182	-16	0	0
84	-17	-9	0	0	326	21	0	0
85	-28	28	0	0	182	229	51	0
86	-38	-82	0	0	328	142	313	0
87	-57	-59	0	0	255	101	109	0
88	43	-96	0	0	139	33	57	0
89	49	-78	0	0	103	-53	57	0
90	-52	39	0	0	50	-77	10	25
91	-94	83	0	0	-76	-16	-32	271
92	+10	49	0	0	-9	-13	82	187
93	-28	-58	0	0	24	39	82	-58
94	80	-41	19	0	-62	155	44	-91
95	-18	-44	198	0	4	102	258	-32
96	-1	0	109	0	117	-18	161	153
97	-2	-8	-76	0	-36	-28	128	187
98	-69	0	-44	0	-23	31	64	-57
99	-11	0	-34	0	-133	-76	-124	-88
2000	-135	0	-16	0	-322	-230	-245	-51

- After the initial surge of immigrants is over, geothermal construction activity fluctuations are likely to produce a net out-migration in a county in any given year as it is to cause a net immigration.
- While both are small, the indirect labor force expansion and associated in-migration is substantially larger than that of the direct labor force.
- Direct use of geothermal energy may cause a few key industries to expand but the overall direct and indirect population impacts will be very small.
- The county appears to be an inappropriate scale for the identification of demographic impacts from geothermal development. Sub-county geographic units (e.g., Cobb Valley) or individual communities appear to be the scale on which impacts may be felt.
- Any immigration impacts from geothermal development have already occurred in Sonoma County, are nearly complete in Lake county,

will probably occur in the late 1980's in Mendocino County, and will occur after 2000 if at all in Napa County.

#### FOOTNOTE AND REFERENCES

\*Condensed from Lawrence Berkeley Laboratory report LBL-10150 (draft)

1. USGS, "Assessment of Geothermal Resources of the United States," United States Geological Survey, Circular 790 (1978).
2. F. E. Goff, J. M. Donnelly, J. M. Thompson and B. C. Hearn, "Geothermal prospecting in the Geysers-Clear Lake area, Northern California," Geology, 5, No. 8, (August 1977).
3. L. Vollintine, L. Kunin and J. Sathaye, "The Lake County economy: Potential socio-economic impacts of geothermal development," Lawrence Berkeley Laboratory, LBL-5944 (1977).
4. D. Hill, California Energy Commission, unpublished data provided through personal communication, June 1, 1979.

## CONSERVATION STRATEGIES FOR COMMUNITY COLLEGES

*B. Krieg and C. York*

### INTRODUCTION

In FY 1978 a pilot project to develop strategies for energy conservation was carried out with five Community Colleges in Northern California. The strategy was based on a program, called TEEM, which had been used by PG&E in K-12 schools in the Fresno area.

In the Total Educational Energy Management (TEEM) system of energy conservation and management, each campus building and activity is considered as a unique system which uses energy to fulfill the specific needs of educational programs. The TEEM system, flexible by design, provides a framework within which the campus community can systematically consider and implement a great number of effective energy-saving practices.

The TEEM system has two basic objectives:

1. Reducing campus energy requirements, and
2. Meeting those reduced energy requirements without adversely affecting the quality of educational programs.

Initially the TEEM system is a labor-intensive approach which required the commitment and participation of all segments of the campus community. The faculty, student body, administration, staff and governing board must be organized into an effective team to analyze and implement energy-saving measures.

The TEEM approach provides this essential organization of the campus community.

To begin the process, the president of the college must adopt the concept of an energy management program. Once the president is willing to commit his institution to such a management program, he must take two actions. First, he must request his governing board to declare, as a matter of policy, that energy conservation on campus will be a high priority. Second, he must appoint an "Energy Conservation Task Force", which is representative of all segments of the campus, to develop and carry out a program for conserving energy on the campus.

Following this simple start, the pilot project was able to demonstrate a "cost avoidance" of \$300,000 in the utility bills of the five campuses involved. Table 1 shows the detailed savings for each school. DOE asked LBL to establish a national program in FY '79 and '80 to attempt to achieve similar results across the country.

### ACCOMPLISHMENTS DURING 1979

If the results of the five college pilot projects could be equaled by all 1230 two year colleges in the U.S., then an annual savings of about 1/30 of a Quad, or  $33 \times 10^{12}$  BTU per year could be anticipated. To achieve this, LBL was asked to launch its national effort at a special workshop of the National Education Business and

Table 1. Program Summary: Energy and dollar savings.

From: Budget year April 1976 - March 1977  
 To: March 1977 - April 1978

College	Diablo Valley Community College	Indian Valley Colleges	College of Marin	Santa Rosa Junior College	Sierra Community College
<u>Electricity</u>					
Savings (KWH x 10 <sup>6</sup> )	1.083	1.300	0.776	0.317	1.382
Use '77-'78	9.604	2.611	5.986	4.489	4.333
Savings (BTU x 10 <sup>9</sup> ) Thermal Fossil Fuel Equivalent	11.10	13.31	7.94	3.25	14.16
<u>Gas</u>					
Savings (Therms x 10 <sup>3</sup> )	6.850	-19.88	193.3	87.95	131.6
Use '77-'78	52.65	82.80	468.0	356.0	227.4
Savings (BTU x 10 <sup>9</sup> )	0.685	-1.988	19.33	8.79	13.16
Total Cost Avoidance	\$47,140	\$57,550	\$75,790	\$32,830	\$97,400
Fuel Cost '77-'78	\$414,580	\$141,600	\$371,700	\$273,140	\$260,890
Percentage of Total Fuel Cost	11.4%	40.6%	20.4%	12.0%	37.3%

Labor Conference on Energy-Related Vocational and Technical Training, Employment and Public Awareness, which was held in Washington in January 1979. The plan was to collaborate with one of the national organizations of the community colleges. The work was to be divided by having this organization serve as the contact with the colleges and LBL would provide data analysis and similar technical support functions. The League for Innovations in the Community Colleges in Los Angeles was chosen as the organization and in March of 1979 contacted all 1230 two year colleges to invite them to join in the project. 304 colleges from all over the country have agreed to participate. In October of 1979 these participants are to submit data on their utility bills from the previous years, 1978-79, and

the first six month period of the operation of their TEEM program of energy conservation. 128 colleges have actually submitted this data.

#### PLANNED ACTIVITIES FOR 1980

The first six months of data will be analyzed and reported to the participating colleges. Computer programs to calculate energy savings and cost avoidance from the submitted data have been written and are in operation. In March 1980 the colleges will submit their utility bill data to determine the effectiveness of their campus programs. We hope to publish the results of these analyses in the Summer of 1980.

# INTERNATIONAL RESIDENTIAL ENERGY CONSERVATION

*L. Schipper*

## INTRODUCTION

The Lawrence Berkeley Laboratory has begun to collect and analyze data on residential energy use for seven countries (Canada, France, West Germany, Italy, Japan, Sweden and the United Kingdom) as part of a project sponsored by the Energy Information Administration. The purpose of the project is to improve our knowledge of future energy demand and conservation opportunities in other countries, as part of our effort to understand the dynamics of the demand for internationally traded fuels, like oil (see Ref. 1 for related analyses).

The first paper in this project, "International Analysis of Residential Energy Use and Conservation," (LBL-9383), was prepared as a preliminary discussion of work done through the summer of 1979. The paper is published in the proceedings of the Second International Conference on Energy Use Management (Pergamon Press, 1979). The paper describes the general problem of analyzing residential energy use in different countries.

## PROJECT OVERVIEW

Residential energy use is analyzed in terms of both a vector of end use activities (e.g., cooking, space heating or cooling, etc.), each of which is measured in physical terms, and of energy intensities that express the energy requirements at the point of use for each unit or activity (Table 1). Additionally, the analyses are segregated where possible by fuel type, though an aggregation will be made at the end of the project. In addition to gathering data on specific energy uses, the first two work tasks included the collection of basic economic and demographic data. Economic data, such as personal disposable income or consumer expenditures, are important for understanding the economic forces that have driven the demand for residential energy use. Demographic information on housing (particularly the size and structure of the housing stock) and population characteristics are very important for quantifying the demand for space conditioning. Thus far we have assembled details of the housing stock, including the size of typical multiple and single family dwellings for many years throughout the study period.

By examining changes in both the structural factors and in energy intensities, the role of each kind of factor in contributing to changes in energy use can be quantified. Additionally the potential for conservation through reductions in energy intensity can be evaluated, and energy uses can be projected based upon a very disaggregated model of demand that takes saturation, conservation, and the effect of energy prices and policies into account. Finally, the relative importance of all the factors that shape energy demand in various countries can be compared. Table 1 lists some of the major energy demands that are being investigated, and gives both measures of intensity sought,

and the structural components relating to economic activity and, where appropriate, to lifestyle or behavior.

Some of the factors that are more easy to quantify include a measure of heating degree days (though conventions vary from country to country), income, house size, indoor temperature (as inferred or measured saturation of appliance stock, and energy prices. Some of the more difficult factors to quantify, or factors for which data is difficult to obtain, include appliance utilization, appliance prices and actual sizes, and the actual split between heating and non-heating uses of fuels.

Indeed, the quantification of each end use has specific problems. When calculating space heating requirements, it is desirable to know the contribution of non-heating appliances (people, the sun, other appliances, and hot water) to the heat balance of the house since extremely well built houses replace most of their heat losses from these sources. In a related project,<sup>2</sup> the factors that account for space heating and conventions for measuring them are discussed. Even though cooking now represents a relatively small energy end use, it is desirable to know the relative intensities of electric and gas stoves, the number of meals eaten in the home, and the nature of a country's cuisine in order to really understand this use of energy. Hot water, however, usually ranks second to space heating for total energy consumption but is relatively poorly understood. In some cases, estimates were found of hot water consumption (in liters/year) and temperature, enabling a careful estimate of energy intensity to be made. In most cases, however, we had to settle for a measure of the average amount of fuel used per device, and the number of devices of each kind in each home as a measure of hot water energy use.

Appliances have been a growing end user of energy with the rise of personal incomes in the study countries between 1960 and 1975. Though there is important evidence of saturation in the ownership of some major appliances (e.g., refrigerators, televisions and clothes washers) in the near future, others (freezers, clothes dryers and dishwashers) are still relatively unsaturated. Utilities have kept relatively detailed statistics on appliance ownership, and some information on appliance size is available. Furthermore, in every country, estimates of unit consumption for each kind of machine are available. Typically these estimates can account for 90 percent of the residential electricity use.

## PLANNED ACTIVITIES FOR 1980

The project has completed the tasks of gathering and submitting economic and demographic data, though some holes in the information still remain. Present activity centers on analyzing the time series of consumption data, on comparing different estimates of end use consumption, and on making



## OVERCOMING SOCIAL AND INSTITUTIONAL BARRIERS TO ENERGY CONSERVATION\*

*C. Blumstein, B. Krieg, L. Schipper, and C. York*

### INTRODUCTION

Energy conservation is becoming an increasingly important response to the continuing energy supply crisis. A persuasive case can be made that conserving energy by increasing the efficiency energy using devices and practices is less expensive than finding additional new supplies of energy. Many energy conserving actions can, in fact, tend to maximize well-being and minimize sacrifice and social cost.<sup>1</sup>

Although they are economically rational responses to the energy crisis, energy conservation actions may be hindered by social and institutional barriers. In the research reported here we explored the nature of these barriers and examined some of the strategies that could be employed to overcome barriers. A more complete description of the results of our research can be found in a Lawrence Berkeley Laboratory technical report.<sup>2</sup>

### THE NATURE OF BARRIERS

Although barriers to energy conservation are not an altogether new topic for policy analysts,<sup>3</sup> previous studies have devoted very little effort to systematic study of the problem. Therefore, we began our effort by defining and classifying various types of social and institutional barriers to energy conservation. Six classes of barriers that occur regularly were identified:

Misplaced Incentives. The economic benefits of energy conservation do not always accrue to the person who is trying to conserve. For example, if an apartment tenant pays the utility bill, the landlord has little incentive to make energy conserving improvements.

Lack of Information. The efficient working of the market depends on the parties to transactions having adequate information. If a consumer is unaware of the cost effectiveness of a conservation measure, he is unlikely to adopt the measure.

Regulation. If a cost-effective conservation measure conflicts with existing codes or standards, its implementation will be difficult or impossible.

Market Structure. Even though a conservation measure or device is cost effective, it may not be on the market.

Financing. Energy conservation measures often require an initial investment; thus the unavailability of financing may be a barrier to some cost-effective measures.

Custom. If a cost-effective conservation measure requires some alteration in the habits of the consumer or seems contrary to some accepted value, such as being considered something that only people of low social status do, it may be rejected.

To gain further insight into the nature of barriers to energy conservation we conducted a series of interviews with people in the building sector: landlords and managers of residential property, managers, owners, and operators of commercial property; and other people connected with the buildings sector such as realtors, representatives of trade associations, and contractors. The interviews (reported in detail in Ref. 2) revealed a variety of views and perspectives. However, some common themes did emerge. A concern with costs was coupled with a lack of information on what the costs are and what the effects of conservation might be. The problem of misplaced incentives recurred in many forms.

### STRATEGIES FOR OVERCOMING BARRIERS

While our study of the nature of barriers did not provide a complete picture of the complex issues involved, we felt that it did provide a starting point for examining possible strategies for overcoming barriers. We identified six types of strategies:

Informing. Where lack of information is a barrier to energy conservation, actions can be taken to provide information in several ways. New information can be produced by sponsoring research; the flow of existing information can be facilitated by supporting libraries and indexing services; and information can be communicated directly to users by providing education and training.

Leading. Energy conserving behavior can be encouraged by leadership. This can be done by example such as the President turning down the White House thermostat, or by persuasion such as the familiar "Don't be Fuelish" advertisements.

Market-Making. A number of actions can be taken to create markets for energy-conserving products or services. Government purchasing policies can be directed toward encouraging the production of energy-efficient products. The government can also create markets in the role of entrepreneur, undertaking development and demonstration projects.

Rule Making. Regulations can be used to encourage or compel energy-conserving actions. For example, rules can require that all residential property be insulated before it is rented or sold.

Pricing. Government policies can influence the incentives to consume or conserve by changing the net price of energy or of energy consuming and conserving commodities. This may be done directly as a seller (of enriched uranium, for example) and by price controls, or indirectly through taxes and subsidies.

Rationing. In principle, the government can use rationing to conserve scarce resources by limiting consumption to some predetermined "correct"

value. However, in practice, rationing is usually used to allocate scarcity: when some commodity becomes scarce, and particularly when the scarcity is dramatic and sudden as in times of war, society may choose to ration the commodity in preference to allowing the price to rise.

In addition to identifying and describing strategies, we developed some criteria for evaluating them. These criteria were divided into two classes: those that relate to the efficiency of a strategy in achieving the goal of energy conservation, and those that relate to the impacts of a strategy on other (possible competing) economic and social goals. In the former class we included such factors as direct costs and benefits, political feasibility, ease of implementation, and leverage. In the latter class we included impacts on economic growth, income distribution, employment, land-use patterns, lifestyle, and individual freedoms.

#### RECOMMENDATIONS

We concluded our work with three recommendations for action directed at overcoming barriers to energy conservation:

Information Programs. We believe that lack of information is a serious and pervasive barrier to energy conservation and that enhanced information programs are one way to attack this problem. One area in need of increased support is the Energy Extension Service.

Demonstration Projects. Many of the possible actions which could be taken to overcome barriers to conservation have a high risk of failure. We believe that before such actions are taken on a national scale, they should be tested in local demonstration projects. The Federal government should assist such projects by providing financial support.

Further Research. The nature of barriers is still incompletely understood and sound systematic methods for evaluating strategies are not well developed. Further research is needed to provide greater understanding and improved methods.

#### FOOTNOTE AND REFERENCES

\*Research supported by the President's Council on Environmental Quality

1. L. Schipper and J. Darmstadter, "The logic of energy conservation," Technology Review, 79, pp. 41-50 (1978).
2. C. Blumstein, B. Krieg, L. Schipper, and C. York, "Overcoming social and institutional barriers to energy conservation," Lawrence Berkeley Laboratory report, LBL-8299 (1979).
3. B. Krieg, "Bibliography on institutional barriers to energy conservation," Lawrence Berkeley Laboratory report, LBL-7885 (1978).

## ENERGY POLICY DECISIONS AND CONSUMER DECISION-MAKING: APPLICATION TO RESIDENTIAL ENERGY CONSERVATION

*J. Corfee, M. Levine, and G. Pruitt\**

#### INTRODUCTION

The National Energy Conservation Policy Act (NECPA) mandates that Appliance Energy Efficiency Standards be prescribed by October of 1980.<sup>1</sup> The law requires that the Standards be designed to achieve the "maximum improvement in energy efficiency" that is "technologically feasible and economically justified." Determination of the economic justification must be based on: the savings in operating costs over the average life of the appliance compared to the increase in the initial purchase price or maintenance costs likely to result from the imposition of the standard; the economic impact of the standard on the manufacturers and the consumers of the appliances; the total projected energy savings likely to result directly from the imposition of the standards; and other relevant factors. Clearly, it is necessary to develop appliance standards that achieve minimum life cycle costs and to evaluate the total impact on residential demand resulting from the implementation of the standards.

The Appliance Efficiency Performance Standards (AEPS) project at LBL will analyze residential ener-

gy demand in support of the appliance standards as outlined in NECPA. The primary tool of the demand analysis will be the ORNL Engineering-Economic Model of Residential Energy Use,<sup>2</sup> which provides detail on the energy use of eight major end-uses by each of four fuel types in the residential sector. Primary in the model are the consumer decision making algorithms determining the saturation of new technology and ultimately the energy use of the appliance stock. Unfortunately, it is the consumer decision algorithms that are considered a major weakness and the least empirically validated components of the model. As a result, a specific research task of the AEPS project has been to improve the consumer decision algorithms of the ORNL model.

#### ACCOMPLISHMENTS DURING 1979

This paper describes the consumer decision research task. Specifically, two methods for improving the ORNL model are described, followed by a summary of preliminary analysis of the refrigerator market in the United States.

## Methods of Improving the ORNL Consumer Decision Algorithms

As previously noted, the consumer decision algorithms are a critical weakness of the ORNL model. Two methods of improving or creating new algorithms are detailed here. The first approach represents an attempt to discover the average effective discount rate used by consumers in their appliance purchases. Ultimately, changes in the average effective discount rate over time indicate the response of consumer decision making to changes in fuel prices. The second approach is an attempt to determine econometrically a meaningful consumer decision algorithm. Both methods focus on the importance of operating costs versus the purchase price in consumers' decisions to buy an appliance.

### Method 1

The first method of discovering consumers' average discount rate is a straightforward life cycle cost calculation. However, there is an assumption that the purchase price of the appliance is a function of the product energy efficiency. It is precisely this assumption to which the refrigerator analysis, described in the next section of the report, is devoted.

A simple form of the life cycle cost equation is:

$$LCC = FC \pm \sum_{i=1}^N [(1 + f_e)/(1 + r)]^i \cdot E_u \cdot P_e \quad (\text{Eq. 1.a})$$

where:  $FC = f(E_u)$  for  $FC$ .

Substituting  $f(E_u)$  for  $FC$ ,

$$LCC = f(E_u) + \sum_{i=1}^N [(1 + f_e)/(1 + r)]^i \cdot E_u \cdot P_e \quad (\text{Eq. 1.b})$$

Finally the derivative of each side with respect to  $E_u$  is taken in Equation 1.c.

$$\partial LCC = \partial f(E_u) / \partial E_u + \partial \left( \sum_{i=1}^N [(1 + f_e)/(1 + r)]^i \cdot E_u \cdot P_e \right) / \partial E_u \quad (\text{Eq. 1.c})$$

$LCC$  = life cycle cost,

$FC$  = first cost,

$N$  = average lifetime of appliance,

$f_e$  = fuel price escalation rate,

$r$  = consumer discount rate,

$E_u$  = average annual energy use of appliance, and

$P_e$  = price of energy.

The minimum of the life cycle cost curve occurs when  $LCC / E_u$  is equal to zero. Therefore, the discount rate is determined by setting the right side of Eq. 1.c equal to zero and solving for the only unknown variable,  $r$ .

### Method 2

The econometric model, illustrated in Eq. 2, attempts to sort out the relative impact of purchase price (the coefficient  $\beta_2$ ) and energy use (represented by the coefficient  $\beta_1$ ) on the consumer choice of buying a certain type of appliance.

$$EMS/TMS = \alpha + \beta_1 (PVFS) + \beta_2 (P_e/P_i) \quad (\text{Eq. 2})$$

$EMS$  = the number of efficient models of the appliance purchased each year,

$TMS$  = the total number of models of appliances purchased each year,

$PVFS$  = present value of fuel savings (an average calculation of the fuel savings resulting from the purchase of the more efficient appliance),

$P_e$  = average price of the efficient models, and

$P_i$  = average price of the inefficient models.

The model uses ratios for the independent variable and one dependent variable so that any strange fluctuation in the market for a given year would affect both the efficient and inefficient. Furthermore, the model is flexible. That is, with additional data, more dependent variables could be included, such as advertising budgets, attribute vectors, and manufacturer reputation. The more complete the data, the more precise one can be in explaining consumer decision-making.

There are some shortcomings to this particular model. First, the approach requires an arbitrary definition of what is an efficient and inefficient approach. Second, there could be a major problem of multicollinearity. According to engineering research, the two independent variables should be negatively correlated in an exponential function (i.e., purchase increasing as energy use goes down).<sup>3,4</sup> If this relationship also exists in the market place, then the research must deal with the problems involved with multicollinearity. However, it is not at all clear how energy efficiency and purchase price are related.

### Refrigerator Analysis

Preliminary analysis indicates that the consumer is not provided with adequate information to make life cycle cost decisions. As this section will reveal, prices and operating costs of refrigerators are only slightly related if at all. In order to postulate that consumers consciously trade off first costs and operating costs (quantitatively represented by a discount rate), we must first demonstrate that consumers are aware of each set of costs and that their choices represent a consistent preference. Ideally, the consumer decision algorithm will capture the dynamics of appliance purchase decisions and the value or lack of value

placed on future energy costs with discount rate that changes over time.

The analysis of refrigerator sales was the logical precedent to an empirical testing of the methods described in the preceding section. Engineering-economic curves of the price versus operating cost always exhibit the trade-off in a negative relationship.<sup>3,4</sup> Thus, the objective of the refrigerator analysis was to test the theoretical relationship, which is the foundation of the methods devised to improve the ORNL consumer decision algorithms.

Refrigerators were selected because adequate data were available and because they represent a major energy end use with little variation in consumption attributable to usage. In addition, consumers generally select their own refrigerator as opposed to buying it "built in" to the house. Finally, main sources of data on refrigerators<sup>5,6</sup> were relatively complete and reliable. Specifically, lists of the retail prices, energy use and models available in the years 1975 and 1977 were used. The statistical analysis included bivariate and multiple regression analysis of purchase price plotted against energy use and/or volume of the refrigerators.

Initially the analysis was intended to demonstrate the relationship between purchase price and efficiency. Both variables were normalized for size of the appliance with kWh per month/total refrigerated ft<sup>3</sup> on the x-axis and purchase price/total refrigerated ft<sup>3</sup> on the y-axis. Refrigerators were separated by 4 types (single door manual defrost, top freezer partial defrost, top freezer automatic defrost and side by side automatic defrost) and each year was run as a separate regression (1975 and 1977).

The bivariate regressions of kWh consumption per month versus purchase price should have reflected the strong negative correlation plotted. This was not the case. The regression revealed a low correlation between energy-consumption and purchase price of refrigerators. In fact, in some cases the correlation exhibited the reverse of the expected relationship, a positive correlation. The proportion of the total variation in the dependent variable (purchase price/total refrigerated volume) explained by the independent variable (kWh per month/total refrigerated volume), which is represented statistically by R<sup>2</sup>, was so low that little can be said about the relationship between the two variables.

The results indicated that the hypothesized simple trade-off of efficiency and purchase price of refrigerators did not exist in the market place of 1975 and 1977. There are three reasons why the regression might not have shown a strong relationship between price and efficiency. Manufacturers are constantly developing energy consuming and price inflating gadgets to build into refrigerators. Because no consistent source of data exists on the specific features of refrigerators, they are likely to confound a statistical analysis of the market. Second, freezer volume might influence the efficiency of refrigerators more than total volume. Third, refrigerators have economies of scale. That

is, by increasing volume by 10%, the kWh usage would increase by a lesser percentage, everything else being equal. Thus, when we normalized energy use and purchase price by dividing them by total refrigerated volume, many other variables could have masked the true relationship.

To test for the influence of freezer volume and economies of scale, various other regressions were run to provide a clearer understanding of the relationship between efficiency and purchase price of refrigerators. Specifically, purchase price was regressed against energy use (normalized by fresh food and freezer volumes), and the three categories of volume (total refrigerated, fresh food and freezer). Thus the following five regressions were run for the 4 types of refrigerators:

- 1) x: kWh/freezer ft<sup>3</sup>  
y: \$/freezer ft<sup>3</sup>
- 2) x: kWh/fresh food ft<sup>3</sup>  
y: \$/fresh food ft<sup>3</sup>
- 3) x: total ft<sup>3</sup>  
y: \$
- 4) x: freezer ft<sup>3</sup>  
y: \$
- 5) x: fresh food ft<sup>3</sup>  
y: \$

(Note: kWh = kWh consumed per month; \$ = purchase price in current dollars; total, freezer and fresh ft<sup>3</sup> = refrigerated volumes)

The results indicated that volumes are better estimators of price, especially with the best selling types of refrigerators, top-freezer automatics and side-by-side automatics. With some notable exceptions, purchase price was influenced more by freezer volumes than by total and fresh food volumes. However, when the kWh/price regression was normalized by freezer volume (see 1 above), there were no negative correlations. Furthermore, the R<sup>2</sup> of these bivariate regressions were low for all types of refrigerators. It must be concluded that freezer volumes do not influence the regression of efficiency and price, although they do appear to be good predictors of purchase price.

In order to sort out the relative importance of refrigerator volume and energy use on purchase price, the following multiple regression equation was developed:

$$\text{purchase price} = \alpha + \beta_1 \text{ total ft}^3 + \beta_2 \text{ kWh/month} \quad (\text{Eq. 3})$$

The regression equation supplied interesting results when run with the refrigerator data. For example, the regression equations for top-freezer automatics were estimated to be:

$$\begin{aligned} \underline{1975:} \quad Y &= 97.5 + 32.9X_1 + .0874X_2 \\ \text{t-ratios:} & \quad - .77 \quad 7.13 \quad .11 \\ R^2 &= 71.6\% \end{aligned}$$

1977:  $Y = 173 + 36.2X_1 + 2.05X_2$   
 t-ratios: 1.48    7.92    -2.20  
 $R^2 = 72.0\%$

(Y = first costs;  $X_1$  = total ft<sup>3</sup>;  $X_2$  = kWh/month)

The t-ratios (parameter estimates over their standard deviations) indicate which variables are statistically significant. A useful generalization is that a t-ratio with an absolute value of 2 or more indicates a parameter estimate that is significant at the 95% level.<sup>7</sup> It is clear that total ft<sup>3</sup> ( $X_1$ ) is a highly significant predictor of the purchase price of a refrigerator. The estimate also has the correct sign; as the total volume of a refrigerator goes up so does its price. For the 1975 regression, the energy use parameter estimate is insignificant; however, the 1977 regression reveals a reverse trend. In 1977, the t-ratio of the energy use parameter is significant at a confidence level of 95% and the sign is correct (negative). In other words, as energy use of a refrigerator increases, the purchase price decreases and vice versa. Note also that the  $R^2$  for each regression is similar to the other and that they are relatively high.

Because it was shown earlier that for some classes of refrigerators the two independent variables (volume and energy use) are correlated, problems of multicollinearity must be considered. In this case, a rule of thumb says that intercorrelation of variables is not necessarily a problem unless it is high relative to the overall degree of multiple correlation.<sup>8</sup> Therefore, with the weak relationship between the two independent variables (fresh food volume and energy use), the problem of multicollinearity is discounted.

The observed trend of energy efficiency influencing purchase price of refrigerators is similar to the theoretical engineering literature discussed earlier in the paper. However, there still exists no clear cut function that explains the trade-off between energy use and purchase price. In fact, it is clear that little or no value has been placed by the purchasing consumer on the future operating costs of major appliances. The lack of sophistication of consumer decisions appears to be a result of the poor information available in the market; specifically, purchase prices rarely indicate the energy efficiency of appliances, thus serving to mask the traditional market relationship between quality and price.

#### PLANNED ACTIVITIES FOR 1980

The primary problem with market analysis of consumer decisions is the lack of data. A new and comprehensive data set collected by DOE from the manufacturers<sup>9</sup> should be made available by the end of 1979. The future of the consumer decision research within the AEPS project will depend partly on the availability and the quality of the manufacturer data. The research will be extended along the same statistical paths outlined in the refrigerator case for other appliances and for more years.

Ideally, the relationships between purchase price and operating costs will be defined through the application of the methods outlined in this paper, even if they exhibit extremely high effective discount rates.

At the present, all consumer decision analysis is focused on the improvement of the ORNL residential demand model. Through application of the model to current practice and AEPS scenarios, the impacts of the standards on residential demand in the United States can be estimated. As a major flow in the ORNL model, the consumer decision algorithms could heavily bias the estimated demand in each scenario. Therefore, it will be necessary to develop new algorithms based on the statistical relationships established. The end result should be an improved version of the ORNL model and consequently, increased accuracy in the AEPS demand analysis.

#### FOOTNOTE AND REFERENCES

\*University of California, Berkeley

1. National Energy Conservation Policy Act. 95th Congress, 2d Session. Report No. 95-1751. October 1978. Title IV, Part 2 - Energy Efficiency Standards for Consumer Products Other than Automobiles.
2. Eric Hirst and Janet Carney, "The ORNL engineering model of residential energy use," Oak Ridge National Laboratory report ORNL/CON-24 (July 1978).
3. Arthur D. Little, Inc., Study of Energy-Saving Options for Refrigerators and Water Heaters, Volume 1: Refrigerators. Prepared for the Office of Transportation and Appliance Programs, Federal Energy Administration, Washington, D.C. 20461, Under Contract No. CO-04-50-28-00. Cambridge, Massachusetts 02140 (May, 1977).
4. Robert A. Hoskins, Eric Hirst, and W. S. Johnson, "Residential Refrigerators: Energy Conservation and Economics", Energy, Volume 3, pp. 43-49. (Pergamon Press, Great Britain, 1978).
5. Association of Home Appliance Manufacturers, 1975 and 1977 Directory of Certified Refrigerators and Freezers. Chicago, Illinois; 1975 and 1977.
6. Dealerscope, 1979 Home Appliance Trade-In Blue Book. Torrance, CA (1979).
7. The general rule can be used because both equations have over 20 degrees of freedom, L. R. Klein, An Introduction to Econometrics, (Prentice Hall, Inc., Englewood Cliffs, N.J., 1962).
8. op. cit. pp. 101.
9. "Consumer Products Survey (Energy Efficiency Standards)", CS - 179, Department of Energy, Consumer Products Efficiency Branch.

## THE USE OF DOE-2 TO EVALUATE ADVANCED ENERGY CONSERVATION OPTIONS FOR SINGLE-FAMILY RESIDENCES

*D. Goldstein, J. Mass, and M. Levine*

### INTRODUCTION

The DOE-2 building energy analysis model<sup>1,2</sup> has been used as the basis for deriving life-cycle cost curves for conservation measures in houses. Buildings were modeled under various conditions of insulation and glazing, and the difference in energy use between two conservation options was calculated from DOE-2 runs. Life-cycle costing procedures were used to compare the energy cost savings predicted with the estimated cost of the conservation measure.

The cost curves were derived for use by the U.S. Department of Energy (DOE) as the basis for the residential Building Energy Performance Standards. The economics of many 'conventional' conservation measures were evaluated. It was found that the cost-minimizing houses went considerably beyond current practice in most regions of the country, and saved about 40% of current energy use.<sup>3,4</sup>

Further conservation measures involving advanced technologies (e.g., residential air-to-air heat exchangers) produced an additional savings of 40% or more. However, these measures are subject to controversy concerning their feasibility of implementation. Thus the use of further conservation measures beyond those currently in use somewhere in the U.S. were excluded from analysis.

As the standards are updated it will be important to study the use of such "advanced" conservation measures - those which are not currently in common use. Analysis of the effect of advanced measures may also be of great interest to builders who want to go beyond the standards and approach minimum life-cycle costs more closely, and to those who wish to find some large energy-saver to trade off against a desired energy-wasting feature (e.g., north-facing view windows or 12-foot ceilings).

### ACCOMPLISHMENTS DURING 1979

Preliminary analysis has been undertaken on two of the many possible (and potentially cost-effective) advanced technologies for houses. At present, the most encouraging such technology appears to be the reduction in infiltration or accidental air leakage into the house combined with the provision of forced ventilation through a heat exchanger. This technology is most effective in the cold regions. For example, in Minneapolis, Minn., the low infiltration/heat recuperator measure cuts heating loads in half, and saves over \$2500 in life cycle fuel bills, at a cost of about \$500. In a warmer area, such as Fresno, Ca., the savings are a small fraction of total heating energy, and a much smaller absolute amount of energy. Costs and benefits for a gas-heated house are approximately equal for Fresno.

To analyze this measure, changes were made in the DOE-2 program to allow the calculation of hourly infiltration loads using a Coblenz-Achenbach formula.<sup>5</sup> Formulas appropriate for present "medium" infiltration levels and projected tighter houses were devised and inserted into DOE-2 formulas.

Passive solar techniques are another possible "advanced" technology which can reduce energy use. The effectiveness of passive techniques in saving energy has been established in many demonstration houses. However, their effectiveness in lowering design energy budgets (which are calculated under tightly prescribed conditions of behavior) must be tested for the application of a performance standard.

Passive solar houses depend heavily for their performance on the ability of the structure of the house to store solar heat collected during the day until a period (night or subsequent day) when heating loads would occur. This heat storage is modeled in DOE-2 using "weighting factors", which were derived for a "typical" room of three different weight ranges. The use of weighting factor techniques will not lead to any serious errors in the analysis, but the present procedure of representing all possible rooms by only 3 sets of weighting factors may lead to problems.

We have analyzed the effectiveness of increasing south-facing "direct gain" windows in houses in a wide range of climates, using both the present DOE-2 weighting factors and a new set of weighting factors derived by Consultants Computation Bureaus<sup>7</sup> for specific geometry and construction of our prototype house. We have found surprisingly small differences between the results using the different sets of weighting factors. Heating energy savings from passive solar appear to range from 15% in the colder regions to over 70% in the milder regions.

### PLANNED ACTIVITIES FOR 1980

Further research on the two advanced technologies already described is necessary to document the expected energy savings and cost effectiveness estimates. Better analysis of latent heat in the study of heat recuperators and of the sizing of the heat exchanger and its fan is needed.

Passive solar analysis will center on the study of heat storage, and the extent to which this can be modeled using the weighting factors. The study will involve the comparison of DOE-2 results with those of other programs and technologies.

In both cases, we hope to study the effect of ventilation assumptions on the savings potential for cooling loads. Present analysis indicate that passive solar buildings begin to show larger cooling loads as south-facing window area increases (even with extensive shading) and that heat exchangers

save very little cooling energy in most climates. Both of these effects may be artifacts of the ventilation algorithm used; we expect to explore this possibility.

Other advanced technologies in which DOE has interest include underground buildings, advanced climate-control systems, and improved window systems. The ability to model these on DOE-2 may depend on the availability of sufficient data to specify the performance of the technology as a function of the relevant variables (e.g., part-load fraction, temperatures or temperature histories, etc.).

#### REFERENCES

1. Metin Lokmanhekim, et al., "DOE-1: (Formerly Cal-ERDA), A new state-of-the-art computer program for the energy utilization analysis of buildings," Lawrence Berkeley Laboratory, LBL-8974. Presented at the Third International Symposium on the use of Computers for Environmental Engineering Related to Buildings, Banff, Alberta, Canada, May 10-12, 1978.
2. Metin Lokmanhekim, et al., "DOE-2: A New State-of-the-Art Computer Program for the Energy Utilization Analysis of Buildings." Presented at the Second International CIB Symposium on Energy Conservation in the Built Environment, Copenhagen, Denmark, May 28-June 1, 1979.
3. M. D. Levine, D. B. Goldstein, M. Lokmanhekim, A. H. Rosenfeld, "Evaluating Building Energy Performance Standards." Presented at the ASHRAE/DOE conference on Thermal Performance of the Exterior Envelopes of Buildings, Orlando, Florida, December 3-5, 1979.
4. "Economic analysis of proposed building energy performance standards," Battelle Pacific Northwest Laboratory, PNL-3044 (1979).
5. P. R. Achenbach and C. W. Coblenz, "Field measurements of air infiltration in ten electrically heated houses," Ashrae Transactions 69, 358-65 (1963).
6. W. A. Schurcliff, Solar Heated Buildings, A Brief Survey, 12th Edition (Schurcliff, Cambridge, Mass., 1976).
7. Computation procedures for weighting factors are discussed in Z. O. Cumali, Interim Report for Contract EM-78-C-01-5221, Dept. of Energy (1979).

## APPLICATION OF THE ORNL RESIDENTIAL ENERGY DEMAND MODEL TO THE EVALUATION OF RESIDENTIAL ENERGY PERFORMANCE STANDARDS

*J. McMahon and M. Levine*

#### INTRODUCTION

The Oak Ridge National Laboratory (ORNL) Residential Energy Demand Model (REDM) was developed to simulate energy use in the residential sector from 1970 to 2000.<sup>1,2</sup> This model can be used as a tool to evaluate the effects of residential energy performance standards and other possible government policies. Application of this model can yield a comparison of a base case (without standards) with the case including implementation of standards. Particular attention will be paid to effects on fuel consumption, fuel costs, and capital costs for new equipment.

The major capabilities of the REDM are that it:

- shows energy demand over time, disaggregated according to fuel type, housing type, and end use;
- considers changes due to economic factors affecting market shares, usage, and technological improvements of appliances;
- distinguishes new equipment energy performance from average energy performance of the total stock;

- calculates economic trade offs between operating cost and capital cost; and
- includes retrofit of existing houses when economically justified.

Effective analysis of proposed standards requires that 1) the REDM simulates energy use reasonably well; and 2) the input data must be the best available, with regard to both accuracy and level of detail. The range of values for inputs should be specified, and the sensitivity of results to various input assumptions must be tested to define the range of values for key effects.

#### ACCOMPLISHMENTS DURING 1979

The model has been obtained from ORNL and installed in an LBL research computer. The input data have similarly been imported and used to verify the integrity of the transferred model.

The results of applying the ORNL model to buildings energy performance standards (BEPS) have been duplicated. Sensitivity of the results to key input economic assumptions are being tested, in order to gain further familiarity with the detailed inner workings of this model.

The methodology programmed into the model (and described in existing documentation<sup>1,2,3</sup>) has been examined in detail. Several aspects of the model are receiving close scrutiny with the intent of replacing some parts with improved formulations based on more recent empirical data.

The new approaches to be implemented are described separately. Of particular interest are: modeling of consumer decision making, and consideration of electricity peak load (not previously included).

A few complete sets of input have been prepared at different geographic levels (national, federal region, and utility service area). The overall effects of appliance standards will be analyzed at the national level, but modeling of peak load requires attention to a utility service area. Inputs include stocks of occupied housing, new construction, equipment ownership (market shares), new equipment installation, annual equipment fuel use, equipment prices, fuel prices, income, new equipment standards, thermal performance standards for new buildings and for retrofit programs, and characteristics of new technologies.

#### PLANNED ACTIVITIES FOR 1980

The ORNL model will be modified to include the most current formulation for consumer decision-making, retirement rates of appliances, and electricity peak loads. Other possible improvements include explicit treatment of solar as a fuel type, and provision for down-sizing of appliances as operating costs increase.

The Residential Energy Demand Model will be applied to proposed national design standards for residential appliances. Comparing the results of two runs of the model (one a base case (without standards), the other the standards case) will

provide detailed information about the effects of standards. Since the two runs share the same economic and demographic assumptions, the difference in key outputs can be attributed to implementation of the standards.

The outputs of particular concern will be fuel use (use by fuel type, end-use function, and housing type), annual fuel costs (total cost and cost by fuel type), annual expenditures for new equipment and for thermal integrity improvements, and total fuel use and expenditures over the period 1980 to 2000.

The net present value - that is, the discounted value over the period of time considered - of fuel costs, equipment costs, and structure improvement costs will be calculated by the model for the two cases. The difference in net present value between the two case yields both fuel costs saved due to standards, and change in equipment costs due to standards. The net economic benefit to society (excluding the cost of government programs) is the difference between fuel costs saved and change in equipment costs.

#### REFERENCES

1. Eric Hirst and Janet Carney, "The ORNL engineering - economic model of residential energy use," ORNL/CON-24 (July, 1978).
2. Janet Carney and Eric Hirst, "ORNL Residential Energy Use Simulation Model: Preparation of Input Cards for Version VI," (December, 1978).
3. Thomas McCormick, "User's Guide to Oak Ridge National Laboratory residential energy demand model," Massachusetts Institute of Technology Energy Laboratory Working Paper No. MIT-EL 79-042WP (August, 1979).

## ENERGY INFORMATION VALIDATION

*M. Horovitz*

#### PROJECT ACTIVITY

The Energy Information Administration (EIA) of the U.S. Department of Energy (DOE) is responsible for conducting a comprehensive energy data and information program. EIA operates over one hundred information systems, numerous models and forecasting procedures, and is required to assess the validity of these systems and the information generated through their use. Such validation studies require investigation of the accuracy, utility and efficiency of the information system.

An Energy Information Validation Project was started at LBL in January 1978 and grew rapidly in scope and size. Validation studies of five energy information systems were carried out; the broader

objectives of the program were to use the experience gained during these first five studies to create methods for efficient validation of the many information systems for which EIA is responsible.

Interim reports<sup>1-5</sup> on validation studies of five information systems were delivered to EIA in December 1978. In January 1979, EIA decided to terminate the LBL Energy Information Validation Project as quickly as possible. The project was closed down by the end of February 1979. During February 1979 it was decided that a small core of the project staff should carry out a review of lessons learned during the previous year's work and document certain findings and knowledge gained. This review was completed in July 1979 with production of four additional reports.<sup>6-9</sup> A study of the

history of oil and gas reserve estimation was also conducted, through a subcontract in FY 1979. The draft report<sup>10</sup> on this study was completed at the close of FY 1979. A report on the techniques developed at LBL for validation of the information systems is being prepared for completion during FY 1980; this constitutes the final item to be produced by the project.

A related but separate study was begun in June 1979 to assess the validity of DOE's energy demand forecasting methods. EIA currently uses the ORNL Engineering Economic Model of Residential Energy Use (Hirst-Carney model) developed at Oak Ridge National Laboratory, to forecast energy demand in the residential sector, to the year 2000. Previously, EIA had carried out this task by using the RDFOR model which was part of the Project Independence Evaluation System (PIES).

A preliminary review of the RDFOR model was carried out at LBL and U.C. Berkeley during the summer of 1979 and drafts of three reports<sup>11-13</sup> were produced and submitted for review at the end of FY 1979. A report on preliminary studies of the Hirst-Carney model is planned for completion during the first half of FY 1980. During FY 1980, this study will be transferred from LBL to the U.C. Berkeley Statistics Department, where it is scheduled for completion during FY 1981.

This first LBL energy information validation project carried out pioneering studies covering a broad range of topics related to the validity of information about energy and created an approach to validation of information systems. Three out of five information systems and one of the models studied were found to have defects which seriously impaired the credibility of information generated through use of these systems.

#### REFERENCES

1. M. O. Stern et al., "Draft interim validation report - domestic crude oil first purchaser system," Lawrence Berkeley Laboratory report LBL-7878, December 1978.
2. P. J. Nagarvala et al., "Draft interim validation report - domestic crude oil entitlements system," Lawrence Berkeley Laboratory report LBL-8436, December 1978.
3. D. H. Hopelain et al., "Interim validation report - middle distillate price monitoring system," Lawrence Berkeley Laboratory report LBL-8437, December 1978.
4. S. Alter et al., "Interim validation report - major fuel burning installation system," Lawrence Berkeley Laboratory report LBL-8434, December 1978.
5. S. Alter et al., "Interim validation report - monthly fuel consumption report manufacturing plants," Lawrence Berkeley Laboratory report LBL-8435, December 1978.
6. M. Horovitz and C. York, "Information validation: a working paper," Lawrence Berkeley Laboratory report LBL-9237, June 1979.
7. M. Horovitz, W. L. Klein and C. M. York, "Review of data analysis on the domestic crude oil entitlements system," Lawrence Berkeley Laboratory report LBL-9184, June 1979.
8. E. B. Deaking, "Sources of information parallel to FRS required information for oil and gas companies," Lawrence Berkeley Laboratory report LBL-9239, June 1979.
9. L. J. Spurrier and B. L. Krieg, "Accounting practices and financial reporting in the petroleum industry, a bibliography," Lawrence Berkeley Laboratory report LBL-9238, June 1979.
10. A Wildavsky, E. Tenenbaum, and P. Albin, "The politics of mistrust: an analytical history of oil and gas estimation," Lawrence Berkeley Laboratory report LBL-9889, Draft-September 1979.
11. D. Freedman and R. Sutch, "The demand for energy in the year 1990: an assessment of the regional demand forecasting method," Lawrence Berkeley Laboratory report LBL-9705, Draft-September 1979.
12. D. Freedman and R. Sutch, "An assessment of the federal energy data system," Lawrence Berkeley Laboratory report LBL-9704, Draft-September 1979.
13. D. Freedman, "Uncertainties in model forecasts," Lawrence Berkeley Laboratory report LBL-9703, Draft-September 1979.

NOTE: For a description of the following projects, see page 2-70 through 2-84 of this Annual Report:

Evaluation of Building Energy Performance Standards for Residential Buildings (BEPS).  
 Energy Efficient Standards for Residential Appliances Including Heating and Cooling Equipment (AEPS).  
 The Impact of Energy Performance Standards on the Demand for Peak Electrical Energy.

# ENERGY EFFICIENT BUILDINGS PROGRAM

## INTRODUCTION

*A. H. Rosenfeld, C. D. Hollowell, S. Berman, and T. Edlin*

The Energy Efficient Buildings (EEB) program conducts both theoretical and experimental research on various aspects of building technology. An important goal of the program is to identify, assess and recommend solutions to problems that interfere with national goals of conserving energy consumed by the buildings sector. Buildings account for approximately 38% of the total energy consumed in the United States, in contrast to automobiles, which consume approximately 18%.

One focus of our investigations during the past several years has been on Building Performance. Building performance is assessed by regarding the building as a system; in this framework, performance is tested in terms of air infiltration rates, thermal characteristics of building components and the behavior of the joiner interface between dissimilar materials. The program devises cost-effective solutions to reduce infiltration and thermal losses, both by retrofitting existing buildings and gathering data on which revised standards for new buildings can be promulgated. This research on air infiltration and thermal performance of the building and its components is conducted in the field, in the laboratory, in our research house and on computer models.

Another major area for the EEB program is Ventilation and Indoor Air Quality (VIAQ). The VIAQ group is identifying, characterizing and monitoring indoor levels of various pollutants in conventional and energy-efficient buildings with specific attention to their impact on indoor air quality. Reducing air infiltration, the most obvious means of improving a building's energy efficiency, can "seal in" indoor air contaminants and have mild to severe repercussions on the health and comfort of building occupants. This group is concomitantly investigating means of preventing and controlling indoor air pollution without compromising energy conservation goals. In this connection, it has tested various ventilation systems with air-to-air heat exchangers at a number of locations throughout the country.

The Windows and Lighting section of the EEB program is emphasizing ways to encourage industry to develop and promote energy-efficient products at cost-effective prices. A primary con-

sideration in the Windows group is to assure that daylight is provided to the building's interior with minimum thermal loss in cool weather and minimum thermal gain in hot weather. To this end, considerable research activity has centered on developing and testing optical coatings for windows as well as evaluating a number of window treatments now available commercially or to be made available in the near future.

The Lighting program is concentrating on developing energy-efficient lighting systems (lamps, ballasts, fixtures and controls) to provide lighting designers with an array of design options to meet occupant needs. One recent development currently being field-tested in several buildings is high-frequency, energy-efficient solid-state ballast for fluorescent lights that effects a 25% savings over conventional core ballasts.

The Building Energy Analysis Group is responsible for developing, improving and documenting the computer program, DOE-2, which has been designated as the national program for calculating building energy performance standards. DOE-2 can also be used by architects/engineers as a means of quickly and effectively optimizing building design to improve its energy efficiency and minimize life-cycle costs. DOE-2 will be systematically updated to incorporate the latest energy-conserving design features (passive and active solar, thermal storage, natural ventilation, daylighting, and evaporative cooling).

DOE has commissioned LBL to develop parametric profiles to quantify the energy requirements of residential buildings, including heating and cooling systems. This work, being accomplished by the BEPS/AEPS Group uses the DOE-2 modeling program to evaluate a wide variety of conservation measures for different house designs and climates in terms of life-cycle costs of implementation.

The reader who is interested in the national energy savings that might be effected as a result of our research is referred to the Summary Section of this chapter which presents data on the potential impact of a national retrofit program and the adoption of energy-efficient building performance standards.

## BUILDING ENVELOPES PROGRAM

*R. C. Sonderegger, R. T. Beerman, A. K. Blomsterberg, W. L. Carroll, J. A. Casey,  
P. E. Condon, R. C. Diamond, D. T. Grimsrud, D. L. Krinkel, C. W. Ma, M. P. Modera,  
A. H. Rosenfeld, M. H. Sherman, and B. V. Smith*

### INTRODUCTION

Residential and commercial buildings account for one-third of the total energy use in the United States today. Approximately 60% of the energy consumption in these sectors is for space heating and air conditioning. Conductive losses through the windows, walls, and roof of the structure account for 2/3 to 3/4 of the 60%, while air infiltration through cracks in the walls, around doors, windows, fireplaces, or any other opening in the building envelope accounts for 1/4 to 1/3 of the 60%.

The Building Envelopes Program was initiated in April 1977 as part of Lawrence Berkeley Laboratory's broad-based study of energy conservation in buildings. The main objective of the program is to provide fundamental information on the thermal performance of a building so that appropriate energy-conserving guidelines and standards governing the design and construction of new buildings as well as retrofit strategies for existing buildings can be recommended or prescribed. A comprehensive research undertaking in this area requires not only systematic study of individual components within the building envelope, but also a careful examination of the energy performance of the building as a whole.

Work carried out during FY 1978 centered around four principal experiments undertaken at LBL's research house in Walnut Creek:

- Tracer gas techniques to measure air infiltration.
- Pressurization tests for air leakage.
- Investigations of heat loss through walls.
- Electric co-heating runs to measure fireplace efficiencies.

The research house is a typical wood-frame, three-bedroom, suburban ranch house built in 1964 (see Fig. 1). After developing the experimental procedures at the research house, we surveyed several houses in the Bay Area to determine the applicability of these procedures to other houses.

### ACCOMPLISHMENTS DURING 1979

Four projects are currently underway: the first three are continuations of past work on air infiltration, thermal performance of walls, and fireplace testing; the fourth is a new effort to provide an audit procedure for energy conservation in residences.



Fig. 1. Research House in Walnut Creek, California. (CBB 7811-14961)

### Air Infiltration Studies

Air infiltration rates are one of the large unknowns in any analysis of building energy use because they involve variable pressures caused by both wind and indoor/outdoor temperature differences, as well as construction features and occupant behavior. Our studies in this area are largely concerned with measuring, modeling, and reducing air infiltration. Considerable attention has been given to correlating air-leakage measurements obtained through fan pressurization of a house with the infiltration rates occurring naturally. An important goal of our research program is to facilitate the development of standards regulating air leakage in residential construction. Several critical issues dealing with air infiltration are discussed in LBL reports concerning Building Energy Performance Standards (BEPS) and Construction Quality Standards.<sup>2,3</sup>

Two general strategies are possible to save dollars and energy lost through air infiltration. The first is to tighten the envelope of existing buildings (by caulking, weatherstripping, etc.) until the infiltration rate is brought down to approximately 0.5 air changes per hour (ach) under typical weather conditions. The second strategy requires careful attention during the construction of new buildings to ensure the integrity of the thermal envelope. In houses where infiltration rates are significantly reduced in order to make them more energy efficient, indoor air quality can deteriorate unless adequate ventilation is provided. Mechanical ventilation systems with heat exchangers

provide sufficient fresh air without excessive heat loss. Research on various aspects of indoor air quality and on residential heat-recovery devices constitute a major part of the Energy Efficient Buildings program and is described elsewhere in this report.

ACCOMPLISHMENTS DURING 1979

Air leakage, surface pressures and air infiltration were measured in several conventional and energy-efficient houses located throughout the United States. Among the houses tested were the Minimum Energy Dwelling (MED I) in Southern California, three energy-efficient houses in the Midwest (two privately built, one a test house at Iowa State University) a group of active-solar houses in Davis, California, and a number of conventional houses in the San Francisco Bay Area. Air-leakage values for these houses are shown in Fig. 2.

Air infiltration measurements taken during the survey were compared with infiltration rates predicted by a simple model combining air-leakage values taken from fan pressurization and measured surface pressures. The comparison between measured and predicted values is shown in Fig. 3.

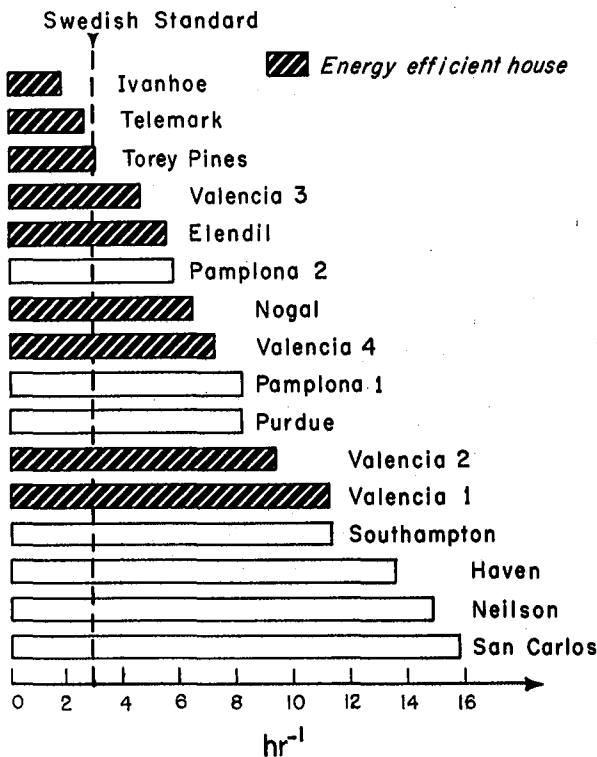


Fig. 2. Air leakage rates, in air changes per hour at a pressure of 50 pascals, for U.S. homes measured in LBL survey. Swedish building standard indicated by dashed line. (XBL-796-1754A)

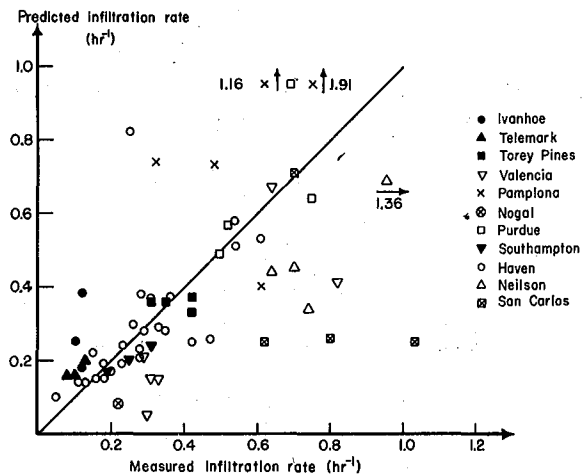


Fig. 3. Predicted vs. measured infiltration rates for survey houses. (XBL-796-1856A)

Two new models were developed to correlate air leakage and infiltration. In addition, a technique that examines the low-pressure leakage function of a residence by means of an oscillating pressure source was developed and tested. The advantage of this method is that it simulates the low-pressure range where natural infiltration occurs, and is independent of weather interactions. Such information is essential in constructing a predictive model of infiltration.

The Envelopes group was also responsible for developing instrumentation for other EEB groups conducting related research. An automated tracer-gas system was designed and built for the EEB mobile trailer and for the Passive Solar Group for their measurements of air infiltration.

A final effort this year has been to establish a U.S. Data Center for infiltration research coordinated with the International Energy Agency Center at BSRIA, England. The data center will hold bibliographical and numerical data for North American research in air infiltration and related studies. The computer software for the data base was completed, and data entries have begun.

PLANNED ACTIVITIES FOR 1980

Work will continue on the infiltration-pressurization correlations, instrumentation development, and the updating and maintaining of the infiltration data center. New work will focus on designing simplified models of infiltration to be used in the LBL Residential Energy Audit and detailed infiltration models to be used in the DOE-2 infiltration algorithm.

To verify these models, a new laboratory is being designed, the Mobile Infiltration Test Unit (MITU), which will allow us to conduct long-term measurements of surface-pressure distribution under different weather conditions and terrains, and with different structural leakage characteristics. Results from these tests will

yield improved confidence limits on infiltration-pressurization correlations.

An important activity begun in FY 1979 and to continue in FY 1980 is the cooperative work with builders, utilities, and other researchers in the building industries. The following projects are already underway: a Johns-Manville/EPRI air-leakage study in Denver, a collaboration with Rochester Gas and Electric and New York State Energy Research and Development Authority on air leakage in new homes, work with Bonneville Power Administration on retrofitting a group of existing houses in Washington state, and work with Pacific Gas and Electric Company in a cooperative program with builders and contractors to reduce air leakage in existing homes.

#### Thermal Performance of Walls

The actual thermal performance characteristics of building walls are largely unknown. Available information is based on theoretical analysis and laboratory tests. Even though a wall may be well designed, differences in construction methods and aging of materials can produce substantial variations in thermal performance. Where actual measurements have been made in buildings, the thermal resistance of the walls is often 20% to 30% less than that predicted by laboratory measurements and standard calculations. Ultimately, recommendations for energy conservation standards should be based on accurate measurements of building walls, rather than on largely unverified inferences from laboratory measurements and computer models. The purpose of this research is to develop techniques for field (or in-situ) measurement of the thermal performance of walls. The improvements being developed fall into two broad categories: better equipment for collecting raw data, and better methods of data reduction using computers.

#### ACCOMPLISHMENTS DURING 1979

In order to measure the thermal resistance and the dynamic thermal response of building walls, a new device, the Envelope Thermal Test Unit (ETTU) was designed and built this year. The prototype ETTU is based on an analysis of complex thermal admittance, and uses a microprocessor for sophisticated on-line computer control and data analysis.<sup>10</sup>

A second, simpler ETTU (ETTU-II) was invented this year. Error analysis for ETTU has shown that the form of the controlled drive signal is not a critical design parameter. Instead of controlling the heat flows through the wall boundaries, as is done in ETTU, the new design uses newly developed heat flow sensors to measure the naturally occurring heat flows. These sensors will measure heat flows and average temperatures across large wall areas (20 to 30 ft<sup>2</sup>).

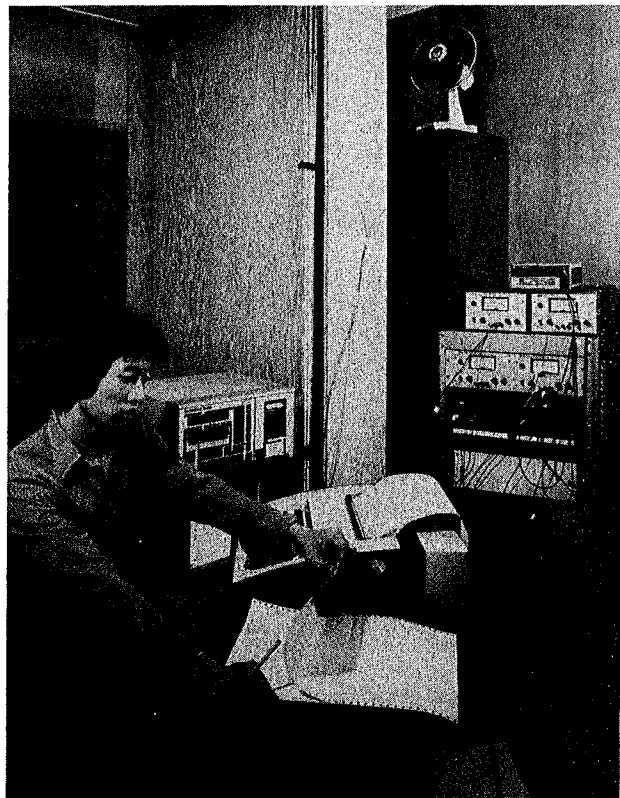


Fig. 4. Envelope Thermal Test Unit (sandwiched between vertical plywood panels) during calibration check at laboratory. (XBB 790-16280)

#### PLANNED ACTIVITIES FOR 1980

We have several goals for the coming year. One project will focus on the use of ETTU as a portable field-testing apparatus to investigate any change in thermal performance with age in a representative sample of actual house walls. Another project is to develop the large heat-flux sensor for the passive system, ETTU-II. The sensor will have a sensitive region of about 1 x 1.5m<sup>2</sup> (3' x 5') and thermal resistance of less than about .002°C m<sup>2</sup>/W (.01°F ft<sup>2</sup> hr/Btu). The technique uses thin film resistors on two sides of a plastic sheet. The temperature difference across the sheet is measured by using the temperature dependence of the electric resistance. Both ETTU systems will be validated by using standard reference materials calibrated in conventional laboratory test facilities. Other projects include the continued collaboration with the ASTM C16 committee on thermal and cryogenic insulating materials in defining appropriate parameters for characterizing thermal wall performance, and the dissemination of the data collection/reduction system developed for ETTU.

#### Fireplace Testing

With the recent surge of interest in heating houses with wood, and the appearance on the market of hundreds of accessories for improving

the efficiency of fireplaces, LBL initiated the development and subsequent testing of a standardized procedure for measuring fireplace efficiency.

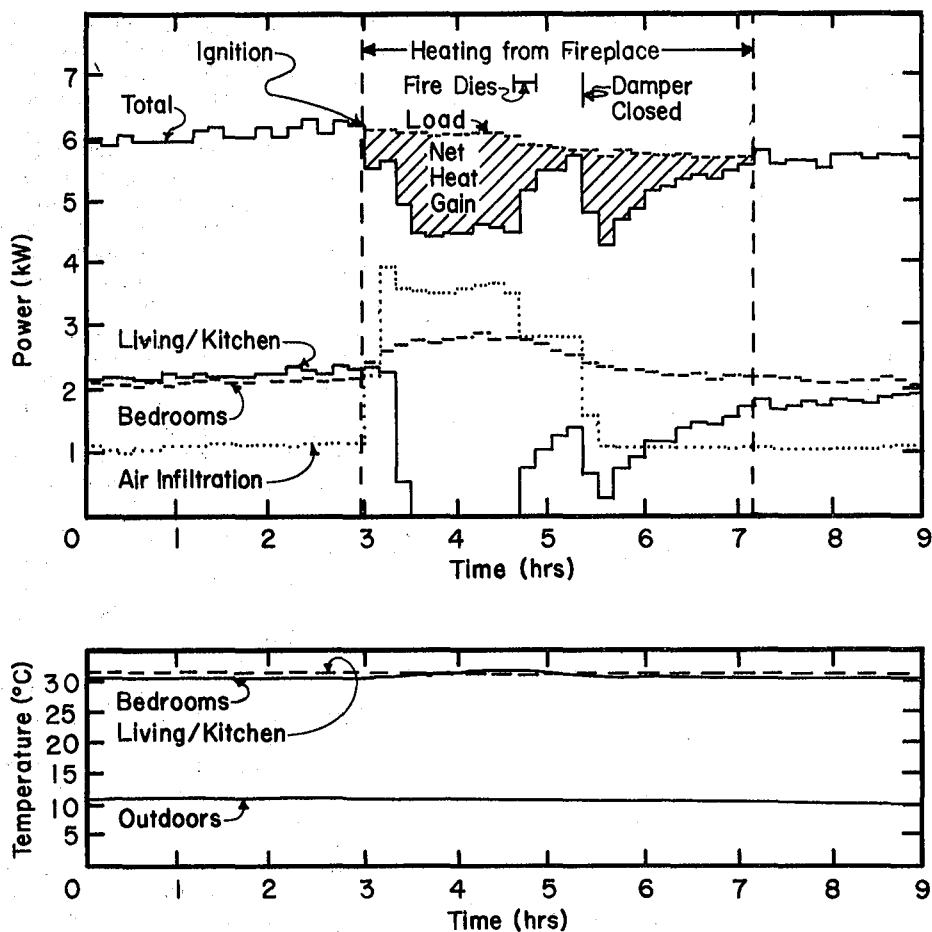
In this procedure, called electric co-heating, several electric heaters are distributed throughout the house. Temperature sensors located in each room ensure that a constant temperature is maintained by the heaters. When the fire is burning, there is a reduction in the heat output of the electric heaters; by measuring the amount of this reduction, we can determine the net efficiency of the fireplace.<sup>11</sup> The advantage of using electric co-heating to measure fireplace efficiency is that it is an in-situ measurement that takes into account the combined effect of the radiant heat gain from the fire and the heat loss from additional air infiltration caused by the chimney draft.

ACCOMPLISHMENTS DURING 1979

Using the co-heating technique, we measured

the efficiency of the fireplace, furnace, and air-conditioning unit in the Walnut Creek research house, where we also tested seven fireplace accessories, ranging from simple convective grates to combination units with blowers and glass doors. The tests were later repeated at a mountain test site where the climate was more severe.

The results from a 9-hour test are shown in Fig. 5. The run is divided into three periods: before, during, and after fireplace operation. The top line is the total electric consumption needed to maintain a constant temperature throughout the house. The lower lines designate the electricity consumption for the heaters in the living room/kitchen (where the fireplace is located) and for the bedrooms. Air infiltration increases significantly while the fire is burning. This increase in air infiltration cools the bedrooms, which are not receiving the radiant energy from the fire. The graph shows this effect as an increase in electrical consumption by the bedroom heaters.



Efficiency Test of Fireplace

Fig. 5: Efficiency test of fireplace. (XBL 7910-12350)

Results of our tests showed that a common masonry fireplace is only about 5% efficient, and that this efficiency decreases in colder weather. The best of the fireplace accessories was 30% efficient, still far below the 70% efficiencies achieved by airtight woodburning stoves.<sup>12</sup> With the cost of wood at \$100 per cord, useful heat from a fireplace at 20% efficiency costs \$21 per million Btu. By comparison, heating with fuel oil at 60% efficiency costs \$9 per million Btu, and heating with natural gas at 70% efficiency costs \$5 per million Btu.

#### PLANNED ACTIVITIES FOR 1980

No new testing is planned. Follow-up activities will be the publication of a technical report on our experiments and a consumer brochure on fireplaces and fireplace accessories.

#### Residential Conservation Service Audit

The Residential Conservation Service (RCS) was established by the 1978 National Energy Conservation Policy Act, which requires that major public utility companies and fuel-oil dealers provide a house energy audit to customers who request it. States have two options in complying: either they submit a plan for DOE approval, or DOE will mandate its own energy audit (currently being developed by ORNL and SERI). In accordance with RCS regulation, this audit will be site- and house-specific, will consider both conservation and renewable resources (solar and wind) in its recommendations, and will give the homeowner a cost-benefit analysis of the recommended measures.

Because of time/cost restrictions inherent in the basic audit, DOE commissioned LBL to develop an expanded residential energy audit. The novel features of this audit are the inclusion of a portable microcomputer for evaluating appropriate retrofits based on input collected during the audit, and the undertaking of several simple retrofits at the time of the visit. (Our current experience in retrofitting at the time of the audit shows a 15-20% reduction in air leakage by caulking and sealing cracks).

The expanded audit will require an initial screening of utility bills and weather data to obtain an "energy signature" for the house. The auditor and assistant then make a three hour visit to the house where they record window types and dimensions, test the envelope for leakage with a blower door that pressurizes or depressurizes the house, identify leaks, plugging the easy ones as they go and noting the more difficult ones to repair later. While the auditor measures furnace efficiency, checks water and air-temperature settings, and estimates envelope R-values, the assistant continues to fix leaks, installs water-heater insulation, changes the air filter in the furnace, calibrates the thermostat and, with the permission of the homeowner, installs a low-flow showerhead and resets the water-heater thermostat.

At the conclusion of the physical inspection, all necessary data are collected and fed to the microcomputer. The auditor then confers with the homeowner on a suitable retrofit package. The computer will scan a master list of possible retrofits stored on a disc that contains conservation measures such as insulation, storm and double-pane windows, insulating shutters, caulking and weatherstripping, and active- and passive- solar retrofits for space and water heating.

The computer will give retrofit packages for several budgets, along with costs and savings of the entire package. Retrofits can be tailored to the preferences of the homeowner with a very short turnaround time. All cost estimates take into account the possibility that the homeowners may provide the labor for doing the retrofits themselves. At the conclusion of the visit, the auditor leaves detailed information on the suggested retrofits with the homeowner.

#### ACOMPLISHMENTS DURING 1979

LBL began work on the energy audit at the end of FY 1979, and will make it a major effort in FY 1980. Several features have already been incorporated that distinguish it from the basic audit and other residential energy audits used by utilities and private businesses:

- The cost-benefit calculations rely heavily on actual data of the thermal characteristics of the house as measured on-site at the time of the audit, and on past fuel consumption data obtained from utility or fuel-dealer records. Past fuel bills will be analyzed to determine marginal heating consumption per additional degree-day, and "free" heat provided by appliances. Both quantities are important for estimating the cost-effectiveness of retrofits and, later, for evaluating the success of the conservation measures adopted.
- The audit is user-oriented, i.e., it allows homeowner preferences for particular retrofits and homeowner plans for house additions to be integrated in the calculations.
- The audit uses state-of-the-art analytical techniques including a simplified calculation of thermal storage effects for estimating energy savings due to heat-loss reduction, solar-gain enhancement and heating efficiency improvements as well as energy savings due to sensible, latent and radiative heat-gain reductions and cooling-system efficiency improvements. (Most audits rely on simplified steady-state load calculations, often without adequate treatment of solar-heat gain and air infiltration).
- The audit will calculate life-cycle costs and savings resulting from installation, operation and replacement of installed retrofits.

## PLANNED ACTIVITIES FOR 1980

Work for FY 1980 will involve the completion of the audit procedure and the validation of this approach with actual measurements on several houses.

## REFERENCES

1. Office of Technology Assessment, "Residential Energy Conservation" U.S. Government Printing Office OTA-E-92, July 1979.
2. D.T. Grimsrud, R.C. Diamond, Building Energy Performance Standards: Infiltration Issues, Lawrence Berkeley Laboratory Report, LBL-9623, (to be published 1980).
3. D.T. Grimsrud, A.K. Blomsterberg, A Construction Quality Standard for Air Leakage in Residential Buildings in the United States, Lawrence Berkeley Laboratory Report, LBL-9416, (to be published 1980).
4. D.T. Grimsrud, M.H. Sherman, R.C. Diamond, P.E. Condon, and A.H. Rosenfeld, "Infiltration - Pressurization Correlations: Detailed Measurements on a California House", ASHRAE Transactions (1979), 85-1, Lawrence Berkeley Laboratory Report, LBL-7824, (December 1978).
5. D.T. Grimsrud, M.H. Sherman, R.C. Diamond, and R.C. Sonderegger, "Air Leakage, Surface Pressures and Infiltration Rates in Houses", Proceedings of 2nd CIB Symposium, Copenhagen (1979), Lawrence Berkeley Laboratory Report, LBL-8828 (March 1979).
6. D.T. Grimsrud, M.H. Sherman, A.K. Blomsterberg, and A.H. Rosenfeld, "Infiltration and Air Leakage Comparisons: Conventional and Energy-Efficient Housing Designs", Proceedings of Intl. Conf. on Energy Use Management, Los Angeles (1979), Lawrence Berkeley Laboratory Report, LBL-9157 (October 1979).
7. M.H. Sherman, D.T. Grimsrud, and R.C. Diamond, "Infiltration - Pressurization Correlations: Surface Pressures and Terrain Effects", ASHRAE Transactions, (1979), 85-II, Lawrence Berkeley Laboratory Report, LBL-8785 (March 1979).
8. A.K. Blomsterberg, M.H. Sherman, and D.T. Grimsrud, "A Model Correlating Air Tightness and Air Infiltration in Houses", Proceedings of DOE/ASHRAE Conference on Thermal Performance of the Exterior Envelopes of Buildings, Orlando (1979), Lawrence Berkeley Laboratory Report, LBL-9625 (to be published 1980).
9. M.H. Sherman, D.T. Grimsrud, and R.C. Sonderegger, "The Low Pressure Leakage Function of a Building", Proceedings of DOE/ASHRAE Conference on Thermal Performance of the Exterior Envelopes of Buildings, Orlando (1979), Lawrence Berkeley Laboratory Report, LBL-9162 (November 1979).
10. P.E. Condon, and W.L. Carroll, "Measurement of In-Situ Dynamic Thermal Performance of Building Envelopes Using Heat Flow Meter Arrays", Proceedings of DOE/ASHRAE Conference on Thermal Performance of the Exterior Envelopes of Buildings, Orlando (1979), Lawrence Berkeley Laboratory Report, LBL-9821 (to be published 1980).
11. R.C. Sonderegger, and M.P. Modera, "Electric co-heating: A Method for Evaluating Seasonal Heating Efficiencies and Heat Loss Rates in Buildings". Proceedings of 2nd International CIB Symposium, Copenhagen (1979), Lawrence Berkeley Laboratory Report, LBL-8949 (March 1979).
12. R.C. Sonderegger, P.E. Condon, and M.P. Modera, "In Situ Measurements of Residential Energy Performance Using Electric Co-Heating", To be presented at the semi-annual ASHRAE conference in Los Angeles (Feb 1980), Lawrence Berkeley Laboratory Report, LBL-10117 (January 1980).

## BUILDING VENTILATION AND INDOOR AIR QUALITY PROGRAM

### INTRODUCTION

*C. D. Hollowell*

The Building Ventilation and Indoor Air Quality (VIAQ) Program is a major component of Lawrence Berkeley Laboratory's (LBL) Energy Efficient Buildings Program (EEB). Funded by the Department of Energy (DOE), Office of Buildings and Community Systems (BCS) and the Office of Health and Environmental Research (OHER), the VIAQ Program is part of a coordinated effort to respond to the need for conserving the nation's

energy while maintaining the health and comfort of occupants of the built environment. The overall objective of the Ventilation Program is to conduct in-depth research and development on existing and proposed ventilation requirements and mechanical ventilation systems in order to provide recommendations for the establishment of energy-efficient ventilation standards and ventilation designs for residential, institutional,

and commercial buildings. LBL is also providing both technical and management support to DOE headquarters for other related ventilation projects.

VIAQ Program activities for FY 1979 represent a continuation of the following tasks:

- 1) field monitoring of indoor air quality;
- 2) laboratory studies of building materials emissions, and health risk assessment studies;
- 3) demonstration and assessment of mechanical ventilation systems utilizing air-to-air heat exchangers;
- 4) continuation of subcontract activities consisting of:
  - assessment of ventilation requirements for odor control in buildings;
  - assessment of hospital ventilation standards;
  - study of automatic variable ventilation control systems based on air quality detection in institutional and commercial buildings.
- 5) completion and implementation of a ventilation-indoor air quality data base.

Residential, institutional, and commercial buildings account for approximately one-third of the energy consumed annually in the United States, (see Fig. 1). More than half of this energy is used to maintain human comfort conditions through the heating, cooling, and ventilating of buildings. Significant savings in the energy used to heat and cool buildings can be realized in at least two ways: 1) by changing the thermal properties of the structure; and 2) by reducing the natural and mechanical ventilation rates. The VIAQ Program is concerned primarily with the latter method.

Air changes in buildings take place through the random introduction of outdoor air by infiltration or its regulated introduction by natural ventilation or mechanical ventilation. In the United States, the latter mechanism is essentially limited to non-residential buildings. Ventilation, in general, is required in order to:

- Establish a satisfactory balance between the metabolic gases (oxygen and carbon dioxide) in the occupied environment.
- Dilute human and nonhuman odors to levels below olfactory threshold.
- Remove contaminants produced in the ventilated space by heating, cooking, construction materials, etc.

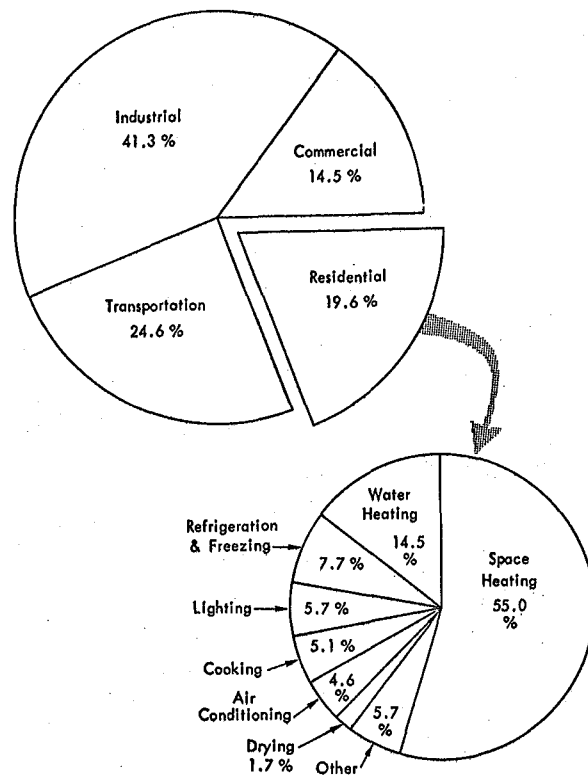


Fig. 1. Primary energy use, U.S., 1970:  
 (a) All sectors ( $\sim 67 \times 10^{15}$  Btu)  
 (b) Residential sector ( $\sim 13 \times 10^{15}$  Btu).  
 [Source: S.H. Dole, Rand Corporation, Energy Use and Conservation in the Residential Sector: A Regional Analysis, Santa Monica, Calif., June 1975, p. VI.]  
 (XBL 7911-12660)

- Remove excess heat and moisture from internal sources.

Ventilation requirements, currently set by state and local governments, vary from one jurisdiction to another. Most of the existing building codes, which contain references to ventilation requirements, are based on rather vague health and safety considerations and, in general, ignore energy conservation.

Through Public Law 94-385, Congress has mandated that Building Energy Performance Standards (BEPS) for new construction be promulgated by 1980 for adoption by state and local government jurisdictions having authority to regulate building construction through building codes and other mechanisms. The Department of Energy (DOE) is developing these standards and it is expected that results of VIAQ Program studies on ventilation requirements will be incorporated in future building energy performance standards.

Because heating or cooling outside air as it is introduced into a building requires a significant amount of energy, energy savings can be achieved simply by minimizing the use of fresh ventilation air. Table 1 illustrates the magnitude of the savings. If ventilation require-

Table 1. Potential energy savings<sup>†</sup> with energy efficient ventilation systems and lowered infiltration.

Total U.S. energy consumption	75 x 10 <sup>15</sup> BTU/yr
Total U.S. energy consumption for buildings	29 x 10 <sup>15</sup> BTU/yr
50% of building energy used to condition air (includes mechanical ventilation systems)	14.5 x 10 <sup>15</sup> BTU/yr
Assume ventilation requirements can be relaxed and infiltration lowered to give a 15% savings in energy used to condition air	
-----	
Potential energy savings	2.2 x 10 <sup>15</sup> BTU/yr
2.5% of national energy budget (7.5% of building energy budget)	1.0 x 10 <sup>6</sup> barrels of oil/day
At present prices of \$30/barrel	Savings of \$30 million/day

<sup>†</sup>1976 energy use estimates from Energy Research and Development Administration, Office of Conservation, "Buildings and Community Systems, Five Year Program Plan."<sup>1</sup>

ments were relaxed and infiltration reduced to save 12.5% of the energy currently used to condition indoor air, oil consumption could be reduced by one million barrels per day (2 quads\* per year). The potential national impact, an annual savings of nearly \$5 billion, is significant. In 1976, the United States imported 7.3 million barrels of oil per day at a cost of approximately \$30 billion.<sup>1</sup> Specifically, this energy savings could be achieved by reducing infiltration by a factor of about two, in approximately two-thirds of existing residential buildings, and decreasing outside air requirements by a factor of two in approximately two-thirds of non-residential buildings.

The introduction of energy-saving measures in buildings, however, may adversely affect indoor air quality. The U.S., unlike some European countries, has not developed mandatory air quality standards specifically for the indoor environment. Nevertheless, we know that low air change rates may contribute to:

- the growth of mold on walls due to high internal humidity:

- the feeling of stuffiness arising from "stale" or polluted air; and
- the buildup of chemical contaminants emitted from building materials and other indoor sources.

It is anticipated that all of the projects in this program will produce data on energy conservation and indoor air quality that will be of important practical use not only to scientists and engineers, but also to building contractors, architects and related building trades people, as well as to the public at large. One of the principal means that will be used to disseminate this information is the LBL ventilation-indoor air quality data base. The main objective of the data base project is to collect research data and other pertinent information on building ventilation and to convert it into a form which allows users easy access through a computerized data management system.

#### REFERENCES

1. Data from Commercial Energy Use: A Disaggregation by Fuel Building Type, and End Use, Oak Ridge National Laboratory Report ORNL/CON-14, (February 1978).

\*One quad equals 10<sup>15</sup> Btu.

## GAS STOVE EMISSIONS

G. W. Traynor

### INTRODUCTION

Field and laboratory measurements carried out thus far have indicated clearly that combustion-generated indoor air pollution may have a significant impact on human health. We have demonstrated that levels of gaseous air pollutants (CO, NO, NO<sub>2</sub> and aldehydes) and respirable particulate carbon and sulfur compounds are elevated in indoor environments where gas appliances are used--in the case of CO, NO<sub>2</sub> and aldehydes, approaching or exceeding promulgated and proposed ambient air-quality standards and in the case of respirable and particulate mass, comparable to those present on a very smoggy day.<sup>1,2,3</sup> Such high levels are unacceptable in terms of human health, safety and comfort, and must be taken into account particularly in energy-efficient structures where the reduction of infiltration may have serious ramifications on indoor air quality. Tables 1 and 2 summarize some of our findings with regard to gas stove oven and gas stove burner emissions, respectively, and present comparative values reported by others.

The work reported here represents the most recent accomplishments of our ongoing laboratory and field studies systematically examining gaseous and particulate air pollutants in residential buildings. The measurement techniques used

in the field and laboratory experiments have been previously described.<sup>2,3</sup>

### ACCOMPLISHMENTS DURING 1979

In our earlier laboratory studies, we quantified emission rates for a wide range of pollutants emitted by gas stoves, now identified as a significant source of pollution in the indoor environment. Tests were made with an environmental chamber about the size of a kitchen. Because the results obtained are not directly applicable to residences without enclosed kitchens, we initiated a project to equip an unoccupied experimental house with a gas stove and air-monitoring instrumentation to study 1) typical simulated exposures to pollutants generated by gas stoves, 2) the pollutant dispersion throughout the house, and 3) the role of infiltration and mechanical ventilation on indoor pollution levels.

A schematic of the Energy Efficient Buildings (EEB) research house used for these studies is given in Fig. 1. Only minor modifications were made to the house in order to reduce natural infiltration rates, e.g., sealing the unused ducts and fireplace. The house contains two mechanical ventilation systems. One is simply a fan-operated range hood installed directly over the gas stove (spot ventilation). The

Table 1. Gas stove oven emission rates ( $\mu\text{g}/\text{kcal}$ )

Pollutant	Lawrence Berkeley Laboratory	The Research Corporation of New England (TRC) <sup>a</sup>		British Gas Corp.	American Gas Assn. Standard
		Old Oven	New Oven	Oven	Oven
<u>Gaseous Emissions</u>					
CO	950(650-1500) <sup>b</sup>	[6] <sup>c</sup>	530	1620	645
CO <sub>2</sub>	200,000(195,000-205,000)	[6]			
NO	29 (14-50)	[11]	91.4	77.9	} 85
NO <sub>2</sub>	62 (44-74)	[11]	73.1	50.4	
SO <sub>2</sub>	0.8 (0.5-1.0)	[11]			
HCN	1.8	[1]			
HCHO	11.4 (9.9-14.2)	[5]			
<u>Particulate Emissions (&lt;2.5 <math>\mu\text{m}</math>)</u>					
Carbon	0.13 (0.05-0.24)	[9]			
Sulfur (as SO <sub>4</sub> <sup>2-</sup> )	(<0.01)	[9]			
kcal/hr	2000		2200	2200	

a. Steady-state emission rate

b. Range of emission rates in parentheses

c. Number of experimental runs in brackets

Table 2. Gas stove burner emission rates ( $\mu\text{g}/\text{kcal}$ )<sup>a</sup>

Pollutant	Lawrence Berkeley Laboratory	British Gas Corporation	American Gas Association Standard
<u>Gaseous Emissions</u>			
CO	890(720-1090) <sup>b</sup>	[4] <sup>c</sup>	645
CO <sub>2</sub>	205,000(196,000-217,000)	[3]	
NO	31(21-47)	[4]	} 136
NO <sub>2</sub>	85(69-100)	[4]	
SO <sub>2</sub>	0.8(0.6-0.9)	[4]	
HCN	0.07	[1]	
HCHO	7.1 (3.6-10.5)	[2]	
<u>Particulate Emissions (&lt;2.5 <math>\mu\text{m}</math>)</u>			
Carbon	0.90(0.86-0.96)	[4]	
Sulfur (as SO <sub>4</sub> <sup>2-</sup> )	0.05 (0.01-0.08)	[4]	
Total Respirable Mass	1.7 (1.0-2.6)	[3]	
kcal/hr. burner	2500		2500

- a. Operated with water-filled and cooking pots  
b. Range of emission rates in parentheses  
c. Number of experimental runs in brackets

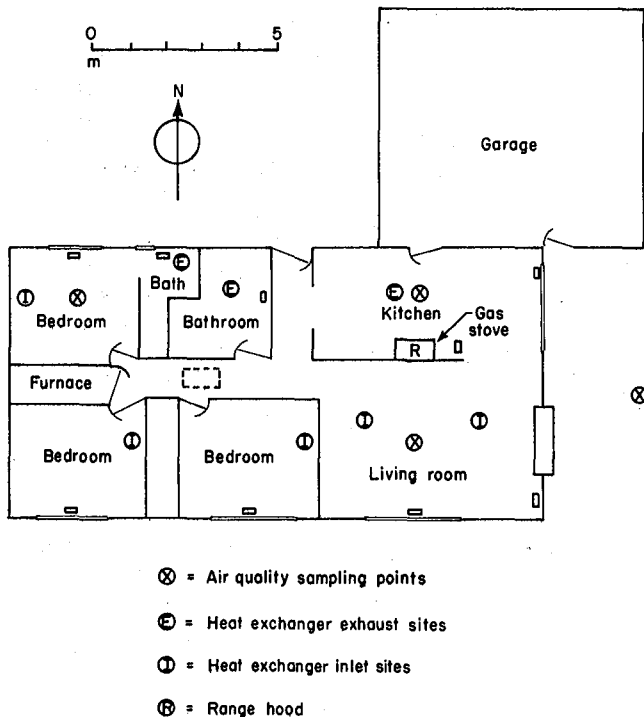


Fig. 1. Energy Efficient Buildings research house (XBL 7910-4489)

other is a heat-exchanging ventilation system which contains a cross-flow air-to-air heat exchanger;<sup>4</sup> the latter provides whole-house ventilation, as does infiltration. Air is exhausted out of the house from the kitchen and both bathrooms; outside air is injected into the living room and all three bedrooms.

Air quality was monitored from the kitchen, the living room, a bedroom, and one outdoor location. Gaseous pollutants (carbon monoxide, carbon dioxide, nitrogen oxide, nitrogen dioxide, and formaldehyde) were measured by drawing air from all monitoring sites to our array of instruments in the Mobile Atmospheric Research Laboratory (MARL).<sup>5</sup> The respirable fractions of particulates were also collected at each monitoring site and analyzed for total carbon, the primary element of particulate emissions from gas stoves. Temperature and dew point measurements were also made at each location.

With the aid of a study conducted by the American Gas Association in 1974,<sup>6</sup> we devised a typical gas stove consumption pattern to simulate actual cooking. These calculations yielded gas consumption values of 0.170 m<sup>3</sup> (6 ft<sup>3</sup>) for both the breakfast and lunch meals and 0.425 m<sup>3</sup> (15 ft<sup>3</sup>) for the dinner meal. Table 3 shows the results of the experiment for NO<sub>2</sub> and CO. No mechanical ventilation was used during the

Table 3. NO<sub>2</sub> and CO concentrations in EEB research house.

	NO <sub>2</sub> (ppm)	CO (ppm)
<b>Peak 1-hour average</b>		
Kitchen	0.452	24.2
Living Room	0.396	21.0
Bedroom	0.235	15.5
Outside	~0.07	0.4
<b>24-hour average</b>		
Kitchen	0.074	5.1
Living Room	0.073	5.1
Bedroom	0.045	4.1
Outside	0.035	0.4
<b>Air exchange rates (air changes per hour-ach)</b>		
morning	0.43	
mid-day	0.33	
evening	0.34	

experiment and natural infiltration varied between 0.33 and 0.43 air changes per hour (ach). As expected, the peak one-hour average pollutant concentration occurred during the dinner meal. The one-hour NO<sub>2</sub> air-quality standard proposed by the Environmental Protection Agency (EPA) is 0.25 ppm. As shown, NO<sub>2</sub> levels in both the kitchen and living room exceed this standard and in the bedroom, NO<sub>2</sub> levels are just under this limit. The one-hour EPA standard for CO is 35 ppm, and this limitation was not exceeded anywhere in the house.

Because of increasing concern about short-term exposure to elevated levels of NO<sub>2</sub>, we tested various ventilation strategies based on our simulation of air-quality conditions during the dinner meal. Figure 2 shows the results of our first set of experiments. The dotted lines represent data points obtained under whole-house ventilation conditions. Although only one set of data is shown for spot ventilation, the advantage of such ventilation can be readily seen. For example, if we were to increase the whole-house ventilation rate to 1.2 ach, we would expect a peak one-hour average NO<sub>2</sub> concentration of about 0.20 ppm in the kitchen; however, by incorporating spot ventilation at the same rate, the peak one-hour average NO<sub>2</sub> concentration was reduced to 0.07 ppm.

These results suggest that an effective energy-conserving strategy for ventilating high levels of gaseous pollutants from a point source (e.g., the gas stove) would be to increase the rate of spot ventilation at the pollutant emission source rather than to increase whole-house ventilation, which can be costly.

Pollutant dispersion throughout the house was also measured under air-quality conditions simulated for the dinner meal. As shown in

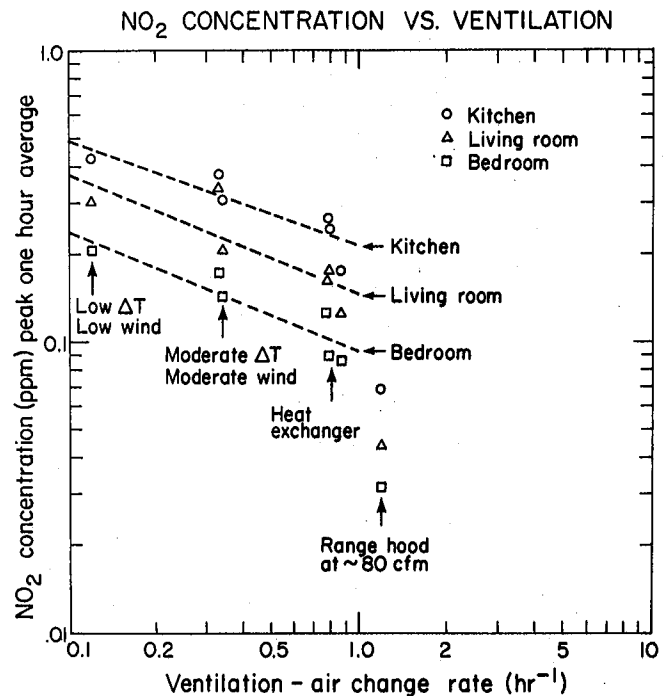


Fig. 2. NO<sub>2</sub> concentration vs. ventilation. (XBL 7910-4476)

Table 4, NO<sub>2</sub> levels in the bedroom are one-half the kitchen levels, while CO levels in the bedroom are two-thirds the kitchen levels. The difference between the two ratios can be explained by the greater reactivity of NO<sub>2</sub> in the indoor environment.

#### PLANNED ACTIVITIES FOR 1980

Our research plans for FY 1980 are to complete the analysis of the data collected at the EEB research house, and to then concentrate on three additional areas: First, we will attempt to use data already collected at the EEB research house for testing, evaluating, and improving various models of indoor air quality in residences. Several models have been published but were either not tested or yielded inadequate predictions of indoor air. Second, we intend to further characterize particulate emissions from the gas stove focusing on the chemical form of carbon--the primary element

Table 4. Pollutant dispersion in EEB research house.

(Peak 1-hour exposures averaged over 8 experiments)

	NO <sub>2</sub>	CO
Kitchen*	100	100
Living Room	77	82
Bedroom	53	68

\*Indexed to equal 100

emitted--and the composition of the remaining particulate emissions. Third, we will attempt to develop a comprehensive passive-monitoring package to determine one-week average pollution levels in various building types. Such a system would allow us to conduct extensive field studies at minimal costs for instrumentation and personnel. Field studies would have the dual goals of testing a wide variety of building types (using different ventilation schemes) and determining actual pollutant levels to which occupants are exposed in the various indoor environments.

#### REFERENCES

1. C.D. Hollowell, R.J. Budnitz, G.D. Case, and G.W. Traynor, Generation of Gaseous and Particulate Air Pollutants from Indoor Combustion Sources: I. Field Measurements 8/75-10/75, Lawrence Berkeley Laboratory Report, LBL-4416 (January 1976).
2. C.D. Hollowell, R.J. Budnitz, and G.W. Traynor, "Combustion-Generated Indoor Air Pollution," in Proceedings of The Fourth International Clean Air Congress, Tokyo, Japan, May 16-20, 1977, pp. 684-7, The Japanese Union of Air Pollution Prevention Associations, Tokyo, Japan (1977).
3. Lawrence Berkeley Laboratory Annual Report, 1978, Energy and Environment Division, pp. 156-163
4. Lawrence Berkeley Laboratory Annual Report, 1978, Energy and Environment Division, pp. 104-106
5. C.D. Hollowell and T. Novakov, "Mobile Atmospheric Research Laboratory," in Novakov, T., et.al., Atmospheric Aerosol Research Annual Report, 1976-1977. Lawrence Berkeley Laboratory Annual Report, 1975-1976, LBL-5214.
6. D.W. DeWerth, "Energy Consumption of Contemporary 1973 Gas Range Burners and Pilot Under Typical Cooking Hoods," American Gas Association Research Report No. 1499 (May 1974).

## ORGANIC CONTAMINANTS

*R. R. Miksch, D. W. Anthon, M. Barnes, L. Z. Fanning, J. Glanville, H. Schmidt, and M. Tashima*

#### INTRODUCTION

The Organic Contaminants Project of the Ventilation Program is currently investigating the pollution of the indoor environment by organic vapors. Research is being actively conducted in several areas; principally: (1) development of laboratory techniques for analyzing formaldehyde levels; (2) development of general methodologies for identifying and characterizing a wide variety of organic contaminants; and (3) development and implementation of a field monitoring program for measuring organic contaminants in indoor environments.

Studies by LBL<sup>1</sup> and others<sup>2-4</sup> clearly show that the levels of organic contaminants in indoor environments often exceed those encountered outdoors. Organic contaminants derive from a variety of sources: formaldehyde can be emitted from common building materials such as plywood, particle board and foam insulation (all of which contain urea-formaldehyde resins), and a wide range of organic contaminants are emitted from such materials as paints or adhesives as well as from combustion processes associated with occupant behavior.

It is generally accepted that the build-up of organic compounds in indoor environments can have adverse effects on the health of building occupants. Organic compounds such as aromatic and chlorinated hydrocarbons that we have encountered in field tests are capable of inducing acute toxic effects when present in high concentrations and, at lower levels of exposure, have been implicated in the etiology of cancer.

In addition, we have detected indoor levels of formaldehyde that exceed European standards for safe exposure limits.

Although methodologies exist for sampling outdoor air or occupational indoor air and for performing subsequent analysis in the laboratory, present capabilities are somewhat limited with respect to sensitivity and the range of compounds that can be identified. At low concentration levels, numerous contaminants are difficult to measure quantitatively with any precision, and instruments for continuous monitoring of organic contaminants in indoor environments do not exist.

A major objective of the Organics Project has been to develop an overall methodology that will encompass both field sampling and laboratory analyses, and be readily transmissible to all those involved in studying or monitoring indoor air quality.

#### ACCOMPLISHMENTS DURING 1979

##### Development of Methods of Analysis

During 1979, the laboratory capabilities of the Organics Contaminants Project were expanded. A second Varian 3700 gas chromatograph and two Nutech thermal desorption devices were purchased. Laboratory space, which had been constricted, was expanded with the acquisition of a new room. Several personnel were added to the

project. These improvements have greatly facilitated the accomplishment of the project tasks discussed below.

Several improvements have been effected in the design of field-sampling instruments for formaldehyde measurements. Air is now drawn through bubblers constructed from straight teflon tubing impingers and polypropylene centrifuge tube bodies. Not only are we now observing lower and more uniform pressure drops across these bubblers but accurate flow control is more easily obtained now that sintered glass frit impingers are not used. In addition, we have found that pooling the contents of two bubblers in series for each sampling line insures a higher and more uniform collection efficiency.

The bubblers have been placed in refrigerators where constant collection efficiency is better maintained and the stability of the samples and of reagents, such as MBTH, are enhanced. Field monitoring work also has been facilitated by these procedures, for not only can we now avoid such mishaps as bubblers going dry under low humidity conditions, but we can store samples for later analysis in the laboratory.

The two formaldehyde field samplers used by the EEB Mobile Laboratory continue to employ the very accurate air flow control system developed at LBL last year. Four other field samplers used for this work utilize critical orifices for flow control. By reducing the size and complexity of these samplers, we have been able to construct them as stand-alone units, i.e., not requiring the support of the EEB Mobile Laboratory. These design features also permit us to use samplers in a wider variety of sampling applications. Details of construction on both kinds of samplers are given in Fig. 1.

The Organics Contaminants Project staff has continued its comparison of various wet chemistry techniques for measuring formaldehyde and total aliphatic aldehydes. A major step forward has been our discovery that the health hazards associated with the pararosaniline technique can be greatly reduced by eliminating the toxic mercury reagent. Coupled with optimization work accomplished to increase the sensitivity of the pararosaniline technique, this method appears to LBL personnel to be superior to the chromotropic acid method given by the National Institute of Occupational Safety and Health (NIOSH) for determining formaldehyde.

Having successfully perfected field-sampling instruments and methods of analysis, the Organics Project is now investigating further ways to improve our ability to measure and analyze formaldehyde levels in indoor environments. Two possibilities are being considered: the use of passive monitors with an appropriate collection medium, and the direct determination of formaldehyde by gas chromatography using an appropriately chosen detector. These two techniques would complement each other for extensive field studies. Significant formaldehyde levels identified through surveys conducted with passive

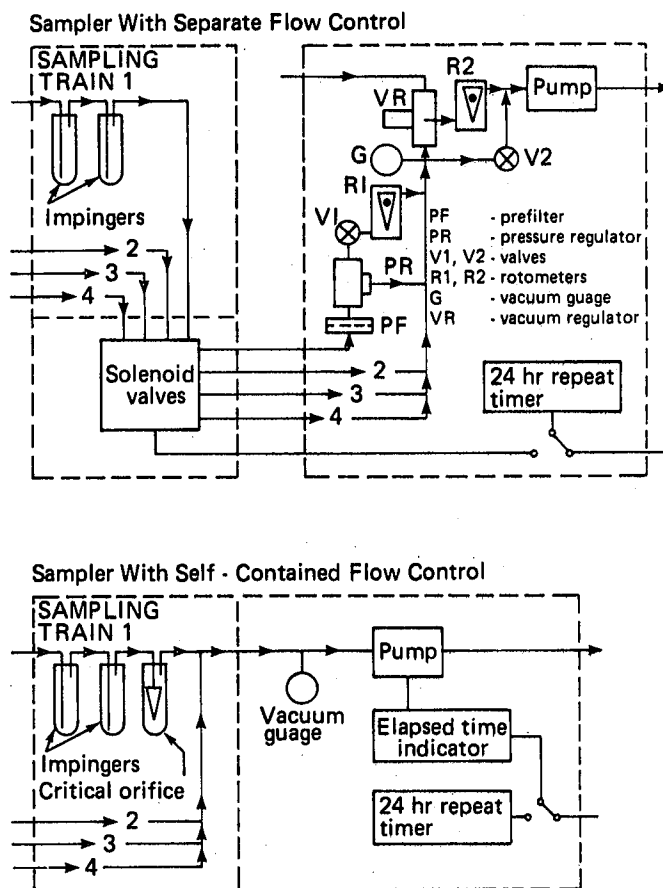


Fig. 1. Schematics of formaldehyde field samplers. Portion inside box labeled SAMPLING TRAIN 1 is contained in refrigerator. (XBL 7910-4484A)

monitors could be quickly validated using the gas chromatograph.

Another aspect of our work this year has been the continued investigation of a sampling and analysis methodology for organic contaminants based on the use of the porous polymer adsorbent, Tenax GC. In this method, field samples are taken by passing air through a glass tube containing Tenax GC. The tube is placed in a screw-top culture tube that is shipped to the laboratory where the sample is analyzed using a Nutech thermal desorption device in conjunction with a Varian 3700 gas chromatograph. The Nutech apparatus contains an oven which is used to thermally desorb organic contaminants from the Tenax GC contained in the glass tube into a cryogenic trap that reconcentrates the organic contaminants. The cryogenic trap is subsequently heated and the organic contaminants are introduced on to the gas chromatograph for separation and quantitative analysis. Figures 2 and 3 show representative gas chromatographs for outdoor and indoor air sampled at an LBL office trailer.

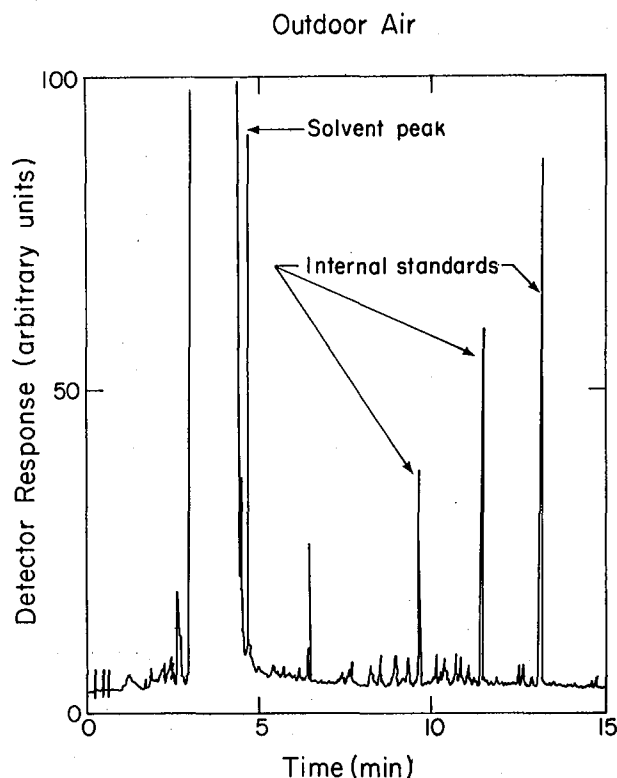


Fig. 2. Representative gas chromatograph showing number and concentration of organic contaminants collected from an outdoor air sample on the porous polymer Tenax GC. The size of the air sample is identical to that in Fig. 3. (XBL 7910-4474)

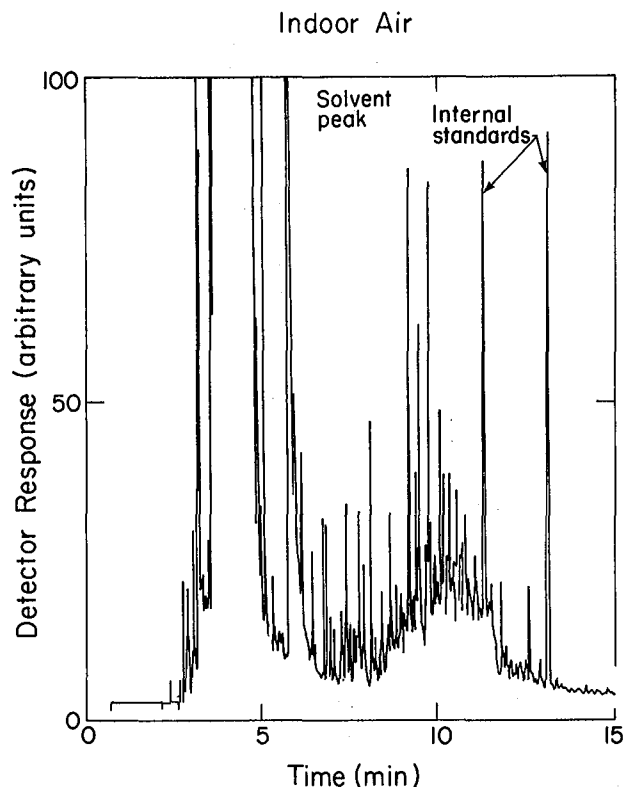


Fig. 3. Representative gas chromatograph showing number and concentration of organic contaminants collected from an indoor air sample on the porous polymer Tenax GC. The size of the air sample is identical to that in Fig. 2. (XBL 7910-4473)

The Nutech thermal desorption device has the advantage of being easily detachable, making it possible to reattach it to a Finnigan 4023 GC/MS available at LBL. The Finnigan mass spectrometer allows us to positively identify many of the organic contaminants contained in a field sample. Once identified, contaminants can be quantified by means of gas chromatography to produce a detailed profile of the organic contaminants present in indoor environments.

A field sampling program using Tenax GC does have limitations, especially for analyzing low molecular weight compounds. We are currently working on alternate approaches such as merely taking a representative grab sample of air in an appropriate container. The use of alternative adsorbents and the possibility of bubbling air through organic solvent are being explored.

#### Field Monitoring of Organic Contaminants

As a continuing part of the Ventilation Program's field monitoring project, formaldehyde and total aliphatic aldehydes were measured this year at the Fairmoor School in Columbus, Ohio, at the NAHB energy Research House in Carroll County, Maryland, and at a Minimum Energy Dwelling (MED II) in Mission Viejo, California.

The data from the Fairmoor School is presented in Fig. 4 in the form of a histogram. As a 20-year old structure, it is not surprising that the indoor concentration of formaldehyde did not vary significantly from ambient outdoor levels, even when air exchange rates were varied from about 2.5 ach (air changes per hour) down to 0.3 ach.

Measurements performed at the NAHB house in Maryland, as shown in Fig. 5, are considerably more interesting. This unoccupied, low ventilation (0.2 ach) house had indoor formaldehyde levels averaging about 80 ppb. The ambient air exposure level recommended in the United States is 100 ppb and an indoor air exposure level of 100 ppb has been recommended or promulgated in several European countries. It is interesting to note that total aliphatic aldehydes in the Maryland house, as determined by means of the MBTH method, averaged somewhat greater than 100 ppb. Outdoor concentrations were less than 10 ppb in both cases, clearly characterizing formaldehyde as an indoor pollutant.

Data taken at the MED-II house in Mission Viejo (see Table 1) are the most interesting of all because they clearly show that furniture and human occupants can be significant sources of indoor formaldehyde. When the house did not

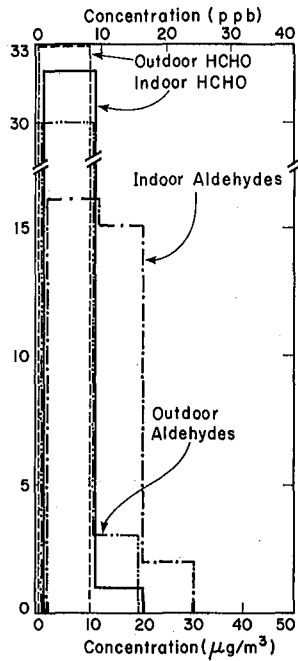


Fig. 4. Histogram of indoor and outdoor formaldehyde and total aliphatic aldehyde concentrations measured in a classroom of Fairmoor School, a 20-year old structure in Columbus, Ohio, during January and February, 1979. The air exchange rates of the classroom were varied from about 2.5 down to 0.3 ach during these measurements. The concentration of HCHO did not vary significantly with air exchange rate. (XBL 796-1748)

contain furniture, formaldehyde levels were below the standard exposure level of 100 ppb; when furniture was added, formaldehyde levels rose to almost twice the 100 ppb level. A further increase was noted when the house was occupied, very likely because of such activities as cooking with gas. When occupants opened windows to increase ventilation, the formaldehyde level dropped substantially. Under all of the conditions noted above, indoor formaldehyde levels were considerably in excess of ambient outdoor levels, which averaged less than 10 ppb.

Preliminary sampling of organic contaminants using Tenax GC was also performed at two sites, an LBL office trailer (90G) and a new San Francisco office building. As the Nutech thermal desorption devices were not available at the time, samples were prepared for gas chromatography/mass spectrometry (GC/MS) analysis by thermal desorption into a small quantity of organic solvent. The solvent was injected by syringe into the GC/MS in order to identify organic contaminants. The results of these tests are displayed in Table 2. The compounds identified fell into three broad categories: (1) aliphatic hydrocarbons; (2) alkylated aromatics; and (3) chlorinated hydrocarbons. Several of these compounds have been identified by the Environmental Protection Agency as "priority pollutants." A smaller number are suspected carcinogens (e.g., benzene). Estimates of concentrations, while necessarily tentative at this stage, invariably showed high indoor-to-outdoor ratios. While preliminary, these findings highlight the urgency of fully assessing the scope and magnitude of organic contaminants in indoor environments.

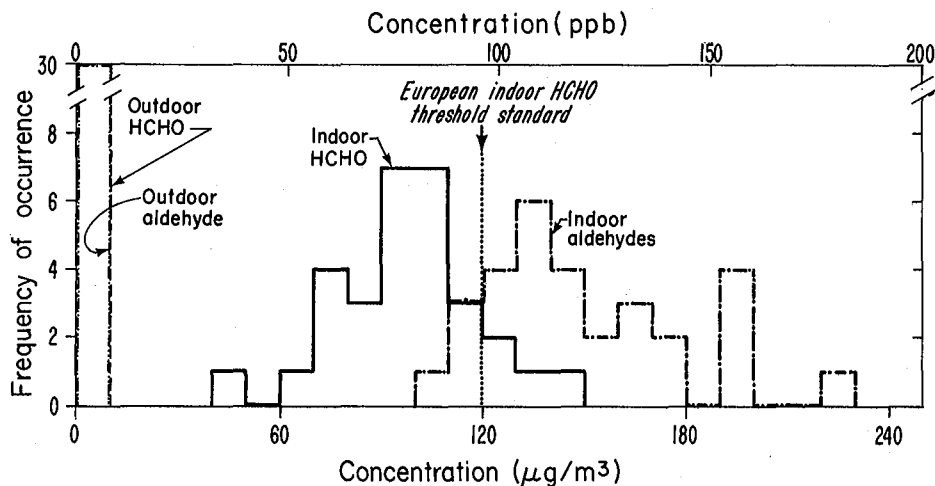


Fig. 5. Histogram of indoor and outdoor formaldehyde and total aliphatic aldehyde concentrations measured at an energy research house in Maryland during March and April, 1979. The air exchange rate of the house is about 0.2 ach. (XBL 795-1458A)

Table 1. Indoor/outdoor formaldehyde and aliphatic aldehyde concentrations measured at the Med-II residence, August 1979

Condition	Number of Measurements	Sampling Time	Formaldehyde (ppb) <sup>a</sup>	Aliphatic Aldehydes (ppb) <sup>b</sup>
Unoccupied, without furniture	3	12	66 ± 9%	74 ± 16%
Unoccupied, with furniture	3	24	183 ± 7%	241 ± 4%
Occupied, day <sup>c</sup>	9	12	214 ± 10%	227 ± 15%
Occupied, night <sup>d</sup>	9	12	115 ± 31%	146 ± 29%

a Determined using pararosaniline method (100 ppb  $\cong$  120  $\mu\text{g}/\text{m}^3$ ). All outside concentrations < 10 ppb.

b Determined using MBTH method, expressed as equivalents of formaldehyde. All outside concentrations < 20 ppb.

c Air exchange rate  $\cong$  0.4 ach.

d Windows open part of time; air exchange rate significantly greater than 0.4 ach and variable.

Table 2. Organic compounds identified in indoor air.<sup>a</sup>

Compound	Approximate Ratio [Indoor] / [Outdoor]	Approximate Concentration (ppb)	Agency Identifying Compound as Potential Health Hazard
<u>Hydrocarbons:</u>			
n-heptane	10	20	
n-octane	80	300	
n-nonane	100	150	
cyclohexane			
hexane			
many other branched aliphatics			
<u>Aromatics:</u>			
benzene	5	25	EPA, NIOSH, OSHA
toluene	5	75	
xylenes	15	150	
trimethylbenzene			
ethylbenzene			
ethylmethylbenzene			
<u>Halogenated Compounds:</u>			
tetrachloroethylene		large	EPA
trichloroethylene		small	EPA, NIOSH
1,1,1 trichloroethane		small	EPA, NIOSH

<sup>a</sup>Compounds identified were present in air sampled at an LBL office trailer (90G) and/or a San Francisco office building. Numerical data is for the San Francisco office building only.

## PLANNED ACTIVITIES FOR 1980

The experimental studies planned for FY 1980 are contained in the various projects already mentioned. With sampling and analytic techniques for formaldehyde determination perfected, our emphasis will turn to examining wholly new approaches for radically increasing sensitivity, decreasing sampling time or increasing sampling capability. The organic sampling methodology based on Tenax GC will continue to be developed, with particular focus on techniques of calibration and field sampling. Alternative techniques, e.g., grab sampling, will be explored.

We will continue to work with the EEB Mobile Laboratory for field monitoring studies of energy efficient buildings throughout the country. Several sites will be added to those currently under investigation, and efforts will be made to correlate specific construction details (e.g. building materials used) and the use of air-to-air heat exchangers with organic contaminant levels.

Finally, we intend to examine explicitly the outgassing of organic contaminants from building materials. Using the methods of analysis developed for field samples, we will identify and quantify the organic contaminants in the headspace vapor over selected building materials

and correlate these findings with field-sampling measurements.

## REFERENCES

1. Chin-I-Lin, Roy N. Anaclerio, Douglas W. Anthon, Leah Z. Fanning and Craig D. Hollowell, Indoor/Outdoor Measurements of Formaldehyde and Total Aldehydes, Lawrence Berkeley Laboratory Report, LBL-9397, (July 1979).
2. I. Johansson, "Determination of Organic Compounds in Indoor Air with Potential Reference to Air Quality." Atmospheric Environment, Vol. 12, 1978, p. 1371.
3. A. Dravnieks, "Organic Contaminants in Indoor Air and Their Relation to Outdoor Contaminants," ASHRAE IRP 183, 1977.
4. I. Andersen, G. R. Lunquist, and L. Molhavi, "Indoor Air Pollution Due to Chipboard Used as a Construction Material," Atmospheric Environment, Vol. 9, 1975, p. 1121.
5. National Institute of Occupational Safety and Health, Manual of Analytical Methods, (2nd Edition), Vol. 1. 1977, pp. 125-1-125-9.

## RADON MEASUREMENTS AND EMANATION STUDIES

*J. V. Berk, M. L. Boegel, J. G. Ingersoll,  
W. W. Nazaroff, B. D. Stitt, and G. H. Zapalac*

The main objective of the Radon Project is to determine the extent to which radon is a contaminant of indoor air in residential buildings. To this end, the program has undertaken three distinct areas of activities:

1. Monitoring conventional and energy-efficient residential buildings for radon levels;
2. Measurement of emanation rates of radon from building materials;
3. Development of appropriate monitors for detecting radon and radon daughters.

Radon-222, an inert gas, is part of the uranium-238 decay chain and, consequently, occurs naturally in the environment. The health hazards associated with radon result from its four short-lived radon daughters, RaA, RaB, RaC and RaC', all of which have half-lives of less than 30 minutes and two of which (RaA, RaC') are alpha-emitters.<sup>1</sup> Airborne radon daughters, when inhaled, can be deposited in the lower respiratory tract. It is known that prolonged exposure to elevated levels of radon daughters is related to increased incidence of lung cancer.<sup>2</sup>

Because radon outgasses from soil and building materials, the concentration of radon and radon daughters may build up in indoor spaces. Other possible radon sources within a building are tap water and natural gas. The potential for radon gas emission from these sources depends to a great extent on the content of radium-226 in the medium (soil, building materials) or on the initial proximity of the medium (water, natural gas) to radium-226-bearing deposits, since radium-226 is the immediate precursor of radon-222 in the uranium decay chain.

When energy-conserving features designed to reduce infiltration of outside air are applied to residential buildings, radon levels as well as levels of other indoor air pollutants may increase. If, as is often presumed in risk-assessment studies, the incidence of cancer from radiation exposure is directly proportional to the dose received,<sup>3</sup> then such an increase in radon levels would result in a higher incidence of lung cancer. The recognition that radon poses a health hazard, generally, and that energy-conservation measures adopted in residential buildings may exacerbate the health risks to building occupants has made indoor air-quality studies a research priority.

For reference purposes, typical levels of radon in outdoor as well as indoor air at representative geographical sites are shown in Fig. 1. Guidelines for remedial action due to industrial contamination that have been adopted by the Atomic Energy Control Board of Canada<sup>4</sup> and guidelines recommended by the U.S. Environmental Protection Agency<sup>5</sup> fall within a range of 1 to 4 nanoCuries per cubic meter ( $\text{nCi}/\text{m}^3$ ).

## ACCOMPLISHMENTS DURING 1979

### Monitoring of Residential Buildings

The principal focus of this part of the program has been the measurement of radon levels in both energy-efficient and conventional houses. We employed three types of measurements to monitor buildings for radon levels: grab-sampling of air, accompanied by measurement of ventilation rates; real-time measurement of radon, radon daughters and ventilation rates; and integrated measurement of radon. Occasionally, we used more than one type of measurement at the same site in order to cross-check the results.

Since the beginning of spring, 1979, we have been monitoring energy-efficient houses across the country for radon concentrations versus air-change rates and other building characteristics that may affect indoor air quality. Of the 16 energy-efficient houses, nine (all located in the New Mexico area) are solar houses. Measurements of radon levels were taken under "worst case" conditions, i.e., closing up the building for several hours prior to the measurement (see

Fig. 2). If the radon source-term were the same for all houses, one would expect all the points to fall on a straight line with a  $45^\circ$  slope in a log-log plot. Obviously, this is not the case.

In a corollary study, we monitored a number of conventional residential buildings in the San Francisco Bay Area from August through September, 1979, in order to compare findings with those obtained in energy-efficient buildings. These measurements were also taken under "worst case" conditions, as previously described. The results of this preliminary survey are shown in Fig. 3, which shows that the majority of the houses monitored had low infiltration rates. What is striking in these results, however, is that even in cases where the infiltration rate was low, radon levels were low, an indication of low radon source strength. It is possible that the very slight indoor/outdoor temperature differences characteristic of Bay Area summers or the lack of winds might be responsible for the low infiltration rates.<sup>2</sup> In any case, these findings should be taken as typical only for conventional houses in the San Francisco Bay Area during the summer.

The National Association of Home Builders (NAHB) house at Mt. Airy, Maryland, was selected for more extensive monitoring because, out of all the houses we measured, it showed the highest radon levels (see Fig. 2). A heat exchanger was installed in that house so that we could vary the ventilation rate and measure corresponding variations in radon levels continuously for two weeks (see Fig. 4). Similar

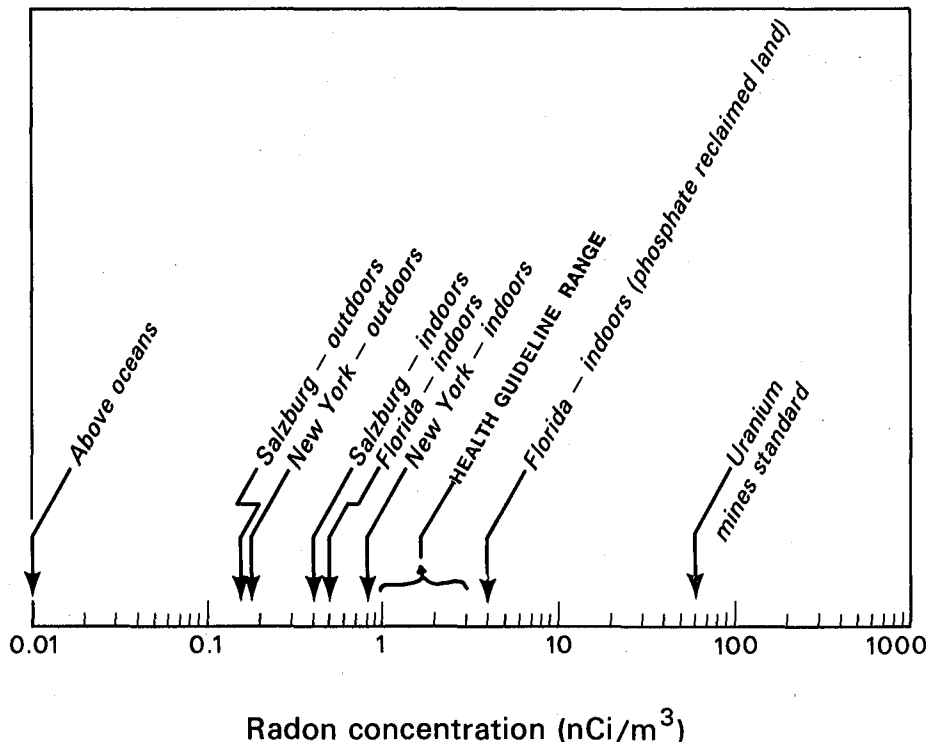


Fig. 1. Typical radon concentrations in air. (XBL 795-1659C)

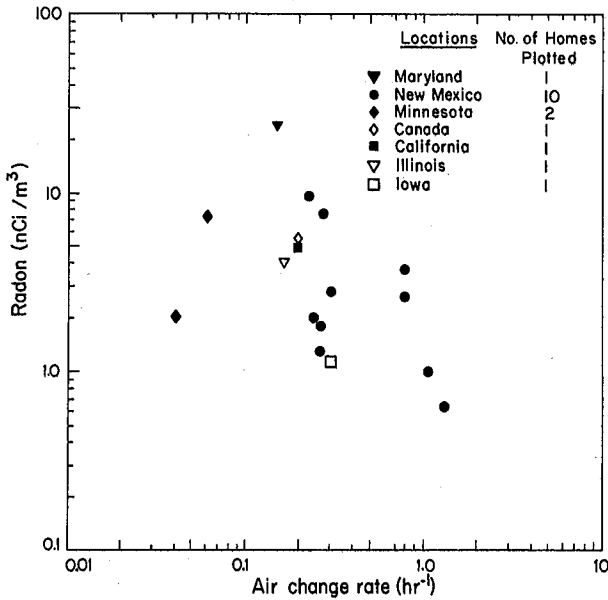


Fig. 2. Radon concentration vs. ventilation in energy-efficient houses. (XBL 796-1875A)

measurements were taken for radon daughter concentration.

Measurement of Emanation Rates from Building Materials

A second major objective of the radon program is to measure radon emanation rates from building material samples from major population centers of the country and, from these data, to compile a listing of frequently used building materials in the U.S., estimating the relative significance of each as an indoor radon source. Concrete was the first building material considered.

A system for measuring radon emanation rates was under development in 1978 and was operative at the end of summer, 1979. The system is schematically shown in Figs. 5 and 6. The sample to be measured is allowed to remain for 24

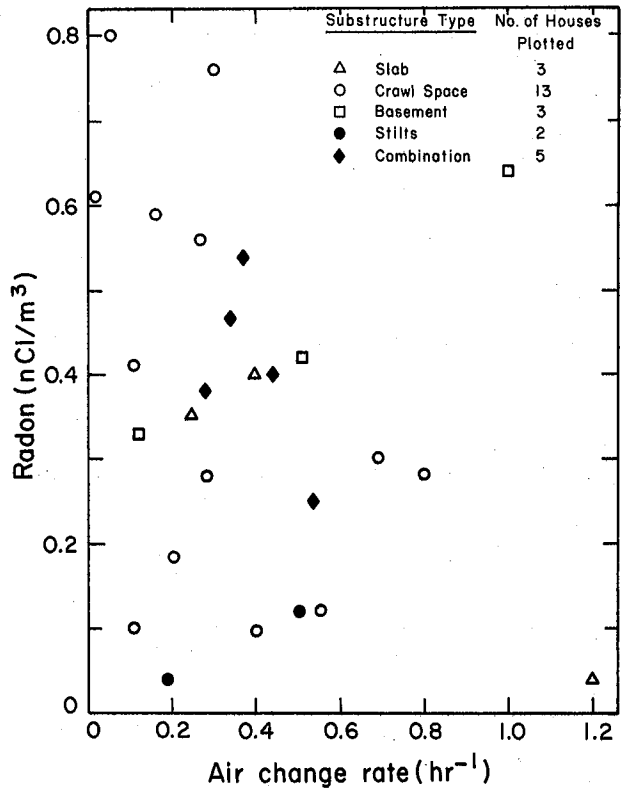


Fig. 3. Radon concentration vs. ventilation in conventional houses (San Francisco Bay Area). (XBL 799-7120)

hours in a sealed chamber, which is a modified paint can. The chamber is then flushed with helium (He) for one hour and the radon is collected by adsorption on glass wool at liquid nitrogen (N<sub>2</sub>) temperature (-196°C). The glass wool trap is evacuated of non-condensed gases while kept at this temperature. It is then left to reach room temperature, at which the radon desorbs from the glass wool surface. Subsequently, the radon is transferred from the trap to a Lucas cell using He as a carrier gas. The emanation rate of the sample is determined by counting the alpha-decay rate of radon and its

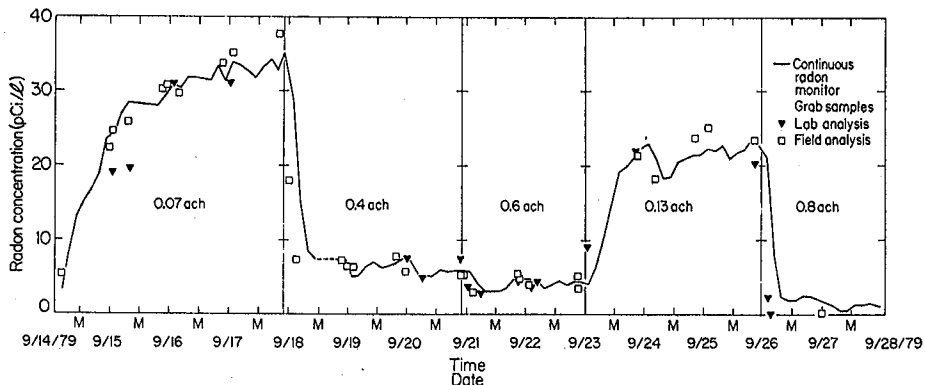


Fig. 4. Indoor radon concentration vs. ventilation rate controlled by a heat exchanger in the NAHB house over a two week period. (XBL 790-4440)

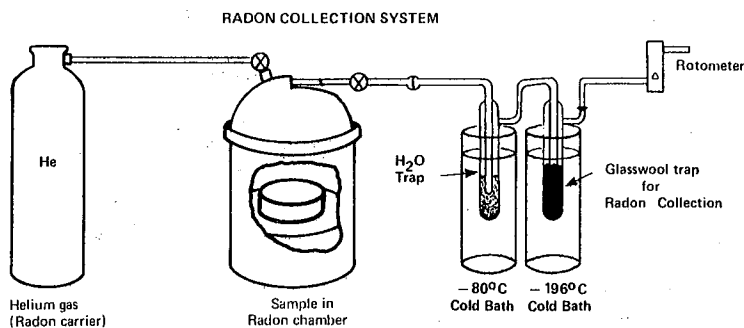


Fig. 5. Radon emanation and collection system.  
(XBL 793-859A)

daughters in the Lucas cell. For calibration, standard radium solutions supplied by the National Bureau of Standards provide radon sources of known strength.

The uncertainty in the emanation measurement ranges from 5% to 15%, depending on the sample. This system, of course, is designed to handle any building material sample. To date, we have built eight radon chambers so that several samples can be measured simultaneously. The concrete samples we have been using are standard American Society for Testing and Materials (ASTM) cylinders (6" in diameter, 12" in height) provided to us by various concrete testing laboratories. Between 6 and 12 cylinders are received from each site.

Each cylinder is cut into 1" and 10" pieces and both pieces are measured for radon. The 10" piece emanates approximately (within 5% to 10%) ten times as much as the 1" piece. This feature enables us to estimate the amount of radon expected to emanate from building walls or slabs made out of the same material. Samples from the San Francisco Bay Area, California; Kansas City, Missouri; Salt Lake City, Utah; Albuquerque, New Mexico; Philadelphia, Pennsylvania; and New York City, New York have been measured already. Measured emanation rates per mass have been in the range of 0.5 to 2.0 pCi/kg.hr.

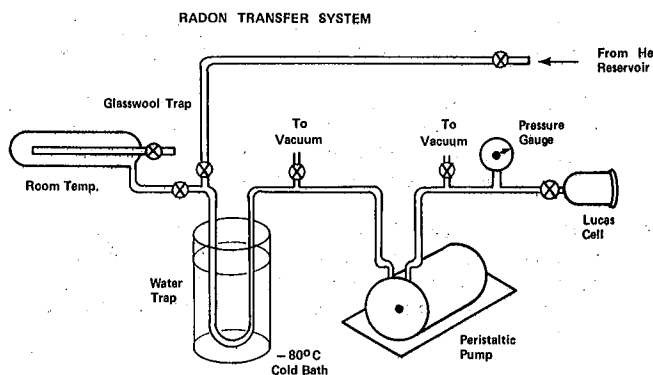


Fig. 6. Radon transfer system. (XBL 793-860A)

Once the emanation rate of radon from concrete has been determined, it is straightforward to calculate the indoor radon levels that can be expected from concrete alone in a typical residential building. As an example, in a house with 1800 ft.<sup>2</sup> floor area, 8 ft. height, a sub-structure consisting of a heavy concrete slab 8" thick, and a ventilation rate of 0.5 ach, the previous emanation rates would contribute 0.1 to 0.4 nCi/m<sup>3</sup> to the indoor radon level. Based on these laboratory measurements of emanation rates, we would conclude that the emanation of radon from the concrete is negligible compared with that measured in most houses.

#### Development of Monitors

Work on passive radon monitors has continued over from 1978, and active radon and radon daughter monitors were developed during 1979.

The 25 Passive Environmental Radon Monitors (PERMs) built in 1978<sup>1</sup> were extensively tested in our calibration box. A number of performance-hampering defects in construction were discovered and corrected, reducing their reproducibility error to less than 20%, including the error in the lithium fluoride TLD chip reading, which was of the order of 13%. Dysprosium-doped, calcium fluoride TLD chips have also been tested in an effort to increase the sensitivity of the instrument. The 25 PERMs are currently used routinely for conducting integrated measurements of radon in residential buildings, as described earlier. Plans for the fabrication of 50 additional PERMs, incorporating several new operational and engineering features deemed necessary from our past experience, are now underway.

For our work on active monitors, we have developed a radon monitor and a radon daughter monitor and have built a continuous monitor based on a prototype developed by others.<sup>6</sup> The continuous radon monitor is shown schematically in Fig. 7. Pre-filtered air, i.e., freed of all radon daughters, is continuously drawn into a two-port 170 ml scintillation flask (Lucas cell) at a rate of 2 liters per minute (lpm). A photomultiplier tube system is used to count the alpha-decays from the radon and the two alpha-emitting radon daughters in the cell. A printer

RADON DAUGHTER MONITOR

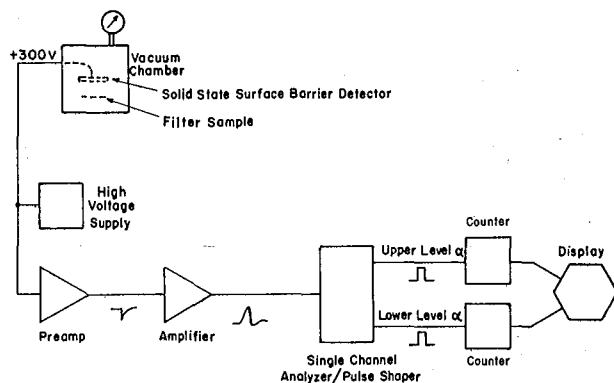


Fig. 7. Radon daughter monitor.  
(XBL 799-7119)

is interfaced with the system so that total counts can be printed out over a pre-set time interval. (We have been using a time interval of 36.4 minutes.) A prototype of this instrument was built in August and has been used since then for field and laboratory measurements of radon concentrations.

The radon daughter monitor, shown in Fig. 8, was developed by members of the radon group. Radon daughters are collected on a teflon filter by drawing air through the filter at a rate of 10 to 15 lpm. After ten minutes of collection time, the filter is placed inside a chamber opposite a solid-state surface barrier detector and the chamber is evacuated to 5" of Hg, absolute. A single-channel analyzer discriminates and separately counts pulses from the two different alpha energies, 6.00 MeV and 7.69 MeV, of the alpha-emitting daughters, RaA and RaC', respectively. In order to determine the nuclide ratio of the three daughters, RaA:RaB:RaC (RaC:RaC'=1 because of the extremely short half-life of RaC') and from that the corresponding Working Level (WL), two consecutive measurements of their alpha activity are necessary. At present, we take the first of the two consecutive measurements between 11 and 33 minutes from the beginning of the 10-minute collection time and the second between 35 and 50 minutes. These time intervals were determined by computer analysis to be optimal for assuring maximum instrument sensitivity as long as the total sampling and counting time does not exceed one hour. Within this time constraint, the radon daughter monitor can measure as low as 0.0025 WL with an error of 10%. The uncertainty in the measurement of each of the daughters is 20% at 1.0 nCi/m<sup>3</sup>. A prototype of this monitor, also built in August, was used for the radon daughter studies conducted at the NAHB house in Maryland in September, 1979.

#### PLANNED ACTIVITIES FOR 1980

In 1980, the radon program will continue the field monitoring of energy-efficient houses

CONTINUOUS RADON MONITOR

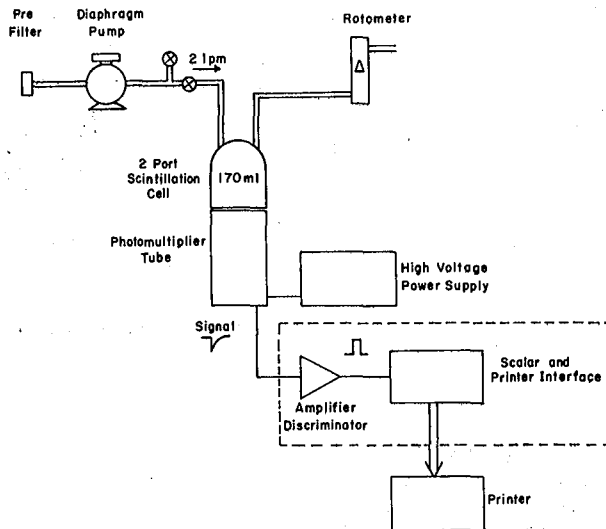


Fig. 8. Continuous radon daughter monitor.  
(XBL 799-7118)

across the country, including solar houses in New Mexico and possibly California. We will also continue monitoring conventional houses in the San Francisco Bay Area as well as elsewhere in the U.S. In all cases, field monitoring will involve measuring both radon and radon daughters.

We plan to complete our measurements of radon emanation rates from concrete samples representative of all major metropolitan areas of the country. Later on, other building materials (bricks, gypsum) may be measured for radon emanation rates.

In the area of instrumentation, we will continue to work on improving active and passive monitors for radon and radon daughters.

Finally, we plan to examine some active and passive radon control strategies.

#### REFERENCES

1. Lawrence Berkeley Laboratory Annual Report, Energy & Environment Division, 1978, p. 100.
2. UNSCEAR, "Sources and Effects of Ionizing Radiation," Annex B, United Nations, Official Records, 32nd Session, Supplement No. 40 (A/32/40), New York, 1977.
3. BEIR Committee, "The Effects on Populations of Exposure to Low Levels of Ionizing Radiation," National Academy of Sciences & National Research Council, Washington, D.C., 1972.
4. Dilworth, Secord, Meagher and Associates, Limited, "Investigation and Implementation of Remedial Measures for the Radiation

Reduction and Radioactive Decontamination of Elliot Lake, Ontario," Atomic Energy Control Board, January 1979.

5. R.J. Guimond, et al., "Indoor Radiation Exposure Due to Radium-226 in Florida Phosphate Lands," U.S. Environmental Protection Agency, EPA 520/4-78-013, February 1979.

6. J.W. Thomas, "A System for Continuous Radon Determination," Health and Safety Laboratory, U.S. Energy and Development Administration, HASL-37, New York, July 1977.

## INDOOR RADON HEALTH RISKS

A. V. Nero

### INTRODUCTION

Radon-222 and its daughters, members of the uranium-238 decay chain present throughout the earth's crust, have long been recognized as significant contributors to natural background radiation. Exposure of the general population to radon and daughters occurs primarily indoors, where concentrations are usually higher than outdoors. While not all energy efficient or retrofitted buildings have low air-exchange rates, a reduction in ventilation rate may result in an increase of indoor radon levels. The purpose of this project is (1) to evaluate the health impact of radon and its daughters as indoor air pollutants and (2) to examine the significance of indoor radon in energy-efficient buildings that are designed (or retrofitted) to reduce infiltration or ventilation. This project is being carried out in close collaboration with the Energy Efficient Buildings Radon Program, which is performing indoor radon measurements and developing monitoring instrumentation.

A basic aspect of assessing health risks of a substance is to determine the dose-response relationship between exposure and increased incidence of disease or pathology. In the case of radon and its daughters, findings that the incidence of cancer is greater among uranium and other miners than among the general population has been correlated with the prolonged exposure of these miners to high radon levels.<sup>1</sup> If the dose-response factor is extrapolated from data on miners and applied to populations exposed to lower radon levels, we can estimate that continuous exposure to 1 picocurie per liter (1pCi/l) of radon and a typical amount of associated daughters would contribute a lung cancer incidence of as much as 100 per million per year, a significant fraction of the current incidence from all causes.<sup>2</sup> This estimate is highly uncertain, since it is based on an extrapolation from high to low doses as well as on other assumptions (e.g., exposure conditions--mines vs residences). However, judging from limited data available on indoor radon concentrations, the estimate of 1 pCi/l is probably within a factor of two of the average value for residences in the United States. Moreover, on the basis of existing data, it appears that a significant portion of conventional residences in areas of the United States that are naturally high in radium have considerably higher radon concentrations than 1 pCi/l. When air-exchange rates are reduced, as occurs in energy-saving

retrofits, indoor radon levels would be even more elevated. Reducing air exchange rates in such houses, or building energy-efficient houses in such areas, may subject occupants to unacceptably high individual risks.

There are, thus, two important aspects to limiting radon and radon daughter levels. One is to limit individual risk by setting numerical limits on indoor radon or daughter concentrations. The second is to develop broad radon control strategies, including a spectrum of control measures for energy-efficient buildings, that would constrain the average increase (if any) in radon exposure to an acceptable level.

### PLANNED ACTIVITIES FOR 1980

We have considered these two viewpoints in examining the impact of increased radon levels for the Residential Conservation Service (RCS) program, which plans to provide low-interest loans nationwide for retrofitting existing homes. The RCS program, to be implemented in 1980, is not expected to have substantial impact on the average air-exchange rate in the nation's homes. This is fortunate since sufficient information is not available to undertake the comprehensive risk-benefit analysis necessary to determine "acceptable" increases in radon exposure. However, it is also clear that in a small percentage of homes affected, radon levels are already unacceptably high. We have therefore recommended that the RCS program include a screening procedure capable of identifying areas with unusually high radon levels so that infiltration-reducing measures would not be recommended in such cases -- at least not without detailed consideration of the impact of retrofits on radon levels and the suggestion of adequate control measures. (For geographical areas where radon levels are particularly high, we would anticipate that remedial measures would be implemented regardless of any RCS program measures affecting air-exchange rates.)

In order to assess the impact of energy-conservation programs on indoor air quality with respect to radon health risks, we will continue to work closely with the Building Energy Conservation Program on three general goals: 1) to assess, on the basis of available information, the health risks from indoor radon levels in existing, new, and retrofitted housing; 2) to indicate how to improve the available information so that it serves as a more adequate

basis for risk assessment, and 3) to evaluate options for controlling the increased risk that may be associated with energy conservation measures and programs.

#### REFERENCES

1. Sources and Effects of Ionizing Radiation, United Nations Scientific Committee on the

Effects of Atomic Radiation, United Nations, New York, 1977.

2. R.J. Budnitz, et.al., Human Disease From Radon Exposures: The Impact of Energy Conservation and Residential Buildings, Lawrence Berkeley Laboratory Report, LBL-7809 (Rev., July 1979).

### FIELD MONITORING OF INDOOR AIR QUALITY

*J. V. Berk, T. A. Boyan, S. R. Brown, I. Ko, J. F. Koonce, B. W. Loo, J. H. Pepper, A. W. Robb, P. C. Strong, I. Turiel, and R. A. Young*

In order to establish criteria for setting energy-efficient ventilation standards, the Ventilation Program staff is conducting a comprehensive assessment of indoor air quality in different types of buildings under a variety of ventilation conditions. Table 1 lists several indoor contaminants that have been identified as potential health hazards, and their sources. The Ventilation Program at LBL is measuring a number of these pollutants and developing techniques for sampling and measuring others.

As part of our ongoing field monitoring of indoor air quality, we have been measuring pollutant levels in prototype energy-efficient residential homes. We are also studying educational facilities and hospitals before and after energy-conserving retrofits are implemented.

Table 1. Indoor air pollutants in residential buildings.

SOURCES	POLLUTANT TYPES
<b>OUTDOOR</b>	
Ambient Air	SO <sub>2</sub> , NO, NO <sub>2</sub> , O <sub>3</sub> , Hydrocarbons, CO, Particulates
Motor Vehicles	CO, Pb
<b>INDOOR</b>	
<b>Building Construction Materials</b>	
Concrete, stone	Radon
Particleboard, Plywood	Formaldehyde
Insulation	Formaldehyde, Fiberglass
Fire Retardant	Asbestos
Adhesives	Organics
Paint	Mercury, Organics
<b>Building Contents</b>	
Heating and cooking combustion appliances	CO, NO, NO <sub>2</sub> , Formaldehyde, Particulates
Furnishings	Organics
Water service; natural gas	Radon
<b>Human Occupants</b>	
Metabolic activity	H <sub>2</sub> O, CO <sub>2</sub> , NH <sub>3</sub> , Odors
<b>Human Activities</b>	
Tobacco smoke	CO, NO <sub>2</sub> , Organics, Particulates, Odors
Aerosol spray devices	Fluorocarbons, Vinyl Chloride
Cleaning and cooking products	Organics, NH <sub>3</sub> , Odors
Hobbies and crafts	Organics

Some of the specific parameters being measured by the Ventilation Program staff and LBL subcontractors are:

- temperatures and relative humidity
- odors
- toxic chemicals (gases and particulates)
- microbial burden

#### EEB Mobile Laboratory

The Energy Efficient Buildings (EEB) Mobile laboratory<sup>1</sup> was completed in 1978 to facilitate field studies of indoor air quality and energy utilization in buildings. The EEB Mobile Laboratory contains sampling, calibrating and monitoring systems that allow us to measure various contaminants of indoor air (see Table 2).

Air-exchange rates have been measured using a tracer gas system<sup>2</sup> developed at LBL in which nitrous oxide is injected and monitored continuously under controlled conditions at the sampling sites. A similar system using ethane as a tracer gas has recently been installed. Air exchange rates and the other continuously monitored parameters are recorded on a microprocessor-controlled floppy disk. The recorded information is transmitted back to LBL by telephone or by sending the floppy disks back to LBL where they may be read into our computer system.

The EEB Mobile Laboratory, shown in Exhibit 1, is positioned outside the building to be studied. Air from three different locations within the structure and from the outside is drawn through teflon sampling lines into the trailer for analysis. By sequentially sampling these lines, the indoor and outdoor air quality are monitored.

For pollutants whose concentrations are too low for direct measurement, such as particulates, formaldehyde, and radon, grab sampling techniques are used. The particulate matter in

Table 2. Instrumentation for Lawrence Berkeley Laboratory ventilation requirements system.

Parameter	Principle of Operation	Manufacturer/Model
Field		
Continuous Monitoring Instruments:		
Infiltration		
N <sub>2</sub> O or C <sub>2</sub> H <sub>6</sub> (Tracer gas)	IR	LBL
Indoor Temperature and Moisture		
Dry-Bulb Temperature	Thermistor	Yellow Springs 701
Relative Humidity	Lithium Chloride Hygrometer	Yellow Springs 91 HC
Outdoor Meteorology		
Dry-Bulb Temperature	Thermistor	Meteorology Research 915-2
Relative Humidity	Lithium Chloride Hygrometer	MRI 915-2
Wind Speed	Generator	MRI 1074-2
Wind Direction	Potentiometer	MRI 1074-2
Solar Radiation	Spectral Pyranometer	Eppley PSP
Metric Rain Gauge	Tipping Bucket	MRI 382
Gases		
SO <sub>2</sub>	UV Fluorescence	Thermo Electron 43
NO, NO <sub>x</sub>	Chemiluminescence	Thermo Electron 14D
O <sub>3</sub>	UV Absorption	Dasibi 1003-AH
CO	NDIR	Mine Safety Appliances-Lira 202S
CO <sub>2</sub>	NDIR	M.S.A. Lira 303
Radon	Alpha Dosimetry	LBL
Particulate Matter		
Size Distribution	Optical Scattering	Royco Particle Counter 225
Radon Progeny	Under Development	LBL
Sample Collectors		
Gases		
Formaldehyde	Chemical Reaction/Absorption (Gas Bubblers)	LBL
Total Aldehydes		
Selected Organic Compounds	Adsorption (Tenax GC Adsorption Tubes) for GC Analysis	LBL
Particulate Matter		
Aerosols (Respirable/Non-respirable)	Virtual Impaction/Filtration	LBL
Bacterial Content	Inertial Impaction	Modified Anderson Sampler
Data Acquisition System		
Microprocessor		Intel System 80/20-4
Multiplexer A/D Converter		Burr Brown Micromux Receiver MM6016 AA Remote MM6401
Floppy Disk Drive		ICOM FD3712-56/20-19
Modem		Vadic VA-317S

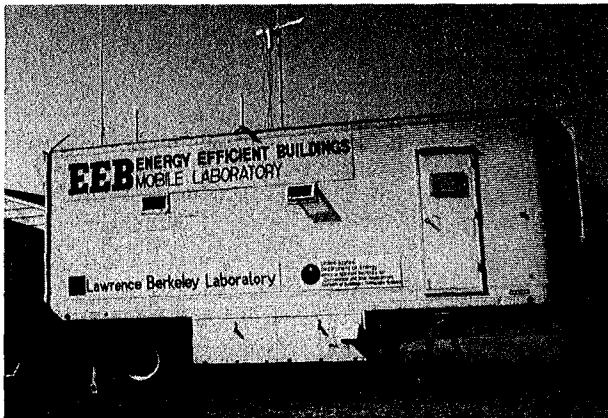


Exhibit 1. The EEB Mobile Laboratory.

(CBB, 790-16251)

the sampled air is measured by automatic dichotomous air samplers developed at LBL to separate aerosols into respirable and non-respirable fractions (below and above 2.5 micron size, respectively). This device uses a flow-controlled virtual impaction system which deposits the particulate matter on teflon filters. The particulates collected on the filters are analyzed by others at LBL using beta-ray attenuation to measure mass concentration, and X-ray fluorescence to determine chemical composition. Radon, formaldehyde, total aldehydes, and bacteria must be collected by means of gas bubblers and other sampling techniques and also require subsequent laboratory analysis.

## ACCOMPLISHMENTS DURING 1979

During 1979, the mobile trailer was used to monitor indoor air quality at four field sites: the Fairmoor Elementary School in Columbus, Ohio (selected by the American Association of School Administrators as a target school for energy-conserving retrofits), "ERHM," (an energy research house in Carroll County, Maryland), MED-II (a production model minimum-energy dwelling in Mission Viejo, California) and Oakland Gardens Elementary School in Bayside, New York. Additional field monitoring, performed by subcontractors, is described later in this section.

Fairmoor School

The ventilation system at the Fairmoor School consists of a single-unit ventilator in the exterior wall of each classroom. Two gas-fired boilers in the school deliver hot water or steam to the unit ventilator in each classroom. The unit ventilator has a thermostatically controlled damper that determines the relative quantities of outdoor and recirculated air to be supplied to the room. Excess room air is vented into the corridor and discharged. For our purposes, manual override switches and a pneumatic control system were installed to control the ventilation rates in two classrooms and one large, multi-purpose room. With outside air supply rates adjusted down from approximately 6.5 cfm per occupant to 1.5 cfm per occupant, indoor air quality was monitored in these classrooms. For comparative purposes, outdoor air was simultaneously monitored.

Ventilation Rates and Chemical Indoor Air Quality

Carbon dioxide was the only pollutant found to exhibit significantly high concentrations inside the school, and the primary sources were the occupants themselves. Fig. 1 shows the frequency distribution of  $\text{CO}_2$  concentrations at various ventilation rates in one of the classrooms. Data points sorted into bins along the horizontal axis represent ten-minute samples taken every forty minutes during regular school hours. Although  $\text{CO}_2$  concentrations did increase inside the classrooms when ventilation rates were reduced, at no time did they exceed 4000 ppm, and only occasionally did they exceed 3000 ppm. (Occupational standards for  $\text{CO}_2$  have been set at 5000 ppm and 10,000 ppm<sup>4,5,6</sup> and refer to time-weighted average concentrations for up to 10-hour workshifts in a 40-hour work week; studies indicate that workers may be exposed to these concentrations day after day without adverse health effects.<sup>4</sup>)

Ventilation Rate and Sensory Perception of Indoor Air Quality (The Research Corporation of New England)

The Fairmoor School was the first site visited by The Research Corporation of New England (TRC) as part of its field monitoring program to determine ventilation requirements for

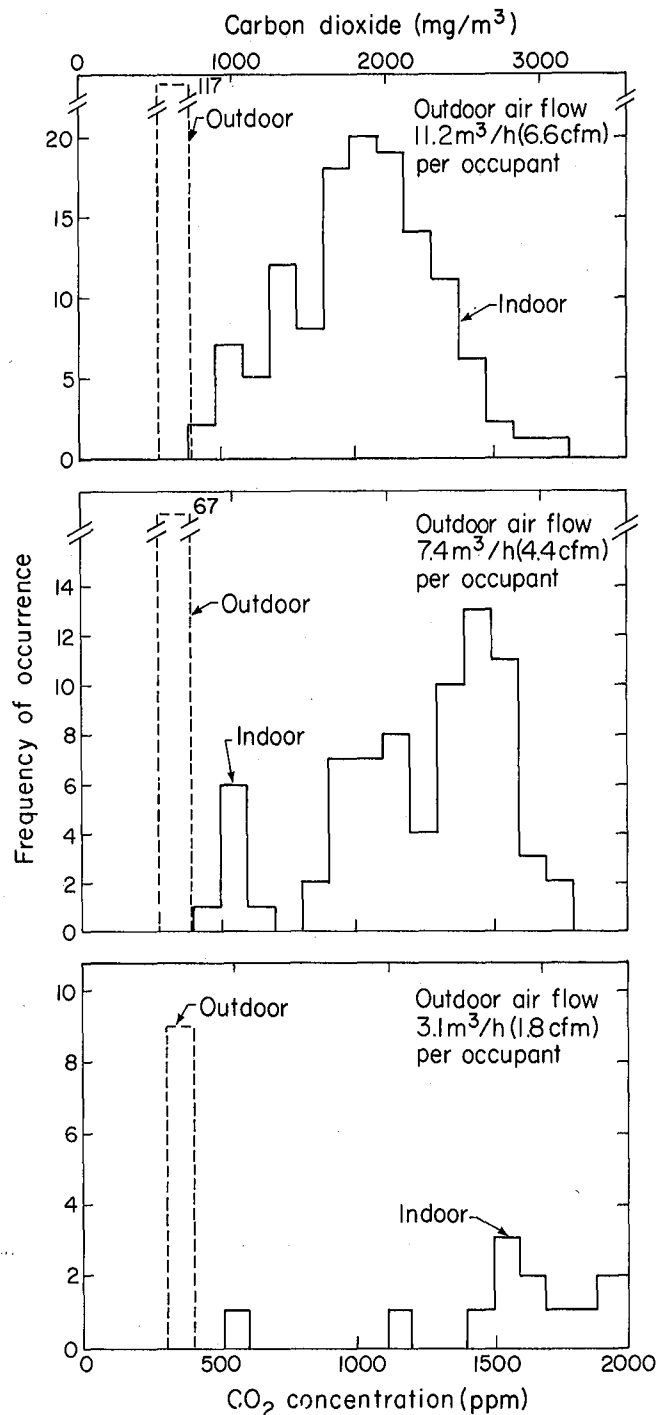


Fig. 1. Frequency distributions of  $\text{CO}_2$  concentrations at Fairmoor Elementary School measured at 3 ventilation rates. The graphs represent data for school days only between 8:00 a.m. and 3:00 p.m. (XBL 7910-4429)

odor control in buildings. Under contract to LBL, TRC and its subcontractors performed two types of studies. In three buildings (one school, one hospital and one office building), the sensory perception of odors, odor acceptability and the chemical composition of indoor air was studied for a two-week period at both

existing and reduced ventilation rates. For twelve other buildings (six schools and six hospitals), the sensory perception of odors and the chemical composition of indoor air were surveyed (for one day) at existing ventilation rates only.

All odor perception measurements were carried out in a mobile laboratory brought to the building site. Odor panelists were recruited from people in the area who are not regular occupants of the building. Air samples within the building are collected in 100-liter Tedlar bags and brought to the mobile trailer.

At all sites, the sensory perception of odors was measured in two ways. The first method employs a forced-choice triangle olfactometer (Exhibit 2) to determine the number of dilutions necessary to bring an odorous air sample to a level where 50% of the members of an odor panel no longer detect it ( $ED_{50}$ ).<sup>7</sup> The olfactometer is equipped with five stations, four of which present dilution ratios of 81, 27, 9 and 3 and the fifth station, the undiluted odor. One glass sniffing port supplies the given dilution level progressing from weakest to strongest (undiluted) concentrations while the other two sniffing ports supply filtered outside air. For each of the five levels of concentration, the odor panelist indicates which of the three ports he or she believes delivers odorous air. Following this process, odor judges are presented with the undiluted odor and using a device called a butanol olfactometer (Exhibit 5) are asked to compare it with progressively increasing concentrations of butanol until a match is made between the intensity of butanol (in ppm) and the intensity of the undiluted sample.<sup>8</sup>

In addition to the procedures described above, both the odor panelists and building occupants filled out a questionnaire (Exhibit 4) twice daily on various "elements" of the room

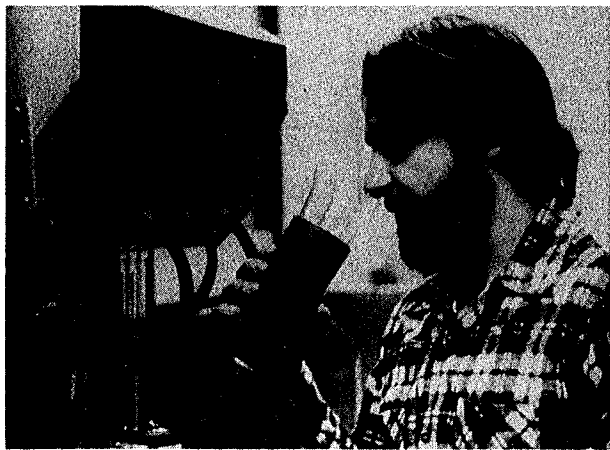


Exhibit 2. Subject using forced-choice triangle olfactometer. One of the three nozzles emits a diluted stream of air taken from the ventilation chamber. The other two nozzles emit pure air. The subject seeks to decide, by smell, which nozzle emits air from the chamber.

(XBB 802-2681)

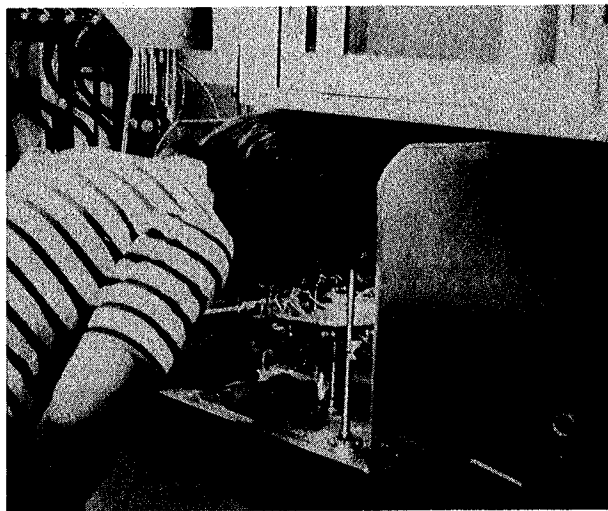


Exhibit 3. Subject using the butanol binary dilution olfactometer to find a level of butanol that matches the perceived intensity of the "occupancy odor" of an occupied ventilation test chamber. (XBB 802-2680)

environment, including odor level, all of which are rated on a nine-point scale. Each aspect of the environment is also rated for "acceptability".

Another aspect of the TRC study at these sites involved collecting air samples on porous polymers which were packed within tubes to facilitate later laboratory analysis for odorant composition. The chemical analyses were carried out by gas chromatographic and mass spectroscopic techniques.

Table 3 summarizes average odor dilution and odor intensity results for the three test rooms at the Fairmoor school at normal and reduced ventilation rates. The odor dilution ratio ( $ED_{50}$ ) under normal ventilation conditions was close to the  $ED_{50}$  for outside air. At reduced ventilation rates, the  $ED_{50}$  doubled in the two classrooms and increased slightly in the gymnasium. The odor intensity, as measured by the butanol olfactometer, exhibited no statistically significant change when the ventilation rate was reduced. The occupants of these rooms found the odor level acceptable at all times; however, the acceptability as perceived by visitors to these rooms (odor panel) decreased in Room 12 under reduced ventilation rates and to a lesser degree in Room 20, where the ventilation rate reduction was somewhat less than in Room 12. The ASHRAE standard 62-73 for odor acceptability of outdoor air calls for agreement of at least 60% of a panel of no fewer than 10 untrained observers that the air is free of objectionable odors. If the present standard were applied to indoor air, the odor levels in the two classrooms where ventilation rates were reduced would have been classified as unacceptable. The outside air ventilation rate under sealed conditions, however, was below the minimum (5 cfm/person) established in ASHRAE Standard 62-73. Criteria for indoor air quality with

Day Number \_\_\_\_\_ Date \_\_\_\_\_ Time \_\_\_\_\_ Room Number \_\_\_\_\_

EVALUATION SHEET

Rating of Individual Elements of the Room Environment		Acceptable	Unacceptable
Cold _____	Hot _____	<input type="checkbox"/>	<input type="checkbox"/>
Humid _____	Dry _____	<input type="checkbox"/>	<input type="checkbox"/>
Drafty _____	Stuffy _____	<input type="checkbox"/>	<input type="checkbox"/>
Stale _____	Fresh _____	<input type="checkbox"/>	<input type="checkbox"/>
No odor _____	Strong odor _____	<input type="checkbox"/>	<input type="checkbox"/>
Loud noise _____	No noise _____	<input type="checkbox"/>	<input type="checkbox"/>
Overall Rating of the Room Environment			
Acceptable _____	Unacceptable _____		

1. Do you have a cold today?  
 Yes  No

2a. If you are a smoker, about how many hours ago today did you have your last smoke?  
 \_\_\_\_\_ hours ago

2b. If you are not a smoker or if you did not smoke today, check this box

Exhibit 4. Questionnaire on indoor air quality.

Table 3. Summary of odor and ventilation data from Fairmoor Elementary School.

	Odor dilution ratio (ED <sub>50</sub> )		Odor intensity Butanol scale (ppm)		Average acceptability (%)	
	Normal vent.	Reduced vent.	Normal vent.	Reduced vent.	Normal vent.	Reduced vent.
<u>Room 12</u>						
a.m.	4	13	57	42		
p.m.	8	9	30	43		
Average	6	11	43	43	76.5	55
<u>Room 20</u>						
a.m.	6	14	50	46		
p.m.	6	10	43	55		
Average	6	12	47	50	67.6	56.3
<u>Multipurpose Room</u>						
a.m.	9	9	44	32		
p.m.	6	9	40	35		
Average	7	9	42	33	94	92

respect to odor levels are now being developed by ASHRAE.

The gas chromatographic mass spectroscopic (GS/MS) results indicate that the odorants collected in these classrooms derive from cleaning compounds, polishes and, perhaps, automotive exhaust, but not body odor; however, odorant concentrations were too low to allow positive identification by gas chromatographic odorogram analysis.

In summary, odorant concentrations are low at both normal and reduced ventilation rates; the occupants of the building find the odor level acceptable under both ventilation conditions; and visitors to the classroom sometimes find the odor level unacceptable at reduced ventilation rates (if acceptability is based on odor criteria for outdoor air.)

#### Ventilation Rates and Microbial Burden

The Naval Biosciences Laboratory was subcontracted by LBL to provide scientific and technical support to the ventilation group on sampling, assay, and data analysis of airborne bacterial content in educational facilities and hospitals where related field monitoring studies are being conducted. NBL was to determine whether energy-conserving changes in ventilation practices would lead to unacceptable levels of airborne microbes; to this end, data was to be analyzed both before and after retrofit.

During FY 1979, NBL performed measurements on airborne microbes at three sites: Fairmoor School, Long Beach Naval Hospital, and a San Francisco office building. (Data from the San Francisco office building are yet to be analyzed.) In addition, they conducted experimental aerosol studies to test filter effectiveness for microbial removal.

At Fairmoor School, instruments that measure airborne microbes<sup>9</sup> in six size ranges were

placed in two classrooms and in a combination auditorium-gymnasium. Samples of airborne microbes were taken by NBL at 8:00 and 10:00 a.m. and at 1:00 and 3:00 p.m. The average number of colony-forming particles/cubic meter of air for all samples are shown in Table 4. A computerized search of the raw data was made to determine whether any parameter(s) showed a significant difference in any room, and it was found that in one instance only -- room 12, 1:00 p.m. sample, respirable colony-forming particles (CFP) -- was there a significant increase caused by reduced ventilation. When each room was examined, individually, for a similar effect; no statistical difference was found among rooms; hence, the effect was not a general one and may have been incidental to ventilation conditions within that particular room. Deleting the data collected from the auditorium did not reveal any new correlations of statistical significance.

Table 5 shows how the mean values of the number of CFP vary with sampling time and follow a repetitive daily pattern corresponding to classroom activity periods.

Table 6 lists mean values of CFP/m<sup>3</sup> found in a number of locations over a two-year period and is representative of a general level of bio-burden at these sites. A comparison between Carondelet High School and Fairmoor under existing conditions indicates that the number of CFP/m<sup>3</sup> at Fairmoor was double that at Carondelet. In looking at classrooms only, we find twice as many CFP/m<sup>3</sup> at Fairmoor (269) than at Carondelet (134) under existing conditions. At Fairmoor, the number of CFP/m<sup>3</sup> increased from 269 to 360 when ventilation was decreased from existing to sealed conditions. A microbial burden in this range is not unusual, as supported by data taken from other buildings.

The number of airborne CFP in the auditorium-gymnasium varied more than in any other room tested at any site. This variation,

Table 4. Mean numbers of CFP/m<sup>3</sup> in two classrooms at Fairmoor Elementary School, excluding 8:00 a.m. sample.

Mode of ventilation	Total particles		Respirable particles		Non-Respirable particles	
	Mean	Stand. dev.*	Mean	Stand. dev.	Mean	Stand. dev.
Normal	269	166	104	68	165	110
Damper closed	253	188	116	74	141	126
Reduced	360	206	182	118	177	99

Note: Because of the large standard deviations, there are no significant differences between any of these means. However, in each case, a consistent increase is evident when the operating mode was changed from normal to reduced.

\*standard deviation.

Table 5. Mean values of CFP/m<sup>3</sup> in classrooms at Fairmoor Elementary School, calculated as a function of time

Time	Normal	Damper Closed	Reduced
8:00 a.m.	13	32	19
10:00 a.m.	243	148	305
1:00 p.m.	256*	323	403*
3:00 p.m.	291	280	370

Note the difference between these two starred values. Since the vents were sealed, we could not have been observing an infiltration of air containing numerous CFP; the explanation could be that rather clean, infiltrating air was acting as a diluent under the normal condition in the rooms.

Table 6. Mean values (no. per cubic meter) of numbers of airborne colony-forming particles (CFP) at various sites.

Fairmoor Elementary School			
Ventilation:	Automatic	Dampers Closed	Sealed
	269	283	360
(Auditorium - Gymnasium had Peak Value of 1200)			
Carondelet High School (Class in session)			
Ventilation Rate (cfm/occupant)		Room 1	Room 2
13.5		160	107
2.5		115	75
Peralta Hospital (Eye Operatory)			40
Sports Arena			200
NBL Conference Room			180
NBL Men's Rest Room			132
Veterans' Administration Hospital (Martinez)			
Cast Room			333
Research House, Walnut Creek			
Sealed and Vacant			17
Blower On and Vacant			550
Long Beach Naval Hospital			
Cast Room			523
Patient Room			900
Proctology			62
Obstetrics			125
Pediatrics			183

from as low as  $12/m^3$  to as high as  $1200/m^3$ , is not unexpected since occupant use of this area is highly variable. Although this factor prevented any analysis of the data in that room with respect to ventilation changes, it does indicate that higher levels of airborne CFP can be tolerated by humans without evident harm.

The following observations were made by NBL from the data amassed: It seems that humans live in air with "bioburdens" of from  $20\text{ CFP}/m^3$  to over 700 without apparent ill effects. There is no evidence that any retrofit situation examined caused an increase in airborne microflora above that present in other usual and common situations. Hence, the probability of infection from aerosols of human origin under normal and usual conditions (excluding the presence of "carriers" or "shedders", which is not really a part of the ventilation evaluation problem) seems vanishingly low. If that very small probability were increased ten-fold as a result of a ten-fold increase in bioburden then a very low probability of infection would still remain.

Data collection from the Oakland Gardens Elementary School is still in progress; data collected from the Fairmoor School and Carondelet High School<sup>10</sup> indicate that ventilation rates of 2.5 cfm/occupant are compatible with acceptable indoor air quality.

#### Energy Efficient Houses

The Maryland house was occupied by our field personnel during the month that this house was studied. The house had electric appliances and incorporated numerous construction features designed to reduce air leakage and energy consumption. Fig. 2 summarizes the air exchange rates, measured on a continuous basis. The average air exchange rate was approximately 0.15 ach, with shifts in weather conditions and routine door openings causing rates to vary from less than .05 to almost 0.3 ach. Levels of for-

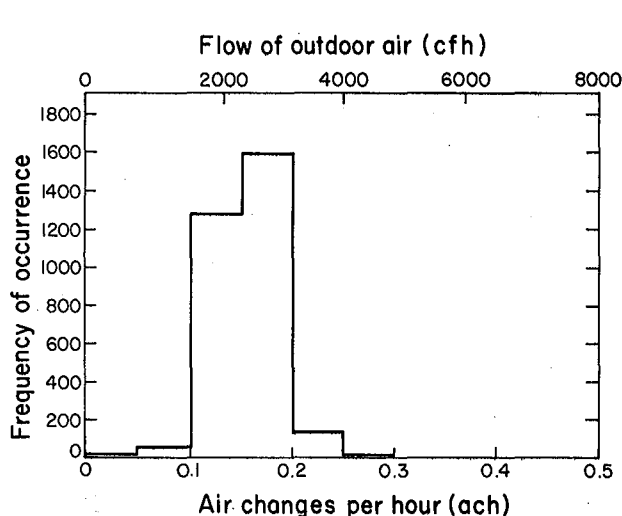


Fig. 2. Frequency distribution of air exchange rates at ERHM. (XBL 7910-4298)

maldehyde and radon in this house were frequently found to exceed existing health standards.

The MED-II minimum energy dwelling in southern California was occupied by a family at the time of monitoring by the EEB Mobile Laboratory. This house was equipped with gas-fired kitchen appliances, which are known to be sources of indoor pollution.<sup>11</sup> Air-exchange rates were found to average approximately 0.4 ach. Pollutants measured in this house and in other buildings tend to fall into three categories: those whose primary sources are indoors (e.g.,  $CO_2$  and aldehydes), those whose primary sources are outdoors (e.g.,  $O_3$  and  $SO_2$ ), and those which have both indoor and outdoor sources (e.g.,  $NO$ ,  $NO_2$ ,  $CO$  and particulates). Those belonging to the first group are generally present in higher concentration indoors than outdoors, and tend to show even higher levels as air-exchange rates are lowered. On the other hand, as buildings are tightened, occupants are shielded from pollutants in the second group, particularly from reactive substances such as  $O_3$  and  $SO_2$ . Substances in the third group may exhibit higher indoor concentrations as air exchange rates are reduced, depending upon the relative indoor and outdoor source strengths.

Fig. 3 shows the frequency distribution of carbon dioxide concentrations at the MED-II house. Although indoor concentrations obviously exceed those outdoors, they do not approach the occupational standard of 5000 ppm. Fig. 4 shows indoor and outdoor ozone concentrations for the same period. This pollutant, a major component of photochemical smog in the Los Angeles area, is highly reactive and, as evidenced from the figure, indoor levels are significantly lower than outdoor levels. Fig. 5 shows the indoor and outdoor concentrations of nitrogen dioxide. Nitrogen oxides are produced from combustion processes, whether outdoors (power plants, automobile exhaust) or indoors (natural gas combustion). As can be seen from the figure, indoor

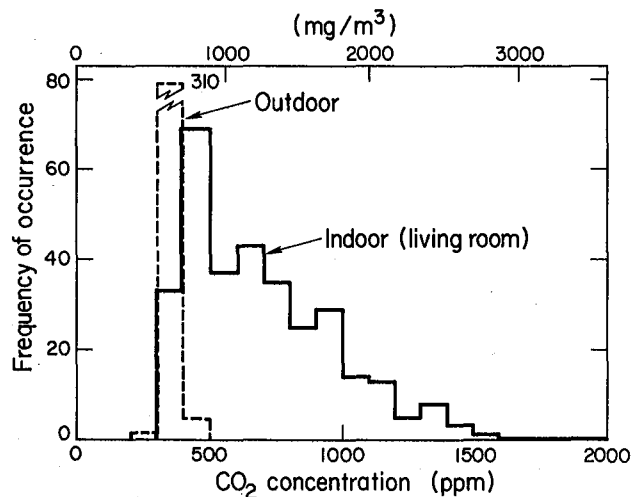


Fig. 3. Frequency distribution of  $CO_2$  concentrations at MED-II house. (XBL 7910-4356)

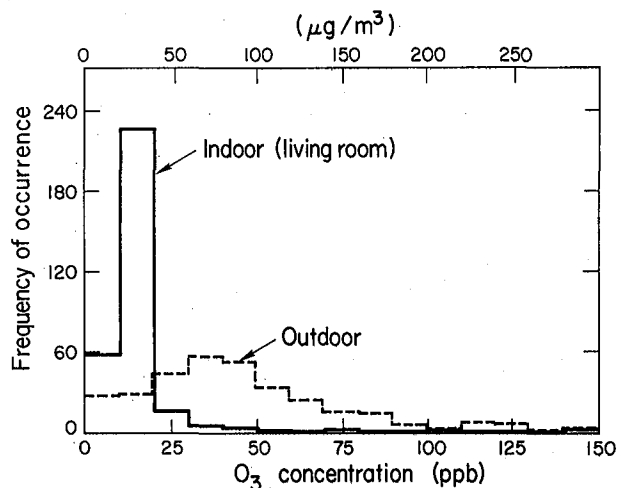


Fig. 4. Frequency distribution of  $O_3$  concentrations at MED-II house. The graph represents data collected between 8:00 a.m. and midnight during occupancy. Indoor concentrations did not exceed 110 ppb. (XBL 7910-4359)

$NO_2$  levels are sometimes higher than those outdoors and these increases have been correlated with cooking activities. The proposed EPA standard for ambient air is  $470 \mu\text{g}/\text{m}^3$ , which was occasionally exceeded in this house. Analysis of the particulate data from the MED-II house indicates that although the outdoor particulate concentrations usually exceed those indoors, again, cooking activities are capable of reversing this situation.

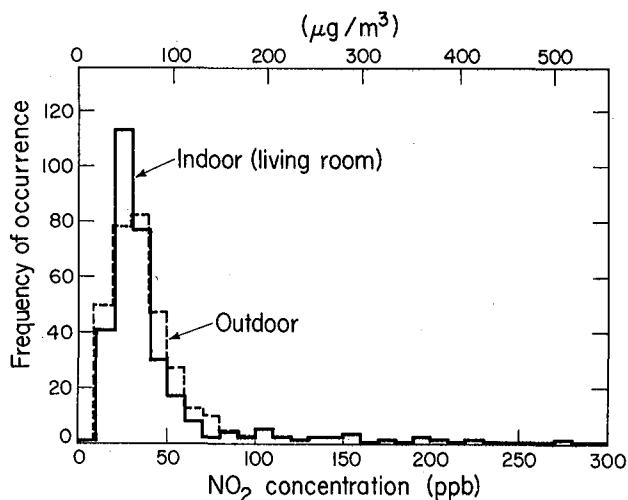


Fig. 5. Frequency distribution of  $NO_2$  concentrations at MED-II house. The graph represents data collected between 8:00 a.m. and midnight during occupancy. (XBL 7910-4361)

Preliminary data collected on energy-efficient residences indicates that a minimum air-change rate of approximately 0.5 ach may be necessary to prevent the indoor concentrations of some pollutants from exceeding existing or recommended U.S. standards for ambient air and standards promulgated by other countries. Air-to-air heat exchangers are effective in maintaining good indoor air quality without sacrificing energy conservation goals. For confined indoor sources of pollutants, such as gas stoves, spot ventilation may be an appropriate solution. These alternatives are documented in more detail elsewhere in this report.

#### Additional Field Monitoring (Subcontractors)

As noted previously, in addition to Fairmoor School, TRC has performed measurements of odor perception, odor acceptability and odorant composition under variable ventilation conditions at the University of Connecticut Medical Center and at a San Francisco office building. The San Francisco office building data was taken during the last two weeks of September and has not yet been fully analyzed.

#### University of Connecticut Medical Center (TRC)

Odor and ventilation rates were measured at the University of Connecticut Medical Center (Hartford, Connecticut) during the month of May. Results of these measurements are presented in Table 7 for three areas of the hospital. As can be seen, only minor elevations in  $ED_{50}$  and odor intensity values (butanol scale) occurred when ventilation rates were reduced. In admissions and in the nurses' area, ventilation rates were reduced by a factor of more than two (to approximately 2.75 ach) which is still higher than the minimum recommendation set forth by Hill Burton or ASHRAE standards. Thus, it is not surprising that we see no significant increase in odor levels at "reduced" ventilation rates. Measurements of acceptability indicated that employees always found the odor level less acceptable than the visiting odor panelists. This finding was unexpected and contrary to usual assumptions. When ventilation was reduced, however, neither group noted a change in odor acceptability.

As with the Fairmoor School classrooms, odorant concentrations were too low to allow positive identification by gas chromatographic odorogram analysis. In general, the nurses' and patients' areas had more organic material in the air than the admissions area, with the nurses' area showing the most. In all areas, reducing the ventilation caused the amount of organic material to approximately double, a finding which correlates well with the fact that, in most cases, fresh air was decreased 50% in the reduced mode. Major compounds identified by GC/MS for the nurses' area were: ethanol, butene, methyl propane, acetone, isopropanol, 2-methyl-1, 3-butadiene, benzene, ethyl benzene, 1, 1, 1-trichloroethane, toluene and xylene.

Table 7. Summary of odor and ventilation data, University of Connecticut Hospital.

	Odor Dilution Ratio (ED <sub>50</sub> )		Odor Intensity Butanol Scale (ppm)		Ventilation Rate (cfm) per person (ach)	
	Normal	Reduced	Normal	Reduced	Normal	Reduced
<b>Admissions</b>						
AM	11.1	9.2	183	134		
PM	8.0	14.5	173	176		
Mean	9.5	11.8	177	155	164 (6ach)	75 (2.8ach)
<b>Nurses' Area</b>						
AM	6.4	5.2	148	141		
PM	8.1	6.3	156	174		
Mean	7.3	5.9	152	158	65 (6.5ach)	27 (2.7ach)
<b>Patient Room</b>						
AM	8.9	5.9	173	116		
PM	7.6	7.8	154	184		
Mean	8.2	6.9	162	150	101 (5.2ach)	79 (4.1ach)

#### East Coast Schools and Hospitals: One-day surveys

Thus far, one-day survey data on odor and ventilation rates have been analyzed for four schools and two hospitals on the East Coast. Table 8 summarizes the results of these surveys. The four schools sampled were found to be free of odor problems. Both the odor dilution ratios and odor intensity levels were low with one exception, Room 15 in the W. H. Grammar School, where the odor intensity level was much higher than would be expected from the odor dilution ratio. In general, the schools were found to be over-ventilated with ventilation rates in classrooms ranging from a high of 41.6 cfm per person to a low of 4.6 cfm per person, for an average of 23.5 cfm per person. This compares to the ASHRAE standard for classroom ventilation rates of 10 cfm per person minimum and 10 - 15 cfm/person recommended.

The two hospitals sampled were also found to be over-ventilated except for the ward room in the Hartford Hospital. Again, there was no existing odor problem in either of these hospitals; ED<sub>50</sub> values and odor intensity were low in all cases except for the outpatient lounge in Hartford Hospital.

#### Experimental Aerosol Studies (NBL)

The purpose of these experiments was to study the effects of particulate filters (0 to 80% efficiency) and varying fresh-to-recirculating air ratios on the removal rate of microbes in hospital spaces.

A 2000 ft<sup>3</sup> experimental chamber was built. The chamber was supplied with facilities for air recirculation, cleaning, and treatment (conditioning) as if it were to be used as a habitat, except that the intake of fresh air (%), recirculation rate, and filter efficiency could be easily varied. Samplers for airborne bacteria and for inert particles, and a spinning-disk aerosol generator, were placed in the room.

Using controlled conditions, a one-minute "burst" of aerosol containing a "tracer" bacterial species was dispersed into the chamber and then sampled at intervals for a period of sixty minutes. The number median diameter (NMD) of the aerosol was 5.5  $\mu$ m.

The following variables that might influence the removal rate of the aerosol were examined: (a) filters of "zero", 20, 60, and 80% efficiency; (b) air exchange ratio of 6 and 12 air changes per hour (67% recirculated air), and (c) 33% or no fresh air intake (100% recirculation).

By comparing observed clearance rates during the first 1/2 hour to the removal rates that prevail when the space is ventilated with 100% fresh air, NBL concluded that it should be possible to reduce fresh-air intake in commercial buildings and, by using combinations of recirculating air, filters, air exchange rates, and recirculation percentages, provide air of essentially the same particulate cleanliness as found in 100% clean fresh air. These studies are described in detail in NBL's April 1979 report to LBL.<sup>9</sup>

Table 8. Odor and ventilation data, six East Coast schools and hospitals.

SITE	Odor Dilution Ratio (ED <sub>50</sub> )	Odor Intensity Butanol Scale/(ppm)	Room Volume (Ft <sup>3</sup> )	Actual Occupancy	Air Changes Per Hour	Ventilation Rate cfm/Occupant
<u>U.C. Dental School (3/20)</u>						
Room L003	2.0	2.8/60	7455	22	5.5	31.2
Room BM031	5.2	2.4/47	9086	55	15.1	41.6
Blue Auditorium	5.2	3.3/86	53360	110	3.0	25.1
<u>S.D. Junior HS (3/21)</u>						
Room 102	8.1	2.3/52	5832	16	2.8	17
Room 109	7.5	3.0/77	5832	22	5.9	26
Gym	8.5	2.8/70	119784	20	1.3	128.
<u>E.W. Grammar School (3/22)</u>						
Room 3	4.4	3.0/83	8125	22	2.6	16.
Room 10	3.6	1.5/32	9315	24	0.7	4.6
Art Room	7.9	2.9	14702	20	1.2	14.3
<u>U.C. Medical Clinic (3/23)</u>						
Patient Room - 2116	10.8	3.0/77	2330	2	6.7	131.0
Nurse's Area - 2nd Fl.	5.9	3.4/107	4770	8	9.4	93.7
Admissions	9.0	3.9/139	16120	10	7.2	193.0
<u>W.H. Grammar School (6/7)</u>						
Room 15	13.0	4.8/264	10008	21	2.5	10.9
Room 16	8.3	3.2/99	10100	20	3.7	31.1
Art Room	15.6	3.2/99	16165	16	2.0	33.7
<u>Hartford Hospital (7/23)</u>						
Outpatient Lounge	46.9	5.3/460	4414	15	6.3	31.0
Ward 522	15.6	3.6/146	2667	6	0.2	1.5
Cafeteria	6.8	3.9/173	95737	200	5.9	47.1
<u>Outside Air Samples</u>						
3/20	30.1*	2.8/60				
3/21	3.4	1.9/40				
3/22	5.2	2.4/52				
3/23	7.9	2.6/58				

\* Sample probably contaminated by Chemistry Lab exhaust.

To reduce energy use in conditioning air without creating a severe increase in the bioburden, NBL suggested the following remedies:

1. Use medium to low efficiency filters.
2. Reduce total volumetric flow rates.
3. Use particulate filters with efficiency approximating "0" to 80% efficiency (ASHRAE Test) in air-recirculating systems.

#### PLANNED ACTIVITIES FOR 1980

The following sites will be included in the field monitoring studies of indoor air quality during FY 1980:

- Oakland Gardens Elementary School, Bayside, New York
- Fridley Jr. High School, Minneapolis, Minnesota
- Two energy efficient research houses, Northfield, Minnesota
- Underground research house, Minneapolis, Minnesota.

TRC will complete its analysis of field data from the San Francisco office building and the six other odor-monitoring sites in FY 1980. One more intensive field-monitoring study will be conducted at Oakland Gardens Elementary School in New York City. When all the data have been analyzed, TRC in consultation with John Pierce Foundation (see Subcontracts section) will recommend ventilation rates for odor control in schools and hospitals.

#### REFERENCES

1. J.V. Berk, C.D. Hollowell, Chin-I Lin and James Pepper, Design of a Mobile Laboratory for Ventilation Studies and Indoor Air Pollution Monitoring, Lawrence Berkeley Laboratory Report, LBL-7817 (April 1978).
2. P.E. Condon, D.T. Grimsrud, M.H. Sherman and R.C. Kammerud, An Automated Controlled Flow Air Infiltration Measurement System, Lawrence Berkeley Laboratory Report, LBL-6849 (March 1978).
3. B.W. Loo, J.M. Jaklevic and F.S. Goulding, Dichotomous Viral Impactors for Large Scale Monitoring of Airborne Particulate Matter,

- Presented at the Symposium on Fine Particles (May 1975). In Fine Particles, Ed., B.Y.U. Liu (Academic Press, New York, 1976).
4. National Institute for Occupational Safety and Health, Criteria for a Recommended Standard...Occupational Exposure to Carbon Dioxides; HEW Pub. No. 76-94 (August 1976).
  5. American Conference of Governmental Industrial Hygienists, Threshold Limit Values for Chemical Substances in Workroom Air Adopted by ACGIH for 1978.
  6. Occupational Safety and Health Administration, 40 FR 23072 (May 28, 1975).
  7. A. Dravnieks and W. H. Prokop, "Source Emission Odor Measurement by a Dynamic Forced-Choice Triangle Olfactometer," Journal of the Air Pollution Control Association 25, 28 (1975)
  8. L. E. Marks, Sensory Processes: The New Psychophysics, Academic Press, New York, 1974
  9. R.L. Dimmick and H. Wolochow, Studies of Effects of Energy Conservation Measures on Air Hygiene in Public Buildings, Lawrence Berkeley Laboratory Report, LBID-045 (April 1979).
  10. J.V. Berk, C.D. Hollowell, C. Lin, I. Turiel, The Effects of Energy Efficient Ventilation Rates on Indoor Air Quality at a California High School, Lawrence Berkeley Laboratory Report, LBL-9174 (July 1979).
  11. C.D. Hollowell and G.W. Traynor, Combustion-Generated Indoor Air Pollution, Lawrence Berkeley Laboratory Report, LBL-7832 (April 1978).

## MECHANICAL VENTILATION SYSTEMS USING AIR-TO-AIR HEAT EXCHANGERS

G. D. Roseme

### INTRODUCTION

Many homes in the United States and in Europe have conserved energy by reducing infiltration. When a house is thus "tightened", however, various indoor air contaminants are sealed in and tend to build up, e.g., odors from human activity, chemical contaminants from cooking and other combustion activity in the household, moisture, formaldehyde emitted from building materials and furnishings, and radon gas from soil, water and building materials. With the broad aim of assuring acceptable indoor air

quality in "airtight" houses without sacrificing the energy efficiency of the house, the Ventilation Program initiated a research project in October, 1978 designed to investigate the use of mechanical ventilation systems incorporating air-to-air heat exchangers.

A heat exchanger or heat recovery device installed directly in the mechanical ventilation system brings the incoming and exhaust air streams into close proximity so that heat can be exchanged between the two air streams (see Figs. 1 and 2). When such devices are installed in an

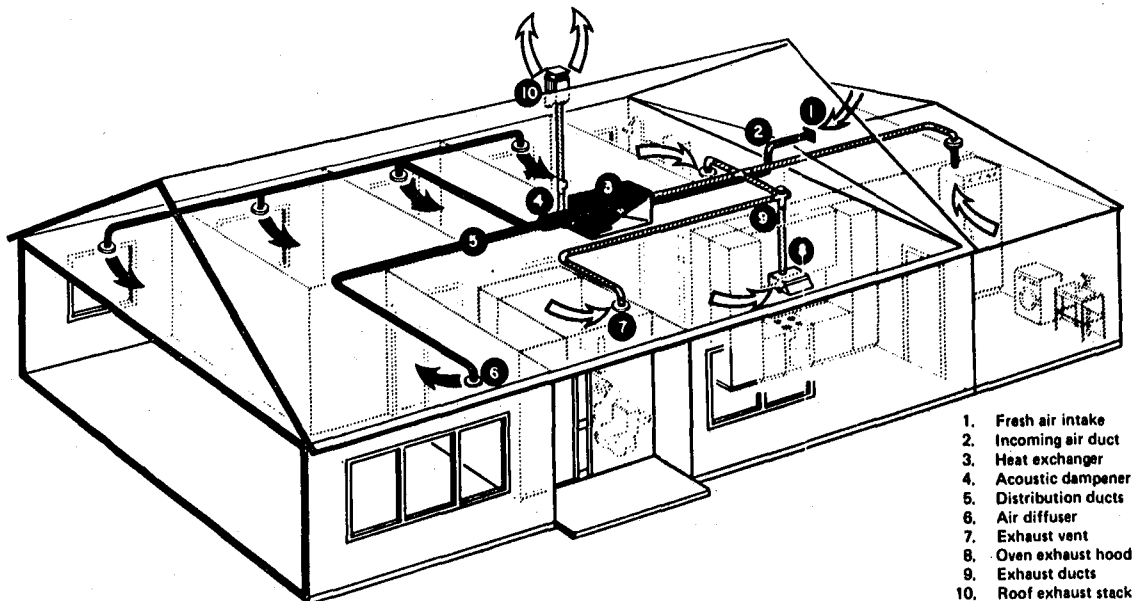


Fig. 1. Residential heat exchanger system. (CBB 791-509)

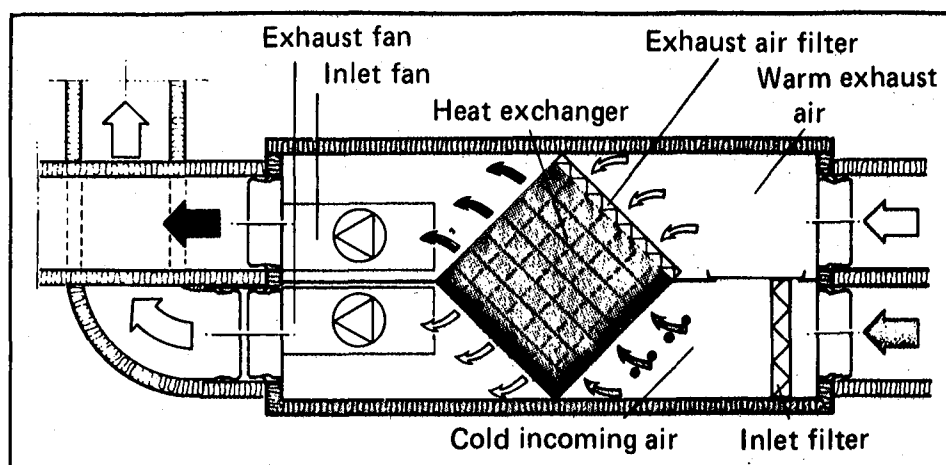


Fig. 2. Principle of operation of heat exchanger.

(CBB 791-507)

energy-efficient house, the concentration of indoor-generated contaminants are reduced without compromising energy-conservation.

The Ventilation Program Staff developed four study areas for this project:

- 1) Analysis and experimental evaluation of air-to-air heat exchangers;
- 2) Testing of a mechanical ventilation system utilizing an air-to-air heat exchanger in the EEB Walnut Creek house;
- 3) A cost-benefit analysis of these systems operating in different climate zones of the United States.
- 4) Installation and testing of a number of systems in occupied homes.

#### ACCOMPLISHMENTS DURING 1979

A heat exchanger test facility has been constructed at the Richmond Field Station of the University of California at Berkeley (see Fig. 3). This facility is capable of measuring the effectiveness, pressure drop, and cross-contamination of residential-sized air-to-air heat exchangers, and can simulate outdoor conditions from 0°F up to 100°F with high relative

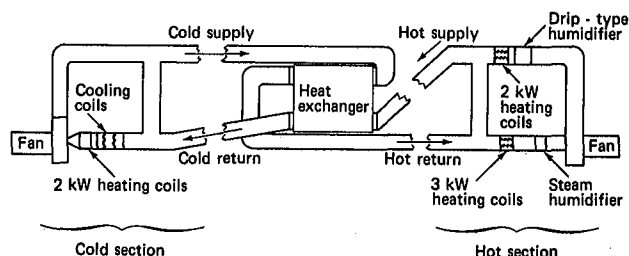


Fig. 3. Heat exchanger test facility.

(XBL 7910-4480)

humidity levels. Actual testing of air-to-air heat exchangers will begin early in FY 1980.

During 1979, heat exchanger systems were installed in two unoccupied research houses. One house, belonging to the National Association of Home Builders and located in Mt. Airy, Maryland, was already determined by our Energy Efficient Buildings (EEB) Mobile Laboratory to have high moisture, radon and formaldehyde levels. Under a subcontract to LBL, the National Association of Home Builders Research Foundation Inc. installed two mechanical ventilation systems and are currently measuring indoor air-quality parameters in the Mt. Airy house as a function of ventilation rate. These parameters include indoor and outdoor dry bulb temperature, relative humidity, formaldehyde concentration and radon concentration.

The second house is an unoccupied house in Walnut Creek, Ca. where we are studying methods of controlling combustion-generated pollutants from gas stoves. We have installed a mechanical ventilation system with an air-to-air heat exchanger and are investigating various ventilation strategies, including spot ventilation to improve indoor air quality in the house.

#### PLANNED ACTIVITIES FOR 1980

Under subcontract to Lawrence Berkeley Laboratory, the Department of Mechanical Engineering of University of California Berkeley, since October 1978, has aided in the design of the Richmond Field Station Heat Exchanger test facility, and has provided us with an analysis of both permeable and non-permeable wall exchangers operating in dry (noncondensing) conditions. Beginning in October, 1979, they will be developing calculation methods for determining heat-exchanger effectiveness as a function of flow rate, for both porous and non-porous wall materials and for exchangers operating with and without condensation and with freezing on the heat-transfer surface. Using these analyses, they will compare their theoretical predictions with experimental performance

as measured at our Richmond Field Station test facility and with manufacturers' specifications.

During the winter of FY 1980, the EEB Mobile Laboratory will measure indoor air-pollutant concentrations in two energy-efficient homes in Northfield, Minnesota. Both of these homes are quite airtight (measured natural infiltration rates of less than 0.2 air changes/hour under windy conditions). One of these houses has a mechanical ventilation system that uses a U.S. manufactured heat-pipe heat exchanger to recover the waste heat from the exhausted air. We are currently negotiating to install a ventilation system with an air-to-air heat exchanger in the second house before the mobile lab arrives.

Contract negotiations are underway with the New York State Energy Research and Development Authority, Rochester Gas and Electric Company, and The Rochester Institute of Technology for a collaborative program to examine the airtightness of approximately 60 homes in the Rochester, New York area. The airtightness of these homes will be measured with a blower door unit supplied by LBL. A number of indoor air-quality parameters will be measured in selected homes. If indoor air-quality problems are found, mechanical ventilation systems with air-to-air heat exchangers will be installed and energy efficiency, operating problems, and indoor air pollution in these houses will be monitored over a period of two years.

## SUBCONTRACT ACTIVITIES

### I. Turiel

#### INTRODUCTION

In addition to activities conducted by the Naval Biosciences Laboratory (NBL) and The Research Corporation of New England (TRC), discussed under "Field Monitoring", and work being performed by the University of Minnesota, described under the Hospitals Program, the Ventilation Program has been directing two other major subcontracts:

- o Assessment of ventilation requirements for odor control (John Pierce Foundation, New Haven, CT)
- o Development of automatic variable ventilation control systems (Honeywell, Inc., Minneapolis, MN)

#### ACCOMPLISHMENTS DURING 1979

##### Odor Control (John Pierce Foundation)

In order to carry out experiments on ventilation requirements for odor control, it is necessary to have a test room where the environment can be regulated at will. The John Pierce Foundation completed construction of a 1,200 ft<sup>3</sup> test chamber in June 1979 at their laboratory in New Haven, Connecticut. The environment in the all-aluminum chamber can be controlled for temperature, humidity and ventilation rate. The objectives of these laboratory experiments are to:

1. Determine how odor magnitude, odor acceptability, and odor detectability vary with the rate and type of contaminant generation, rate of ventilation, temperature and humidity.
2. Compare air acceptability as perceived by occupants in an experimental chamber with that perceived by visitors to the chamber.

3. Assess the efficiency of solid granular media for controlling odors under conditions of reduced ventilation.

In all experiments planned, the primary independent variables are:

- a. type of contaminant
- b. rate of contaminant generation
- c. rate of ventilation
- d. presence/absence and type of filter media and
- e. environmental conditions

One experiment on body odor serves as a typical example: Variables c, d, and e above are predetermined for each experiment. Occupants enter to serve as odor generators. Persons are stationed at a sniffing port outside the chamber (where air from the chamber is exhausted) to act as odor judges. At periodic intervals, judges record odor detectability, intensity, and acceptability. (The same type of olfactometers are used as in the TRC odors field work described in the Field Monitoring section.)

Figure 1 presents results on body odor experiments at ventilation rates of 3.3, 5.0 and 10 cfm per occupant, three temperature settings, and two humidity conditions. Although the air space per person (100 ft<sup>3</sup>) is quite low compared with typical occupied spaces in buildings, the air was found to be generally acceptable. As indicated on the figure, an odor-intensity reading of 4 or less means that 80% of the judges found the air odor acceptable. When the temperature is kept below 25.5°C and the relative humidity below 70%, a ventilation rate of 5 cfm/person appears adequate to maintain acceptable odor level even under such crowded occupancy conditions. This finding is in contrast with earlier results reported by Yaglou, et al.<sup>1</sup>

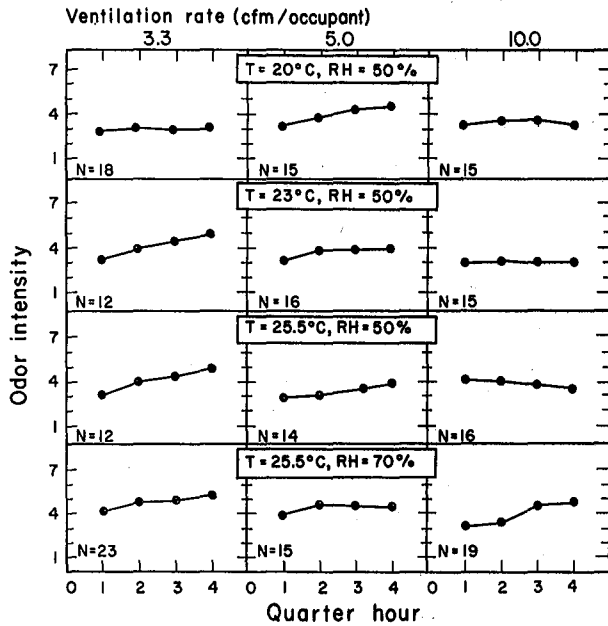


Fig. 1. Odor intensity as a function of temperature and relative humidity.  
(XBL 801-72)

which specified that 25 cfm/person was required to produce an acceptable odor level under the above occupancy conditions. These results from the John Pierce Foundation are only preliminary, however.

Continuing experiments in this area will test other odorous substances. From these findings, it will be possible to construct "families" of psychophysical functions relating perceived odor magnitude in steady-state or quasi steady-state conditions to levels of concentration of an odorous contaminant, number of occupants, rate of ventilation, etc.

Corollary work undertaken by the John Pierce Foundation -- a review of existing regulations for odor control in buildings and their underlying data base -- together with a discussion of odor-measurement techniques and air-treatment systems for odor control in buildings, has been completed and published as an LBL report, Ventilation and Odor Control: Prospects for Energy Efficiency.<sup>2</sup>

#### PLANNED ACTIVITIES FOR 1980

In FY 1980, the John Pierce Foundation will continue experiments on ventilation requirements for control of body and tobacco odors with the objective of establishing ventilation rate recommendations under various conditions of occupancy and thermal environment. The ability of several solid materials to adsorb odors under various conditions will also be assessed.

#### Variable Ventilation Control Based on Air Quality Detection

Honeywell, Inc. was subcontracted to develop and demonstrate an automatic variable ventilation control system based on air-quality detection for various institutional and commercial building types. The air-quality detector was to be sensitive to changes in the number of occupants and activity loads. Field work in schools and office buildings has indicated that CO<sub>2</sub> concentration and occupancy are closely related.<sup>3</sup>

At the end of FY 1979, Honeywell installed a variable ventilation control system in the music wing of Fridley Junior High School, located in the greater Minneapolis area.

Occupancy/activity levels are sensed by fluctuations in CO<sub>2</sub> concentration, and the detector output signal controls the outside air damper. The HVAC system was modified to allow measurement of air velocities, temperature, and relative humidity in several return and supply air ducts, and also to measure the energy consumed by the hot water reheat coils.

For space heating, the HVAC system can be operated in three modes. The first mode, the "BEFORE" mode, supplies air at 55°F to the reheat coils which reheat the air to maintain space conditions; the second mode is an ENERGY EFFICIENT mode where the air temperature supplied to the reheat coils is reset so that it is no colder than required to keep the warmest reheat zone from over-heating; the third mode, also an ENERGY EFFICIENT mode, is the automatic variable ventilation mode where the amount of outdoor air introduced will be the minimum amount required to prevent the CO<sub>2</sub> level in the occupied zones from rising above the control level for CO<sub>2</sub>, or the amount of outdoor air required to prevent overheating while the HVAC system is operating on the "free" outside air cooling cycle. When operating in this last mode, ventilation air is introduced through an outside air-damper section (Fig. 2) and an air measurement device. This damper section, as well as the thermal outside air damper and the exhaust air damper, are of a "low leakage" design to minimize the introduction of unwanted outside air. Two small exhaust fans in the HVAC system were disabled and sealed off so that the only exhaust capability of the tested area will be that of the central return-exhaust fans.

#### PLANNED ACTIVITIES FOR 1980

During 1980, the control system will be tested for its reliability in maintaining adequate indoor air quality with maximum energy conservation. Energy consumption data from these three modes of operation will be normalized for weather variance and compared with each other to evaluate the benefits derived from ventilation control systems based on CO<sub>2</sub> detection.

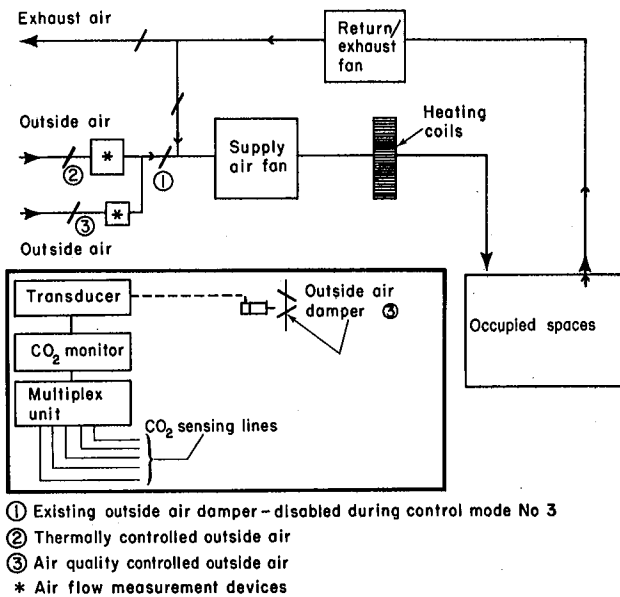


Fig. 2. Control modifications to heating, ventilation and air conditioning system at Fridley Junior High School. (XBL 801-73)

A similar evaluation will be conducted for the "peak" cooling period of operation. The "peak" cooling period occurs during those occupied times when the outdoor air has a higher enthalpy (more heat) than the return air. The control modes will again be "BEFORE," "ENERGY EFFICIENT" and an ENERGY EFFICIENT mode where the amount of outside air is minimal and controlled to maintain interior air quality as measured by CO<sub>2</sub>

## VENTILATION - INDOOR AIR QUALITY DATA BASE

R. Langenberg

### INTRODUCTION

The Ventilation Indoor Air Quality (VIAQ) data base is a computerized information service developed by the Ventilation Program, a major component of the Lawrence Berkeley Laboratory Energy Efficient Buildings Program. This program is part of a coordinated effort to respond to the need for national energy conservation, while concurrently ensuring satisfactory indoor air quality for building occupants. To this end, Lawrence Berkeley Laboratory (LBL) is conducting research and development on existing and proposed ventilation requirements and mechanical ventilation systems. The program will produce recommendations for energy-efficient ventilation standards and designs for residential, institutional and commercial buildings.

Various segments of the professional community have expressed a growing interest in energy conservation as applied to the built environment. A partial listing of those concerned

content in the occupied spaces. The occupants of the music wing will be asked to complete a questionnaire daily, as a means of assessing their perception of the indoor air quality under various ventilation conditions.

As indicated under "Field Monitoring," the LBL EEB Mobile Lab will be brought to Fridley Junior High School during the month of February to determine the effectiveness of the ventilation control system in maintaining acceptable indoor air-quality. In addition, Honeywell will proceed with the following tasks:

- Determine the cost-effectiveness of variable ventilation control systems and estimate expected national energy savings.
- Assess commercialization potential of variable ventilation control systems.

### REFERENCES

1. C.P. Yaglou and W.N. Witheridge, "Ventilation Requirements," Transactions of the American Society of Heating and Ventilation Engineers, Vol. 42, pp. 133-63 (1936).
2. W.S. Cain, L.G. Berglund, R.A. Duffee and A. Turk, Ventilation and Odor Control: Prospects for Energy Efficiency, Lawrence Berkeley Laboratory Report, LBL-9635 (November 1979).
3. I. Turiel, C.D. Hollowell and B.E. Thurston, Variable Ventilation Control Systems: Saving Energy and Maintaining Indoor Air Quality, Lawrence Berkeley Laboratory Report, LBL-9380 (June 1979).

include: architects, building contractors, design engineers, legislators/administrators, mechanical engineers, professors/educators, public health officials, researchers and scientists.

In an effort to meet the needs of these specific groups, as well as the commercial sector and the general public, LBL is in the process of establishing an information clearing-house for ventilation indoor air quality research (VIAQ). The basic objective of the VIAQ Data Base project is to consolidate existing information with current research developments and to make this information directly accessible to user groups throughout the country.

Access to the data base will occur via an interactive session between the user and VIAQ. Communication (data links) may be established through commercial telephone lines, or high-speed computer networks. User equipment requirements are minimal--a telephone, a computer ter-

minal, and an acoustic coupler. Once the connection has been achieved, the typical user will be interactively guided through selected resource modules.

When the VIAQ data base is fully operational, it will include information on the following items:

1. Air Quality Resources
2. Bibliography
3. News
4. Seminars, Workshops and Conferences
5. Who's Who
6. Ventilation-Research and Development Projects
7. Ventilation-Business and Finance
8. Ventilation-Standards and Guidelines
9. Models
10. Analysis Programs
11. User Alert Service
12. Hard-Copy Output
13. Utility Routines
14. Help

In the prototype version, LBL is preparing to bring on-line the following modules:

Module 1: A current listing of data base resources to inform users of existing search facilities.

Module 2: The bibliographic resource including bibliographic references, abstracts, and thesaurus, covers subject areas such as indoor air quality, airborne contaminant control, hospital ventilation and energy conservation, infiltration, windows and lighting, and radon. Each bibliographic entry includes source reference information including: author name and affiliation, publication type, language of the original article, abstract and keywords. Abstracts are maintained on-line to aid the user in determining whether he/she wishes to obtain the complete document. Original author-prepared abstracts are utilized wherever possible; however, LBL has supported abstracting activities to ensure adequate subject coverage. The indexing process, a vital part of bibliographic control, employs a consistent vocabulary (thesaurus) of keywords to describe the content of each document. The VIAQ on-line thesaurus conceptually structures

keywords into broad, narrow and/or related terms, which will be used in the retrieval process.

Module 3: Current information and announcements, including data base updates, are obtainable in News.

Module 5: Who's Who is a listing of names, affiliations, and interest areas for researchers and officials working in building ventilation/indoor air-quality activities. The module may be used to generate specialized mailing lists or to link with the bibliographic module to immediately provide addresses and telephone numbers for authors of interest.

Module 12: When a session is terminated, final results may be printed on a hard copy peripheral to the user, or hard copy may be requested from LBL.

Module 14: Should the user have difficulty during a session, he/she may summon "help" at virtually any phase in the dialog, and instructions will be issued suggesting an appropriate remedy.

#### WHO'S WHO IN VENTILATION DATA BASE RESOURCE

Data collection is currently underway for module 5, the "Who's Who" resource module of VIAQ. This listing will facilitate contact among individuals by providing the user with pertinent information regarding other researchers who are involved in the ventilation/indoor air quality field. Searchable fields for this resource are name, affiliation and area(s) of interest.

Typical interest areas are as follows:

1. Airborne Microbes
2. Administration/Management
3. Building Envelope
4. Computer Analysis
5. Energy Conservation
6. Energy Efficient Buildings
7. Epidemiology
8. Field Studies
9. Formaldehyde
10. Heat Exchangers
11. Indoor Air Quality
12. Infiltration
13. Instruments/Instrumentation
14. Mathematical Models

- 15. Odors
- 16. Organics
- 17. Radon
- 18. Standards/Guidelines

## ACCOMPLISHMENTS DURING 1979

Information analysis activities in FY 1979 centered on the following bibliographics:

In the area of air quality and energy conservation in hospitals, emphasis is placed on the patient environment, with respect to heating, ventilating, and air conditioning parameters. Topics include 1) general air hygiene, hospital-acquired infections, 2) characterization of gaseous chemical contaminants detected in the hospitals, 3) hospital-specific contaminant control procedures, and 4) variables affecting patient comfort, such as temperature, humidity and odor level.

The survey of literature by the Infiltration Group includes studies of single-family struc-

<u>Area</u>	<u>Source</u>	<u>Processing</u>
Organic Chemistry*	LBL	data entry
Radon	LBL	validation, data entry
Odors	John B. Pierce Foundation	data entry
Contamination Control	LBL	validation
Hospitals	University of Minnesota	validation
Infiltration	LBL	coordination between infil- tration and VIAQ group
Windows and Lighting	LBL	Coordination between Win- dows and Light- ing Group and VIAQ.

The radon literature survey contains studies relating to the physical properties of radon and its daughters, instrumentation for their measurement, health effects, air-concentration surveys, and regulatory measures.

Literature surveyed by the John Pierce Foundation is an extension of the LBL contamination control survey. It encompasses existing and proposed ventilation requirements for odor control in buildings; odor measurement techniques, both analytical and subjective; and air treatment systems for odor control in institutional and commercial buildings.

In the area of contamination control, the literature survey is restricted to contaminant control theory and application in residential, commercial and public buildings. Areas of emphasis are toxic gas control, general odor control, and non-viable particulate control.

tures as well as high- and low-rise commercial buildings. Measurement techniques used include tracer gas, pressurization, and wind tunnel investigations. Influences due to wind, temperature, humidity, and terrain are also covered.

The Windows and Lighting Group is gathering bibliographic citations, patents, and standards on energy conservation as it relates to windows, and lighting.

A single hierarchical thesaurus of approximately 2,000 main terms has been established for keywording and searching the above bibliographics. The thesaurus contains synonyms and scope notes, and supports the standard binary relations between main terms (broader term, narrower term, related term). Data entry formats for technical bibliographic material (books, serials, analytics, "other") were established and

underwent testing. A table-driven data entry program (UNIX software) was developed to accept these formats as record definitions, producing an interactive program that prompts the key operator for the appropriate information, validates when possible, and formats the output according to the requirements of a specific data-base management system.

The viability of modular design was demonstrated by bringing up various portions of the data safe on a PDP 11/70, utilizing UNIX and the Ingres data management system. By mid-July 1979, it became clear that VIAQ required a more production-oriented computer system, and the application was moved to an IBM 3033 housed at Stanford University. Existing data structures (primarily bibliographic records) were redesigned and programmed as file definitions in SPIRES, the general purpose data management system running on the IBM 3033.

#### PLANNED ACTIVITIES FOR 1980

The move to SPIRES delayed opening of the prototype data safe beyond FY 1979. It is currently scheduled for late January, 1980 and includes modules 1, 2, 3, 5, 12 and 14. Hard copy documentation of VIAQ modules will be generated in the 2<sup>nd</sup> and 4<sup>th</sup> quarters of FY 1980.

Tasks for FY 1980 are as follows:

Task 1: Continue to add program modules 3, 4, 6, 7, 8, 9, 10 and 11 to prototype version.

Task 2: Expand the data base to include information consolidation and dissemination tasks of other components of the EEB Program, e.g., Windows and Lighting Group, Infiltration. Generalized data storage structures have been established, and custom-user interface software will be provided to specific EEB user groups.

The full text and reduced data of EEB publications (e.g., "Windows") will be entered into the data base, allowing convenient editing, searching, and recall. High-quality hard-copy output of reports will be quickly available for widespread circulation.

Task 3: Begin software development to automatically monitor public use of the data base. Heavy-demand modules will be improved in terms of execution efficiency and user sophistication, while lower-demand modules may be reduced or eliminated.

Task 4: Coordinate efforts with related data base elsewhere. Export Ventilation Data Base to IEA Data Management Center.

In its final form, VIAQ will offer a leading-edge information service specializing in energy conservation and air quality in the built environment. In addition to the core subject matter, distinguishing features include wide public access, thoroughly indexed information, and direct user-to-data interface in a friendly computer environment.

## DOE-2 COMPUTER PROGRAM FOR BUILDING ENERGY ANALYSIS

*W. F. Buhl, R. B. Curtis, S. D. Gates, J. J. Hirsch, S. P. Jaeger, M. Lokmanhekim,  
A. H. Rosenfeld, J. V. Rudy, and F. C. Winkelmann*

#### INTRODUCTION

For the past three years, LBL has been developing a comprehensive computer program for predicting energy use in buildings. Collaborating in this effort are LBL and Los Alamos Scientific Laboratory (LASL). LBL performs the role of lead laboratory. This program was formerly called Cal-ERDA and DOE-1.

The DOE-2 computer program is a tool that architects, engineers, and others can use to design new energy-efficient buildings and to analyze existing buildings for cost-effective energy-saving modifications.

The program has four main sub-programs:

1. **LOADS**--Computes hourly heating and cooling loads for each space in the building. The program differentiates loads

due to infiltration, heat conduction, solar gain through windows, and internal gains generated by people, lights, appliances, and other equipment.

2. **SYSTEMS**--Simulates the operation of the HVAC distribution systems that heat and cool each space in the building and (in large buildings) distribute fresh conditioned air.

3. **PLANT**--Simulates the operation of the building's primary heating, cooling, and electrical plant, and calculates the hourly, monthly, and yearly energy requirements for the building.

4. **ECONOMICS**--Calculates the life-cycle cost of the building's mechanical system and energy-related features, including capital costs as well as maintenance,

operating and energy costs. This sub-program also performs a cost-benefit analysis; i.e., the user can input different design options which will be ranked on the basis of cost and/or energy use.

DOE-2 differs from its predecessor programs in two major respects:

1. It executes faster in the computer than other programs with similar purposes, and it is approximately five times cheaper to run. These features permit more alternative design options to be considered by the user as a basis for determining those most acceptable from a cost and energy-consumption point of view.
2. Where earlier programs read data cards filled with numbers punched in fixed format from forms filled in by the user, DOE-2 reads a "Building Description Language" (BDL), designed to increase speed, flexibility, and reliability of input. Special commands and keywords permit the user to specify building properties and parameters such as geometry, construction materials, schedules, HVAC systems, fuel costs, etc. Environmental data are provided via standard meteorological tapes of hourly weather conditions.

The overall logic and energy-flow diagram for primary HVAC systems of commercial buildings under DOE-2.1 are given in Fig. 1 and Fig. 2, respectively.

ACCOMPLISHMENTS DURING 1979

During 1979, two updates, DOE-2 and DOE-2.0A, were completed. Work is substantially underway on DOE-2.1, an expanded program selected by the Department of Energy as the benchmark for certifying compliance with the Building Energy Performance Standards (BEPS) to go into effect in 1980. This version of the program will include residential and packaged system simulation routines and will give the user the choice of (1) ASHRAE Weighting Factors and (2) Customized Weighting Factors as a basis for calculating heating and cooling loads for a given building.

Documentation was completed for the DOE-1, DOE-2, and DOE-2.0A programs. A new site manual for "Using DOE-2 at Lawrence Berkeley Laboratory" was completed by a sub-contractor (Jewson Enterprises).

DOE-2 is currently running at 47 sites, including: five national laboratories; ten universities; eight computer service bureaus; seven foreign sites; and two state energy commissions. These users, as well as others knowledgeable in building energy analysis, have been surveyed for advice on future developments of DOE-2. The DOE-2 User Coordination Office at LBL responded to nearly 400 telephone inquiries and/or requests for assistance in running DOE-1 and DOE-2.

The three-year verification project, assigned to LASL in 1978 by the Department of Energy, involves: (1) laboratory measurements of HVAC system components and comparison with DOE-2 simulations; (2) comparison of DOE-2 results

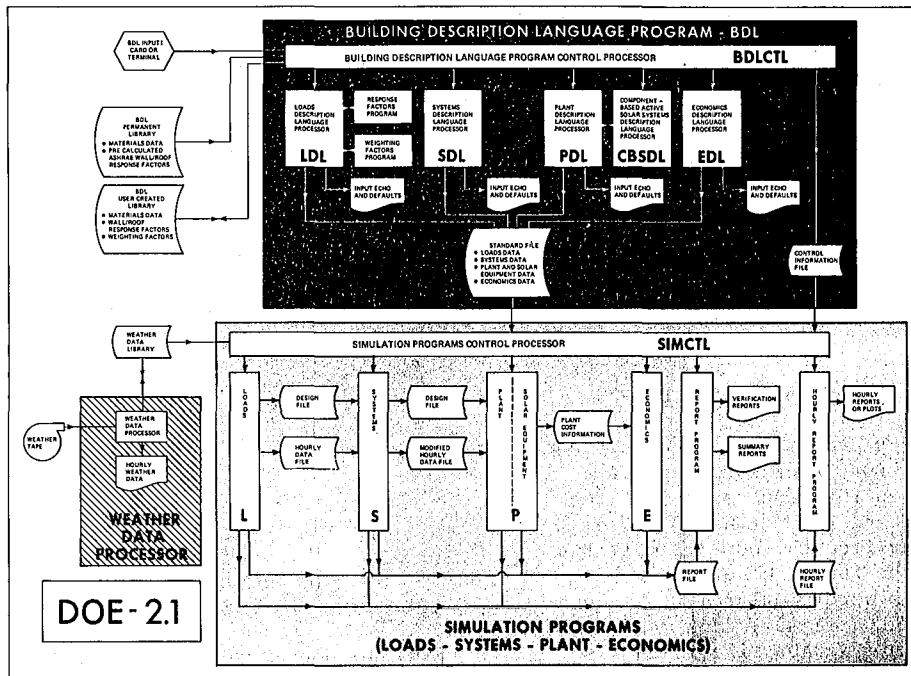


Fig. 1. DOE-2.1 simulation program for predicting energy use: overall logic. (XBL 7910-4353A)

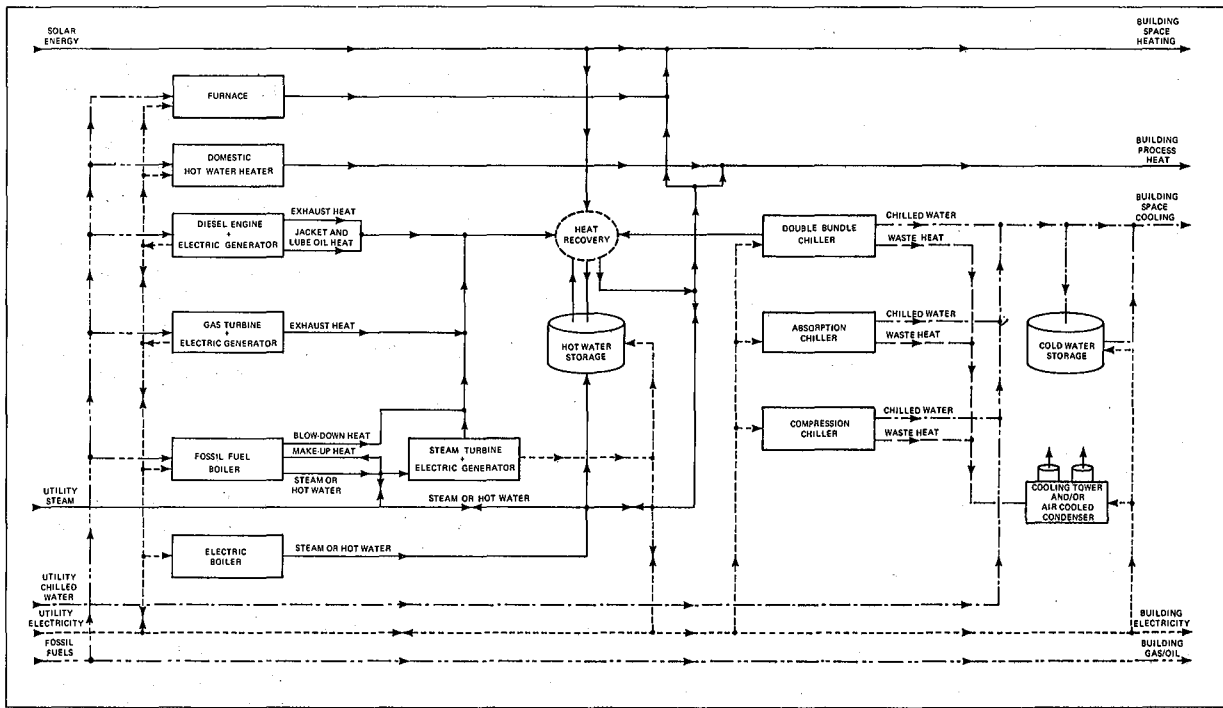


Fig. 2. Plant energy flow diagram for primary HVAC systems in commercial buildings. (XBL 7910-4354A)

with standard manual calculations; and (3) comparison of DOE-2 results with the actual energy consumption of six different commercial buildings.

In 1979, International Energy Agency (IEA) activities continued to perform: (1) energy use analysis of the Avonbank building, located in Bristol, England; (2) parametric studies on the energy use of the Avonbank building; and (3) comparisons of the energy use of the Avonbank building calculated by using different types of ASHRAE and Custom Weighting factors. The results of Task 1 were presented at the meeting of the International Energy Agency Executive Committee on Buildings and Community Systems in Copenhagen, Denmark (May, 1979). The results of Tasks 2 and 3 were presented at the meeting of the International Energy Agency Executive Committee on Buildings and Community Systems in Zurich, Switzerland (December, 1979).

Sample Energy Conservation Study with DOE-2

Significant energy and financial savings can be achieved by using DOE-2 for studying HVAC systems. Fig. 3 shows the results of 7 of the 10 different SYSTEMS and PLANT runs of a 31-story office building from the DOE-2 Sample Run Book 1. (Three of the runs are not shown because the buildings were simulated with unconventional primary HVAC systems.) Each run employed the same hourly LOADS file which was generated using Chicago TRY weather data. Results of other studies have been also incorporated in Fig. 3 in order to aid comparison.

The building typified 1974 construction, which did not quite conform to ASHRAE Standard 90-75. Details on Figure 3

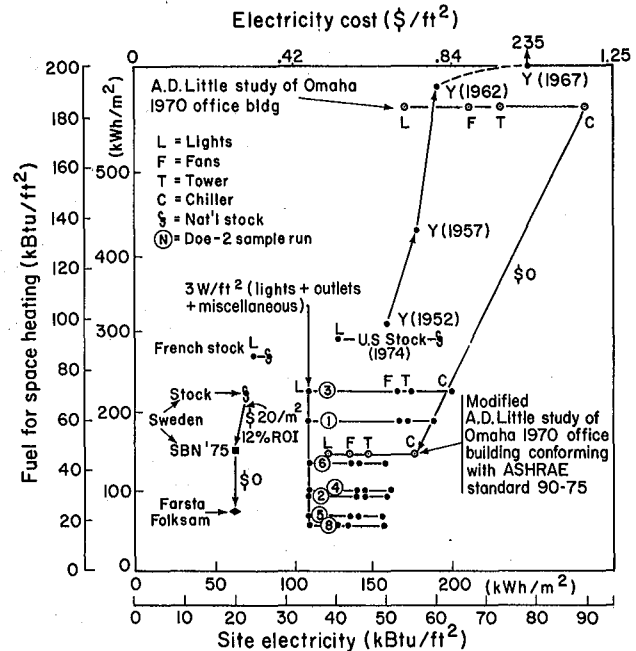


Fig. 3. Energy use in office buildings: fuel for space heating vs. site electricity (i.e., 1 kWh<sub>e</sub> counted as 3600 kJ = 3414 Btu).<sup>3</sup> (XBL 793-891)

Each combination of a primary and secondary HVAC system is designated by a horizontal bar labeled by the run (system) number. The height of the bar indicates the amount of fuel consumed for space heating. Electricity consumed by the lights, outlets and miscellaneous building-wide operations is identical for all runs, and indicated by the dot on the bar labeled L. Electricity used by the fans, cooling tower and chiller is indicated by the dots labeled F, T and C, respectively; point C also indicates the cumulative total electrical consumption of the building.

The line at the top labeled "A.D. Little Study of Omaha 1970 Office Building"<sup>2</sup> corresponds to the calculated energy use of a 1970-style office building, built and operated energy-intensively. Energy use of the building was then recalculated to conform with ASHRAE Standard 90-75 and replotted. The line labeled "\$0" connects the results of the two calculations and indicates that redesign led to no increase in first cost, despite reductions in site electricity use from 90 to 55 Kbtu per ft<sup>2</sup> and in fuel use for space heating from 184 to 46 Kbtu per ft<sup>2</sup>.

The four Y's indicate energy used in large New York City office buildings constructed during 5-year intervals between 1950 and 1970. These buildings are equipped with absorption chillers in order to use cheap urban steam. Presumably, as demonstrated in the ADL study<sup>2</sup>, use of steam power in large office buildings will decrease in new construction.

The three points plotted as f represent French, Swedish and U.S. national energy consumption which is less than the non-cooling part of the U.S. average. The energy consumption in Sweden, with a cold climate and expensive oil, is slightly less than the French average.

Two other Swedish points are also plotted: Swedish Building Norm 1975 (SBN-75) and Farsta-Folksam 5. SBN-75 represents redesign of an office building, typically triple-glazed, with 25 cm of rockwool insulation, and heat recovery for fresh air, yielding an annual ROI of 12%. Farsta-Folksam represents a new suburban Stockholm building which stores heat by circulating air through hollow cores in the concrete roof/floor slab at no increase in first cost. In this design, total annual site energy consumption has been reduced to 45,000 BTu per ft<sup>2</sup>; however, in the most economical DOE-2 run of a 31-story office building, consumption was calculated to be 70,000 Btu per ft<sup>2</sup> and average consumption for U.S. stock is 130,000 Btu per ft<sup>2</sup>. These comparisons demonstrate that by careful study of alternative HVAC systems, and by storing heat and coolth, energy consumption in a typical U.S. office building can be reduced by 1/2 to 2/3 with little or no increase in first cost.

The 25-year life-cycle cost (LCC), calculated by using first costs of the HVAC systems plus present values of fuel, electricity and maintenance costs, are tabulated for the seven systems in Table 1.

Annual resource energy consumption for each system is also shown in the table. As can be seen, LCC's for constant air volume systems (CAV) 1, 3 and 8 range from \$21 to \$36 per ft<sup>2</sup>, while LCC's for variable air volume systems (VAV) 2, 4, 5 and 6 range from \$25 to \$27 per ft<sup>2</sup>. Since the least expensive system, at \$21 per ft<sup>2</sup>, is also the least attractive from the point of view of comfort, system 5 represents the most economical investment with new construction. CAV systems 1 and 3, popular when energy costs were negligible, waste more energy at a correspondingly high expense. Remarkable annual returns on investment (ROI) can be achieved by retrofitting CAV

Table 1. Annual resource energy consumption and Life Cycle Costs for a 31-story office building with conventional primary (boiler, chiller and cooling tower) and different secondary HVAC systems.

System No.	Secondary HVAC System	Annual Resource Energy Consumption		Life Cycle Cost	
		KBTU/ft <sup>2</sup>	KWh/m <sup>2</sup>	\$/ft <sup>2</sup>	\$/m <sup>2</sup>
1	DD - CAV	238	752	29	312
2	DD - VAV (50%)	181	572	27	291
3	SD - CAV - Reheat	262	828	36	387
4	SD - VAV (50%) - Reheat <sup>a</sup>	184	581	26	280
5	SD - VAV (30%) - Reheat <sup>a</sup>	170	537	25	269
6	Interior	192	607	26	280
	Exterior				
8	SD - VAV (10%) DD - CAV	168	531	21	226

DD = Double Duct, SD = Single Duct  
CAV = Constant air volume, VAV = Variable air volume  
a. Reheat systems are controlled by space thermostats.  
b. Baseboard systems are controlled by outside thermostats.

systems with VAV systems, i.e., converting from system 1 to system 2, or from system 3 to system 4. A retrofit from 1 to 2 costs \$30 per mixing box, yielding an annual ROI of 900%; a retrofit from system 3 to 4 costs \$350 per mixing box, yielding an annual ROI of 100%.

#### PLANNED ACTIVITIES FOR 1980

After the completion of DOE-2.1 and its documentation early in 1980, LBL's efforts will be directed toward improving the program in areas recommended by a newly-formed advisory committee and approved by the Department of Energy. This new committee will be comprised of two sub-committees of five members each. One sub-committee consists of practicing building professionals; the other, of computer program theoreticians. In preparing its consensus opinion on program improvement for presentation to the Department of Energy, the committee will consider optimum program structure, the needs of the Department of Energy, and the needs of the user community, as generated by the user survey conducted in FY-1978. The User Coordination Office at LBL will be expanded to respond to the needs of an enlarged user community.

#### REFERENCES

1. Building Energy Analysis Group, DOE-2 Sample Run Book, Lawrence Berkeley Laboratory Report, LBL-8678 (February 1979).
2. A.D. Little Co., "Energy Conservation in New Building Design: An Impact Assessment of ASHRAE Standard 90-75", FEA Conservation Paper No. 43B, 1976.
3. A.H. Rosenfeld, et al., Building Energy Use Compilation and Analysis (BECA), An International Comparison and a Critical Review, Lawrence Berkeley Laboratory Report, LBL-8912 (June 1979).
4. L.O. Andersson, K.G. Bernander, E. Isfalt, and A.H. Rosenfeld, "Storage of Heat and Coolth in Hollow-Core Concrete Slabs: Swedish Experience and Application to Large American-Style Buildings," to be submitted to ASHRAE Journal; Lawrence Berkeley Laboratory Report, LBL-8913 (October 1979).

## HOSPITALS PROGRAM

*R. Pollack and I. Turiel*

#### INTRODUCTION

As energy-intensive buildings, hospitals have been singled out for special study by Lawrence Berkeley Laboratory's Energy Efficient Buildings (EEB) Program. Energy conservation in hospitals involves a number of special considerations, not only because hospitals are high-intensity users, especially for their HVAC needs (heating, ventilation and air conditioning), but because their patient-care responsibilities place unique demands on the type and level of energy-conserving modifications implemented, or recommended, as general standards nationwide. For example, it is believed that hospital patients are more susceptible than the general population to airborne infections, to the deleterious effects of odors and chemical contaminants, and to changes in temperature and relative humidity. In addition, a significant body of literature substantiates the fact that infections whose onset is in the hospital and which are unrelated to the patient's condition (nosocomia) are associated with the high-risk environment of the hospital itself. Finally, as institutions serving health and medical needs of the general public, complex policy questions are raised more sharply than in other institutional buildings considering energy-conservation-related changes in design and procedures. Thus, the ultimate objectives of the Hospitals Program are 1) to develop energy-conservation strategies that do not compromise the health, safety and comfort of patients and staff, and 2) to support

DOE/HEW/LBL efforts to promote energy-efficient ventilation and thermal standards for hospitals.

Because more than 50% of the energy consumed in hospitals is accounted for by their HVAC systems, with lighting and water the next largest consumers, the Hospitals Program has been closely tied to LBL's Ventilation Program. Two subcontracts were awarded by LBL to complete those tasks regarded by Hospitals Program staff as priority needs: 1) the University of Minnesota (School of Public Health) was charged with reviewing current hospital ventilation and thermal standards and recommending opportunities for energy conservation compatible with the health, safety and comfort of the patients and staff; and 2) Hittman Associates, Inc. was charged with studying energy-efficient water use in hospitals.

#### UNIVERSITY OF MINNESOTA

As an outgrowth of an international working conference presented in February, 1978, the University of Minnesota conducted an opinion poll of panelists to pursue some of the issues that had remained in question and unresolved. The poll listed various factors related to hospital-acquired infections, thermal comfort, odors and toxic chemicals and requested panelists to rank each in terms of their relative importance. The results tabulated thus far indicate that in the area of nosocomial infections, airborne contaminants were rated next to

the least important, and techniques related to quality patient care were regarded as more important than hospital ventilation design criteria.

#### ACCOMPLISHMENTS DURING 1979

A similar poll is now being conducted among members of the Association of Practitioners and Infection Control, an association of 4,500 members, approximately 85% nurses and 15% doctors and other professionals primarily employed as infection control officers. Preliminary tabulation of these returns has corroborated findings revealed by the limited poll of conference panelists. Handwashing was consistently viewed as the most important of the ten factors presented in relation to nosocomial infections, and the importance of airborne contaminants rated 5th or 6th.

In their survey of existing ventilation standards, the University of Minnesota reported that national standards related to hospital ventilation and thermal requirements rely essentially on:

1. U.S. Department of Health, Education and Welfare, Public Health Service, Health Resources Administration: Minimum Design and Construction Requirements under the Hill-Burton Program.
2. American Society of Heating, Refrigerating and Air Conditioning Engineers, Inc.: Applicable Engineering Standards.
3. National Fire Protection Association: Life Safety Code (NFPA).

In addition, they note the following:

1. Nineteen states adopted their own standards. (ASHRAE).
2. Seventeen states and one territory adopted the Hill-Burton standards.
3. Seven states adopted the NFPA Life Safety Code.
4. Two states adopted an ASHRAE standard.
5. Five states do not have any standard.

Following outside review of its recommended standards and careful analysis of written comments received, the University of Minnesota has developed the following set of principles:

1. Except for those spaces used directly for patient care or where other unusual health or safety hazards exist, ASHRAE energy conservation standards can be applied.
2. Ventilation requirements do not need to be based on control of airborne microorganisms, except for those sensitive

areas where the patient is particularly at risk.

3. Acute odors should be controlled at their source, not by ventilation air.
4. An outdoor air requirement for control of the airborne chemical contaminant load needs to be established.
5. Humidity control need not be based on patient comfort or control of airborne microorganisms.
6. A temperature range can be specified for patient care spaces.

These principles were incorporated in a Draft Discussion Paper: "Modification of Hospital Ventilation and Thermal Standards for Energy Conservation" sent to 500 knowledgeable professionals around the country. A 26% response was received and comments from this group were incorporated in their "Proposed Pressure Relationship, Ventilation and Thermal Requirements of Certain Hospital Areas."

The University of Minnesota also has completed a study of chemical contaminants of hospital air, and their final report<sup>1</sup> is now being reviewed by members of the Ventilation Program staff. Briefly, their findings can be summarized as follows:

1. The general public is misinformed about the quality of sanitation practices in hospitals;
2. Most hospital workers focus, justifiably, on the hazards of chemical contaminants to employees, whose exposure is prolonged in contrast to that of patients whose exposure is short-term.
3. Hospital housekeeping staffs are as much influenced by commercial advertising of chemical products as the general public and restraint in their use is the best answer for both groups.
4. Spot ventilation specifically designed for hospital laboratories should be promoted as a control measure for chemical contamination.
5. Ventilation systems in hospital laboratories should exhaust directly outdoors and, again, be designed according to the heat load generated by the specific instrumentation housed.

The University of Minnesota investigated hospital laundry water use to determine whether the quality of finished laundry with respect to stain removal, whiteness, and sanitation could be maintained under the new (1979) DREW minimum hot water requirement of 160°F. From their review of the literature, they concluded generally that a water temperature of 140°F or 150°F was adequate for removal of stains as well

as for whiteness, as long as the soaps, detergents and bleaches were appropriately used. For example, hospitals generally use medium-titre soaps which dissolve at 130°F to 140°F. In terms of bleaches, water temperatures below 160°F will require a slightly longer immersion time but are otherwise acceptable for assuring stain removal and whiteness.

The problem of transmitting diseases or infections by means of inadequately laundered linens appears to be a real one. Various organisms (Staphylococcus, polio virus, vaccinia virus and Salmonella typhimurium) can persist on fabrics for days or weeks after contamination first occurs. Apparently, today's standards in this area are based on an early study of Arnold in 1938. In his year-long study of 54 hospitals, Arnold determined a formula that called for 165°F water temperature and the addition of a "sour" to the final rinse as a means of eliminating bacteria. Ironing fabrics also kills most bacteria (see Table 1). A summary table of effective wash temperatures for various organisms is presented in Table 2. From these data (a compilation of 12 reports published since 1938) it seems that a water temperature of 140°F is effective in killing most vegetative organisms and 150° is effective for the remaining.

The University of Minnesota concurs with Hittman's recommendations that carefully controlled studies need to be initiated in a University setting, with input from experts on microbial contamination as well as from health departments and infection control personnel. Their program plan for such a comprehensive project is being reviewed by LBL.

Ultimately, the findings from these foregoing studies must be related to broader policy questions which DOE and HEW will need to consider in meeting uniform standards for efficient use of energy in the nation's hospitals. For example,

- Hospital staff and administrators must be made aware of energy conservation opportunities and must be given access to the technical knowledge needed to implement changes;
- A financial environment must be created that effectively removes institutional barriers to energy conservation;
- The progress of energy management in hospitals must be monitored to determine what additional assistance is needed to produce effective conservation programs;
- Energy-related design and operating standards which are unnecessarily restrictive must be re-evaluated and changed, where appropriate, to allow energy-efficient operation.<sup>5</sup>

#### HITTMAN ASSOCIATES, INC.

The scope of work assigned to Hittman Associates was as follows:

1. Define water and water heating energy use in hospitals with respect to functional areas, e.g., diet kitchen, cafeteria, laundry, etc.
2. Review existing and proposed energy conservation measures for diet kitchen and laundry hot water.
3. Survey existing and proposed methods for energy-efficient water use with emphasis on diet kitchen and laundry applications, and review standards and regulations.

Preliminary work accomplished in these areas by Hittman Associates is reported in LBL's Annual Report for 1978.<sup>2</sup> The results of their continued study of hospital use of water in laundry and diet kitchen areas were published in July 1979 as an LBL report, Energy Efficient Water Use in Hospitals, Final Summary Report. The authors note that the data reported reflect criteria based on commercial acceptability factors, and recommend strongly that a research program be developed based on broad-based statistical sampling, using criteria that meet scientific standards for determining energy-efficient use of water in prototypic hospital settings.

Recommended for immediate implementation by hospitals are the following, none of which involves major expenditures:

- Comprehensive maintenance programs
- Laundry formula and equipment upgrading
- Use of 160°F water in laundries
- Use of cold water in floor and bathroom cleaning and dishwasher prerinse
- Use of low temperature water in dishwashers
- Reduction of water flow rate in X-ray film processing to two gallons/minute and/or install demand-only film processors
- Lowering of supply water temperature to 120°F
- Investigate the benefits of installing a laundry water heat reclaim system.

Hittman's investigation of federal, state and local health codes and standards related to hospital laundries and diet kitchens revealed great variability, which they regard as added reason for a comprehensive research program that would provide universally acceptable methods for contamination control in hospital procedures.

Table 1: Effectiveness of drying and ironing in destroying bacteria.

<u>Organism</u>	<u>Conditions</u>	<u>Log reduction in counts</u>	<u>Source</u>
A. Drying			
<u>E. coli</u> T3 phage	115°F <sup>a</sup> (washed at 100°F)	1.69 <sup>b</sup>	Wiksell et al., 1973
<u>Serratia marcescens</u>	115°F <sup>a</sup> (washed at 100°F)	3.84 <sup>b</sup>	Wiksell et al., 1973
<u>S. aureus</u>	115°F <sup>a</sup> (washed at 100°F)	3.23	Wiksell et al., 1973
<u>S. aureus</u>	185°F for 30 min.	b	Spillard, 1964
<u>B. stearothermophilus</u>	115°F <sup>a</sup> (washed at 100°F)	0.78	Wiksell et al., 1973
<u>M. pyogenes</u> ( <u>S. aureus</u> )	160°F for 30 min.	1.78	Ridenour, 1952
<u>M. pyogenes</u> ( <u>S. aureus</u> )	151°F for 15 min.	0.70	Ridenour, 1952
<u>S. aureus</u>	(washed at 100°F)	2.36	Walter & Shilling- inger, 1975
<u>Klebsiella pneumoniae</u>	(washed at 100°F)	0.59 <sup>b</sup>	
Undentified	180°F for 25 min.	b	Johnston, 1958
<u>Clostridium butyricum</u>	185°F for 30 min.	b	Spillard, 1964
<u>E. coli</u>	185°F for 30 min.	b	Spillard, 1964
<u>Pseudomonas arginosa</u>	185°F for 30 min.	b	Spillard, 1964
B. Ironing			
<u>Bacillus subtilis</u>	a	b	Arnold, 1938
<u>B. welchii</u>	a	b	Arnold, 1938
<u>B. megatherium</u>	a	b	Arnold, 1938
<u>B. coli</u>	a	b	Arnold, 1938
<u>B. pyocyaneus</u>	a	b	Arnold, 1938
<u>Streptococcus</u> sp.	a	b	Arnold, 1938
<u>Staphylococcus</u> sp.	a	b	Arnold, 1938
<u>M. pyogenes</u>	twice at cotton setting	3.91	Ridenour, 1952
Mainly <u>S. aureus</u>	350°F	0.4 to 1.4	Church & Loosli, 1953
Undentified	338°F for 1 min.	b	Johnston, 1958

<sup>a</sup>Details not further specified.

<sup>b</sup>Authors report no survivors.

Table 2. Reduction in counts of microorganisms after washing at various temperatures.

<u>Organism</u>	<u>Wash Temp. (°F)</u>	<u>Time</u>	<u>Log reduction in counts</u>	<u>Source</u>
Unidentified	165°	27 min.	>5 <sup>a,b</sup>	Arnold, 1938
<u>E. coli</u> T3 phage	154°	c	4.41	Wiksell, et al., 1973
<u>Serratia marcescens</u>	135°	c	5.19 <sup>a</sup>	Wiksell, et al., 1973
<u>Staphylococcus aureus</u>	135°, 155°	c	4.5	Wiksell, et al., 1973
<u>Staphylococcus aureus</u>	77°, 20 ppm Cl	c	>6	cited in Foter, 1960
<u>Staphylococcus aureus</u>	140°	5 min.	6.18 <sup>a</sup>	Walter & Schilling- inger, 1975
<u>Staphylococcus aureus</u>	140°	5 min.	>5	pers. comm.
<u>Staphylococcus aureus</u>	141°	5 min.	>5	Crone, 1958
<u>M. pyogenes var. aureus (S. aureus)</u>	140°	1 min.	4.27	Ridenour, 1952
<u>M. Pyogenes var. aureus (S. aureus)</u>	100°, 5 ppm Cl	15 min.	>4	Ridenour, 1952
<u>E. coli</u>	140°	1 min.	4.32	Ridenour, 1952
<u>E. coli</u>	100°, 100 ppm Cl <sup>d</sup>	5 min.	2.33	Ridenour, 1952
<u>B. stearothermophilus</u>	154°	c	1.71	Wiksell, et al., 1973
<u>B. stearothermophilus spores</u>	160°	15 min.	2.7	Ridenour, 1952
Polio virus	130°	10 min.	(no virus recovered)	Jordan, et al., 1969
Polio virus	110°, 200 ppm Cl	10 min.	(no virus recovered)	Jordan, et al., 1969
Polio virus	129° to 140°	c	>4.6	Sidwell, et al., 1971
Coliforms	123°, 15 ppm Cl	13 min.	4 <sup>a,b</sup>	Sandiford, et al., 1959
Coliforms	140°	13 min.	>6 <sup>a,b</sup>	Sandiford, et al., 1959
<u>Streptococcus faecalis</u>	149°	5 min.	>7	Jerram, 1958
<u>Chromobacterium prodigiosum</u>	140°	5 min.	>7	Jerram, 1958
<u>Klebsiella pneumoniae</u>	120°	13 min.	5.28	Walter & Shilling- inger, 1975

<sup>a</sup> Authors report no surviving bacteria.

<sup>b</sup> Counts in final rinse water.

<sup>c</sup> Time not specified.

<sup>d</sup> Not under actual washing conditions; washing E. coli seeded swatches produced 99.99% (4 log) reduction by removal by mechanical action alone.

## PLANNED ACTIVITIES FOR 1980

Final recommendations for revising ventilation and thermal standards for hospitals will be submitted in FY 1980.

## REFERENCES

1. David Rainer and George S. Michaelson, Chemical Contamination of Hospital Air, School of Public Health, University of Minnesota, Minneapolis, MN 55455, Lawrence Berkeley Laboratory Report, LBL-10475, EEB-Hosp 79-6 (January 1980).
2. Lawrence Berkeley Laboratory Annual Report, 1978, LBL-9576.
3. T. Alereza, A.J. Benjamin and B.R. Gilmer, Energy Efficient Water Use in Hospitals, Final Summary Report. Hittmann Associates. Lawrence Berkeley Laboratory Report, LBID-082 (July 1979).
4. D.R. Battles, D. Vesley and R.S. Banks, Hospital Laundry Standards and Energy Conservation: A Program Plan, Lawrence Berkeley Laboratory Report, LBID-156 (in process).
5. R. Pollack, Energy Conservation in Hospitals: Actions to Improve the Impact of the National Energy Act, Lawrence Berkeley Laboratory Report, LBID-111 (February 1980).

## ENERGY EFFICIENT WINDOWS PROGRAM

*S. Berman, R. Johnson, J. Klems, M. Rubin, S. Selkowitz, and R. Verderber*

## INTRODUCTION

Approximately 20% of the annual energy consumption in the United States is used for space conditioning of residential and commercial buildings, and about 25% of that figure is required to offset heat loss and gain from windows. In other words, 5% of national energy consumption, 3.5 quads annually, or the equivalent of 1.7 million barrels of oil per day, is tied to the thermal performance of windows.

An important aim of the Windows Program is to develop and commercialize innovative and effective window designs, materials and accessories that support national energy conservation goals. Of critical importance to our program is that design professionals and the public-at-large recognize, accept and use these products. To that purpose, we have developed a broad-scale program encompassing research and development activities, field demonstrations, market studies and an education and public information program. While the technical management of these projects is the responsibility of the Windows Group, certain portions of the work are subcontracted out.

## ACCOMPLISHMENTS DURING 1979

The work accomplished in FY 1979 comprises three major areas: (1) program planning and management, (2) performance testing and analysis, and (3) design strategies, materials, and prototype developments. Projected activity for 1980 is included in the detail presented below.

Program Planning and Management

The Windows Program Plan is being developed to outline and coordinate all DOE-supported energy conservation activities related to windows, and will interface with the DOE Thermal

Envelopes and Insulating Materials Program Plan and the Passive Solar Program Plan. Substantial efforts were made in 1979 to better coordinate with the DOE Passive Solar Program to avoid unnecessary duplication of effort. As a result of this activity, several joint programs are in progress or under discussion.

In our continuing concern that research activities have commercial potential and applicability, we have looked in detail at several subsectors of the window accessories market to understand the relationships between product manufacturers and the distribution and sales networks that provide building designers and managers as well as homeowners with product selections. Our immediate next concern is that technical data and non-technical information on energy-conserving window designs be readily transmitted to relevant professionals. To this end, we developed a publication, "Windows for Energy-Efficient Buildings," which reports on latest developments, patents, new materials and products, legislation, etc., and is circulated widely to architects, engineers, manufacturers, inventors, suppliers, code officials, and researchers. In the process of generating material for this publication, extensive product files, patent files, bibliographies and related information resources have been compiled.

Performance Testing and Analysis

Thermal Performance Testing. We have set up a Building Technology Laboratory in the College of Environmental Design of the University of California, Berkeley, to support our research and development activities, to provide independent tests and evaluations of materials and products submitted by subcontractors, and to permit evaluation of new products being introduced to the market. Testing facilities include a calibrated hot box (shown in Fig. 1), which is now being used to test the thermal performance of

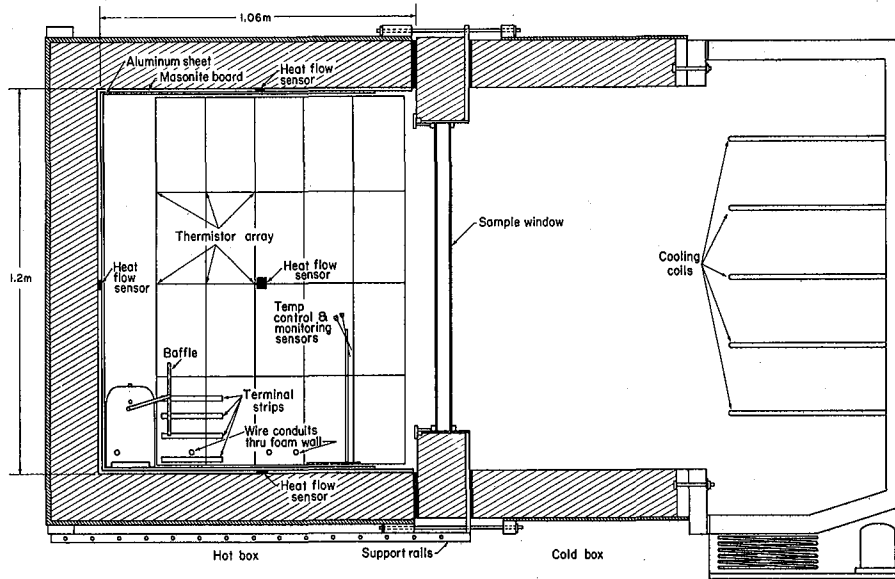


Fig. 1. Section through calibrated hot box showing hot and cold box chambers and sample window. (XBL 799-2921)

windows and associated energy-conserving accessories. Sample results are shown in Fig. 2. Infiltration tests on windows can now be made in our laboratory with the apparatus shown in Fig. 3. The heat loss and heat gain rate of windows can be improved with the use of thin-film coatings on glazing materials. We now have capabilities for measuring a range of optical properties of glazing materials and coatings, and additional measurement capabilities will be added in 1980. A solar calorimeter for measuring the solar heat-gain properties of windows is under construction and should be completed in FY 1980.

A major goal of our program is to develop and promote managed window systems, i.e., windows whose thermal/optical properties can be manually or automatically changed by building occupants. The laboratory testing facilities described above were designed primarily to conduct steady-state measurements of static materials and devices. Accordingly, we are designing a Mobile Window Thermal Test (MoWITT) facility to test the performance of managed window systems (see Fig. 4). As conceived, such a facility will permit the testing of net thermal performance of windows (combined infiltration, conduction/convection, radiation effects) as a function of window orientation and changing weather conditions throughout the day. Winter testing will be conducted in a cold, mountainous location and summer testing in a desert area. The thermal properties of each of the four test chambers in the MoWITT facility can be varied in terms of insulation level, thermal mass, and air-leakage rate, enabling us to simulate a wide range of building conditions. From these experimental results, we will be able to rank the performance of various window-management strategies as well as validate our analytical

models. Working drawings for the MoWITT facility are nearing completion, and construction is scheduled for late 1980. Development of software for its data-acquisition system is in progress.

**Analysis and Computer Modeling.** A detailed analytical model of the net heat transfer through a window assembly composed of an array of glazing elements and optical coatings was also developed this year. This model will also predict the performance of multiple-glazed windows in which the airspace has been filled with a low-conductivity gas. Additional capabilities will be added in the coming year.

A computer model for calculating optical constants for a variety of multilayer optical films was also completed. We calculated the spectral properties of various coatings in order to generate optical coefficients for analysis of visible and solar radiation transmission through windows, as well as thermal transfer between glazing layers.

In order to determine the effectiveness of window-management strategies, the performance of the window must be assessed in the context of the performance of the entire building. For these studies, we have used the Building Energy Analysis Program (DOE-2), modified to incorporate a variety of window management strategies such as movable shades and shutters and to provide detailed quantitative information on the hourly performance of windows and a more qualitative graphic perspective of the net gains and losses of windows on an hour-by-hour basis over the year. The performance of a variety of movable insulating devices for windows has been calculated by means of this model. Figure 5 shows the annual heating loads of a house in

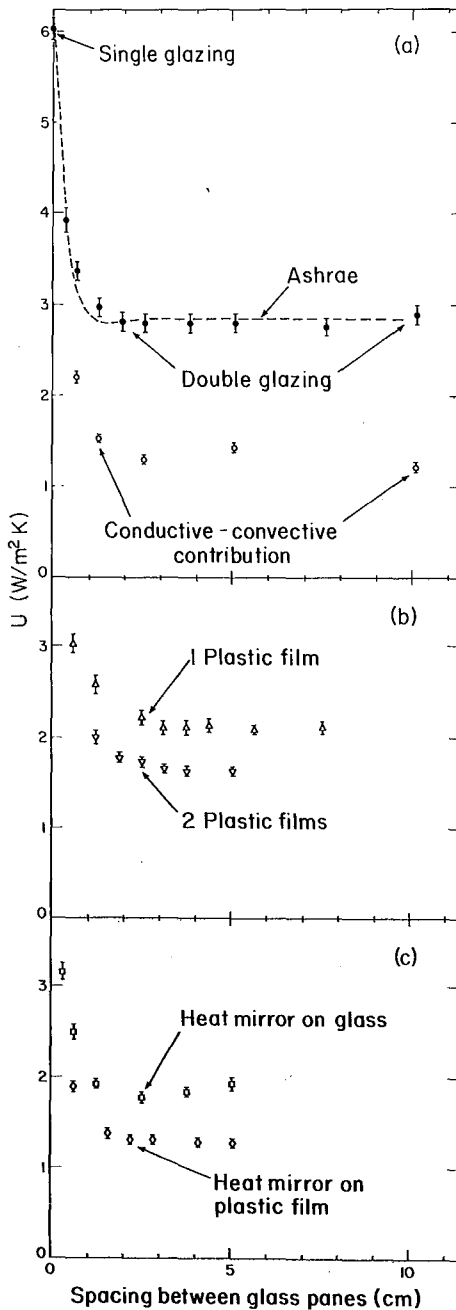


Fig. 2. Sample Thermal Transmittance vs. Glass Spacing for the Prototype Windows. (XBL 799-2917A)

- Ordinary double glazing (solid points) and double glazing with aluminum foil on inside of both glass panes (open circles).
- Double glazing with one (triangles) or two (inverted triangles) plastic films.
- Double glazing with heat mirror coating on plastic film, where the plastic film is mounted on the surface of one glass pane (squares) or suspended between panes (diamonds).

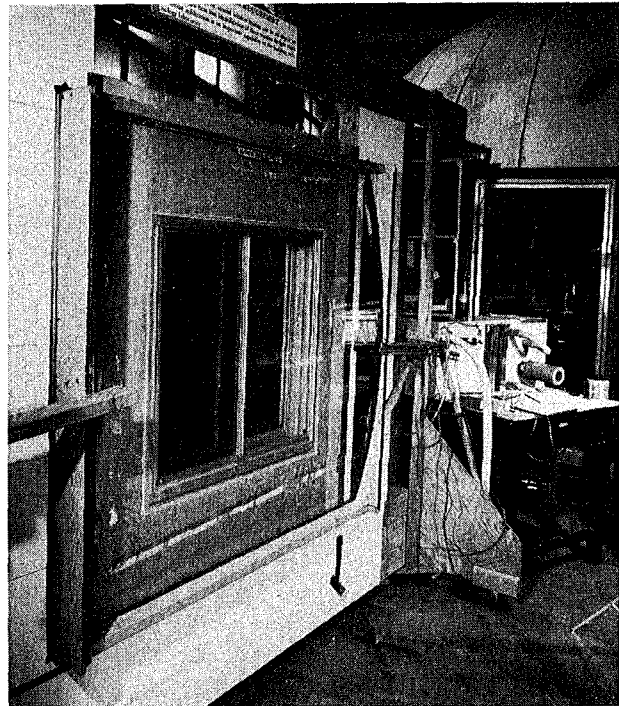


Fig. 3. View of apparatus for measuring air leakage of windows. (CBB 793-3731)

Minneapolis whose single- and double-glazed windows were fitted with a variety of insulating coverings that were closed for 12 hours each night. The effects of window orientation, window area, hours of operation and air-leakage characteristics of the window coverings may be just as important as the insulating value in determining annual energy savings. The foregoing studies are concerned with winter performance; in FY 1980, we will extend this work to include the effect of movable shading devices on cooling loads.

#### Design Strategies, Materials, Prototype Developments

**Daylighting.** Windows and skylights provide visible daylight in buildings, thus reducing lighting energy and peak power requirements. In addition, natural lighting has always been valued by architects and building occupants for qualitative reasons. In FY 1979, our daylighting program activities were significantly expanded.

In order to predict annual energy savings, data on daylight availability (including the frequency and intensity of daylight) must be collected. No source for such data currently

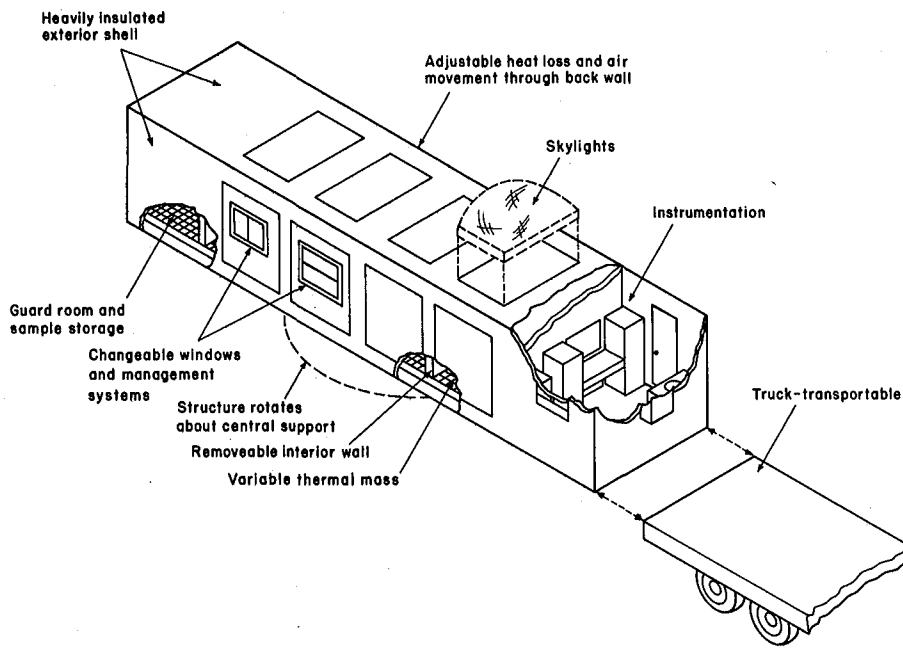


Fig. 4. Schematic view of Mobile Window Thermal Test (MoWITT) facility. (XBL 796-1848)

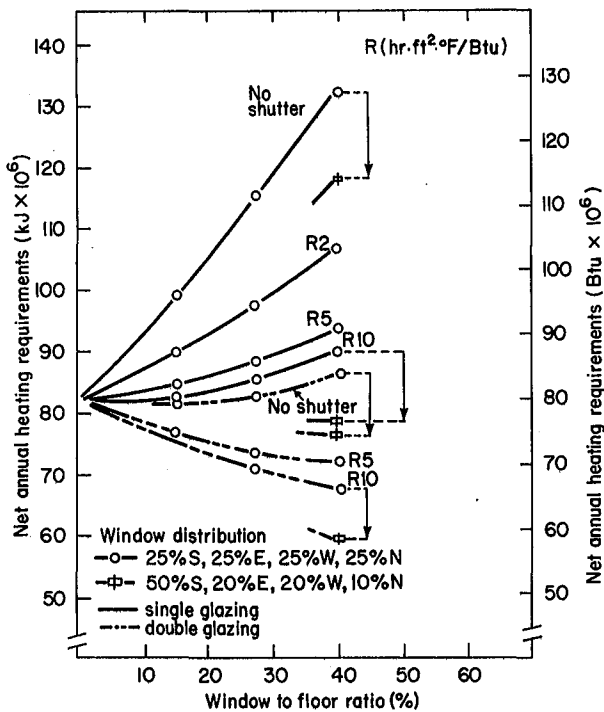


Fig. 5. Annual heating energy requirements for a house in Minneapolis based upon various glazing and insulating shutter options. (XBL 796-10097)

exists for most of the United States. The Pacific Gas & Electric Company Building in San Francisco has been instrumented to collect and record the amount of solar and visible radiation available at all building surfaces. An array of thirteen pyranometers and photometers has been installed to feed readings to a data-acquisition system at fifteen-minute intervals (see Fig. 6). Preliminary results for the first year of monitoring suggest strong linear correlations between illumination and insolation -- a finding which encourages us to believe that daylight availability data can be generated from existing measurements of solar radiation. A generalized method for developing illumination availability data from insolation is being developed.

Accurate and efficient daylighting design methods must be conveyed to building designers if they are to successfully incorporate daylighting designs in buildings. Three different approaches are in progress as part of the overall LBL program in this area: Under subcontract, Renssalleer Polytechnic Institute is developing a computer program to predict daylight illumination in interior spaces; a team at the University of Washington is developing a graphic design method which employs transparent overlays for daylight predictions; and, finally, an LBL project is underway to simplify design techniques (computational and graphic) for predicting daylight illumination from clear and overcast skies (Fig. 7). Activity in these

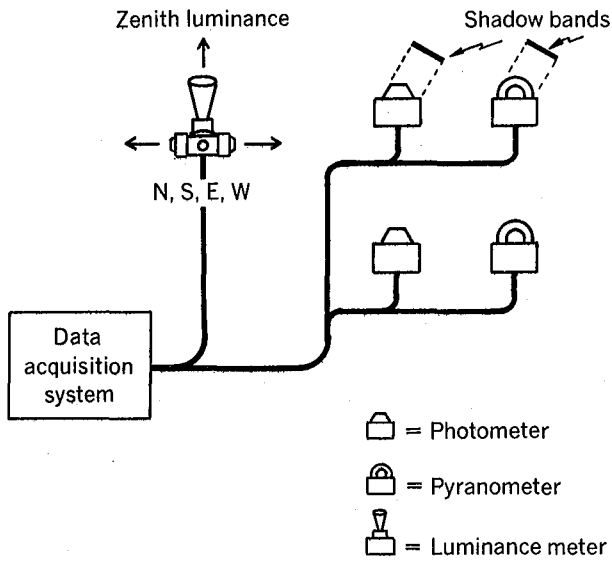


Fig. 6. Schematic of rooftop photometric and radio-sensor array for determining insolation/illumination correlations. (XBL 796-10182)

areas will continue in 1980 and a small effort to add daylighting analysis capabilities to a building energy analysis program (DOE-2) will be expanded.

Physical models are useful for studying alternative daylighting systems. To facilitate these studies, an artificial sky dome has been designed and built on the U.C. campus (Fig. 8). Luminance distributions for both clear and overcast skies will be reproduced on the underside of the hemisphere; by measuring light levels in a scale model building under this "artificial sky," we will be able to predict actual values expected in a real building. The addition of the lighting control system and an associated photometric measurement system in 1980 will make the artificial sky fully operational.

Direct sunlight is the only natural light source with sufficient intensity and collimation to illuminate interior spaces deep in the building, and various design approaches have been studied to exploit beam daylighting in buildings. Over the past two years we have examined

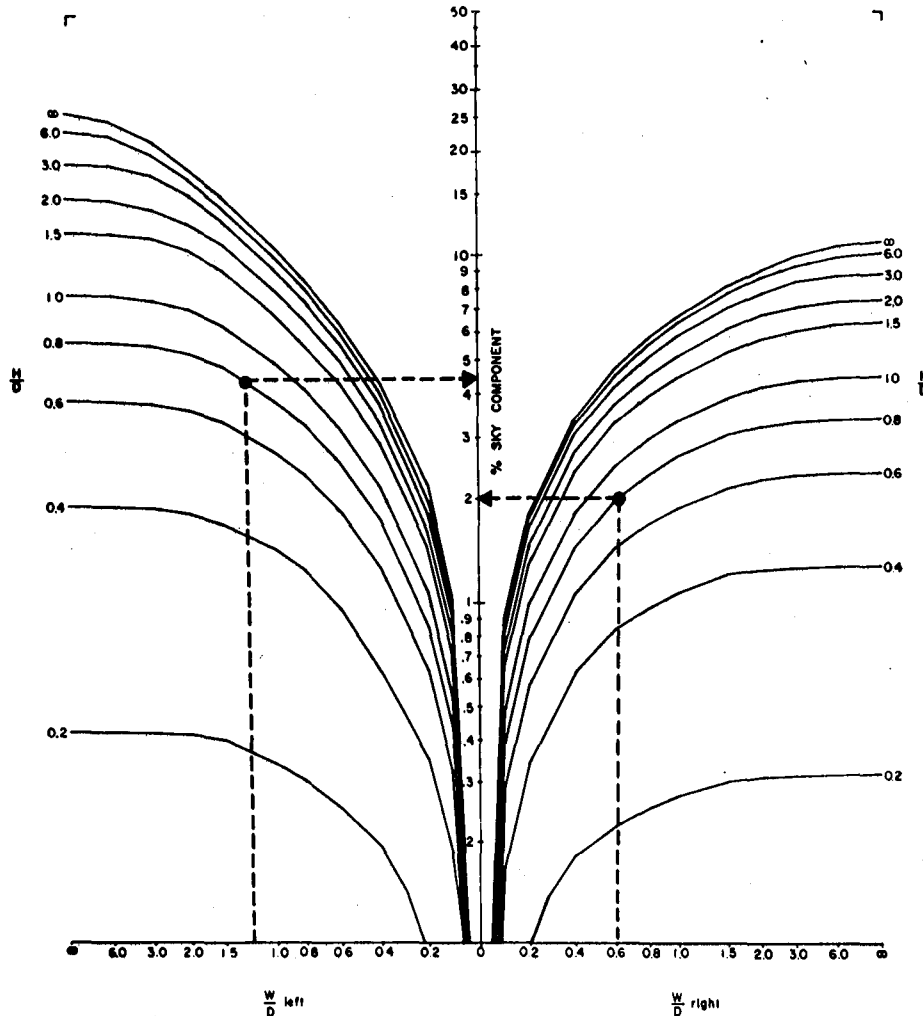


Fig. 7. Graph for determining sky component of daylight factor for clear sky conditions, sun altitude 40°. (XBL 803-8642)

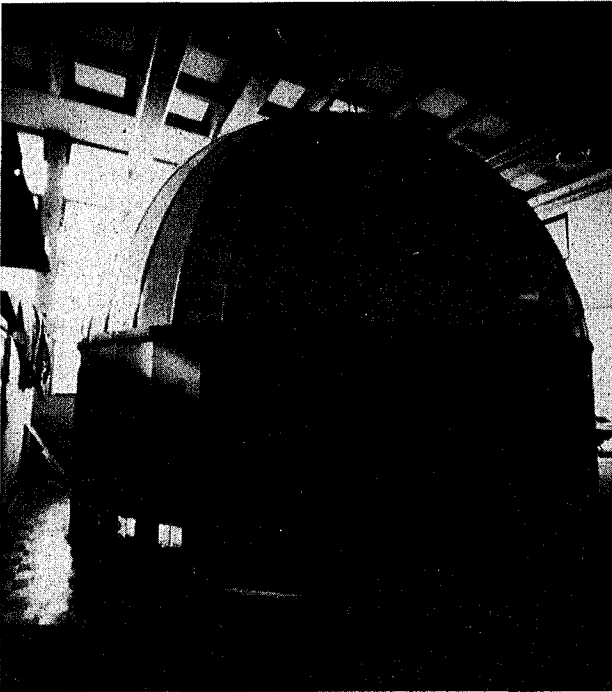


Fig. 8. Exterior view of artificial sky dome for daylighting studies. (CBB 803-2837)

the feasibility of using reflective devices mounted at the windows to take advantage of direct sunlight. In 1979, attention turned to using linear fresnel lenses as a possible alternative to mirror systems. Computer simulation and model testing in this area will continue in 1980.

We believe that daylighting techniques would be more widely used by architects and builders if technically accurate information was more accessible to them. For this reason, LBL has taken a lead role in developing a comprehensive educational program to fill this gap. A draft of our "Daylighting Resource Package," directed to educators and building designers and prepared in collaboration with the Illuminating Engineering Society, several universities, and daylighting experts throughout the country, will be available in summer, 1980. Over the next two years, the resource package will be refined, expanded, and disseminated widely.

Heat Mirror Commercialization. A transparent heat mirror is an optical coating applied to a glass or plastic glazing material that transmits the full solar spectrum but reflects long-wave infrared radiation emitted by room temperature surfaces. By reducing the radiative component of thermal losses, the heat transfer coefficient of a single- or double-glazed window is greatly reduced.

The development of transparent heat mirror coatings for plastic films has been successfully undertaken by subcontractors, although abrasion and corrosion resistance of the deposited coatings remains a problem area. It is possible

that heat mirrors may find their first use in sealed airspaces of new windows rather than as retrofits to single-glazed windows, as originally envisioned. For new windows, the coating can be deposited directly on glass or on plastic films which are then glued to the glass surface or stretched across the double-glazed airspace.

We have examined various window configurations incorporating multiple glass, plastic and coating layers (Fig. 9). Note that the best of the heat mirror window systems has a U-value approaching that of a well-insulated wall. A number of prototype window systems incorporating heat mirrors in different configurations were fabricated and tested in our calibrated hot box. The experimental results agree well with our computational models. We are currently planning to install prototype windows incorporating heat mirrors in test buildings to monitor their performance under field conditions. In 1980, we expect that several firms may be ready to introduce these heat-mirror windows to the market.

#### Convection-Suppression Window Prototypes.

Double-glazed windows frequently incorporate venetian blinds or similar devices between the glass panes to control light and glare as well as to provide privacy. These devices also help to reduce heat loss, although they have not been designed for that purpose. The Mechanical Engineering Department at the State University of New York, Stonybrook, is investigating the design and performance of mechanisms installed in the air space of double-glazed windows to suppress convective heat transfer (see Fig. 10). It appears that this modification of double-glazed windows may yield a heat-transfer rate approximating that of an insulated wall. Prototypes of such devices with a thermal resistance of R5 in an open mode and R10 in a closed mode have been built and tested. A heat-transfer gauge with a cross section of approximately 20 ft<sup>2</sup> was built so that full-sized windows could be tested. Interferometric techniques were used to examine heat transfer in the airspaces created by the parallel slats. Initially, ideal airspaces, i.e., with no air leaks, were examined. When the slat-to-glass clearance was increased to as much as 1/8 inch, the heat-transfer rate was not seriously increased. These results suggest that building products with a comparable level of thermal performance could be successfully manufactured.

Triple and quadruple glazing systems will further reduce heat loss through windows although solar gain may be sacrificed due to surface reflection losses. Replacing window glass with a thin plastic film coated to be anti-reflective solves this problem effectively. These lightweight, high-performance window systems have been studied by means of computer simulation, and prototypes tested in our laboratory show good agreement with the model. Although the performance of these systems does not match that of multi-glazed units incorporating transparent heat mirrors, they are not as susceptible to corrosion as units using heat mirrors.

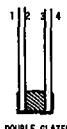
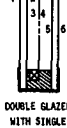
	TOTAL GAP (cm)	c	SURFACE	GAS	ΔT (K)	SOLAR TRANSMITTANCE	U (W/m <sup>2</sup> ·K)	CALCULATED OR REQUIRED	SOURCE (Ref)
 DOUBLE GLAZED WINDOW	.6	.065	3	Air	10	--	2.7	meas.	Glaser (19)
	1.2	.065	3	Air	10	--	1.8	meas.	Glaser
	1.2	.065	3	Krypton	10	--	1.0	meas.	Glaser
	1.6	.065	3	Air	10	.45 visible (est)	1.6	meas.	Glaser
	2.0	.1	3	Air	20	.37 visible	1.5	calc.	Karlson & Ribbing (34)
	1.2	.15	3	Air	--	--	1.9	calc.	Rafilio (16)
	1.27	.20	3	Air	22	.70	1.99	calc.	(ASHRAE Data)
	1.27	.05	3	Air	22	.63	1.70	calc.	(ASHRAE Data)
	1.2	.06 (est)	3	Low Cond	--	.15-.49	1.4-1.5	meas.	Flachglas literature
	.64 - 1.27	.1	3	Air	22	.04-.3	1.7-2.8	meas.	Commercially Available
 DOUBLE GLAZED WITH SINGLE PLASTIC INSERT	3.8	.20	3,4	Air	--	.59	.89	calc.	Johnson (36)
	2.54	.05	4	Air	10	.56	1.19	calc.	
	1.8	.05	4	Air	10	.56	1.43	calc.	
	1.8	.05	4	Argon	10	.56	1.33	calc.	
	1.8	.05	4	Krypton	10	.56	.87	calc.	
	1.8	.20	4	Air	10	.63	1.60	calc.	
	2.54	.05	5	Air	10	.50	1.01	calc.	
	1.8	.05	5	Air	10	.50	1.25	calc.	
	1.8	.05	5	Argon	10	.50	1.15	calc.	
	1.8	.05	5	Krypton	10	.50	.72	calc.	
 DOUBLE GLAZED WITH DOUBLE PLASTIC INSERT	3.8	.06	7	Air	10	.46	.49	calc.	
	1.8	.05	7	Air	10	.46	1.24	calc.	
	1.8	.05	7	Argon	10	.46	.97	calc.	
	1.8	.05	7	Krypton	10	.46	.64	calc.	
	3.8	.06	3,6	Air	10	.42	.44	calc.	
	1.8	.05	3,6	Air	10	.42	1.24	calc.	
	1.8	.05	3,6	Argon	10	.42	.95	calc.	
	1.8	.05	3,6	Krypton	10	.42	.61	calc.	

Fig. 9. Thermal performance characteristics of various high performance window designs. (XBL 796-10098)

**Movable Insulation.** We have calculated and measured the thermal performance of a large number of movable insulation systems for windows. (Some results are described in the Analysis and Computer Modeling Section.) Calculations and laboratory measurements are now being supplemented with large-scale field testing of products in buildings.

The Insulating Shade Company in Branford, CT, has developed a multilayer, aluminized plastic roll-up shade with a thermal resistance of 12 in its deployed mode (Fig. 11). Two hundred such shades have been installed in a college dormitory, and energy savings are being monitored by means of a data-acquisition system designed and built at LBL. Patterns of occupant use of these shades will be studied and attempts may be made to motivate occupants to use the insulating devices more effectively.

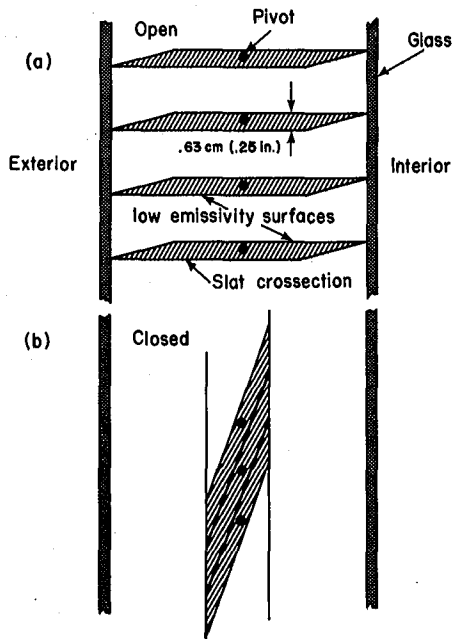


Fig. 10. Schematic cross-section of open and closed convection suppression window prototype. (XBL 796-1099)

**Selective-Reflectance Coatings.** Reflective and/or tinted glass is widely used in many commercial buildings to reduce solar impact and, thus, energy requirements for air conditioning. However, this glazing will also reduce the amount of daylight illuminating interior spaces and thus increase energy used for electrical lighting.

Since approximately one-half of the sun's radiation is short-wave infrared, which contributes nothing to illumination, an optical coating that selectively reflects this infrared but transmits visible light could, ideally, reduce cooling loads by 50% without reducing available illumination. Under subcontract, Kinetic Coatings, Inc., has used novel ion-beam sputtering techniques to produce durable, weather-resistant selective coatings that can be applied to the outside of a window where they function effectively in a solar-control mode. A wide range of selective-reflectance coatings and protective layers has been produced and tested for both optical performance and weatherability (Fig. 12). In 1979, Kinetic Coatings, Inc., focussed their efforts on scaling-up the sputtering deposition system to provide coating uniformity over a larger sample size. Results to date show a uniformity of ± 5% in optical properties over a

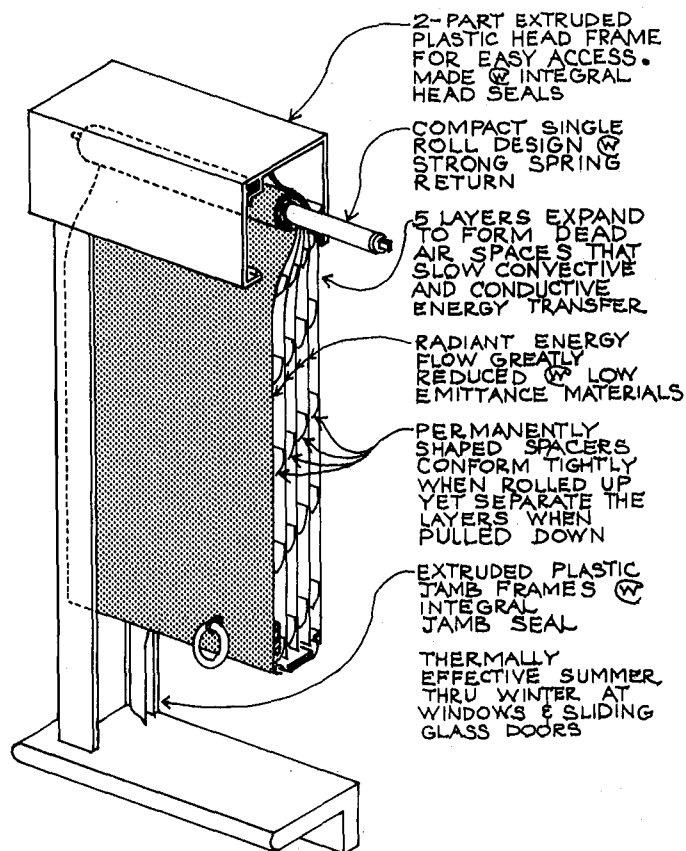


Fig. 11. Cross-section of multilayer insulating window shade. (XBL 803-8641)

1.5 ft<sup>2</sup> area. Indications are that these methods can be further refined so that glass of architectural size can be coated with equal or better uniformity.

**High-Performance Sun Control Systems.** Conventional venetian blinds are reasonably successful in reducing solar heat gain through windows. To improve their performance, Stevens Institute of Technology in Hoboken, NJ, is testing and evaluating a new class of highly reflective venetian blinds expected to transmit 50% less summer heat than conventional blinds. Test results from this program will be compared with existing methods of calculating the performance of blinds.

**Air-Flow Window Systems.** Among the options being studied for high-performance window systems are those designed to control heat transfer by using air flow between multiple panes of glazing. These systems offer thermal performance advantages in winter (by reducing net heat losses through the windows and collecting useful solar gain) and in summer (by reducing cooling loads) without sacrificing daylighting potentials year-round.

One such window system of interest to our program is the "Clearview" solar-collector win-

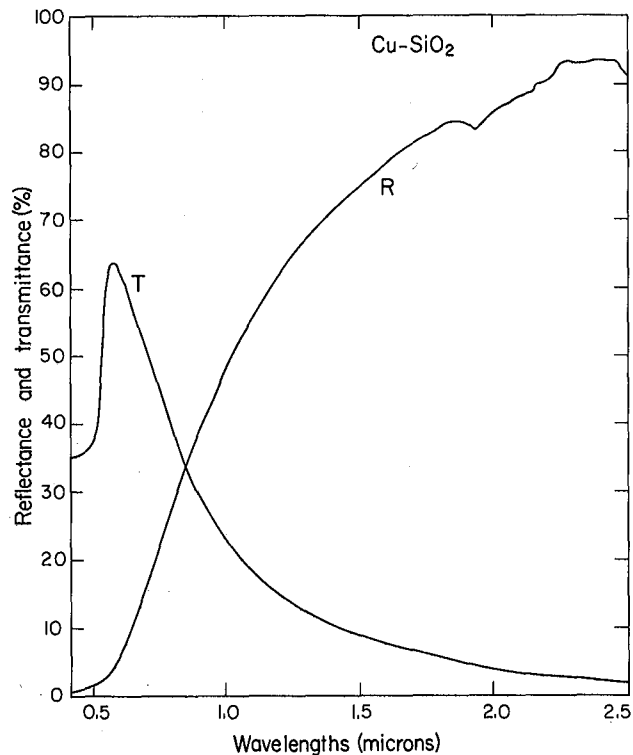


Fig. 12. Normal spectral transmittance and reflectance of selective solar control film with increased visible transmittance; glass substrate (1/8") - Cu (78A) - SiO<sub>2</sub> (500A); weighted spectral averages, T solar = 42%, T visible = 60%.

(XBL 792-512)

dow developed by researchers at the Environmental Research Laboratory (ERL) at the University of Arizona. Designed for residential applications, this window system is being analyzed in detail by ERL for its performance capabilities, and will be field-tested in the upcoming heating and cooling season.

Another approach to designing air-flow windows has been used in Europe for many years. Windows are constructed with cavity ventilating ports that permit air to pass between double or triple glazing at rates controlled by HVAC system pressures (Fig. 13). Venetian blinds in the glazing cavity absorb the sun's heat in the winter and the air flow over the blinds carries the heat throughout the building. Similarly, the heated air can be exhausted from the building in summer to reduce cooling loads. This approach lends itself to many different system configurations that will be investigated by the University of Utah under subcontract. The performance of exhaust air windows and conventional multiple glazed windows will be compared, side-by-side, in a test building designed to rotate so that all window orientations can be evaluated. Test results will be used to assess their marketability in the United States.

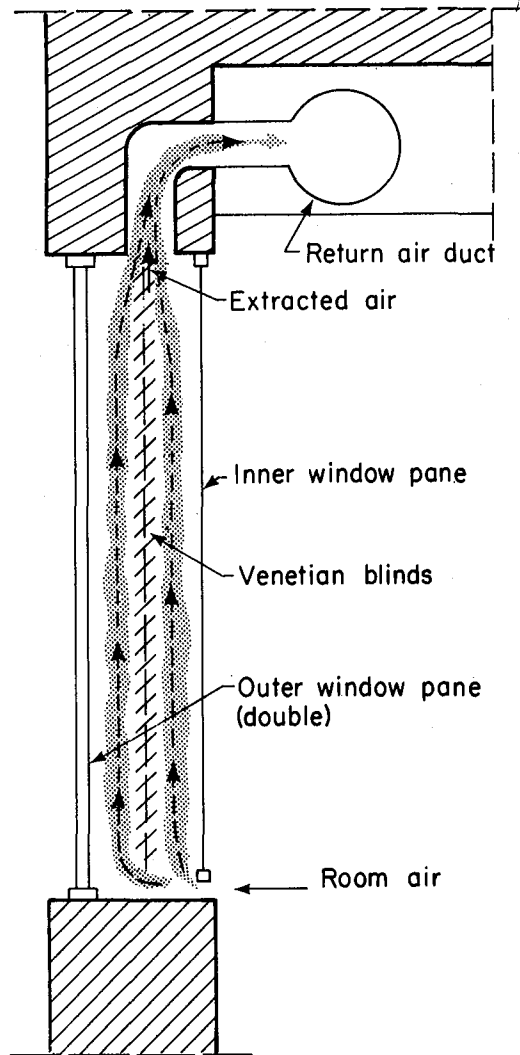


Fig. 13. Schematic cross-sections for air-flow window system. (XBL 7912-13366)

## ENERGY EFFICIENT LIGHTING PROGRAM

*S. Berman, R. Clear, J. Klems, F. Rubinstein, S. Selkowitz, and R. Verderber*

### INTRODUCTION

The Energy-Efficient Lighting Program of the Lawrence Berkeley Laboratory is carrying out comprehensive research, development, and demonstration activities emphasizing the commercialization of energy-efficient and cost-effective lighting.

Lighting accounts for 25% of the electrical energy generated in this country every year or about 6% of total energy consumption. This amounts to some 440 billion kilowatt-hours of electricity, which may be broken down by end-use as follows:

	Percentage
Residences	20
Stores	19
Industry	19
Offices	10
Outdoors	8
Schools	7
Streets and highways	3
Other indoor uses	14

We estimate that approximately 50% of the electrical energy consumed for lighting, or

about 12% of total electrical sales, could be saved by replacing existing lighting with energy-efficient lighting. This changeover is timely, given the widespread concern about the rising cost of electrical energy. Furthermore, the rapid turnover in most lighting stocks is conducive to the substitution of new, more efficient products.

The broad objectives of our program are:

1. To foster the development of energy-efficient lighting technologies, strategies, and design methods by helping the lighting community (product manufacturers, design firms, professional organizations, and government agencies) to achieve energy-efficient lighting.
2. To minimize any possible adverse social, economic, and environmental impact connected with introducing energy-efficient lighting technologies and lighting-design practices.
3. To provide information so that lighting users, designers, and purchasers can make informed choices on lighting effectiveness and cost/benefit.
4. To assist in removing institutional barriers to adopting efficient lighting.

An important activity of the Energy-Efficient Lighting Program is to make the public aware of LBL's commercialization efforts. We provide information by distributing reports, giving public addresses, and holding meetings, and by maintaining contacts with private persons and many public and professional organizations concerned with lighting.

Among the more prominent organizations with whom we regularly exchange information are the Illuminating Engineering Society, the Institute of Electrical and Electronic Engineers, the American Institute of Architects, the American National Standards Institute, and the Underwriter's Laboratory. As for consumer organizations, we have contacts with trade associations such as the Building Owner's Management Association and government purchasing groups such as the General Services Administration. Most of our information comes from research and development carried out by subcontractors, by the LBL Lighting Laboratory, and by the demonstration projects managed by LBL.

Prior to 1979 we worked primarily on developing new lighting technologies for the commercial and industrial sector. In 1979 we extended our work to the residential sector. The technologies being developed are described in the following paragraphs.

## ACCOMPLISHMENTS DURING 1979

### High-frequency Solid-state Fluorescent Ballast

The two-and-a-half-year project on developing high-frequency solid-state fluorescent ballasts for the two 40-watt T-12 lamps is expected to be completed this year. The ballasts were developed for LBL by Stevens Luminoptics and IOTA Engineering, and have been used successfully for over a year and a half in a demonstration project at the Pacific Gas and Electric Company (PG&E) headquarters' office building in San Francisco. The ballasts reduced energy consumption for in situ lighting by at least 25% and operated safely and reliably, causing no discomfort to users. In 1980, small quantities of these solid-state electronic ballasts will be available for purchase, and stocks will be built up rapidly in the following years. A summary report on the demonstration data was presented at the International Illuminating Engineering Society meeting in Japan in August 1979. The general lighting community concurs with LBL that the project has been a success.

Complementary to the work of the lamp industry, a test of standard fluorescent lamp life has been carried out in the LBL Lighting Laboratory (located in Wurster Hall at the University of California, Berkeley), and the positive result has advanced the commercialization of the electronic ballast. The fluorescent lamps driven by the Stevens ballast are still functioning properly after 12,000 hours of testing, confirming that operation at high frequencies will not shorten lamp life.

### Efficient Fixtures

The successful work on the electronic ballast stimulated an attempt to develop an energy-efficient fixture that would take advantage of the lighter-weight ballast and use coatings to increase transmission and reflection abilities.

A lighting fixture has a pronounced effect on the overall efficiency of a lighting system by virtue of its coefficient of utilization. One way of raising the coefficient is to increase the useful light delivered by a fixture by improving the reflectivity and transmissivity of reflectors and lenses. The Optical Coating Laboratory, Inc., under contract to LBL, has applied multilayered, thin-film coatings to reflectors and lenses to see how the coatings would affect fixture performance. Two types of high-intensity-discharge (HID) fixtures have been designed, one for outdoor and one for indoor use. The outdoor fixture employs a high-pressure sodium lamp and the indoor fixture a metal halide lamp. The fixtures have been tested for efficiency with and without the thin-film coatings; results are given in Table 1.

Table 1. Reflectance of Coilzak<sup>(R)</sup> specular lighting sheet with and without optical coatings.

	(Percentage)			
	Single reflection		Multiple Reflections	
	Hemispherical		2nd	4th
Total**	Specular**			
Coated	94	92	85	72
Uncoated	83	78	61	37

\*Dian TR-1 Reflectometer  
 \*\*Cary 14 Spectrophotometer  
 (R) Alcoa Trademark

For a single reflection, the reflectivity of the coated Coilzak<sup>(R)</sup> improves by more than 10%. For multiple reflections (very common in fixtures), the improvement is more than 50%. According to Lighting Science, Inc., an independent testing laboratory, the improved performance increases the coefficient of utilization as follows:

Reflector	Lens	Coefficient of Utilization (%)
Uncoated	Uncoated	63.55
Coated	(No lens)	79.73
Coated	Coated	75.42

In further studies, we intend to determine the cost-effectiveness of the coating procedure.

#### Residential Adaptive Circline Fluorescent Lamps

LBL awarded a contract to the EETech Corporation to develop a solid-state ballast for the operation of a circline fluorescent lamp. The system will be packaged with an Edison-type base so that it will fit standard residential incandescent light-bulb sockets.

The ballast circuit has been designed to be manufactured as an integrated circuit, which will reduce the size, weight, and cost of the ballast. The light output is equivalent to that of a 150-watt incandescent bulb (2,200 lumens). In addition, the ballast permits the fluorescent lamp to be dimmed to accommodate different lighting needs.

EETech has delivered eight ballast-lamp systems to LBL. Table 2 compares the performance of the EETech system using the electronic ballast with other circline lamps operated with commercial core-coil ballasts and incandescent lamps. As indicated, the EETech design is >10% more efficient than the core-coil types.

Note: The lamp designations may be decoded as follows: "FC" is circline fluorescent; "12," "6," "10," is the lamp diameter in inches; "T10," "T9" is the diameter of the lamp tube in one-eighth inches (i.e., 10/8 inches);

"ww" means warm white color; and "sw" means soft white color. The second set of data (in parentheses) for the EETech system shows its performance when dimmed.

Figure 1 shows two photos of the adaptive circline lamp and ballast fitted into the ceiling socket for a standard incandescent lamp. Once the diffuser is in place (Fig. 1b), the occupant cannot tell whether the lamp is fluorescent or incandescent. Compared to the incandescent lamp, the circline fluorescent improves efficiency by more than 60%.

#### Switching and Controls

Few buildings today have lighting-control systems; yet the energy savings that could be achieved if controls were used is estimated at over 50%. Our objective is to compare the performance and cost-effectiveness of several systems and to publicize our findings. We anticipate that the widespread commercialization of control systems--those available today as well as those still in the research and development stage--will gain in importance and that demand for these systems will increase as their usefulness becomes known.

LBL has organized two demonstrations to assess the energy savings of different switching and control strategies. Honeywell, Inc. has supplied the lighting-control system for the first demonstration, and we have installed it on one floor of the San Francisco PG&E building and are collecting data. The system controls groups of lamps and can dim the lamps over a continuous range of lighting levels. General Electric will supply the control system for the second demonstration, to be carried out in the World Trade Center in New York. This system allows only on-off control, but fixtures can be individually controlled. The second demonstration will start in early 1980. Both contractors have done marketing studies that indicate a large potential market, primarily for new construction. At present, it is not cost-effective to install these control systems in existing buildings because of the block manner in which lighting systems have been wired. However, wiring codes in California require that the periphery light-

Table 2. Comparative performance of circline fluorescent-lamp systems and 100-watt incandescent lamps.

Lamp	Commercial products with core-coil ballasts			EETech system with electronic ballasts	Incandescent
	FC12T10ww	FC6T9ww	FC10T9sw	FC10T9sw	
Power (watt)	35	21	44	44 (19.5)	100 W
Light (lumens)	1226	700	1812	2018 (790)	1750
Efficacy (lumens/watt)	35	33.3	41.2	45.8 (40.5)	17.5

ing of new buildings be independent of the interior lighting, a modification that will substantially reduce the cost of installing automatic control systems.

The demonstration data on the two systems will help in evaluating different control strategies, such as daylighting, group vs. single, continuous vs. step-dimming. For instance, the data will be used to verify the accuracy of a computer program being developed by Smith, Hinchman, and Grylls, under subcontract to LBL, to predict the energy savings that can be realized by using various types of lighting controls, strategies, and maintenance practices.

Daylighting projects related to lighting controls are covered in the Windows section of this report.

#### Solid-state Ballasts for High-intensity-discharge Lamps

LBL awarded contracts to three firms for developing a solid-state ballast for operating high-intensity-discharge (HID) lamps. Each contractor has been required to deliver six units for testing at the LBL Lighting Laboratory. The

preliminary results indicate that high-pressure-sodium (HPS) lamps are 15-20% more efficient when operated at high frequency with solid-state ballasts (combined ballast and lamp efficacy).

#### Energy-Efficient Light Bulbs

During 1979, we also made preliminary plans for initiating a new project to develop an energy-efficient replacement for the standard incandescent lamp. The project will begin in 1980 with a public competition inviting companies in the lamp-development field (by a Request for Proposal procedure) to elaborate a cost-sharing proposal aimed at achieving accelerated commercialization of an energy-efficient incandescent replacement. The project will have three phases, the first of which should be completed in the latter part of 1980 with the delivery of a pre-manufacturable prototype for testing at LBL. We intend to have several firms working on the problem so that a number of different concepts can be evaluated.



Fig. 1a. Adaptive circline fixture.  
(CBB 790-15389)

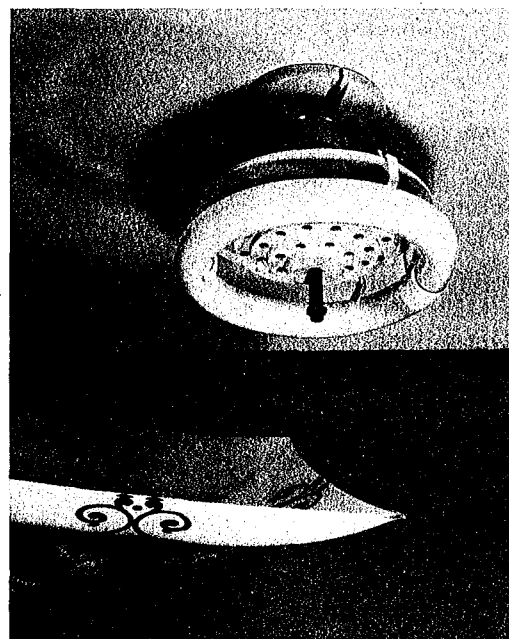


Fig. 1b. Adaptive circline fixture with  
diffuser.  
(CBB 790-15387)

## PLANNED ACTIVITIES FOR 1980

Besides continuing the above projects, we will begin work in two new program areas: sensors and controls, and visual performance. To study sensors and controls we will set up two new demonstration projects. The sensors project will test the energy that can be saved by introducing a personnel detector that senses room occupancy, turning lights on or off according to the presence or absence of occupants. The demonstration will take place in an office building in New York City; work will be carried out in conjunction with the New York State Energy Research and Development Authority and the Tishman Research Company. The controls demonstration, which will also take place in an

office building, will determine the appropriate placement of photodetectors to optimize the performance of control systems in daylight spaces.

The visual-performance program will analyze the theoretical implications of previous research and initiate simple and direct experiments in cooperation with the faculty of the University's School of Optometry. We intend to examine the information requirements that relate energy efficiency in lighting to lighting standards. We will consider the impact of visibility, visual performance, and overall productivity on both the introduction of new lighting technologies and the development of energy-performance standards for the entire building.

## CONSERVATION POTENTIALS: COMPILATION, PUBLICATION, AND DEMONSTRATION

*A. H. Rosenfeld, H. Arin, M. Maulhard, A. Meier, J. Poling, L. Schipper, L. Wall,  
and J. Wright*

The Building Energy Compilation and Analysis (BECA) Group, initiated in 1976, compiles the results of energy-conservation research performed at LBL and other laboratories worldwide, and publishes comprehensive tables of conservation options, ordered by annual return on investment. We advise utility companies, local governments, and the State of California on conservation options, and promote demonstrations and training in retrofitting.

### PUBLISHED REPORTS, DATA BASE AND OTHER ACTIVITIES

#### Some Potentials for Energy and Peak Power Conservation in California.<sup>1</sup>

In this report, we analyzed known conservation measures for buildings and appliances, and ranked them by cost of conserved energy (in \$/barrel saved). Tables of conservation options were presented in order of maximum return on investment. We calculated that, if these options were implemented over 10 years, the following savings would result: about 30% each in natural gas and electric energy, and nearly 50% in peak power, compared with 1975 consumption. The annual savings to the California consumer would be about \$1 billion in natural gas and \$1 billion in electric bills (at 1975 prices). This saving, if redirected from energy purchases to more typical and labor-intensive purchases, would create about 60,000 jobs in California. Moreover, the \$5 billion initial cost of a 10-year program would be more than offset by a 12 gigawatt reduction in peak-power demand, which would permit deferring the construction of new plants, whose total cost would be about \$10 billion.

In a similar vein, we published Energy Conservation through Appliance Labelling: Facts and Fact Sheets<sup>2</sup> in 1978; Conservation Options in Residential Energy Use<sup>3</sup> in 1977; and Saving Half of California's Energy and Peak Power by Long-range Standards and Other Legislation<sup>4</sup> in 1978. We are now expanding the data base on end-use of energy and conservation options on which these reports were based. New projects are:

Low-Cost/No-Cost Residential Conservation Measures. During 1979, as prices for home heating oil rose toward \$1/gallon, there was revived interest in retrofitting homes and in legislation providing new incentives for home audits and retrofitting. Accordingly, we updated our existing data on California and collected additional data on cities in other parts of the country. Some of this work is reproduced in Fig. 1 and Tables 1 and 2.

BECA: An International Comparison and Critical Review. The Review will consist of three parts, which are to be updated and republished regularly:

Part A: Single-Family Residences

Part B: Retrofitting of Residences

Part C: Commercial Buildings

Part A will be published for the first time in Energy and Buildings in April 1980; it was compiled by eleven researchers from North America and Western Europe.<sup>5</sup> It gives data on the fuel energy used for space heating in single-family residences in the U.S., Canada, and

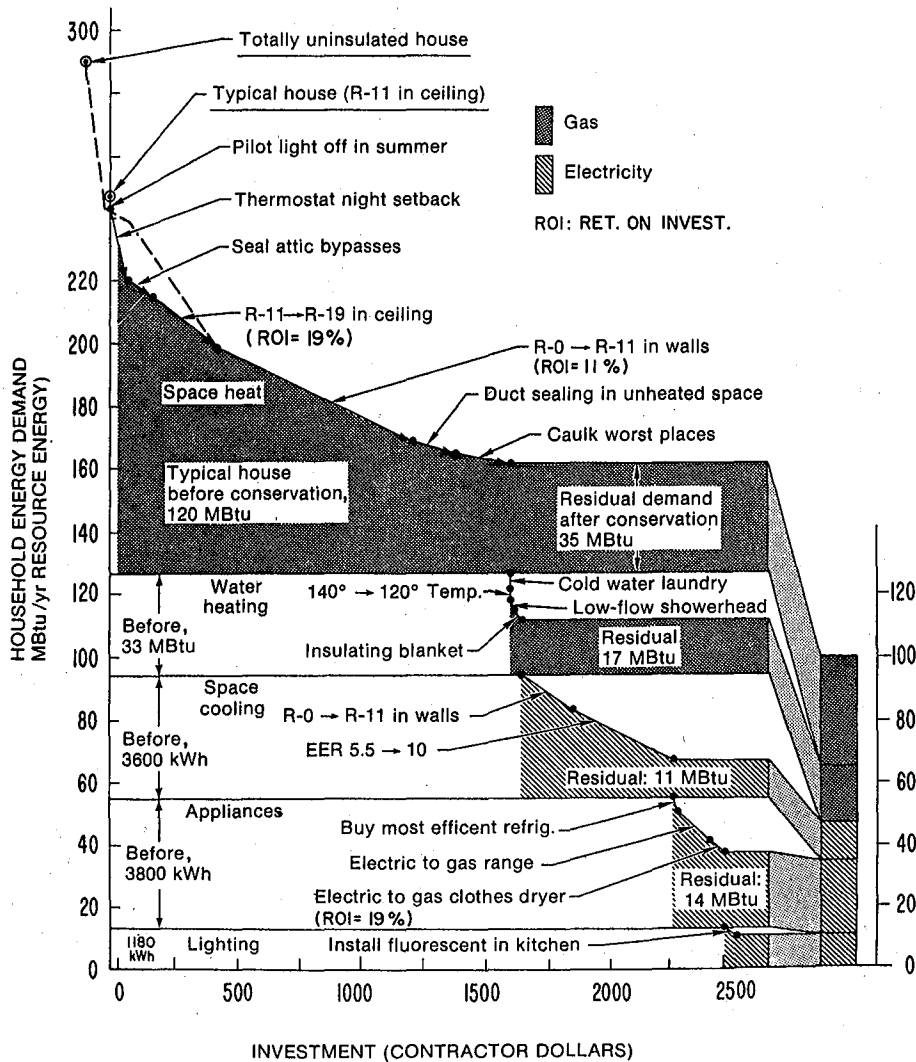


Fig. 1. Conservation potential for a Northern California single family home (1200 ft.<sup>2</sup>, 3000 heating degree days). From Maulhardt, Meier, Newbold, Rosenfeld, and Wright, LBL-5926 (rev. 11/79), Lawrence Berkeley Laboratory, Berkeley, CA. (XBL 7910-13101)

Western Europe. Three classes of data are plotted and compared: (1) calculated data determined by computer simulation or by simplified calculation, (2) housing-stock data obtained from gross consumption figures in given countries for a given year, and (3) measured data for individual dwellings built as (or modified into) energy-efficient houses. The computer simulations calculate the energy used to heat a residence constructed according to current building codes or practice. A description of optimum construction, based on minimum life-cycle cost, is given for the U.S., and data on the cost of moving from one construction level to another are provided. The combined results on actual houses show the low annual fuel requirements for space heating that can be achieved in new houses and by retrofitting existing ones. In most existing houses, the space-heating requirements can be reduced by about 50% with an investment of \$1,500. In new houses, a reduction of more than 60% can be achieved by investing \$1,500 in

improvements over and above those called for in current practice.

Topics covered briefly in Part A are: other energy-conservation designs such as passive solar heating and insulating shutters or shades; and indoor air quality in tight houses, including radon concentrations.

Figures 2, 3, and 4 are from BECA, Part A.

Storage of Heat and Coolth in Hollow-Core Concrete Slabs. Swedish Experience, and Application to Large, American-Style Buildings.<sup>6</sup> We have collaborated with a team of Swedish researchers to produce a report on the storage of heat and "coolth" in hollow-core concrete slabs. We analyzed the Folksam office building in Farsta, near Stockholm, which has been functional since December 1977, with an energy use for direct space heating of only 60 kWh/m<sup>2</sup> (19,000 Btu/ft<sup>2</sup>), half the Stockholm average for

Table 1. Lo-cost/no cost residential conservation measures - Northern California (Travis AFB).

We assume a 1200 square foot house, with R-11 in the attic, and no night thermostat setback in a climate of 2400 heating degree days and 1200 cooling degree days. Before retrofit, the house used 1200 therms (or 21,200 kWh) for space heating, 3600 kWh for air conditioning, 330 therms (or 5000 kWh) for water heating and 1200 kWh for refrigeration. The seasonal efficiency of the furnace/duct system before retrofit was taken as 60%.

Measure	Alternative Costs			Annual Savings			
	By			Electric kWh	Natural Gas		
	Contractor	Deluxe	Simple		@5c/kWh	Therms	@30c/Th
1. <u>Low Temperature Laundry</u> warm wash/cold rinse or (all cold water)	\$0 (\$0)	\$0 (\$0)	\$0 (\$0)	600 (1000)	\$30 (\$50)	35 (50)	\$11 (\$15)
2. <u>Reduce Hot Water Temperature</u> 140 deg. to 120 deg. or (140 deg. to 110 deg.)	\$0 (\$0)	\$0 (\$0)	\$0 (\$0)	350 (520)	\$17 (\$26)	25 (35)	\$8 (\$11)
3. <u>Shower Flow Restrictors</u>	\$20 <sup>a</sup>	\$8	\$1	750	\$38	35	\$11
4. <u>Blanket on Water Heater</u>	\$30 <sup>a</sup>	\$20	\$5	350	\$18	24	\$7
5. <u>Other Turnoffs</u>							
a. Furn. Pilot Off in Summer	\$0	\$0	\$0	-	-	35	\$11
b. Refrig. Anti-Sweat Switch	\$0	\$0	\$0	120 <sup>b,c</sup>	\$6	-	-
c. Second Refrigerator	\$0	\$0	\$0	900 <sup>b,c</sup>	\$45	-	-
6. <u>Heating and Cooling Systems</u>							
a. Set Back Furnace Fan Thermostat	\$15 <sup>a</sup>	\$5	\$0	-	-	30	\$9
b. Night Thermostat Setback to 60 deg.	\$75 <sup>a</sup>	\$60	\$0	4100	\$200	230	\$70
7. <u>Plug Fireplace Flue</u>	\$35	\$15	\$5	230	\$11	15	\$5
8. <u>Seal Air Bypass Paths to Attic</u>	\$100 <sup>a</sup>	\$40	\$10	750	\$37	35	\$11
9. <u>Seal and Insulate Ducts</u> in Unheated Areas	\$175	\$50	\$25	550	\$28	30	\$10
10. <u>Caulk and Seal Build. Shell</u> Heating Cooling	\$220	\$60	\$15	620 200 <sup>c</sup>	\$31 \$10	35 -	\$11 -
<b>TOTALS</b> (see note c)	\$670	\$260	\$60	1200 <sup>c</sup> (25%)	\$60 <sup>c</sup>	530 <sup>c</sup> (35%)	\$160 <sup>c</sup>

a. assumes the measure was part of a contractor package job.

b. not included in total because original requirements did not include appliances.

c. For total savings, to avoid double counting, we assume gas used for space and water heating, electricity for cooling and refrigeration (where the gas columns show a dash).  
2-2 setback  
17 oct rev.

new buildings. To this amount must be added another 60 kWh/m<sup>2</sup> for lights, equipment, fans, etc. New Swedish buildings are so well insulated that their temperature rises during winter working days. In the Folksam building, the surplus heat from the 40 hours per week that the building is occupied is stored in hollow-core concrete slabs and then used to compensate for the heat losses during the 128 remaining hours. The energy transport and storage system necessary to keep the indoor temperature comfortable, summer and winter, is called Thermodeck; it is described in detail in the report.

Fig. 5, taken from the report, shows how the Thermodeck system can also eliminate the need for daytime air conditioning.

#### California Policy Seminar

We received a grant from the California Policy Seminar to update the report on potentials for conserving energy and peak power in California<sup>1</sup> and to consider further savings that might be realized if long-range standards for buildings and appliances were adopted. We are also

computerizing our data base and writing several policy papers under this grant.

#### Energy "Points" for Real-Estate Appraisers

In a project related to our Low-Cost Residential Conservation Measures, we are calculating the energy savings of applying residential conservation options in ten cities. The results will be listed as points on a form intended for use by real-estate appraisers.

#### Retrofitting Projects

In collaboration with Princeton University, we have developed the practice of partially retrofitting a residence as it is being audited in accordance with the Residential Conservation Service legislation. If we assume a situation in which gas or oil use in a partially retrofitted house is reduced by 25%, then a homeowner who spends \$250 on the retrofitting procedures can save \$100/year in energy costs, which works out to 25¢/MBtu or \$1.50/barrel.

Table 2. Lo-cost/no cost residential conservation measures - Chicago/Boston

We assume a 1200 ft.<sup>2</sup> house, with R-11 insulation in the ceiling, R-7 in the walls, no night thermostat setback, and 6000 heating degree-days per year. Before retrofit the house used 2200 therms (32,000 kWh or 1570 gal. of oil) for space heating and 300 therms. (or 5000 kWh) for hot water. Air conditioning in Chicago uses 2300 kWh, but we do not consider a/c savings. Gas and oil seasonal furnace/duct system efficiency before retrofit was taken to be 50 percent.

Measure	Alternative Cost				Annual Savings				
	Work By Contr.	By Homeowner		Electric kWh	Electric @5¢/kWh	Natural Gas		Oil gal @85¢/gal	
		Deluxe	Cheap			Therms @37¢/Th			
1. <u>Low Temperature Laundry</u> warm wash/cold rinse, or (all cold water)	\$0	\$0	\$0	600	\$30	50	\$19	-	-
	\$0	(\$0)	(\$0)	(1000)	(\$30)	(55)	(\$20)	-	-
2. <u>Reduce Hot Water Temp.</u> 140 deg. to 120 deg. or (140 deg. to 110 deg.)	\$0	\$0	\$0	350	\$17	25	\$9	-	-
	\$0	(\$0)	(\$0)	(520)	(26)	(35)	(\$13)	-	-
3. <u>Shower Flow Restrictor</u>	\$20 <sup>a</sup>	\$8	\$1	750	\$38	35	\$13	-	-
4. <u>Blanket on Water Heater</u>	\$30 <sup>a</sup>	\$20	\$5	350	\$18	24	\$9	-	-
5. <u>Other Turnoffs</u>									
a. Furn. Pilot Off In Summer	\$0	\$0	\$0	-	-	30	\$11	-	-
b. Refrig. Anti-Sweat Switch	\$0	\$0	\$0	120 <sup>b</sup>	\$6	-	-	-	-
c. Eliminate Second Refrig.	\$0	\$0	\$0	900 <sup>b</sup>	\$45	-	-	-	-
6. <u>Heating and Cooling Systems</u>									
a. Set back Furn. Fan T'stat	\$15 <sup>a</sup>	\$5	\$0	-	-	30	\$11	21	\$18
b. Night Thermostat Setback to 60 deg.	\$75 <sup>a</sup>	\$60	\$0	5500	275	320	\$120	230	\$194
c. Furnace Tuneup	\$35 <sup>a</sup>	-	-	-	-	220	\$81	157	\$133
7. <u>Plug Fireplace Flue</u>	\$35	\$15	\$5	900	\$45	60	\$22	43	\$37
8. <u>Seal Bypass Paths To Attic</u>	\$100 <sup>a</sup>	\$40	\$10	1400	\$70	80	\$30	57	\$48
9. <u>Seal And Insulate Ducts</u> In Unheated Areas	\$175	\$50	\$25	1900	\$95	130	\$48	93	\$79
10. <u>Caulk And Seal Building</u> Shell, Worst Places Only	\$220	\$60	\$15	1500	\$75	100	\$37	71	\$60
TOTALS (see note d)	\$700	\$260	\$60			1100 (44%)	\$410	670 <sup>d</sup> (43%)	\$570 <sup>d</sup>

a. assumes measure was part of a contractor package job.

4 Oct 79 Rev. 1

b. Not included in total because original requirements did not include appliances.

d. Oil savings apply for space heating alone; domestic water heated by gas.

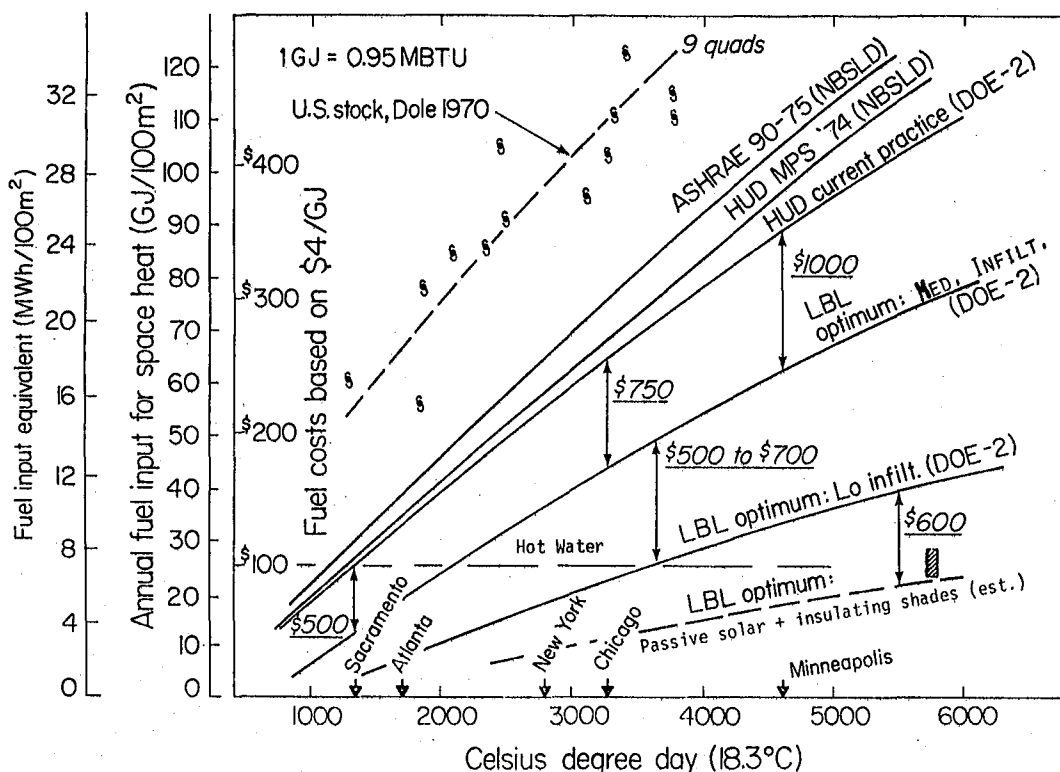


Fig. 2. U.S., fuel for single-family residential space heating. (XBL 795-1396A)

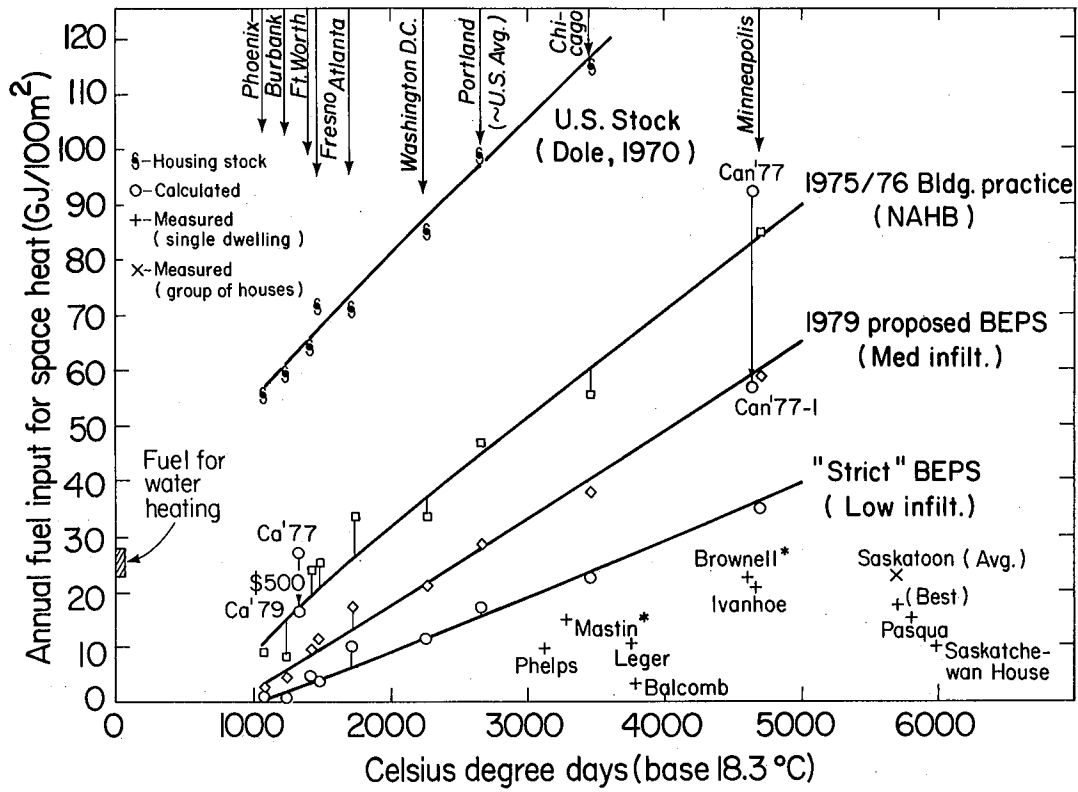


Fig. 3. North America, fuel for single-family residential space heating. (XBL 807-1680)

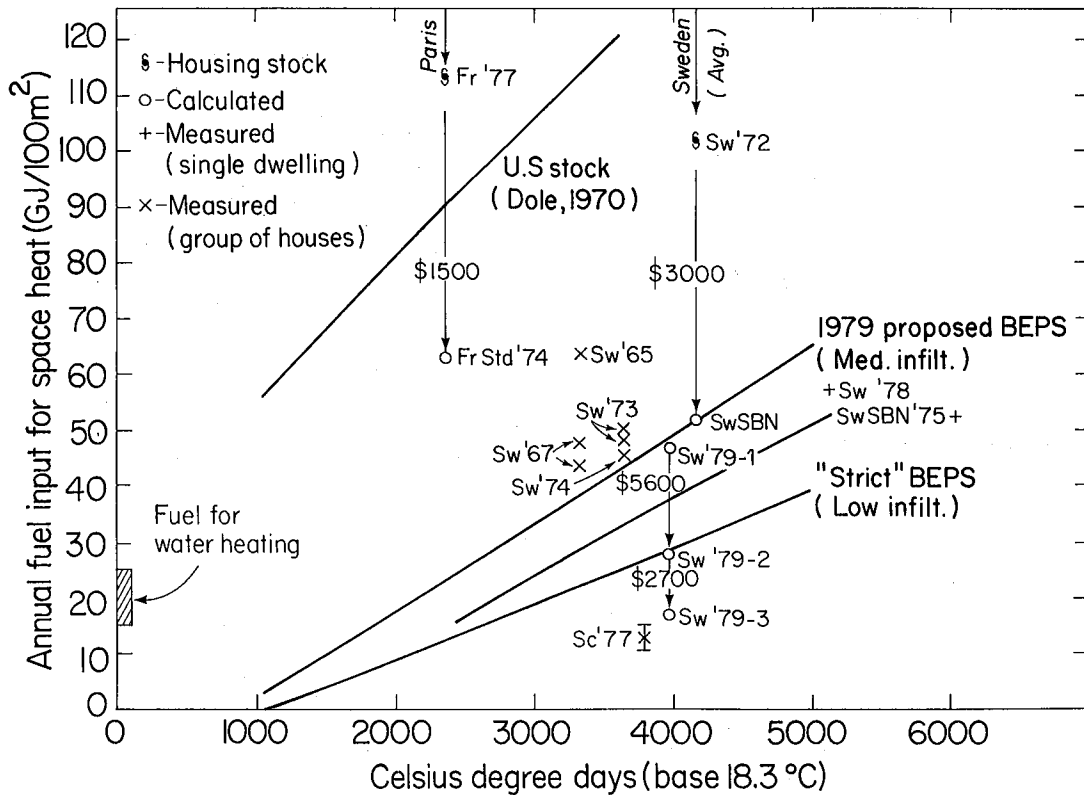


Fig. 4. Europe, fuel for single-family residential space heating. (XBL 807-1679)

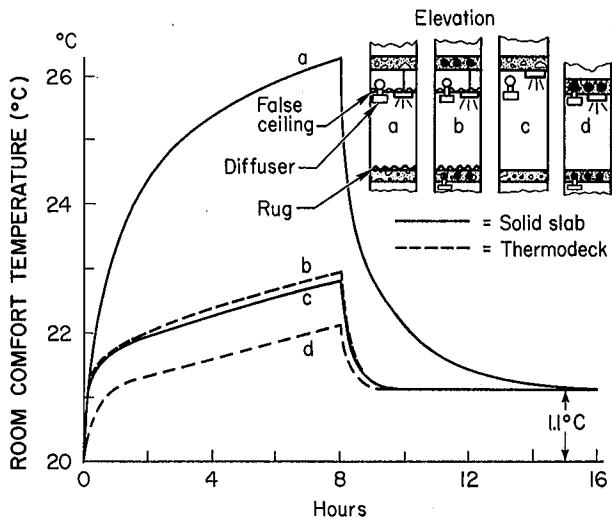


Fig. 5. Response/relaxation curves calculated by the BRIS-program for equal rooms with two different slabs, each with a heat capacity of  $100 \text{ Wh/m}^2\text{K}$ . The surroundings are assumed symmetric on all sides (as in an office in the core of a building).  $15 \text{ W/m}^2$  of lighting (50% radiation) is turned on for the first eight hours of each run. The cases are as follows:

- 20-cm thick solid concrete slab, with rug, insulated, suspended ceiling, and plenum. Resistances assumed were: rug --  $0.1 \text{ (W/m}^2\text{K)}^{-1}$ ; insulated false ceiling --  $0.5$ ; plenum --  $0.17$ .
- Same as a., but slab is 30-cm thick Thermodeck.
- 20-cm thick concrete slab, but bare -- no rugs, suspended ceilings, plenum.
- Same as c., but slab is 30-cm thick Thermodeck.

(XBL 7910-13104)

To test and demonstrate the economics of retrofiting, we are working with the Pacific Gas and Electric Company to partially retrofit 20 homes in Walnut Creek, California, and then to fully retrofit six of them. This activity is part of a broader program, covering 150 homes, that has been organized by Princeton University.

Also with Princeton, we are proposing to carry out a demonstration project in which 1,000 homes would be retrofitted. The project would also be used to train "house doctors" (persons skilled in diagnosing sources of energy waste in a house) and to give utility company personnel experience in conducting audits and in partially and extensively retrofitting homes.

#### REFERENCES

- A. H. Rosenfeld, Some Potentials for Energy and Peak Power Conservation in California, Lawrence Berkeley Laboratory Report, LBL-5926 (October 1977).
- D. B. Goldstein and A. H. Rosenfeld, Energy Conservation in Home Appliances through Comparison Shopping: Facts and Fact Sheets, Lawrence Berkeley Laboratory Report, LBL-5910 (March 1978).
- L. Wall, T. Dey, A. Gadgil, A. Lilly, and A. H. Rosenfeld, Conservation Options in Residential Energy Use: Using the Computer Program Twozone, Lawrence Berkeley Laboratory Report, LBL-5271 (August 1977). Preprint.
- D. B. Goldstein and A. H. Rosenfeld, Saving Half of California's Energy and Peak Power in Buildings via Long-range Standards and Other Legislation, Lawrence Berkeley Laboratory Report, LBL-6865 (May 1978). [Submitted to the California Policy Seminar]
- A. H. Rosenfeld, et al., Building Energy Use Compilation and Analysis (BECA): An International Comparison and Critical Review. Part A: Single-Family Residences, Lawrence Berkeley Laboratory Report, LBL-8912 (October 1978).
- L. Andersson, K. Bernander, E. Isfalt, and A. H. Rosenfeld, Storage of Heat and Coolth in Hollow-Core Concrete Slabs. Swedish Experience, and Application to Large, American-style Buildings, Lawrence Berkeley Laboratory Report, LBL-8913 (October 1979).

## SUMMARY AND DISCUSSION OF POTENTIAL SAVINGS IN THE BUILDINGS SECTOR

A. H. Rosenfeld

### OVERVIEW

In 1979 the U.S. consumed about 79 quadrillion Btu's of resource energy (1 quad per year =  $1/2$  million barrels of oil per day). Because automobiles are so visible, many Americans first think of energy consumption in terms of gasoline used to fuel cars; in fact, gasoline use was only 14 quads. The next highest energy consumer

in the minds of the public is industry, and, at the bottom of the list, our homes and workplaces. To the surprise of most, our homes and workplaces in 1979 used as much energy as industry -- 29 quads each.

Table 1 shows a breakdown of energy consumption by sector (residential, commercial, industrial, transportation) and by supply (fossil

Table 1. Comparative energy consumption by sector and resource (United States, 1977)

	Resource Energy (Quads)					
	Fossil Fuel		Electricity		Total	
<b>Buildings:</b>						
• Residential	10	(3)*	7	(3)	17	(6)
• Commercial	4	(1)	7	(2)	11	(3)
All Buildings	14	(4)	14	(5)	28	(9)
Industry	21	(21)	8	(8)	29	(29)
<b>Transportation:</b>						
• Gasoline	14	(7)	---	---	14	(7)
• Other	7	(7)	---	---	7	(7)
All Transportation	21	(14)	---	---	21	14
<b>TOTAL</b>	<b>56</b>	<b>(39)</b>	<b>22</b>	<b>(13)</b>	<b>78</b>	<b>(52)</b>

\*Figures in parentheses represent estimated energy use if all homes, buildings and appliances were replaced with new ones, optimized to minimize life-cycle energy cost, and autos meet the 1985 standard of 27.5 mpg.

fuel vs. electricity) for 1977. Note that residences alone use more energy than motor cars, and that buildings and appliances use 60% of our electricity. Figures in parentheses reflect our estimate of energy consumption if all homes and buildings were magically retrofitted or replaced with new ones whose energy use has been optimized to minimize life-cycle energy costs, and if automobiles were brought up to 1985 fuel-economy standards. Based upon our projections, we estimate potential energy savings of 19 quads in the building sector and 7 quads in the transportation sector. The result is that the 29 quads used by the buildings sector would drop to 9, and the 21 quads used for transportation would drop to 14.

#### RETROFITTING

Although it would take 50-100 years to replace all our homes and buildings, that somber fact does not mean that national energy conservation is a utopian prospect. Results of our research on retrofitting existing buildings suggest that energy requirements for space heating can be reduced by 50% (14 quads to 7) and electricity by approximately 35% (14 quads to 10). It is this potential supply of "conserved energy" (11 quads) that gives rise to articles with such exuberant titles as "Drilling for Oil and Gas in our Buildings."<sup>1</sup> By comparison, it is instructive to look at the National Energy Plan that would invest \$88 billion in plants to produce annually 5 quads of synthetic fuel and unconventional oil and gas. To this \$88 billion must be added a continuing annual cost of primary fuel inputted to the synfuel plant. Retrofitting existing buildings, on the other hand, will save 11 quads of energy for a gross capital investment of \$140 billion, or, if federally-financed, an annual carrying cost of approxi-

mately \$16 billion. In other words, such a national conservation program, for a smaller one-time initial investment, could produce twice what the synfuel program is projected to produce — not only at less cost but with a shorter pay-back time, some immediate benefits, and a higher probability of minimizing U.S. dependence on foreign energy sources in the near future.

Figure 1 of the article on "Conservation Potentials" in this chapter shows 20 steps designed to reduce existing energy use in a typical Northern California house by 60%, thus saving 140 MBtu/year. Assuming an average retrofit life of twenty years and an investment of \$2,500 to accomplish these retrofits, then at a 10% discount rate the 140 MBtu/year saving would cost \$294/year. The "conserved energy" cost is thus  $\frac{\$294}{140\text{MBtu}} = \$2.10/\text{MBtu}$ , or \$12.18/barrel.

#### REDUCING INFILTRATION

The most novel and cost-effective retrofit measure is to reduce natural infiltration of outside air. In the typical U.S. house which contains 80 lb. of air, infiltration averages 1 ach (air changes per hour). In winter, this incoming outside air must be heated hourly, and in summer the air must be cooled and dried in regions where air conditioning exists.

To heat all infiltrating air in a typical Boston house for one heating season adds to the normal heating load the energy and costs tabulated below:

Heating System	Furnace Efficiency	Fuel	Unit Price	Annual Heating Bill
Natural Gas	60%	450 therm	40c/ea.	\$180
Oil	60%	340 gal	\$1/gal	\$340
Electric Resistance	100%	13,000 kWh	5c/kWh	\$650

A good job of air-tightening this house could reduce infiltration by 25% to 50% and save a corresponding amount of energy and dollars.

Increased energy prices have encouraged builders to tighten construction in new houses where, on the average, infiltration has been reduced to about 0.6 ach. There are even examples of energy-efficient houses which have been built with 0.1 - 0.2 ach; however, when infiltration is reduced, indoor pollutants such as odors, moisture, formaldehyde, radon gas, and combustion products from cooking with a gas stove, all build up, and indoor air quality becomes unacceptable. One promising solution is to install a fan to supply fresh air and exhaust stale air through an air-to-air heat exchanger. The EEB program is addressing this problem (see Ventilation Program).

#### NEW BUILDINGS

In addition to exploring retrofit possibilities in existing houses, the EEB program is concerned with new energy-efficient designs in

buildings. Indeed, the various research programs described in this chapter have the common aim of providing baseline data needed to establish building energy performance standards (BEPS) which Congress has mandated for 1980. The BEPS program is discussed in detail in the following article. Figs. 2 and 3 in "Conservation Potentials" show some of the improvements to be included in building standards for single-family housing stock in various geographical locations, and the energy savings that can be achieved by incorporating these energy-conserving features. For a typical house in Chicago, space heating requirements (gas) can be reduced by 85% (from 65 MBtu = \$260 to 10 MBtu = \$40) by using better windows, adding insulation, reducing infiltration, installing heat exchangers, and utilizing solar gain.

#### REFERENCES

1. R. Williams, M. Ross, "Drilling for Oil and Gas in Our Buildings," Princeton University, Center for Energy and Environmental Studies, Report PU/CEES 87, July 17, 1979, to be published in Technology Review, 1980.

## EVALUATION OF BUILDING ENERGY PERFORMANCE STANDARDS FOR RESIDENTIAL BUILDINGS

*M. Levine, D. Goldstein, M. Lokmanhekim, J. Mass, and A. Rosenfeld*

#### INTRODUCTION

In August of 1976, in response to the need for encouraging greater conservation of depletable energy resources in new buildings, Congress passed the Energy Conservation Standards for New Buildings Act of 1976. The Act mandated the development, promulgation, implementation, and administration of energy performance standards for all new buildings constructed in the United States after 1981.

The importance of the Building Energy Performance Standards (BEPS) program in the residential sector is underscored by results showing that setting the residential standard at the minimum in life-cycle costs using only traditional energy conservation measures can:

- reduce energy use for space conditioning by about 30% - 40% from current building practice (or 60% - 70% from an average house built before the OPEC oil embargo of 1973)
- produce a net savings in life-cycle costs of more than \$1,000 to an average new homeowner.

Lawrence Berkeley Laboratory (LBL) was assigned primary responsibility for the support of the U.S. Department of Energy's (DOE's) development of the energy performance standards for single-family residential buildings in December, 1978. During

Fiscal Year 1979, LBL completed the following tasks in support of the standards development:

1. Development of prototype designs for single-family residential buildings;
2. Description of conservation measures and building operating conditions for residential dwellings;
3. Building energy simulations using a state-of-the-art energy analysis computer program (DOE-2) of four buildings in ten locations with approximately twelve combinations of energy conservation measures for each building;
4. Development and application of a computer program to evaluate the life-cycle costs of the conservation measures in the residential buildings;
5. Analysis of the sensitivity of the life-cycle cost curves to variations or uncertainties in key economic parameters and building and climate characteristics;
6. Preparation of a series of memos and issued papers on the key policy issues resulting from the analysis of residential Building Energy Performance Standards (BEPS); and

7. Active participation with DOE in the preparation of the Notice of Proposed Rulemaking for the BEPS.<sup>1</sup>

The LBL research effort during Fiscal Year 1980 will focus on: (1) key issues that need to be resolved for the final rulemaking; (2) planning of a research effort to increase the energy conservation potential in residential buildings, in support of an update of the standards anticipated in 1985; (3) initiation of selected research tasks treating advanced energy conservation technologies (discussed in an article in this volume by D. B. Goldstein, J. Mass, and M. D. Levine); (4) support for DOE in its efforts on commercial buildings and mobile homes; and (5) participation in DOE's public information program on BEPS.

#### METHOD OF APPROACH

The approach followed in the analysis of residential space conditioning energy performance standards involves the following steps:

1. Development of residential prototypes,
2. Selection of conservation measures to be evaluated,
3. Description of standard building operating conditions,
4. Development of economic data, projections, and assumptions,
5. Computer simulation of building energy requirements in different climatic regions,
6. Analysis of life-cycle costs of energy conservation measures,
7. Sensitivity analyses on building characteristics, operating conditions, conservation measures, and economic parameters, and
8. Analysis of impacts of alternative energy budget levels, in which the alternative budget levels are based on steps 1 through 7.

The basis of the analysis method is the use of life-cycle costing. The objective of achieving a minimum in life-cycle costs is a reasonable basis for establishing energy conservation policy because it provides a rational framework for trading off scarce energy resources and other resources (e.g., labor and capital) in achieving a particular goal (in this case, space conditioning in residential buildings).<sup>2</sup> The use of an economic approach to energy conservation--and the increasing public awareness of how economics can help resolve issues--can be greatly enhanced by a government decision to use life-cycle costing as one of the major elements of its energy conservation policy.

#### Specifics of Approach and Assumptions

The most important specific elements of the approach to evaluating the life-cycle cost of energy

conservation measures for single-family residential buildings are summarized below. More detailed information on the assumptions used in the analysis is found in Ref. 3. More detailed information about the results of sensitivity analyses is found in Chapter 4 and appendices A and I of Ref. 4.

#### Residential Prototypes

- Four designs selected, following Hastings:<sup>5</sup> single story ranch, two story, townhouse, and split level house.
- Window area taken to be 15% of floor area for all designs.
- Windows equally distributed on all four sides of house (two sides for townhouse).
- Sensitivities of prototypes performed:
  - window area
  - window orientation
  - house size and orientation
  - aspect ratio of house
  - thermal mass of house
  - conservation measures (see below)
  - building operating conditions (see below)

#### Conservation Measures

- Windows: up to triple glazing (or double glazing plus storm window).
- Exterior wall: up to R-25 (using 2" x 6" studs plus insulating sheathing).
- Ceiling: up to R-38 insulation.
- Excludes: exterior wall with double studs (two 2 x 4 or 2 x 8 studs with insulation); ceiling insulation greater than R-38; infiltration reduction (with or without heat recuperator); any conservation measure requiring a change in behavior; other advanced energy conservation technologies.

#### Building Operating Conditions

- Thermostat set points: 70°F for heating; 78° for cooling; no night setback.
- Average air infiltration rate: 0.6 air changes per hour.
- Average internal loads: 50,000 Btu/day, Highest in early morning (cooking, occupants, lighting) and evenings (cooking, lighting, occupants, TV).
- Natural ventilation: windows open when indoor temperature greater than 78°F and outdoor temperature low enough to cool house to 78° in less than one hour. Non-opening windows considered as a sensitivity case.

#### Economic Data, Projections, and Assumptions

- E.I.A. average energy price projections

(Series B)

- Gas prices escalate at 2.8% per year above inflation,
- Electricity prices escalate at 1.5% per year above inflation.

- Installed cost of energy conservation measures from N.A.H.B.
- Discount rate chosen to equal cost of borrowed capital for a new house (3% above inflation).
- Possible future changes in assumptions:
  - marginal energy prices
  - updated conservation costs
  - regional prices

Building Energy Simulations

- Use of DOE-2 computer program, checked against TWOZONE and BLAST.
- Change in infiltration and ventilation algorithms.
- Run for 4 prototypes, about 12 groups of conservation measures per prototype, two ventilation algorithms and 10 cities.

RESULTS

Gas Heated Houses

Table 1 contains the detailed results obtained by minimizing the life-cycle costs of energy conservation investment and a discounted stream of payments for fuel over the lifetime of the house mortgage, for a house with natural gas heating (assuming a system efficiency of 70 percent) and electric cooling. The first column lists the climatic regions. The second column presents the representative city for which the thermal analysis of the residence was performed. Columns 3 and 4 show the long-term average heating and cooling degree days for each of the cities. The heating degree days are presented with a base of 65°F and, in parentheses, a base of 53°F. The cooling degree days are presented with a base of 65°F and, in parentheses, a base of 68°F. (The 53°F base for heating and 68°F for cooling are included because space heating and cooling loads for a well-insulated house are expected to be more nearly linear with degree days calculated on this basis than for the traditional base of 65°F.)

Column 5 presents the insulation levels and column 6 the number of glazings in the prototype house which minimized life-cycle costs.\* These

\*For regions in which a crawl space is the common form of basement, the floor insulation levels are noted in Table 1. For unheated full basements, the assumption is made that heat losses and gains balance. Slab on grade and basement construction is assumed to have adequate perimeter insulation, as described in Ref. 1.

insulation levels would bring most houses into compliance with the energy budgets. Of course, many other configurations would also comply. Triple glazing is used in climates as cold as Washington, D.C., and in areas with very large cooling load, and double glazing is used in all other climates modeled. Typical insulation levels for all but the extreme climates (coldest or mildest) are R-38 ceiling and R-19 walls. Column 7 contains the estimated increase in investment (for an 1176 square foot house) for the conservation measures compared with current investment in conservation in the different climates. (The estimates of current conservation investment are based on a NAHB survey, results of which are contained in Table 2.6) Column 8 contains the energy budget at the life-cycle cost minimum, which we have previously defined as the Design Energy Budget of a house. We have expressed these budgets in terms of primary energy use and use at the building boundary.

There are numerous ways that the Design Energy Budgets can be met in the different climates. Table 3, taken from Refs. 1 and 7, illustrates two or three alternative ways of achieving the Design Energy Budgets in three climates.

Electric Resistance Heated Houses

Table 4 summarizes the life-cycle costing results for electric resistance heating. Columns 5 and 6 show the standard insulation and glazing levels that will meet the designed energy budgets of the nominal case: R-38 ceiling and triple glazing insulation is used in all climates except the most mild (Burbank); R-25 wall insulation is used in all climates as cold as or colder than Washington, D. C. and R-19 wall insulation in all other climates. Thus, in all climates except region 1 (Minneapolis), the standard conservation

Table 2. Standard energy conservation measures for residential houses constructed in 1975, based on data from the 1977 NAHB survey.

City	Standard Practice, 1975			
	C	W	F	G1 <sup>a</sup>
Minneapolis	22	11	--	2
Chicago	19	11	--	2
Portland	19	11	7	2
Washington, D.C.	19	11	--	2
Atlanta	19	11	7	1
Fresno	19	11	--	1
Burbank	19	11	--	1
Phoenix	19	11	--	1
Houston	19	11	--	1
Ft. Worth	19	11	--	1

<sup>a</sup> C = ceiling R-value; W = wall R-value; F = floor R-value (if applicable); G1 = number of glazings for all windows.

Table 1. Results of the life-cycle cost analysis of energy conservation measures for single story houses heated by natural gas and cooled by electricity.

1 Climate Region	2 Representative City	3 Heating Degree- Days <sup>a</sup>	4 Cooling Degree- Days <sup>a</sup>	5 Insulation Levels of Nominal Case (R-Value)			6 Glazing of Nominal Case	7 Conservation Investment, \$1978	8 Natural Gas Energy Budget	
				Ceiling	Wall	Floor			Primary Energy, MBtu/sq. ft./yr	Building Boundary, MBtu/sq. ft./yr
1	Minneapolis	8310 (5260)	530 ( 370)	38	25	--	3	\$1,160	66.1	54.5
2	Chicago	6130 (3540)	930 ( 620)	38	19	--	3	\$ 900	42.9	35.0
3	Portland	4790 (1840)	300 ( 150)	38	19	19	3	\$1,050	30.9	25.9
3	Washington, D.C.	4210 (1980)	1420 (1010)	38	19	--	3	\$ 900	33.7	22.4
4	Atlanta	3100 (1230)	1590 (1130)	38	19	11	2	\$ 900	28.2	18.3
4	Fresno	2650 ( 770)	1670 (1220)	38	19	--	2	\$ 850	31.9	16.1
5	Burbank	1820 ( 170) <sup>b</sup>	620 (310) <sup>b</sup>	19	11	--	2	\$ 380	15.7	7.2
6	Phoenix <sup>C</sup>	1550 ( 320)	3510 (2960)	38	19	--	3	\$1,280	35.8	12.0
6	Houston	1430 ( 360)	2890 (2240)	30	11	--	2	\$ 520	34.4	15.1
7	Ft. Worth <sup>C</sup>	2830 ( 810)	2590 (2030)	38	19	--	3	\$1,280	32.3	15.2

<sup>a</sup>Heating and cooling degree-days base 65°F presented; heating degree-days base 53°F in parentheses; cooling degree-days base 68°F in parentheses.

<sup>b</sup>Degree-days for Los Angeles reported.

<sup>C</sup>Under the EIA Medium Price Projections (December 17, 1978) both Phoenix and Ft. Worth would have used double glazing at a conservation investment of \$850. Primary energy use was 40.1 and 36.8 MBtu/sq. ft./yr for Phoenix and Ft. Worth, respectively.

Table 3. Illustrative ways of meeting the design energy budgets for single family residences in three locations: gas heated homes.

Location	Sets of Options
Chicago, IL	<ol style="list-style-type: none"> <li>1. Average window area and distribution;<sup>a</sup> triple glazing;<sup>b</sup> R-38 ceiling and R-19 wall insulation.</li> <li>2. Windows redistributed so that south facing window area increased by 75% and east, west, and north facing window area decreased by 25%; double glazing; R-38 ceiling and R-9 wall insulation.</li> <li>3. Active solar domestic water heating system;<sup>d</sup> double glazing; R-38 ceiling and R-11 wall insulation.</li> </ol>
Atlanta, GA	<ol style="list-style-type: none"> <li>1. Average window area and distribution;<sup>a</sup> double glazing; R-38 ceiling, R-19 wall, and R-11 floor<sup>c</sup> insulation.</li> <li>2. Windows redistributed so that south facing window area increased by 75% and east, west and north facing window area decreased by 25%; double glazing; R-30 ceiling, R-11 wall and R-11 floor insulation.</li> <li>3. Active solar domestic water heating system;<sup>d</sup> double glazing; R-19 ceiling, R-11 wall and R-7 floor insulation.</li> </ol>
Houston, TX	<ol style="list-style-type: none"> <li>1. Average window area and distribution;<sup>a</sup> double glazing; R-30 ceiling and R-11 wall insulation.</li> <li>2. Active solar domestic water heating;<sup>d</sup> R-19 ceiling and R-11 wall insulation.</li> <li>3. Other alternatives, such as passive solar design and redistribution of windows, not evaluated for Houston.</li> </ol>

<sup>a</sup>The average window area is 15% of total floor area. The windows are distributed equally among the exterior walls.

<sup>b</sup>Double glazing plus storm windows can substitute for triple glazing with little change in the Design Energy Consumption of the house.

<sup>c</sup>Floor insulation is noted in Atlanta, Georgia, and all other areas where crawl-space basements are used.

<sup>d</sup>The active solar domestic water heating is assumed to be sized at 60% of the water heating load in a 1500 square foot house for the purpose of this illustration.

Table 4. Results of the life-cycle cost analysis of energy conservation measures for single story houses heated and cooled by electric heating (other than heat pumps).

1 Climate Region	2 Representative City	3 Heating Degree-Days <sup>a</sup>	4 Cooling Degree-Days <sup>a</sup>	5 Insulation Levels of Nominal Case (R-Value)			6 Glazing of Nominal Case	7 Conservation Investment, \$1978	8 Electrical Energy Budget	
				Ceiling	Wall	Floor			Primary Energy, MBtu/sq. ft./yr	Building Boundary, MBtu/sq. ft./yr
1	Minneapolis	8310 (5260)	530 ( 370)	38	25	--	3	\$1,160	132.2	38.9
2	Chicago	6130 (3540)	930 ( 620)	38	25	--	3	\$1,190	80.0	23.5
3	Portland	4790 (1840)	300 (1010)	38	25	19	3	\$1,350	58.5	17.2
3	Washington, D.C.	4210 (1980)	1420 (1010)	38	25	--	3	\$1,190	53.7	15.8
4	Atlanta <sup>C</sup>	3100 (1230)	1590 (1130)	38	19	19	3	\$1,433	39.6	11.6
4	Fresno	2650 ( 770)	1670 (1220)	38	19	--	3	\$1,280	38.6	11.4
5	Burbank	1820 ( 170) <sup>b</sup>	620 (310) <sup>b</sup>	30	19	--	2	\$ 760	15.1	4.4
6	Phoenix	1550 ( 320)	3510 (2960)	38	19	--	3	\$1,280	38.5	11.3
6	Houston	1430 ( 360)	2890 (2240)	38	19	--	3	\$1,280	33.6	9.9
7	Ft. Worth	2830 ( 810)	2590 (2030)	38	19	--	3	\$1,280	43.0	12.6

<sup>a</sup>Heating and cooling degree-days base 65°F presented; heating degree-days base 53°F in parentheses; cooling degree-days base 68°F in parentheses.

<sup>b</sup>Degree-days for Los Angeles reported.

<sup>c</sup>Under the EIA Medium Price Projections (December 17, 1978) Atlanta used R-11 floor insulation for a conservation investment cost of \$1,330 and a primary energy budget of 40.7 MBtu/sq. ft./yr.

measures for houses using electric resistance heating are stricter than those for natural gas-heated houses. The investment in energy conservation for the electric resistance heated houses reflects the use of tighter measures for all climates except Minneapolis. The increased investment in energy conservation (beyond estimated 1975 current practice) is between \$1,160 and \$1,433 for the 1176-ft<sup>2</sup> wood frame prototype house.

#### Houses Heated and Cooled with Heat Pumps

Table 5 summarized the life-cycle costing results for heating and cooling with an electric heat pump. Column 8 in Table 5 presents the seasonal coefficients of performance (COP) of heat pumps in the heating mode in ten climates. These COPs are based on the simulation of available efficient heat pumps in ten climates by the Oak Ridge National Laboratory.<sup>8</sup> The COP for a heat pump is reported as 10% lower than can presently be achieved by commercial models to account for heat losses in the ductwork associated with the heat pump.

Comparison of the Design Energy Budgets for the electric heat pump (column 9 in Table 5) with electric resistance heating (column 8 in Table 4) reveals that the heat pump budget is lower than the electric resistance budget in almost all cases. The heat pump budget is significantly lower in cool and cold climates. An economic evaluation of electric heating using heat pumps and using resistance heating indicates that the heat pump system has lower life-cycle costs than resistance heating in cool and cold climates, in spite of the higher first costs of the heat pump.<sup>9</sup>

Table 6 illustrates alternative ways of meeting the Design Energy Budgets that were obtained for homes heated and cooled by heat pumps in three climates.<sup>1,7</sup>

#### Comparison with Current and Past Energy Conservation Construction Practice

Figure 1 presents a comparison of fuel requirements for space heating using natural gas for a large number of different cases. The upper curve, labeled "U.S. stock, Dole 1970," is the best available estimate of the fuel requirements for space heating the 1970 stock of houses in the United States.<sup>10</sup> The fourth curve from the top labeled "Current Practice (DOE-2)," is our best estimate of the current construction practice in houses built after the 1973 oil embargo. This curve is based on survey data for the years 1975 and 1977 and on results of DOE-2<sup>11</sup> computer calculations performed at LBL.<sup>4</sup> The fifth curve from the top, labeled "LBL optimum medium infiltration," contains the results of life-cycle costing analysis for gas heated houses. The sixth curve, labeled "LBL optimum: low infiltration (DOE-2)," illustrates the energy requirements for a house with infiltration levels reduced from 0.6 to 0.2 air changes per hour. For this case the assumption is made that mechanical ventilation through a heat recuperator restores the outside air exchange rate to 0.6 air changes per hour.

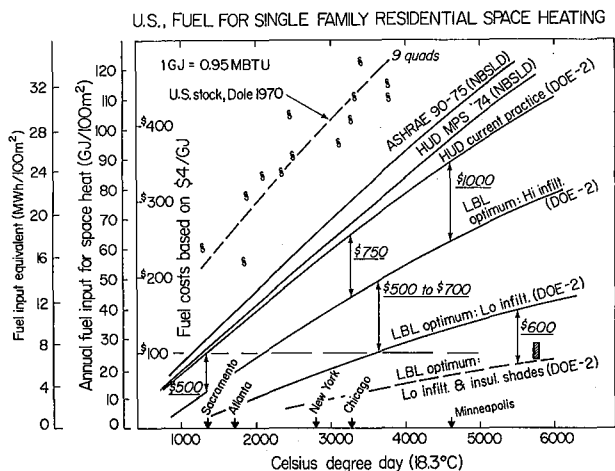


Fig. 1. Fuel for single family residential space heating (U.S.). (XBL 795-1396)

#### CONCLUSIONS

Figure 1 indicates that very large energy savings can be accomplished by requiring all new houses to use all commonly available cost effective energy conservation measures. BEPS can result in a substantial improvement in the thermal integrity of new houses in the United States and at the same time save the consumer money. The magnitude of the energy savings is sufficiently great as to go a long way toward reducing growth in energy demand in the Nation. (About 35% of energy in the Nation is consumed in buildings with about half of this amount consumed in residential buildings.)

If BEPS is set at the minimum in the life-cycle cost curves (as proposed in DOE's NOPR)<sup>1</sup> and if all new residential buildings meet BEPS then:

- a reduction of 30% to 40% in the average energy use for residential space conditioning (from current building practice) is accomplished. This is a reduction of 60% to 70% from the energy use of an average existing house, built before the OPEC oil embargo in 1973.
- simple payback on conservation investment occurs in 1 to 4 years for electric heat and 3 to 10 years for gas heat;
- an increased investment of \$0.50 to \$1.00 per square foot for a new house is required (i.e., an increased initial investment of 1.5% to 3%); and
- the new home owner achieves a net savings of \$800 to \$1500 over the life of the house mortgage, in addition to a higher selling price of the house.

If the list of conservation measures is expanded to include just one conservation technology (reduced air infiltration combined with mechanical

Table 5. Results of the life-cycle cost analysis of energy conservation measures for single story houses heated and cooled by electric heat pumps.

1 Climate Region	2 Representative City	3 Heating Degree- Days <sup>a</sup>	4 Cooling Degree- Days <sup>a</sup>	5 Insulation Levels of Nominal Case (R-Value)			6 Glazing of Nominal Case	7 Conservation Investment, \$1978	8 Heat Pump Seasonal COP	9 Electrical Energy Budget	
				Ceiling	Wall	Floor				Primary Energy, MBtu/sq. ft./yr	Building Boundary, MBtu/sq. ft./yr
1	Minneapolis	8310 (5260)	530 ( 370)	38	25	--	3	\$1,160	1.38	98.3	28.9
2	Chicago	6130 (3540)	930 ( 620)	38	25	--	3	\$1,190	1.52	54.6	16.1
3	Portland	4790 (1840)	300 (1010)	38	19	19	3	\$1,050	1.87	34.9	10.3
3	Washington, D.C.	4210 (1980)	1420 (1010)	38	19	--	3	\$ 900	1.79	37.7	11.1
4	Atlanta	3100 (1230)	1590 (1130)	38	19	11	3	\$1,330	1.82	27.0	7.9
4	Fresno	2650 ( 770)	1670 (1220)	38	19	--	3	\$1,280	2.02	28.6	8.4
5	Burbank	1820 ( 170) <sup>b</sup>	620 (310) <sup>b</sup>	30	11	--	2	\$ 520	2.02	4.6	4.3
6	Phoenix	1550 ( 320)	3510 (2960)	38	19	--	3	\$1,280	1.92	36.0	10.6
6	Houston	1430 ( 360)	2890 (2240)	38	19	--	3	\$1,280	1.83	28.5	8.4
7	Ft. Worth	2830 ( 810)	2590 (2030)	38	19	--	3	\$1,280	1.83	33.9	10.0

<sup>a</sup>Heating and cooling degree-days base 65°F presented; heating degree-days base 53°F in parentheses; cooling degree-days base 68°F in parentheses.

<sup>b</sup>Degree-days for Los Angeles reported.

Table 6. Illustrative ways of meeting the design energy budgets for single family residences in three locations: electric heated homes.

Location	Sets of Options
Chicago, IL	<ol style="list-style-type: none"> <li>1. Average window area and distribution;<sup>a</sup> triple glazing;<sup>b</sup> R-38 ceiling and R-25 wall insulation; heating supplied by a heat pump.</li> <li>2. Windows redistributed so that south facing window area increased by 36% and east, west, and north facing window area decreased by 12%; triple glazing; R-38 ceiling and R-19 wall insulation; heating supplied by heat pump.</li> <li>3. Active solar domestic water heating system;<sup>d</sup> double glazing; R-38 ceiling and R-25 wall insulation; heating supplied by electric resistance.</li> </ol>
Atlanta, GA	<ol style="list-style-type: none"> <li>1. Average window area and distribution;<sup>a</sup> triple glazing;<sup>b</sup> R-38 ceiling, R-19 wall, and R-11 floor<sup>c</sup> insulation; heating supplied by heat pump.</li> <li>2. Windows redistributed so that south facing window area increased by 80% and east, west, and north facing window area decreased by 27%; double glazing; R-38 ceiling, R-19 wall, and R-11 floor<sup>c</sup> insulation; heating supplied by heat pump.</li> <li>3. Active solar domestic water heating system;<sup>d</sup> double glazing; R-30 ceiling, R-19 wall, and R-11 floor<sup>c</sup> insulation; heating supplied by electric resistance.</li> </ol>
Houston, TX	<ol style="list-style-type: none"> <li>1. Average window area and distribution;<sup>a</sup> triple glazing;<sup>b</sup> R-38 ceiling and R-19 wall insulation; heating supplied by heat pump.</li> <li>2. Active solar domestic water heating system;<sup>d</sup> R-19 ceiling and R-11 wall insulation.</li> </ol>

<sup>a</sup>The average window area is 15% of total floor area. The windows are distributed equally among the exterior walls.

<sup>b</sup>Double glazing plus storm windows can substitute for triple glazing with little change in the Design Energy Consumption of the house.

<sup>c</sup>Floor insulation is noted in Atlanta, Georgia, and all other areas where crawl-space basements are used.

<sup>d</sup>The active solar domestic water heating is assumed to be sized at 60% of the water heating load in a 1500 square foot house for the purpose of this illustration.

venting through a heat exchanger), then

- a reduction of 50% to 60% in average energy use for residential space conditioning (from current building practice) can be accomplished. This is a reduction of 75% to 85% from the energy use of an average existing house;
- this requires an increased initial investment of \$0.75 to \$1.50 per square foot.
- the net savings is \$1500 to \$4000 to the new house owner, in addition to a higher selling price of the house.

#### PLANNED ACTIVITIES FOR 1980

The BEPS program at LBL has been expanded for Fiscal Year 1980. The following activities are either underway or planned:

1. Analysis in support of Final Rulemaking:
  - development of new prototype,
  - detailed assessment of the economics and thermal performance of residential heating and cooling equipment (including heat pumps) and water heaters,
  - application of life-cycle costing to heating and cooling equipment, water heaters, and the building envelope,
  - continued analysis of the economics and energy performance of exterior masonry walls,
  - final computer curves of conservation measures for four prototypes in 32 locations,
  - sensitivity studies of the effects of changing window size and orientation, conservation measures, internal thermal mass, and other building characteristics,
  - continuing analysis of the impact of uncertainty in key economic parameters on the development of the standards (see paper by P. P. Craig, M. D. Levine, and J. Mass on this subject in Energy, in press),
  - study of other key issues related to the promulgation and implementation of standards:
    - computer program comparison and validation,
    - credits for the use of renewable resources,
    - assessment of how many energy budgets are needed,
    - continued analysis of how energy budgets for different fuels are compared.

2. Planning of energy conservation research to support an update of the standards in 1985.
3. Research on selected advanced energy conservation measures, including infiltration with mechanical ventilation through a heat exchanger, direct gain passive solar, and advanced concepts for energy conservation in windows.
4. Support for DOE in its analysis of commercial buildings and mobile homes.
5. Participation in DOE's public information program on the Building Energy Performance Standards.

#### REFERENCES

1. U.S. Department of Energy, "Notice of Proposed Rulemaking for the Building Energy Performance Standards," in press, 1979.
2. L. J. Schipper, J. Hollander, M. D. Levine, and P. P. Craig, "The National Energy Conservation Policy Act: An Evaluation," Natural Resources Journal, in press, 1979.
3. D. B. Goldstein, M. D. Levine, and J. Mass, "Residential energy performance standards: Methodology and assumptions," Lawrence Berkeley Laboratory report, LBL-9110, in press, 1979.
4. Pacific Northwest Laboratory, Lawrence Berkeley Laboratory, and Oak Ridge National Laboratory, "Economic Analysis of Proposed Building Energy Performance Standards," PNL-3044, September 1979, (Chapter 4 and appendices A and I by M. D. Levine and D. B. Goldstein).
5. S. R. Hastings, "Three proposed typical house designs for energy conservation research," NBSIR, 77-1309, 1977.
6. National Association of Homebuilders, "A National Survey of Characteristics and Construction Practices for all Types of One Family Houses" (1977).
7. M. D. Levine, D. B. Goldstein, and D. O'Neal, "Residential energy performance standards: comparison of HUD minimum property standards and DOE's proposed standards," Lawrence Berkeley Laboratory report, LBL-9817, in press, 1979.
8. Dennis O'Neal, personal communication to the authors, August, 1979.
9. See Reference 4, Appendix I.
10. A. H. Rosenfeld, W. G. Colborne, C. D. Hollowell, L. J. Schipper, Bo Adamson, M. Cadiergues, Gilles Olive, Bengt Hidemark, G. S. Leighton, H. Ross, N. Milbank, and M. J. Uyttenbroeck, "Building energy use compilation and analysis (BECA): an international comparison and critical review," Lawrence Berkeley Laboratory report LBL-8912, (July, 1979).

11. M. Lokmanhekim, et al., "DOE-2 : A New State-of-the-Art Computer Program for the Energy Utilization Analysis of Buildings," presented at the Second International CIB Symposium on Energy Conservation in the Built Environment, Copenhagen, Denmark, May 28 - June 1, 1979.
12. A. J. Gadgil et al., "TWOZONE user's manual," Lawrence Berkeley Laboratory report LBL-6840 (1978).
13. BLAST - The Buildings Loads Analysis and System Thermodynamics Program, Published by CERL, Technical Report E-153 (June, 1979).
14. T. Kusuda, NBSLD, "Computer Program for Heating and Cooling Loads in Buildings," NBS Build-Science Series 69 (1976).
15. A. Gadgil, D. Goldstein, R. Kammerud, and J. Mass, "Residential Building Simulation Model Comparison Using Several Building Energy Analysis Programs," Proceedings of the Fourth National Passive Solar Conference, Kansas City, October, 1979.
16. A. Gadgil, D. Goldstein, and J. Mass, "A Heating and Cooling Loads Comparison of Three Building Simulation Models for Residences: TWOZONE, DOE-1 and NBSLD," Proceedings of the International Conference on Energy Use Management II, Los Angeles, October, 1979.

## ENERGY EFFICIENCY STANDARDS FOR RESIDENTIAL APPLIANCES INCLUDING HEATING AND COOLING EQUIPMENT

*M. Levine, S. French, J. McMahon, R. Pollack, and I. Turiel*

### INTRODUCTION

The National Energy Conservation Policy Act (NECPA) mandates that Appliance Energy Efficiency Standards be prescribed by October of 1980. The law requires that the standards be designed to achieve the "maximum improvement in energy efficiency" that is "technologically feasible and economically justified." Determination of the economic justification must be based on: the savings in operating costs over the average life of the appliance compared to the increase in the initial purchase price or maintenance costs likely to result from the imposition of the standard; the economic impact of the standard on the manufacturers and the consumers of the appliances; the total projected energy savings likely to result directly from the imposition of the standards; and other relevant factors. Clearly, it will be necessary to systematically develop appliance standards that achieve minimum life cycle costs and to evaluate the total impact on residential energy demand resulting from the implementation of the standards.

The Appliance Efficiency Performance Standards (AEPS) program at LBL will perform analysis of residential energy demand in support of the appliance standards as outlined in NECPA. One major tool of the demand analysis will be the Oak Ridge National Laboratory (ORNL) Engineering-Economic Model of Residential Energy Use, which provides detail on the energy use of eight major end uses by four fuel types in the residential sector. A second important tool is the DOE-2 Model, which analyzes the energy use of buildings. The DOE-2 Model needs to be extended to simulate the performance of residential heating and cooling equipment for it to be used in the evaluation of energy efficiency standards for this equipment. Two additional analytic tools are under development at LBL in support of the appliance efficiency standards: (1) a model to assess the bases of consumer decision making in the purchase of appliances, with particular emphasis on the factors influencing

the efficiency of consumer products purchased, and (2) a model to assess the effects of alternative standards for residential energy use on the peak loads of electric utilities.

### PROGRAM OVERVIEW

The purpose of the Appliance Energy Performance Standards (AEPS) program at LBL is to provide assistance to the U.S. Department of Energy (DOE) in the formulation of energy efficiency standards for appliances. This purpose will be achieved by establishing base cases for energy demand with and without appliance efficiency standards (with appropriate sensitivity analyses), by evaluating the efficiencies of heating and cooling equipment in different climates and in houses with differing levels of conservation (by performing hourly computer simulations over the course of a typical year), by assessing the effects of appliance efficiency standards on peak loads of utilities, and by assisting DOE in its development of an overall methodology for evaluating alternative energy performance standards.

The specific primary tasks for F.Y. 1980 are:

- Task 1: Establish base case projections of appliance energy use using the ORNL residential energy demand model.
- Task 2: Perform preliminary assessment of consumer decisionmaking in the purchase of appliances; use results to refine the ORNL base case projections (in Task 1).
- Task 3: Analyze the weather sensitivity of heating and cooling systems, using DOE-2 computer program for houses of varying conservation levels.
- Task 4: Assess the life-cycle costs of a wide range of energy conservation

measures for heating and cooling equipment, using the results of Task 3 and engineering/economic data supplied by DOE.

**Task 5:** Assess impacts of appliance efficiency standards on utility peak loads, using results of Task 4 and peak load data from selected utility service areas.

**Task 6:** Assist DOE in developing ranking methodology to assess alternative standards; apply methodology to establish alternative standards.

Original analysis on performance of equipment in different climates and types of houses, specified in Task 4, is limited to heating and cooling systems and does not cover other appliances.

#### SPECIFIC DETAILS OF APPROACH

Table 1 shows the relationships among the tasks (and subtasks) of the research effort and indicates how the results can be used to support the development of energy performance standards for residential appliances.\*

An explanation of the information flows in the project, as designated by the letters A through O, on Table 1, provides an understanding of how the individual tasks support the establishment of standards. The information flows in Table 1 are as follows:

- A: assessment of elements of ORNL model projection in need of improvement,
- B: improvements in ORNL model; preliminary consumer decision-making model,
- C: derivation of annual heating and cooling energy use from hourly simulations,
- D: Sensitivities of annual heating and cooling energy use to weather; building envelope conservation measures; equipment size; equipment performance characteristics,
- E: impact of different appliance energy standards on peak load performance of utilities,
- F: refined data base for ORNL model (energy use of appliances and cost of efficiency improvements),
- G: refined data for complete life-cycle cost analysis,

Table 1. Overview of LBL Appliance Performance Standards (AEPS) Program.

Task No.	Title	Output Information Flow	Feeds In-to Tasks	Program Output
1	Base Case Analysis (no standards)	A*	1-1	
2	Improve ORNL Model (emphasis on consumer decisionmaking)	B J M	1-1 1-2 6	consumer decision-making & energy growth Analysis & policy consideration
3	Extend DOE-2 Model for Residential Heating & Cooling Equipment	C D	4 4-1	
4	Preliminary Life-Cycle Cost Analysis	F G	1-1 4-1	
1-1	Assess Base Case	---	1-2	
5	Peak Load Analysis	E H	--- 4-1	Effects of Standards on Peak Loads
4-1	Extended Life-Cycle Cost Analysis	I K K	1-2 6 ---	Life Cycle-Cost Curves; Sensitivities
1-2	Assess Standards Case, Reasses Base Case	L N	6 ---	Residential Energy Projections with and without Standards; Net Present values; sensitivities
6	Policy Analysis of Alternate Standards	O	---	Economic Impacts of Alternate Energy Performance Standards for Residential Appliances

\*Capital letters refer to Information Flows discussed in the text.

- H:\* peak power use by appliances and cost of peak power; oil use (through use of peak power),
- I: final data base on costs of energy conservation measures and associated energy savings,
- J: final improvements in ORNL model; refinement of consumer decision-making algorithm,
- K: final results of life-cycle cost analysis, including sensitivities (see C and D),
- L: results of residential energy projections with and without standards; results of net present value analysis,
- M: effects of alternative policy approach on consumer decision-making and vice-versa,

\*Although the approach can be applied to any appliance, LBL's effort will place greatest emphasis on residential heating and cooling equipment.

\*This information will not be available except in very preliminary form during F.Y. 1980.

- N: final results of residential energy use projections and net present benefit (cost) of alternative standards,
- O: final results of selected direct economic impacts of alternative formulations of standards (including regional versus national standards) and levels of standards.

#### FUTURE PLANS

LBL intends to continue its Appliance Energy Performance Standards program after the final rule is issued in F.Y. 1980. In particular, the following four tasks will be pursued:

- determinants of residential peak loads and the impact of federal policies (including energy performance standards) on peak loads,
- elements of consumer decision-making that affect purchase of energy efficient products; policy implications of consumer decision-making,
- improvements and application of residential energy forecasting tools (especially the ORNL model),
- analysis in support of updating the appliance energy performance standards.

## THE IMPACT OF ENERGY PERFORMANCE STANDARDS ON THE DEMAND FOR PEAK ELECTRICAL ENERGY

*M. Levine, J. McMahon, S. French, and R. Pollack*

#### INTRODUCTION

A major issue in the assessment of residential energy performance standards (the subject of two LBL programs--residential building and appliance standards analysis--discussed in this volume) is the effect of standards on the peak loads of electric utilities. The importance of this issue is twofold:

- If the standards reduce the use of peak power more than they reduce base power demand, then they will provide benefit to utilities in reducing the peak to base ratio (and thus reduce the requirement for new generating capacity). This will save the utilities and utility customers money, both because of the reduced growth of generating capacity and because of the reduced demand for peak power (which is generally two to four times as expensive as baseload power).
- To the extent that an appliance consumes peak rather than base electricity, the economics of energy conservation should be evaluated against the price of peak power in evaluating the cost effectiveness of an energy performance standard. This will have the effect of significantly tightening the level of the energy performance standard for those appliances that draw a substantial fraction of their power during periods of peak demand for electricity.

This project is designed to evaluate these two issues. Many tools are available to project the growth of average electrical demand in a utility service area. However, the analysis of the determinants of peak power is in relatively early stages of development. As a result, this project is seen as a multi-year effort and its primary goal is to advance the state of the art in the understanding

of the factors influencing the growth of peak electrical demand. In the near term, the results will emphasize the qualitative and quantitative assessment effects of the residential energy standards (building and appliances) on peak power and the effects of the peak power impacts on these standards. In the long term, the project output should be particularly useful in two additional areas: (1) assessing the interactions among a wide range of federal energy policies and growth in demand for peak power and (2) utility load management planning to achieve a reduction in the growth in demand for peak electrical power.

#### UNIQUE ASPECTS OF THE STUDY

Utility planning for installation of new capacity requires load forecasting with particular emphasis on annual peak demand. Utility operations require similar forecasts of daily load curves. Existing methods accomplish these forecasts without an understanding of the instantaneous demand at the end use level. This reduces the reliability of the demand forecasts as well as severely limiting their utility in assessing impacts of energy performance standards on electric utilities and users of electricity.

This project investigates the shape of the load curve by starting at specific end uses and building upwards from the household demand, to system load. This is the opposite approach to current analyses, which collect data about some aggregate load and seek correlation with averaged data (e.g., saturation of air-conditioners).

Analysis is directed toward clarification of coincidence of use among different appliances in the same household in addition to the more traditional coincidence of use for the same appliance among a population of households (diversity). This approach, expanded to treat industrial and commercial end uses, can explain the difference

in time between the system peak and the residential air-conditioning peak in certain summer peaking utilities.

The greater level of detail achieved by considering individual end uses should result in a better understanding of causes of variability in weather and time-dependent demand. For example, present forecasting methods work well for predicting the average dependence of load on temperature, while the proposed method should reduce the range of error of such forecasts.

#### DESCRIPTION OF RESEARCH TASKS

##### Task 1: Collection of Existing Data

Much data is currently available bearing on time and weather demand, although only a small subset deals with demand at the end use level required for this analysis. Accessible data include:

- LBL data bases obtained from load surveys of residential end uses (including lighting);
- California Energy Commission forecasts and background information;
- Dynamics of total energy systems (Ref. 1).
- Office of Technology Assessment Solar Study (Ref. 2);
- Effects of weather variability on load (Ref. 3);
- Utility load curves, including:
  - Connecticut peak-load pricing experiment data and related analysis (Refs. 4 and 5).
  - Detroit Edison Company Summer 1975 air conditioning study (Ref. 6);
  - New York State Department of Public Service (Ref. 7); and
- U.S. Washington Center for Metropolitan Studies aggregate data on residential energy consumption for 1973 and 1975.

##### Task 2: Development of Peak Power Simulation Model

A preliminary methodology for analyzing aggregate demand as a function of constituent end use demands has been established. Inputs for each end use include: (1) capacity (or maximum load) of appliance; and (2) coefficient of use for each consumer class as a function of time of day, temperature and policy.

Calculations performed by the model include successive aggregation of the input data and derivation of diversities and average demands where appropriate. The general form of the calculation of demand by the  $j^{\text{th}}$  household for a time period (e.g., one hour) is:

$$D_{HH,h,T}^{(j,k)} = \sum_i \text{COU}_{k,i}(h,T,p) \cdot (\text{SA}_i) \cdot \text{UEC}_i(m)$$

where:

- $\text{UEC}_i(m)$  is the hourly energy consumption of appliance  $i$  of type  $m$  (brand  $x$ );
- $\text{SA}_i$  is the "saturation" (= 1 if household has appliance  $i$ ; =  $\emptyset$  if not);
- $\text{COU}_{k,i}(h,T,p)$  is the coefficient of use appliance  $i$  at hour  $h$  for consumer class  $k$  given condition of policy (or price)  $p$  and temperature (or season)  $T$ .

Appropriate summations give the daily demand of the household, the demand of all households of a given consumer class, and the total demand within a utility service area. Further calculations include coincidence of use of different appliances in a single household as well as coincidence of use for the same appliance among different households, and the diversified demand for the complete set of households in a specific utility service area.

Output from the model calculation will include: (1) aggregated demand (several households) versus time of day, i.e., daily load curve; (2) peak demand as a function of constituent end uses; (3) daily energy consumption per end use per household; (4) "diversity" of use for the same appliance in all households; and (5) "diversity" of use of different appliances in the same households. The model will be run first for a case in which no energy standards are assumed, based on the projection developed in other parts of the Appliance Energy Performance Standards (AEPS) program using the Oak Ridge National Laboratory (ORNL) Residential Demand Model. A second set of runs will analyze cases in which different energy standards are implemented by the government. The difference between the first and second sets of runs will provide a quantitative estimate of the effect of alternative standards on the peak loads of electric utilities.

##### Task 3: Application of Results to the Setting of the Levels of the Energy Performance Standards

The results of the model calculations will provide a basis for estimating the following parameters:

- fraction of peak power used by different residential appliances (including heating and cooling equipment);
- the sensitivity of peak power requirements of residential appliances to weather, conservation in the building shell, and appliance size and performance characteristics;
- the cost of the peak power requirements of the different appliances in different environments and locations; and
- the amount of oil and gas that is consumed by appliances as a result of their use of peak electrical power.

These data will be used directly to refine and improve the evaluation procedure for establishing the levels of the standards (see article in this volume on the appliance energy performance standards). Specifically, the life-cycle costing will take into account the cost or value of electricity used by different appliances, thus increasing the stringency of the standards for the appliances that draw a large fraction of peak power.

#### Task 4: Extension of Analysis to Other Key Policy Areas

This methodology will make possible an in-depth analysis of various load management strategies as they affect daily energy consumption and peak demand. The existence of different consumer classes as a function of daily activity patterns and demographic variables allows explicit treatment of changes in energy demand as a function of social or behavioral change. As more data on responses to different pricing schemes becomes available, these elasticities can also be added.

Some strategies of interest that may be examined with this model are:

- Direct load control by the utility. Experiments are already under way in some service areas where radio control of certain devices (air conditioners, water heaters) is initiated at high demand levels. This may involve complete interruption, or cycling of service to particular end uses when a certain demand level is exceeded (Ref. 6).
- Rate incentives to consumer. This voluntary measure provides economic incentives to utility customers to shift part of their demand to cheaper, off-peak times and has been shown to have significant effects in residential daily load curves.
- Conservation measures. As noted, the primary focus of the F.Y. 1980 effort has been the analysis of the effects of energy performance standards on peak loads. Additional research could analyze the effects of other energy conservation policies on peak loads: e.g., tax incentives, government financing strategies, involvement of utilities in billing for energy consuming consumer durables.
- Dispersed energy storage. Intuition leads to the expectation that dispersed storage will smooth load profiles; a quantitative estimate of those effects will be very valuable and can contribute to a clearer understanding of the economic trade-offs involved between investments in storage systems and in added generating capacity.
- Solar space heat/cooling. A significant penetration of solar systems into the market for home heating and cooling can have major effects on the shape of energy demand due to the possible weather-driven correlation of behavior of all such systems in a service area. This model provides a useful tool for evaluating the impacts of such a transition.

Finally, this model may be used for an estimation of peak demand under a wide range of conditions, but even more important than the estimation of that single measure is the attendant understanding of the components most responsible for growth in peak demand and of possible strategies for mitigating that growth.

#### REFERENCES

1. J. W. Stetkar and M. W. Golay, "TDIST, a program for community energy demand analysis and total energy system response simulation," Final Report, Massachusetts Institute of Technology, Cambridge (August 1976).
2. \_\_\_\_\_, Application of Solar Technology to Today's Energy Needs, Volume 1, Office of Technology Assessment, Washington, D.C. (June 1978).
3. E. R. Reiter and A. M. Starr, "Effects of atmospheric variability on energy utilization and conservation," Final Report, Colorado State University, Fort Collins, Department of Atmospheric Sciences (February 1978).
4. C. W. J. Granger, R. F. Engle, R. Ramanathan and A. Andersen, "Long-term residential load forecasting," Volume 1, Final Report, Electric Power Research Institute, Research Project 943-1 (February 1976).
5. A. Lawrence (ed.), "Forecasting and modeling time-of-day and seasonal electricity demands," Electric Power Research Institute, EA-578-SR, Palo Alto (December 1977).
6. T. S. Yau and C. J. Frank (eds.), "Power system planning and operations: Future problems and research needs," Electric Power Research Institute, EPRI EL-377-SR, Palo Alto (February 1977).
7. P. D. Mathusa, "An examination of the integrated effects of adopting various energy conservation and load leveling policies for the metropolitan area of New York City," Final Report, New York State Department of Public Service, Albany (February 1978).

# SOLAR ENERGY PROGRAM

## INTRODUCTION

Solar energy has become a major alternative for supplying a substantial fraction of the nation's future energy needs. The Department of Energy (DOE) supports activities ranging from the demonstration of existing technology to research on future possibilities; and at LBL projects are in progress which span that range of activities.

To assess various solar applications it is important to quantify the solar resource. In one project, LBL is cooperating with the Pacific Gas and Electric Company in the implementation and operation of a solar radiation data collection network in northern California. Special instruments have been developed and are now in use to measure the solar and circumsolar (around the sun) radiation. These measurements serve to predict the performance of solar designs which use focusing collectors (mirrors or lenses) to concentrate the sunlight.

Efforts are being made to assist DOE in demonstrating existing solar technology. DOE's San Francisco Operations Office (SAN) has been given technical support for its management of commercial-building solar demonstration projects. The installation of a solar hot water and space heating system on an LBL building established model techniques and procedures as part of the DOE Facilities Solar Demonstration Program. Technical support is also provided for SAN in a DOE small scale technology pilot program in which grants are awarded to individuals and organizations to develop and demonstrate solar technologies appropriate to small scale use.

In the near future it is expected that research will exert a substantial impact in the areas of solar heating and cooling. An absorption air conditioner is being developed that is air cooled yet suitable for use with temperatures available from flat plate collectors. With inexpensive but sophisticated micro-electronics to control their operation, the performance of many-component solar heating and cooling systems may be improved, and work is under way to develop such a controller and to evaluate commercially available units.

Research is continuing on "passive" approaches to solar heating and cooling where careful considerations of architectural design, construction

materials, and the environment are used to moderate a building's interior climate. Computer models of passive concepts are being developed in a collaborative project with Los Alamos Scientific Laboratory. These models will be incorporated into public domain building energy analysis computer programs to be used in systems studies and in the design of commercial buildings on a case study basis. The investigation of specific passive cooling methods is an ongoing project; for example, a process is being studied in which heat storage material would be cooled by radiation to the night sky, then provide "coolness" to the building.

The laboratory personnel involved in the solar cooling, controls, and passive projects are also providing technical support to the Solar Heating and Cooling Research and Development Branch of DOE in developing program plans, evaluating proposals, and making technical reviews of projects at other institutions and in industry.

Low grade heat is a widespread energy resource that could make a significant contribution to energy needs if economical methods can be developed for converting it to useful work. Investigations continued this year on the feasibility of using the "shape-memory" alloy, Nitinol, as a basis for constructing heat engines that could operate from energy sources such as solar heated water, industrial waste heat, geothermal brines, and ocean thermal gradients.

Several projects are investigating longer-term possibilities for utilizing solar energy. One project involves the development of a new type of solar thermal receiver that would be placed at the focus of a central receiver system or a parabolic dish. The conversion of the concentrated sunlight to thermal energy would be accomplished by the absorption of the light by a dispersion of very small particles suspended in a gas. Work continued this year on chemical storage processes (such as  $2SO_3 = 2SO_2 + O_2$ ) that could play an important role in providing long-term storage for high temperature power generation cycles. Another project is exploring biological systems. The possibility is being explored of developing a photovoltaic cell, based on a catalyst (bacteriorhodopsin) which converts light to electrical ion flow across the cell membrane of a particular bacteria.

# ULTRAFINE PARTICLE SUSPENSIONS FOR SOLAR ENERGY COLLECTION\*

A. J. Hunt

## INTRODUCTION

Solar energy is being considered as a practical source of high temperatures to operate very efficient heat engines and provide industrial process heat. Many current concepts for conversion of sunlight to heat are based on traditional, nonsolar technologies. This project uses a novel approach to match the characteristics of concentrated sunlight to the requirements of heating a gas.

The purpose of the work is to develop a new type of solar thermal receiver that utilizes a dispersion of very small particles suspended in a gas to absorb the radiant energy directly from concentrated sunlight. The Small Particle Heat Exchange Receiver (SPHER) operates by injecting a very small mass of fine, light-absorbing particles into a gas stream. The air-particle mixture then enters a transparent chamber that forms the solar thermal receiver. Sunlight is focused through the window of the receiver by a concentrating solar collector (a parabolic dish or a field of heliostats). Suspended particles absorb the radiation and, because of their very large surface area, quickly transfer the heat to the surrounding gas. The air-particle mixture heats to the desired temperature until the particles vaporize or oxidize. The gas may be heated to medium or high temperatures as suitable for a variety of power or industrial process heat requirements. Mechanical power can be produced if the gas is compressed before it is heated and subsequently expanded through a turbine or other device such as a Brayton cycle engine. The resulting shaft rotation can be used to turn an electrical generator or provide mechanical power for other purposes.

The most important characteristic of these small particles is their extremely large surface area per unit mass of absorber material. (One gram of particles for this application has a surface area of the order of 100 square meters.) This results in a high absorption coefficient for the incoming sunlight and a high optical efficiency for the receiver. The combination of the large surface area and the small size of the particles insures that the particle temperature stays to within a fraction of a degree of the gas temperature. Thus, the highest temperature present in the receiver is essentially that of the working gas. This results in considerably lower radiant temperatures in the chamber compared to other solar receivers that produce gas of the same temperature. Since the chamber window inhibits infrared reradiation from the heated particle-gas mixture, the receiver has a high overall efficiency.

There are several other important advantages to the use of small particles as heat exchanger elements. SPHER eliminates the need for heavy and complex heat exchanger elements, since its receiver basically consists of a hollow chamber with a window, resulting in a very lightweight structure.

Because the heat exchanger is uniformly distributed throughout the chamber, the gas need not be pumped through pipes or small orifices. Therefore the amount of energy required to overcome pressure losses is considerably reduced. Because the heat exchanger is vaporized in the process of performing its function, problems associated with maintenance, failures, heat stress, or corrosion, which occur with conventional heat exchanger elements, are eliminated.

The basic small particle gas receiver can be scaled to any size. Upper size limitations are determined by window design, by the use of multiple windows, a matrix of transparent quartz tubes, or other modular designs; this technique is applicable to sizes characteristic of the solar central receiver program. The concept can also be applied on a small scale by using a parabolic dish concentrator and off-the-shelf gas turbines in the 10 kW size range.

Because there are no temperature limitations on the heat exchanger in the usual sense, SPHER is applicable to the field of high-temperature solar process heat. The ultimate temperatures achievable using SPHER are limited only by the chamber walls, the window (if pressurized operation is desired), and the second law of thermodynamics. It appears that gas temperatures in excess of 2000°C are achievable.

Calculations performed earlier quantify the optical and physical processes of absorption and heating of the particles.<sup>1,2</sup> Related considerations investigated include particle production methods, window and chamber designs, hybrid fossil-solar compatibility, as well as environmental and safety factors. Analyses confirm that the operating parameters are flexible and suitable to a variety of solar thermal power applications. A modest laboratory apparatus built earlier successfully demonstrated the SPHER concept.<sup>3</sup>

## ACCOMPLISHMENTS DURING 1979

In FY 1979 the operation of the various subsystems was investigated and the overall efficiency and system parameters were determined. Theoretical work was performed to determine the efficiency and operating conditions of a high-temperature receiver utilizing a transparent window. Two different window designs were evaluated, material and sealing considerations were addressed, and window costs were determined. A new type of heat engine utilizing the SPHER concept was studied to determine its thermodynamic efficiency. An experimental program was initiated to produce and characterize the particle suspensions. A patent application was filed on the SPHER concept with the rights held by DOE.<sup>4</sup>

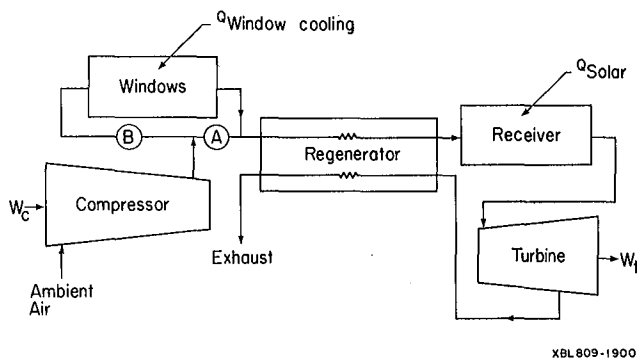
### Windowed Receiver Studies

A study of the optical and thermodynamic efficiencies of single- and double-windowed high-temperature gas receivers was completed.<sup>5</sup> The two-window design utilized a cooling gas flow between the windows. Calculation of receiver performance is based on a detailed window energy balance that includes the energy flows resulting from both radiative and convective transfer to and from the window(s). Equations governing the energy flows were written using conservative estimates for the quantities involved. Parameters were varied by an iterative process until a self-consistent solution was obtained. Once the window temperatures were determined by this process, the total energy loss and the receiver collection efficiency were calculated.

The analysis is based on the assumption that the receiver is sized to 4 MW(t) per module. In the double window design, cooling air flowing between the windows comes directly from the compressor and then passes on to the recuperator. Receiver efficiencies obtained for a gas temperature of 1000°C using high silica windows spanning a 1.7-m opening were 93.8% and 95.4% for the single- and double-window designs respectively. Losses due to each mechanism are computed and their relative contributions assessed.

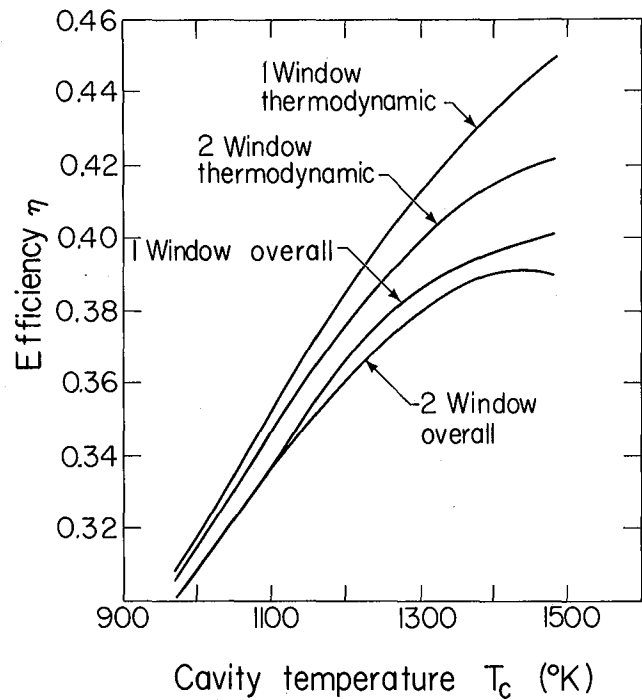
It is important to consider the overall system efficiency as well as that of the receiver alone. Figure 1 illustrates a Brayton cycle turbine system connected to a SPHER. In the case of a single windowed receiver, the air from the compressor passes directly to the recuperator that recovers heat from the exhaust gases. In the double window design, the compressed air first passes between the windows to provide cooling.

Single and double window systems are compared in overall thermodynamic efficiency (product of the receiver and Brayton cycle efficiencies) as a function of turbine inlet temperature in Fig. 2. Note that the thermodynamic cycle efficiency



XBL 809-1900

Fig. 1. System diagram for a Brayton-cycle turbine combined with a SPHER. Path A is used for the single-window design, and Path B for the double-window design. (XBL 809-1900)



XBL 809-1899

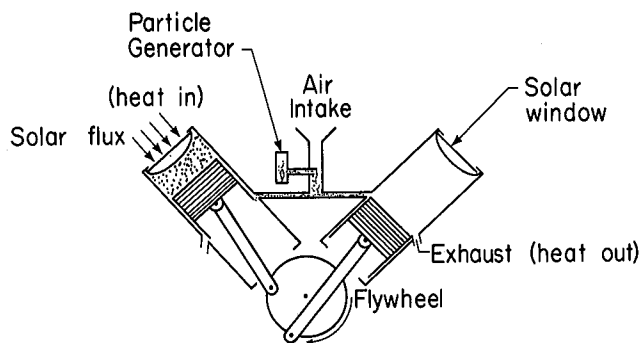
Fig. 2. Thermodynamic and overall efficiencies for one and two window systems. Note: Overall efficiency is defined as the product of thermodynamic and receiver collection efficiency. (XBL 809-1899)

associated with the single window is significantly higher than that for the two-window design. This occurs because the cooling air for the two-window system passes into the recuperator at a higher temperature, reducing the amount of heat recovered from the exhaust gases. The overall effect of this is to make the single-window system more efficient even though the efficiency of the double-window receiver alone is higher.

Sensitivity studies performed by varying each parameter from the baseline design indicate their effects on system efficiency. Techniques used in this analysis are not restricted to receivers of the SPHER type but are general enough to be applied to a number of windowed receiver designs.

### Efficiency Study of New Type of Heat Engine

Early in the program, it was realized that the basic concept of the direct absorption of sunlight in a gas could be applied to a number of situations; in particular, it presented possibilities for new types of heat engines. To investigate the feasibility of reciprocating engines in which the solar flux is deposited into the cylinder, a preliminary investigation of the associated thermodynamic cycle efficiencies was initiated.<sup>6</sup> The basic concept is illustrated in Fig. 3. The cylinder induces a charge of cool air that contains a suspension of small heat-absorbing particles. At some point in the cycle, an optical valve opens, allowing concentrated sunlight to be focused through the top of the cylinder by a quartz window acting as a lens.



XBL 809-1897

Fig. 3. Schematic view of simple two-cylinder solar engine. Cylinder on the left is near end of compression stroke. At this point, solar flux is directed into cylinder. Cylinder on right is near the end of work stroke. Particles in this cylinder have oxidized. (XBL 809-1897)

The air-particle mixture absorbs the sunlight directly and heats the gas. As the heated gas expands, work is done on the piston providing mechanical power. The cycle efficiency for different periods and phases of the heat injection is being investigated.

The thermodynamic question can be posed as follows: given a constant rate of heat input, and a period equal to the reciprocal of the number of cylinders, what is the optimum timing and the corresponding efficiency? Preliminary results indicate that the efficiency for a two-cylinder engine is about 50% for a compression ratio of 12 when heat injection starts well before the top dead center position of the piston.

#### Experimental Particle Production

A laboratory has been obtained, equipped, and is in operation. Work has begun on two alternative methods of producing carbon particles suitable for high-temperature receiver work. One method utilizes an enclosed diffusion flame and has successfully produced very dense particle streams. The second method relies on a high-intensity arc in an inert gas atmosphere. Work is under way on the experimental chamber and a set of remotely controlled electrode holders are being fabricated.

#### PLANNED ACTIVITIES FOR 1980

The experimental program for next year will have three main emphases: particle production, particle characterization, and the determination of the performance of the particle-gas mixture as a heat exchanger. Work will continue on using rich-burning flames with various feed gases and combustion parameters. High-intensity arcs will be used as a means of producing particles of a variety of carbon allotropes. Once good candidates

for particle generation are obtained, measurements will be performed to characterize the particles and determine their operating parameters in a receiver.

Opacity measurements will be performed on the particle-gas mixture as well as on collected samples of the particles. Oxidation properties will be determined by optical measurements on particle samples in a high-temperature furnace. Electron microscopy will be used to determine the size, size distribution, and shape of the particles.

An analytical program will be used for guidance and interpretation of the laboratory work. Computer codes to analyze the optical and thermodynamic properties of the system will be written.

A chamber will be constructed to determine the temperature rise and energy exchange to a particle-gas stream. It will utilize a tungsten halogen light source to simulate the sun. The goal is to gain enough experience to design a test receiver to operate with a solar collector. If enough interest is expressed, future plans include the fabrication of a larger SPHER and a testing program at a National Solar Thermal Test Facility.

#### FOOTNOTE AND REFERENCES

\*This work has been supported by the U.S. Department of Energy under contract no. W-7405-ENG-48.

1. A. J. Hunt, "Small particle heat exchangers," Lawrence Berkeley Laboratory report LBL-7841 (1978).
2. A. J. Hunt, "A new solar thermal receiver utilizing small particles," Presented at the 1979 ISES Congress, Atlanta, Georgia, May 28 to June 1, 1979, Lawrence Berkeley Laboratory report LBL-9317.
3. A. J. Hunt, "A new solar thermal receiver utilizing a small particle heat exchanger," Proceedings of the 14th Intersociety Energy Conversion Engineering Conference, Boston, Massachusetts, August 5-10, 1979, and Lawrence Berkeley Laboratory report LBL-8520.
4. A. J. Hunt, "Radiant energy collection and conversion apparatus and method," patent pending.
5. W. Fisk, D. Wroblewski, and A. J. Hunt, "Performance analysis of a windowed high temperature gas receiver using a suspension of ultra-fine carbon particles as the absorber," Lawrence Berkeley Laboratory report LBL-10100 (1980).
6. P. Hull and A. J. Hunt, "A reciprocating solar heated engine utilizing direct absorption by small particles," draft, to be submitted to the J. of Solar Energy Engineering.

# SENSIBLE HEAT STORAGE FOR A SOLAR THERMAL POWER PLANT\*

T. Baldwin, S. Lynn, and A. Foss

## INTRODUCTION

The energy input to a solar power plant depends on the amount of insolation reaching the collection field. Maintenance of a constant level of power generation through the early evening hours or through a period when the cloud cover varies requires integration of the heat collection and power generation units with some type of energy storage unit.

This work examines in detail one possible configuration for a solar power plant with a sensible-heat storage unit. The proposed flow sheet allows thermal energy storage between the heat collection unit and the power generation unit without a reduction in the thermodynamic availability of the energy supplied to the power turbines. Energy is stored by heating a checkerwork of magnesia bricks. A gas that is circulated from the solar collector through the storage unit and the power plant boiler serves as the heat-transfer medium. A standard steam Rankine cycle is used in power generation. The process configuration is shown in Fig. 1.

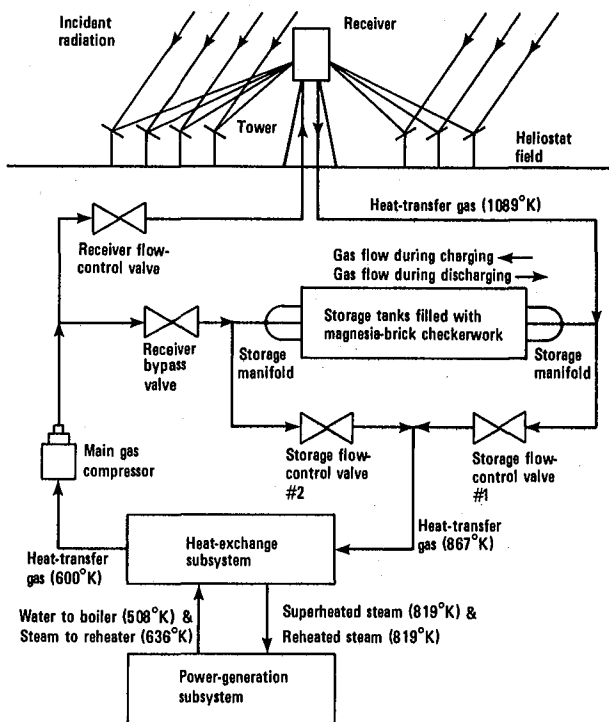


Fig. 1. The proposed flowsheet for a solar power plant with sensible-heat storage.

(XBL 797-2191)

This work was begun in 1977 to compare power costs of a process using sensible heat storage to those of a process using the sulfur-oxide chemical heat storage concept.<sup>1,2</sup>

## ACCOMPLISHMENTS DURING 1979

A computer model was developed to predict the behavior of the sensible-heat storage unit and to aid in sizing the storage unit. Procedures were developed to estimate the cost of electricity generated by the solar power plant. These procedures illustrate the effect of changes in the energy storage unit on the cost of electricity. The effects on the storage unit and on the total plant design of changing several process and design parameters were then evaluated.

The proposed configuration for a solar power plant with sensible-heat storage for nighttime electricity generation produces electricity at a cost of 8.7¢/kW(e)-hr. If one forgoes storage for nighttime power generation, the cost drops to 7.6¢/kW(e)-hr. Both of these power plants convert 32% of the energy absorbed by the central receiver into usable electric energy. These costs and efficiencies are more favorable than those of the sulfur-oxide storage system<sup>1</sup> for which the cost was 10.7¢/kW(e)-hr at 25% efficiency, but they are not so favorable as those of Tyson et al.<sup>3</sup> who estimated the cost and efficiency for a sulfur-oxide storage system combined with a hybrid Brayton-Rankine cycle to be 7.7¢/kW(e)-hr and 39%.

Modifications in the sensible-heat storage process to incorporate a Brayton cycle as topping for the steam cycle showed no advantage in power cost.

Because power costs for plants with sensible-heat systems are close to those of sulfur-oxide systems and because the uncertainties in technical aspects are less for the sensible-heat systems, it appears that they will serve best for short-term storage at the present time.

## PLANNED ACTIVITIES FOR 1980

This work is completed and no further work is planned.

## FOOTNOTE AND REFERENCES

\*This work was funded during FY 1979 entirely by the Department of Energy, Division of Energy Storage Systems.

1. J. Dayan, S. Lynn, and A. Foss, "Evaluation of a small oxide chemical heat storage process for a steam solar electric plant," Lawrence Berkeley Laboratory report, LBL-7868 (July 1979).
2. T. F. Baldwin, S. Lynn, and A. Foss, "Sensible heat storage for a solar thermal power plant," Lawrence Berkeley Laboratory report, LBL-9321 (July 1979).
3. G. Tyson, S. Lynn, and A. Foss, "A solar heated gas-turbine process using sulfur oxides for power production and energy storage," Lawrence Berkeley Laboratory report, LBL-9472 (September 1979).

## PASSIVE SYSTEMS ANALYSIS AND DESIGN\*

*R. Kammerud, H. Akbari, B. Andersson, F. Bauman, C. Conner, M. B. Curtis,  
M. Daneshyar, A. Gadgil, A. Mertol, W. Place, T. Webster, K. Whitley, and T. Borgers*

### INTRODUCTION

The Passive Systems Analysis and Design Group began in response to a void in passive solar technical information and passive solar analysis tools. Historically, the primary focus of the program has been computer modeling. This work has been a joint undertaking of the Solar Group at LBL and the WX-4 group at Los Alamos Scientific Laboratory, which had responsibility for the development of the active solar simulation capabilities in DOE-I and DOE-II. Computer work is being coordinated with the conservation group at LBL, which has primary responsibility for the development of conventional building analysis capabilities of DOE-II. Some of the passive solar analysis and design projects are also related to work being done in the Windows and Lighting program at LBL. We are currently shifting the focus of our activities from the residential to the commercial sector.

Recently the group has expanded its efforts to include building design projects. Projects of this nature provide a framework for development of concepts, design tools, and technical information directly related to commercial buildings and the design community's needs. The Passive Solar Program at LBL continues to provide support for related DOE activities in the areas of national program planning, solicitation preparation, contracting, and contract technical monitoring.

### ACCOMPLISHMENTS DURING 1979

#### Heat Transfer Analysis

Theoretical and experimental heat-transfer studies accounting for thermocirculation, single-zone convective heat transfer, and convective heat transfer through doorways and other wall openings were performed.

A detailed thermal analysis of both laminar and turbulent flow in thermocirculation systems was completed, documented, and successfully compared to laboratory data found in the literature. This detailed loop model (DLM) was used to generate simplified algorithms capable of deriving the outlet temperature and flow rate. Specifications were

written to include these algorithms in the public domain computer program BLAST (Building Loads Analysis and System Thermodynamics), extending its capabilities to storage walls and massless vertical collectors.

A small-scale experiment designed to measure convective heat transfer was designed and assembled. The apparatus was used to generate data for comparison with the previously cited algorithms. Exploratory studies of the two-zone problem were initiated using the apparatus.

A model designed to simulate the thermal performance of roof pond systems was developed. The model includes options, such as an evaporative water layer over water containment bags; and movable insulation between both the roof pond and the environment, and between the occupied space and the roof pond. Compared to currently available models, this model performs a more detailed analysis of the interaction of water layers and the environment.

Other refinements and extensions of BLAST were completed: successful comparisons were made between BLAST and thermal data from test cells located at LASL; algorithms describing ventilative cooling were inserted; and BLAST specifications were written to include movable insulation.

#### Building Performance Studies

Building experiments can provide detailed data for validating thermal simulations of well-established passive systems or can serve as a tool for exploring the behavior of new passive concepts. In the former category of experiments, a number of test cells and passive residences in the U.S. have been heavily instrumented for acquiring weather, auxiliary consumption, and internal temperature data. The major unknown in each of these structures is the level of infiltration. In contribution to the national program for passive system data acquisition and thermal simulation validation (more specifically, in support of BLAST validation), the LBL Passive Solar Group has built an infiltration measuring apparatus modeled after a similar device developed by the LBL Building Envelopes

Group. This device will be used on a variety of instrumented passive structures to produce the full complement of data required for proper validation of building energy analysis computer programs. In addition to these validation-related experiments, exploratory studies were initiated on a double-envelope, convective-loop residence in Martinez, California.

BLAST was used extensively to study the sensitivity of residential heating and cooling to structural mass and thermostatic controls.

Plans were made for using BLAST in commercial building parametric sensitivity studies. A review of various commercial building energy consumption studies was made in order to:

- identify the building types which account for sizeable fractions of the national energy consumption.
- identify the nature of the energy demand.

Based on that review, the decision was made to:

- emphasize retail-wholesale, office-public, and educational building types
- give balanced consideration in accounting for space heating, space cooling, lighting and distribution energy.

#### Passive Solar Building Design and Design Tools

Design and analysis assistance was given in varying amounts to several building projects with the aims of (1) assisting in the design of better passive buildings, and (2) identifying design requirements not fulfilled by commonly understood and available tools.

At the request of the Pittsburgh Energy Technology Center, LBL conducted extensive analysis on a proposed energy conservation building to determine the energy savings of passive design elements compared to those of the original design, and to assist in design refinement. Several helpful design tools were identified, including better methods of displaying weather information, shade design using sun charts and a graphic technique, and analysis of window placement and construction.

Design assistance was given to several projects which asked for help in assessing the energy impacts of their designs, and critiques of their integration of architectural and energy considerations. The designers of the Heavy Ion Institute at Oak Ridge National Laboratory received advice on the architecture, energy design, and instrumentation of their underground/passive building. The designers of a two-unit residential passive retrofit came to us for advice on their own passive design. LBL involvement resulted in a much simpler, less expensive system capable of delivering more heat than the original design.

Members of the Passive Solar Group have worked closely with the design team for the Colorado Mountain College Classroom and Administration building(s). Several important decisions have been

made with regard to structure, glazing areas, and mechanical systems as a result of energy analysis by the Passive Solar Group.

All of these passive solar design activities have been used to identify tools useful during the design process. Participation of LBL personnel as designers, experts in building thermal analysis computer programs, and as observers of the design process have highlighted the need for analysis tools and capabilities, simpler design tools, graphic design techniques, and simple calculations. This information allowed the Passive Solar Group to direct its development of BLAST toward these capabilities most needed by passive solar designers, and to encourage the development of building thermal analysis programs suitable to architects' most immediate needs.

#### Headquarters Support

The year's activities in the area of headquarters support vary from preparation of a marketable products solicitation to preparation and publication of a report on passive and hybrid solar heating<sup>1</sup> to completion by an LBL subcontractor of a passive solar design workbook for residential-scale buildings.

#### PLANNED ACTIVITIES FOR 1980

##### Heat Transfer Analysis

The thermosiphon DLM will be completed and used to generate algorithms describing system performance as a function of solar input, ambient weather conditions, load profile, collector characteristics, and heat exchanger properties. Thermosiphon experiments will be used to validate the general behavior of the theoretical models and to establish the effective heat-transfer coefficient for use in those models.

The single-zone room convection model will be extensively explored and sensitivity studies performed to assess the need for more sophisticated convection calculations in the BLAST loads program. Results from the interzonal convective transfer experiment will be used, along with data from related experiments at LASL and NBS (National Bureau of Standards), to generate algorithms for inclusion in BLAST. The roof pond model will be completed and checked, and software written for inclusion in BLAST.

By the end of the fiscal year, the research version of BLAST/Passive will contain the following new capabilities:

- A detailed model describing the interaction of storage roof systems with occupied space.
- A daylighting algorithm. (This project will be performed in conjunction with the Windows and Lighting program at LBL.)
- An algorithm describing convective heat exchange between thermal zones.
- Analysis techniques for shaded roof aperture systems.

- Routines for innovative glazing materials and glazing coatings.
- Algorithms for thermocirculation systems.

A documented version of BLAST/Passive will be made available to the design community. The following capabilities will be included:

- Direct-gain systems with movable insulation.
- Thermocirculation systems with massive and nonmassive absorbers.
- Direct ventilation cooling of the occupied space.
- Direct conductive coupling between thermal zones.

#### Passive Solar Building Design and Design Tools

LBL will continue its cooperation with the designers of the Colorado Mountain College. Two other case study projects will be added: a small passive solar commercial building in Santa Rosa, CA, which will serve as both office space and laboratory, and a large passive multistory shopping center in Newport Beach, CA. All three projects have received grants from DOE for their passive solar design.

Requirements for an architect's energy analysis tool will be further refined. Informative booklets to assist with design of fixed shading devices and selection of window orientation and construction will be produced and distributed. More design tools will be identified during the case studies, and their development will be pursued.

#### Building Performance Studies

Infiltration measurements will be made on a variety of passive solar structures and BLAST predictions will be compared to the data from direct-gain and Trombe Wall test cells and residences. Exploratory studies will continue on the double-envelope house; data will be collected on weather conditions, solar radiation, interior temperatures, convective flow rates, infiltration ground temperatures, and auxiliary consumption. BLAST applications for residential parametric sensitivity studies will continue. Thermal mass and thermostatic control studies will be extended to more climates, glazing distributions, shading operations, and building configurations; effects

of ventilative cooling and movable insulation will be investigated. Simplified methods will be devised for evaluating the thermal effects of massive construction. Parametric studies will be performed using the thermocirculation, room convection, and roof pond models.

BLAST applications for commercial parametric sensitivity studies will focus on: building size, proportion and orientation; glazing area and distribution; human, lighting and equipment loads; zoning; movable insulation; ventilative cooling; thermal mass; occupant use patterns; and electric lighting control strategies. Daylighting will be investigated for various room geometries and lighting control strategies using experimental models. The output of these experiments will provide instructions to BLAST regarding electric lighting levels for various conditions of sunlight. In addition to energy consumption, considerable attention will be given to the comfort/productivity implications of the factors listed above.

#### Headquarters Support

A diverse set of headquarters support activities are planned for 1980. These include issuance of the marketable products solicitation written in 1979 and completion of its concomitant proposal review and contract writing tasks; issuance of a basic physical studies research and development solicitation; completion of program area plans for commercial buildings, basic physical studies, products and materials, and commercial building design tools; and completion of the design of a test facility for evaluation of design concepts for commercial passive solar building systems.

#### FOOTNOTE AND REFERENCE

\*This work was supported by the Passive and Hybrid Systems Branch, Systems Development Division, Office of Solar Applications, U.S. Department of Energy, under contract No. W-7405-ENG-48.

1. Draft Interim Report: "National program plan for passive and hybrid solar heating and cooling," prepared by Energy and Environment Division, Lawrence Berkeley Laboratory, University of California; Solar Energy Research Institute; Heating and Cooling Research and Development Branch - Office of Conservation and Solar Applications of the U.S. Department of Energy, January, 1979. (Also Lawrence Berkeley Laboratory report, LBL-8606 Revised, February 1979).

## NITINOL ENGINE DEVELOPMENT\*

*R. Banks, W. Hubert, R. Kopa, M. H. Mohamed, and M. Wahlig*

### INTRODUCTION

Low-grade heat, in the form of thermal energy at temperatures below the boiling point of water, is a widespread energy resource that could make a significant contribution to worldwide energy needs if an economical technology can be developed for converting it to useful work. The Nitinol Engine Development project is investigating the feasibility of using the thermally-activated shape change phenomenon in certain intermetallic Shape Memory Alloys, particularly the nickel-titanium compound "55-Nitinol", as the basis for thermal-to-mechanical energy conversion at temperatures available from such sources as industrial waste heat, low-temperature geothermal brines, solar-heated water, or the moderate temperature differences that exist in the ocean thermal gradient. An important advantage in using a solid rather than a fluid working medium in such applications is the possibility of eliminating the heat exchangers required by closed-cycle fluid systems, which often constitute major cost and maintenance items in conventional low-temperature energy conversion technologies.

A prototype Nitinol heat engine has been in operation at the Lawrence Berkeley Laboratory since August 1973. Since that time, several iterations of engine design have led to an improved understanding of the important practical considerations in applying this material to energy conversion in continuously cycling heat engines. These studies, as well as experimental and theoretical investigation of the material's thermodynamic and metallurgical properties, have confirmed that Nitinol engines for the recovery of thermal energy from low-grade or waste heat can be constructed; however, the question of economic feasibility is still open.

### ACCOMPLISHMENTS DURING 1979

The work of the past year has been focused on experimental investigation of cycling and thermodynamic characteristics of Nitinol through three parallel approaches using specialized test instruments designed and fabricated at the Laboratory during this year and previously. The first of these, an electronically controlled and instrumented Cycle Simulator, was used to compare the effects of performance and lifetime of Nitinol wires cycled under differing thermomechanical conditions (e.g., heating at constant strain versus heating under uniform load.) The Cycle Simulator has the flexibility to vary and control a number of parameters that are critical to practical engine design, particularly in the area of phasing the shape-memory response in the working material with the mechanical response time of engine power take-off components. Based on data derived from the Cycle Simulator studies, comparative efficiencies for the various types of cycles investigated were derived.

A second approach to identifying optimum cycling and work output conditions for Nitinol wires was carried out using a high resolution, laser-beam dilatometer. This instrument, which magnifies axial displacement in a Nitinol specimen by a factor of 200, makes possible observation of variation in the rate of change throughout the complete thermal transition range under controlled and uniform heating rates and stress conditions. Correlating stress and displacement data with calculated heat input values, comparative conversion efficiencies were predicted for a range of thermal cycle conditions.

The third experimental instrument, a Tensile Fatigue Test Stand, fabricated at LBL in early 1979, has subjected Nitinol wire elements to actual engine working conditions for more than one million cycles, the highest limit now known for reproducible cycling of wires working in the mode of linear (axial) strain. This machine, which appears to have overcome many of the problems encountered in previous engine concepts, is the first device since the original 1973 prototype to exceed the million-cycle limit. As in the case of the first engine, systematic improvement in performance of the Nitinol working elements was observed throughout the period of the initial run.

### Cycle Simulator Studies

The Cycle Simulator was used this year primarily in the systematic investigation of two types of cycling conditions: the constant strain cycle, and the stress-limited cycle. In the constant-strain cycle, a single Nitinol wire is heated by immersion in a water bath while held at a constant length. Recovery stresses developed in the wire are allowed to come to a maximum before being relieved by controlled relaxation of the simulator mechanism. Stress and strain data are displayed on a storage oscilloscope, and computation of the area enclosed in the oscilloscope gives the work output for that particular cycle. A typical trace for the constant-strain cycle is shown in Fig. 1.

It was found that heating a Nitinol wire through its thermal transformation range prior to initiating shape recovery severely limits the percentage of initial strain that may be imposed on the specimen prior to heating. This also limits the work output per cycle that can be realized over a large number of reproducible cycles. For a wire lifetime expectancy of  $10^4$  cycles, a strain of 1.0% was found to be the limit for the materials tested, and the maximum calculated conversion efficiency was 1.2% (approximately 6% of the Carnot maximum for the temperatures of the experimental cycle). Limits imposed in heating Nitinol at constant strain have to do with the magnitude of the recovery stresses that develop during the transformation (in excess of 100 Kpsi at 8% strain) and which can effectively exceed the practical yield strength of the material. In addition to being

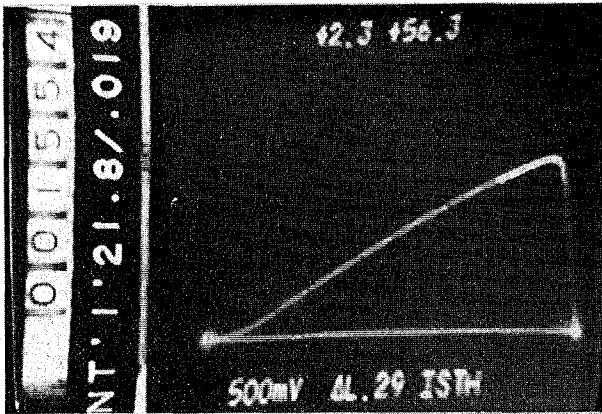


Fig. 1. Video record of a typical constant-strain isothermal cycle. (XBB 786-7388)

an energy transducer, Nitinol is, of course, a realistic engineering material and therefore subject to conventional fatigue constraints like any other metal. The relationship between maximum recovery stress and practical yield strength in Nitinol is closely related to the discrepancy that exists between the calculated strength of pure metals and their observed experimental values. In the case of Nitinol, the recovery stresses generated internally during transformation, must not be allowed to build up to the practical yield strength as a result of external restraining forces, or progressive elongation leading to ultimate failure of the material will result.

For the second series of tests, the Cycle Simulator was modified slightly to apply the shape recovery stress of the Nitinol specimen directly to the lifting of a weight. In this constant-stress cycle, a feasible and reproducible strain limit of 5.0% was observed, with a corresponding increase in indicated conversion efficiency of a factor of  $\geq 2$ . To date, these tests have been conducted at a stress limit of 29 Kpsi, substantially below the theoretical practical limit for the material. With increase in applied stress, and resulting increase in work output per cycle, the conversion efficiency of the constant-stress cycle may reasonably be expected to increase even further.

In addition to the simulated engine cycle tests performed on the Cycle Simulator this year, the instrument was also used to evaluate the effects of an alternative approach to heating the wire by controlled electric pulse rather than immersion in a bath. Timed delivery of the electric pulse was adjusted to correspond to the conditions of normal heat delivery (by immersion), and the cycles produced on the oscilloscope were compared. The area of the work diagram for the electric heating technique was found to be almost identical to that produced by continuous heat delivery in the bath. However, in the case of heating the wire with the electric pulse, all of the energy is absorbed by the wire while it is held at constant strain. From this observation, it was deduced that Nitinol wires absorb the latent heat of transformation prior to the shape recovery event, not during the contraction part of the cycle as had been

assumed by most prior investigators. This is an important new piece of information in our understanding of the basic mechanism of the shape memory cycle.

#### Laser Beam Dilatometer

The Laser Beam Dilatometer, shown in Fig. 2, was originally fabricated in 1977 for the purpose of precisely correlating changes in Nitinol thermal transformation thresholds with variation of externally applied stress; it has subsequently proven useful for a number of other applications. Because of the sensitivity of the amplification mechanism of this device, it is possible to isolate macroscopic changes in shape of a specimen due to the shape memory effect from changes solely due to thermal expansion and contraction. Thus it is possible to demonstrate visually that, at the transition thresholds, changes in the thermoelastic properties of Nitinol are essentially discontinuous with continuous variation of stress and temperature.

Of particular interest is the observation that during a complete thermal transformation cycle (complete establishment of the low-temperature phase on cooling, and complete reversion to the high-temperature phase on heating), there is a sensitive region at approximately the middle of the cycle in which the majority of the shape recovery takes

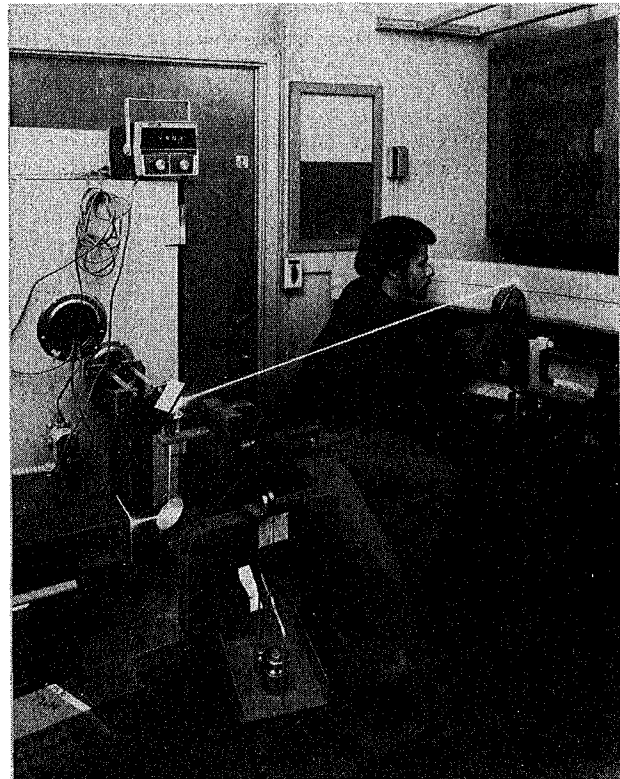


Fig. 2. Laser-Beam Dilatometer, used to measure small axial displacements in a Nitinol wire. (Test specimen is mounted in a temperature-controlled environmental chamber in the background of the photograph). (CBB 796-8367)

place. As heating and cooling is effected (at slow and uniform rates), this most active region is approached by a gradual acceleration in shape-change with respect to rise or fall in temperature, increasing to a change-rate maximum at about the midpoint of the thermal cycle; subsequently, there is again a gradual deceleration in shape-change until the target temperature is reached. This non-uniformity in rate of change, with uniform change in temperature, appears to be enhanced by a directionality that develops in the microstructure of the Nitinol wire. It is a well-known feature of the Shape Memory Effect (SME) in Nitinol that apparent ductility of the low-temperature phase is the result of preferential growth of certain favorably oriented crystal domains (twinned martensite) and shrinkage of others. With repeated cycling (as in the working element of a heat engine), certain of these favored orientations become dominant upon transformation, and the wire develops a "second memory"--a shape change unassisted by externally applied stress--on cooling, a process which has been described as "training". Because transformation threshold temperatures are controlled in part by applied stress, it is to be expected that all martensites of identical orientation (with respect to stress) will be subject to the same local stress conditions, and will transform as a coherent group once the threshold temperature has been exceeded. The appearance of a sensitive thermal region where the SME is at an optimum is therefore interpreted as a reflection of the training process, or a progressive increase in the volume fraction of martensite variants which nucleate in orientations best favored for shape recovery on heating.

After the maximum work output for a "complete" thermal cycle was established by heating and cooling a trained Nitinol specimen to temperatures beyond which there was no observable thermally activated shape change, a series of restricted thermal cycles was performed to determine if work output per cycle would decrease linearly with decrease in  $\Delta T$ . This was found not to be the case. In a series of experimental trials, the thermal extrema of the cycle were reduced from  $\Delta T_{\max} = 120^{\circ}\text{C}$  to  $\Delta T = 30^{\circ}\text{C}$ . For the reduced cycle, a work output was achieved that was equal to 51% of the total work of the larger (reference) cycle, although the sensible heat required to produce the work was reduced by a factor of 4. From this it was calculated that the work of the original (reference) cycle could be reproduced by cycling twice the volume of material in the restricted thermal range, but with a net saving in sensible heat input on the order of 50% for the restricted cycle. It thus appears that the work output (and therefore the conversion efficiency) of Nitinol does not increase linearly with increasing  $\Delta T$ , but that the most favorable range for a practical engine cycle, based on currently available materials, will be in the order of  $15^{\circ}\text{C} \leq \Delta T \leq 35^{\circ}\text{C}$ . Correlating measured work outputs with calculated heat inputs, conversion efficiencies were predicted for cycles in which  $\Delta T = 120^{\circ}\text{C}$ ,  $60^{\circ}\text{C}$ ,  $30^{\circ}\text{C}$ ,  $20^{\circ}\text{C}$ , and  $10^{\circ}\text{C}$ , respectively. The absolute efficiency attained was 2.6% for the  $\Delta T = 30^{\circ}$  cycle, which corresponds to 27% of the Carnot maximum for temperatures of  $25^{\circ}$ – $55^{\circ}\text{C}$ . The highest Carnot fraction calculated was 64% for the cycle at  $\Delta T = 10^{\circ}\text{C}$ , which had an absolute efficiency of 2.0%. As a corollary to this

experiment, a cycle was hypothesized in which  $\leq 50\%$  of the sensible heat rejected on cooling could be stored and recovered in a regenerator. This component, which has not yet been evaluated experimentally, could theoretically increase the computed efficiency values by a factor of as much as 1.4.

During the latter part of the year, the dilatometer has been used to evaluate changes that have occurred in the performance characteristics of Nitinol wires taken from the Fatigue Test Stand at various intervals. A specimen which had withstood  $5 \times 10^5$  cycles in the Test Stand at 1.4% strain was investigated, and an increase of  $>10\%$  work output per cycle was measured as a result of its "training" during Test Stand operation.

#### Tensile Fatigue Test Stand

The Tensile Fatigue Test Stand was originally constructed with the objective of providing a facility in which the performance of Nitinol wire elements could be observed over many working cycles. Mechanical energy for operation of the test stand comes from the SME recovery stress of a number of Nitinol wires (0.5 m in diameter, 38 cm in length) cycled in parallel between baths of hot and cold water. As a self-powered unit, it is therefore, in a sense, a primitive engine concept as well as a test machine. Mechanical features of interest include relative simplicity of design, and reduction of precision requirements for fabrication by amplification of the modest displacement of the Nitinol wires (approximately 5.3 mm) through a compound lever system. In its present configuration, the machine bears some resemblance to the early steam engines of the 18th century--the walking-beam or Newcomen engine. Heating and cooling of the Nitinol working elements is effected by dipping of the elements in water through front-end reciprocating oscillation of a dynamically balanced pivoting system suspended from above, as a sort of inverted pendulum. Because the rotational momentum of the components carrying the working elements rapidly decreases as soon as the wires reach the surface of the water, parasitic losses due to mass transfer and hydrodynamic friction (a serious limitation to scale-up, if wires are passed continuously through a liquid heat transfer medium) are minimized.

Design-point operating parameters for the machine (anticipated cycling rate of 60–80 cpm at a  $\Delta T$  of approximately  $20^{\circ}\text{C}$ , under no-load conditions) were not initially achieved. For the initial run-in (early July 1979) it was found that chilled water was required for sustained operation, and water from the engine was put through an ice-water bath. At one point during the early hours of testing, the supply of ice ran out, but the machine continued to operate. It was then switched to the in-house hot and cold tap-water supply ( $T_H \approx 42^{\circ}\text{C}$ ;  $T_C \approx 21^{\circ}\text{C}$ ) and a gradual acceleration from about 42 cpm to 60 cpm was observed over the first few thousand cycles. This improvement, due in part to refinements in timing adjustment and mechanical break-in, is also interpreted as an indication of the ability of Nitinol to accommodate, to some extent, to available operating temperatures.

The machine was subsequently installed in a test facility where closed heating and cooling

loops are available and tested under various conditions for the balance of the first million cycles. Part of this test included running under load for 250,000 cycles, during which an electric generator was attached to the machine, powering a dial tachometer and conventional flashlight bulb. When the generator was removed, a significant increase in speed of operation (from ~80 cpm to >90 cpm) was observed under no-load conditions and at reduced  $\Delta T(T_H \approx 38^\circ\text{C}; T_C \approx 20^\circ\text{C})$ . One interpretation of this improvement is that the "training" effects of continuous cycling are enhanced, or accelerated, by cycling under load.

The wire stock selected for fabrication of the first power element had been recycled from experiments in earlier phases of the project, without any attempt to heat treat or reanneal the material. It was known to be embrittled and, in fact, a number of wires were fractured in assembly of the first set before it was even installed on the machine. The rationale for using distressed material for the first run was the anticipation that inadequacies in the machine design (improper provision for the mechanical cycling of the Nitinol wires) would become apparent on the order of thousands of cycles, rather than many millions of cycles. As a result of this initial embrittlement, imperfections in mounting procedures, and maladjustments of the machine during the initial experimental learning period, a substantial number of fractures were encountered in the wires, all occurring at the ends where the Nitinol was pressed into stainless steel ferrules. Although undesirable, these features were anticipated and provided valuable guidelines for the assembly of the second working wire set. Again, recycled and unannealed wire was used (for the same reason as previously), but mounting procedures were modified to reduce point load on the surface of the Nitinol at the fixture end, and to eliminate a bending moment which inadvertently resulted from the geometry of the first mounting assembly. Considerable care was taken to ensure uniformity of length in the wires of the second set, and it has now sustained 2,500 hand cycles, prior to installation on the machine, without mishap.

#### PLANNED ACTIVITIES FOR 1980

Activities planned for the coming year include broadening of the three main areas of current investigation: cycle simulator studies, dilatometric measurements and wire fatigue lifetime testing. In addition a new research component, the need for which has been increasingly emphasized in this past year's work, will be included: direct experimental measurement of the thermal properties of Nitinol during transformation. In the past, theoretical and experimental determinations of the values for latent and sensible heat transfer in conventional Nitinol materials have been in sufficiently good

agreement that they were serviceable to a first approximation for estimates of the properties of relatively uncharacterized commercially available materials. Changes which take place in the performance of Nitinol over the course of many thousands of working cycles, however, indicate that differences in the thermomechanical properties of as-delivered Nitinol materials and partially stabilized, "trained" materials may be sufficiently great that measurements made on uncycled stock may be substantially invalid. As the Laboratory is now in the unique position of having available wires which have sustained over a million cycles in uniform axial strain, investigation of the changes--both structural and thermodynamic--that this cycling history may have produced in the material appears essential. As the thermal and mechanical properties of the material cannot be considered in isolation, this task will require some ingenious modification of standard calorimetric techniques, and various experimental methodologies are currently under consideration.

Cycle Simulator Studies will be continued, especially in the area of stress-limited or constant stress cycles, to identify the practical limits for the work output per cycle that can be realized from both new and stabilized materials. The simulator will also be used for controlled and automated break-in of wire working elements prior to installation on the Fatigue Test Stand.

The Fatigue Test Stand, used this year primarily to assign lower-limit values for the working lifetime of Nitinol wires deformed in axial strain, will be modified to perform direct work-output measurements and empirical efficiency measurements. Modification will include instrumentation of the machine to facilitate direct readout of stress levels, temperature and speed variables, and construction of a simple regenerator chamber to evaluate the feasibility of partial recovery of sensible heat, now largely lost to the atmosphere during transfer of the working element from bath to bath.

Preliminary studies made on the Laser Beam Dilatometer in the past year, correlating specific work output of Nitinol with varied thermal cycling conditions, will be systematically pursued. Tests made on relatively new wires will be reproduced to fill in missing thermal data points, and the investigation extended to include comparative evaluation of properties of cycled wires from the Tensile Fatigue Test Stand.

#### FOOTNOTE

\* This work has been supported by the Division of Fossil Fuel Utilization, Office of Energy Technology, U.S. Department of Energy, under Contract No. W-7405-ENG-48.

## APPROPRIATE ENERGY TECHNOLOGY\*

*C. Case, H. Clark, J. Kay, F. Lucarelli, J. Morris, J. Rees, and S. Rizer*

### INTRODUCTION

In the spring of 1977, the Building and Community Systems Division of the Energy Research and Development Administration (ERDA), responding to the 1977 ERDA Authorization Act, instructed its San Francisco Operations Office (SAN) to establish a small grants pilot program for appropriate energy technology projects within Federal Region IX (Arizona, California, Hawaii, Nevada, and the western Pacific). Following program guidelines, SAN made these grants available to small businesses, individuals, nonprofit agencies, public agencies, and Indian tribes. The purpose of the grants was to design, construct, and/or demonstrate small-scale energy technologies which conserve depletable fossil fuels or which use renewable energy resources.

With \$500,000 to distribute in grants up to \$50,000, SAN accepted applications from September to November, 1977. They received 1100 applications requesting \$21.3 million. After technical, economic, and peer reviews by a variety of state and university institutions and after receiving an additional \$750,000 from other DOE Divisions, SAN awarded 108 grants for \$1.25 million in April, 1978. The grants covered a complete spectrum of small-scale energy technologies including solar active and passive systems, wind machines, biomass conversion systems, energy conservation devices, recycling methods, aquacultural and agricultural systems, hydroelectric devices, geothermal systems, and integrated methods.

In the spring of 1979, DOE created the Office of Small Scale Technologies, transferring the program administration to this new office. With a FY 1979 budget of \$8.5 million, the program has expanded into all ten federal regions. These regions have received over 10,000 applications requesting \$200 million and are just completing their review processes and awarding grants. Federal Region IX received another 1100 applications during the winter of 1979 and has distributed \$500,000 in 34 additional grants.

During the late winter of 1980, DOE plans to offer a third national program cycle. Details of this cycle will be similar to the others, and DOE is deciding on the amounts to be distributed for each region.

### ACCOMPLISHMENTS DURING 1979 AND PLANNED ACTIVITIES FOR 1980

The LBL role in the Appropriate Energy Technology Program is evolving from a technical advisory one on a regional basis to a policy analysis role on a national level. During 1977 and 1978, we offered technical assistance to the SAN Office; reviewed a sizeable number of applications for technical/economic merit; provided technical assistance to the grantees; and monitored

projects in Arizona, Nevada, and the western Pacific. The program has now become a national one, and the Region IX jurisdictions do most of their own reviewing and monitoring; therefore, DOE has asked LBL to change the focus of the work to include various policy studies for implementing the national program. The next sections describe our traditional role and our policy studies for FY 1979 and FY 1980.

### Technical Assistance

Since the program's inception, we have been providing DOE with general technical support. This support includes a wide variety of tasks ranging from representing DOE at a Micronesian/Peace Corps workshop in Guam and providing technical backup support and energy efficiency data at regional managers' meetings to designing project evaluation forms. We gave technical advice on the proposed Golden Gate Energy Center and outlined ways for determining which projects have exceptional commercial potential. These tasks will continue with a more national than local perspective as the states assume more technical responsibilities. We will continue helping with logistical chores such as prescreening applications from the program cycles and reviewing applications which the states do not have the technical expertise to evaluate.

### Monitoring Projects

During FY 1979 we visited and reviewed 45 projects in Arizona, Nevada, and the western Pacific. During these visits we checked the projects for progress, budget and technical problems, demonstration and commercial potential, and general well-being. In addition, we gathered data for various reports. With encouragement from DOE and LBL, these jurisdictions have now set up their own mechanisms for monitoring during FY 1980. We will continue to visit various projects in Region IX and other regions in order to compile current data for reports.

### Energy Savings Studies

DOE is evaluating the grant program's effectiveness. As part of this evaluation, we have assessed the energy savings potential and cost-effectiveness of 20 projects in Region IX.<sup>1</sup>

The projects in our sample are representative of the 108 projects funded during the first cycle. The projects have developed a variety of energy technologies and have end use applications in the residential, commercial, industrial, and agricultural sectors. Funding levels for the projects vary from \$1,995 to \$46,874, and average \$15,270.

We evaluated the projects for direct and indirect energy savings, defining direct savings as those from the original project and indirect

savings as those from secondary applications of the project. We express these savings in terms of end use and primary energy savings. Using a conservative approach for evaluating indirect energy savings, our study estimates these savings at 1.2 trillion Btu annually and 22.1 trillion Btu over the project lifetimes. Primary energy savings from these indirect applications are estimated at 2.9 trillion Btu annually. Over their lifetimes, the 20 projects can save 5.7 trillion Btu of primary energy--the energy equivalent of 9.8 million barrels of oil.

Achieving indirect energy savings requires that each project be cost-effective. To evaluate cost-effectiveness, we compared the annualized cost of producing energy from each project with the annualized price of an equivalent amount of displaced fuel. Those projects which produce energy at a cost lower than the cost of displaced fuel are considered cost-effective. Based on this criterion, 13 of the 20 projects are cost-effective. This conclusion may be overly optimistic because most consumers and businesses do not apply life-cycle costing methods to energy investments. Instead, they use a more stringent test of economic viability, the five-year payback period. If this more stringent criterion is applied, only eight projects are cost-effective.

The study concludes with a discussion of ways DOE can improve the program's effectiveness for saving energy. Specifically, we concluded that for the 20 projects and others to achieve their full energy savings potential, DOE must develop innovative programs to assist with project commercialization and to disseminate information on individual projects.

During FY 1980, we will expand this study to include energy savings of projects from other regions, including projects from the Northwest, Southwest, and East Coast. We also plan to develop standard methods for evaluating the energy savings and cost-effectiveness of additional technologies such as wind and biomass conversion.

#### Fact Books

We are preparing a series of six reports, or Fact Books, synthesizing the technical and economic data assembled so far from the 108 projects. The purpose of these reports is to assist DOE management in understanding the nature of the projects, identifying constituencies served by the program, quantifying energy impacts of the program, and clarifying objectives for later cycles. In addition, these documents will provide Congress and the public with easy-to-read reports acquainting them with a few of the general and technical accomplishments of the grants program.

We have developed a descriptive format which will be used for Region IX and for all DOE/AET projects nationally. To test this format, DOE, LBL, and the California Office of Appropriate Technology selected 18 projects for the initial report.<sup>2</sup> We used a two-page description for each project, including a diagram or picture. The description includes a simple entry for the project title and number; applicant name, address, and

group type; project type; amount of award; project duration, date started, and date completed. One or two paragraphs describe the project in general terms, and another paragraph gives brief technical details. A final section presents project results, including details on direct and indirect energy savings. Also included are information on innovative features, regional or national demonstration possibilities, and aspects of the project which can be replicated elsewhere on either a regional or national scale.

We are issuing a second report describing another 18 projects,<sup>3</sup> and we plan to complete the series, which will describe all 108 projects, by mid FY 1980. We are also developing a loose-leaf notebook format to be used for projects from this and other regions.

#### California Biomass Potential

We are studying the resource limits and economic feasibility of using California biomass as a source of liquid fuels. The study assesses five categories of biomass for annual yield, seasonal availability, and cost of collection. These categories include municipal, forestry, agricultural wastes, feed grains, and harvest from chaparral and brushland.

Annual yields are estimated for 1976 with projections to 2025. To determine the cost-effectiveness of producing liquid fuels from biomass, we have made two comparisons. The first compares the cost of producing alcohol from biomass to the cost of using biomass for producing alternative fuels, such as low Btu gas, electricity, and steam. The second compares the cost of producing each fuel from biomass with projected prices of fossil fuels. Additionally, the study assesses the environmental impacts of biomass collection and the role that government agencies can play in a large-scale biomass program. The study concludes by discussing the implications for achieving a renewable energy resource future totally reliant on biomass for liquid fuels.

#### The Labor Impacts of Selected Appropriate Energy Technology Projects

We are beginning a study assessing the labor impacts from a sample of projects funded during the first program cycle. The labor impacts will include four categories: direct, indirect, induced, and employment impacts from responding. We will examine 20 projects, comparing their quantitative labor effects with those of conventional energy systems. To provide data for assessments, we will attempt to identify and use available methods and models. The final report will provide data to DOE for evaluating the program and for clarifying the complex conceptual issues in measuring labor impacts.

#### Aquacultural Studies

To complement our technical assistance, project monitoring, and policy studies, we have developed a laboratory research component for an aquaculture problem. During FY 1979 and FY 1980, we are studying the laboratory mass cultivation of

Daphnia magna, a freshwater cladoceran, as a potential live food source for aquaculture systems. Attributes such as ready availability, nutritional acceptability, and parthenogenic reproduction allowing for large population accrual in a relatively short period of time, may encourage using Daphnia magna and related genera in small aquaculture systems. However, users have experienced certain problems in mass cultivation. For our research, we performed a number of trials to determine which medium or combination of media provides the best growth of Daphnia magna. We then tested these combinations for two runs of preliminary experiments to evaluate growth and reproduction patterns in a variety of conditions.

Daphnia magna (Straus 1820), reared on a defined medium in 4 liter flasks with controlled light, temperature, and species of algae food, were found to be tolerant to high levels of ammonia, up to 108  $\mu\text{M}$ , at high pH (>10). Parthenogenic reproduction may be inhibited, though, at these high levels. Scenedesmus quadricada and Ankistrodesmus species were found to be satisfactory food sources. Densities of greater than one animal per ml in culture were attained utilizing Ankistrodesmus species as a food source at a pH of 7.7. Maintenance of pH at about 7-8 appears to be important to successful cultures. Therefore, during FY 1980, we plan to undertake our experiments with controlled pH.

#### Library, Bibliography, and How-To-Books

During the course of our work, we have assembled a library of books on small-scale technology. The library is intensively used by others outside of our program, and in order to facilitate cataloging and browsing, we have developed a simple color-coded system for cataloging the material. In response to a request from DOE, we issued a bibliography listing the books in our library and describing the cataloging system.

For FY 1980, we plan to issue a series of non-technical how-to books or brochures describing how

to construct or duplicate some of the successful projects or how to complete successfully some of the paperwork required by the program. A few of the potential topics include how-to build a solar beeswax melter, how-to run a small scale energy workshop, how-to write a how-to booklet, and how-to complete a grants application.

#### FOOTNOTE AND REFERENCES

\* This work has been supported by the Office of Inventions and Small Scale Technologies within the Buildings and Community Systems Division, Office of Conservation and Solar Applications, U.S. Department of Energy under Contract no. W-7405-ENG-48.

1. F. B. Lucarelli, J. Morris, J. M. Kay, S. Rizer, C. W. Case, and H. R. Clark, "The Energy Savings Potential of the Region IX Appropriate Energy Technology Grants Program: An Assessment of Twenty Projects," Lawrence Berkeley Laboratory report LBL-9715 (1979).
2. C. W. Case, F. B. Lucarelli, J. Morris, and H. R. Clark, "Projects from Federal Region IX DOE Appropriate Energy Technology Pilot Program - Part I," Lawrence Berkeley Laboratory report LBL-9642 (1979).
3. C. W. Case, F. B. Lucarelli, H. R. Clark, J. M. Kay, and S. Rizer, "Projects from Federal Region IX Department of Energy Appropriate Technology Pilot Program - Part II," Lawrence Berkeley Laboratory report LBL-10098 (1979).
4. J. T. Rees and J. M. Oldfather, "Small Scale Culture of Daphia Magna Straus" (in press).
5. F. B. Lucarelli, "The California Biomass and its Energy Potential," Lawrence Berkeley Laboratory report LBL-10058 (in press).
6. H. R. Clark, "Appropriate Energy Technology Library Bibliography," Lawrence Berkeley Laboratory report LBL-9391 (1979).

## ENERGY CONVERSION BY HALOBACTERIA\*

*L. Packer, R. Mehlhorn, A. Quintanilha, C. Carmeli, P. Scherrer, N. Kamo, P. Sullivan, S. Tristram, J. Herz, T. Racanelli, I. Probst, and A. Pfeiffhofer*

### INTRODUCTION

The purple membrane found in the halophilic bacterium Halobacterium halobium contains the simplest biological light-to-electrical energy converter known. The component of this organism responsible for the light energy conversion process is the relatively small and simple protein bacteriorhodopsin. Our understanding of this protein is expanding rapidly, and we now know its complete amino acid sequence, its electron density profile

in the membrane, the probable location of the chromophore (retinal), and many details of the photocycle which involves a number of distinct spectral intermediates occurring over a seven millisecond time span at room temperature. Much of the current research on bacteriorhodopsin is concerned with the molecular details of how these spectral intermediates are related to the movement of protons across the purple membrane. Considerable added interest in the halobacteria has been stimulated by the recent discovery that their membranes contain a

second light-driven ion pump which accomplishes charge movement without the obligatory participation of protons. Evidence is mounting that this photocatalyst achieves sodium pumping, a hitherto unsuspected biological process. This discovery is of great significance for potential photocell applications because sodium currents can provide considerably more electrical power than protons since the latter eventually give rise to deleterious pH changes in the course of photocurrent production.

In previous years, our laboratory constructed a photocell derived from bacteriorhodopsin, and characterized the efficiency and stability of the cell, thus paving the way for constructing similar devices from other membrane-derived ion pumps. We chemically modified bacteriorhodopsin and showed that the amino acids tyrosine and tryptophan were involved in proton translocation driven by the photocycle, and applied spin label assays for analyzing light-dependent electrochemical potentials on isolated purple membrane surfaces and across sealed membrane preparations.

#### ACCOMPLISHMENTS DURING 1979

##### Energy Transduction by Bacteriorhodopsin

To clarify the process of proton translocation by bacteriorhodopsin in purple membranes of halobacteria, we have exploited specific chemical modification of selected amino acid residues.<sup>1,2</sup> The simple amino acid composition of the protein has been a considerable asset for these studies.<sup>3,4</sup> Our attention has been focused on the ionic amino acids, including glutamate, aspartate and arginine, which can be protonated in the physiological pH range, and thus are potential elements of the proton pathway through the protein. The molecular model of the protein revealed a high density of these amino acids at the cytoplasmic membrane interface.

Carboxyl-containing amino acids were specifically modified with water soluble carbodiimides, in reactions which caused their negative charges to be either neutralized or become positive.<sup>5</sup> These modifications caused slowing of the photocycle during the stages corresponding to the uptake of a proton by bacteriorhodopsin. The onset of the photocycle which is related to proton release was unaffected by the modifications. Partial resolution of the carboxyl groups involved in proton uptake was achieved by means of trypsin digestion of a polar fragment of the protein; this treatment has no effect on the photocycle, even though this fragment includes five carboxyl containing amino acids. Positively charged arginine residues were modified with two reagents such that three to five of the seven residues were modified. The general effect of arginine modification was very similar to the effect of carboxyl modification; negative charges were either neutralized or became positive, and slowing of the photocycle was observed during stages corresponding to the uptake of a proton by bacteriorhodopsin (Table 1). These results indicate that both carboxyl groups and guanidinium groups are essential for the proton translocation process.

Previously, we observed that proton pumping by bacteriorhodopsin was affected by iodination of tyrosine residues,<sup>6</sup> although the location of the critical residues could not be ascertained. Tyrosines are of special interest because of the possible involvement of their phenolic hydroxyl group in proton translocation. In the past year,<sup>7</sup> we succeeded in iodinating tyrosines much more specifically with the enzyme glucoseoxidase lactoperoxidase, whose bulk and solubility characteristics should make it mainly a surface specific reagent in the early stages of reaction, and a modifier of hydrophobic tyrosines in the later stages. Experiments in collaboration with Dr. Stanley Seltzer of Brookhaven National Laboratory have revealed that iodination of the lipid of the purple membrane and of the retinal chromophore is insignificant.

Table 1. Effect of treating purple membranes with carboxyl and arginine specific reagents on photoreaction cycle linked to proton translocation.

Modification	570 nm Chromophore		412 nm Intermediate		Photostationary State Absorbance Relative Percent
	Absorbance (percent)	Rise ( $t_{1/2}$ , $\mu$ sec)	Phase of Decay Initial ( $t_{1/2}$ , msec)	Second	
<u>Carboxyl Specific</u>					
Control	100	40	5.6	-	100
EDC-Treated	85.7	40	15.0	280	527
<u>Arginine Specific</u>					
Control	100	39.2	2.8	-	100
2-3-Butanedione-Treated	91.3	68.4	34.6	174	1922

nificant compared to the iodine labeling on the protein. Using lactoperoxidase on normally oriented and inverted bacteriorhodopsin molecules in sealed vesicle systems, we have been able to show with short reaction times that the most iodine sensitive tyrosines are located on the cytoplasmic membrane surface. This supports our earlier suggestion that proton uptake from the cytoplasm may require a tyrosine residue.

More extensive tyrosine modification eventually causes four tyrosines to become iodinated. Structural information from our schematic model of bacteriorhodopsin shows that several tyrosines are located in close proximity to the region where the  $\beta$ -ionone ring may be located. Extensive iodination slows down the decay, but interestingly accelerates the formation of the  $M_{412}$  intermediate. A group of investigators in Cambridge, England have recently made extensive modification of tyrosine residues with tetranitromethane,<sup>8</sup> which also revealed that when up to 30% of the 11 tyrosine residues were altered, an acceleration of  $M_{412}$  formation occurred.

Raman spectroscopy is a sensitive tool for studying the environment of the retinal chromophore. Rapid flow techniques were used to measure Raman spectra of both the BR570 ground state and the  $M_{412}$  intermediate of the chromophore in the laboratory of Dr. R. Mathies, School of Chemistry, University of California, Berkeley. The results were quite different for the two states; there was a considerable alteration in the spectrum of the ground state in the extensively iodinated protein while the  $M_{412}$  state was essentially identical to that seen in the untreated protein. One interpretation of this result is that a conformational change occurs in the protein which causes one or more of the iodinated tyrosines to move away from the chromophore in the excited state. Furthermore, since this observation is seen only in extensively modified bacteriorhodopsin, the tyrosine which interacts with the chromophore appears to be distinct from the tyrosine which seems to act as a proton donor.

#### Surface Electrical Potential Measurements

Previously, we demonstrated that electrical surface potential changes occurred in spinach chloroplasts upon illumination,<sup>9</sup> by means of a new spin probe method developed in our laboratory, based on the partitioning of permanently charged hydrophobic molecules between the aqueous medium and membrane bound populations. This method enabled us to monitor electrical surface charges with high sensitivity and rapid response time.<sup>10,11</sup>

Electrical surface potential changes in purple membranes were of interest because they might provide information about proton binding sites and perhaps conformational changes in the protein.<sup>11,12</sup> We used the amphipathic spin probe  $CAT_{12}$ , an analogue of trimethyl dodecyl ammonium bromide to estimate surface charge changes occurring during illumination of bacteriorhodopsin. At room temperature, when purple membranes are illuminated in low ionic strength media, small surface potential changes are observed. However, when the photocycle is slowed, thereby increasing the amount of  $M_{412}$

intermediate in the photostationary state, surface potential changes also increase. When the photocycle is slowed by chemical modification of tyrosine, arginine and carboxyl containing residues in purple membranes or by lowering of the temperature, larger surface charge changes are recorded. Figure 1 shows that the partitioning of the probe into aqueous domains (narrow lines) and membrane domains (broad lines) changes slightly under illumination and hence the effective surface potential seen by the probe increases. When these data are interpreted in terms of the Gouy Equation, which relates interfacial charge densities to surface potentials, the changes correspond to about one charge per  $M_{412}$  intermediate of the photocycle. The kinetics of the surface potential changes and of the rise and decay of the  $M_{412}$  are of the same order of magnitude. The experiments with  $CAT_{12}$  suggest that, at low ionic strength and with positively charged purple membranes, the proton leaves the membrane entirely. It is also known that the Schiff base nitrogen becomes deprotonated in the  $M_{412}$  state, but it cannot be ascertained if it is this proton which is released from the purple membrane.

#### Hypothesis for Light Energy Transduction by Bacteriorhodopsin

All data obtained thus far have led us to propose a scheme for relating proton translocation to the photocycle of bacteriorhodopsin (Fig. 2). Based on results of others, theoretical considerations,<sup>13</sup> and our research, we have updated a scheme that attempts to relate the proton translocation by bacteriorhodopsin to its photoreaction cycle. We hypothesize that photon absorption shifts the electron distribution in the polyene side chain toward the Schiff base nitrogen, resulting in a decrease of its positive charge. This results in a structural change of the polyene chain and a charge separation between the Schiff base nitrogen and a nearby  $R^-$  group. Charge separation may be the primary event of light energy conversion as it is rapidly (in 30  $\mu$ sec) followed by proton release from the Schiff base N and at the extracellular surface of the purple membrane. Reprotonation occurs in a relatively slow process (3-5 msec) from the cytoplasmic surface. No precise quantities of absorbed photons and released  $H^+$  have

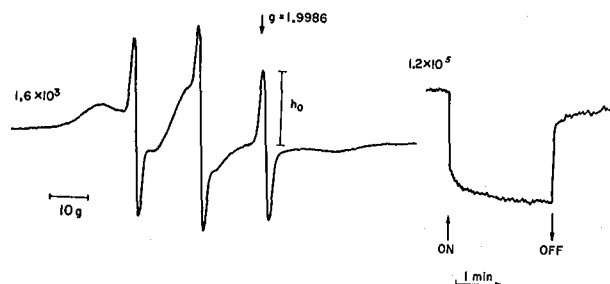


Fig. 1. EPR spectrum and light induced amplitude changes of the high field aqueous  $CAT_{12}$  signal,  $h_0$ , in a purple membrane suspension.

(XBL 797-10700)

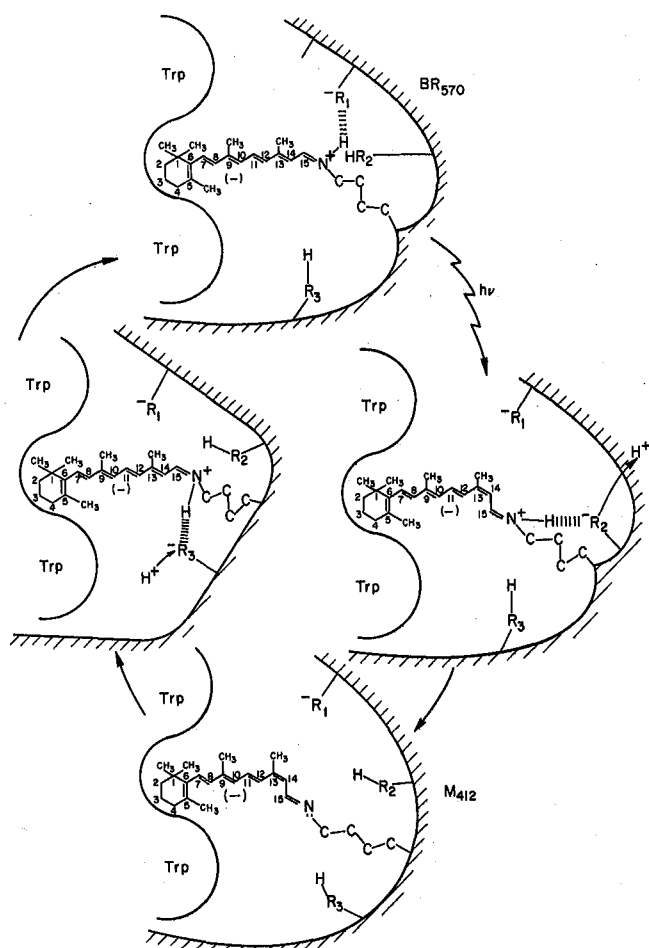


Fig. 2. Light energy conversion by bacteriorhodopsin. Light initiates a chain of events which perturb the structure of this photocatalyst such that protons are released and taken up at different surfaces of the purple membrane in which bacteriorhodopsin is located. When bacteriorhodopsin absorbs a photon, the retinal chromophore isomerizes. This causes a charge separation between a proton on the Schiff base nitrogen ( $-N^+$ ) and a nearby negatively charged group ( $R_1$ ); this is believed to be how energy is initially conserved. This, in turn, initiates the release and uptake of protons from other groups in the protein ( $R_1$ ,  $R_2$ ,  $R_3$ , etc.); our studies indicate that tyrosine is one of the important groups in this process. There is evidence that aromatic amino acids like tryptophan (trp) help to form the proper environment for retinal.

(XBL 7911-3903)

yet been established, and no experiments have yet demonstrated whether it is the Schiff base ( $C=NH$ ) proton which is translocated, or whether proton translocation occurs via another route. Nevertheless, our chemical modification studies reveal that certain groups of charged amino acids are of great importance for the reprotonation process. A precise structural arrangement of arginine and carboxyl groups, probably in complexation with one another, and at least one tyrosyl group near the cytoplasmic

surface, is required as are protein conformational changes. The latter has been deduced from chemical crosslinking studies of  $\alpha$ -amino groups of lysine which inhibit reprotonation and  $M_{412}$  decay. At least one tyrosyl group is also important in the immediate environment of the chromophore, as perturbing it by two methods of chemical modification results in acceleration of proton release. Not enough knowledge is yet available on the tertiary structure and the precise localization of the groups affected to determine whether it is merely configuration of these groups which is important for proton movement through the protein, or whether they participate directly in the precise translocation of protons.

#### Light-Dependent Energy Conservation in Mutant Strains of Halobacteria

Characterization of the electrochemical gradients developed by halobacteria is essential in understanding how light energy is conserved. We are studying two bacteriorhodopsin-deficient mutant bacteria (red and white strains) in collaboration with Yasuo Mukohata of Osaka University. These strains contain a retinoprotein that results in proton translocation in an opposite direction to that of bacteriorhodopsin.

Critical questions being investigated in our laboratory are: What is the nature of the primary light energy converter in the mutant cells, and what is the feasibility of isolating this converter for subsequent incorporation into synthetic membranes? To answer these questions, it is important to characterize the primary ion pump by identifying pathways of cation movement across the membrane. Identification of these cation pathways will also assist us in moving toward the construction of a photodesalination device.

To monitor proton movements, we are using two independent experimental approaches: (1) pH electrodes which respond to proton concentrations outside of intact cells and cell vesicles, and (2) spin probes which monitor intracellular and intravesicular concentrations.<sup>14,15</sup> The judicious combination of these approaches can give quite accurate information about the salt economy of the cell. A spin-labeled weak acid and amine were used to measure transmembrane pH gradients in *H. halobium* cell envelope vesicles during illumination. By quenching the probe signal outside the vesicles with the impermeable paramagnetic ion ferricyanide, uptake of the acid and release of the amine were observed (cf. Fig. 2 of Probst et al.<sup>15</sup>). The pH gradients calculated from the data ranged from zero at an external pH of 9.3 to 2.0 at pH 5.0.

Volume measurements are needed to calculate accurately the pH gradients with any method. We have developed a spin probe method which allows simultaneous and accurate cell volume determinations to be made by measuring the intracellular concentration of a permeable probe which equilibrates across the membrane independently of pH and electrical gradients. A perdeuterated, spin-labeled ketone nitroxide, designated as  $^2H$  Tempone, which exhibits very narrow spectral lines in aqueous environments, has proven most useful for this purpose.

Membrane permeable lipophilic anions and cations can be used for measuring electrical gradients by developing electrodes which measure their external concentrations.<sup>16,17</sup> Upon illumination of intact cells, a potential of about 150 to 180 mV is observed, negative inside. This potential is consistent with electrogenic proton extrusion from the cell which can be simultaneously measured with the pH electrode technique.

To increase the time resolution of the electrical transmembrane potential measurements, spin-labeled permeable cations (phenylated phosphonium derivatives) have been developed. Probes synthesized thus far exhibit considerable membrane binding in their spectra. The spin probe method has a critical advantage over other procedures because binding of the probe can be measured so that this effect can be corrected for in calculations of the membrane potential. Computer interfacing of our EPR instrument this year has made it possible to observe and quantify the population of probe molecules that are bound to the membrane and correct for this common source of error. Computer interfacing is also used to analyze kinetics of the photoresponse, to perform data averaging or subtracting, and to obtain concentrations of the probe in different environments by double integration of the individually resolved spectral components. With these techniques, absolute transmembrane potentials are being determined and the relationship among these gradients elucidated.

#### PLANNED ACTIVITIES FOR 1980

We will continue to refine our understanding of the molecular mechanism of light energy transduction by bacteriorhodopsin by further exploring the role of specific amino acids in proton translocation. Results of flash photolysis studies of photocycle intermediates will be correlated with measurements of the electrical surface and transmembrane potentials, and direct methods for proton production. These investigations will include more selective chemical modification with emphasis upon protein chemistry and the use of spin-labeled reagents to determine the specific groups modified; studies on deuterated purple membranes; and the effect of D<sub>2</sub>O on light energy conversion in purple membranes and reconstituted proton translocation systems. We expect that these studies will advance to a stage at which we may be able to decide among several alternative hypotheses for the mechanism whereby this photocatalyst generates electrochemical gradients.

The recent discovery of a new retinoprotein pigment with different light energy transduction properties, indicating that it may act as a direct light-energy driven transmembrane device for sodium transport, will be explored in halobacteria cells and vesicles. These experiments will involve simultaneous measurements of changes in parameter of the electro-chemical potentials,  $\Delta\text{pH}$ , and  $\Delta\Psi$  by newly developed electrode and spin-probe techniques which will enable us to quantify the converted energy. These studies will be made in mutant species of halobacteria and membrane vesicles prepared from them, in which the function of this new retinoprotein can be distinguished from that of bacteriorhodopsin.

#### FOOTNOTE AND REFERENCES

\*This research was supported by the Office of Basic Energy Sciences, Division of Chemical Sciences, of the U.S. Department Energy.

1. L. Packer and T. Konishi, "Chemical Modification of Bacteriorhodopsin: An Approach to the Mechanism of Proton Translocation," in Energetics and Structure of Halophilic Microorganisms, Proceedings of the EMBO Workshop on Halophilism held at the Weizmann Institute of Science, Rehovot/Arad, Israel, May 14-19, 1978), S. R. Caplan and M. Ginsburg, eds. (Elsevier/North-Holland Biomedical Press, The Netherlands, pp. 143-163) 1978.
2. T. Konishi, S. Tristram, and L. Packer, "The Effect of Cross-Linking on Photocycling Activity of Bacteriorhodopsin," Photochem. Photobiol. 29, 353-358, 1979.
3. Y. A. Ovchinnikov, N. G. Abdulaev, M. Feigina, A. V. Kiselev, and N. A. Lobanov, "Recent Findings in the Structure-Functional Characteristics of Bacteriorhodopsin," FEBS Lett. 84, 1-4, 1977.
4. G. E. Gerber, R. J. Anderegg, W. C. Herlihy, C. P. Gray, K. Biemann, and H. G. Khorana, "Partial Primary Structure of Bacteriorhodopsin: Sequencing Methods for Membrane Proteins," Proc. of the Nat. Acad. Sci. (USA) 76, 227-231, 1979.
5. L. Packer, S. Tristram, J. Herz, C. Russel, and C. L. Borders, "Chemical Modification of Purple Membranes: Role of Arginine and Carboxylic Acid Residues in Bacteriorhodopsin," FEBS Lett. 108, 243-248, 1979.
6. T. Konishi and L. Packer, "The Role of Tyrosine in the Proton Pump of Bacteriorhodopsin," FEBS Lett. 92, 1-4, 1978.
7. P. Scherrer, C. Carmeli, P. Shieh, and L. Packer, "The Effect of Chemical Modification of Tyrosyl Residues on Proton Conductivity Mediated by Bacteriorhodopsin (Abstract)," Biophys. J. 25, 207a, 1979.
8. M. Campos-Cabieres, T. A. Moore, and R. N. Perham, "Effect of Modification of the Tyrosine Residues of Bacteriorhodopsin with Tetranitromethane," Biochem. J. 179, 233-238, 1979.
9. A. T. Quintanilha and L. Packer, "Outer Surface Potential Changes Due to Energization of the Chloroplast Thylakoid Membrane," Arch. Biochem. Biophys. 190, 206-209, 1978.
10. R. Mehlhorn and L. Packer, "Membrane Surface Potential Measurements with Amphiphilic Spin Labels," Methods in Enzymology vol. LVI, part G, pp. 515-526, (Academic Press, New York), 1979.
11. C. Carmeli, A. Qunitanilha, and L. Packer, "Light Induced Surface Potential Changes in Purple Membranes and Bacteriorhodopsin Lipo-

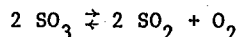
- somes," in Membrane Bioenergetics (C. P. Lee et al., Eds.) Addison-Wesley, p.547-558 (1979).
12. C. Carmeli, A. Quintanilha, and L. Packer, "Relation Between Surface Charge Changes in Purple Membranes and the Photoreaction Cycle in Bacteriorhodopsin", Proc. Nat. Acad. Sci. (USA), in press.
  13. B. Honig, T. Ebrey, R. Callender, H. Dinur, and M. Ottolenghi, "Photoisomerization, Energy Storage and Charge Separation: A Model for Light Energy Transduction in Visual Pigments and Bacteriorhodopsin," Proc. Nat. Acad. Sci. (USA) 76, 2503-2507, 1979.
  14. I. Probst, R. Mehlhorn, A. Quintanilha, J. Lanyi, and L. Packer, "Light Induced Transmembrane Proton Fluxes Across Envelope Vesicles of Halobacterium halobium Measured with Spin Probes," Biophys. J. 25, 308a, 1979.
  15. I. Probst, R. J. Mehlhorn, J. K. Lanyi, and L. Packer, "Light Induced pH Gradients Across Halobacterium halobium Cell Envelopes Vesicles Measured with Spin Labeled Amine and Carboxylic Acid Probes," Lawrence Berkeley Laboratory report LBL-9674, 1979.
  16. L. L. Grinius, A. A. Jasaitis, Yu. P. Kadsiauskas, E. A. Liberman, V. P. Skulachev, V. P. Topali, L. M. Tsofina, and M. A. Bladimirova, Conversion of Biomembrane Produced Energy into Electric Form. Biochim. Biophys. Acta, 216, 1-12, 1970.
  17. N. Kamo, M. Muratsugu, R. Hongoh, and Y. Kobatake, "Membrane Potential of Mitochondria Measured with an Electrode Sensitive to Tetraphenyl Phosphonium and Relationship Between Proton Electrochemical Potential and Phosphorylation Potential in Steady State," J. Membrane Biol. 49, 105-121, 1979.

## A SOLAR-HEATED GAS-TURBINE PROCESS USING SULFUR OXIDES FOR POWER PRODUCTION AND ENERGY STORAGE\*

G. Tyson, S. Lynn, and A. Foss

### INTRODUCTION

If any system of solar power generation is to provide a significant fraction of the power requirements of a community, some means of economical energy storage must be used. The purpose of this study is to develop and evaluate a process configuration using the heat of reaction of:



for energy storage. The forward reaction is endothermic and is used to absorb energy. The reverse reaction is exothermic and releases the energy that has been stored. This process uses the sulfur oxides directly in a gas turbine in a hybrid Brayton-Rankine cycle to produce electricity. Heat for the system is supplied during sunlight hours by a field of heliostats focused on a central solar receiver. When sunlight is not available, the storage system provides the heat to drive the gas turbine.

This work was begun in 1978 as a natural extension of a chemical storage system<sup>1</sup> which employed only a steam Rankine cycle for power generation.

### ACCOMPLISHMENTS DURING 1979

An efficient process configuration for this power cycle was developed, and flow sheets for it are given in Figs. 1 and 2. Detailed material and energy balances were made for a base case that represents a middle range of expected operating conditions. Sensitivity of this process to variations in the key operating parameters was determined. Equipment sizes and costs were estimated for the base case to determine an approximate cost for the electricity produced by this process.

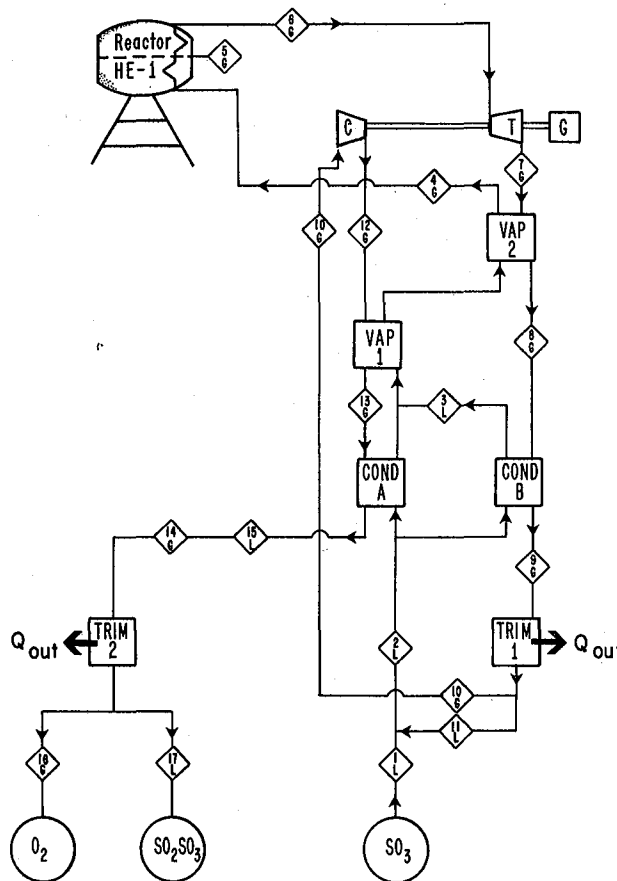


Fig. 1. Block flow diagram of the daytime (charge) process. (XBL 797-2228)

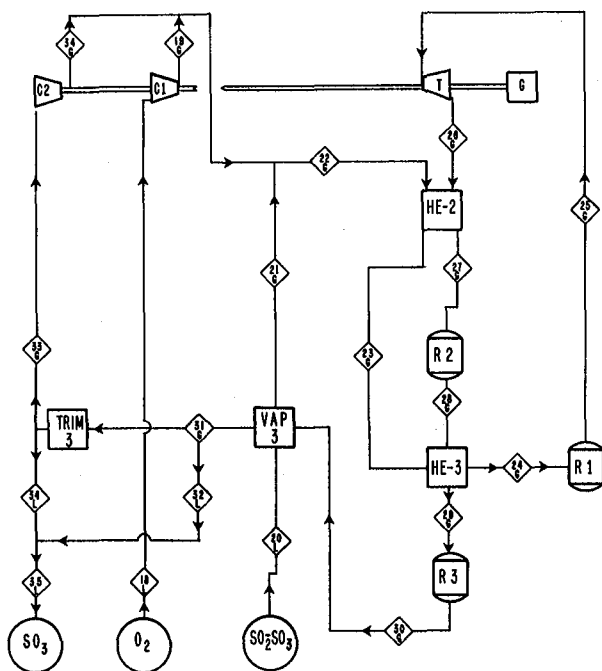


Fig. 2. Block flow diagram of the nighttime (discharge) process. (XBL 797-2229)

In the base case, the solar receiver absorbs heat at a rate of 230 MW(t) for a period of eight hours during the day. Daytime electricity generation is about 52.3 MW(e). Nighttime generation is about 19.0 MW(e) for a period of 16 hours. The overall efficiency of converting heat into electricity is thus about 39%. Total capital cost for the base case is \$71.7 million, of which 69% is for the tower and heliostat field. Average cost of the electricity produced is estimated to be 7.7¢/kW(e)-hr.

The economics of electricity production using the gas-turbine process developed in this work

appears to be attractive. The estimated power cost of 7.7¢/kW(e)-hr is high compared to current fossil-fuel-fired power sources but only by a factor of about 2. This power cost is substantially lower than the 10.7¢/kW(e)-hr that was projected for a process using the same sulfur-oxide storage concept but using only a steam Rankine cycle for power production.<sup>1</sup>

The principal reason for the improved power cost is an increase in efficiency, 39% in the present process compared to 26% in the earlier process.

The primary uncertainty in the economic estimates presented arises from the corrosiveness of the fluids in the sulfur-oxide system at the temperatures of the process. A developmental program will be needed to determine whether economically as well as technically feasible solutions exist for the materials problems that would be faced in an application of this process.

#### PLANNED ACTIVITIES FOR 1980

This project is completed, no further funding is sought at the present time, and our activities in this area have ceased.

#### FOOTNOTE AND REFERENCES

\*This project was funded during FY 1979 entirely by the Department of Energy, Division of Energy Storage Systems.

1. J. Dayan, S. Lynn, and A. Foss, "Evaluation of a sulfur oxide chemical heat storage process for a steam solar electric plant," Lawrence Berkeley Laboratory report, LBL-7868 (July 1979).
2. G. Tyson, S. Lynn, and A. Foss, "A solar-heated gas-turbine process using sulfur oxides for power production and energy storage," Lawrence Berkeley Laboratory report, LBL-9472 (September, 1979).

## EXPERIMENTAL AND THEORETICAL EVALUATION OF CONTROL STRATEGIES FOR ACTIVE SOLAR ENERGY SYSTEMS\*

M. Warren, S. Schiller, M. Martin, M. Wahlig, and G. Sadler

### INTRODUCTION

Improved solar energy control systems will reduce the need for using non-renewable fuel sources for heating building spaces and domestic hot water. The LBL solar controls program has four principal objectives: (1) to construct a test facility capable of experimentally evaluating the relative performance of different solar heating

and cooling control strategies under a variety of input meteorological conditions and output load demands (performance of control strategies is measured by the ratio of useful heating by solar divided by the auxiliary and parasitic energy required); (2) to use the test facility to test an electronic controller developed at LBL and to evaluate other controllers; (3) to carry out theoretical studies of collector and load loop perform-

ance in support of the experimental work; and (4) to perform technical support activities as part of the Systems Analysis and Controls program element of the DOE solar heating and cooling R and D program.

Experimental evaluation of the cost effectiveness of controllers and control strategies is expected to be the primary output of this project.

#### ACCOMPLISHMENTS DURING FY 1979

In the past year, the test facility has been brought to an operational status with emphasis on refinement of system instrumentation and the development of the necessary computer software to operate the facility and perform data analysis. The test facility is described in detail elsewhere.<sup>1,2,3</sup> Other work this year has included the application of theoretical models to describe dynamic collector operation and building temperature response. The specific building and solar-heating system that will be simulated have also been determined.

#### Instrumentation and Data Analysis System

A disk drive and operating system for the hp-9825A microcomputer that controls and monitors the test facility was installed this past year and is now operational. Software requirements for data acquisition, adjustment of the load and pseudo-collector simulators, and intermediate data analysis are extensive, exceeding the limits of the computer memory. Therefore, the software has been rewritten in an overlay mode, greatly extending the system capability. Segments containing the main program, subroutines for operation of the data logger and output devices, experiment initiation, data analysis, and control procedures are now stored on different files. Various routines are loaded into memory from the disk as they are required. Auxiliary gas consumption for back-up heat, and parasitic power requirements for the pumps and fans, are now measured electronically.

#### Solar Input Simulator (Pseudo-Collector)

To make comparisons between alternative control strategies, the heat input and the load conditions must be reproducible. Therefore, solar energy input to the system and building energy requirements are simulated to allow repeated runs under identical external conditions.

The solar input simulator, the pseudo-collector, is a boiler with a controlled mixing valve that allows adjustment of the fluid input-output temperature difference. This year the pseudo-collector solar input simulator has been brought under full computer control. Values of solar insolation, ambient temperature, the boiler inlet temperature and flow rate, along with typical collector parameters, are used to calculate the expected inlet-outlet temperature difference using a steady state collector model.

Figure 1 shows the collector loop. The high- and low-fire gas burners of the boiler, as well as the position of the three-way mixing valve, are all controlled by the hp-9825A. Under no-flow conditions in the collector loop, the value of the collector sensor, TS-4, is set to the calculated

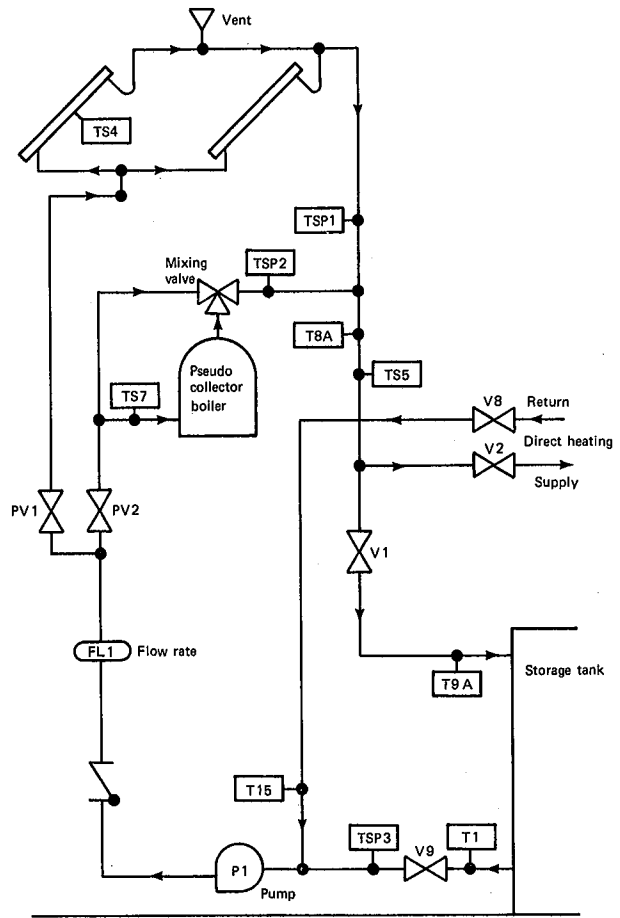


Fig. 1. Solar controls facility collector loop. (XBL 794-1152)

collector stagnation temperature through an output device. When the collector loop pump is on, the collector output temperature is calculated from the collector model, and the boiler output is adjusted accordingly. The apparent collector temperature and boiler control are updated every 60 seconds.

The PROM system controller turns on the collector loop pump, P1, when the apparent collector temperature reaches the "on" set point, given by the storage tank temperature plus a temperature differential,  $\Delta T_{on}$  of  $11^{\circ}\text{C}$ . The pump is turned off if the collector temperature falls below the "off" temperature, given by the storage tank temperature plus a temperature differential,  $\Delta T_{off}$  of  $2^{\circ}\text{C}$ .

Figure 2 shows the inlet temperature and the calculated and observed collector outlet temperature over a four hour period of increasing and decreasing insolation. If the collector outlet temperature under flow conditions is less than the "off" temperature and the collector stagnation temperature is greater than the "on" temperature, then the collector loop pump will cycle on and off. Such cycling is typical of solar collector systems. The steady-state collector model does not adequately describe this cycling, and work is continuing to implement a dynamic collector model as part of the solar input simulator.

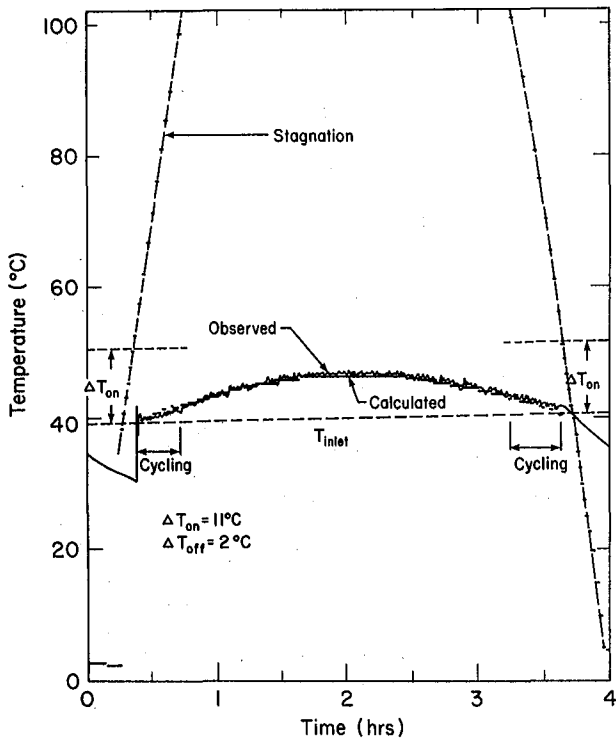


Fig. 2. Pseudo-collector output. Calculated temperature (no flow), calculated outlet temperature (flow), and observed pseudo-collector outlet temperature. (XBL 7912-13155)

Load Simulator

The load simulator is an air channel that simulates a building's heating system, consisting of a return air duct, fan, and heating and cooling coils. The inlet air temperature is adjusted by an electric resistance heater and an air conditioner under the control of the hp-9825a. A schematic of the building load loop and air channel is shown in Fig. 3.

The building heating requirements to be satisfied by the solar energy system are modeled in the microcomputer. A simple thermostat model is used to control the heat delivery system which, as determined by McBride<sup>4</sup> in experimental studies, is on for a fixed interval of about 5 minutes. The energy delivered to the load by the heating coil is measured and compared with the building load to determine how often heat must be supplied and whether auxiliary energy is required.

Energy Balance Tests

Energy balances are performed during the experiment by (1) determining the energy delivered by the pseudo-collector, (2) determining the energy stored at the beginning and end of a period, and deducting estimated losses from storage, (3) determining the amount of energy delivered to the load, and (4) estimating piping heat loss.

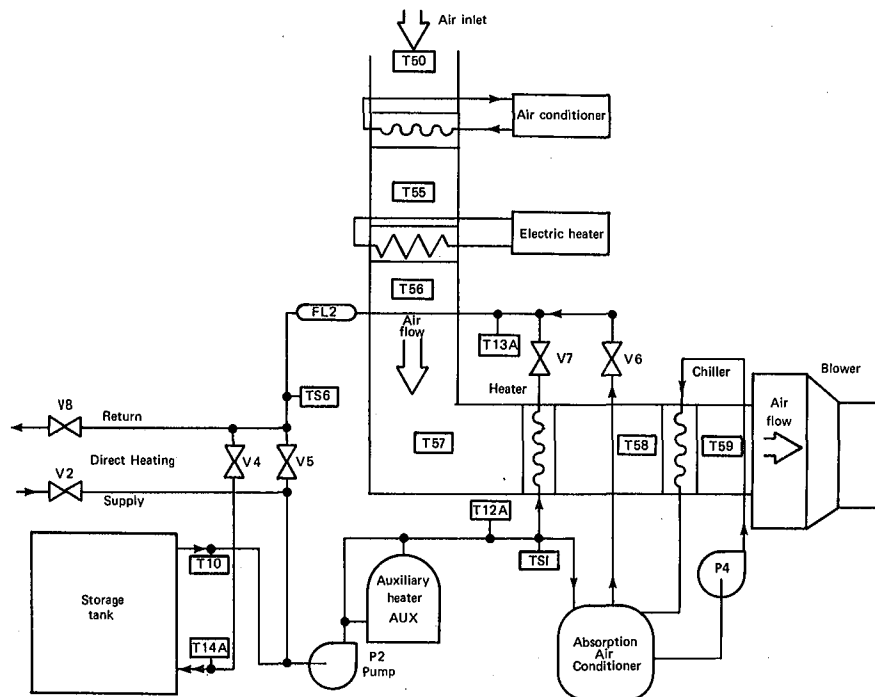


Fig. 3 Solar controls facility load simulator. (XBL 794-1150)

### Collector Loop Energy Balance

Preliminary energy balance experiments were done with simulated solar heat input from the pseudo-collector, with the apparent collector temperature determined by the hp-9825a, and with the operation of the collector and load loop determined by the LBL electronic controller. Energy supplied by the pseudo-collector was calculated at 60 second intervals and the amount of energy in the storage tank was calculated at 30 minute intervals as the apparent solar insolation was increased from zero to a maximum of  $950 \text{ W/m}^2$  and then back to zero. The duration of each experiment was 4 hours.

An energy balance summary for two 4 hour experiment and for a 22 hour total of successive experiments is shown in Table 1. The measured change in storage tank energy,  $\Delta Q_{\text{storage}}$ , plus the loss from storage during the period,  $\Delta Q_{\text{loss}}$ , gives the total heat input to storage,  $\Delta Q_{\text{storage}}$ . Heat input from the pseudo-collector boiler is calculated using the measured flow rate and the temperature difference between inlet and outlet.  $Q_2$ , the total heat supplied to the fluid stream, is calculated using thermocouples just before and after the boiler.  $Q_4$ , the heat supplied to storage, is calculated using thermocouples before the boiler, and at the storage return and is slightly smaller because of piping losses. Estimates are made for heat losses from the system piping and from the storage tank, which contains 11,400 kg of water. Previous experiments indicated that the heat loss coefficient should be approximately  $25 \text{ W/}^\circ\text{C}$  for the collector loop piping and  $24.6 \text{ W/}^\circ\text{C}$  for the storage tank. Estimated piping energy losses are indicated in Table 1 and compared with the differences between  $Q_2$  and  $Q_4$ . The differences between

$Q_2$  and  $Q_4$  only account for piping losses in the return side of the collector loop. Additional losses are found in the supply side. Energy input during each four hour period was repeatable as shown in Table 1. The energy balance over a single measurement period of 4 hours is not precise primarily because of uncertainty in the storage tank energy measurements. Even though the storage tank energy is calculated from the weighted average of 6 thermocouples, errors of 10 MJ are produced as stratification of the tank temperature changes. However, over a long experimental run of 22 hours, the energy balance is quite acceptable.

### Load Loop Energy Balance

Preliminary energy balance experiments were run with heat delivered from the storage tank to the heating coil located in the air duct. Power discharged in the heating coil,  $Q_H$ , was measured every thirty seconds using a differential thermocouple, DT13, and the load loop flow measurement, FL2. Power delivered to the load was typically 12 kW. The load loop experiment summarized in Table 2 was run for a period of 18 hours, with the building load calculated for a constant outdoor temperature of  $0^\circ\text{C}$  and a building loss coefficient of  $500 \text{ W/}^\circ\text{C}$ . The overall energy balance for the 18 hour run is quite acceptable.

### Theoretical Studies to Support Experimental Program

#### Development of Dynamic Collector Model

The dynamic response of a solar collector was simulated using a collector energy balance equation which accounts for collector thermal capacitance. The equation was numerically solved to describe the

Table 1. Collector loop energy balance summary (in megajoules).

<u>Duration of tests</u>	<u>4 hr</u>	<u>4 hr</u>	<u>22 hr</u>
<u>Storage Tank</u>			
$\Delta Q_{\text{storage}}$	113.0 MJ	118.5 MJ	663.9 MJ
$\Delta Q_{\text{loss}}$	4.6 MJ	5.6 MJ	28.4 MJ
$\Delta Q_{\text{storage}}$	117.6 MJ	124.1 MJ	692.3 MJ
<u>Heat Input</u>			
$Q_2$	131.9 MJ	128.6 MJ	705.2 MJ
$Q_4$	128.6 MJ	126.1 MJ	692.3 MJ
<u>Estimated Piping Losses</u>			
$Q_2 - Q_4$	3.3 MJ	2.5 MJ	12.8 MJ
$Q_{\text{piping}}$	3.7 MJ	4.9 MJ	25.2 MJ
<u>Net Energy Balance</u>			
$Q_{\text{storage}}$	117.6 MJ	124.1 MJ	692.3 MJ
$-Q_2$	-131.9 MJ	-128.6 MJ	-705.2 MJ
$+Q_{\text{piping}}$	3.7 MJ	4.9 MJ	25.2 MJ
<u>Net Balance</u>	-10.6 MJ (-9.0%)	-0.4 MJ (0.3%)	12.3 MJ (1.7%)

Table 2. Load loop energy balance summary (in megajoules) for 18 hour period.

Storage tank energy balance	
$\Delta Q_{\text{storage}}$	-561.4 MJ
$\Delta Q_{\text{loss}}$	21.8 MJ
Piping losses (estimated)	<u>24.3 MJ</u>
Net delivered to load	-515.3 MJ
Measured heat to load, $Q_H$	<u>-536.7 MJ</u>
Net energy balance	-21.4 MJ (4%)

circulating fluid temperature as a function of time and space. Figure 4 shows a typical collector outlet temperature history derived by the model.

The model is used to evaluate the performance of proportional and on/off collector loop control for various set points, flow rates, insolation levels and patterns (clear and cloudy days), and ambient temperature conditions. In proportional control, the collector loop fluid flow rate is proportional to the temperature rise across the collector. With on/off control, the fluid flow is either on or off. Evaluation of control strategies is based on the following criteria: collection efficiency, percent of maximum steady-state efficiency, pump running time (parasitic power demands), and cycling. Results of comparisons have been presented along with methods for determining controller set points.<sup>5</sup>

Typical results for collection efficiency for a clear day are shown in Fig. 5. Results indicate that the turn-on set point is not always a critical factor in the collection of energy because the collector stores energy while it is warming up and during cycling. This energy is transferred to the storage tank once the fluid begins to circulate.

Figure 6 shows results obtained for an overcast day with lower solar gain. Proportional flow controllers provide improved energy collection only during periods of interrupted or very low insolation when the maximum possible energy collection is relatively low. Although proportional controllers initiate flow at lower insolation levels than on/off controllers, they produce lower flow rates and higher average collector temperatures and thus slightly lower instantaneous collection efficiencies.

#### Study of Building Load Dynamics

Work has also begun on development of a residential building temperature response model to simulate the effects of heat input on room air

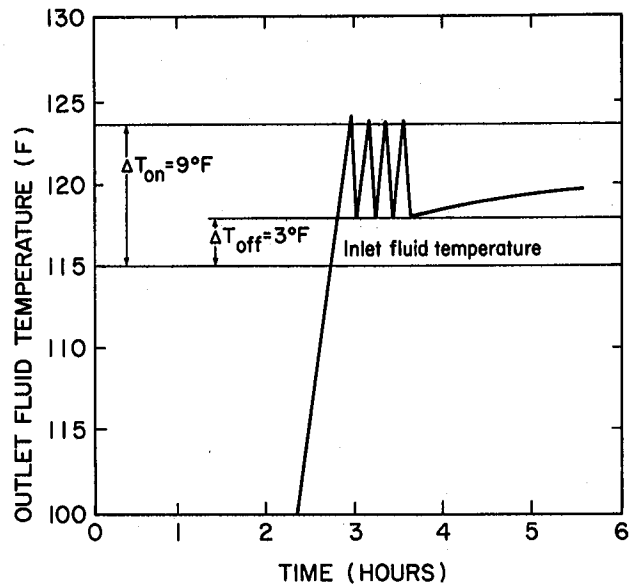


Fig. 4. Collector outlet temperature for a typical day with cycling. (XBL 7911-13120)

dynamics.<sup>6</sup> The model has three nodes: the building shell, the air, and the interior walls. This model gives the short time constant response appropriate for the heating of air within the structure and the long time constant response associated with the building structure. The model will be used in the test facility for evaluating advanced control strategies and controllers.

#### Technical Support Activities

This past year the Laboratory has been actively involved in proposal review and contract monitoring for the Controls Element of the DOE solar heating and cooling R and D program. Activities have included coordination with SERI on the controls part of the systems plan, conducting site visits, and reviewing the work of DOE controls contractors.

#### PLANNED ACTIVITIES FOR 1980

Plans for 1980 include a series of experimental tests of on/off control strategies for a variety of meteorological conditions. Experiment modifications are underway to permit variable-flow and proportional-flow control of the collector loop. A series of experimental comparisons of proportional and on/off collector loop strategies are planned. The design of the necessary modifications to test combined domestic hot water and heating systems are also planned. Papers have been submitted for presentation at several energy conferences and for publication in solar energy journals. Technical program support activities, in cooperation with SERI, will be continued.

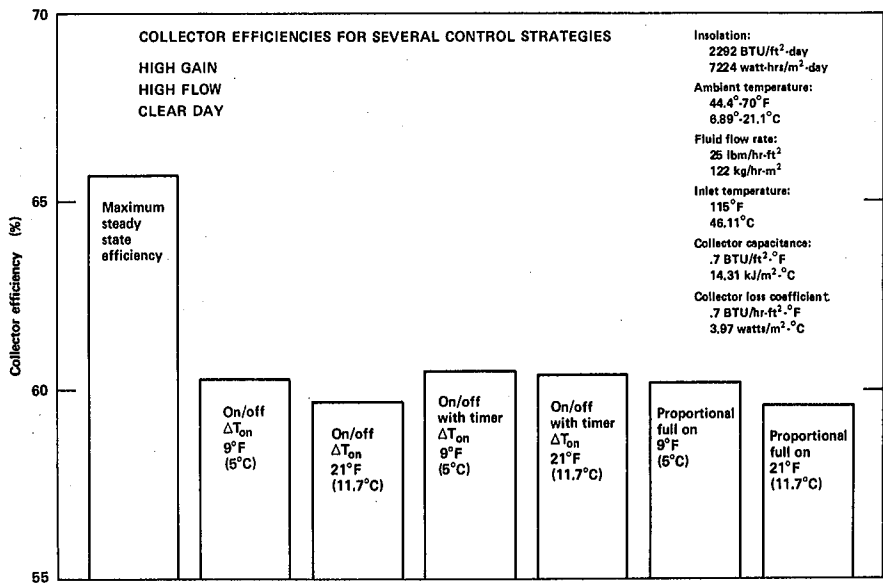


Fig. 5. Collector efficiencies for several control strategies--clear day, high gain cases. (XBL 796-1884)

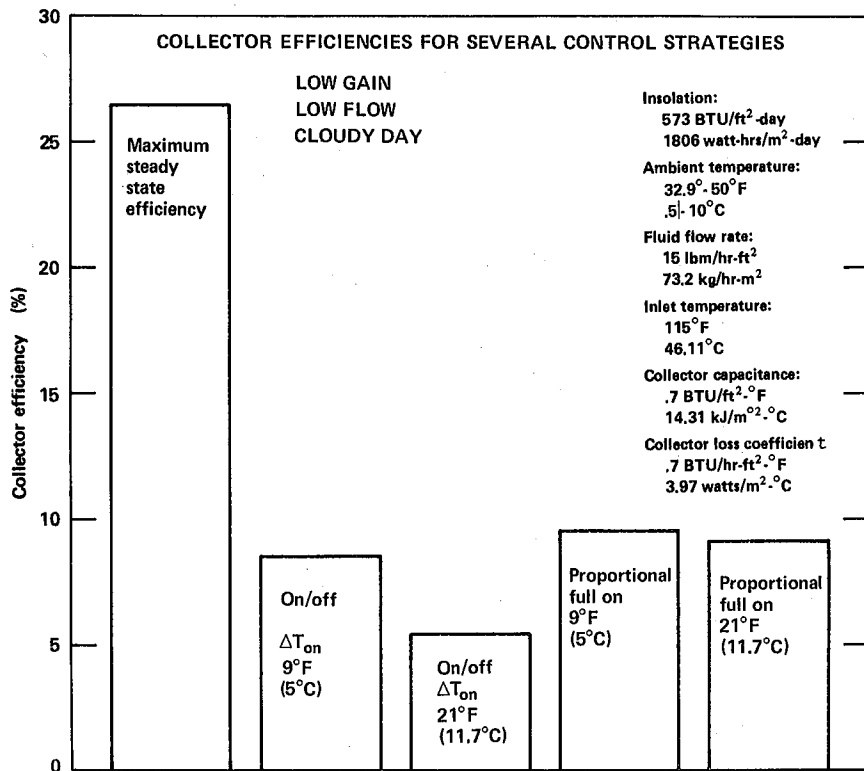


Fig. 6. Collector efficiencies for on/off and proportional control--cloudy day low gain cases. (XBL 796-1891)

## FOOTNOTE AND REFERENCES

\*This work has been supported by the Systems Analysis and Design Branch, Systems Development Division, Office of Solar Applications, U.S. Department of Energy.

1. M. Majteles, H. Lee, M. Wahlig and M. Warren, "Experimental Test Facility of Solar Control Strategies," Proceedings of Workshop on Control of Solar Energy Systems for Heating and Cooling, Hyannis, MA, May, 23-25, 1978. (Lawrence Berkeley Laboratory report LBL-8308, 1978).
2. M. Wahlig and M. Warren, "Electronic Controller Development and Evaluation of Control Strategies," Proceedings of Third Annual Solar Heating and Cooling Research and Development Branch Contractors' Meeting, September 24-27, 1978. Washington, D.C. (Lawrence Berkeley Laboratory report LBL-8381, 1978).
3. M. L. Warren, S. R. Schiller, and Wahlig, "Experimental test facility for evaluation of controls and control strategies," Second Annual Systems Simulation and Economic Analysis Conference, January 23-25, 1980, San Diego, CA.
4. M. F. McBride, "Measurement of Residential Thermostat Dynamics for Predicting Transient Performance," ASHRAE, 85 (1979), PH-79-7A.
5. S. R. Schiller, M. L. Warren, and D. M. Auslander, "The comparison of proportional and on/off solar collector loop control strategies using a dynamic collector model," Second Annual Systems Simulation and Economics Analysis Conference, January 23-25, 1980, San Diego, CA.
6. M. L. Warren, F. Sakkal, and S. R. Schiller, "Predicting the time response of a building under heat input conditions for active solar heating systems," Second Annual Systems Simulation and Economic Analysis Conference, January 23-25, 1980, San Diego, CA.

## DEVELOPMENT OF SOLAR DRIVEN ABSORPTION AIR CONDITIONERS\*

*K. Dao, M. Wahlig, and E. Wali*

### INTRODUCTION

The objective of this project is to develop absorption refrigeration systems for active solar heating and cooling applications. As of the conclusion of the first phase of this project, it has been experimentally demonstrated that the conventional single-effect ammonia-water absorption cycle can be used for solar cooling.<sup>1</sup> Optimum operating temperature ranges for this kind of system are:

- heat source input temperatures:  
 $200^{\circ}\text{F} < T_s < 230^{\circ}\text{F}$  (condenser)
- absorber cooling air temperature:  
 $T_0 = 95^{\circ}\text{F}$  (chilled water)
- output temperature:  $50^{\circ} > T_E > 40^{\circ}\text{F}$ ,  
coefficient of performance (COP) =  
0.65 to 0.70

The second phase of this project explores the commercial potential of the  $\text{NH}_3/\text{H}_2\text{O}$  single effect absorption air conditioner. A completely new 3-ton, single-effect unit was engineered and designed to achieve high performance and low cost.<sup>2,3</sup> Key components of this new unit are tube-in-tube heat exchangers for high effectiveness and low cost, and a pair of piston drivers and pumps for recuperation of mechanical energy from the returned weak solution. Estimated production cost of this unit is in the range of \$300-\$500/ton of rated capacity, depending on the choice of materials. The lower estimate applies when all components are made of welded carbon steel tubing. If stainless steel is used for some components, the cost approaches the higher estimate.

Success of the single-effect unit will not obviate the need for development of more advanced chillers with higher COP's compatible with high temperature collectors (above  $230^{\circ}\text{F}$ ). Accordingly, the third phase of this project is the development of advanced absorption cycles whose COP increases with temperature, maintaining a relatively constant fraction of the current COP over a wide range of operating temperatures.

### ACCOMPLISHMENTS DURING 1979

The fabrication and installation of the new single-effect  $\text{NH}_3/\text{H}_2\text{O}$  absorption conditioner has been completed. Preparation is now under way for its performance tests.

The development of the piston circulation pumps has been completed. Vibrations and banging have been reduced to an acceptable level and volumetric efficiency has been improved to above 90 percent. Two of these piston pumps are used to replace the conventional electric diaphragm circulation pump. One pump uses the high pressure weak solution as a driving medium while the other (called the make-up pump) uses high pressure vapor.

Detailed computer analysis of the new advanced absorption cycle (called cycle 2R for double effect regenerative absorption refrigeration cycle), completed this year, served as the basis for the design of the components of the "2R chiller." The configuration of the 2R chiller is shown in Fig. 1; its operation is described below (more details on cycle 2R can be found in Ref. 4).

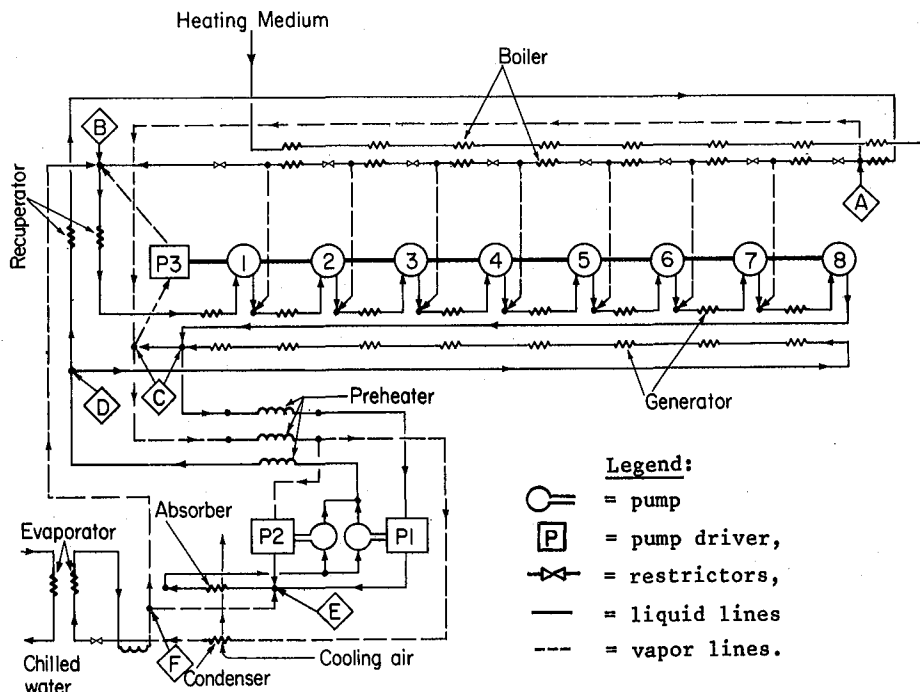


Fig. 1. Schematic diagram of cycle 2R chiller to be developed in phase 3 of the project.

(XBL 809-1894)

Heat is transferred from the heating medium to the ammonia solutions boiling at eight different pressure stages in the boiler. At the end of each boiling, vapor is extracted and reabsorbed in one flow side of the generator. The heat of absorption produced in this side of the generator boils the solution flowing in the other side of the generator. The  $\text{NH}_3$  vapor produced by the generator at C is fed to the condenser through the preheater. A small amount of this vapor is bled off to run the piston driver P3 of the multistage pump (stages 1-8). After condensation in the condenser, the liquid  $\text{NH}_3$  expands through a restrictor (or expansion valve) to the evaporator where it boils and chills the chilled water. The  $\text{NH}_3$  vapor leaving the evaporator at F is absorbed in the absorber at E and in the recuperator at B. The heat of absorption produced in the absorber is rejected to the cooling air. Heat of absorption produced in the B side of the recuperator boils the solution flowing in the D channel of the recuperator. Vapor generated by this boiling process DA is collected at A to be subsequently condensed in the condenser. At the outlet of the absorber, the solution rich in  $\text{NH}_3$  is pumped by pumps P1 and P2 to D through the preheater. At D the solution is split into two streams. The first stream (82%) boils in the generator and the second stream (18%) boils in the recuperator. Essentially the cycle 2R is constructed by adding a boiler and a recuperator to the basic conventional single-effect cycle which consists of the generator, the preheater, the absorber, the condenser and the evaporator. Note that the boiler does not directly produce any  $\text{NH}_3$

vapors that can be used in the evaporator. The function of the boiler is to transfer heat from the heating medium to the generator and to benefit from the high temperature of the heat source to produce a very weak solution at B.

The amount of heat received by the boiling solution from A to B in the boiler is transferred essentially without losses to the generator in the form of latent heat from the vapors generated by the different stages of the boiler. Upon reabsorption these vapors release their latent heat to the boiler side of the generator.

The very weak solution at B is at lowest pressure and can absorb  $\text{NH}_3$  vapor from the evaporator. Absorption of this very weak solution B rejects heat at temperatures high enough to boil stronger solutions in the D side of the recuperator, at condenser pressure. The vapor produced by the boiler solution from D to A adds up to the vapor produced by the generator at C to increase the cooling capacity of the cycle, thus improving the COP. The larger the temperature spread between B and C, the higher the COP. The single-effect cycle part of cycle 2R is designed to operate near cut-off conditions, independently of the heating medium temperature; for instance, the temperature at C is always  $216^\circ\text{F}$  when the temperature of the condenser absorber is  $110^\circ\text{F}$  and the evaporator temperature is  $40^\circ\text{F}$ .

In Fig. 1, all check valves' connections are left out for clarity. With five check valves

properly located, the cycle 2R also operates when the heating medium temperature is below the cut-off generator temperature of the single-effect subcycle. This is possible because the boiler and recuperator perform as a heat pump that can pump heat from the low temperature (say 170°F) heat source to a temperature high enough to operate the single-effect subcycle. The design, drawing, and fabrication of the multistage pump P3 has been completed. Performance tests will follow soon. The design and drawing of the remaining components of the 2R chiller is almost 50 percent completed. All heat exchangers are of tube-in-tube configuration.

Design rated capacity is 3 tons; for an anticipated net COP of 0.87, design operating temperatures are:

heat source: 280°F (input to the boiler);  
 heat source: 95°F (condenser absorber cooling air);  
 cold source: 45°F (chilled water outlet).

Net COP is defined as the COP obtained after deduction of the amount of generated vapor bled to run the pumps P2 and P3.

Off-design performance of this 2R chiller is summarized in Table 1 and Fig. 2.

#### PLANNED ACTIVITIES FOR 1980

Reports on the testing of the phase 2 single-effect chiller will be completed in 1980.

The multistage (8 stage) pump (pump P3 in Fig. 1) will be tested, "debugged," and improved during 1980 so that it can be ready for assembly with the cycle 2R chiller in 1981.

The design and drawings of all components of the 2R chiller will be completed in 1980. Fabrication of some components of the 2R chiller may proceed in late 1980.

Table 1. Off-design performance of 2R chiller.

	Temperature of solution leaving generator at C, °F					
	160	182	210	240	270	300
Chilled water outlet temperature, °F	45	45	45	45	45	45
Cooling air temperature, °F	95	95	95	95	95	95
Condenser absorber temperature, °F	101	103	106	108	110	112
Input temperature, °F	165	190	220	250	280	310
Capacity, tons	0.9	1.5	2.1	2.5	3.0	3.3
Net COP	0.33	0.50	0.67	0.79	0.87	0.93
Cond/absorber fan power, watts	450	450	500	500	500	500

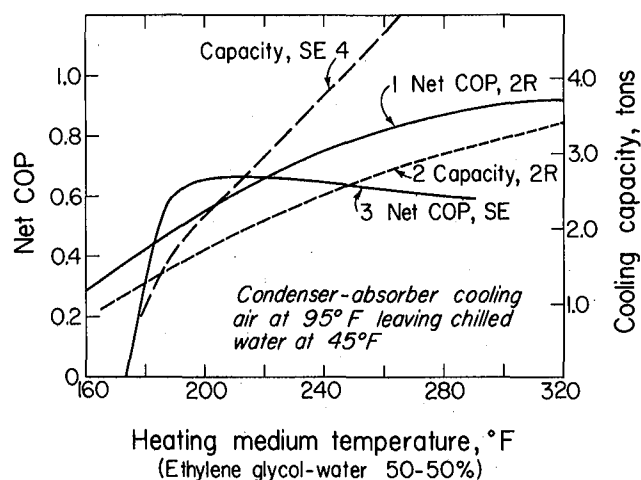


Fig. 2. Estimated performance characteristics of the phase 3 2R chiller as compared to those of the phase 2 single-effect (SE) chiller. (XBL 809-1895)

Investigations of other possible advanced cycles (such as cycle 1R, Ref. 5), and the search for an advanced cycle that may have better performance and lower production cost than the cycle 2R will continue in 1980.

The search for higher-temperature refrigerant absorbant pairs suitable for advanced cycles (particularly for cycle 1R, Ref. 5) will continue in 1980. The search consists of subcontracting the measurements of key properties of a number of pairs:

- heat of mixing at constant temperature: 25°C;
- vapor pressure of the pure fluids;

- specific heat capacity of the pure fluids, and mixtures;
- vapor pressure of mixtures over a temperature range.

From the key properties, approximate mixture properties will be calculated over the whole range of interest using appropriate thermodynamic relations. Cycle analysis using the approximate properties will determine the best pair. Properties of the selected pair will then be measured accurately over the whole range of interest. Other properties such as viscosity, thermal conductivity, chemical stability at high temperature, and compatibility with various materials of construction will also be determined.

#### FOOTNOTE AND REFERENCES

\*This work was supported by the Active Building Systems Branch, Systems Development Division, Office of Solar Applications, US Department of Energy.

1. Annual Report 1976, Energy and Environment Division, Lawrence Berkeley Laboratory report LBL-5952, p. 71-73, 1976.
2. Annual Report 1977, Solar Energy Program, Energy and Environment, Lawrence Berkeley Laboratory, Pub 248, p. 13-16, 1977.
3. Annual Report 1978, Solar Energy Program, Energy and Environment Division, Lawrence Berkeley Laboratory report LBL-9630, p. 15-18, 1978.
4. K. Dao, "Conceptual design of an advanced absorption cycle. The double effect regenerative absorption refrigeration cycle," Lawrence Berkeley Laboratory report LBL-8405, 1978.
5. K. Dao, "A new absorption cycle: The single effect regenerative absorption refrigeration cycle," Lawrence Berkeley Laboratory report LBL-6879, 1978.

## PASSIVE COOLING\*

*M. Martin, P. Berdahl, F. Sakkal, and M. Wahlig*

### INTRODUCTION

The major objective of this project is to evaluate radiative and passive cooling systems for various parts of the United States. The long-range goal is to displace electricity used for air conditioning. The primary emphasis in this project to date has been infrared radiative cooling.

Infrared radiative cooling systems are composed of a radiator surface which is exposed to the sky, an infrared-transparent windscreens to reduce convective intrusion of heat from the air, and a means for transporting heat from the building's interior to the radiator surface. The current work includes measurement of atmospheric infrared emission characteristics in order to identify geographical regions in which selective and nonselective radiators may be effective. Both atmospheric radiation models and experimental sky radiation measurements are employed in this effort. A computer analysis of radiative cooling will model the entire system, including the atmospheric characteristics, the blackbody or selective radiating surface, and the building load. Promising radiator surfaces and infrared-transparent windscreens will be experimentally evaluated at an outdoor test facility at LBL. Finally, convective and evaporative cooling systems will be integrated into the study so that other aspects of passive cooling will be included.

In order to predict accurately the net heat exchange between the sky and a surface of known

infrared characteristics, it is necessary to have a knowledge of the intensity of infrared radiation produced by the atmosphere as a function of both zenith angle and wavelength. Most measurements in the literature pertaining to the spectral radiance of the sky were obtained on one or two nights, or were made only under clear sky conditions. It therefore became necessary to make measurements, day and night, over periods of months, to obtain data on which estimates of cooling system performance can be based. During 1978, a major effort was devoted to construction of four spectral infrared sky radiometers and the siting of three of these instruments at Tucson, San Antonio and Gaithersburg. These sky spectrometers were set up to measure the radiance of the zenith sky at half hour intervals in 6 wavelength bands ranging from 8 to 22 microns. Auxiliary measurements performed consisted of total infrared sky radiance (with a pyrgeometer), air temperature, and dewpoint. Further details of the measurement system may be found in last year's Annual Report,<sup>1</sup> and elsewhere.<sup>2-5</sup>

### ACCOMPLISHMENTS DURING 1979

A major activity in FY 1979 was the operation and improvement of the infrared radiometer systems. The fourth system was sited at St. Louis in June. As data acquisition became routine, it was possible to devote some effort to data analysis. A major new activity this year has been the design and construction of the experimental test facility for selective radiative cooling systems. At year's end, the facility was nearly complete.

### Spectral Radiometer Measurement Systems

During winter and spring months, efforts were directed toward maximizing the quality and quantity of sky radiance data to be acquired during the summer. Several improvements were implemented.

Radiometer improvements resulted in reduced mirror emissivity corrections. Formerly, a front-surfaced aluminum mirror overcoated with silicon monoxide was used. In the 8 and 9 micron spectral regions, corrections for the mirror emissivity were typically 10%. Although these values are determined automatically during computer processing of the data at LBL, they are not accurately known. New mirrors, with a reflecting surface composed of a thin layer of bare gold, reduced typical emissivity corrections to 3%.

Calibration techniques were also improved. Radiometer calibration is performed by measuring the radiance of a black body of known temperature as it cools from 70°C down to ambient temperature. Formerly, this procedure was initiated manually by personnel at the radiometer site. This function is now under the control of the on-site microprocessor, making it possible to perform calibrations daily. More frequent calibrations aid detection of possible instrument malfunctions.

The most significant improvement implemented was the introduction of new viewing angles. (This extension in capability had been planned from the project inception, subject to the availability of funds.) Prior to this summer, the radiometer viewed only the zenith. However, the hardware and software are now modified so that the instrument can measure the radiance at zenith angles of 0°, 20°, 40°, 60°, and 80°, on an arc from the zenith to the north horizon.

For the summer period, data sets actually obtained range from 67% complete at San Antonio to 88% complete at Tucson. The primary problems which caused loss of data were:

- pyroelectric detector failure;
- rain detector failure (the system "thought" it was raining and did not make measurements);
- rare but recurring hardware failure of unknown origin which interacted with software "bug" to disable microprocessor;
- telephone line failure (data could not be transmitted to LBL);
- broken microswitch; and
- power outages.

Although these problems were significant, they did not substantially impair usefulness of the data.

### Analysis of the Sky Radiance Data

Analysis of the sky radiance data to date has provided rough estimates of the resource for radiative cooling. For example, a 100% efficient

idealized radiative cooling system with a radiator temperature of 25°C (described in Ref. 3), located in Tucson from August 16-31, 1978, would have rejected an average of 88 W/m<sup>2</sup> to the sky, 24 hr/day.<sup>3</sup> The same system, sited at San Antonio for the last week in September, 1978, would have rejected 69 W/m<sup>2</sup>.<sup>3</sup> After further data analysis, estimates such as these will be available for various types of cooling systems, based on longer periods of data.

An important aspect of the data analysis is the verification of the atmospheric model of sky radiance developed at LBL, based on the public domain computer model LOWTRAN 3B.<sup>6</sup> Such a verification is not practical for cloudy skies because an adequate characterization of clouds is not usually available from meteorological measurements. However, for clear skies, it is possible to use radiosonde measurements of the atmospheric profile of temperature and humidity. These measurements are made at 12 hour intervals by the National Weather Service. Incorporating typical profiles for ozone, carbon dioxide, and aerosols, one has enough information to produce a calculated spectrum of the sky radiance. For the 8.1-13.7 micron filter of the spectral radiometer, these calculated radiances are plotted on the horizontal of Fig. 1. (The spectral radiances produced by LOWTRAN have been averaged over the 8.1-13.7 spectral interval, using the spectral transmissivity of the radiometer system as a weighting function in performing the

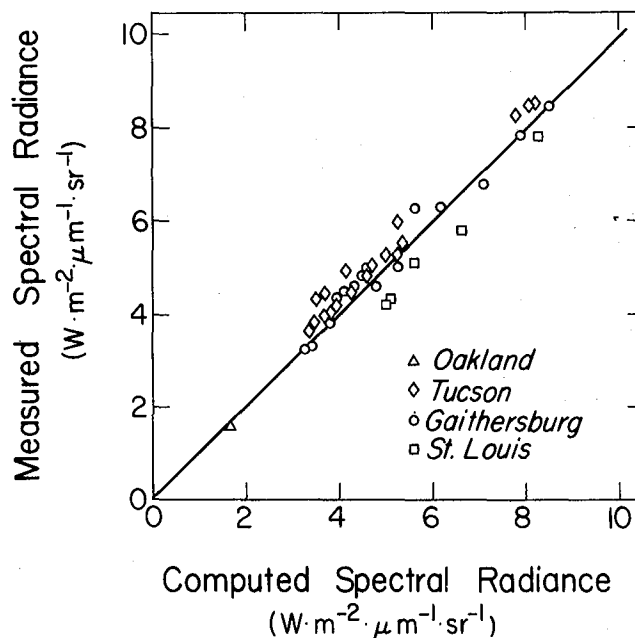


Fig. 1. The measured spectral radiance of clear skies in the 8.1-13.7 band, plotted versus calculated radiances based on measured atmospheric profiles of water vapor and temperature. Except for the single measurement at Oakland, all results are for the summer season. Points to the right in this diagram correspond to measurements near the horizon, where the atmosphere is "warmer".

(XBL 809-1898)

average.) The measured values of the average spectral radiance for this filter are plotted along the vertical axis. Most of the scatter in this plot is due to deviations of the radiosonde profile from the actual temperature and water vapor profile along which the radiometer was viewing. To support this contention, Fig. 2 displays the subset of the data in Fig. 1 in which the surface temperature and dew point, as measured at the radiometer site, agree to within  $\pm 1^\circ\text{C}$  with the values reported from the radiosonde sounding. The improvement in the data scatter is evident. The computer model verifies that errors of  $1\text{-}3^\circ\text{C}$  in the dew point temperature are large enough to cause the increased scatter seen in Fig. 1. The small systematic deviation remaining in Fig. 2 between the measured and computed spectral radiance is probably significant; however, more work is required to determine its origin.

Based on the foregoing comparison, one may state that the systematic errors in the radiometer measurements are probably less than  $0.3 \text{ W/m}^2 \mu\text{sr}$ , for the  $8.1\text{-}13.7 \mu$  band. The errors in computed estimates of clear sky radiance are also less than  $0.3 \text{ W/m}^2 \text{ Mm sr}$ , provided the atmospheric profiles of temperature and water vapor are adequately known.

#### Experimental Test Facility for Selective Radiative Cooling Systems

This new facility, located on a rooftop at LBL, will permit measurements of the performance

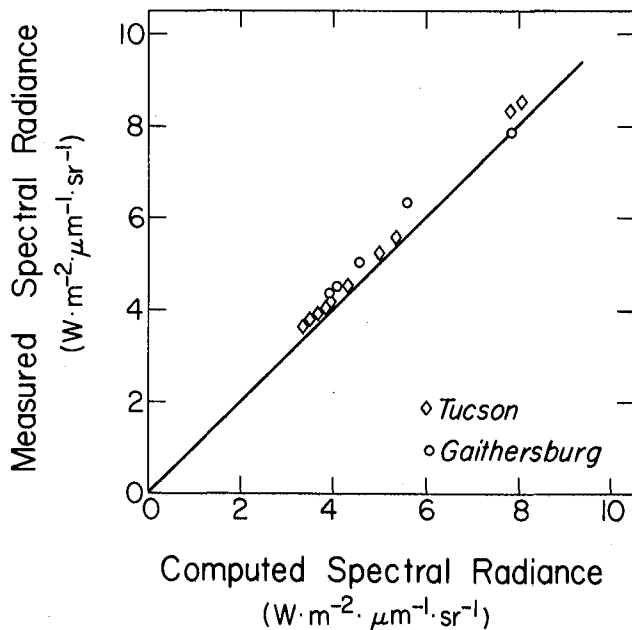


Fig. 2. This figure shows a subset of the points in Fig. 1. Eliminated were those measurements made when the ground level temperature and dew point of the radiosonde measurement did not agree to within  $1^\circ\text{C}$  of the values measured at the radiometer. (XBL 809-1896)

of candidate radiator and windscreen materials. Eight radiator assemblies have been mounted on a rooftop rack. Each assembly consists of an insulated Kydex (Acrylic and PVC) box having outside dimensions  $108 \times 66 \times 12.7 \text{ cm}$ , as shown in the cross-sectional view of Fig. 3. The insulation, which fills the  $10\text{-cm}$ -thick interior of the box, consists of injected styrofoam.

A recess in the upper surface of the box holds a  $0.8 \text{ mm}$ -thick aluminum radiator plate of dimensions  $50 \times 90 \text{ cm}$ . Convection losses above the radiator are suppressed by means of a  $0.050 \text{ mm}$ -thick polyethylene windscreen located approximately  $3 \text{ cm}$  above the plate. A resistive heating element is glued to the bottom side of the radiator plate and the upper side is painted or specially treated to form the radiating surface. The heater capacity is  $140 \text{ W}$  which allows a maximum net outgoing thermal flux of approximately  $311 \text{ W/m}^2$  to be radiated.

A microprocessor-based data acquisition system will be used to control and measure the heater outputs as well as to make measurements of radiator and windscreen temperatures. Auxiliary measurements are to be air temperature, dew point, and total infrared sky radiance using a pyrgeometer.

Preliminary experiments with the test facility have been performed, and results were reported at the Fourth National Passive Solar Conference.<sup>7</sup> More extensive tests will be initiated during the summer of 1980 upon completion of the automatic temperature control and data acquisition system. Improvements on results obtained elsewhere in similar tests<sup>8-15</sup> are expected through the use of more accurate characterization of atmospheric conditions because a pyrgeometer is used to measure infrared sky radiance.

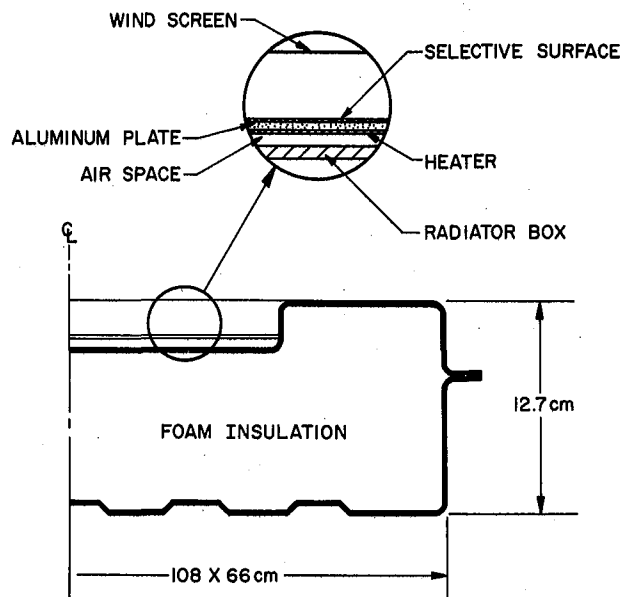


Fig. 3. Radiator assembly showing insulating box, radiator, and windscreen. (XBL 798-10763)

## PLANNED ACTIVITIES FOR 1980

All four spectral infrared sky radiometer systems will continue to collect data through the summer of 1980. Two systems have been moved to permit data sets to be accumulated in other (warm) climate regions of the United States. The new sites are West Palm Beach, Florida, and Boulder City, Nevada, which represent extremes of humid and dry climatic conditions.

A major effort in 1980 will be devoted to the analysis of the sky radiance data in order to produce information useful for the design of passive cooling systems which utilize radiative cooling. This effort will have two primary components. First, tabulated values of cooling rates for various systems will be computed, taking into account system operational characteristics, such as the spectral emissivity of the radiator, radiator aspect angle, and whether or not the system will be operated during daylight hours. Second, the radiometer data will be correlated with both meteorological and pyrgeometer data in an effort to establish techniques for estimating spectral data from more conventional measurements.

The experimental test facility for selective radiative cooling systems will be fully operational. The facility will be used to establish the relative and absolute merits of various radiator and wind screen materials. Other issues to be investigated include the effectiveness of honeycombs for suppressing convective losses, the use of infrared reflectors to "concentrate" the cooling resource, the use of infrared-transparent glazings which can reflect sunlight to permit daytime cooling, and the control or elimination of the condensation of atmospheric moisture within the cooling apparatus.

## FOOTNOTE AND REFERENCES

\*This work was supported by the Passive and Hybrid Systems Branch, Systems Development Division, Office of Solar Applications, U.S. Department of Energy, under Contract No. W-7405-ENG-48.

1. M. Martin et al., "Radiative and passive cooling," Lawrence Berkeley Laboratory report LBL-8619, 58 (1978).
2. P. Berdahl and M. Martin, "Infrared Radiative Cooling," Proceedings of the 1979 International Congress of the International Solar Energy Society, Atlanta, GE (1979).
3. P. Berdahl and M. Martin, "Spectral Measurements of Infrared Sky Radiance," Proceedings of the Third National Passive Solar Conference, San Jose, CA, 443 (1979).
4. P. Berdahl, "Routine Spectral Measurements of Infrared Radiation from the Atmosphere," Proceedings of the Second International Conference on Infrared Physics, Zurich, Switzerland, 406 (1979).
5. M. Martin and P. Berdahl, "Description of a Spectral Atmospheric Radiation Monitoring Network," Proceedings of the Third Conference on Atmospheric Radiation, Davis CA, 148 (1978).
6. J. Selby et al., "Atmospheric Transmittance from 0.25 to 28.5 M: Supplement LOWTRAN 3B," available from NTIS.
7. F. Sakkal et al., "Experimental Test Facility for Selective Radiative Cooling Surfaces," Proceedings of the Fourth National Passive Solar Conference, Kansas City, MI (1979).
8. S. Catolanotti et al., "The Radiative Cooling of Selective Surfaces," Solar Energy 17, 83 (1975).
9. A. Addeo et al., "Selective Covers for Natural Cooling Devices," Il Nuovo Cimento 1C, 419 (1978).
10. D. Michell, "Selective Radiation Cooling, Another Look," Report on the CSIRO Division of Tribophysics, University of Melbourne, Parkville, Victoria, 3052, Australia (1976).
11. B. Landro and P. G. McCormick, "Effect of Surface Characteristics and Atmospheric Conditions on Radiative Heat Loss to a Clear Sky," to be published in the International Journal of Heat and Mass Transfer (1979).
12. W. C. Miller and J. O. Bradley, "Radiative Cooling with Selective Surfaces in a Desert Climate," Proceedings of the Fourth National Passive Solar Conference, Kansas City, MI (1979).
13. E. Hernandez and E. Mayer, "Nocturnal Infrared Radiative Cooling Experiments in Mexico," Proceedings of the International Conference on Solar Building Technology, London, England (1977).
14. F. Trombe, "Devices for Lowering the Temperature of a Body by Heat Radiation Therefrom," U.S. Patent #3,310,102 (1967).
15. P. Grenier, "Refrigeration Radiative: Effet de Serre Inverse," Revue de Physique Appliquee 14, 87 (1979).

# LBL SOLAR DEMONSTRATION PROJECT\*

T. Webster

## INTRODUCTION

The LBL Solar Demonstration Project in Building 90 (Fig. 1) is one of eleven projects selected to be part of the FY 1977 Department of Energy (DOE) Facilities Solar Demonstration Program, a pilot program for the Solar Federal Buildings Program authorized by the National Energy Act. The objectives of this pilot program were to establish procedures and techniques for assessing and implementing solar systems for federal facilities, and to assist in energy use reduction within DOE facilities.

The following criteria were used to select projects for this initial program:

- Buildings should be suitable for retrofitting, i.e., their orientation, location and configuration should be suitable for solar energy use.
- Solar space and hot-water heating should be emphasized.
- Buildings should be typical government buildings.
- Design and construction should not cost more than \$200,000.

The LBL project was funded by the DOE Solar Energy Division through the Construction, Planning,

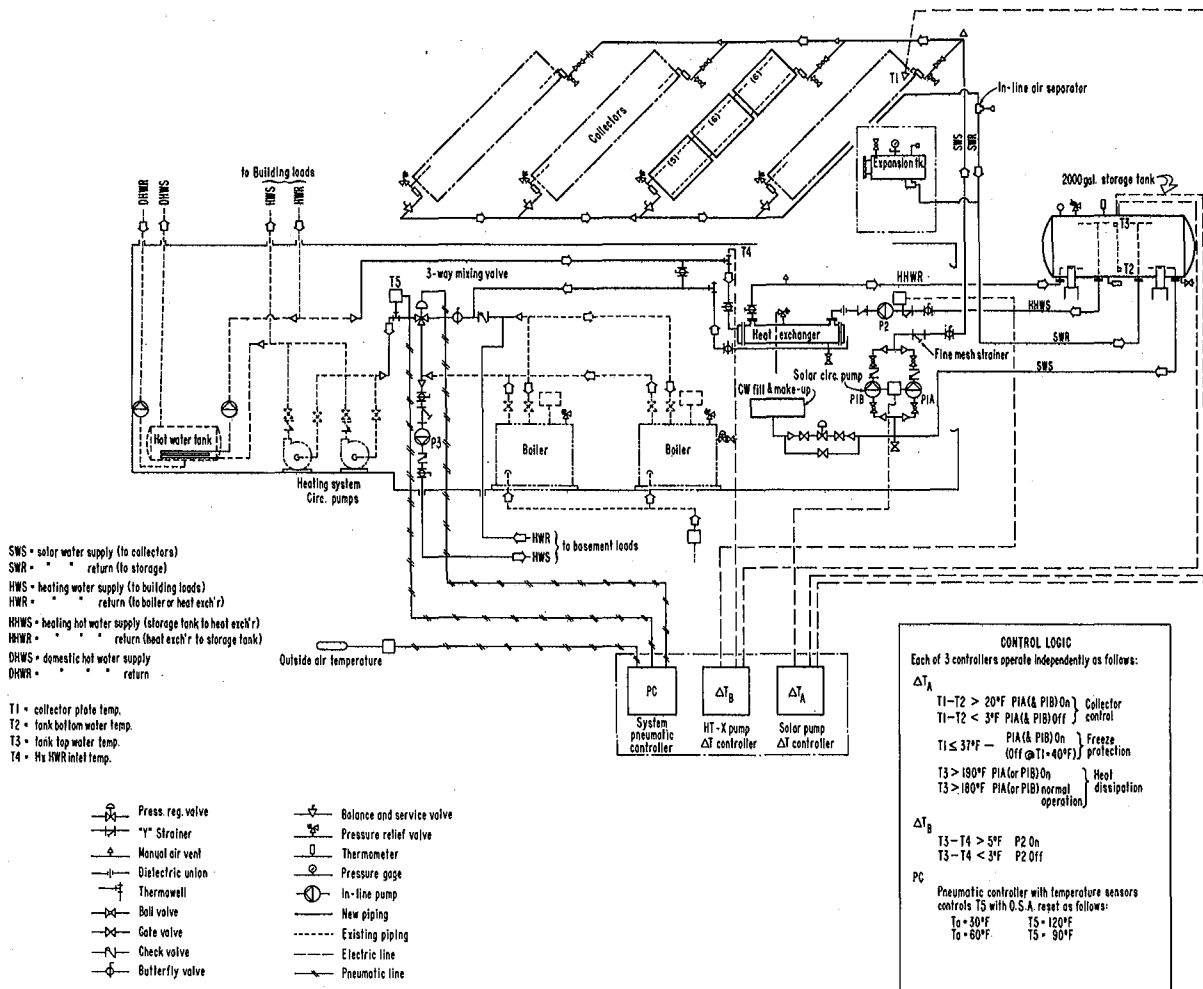


Fig. 1. Building 90 solar retrofit piping and control schematic. Engineering Drawing 4B90-PO43-B. (XBL 791-102)

and Support Division. LBL Plant Engineering was responsible for design and construction of the project with assistance provided by the LBL Solar Group. A detailed description of the building, solar systems, preliminary and final design considerations, and initial construction is contained in the 1977 Energy and Environment Division Annual Report, 1978.

#### ACCOMPLISHMENTS DURING 1979

The solar system construction was completed during 1979. Among significant events and problems during system construction and initial operation were:

- erroneous Unistrut locations (for collector attachment) requiring field modifications;
- rerouting existing piping in the basement to allow installation of solar piping;
- leaking 3-way control valve due to piping misalignment;
- installation of a bulb type collector freeze protection sensor that was unable to take high collector temperatures; this sensor was replaced with an electric, resistance type sensor with a  $\Delta T$  controller;

- flow anomalies in the heating system which were traced to a check valve that would isolate the boiler from the system in some modes of operation; the valve was found to be unnecessary and was removed;
- differential expansion between the urethane foam insulation surrounding the tank and the steel tank shell caused cracking in the tank's insulation and outer aluminum cover. The problem was corrected by resealing the shell.

Construction of the system was completed in April 1979. Peripheral items such as IBM instrumentation and stairs and walkways were completed in September. Although the system is complete and ready to operate, the collector-to-storage loop is the only part of the system currently operating; a return-air recirculating system has not yet been installed, so the solar system is not capable of operating effectively at the temperatures currently required by the heating system. This system is slated for installation soon.

#### FINAL SYSTEM COSTS

Table 1 is a summary of final system construction costs as reported by the contractor.

Table 1. System costs

Systems	Materials	Labor	Total
<u>Collector Subsystem</u>			40,866
Collectors and mounting	19,123	5,920	25,051
Collector supports	8,762	4,716	13,478
Collector piping		960	960
Collector piping insulation			1,377
<u>Storage Subsystem</u>			8,334
Tank and Installation	4,449	1,130	5,579
Insulation			2,755
<u>Other</u>			36,856
Piping, pumps, heat exchanger	7,255	10,696	17,151
Insulation			2,755
Controls			7,050
Electrical			4,101
Painting			2,200
Contractor overhead and profit			2,799
<u>Total System Costs</u>			86,056
Cost per square foot gross collector area			60.3
Cost per square foot net collector area			67.1
Contract amount			79,700
Extras			6,356

Among the lessons learned (and recommendations for future systems of this type) are the following:

- As shown by the actual costs above, the collector structural supports (at 15%) is a significant part of the system costs. The structure was redesigned three times in an attempt to reduce these costs without much success. Alternative structures that require less structural steel and less reinforcement of building structure beams should be explored.
- While internal collector manifolding is highly recommended, spacing of the collectors should be increased to at least 2 in. to allow easier access for soldering and installation of insulation.
- Expansion joints should be provided when urethane foam insulation is used for tank insulation.
- All minor details, such as valve locations and positions, collector attachment locations and details, insulation details, and clearances should be carefully worked out and double-checked during design and construction to reduce costs and insure durability of the installation.
- Although this was a federal project which usually results in high costs, the overall cost per square foot of collector area is not unreasonable compared with commercial system costs in the private sector. However, the contractor's overhead and profit is quite low at 3%; comparable low bids for this type of work would probably be the exception rather than the rule. On the other hand, because this system is industrial quality and probably is about as difficult a retrofit as is reasonable to undertake, the overall costs are probably typical for future systems of this type.

#### FUTURE ACTIVITIES

Funding for this project has been terminated as of September 1979. IBM instrumentation will be activated in early FY 80 and performance data collection will commence as soon as the recirculating air system is installed.

#### FOOTNOTE

\*This work has been supported by the Solar Heating and Cooling Demonstration Branch, Office of Conservation and Solar Applications, U.S. Department of Energy under Contract No. W-7405-ENG-48.

## SUPPORT FOR COMMERCIAL SOLAR DEMONSTRATION PROGRAM\*

*F. Salter, S. Peters, and T. Webster*

#### INTRODUCTION

The Solar Applications Group at LBL provides technical consulting and management services to support the DOE San Francisco Operation Office's (DOE/SAN) overall management of commercial-building solar demonstration projects and hotel/motel hot water solar projects located throughout the Northwestern States and Hawaii. These projects are part of the National Solar Heating and Cooling Demonstration Program,<sup>1</sup> whose primary objectives are to stimulate a solar industry and to promote the use of solar energy as a means of reducing demand on conventional fuel supplies.

The group is currently involved in support for projects in this program as follows:

Projects	Program solicitation	
1	NSF-1	Cycle I
13	DSE-76-2	Cycle II <sup>2</sup>
11	PON 4200	Cycle III <sup>3</sup>
3	PON 1450	Hotel/motel <sup>4</sup>

A detailed description of activities of this group is contained in the Energy and Environment Division Annual Report for 1977.

#### ACCOMPLISHMENTS DURING 1979

Technical consulting and management activities continued on all projects. One Cycle III project was cancelled due to participant funding problems. LBL's participation in these demonstration projects will cease at the end of FY 1980, and accordingly, one Cycle II and five Cycle III projects, which have been delayed primarily because of funding problems and will not be complete by the end of FY 80, have been transferred to Energy Technology Engineering Center (ETEC) in Southern California.

At the end of FY 1979, construction was complete, or near complete, on the following projects:

Program Cycle	Construction Completion	
	100%	>95%
Cycle I	1	1
Cycle II	7	12
Cycle III	1	4
Hotel/motel	2	2

Even on projects that are operational, some consulting and management effort is required to follow the project, deal with occurring operational problems, gather and review Final Reports and Data

Collection Reports. On two Cycle II projects, contracts have been written for refurbishment work to improve the overall systems efficiencies and to make the systems more reliable and serviceable. This work is primarily related to piping, insulation and control modifications. At present, investigations are in progress on three other projects which appear to be potential candidates for similar refurbishment contracts.

#### PLANNED ACTIVITIES FOR 1980

For FY 1980, activities have been reduced from three to one man-year of effort. LBL's involvement in these projects will cease at the end of FY 1980. Efforts will be directed toward completing as many projects as possible; however, it is likely that additional projects will be transferred to DOE/SAN or ETEC during the course of the year.

#### FOOTNOTE AND REFERENCES

\* This work has been supported by the Solar Heating and Cooling Demonstration Branch, Office of Conservation and Solar Applications, U.S. Department of Energy.

1. National Program for Solar Heating and Cooling of Buildings, ERDA 76-6 (November 1976).
2. Commercial Integrated Projects for Use in Demonstrations of Solar Heating and Cooling, PON DSE 76-2, ERDA (1976).
3. Commercial Integrated Projects for Use in Demonstrations of Solar Heating and Cooling, PON EG-78-N-01-4200, DOE (1978).
4. Hot Water Initiative for Hotel/Motel Installations, PON EG-77-N-03-1450, ERDA (1976).

## MEASUREMENT AND ANALYSIS OF CIRCUMSOLAR RADIATION\*

*D. Evans, D. Grether, A. Hunt, and M. Wahlig*

### INTRODUCTION

Instrument systems called "Circumsolar Telescopes" are used to measure the solar and circumsolar radiation for application to solar energy systems that employ lenses or mirrors to concentrate the incident sunlight. Circumsolar radiation results from the scattering of direct sunlight through small angles by atmospheric aerosols (dust, water droplets, or ice crystals in thin clouds, etc.). The solar energy system will typically collect all of the direct solar radiation (that originating from the disk of the sun) plus some fraction of the circumsolar radiation. The exact fraction depends upon many factors, but primarily upon the angular size (field-of-view) of the receiver. A knowledge of the circumsolar radiation can be used as a factor in the optimization of a receiver design, as one measure of the suitability of a geographic region for concentrating systems, or as input to comparison studies of competing designs at a particular location.

Design and construction of the circumsolar telescope was one of the first tasks completed in this project. The instrument system has a "scanning telescope" mounted on a precision solar tracker. The telescope mechanically scans through an arc of  $6^\circ$  with the sun at the center of the arc. A digitization of the sun's brightness or the brightness of the circumsolar radiation is taken every 1.5' of arc, with a complete scan taking one minute of time. In all, four such instruments were constructed. Auxiliary instruments include a pyrheliometer, a collimating instrument with a fixed field of view (typically  $5-6^\circ$ ) that provides an estimate (called the "normal incidence" reading) of the direct solar radiation. The telescope and pyrheliometer have matched ten position filter

wheels: one open position, eight interference filters that divide the solar spectrum into eight intervals of roughly equal energy content, and one opaque filter to monitor detector noise. The data are recorded on magnetic tape, with one tape holding a week's worth of data per telescope.

The telescopes have been primarily operated at locations for which the instruments can play a dual role: (1) characterization of a region or climate, and (2) provision of site-specific data for proposed or actual concentrating solar energy systems.

The data are used at LBL and other DOE-supported institutions [e.g., Sandia Laboratories and Solar Energy Research Institute (SERI)] in consideration of the concentrating system's performance. In order to extend the analyses to areas not covered by the instruments, efforts are underway to understand the relationship of the circumsolar radiation to atmospheric conditions and to other, more routine, solar and meteorological measurements.

Details of the instrument system, and examples of the measurements and data summaries have been given in previous annual reports.

### ACCOMPLISHMENTS DURING 1979

#### Measurement Program

Telescopes were operated this year at Sandia Laboratories, Albuquerque (location of the Central Receiver Test Facility (CRTF) and other concentrating systems); on a Southern California Edison (SCE) building at Barstow, California (near the site of a future 10 Mw(e) Central Receiver Pilot

Plant), and at Atlanta (site of a Georgia Tech central receiver test facility).

The remaining telescope underwent an upgrading program at LBL, with a number of modifications made to improve weatherability. An automated sun photometer (of the Volz type) was installed, and some electronic modifications were made to increase the precision with which the output of the pyrheliometer is recorded.

#### Data Summary for Atlanta

The basic telescope measurement (brightness of the sun and circumsolar region as a function of angular distance from the center of the sun) is in arbitrary units. The scan is converted to energy units ( $W/m^2$ -steradian) by normalizing to the pyrheliometer reading. Unfortunately, the data from Atlanta showed the effects of periods of time when the pyrheliometer was not working properly, or was at the manufacturer's for repair. Correlations were obtained between the pyrheliometer reading and other measures of the solar radiation for "good" periods, and were then used to estimate the pyrheliometer value during "bad" periods.<sup>1</sup>

With the estimated pyrheliometer values, the analysis and summary of the Atlanta data could proceed. In particular, a comparison could be made of the average effect of the circumsolar radiation for the relatively humid climate of Atlanta, to that for a more arid area. Figures 1a and 1b are for a year's worth of data from Atlanta and Barstow, respectively. The quantity plotted is the overestimate that would be made by a pyrheliometer in estimating the solar radiation available to a concentrating solar plant, when the plant is described in terms of two simplified parameters. The first parameter is the operating threshold; the plant is assumed to be in operation whenever the solar radiation exceeds the threshold. The second is the effective aperture radius (half the field of view) of the receiver. Figure 1 is for a threshold of  $50 W/m^2$  and for various radii as indicated. The overestimate is generally greater for Atlanta (corresponding to generally higher circumsolar levels), but not dramatically so. At least for this year, the two locations appear to have quite different seasonal dependencies. Two cautionary comments are in order. First, the winter months for 1977-78 in Barstow were particularly cloudy, and the values may not be representative of average conditions. Second, the figures do not give the total energy available at Barstow as compared to Atlanta. This total is significantly higher for Barstow. Additional results are in Ref. 2.

#### Circumsolar Slope

One approach to extending the circumsolar measurements to locations not covered by the telescopes is to relate the measurements to the atmospheric scattering processes. As one part of such an effort, the "circumsolar slope" has been investigated. Figure 2 shows a sample scan in log-log space, with the brightness of the solar and circumsolar radiation plotted versus angular distance from the center of the sun. The straight line through the data points in the circumsolar region and the corresponding slope value are from a simple

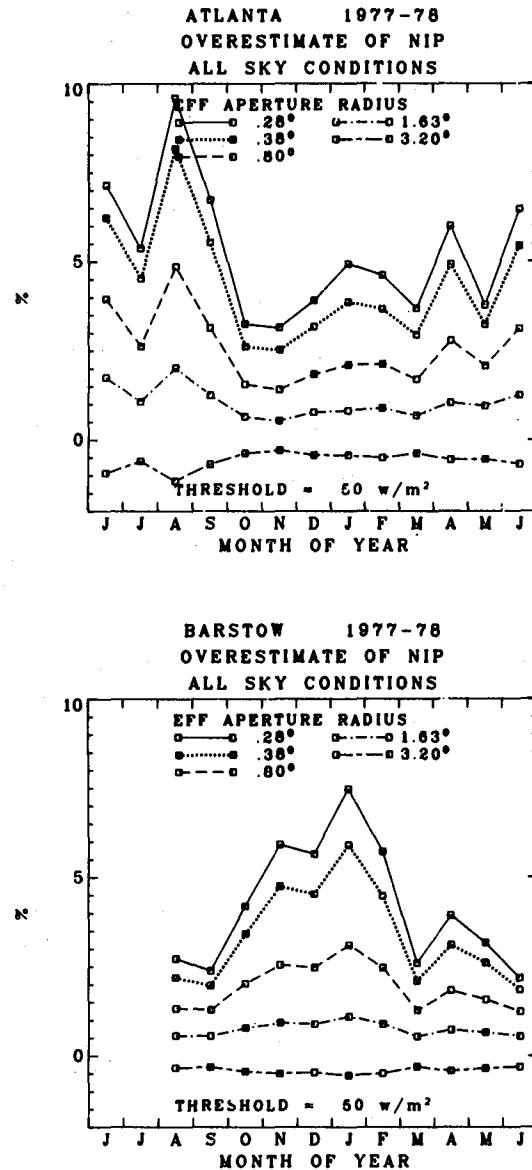


Fig. 1. (a) Overestimate made by a pyrheliometer in estimating the energy available to a concentrating solar energy system for a particular threshold and series of effective apertures (see text). The data are for June, 1977 through June, 1978 at Atlanta, Georgia. (b) Same as for (a), but for Barstow, California.

computer algorithm. In general, such a straight line provides a reasonable description of the circumsolar radiation for angles between  $0.5^\circ$  and  $3^\circ$  in log-log space. The slope of the line then provides one method of characterizing the data, in addition to the circumsolar ratio (ratio of energy content in the circumsolar region to energy content of the solar plus circumsolar,  $C/(C+S)$  in the figure), and the normal incidence reading of the pyrheliometer (NI in the figure).

Plotted in Fig. 3 is the circumsolar slope versus the circumsolar ratio for a month's data

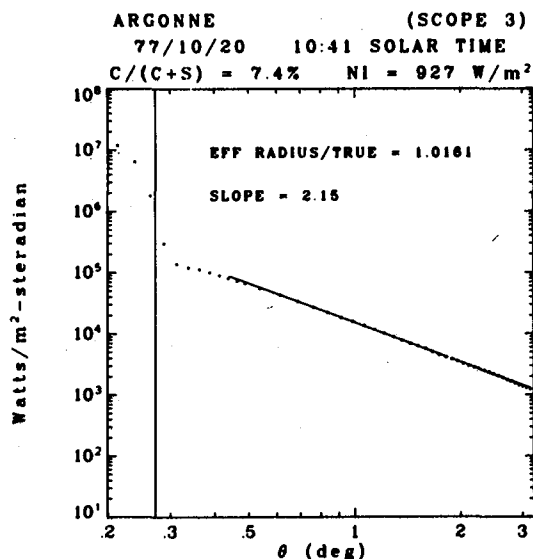


Fig. 2. Sample of a telescope scan in log-log space. The solid, vertical line represents an "effective radius" of the sun. The center of the sun is off-scale.

from Barstow. The dense cluster of points at relatively low slope (~1.5) and low circumsolar ratio correspond to clear-sky conditions. The high slopes (~2.5) are seen to be associated with high circumsolar ratios. In terms of scattering properties of aerosols, a relatively steeper slope indicates that relatively larger particles are responsible for the scattering. The interpretation is that for the atmospheric conditions that give rise

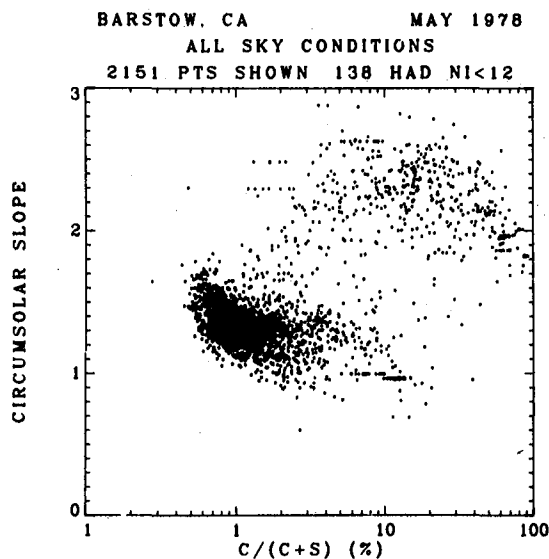


Fig. 3. Plot of the circumsolar slope versus the circumsolar ratio for the month of May, 1978 in Barstow. "138 HAD NI<12" refers to measurements for which the normal incidence reading of the pyrheliometer was essentially negligible. These points are excluded from the graph.

to high levels of circumsolar radiation (e.g., haze or thin clouds) the light-scatterers tend to be rather large.

Some work has been done on comparing these slopes to the predictions of the so-called Mie Theory for light scattering from aerosols, with the aerosols approximated by dielectric spheres of a specified size distribution and complex index of refraction. In terms of this model, slopes on the order of 2.5 would imply that the scattering is dominated by particles with dimensions greater than about 20  $\mu$  in diameter.

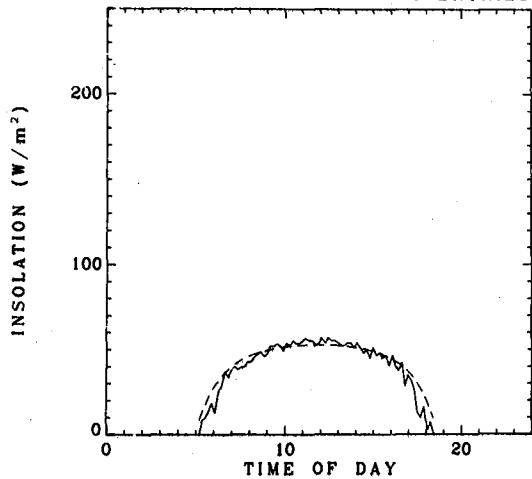
#### Colored Filter Data

The emphasis in the project has been on the "clear" filter measurements, because these data are most relevant to concentrating collectors employing thermal receivers (which use black surfaces to absorb the solar radiation). However, there are also applications for which the receiver would be a photovoltaic cell, which is highly wavelength selective. So few systematic measurements of the wavelength dependence of solar radiation are available that the colored filter pyrheliometer data are of considerable interest in themselves, apart from the telescope scans. Thus the first priority has been to extract the normal incidence spectral data. To do this, the transmission of each filter as a function of wavelength must be accurately characterized.

Curves of transmission versus wavelength (obtained on a spectrophotometer) were supplied by the manufacturer when the filters were new. However, such filters may degrade with time. This year, transmission curves were obtained for the filters from one of the telescopes, using an LBL spectrophotometer. These measurements showed that while some of the filters were essentially unchanged, others had a reduced overall transmission and (sometimes) a broader pass band. An effort was then initiated to use the data themselves to track the effective change in filter characteristics between spectrophotometer measurements. The technique (outlined in Ref. 3) would utilize pyrheliometer readings from clear days, when atmospheric conditions are relatively stable and the atmospheric attenuation of the solar radiation is generally thought to be well understood. The computer program Lowtran<sup>4</sup> has been investigated as a model for the atmospheric attenuation.

As a check on the applicability of Lowtran, the model has been compared to actual pyrheliometer values for selected clear days. Figure 4 shows the comparison for Barstow for two filters, one at the blue end of the solar spectrum and the other at the infrared (IR) end. For this comparison, the atmospheric transmission values from Lowtran have been combined with a standard extraterrestrial solar spectrum and with the manufacturer-supplied transmission curve so as to simulate the reading of a pyrheliometer taken through the corresponding filter. As is indicated by Fig. 4, the Lowtran calculation tends to agree with the data at the blue end of the solar spectrum, but to yield higher values towards the red/IR end of the spectrum. A certain number of assumptions were made in order to carry-out the Lowtran calculation, and the validity

LOWTRAN VS DATA  
 .38 TO .46 MICRONS  
 74 ENTRIES



LOWTRAN VS DATA  
 1.25 TO 3.00 MICRONS  
 74 ENTRIES

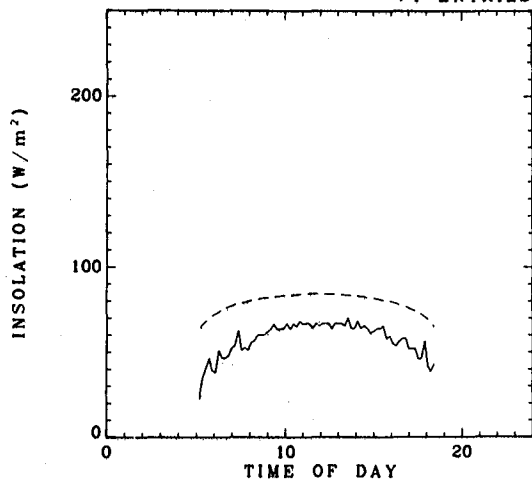


Fig. 4. (a) Pyrliometer reading versus time of day for July 24, 1978 at Barstow, CA for a filter near the blue end of the solar spectrum. The solid curve is the actual pyrliometer value, the dotted curve the calculation based on the atmospheric transmission computer program Lowtran. (b) Same as (a), but for a filter at the red/IR end of the solar spectrum.

of these assumptions needs to be examined. However, if the discrepancy holds, then there are implications beyond the immediate problem of filter calibration. In particular, Lowtran has been recently recommended as a suitable tool for calculating the solar radiation available to photovoltaic cells on clear days.<sup>5</sup>

#### Other Activities

The Solar Energy Research Institute (SERI) is examining the effect of circumsolar radiation

on a variety of concentrating systems.<sup>6</sup> As input to this study, LBL prepared selected data in a form usable by SERI.

A DOE-supported engineering firm (Watt Engineering, Limited) is examining the correlations of average values of circumsolar radiation with other solar and meteorological parameters, using data from LBL and other sources. LBL, working with Watt Engineering, prepared several data tapes for use in the analysis.

During actual tests of concentrating systems or components, circumsolar data can be of importance in comparing the actual to predicted performance of the system. Individual scans of the telescopes, taken in parallel with tests of the CRTF at Albuquerque, were provided to Boeing (Brayton cycle receiver tests) and Sandia Laboratory (heliostat tests).

#### PLANNED ACTIVITIES FOR 1980

The measurement program will continue. Plans originally were for the upgraded telescope to be moved to SERI in Colorado. For various reasons, this move did not prove feasible. Revised plans are for this instrument to be located at the Jet Propulsion Laboratory (JPL) test station at Edwards Air Force Base. The instrument would provide site-specific data for point concentrating collectors (paraboloidal dishes) that are undergoing tests by JPL. The instrument would also provide characterization of the Mojave desert area, a role heretofore played by the telescope at Barstow. This latter instrument would then be returned to LBL for upgrading and eventual relocation.

The various analyses will continue with the overall goal of better understanding of the relationship of circumsolar radiation to atmospheric characteristics and to the performance of concentrating solar energy systems. The extraction of the colored filter data will be particularly emphasized.

#### FOOTNOTE AND REFERENCES

\*This work has been supported by the Department of Energy through Conservation and Solar Applications (Systems Development Division of the Office of Solar Applications), and through Solar Geothermal, Electric, and Storage Systems (Central Solar Technology-Solar Thermal Branch, and Distributed Solar Technology Photovoltaics Branch), under Contract No. W-7405-ENG-48.

1. D. F. Grether, D. Evans, A. Hunt and M. Wahlig, "Measurement and Analysis of Circumsolar Radiation," Proceedings of the DOE Division of Distributed Solar Technology Contractors' Program Review, Denver, April 1979, and Lawrence Berkeley Laboratory report LBL-9214 (1979).
2. D. F. Grether, D. Evans, A. Hunt and M. Wahlig, "Application of Circumsolar Measurements to Concentrating Collectors," Proceedings of the 1979 International Congress of the International Solar Energy Society, Atlanta, and Lawrence Berkeley Laboratory report LBL-9412 (1979).

3. D. F. Grether, D. Evans, A. Hunt and M. Wahlig, "Measurement and Analysis of Circumsolar Radiation," Proceedings of the DOE Division of Distributed Solar Technology Insolation Assessment Contractors' Program Review, Bethesda, MD, October, 1979, and Lawrence Berkeley Laboratory report LBL-10243 (1979).
4. J. E. A. Selby et al., "Atmospheric Transmittance from 0.25 to 28.5 microns: Computer Code Lowtran 2," Air Force Cambridge Research Laboratory.
5. P. J. Ireland, S. Wagner, L. L. Kazmerski and R. L. Hulstrom, "A Combined Irradiance-Transmittance Solar Spectrum and Its Application to Photovoltaic Efficiency Calculations," Science, 24, May 1979.
6. P. Bendt and A. Rabl, "Effect of Circumsolar Radiation on Performance of Focusing Collectors," Presented at the 1979 International Congress of the International Solar Energy Society, Atlanta, June, 1979.

## INSTRUMENTATION AND DATA PROCESSING MODIFICATIONS IN THE PG&E/SOLAR DATA NETWORK\*

*D. Anson*

### INTRODUCTION

A six station network of solar radiation measuring instruments (pyranometers) has been operating in Northern California for the past three years. The network is a cooperative project between LBL and Pacific Gas and Electric Company (PG&E). Each organization contributes its own unique and complementary resources to the implementation of the network. LBL provides technical guidance in the areas of hardware selection, software for analysis and reporting, and calibration and routine maintenance assistance. PG&E coordinates the project and contributes the physical site and personnel to change tapes and check instruments.

Five years have elapsed since the project began, and unfortunately the first two and one-half years were largely consumed by delays caused by funding uncertainties. More recently, though, data has been routinely collected, and, in several locations, has been collected for as much as two and one-half years.

The original purpose of providing quality solar energy research and design data in microclimatic regions with no current or previous solar data records continues to be emphasized by the project. High-quality instruments and data-monitoring practices have also been a high priority with the project. This is important for both system reliability and data credibility.

Considerable interest in the data has been expressed in a variety of ways. A state agency, for example, is eager to include these measurements in a larger, state-wide publication on solar data. A number of colleges have volunteered to operate additional instruments if they become available and assist with certain data analysis functions. There has also been some interest in establishing a "grass-roots" type of network in which responsible and knowledgeable individuals would oversee measurements at their residences and report them each month for publication.

### ACCOMPLISHMENTS DURING 1979

Accomplishments during the past year have been in four major areas: (1) improved translation and archival of raw data tapes, (2) receipt of seven new Eppley model PSP pyranometers and a microprocessor-based recorder for testing, (3) arrangements for a number of additional stations, and (4) coordination for acquiring unreported raw data from other agencies.

In the field, all six stations continued to operate routinely throughout 1979. From the perspective of raw data processing at the PG&E general office in San Francisco, a major change occurred in the way the small magnetic tapes were translated and the data transferred onto a 9-track tape. This was significant in almost completely eliminating data losses with respect to computer processing procedures. This consisted of two procedural changes. First, a 9-track tape was established for permanent archival of all unprocessed data. Each new monthly receipt of data is now automatically added onto the tape. Secondly, the erasure and return of the small recorder tapes was delayed until all data had been successfully transferred to the 9-track archive tape, to punched cards, and to a print-out. As much as six months of data had been lost at some stations prior to these new procedures.

Because LBL funding of the part-time network coordinator position ceased, PG&E picked up the person (Dean Anson) who had been coordinating this work. This served to maintain project continuity.

Seven new Eppley model PSP pyranometers were recently received to replace the original units in the network. These first class pyranometers will serve to upgrade the accuracy from that achieved with the second class instruments (Eppley model 8-48) in use. The 6 model 8-48 (also known as "black and white") pyranometers are still quality sensors and will be moved to locations where solar data is not currently available. Also, a complementary instrument has been procured for use in

testing, performance evaluation, and measurements of direct solar radiation. This unit is an Eppley NIP pyrhelimeter, a device that tracks the sun throughout the day.

A new recorder (Campbell Scientific CR-21) is on order for possible use at each of the stations. This is a microprocessor-based device that can be remotely interrogated by telephone. This is similar to units being used for two other data collection projects managed by LBL.

Preliminary arrangements have been made to add a station in San Ramon, where PG&E's Department of Engineering Research is located. A solar test facility and experienced technicians are available to assure accurate data is collected at the site. Additional sites are being considered at San Francisco City College, University of California at Santa Cruz, and Napa.

A number of organizations are known to collect solar energy data that is not reported or generally available. Lawrence Livermore Laboratory (LLL) has nearly 5 years of quality data available. These data and those from the University of California at Davis, for example, would make valuable additions to a publication of solar data in Northern California.

This project has also done some calibrations of photovoltaic-type pyranometers for local colleges. On one occasion, a spare pyranometer was loaned to a local solar firm for final solar system performance tests after installation.

Overall, the main accomplishments have been in the areas of raw-data processing and new-equipment procurement. The remaining area needing the most attention is in data reduction and reporting.

#### PLANNED ACTIVITIES FOR 1980

Next year is viewed as one in which final arrangements will have been made for so-called

"routine" network operation. With respect to hardware, the final details of pyranometer and recorder installation will be completed, and older units will be relocated.

The highest priority during FY 1980 is to process all solar data as of the end of FY 1979 and, by early 1980, make it widely available.

It is hoped that the concept of a "grass-roots" solar network can be tested using the low-cost and accurate solar-cell-based pyranometer by Li-Cor, Inc. (model LI-200S). This sensor has been carefully tested by the Solar Radiation Laboratory (NOAA) in Boulder, Colorado and was found to perform nearly as well as the Eppley model PSP.<sup>1</sup> A solid state integrator (Li-Cor, Inc. LI-175) is being considered for recording the solar data. It is low in cost and allows a pyranometer-and-recorder combination to be purchased for about \$500. This hardware would be supplemented with a user's manual and a contact person to answer questions.

#### ACKNOWLEDGMENTS

The continuation of the PG&E/LBL solar data network is largely a result of the efforts of Mike Wahlig, Solar Group Team Leader at LBL and of Stan Blois, Technical Services Coordinator of PG&E. I sincerely appreciate their contributions to this cooperative project.

#### FOOTNOTE AND REFERENCE

\*The solar data network project is jointly funded by PG&E and the Lawrence Berkeley Laboratory Solar Energy Program.

1. E. C. Flowers, "Comparison of Solar Radiation Sensors from Various Manufacturers," Annual Report, Nat'l Oceanographic and Atmospheric Administration, Environmental Research Laboratories, Solar Radiation Facility, Boulder Colorado (1978).

## SUPPORT ACTIVITIES FOR DOE SOLAR HEATING AND COOLING RESEARCH AND DEVELOPMENT PROGRAM\*

*M. Wahlig, M. Martin, R. Kammerud, W. Place, B. Boyce, M. Warren, and A. Heitz*

#### INTRODUCTION

This project consists of technical support activities for the Systems Development Division (formerly the Solar Heating and Cooling Research and Development Branch) of the DOE Office of Solar Applications. Areas in which LBL provides program support are controls for solar heating and cooling systems, passive cooling, active solar cooling, and passive solar analysis and design. These activities include the following: (1) peer review of unsolicited proposals; (2) preparation and evaluation of program solicitations; (3) technical monitoring of projects performed both by DOE contrac-

tors and by LBL subcontractors; (4) program planning, reviews and summaries; and (5) inter-laboratory coordination of support activities. Program responsibilities of the Laboratory have increased due to implementation of a program decentralization plan approved in the fall of 1978. Under this plan, LBL and the San Francisco Operations Office of DOE (SAN) work together to manage the national R&D program in these assigned areas, with SAN providing project management and LBL providing the technical support. DOE headquarters transfers block funds to the SAN office to support outside research and development contracts being performed under these program elements. Most of

the staff members of the Solar Energy Group have participated to some extent in this effort during 1979.

#### ACCOMPLISHMENTS DURING 1979

##### Review of Unsolicited Proposals

The LBL Solar Energy Group conducted a formal review session for unsolicited active solar cooling proposals at the Solar Energy Research Institute (SERI) in Golden, Colorado in late October 1978. The results of these reviews were then sent to DOE in Washington, D.C. along with recommendations for action. In addition, some nine individual unsolicited proposals for active cooling projects were reviewed during FY 1979. Preparations were begun to develop a standard evaluation process for new proposals (as well as follow-on proposals for contracts in progress) that can be used for making decisions about future funding.

##### Preparation and Evaluation of Program Solicitations

LBL staff members participated in the development of a computerized evaluation process to evaluate the solar cooling proposals submitted to SERI as part of the joint U.S./Saudi Arabian program (SOLERAS). Additional input was provided to carry out the proposal evaluation and make recommendations for funding. As a result of this program, four contracts were awarded to install solar cooling systems in U.S. locations that have climates similar to those of Saudi Arabia.

LBL staff also participated in the preparation and evaluation of DOE solicitations for Marketing Studies for Solar Heating and Cooling Systems, and for a marketable passive products solicitation.

##### Technical Monitoring of Projects

Early in FY 79, LBL was given responsibility for the technical monitoring of Absorption and Rankine solar cooling projects that were previously being monitored by Brookhaven National Laboratory (BNL). Initially, five Absorption and four Rankine contracts were included; two additional Absorption contracts have since been added. Project monitoring consists of the continuous technical evaluation of projects being performed by other contractors, including site visits, review of progress reports, and organization of contractor meetings as appropriate. During FY 79, site visits to all active solar cooling contractors were conducted by LBL review teams, whose members included nonLBL technical experts as well as LBL staff. Detailed status reports and action item lists have been generated from these site visits to provide DOE with information on the current condition of each project.

A workbook intended for residential-scale use was developed by an LBL subcontractor under direction of LBL staff. The workbook is slated to be published sometime in FY 80.

##### Program Planning, Reviews and Summaries

LBL has played an active role in the formulation of three international solar programs during

FY 79: the U.S./Saudi Arabia (SOLERAS), U.S./Israel and U.S./Mexico solar programs. The SOLERAS project is mentioned earlier in this article. LBL participated in negotiations in Israel to develop joint active solar cooling and passive cooling projects that would be beneficial to both countries. Both active solar cooling (solar refrigeration) and passive cooling projects were also involved in LBL's negotiations with representatives of the Mexican solar energy program.

LBL has assisted DOE in the formulating and review of a number of program planning and summary documents, including a Decentralized Field Management Plan, Solar Heating and Cooling R&D Project Summary Book, Commercial Readiness Assessments, Multiyear Plans for Active Systems and for Passive Systems for Heating and Cooling of Buildings, and National Program Plan for Passive and Hybrid Solar Heating and Cooling.

The Passive Cooling Program support effort has increasingly shifted from program implementation to program planning. Preparation of a Passive Cooling Area Plan began during FY 1979 and this document is slated to be incorporated into a DOE Multiyear Plan for heating and cooling. Tasks identified in the Area Plan for near-term funding are the subject of three major solicitations to be written by LBL and issued during the spring of 1980. One solicitation is for the construction and operation of a Passive Cooling Experimental Facility in a hot arid climate, and the other two contain numerous tasks covering the entire range of passive cooling technologies. A project management plan is in preparation for monitoring the projects which will result from the solicitation.

LBL involvement in controls program support activities has centered on development of a solar controls program plan that integrates ongoing and planned controls projects into a coherent program. Contact with individual controls projects involved review of periodic progress reports, telephone discussions, visits to contractor sites, and invitations to contractors to come to LBL for project reviews.

##### Interlaboratory Coordination

A number of meetings have been held during FY 1979 for purposes of program definition, planning, and coordination of activities for both the Active and Passive Heating and Cooling Programs. Included in such meetings have been representatives of many organizations; for example, national laboratories (LBL, LASL, ANL, BNL, LLL), DOE field offices (SAN, CHO, ALO), DOE headquarters, SERI, NBS, NCAT, as well as DOE consultants and support contractors.

LBL has had major input to the controls program planning process in meetings with SERI and SAN in developing and implementing an overall Systems Analysis Program Plan that includes a well-defined controls element and that addresses both currently recognized field problems and longer range research questions. LBL will also be participating in the DOE Technical Managers Coordination Meeting for the Active Solar Heating and Cooling Program, and the DOE Active Systems Contractors Review Meeting, both to be held in March 1980.

## PLANNED ACTIVITIES FOR 1980

Activities in all of the above areas will continue throughout FY 1980. Unsolicited proposals will be reviewed and evaluated as they are received. LBL will assist the SAN and CHO field offices in the preparation and evaluation of a number of program solicitations, including those for Passive Products, Passive Manufactured Buildings, Passive Commercial Buildings, Passive Cooling and Materials Studies, and Fluids for Active Cooling Applications. Technical monitoring of projects will likely expand in scope as new projects are initiated as a result

of the new program solicitations. LBL will participate in the next round of program planning exercises that will inevitably follow the latest DOE reorganization. A number of headquarters, field office, and laboratory coordination meetings are scheduled for FY 1980, and LBL will take an active role in these activities.

## FOOTNOTE

\*This work has been supported by the Systems Development Division, Office of Solar Applications, U.S. Department of Energy.

# CHEMICAL PROCESS RESEARCH AND DEVELOPMENT PROGRAM

## INTRODUCTION

The Chemical Process Program focuses upon three principal areas--1) production of synthetic fuels, and 2) processing of effluent or recycle water and gas streams to achieve environmental compatibility, and 3) energy storage. The common thread is the use of principles of transport, thermodynamics, kinetics, separations and physical chemistry to improve fundamental, mechanistic understanding, and to develop improved processing approaches.

Two major projects are concerned with conversion of biomass (wood chips, agricultural waste, newsprint, etc.) to fuels. In one of these, a fungus enzyme is used to convert cellulose to glucose, which is then converted to ethanol by fermentation. Ethanol is a candidate as an alternative to, or a diluent for, gasoline (e.g., "gasohol"). The energy efficiency of such a process is critically dependent upon the energy consumed for separation of ethanol from water; improved distillative methods for carrying out that separation are being sought. Related research on fundamentals of fermentation and enzymatic processes supports this project. The second major endeavor deals with direct, reductive conversion of biomass to a fuel oil, using homogeneous catalysis. Here LBL monitors a process-demonstration unit in Albany, Oregon, operated under DOE contract, and at the same time carries out more fundamental research directed towards improvements of various components of that process. A signal accomplishment in 1979 was production of the first barrel-sized quantities of oil from the PDU, following a breakthrough in methodology for catalysis and digestion of wood chips.

Another project directed toward production of synthetic fuels concerns coal liquefaction. Lewis-acid homogeneous catalysts, such as zinc chloride, mixed with certain organic solvents, such as tetralin, provide substantial liquefaction of coal at temperatures markedly lower than those contemplated for other coal-liquefaction processes. Current research is directed toward understanding fundamental aspects of the underlying chemical reactions, as well as the influence of the pore structure of coal and transport characteristics.

In the area of processing for environmental control, one project deals with desulfurization of coal before combustion. Work to date has involved comparison of the relative capabilities of several different oxydesulfurization processes for removing both pyritic and organic sulfur, as well as chemical research probing mechanisms of reaction of coal sulfur in metallic sodium dispersions, sodium sulfide, or acidic aqueous media. These latter studies could lead to novel and more effective methods for sulfur removal from coal.

Sulfur can also be removed from flue gases formed after combustion. In a recently started project, we are exploring solution chemistry (thermodynamics and kinetics) underlying aqueous-scrubbing methods for removal of  $\text{SO}_2$  and  $\text{NO}_x$  from combustion flue gases. Particular attention is being paid to iron chelates, which offer the possibility of simultaneous removal of  $\text{SO}_2$  and  $\text{NO}_x$ .

Nearly all approaches for converting coal, oil shale, or biomass to liquid and/or gaseous fuels produce large amounts of process-condensate water, which is highly contaminated with organics, ammonia, sulfides, etc. These waters have proved to be very difficult to treat by conventional biological processing. We are exploring and evaluating the use of physico-chemical techniques alone as a roughing treatment for such waters, removing enough chemical oxygen demand and ammonia to allow recycle of the water as cooling-tower make-up. Particular attention is being paid to the use of novel solvents to allow effective removal of mono- and poly-hydric phenols by solvent extraction, and to innovative ways of combining solvent extraction and stripping to reduce the very considerable energy requirement for stripping of ammonia.

In the final area of energy storage, new programs are directed toward improved batteries, such as are needed to enable widespread use of electric cars.

## PROCESS DEVELOPMENT STUDIES ON THE BIOCONVERSION OF CELLULOSE AND PRODUCTION OF ALCOHOL\*

C. R. Wilke, H. W. Blanch, S. L. Rosenberg,  
S. K. Tangnu, A. F. Sciamanna, and R. P. Freitas

### INTRODUCTION

In most lignocellulosic materials, that are considered as residues, the cellulose is relatively inaccessible to hydrolysis by enzymes. This is mainly due to the crystalline structure of the cellulose and the presence of protective and interspersed layers of lignin and pentosans.

One aspect of increasing the accessibility is by changing the crystalline structure of cellulose to a less ordered system. There are various physical and chemical treatments that can be performed to accomplish this, however, these methods must be relatively very low in cost. Most physical methods are relatively expensive.

Various agricultural and forest residues have been subjected to various chemical pretreatments as part of the ongoing studies on raw materials and process evaluation performed in our laboratory.

The most economical of the pretreatments studied has been the dilute acid process whereby, generally, at least one half of the pentosans, the so-called "hemicellulose fraction," is hydrolyzed to pentoses. Thus, a partial separation of the pentoses from the hexosans is obtained. There is the additional feature of generally doubling the conversion of the carbohydrates to sugars as otherwise occurs on enzymatic hydrolysis of the natural state of these residues.

Promising results have been obtained and reported<sup>1</sup> on the agricultural residues such as the straws of wheat, barley, rice, sorghum, rice hulls, and corn stover. The forest residues such as populus, sycamore, sweet gum, and spruce were studied. These woods are considerably more resistant to attack and stronger chemical treatment were tried with moderate degrees of improvement.<sup>2</sup>

### BIOCONVERSION OF CELLULOSE

Most recently, two fractions of bagasse were analyzed in the continuing work on raw materials analysis and evaluation. The rind fiber and pith fractions were analyzed and enzymatically hydrolyzed. They were also subjected to acid pretreatment followed by enzymatic hydrolysis. The acid pretreatment was accomplished by boiling the above substrates in about 6 w% suspensions for 5 1/2 hours in 0.9 w% sulfuric acid. On enzymatic hydrolysis of the rind fiber fraction there was a 5.7% carbohydrate conversion, and with the pith fraction there was about an 18% conversion. Enzymatic hydrolysis with the acid treated substrates above and including the sugars in the acid liquors, there was a 35% and 57% carbohydrate conversion, respectively.

It would appear that bagasse pith fraction is well worth retaining for hydrolysis and the rind fiber fraction used for direct power production.

Because of the encouraging results obtained with the sulfuric acid hydrolysis's on ground wood such as populus and reported,<sup>2f</sup> work was extended to try other acids, especially those with appreciable vapor pressures at moderate vacuum, thus leading to acid recovery and recycle.

### Enzymatic Hydrolysis

In the past year, a new strain of cellulolytic fungus produced at Rutgers University, and labelled Rut-C-30, was introduced for general study by interested groups throughout this country. Preliminary studies on its performance on corn stover, as a base case, can conservatively be called outstanding relative to the strain T. reseei QM-9414.

### Batch Cellulase Production (Rut-C-30).

Fermentation operations were conducted in 5 and 14 liter New Brunswick fermentors. Three cellulose concentrations, S<sub>0</sub>, (1, 2.5 and 5.0%) were tested to determine the maximum levels of cellulase activity obtainable in submerged culture. Temperature-pH profiling was tried to increase viable cell mass to maximum levels and thereby enhance fermentor productivity at the higher substrate levels. The effect of Tween-80 and urea concentration on cellulase production were also determined.

Various batch experiments were undertaken to determine the optimum conditions for cellulase production. Various combinations of temperature and pH programming were examined, and the results are summarized in Table 1.

From the above concentrations it can be concluded that a temperature of 25°C and pH controlled not to go below 5.0 are optimum for enhanced cellulase production.

In runs #15 and 16, higher levels of cellulase (2.5 and 5.0%), respectively, were used. There is a substantial increase in cellulase activities as well as in soluble production.

Table 2 shows the comparison of Rut-C-30 with Trichoderma viride QM-9414. If we compare runs #2 and 3, the filter paper activity in #3 is slightly higher but  $\beta$ -glucosidase activity is higher by 10 times versus run #2. This higher level of  $\beta$ -glucosidase would permit more rapid conversion of cellobiose to glucose. This would then decrease the cellobiose inhibition of the C<sub>1</sub> enzyme and hence increase the rate of depolymerization of crystalline cellulose.

If we compare runs #1 and 3, there is an increase in filter paper activity,  $\beta$ -glucosidase and soluble protein by about 3.7, 2.5, 7 and 1.6 times, respectively. All of these experiments demonstrate the superiority of Rut-C-30 over T. viride QM-9414.

Table 1. Effect of environmental conditions on enzyme activity of Rutgers C-30.

Operating Conditions						(%)				
Run	pH	Temp °C*	S <sub>0</sub> (%)	T-80 (%)	C/N	FPA	β-glu.	C <sub>1</sub>	C <sub>x</sub>	S.P.
1	4 up to 48 hrs, after 48 hrs decrease to 3.3 and was controlled not to go below 3.3	31° 0-2D	1.0	0.02	8.4	1.6	2.3	0.06	38	3.4
2		28° 2-8D	1.0	0.02	8.4	1.7	2.3	0.06	40	3.3
3	Controlled not to go below 4.0	31° 0-2D	1.0	0.02	8.4	2.0	3.55	0.169	44	3.4
4		25° 2-8D	1.0	0.02	8.4	2.1	3.35	0.173	44	3.25
5	Controlled not to go below 5.0	31° 0-36H	1.0	0.02	8.4	2.1	4.25	0.2	40	3.45
6		25° RT	1.0	0.02	8.4	2.1	4.75	0.17	40	3.2
7	Controlled not go below 5.0	31° 0-9H	1.0	0.02	8.4	2.6	2.75	0.18	59	2.78
8		25° RT	1.0	0.02	8.4	3.1	3.3	0.195	84	3.3
9	Controlled not to go below 5.0	25° 0-8D	1.0	0.02	8.4	3.0	4.3	0.26	105	3.3
10		28° 0-2D	1.0	0.02	8.4	2.9	3.9	0.23	115	3.45
11	Controlled not to go below 4.0	25° 0-8D	1.0	0.02	8.4	2.6	1.85	0.2	54	3.15
12		25° 0-8D	1.0	0.02	8.4	2.1 <sup>a</sup>	1.6	0.23	50	3.35
13	Controlled at 4.0	25° 0-8D	1.0	0.02	8.4	2.8	3.3	0.24	110	3.6
14	Controlled at 6.0	25° 0-8D	1.0	0.02	8.4	2.5	3.1	0.17	70	2.6
15	Controlled at 5.0	25° 0-8D	2.5	0.02	10.29	5.2	10	0.48	210	8.2
16	Controlled not to go below 5.0	25° 0-8D	5.0	0.02	8.1	14.4	26	1.03	348	20

<sup>a</sup>With urea (0.3 g/L).

\*D = Days, H = Hours, RT = Remainder of Time

Table 2. Comparison of *T. viride* strains Rut-C-30 and QM-9414.

Run No.	S <sub>0</sub> (%)	Strain	FPA U/mL	β-Glucosidase U/mL	Solution Protein mg/mL	Remarks
1	5.0	Rut-C-30	14.4	26	20	pH 5.0, T-80 level = 0.02%, 25°C
2	2.5	Rut-C-30	5.2	10	8.2	pH = 5.0, T-80 level = 0.02%, 25°C
3	5.0	QM-9414	6.1	1.01	12.68	(0-1 day) pH allowed to fall to 4 (1-2 day) pH allowed to fall to 2 (2 day) raised to 3.3 and controlled not to go below pH 3.3
4	2.5	QM-9414	4.3	1.15	5.94	same as above

Continuous Cellulase Production (*T. viride* strain QM-9414). It was observed in previous work that increasing the cell density or substrate concentration did not proportionally increase enzyme productivity. Extensive studies were carried out in order to optimize individually the 1st and 2nd stage of the two-stage continuous system for cellulase activity by manipulating pH, temperature, Tween-80 level, substrate concentration and dilution rates. The results are shown in Table 3. The experiments were run continuously for about 3 1/2 months.

Runs #1 and #2 show that decreasing Tween-80 level by half increases the filter paper activity by 60% in the first stage of the two-stage fermentation. There is a considerable drop in the filter paper activity in the first stage at pH 5.0 than at other pH levels which severely affects the productivity in the second stage. Although, the filter paper activity of run #1 in the first stage is about 70% less than in run #3, the productivity is higher in the second stage. If run #1 was operated with 0.1% Tween-80 level, it could lead to higher productivity. Similarly, if the second stage of run #2 was operated at pH 5, it could also lead to higher productivity. Hence for all practical purposes the first stage can be operated between a pH range of 3.75--4.25 and the second stage at pH 5. In terms of inlet substrate concentration, 1.75% gives as good a filter paper activity as 2.5%. If the first stages of run #2 and run #9 are compared, it is seen that there is a decrease in filter paper activity and enzyme productivity from 4.2 and 0.084 to 2.54 and 0.053, respectively. If enzyme activity and production in the second are taken into consideration, then it would be profitable to use SW-40 rather than BW-200, as the substrate. Table 4 gives the optimum operating conditions of the two-stage continuous cellulase production system using *T. viride* QM-9414.

Xylanase Production. In shake flasks, *Streptomyces xylophagus* nov. sp. grows in pellet

Table 4. Optimum operating conditions for cellulase production by *T. viride* QM-9419.

Control Variables	1st Stage	2nd Stage
pH	3.75-4.25	5.0
Temperature (°C)	28°	28°
Dilution Rate (hr <sup>-1</sup> )	0.02	0.027
Inlet Substrate (%) Conc.	1.75	--

form. The size of pellets varies from flask to flask, some being very fine and the largest about 1 mm in diameter. As pellets grow, the color of the broth changes from milky white to brown. The organism growing in wheat bran medium is thus difficult to observe directly.

The results of batch growth studies are shown in Table 5. The enzyme production rate in shake flask and 14-liter fermentor showed a marked difference in final enzyme activity in using washed wheat bran compared with washed-dried wheat bran. In the 14-liter fermentor where the pH was controlled, wheat bran shows a considerable improvement in enzyme activity as compared to shake flask studies.

In continuous culture, a dilution rate of 0.027/hr gives an enzyme activity of 7.25 mg/mL-hr while lower or higher dilution rates seem to affect the enzyme activity, soluble protein and cell dry weight. It thus appears that a dilution rate of approximately 0.027/hr is optimal.

Composition of Cellulase. Cellulase is composed of three distinct types of activities. These are roughly characterized by activity towards crystalline cellulose, amorphous cellulose and cello-

Table 3. Two-stage continuous production of cellulase from QM-9414.

Run No.	Controlled Variables								Results <sup>a</sup>				Results (Past Process)		
	Inlet Sub <sup>b</sup> Conc. (g/L)	Tween-80 Level (%)	Temp (°C) F <sub>1</sub> F <sub>2</sub>	pH F <sub>1</sub> F <sub>2</sub>	Dilution Rate (hr <sup>-1</sup> ) F <sub>1</sub> F <sub>2</sub>	Productivity F <sub>1</sub> F <sub>2</sub>	FPA F <sub>1</sub> F <sub>2</sub>	System	S <sub>0</sub> (g/L)	D (hr <sup>-1</sup> )	FPA				
1	25	0.2	28 28	4.0 5.0	0.02 0.02	0.053 0.112	2.64 5.6	Single-stage	7.5	0.02	2.7				
2	25	0.1	28 28	4.0 4.0	0.02 0.02	0.084 0.087	4.2 4.36	no re-cycle	7.5 1.50 1.50	0.03 0.03 0.02	1.9 1.4 2.5				
3	25	0.1	28 28	3.75 3.3	0.02 0.02	0.089 0.105	4.44 5.24								
4	25	0.1	28 28	4.25 4.0	0.02 0.02	0.088 0.104	4.39 5.2	Single-stage	10	0.02	3.7				
5	25	0.1	28 28	5.0 3.75	0.02 0.02	0.025 0.053	1.25 2.66	recycle							
6	25	0.1	28 28	4.0 5.0	0.027 0.027	0.054 0.116	2.0 4.3								
7	17.5	0.1	28 28	4.0 5.0	0.027 0.027	0.054 0.11	2.0 4.1								
8	17.5	0.1	28 28	4.0 5.0	0.054 0.054	0.038 0.099	0.7 1.84								
9	17.5 <sup>c</sup>	0.1	28 28	4.0 4.00	0.02 0.02	0.05 0.096	2.54 4.8								

<sup>a</sup>For non-recycled system F<sub>1</sub> = first stage; F<sub>2</sub> = second stage

<sup>b</sup>Ball-milled Solka Floc (200 mesh)

<sup>c</sup>Solka Floc (40 mesh)

Table 5. Xylanase production.

Mode of Operation	Type of Substrate	Results		
Shake Flask (200 mL medium in 500 mL flask)	Larchwood (L) 1% Wood Gum (WG) 1% Wheat Bran (W) 7%	Final Enzyme Activity		
		6.97+ 5.17 3.11++	6.89* 7.55 4.19**	
		+Bacto peptone 3g/L *Bacto peptone 8g/L	++Washed & dried wheat bran **Washed wheat bran	
Submerged Fermentation  Fer vol = 14L Liq vol = 10L	L; WG; W  1% 1% 7%	9.82*    8.53* (1.61)+; pH, 7.4 6.08 (1.75)    pH, 7.9 6.83 (1.79)    pH, 8.4 7.77 (1.81)    pH, uncontrolled 7.83 (1.56)    pH, 8.4 bacto-pep-2g/L <sup>-1</sup> 2.79    pH 8.4, no bacto-peptone	9.44 (3.16+)	
		*Enzyme activity (mg/mL) +Soluble protein (mg/mL)		
Continuous (in 14-litre fermenter)	WG(1%)	Dilution rate (hr <sup>-1</sup> )	Steady-State Value	
		0.02 0.027 0.034 0.04	6.75*(1.6)** (5.25)*** 7.25 (1.75) (6.5) 5.7 (1.5) (7.25) 3.25 (1.4) (5.5)	
		*Enz. Act (mg/mL)	**Soluble protein (mg/mL)	***Cell dry wt. (g/L)

biose. To describe the kinetics of cellulose hydrolysis, these components of the cellulase complex are separated.

Figure 1 shows a scheme for such a separation. The raw culture filtrate, in 0.05 M citrate buffer, pH 5.0, 0.02% Na<sub>3</sub>, is concentrated by ultrafiltration with an Amicon UM2 membrane, which removes material of molecular weight less than 1,000. The concentrate is then subjected to gel permeation chromatography (GPC), which results in two fractions. The low-molecular weight fraction contains nonessential material. The high-molecular weight fraction containing enzyme is concentrated by freeze-drying, resuspended in citrate buffer, and subjected to ion-exchange chromatography in a 95 x 1.5 cm column packed with DEAE-Sephadex and eluting with an ionic gradient from 5 mM citrate to 50 mM citrate at pH 5.5.  $\beta$ -glucosidase is eluted first, followed by two separate components of C<sub>x</sub> and a single C<sub>1</sub> component.

Two dimensional polyacrylamide gel electrophoresis was used for the analysis and detection of the enzyme at various stages in the separation. This technique gives the molecular weights and isoelectric points of the four components which were resolved. Xylanase and protease activities have not localized in a single fraction.

#### PRODUCTION OF ALCOHOL

##### Ethanol Production

Optimization of the Ethanol Fermentation Medium. According to the processing cost distribution of Wilke, Yang, Sciamanna and Freitas<sup>3</sup> for the bioconversion of corn stover to ethanol, the greatest cost for ethanol production exclusive of the sugars cost is that for the medium chemicals going

Culture filtrate of  
C-30 strain of T.V.

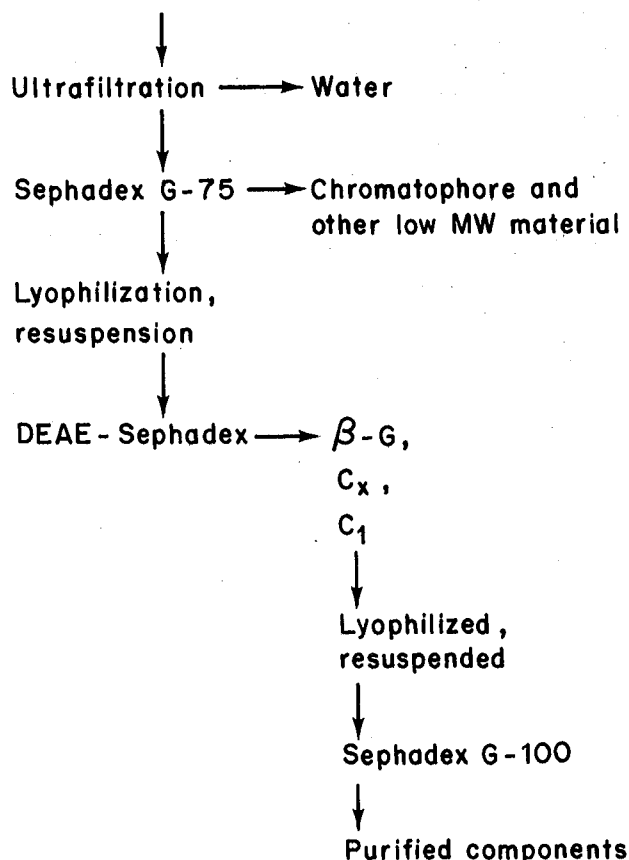


Fig. 1. Separation scheme for cellulase complex. (XBL 801-76)

into the ethanol fermentation. Of the chemical costs, 95% can be attributed to the protein nutrients in the form of antolyzed yeast. To reduce these chemicals cost, basic studies have been undertaken to determine the active components of yeast extract and their quantitative requirements as well as the minimal minerals requirement. It will then be possible to optimize the source and quantity of these active components and minerals for various raw materials.

The following conclusions were drawn from batch ethanol fermentations using glucose as the substrate.

From Shake Flasks:

1. *Saccharomyces cerevisiae* var. *Anamensis* (ATCC-4126) can synthesize all growth factors needed with sufficient time (Fig. 2).
2. Vitamin deficient media produce lower cell mass yields but higher ethanol yields (Fig. 3).
3. Biotin synthesis is the rate-limiting step in cell growth if no external growth factors are added (Fig. 2).

From 1 liter batches:

1. Vitamins and amino acids can increase the specific growth rate. A synthetic mix of vitamins can achieve 85% of the maximum specific growth rate produced with yeast extract (Fig. 4).

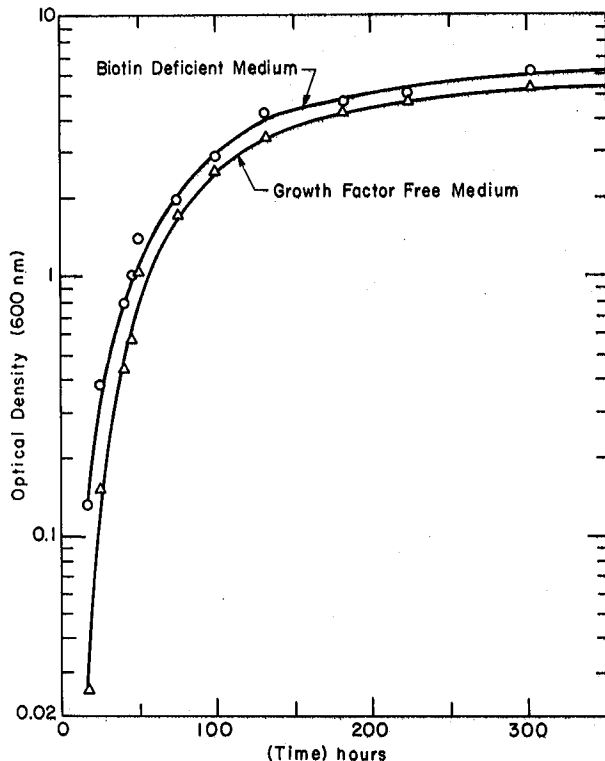


Fig. 2. Comparison of growth in biotin deficient and growth free medium. (XBL 795-6359)

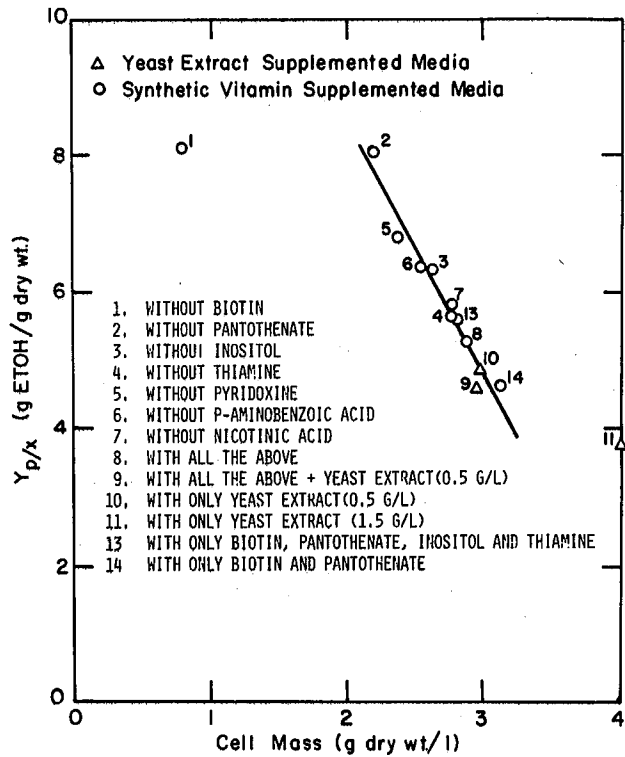


Fig. 3. Effect of various growth factor combinations on cell yield and ethanol yield per gram of cells in shake flasks. (XBL 795-6358)

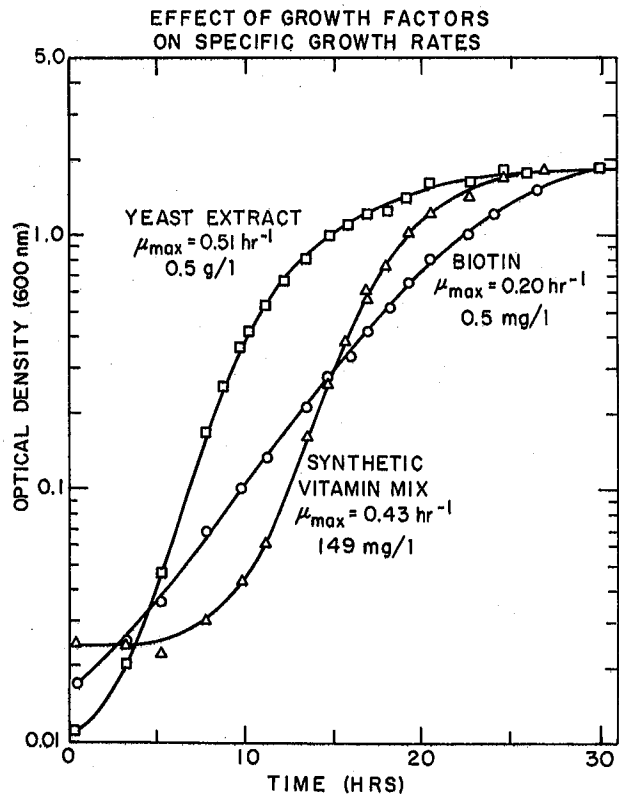


Fig. 4. Effect of growth factors on specific growth rates. (XBL 795-6365)

After the identification of the important growth factors in batch fermentation, continuous cultures were started to determine the optimum levels of all the medium components in ethanol fermentation. A novel procedure extending developments by Mateles and Battat<sup>4</sup> was employed. Each medium component is made the limiting substrate in terms of cell and ethanol yields. The limiting nutrient is first determined by observing which components when injected as a concentrated shot directly into the fermenter produces a transient increase in cell mass and/or ethanol. When this limiting nutrient is found, its concentration in the feed reservoir which is feeding at a steady state dilution rate, is increased such that it is no longer yield limiting up to a given level of cell mass and ethanol. When the component was limiting from the steady-state yield, then the stoichiometric requirement of that component per quantity of cell mass as well as the ethanol yield per quantity of cell mass can be determined. This component can then be eliminated from further testing as the other components in turn are each made yield limiting.

Using this procedure, the effect of the important growth factors for yeast growth in continuous culture was determined for 10 g/L glucose concentrations that are summarized in Table 6. With a minimal level of yeast extract of 0.1 g/L, the cell yield in grams/liter dry weight (which is approximately equal to the optical density) was about 0.33. Increasing the yeast extract to 0.35 g/L resulted in total sugar utilization and about 1.22 g/L dry weight, indicating the growth limiting factors were in yeast extract.

It was then shown that the first growth factor deficiency which has to be satisfied before the effects of the other vitamin deficiencies could be discerned is that for biotin. Increasing the concentrations of the other vitamins had no effect with biotin was not added. With biotin added, increasing the pantothenic acid and then the pyridoxine concentrations each increased the cell yield.

With these three vitamins in excess, further addition of other vitamins had no significant effect

on cell yield but may have increased the ethanol yield. In fact, with all the vitamins in excess it appeared that the sugar was totally utilized but with more ethanol and less cell mass than with high (0.35 g/L) yeast extract concentration.

Work is now in progress to determine the effects of decreasing the present levels of growth factors and minerals and increasing the level of glucose for scaleup to the higher sugar concentrations called for in the vacuum fermentation systems described elsewhere. The above results for batch and the initial results for continuous ethanol fermentation were presented at the annual meeting of the American Society for Microbiology.<sup>5</sup>

Ethanol Production from Xylose. Xylose represents the most significant component monomer of hemicellulose, and work has been undertaken to convert pentose sugars, arising from hemicellulose hydrolysis, to ethanol. The organism Bacillus macerans has been selected as the most promising ethanol producer.

Early work was performed in batch cultures. Figure 5 shows a typical batch culture on 2% xylose. The maximum specific growth rate is 1.5/hr and with a significant amount of unconverted substrate remaining even though growth is essentially finished. The curve for acetic acid departs from that for ethanol at about 0.07% (after 45 hr). This departure coincides with the slowing of the specific growth rate and is followed by the appearance of acetone. More precisely, when the concentration of acetate in the medium reaches approximately 0.07%, the organism begins shifting its metabolic pathway so that it produces more acetone and less acetate. When B. macerans produces acetate, it makes an extra ATP. When it slows acetate production it makes less ATP per xylose molecule, hence the growth rate slows. It should be pointed out that to balance oxidation states, Bacillus macerans must make one mole of acetate for every mole of ethanol or one mole of acetone for every two moles of ethanol. It also produces formic acid which it is also capable of converting to hydrogen and carbon dioxide. It does not produce lactic acid.

Table 6. Effects of growth factors on continuous yeast cultures for 10 g/L glucose.

Growth Factors	Optical Density dry wt. (g/L)
Yeast extract (0.1 g/L)	0.33
Yeast extract (0.35 g/L)	1.22
Yeast extract (0.1 g/L) + Biotin (4µg/L)	0.43-0.53
Yeast extract (0.1 g/L) + Biotin (4µg/L) + Pantothenic Acid	0.733
Yeast extract (0.1 g/L) + Biotin (4µg/L) + Pantothenic Acid + Pyridoxine (1.25 mg/L)	0.91
Above + all other vitamins	0.95

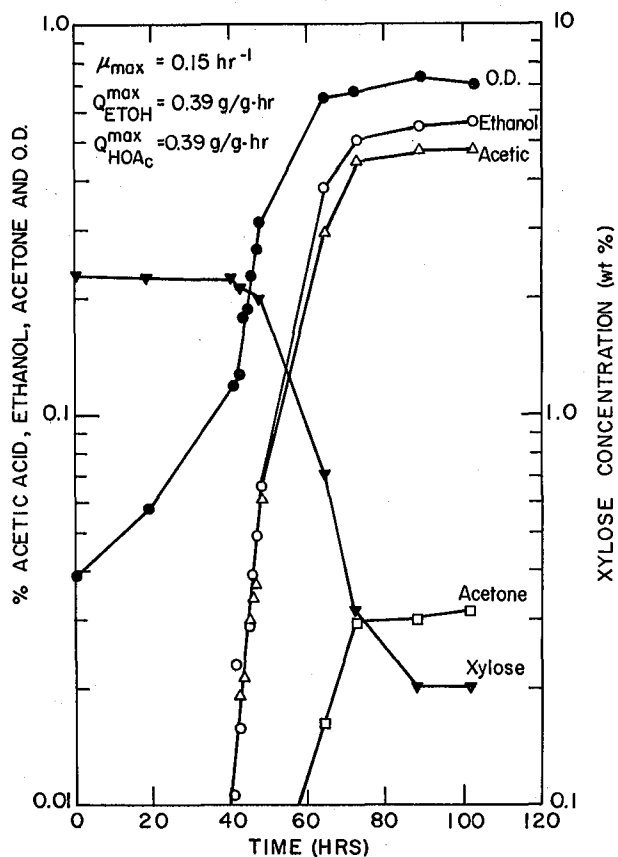


Fig. 5. *Bacillus macerans* growth on xylose.  
(XBL 795-6364)

Following batch culture experiments, continuous culture experiments were begun. Several runs were made using 2% xylose at dilution rates of approximately 0.03, 0.06 and 0.09/hr, i.e., 20%, 40% and 60% of  $\mu_{max}$ , respectively. Several runs were made at the same dilution rates, but with 0.5% ethanol added to the inlet medium. For all of these, nitrogen was sparged through to sweep out  $CO_2$ . The sparging rate was 0.05 VVM. The results showed a

good conversion to ethanol. The theoretical maximum yield by the metabolic pathways of *Bacillus macerans* is 26%. The yields obtained were poor. At a dilution rates of 0.09/hr only half of the xylose was consumed. The lower dilution rates showed better consumption, up to 98% utilization at 0.03/hr. The addition of ethanol to the feed caused poorer utilization, but no significant decrease in cell density.

Future work will include quantifying inhibition by ethanol, acetone, and acetate. The nitrogen sparging rate will be changed to determine if  $CO_2$  is an inhibitor. There is some evidence that xylose is an inhibitor at concentration in the range of 6 to 8 w% and above.

#### FOOTNOTE AND REFERENCES

\*This work was supported by the Assistant Secretary for Energy Technology, U.S. Dept. of Energy.

1. A. F. Sciamanna, R. P. Freitas, and C. R. Wilke, "Composition and Utilization of Cellulose for Chemicals from Agricultural Residues," Lawrence Berkeley Laboratory Report LBL-5966 (1977).
2. C. R. Wilke and H. W. Blanch, Process Development Studies on Bioconversion of Cellulose and Production of Ethanol, Progress Reports:
  - (a) LBL-6859 (Jan., 1977)
  - (b) LBL-6860 (June, 1977)
  - (c) LBL-6861 (Sept., 1977)
  - (d) LBL-6881 (Feb., 1978)
  - (e) LBL-7880 (Sept., 1978)
  - (f) LBL-8658 (Dec., 1978).
3. C. R. Wilke, et al., "Raw Materials Evaluation and Process Development Studies for Conversion of Biomass to Sugars and Ethanol," Lawrence Berkeley Laboratory Report LBL-7847 (1978). Submitted to Biotechnol. and Bioeng.
4. R. I. Mateles and E. Battat, Applied Microbiology 28, 6, 901-905 (1974).
5. H. Wong, H. W. Blanch, and C. R. Wilke, "Media Development and Kinetics of Ethanol Fermentation," presented at the 79th Annual Meeting of the American Society for Microbiology, Los Angeles, Ca., May 4-8, 1979.

# LOW-COST, LOW-ENERGY FLASH ETHANOL FERMENTATION\*

B. Maiorella, H. W. Blanch, and C. R. Wilke

## INTRODUCTION

Ethanol production from renewable agricultural resources is an important potential supplement for petroleum-derived fuels and chemicals. Ethanol can be mixed in up to a one to nine ratio with gasoline for automotive fuel without modification to the standard auto engine. With modifications (primarily to the carburetor) ethanol can be used exclusively. After a chemical shift to ethylene, a wide range of petrochemicals can be synthesized from fermentative ethanol.

Two major problems are associated with the use of ethanol to replace petroleum derived fuel and chemicals. The cost of fermentation derived ethanol is high (Table 1) and large amounts of energy are required for ethanol production.

The major cost component of fermentative ethanol is sugar costs (63% of finished product cost). Currently, sugar from molasses sells<sup>1</sup> for \$0.19/kg, which alone accounts for a charge of \$0.32/ liter for ethanol.

The second major cost factor is fermentation plant production cost. Fermentative ethanol is traditionally produced by labor and capital intensive batch techniques. Based on 94.6 M liter-per-year batch-plant design by Cysewski and Wilke,<sup>2</sup> the capital cost of a new batch fermentation plant would be 25.4 million dollars, with an ethanol manufacturing cost, exclusive of feed materials costs and without profit, of \$0.14/liter.

Production of sugar by hydrolysis of agricultural wastes is under study by many researchers<sup>3,4</sup> and offers promise of major reductions to the raw material costs. New fermentation techniques, described here, greatly reduce production costs.

Energy requirements for fermentative ethanol production must be considered on a global basis, including energy consumed in farming (Table 2).

A substantial net positive energy return can be claimed by including energy from the burning of farm by-products.<sup>5</sup> If sugar is to become less costly though, the by-products must be used for hydrolysis to produce more sugar raw material, and not for plant steam production. The distillation energy requirement is equivalent to almost one-half of the energy available in the ethanol produced, and this energy requirement must be reduced.

## VACU-FERM PROCESS

The vacu-ferm process, developed concurrently by Cysewski and Wilke,<sup>6</sup> and Ramalingham and Finn<sup>7</sup> was a major step forward in reducing capital equipment and production costs for fermentative ethanol manufacture and is shown in Fig. 1. Fermentation is conducted under vacuum (51 mm Hg). Ethanol is boiled away at 35°C as it is produced, maintaining beer ethanol concentration at 3.5 wt%. Thus, end product inhibition is removed. Specific ethanol productivity is increased from 0.6/hr, the average rate over the course of an atmospheric batch fermentation, to a continuous 0.8/hr for vacu fermentation. With cell recycle to achieve high cell concentrations (123 g/L) in the continuous vacuum fermentor, overall productivities of 80 g ethanol/L-hr are achieved. The twenty-eight, 189 m<sup>3</sup> fermentors of the batch plant can be replaced by a single, high efficiency, 151 m<sup>3</sup> continuous vacuum fermentor.

Energy for boil-up in the vacuum fermentor could be provided by external heating. To reduce energy requirements, vapor recompression heating is used instead. Rather than compressing the vapor mixture entirely to atmospheric pressure, the main compressor compresses the vapor to only 118 mm Hg. At this pressure, the vapors can be passed through a fermentor reboiler with heat exchange providing for boil-up in the fermentor. The liquid ethanol-water mixture can now be pumped with low energy costs to distillation column pressure. A second compressor is required to remove the noncondensable CO<sub>2</sub> and O<sub>2</sub> gases (along with an equilibrium amount of ethanol and water) from the system.

Table 1. Ethanol production and market costs.

Fermentative Ethanol Manufacturing Cost: (94.6 M Liter per year from conventional operating batch plants not including profit)	\$0.47/liter
Ethanol Chemical Market Price:	\$0.34/liter
Cost of Energy Equivalent Gasoline: (One liter of ethanol contains the same chemical energy as 0.7 liters of gasoline.)	\$0.18/liter
Federal Supported Price for Fermentative Ethanol Blended into Gasohol: <sup>a</sup>	\$0.45/liter

<sup>a</sup>Additional tax supports are provided by many states.

Table 2. Estimated global energy balance for production of ethanol from molasses (energies are in kJ per liter anhydrous ethanol).<sup>a</sup>

Energy Consumption		Energy Production	
Farming	13,155	Ethanol	21,071
Sugar Milling and Concentration	6,912	Fusel Oils and Aldehydes	307
Feed Sterilization	139	Farm By-products (cane bagasse for steam generation)	34,700
<u>Distillation</u>			
To Azeotrope	6,996		
To Anhydrous	2,090		
Yeast Product Drying	390		
Subtotal	29,672		56,078
		Net Energy Production	26,406

<sup>a</sup>Compiled from estimates by Vogelbush, Scheller, Black, and Cysewski.

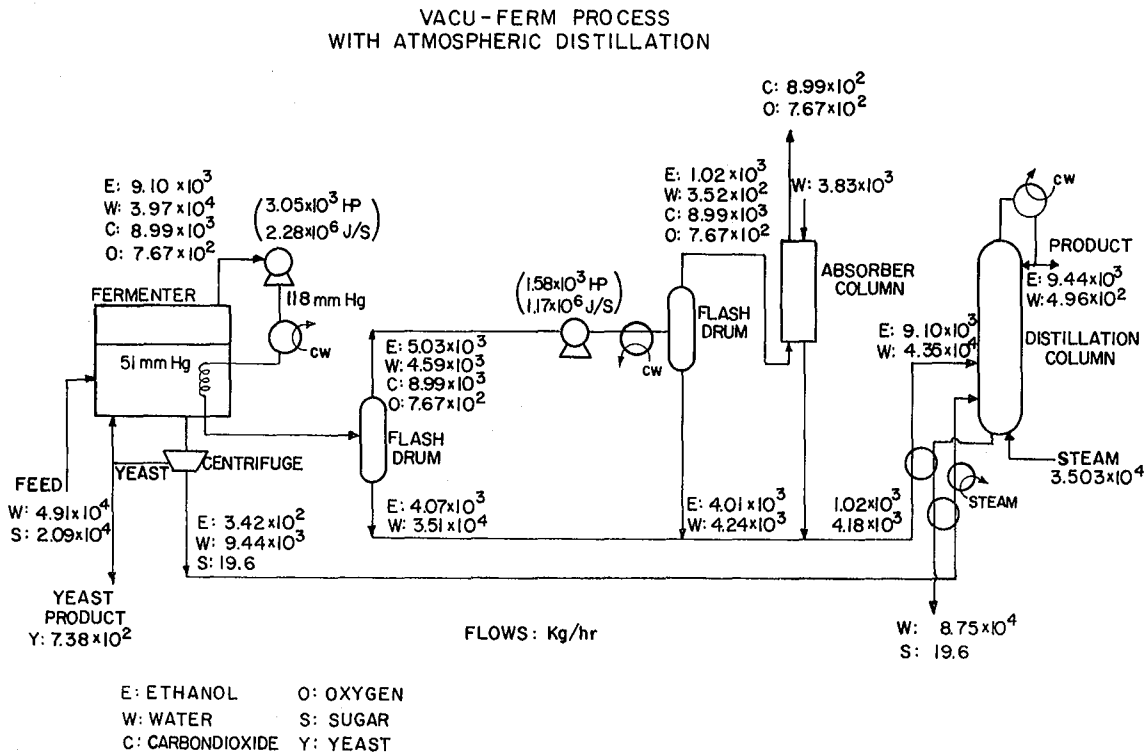


Fig. 1. Flash-ferm process with vacuum distillation.  
(XBL 799-7051)





Table 3. Ethanol separation energy requirements J/L 95 wt%.<sup>a</sup>

Process	Compressors	Column Feed Preheat	Column Reboiler Energy	Total
Batch Fermentation and Atmospheric Distillation	0	$2.58 \times 10^5$	$6.74 \times 10^6$	$7.00 \times 10^6$
Vacuum Fermentation and Atmospheric Distillation	$1.26 \times 10^6$	$1.64 \times 10^5$	$6.58 \times 10^6$	$8.00 \times 10^6$
Flash-Ferm and Atmospheric Distillation	$1.07 \times 10^6$	$1.26 \times 10^5$	$6.63 \times 10^6$	$7.83 \times 10^6$
Flash-Ferm and Vacuum Distillation	$1.07 \times 10^6$	$9.17 \times 10^4$	$2.41 \times 10^6$	$3.57 \times 10^6$

<sup>a</sup>These figures do not include scavenging of 600 psia compressor exhaust steam.

Table 4. Manufacturing cost comparison of processes.

	Batch-Ferm (1 ATM Column) ¢/L	Vacu-Ferm (1 ATM Column) ¢/L	Flash-Ferm (1 ATM Column) ¢/L	Flash-Ferm (Vacuum Column) ¢/L
Direct Costs:				
Raw Material	33.180	33.748	33.180	33.180
Operation	<u>9.138</u>	<u>4.766</u>	<u>4.731</u>	<u>3.838</u>
Total Direct Cost	42.336	38.514	37.914	37.121
Fixed Cost	3.027	1.662	1.617	1.712
Plant Overhead	<u>1.432</u>	<u>0.642</u>	<u>0.631</u>	<u>0.655</u>
Total Manufacturing Cost	46.795	40.820	40.162	39.385
General Expenses	<u>3.260</u>	<u>1.992</u>	<u>1.944</u>	<u>2.039</u>
Total Production Cost	50.108	42.809	42.106	41.425
Gross Income				
Ethanol Sales	44.909	44.909	44.909	44.909
Yeast Sales	5.944	5.944	5.944	5.944
Gross Profit	0.745	8.044	8.747	9.428
Tax (50% gross profit)	0.372	4.021	4.375	4.713
Net Profit (annual after tax)	0.372	4.021	4.375	4.713
Return on Investment	1.45%	28.12%	31.43%	32.00%

flashing operation is taken advantage of, and energy requirements are reduced to very low levels.

With these improvements, the fermentation and distillation processes have been optimized. Further steps toward reducing fermentative ethanol cost must come from development of cheap supplies of sugar raw material.

#### ACKNOWLEDGMENT

The assistance of Tom Glenchur in carrying out many of the detailed design and economic calculations is gratefully acknowledged.

#### FOOTNOTE AND REFERENCES

\*This work was supported by the Director, Energy Research, U.S. Dept. of Energy.

1. Chemical Marketing Reporter, January 15, 1979, Schnell Publishing Co., Inc.
2. C. R. Cysewski and C. R. Wilke, "Process design and economic studies of alternative fermentation methods for the production of ethanol," Biotechnol. and Bioeng. XX, pp. 1421-1444 (1978).
3. G. T. Tsao, "Fermentable sugars from cellulosic wastes as a natural resource," J. Chin. Inst. Chem. Eng. 9(1), 1-8 (1978).
4. C. R. Wilke, et al., "Raw materials and process development studies for conversion of biomass to sugar and ethanol," Proceedings: The Second Annual Symposium on Fuels from Biomass (1978).
5. A. E. Humphrey, E. J. Nolan, Report to the Office of Technology Assessment: Biological Production of Liquid Fuels and Chemical Feedstocks, Govt. Printing Office #052-003-00706.
6. G. R. Cysewski and C. R. Wilke, "Rapid ethanol fermentation using vacuum and cell recycle," Biotechnol. and Bioeng., XIX, pp. 1125-1143 (1977).
7. A. Ramalingham and R. K. Finn, "The vacu-ferm process: A new approach to fermentation alcohol," Biotechnol. and Bioeng., XIX, pp. 583-589 (1977).
8. C. R. Wilke, Personal communication to G. Cysewski, Univ. of Calif. Dept. of Chemical Engineering (March 1977).
9. C. R. Wilke and R. Yang, "Process Development Studies on the Bioconversion of Cellulose and Production of Ethanol," Lawrence Berkeley Laboratory Report LBL-6881 (1978).
10. A. H. Beebe, K. E. Coulter, et al., Ind. Eng. Chem. 34, 1501, (1942).

## STUDIES ON THE PHYSIOLOGY AND ENZYMOLOGY OF LIGNIN DEGRADATION\*

*S. L. Rosenberg and C. R. Wilke*

Studies of biological lignin degradation were undertaken in order to see if this process could be incorporated in our current scheme for the bioconversion of lignocellulosic materials to ethyl alcohol. The presence of lignin in natural cellulosic materials protects some of the cellulose and other carbohydrates from enzymatic attack. Removal of the lignin increases the amount of carbohydrate subject to enzymatic saccharification and, thus, the amount of ethanol obtainable. The goal of this research was the demonstration of a cell-free lignin-degrading enzyme system.

Before a cell-free system could be demonstrated, it was necessary to learn how to grow the organisms (molds) rapidly under conditions where lignin degradation was actually occurring. It was found that both intimate cell-substrate contact and high oxygen concentrations were required for lignin (but no carbohydrate) degradation. Figures 1-3 illus-

trate these conclusions. Only in stationary, non-submerged cultures (Fig. 2) or in submerged but oxygenated cultures (Fig. 3) was lignin degraded to a significant degree.

Having a culturing system where rapid lignin degradation was known to occur (Fig. 2) we next attempted to extract the enzymes involved by a number of conventional methods and demonstrate their activity in the absence of the living cells. These attempts were unsuccessful.

Since it was possible that the presence of cells was necessary for the regeneration of needed co-factors or the continued production of unstable components, an apparatus was developed to indicate the presence of diffusible enzyme systems in the presence of growing cells. The apparatus, termed a diffusion chamber is shown in Fig. 4. The top and bottom compartments are separated by a bacterio-

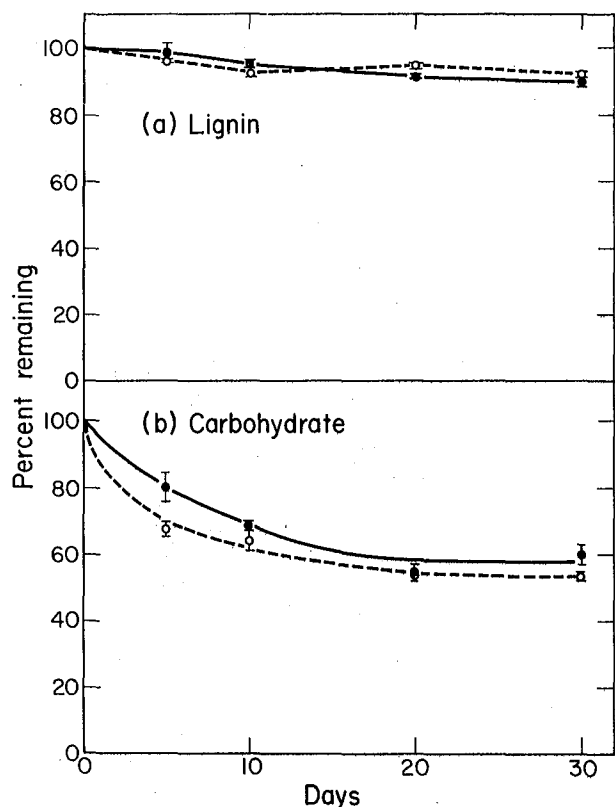


Fig. 1. Lignin and carbohydrate loss in shaking submerged cultures of *C. pruinosa* grown in mineral medium plus manure fiber in the presence of air ●—● or oxygen ○---○. Each data point represents the average of two cultures.

(XBL 784-659)

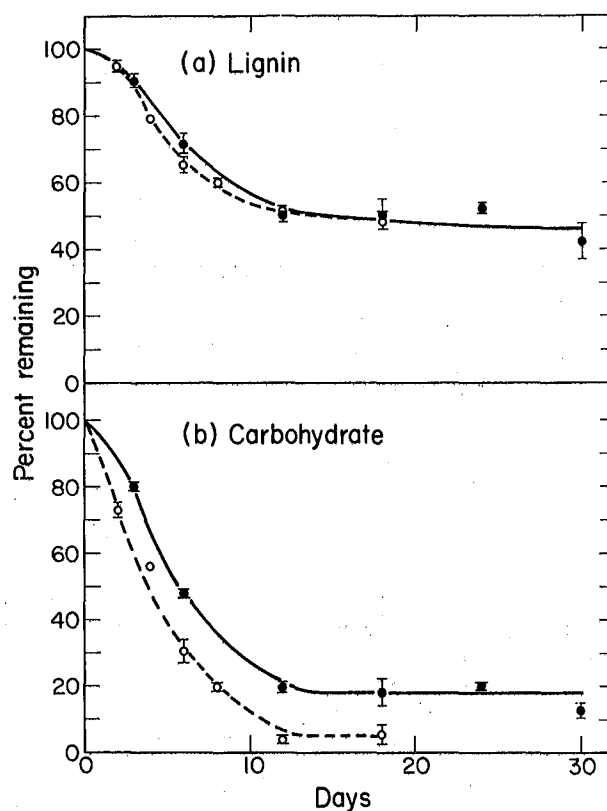


Fig. 2. Lignin and carbohydrate loss in damp manure fiber cultures of *C. pruinosa* grown on the surface of mineral agar plates in the presence of air ●—● or oxygen ○---○. Each data point represents the average of two cultures. (XBL 784-660)

logical membrane filter. Sterile lignocellulose is pressed against the underside of the filter by a sponge plug. The top compartment contains a mold inoculum plus or minus lignocellulose. The presence of diffusible lignin and cellulose-degrading enzyme systems is indicated by the loss of solid lignin and carbohydrate from the bottom compartment.

A number of known lignin-degrading molds was tested in this apparatus, and none gave evidence of producing significant levels of diffusible lignin degrading activity, although many showed diffusible carbohydrate-degrading activity. Data for most of the organisms tested are presented in Fig. 5. The simplest interpretation of the results is that one or more components of the lignin-degrading system produced by these organisms is bound to the cell surface or otherwise immobilized close to the site of production. For some of these organisms this appears to be true of the cellulase enzymes as well. Members of group-1 showed excellent lignocellulose-degrading ability when in contact with the substrate and might be considered for the production of single cell protein from ligno-

cellulosic wastes. A more complete description of this work can be found in references 1 - 3.

#### FOOTNOTE AND REFERENCES

\*This work was supported by the National Science Foundation.

1. S. L. Rosenberg, "Physiological studies of lignocellulose degradation by the thermotolerant mold *Chrysosporium pruinosa*," Devel. in Indust. Microbiol., **20**, 133-142 (1979).
2. S. L. Rosenberg and C. R. Wilke, "Lignin biodegradation and the production of ethyl alcohol from cellulose," in Lignin Biodegradation: Microbiology, Chemistry and Applications, T. K. Kirk, T. Higuchi, and H.-m. Chang, Eds. CRC Press, West Palm Beach, Fla. (In press).
3. S. L. Rosenberg, "Patterns of Diffusibility of Lignin and Carbohydrate Degrading Systems in Wood-Rotting Fungi," Lawrence Berkeley Laboratory Report LBL-9863 (1979).

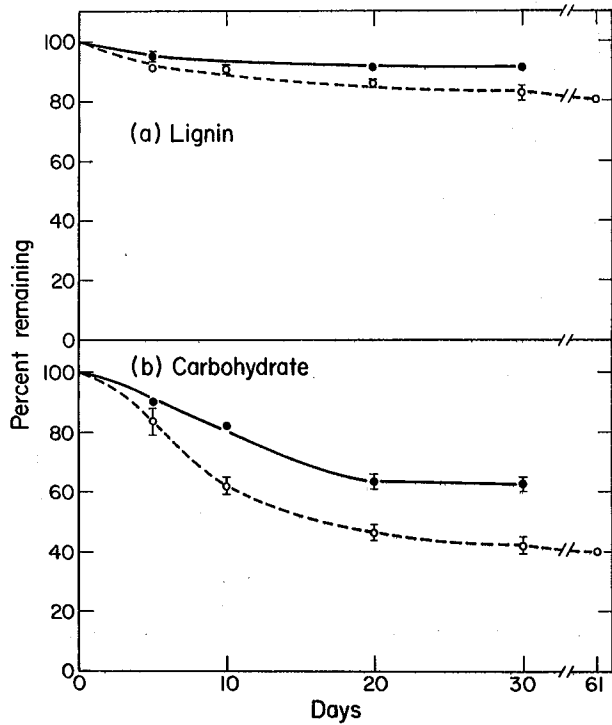


Fig. 3. Lignin and carbohydrate loss in stationary submerged cultures of *C. prunosum* grown in mineral medium plus manure fiber in the presence of air ●—● or oxygen ○—○. Each data point represents the average of two cultures. (XBL 784-661)

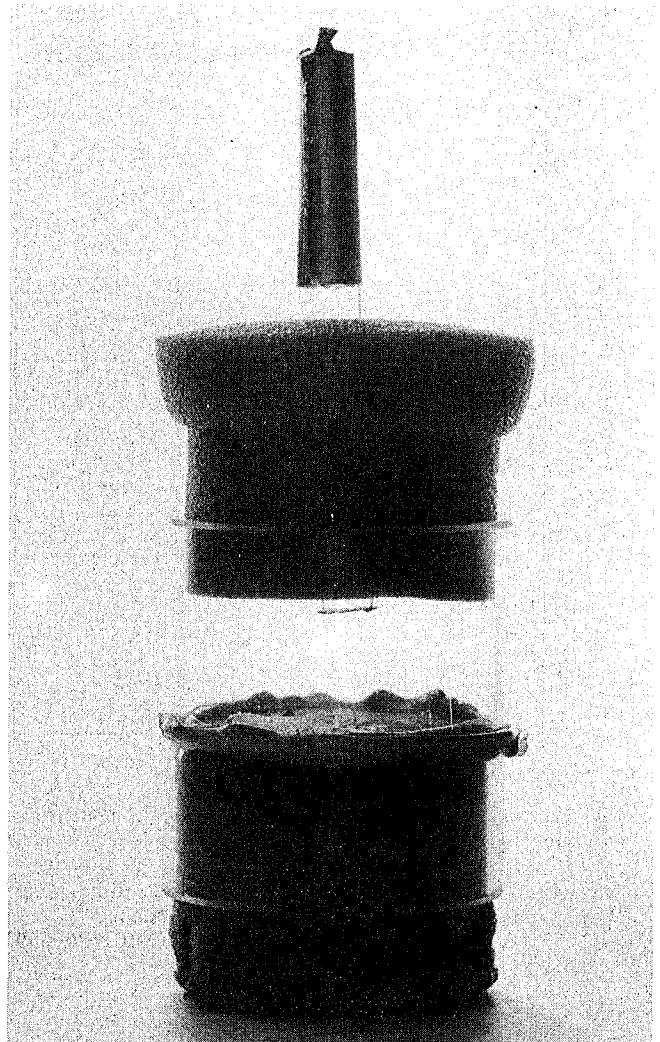


Fig. 4. Diffusion Chamber. Top plug has been raised and bottom foil cover has been removed to show details of construction. (CBB 783-2637)

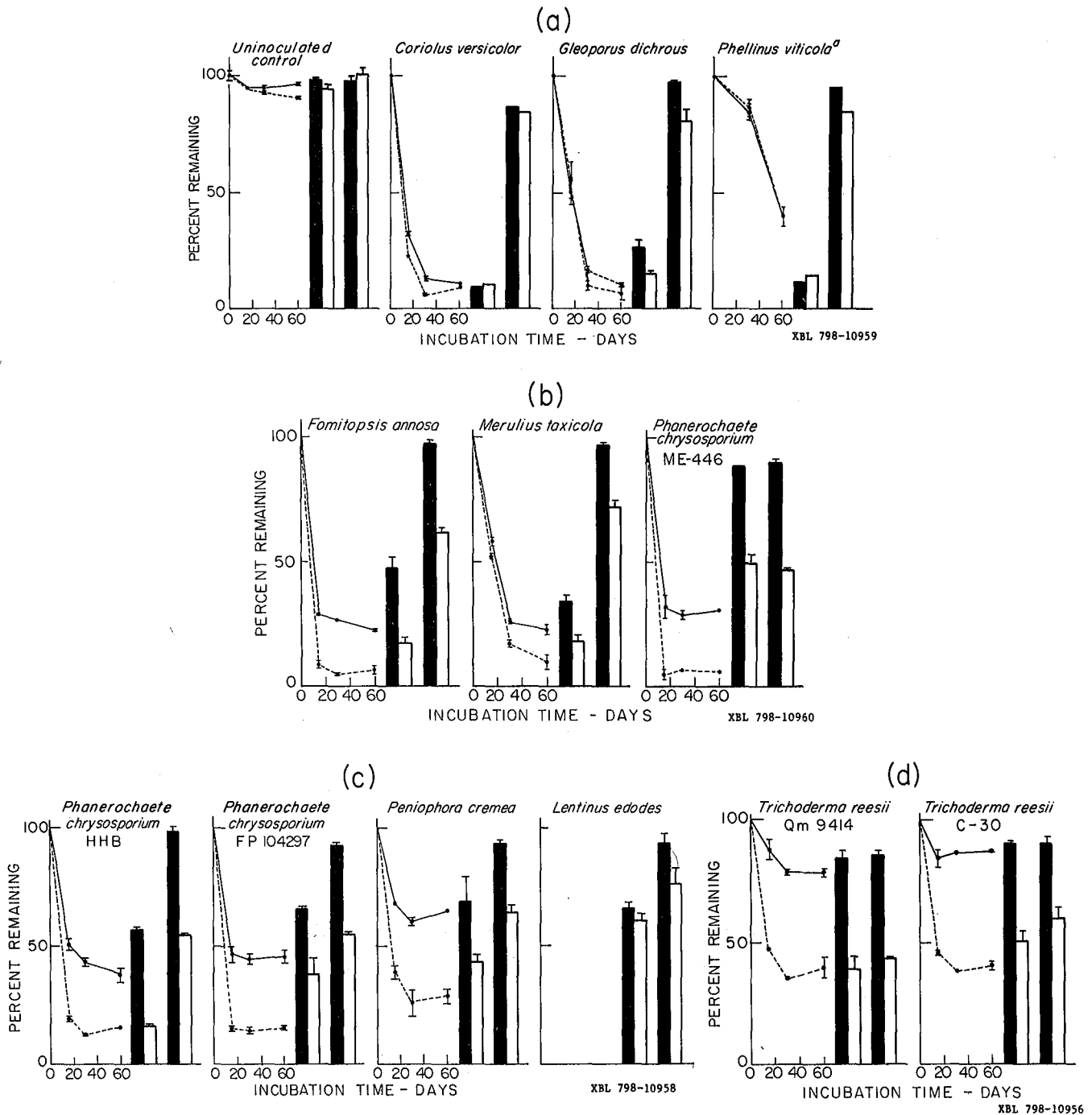
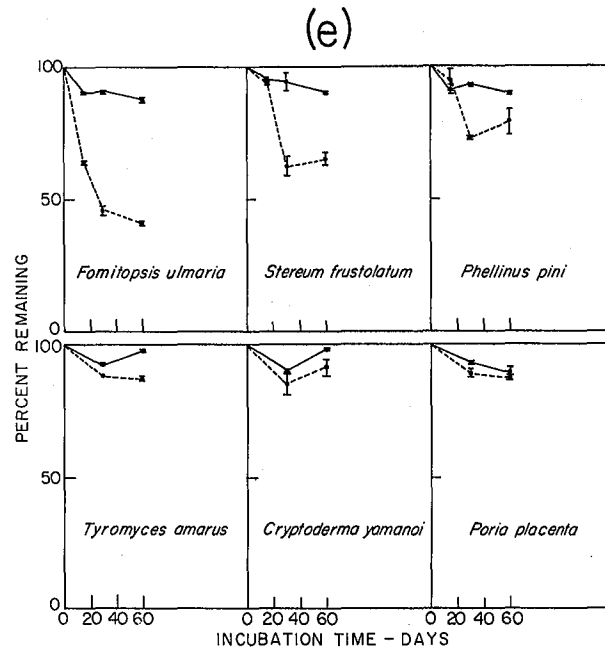


Fig. 5. (a-d) Lignin and carbohydrate remaining in washed manure fiber degraded by cellulolytic and ligninolytic fungi. —lignin and ----carbohydrate remaining in agar plate cultures. Lignin (dark bar) and carbohydrate (light bar), remaining in diffusion cultures. Left-hand bar pair = residual lignocellulose in top (inoculated) chamber. Right-hand bar pair = residual lignocellulose in bottom (sterile) chamber. Error bars indicate range of variability in replicate samples. No-error bar means only one sample processed. Diffusion cultures were incubated for 30 days except for the *P. viticola* culture which was incubated for 60 days.



XBL 798-10957

Fig. 5(e). See caption on previous page for key.

## STATUS OF BIOMASS LIQUEFACTION AT LAWRENCE BERKELEY LABORATORY

S. Ergun

Conversion of biomass into oil or gas is not a new idea, nor is the recognition that synfuels derived from wood wastes or wood grown for such a purpose could meet a substantial portion of America's needs of energy and chemicals. Suffice it to state that there was a genuine interest in the early 1940s for fuels from wood, which was lost upon the discovery of huge oil fields in the Arabian peninsula soon after.

The interest in synthetic fuels from biomass was revived some thirty years later for reasons that need no elaboration. The current biomass liquefaction program of DOE has evolved from the lignite liquefaction program of the Bureau of Mines (BOM) in the late 1960s and early 1970s. Noting the widespread interest in municipal waste disposal,

the Bureau of Mines researchers explored the effectiveness of a process particularly well suited for lignite to liquefy organic municipal waste. They found that organic municipal waste and other biomass wastes such as sawdust and manure, liquefied with greater ease under milder conditions than did lignite.

Encouraged by the results of bench-scale research and economic feasibility analysis, the Bureau of Mines proceeded with the design and construction of a process development unit (PDU) capable of processing 3 tons of wood daily or to yield roughly 5 barrels of oil daily. The plant site chosen was adjacent to the Experimental Metallurgical Station of the Bureau of Mines at Albany, Oregon.

In October 1977, DOE contracted with LBL to monitor both the development program at Albany and the supporting activity, to provide a third-party objectivity in the evaluation of results, to make recommendations regarding the future course of the program, and to provide assistance and appraisal to the operators of the facility.

LBL was also given the responsibility of monitoring the supporting research activity on biomass liquefaction in order to utilize the results in the development program at Albany. Also, LBL has conducted supporting engineering and development studies to provide optional approaches to biomass liquefaction. Accordingly, process modifications and/or new process options had to be researched and a data base provided for testing at Albany.

As lead laboratory for Biomass Liquefaction, LBL has undertaken the following objectives:

1. To provide a continual independent evaluation for the Biomass Energy Systems (BES) Branch of the Department of Energy (DOE) of the technical progress made in biomass liquefaction projects sponsored by DOE.
2. To monitor the operations of the Biomass Liquefaction Facility at Albany, Oregon and to provide technical operating directives for the test runs to be conducted at Albany.
3. To undertake engineering and bench scale experimental studies to enhance the progress of the biomass-to-oil program of DOE.

The following reports summarize LBL's efforts over the past year.

## PRETREATMENT OF BIOMASS PRIOR TO LIQUEFACTION\*

*L. Schaleger, N. Yaghoubzadeh, and S. Ergun*

### INTRODUCTION

The preparation of a concentrated slurry of biomass and its introduction into a high-pressure reaction system are critical operations in the DOE-Albany waste wood-to-oil process. The original Bureau of Mines scheme called for green wood chips to be dried and milled to a flour. The flour was to be blended with a carrier oil and then pumped into the reactor at a solids concentration of 30%. Unfortunately, in practice it has not been possible to pump slurries more concentrated than 10% on a continuous basis. This has had a large negative impact on the economic feasibility of the process since the lower the concentration of biomass in the feed to the reaction system, the larger the plant must be for a given production rate.

Studies at LBL have therefore been directed toward finding alternatives to the Bureau of Mines scheme for injecting biomass into a liquefaction system. Work has centered on chemical pretreatment for the purpose of producing slurries which are pumpable at high concentrations of solids. Physical pretreatment, that is drying and grinding, accounted for 22% of processing costs in the original scheme and has therefore been eliminated from the LBL process development concept. The most promising method of chemical pretreatment found was hydrolysis promoted by mild aqueous acid. The major objectives of the FY 79 research program in pretreatment were: (1) to provide an engineering data base for hydrolytic pretreatment through bench-scale research; (2) to evaluate the resulting slurries of hydrolyzed wood as to liquefiability; and (3) to investigate means of integrating chemical pretreatment and catalytic liquefaction in a continuous manner.

This subproject was begun in October, 1978, using the facilities of the UC Forest Products Laboratory at the Richmond Field Station. After 1 June 1979, research was conducted in the group's permanent facility in Bldg. 934.

### ACCOMPLISHMENTS DURING 1979

A series of bench-scale experiments on the hydrolysis of green wood chips were conducted and a set of conditions which resulted in the production of a slurry having superior rheological properties was established. After appropriate procedural and equipment modifications were made, these results were duplicated on a 200-gal scale by Rust Engineering Corp., operators of the DOE-Albany facility. A subsequent liquefaction run at Albany succeeded in producing 6 bbls of purely wood-derived oil from prehydrolyzed wood slurry. Thus the chemical feasibility of the LBL approach was demonstrated. In this report the studies on pretreatment which culminated in the successful production of oil at Albany are detailed.

### Chemistry of Pretreatment

Wood is composed of carbohydrate, which includes cellulose (about 40%) and hemicellulose (25-30%), and lignin (25-30%). When treated with aqueous acid at elevated temperatures and pressures, the carbohydrate fraction is broken down to its constituent monosaccharides, cellulose yielding glucose and hemicellulose yielding a mixture of mannose, glucose, xylose, galactose, and arabinose. Hemicellulose undergoes hydrolysis much more rapidly than cellulose. Continued exposure to hot, aqueous acid causes the degradation of monomeric sugars to fur-

fural derivatives. Hydrolysis also liberates small amounts of acetic acid, uronic acids, fatty acids, and resinous substances. These are the facts concerning hydrolysis which were taken into account in the design of a suitable pretreatment option.

#### Data Base for Hydrolysis

Initially we found that the reaction of green Douglas Fir wood chips with water at 250°C gave a char unsuited for pumping or liquefaction. However, the fact that extensive size reduction of the wood chips had occurred by means of chemical action encouraged further efforts along these lines. It was found that the addition of dilute sulfuric acid to the aqueous phase permitted the use of milder conditions for the same degree of size reduction. Approximately a dozen experiments were conducted; the conditions shown in Table 1 were found to be optimal.

Table 1. Data Base for hydrolysis.

Wood/Water Ratio	23/77
Heat-up Time	12 min.
Temperature	180°C
Acid	650 ppm H <sub>2</sub> SO <sub>4</sub>
pH	2.0
Retention Time	45 min.

Under the conditions specified, the hemicellulose portion is nearly completely hydrolyzed with minimal degradation of the liberated sugars. The reaction mixture is vigorously agitated in order to enhance particle size reduction. This combination of chemical and physical action results in the reduction of the major fraction of wood chips to fine, non-fibrous particles having a bulk density of about 1.4 g/mL. Approximately 30% of wood solids become solubilized so that the concentration of insoluble solids is reduced from 23 to a more manageable 16% during the course of the reaction.

The resulting slurries are quite fluid and appear to be pumpable. However it was found that a minor fraction of partially hydrolyzed wood chips always remain. These could be removed by screening. However, since they are easily crumbled between the fingers, further mechanical treatment such as disc refining may suffice to prepare the slurry for injection into a liquefaction loop.

Ferric chloride and hydriodic acid have also been found to be suitable pretreatment catalysts

provided that the initial pH is 2.0. Material, carbon, hydrogen and energy balances have been found to be 85% or greater.

Several experiments designed to test the liquefiability of prehydrolyzed wood slurries were performed. Under identical conditions prehydrolyzed wood was found to give a slightly higher yield of oil than wood flour.

The results indicate that acid pretreatment affords a promising option to drying and grinding as a method for preparing wood for catalytic liquefaction. Further work will be necessary to establish the technical feasibility of incorporating acid pretreatment into an integrated biomass liquefaction process.

#### PLANNED ACTIVITIES FOR 1980

A major fraction of the FY 80 effort will be devoted to process development considerations. One major task will be to undertake an investigation of the rheological properties of prehydrolyzed wood slurries. These will be characterized as to viscosities, settling rates, concentration limits and other factors pertinent to the question of their pumpability. Pumpability tests will be conducted in a laboratory scale pumping loop under construction.

Neutralization presents another difficulty. The current liquefaction scheme calls for acid pretreatment slurry to be neutralized with sodium carbonate prior to liquefaction. While neutralization is not a problem technically, it is wasteful and adds expense. Pretreatment and liquefaction could be more economically integrated if either a satisfactory basic pretreatment catalyst or an acidic liquefaction catalyst could be found. Exploratory research along these lines will be continued.

#### FOOTNOTE AND REFERENCE

\*This work was supported by the Assistant Secretary for Energy Technology, U.S. Dept. of Energy.

1. L. Schaleger, N. Yaghoubzadeh, and S. Ergun, "Pretreatment of Biomass Prior to Liquefaction," Lawrence Berkeley Laboratory Report LBL-9190, (1979).

# CATALYTIC LIQUEFACTION OF BIOMASS\*

M. Seth, R. Djafar, G. Yu, S. Ergun,  
and T. Vermeulen

## INTRODUCTION

Work on this project began in November 1978. We reviewed the literature on the hydrogenation and hydrogenolysis of wood, cellulose, lignin, and sugars. Based on this review, 20 potential catalysts were screened. Both the review and the results of the screening experiments have been reported.<sup>1</sup> These experiments led to the identification of ferric chloride as an effective reagent for wood liquefaction.

The objectives of this project are:

- To undertake bench-scale studies leading to improvements in the present liquefaction process.
- To formulate and conduct exploratory research for the identification and development of new, integrated processes for biomass liquefaction.
- To investigate the characteristics and stability of biomass liquids.
- To explore and develop options for the upgrading and utilization of liquids from biomass.

The selection and development of integrated process concepts generally proceeds in three phases. The first phase involves exploratory catalyst screening. Several potential catalysts are screened at standard conditions based on the chemical approach being pursued. The effect of process variables is then investigated for the most promising catalytic systems. Finally, changes that could result in improved process economics or process operation are tested and evaluated. Two related aspects of the project are concerned with the analysis and characterization of products and with product upgrading and utilization.

## ACCOMPLISHMENTS DURING 1979

### Exploratory Research on Catalysis

In the task of exploring new catalysts, two chemical approaches are being tested for their application to wood liquefaction. The first relies on the solvolytic depolymerization of cellulose and/or lignin using acidic mixtures of water and wood-derived organic solvents. Hydrogen transfer from partially hydrogenated lignin-derived solvents is the second approach being tested. In this approach tests are being run to see if hydrogen can be added to wood by the acid catalyzed hydride transfer reaction. We will also test the use of organometallic catalysts and other hydrogenations and decarboxylation catalysts.

### Solvolytic Degradation/Hydrogenation System

Several hydrogenation catalysts have been tested for the production of liquids from wood, cellulose, lignin and sugars.<sup>2,3,4</sup> In order to hydrogenate wood over a solid catalyst, the wood must first be depolymerized to fine particles or to material soluble in a carrier solvent. The depolymerization and hydrogenation steps could be integrated if a fraction of the products of wood hydrogenation could be used as the carrier solvent. Solvolysis in an acidic medium could be used for the depolymerization of cellulose (and lignin). If the carrier liquid is also a good solvent for the products of solvolysis, a substantial fraction of the wood could be put into solution.

Methanol, ethanol, propanol, ethylene glycol and glycerol were screened in order to test the effectiveness of alcohols as recycled solvents for the solvolytic degradation of wood. Phenol and catachol were selected as representative lower molecular weight lignin-derived solvents for testing

All screening experiments were run in a 300 mL Parr reactor. About 15g of wood, 30g of acid and 30g of the organic solvent were weighed into a glass liner. The liner was then placed in the reactor and the reactor sealed. The reactor was charged with 200 psig hydrogen and 200 psig carbon monoxide. The reactor was then heated to temperature and held there for one hour. At the end of the run the reactor was quickly quenched to room temperature.

Products were separated into fractions soluble in toluene, acetone, reaction liquor (i.e., the acidic-solvent medium), and the remaining insoluble residue. Toluene solubles ranged from about 1% of dry wood for hydrolysis (in a pH of 2.5), to 22% for propanol. With most other organic solvents the toluene soluble material ranged between 2 and 10%. Acetone solubles ranged about 5% for solvolysis with propanol to about 36% with catachol. Up to 60% of the wood was converted to material soluble in the reaction medium at room temperature. Catachol and phenol gave the lowest yields of insoluble material (2% and 9% of the wood, respectively). Ethylene glycol was the solvent that resulted in the lowest yield of insoluble residue amongst the alcohols (18%).

### Hydride Transfer

Hydrogenation of solid hydrocarbons such as coal can occur by the donation of hydrogen from organic liquid molecules. Thermal cleavage of bonds followed by hydrogen abstraction from the solvent is the basis of SRC-type coal liquefaction processes. It may be possible to catalytically transfer hydrogen from hydrogen-rich solvents and so effect the reduction of hydrocarbonaceous feeds at lower temperatures.

Two representative solvents, cyclohexadiene and  $\alpha$ -phellandrene (5-isopropyl - 2-methyl - 1,3-cyclohexadiene), were selected for testing. Each solvent was run at 250°C for one hour with aqueous sulfuric acid pH of about 2.5 and 3. The reaction procedures used were exactly the same as those for the solvolytic degradation experiment.

In the experiments, about 75-80% of the wood was solubilized. Acetone soluble yields were between 30 and 35% with cyclohexadiene and 22% with  $\alpha$ -phellandrene within the range of our tests acid pH seemed to make little difference to yield and atomic H/C and O/C of product fractions for both solvents. Extensive alkylation of products occurred when  $\alpha$ -phellandrene was used as the solvent.

During the next year we will extend the study to other potential hydride transfer solvents. The effect of acid pH, reaction time and reaction temperature on the yield and quality of products will be explored. Spent solvents will be analyzed to determine the extent of hydrogen transfer.

#### Investigation of Process Variables

The effect of process variables are being studied for three catalytic systems. Sodium carbonate catalyzed liquefaction in an aqueous medium (LBL process) is the first catalytic system undergoing tests. The effect of catalyst concentration, reaction time, and slurry concentration are being determined at a reaction temperature of 360°C. In the second catalytic system, the effects of catalyst concentration, slurrying solvent, and reaction time are being tested for the ferric chloride at reaction temperatures of 250 and 360°C. We expect to begin testing the hydrogen iodide system, our third catalytic system in the near future.

#### Aqueous Sodium Carbonate System

The Bureau of Mines (BOM) process uses a mixture of aqueous sodium carbonate and recycled oil as the carrier solvent for wood liquefaction, whereas the LBL option relies on the acidic hydrolysis of wood chips followed by sodium carbonate catalyzed liquefaction in an aqueous medium. The effect of process variables on the aqueous (LBL) system has, however, never been systematically evaluated. We have recently begun to determine the effect of catalyst concentration, slurry concentration and reaction time on the yield and quality of the products obtained during aqueous sodium carbonate catalyzed liquefaction.

All sodium carbonate experiments were run in a one-liter autoclave reactor. About 50g of wood flour and 220g of aqueous sodium carbonate solution was used for each run. The autoclave was charged with 300 psig of H<sub>2</sub> and 300 psig of CO. The reactor and its contents were heated to 360°C in 40-55 min and held there for the desired reaction time. At the end of the run the autoclave was cooled and the products removed.

Total water solubles (i.e., material soluble in the reaction liquor plus material obtained by water extraction) were determined for selected

experiments. In each case between 17 and 19% of the starting wood appeared as water-solubles. In the absence of sodium carbonate only 4% of the products dissolved in water.

Insoluble residue ranged from 2 to 8% of the wood and generally increased with decreasing sodium carbonate concentration. When no sodium carbonate was present about 25% of the wood was obtained as an insoluble residue.

Between 42 and 47% of the original wood was accounted for in each run where catalyst was present, and about 50% of the original wood was recovered in the absence of a catalyst.

To characterize product fractions, ultimate analysis was done for each fraction of products obtained. Among the soluble fractions, the toluene solubles contained the least amount of oxygen per carbon atom (O/C = 0.11). Atomic O/C ratios of the acetone solubles were comparable to those of the toluene soluble material. The toluene soluble fraction had an atomic H/C of 1.25 which was significantly higher than that of the acetone soluble fraction (H/C = 0.18). Fractions soluble in water had similar O/C ratios (about 0.66), whereas product soluble in the reaction liquor had a considerably higher H/C ratio than product obtained by extraction with water. About 67% of the initial carbon was recovered in the various product fractions.

Average molecular weights and spectroscopic analysis of different product fractions is underway. More conclusive comments on the nature of the products may be possible when additional information becomes available.

#### Ferric Chloride System

In the LBL modification of the BOM process, wood chips are hydrolyzed with dilute acid to form a pumpable slurry which is then liquefied using a basic catalyst (sodium carbonate). Another option would be to use an acidic catalyst effective both for hydrolysis and liquefaction. Initial screening experiments<sup>1</sup> indicated that ferric chloride may be a good reagent for liquefaction. Dilute solutions of ferric chloride may be a good reagent for liquefaction. Dilute solutions of ferric chloride were also found to hydrolyze wood chips. The ferric chloride system is being further evaluated by testing for the effect of process variables on the yield and quality of the products.

The effect of ferric chloride concentration, reaction time and reducing gases on the yield of product fractions were determined both for wood flour and pre-hydrolyzed slurries at 180 and 250°C. Products were fractionated into acetone and toluene solubles.

The insoluble residue obtained usually varied between about 28 and 45% of the starting wood. Within this range an increase in ferric chloride concentration led to a small reduction in insoluble solids at 180°C. Ferric chloride concentrations higher than 1.2% appeared to have little effect on the yield of insoluble solid at 250°C for reaction times of 1 hour or more.

Where no reducing gases were used, the toluene-soluble fractions of the product appeared to depend on reaction time and ferric chloride solution concentration at 180 and 250°C. At the lower temperature an increase in residence time from 1 to 2 hrs resulted in a decline in toluene solubility from about 14 to 0.4%.

Our research on the Ferric Chloride System indicates the following:

- Presence of reducing gases (CO/H) is beneficial for liquefaction with ferric chloride.
- A complex set of reaction occur where toluene-soluble materials are further converted to products soluble in either water or acetone.
- Reaction conditions could be tailored to obtain any of a wide span of products (as indicated by their solubility characteristics)
- In order to be of possible commercial use, the ferric-chloride system must be modified so as to convert the large fraction of insoluble material to more desirable products.

We plan to continue studying the ferric chloride system in the future. The feasibility of using co-catalysts that enhance the yield of liquids and the use of non-aqueous slurries will be explored.

#### Product Characterization and Stability Studies

So far the major effort in this task was geared toward developing adequate separation procedures. Methods for separation of products for each catalytic system have been discussed in the appropriate sections.

We have also begun spectrometric analysis and molecular weight determinations of selected product fractions, which will enable us, we hope, to better understand possible chemical structures in product fractions.

During the next year we plan to test a variety of methods for the characterization of wood-derived liquids. Thermal and oxidative stabilities of liquid products will also be evaluated.

#### PLANNED ACTIVITIES FOR 1980

Activities planned for 1980 have been mentioned above. Other work, to begin in March 1980, is briefly summarized below.

#### Investigation of Process Improvement Options

The objective of this task will be to test and evaluate modifications that could lead to improved process economics. In particular, changes that could result in higher slurry concentrations, better product quality, higher oil yield, and reduced heat transfer and separation costs will be identified and tested. As a first step, we plan to evaluate changes in slurry solvent composition and the use of co-catalysts. As more information is collected other areas of interest may become apparent, and these will be further evaluated if necessary.

#### Product Upgrading Utilization Options

The objective of this task will be to screen several potential methods for upgrading the utilization of products obtained from biomass liquefaction. Potential uses for biomass liquids will be suggested once sufficient chemical and physical characterization has been completed. Several solid hydrogenation, hydrogenolysis, and decarboxylation catalysts will be tested for their effectiveness in further upgrading biomass liquids so as to obtain a wider range of liquid fuels.

#### FOOTNOTE AND REFERENCES

\*This work was supported by the Assistant Secretary for Energy Technology, U.S. Dept. of Energy.

1. M. Seth and T. Vermeulen, Liquid Fuels from Biomass: Catalyst Screening and Kinetic Studies Ph.D. Thesis, University of California, Lawrence Berkeley Laboratory (1979) (In press).
2. B. L. Browning, The Chemistry of Wood, (Wiley-Interscience, New York, 1963).
3. J. A. Pearl, The Chemistry of Lignin (M. Dekker Inc., New York, 1967).
4. K. V. Sarkanen and C. H. Ludwig, Eds., Lignins (Wiley-Interscience, New York, 1971).

## MONITORING THE BIOMASS LIQUEFACTION PROCESS DEVELOPMENT UNIT AT ALBANY, OREGON\*

*S. Ergun, C. Figueroa, and C. Karatas*

### INTRODUCTION

Serious efforts to convert biomass to oil were initiated by the Bureau of Mines, Department of Interior, during the late 1960s. The Bureau's efforts were culminated by the design and construction start-up of a process development unit (PDU) at Albany, Oregon early in 1974. It was expected that the construction of the facility would be completed during the third quarter of 1975 and supporting research and analytical work necessary for the development activity would be provided by the Pittsburgh Energy Research Center and Albany Metallurgical Research Center of the Bureau of Mines.

During 1974, the Energy Research and Development Agency (ERDA) was established and the biomass liquefaction program was transferred to ERDA's Solar Energy Division. During the transition period, ERDA authorized a number of reevaluation studies regarding the economics of producing oil from biomass, best use of the facility under construction, options for modifying the PDU and experimental programs that could be undertaken. In all of these studies construction completion and a genuine effort for process development were recommended.

The construction of the PDU was completed at the end of December 1976. Bechtel National, Inc. was awarded the contract to commission the facility, affect the modifications indicated in the earlier ERDA studies and to conduct some test runs. The Bechtel contract was for one year; it was extended for another six months (on a monthly basis) pending the responses to an RFP issued by ERDA for a two year development program. The Rust Engineering Company was awarded the contract to operate the facility for two years starting July 1978.

The following is a brief account of the results of the monitoring efforts undertaken by LBL in biomass liquefaction.

### ACCOMPLISHMENTS DURING 1979

LBL monitored the Albany operations through an independent analysis of the raw data obtained, and plant modifications proposed and planned. LBL stationed a chemical engineer at Albany for a period of three months in order to become fully familiar with equipment, operating procedures, and data acquisition.

Analysis of production difficulties, coupled with in-house research, led LBL researchers to seek alternative processes. A literature survey by LBL revealed that catalysts other than sodium carbonate had been utilized by researchers in converting wood and wood components (especially lignin and cellulose) into oil and chemicals (phenols, high boiling alcohols, etc.). Promising catalysts were evaluated.

An LBL analysis of all of the data obtained at Albany led to the following conclusions regarding the involuntary termination of all of the runs conducted during 1977 and 1978:

- 1) Remedy for operational problems is not likely to be found by altering the operating conditions (wood/oil ratio, catalyst/wood ratio, temperature, pressure, residence time, agitation levels, etc.).
- 2) The cause of the difficulty is likely to be related to the process chemistry.
- 3) It could be pinpointed by investigating the performances of the various process units one by one, by isolation if possible.

Researchers conducted a comprehensive test run that established the following conclusions about the existing process:

- 1) A major portion of sodium salts remained in the solid residue, and not in the aqueous phase.
- 2) The centrifuge was not designed properly to separate relatively small amounts (<10%) of aqueous phase from an oil phase.
- 3) Densities of oil and salt-laden solid residue being about the same, neither the available three-phase centrifuge or a rented sludger could separate the solid phase.

In April, 1979, after consultation with Rust Engineering Company (the plant operators), LBL issued an operating directive to test the chemical and technical feasibility of a modified process that appeared promising on the basis of results obtained at LBL. This test run was conducted during the first week of May, 1979, and for the first time an oil derived from wood was obtained in large quantities.

Noting that the number of tests that can be conducted at Albany are limited and would be insufficient for a systematic investigation of the influences of the various process variables to arrive at optimum conditions, LBL proposed the construction of a continuous process evaluation unit that would simulate the Albany Facility and incorporate a tubular reactor that is lacking at Albany. During FY 79, LBL designed, fabricated and procured the necessary equipment for the continuous unit shown schematically in Fig. 1. The objectives of this engineering effort are:

- 1) To screen the influences of process variables and provide a data base for

the test runs that can be conducted at Albany.

- 2) To provide engineering data regarding heat, momentum transfer, and reaction rates for the design of a reactor and other process units that may be (or has to be) incorporated into the Albany facility.
- 3) To screen, under continuous flow conditions, promising process concepts that may come from bench-scale batchwise experiments being conducted at participating laboratories and to provide firm data base for pilot scale reactor design.

The construction of this unit will be completed in December 1979. It is anticipated that the unit will be operational during February, 1980. The expected oil production rate is between 2.5 to 5 gallons per day if operated on a 24 hour basis.

In summary, the PDU monitoring effort by LBL consisted of the following efforts:

- 1) To overcome the mechanical and operational difficulties of the existing facility.
- 2) To examine the chemical, technical, and economic feasibility of the Bureau of Mines Liquefaction Process.
- 3) To develop and evaluate the feasibility of an alternative process.
- 4) To undertake supporting research.

#### PLANNED ACTIVITIES FOR 1980

##### Project Evaluations and Novel Process Concepts

Various research institutions are conducting research solely dedicated to biomass liquefaction. LBL will provide DOE with an independent evaluation of the technical progress made in the projects authorized by DOE based on reviews of reports issued and analyses of data provided. As in FY 79, LBL

will provide DOE with evaluation of projects that may have produced promising results or may have been brought to the attention of DOE because of attractive claims or discoveries. The technical approach by LBL for the evaluation and enhancement of such results and/or claims will be the same as in FY 79.

In FY 80, it is anticipated that LBL will follow a process scheme advanced by SRI that involves molybdate salts as a catalyst. The preliminary results reported indicate the synthesis of a high quality oil (toluene soluble) with reasonable large yields (57%). Another scheme worthy of following is the biomass thermolysis advanced by Wright-Malta and Pacific Northwest Laboratory.

The third promising scheme planned for investigation concerns dissolution of wood by chemicals derived from hydrogenation followed by catalytic hydrogenation of dissolved wood. It is now under scrutiny.

##### Monitoring

In FY 80, LBL formulated and issued an operating directive to remedy or correct the short-cuts or improvisations made at Albany in producing six barrels of oil using the LBL process, because they concern the technical and economic feasibility of the process in question. If this operating directive is successfully carried out, LBL will issue an operating directive to test the new process option under the condition that assures its technical feasibility.

##### Research and Engineering Studies

This task is the core of the LBL in-house program. It consists of:

##### Prehydrolysis and Slurrying Studies

The objectives of this task are 1) to find conditions that maximize wood/water ratio and 2) to provide a data base for design of a continuous prehydrolyzer. The base-line water/wood ratio in

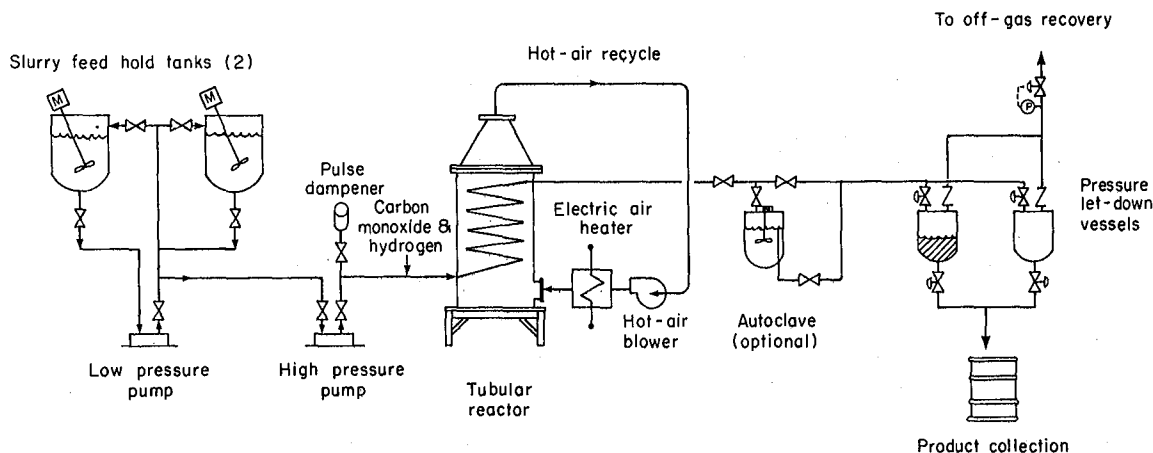


Fig. 1. Biomass liquefaction process evaluation unit LBL process. (XBL 7910-4293)

the LBL process (based on estimates from batchwise experiments) was  $77/23 = 3.35$ . Recirculation studies already conducted (during October–November, 1979) showed that this base-line condition is technically feasible in a continuous mode of injection. If this ratio can be reduced to  $69/31 = 2.23$ , it would result in 35% increase in oil production per unit reactor and, at the same time, a 34% decrease in reactor heat input requirement, i.e., the economics of the wood liquefaction process would improve tremendously. For this reason LBL will explore the influences of pH, temperature, time on prehydrolysis. This effort requires tedious analytical work and physical experimentation.

#### Catalysis Studies

The objective of this subtask is to provide a database for the chemistry and kinetics of liquefaction, product upgrading, etc. This will be accomplished through exploratory research on catalysis, investigation of the influence of process variables and process improvement options, and catalytic hydrogenation of product oil.

#### Engineering Development

The scope of the engineering development progress is given below:

##### Continuous Process Evaluation Experiments

- Installation of process evaluation unit (PEU)
- Calibration and shakedown tests

- PEU performance evaluation
  - Evaluation of process variables
  - Database for design
- Exploratory Design Investigations
- Definition of design parameters
  - Acquisition of data required
- Integrated Plant Concepts
- Process flowsheet developments
  - Comparative economic feasibility assessments

#### FOOTNOTE AND REFERENCES

\*This work was supported by the Assistant Secretary for Energy Technology, U.S. Dept. of Energy.

1. S. Ergun, "Economic Feasibility Assessment of Biomass Liquefaction," Lawrence Berkeley Laboratory Report LBL-9192 (1979).
2. S. Ergun, "An Overview of Biomass Liquefaction," Lawrence Berkeley Laboratory Report LBL-9188 (1979).
3. C. Figueroa and S. Ergun, "Direct Liquefaction of Biomass: Correlative Assessment of Process Development," Lawrence Berkeley Laboratory Report LBL-9189 (1979).

## LBL CONTINUOUS BIOMASS LIQUEFACTION PROCESS ENGINEERING UNIT (PEU)\*

*S. Ergun, C. Figueroa, C. Karatas, and J. Wrathall*

#### INTRODUCTION

Ever since the commissioning and subsequent operation of the Albany, Oregon Biomass Liquefaction Process Development Unit (PDU) in 1977, it became very evident that the PDU would be unable to provide basic reactor design data for a commercial-sized plant. Beginning in 1977, LBL was contracted to provide technical monitoring followed in 1978 by supporting research. LBL research efforts were divided into three areas:

- 1) Biomass liquefaction catalysis
- 2) Biomass pretreatment-hydrolysis
- 3) Construction of a continuous biomass liquefaction PDU.

Discussion centers on the latter of these three areas.

#### ACCOMPLISHMENTS DURING 1979

The intent of the PEU was to provide engineering support to the Albany, Oregon PDU. However, it later became clear that basic engineering design data for slurry pumping and the reactor would be the final product. Undertaking this task meant long-term planning as high-pressure equipment generally have long delivery times. By January 1979, a detailed schematic for the PEU was finalized as shown in Fig. 1. Major or minor equipment investigations, specifications, and procurement commenced and proceeded into late 1979.

Completion of major piping, electrical, and instrumentation is expected by December 1979. Preliminary shakedown testing will continue for three months, after which a preliminary liquefaction run is expected by March 1980.

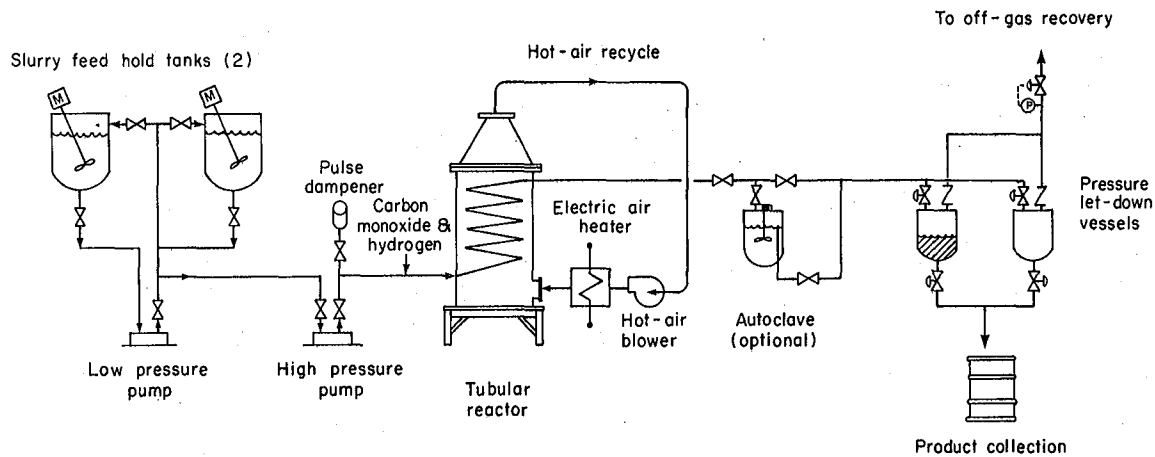


Fig. 1. Biomass liquefaction process evaluation unit LBL process. (XBL 7910-4293)

During the months of October and November, 1979, extensive testing of the PEU slurry pumping capabilities took place and is the subject of an unpublished report.<sup>1</sup> Findings from this study indicate that hydrolyzed biomass slurries of 20% can be easily pumped without any difficulties. The key to this capability apparently lies with the slurry ability to uptake gas (approximately 10% by volume).

#### FOOTNOTE AND REFERENCE

\*This work was supported by the Assistant Secretary for Energy Technology, U.S. Dept. of Energy.

1. J. A. Wrathall, "Hydrolyzed Wood-Slurry Flow Modeling," Lawrence Berkeley Laboratory Report LBL-10093 (In press).

## SELECTIVE HYDROGENATION OF COAL\*

*E. A. Grens, T. Vermeulen, J. T. Edwards,  
F. Hershkowitz, P. J. Joyce, J. A. Maienschein,  
C. O. Onu, J. H. Shinn, and G. H. Zieminski*

### INTRODUCTION

Coal liquefaction processes currently under development operate by thermal decomposition (pyrolysis) of the coal in a hydrocarbon medium followed by hydrogenation of the initial pyrolysis products, often with the aid of heterogeneous catalysts. The thermal degradation reactions are not selective, and do not take advantage of reactive bond types in the coal structure. They produce a wide range of products, including light hydrocarbon gases and refractory char. The former contribute to high hydrogen consumption while the latter require special processing (e.g., gasification) for their utilization. The coal pyrolysis is required because pyrolysis temperatures, and solid catalysts can not promote the reaction of the solid coal material.

The objective of this project is to convert coal to liquid products by the use of homogeneous catalysts that promote selective scission of certain bonds in the coal structure below coal pyrolysis temperature. The bonds to be attacked are those

linking conjugated hydroaromatic groups in the coal, including aliphatic bridges and oxygen links (e.g., ether bridges). The catalysts are dissolved in, or constitute, a liquid reaction medium and have access to the extensive interior pore surfaces in the coal.

Included in this research program are studies of the interaction of organic solvent media with coals, the effects of homogeneous catalysts in promoting reactions at moderate temperatures, and the use of inorganic Lewis-acid type melts as catalytic media for coal conversion. The action of the catalytic treatments on model chemical compounds containing certain types of bond structures found in coal is examined to elucidate the mechanisms of coal decomposition. Transport processes for coal reaction products and dissolved hydrogen gas are considered to determine the extent to which these processes may limit conversion rates.

This project was initiated in January 1974, and during its first three years concentrated on

studies of the action of organic and inorganic reaction media on sub-bituminous coal and on model compounds. The inorganic melts examined as catalysts include phosphoric acid, sodium hydroxide, and zinc chloride. In 1977, the studies began to focus on use of mixed organic-inorganic treatment media, in particular zinc chloride melts in combination with hydroaromatic solvents (e.g., tetralin) or with alcohols (e.g., methanol). This type of coal treatment was found to be much more effective than treatment with either organic or inorganic media separately, doubling or tripling conversions compared to those obtained with treatment and single medium under the same temperature conditions.

#### ACCOMPLISHMENTS DURING 1979

The project activities planned for 1979 were directed mainly to investigation of the effect of treatment parameters on the conversions of coal in zinc chloride/organic mixed media. The work utilized sub-bituminous coal because of its high reactivity under these treatments. The reaction paths were explored by successive treatments at different temperatures and of fractionated intermediate reaction products. Product analyses and characterization were emphasized to provide insight into the manner by which treatment parameters influence conversion, and proposed reaction mechanisms were treated through model compound studies. Reaction rate studies were also conducted for coal-solvent and coal-melt-solvent interactions.

#### Interaction of Coal with Organic Solvents

(Grens, Zieminski)

The rate of dissolution of coal in hydroaromatic organic solvents was studied over the temperature range 200-300°C in specially designed apparatus having a time resolution of about 30 s (heating, cooling, and sampling times of the order 10 s). The rates of such interactions are important because these solvents serve to promote access of reactive species and catalysts to the coal interior structure and to remove reaction products from the coal.<sup>1</sup> Studies of Wyodak coal in tetralin show relatively slow overall dissolution kinetics (70% of ultimate in 20 minutes) with modest influence of coal particle size. The initial extraction rates for -100 mesh coal significantly exceeded those for -30 mesh, but after 10 minutes the rates were comparable. Stirring rates beyond those required to achieve uniform coal mixing in the solvent had no significant effect. The initial dissolution reaction shows an apparent activation energy of around 8 kcal/gmole, and apparently is both reaction and pore diffusion controlled. The dissolution mechanisms will be further examined in the coming year.

#### Coal Conversion in Zinc Chloride/Tetralin Mixtures

(Grens, Edwards, Hershkowitz, Maienschein)

During the past year, our investigations of coal conversion in mixed organic-inorganic media have been primarily on one two-phase system, zinc chloride/tetralin, and one single-phase system, zinc chloride/methanol. In both cases detailed investigations of reaction conditions and product properties have been undertaken.

The treatment of coal in zinc chloride/tetralin media has usually involved 50 g of Wyodak sub-bituminous coal with 300 g of ZnCl<sub>2</sub> melt (10% H<sub>2</sub>O) and 50 g of tetralin.<sup>2</sup> The rates of conversion to oils (cyclohexane solubles), asphaltenes (incremental toluene solubles), and preasphaltenes (incremental pyridine solubles), have been determined in the 200-300°C temperature range (initial coal pyrolysis is at about 325°C). As shown in Fig. 1, for 300°C treatment, the conversion to preasphaltenes is quite rapid, with subsequent slower conversions to asphaltenes and oils. Experiments in which products were fractionated (into oils, asphaltenes, preasphaltenes, and residue) after short reaction time, and then separately treated for additional time, establish that conversion proceeds through preasphaltenes and asphaltenes to oils, as well as directly from preasphaltenes to oils.

It has been previously noted that conversion of Wyodak coal by this procedure is accompanied by large reductions of the oxygen content of the coal, and certainly involves catalytic scission of oxygen linkages in the coal. We have examined this phenomenon in more detail by chemical analyses of the coal and coal products, for hydroxyl and carbonyl oxygen, and by difference for other (largely ether) oxygen content. These studies have established that the conversion of coal to preasphaltenes involves major reductions in ether oxygen (the carbonyl oxygen content is small), while the conversion of preasphaltenes to oils involves removal of hydroxyl oxygen.

The analysis of soluble products from the reactions indicates a relatively uniform decrease in molar H/C ratios of these products with increasing extent of conversion, as illustrated in Fig. 2, extending over a wide range of treatment media and temperatures. The products of more complete conversion have lower H/C ratios than the original coal (1.0 in the coal). Examination of residues as well as extracts indicates significant internal hydrogen transfer in the processes.<sup>3</sup> The molecular-weight distribution in the products is characterized by gel-permeation chromatography in pyridine and (for oils) in tetrahydrofuran. Representative

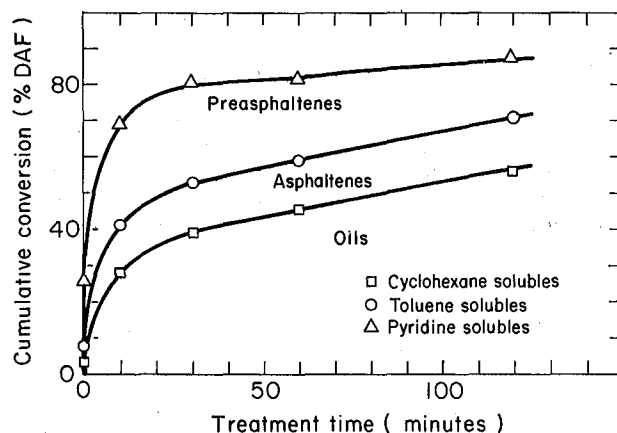


Fig. 1. Effect of treatment time at 300°C. 50 g Wyodak coal + 275 g ZnCl<sub>2</sub> + 50 g tetralin + 35 bar H<sub>2</sub>. (XBL 801-75)

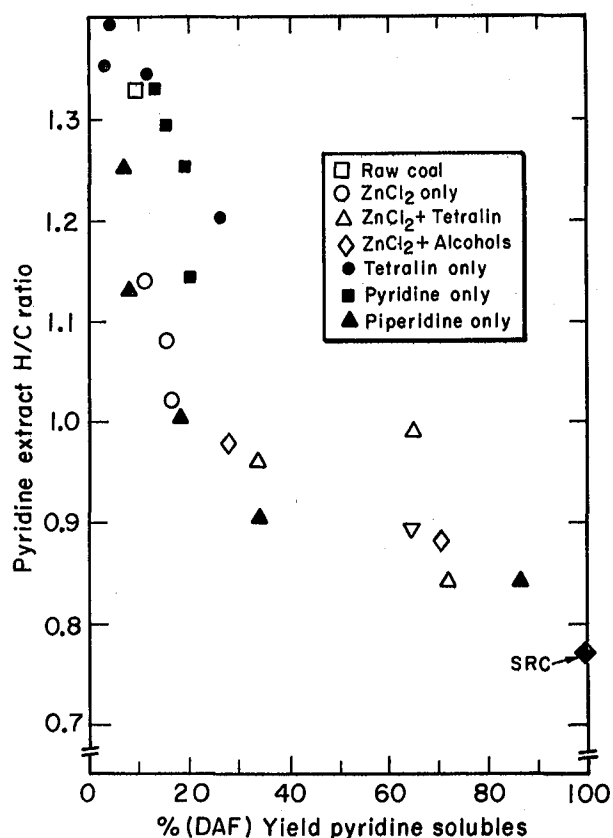


Fig. 2. Wyodak coal extracts after treatments in various media at 200 to 300°C. (XBL 7811-3698)

chromatograms are given in Fig. 3; the high-MW peak for preasphaltenes represents colloidal material that slowly precipitates in the pyridine solution. The wide molecular-weight ranges, and large degrees of overlap, of these fractions is apparent. Although the characterization into oils, etc., by fractional solubility is a standard procedure in coal research, its validity as a measure of meaningful product characteristics is extremely limited, and alternate characterizations are being investigated.

The coal conversion products also are examined by proton NMR spectrography for the aromaticity of their hydrogen content and, indirectly, of their carbon structure. Typically the oils produced have aliphatic-to-aromatic hydrogen ratios of about 1.7, and Brown-Ladner carbon aromaticities of about 0.7; these are far less aromatic materials than those produced by higher temperature conversion methods such as the solvent-refined coal process.

The zinc chloride/tetralin treatment studies are now being extended to determine the effect of inorganic melt acidity and water content on product yields and properties. The treatments are also being applied to model compounds, including those with hydroaromatic and aromatic nuclei linked by ether and aliphatic bridges, to investigate the mechanisms and kinetics of action on specific bond types.

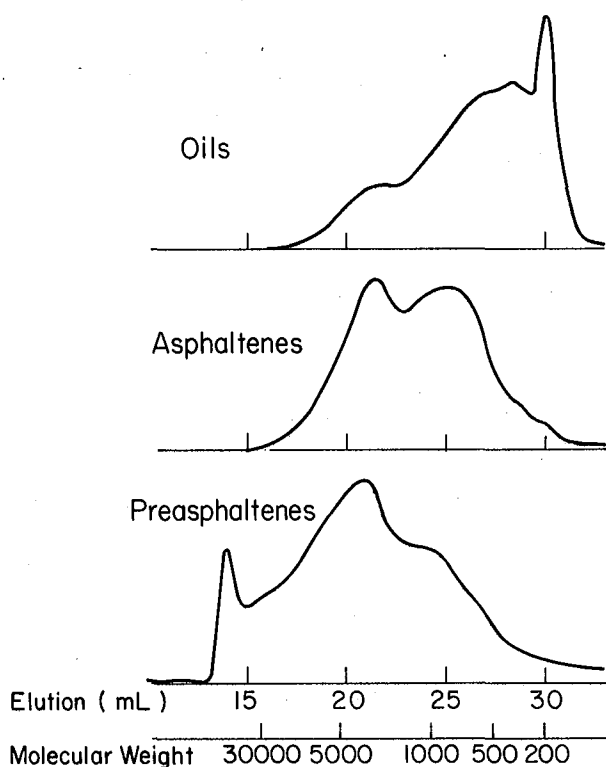


Fig. 3. Gel permeation chromatogram of products Wyodak coal with  $ZnCl_2$  + tetralin 300 C and 25 bar  $H_2$  for 1 hour. Pyridine carrier - 1 mL/min 100A + 500A + 1000A styragel 313 nm UV detector.

(XBL 801-74)

#### Coal Conversion in a Zinc Chloride/Methanol Melt

(Vermeulen, Onu)

When methanol addition is used in zinc chloride melt treatment of sub-bituminous coal (serving to depress the  $ZnCl_2$  melting point), relatively high conversions to solvent-soluble products are obtained. Total-conversion levels approaching 90% at 250°C, and 95% or better at 275°C, were reported for 1978.<sup>3,4</sup>

Efforts to extract the products from the melt-coal suspension at 250°C with decalin or other high-boiling solvents have been only partially successful, suggesting that the preasphaltene fraction is strongly complexed with the zinc chloride. This finding has focused special attention on the need to obtain a high conversion of preasphaltenes to lower-molecular-weight products.

Two effects have been utilized to reduce the preasphaltene content of the products--addition of zinc metal to the  $ZnCl_2$  melt, and staged increases in processing temperature.

Higher molar hydrogen-carbon ratios appear to correlate with increased production of oils. The addition of metallic zinc to the zinc chloride/

Table 1. Effect of zinc metal addition to  $ZnCl_2$  melt, in treatment of Wyodak coal at 275°C (or 300°C) for 30 minutes (50 g coal with 30 g melt).

Run No.	Pressure of $H_2$ (bar)	Additives	Extractibles, daf Basis %			Atomic H/C
			Oil	Asph.	Preasph.	
5	35	10% $CH_3OH$ , 10% $CaCl_2$	17	14	57	0.89
2	35	same + 1.5% Zn	28	11	35	1.02
43	55	14% $CH_3OH$	22	15	63	1.01
44	55	14% $CH_3OH$ , 1.5% Zn	30	16	54	1.03
51	55	14% $CH_3OH$ , 3% Zn	32	15	53	1.05 est.
54 <sup>a</sup>	55	10% $CH_3OH$	17	14	61	0.88
77 <sup>a</sup>	55	14% $CH_3OH$ , 3% Zn	33	17	50	1.04

<sup>a</sup>300°C

Table 2. Effect of temperature staging in treatment of Wyodak coal at 55 bars hydrogen, with 3% Zn and 14%  $CH_3OH$  (50 g coal with 300 g melt).

Run No.	Temp (°C)	Time (min)	Extractibles, daf Basis, %			Atomic H/C
			Oil	Asph.	Preasph.	
70	275	15	31	14	54	1.00
51	275	30	32	15	53	1.05 est
63	275	45	35	15	48	1.09
76	{ 275 300 }	{ 15 15 }	37	18	45	1.10
69	{ 275 300 325 }	{ 15 15 15 }	46	10	44	1.10
73	{ 275 300 325 }	{ 15 15 30 }	54	10	36	1.19
74	{ 275 300 325 340 }	{ 15 15 15 15 }	51	9	40	1.13
79 (without Zn)	{ 250 275 300 325 }	{ 10 10 10 10 }	27	10	63	1.09
78 with Zn)	{ 250 275 300 325 }	{ 10 10 10 10 }	40	15	45	1.06

methanol melt appears to increase the yield of oils and also to prevent low H/C values, as is shown in Table 1. It appears possible that the zinc dissolves into the melt to form catalytically active monovalent-zinc ions such as  $Zn_2^{++}$ .

The question of time-temperature relations and the selection of optimum temperatures sequences has been studied in several comparative runs for the  $ZnCl_2$ /methanol treatment. It has appeared likely that different types of bonds have different thresholds for  $ZnCl_2$ -catalyzed scission, as well as for thermal pyrolysis, and hence that higher-temperature treatment will give more complete conversion.

In Table 1, comparison between run 51 at 275°C and run 77 at 300°C shows almost no advantage for the higher temperature. However, in Table 2, run 76 at 275°C and 300°C in succession is clearly superior to run 51 entirely at 275°C (both for 30 minutes). Adding 15 minutes at 325°C (run 69) or 30 minutes at 325°C (run 73) produces highly significant improvement. The results for run 77 may show that treatment at 300°C or above should be preceded by treatment at 275°C.

Pushing the reaction mixture of 340°C for 15 minutes (run 74) appears to reverse the beneficial effect of 325°C, possibly by fostering coke-forming reactions. Run 78 can be considered kinetically similar to 15 minutes at 275°C and 15 minutes at 325°C, and indeed comes out between runs 76 and 69. Thus, while pretreatment at 275°C appears beneficial, pretreatment at 250°C seems to impart no further advantage.

The inference from these runs is that a sequence of 275°C briefly and 325°C for a longer period will give the lowest residual preasphaltene in the shortest total time. The possibility remains that tetralin added to the methanolic  $ZnCl_2$  will give still better conversion. Comparison of run 73 with the tetralin/aqueous  $ZnCl_2$  results (Fig. 1) shows about the same total for preasphaltene plus insoluble residue after 60 minutes of treatment. These combined treatments will be further studied during the coming year.

#### Slurry-Reactor Development for Coal Conversion by Zinc Chloride Melt

(Vermeulen, Joyce)

In a consideration of large-scale reactor concepts for melt treatment of coal, it has been concluded that a plug-flow type of reactor can be used, with minimum costs for both construction and maintenance. The reactor should operate with downflow of slurry and counterconcurrent (upward) flow of hydrogen. To achieve a relatively uniform gas flow of hydrogen and minimize the excess input of hydrogen, the input hydrogen can be fed at several levels (perhaps five).

Because water is produced from the original oxygen content of the coal, residual hydrogen should be withdrawn near the mid-height of the reactor to insure that water does not accumulate by reflux in the melt and correspondingly lower its catalytic activity.

It is projected that slotted trays could be used to reduce backmixing of the slurry by equalizing the pressure drop throughout each cross section of the reactor. The trays would restrict axial mixing in the slurry, and might also enhance the hydrogen holdup and the interfacial area available for gas-liquid mass transfer.

Exploratory mass-transfer measurements at room temperature have been made (on helium in a nitrogen carrier gas stream) with zinc chloride solutions in water, glycol, and glycerol, to determine whether zinc chloride exerts any special adverse physical effects (such as foam formation) on mass transfer. Slurry viscosities up to 100 centipoise, simulated by viscous solutions, showed an inverse square-root dependence of mass-transfer rate upon viscosity, in agreement with existing correlations. Even at the upper viscosity level, the mass-transfer rate projected for hydrogen under reaction conditions is approximately ten times the anticipated chemical rate of hydrogen consumption by the coal contained in the slurry.

#### FOOTNOTE AND REFERENCES

\*This work was supported by the Director, Energy Research, U.S. Dept. of Energy.

1. E. C. Harris and E. E. Petersen, "Change in Physical Characteristics of Roland Seam Coal with Progressive Solvent Extraction," in press for Fuel (1979).
2. E. A. Grens, F. Hershkowitz, R. R. Holten, J. H. Shinn, and T. Vermeulen, "Coal Liquefaction Catalysis by Zinc Chloride Melts in Combination with Organic Solvents," Lawrence Berkeley Laboratory Report LBL-9372 (1979).
3. J. H. Shinn and T. Vermeulen, "Coal Conversion Catalysis using Zinc Chloride in Organic Media," Lawrence Berkeley Laboratory Report LBL-9372 (1979).
4. J. H. Shinn and T. Vermeulen, "High-Yield Coal Conversion in a Zinc Chloride/Methanol Melt under Moderate Conditions," Preprints of the Division of Fuel Chemistry, American Chemical Society, 24, No. 2, pp. 80-88 (Honolulu, April 1979).
5. T. T. Derencsenyi and T. Vermeulen, "Kinetics and Mechanism of Metal-Carbonyl-Catalyzed Hydrogenation of Aromatic Hydrocarbon Models for Coal Constituents," Lawrence Berkeley Laboratory Report LBL-9777 (1979).

## COAL DESULFURIZATION\*

S. Ergun, S. Lynn, E. E. Petersen, T. Vermeulen,  
J. A. Wrathall, L. Clary, G. Cremer, J. Meshner,  
D. A. Mixon, and M. C. Smith

### INTRODUCTION

The many coals of the United States were formed under a wide variety of conditions and, as a result, display a wide range in all properties of interest. For example, pyrite weight percent varies from nearly 0 to 20%, while organic sulfur varies from 0 to 10%. These two properties can be used to classify coals for optimum end use.

Coal is most economically used as a direct boiler fuel. However, motor fuel supply cannot drop significantly without serious economic and social disturbance. Thus coal, by necessity, must also serve as a feedstock for liquefaction processes as petroleum availability declines.

#### Direct Burning of Coal

A combination of environmental and economic considerations dictates the amount of sulfur that can be emitted by coal-fired facilities. This, in turn, sets limits on the amount of sulfur in the coal to be burned. Other properties, such as free-swelling index, mineral matter composition, and volatility determine whether a particular coal can serve as a boiler fuel. Thus, both environmental and technical considerations enter into selection of boiler fuels.

#### Applicability of Cleaning Processes to U.S. Coals

Since current coal cleaning processes remove only a fraction of the total sulfur,<sup>1</sup> the question arises as to what fraction of U.S. coals can be cleaned to comply with current EPA new source standards (1.2 lb. SO<sub>2</sub> per MBtu). A number of studies have shown the fraction to be encouragingly large. A report on the applicability of the Meyers process<sup>2</sup> estimates, on the basis of 35 coals sampled, that 40% of the samples could be burned cleanly after some combination of physical separation and chemical leaching.

A report by Ergun<sup>3</sup> on coal cleaning gives the higher estimate of cleanability of 56%, based on 455 samples properly weighted between Eastern and Western coals. Beyond this figure, Ergun estimates an additional 17% is cleanable if 30-40% of the organic sulfur is removed, bringing the total cleanable to 73%.

Data from a study by Cavallaro,<sup>4</sup> with coal reserves taken from a study by Beekers,<sup>5</sup> give an estimate in agreement with that of Ergun on the amount of coal cleanable by pyrite removal.

In summary, it can be seen that cleanable coal reserves increase by 33% if processes are used which can remove what are probably the more reactive organic sulfur species,<sup>6</sup> such as aliphatic

mercaptans, sulfides, and disulfides. A process which attacks the refractory thiophenic sulfur could conceivably increase the cleanable coal reserves by another 20 - 30%, assuming roughly equal distribution between reactive and refractory organic sulfur.

#### History of the Project

Prior work concentrated on developing and evaluating separate methods for removing both inorganic and organic sulfur from coal. A kinetic study of reductive desulfurization of heteroaromatic coal subunits (organic sulfur) was extended to the upgrading of a heavy residuum produced by solvent refining of coal.<sup>7</sup> Exploratory work on combustion of coals with sulfur-trapping salts indicated the possibility of a technically and economically feasible method of coal utilization that could be implemented with a minimum of process development.<sup>8</sup>

Sodium sulfides were found to attack pyrite (inorganic sulfur) with limited success,<sup>9</sup> while preliminary research into oxidative pyrite leaching showed that a concentrated ferric acid solution (Fe<sub>2</sub>(SO<sub>4</sub>)<sub>3</sub> + H<sub>2</sub>SO<sub>4</sub>) offered both kinetic and by-product recovery advantages over a similar process developed elsewhere.<sup>10</sup>

#### ACCOMPLISHMENTS DURING 1979

LBL is involved in five aspects of research on pretreatment of coal prior to combustion to decrease sulfur emissions.

The first aspect is development of an acidic oxidative leach process involving H<sub>2</sub>SO<sub>4</sub>, (a cheap and readily available bulk chemical) in combination with Fe<sub>2</sub>(SO<sub>4</sub>)<sub>3</sub> and O<sub>2</sub> or possibly H<sub>2</sub>O<sub>2</sub>. Pyrite oxidation is complete under mild conditions (160°C, 30 atm oxygen pressure). These process conditions have the advantages of recycling the reaction by-products, making it possible to remove the surplus byproducts in a relatively concentrated form that will permit economic recovery, minimizing the costs of chemical feeds for neutralization and of waste disposal, minimizing the raw-water requirements for such a process, and avoiding the formation of elemental sulfur, which requires an additional extraction step in similar presently available processes. As yet, the effect of the acid solution on organic sulfur is minor.

The second aspect involves development of techniques for independent analysis of sulfur forms other than pyrite or sulfate. The first has been directed toward spectrophotometric identification of elemental sulfur, which may be an unwanted by-product of pyrite oxidation, and also a component of raw coals. Both sulfur analysis and pyrite

oxidation are discussed in more detail in Lawrence Berkeley Laboratory Report LBL-9963.10

Another study has dealt with direct identification of organic sulfur, using x-ray fluorescence. Hitherto, this component has been determined as a difference between inorganic sulfur (pyrite, sulfate, elemental) and total sulfur.

The third aspect considers the question of whether the organic sulfur species in coal can be effectively converted to water-soluble products without serious loss in the coal's calorific value.

The fourth aspect is reductive desulfurization of primary conversion products from raw coal, for example high-sulfur forms of solvent-refined coal. The catalytic action of pyrite in hydrodesulfurization and the physical and chemical factors affecting that catalyses have been an area of study.

The fifth aspect is combustion of coal that has been treated with a "trapping agent," notably an alkali metal base or salt. Chemical costs for such treatment will probably be comparable to those for alkaline or neutral desulfurization, or lower if the cost of oxidizing agent ( $O_2$ , air,  $H_2O_2$ ) is included.

The last three activities and the x-ray analysis technique are discussed in Lawrence Berkeley Laboratory Report LBL-10118.11

#### PLANNED ACTIVITIES FOR 1980

Prior to any studies of reductive or oxidative coal desulfurization processes in the continuous units at the Coal and Biomass Laboratory at LBL, flow modeling of coal or related slurries will be carried out in order to determine the operating conditions necessary to overcome such problems as settling, channeling, slug flow, and solids holdup.

Several reactor heat exchange systems will be evaluated to determine which is most applicable to the processes being considered. Preliminary kinetic parameters will be developed for the ferric acid pyrite leach, as well as rough cost estimates for any new permutations of the process. A mathematical treatment of the sulfation reaction will be developed and tested with data from either a single-particle or fluid bed flow furnace, in order to obtain a better understanding of sulfur-trapping during coal combustion.

#### FOOTNOTE AND REFERENCES

\*This work was supported by the Assistant Secretary for Energy Technology, U.S. Dept. of Energy.

1. S. Ergun et al., "Analysis of Chemical Coal Cleaning Processes," BOM/USDI Report J0166191 (1977).
2. J. Hamersma et al., "Meyers Process for Coal Desulfurization;" in Wheelock, Coal Desulfurization, ACS Symp. Ser 64 (1977).
3. S. Ergun, "Analysis of Technical and Economic Feasibility of Coal Cleaning by Physical and Chemical Methods," Nov. 1977. LBL Report to be published.
4. J. A. Cavallaro et al., Sulfur Reduction Potential of U.S. Coals. USDI/BOM RI 8118 (1976).
5. T. F. Beekers and R. E. C. Weaver, Coal Use in Louisiana, State of Louisiana Dept. of Natural Resources, Baton Rouge (1978).
6. E. Mendizabal, Low Temperature Processes for Coal Desulfurization, M. S. thesis, U. C. Berkeley (August 1976).
7. J. Wrathall and E. E. Petersen, "Desulfurization of Coal Model Compounds by Sodium Dispersion," 71st AICHI Meeting, Miami (1978).
8. J. Wrathall and E. E. Petersen, "Desulfurization of Coal Model Compounds and Coal Liquids," Lawrence Berkeley Laboratory Report LBL-8576 (1979).
9. J. Mesher and E. E. Petersen, "Coal Desulfurization via Chemical Leaching with Aqueous Solutions of Sodium Sulphide and Polysulphide, Lawrence Berkeley Laboratory Report LBL-9386 (1979).
10. D. A. Mixon and T. Vermeulen, "Oxydesulfurization of Coal by Acidic from Sulfate Solutions," Lawrence Berkeley Laboratory Report LBL-9963 (1979).
11. S. Ergun, T. Vermeulen, and J. A. Wrathall, "Coal Desulfurization Prior to Combustion," Lawrence Berkeley Laboratory Report LBL-10118 (1979).

## PROCESSING OF CONDENSATE WATERS FROM SOLID-FUEL CONVERSION

C. J. King, S. Lynn, D. N. Hanson,  
D. C. Greminger, G. P. Burns, D. H. Mohr,  
J. D. Hill, and N. E. Bell

### INTRODUCTION

Nearly all approaches for converting solid fuels (coal, oil shale, biomass) to gaseous or liquid fuels produce substantial amounts of process-condensate water. This water is formed by condensation from the reactor effluent as it is cooled. It typically contains large amounts of ammonia, carbon dioxide and dissolved organics. In some cases there are also substantial quantities of nonvolatile salts and sulfur-containing compounds. There are also toxic substances, such as polynuclear aromatics, nitrogen heterocyclics, and cyanides. Water supply, environmental considerations and process economics dictate that such waters be purified sufficiently to allow a high degree of recycle.

Conventional biological treatment has often given poor results for these condensate waters. Also, biological-treatment processes are highly sensitive to upsets in feed concentration and are of questionable value for various refractory substances, such as trihydric phenols (trihydroxybenzenes). Consequently, the thrust of this project is process research directed toward physico-chemical treatment methods, such as combinations of solvent extraction and stripping, followed by carbon adsorption if necessary, to provide sufficient removal of organics and ammonia to allow recycle as cooling-tower make-up.

Process condensates from coal conversion contain large amounts of phenols. Among these, the di- and trihydric phenols are the most difficult to remove. They are also strong precursors of color. Hence the project is directed toward development of effective extraction solvents for these compounds. Another area of concern is innovative and effective combination of stripping and extraction processes to reduce the large energy (steam) requirement for stripping of ammonia. Ammonia is difficult to strip because of chemical interaction of the basic ammonia with CO<sub>2</sub>, H<sub>2</sub>S and carboxylic acids in aqueous solution.

The project was started in October 1977. Through 1978, accomplishments included characterization of phenolic compounds present in process condensates from the SRC liquefaction process and the Synthane gasification process, using flame-ionization gas chromatography, mass spectrometry and high-performance liquid chromatography.<sup>1</sup> It was confirmed that darkening of the waters is associated with pyrocatechol, resorcinol, and possibly other polyhydric phenols as well. Initial explorations were made of the effect of pH on equilibrium distribution coefficients for extraction of phenolics. This question is of importance since the pH of condensate waters tends to be in the range 8.0 to 9.5, where applicable fractions of the phenolics can be ionized.

### ACCOMPLISHMENTS DURING 1979

#### Analysis of Water Samples

The analyses by gas chromatography and liquid chromatography (HPLC) described in the 1978 report were extended to demonstrate the existence of 610 ppm of a trihydric phenol, phloroglucinol (1,3,5-trihydroxybenzene), in an aged sample of condensate water from the SRC coal-liquefaction demonstration plant in Ft. Lewis, Washington.<sup>1</sup> This is the first quantitative report of a trihydric phenol and is significant since nearly all previous analyses of coal-conversion condensate waters have been conducted in ways that would not reveal trihydric phenols, and since the trihydric phenols are quite resistant to biological oxidation.

#### Extraction of Phenols

Measurements of equilibrium distribution coefficients for solvent extraction of various phenols from synthetic aqueous solutions were made for several purposes--(1) to assess the relative capacities of different solvents, (2) to determine the relative distribution coefficients for different mono-, di-, and tri-hydric phenols, (3) to quantify the effect of pH on the equilibrium distribution coefficients for different phenols in various physical solvents, and (4) to determine the effect of temperature on the equilibrium distribution coefficient.

#### Effect of pH

Figure 1 shows equilibrium distribution coefficients for extraction of resorcinol (1,3-dihydroxybenzene) from water into diisopropyl ether (DIPE) as a function of aqueous-phase pH.<sup>1</sup> DIPE is the solvent in the Lurgi Phenosolvan process. The solid curve represents the prediction of a model based upon the assumption that the non-ionized portion of the resorcinol distributes between phases in accord with the distribution coefficient at low pH, while the ionized portion is totally non-extracted:

$$K_D = \frac{K_{D, \text{low pH}}}{(K_a/[H^+]) + 1} \quad (1)$$

Here,  $K_D$  is the equilibrium distribution coefficient (wt. fraction in solvent phase/wt. fraction in aqueous phase), and  $K_a$  is the acid dissociation constant for resorcinol.  $K_{D, \text{low pH}}$  is a fitted parameter, and  $K_a$  is taken from the literature. Similar results for extraction of other phenols into DIPE and MIBK also confirm the applicability of Eq. 1, based upon literature values of  $K_a$ .

Table 1 gives values of  $K_{D, \text{low pH}}$  determined for different phenols extracted from water into DIPE and methyl isobutyl ketone (MIBK), along with

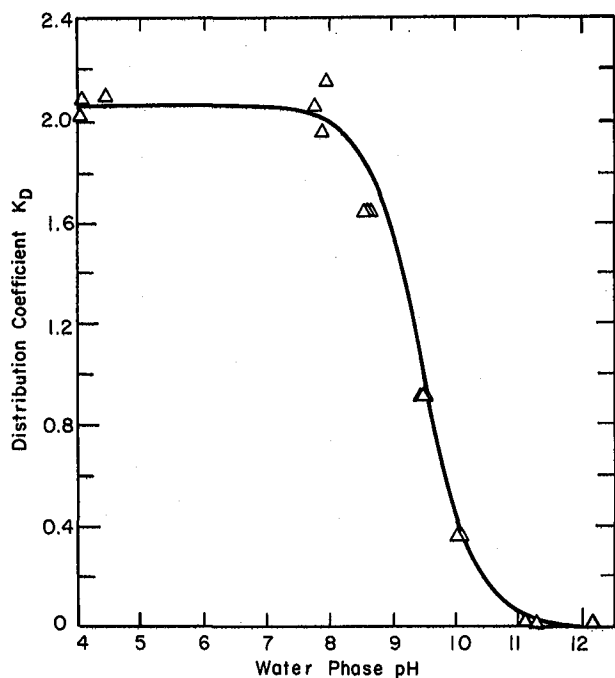


Fig. 1. Equilibrium distribution coefficient of resorcinol at high dilution between DIPE and water vs. pH at 298 K. Solid curve is based upon Eq. 1, with  $K_{D, \text{low pH}} = 2.06$  and  $K_a = 3.36 \times 10^{-10}$ .  
(XBL 795-6299)

values of  $K_a$  determined from the literature.<sup>1</sup> Since condensate waters from solid-fuel conversion processes typically fall in the pH range between 8 and 9.5, one can see from Eq. 1, Fig. 1 and Table 1 that ionization of the different phenols can substantially reduce  $K_D$  below the low-pH values.

#### Polyhydric Phenols

From Table 1 it is apparent that the dihydric phenols are much less extracted than phenol itself, and that the trihydric phenols are even less extracted than the dihydric. This is a direct result of the very low activity coefficients of the polyhydric phenols in water; adding more -OH groups increases water compatibility. Since the polyhydric phenols are known to be present in substantial quantities in coal-conversion condensate waters, they will be substantially more difficult to extract than phenol, cresols, xylenols, etc.

#### MIBK vs. DIPE

Table 1 also shows that MIBK is much more effective than DIPE for removing polyhydric phenols. An extraction process requires that  $K_D S/W$  be 1.5 or more for good removal, where  $S$  = solvent flow and  $W$  = water flow. Therefore, very high solvent-to-water ratios ( $S/W = 1.5$  or more) would be required to remove the dihydric phenols using DIPE, even at low pH, while  $S/F$  of 8 or more would be required to remove trihydric. Such large solvent flows would pose a great economic penalty.

Table 1. Equilibrium distribution coefficients determined at low pH (3.8 - 5.8) for different phenols, along with literature values of  $pK_a$ .<sup>\*</sup> All values are for 298 K.

Solute	$K_D, \text{low pH}$		$pK_a$
	DIPE	MIBK	
Phenol	36.5	(90)**	9.98
Pyrocatechol (1,2-dihydroxybenzene)	4.9	18.7	9.48
Resorcinol (1,3-dihydroxybenzene)	2.1	17.9	9.47
Hydroquinone (1,4-dihydroxybenzene)	1.03	9.9	10.1
Pyrogallol (1,2,3-trihydroxybenzene)	ND	3.6	9.01
Hydroxyquinol (1,2,4-trihydroxybenzene)	0.18	5.0	NA
Phloroglucinol (1,3,5-trihydroxybenzene)	ND	3.9	8.44

<sup>\*</sup> -  $pK_a = \log_{10} [(K_a)^{-1}]$ . The value of  $pK_a$  is also the value of pH at which the solute is exactly half ionized.

\*\* - 303 K (Reference 2)

ND - not determined

NA - not available

### Effect of Temperature

Since condensate waters are available at temperatures above ambient, extraction at the source temperature would be attractive from the standpoint of minimizing heat exchange.  $K_D$  for phenol from water into MIBK was measured as a function of temperature, with the result that  $K_D$  decreases as temperature increases, dropping from 90 at 303K to 37 at 348K.<sup>2</sup> Thus the operating temperature for extraction should represent a compromise between lower  $K_D$  at higher temperatures and less cost for heat exchange at lower temperatures.

### Stripping of Residual Solvent

Solvents such as DIPE and MIBK have solubilities in waters of order 1%. Hence it is necessary to remove residual solvent before recycle of the water to a cooling tower. Alternatives include atmospheric and vacuum steam stripping, inert-gas stripping, and extraction with a hydrocarbon, such as isobutane. Conceptual-design studies were made for recovery of butyl acetate, DIPE or MIBK by vacuum steam stripping, operating at a pressure near the vapor pressure of water at the feed-water temperature. It was shown that the properties of MIBK are particularly well suited to this sort of recovery process, and that the vacuum steam-stripping approach is economically attractive for recovery of MIBK. This lends further incentive to the use of MIBK as a physical solvent for removal of phenols.

### Chemically Complexing Solvents

DIPE and MIBK are solvents which should interact with phenols through simple hydrogen bonding. Solvents which complex chemically in other ways were explored in a search for substances which would give higher  $K_D$  values for di- and tri-hydric phenols. Tertiary amines in the tri-C<sub>8</sub> to C<sub>10</sub> range have been found to be very effective for extraction of acetic acid, when mixed with a suitable diluent or co-solvent.<sup>3</sup> A commercial mixture of such amines (Alamine 336, General Mills, Inc.) was therefore tested as an extractant for the more weakly acidic phenolics.

For resorcinol,  $K_D$  was measured for Alamine 336 with four diluents (1/1 volume ratio, amine/diluent) -- 2-ethyl-1-hexanol (2EH), diisobutyl ketone (DIBK), Chevron Solvent 25 (a mixture similar to butylbenzene), and kerosene. Of these, Alamine 336 in 2EH gave the highest  $K_D$ , which was 5.0. However, 2EH by itself gave  $K_D = 3.7$ , so the effect of the amine was not large. For pyrogallol,  $K_D$  was 0.9 in 1/1 Alamine 336/2EH, and was 0.7 in pure 2EH. There were also problems of material-balance non-closure for resorcinol and of darkening, suggesting an undesirable loss of the amine as well.

In related EPA-sponsored research, tricresyl phosphate (TCP) was studied as an extractant for phenolics.  $K_D$  for phenol into undiluted TCP was 72, and  $K_D$  for phenol extracted into mixtures of TCP with MIBK, 2EH, and Chevron Solvent 25 was approximately what would be expected from a simple linear blend of the  $K_D$  values for TCP and for the pure diluents. Resorcinol and pyrogallol gave  $K_D$  values of 12 and 1.5, respectively, in pure TCP.

Phosphine oxides are stronger bases than phosphates, because of the greater electronegativity imparted to the phosphoryl oxygen by the presence of R- groups rather than RO- groups. Tri-n-octyl phosphine oxide (TOPO) [(C<sub>8</sub>H<sub>17</sub>)<sub>3</sub>PO], diluted in DIBK (1 part TOPO to 3 parts DIBK, by volume), was tested as a solvent for pyrogallol, giving a strikingly high  $K_D$  value of 110. Some unanswered questions still surround this result, however. Although commercial TOPO has a rather high cost--around \$10/lb--it is obviously worthy of further study as an extractant for polyhydric phenols.

### Stripping of NH<sub>3</sub> and CO<sub>2</sub>

We have assembled a batch, one-stage nitrogen-stripping apparatus for investigating removal of ammonia and carbon dioxide from condensate waters. We have also implemented and confirmed ion-selective electrodes as means of monitoring these two substances in solution. Initial tests have been carried out with synthetic solutions of NH<sub>4</sub>HCO<sub>3</sub> and (NH<sub>4</sub>)<sub>2</sub>CO<sub>3</sub> in water, with results for ammonia stripping which agree well with predictions from the equilibrium data of van Krevelen, et al.<sup>4</sup>

### Wastewater Workshop

Participants from the project organized and conducted a workshop on processing of waters from coal-conversion, shale-retorting and biomass-pyrolysis processes held at DOE headquarters in Germantown in June 1979. The proceedings are in press.<sup>5</sup>

### PLANNED ACTIVITIES FOR 1980

A short conceptual-design study will be made to assess the potential for fully physico-chemical, as opposed to biological, processing of condensate waters as a roughing treatment to enable recycle to a cooling tower. This will also identify the more critical questions and opportunities associated with bulk reduction of chemical oxygen demand (COD) by extraction, coupled with NH<sub>3</sub> stripping. Experimental studies of solvent extraction will be directed toward (1) identifying the most effective extraction solvent(s) and processing scheme for bulk COD reduction, and (2) development of improved extractants for polyhydric phenols. TOPO will be examined further as a solvent for phenols, as will any other substance identified as having comparable promise.

These efforts will be supported as needed by analytical studies of condensate waters from demonstration plants. One or more new samples of condensate water from the SRC demonstration plant at Ft. Lewis, Washington will be used to confirm and extend identifications of polyhydric phenols and to make a specific comparison of measured COD with the theoretical oxygen demand (TOD) predicted by adding contributions from individually identified constituents.

The apparatus for batch, one-stage stripping will be used to monitor rates of stripping of NH<sub>3</sub> and CO<sub>2</sub> from water samples from actual processes. These rates will then be interpreted in terms of the equilibrium data of van Krevelen, et al.,<sup>4</sup> as implemented by Edwards, et al.<sup>6</sup> and modified to allow for the presence of non-volatile anions and

cations. We shall also initiate experimental and conceptual design studies to assess the potential of an approach which uses two separation processes (e.g., stripping and extraction) simultaneously to remove both acid and basic substances, at a steam consumption less than that required for stripping alone.<sup>7</sup>

#### REFERENCES

1. D. C. Greminger and C. J. King, "Extraction of Phenols from Coal Conversion Process Condensate Waters," Lawrence Berkeley Laboratory Report LBL-9177 (1979).
2. G. P. Burns, D. N. Hanson, and S. Lynn, "Energy Reduction in Phenol Recovery Systems," Lawrence Berkeley Laboratory Report LBL-9176 (1979).
3. N. L. Ricker, J. N. Michaels, and C. J. King, J. Separ. Process Technol., 1, 36 (1979);  
N. L. Ricker, E. F. Pittman, and C. J. King, ibid., No. 2, in press.
4. D. W. van Krevelen, P. J. Hoftijzer, and F. J. Huntjens, Rec. Trav. Chim. Pays-bas, 68, 191 (1949):
5. C. J. King, S. Lynn, D. N. Hanson, and D. H. Mohr, Eds., "Processing needs and methodology for wastewaters from the conversion of coal, oil shale and biomass to synfuels," U.S. Dept. of Energy, Division of Environmental Control Technology, report in press.
6. T. J. Edwards, G. Maurer, J. Newman, and J. M. Prausnitz, AIChE Jour., 24, 966 (1978).
7. R. P. Cahn, N. N. Li, and R. M. Minday, Environ. Sci. & Technol., 12, 1051 (1978).

## APPLIED BATTERY AND ELECTROCHEMICAL RESEARCH PROGRAM

*E. J. Cairns and F. R. McLarnon*

#### INTRODUCTION

LBL, together with the San Francisco Operations Office (SAN), has assumed field management responsibility for the contracts comprising the Applied Battery and Electrochemical Research Program supported by the Energy Storage Systems Division (STOR) of the Department of Energy (DOE). This program provides the applied research base which supports all of the Electrochemical Systems missions in STOR, and the general objective of the program is to help provide electrochemical systems that satisfy economic, performance and schedule requirements. The specific goal of the project is to identify the most promising electrochemical technologies and transfer them to industry and/or another DOE program for further development and scale-up. The LBL participants in the program are: E. J. Cairns, L. C. DeJonghe,\* J. W. Evans,\* F. R. McLarnon, R. H. Muller,\* J. S. Newman,\* P. N. Ross,\* and C. W. Tobias.\*

#### ACCOMPLISHMENTS DURING 1979

This program started during July 1979, and an implementation plan has been prepared, describing how LBL, in cooperation with SAN, will conduct the management responsibilities, delineating appropriate managerial controls to meet the program objectives. LBL is contracting with and directing the activities of project participants. LBL is overseeing the technical status, costs and schedules of the technical projects, providing reports of same to STOR, and establishing appropriate project modifications. LBL maintains overall accountability for successful field management of the program.

#### PLANNED ACTIVITIES FOR 1980

The technical direction of the Applied Battery and Electrochemical Research Program for FY 1980 and beyond is described in the implementation plan and is designed to support the DOE Electrochemical Systems missions: electric vehicles, solar electricity, dispersed electric load-leveling, and energy and resource conservation. General problem areas addressed by the program include the identification of new electrochemical couples for advanced batteries, the determination of technical feasibility of the new couples, improvements in components of batteries under development by other Electrochemical Systems projects funded by STOR, and the establishment of engineering principles applicable to batteries and electrochemical processes. Major emphasis will be on applied research which will lead to superior technical performance and lower life cycle costs. The program is divided into three major research areas: Exploratory Battery R&D, Engineering Science Research, and Materials Research.

The Exploratory Battery R&D area provides for the study of new electrochemical couples, or of new approaches to known battery systems, and offers the prospect of developing better-performing, simpler, longer-life, safer, and/or lower-cost batteries. Research on the calcium/metal sulfide cell will progress toward the technology transfer stage, and exploratory work on such systems as solid electrolyte, organic electrolyte, and molten-salt cells will be pursued.

Engineering-Science Research will include morphological studies that address problems hindering the timely development of near-term batteries (lead/lead dioxide, iron/nickel oxide, and/or zinc/nickel oxide); phenomenological studies to provide basic information needed for the rational design, operation and control of electrochemical processes; studies on physiochemical methods for electrochemical research to aid the development of such advanced tools as ellipsometry and spectrometry for the detailed study of battery materials and processes; and modeling studies aimed at quantitative prediction of the dynamic behavior of cells, cell components and batteries.

Materials Research seeks to identify, characterize, and improve the materials and components to be used in batteries and electrochemical processes. Investigations of solid electrolytes, including those of ceramic (beta-alumina, NASICON), glass, and polymeric compositions, will continue, and advanced liquid electrolytes, such as low-temperature molten-salt mixtures and ionizing organic liquids, will be studied.

#### FOOTNOTE

\*Materials and Molecular Research Division of Lawrence Berkeley Laboratory.

## BATTERY ELECTRODE STUDIES\*

*E. J. Cairns and F. R. McLarnon*

### INTRODUCTION

The purpose of this work is to study the behavior of electrodes for rechargeable batteries, and to investigate means for improving their performance and lifetime. For example, some aqueous electrolyte batteries exhibit a redistribution of active material over the face of one or both electrodes, causing a significant loss in the cell's capability of storing energy. In cases such as this (e.g., Zn), the purpose of the work will be to investigate the mechanism(s) by which the redistribution of active material takes place, and to evaluate means of minimizing or eliminating the redistribution and thereby increase the electrode life. Other related purposes include the investigation of morphology changes, nucleation, and current density distribution. In the case of batteries with molten salt electrolytes, the purpose of this work will be to investigate the mechanisms of capacity loss of the electrodes and means for eliminating this loss.

The goal of this research program is to aid the development of rechargeable batteries for vehicle propulsion and energy storage applications, an area beset with significant problems in achieving adequate performance and lifetime at an acceptable cost. There are electrodes available with acceptable performance and potentially acceptable cost, but inadequate lifetime. In some cases, inadequate information is available concerning the precise cause(s) of short lifetime.

In the case of the zinc electrode, there are many theories concerning the cause(s) of active material redistribution over the face of the electrode, but none is recognized as being correct, or even in good agreement with observations. This is a significant problem because the cycle life of cells with zinc electrodes is inadequate for many applications, but the performance and projected cost are both acceptable. Furthermore, there are

several important cells that use zinc electrodes, and therefore could benefit from added knowledge about the zinc electrode. Examples of cells with zinc electrodes are: Zn/NiOOH, Zn/AgO, Zn/Br<sub>2</sub>, ZnCl<sub>2</sub>, Zn/Air, and Zn/MnO<sub>2</sub>.

High-temperature cells with molten salt electrolytes have been under investigation for at least two decades. During this period, a number of electrodes have been investigated for use as either the positive or negative electrode. The early work was concentrated on active materials which were liquid under cell operating conditions. These early cells (e.g., Li/S, Li/Se, Li/Te) demonstrated very high performance, but inadequate lifetime. Gradually, efforts have shifted to solid electrodes of more complex geometry and composition. At the same time, the cell performance was decreased, and the cell lifetime has increased. Present cell lifetimes are in the neighborhood of 10,000 h, with the goal being 3 to 10 times that, depending upon application. Cell performance is presently about 2/3 of the minimum goal. Examples of molten-salt cells of current interest are Li-Al/FeS, Li-Al/FeS<sub>2</sub>, Li-Si/FeS, Li-Si/FeS<sub>2</sub>, and Na/β-Al<sub>2</sub>O<sub>3</sub>/NaCl-AlCl<sub>3</sub>-SCl<sub>4</sub>.

The approach used in these investigations will be to study the problems discussed above under realistic cell operating conditions, with modern instrumental techniques for monitoring the behavior of the electrodes during operation. Post-test examination and analysis will also be carried out. The results will then be analyzed and used to test theories and candidate explanations for the behavior of the electrode. Using the results and compatible theories, improvements in the electrodes will be proposed and investigated.

### ACCOMPLISHMENTS DURING 1979

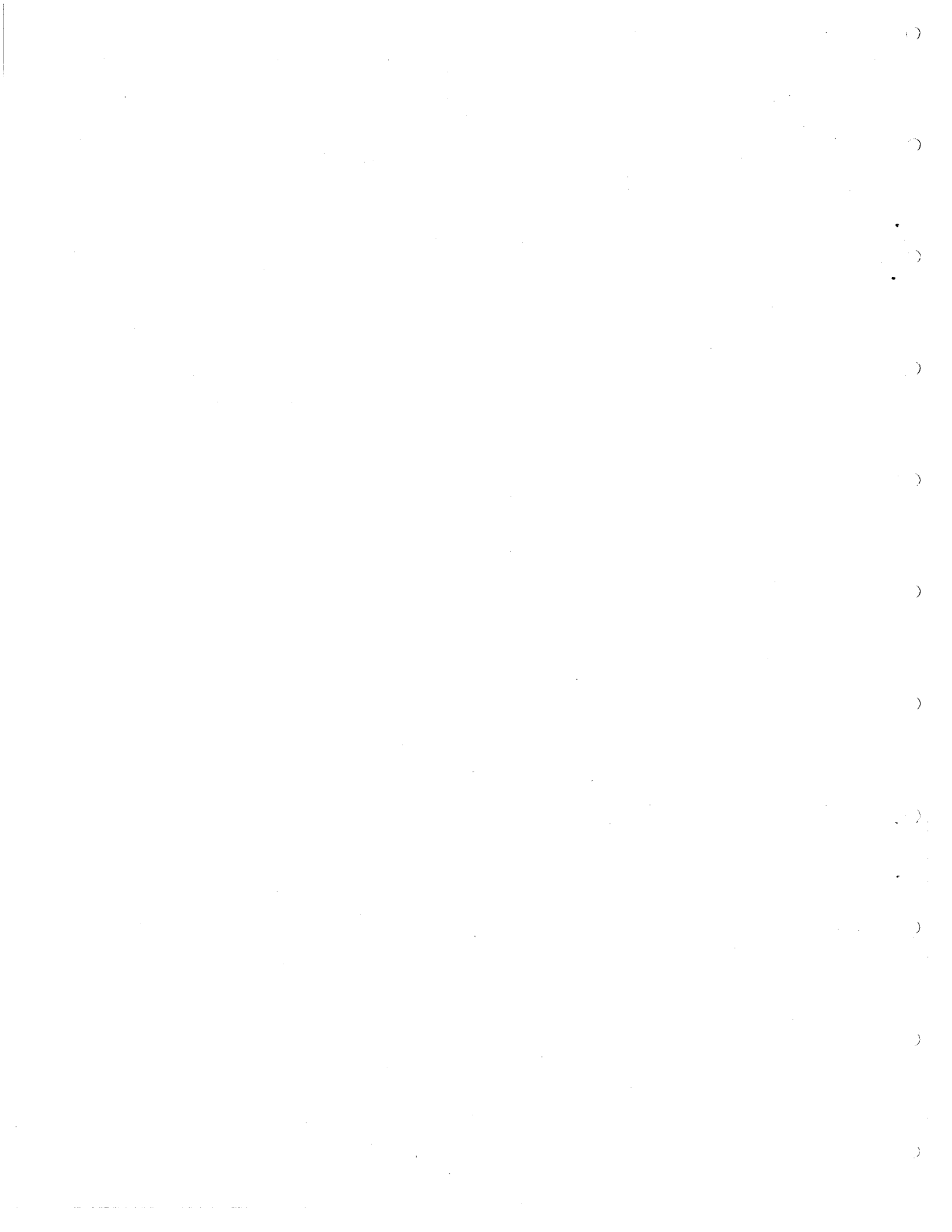
This is a new project starting in FY 1980.

## PLANNED ACTIVITIES FOR 1980

Equipment for the characterization and cycle life testing of electrodes will be designed, ordered and set up. Details of the first phase of experimentation will be planned, and investigations will be initiated.

## FOOTNOTE

\*This project is part of a larger effort, "Electrochemical Synthesis and Energy Storage," the remainder of which is reported in the Materials and Molecular Research Division 1979 Annual Report. This work was supported by the Energy Storage Systems Division of the Department of Energy.



# OIL SHALE RESEARCH

## INTRODUCTION

Vast resources of oil shale -- in excess of 1.8 trillion barrels of oil -- exist in the tri-state area of Colorado, Utah, and Wyoming. Some 80 billion barrels of this oil are recoverable with technology available today -- more energy than is contained in all of the known oil and gas reserves in the United States. The U.S. Department of the Interior has estimated that with more advanced technology and under different economic conditions, oil shale deposits in the U.S. might yield as much as 800 billion barrels of oil.

Oil shale is a layered, greyish, sedimentary rock that was deposited eons ago in fresh water lakes. It contains about 20 percent organic material, primarily kerogen, which originated from algae and other micro-organisms and wind-blown or water-borne pollen and spores. The inorganic material is a dense, tough marlstone composed primarily of the two carbonaceous minerals, dolomite and calcite. The shale may exist anywhere from 100 to 3000 feet beneath the surface interbedded with varying amounts of tuff, siltstone, sandstone, and claystone and laced with groundwater aquifers.

Oil may be extracted from the shale by heating the rock to break down the kerogen, a high molecular weight polymer, into smaller molecules. This process, termed pyrolysis, may be carried out in a surface retort or in the ground (in-situ processes). The technology for surface retorting is further advanced but is limited by economic and environmental factors. Large volumes of rock must be mined, crushed, transported, and disposed of. The processing requires large volumes of water and generates large quantities of noxious gases. In the in-situ processes, the majority of the resource is pyrolyzed in the ground (a small amount, usually about 20 percent, is removed to create void space). This approach to processing oil shale is presently under intensive study by industry and the Department of Energy as an economic and environmentally superior alternative to surface processing.

The existence of these rich Rocky Mountain oil shale deposits has been known for more than a century, and the exploitation of them has been considered, off and on, from just about every conceivable angle -- technologically, economically, politically, and most recently, environmentally.

The Oil Shale Program at the Lawrence Berkeley Laboratory is concerned with the environmental aspects of oil shale production -- air, solid waste, and water problems -- of far-reaching consequences. The program has identi-

fied a number of previously unrecognized or little understood environmental concerns -- in-situ leaching, air emission of toxic trace elements, aqueous effluent disposal -- and is conducting basic and applied research in these areas. The goal of the program is to develop the scientific information necessary to understand and, ultimately, to control environmental problems.

Information on the chemical composition of oil shale and its by-products is being developed to assess environmental impacts and to select and develop suitable control strategies. Lawrence Berkeley Laboratory is characterizing the gases, oils, waters, and solids produced by oil shale retorting. This work has indicated that the primary elements of environmental concern are As, Se, Cd, Hg, F, and B, and that inorganic and organometallic species, including arsenate and methylarsonic acid, are present in retort waters. Methods are being developed to measure organometallic and organic compounds present in aqueous effluents and to assess their impact on aquatic biota. In-depth geochemical investigations of the Green River Formation in Colorado are being conducted which indicate a remarkable uniformity in most major, minor, and trace element concentrations throughout the formation. Detailed elemental mass balances have been completed on some 30 runs of several pilot-scale retorts, and the effect of retort operating conditions on trace element distribution is being investigated.

Pyrolysis of oil shale produces from 70 to about 15,000 standard cubic feet of gas per ton of shale processed. The proper use and disposal of this low-Btu gas represents a significant challenge to the oil shale industry. This gas contains a significant fraction of the recoverable energy and is highly corrosive, has a low heating value, and may contain high concentrations of such toxic trace elements as Hg, As, Se, and Cd. Lawrence Berkeley Laboratory is developing real-time instrumentation to measure toxic trace elements in oil shale gases and is using this instrumentation to measure As, Se, Cd, Hg, and Pb in gases from laboratory, pilot, and field retorts. A Zeeman atomic absorption spectrometer capable of making real-time, in-place measurements has been developed and used to demonstrate that Hg emissions from in-situ retorts may be nonuniform and that the majority of the Hg released occurs as a pulse towards the end of a run.

Oil shale processing may also produce from 0.1 to 22 barrels of water per barrel of oil. This water, which is highly contaminated, represents a potential resource for the arid oil

shale region if it can be upgraded. Lawrence Berkeley Laboratory is exploring the use of various physical, chemical, and biological processes to upgrade this water for in-plant use or discharge. This research has led to the development of a novel technique, termed spent shale treatment, to reduce inorganic and organic carbon, color, and odor of these waters.

Leachates produced by the interaction of rain or groundwater with spent residuals may degrade local water resources. Since the rich oil shale deposits are laced with groundwater, in-situ processing may result in significant

underground contamination. Lawrence Berkeley Laboratory is investigating in-situ leaching and chemical transport in laboratory studies and by computer modeling and is searching for solutions to mitigate this phenomenon. This work has led to the identification of several possible control strategies and the development of a high-strength hydraulic cement from spent residuals which may be used to seal underground retorts.

This report summarizes progress on these and other oil shale programs for the calendar year ending December 31, 1979.

## CHARACTERIZATION STUDIES

## TRACE CONTAMINANTS IN OIL SHALE RETORT WATER\*

M. J. Kland, A. S. Newton, and H. L. Eaton

## INTRODUCTION

The prospect of commercial development of oil shale as a source of fuel raises some difficult environmental questions particularly with respect to ground and surface waters, since some of the richest oil shale deposits in the U.S. occur in the semi-arid tri-state region of Colorado, Wyoming, and Utah.

Water derived from in-situ oil shale retorting is heavily contaminated with organic and inorganic constituents. It is generally alkaline (pH 8-9.5) and contains a variety of polar organic species, including carboxylic acids, bases (amines, N-heterocyclics, N-aromatics), and organic oxygen and sulfur compounds (phenols, pyrans, thiophenes).

Inorganic content of retort waters is also high, including the following anions:  $\text{HCO}_3$ ,  $\text{CO}_3$ , Cl, F,  $\text{S}_2\text{O}_3$ , SCN, and  $\text{SO}_4$ . The principal dissolved cations are Na,  $\text{NH}_4$ , Mg, Fe, and the amphoteric forms of Al and Si which exist as complex anions under alkaline conditions. Trace elements of environmental concern include As, Se, Hg, Zn, Mo, and B.

Hetero-organics, in addition to their own specific toxicities, may also increase the mobility of some elements such as As and Se by virtue of their complexing power. The relationship of biotoxicities of As, Se, Hg, and other transition metals to their biomethylation in living systems is well known.<sup>1</sup> Thus, the presence of even very low levels of organometallic forms of the toxic metals, which may enhance their biological uptake and movement through an ecosystem, may multiply their toxic potential to sensitive species by orders of magnitude. It is therefore important to identify the organic forms of trace metals present in process waters

as well as their inorganic counterparts which are generally present in much higher concentrations. Work toward this end is reported separately elsewhere in this Annual Report.<sup>2,3</sup>

This paper reports some of the exploratory work completed in 1979 on organic and inorganic contaminants found in process waters. The purpose of this program was to identify and quantify trace contaminants in oil shale process waters using appropriate separation techniques.

## ACCOMPLISHMENTS DURING 1979

Each of several oil shale process waters was separated into methylene chloride ( $\text{CH}_2\text{Cl}_2$ )-soluble and  $\text{CH}_2\text{Cl}_2$ -insoluble alkaline and acid fractions as shown in Fig. 1. Acid extracts were esterified with dry HCl-methanol before gas chromatography-mass spectrometry (GC-MS) analysis. After appropriate preprocessing of  $\text{CH}_2\text{Cl}_2$  extracts of the original (pH 8.5-9.5) and acidified (pH 2) waters, the organic extracts were examined for trace metals by x-ray fluorescence spectrometry (XRF), inductively coupled plasma emission spectroscopy (ICP), and Zeeman atomic absorption spectroscopy (ZAA), and for trace organic constituents by GC-MS. Separations were followed by differential ultraviolet (UV) spectrophotometry and thin-layer chromatography (TLC) where feasible. The use of TLC in the separation of trace metals and organics, and as a tool in the measurement of organic carbon recovery, was also briefly investigated. The waters examined included Omega-9 retort water from Laramie Energy Technology Center's (LETC) Site-9 true in-situ experiment, retort water from a combustion run of LETC's 150-ton retort (150-ton), retort water and gas condensate from a steam-combustion run of Lawrence Livermore Laboratory's (LLL) 6000-kg retort (L-2), and three process waters from Occidental's Retort 6

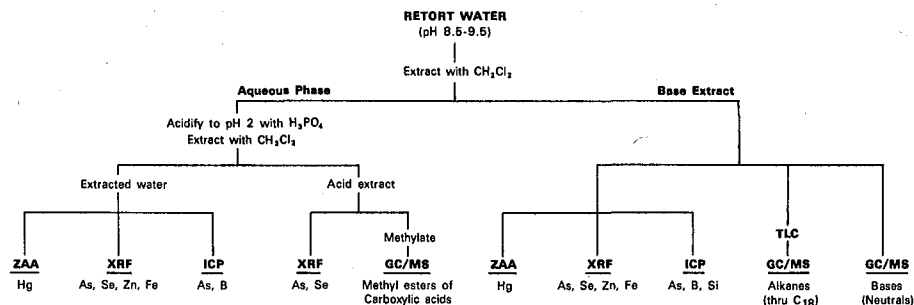


Fig. 1. Flow chart for  $\text{CH}_2\text{Cl}_2$  extraction of trace contaminants from oil shale process waters (ZAA = Zeeman atomic absorption spectroscopy; XRF = x-ray fluorescence spectrometry; ICP = inductively coupled plasma emission spectroscopy; TLC = thin layer chromatography).

(XBL 806-1129)

at Logan Wash -- retort water, heater-treater water, and boiler blowdown. These waters are described elsewhere in this report by Fish et al.<sup>2,3</sup>

#### Trace Organics

Reconstructed ion chromatograms of a base extract and methylated acid extract of 150-ton retort water are shown in Figs. 2 and 3. Tentative identifications are noted above each peak. Figure 2 shows that, of the basic components in 150-ton retort water, the alkylpyridines were predominant. Neutral compounds included three cycloalkanes and two alkynes. The heptane-soluble fraction of methylated 150-ton acid extract (Fig. 3) contained both mono- and dicarboxylic acid esters. Dicarboxylic acids may result from the oxidative cleavage of hydroxy and unsaturated monocarboxylic acids. A similarly treated acid extract of a sample of L-2 retort water had a simpler spectrum of monocarboxylic methyl esters from valeric through decanoic acids. Aromatics and dicarboxylic esters were absent. These differences reflect differences in retort operating conditions that produced the two samples.

In addition to the extracted polar constituents, GC-MS examination of an eluate from an early thin-layer chromatogram of the 150-ton extract (benzene-acetone, 95:5) showed the alkanes pentadecane through octadecane and a number of unidentified hydrocarbons. Although this TLC finding is subject to further verification, later column chromatographic analysis confirmed the presence of these hydrocarbons.

#### Trace Metals

The purpose of this work was to isolate, identify, and quantitate trace metals of environmental concern associated with organics in oil shale retort waters. The work was divided into two phases. Initially the  $\text{CH}_2\text{Cl}_2$  extraction procedure shown in Fig. 1 was used to separate metals into  $\text{CH}_2\text{Cl}_2$ -soluble and  $\text{CH}_2\text{Cl}_2$ -insoluble fractions at acid and basic pH. These "acid" and "base" extracts contained a mixture of trace metals which were then identified and quantitated using standard analytical techniques.

X-ray fluorescence analyses (XRF) were carried out on ammonium hydroxide ( $\text{NH}_4\text{OH}$ ) solutions of the metals after removal of the organic solvent. For  $\text{NH}_4\text{OH}$ -insoluble residues, methanol and ethanol-water (1:1) were used as solvents. More recently the use of a solid substrate of microcrystalline cellulose acetate to adsorb the organic metal extracts directly has replaced direct analysis of the aqueous sample. Inductively coupled plasma emission spectroscopy (ICP) analyses were used for boron, arsenic, and other metals in organic extracts. These analyses were carried out in dilute acid solutions. The use of neutron activation analysis (NAA) was confined to one experiment, in which the aqueous eluates from zones of a thin-layer chromatogram of 150-ton extract were examined for metals. Zeeman atomic absorption spectroscopy (ZAA) was used to measure mercury extracted into the

$\text{CH}_2\text{Cl}_2$  phase from 150-ton retort water.

The unextracted water, the base and acid extracts, and the extracted water were analyzed by ICP or XRF. The base extract was obtained by extracting the filtered water at its original pH. The acid extract was obtained by acidifying the aqueous phase from the initial base extraction and re-extracting it with  $\text{CH}_2\text{Cl}_2$  at pH 2. The extracted water is the aqueous phase remaining after the acid extraction. Thus, the sum of the measured concentrations for the base extract, the acid extract, and the extracted water should equal the unextracted water, within the limits of experimental error. An analysis of the data indicates that good mass balances were obtained on all elements for which there were adequate data.

The above data plus other data not reported here indicate that As, Se, Fe, Co, Ni, Zn, Cu, Pb, Cr, Br, Mo, Sb, U, and B, among others, are extracted from process water by  $\text{CH}_2\text{Cl}_2$ . Additional work is required to determine whether these elements are organically complexed or bound.

Two observations of interest emerge from the study. First, only transition elements are extracted. Secondly, only a small fraction of each element present, usually less than 10 percent, is extracted into the organic phase. Control experiments with inorganic arsenic-doped 150-ton retort water showed that it is not extracted under these conditions. Neither is phenylarsonic acid which was isolated in trace quantities from retort waters.<sup>2</sup> Arsenic and Se are primarily present in the acid extracts while the other transition metals (Cu, Zn, Cr, Ni, and Pb) were usually predominant in the base extract. These metals can form complexes with the organic nitrogen compounds which are present in process waters. In the presence of phenols, phenolcarboxylic acids, and acids containing other hetero atoms such as nitrogen, chelation may also solubilize these metals in  $\text{CH}_2\text{Cl}_2$ .

Although arsenic is a major trace contaminant of biological concern in process waters, others (Se, Zn, Cu, Pb, and Cr) can have serious negative environmental effects. All are toxic to biota, some forms of As, Pb, and Cr are known or suspect carcinogens, and Pb and Hg are neurotoxins. The inorganic forms of toxic metals generally undergo biological conversion (e.g., methylation) to more assimilable forms before they can be incorporated into biological systems. Thus, any organically soluble form of a metal, whatever its form, poses an environmental hazard, often out of all proportion to its concentration. Greater lipid solubility increases its rate of uptake by plant and animal tissue, resulting in rapid biomagnification of the toxicant. Thus, a measure of the organically bound metals in a sample would be useful information. The methylene chloride extractability of metals from retort waters could be used routinely as such an environmental indicator of potential toxicity.

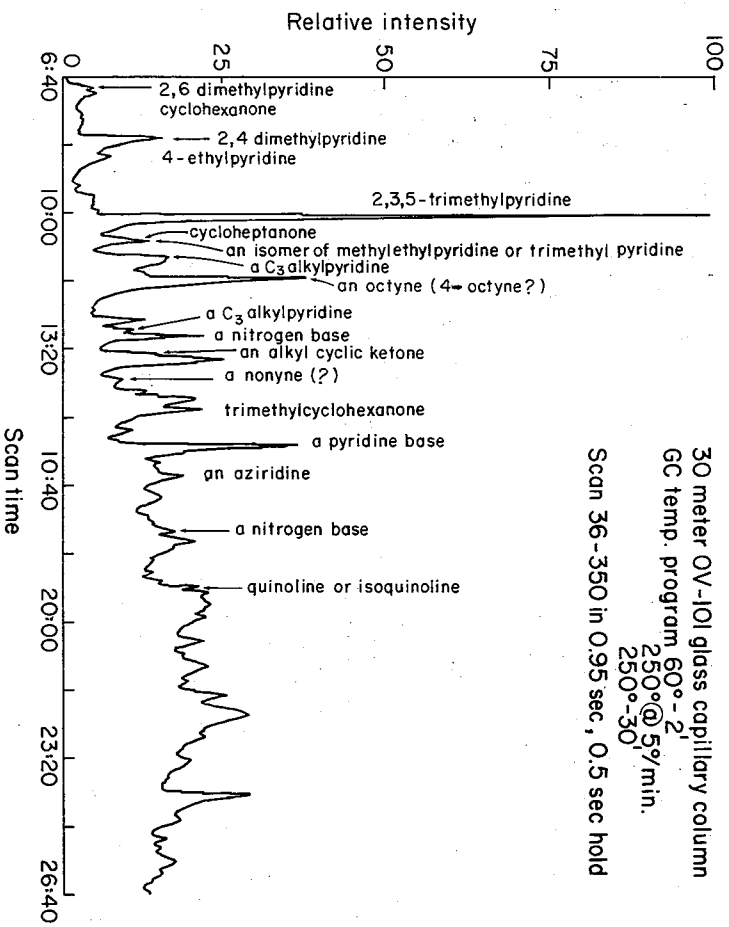


Fig. 2. Reconstructed ion chromatogram of 150-ton base extract (filtered). (XBL 806-1130)

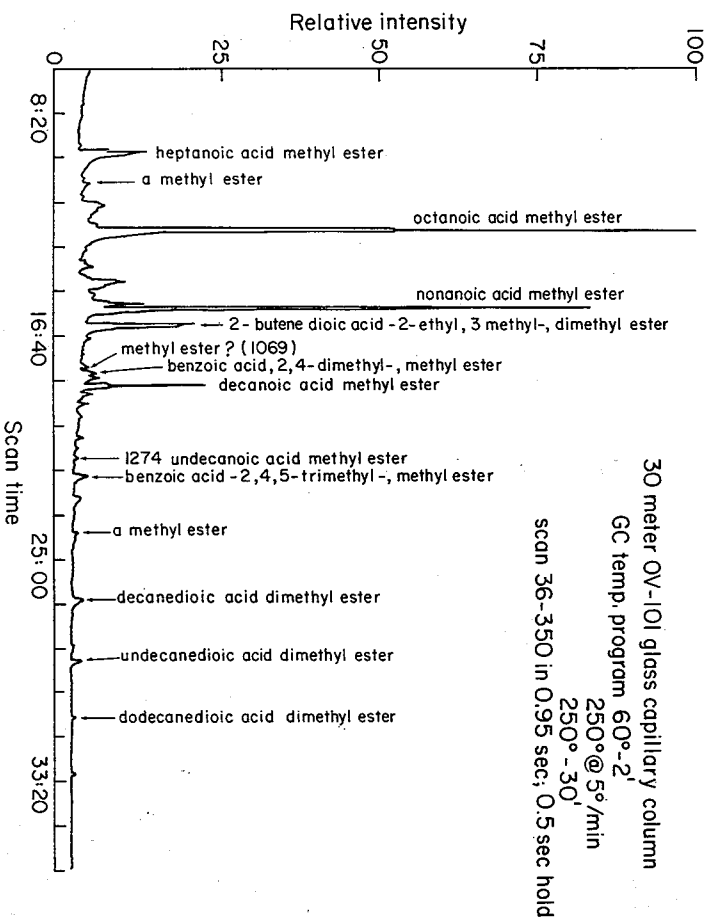


Fig. 3. Reconstructed ion chromatogram, heptane-soluble fraction of methylated acid extract of 150-ton retort water. (XBL 806-1131)

## Major Elements

The purpose of this work was to quantitate the major elements C, H, N, and S in acid and base extracts. Carbon, H, and N were determined by the Perkin-Elmer Model 240 CHN analyzer and S was determined by the Grote combustion method followed by gravimetric analysis. Table 1 summarizes the results of these analyses for various acid and base extracts for nine separate oil shale process waters.

In general, the compositions of  $\text{CH}_2\text{Cl}_2$  extracts of process waters are similar, containing many of the same lower molecular weight polar and nonpolar organic compounds. Variations in the relative ratios of low molecular weight polar components are related to differences in retorting temperatures and other process variations (steam or gas injection, etc.). These are reflected in the ratios of acid to base extracted by  $\text{CH}_2\text{Cl}_2$  and in their elemental composition and ratios. Most waters had base extracts of higher carbon content than their acid fractions, and two (Omega-9 and L-3) analyzed lower for carbon in the base extracts. All of the waters had higher N in the base extracts than in

the acid extracts, and acid fractions were generally higher in percent H and S. The difference between the sum of C, H, N, and S present and 100 percent reflects the combined oxygen and/or metals present.

Carbon-hydrogen ratios give some indication of the degree of unsaturation or aromatization. They are consistently higher in the base fractions (Omega-9 excepted), and may also reflect the degree of oxidation. Where carbon-sulfur ratios are comparable in the acid and base fractions, the S is primarily of the neutral type (e.g., thiophene). The presence of acidic sulfur ( $\text{RSO}_2\text{H}$ ,  $\text{RSO}_3\text{H}$ ) will reduce the carbon-sulfur ratio of the acid fraction vis à vis the base fraction.

## FUTURE ACCOMPLISHMENT

This phase of the work is complete.

## Acknowledgements

Thanks are due R. D. Giaque for XRF analyses and R. E. Heft for ICP and NAA analyses.

Table 1. Elemental analysis of unfiltered oil shale process water extracts for  $\text{C}^a$ ,  $\text{H}^a$ ,  $\text{N}^a$ , and  $\text{S}^b$ . Reported values are weight percent.

Sample	C	H	N	S	100- ΣC,H,N,S	C/H	C/N	C/S
<u>150-ton Retort Water</u>								
Base extract	65.48	8.40	8.34	2.3*	15.48	7.80	7.85	28.47
Acid extract	63.46	8.85	2.35	0.53	24.81	7.17	27.00	119.74
<u>L-2 Retort Water</u>								
Base extract <sup>c</sup>	69.17	8.64	8.47	0.36	13.36	8.00	8.16	192.00
Acid extract <sup>c</sup>	62.92	9.65	1.50	0.40	25.53	6.52	41.95	157.30
<u>L-2 Gas Condensate</u>								
Base extract <sup>c</sup>	66.77	8.19	1.66	1.04	22.34	8.15	40.22	64.20
Acid extract <sup>c</sup>	59.53	8.94	1.42	4.13	25.98	6.66	41.92	14.41
<u>L-3 Retort Water</u>								
Base extract	62.92	8.10	7.60	0.78	20.60	7.77	8.28	80.67
Acid extract	64.69	9.94	1.24	0.08	24.05	6.51	52.17	808.63
<u>L-3 Gas Condensate</u>								
Base extract	60.51	8.31	7.58	0.62	22.98	7.28	7.98	97.60
Acid extract	57.71	8.77	1.52	2.58	29.42	6.58	37.97	22.37
<u>Omega-9 Retort Water</u>								
Base extract	58.92	8.41	7.04	0.14	25.49	7.01	8.37	420.86
Acid extract	62.65	8.93	2.55	1.12	24.75	7.02	24.57	55.94
<u>Occidental Heater-Treater Water</u>								
Base extract	67.05	8.18	7.21	2.23	15.33	8.20	9.30	30.07
Acid extract	63.65	9.22	1.53	2.73	22.87	6.90	41.60	23.32
<u>Occidental Boiler Blowdown Water</u>								
Base extract	67.58	8.21	10.38	0.0	13.83	8.23	6.51	--
Acid extract	64.04	9.50	0.80	0.40	25.26	6.74	80.05	160.10
<u>Occidental Retort Water</u>								
Base extract	67.78	8.22	7.96	0.27	15.77	8.25	8.52	294.70
Acid extract	64.73	9.73	2.19	0.63	22.72	6.65	29.56	95.19

\*Insufficient sample

<sup>a</sup>Perkin-Elmer Model 240 CHN analyzer.

<sup>b</sup>Grote combustion method followed by gravimetric analysis.

<sup>c</sup>Filtered through 0.45 μm Millipore filter.

## FOOTNOTE AND REFERENCES

\*This program was funded by the Department of Energy's Division of Oil, Gas, and Shale Technology.

1. "Organometals and Organometalloids: Occurrence and Fate in the Environment," A.C.S. Symp. Ser. 82, F.E. Brinckman and J. M. Bellama, Eds., ACS, Washington, D.C. (1978).
2. R. H. Fish, J. P. Fox, F. E. Brinckman, and

K. L. Jewett, "Speciation of Inorganic and Organic Arsenic Compounds in Oil Shale Process Waters," Energy and Environment Division Annual Report 1979, Lawrence Berkeley Laboratory Report, LBL-10486 (1980).

3. R. H. Fish, Amos Newton, A. M. Bowles, and P. C. Babbitt, "Use of Capillary Column Gas Chromatography-Mass Spectrometry to Identify Organic Ligands of Metals in Oil Shale Process Waters," Energy and Environment Division Annual Report 1979, Lawrence Berkeley Laboratory Report, LBL-10486 (1980).

## SPECIATION OF INORGANIC AND ORGANIC ARSENIC COMPOUNDS IN OIL SHALE PROCESS WATERS\*

R. H. Fish, J. P. Fox, F. E. Brinckman,<sup>†</sup> and K. L. Jewett<sup>†</sup>

### INTRODUCTION

Oil shale retorting produces a number of solid, liquid, and gaseous wastes that may reach the environment through direct discharge or accidental spills. In-situ retorting of one ton of 24 gallon per ton shale produces approximately half a barrel each of retort water and shale oil, about 10,000 standard cubic feet of low Btu gas, about 0.8 ton of retorted shale, and various other solid and liquid waste products including spent catalysts, treatment plant sludges, and blowdown streams. Toxic and trace elements initially present in the raw shale may be distributed to these various products and to the environment during heat treatment of the shale, combustion or other end use of the oil, and leaching of the solid waste. Because of the chemical and physical environment in which these processes occur, a range of organometallic and inorganic compounds may be either synthesized or released. The organometallic forms may increase trace element mobility and toxicity and interfere with various refinery processes.

The purpose of this program is to identify and quantify the organometallic and inorganic species present in shale oils, process waters, gases, and leachates from solid wastes and to interpret the data in an environmental framework.

### ACCOMPLISHMENTS DURING 1979

In 1979, a high-performance liquid chromatograph coupled to a graphite furnace atomic absorption detector (HPLC-GFAA) was used to identify organic and inorganic arsenic compounds in several process waters from field and simulated in-situ retorts. This work revealed that each water has a distinctive arsenic fingerprint and that arsenate, methylarsonic acid, and phenylarsonic acid are present in several of the waters while arsenite and dimethylarsinic acid are not observed. Arsenic was selected for these

investigations because previous work at this Laboratory revealed that total arsenic concentrations in oil shale process waters and shale oils were high, ranging from 0.3 to 15.3 ppm in the waters and 0.5 to 19.8 ppm in shale oils.<sup>1</sup> The results of this investigation are summarized here.

### Samples

The work this year has focused on process waters from several simulated and field in-situ oil shale retorting processes. Most of these were retort waters or concentrates and various mixtures of retort water. Retort waters are produced within the retort with the oil as a vapor that is condensed from the gas stream and is separated from the oil by heat treatment and decantation. The waters originate from mineral dehydration, combustion, groundwater seepage, and steam and moisture in the input gas.

A summary of the waters that we investigated and their distinguishing factors are presented in Table 1. Simulated waters are produced in pilot-scale laboratory retorts designed and operated to simulate large-scale modified in-situ retorts. We studied two such waters, one from a steam-combustion run of Lawrence Livermore Laboratory's (LLL) 6000-kg retort (L-2),<sup>2</sup> and the other from a combustion run of Laramie Energy Technology Center's 150-ton retort (150-ton).<sup>3</sup> Field in-situ process waters are produced during demonstration-scale field experiments conducted by industry and the Department of Energy to develop oil shale technology. We studied process waters from Geokinetics' horizontal true in-situ process,<sup>4</sup> from LETC's Rock Springs Site 9 true in-situ experiment (Omega-9),<sup>5</sup> and three process waters from the Occidental Logan Wash modified in-situ process.<sup>6</sup>

The origin of the three process waters--

Table 1. Water types and sources and retort operating conditions for samples used in arsenic speciation study.

Water	Retort/ Process	Shale Source	Retorting Atmosphere	Retorting Temperature
SIMULATED IN-SITU RETORTS				
L-2 Retort Water	LLL 6000-kg/ modified in-situ	Anvil Points, Colorado	air/steam	887°C
150-ton Retort Water (Run 13)	LETC 150-ton/ modified in-situ	Anvil Points, Colorado	air	816°C
FIELD IN-SITU RETORTS				
Omega-9 Retort Water	LETC Site 9/ true in-situ	Rock Springs, Wyoming	air	(a)
Geokinetics Retort Water	Retort 16 true in-situ	Book Cliffs, Utah	air	(a)
Occidental Retort Water	Retort 6 modified in-situ	Logan Wash, Colorado	air/steam	(a)
Occidental Boiler Blowdown	Retort 6 modified in-situ	Logan Wash, Colorado	air/steam	(a)
Occidental Heater-Treater Water	Retort 6 modified in-situ	Logan Wash, Colorado	air/steam	(a)

(a) Field retorting temperatures are not accurately known due to corrosion problems with thermocouples. However, mineral analyses of spent shales from the Geokinetics and Occidental processes suggest temperatures may locally reach 1000°C.

retort water, boiler blowdown, and heater-treater water--is shown in Fig. 1. Retort water and oil are collected together in an underground sump at the bottom of the retort. These two products are introduced into a Separator Tank where the majority of the water is separated from the oil by decantation. The water collected from the Separator Tank is referred to here as "retort water." The oil from the Separator Tank is then introduced into the Heater-Treater to remove any residual moisture, usually less than five percent by weight. The oil is heated and the water is separated by decantation. The water collected from the Heater-Treater is referred to here as "heater-treater" water. The aqueous streams from the Separator Tank and the Heater-Treater are then introduced into a low-pressure boiler, together with makeup water from local surface streams, and the mixture is used to generate process steam. About 20 percent of the input water is blown down to maintain operation of the unit. This underflow is a concentrated stream which contains greater than 90 percent of the original organics and inorganics in 20 percent of the original volume of water. This water is referred to here as boiler blowdown.

The sample waters are rich in organics and particulates, and appear to be microbiologically active if unrefrigerated. Samples chilled to 4°C were received and maintained at this temperature throughout the study except for filtering and chromatographic sampling.

The processes investigated in this work do not represent commercial technology because additional work is required to resolve a number of technical problems, including rubblization and process control. This additional work may lead to the development of a process that is very different from those that generated the

waters we studied. Therefore, the reader is cautioned that these results should not yet be extrapolated to a commercial oil shale industry.

#### Experimental

A high performance liquid chromatograph was coupled to a graphite furnace atomic absorption spectrometer (HPLC-GFAA), using a laminar-flow cell, to separate and detect five known arsenic compounds. The technique used has been described elsewhere<sup>7,8</sup> and is shown schematically in Fig. 2. Five known arsenic compounds--arsenite

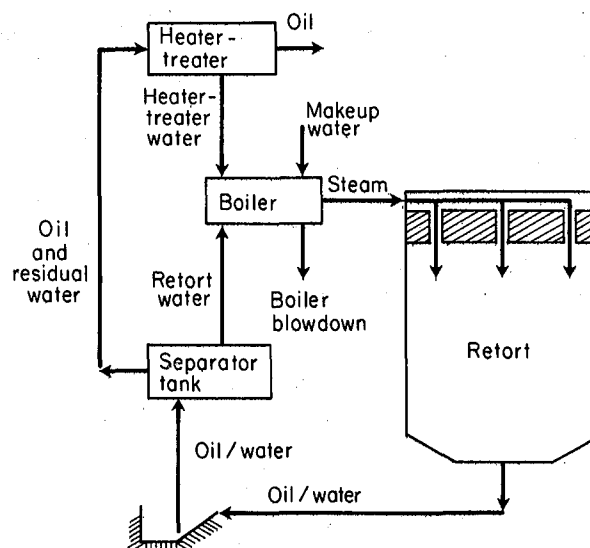


Fig. 1. Aqueous waste streams of Occidental Logan Wash Retort 6. (XBL 805-971)

(AsO<sub>2</sub><sup>-</sup>), dimethylarsinic acid ((CH<sub>3</sub>)<sub>2</sub>As(O)OH), methylarsonic acid (CH<sub>3</sub>As(O)(OH)<sub>2</sub>), phenylarsonic acid (φ-As(O)(OH)<sub>2</sub>), and arsenate (AsO<sub>4</sub><sup>3-</sup>) were separated on a Dionex anion exchange column using a solvent gradient program of water/methanol (80/20 v/v) to 0.02 M ammonium carbonate in water-methanol (85:15, v/v) at 10% per min.<sup>9</sup> Seven oil shale process waters (Table 1) were filtered through 0.45 μm filters, separated by HPLC using the Dionex column, and were automatically analyzed for arsenic at 193.7 nm, following recording the UV absorption signal (254 nm) of the HPLC column eluate.

### Results and Discussion

Results of the arsenic speciation studies are summarized in Table 2 and a typical chromatogram is shown in Fig. 3. This figure shows an arsenic fingerprint and the UV absorption signals for the three water samples from the Occidental modified in-situ process. The chromatogram obtained for each sample consists of a series of peaks which represent one or more arsenic compounds eluting from the Dionex column. The UV absorption signal, also shown in Fig. 3 superimposed on the AA pulsed output, represents the complex mixture of aromatic organic compounds typically seen in the samples. An arsenic standard, which consisted of an aqueous solution of sodium arsenite, cacadylic acid, methylarsonic acid, and sodium arsenate, is shown in the top segment of Fig. 3. Table 2 summarizes the retention times of the tentatively identified species and additional unidentified species for each water.

Table 2 indicates that arsenate, methylarsonic acid, and phenylarsonic acid are the predominant identified arsenic species in the oil shale process waters studied. No arsenite or

dimethylarsinic acid was detected in any of the samples, and all of the samples had a neutral (nonionic) arsenic compound that eluted with the solvent front. Arsenate and methylarsonic acid were identified in all of the samples, and phenylarsonic acid was identified in all samples except 150-ton retort water.

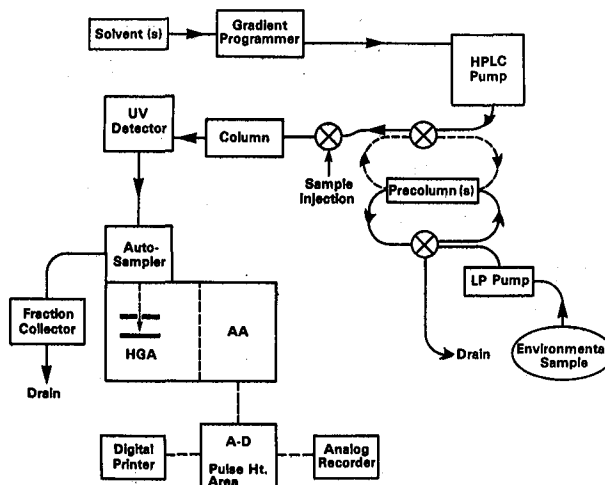


Fig. 2. Schematic of automated graphite furnace atomic absorption detector (GFAA) coupled with programmed gradient-flow high-performance liquid chromatograph (HPLC). At pre-selected intervals (ca. 45 s) 10 μL segments of the HPLC eluant are sampled and selectively analyzed for arsenic (or another element) to give the element-specific AA chromatograms illustrated in Fig. 3. (XBL 803-8498)

Table 2. Tentative identification of inorganic and organoarsenic compounds by HPLC-GFAA in various oil shale process waters<sup>a</sup>.

Sample	NaAsO <sub>2</sub> Sodium Arsenite	(CH <sub>3</sub> ) <sub>2</sub> As(O)(OH) Dimethylarsinic Acid	CH <sub>3</sub> As(O)(OH) <sub>2</sub> Methylarsonic Acid	φ-As(O)(OH) <sub>2</sub> Phenylarsonic Acid	Na <sub>2</sub> AsO <sub>4</sub> Sodium Arsenate	Unknown
Calibration	2.11 ± 0.43	16.28 ± 1.84	25.37 ± 0.44	35.7 ± 0.44	44.81 ± 1.1	--
SIMULATED IN-SITU RETORTS						
L-2 Retort Water	--	--	25.19 (+)	35.64 (+)	42.89 (+)	1.04
136-tonne Retort Water (150-ton)	--	--	23.79 (+)	--	43.91 (+)	0.46
FIELD IN-SITU RETORTS						
Omega-9 Retort Water	--	--	25.19 (+)	34.88 (+)	43.71 (+)	1.37 20.37
Geokinetics Retort Water	--	--	26.01 (+)	33.25 (+)	44.51 (+)	1.08 20.38
Occidental Heater-Treater Water	--	--	25.11 (+)	36.36 (+)	46.82 (+)	0.96 14.64
Occidental Boiler Blowdown Water	--	--	24.90 (+)	34.55 (+)	44.20 (+)	0.75
Occidental Retort Water	--	--	24.63 (+)	35.88 (+)	44.75 (+)	0.51 14.99

<sup>a</sup>A dash (--) signifies that the species was not detected. A plus (+) signifies that the species was tentatively identified. The numerical values are the retention times at which the species or unknown peaks were detected.

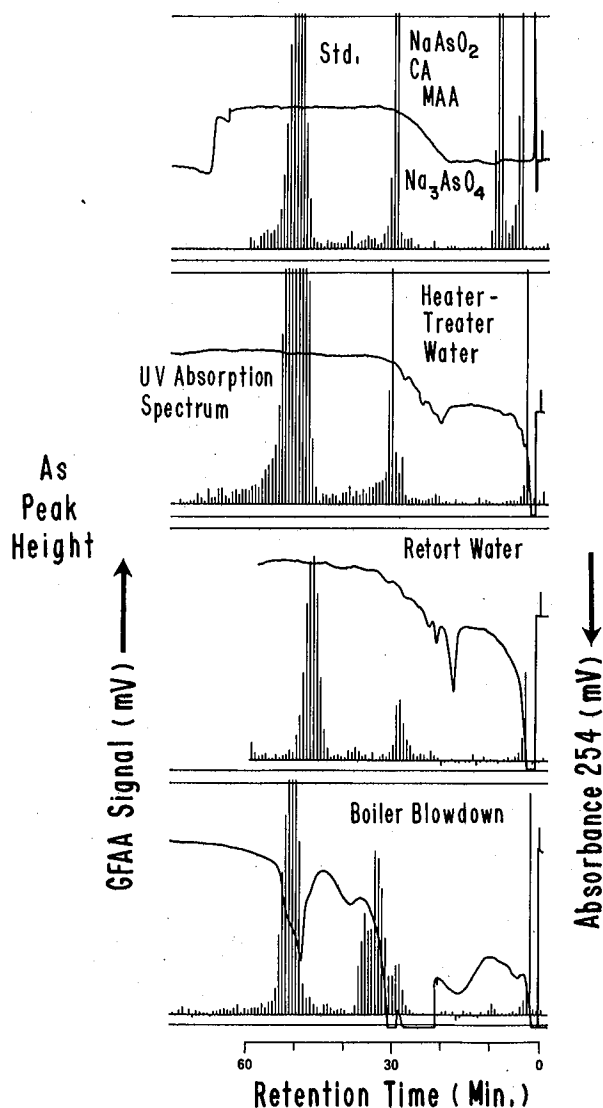


Fig. 3. Fingerprint of arsenic species and UV absorption signal of three waters from the Occidental modified in-situ process, Retort 6, Logan Wash, Colorado. The standards (std) are sodium arsenite ( $\text{NaAsO}_2$ ), cacadylic acid, i.e., dimethylarsinic acid (CA), methylarsonic acid (MAA), and sodium arsenate ( $\text{Na}_3\text{AsO}_4$ ), 200 ng each as As. (XBL 803-8499A)

The origin of the separated species is not fully understood at this time and can only be inferred from what is known about the retorting process and from environmental arsenic chemistry. The arsenic species present in the process waters probably originate from partitioning between the oil, gases, and raw shale and the water. In in-situ retorting, a hot reaction zone is propagated vertically down a packed bed of shale. The oil, water, and gas move over unretorted shale in front of this reaction zone. Therefore, the retort water, which is produced from combustion, mineral dehydration, and input steam in the reaction zone, is in intimate contact with oil, gases, and unretorted shale.

Arsenic compounds present in these oils, gases, and the shale may partition into the water phase during transit from the reaction zone to the exit of the retort where the products are collected. Reactions may also occur after the water is collected at the exit of the retort. For example, arsenic in the water or oil may be biologically methylated<sup>10</sup> while changes in the water temperature and pH may result in further chemical reactions. Additional work is required to identify the origin of each arsenic compound in these waters.

#### PLANNED ACTIVITIES FOR 1980

This work will be expanded to include additional samples and elements. Other oil shale wastewaters from additional processes will be characterized. Organometallic species in shale oils and leachates will be included in future work, and other retorting processes, including Paraho and the Rio Blanco Oil Shale Project process, will be characterized. Methods will be developed to speciate other elements including Se, Hg, and Zn. Experiments will be conducted to determine the origin of the identified organometallic species and the toxicological implications of identified compounds will be explored.

#### FOOTNOTES AND REFERENCES

\*This program is funded by the Department of Energy's Division of Oil, Gas, and Shale Technology and jointly carried out by the Chemical Stability and Corrosion Division, NBS, and the Energy and Environment Division, LBL.

† Center for Materials Science, National Bureau of Standards.

1. J. P. Fox, The Partitioning of Major, Minor, and Trace Elements during Simulated In-Situ Oil Shale Retorting, Ph.D. Dissertation, University of California, Berkeley (1980).
2. W. A. Sandholtz and F. Ackerman, "Operating Laboratory Oil Shale Retorts in an In-Situ Mode", paper presented at Society of Petroleum Engineers 52nd Annual Meeting, Denver, Colorado, October 9-12, Lawrence Livermore Laboratory Report, UCRL-79035 (1977).
3. A. E. Harak et al., "Oil Shale Retorting in a 150-ton Batch-Type Pilot Plant", U.S. Bureau of Mines, Report of Investigations No. 7995 (1974).
4. M. A. Lekas, "Progress Report on the Geokinetics Horizontal In Situ Retorting Process", Twelfth Oil Shale Symposium Proceedings, Colorado School of Mines, 228 (1979).
5. J. P. Fox, D. S. Farrier, and R. E. Poulson, "Chemical Characterization and Analytical Considerations for an In-Situ Oil Shale Process Water", Laramie Energy Technology Center Report, LETC/RI-78/7 (1978).

6. R. A. Loucks, Occidental Vertical Modified In-Situ Process for the Recovery of Oil from Oil Shale: Phase I, Volume I Summary Report, November 1, 1976 - October 31, 1977.
7. F. E. Brinckman, W. R. Blair, K. L. Jewett, and W. P. Iverson, "Application of a Liquid Chromatograph Coupled with a Flameless Atomic Absorption Detector for Speciation of Trace Organometallic Compounds", *Journal of Chromatographic Science*, 15, 493 (1977).
8. F. E. Brinckman, K. L. Jewett, W. P. Iverson, K. J. Irgolic, K. C. Ehrhardt, and R. A. Stockton, "Graphite Furnace Atomic Absorption Spectrophotometers as Automated Element Specific Detectors for High-Pressure Liquid Chromatography: The Determination of Arsenite, Arsenate, Methylarsonic Acid and Dimethylarsinic Acid", *Journal of Chromatography*, 191, 31 (1980).
9. E. A. Woolson and N. Aharonson, "Speciation of Arsenical Pesticide Residues and Some of their Metabolites by High Pressure Liquid Chromatography - Graphite Furnace Atomic Absorption Spectrometry," *J. Assoc. Official Anal. Chem.*, in press (1980).
10. M. O. Andrae and D. Klumpp, "Biosynthesis and Release of Organoarsenic Compounds by Marine Algae," *Environ. Sci. Technol.*, 13, 738 (1979).

## USE OF CAPILLARY COLUMN GAS CHROMATOGRAPHY-MASS SPECTROMETRY TO IDENTIFY ORGANIC LIGANDS OF METALS IN OIL SHALE PROCESS WATERS\*

*R. H. Fish, A. S. Newton, A. M. Bowles, and P. C. Babbitt*

### INTRODUCTION

Oil shale retorting produces a number of aqueous effluents that may reach the environment by accidental spills or discharge to surface and groundwaters. These include retort water, gas condensate, leachate, and boiler blowdown. Retort water and gas condensate, the most voluminous and highly contaminated waters, are co-produced with the oil. They originate from combustion, mineral dehydration, steam and moisture in the input gas, and groundwater seepage into in-situ retorts. The retort water is condensed at elevated temperatures while the gas condensate is condensed at lower temperatures, from 15 to -15°C. Blowdown is a concentrated underflow stream produced in the boiler used to make process steam. Leachates are produced by the interaction of rainfall and snowmelt with surface piles of spent shale or by groundwater trickling through in-situ spent shales. These four types of water may contain a number of toxic trace metals, including As, Se, Zn, B, and Fe, which may be complexed by organic ligands. The organic ligands increase the mobility of the trace elements, increase their biological uptake rate, enhance their toxicity, and interfere with various oil refining and water treatment processes.

The purpose of this program is to identify organic ligands that may be associated with trace metals in oil shale process waters.

### ACCOMPLISHMENTS DURING 1979

We used a capillary column gas chromatograph coupled to a mass spectrometer (GC-MS) to separate and identify fatty acids and substituted nitrogen aliphatic and aromatic heterocyclic

compounds in retort waters, gas condensate, and boiler blowdown from field and simulated in-situ retorts. This work revealed that each water has a distinctive fatty acid fingerprint with C<sub>4</sub> through C<sub>16</sub> mono- and C<sub>8</sub> through C<sub>15</sub> dicarboxylic acids present. Substituted pyridines, quinolines, and aliphatic nitrogen compounds were also identified as possible ligands for trace metals.

The work focused on process waters from several simulated and field in-situ oil shale retorting processes. These samples were described in a previous article in this Annual Report.<sup>1</sup>

### Fatty Acids

Since the higher molecular weight fatty acids are not volatile and thus not readily amenable to analysis by GC-MS, we converted the fatty acids to their methyl esters. This was accomplished by lyophilizing 20 ml filtered samples of each water (pH<sup>9.0</sup>) and subsequently reacting the residue with a 14 percent solution of boron trifluoride in methanol. This was followed by an hydrolysis step and extraction of the aqueous layer with benzene. The benzene extracts for the seven waters were analyzed for their fatty acid methyl ester content using capillary column gas chromatography (10 m x 0.025 mm column coated with SP 2100 and programmed from 50 to 250°C, 3°C/min).

Figure 1 shows the fatty acid methyl ester capillary column gas chromatograms of the seven waters and indicates that each water has a distinctive fatty acid methyl ester profile and that there is an homologous series of methyl esters present. Several process-related simi-

Table 2. Substituted aliphatic and aromatic heterocyclic compounds found in pH 9.2 methylene chloride extract of heater-treater water by GC-EIMS<sup>a</sup>.

Scan Number <sup>b</sup>	Formula	Compound <sup>c</sup>
1	C <sub>8</sub> H <sub>11</sub> N	2,3,5-trimethylpyridine
2	C <sub>10</sub> H <sub>13</sub> ON	2(pent-1-one)-Pyridine
3	C <sub>8</sub> H <sub>17</sub> N	1-ethyl-2-methylpiperidine
4	C <sub>9</sub> H <sub>19</sub> N	3-methyl-1,2-diisopropyl-aziridine
5	C <sub>10</sub> H <sub>9</sub> N	2-methylquinoline
6	C <sub>11</sub> H <sub>11</sub> N	2,4-dimethylquinoline

<sup>a</sup> Finnigan 4023 equipped with a 30 m x 0.25 mm glass capillary column coated with OV101. Programmed from 40-250°C at 5°/min.

<sup>b</sup> See Figure 2 for scan number mass spectrometry assignment of a particular peak for the GC analysis.

<sup>c</sup> From data base of known compounds.

## CHARACTERIZATION OF TWO CORE HOLES FROM THE NAVAL OIL SHALE RESERVE NO. 1\*

R. D. Giauque, J. P. Fox, J. W. Smith,<sup>†</sup> and W. A. Robb<sup>†</sup>

### INTRODUCTION

Green River oil shale is a marlstone that contains about 20 percent organic material. It was deposited from an ancient lake that covered parts of Colorado, Utah, and Wyoming. This lake was probably permanently stratified. The upper portion supported life, and the lower layer was probably a sodium carbonate solution with a pH of 11 to 12. Oil shale was formed by lithification of sediments accumulated at the bottom of this lake. These materials entered this lake by overland runoff and atmospheric fallout of dust, pollen, and volcanic ash.

The purpose of this program (initiated in June 1978) is to characterize two cores, Core Holes 25 and 15/16, from the Naval Oil Shale Reserve No. 1. The resulting data are being analyzed to shed some light on the geochemistry of these deposits, to assess environmental impacts of oil shale production, and to develop information required to assess the deposit's commercial potential. The stratigraphy of the Green River Formation is shown in Fig. 1.

The distribution of minerals, elements, and Fischer Assay products was determined as a function of the stratigraphic position for core segments from the Naval Oil Shale Reserve No. 1.

Correlation analyses were performed to determine significant relationships between Fischer Assay oil yields, water yield, eight minerals, and 48 elements. Correlations were carried out for samples from individual stratigraphic zones which were composited at five-foot intervals or less. Correlations showing greater than 95 percent probability of not being zero were deemed to be significant.

### ACCOMPLISHMENTS DURING 1979

Previously, two cores from the Naval Oil Shale Reserve No. 1 were sectioned and composited into 284 samples at 1, 2, 25, or 50 foot intervals based on stratigraphy,<sup>1</sup> and chemical measurements on these samples were initiated. This year, the chemical measurements were completed, and statistical procedures were developed and used to analyze the data from Core Hole 25.

The 284 samples were analyzed for 57 major, minor, and trace elements by neutron activation analysis, x-ray fluorescence spectrometry, Zeeman atomic absorption spectroscopy, and other instrumental and wet chemical techniques. The major mineral phases, dolomite, calcite, analcime, K and Na feldspars, and quartz, were determined by x-ray diffraction analysis at

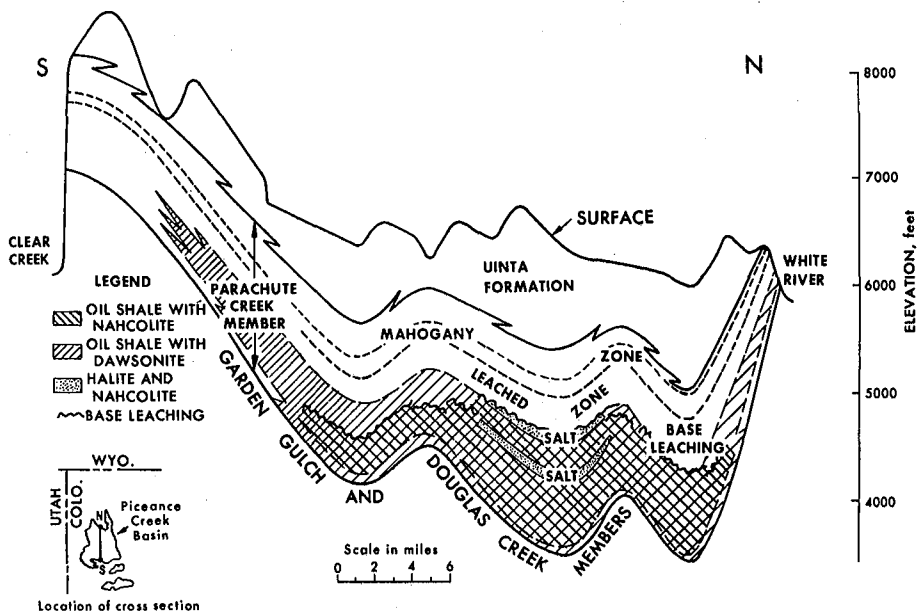


Fig. 1. South-north diagrammatic cross-section of the Green River Formation in Colorado's Piceance Creek Basin (Ref. 3)

(XBL 7911-12837)

Laramie Energy Technology Center (LETC). Fischer Assay, a standard test used to determine the oil yield of oil shale, was run at LETC on each sample, determining the weight percent oil, water, spent shale, and gas. These data were entered into a computerized data base system and statistical procedures were developed to analyze the data. These procedures, which included the computation of Pearson correlation coefficients and statistical significance coefficients, were used to investigate relationships between the measured variables. This section describes the results of the measurements and analyses for Core Hole 25.

Table 1 lists the four stratigraphic zones, the depth of the zones, and the composite sampling intervals for Core Hole 25. The determination of significant relationships between minerals, Fischer Assay products, and the elements is complicated by the fact that the oil shale was formed by a very slow sedimentation process which produced numerous thin geologic laminations. An oil shale composite section one-foot in depth can easily represent hundreds to thousands of years of deposition.<sup>2</sup> Such a section would contain a great many geologic laminations, each representing a specific set of deposition conditions. These conditions probably changed during the very long time intervals represented by a composite sample. Thus, many geochemical relationships may be obscured, while certain others may have prevailed over geologic time.

Figures 2-4 are typical histograms of mineral analyses, Fischer Assay data, and elemental data for the stratigraphic zones of interest. In the oil-rich Mahogany Bed and Mahogany Zone, high oil yields coincided with high concentrations of aluminum silicate minerals and Na and K feldspars as shown in Fig. 2. Additionally, a significant correlation was obtained between water yields and analcime for all four stratigraphic zones.

Table 1. Core Hole 25 composite samples used for correlation analysis.

Stratigraphic Zone <sup>a</sup>	Depth (feet)	Composite Interval (feet)
Overlying Oil Shale	388-634	5
Upper Mahogany Zone	634-670	2
Mahogany Bed	670-690	1
Lower Mahogany Zone	690-705	2

<sup>a</sup>See Figure 1 for appropriate locations of these zones.

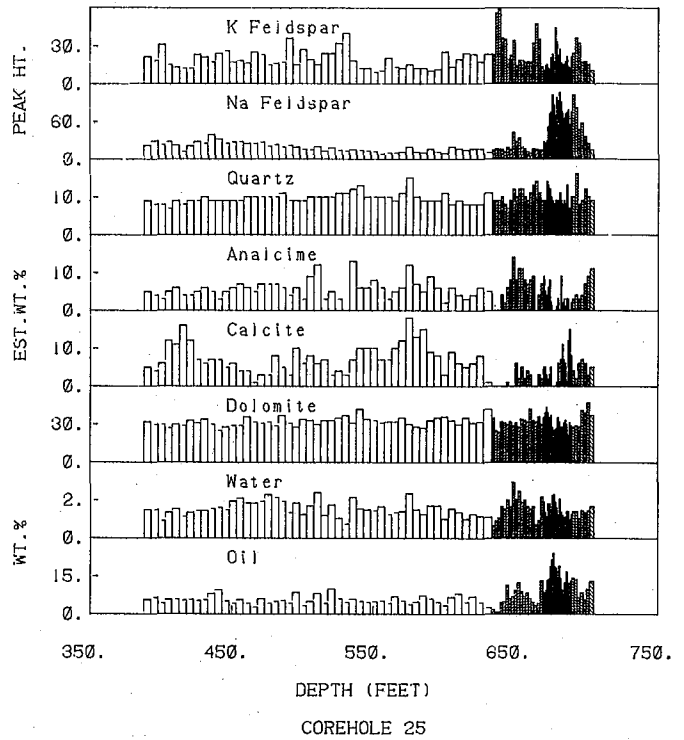


Fig. 2. Histogram of results for six minerals and Fischer Assay water and oil yield. (FXBL 804-9106)

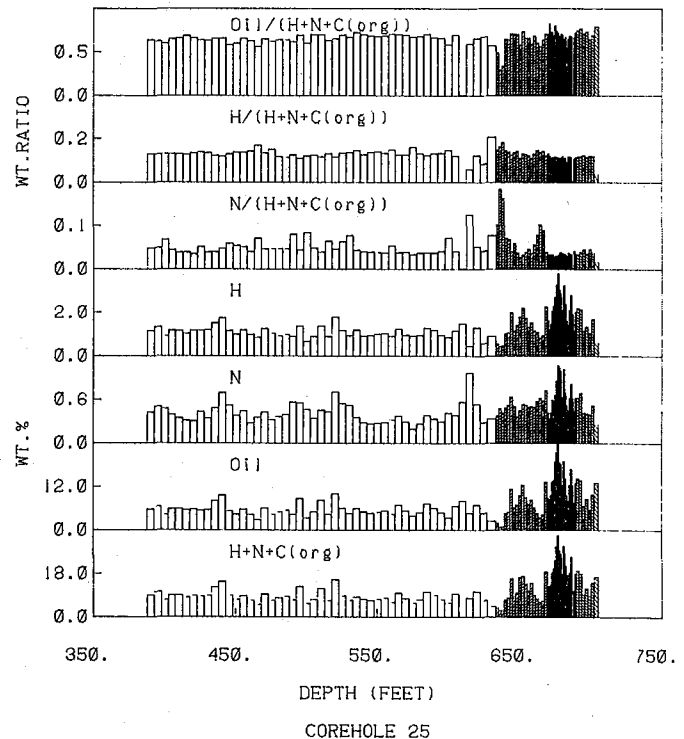


Fig. 3. Histogram of results for organic elements and Fischer Assay oil yield. (FXBL 804-9107)

Total hydrogen (this includes organic hydrogen and hydrogen associated with the produced water) correlated with oil yields in the upper three zones as shown in Fig. 3. The amount of hydrogen present relative to organic carbon was essentially constant and corresponded to a 1.7:1 atomic weight ratio. However, nitrogen was more variable relative to organic carbon. The oil yield typically represented about 65 percent of the total organic content as illustrated in this same figure.

In Fig. 4, positive correlations between Pb, Cu, and Co are easily observed. The concentrations of As, Se, and Hg, elements of potential environmental significance, were at maximum in the zones which yielded the highest oil assays. These same three elements had positive correlations with oil yield for most of the stratigraphic zones.

#### PLANNED ACTIVITIES FOR 1980

Data acquired for Core Hole 25 along with that obtained for Core Hole 15/16, which is closer to the depositional center of the oil shale formation, will be statistically evaluated. Significant relationships that exist among minerals, Fischer Assay data, and elemental abundances will be determined. In turn, the geochemistry of these two core holes will be postulated.

#### FOOTNOTES AND REFERENCES

\*This program is jointly funded by the Laramie Energy Technology Center (LETC), the Department of Energy's Division of Environmental Control Technology and Division of Oil, Gas, and Shale Technology, the U.S. Navy, and the Environmental Protection Agency.

†Laramie Energy Technology Center

1. B. Branstetter, R. D. Giauque, H. V. Michel, J. P. Fox, R. B. Garrett, and L. Y. Goda, "Geochemical Studies of an Oil Shale Deposit," Energy and Environment Division Annual Report 1978, Lawrence Berkeley Laboratory Report, LBL-9857 (1979).
2. W. A. Robb, J. W. Smith, and L. G. Trudell, "Mineral and Organic Distributions and Relationships across the Green River Formation's Saline Depositional Center, Piceance Creek Basin, Colorado," Laramie Energy Technology Center Report, LETC/RIU-78/6 (1978).
3. John Ward Smith, Thomas N. Beard, and Laurence G. Trudell, "Colorado's Primary Oil-Shale Resource for Vertical Modified In-Situ Processes," Laramie Energy Technology Center Report, LETC/RI-78/2 (1978).

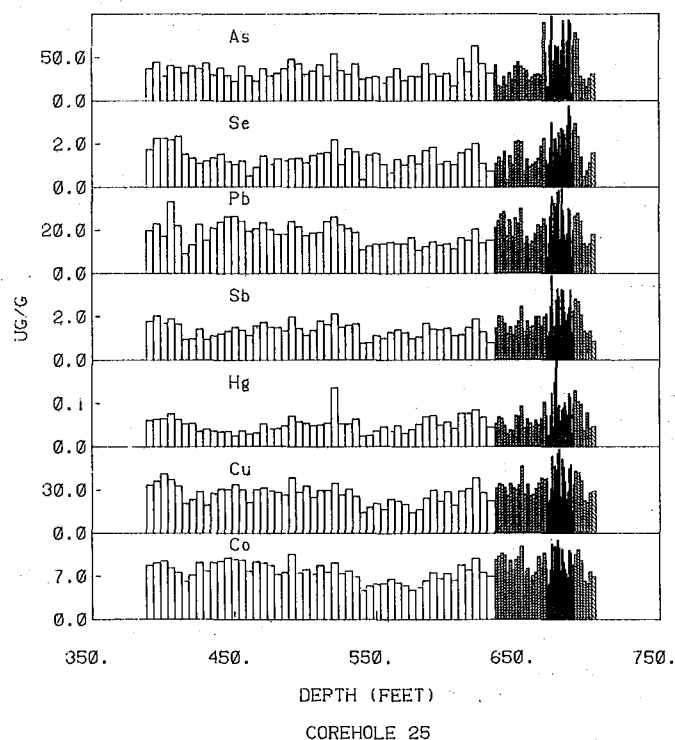


Fig. 4. Histogram of results for As, Se, Pb, Sb, Hg, Cu, and Co. (FXBL 804-9104)

## ECOLOGICAL STUDIES

### THE EFFECTS OF OIL SHALE RETORT WATER ON SOME BENTHIC FRESHWATER ORGANISMS\*

P. P. Russell, A. J. Horne,† J. F. Thomas,† and V. H. Resh†

#### INTRODUCTION

Production of synthetic crude from oil shale generates from 0.10 to 22 barrels of water per barrel of oil, depending on the specific process used. This water, referred to as retort water, originates from combustion, mineral dehydration, steam and moisture in the input gas, and from groundwater intrusion (in-situ processes only). The organic content of retort water may reach three percent while inorganic concentrations of as much as five percent are typical. The principal inorganic components of the wastewater are ammonium, sodium, and bicarbonate, with lesser but significant amounts of thiosulfate, chloride, sulfate, and carbonate.

The goal of this project is to investigate the probable effects of accidental or intentional discharge of retort water on attached microorganisms (aufwuchs) and caddisfly larvae in streams of the oil shale region. Current industry development plans envision zero discharge of retort water, but nevertheless, unintentional release through spills and leakage is a real possibility.

Aufwuchs are sensitive indicators of the effect of a pollutant on the food chain. Aufwuchs typically consist of an attached mat of algae, protozoa, bacteria, fungi, and some associated metazoans. Caddisfly larvae, on the other hand, are used as water quality indicators for freshwater lotic habitats due to their nearly ubiquitous occurrence, their frequent dominance in both diversity and abundance, and the narrow pollution tolerances of many species.

The approach used in this investigation was to employ laboratory-scale model streams. Standardized growth surfaces upon which aufwuchs could develop were located in riffle reaches of the streams. Caddisfly larvae were contained in cages located in pools at the downstream end of each riffle reach.

This program was initiated in 1977 and will be completed in 1980.

#### ACCOMPLISHMENTS DURING 1979

Previously, a laboratory-scale model stream system had been constructed and tested and used to study the effect of two retort waters on aufwuchs and caddisfly larvae. This year, the data collected from those experimental runs were analyzed using statistical techniques and work was initiated on final report preparation. The results of these investigations are summarized here.

#### Model Streams

Laboratory-scale model streams were designed and constructed to simulate conditions expected in the streams of northwestern Colorado where early development of oil shale is anticipated. A schematic of the model-stream apparatus with one of the four streams shown is presented in Fig. 1. Each stream consisted of a riffle reach 122 cm long bounded by a pool at each end. The width of the riffle and pool reaches was 9.5 cm and the capacity of each stream was 12 liters. Flow was produced in the streams by pumping water from the lower pools to the respective upper pools. A nominal flow rate of 45 cm/s and water depth of 2 to 3 cm were obtained by simultaneously adjusting the slope of the stream beds and the throttle valves on the discharge of the centrifugal pumps used for recirculation. Fluorescent tubes suspended over the riffle reaches provided illumination. A 15 hour : 9 hour light : dark photoperiod was employed. Temperature control was effected by means of a cooling coil in the lower pool of each stream. Stream temperature was monitored daily, and the cooling system maintained the mean temperature of the four streams between 20.9 and 25.2°C. Chemical constancy of the stream waters was maintained by metering makeup water to the streams on a continuous basis. The makeup water source was Berkeley (East Bay Municipal Utilities District) tap water, dechlorinated by passage through a column of activated carbon. Nutrient salts were added to the makeup water to promote primary productivity. The wastewater load for each stream was fed with this makeup water, and metered makeup water displaced an

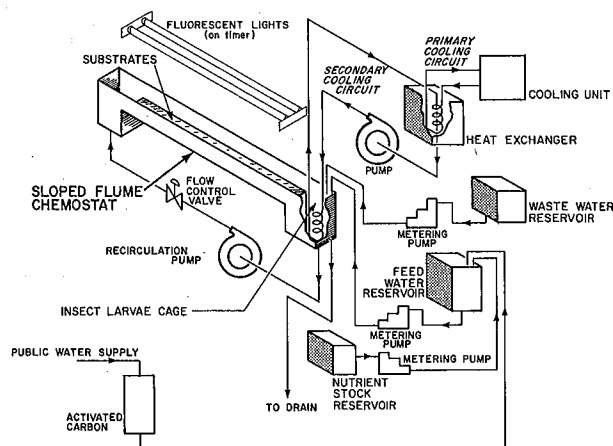


Fig. 1. Schematic of model streams.

(XBL 779-1907B)

equal volume of stream water to waste which left the system via overflow ports in stilling wells connected to each stream. The rate of makeup water feed was adjusted to deliver six stream volumes per day for a mean residence time of four hours.

### Samples

Two oil shale retort waters were studied. One sample came from a combustion run of Laramie Energy Technology Center's (LETC) 150-ton retort facility (150-ton retort water). The other was produced during the Rock Springs Site-9 true in-situ oil shale processing experiment (Omega-9 water) near Rock Springs, Wyoming. Filtered and unfiltered samples of the Omega-9 water were investigated to assess the effect of wastewater suspended solids, oil and grease, and tarry materials present in the unfiltered samples. The 150-ton water was used unfiltered. In addition, an ammonium carbonate solution was used in one run. This solution was tested to determine if two of the principal ions in retort waters, ammonium and carbonate, were responsible for observed effects on the aufwuchs and caddisfly larvae.

These retort waters are not necessarily representative of waters which may be produced during other oil shale processing experiments, and the results obtained are strictly indicative of these waters only. Nevertheless, probable aufwuchs responses from the retort waters of future full-scale oil shale processing can be estimated using this methodology.

### Aufwuchs

Six experimental runs were performed using unfiltered Omega-9 water, Omega-9 water filtered through a 0.4  $\mu\text{m}$  membrane (two runs), unfiltered 150-ton retort water, and an ammonium carbonate solution. Dilutions of these effluents ranging from 0.013 percent to 2.12 percent for contact periods of nine days were studied. Development and metabolism of aufwuchs on initially clean growth surfaces in the riffles of each stream were measured on the third, sixth, and ninth day of each experiment. Seed organisms were obtained by collecting stones (5 cm diameter) from the Stanislaus River, California (1300-m elevation) and transporting them in chilled containers to the laboratory. The stones were distributed to the lower reservoirs of the four streams. Assays of total solids, percent volatile solids, chlorophyll *a*, photosynthesis, respiration, and adenosine triphosphate (ATP) were performed, and microscopic examination was used to determine species distribution.

The effects of Omega-9 water on total solids, volatile solids, percent volatile solids, chlorophyll *a*, and respiration rates of aufwuchs are summarized in Fig. 2. Parameter values are given on a per substrate basis rather than per unit area to adjust for growth heterogeneities. An analysis of variance was performed on the data plotted in Fig. 2 and other study results. Three factors were used in the analyses: sampling time, stream identity, and Omega-9 water

dilution. This three-factor model was very significant ( $p = 0.001$ ) in explaining the variance observed in measurements of each of the variables.

These studies indicate that the laboratory-scale model stream apparatus and developed methodology can yield reproducible results for the biomass variables: total solids, volatile solids, and percent volatile solids. Growth and composition of the aufwuchs varies in the range of 10 percent to 25 percent under the no-load condition. The variance in the chlorophyll *a* and respiration rate data is enlarged through analytic error. Simple improvements to increase pigment extraction efficiency could lower the variation in the data. The respiration rate methodology is in need of more extensive refinement.

Filtered Omega-9 water stimulated aufwuchs growth at concentrations of 0.5 percent and less. Higher concentrations inhibited aufwuchs growth. Unfiltered Omega-9 water stimulated aufwuchs growth at concentrations of approximately 0.25 percent and less. Inhibition was suggested but not statistically confirmed at the highest concentration tested, one percent unfiltered Omega-9 water. Samples collected on day three of the nine-day experiments generally showed stimulated growth at all dilutions. Measurements on days six and nine, however, had lowered levels of growth at one percent or more filtered Omega-9 water concentration. The more dilute effluent loads stimulated growth throughout the test period. The most marked effect of Omega-9 water was to lower the proportional contribution of diatoms to the aufwuchs biomass. Dominance was shifted from diatoms to green algae. The ramifications of this species shift on other food chain components require further investigation.

The 150-ton retort water did not stimulate aufwuchs growth at the concentrations tested, 0.1 to 0.7 percent. Inhibition of aufwuchs growth was produced by this effluent, especially at the higher concentrations. Ammonium carbonate dilutions in the range of 0.5 to 4.5 mM did stimulate aufwuchs growth and no growth inhibition was observed.

### Caddisfly Larvae

Three experimental runs were performed using filtered and unfiltered Omega-9 water and an ammonium carbonate solution. The response of the caddisfly larvae, *Gumaga nigricula* and *Dicosmoecus gilvipes*, was monitored by surveying the state of the larvae at the end of each day. The caddisfly larvae were confined in cages of PVC screen located in the lower pool of each stream. A minimum of 16  $\text{cm}^3$  was provided for each individual.

The results of this investigation are summarized in Table 1 which details the response of the caddisfly larvae for each of the four runs. The disposition of the initial number of larvae in each stream is partitioned into the categories "active," "prepupae," "pupae," "dead or moribund," and "missing."

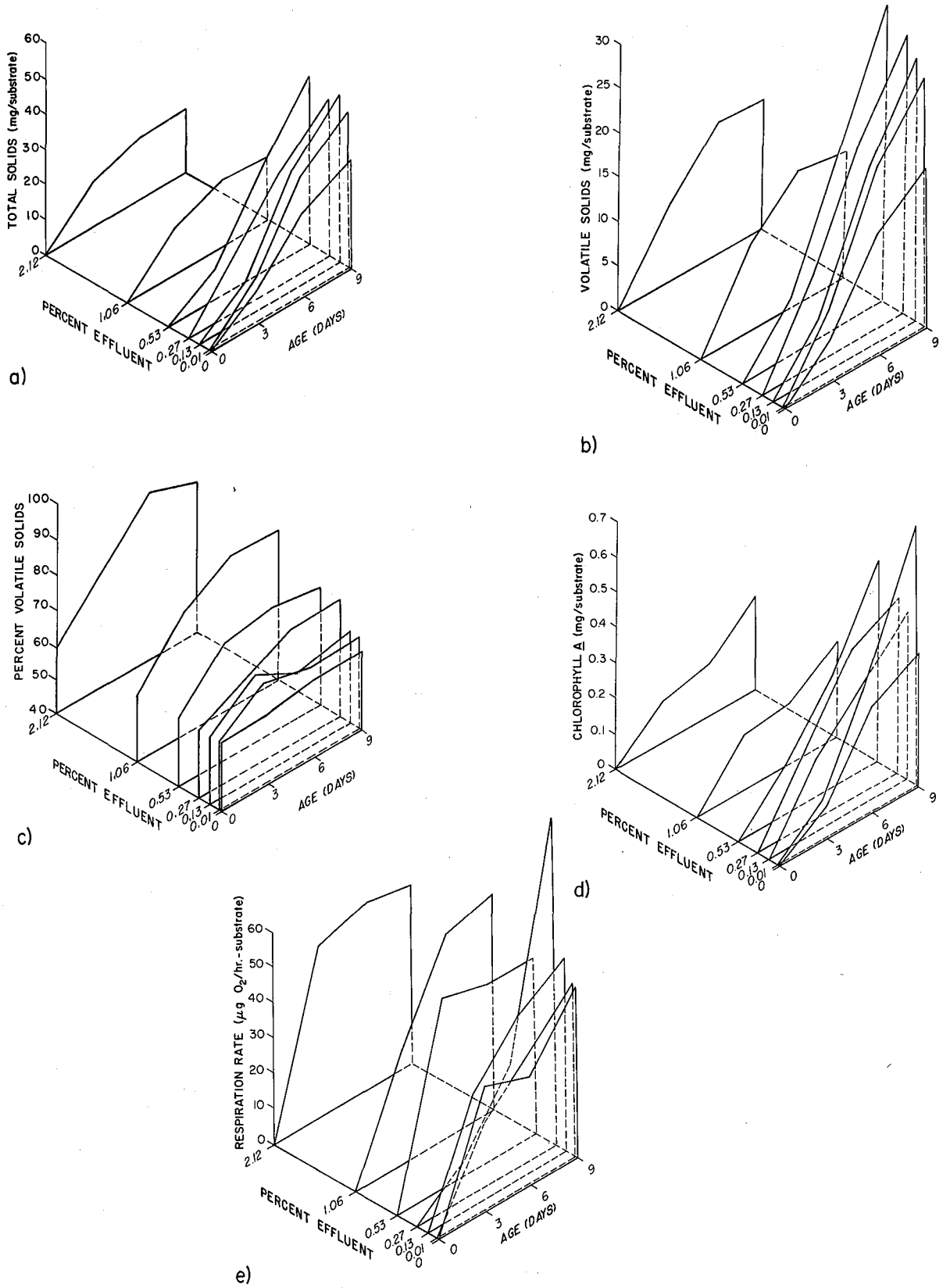


Fig. 2. The effect of various dilutions of filtered Omega-9 retort water on total solids, volatile solids, percent volatile solids, chlorophyll a, and respiration rate of aufwuchs.  
 a) XBL 7811-12619; b) XBL 791-97; c) XBL 7811-12618; d) XBL 791-98;  
 e) XBL 791-152

These results indicate that Gumaga nigricula larvae can be maintained in the laboratory model streams with no effluent loading at nearly 100 percent survival for at least 12 days. Filtered and unfiltered Omega-9 water had no statistically significant effect on the survival of this species for the dilutions and exposure times studied here. Concentrations of filtered Omega-9 water up to 2.12 percent, of unfiltered Omega-9 water up to 1.06 percent, and of ammonium carbonate up to 4.52 mM, produced no demonstrable reductions in Gumaga nigricula activity after nine days of exposure in the model streams. Dicosmoecus gilvipes larvae, on the other hand, were more sensitive to the ammonium carbonate solution than Gumaga nigricula. The activity of Dicosmoecus gilvipes was significantly reduced when fed ammonium carbonate con-

centration of 4.52 mM. Thus, they are potentially more sensitive indicators of environmental stress for retort waters which have high ammonium carbonate concentrations than are Gumaga nigricula larvae.

#### PLANNED ACTIVITIES FOR 1980

The data analysis will be completed and a final report on the study published.

#### FOOTNOTE

\*This work was funded by the Department of Energy's Laramie Energy Technology Center and the U.S. Department of the Interior.

†University of California, Berkeley, CA.

Table 1. Insect larvae bioassay results.

		INITIAL NO.	ACTIVE	PREPUPAE	PUPAE	DEAD OR MORBUND	MISSING
<u>Gumaga nigricula</u>	0%	17	16	0	1	0	0
	0.27%	15	15	0	0	0	0
	1.06%	15	14	1	0	0	0
	2.12%	16	14	2	0	0	0
<u>Gumaga nigricula</u>	0%	18	13	2	2	1	0
	0.27%	14	9	2	3	0	0
	Unfiltered Omega-9 Water	18	12	3	2	1	0
	1.06%	18	13	2	0	3	0
<u>Gumaga nigricula</u>	0 mM	9	5	2	1	0	1
	0.56 mM	11	8	3	0	0	0
	Ammonium Carbonate	10	5	3	1	1	0
	4.52 mM	9	4	3	1	1	0
<u>Dicosmoecus gilvipes</u>	0 mM	10	9	0	0	0	1
	0.56 mM	9	8	0	0	1	1
	Ammonium Carbonate	9	2	0	0	3	4
	4.52 mM	10	4	0	0	4	2

## TRACE ELEMENT STUDIES

MASS BALANCE AND PARTITIONING STUDIES OF SIMULATED  
IN-SITU RETORTS\*

J. P. Fox

## INTRODUCTION

Oil shales contain organic material in a matrix which includes significant quantities of such environmentally sensitive elements as U, Zn, Cu, Pb, As, Se, Hg, Cd, and Co. These elements could be released to the environment by the disposal of by-products, by leaching of solid wastes, or by refining and using shale oil.

Oil shale retorting produces shale oil, gas, a solid referred to as spent shale, and an aqueous effluent known as retort water. Elements initially present in the oil shale are partitioned or distributed to those products during the retorting process. The quantity of each element distributed among the products depends on the mineralogy of the oil shale and on retort operating conditions.

The purpose of this program (initiated in 1976) is to study the partitioning of fifty elements during in-situ oil shale retorting. In this program, products from pilot-scale and field-scale retorts are collected and analyzed for major, minor, and trace elements using neutron activation analysis, x-ray fluorescence spectrometry, Zeeman atomic absorption spectroscopy, and other techniques. The effects of retort operating conditions and oil shale source, grade, and particle size on elemental partitioning are being studied. The resulting data are used to complete elemental mass balances and to investigate the effect of operating conditions, such as temperature and input gas composition, on the distribution of the elements. Environmental implications of observed trends are determined and control of partitioning by modification of retorting parameters is explored. The program has focused on products produced by Laramie Energy Technology Center's (LETC) controlled-state retort and Lawrence Livermore Laboratory's (LLL) two pilot-scale retorts.

## ACCOMPLISHMENTS DURING 1979

Previously, products from 15 runs of the LETC controlled-state retort and nine runs of the LLL retorts were collected and analyzed for major, minor, and trace elements. This year, these data were used to complete material balances for each run and to study the effect of a range of retorting conditions on partitioning trends. The retort operating conditions for the 24 runs studied here are reported in Ref. 1. A range of conditions were investigated, including temperatures from 494 to 1200°C; nitrogen, air, and steam atmospheres; isothermal advance rates from 1.3 to 2.6 m/day; shale grades from 40 to 248 liters per tonne; and shales from

Colorado, Utah, Michigan (Antrim), and Morocco.

Mass Balance Studies

Mass balances were computed for each run and used to study partitioning trends and to assess the adequacy of sampling and analysis procedures. The elemental mass balances were computed as:

$$M_{x,IG} + M_{x,R} = M_{x,W} + M_{x,O} + M_{x,OG} + M_{x,S} \quad (1)$$

where

IG = input gas  
R = raw shale  
W = water  
O = oil  
OG = output gas  
S = spent shale

and  $M_x$  is the product of the elemental concentration  $C_x$  and the product mass  $m$ , and  $x$  is a subscript designating an individual element.

The degree of elemental mass balance closure was assessed using the elemental closure. The elemental closure is defined as the elemental mass recovery and is the percentage of the total elemental mass present in the raw oil shale and input gases that is accounted for in the products -- the spent shale, oil, water, and gas. It is computed from Eq. (1) as the ratio of elemental outputs to elemental inputs and is given by:

$$\left( \text{Elemental closure} \right)_x = 100 \frac{M_{x,S} + M_{x,O} + M_{x,W} + M_{x,OG}}{M_{x,R} + M_{x,IG}} \quad (2)$$

The elemental closures for each run and each element computed using Eq. (2) are summarized and reported elsewhere.<sup>1</sup> These data indicate that the elemental closure for LETC runs ranges from 15 percent to 240 percent and averages  $101 \pm 7$  percent (excluding Hg and Cd), and that for LLL runs it ranges from <25 percent to 360 percent and averages  $101 \pm 10$  percent (excluding Hg and Cd).

The data indicate that, within the limits of error, 100 percent of all measured elements, except Hg and Cd, was recovered. About 68 percent of the Cd and slightly less than 39 percent of the Hg originally present in the raw oil shale in LETC runs were recovered in the spent shale, oil, and water, while in the LLL runs, 88 percent of the Cd and slightly less than 35 percent of the Hg were recovered. The balance was

probably removed from the retort in the gas stream.

There are some noteworthy aspects of the closure data. The Zn, Pb, Cu, and Ni closures for the LLL runs are all greater than 100 percent, and the coefficients of variation are all larger than would be expected based on error propagation theory. Some of the Cu, Pb, and Zn closures are spuriously high, suggesting contamination.

The elements Cu, Pb, Ni, and Zn are typically alloyed with the stainless steels and brass used in grinding and sieving equipment. Hence, they could easily be introduced into samples during sample handling. If both the raw oil shale and spent oil shale are handled identically, any contamination introduced from sample handling would not significantly affect the mass balance since both samples would be contaminated approximately equally. However, if the spent shale is processed to a greater extent than the raw shale, contamination introduced during the additional processing would appear as a net increase in elemental mass. This is consistent with the actual handling received by the LLL samples. The spent shale from the LLL retorts, except Run S-10, received additional handling beyond that received by the raw oil shale. Therefore, it is concluded that a spurious contamination problem resulted for Cu, Pb, Ni, and Zn in LLL spent shales.

#### Partitioning Studies

The mass balances discussed in the previous section were used to study elemental distribution among the spent shale, retort water, oil, and gas. The mass distribution patterns of the more mobile elements are presented and discussed, and the effect of retort operating conditions on partitioning trends is inferred.

The mass balances computed for each run were analyzed to determine the mobility of each element where:

$$(M_x) = 100 \left( \frac{M_{x,O} + M_{x,W} + M_{x,OG}}{M_{x,S} + M_{x,O} + M_{x,W} + M_{x,OG}} \right) \quad (3)$$

Thus, the mobility is the percentage of the total elemental mass originally charged to the retort that is distributed to the oil, gas, and water phases as a consequence of retorting.

Table 1 compares the mobilities of Green River oil shales retorted in LETC and LLL retorts with those of Antrim and Moroccan shales retorted in the LETC retort. The Green River mobilities are the average ( $\bar{x}$ ) and one standard deviation ( $\sigma$ ) for all runs with Green River oil shales (Colorado and Utah). The Antrim and Moroccan mobilities are each for a single run. The data in Table 1 indicate that there are some significant differences in the mobilities of the Green River, Antrim, and Moroccan shales and between mobilities of Green River shales retorted in LETC and LLL retorts.

The Green River mobilities were ranked according to magnitude and three separate groups delineated. These groups are:

Group 1: (10% - 100%)	H, Hg, C, N, S, Cd
Group 2: (1% - 10%)	Se, Ni, As, Co
Group 3: (<1%)	Cr, Sb, Zn, Cu, Na, Mo, V, Ga, Fe, Mn, U, Ba, Dy, La, K, Mg, Sm, Cs, Eu, Hf, Rb, Ce, Sr, Ti, Th, Al, Sc, Yb, Ca.

Similar rankings were not attempted for the Antrim and Moroccan shales -- the data were too limited to permit assessment of variability.

Mass distribution patterns for the Group 1 elements are summarized in Fig. 1 (LETC) and Fig. 2 (LLL) for various retort operating conditions and shale types. These figures and the mobilities in Table 1 indicate that Group 1 elements are significantly mobilized during retorting and are characterized by a large oil and gas component. The majority of the H is removed from the shale matrix while the other Group 1 elements - C, N, S, Cd, and Hg - have a significant spent shale component except high temperature runs of the LLL retorts (Fig. 2). This is proposed to be related to the relative volatilities of these elements. The H, N, organic C, and some of the S are initially present in kerogen in Green River shales and are readily converted to oil and gases by pyrolysis at about 500°C or higher. The remainder of the S and the Cd, Hg, and inorganic C are largely present in the mineral phase of the shales and are released when the retorting temperature is high enough to decompose them. Thus, H is the most volatile element followed by Hg, C, N, S, and Cd. The elements H, N, and C are distributed primarily to the oils and gases in Green River shales; more than 35 percent of the H, N, and C is distributed to the oil (except air-stream runs on the LLL retorts) compared to less than 15 percent of the S, Cd, and Hg (except high temperature runs of the LLL retorts).

Very little ( $\leq 1$  percent) of the Group 1 elements, except N and H, is distributed to the water. The large mass distribution of N to the water may be related to significant solubility in water of the N compounds produced during retorting, while the similar trend for H is probably due to both production of water during retorting and to dissolving of H-containing organic compounds.

All of the Group 1 elements, except N, have a significant gas-phase component for most runs. Over 20 percent of the S, Cd, and Hg is distributed to the gas phase while less than 5 percent of the N and 20 percent of the C is distributed to the gas phase.

Figures 1 and 2 also show the effect of various retort operating conditions on partitioning trends. The percentage of H, N, and C remaining in the spent shale decreases with the addition of steam and as the temperature increases. For example, 33 percent and 40 percent of the C during N<sub>2</sub>-steam and N<sub>2</sub> runs (Fig.

Table 1. Mobility of some major, minor, and trace elements in Green River, Antrim, and Moroccan oil shales.

Group	Constituent	Mobility, % <sup>a</sup>			
		Green River		Antrim	Moroccan
		LETC	LLL		
1	H	94 ± 3	99 ± 1	79	88
	Hg	70 ± 20	88 ± 19	46	67
	C	64 ± 7	98 ± 1 <sup>c</sup>	41	41
	N	49 ± 7 <sup>b</sup>	-	16	35
	S	44 ± 8	-	46	72
	Cd	29 ± 7	23 ± 6	53	-
2	Se	5.1 ± 1.0	19 ± 13	2.6	7.5
	Ni	4.7 ± 1.3	1.9 ± 1.3	0.13	0.62
	As	3.8 ± 1.3	3.1 ± 1.2	0.22	1.5
	Co	3.8 ± 0.8	1.6 ± 0.6	0.005	0.16
3	Cr	0.38 ± 0.78	0.37 ± 0.72	0.0085	0.0060
	Sb	0.28 ± 0.15	0.29 ± 0.38	0.70	1.2
	Zn	0.27 ± 0.28	0.43 ± 0.37	0.65	0.059
	Cu	0.27 ± 0.33	4.0 ± 3.1	0.013	0.020
	Na	0.19 ± 0.10	0.01 ± 0.01	0.15	1.0
	Mo	0.18 ± 0.11	0.34 ± 0.16	0.076	0.055
	V	0.11 ± 0.03	0.052 ± 0.042	0.033	0.20
	Ga	0.10 ± 0.07	0.045 ± 0.022	0.023	0.17
	Fe	0.084 ± 0.081	0.026 ± 0.016	0.0006	0.008
	Mn	0.056 ± 0.071	0.016 ± 0.022	0.003	0.008
	U	0.040 ± 0.023	0.063 ± 0.075	0.076	0.063
	Ba	0.035 ± 0.022	-	0.004	0.03
	Dy	0.034 ± 0.017	-	-	0.026
	La	0.024 ± 0.019	0.0018 ± 0.0020	0.0007	0.002
	K	0.023 ± 0.022	0.0029 ± 0.0024	0.016	0.050
	Mg	0.021 ± 0.019	0.0010 ± 0.0010	0.009	0.008
	Sm	0.020 ± 0.019	0.016 ± 0.026	-	0.18
	Cs	0.019 ± 0.019	-	0.034	0.016
	Eu	0.018 ± 0.013	0.020 ± 0.024	0.0004	-
	Hf	0.014 ± 0.028	-	0.003	-
	Rb	0.014 ± 0.009	0.0029 ± 0.0023	0.028	0.052
	Ce	0.013 ± 0.007	0.0017 ± 0.0004	0.0005	-
	Sr	0.012 ± 0.016	-	0.015	0.0028
	Al	0.0062 ± 0.0035	0.00060 ± 0.00042	0.0002	-
	Ca	0.003 ± 0.005	0.00042 ± 0.00034	0.008	0.0004
	Sc	0.0057 ± 0.0025	0.0011 ± 0.0009	-	0.0002
	Ti	0.0090 ± 0.015	0.019 ± 0.024	0.005	-
	Yb	0.0033 ± 0.0010	0.022 ± 0.006	-	-
Th	0.0076 ± 0.0081	0.0043 ± 0.0037	0.049	-	

<sup>a</sup>Percent of elemental mass present in raw oil shale that is distributed to the oil, water, and gas phases.

<sup>b</sup>Excludes the N<sub>2</sub>-steam-O<sub>2</sub> runs (CS-69, CS-74) which were significantly different from others in set. The mobility of N for these runs is 88% and of C, 92%.

<sup>c</sup>Excludes the single N<sub>2</sub> run (S-9) which was significantly different from others in the set. The mobility of N for run S-9 is 55%; of H, 86%; and of Hg, 63%.

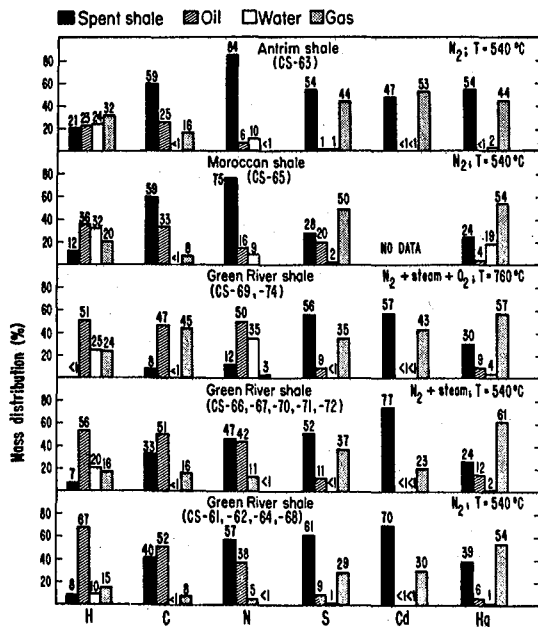


Fig. 1. Mass distribution patterns for Group 1 elements in LETC's controlled-state retort. (XBL 795-1651B)

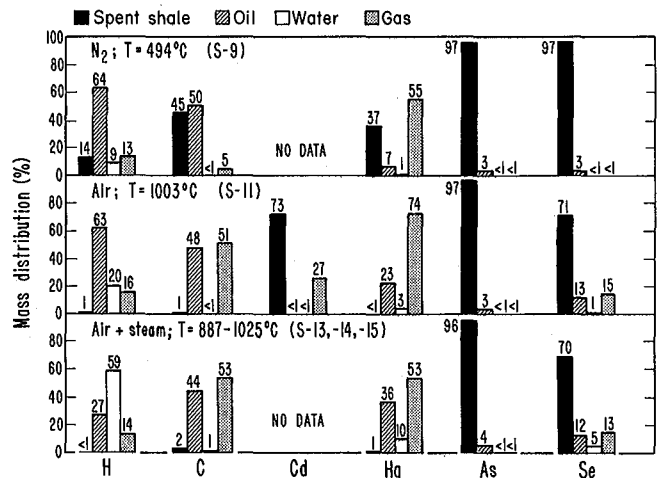


Fig. 2. Mass distribution patterns for Group 1 elements in LLL's 125-Kg retort. (XBL 805-962)

2), respectively, remain in the spent shale and only 8 percent remains in the spent shale produced from the  $N_2$ -steam- $O_2$  runs. In the high temperature  $N_2$ -steam- $O_2$  runs (Figure 1), a larger fraction of the H, N, and C is distributed to the byproducts than during  $N_2$  or  $N_2$ -steam runs at lower temperatures.

The  $N_2$  and  $N_2$ -steam runs of the LETC retort (Fig. 1) have identical mass distribution patterns, with the exception of H, for which a larger fraction of the total mass of H is distributed to the water in the  $N_2$ -steam runs than in the  $N_2$  runs. The LLL retorts also have a larger fraction of the H mass distributed to the water in air-stream runs than in  $N_2$  runs (Fig. 2). This is because the steam charged to the retort appears as retort water, resulting in a larger percentage mass distribution of H to the water phase.

There are also statistically significant differences in the C and N mass distributions between the  $N_2$ -steam- $O_2$  runs ( $T = 760^\circ\text{C}$ ) and other runs of the LETC retort with Green River shales; a larger fraction of the C is distributed to the gas, and of the N, to the water. These differences are due to the more complete conversion of kerogen and decomposition of carbonates at the elevated temperatures (the  $N_2$ -steam- $O_2$  runs were at  $760^\circ\text{C}$  and other runs were at  $540^\circ\text{C}$ ) and to reactions of  $O_2$  in the input gas with constituents in the oil shale.

The retort operating conditions studied here had little effect on the distribution patterns of Hg, Cd, and S and there are no significant differences between the patterns shown in Fig. 1 for  $N_2$ ,  $N_2$ -steam, and  $N_2$ -steam- $O_2$  and in Fig. 2 for  $N_2$ , air, and air/steam.

Figure 1 also indicates that there are some differences between the mass distribution patterns for Green River, Moroccan, and Antrim shales. A larger fraction of the H, N, and C remains unconverted in the spent shale in Moroccan and Antrim shales than in Green River shales. Consequently, a smaller fraction of the H, N, and organic C is distributed to the oil in Antrim and Moroccan shales than in Green River shales retorted under equivalent conditions. It is hypothesized that this is due to differences in mineral and organic composition of the various shales. This suggests that different retorting conditions will be required to optimally extract oil from various shales and illustrates that the data developed for one shale should not be generalized to others. The mass distribution patterns for S, Cd, and Hg in Moroccan and Antrim shales are consistent with those for Green River shales.

Mass distribution patterns for the Group 2 elements are summarized in Table 2 in which the Green River, Antrim, and Moroccan shales are compared. Tables 1 and 2 indicate that from one percent to five percent of the elemental mass of Green River shales for Group 2 elements is mobilized, and about 95 percent of that is distributed to the oil. Less than one percent of these elements is distributed to the water and gas except for Se.

The retort operating conditions studied here had no statistically significant effect on the mass distribution patterns of Green River oil shales for any of the Group 2 elements except Se. The LLL mass balance data suggest that Se is vaporized and removed from the retort at temperatures greater than approximately  $900^\circ\text{C}$ .

The principal differences in mass distri-

Table 2. Mass distribution patterns of Group 2 elements, percent.

	Green River		Antrim	Moroccan
	LLL	LETC		
Nickel				
Spent shale	98.0 ± 1.4	95.4 ± 1.0	99.9	99.3 ± 0.1
Oil	1.3 ± 0.4	4.4 ± 1.0	0.1	0.5 ± 0.01
Water	0.3 ± 0.5	0.2 ± 0.1	0.0	0.2 ± 0.1
Gas	0.0	0.0	0.0	0.0
Cobalt				
Spent shale	99.2 ± 0.4	96.2 ± 0.9	100.0	99.8
Oil	0.8 ± 0.4	3.7 ± 0.8	0.0	0.1
Water	0.0	0.1 ± 0.1	0.0	0.1
Gas	0.0	0.0	0.0	0.0
Arsenic				
Spent shale	96.9 ± 1.2	96.3 ± 1.2	99.8	97.8 ± 0.9
Oil	3.0 ± 1.2	3.4 ± 1.2	0.0	1.1 ± 0.8
Water	0.1 ± 0.1	0.3 ± 0.1	0.2	1.1 ± 0.1
Gas	0.0	0.0	0.0	0.0
Selenium				
Spent shale	71.9 ± 4.6 <sup>a</sup>	94.9 ± 1.0	64.4	92.2 ± 0.4
Oil	9.5 ± 4.2 <sup>a</sup>	4.6 ± 0.8	1.2	5.4 ± 0.4
Water	2.8 ± 2.0 <sup>a</sup>	0.5 ± 0.5	0.5 <sup>b</sup>	2.3 ± 0.8
Gas	15.9 ± 6.4 <sup>a,b</sup>	0.0	15.2 <sup>b</sup>	0.0

<sup>a</sup>These values are for S-11 through S-15 and L-1. The mass distribution pattern for S-9 and S-10 was: spent shale =  $96.7 \pm 0.8$ ; oil =  $2.8 \pm 0.2$ ; water =  $0.6 \pm 0.6$ ; gas = 0.0.

<sup>b</sup>Computed by difference.

bution patterns for Group 2 elements occur for shales retorted in different retorts and of different geological origins, namely, Green River, Antrim, and Moroccan. The mass distribution of both Ni and Co to LLL oils is significantly lower than to LETC oils while the mass distribution of Se to LLL oils is higher. There is no statistically significant difference in the distribution of As nor of Ni and Co to the water between the LLL and LETC retorts. It is significant that both Co and Ni, which are chemically similar, behave differently in the LLL and LETC retorts. The cause for this is uncertain and may be related to differences in retort operation, such as condenser design and operation, not reflected in the variation of retorting parameters as reported elsewhere.<sup>1</sup>

Geological origin of the shale also influences the mass distribution pattern for Group 2 elements. Significantly less Ni, Co, and As is distributed to the oil and water in Antrim and Moroccan shales than in Green River shales. Although the distribution pattern of Se in Moroccan shale is similar to that of LETC Green River shales, the pattern for Se in Antrim shale is very different, with about 15 percent of the Se leaving the retort in the offgas. Because it is based on a single retort run, additional and corroborative work is required to verify and support this latter conclusion.

The elements in Group 3 all have mobilities that are less than one percent and large coefficients of variation (27 percent - 205 percent) (Table 1). The large coefficients of variation

are due to experimental error rather than retort operating conditions. Because the concentration of these elements in the oil and water phases is near the detection limit of many of the techniques used, the analytical errors are large. No significant relationships between operating conditions and mobility in any phase or combination of phases for Group 3 elements were observed. The variation in the mobility of those elements recorded in Table 1 is hypothesized to be due to propagation of experimental errors.

#### PLANNED ACTIVITIES FOR 1980

Chemical thermodynamic calculations will be used to assess partitioning results and predict elemental volatility. Reaction mechanisms postulated to control elemental partitioning will be investigated in laboratory studies. Mass balance and partitioning studies will be conducted on samples from field retorts including Occidental's Logan Wash site, Rio Blanco Oil Shale Project's C-a site, and Geokinetics' Utah site.

#### FOOTNOTE AND REFERENCE

\*This program is funded by the Department of Energy's Division of Oil, Gas, and Shale Technology.

1. J. P. Fox, The Partitioning of Major, Minor and Trace Elements during Simulated In-Situ Oil Shale Retorting, Ph.D. Dissertation, University of California, Berkeley (1980); Lawrence Berkeley Laboratory Report, LBL-9062 (1980).

## PARTITIONING OF As, Cd, Hg, AND Se DURING SIMULATED IN-SITU OIL SHALE RETORTING\*

A. T. Hodgson, D. C. Girvin, G. Winston, and S. Doyle

### INTRODUCTION

Oil shales from the Green River Formation in Colorado and Utah contain significant quantities of potentially mobile, toxic trace elements such as As, Cd, Hg, and Se. These elements could be released to the environment as the result of commercial exploitation of the oil shale resource through disposal of liquid and gaseous by-products, through leaching of solid wastes, and through refining and use of the oil. Concern about toxic trace element mobilization and the potential public health and environmental consequences has led to several recent investigations of elemental distributions in oil shales from the Green River Formation.<sup>1-4</sup> These studies have revealed that As, Mo, Sb, Se, and Zn, which are conventionally sulfide-forming elements, are significantly enriched in the shales while most other elements in the shales have abundances which are similar to average crustal abun-

dances.<sup>3</sup> Although Cd and Hg, with typical concentrations of 0.1 to 1 ppm, are not significantly enriched in oil shales, they are included among the potentially mobile elements because of their high volatilities.

Retorting of oil shale results in the production of shale oil, retort offgases, an aqueous effluent known as retort water, and a solid referred to as spent shale. The elements initially present in the oil shale are distributed, or partitioned, to these products during the retorting process in a manner which is dependent upon the mineralogy of the oil shale and the retort operating conditions.

Some limited information is available on elemental partitioning during oil shale retorting. Studies completed to date<sup>2,3,5</sup> have demonstrated that most elements remain in the shale. The notable exceptions among trace ele-

ments are As, Cd, Co, Hg, Ni, and Se. Due to the high volatilities of Cd and Hg, about 30 and 70 percent of the respective elemental masses of these elements partition into the gas phase. Approximately four percent of the elemental masses of As, Co, Ni, and Se are released from the shale with about 95 percent of that distributed to the oil.

The purpose of this program, which is entering its second year, is to investigate the partitioning of As, Cd, Hg, and Se during simulated and pilot-scale in-situ oil shale retorting. The investigation will be accomplished by making careful measurements of the four elements in the starting material and in the retorting products from a 6-kg, laboratory-scale retort and from various pilot-scale retorts. The laboratory retort, which was specifically designed and built for this program, will be used to determine the effects of retort operating conditions, such as temperature regime and gas composition, on elemental partitioning. Gas monitoring instrumentation is being developed to make measurements of As, Cd, Hg, and Se in retort offgases. Conventional analytical methods are being adapted, as necessary, and applied to the measurement of these elements in shale oils, retort waters, and raw and spent shales.

## ACCOMPLISHMENTS DURING 1979

### Laboratory Retort

A major achievement during the first year of this program was the design and construction of an oil shale retort (Fig. 1 and 2) for the purpose of conducting environmental research in the laboratory under simulated in-situ retorting conditions. The retort will be used to evaluate the effects of various gas environments, flow rates, and heating conditions on trace element volatilization and partitioning. These objectives dictated retort design. Consequently, provisions have been made for the separation and collection of liquid products, for the accurate measurement of the volume of offgas produced, and for the on-line installation of the ZAA gas monitor. In addition, construction materials were carefully selected in order to minimize contamination during retorting and sample collection.

The laboratory retort can batch-process 6 kg of raw shale at temperatures up to 1200°C. Initially, hot-inert-gas retorting will be used. However, the retort is versatile and can be modified in the future for combustion retorting. A basic description of the major components is given below.

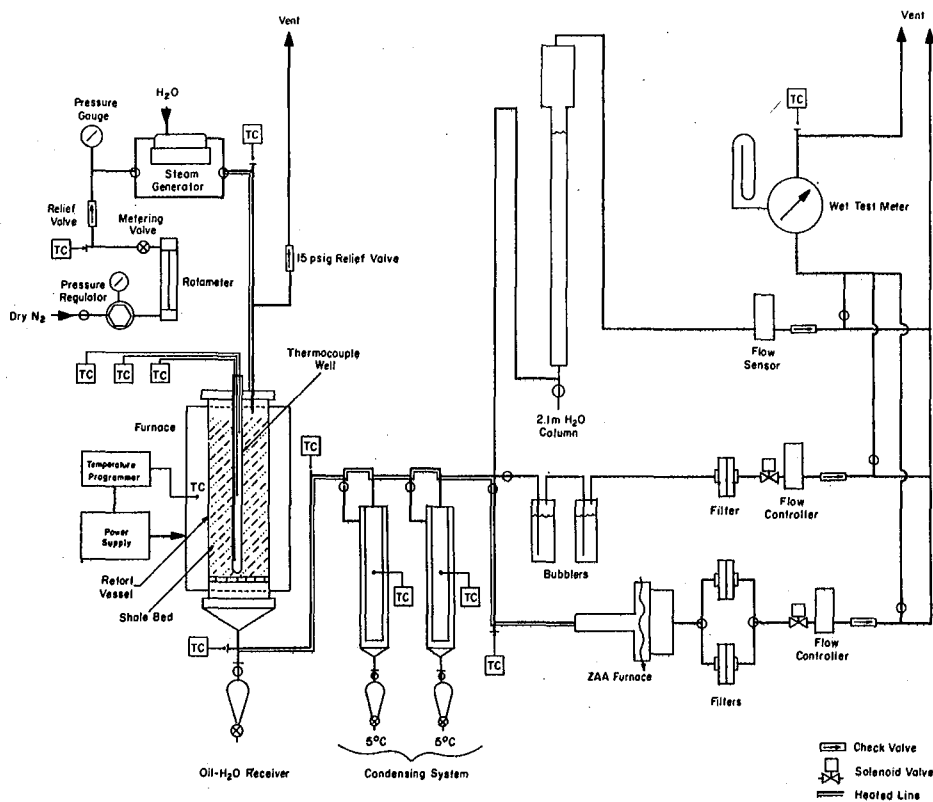


Fig. 1. Schematic of 6-kg laboratory retort. (XBL 802-8238)

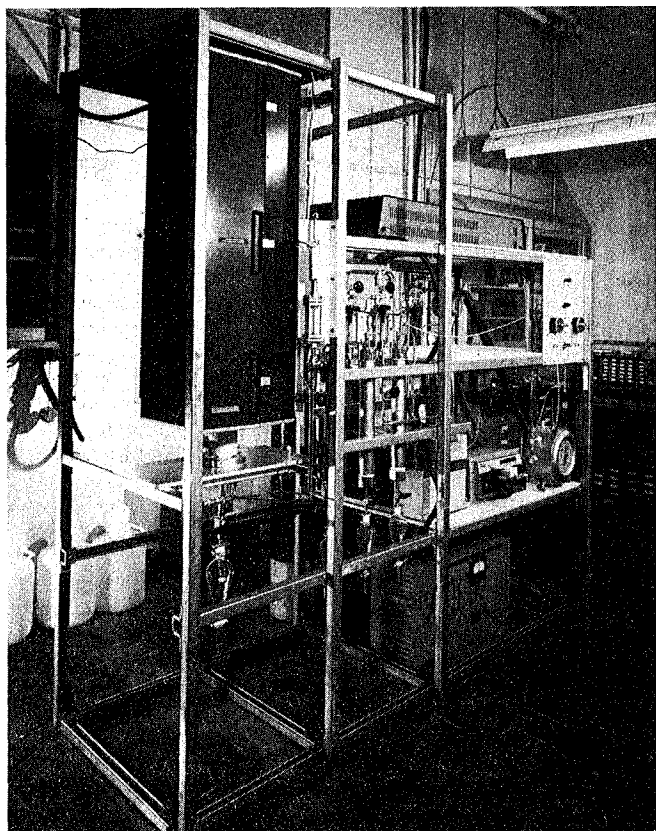


Fig. 2. Overall photographic view of 6-kg laboratory retort. (XBB 798-10748)

The retort vessel is a mullite ceramic tube, 9 cm ID by 160 cm long, with removable stainless steel flanges mated to both ends. An inner mullite tube and ceramic grate support the 80 cm-long shale column. The retort vessel is heated by a single zone tube furnace designed for a 1200°C maximum operating temperature. A programmer provides a heating ramp of 0.4 to 9.9°C/min over the calibration range of the control console. A small mullite tube extends down through the axis of the shale column and serves as a thermocouple well. Thermocouple junctions are positioned in the well at the center and ends of the column.

Oil and water which drain from the retort vessel are collected in a receiver located immediately below the retort. Offgases exit the retort and pass through a section of electrically heated, stainless steel tubing to two variable temperature condensers. The plumbing system is designed so that the offgases can be routed past either or both of these units.

The Zeeman atomic absorption (ZAA) gas monitor is connected to the offgas line downstream of the condensers. Flow through the ZAA monitor is regulated with an electronic flow controller. Provision has also been made to pass a portion of the offgas flow through a series of bubblers in order to chemically trap out the elements of interest. Excess flow bubbles through a 2.1 meter high water column which serves as a back

pressure regulator. A wet test meter is used to calibrate the flow controllers.

#### Analytical Methods

Adequate analytical methods are essential for elemental partitioning studies. The methods used must be sufficiently sensitive, precise, and accurate so that an acceptable degree of confidence in elemental mass closure equations can be obtained. Since oil shale and its products are complicated matrices, standard analytical procedures are often inadequate. Consequently, we have developed new methods or adapted conventional methods for the analysis of these materials.

Our major analytical emphasis during the first year of the program has been placed on developing on-line, gas-phase measurement capabilities for the elements of interest. To date, we have successfully modified a ZAA spectrometer for continuous on-line Hg monitoring in oil shale offgases and have initiated development of similar instrumentation for As, Cd, and Se. This work is discussed in detail in another article of this report.<sup>6</sup> We have also adapted and evaluated analytical methods for As, Cd, Hg, and Se in shale oils and retort waters.

We first examined energy-dispersive x-ray fluorescence (XRF) spectrometry for analysis of As, Cd, Hg, and Se in shale oils and retort waters and found it to be generally adequate for analyses of As and Se, but not sensitive enough for Cd and Hg analyses. These limitations necessitated the expansion of our analytical capabilities.

Graphite furnace atomic absorption (GFAA) spectroscopy was selected as an alternative method because of its high sensitivity for the elements of interest and its moderate cost. With GFAA we were able to analyze a variety of retort water samples for As, Cd, and Se without extensive sample pretreatment. Chemical and background matrix interferences were reduced to acceptable levels by careful temperature control during the furnace heating cycle, simple matrix modifications, and moderate dilution of the sample. Preliminary attempts to analyze shale oils by GFAA have produced promising results; however, additional evaluation is required.

Direct analyses of Hg in shale and diluted oil are performed with a batch-type ZAA, while a conventional cold vapor atomic absorption technique is used for Hg analyses of retort water because higher sensitivity is required. The cold vapor technique necessitates the use of an oxidation step to destroy organometallic compounds and organic complexing agents prior to analysis. Organics in retort water samples have been successfully oxidized by ozone in combination with ultraviolet radiation from a low-pressure Hg vapor lamp.

#### PLANNED ACTIVITIES FOR 1980

Our efforts to develop on-line ZAA gas monitors for trace elements other than Hg will

continue. The Hg gas monitor and the new gas monitors will be used in experiments with the laboratory retort to investigate the partitioning of As, Cd, Hg, and Se during inert gas, simulated in-situ retorting. The temporary installation of the Hg gas monitor at a large pilot-scale in-situ retort is also planned.

#### FOOTNOTE AND REFERENCES

\*This program is funded by the U.S. Environmental Protection Agency.

1. G. A. Desborough, J. K. Pitman, and C. Huffman, Jr., "Concentration and Mineralogical Residence of Elements in Rich Oil Shales of the Green River Formation, Piceance Creek Basin, Colorado, and the Uinta Basin, Utah--A Preliminary Report," *Chemical Geology*, 17, 13-26 (1976).
2. J. P. Fox, K. K. Mason, and J. J. Duvall, "Partitioning of Major, Minor, and Trace Elements during Simulated In-Situ Oil Shale Retorting in a Controlled-State Retort," Twelfth Oil Shale Symposium Proceedings, Colorado School of Mines, Golden, CO (1979).
3. J. P. Fox, The Partitioning of Major, Minor, and Trace Elements during Simulated In-Situ Oil Shale Retorting, Ph.D Dissertation, University of California, Berkeley (1980).
4. R. D. Giaque, J. P. Fox, J. W. Smith, and W. A. Robb, "Geochemical Studies of an Oil Shale Deposit," Energy and Environment Division Annual Report 1979, Lawrence Berkeley Report, LBL-10486 (1980).
5. J. P. Fox, J. J. Duvall, K. K. Mason, R. D. McLaughlin, T. C. Bartke, and R. E. Poulson, "Mercury Emissions from a Simulated In-Situ Oil Shale Retort," Eleventh Oil Shale Symposium Proceedings, Colorado School of Mines, Golden, CO (1978).
6. D. C. Girvin and A. T. Hodgson, "On-line Measurement of Trace Elements in Oil Shale Offgases by Zeeman Atomic Absorption Spectroscopy," Energy and Environment Division Annual Report 1979, Lawrence Berkeley Laboratory Report, LBL-10486 (1980).

## ON-LINE MEASUREMENT OF TRACE ELEMENTS IN OIL SHALE OFFGASES BY ZEEMAN ATOMIC ABSORPTION SPECTROSCOPY\*

*D. C. Girvin, A. T. Hodgson, and S. Doyle*

#### INTRODUCTION

Recent emphasis on the development of synfuel processes has renewed interest in the vast oil shale deposits of Colorado, Utah, and Wyoming and the technology needed to recover and utilize this source of domestic oil. Accompanying the development of oil shale recovery processes are a number of important environmental concerns such as the mobilization and release to the atmosphere of toxic trace elements. Preliminary mass balance studies of pilot-scale in-situ oil shale retorting processes indicate that significant quantities of the toxic trace elements Hg, Cd, As, and Se originally present in the raw shale are volatilized during retorting and are subsequently swept from the retort into the atmosphere in the stream of process offgases. Based on preliminary information, the magnitude of these emissions for each of these elements could be on the order of several metric tones per day for a 100,000 barrel per day commercial in-situ oil shale facility.

Assessment of this potential problem and development of the control technology to minimize emissions depend upon reliable direct measurements. The lack of data is due to the fact that measurements of Hg, Cd, As, and Se are very difficult to make in a matrix as complex and corrosive as oil shale offgases. No direct on-line offgas measurements of As, Cd, or Se exist while direct on-line mercury measurements

have been made. These preliminary measurements in the offgas of a pilot-scale in-situ oil shale processing plant were made by LBL scientists<sup>1</sup> using Zeeman atomic absorption spectroscopy (ZAA). This successful use of a prototype ZAA spectrometer demonstrated that the unique background correction capability of ZAA makes it suitable for continuous on-line analysis of trace elements in a highly complex organic-rich gas matrix.

The purpose of this program, which is entering its second year, is to develop and apply ZAA spectroscopy for direct on-line trace element analysis of gases. The specific objectives are: (1) to develop highly stable light sources and accurate calibration techniques for each of these elements; (2) to design and build two ZAA spectrometers for analysis of gas streams, one for Hg for field and laboratory use and a second for As, Cd, and Se for lab use; (3) to design and build appropriate gas sampling and metering systems; and (4) to test these instruments in the offgas streams of laboratory-scale and pilot-scale oil shale retorts.

#### ACCOMPLISHMENTS DURING 1979

A field Zeeman atomic absorption (ZAA) spectrometer capable of continuous on-line mercury measurements and a gas handling and calibration system were designed, built, and tested during a steam-combustion run of the

Lawrence Livermore Laboratory's (LLL) 6000-kg simulated in-situ retort. The field ZAA instrument shown in Fig. 1 incorporates some significant advances in state-of-the-art Zeeman atomic absorption spectroscopy and gas monitoring. A new light source, furnace, and gas sampling and calibration system were developed and electronics were redesigned to facilitate parts replacement and to improve stability for long-term field use.

#### Instrumentation Development

The new spectrometer includes a new light source, furnace assembly, and electronics developed to accommodate mercury analysis under severe field conditions. A new gas sampling-metering system was developed which includes both a heated sample probe and a heated sample transport line to minimize the loss of mercury during sampling. Finally, a dynamic mercury calibration device, similar to that described by Nelson<sup>2</sup>, was built which enables a stream of inorganic mercury vapor of known concentration to be added directly to the sample gas for calibration of the ZAA spectrometer.

#### Mercury Light Source.

The mercury ZAA will be used in field applications where significant temperature fluctuations are likely to occur. By far the most temperature-sensitive component of this ZAA is the light source. A new, low pressure mercury gaseous discharge lamp was built and tested. This new lamp resolves the previous problem of baseline drift with temperature and eliminates radio-frequency pickup previously encountered; the 2537 Å line intensity is approximately 50 percent greater than with the previous radio-frequency excited electrodeless discharge lamp

(EDL). This new lamp, shown in Fig. 2, consists of a U-shaped quartz tube containing argon and a small quantity of mercury. Minute electrodes are sealed in each end of the tube. The outer diameter of the tube is 7 mm. The lamp is surrounded by a soft iron water jacket fitted with a quartz window. The lamp water-jacket assembly, shown in Fig. 2, fits between the pole tips of the permanent magnet which produces the Zeeman splitting of the resonance lines. The argon plasma and mercury resonance lines are produced by a 700-Hz high voltage driver.

Changes in light source intensity can be a problem in field applications where significant temperature fluctuations are likely to occur. The change in the intensity of the 2537 Å line with variations in the light source temperature is shown in Fig. 3a. The intensity increases by a factor of three from 12°C to 31°C because of an increase in the mercury vapor pressure within the lamp. However, the ZAA response to a constant mercury concentration remains stable within measurement errors over this temperature range (Fig. 3b). Stability is achieved by routing the photomultiplier tube signal through a log amplifier before it enters the tuned amplifier section of the lock-in-amplifier. This electronic processing effectively "filters out" the effect of light intensity changes due to changes in temperature.

However, there is another temperature effect which is not "filtered out" by the electronics. The relative intensity of the Zeeman split analytical lines is altered by self-absorption within the plasma of the lamp. This effect, which increases with temperature, manifests itself as a change in instrumental baseline voltage and, thus, is indistinguishable from the signal produced by mercury in the sample gas.

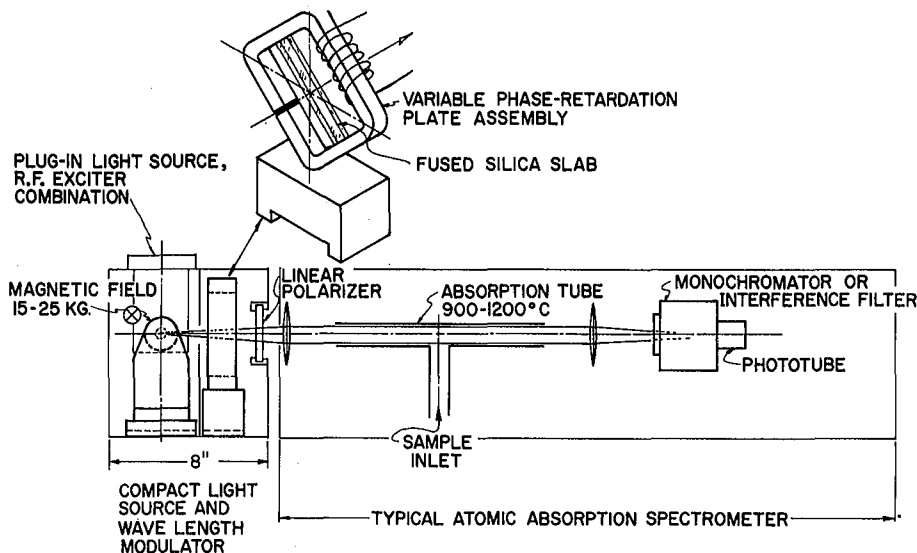


Fig. 1. Schematic of Zeeman atomic absorption spectrometer designed to make continuous on-line measurements of mercury in gas. (XBL 793-8742)

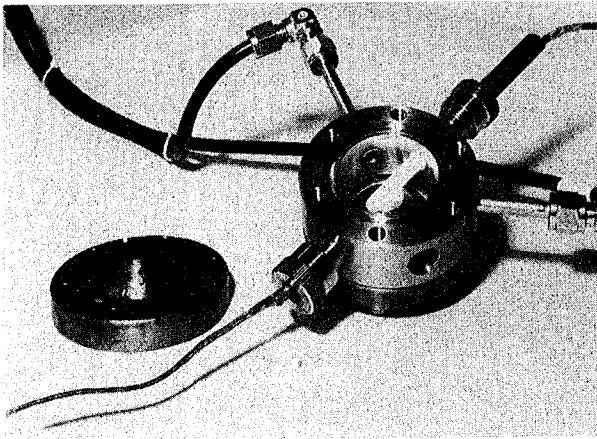


Fig. 2. Light-source water-jacket assembly. The low pressure mercury light source screws into the upper right hand corner. (CBB 793-3220)

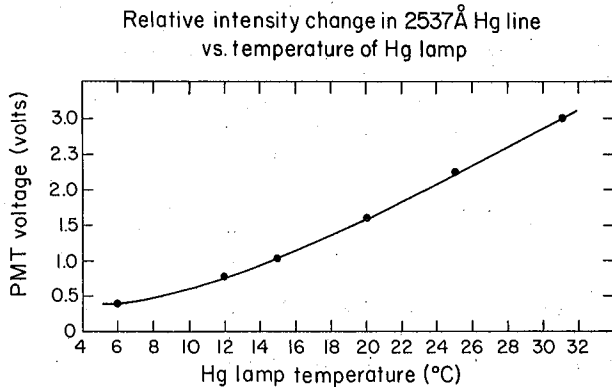


Fig. 3a. Change in intensity of gaseous mercury discharge lamp with temperature. (XBL 793-869)

The magnitude of this effect is shown in Fig. 3c. In the absence of mercury, a 12-31°C change in temperature produces a 220 millivolt ZAA voltage as shown by the lower curve in Fig. 3c. The upper curve shows this change in parts per billion (ppb) of mercury. If the lamp is operated at 25°C, a variation of  $\pm 2^\circ\text{C}$  produces a 5 ppb error, which is significant when levels are 60 ppb or lower. Temperature control of the light source was not possible with the old EDL. However, with the new light source, the problem has been eliminated by enclosing the lamp in the water-jacket assembly described above and coupling it to a small thermoelectric constant-temperature water bath, mounted within the instrument. This arrangement allows the temperature of the new lamp to be controlled to within  $\pm 0.4^\circ\text{C}$ , which is equivalent to an error of only  $\pm 0.1$  ppb of mercury.

#### Arsenic, Cadmium, and Selenium Light Sources.

New highly stable ZAA light sources for As, Cd, and Se have been developed and tested under a separate DOE contract. These light sources are similar in concept to those now used for mercury,

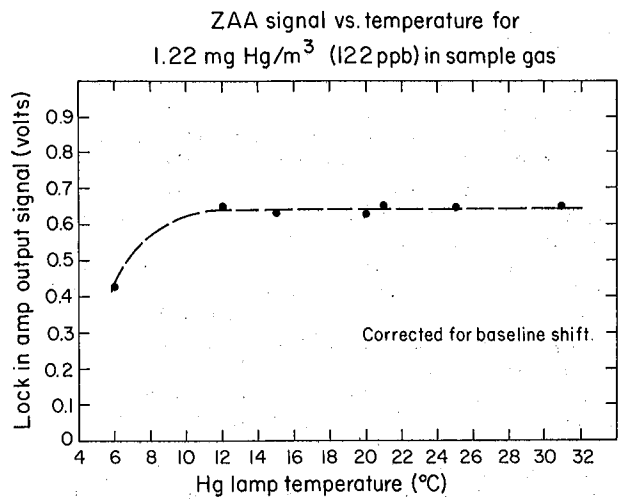


Fig. 3b. Temperature dependence of ZAA response to a constant concentration of mercury. (XBL 793-870)

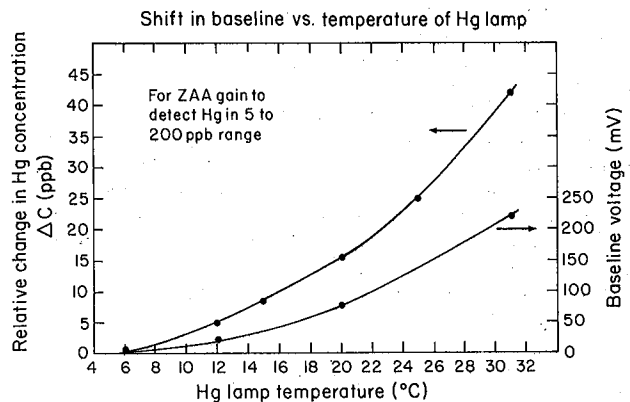


Fig. 3c. Change in ZAA output voltage due to temperature-induced self reversal in the absence of mercury in the sample gas. (XBL 793-868)

except that two heating coils are used to maintain the vapor pressure of the analyte constant inside the quartz lamp. The electronics used to excite the plasma discharge are also of new design. These new lamps have been tested and used with a batch-type ZAA to make the analytical measurements. Excellent sensitivity and precision were obtained for solid and liquid samples. Of major importance for continuous gas analysis is the stability of the lamp intensity and instrumental response. For typical operation, intensity and instrumental response varied less than 1 percent over a 24-hour period for all lamps. These new light sources will be used with the ZAA which has been built for As, Cd, and Se gas analysis. However, the ZAA furnace for gas analysis of these elements must be completed before this new spectrometer can be tested on the lab-scale oil shale retort.

### Furnace.

A new furnace for continuous on-line analysis of mercury in gas streams was constructed and successfully operated at temperatures as high as 900°C for extended periods. The furnace (Fig. 4) is constructed of 1.25 cm OD, 0.12 cm thick wall, 321 stainless steel (SS) tubing welded into a tee. The tubing is alonized to lessen corrosion. Incoming gases first pass through the atomization-combustion chamber which is maintained at temperatures between 750 and 900°C by joule heating. This chamber is filled with ceramic beads to break up the gas flow and increase the thermal contact area. The gases then pass through a small opening into the absorption chamber which is aligned along the optical path of the spectrometer. Quartz windows at the ends of the absorption chamber pass the 2537 Å mercury resonance lines while isolating the hot sample gases from the ambient air. Gases exit the furnace through tubes located near each end of the absorption chamber. For operating temperatures between 750°C and 900°C, the corrosive attack of the hydrogen sulfide in the offgas would destroy the furnace within a few hours. To retard this attack and extend furnace lifetimes, stainless steel surfaces have been conditioned with a protective layer of alumina by a process termed alonization. To obtain an estimate of alonized furnace lifetime, corrosion tests were conducted using a highly sulfidizing inert atmosphere, simulating actual furnace operating conditions. These tests indicate that lifetimes on the order of 70 to 100 hours can be expected for continuous operation at 900°C with 2 percent by volume of hydrogen sulfide in the offgas.

### Testing and Use of Instrumentation

Following extensive laboratory testing, the ZAA mercury monitor was field tested in May 1979 during Lawrence Livermore Laboratory's 6000-kg oil shale retort experiment, L-3. The objectives of the field test were to evaluate the new ZAA spectrometer, to test the new gas handling-metering system and the new calibration system, and to make long-term mercury measurements at an in-situ oil shale retort.

Run L-3 retorted a graded mix of lean and rich Colorado shale in a 50-50 volume percent mixture of air and steam. The maximum retorting temperature was 1000°C. This run was terminated because of a vessel leak before the last 1 meter of raw shale had reached retorting temperature.

The four day field test of the ZAA monitor was highly successful. The instrumentation was evaluated and several necessary modifications were made during the first half of the retort run. The remainder of the test was primarily devoted to on-line measurement of mercury in the offgas. The ZAA was found to be capable of measuring concentrations of mercury as low as 10 ppb with up to 85 percent extinction of the analytical line due to broadband UV absorption by organics in the offgas.

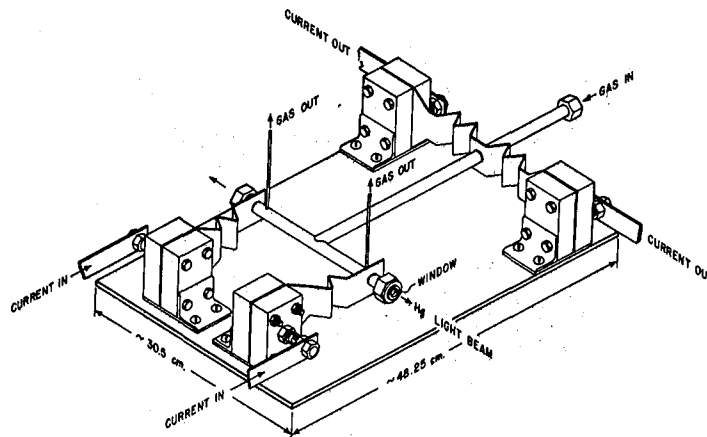


Fig. 4. New furnace for mercury analysis in offgases. (XBL 792-481)

Matrix effects necessitated the use of standard additions to quantify mercury levels in the offgas. These matrix effects were not directly related to the broadband UV extinction of the 2537 Å analytical line. The matrix effect manifested itself as a factor of two reduction in the slope of the standard addition curves obtained in offgas, relative to the slope of the standard addition curves in a stream of air. This matrix suppression is thought to be due to the reaction of inorganic mercury, used for calibration, with hydrogen sulfide and other sulfur-containing compounds in the retort offgas.

Several modifications of the instrumentation have been made as a result of the L-3 test. These have improved its performance and include changes in the furnace, light source assembly, and the electronics.

ZAA mercury monitoring was initiated on May 9, 28 hours after ignition of the retort. The mercury concentrations in the L-3 offgas were low throughout this interrupted retort experiment (Fig. 5). During the subsequent 72 hours of the retort run, a total of 25 hours of quantitative mercury data were obtained. Offgas mercury concentrations are plotted in Fig. 5 as a function of time after ignition. The data shown in the figure are one-half hour time averages. Time averages which were less than or equal to 10 ppb are plotted at the 10 ppb level. Analytical precisions, as determined by the coefficient of variation, are not shown in the figure but were approximately  $\pm 5$  ppb for all data.

Evaluation of the ZAA was the primary objective during the first 50 hours of the retort run. Consequently, adjustments and modifications to the system limited the collection of mercury data during this period. Also, data were not collected between midnight and 8 AM except on the morning of May 12. All data obtained from May 9 through May 11 were for offgas sampled at port S2, downstream of the condenser system. Sampling was initiated at port S1, ahead of the condenser system, on the morning of May 12 and continued for four hours. Then, sampling was switched back to S2 for one hour until excessive temperatures resulted in instrument failure.

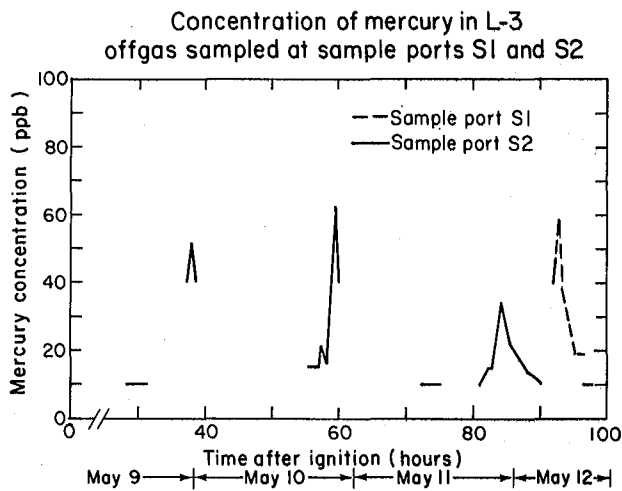


Fig. 5. Concentration of mercury in the offgas from LLL retort run L-3. (XBL 805-1117)

Concentrations ranged from less than 5 ppb to 65 ppb. The data obtained from L-3 can be compared to the ZAA offgas data obtained during a previous retort experiment using a prototype ZAA.<sup>1</sup> Mercury concentrations in that work were less than 10 ppb for the first 2/3 of that run, and subsequently, several large pulses of mercury were observed with maximum concentrations reaching 8 ppm.

No mercury pulses of comparable magnitude were observed during L-3 because the run was not completed. It has been hypothesized that mercury originally present in the raw oil shale is volatilized by the retorting (pyrolysis) front as it descends down the retort's vertical shale column. This mercury is swept ahead of the front by the carrier gas and then condenses on a layer of cool raw oil shale below the reaction zone.<sup>1</sup> If this process continues as the front propagates down the retort bed, mercury eventually becomes concentrated in the lowest layer of raw shale.

The reason why no large pulses of mercury were observed in L-3 offgas is that the mercury in the lowest enriched layer was not volatilized into the carrier gas. This suggests early termination of the retorting process as a control strategy for minimizing mercury emissions.

#### PLANNED ACTIVITIES FOR 1980

Calibration techniques and a ZAA furnace will be developed for on-line analysis of As, Cd, and Se in gas streams. The ZAA and As-Cd-Se spectrometers and the sampling and calibration strategies will be tested in offgas streams from the LBL simulated in-situ oil shale retort. The mercury spectrometer will also be field tested at a pilot-scale retorting experiment. The nature of offgas matrix effects on ZAA gas analyses will be investigated in laboratory and field experiments. Improvements resulting from these tests and experiments will be incorporated, and instrumentation will be used during one or more commercial-scale in-situ field retort runs.

#### FOOTNOTE AND REFERENCES

\*This program is funded by the Environmental Protection Agency and the Department of Energy's Division of Oil, Gas, and Shale Technology.

1. J. P. Fox, J. J. Duvall, K. K. Mason, R. D. McLaughlin, T. C. Bartke, and R. E. Poulson, "Mercury Emissions from a Simulated In-Situ Oil Shale Retort," Eleventh Oil Shale Symposium Proceedings, Colorado School of Mines, Golden, CO (1978).
2. G. O. Nelson, "Simplified Method for Generating Known Concentrations of Mercury Vapor in Air," Rev. Sci. Instr., 41, 776 (1970).

## RETORT ABANDONMENT

### CONTROL STRATEGIES FOR ABANDONED IN-SITU OIL SHALE RETORTS\*

*P. Persoff and J. P. Fox*

#### INTRODUCTION

Vast resources of oil shale--more than 80 billion barrels or recoverable syncrude--exist in the Green River Formation in Colorado, Utah, and Wyoming. The richest of these deposits and the ones scheduled for early development are located in the Piceance Creek Basin of western Colorado. The rich oil shale layer, the Mahogany Zone, which is largely impermeable, separates layers of fractured leaner shale which act as confined or unconfined aquifers.

Current industrial plans call for the development of this resource by vertical modified in-situ (VMIS) retorting. Figure 1 shows a schematic of the relative positions of the Mahogany Zone, fractured oil shale, artesian aquifers, and VMIS retorts. Large chambers of underground shale about 300 to 750 feet high and 200 feet square in cross section, will be formed some 1000 to 2000 feet below the surface by mining out 20 to 40 percent of the in-place shale and explosively blasting the balance into the mined-out void. Large vertical pillars, representing nearly 50 percent of the in-place shale, will be left between the retorts to support the overburden. The retort chambers will be pyrolyzed vertically from the top to the bottom by propagating a reaction zone down the packed bed of shale using air and steam. Oil, water, and gaseous products will drain to the bottom of the retort and will be pumped to the surface for processing. Following processing, the retort will be abandoned and large underground chambers of retorted shale will be left behind.

This type of oil shale processing may result in a number of environmental impacts, including aquifer disruption, subsidence, and low resource recovery. During processing, the surrounding aquifers will be dewatered. On abandonment, groundwater will reinvade the area, leaching retorted shale and transporting leached material into the aquifers where it may be withdrawn in wells or discharged to springs and streams that feed the Colorado River system. Additionally, formerly separated aquifers will be in communication, allowing waters of different quality to mix. And there is considerable concern that the large overburden, and high void fraction (about 40 percent) presently under consideration, will result in pillar failure and subsidence over the retorts. Finally, resource recovery in VMIS retorting is poor because of the necessity of leaving large pillars in place to support the overburden.

The purpose of this program is to identify, develop, and demonstrate control technologies to prevent aquifer disruption and overburden subsi-

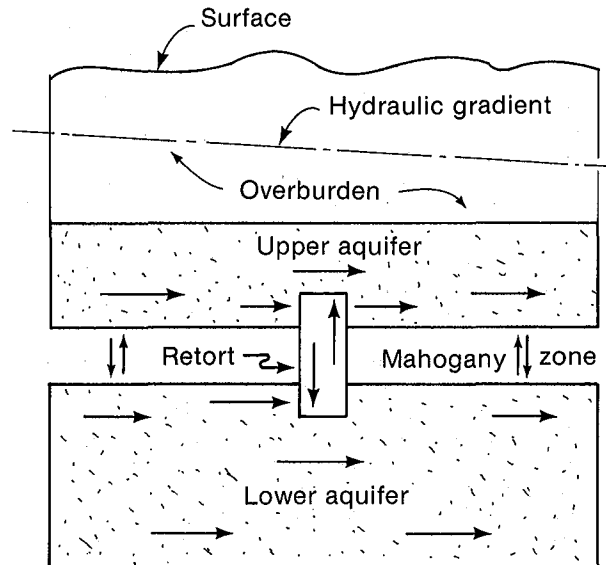


Fig. 1. Schematic of retort-aquifer configuration in Piceance Creek Basin. (XBL 786-994)

dence and to improve resource recovery when VMIS retorts are used to extract syncrude from oil shale in the Piceance Creek Basin. Some of the options being evaluated include: (1) making the retorts impermeable to groundwater flow and strengthening them by forming calcite in the retorts or by filling them with a grout based on retorted shale; (2) modifying the geohydrologic regime to route groundwater flow around rather than through retorts; (3) injecting a slurry of bentonite and/or ion exchange resin into the retorts to remove leachables as they are formed; (4) intentionally leaching the retorts with groundwater that would be recovered, treated, and reused; and (5) modifying the retorting process to minimize leachables in retorted shale. Only the first of these, filling the retort with either a grout or calcite, simultaneously achieves all three goals--mitigation of groundwater disruption, protection against subsidence, and improved resource recovery.

This program is being implemented by literature surveys, laboratory studies, and computer modeling. Literature surveys were conducted to assess the problem of aquifer disruption and to identify technically and economically viable control technologies to mitigate aquifer disruption and other environmental problems. Based on the results of these surveys, an experimental and analytical program was designed to evaluate each of the candidate control technologies.

This experimental program will study a number of technologies that are technically feasible, and it will develop design parameters sufficient to scale the technology up for field testing. This information will be used in a computer model of the local hydrology and rock mechanics to evaluate the ability of each technology to solve environmental problems. Simultaneously, each technology will be costed and one or more will then be selected for more detailed field testing.

#### ACCOMPLISHMENTS DURING 1979

Literature surveys and calculations were completed to place in perspective potential water quality impacts and technologies required to control them. Based on these investigations, a laboratory program was designed and implemented. This article describes the results of the literature survey to identify potentially viable control technologies. Subsequent articles in this report by Fox; Hall and Selleck; and Mehta and Persoff will describe other work completed under this program.

The literature from a range of fields, including construction engineering, cement chemistry, oil and gas, and coal mining was reviewed to identify methods to mitigate aquifer disruption, subsidence, and low resource recovery resulting from VMIS recovery of oil shale. The resulting data were interpreted in the framework of problems unique to oil shale, and preliminary cost estimates were performed on candidate control technologies to help focus research.

In-situ leaching of spent shale may be prevented or mitigated using several different control strategies. These include selection of dry sites, grouting of individual retorts, various hydrogeologic modifications, intentional leaching, in-place adsorption of leachables, and continuous dewatering. Some of these approaches will simultaneously address other environmental and technical issues, including subsidence, resource recovery, and disposal of surface spent shales. Site selection may be adequate on a case-by-case basis but will have a limited area of applicability, as the target of VMIS retorting, deep rich seams, is located in the center of the basin where groundwater abounds. Perpetual dewatering is not economic and long-term operator responsibility would be required. The remaining options may be both technically and economically feasible and are discussed here.

#### Grout Individual Retorts

Retorts may be isolated from groundwaters by backfilling with a material that is less permeable than the surrounding aquifers. This process, referred to as grouting, involves completely filling abandoned retorts with a material that will reduce permeability. If this material also increases the strength of the retort, the risk of subsidence may be reduced, and it may be feasible to retort the pillars to improve resource recovery.

A variety of grouting materials is available, ranging in cost upward from soil-cement mixtures, at less than \$1/ft<sup>3</sup>, and neat portland cement, at about \$2/ft<sup>3</sup>, to chemical grouts with controllable gel times and viscosities, costing more than \$20/ft<sup>3</sup>. Even the cheapest commercially available grouting materials are too expensive for grouting abandoned retorts because of the large volumes that need to be filled. Oil shale is a low organic carbon resource and for each barrel of oil extracted, 8-13 ft<sup>3</sup> of voids remain to be filled. Thus, cheap materials are required for grouting abandoned retorts.

Review of the literature suggests that spent shale may have properties which make it suitable for use as a grout. Spent shale from some retorts (Lurgi, TOSCO) is finely ground, and thus can be easily slurried and pumped. Investigators studying stability of spent shale disposal piles have found that the permeability of these piles is low and decreases with time and that compressive strengths increase with time. Unconfined compressive strengths up to 200 psi were found for compacted Paraho spent shale<sup>1</sup>, up to 500 psi for compacted TOSCO spent shale,<sup>2</sup> and up to 300 psi for compacted surface retorted shales from a laboratory retort<sup>3</sup>. Mechanisms postulated for strength development include growth of an interlocking crystal structure, hydration of free lime (CaO) in spent shales, and pozzolanic reactions.

Retort grouting is the only candidate control technology that would simultaneously strengthen abandoned retorts and prevent leaching of spent shale. It would also reduce the problem of disposal of surface-retorted spent shale and mixing of waters of the two aquifers. Design criteria for such a grouting operation have not been established, but the following requirements are likely:

- (1) Low permeability of the grouted retort, probably on the order of 10<sup>-6</sup> cm/sec.
- (2) Sufficient stiffness and strength to support the roof of the retort without tensile fracture of the overburden and, if possible, to permit the pillars (undisturbed rock between retorts) to be retorted afterward. A modulus of 50 x 10<sup>3</sup> psi may be adequate for the former requirement, and 500 x 10<sup>3</sup> for the latter.
- (3) Long-term stability.

Two major technical problems remain to be solved for this technology to be successfully demonstrated. One is the preparation of a grout that would satisfy the criteria listed. This is discussed in another article in this report by Mehta and Persoff. The other is ensuring good penetration of the grout into the voids of an abandoned retort without incurring excessive drilling and injection costs. This is discussed in a subsequent article by Persoff.

## Hydrogeologic Modifications

Retorts may be hydraulically isolated by surrounding a retorted area with a grout curtain or by providing a hydraulic bypass around the area. Figure 2 shows a schematic of a grout curtain used in conjunction with an in-situ retorting operation. A curtain of conventional grouting material such as portland cement would be formed around a large block of retorts. Flow in aquifers would then be detoured around the curtain. Flow through the retort block would be limited to leakage through the curtain which would be several orders of magnitude lower than would otherwise occur. The economic attractiveness of this approach requires that a large number of retorts (about 150) be surrounded by such a curtain. The technology of grout curtains is well established for smaller scale application. The application of this technology to large retort blocks may have some important technical limitations. Faults or fractures may limit the area which can be surrounded by a single grout curtain. Drilling and grouting at depths up to 1500 feet may be technically difficult or costly.

Alternatively, flow through a retorted area may be limited by providing a hydraulic bypass around the area. Concentrations of leachate in groundwater would then be reduced by dilution. A hydraulic bypass arrangement could be a palisade of wells short-circuiting the lower to the upper aquifer, as shown schematically in Fig. 3. Alternatively, a grout curtain and hydraulic bypass could be used together.

### Recover and Treat Leachate

Control technologies considered thus far have focused on retarding flow through the retorts. Another means of minimizing aquifer disruption is intentional leaching. Laboratory studies have shown that most of the leachable material is removed in the passage of the first few pore volumes of water. Thus, a finite amount of leachate can be pumped to the surface, treated, and disposed of.

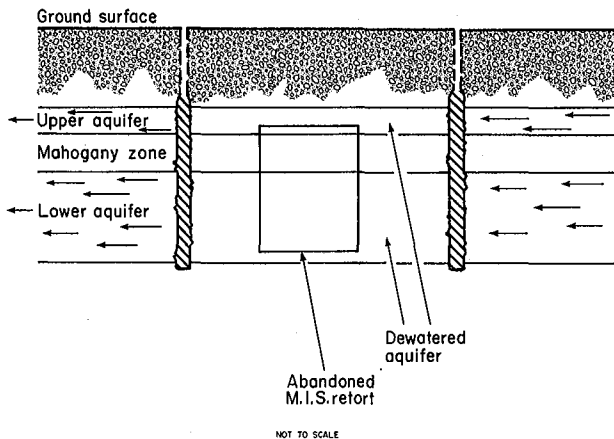


Fig. 2. Schematic of grout curtain to prevent groundwater re-invasion of abandoned retorts. (XBL 793-704)

For most spent shales, two to six pore volumes are sufficient to remove most of the leachables. Figure 4 shows typical experimental results<sup>4</sup> for spent shale from run S-55 of Laramie Energy Technology Center's 10-ton retort. Similar results were obtained for inorganics leached from spent shale recovered from one of Occidental Oil Shale's experimental retorts.<sup>5</sup> Thus, after some limited volume of leachate is recovered and treated, additional leachate may be allowed to enter the aquifers and pollutant transport will be minimal. Conventional technology is adequate to treat leachate. Adsorption on activated carbon followed by reverse osmosis would probably produce an effluent suitable for use or disposal. Other demineralization technologies, such as electrodialysis and ion exchange, are generally more costly for waters in the expected range of salinity.

The effect of particle size on the volume of leachate to be treated must be resolved before this technology can be applied. Another problem is the volume of brine (rejected from the reverse osmosis process) to be disposed of. The brine flow, about 10 percent to 20 percent of the leachate treated, would have to be disposed of in lined evaporation ponds. For a 50,000 bbl/day production rate,  $10-12 \times 10^6$  gal/day of leachate would have to be treated and disposed. This would require about 300-400 acres of ponds for a net evaporation rate of 4 ft/yr, typical of the Piceance Creek Basin.

It would theoretically be possible to allow reinventing groundwater to leach the retorts. The disadvantage of this is that control measures would only be implemented after retorting in an area had ceased, and it would have to continue for a long period of time (on the order of 100 years).

### In-Place Treatment by Adsorption

Some clays have large adsorptive capacities for organics. Industrial applications of bentonite, such as refining oils and de-inking

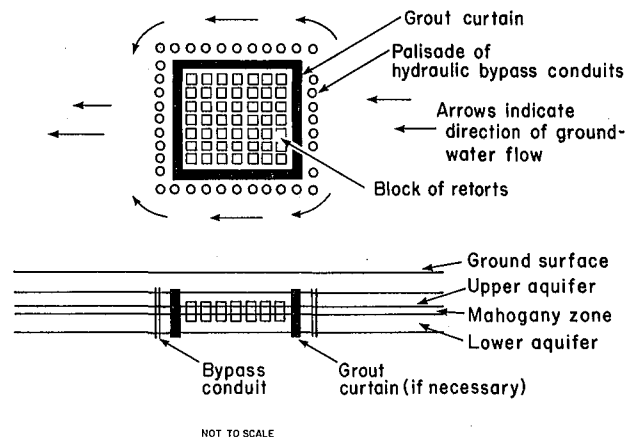


Fig. 3. Schematic of hydraulic bypass around block of retorts. (XBL 793-712)

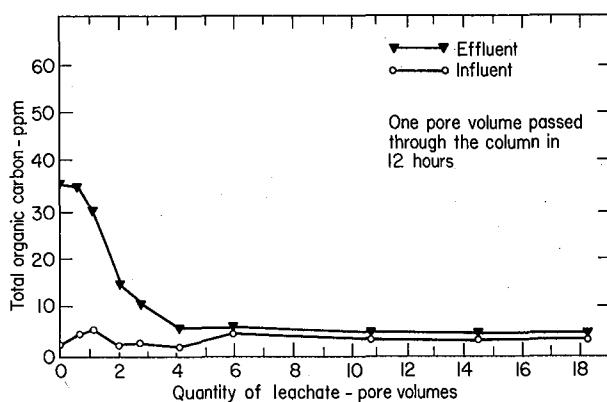


Fig. 4. Progressive decrease in leachate strength - most organic carbon is leached by first six pore volumes. (XBL 791-246)

newsprint, make use of this property. Under certain retorting conditions, it may be possible to treat leachate by removing only organics. In this situation, the adsorbent could be placed into abandoned retorts to contact leachate. The adsorbent would act to "meter out" the pollutants which would be transported away from the retorts at a rate low enough to protect receiving water quality. Eventually, most of the pollutants would be disposed of by dilution and dispersion.

#### Modify Retort Operating Conditions

Several studies have shown that the leach-

ability of spent shale depends upon retorting conditions. Spent shale retorted in an oxidizing atmosphere contains less leachable organic carbon than if retorted in an inert atmosphere; recycling retort offgases through the retort contributes to leachable organic carbon.<sup>6</sup> Retorting at high temperatures in the presence of steam promotes the formation of relatively insoluble silicates rather than leachable oxides in the spent shale.<sup>7,8</sup>

These results suggest that the leachability of organics and inorganics can be minimized by combustion retorting (to burn off char) at high temperatures (about 1000°C) in a steam-rich atmosphere using a low retorting rate (to expose the shale to high temperatures for long times). None of these conditions conflicts with the primary goal of efficient oil recovery. However, tight control of retort conditions may be difficult to achieve.

#### Cost Projections

Preliminary cost projections were performed to focus attention on controls that have a potential for commercial application. Control costs in excess of about \$3/bbl or 10 percent of the cost of a barrel of shale oil may seriously affect the economics of oil shale production. Table 1 summarizes unit costs for some of the control technologies discussed and the assumptions upon which the cost projections are based. These cost figures assume 24 gal/ton shale grade, 40 percent voids in tract C-a retorts and 23 percent voids in tract C-b retorts, and 65

Table 1. Cost projections for control technologies.

Control technology	Technical problems to be resolved	Projected Cost, \$/bbl		Cost assumptions
		Tract C-a	Tract C-b	
Grout abandoned retorts with spent shale slurry <sup>a</sup>	Development of spent shale with adequate cementing properties  Distribution of grout through retort	0.49 <sup>b</sup>	0.35 <sup>b</sup>	Grout injection holes on 50 foot centers  \$20/ft to drill through rock, \$10/ft through rubble  \$2/ton to treat, slurry and inject spent shale
		0.65 <sup>c</sup>	1.30 <sup>c</sup>	
Construct grout curtain around block of retorts	Engineering feasibility of constructing grout curtain (not routine)  Computer modeling to evaluate effectiveness	0.84	2.88	\$20/ft to drill  \$2/ft <sup>3</sup> for grout material
Construct hydraulic bypass around block of retorts	Computer modeling to evaluate effectiveness	0.52	1.77	Bypass wells placed around perimeter at 5-ft centers  \$20/ft to drill
Collect leachate and treat on surface by activated carbon and reverse osmosis	Disposal of brine  Volume of leachate that must be treated — depends on kinetics of leaching large blocks	0.64	0.52	Must treat 2 pore volumes of leachate

<sup>a</sup>This control option may also strengthen abandoned retorts, permit additional resource recovery, and allow disposal of part of the surface spent shale.

<sup>b</sup>Assumes grout injection is performed from the air level above the retorts.

<sup>c</sup>Assumes grout injection is performed from the ground surface.

percent oil recovery by in-situ retorting and 90 percent by surface retorting. Retort/aquifer geometry from the detailed development plans<sup>9,10</sup> for tracts C-a and C-b were used in these estimates. Costs for tract C-b are higher than for tract C-a due to the greater depth of overburden on tract C-b and associated greater proportion of the costs due to drilling.

While these cost projections are preliminary and require verification by laboratory and field data, they do indicate that environmental control may be economically feasible and that selection of control technology will be site specific.

#### PLANNED ACTIVITIES FOR 1980

The literature survey described here is completed and will be published in 1980. This report will be periodically updated as new research results are made available.

#### FOOTNOTE AND REFERENCES

\*This program is jointly funded by the Department of Energy's Division of Environmental Control Technology and Division of Oil, Gas, and Shale Technology.

1. Woodward-Clyde Consultants, "Disposal of Retorted Oil Shale from the Paraho Oil Shale Project," Report to U.S. Bureau of Mines (1976).
2. W. J. Culbertson, T. D. Nevens, and R. D. Hollingshead, "Disposal of Oil Shale Ash," Quarterly of the Colorado School of Mines, 65, 4, 89-132 (1970).
3. C. B. Farris, "Natural Cementation of Retorted Oil Shales," Colorado School of Mines (1979).
4. J. P. Fox, W. G. Hall, R. E. Selleck, and J. F. Thomas, "Control Technology for In-Situ Oil Shale Retorts," Quarterly Progress Report for Period June 1, 1978-October 31, 1978 (1978).
5. M. C. T. Kuo, W. C. Park, A. E. Lindemanis, R. E. Lumpkin, and L. E. Compton, "Inorganics Leaching of Spent Shale from Modified In-Situ Processing," Twelfth Oil Shale Symposium Proceedings, Colorado School of Mines, Golden, CO (1979).
6. G. Amy and J. Thomas, "Factors that Influence the Leaching of Organic Material from In-Situ Spent Shale," Second Pacific Chemical Engineering Congress, A.I.Ch.E. (1977).
7. J. H. Campbell, "The Kinetics of Decomposition of Colorado Oil Shale: II. Carbonate Minerals," Lawrence Livermore Laboratory Report, UCRL-52089, part 1 (1978).
8. A. K. Burnham, C. T. Stubblefield, and J. H. Campbell, "Effects of Gas Environment on Mineral Reactions in Colorado Oil Shale," Lawrence Livermore Laboratory Report, UCRL-81951 (1978).
9. Gulf Oil Corp. and Standard Oil Co. (Indiana), "Rio Blanco Oil Shale Project Revised Detailed Development Plan, Tract C-a." Submitted to Area Oil Shale Supervisor (1977).
10. Ashland Oil, Inc. and Occidental Oil Shale, Inc., "Oil Shale Tract C-b Modifications to Detailed Development Plan." Submitted to Area Oil Shale Supervisor (1977).

## HYDRAULIC CEMENT PRODUCTION FROM LURGI SPENT SHALE\*

*P. K. Mehta† and P. Persoff*

#### INTRODUCTION

Oil shale production by vertical modified in-situ (VMIS) retorting of the Mahogany Zone may result in a number of environmental problems including degradation of local aquifers, subsidence and overburden cracking, and low resource recovery. Local aquifers may be contaminated by materials leached from the abandoned retorts. These materials may be discharged into local surface streams which are part of the Colorado River System, thus contaminating municipal, agricultural, and industrial water supplies. Void space introduced by mining the in-place shale may result in long-term subsidence over

the retort site which could damage local structures and affect the hydrology of underlying aquifers. And finally, resource recovery of the VMIS process is low due to the necessity of leaving large pillars between the retorts to support the overburden.

Backfilling the abandoned retorts with a grout is a possible solution to these problems. The grout would improve the strength and stiffness and reduce the permeability of the abandoned retort. The increased strength and stiffness would provide protection against subsidence. If adequate strength could be developed in the retort, it might even be feasible to

extract oil from the pillars between the retorts, thus improving resource recovery. The grout would also reduce the permeability of the abandoned retort by filling the voids. This would minimize the flow of groundwater through the retorted area and thus minimize the leaching of materials from the retorted shale.

The purpose of this program, begun in June 1978, is to investigate the production of a grout from on-site waste products. The large void space that must be filled, about 9 ft<sup>3</sup> per barrel of oil extracted, precludes the use of conventional grouts such as portland cement due to the high costs involved (\$14 to \$300 per barrel of oil recovered). The 20 to 40 percent of the in-place shale which is mined for VMIS retorting is brought to the surface and processed in a surface retort such as Lurgi, Paraho, or TOSCO. The spent shale from these surface processes has physical and chemical properties similar to portland cement. By the use of additives and post retorting treatment, it will be possible to manufacture a cheap grout from surface spent shale.

The spent shale used in this investigation was Lurgi spent shale. This shale was selected because both of the commercial VMIS oil shale ventures, Occidental and Tenneco on tract C-b and Rio Blanco Oil Shale Project on tract C-a, have proposed to use the Lurgi process to retort the mined-out shale.

#### ACCOMPLISHMENTS DURING 1979

A cement was developed from Lurgi spent shale. This cement is produced by calcining a 1:1 weight mixture of Lurgi spent shale and limestone at 1000°C for 1 hour. The resulting material has a 28-day compressive strength of 3150 psi and is estimated to cost about \$20 per ton of material. By comparison, portland cement has a 28-day compressive strength of about 5000 psi and costs about \$60 per ton. These results indicate that a cheap cement can be produced from on-site waste materials. This cement is adequate for grouting of abandoned retorts and may be used for on-site construction or sold outside of the oil shale region for general construction purposes. This section describes the development of the Lurgi spent shale grout.

#### Experimental

Lurgi spent shale is a fine powder containing little residual carbon. Chemical and mineral analyses of this material are shown in Table 1. In a preliminary investigation, small samples of Lurgi spent shale were ignited in an electric muffle furnace. A modification of ASTM test method C 109 was used to evaluate cementing properties. Lurgi spent shale was found to have no cementing strength when measured by this method, either as received or after heating for one hour at 800, 900, or 1000°C. No free CaO or hydraulic calcium silicates were detected in any of the ignited samples. However, large amounts of akermanite were present in each of them. X-ray diffraction analysis for mineral

forms showed that as-received spent shale contained primarily minerals present in raw shale. After heat treatment, the carbonates decomposed to form the oxides, MgO and CaO, which reacted with quartz to form non-cementing silicates such as akermanite, Ca<sub>2</sub>MgSi<sub>2</sub>O<sub>7</sub>. The presence of large quantities of calcite and dolomite in the Lurgi spent shale shows that the temperature of the retorting process was not high enough to cause decomposition of the carbonate minerals present in the raw shale.

From the above, it was obvious that some changes had to be made in the composition of the spent shale if hydraulic cement of adequate strength was to be developed from it. A comparison between chemical analyses of Lurgi spent shale and a typical portland cement raw mix showed that for the formation of hydraulic calcareous compounds, the spent shale has excess SiO<sub>2</sub> and MgO and was deficient in CaO. The principal compound in portland cement, typically more than 50 percent by weight, is 3CaO·SiO<sub>2</sub> (C<sub>3</sub>S)<sup>††</sup> the formation of which requires a lime-silica ratio of 2.7 by weight and temperatures in the range of 1500 to 1600°C. The lime-silica ratio of Lurgi spent shale is 0.7. Thus, the production of C<sub>3</sub>S from Lurgi spent shale would require high temperatures and a large amount of imported lime.

The second most abundant compound in portland cement (typically about 25 percent by weight) is 2CaO·SiO<sub>2</sub> (C<sub>2</sub>S). Its reactivity is considerably less than that of C<sub>3</sub>S, but it is formed at lower temperatures and requires a lower lime-silica ratio. The two minor compounds in portland cement, usually totaling together less than 20 percent by weight, are 3CaO·Al<sub>2</sub>O<sub>3</sub> (C<sub>3</sub>A) and 4CaO·Al<sub>2</sub>O<sub>3</sub>·Fe<sub>2</sub>O<sub>3</sub> (C<sub>4</sub>AF). The C<sub>3</sub>A is highly reactive and can contribute to the quick setting phenomenon in portland cements unless its reactivity is retarded by the addition of about 5 percent gypsum. Calcium sulfoaluminate hydrate (ettringite) formed by the reaction of C<sub>3</sub>A with gypsum and water also contributes binding properties to portland cement.

Based on the observed properties of Lurgi spent shale, it appeared that higher temperatures would be necessary for decomposition of the carbonate minerals, and that addition of some CaCO<sub>3</sub> would be necessary to develop reasonable cementing properties. The first experiment, series A, involved preparation of blends of Lurgi spent shale with commercial-grade CaCO<sub>3</sub> powder in 1:1 proportion by weight, heating the mixture in air at 900, 950, 1000, and 1100°C for one hour, grinding the resulting clinkers to powder, and determining the mineralogical composition and cementing properties of the cements produced. This experiment was expected to provide preliminary information on the optimum temperature of heat treatment to develop adequate strength.

<sup>††</sup>Abbreviated formulae used by cement chemists are: C = CaO, S = SiO<sub>2</sub>, A = Al<sub>2</sub>O<sub>3</sub>, F = Fe<sub>2</sub>O<sub>3</sub>. Thus for example, C<sub>4</sub>AF = 4CaO·Al<sub>2</sub>O<sub>3</sub>·Fe<sub>2</sub>O<sub>3</sub>.

Table 1. Properties of Lurgi spent shale as received.

Mineralogical analysis <sup>a</sup>		Chemical analysis, % <sup>b</sup>		Particle size analysis, % <sup>c</sup>	
Quartz	present	Na <sub>2</sub> O	2.3	> 30.3 μm	0.6
Calcite	present	MgO	7.5	17.9-30.3 μm	2.1
Dolomite	present	Al <sub>2</sub> O <sub>3</sub>	7.2	10.0-17.9 μm	4.9
Feldspar	present	SiO <sub>2</sub>	32.0	6.6-10.0 μm	9.0
Free lime	not detected	CaO	21.8	3.94-6.6 μm	25.7
		Fe <sub>2</sub> O <sub>3</sub>	2.7	> 3.94 μm	57.7
		Ignition loss	20.0		
		(mainly carbonate)			

- a) by x-ray diffraction  
b) by x-ray fluorescence  
c) analysis supplied by Lurgi

The next experiment, series B, was to provide information on the optimum ratio of CaCO<sub>3</sub> to spent shale which would yield cements of good strengths when mixtures were heated at the temperature selected in series A. The following weight ratios of CaCO<sub>3</sub> to spent shale were investigated: 0.5, 0.75, 1.0, 1.25, 1.5, 1.75, and 2.0 to 1.

In order to investigate the effect of gypsum addition on cement strength, a cement selected from series B was tested with and without 5 percent gypsum addition after grinding.

Mixtures of CaCO<sub>3</sub> powder and Lurgi spent shale were wet blended in the presence of a small amount of water. The resultant slurry was dried at 110°C and cut into cakes of about 2 x 2 x 1/4 inches. These cakes were stacked on a periclase hearthplate in an electrical muffle furnace. The furnace temperature was raised to the desired level and held there for one hour. The heat-treated material (clinker) was pulverized to about 10 percent residue on 200 mesh sieve (74 microns). The cement thus produced was subjected to physical and chemical tests.

Qualitative mineralogical analysis was carried out by x-ray diffraction (XRD), using Cu Kα radiation. Free CaO was determined chemically by ASTM method C 114. Compressive strengths of cements were determined by a modification of ASTM C 109, compressive strength of mortar cubes. This standard calls for a sand-cement ratio of 2.75, using standard graded sand, and a water-cement ratio of 0.5. All conditions of ASTM C 109 were met except the water-cement ratio. A water-cement ratio of 0.625 was needed to obtain the desired flow characteristics because of the fine particle size of the cements. The mortar cubes were stored under humid conditions at room temperature until the test age when they were crushed to failure with a hydraulic test machine.

### Results and Discussion

The data in Table 2 show the results of mineralogical analyses and compressive strength tests on cements of series A, namely the cements produced by heat treatment of the mixtures containing equal parts by weight of CaCO<sub>3</sub> and Lurgi spent shale at temperatures from 900° to 1100°C. Comparison of the data in Table 1 and Table 2 shows that the addition of CaCO<sub>3</sub> to the Lurgi spent shale prevented the formation of akermanite, a non-cementing compound, and shifted the reaction equilibrium in favor of formation of the cementing compounds β-C<sub>2</sub>S and C<sub>3</sub>A. This was especially true at temperatures of 1000°C and 1100°C by which most or all of the CaCO<sub>3</sub> present had decomposed to provide enough lime for β-C<sub>2</sub>S and C<sub>3</sub>A formation.

The compressive strength data in Table 2 show that higher strengths are developed at 1000°C and 1100°C than at lower temperatures of heat treatment. Maximum strength results at 1000°C even though some undecomposed CaCO<sub>3</sub> is still present. This can be attributed to partial loss of reactivity of the cementitious compound, β-C<sub>2</sub>S, due to crystal growth at the higher temperature of heat treatment. The 28-day strength (2720 psi) of the 1000°C cement is considered adequate for use as an ingredient of a spent shale grout or for structural use. Therefore, this temperature (1000°C) was selected for series B experiments.

The results of mineralogical analyses, free CaO determination, and compressive strength tests of the cements of series B, which were made by 1000°C heat treatment of various CaCO<sub>3</sub> - spent shale mixtures, are shown in Table 3. The XRD data for some of the mixtures are also illustrated in Fig. 1. The compressive strength data indicate that for the 1000°C heat treatment, the 1:1 mixture represents the optimum composition. Under moist curing conditions at ambient temperature, the cement made

Table 2. Mineralogical analysis and compressive strength of cement made by one hour heat treatment of a mixture of equal parts by weight of  $\text{CaCO}_3$  and Lurgi spent shale.

Minerals present <sup>a</sup>	Temperature of heat treatment			
	900°C	950°C	1000°C	1100°C
Akermanite	N	N	N	N
$\text{C}_3\text{S}$	N	N	N	N
$\beta\text{-C}_2\text{S}$	W	W	M	M
$\text{C}_3\text{A}$	W	W	W	W
$\text{CaCO}_3$	VS	S	W	N
Compressive strength, psi <sup>b</sup>				
3 day	190	280	470	295
7 day	450	630	950	650
28 day	925	1400	2720	2100

a) by x-ray diffraction; N = none, W = weak, M = medium, S = strong, VS = very strong

b) by modified ASTM C 109

Table 3. Mineralogical analysis, free lime, and compressive strength of cements made by heat treatment of various proportions of  $\text{CaCO}_3$  and Lurgi spent shale, 1 hr @ 1000°C.

Minerals present <sup>a</sup>	$\text{CaCO}_3$ : spent shale ratio by weight							
	2:1	1.75:1	1.5:1	1.25:1	1:1	0.75:1	0.5:1	0:1
$\text{CaCO}_3$	VS	VS	W	W	N	N	N	N
Akermanite	N	N	N	N	N	N	M	VS
$\text{C}_3\text{S}$	N	N	N	N	N	N	N	N
$\beta\text{-C}_2\text{S}$	W	W	M	M	M	M	W	N
$\text{C}_3\text{A}$	W	W	M	M	M	M	W	N
CaO	S	S	S	S	W	N	N	N
% Free CaO <sup>b</sup>								
	12.2	9.0	7.9	6.0	3.1	1.5	0.64	0
Compressive strength, psi <sup>c</sup>								
3 day	120	250	140	170	340	375	poor	nil
7 day	380	630	390	395	670	455	poor	nil
28 day	840	1210	1200	890	2600	NA	poor	nil
90 day	1310	1690	1910	1600	3340	NA	poor	nil

a) by x-ray diffraction; N = none, W = weak, M = medium, S = strong, VS = very strong

b) by ASTM C 114

c) by modified ASTM C 109

from this composition continued to develop strength up to the test age of 90 days which shows the long-term stability of the products of this cement in moist environments. The poor strength of cements made with lower proportions of  $\text{CaCO}_3$  was due to the formation of lesser amounts of the cementitious compounds. Lower strength of the cements made with 1.25 or larger parts of  $\text{CaCO}_3$  per unit part of the spent shale was due to microcracking of the specimens caused by delayed hydration of free  $\text{CaO}$  which was present in significantly large quantities.

Although the compressive strengths of the 1:1  $\text{CaCO}_3$  - spent shale mixture heat treated at  $1000^\circ\text{C}$  are considered adequate for many applications, it is possible to obtain further improvements in strength by lowering the water-cement ratio and by adding suitable strength accelerators to the cement, such as 5 percent gypsum by weight of the cement. The water-cement ratio in the test mortar was reduced by using a locally available coarser sand instead of the ASTM standard C 109 graded sand for a series of tests. The use of this sand permitted the lowering of the water-cement ratio from 0.625 to 0.52. The relevant compressive strength data from this test are shown in Table 4.

In summary, calcareous hydraulic cement having adequate strength characteristics cannot be produced from as-received Lurgi spent shale due to the low  $\text{CaO}:\text{SiO}_2$  ratio of the material. It is possible to make adequate quality hydraulic cements from this shale by blending about equal parts by weight  $\text{CaCO}_3$  and heat treating the mixture at  $1000^\circ\text{C}$ . Due to presence of reactive  $\text{C}_2\text{S}$  and  $\text{C}_3\text{A}$ , the hardening and the hydraulic (water resistant) properties of the cements produced were satisfactory.

#### PLANNED ACTIVITIES FOR 1980

Work will be continued to develop spent shale grouts. Cementitious properties of spent shale from other surface retorts, such as Paraho and TOSCO, will be investigated and experiments conducted to promote these properties by post-retorting treatment or by the use of additives. Direct use of spent shale, with no additives or other treatment, will be investigated.

A numerical model of a retort field will be used to determine the strength and stiffness of grouted retorts necessary to prevent overburden subsidence and cracking and permit additional

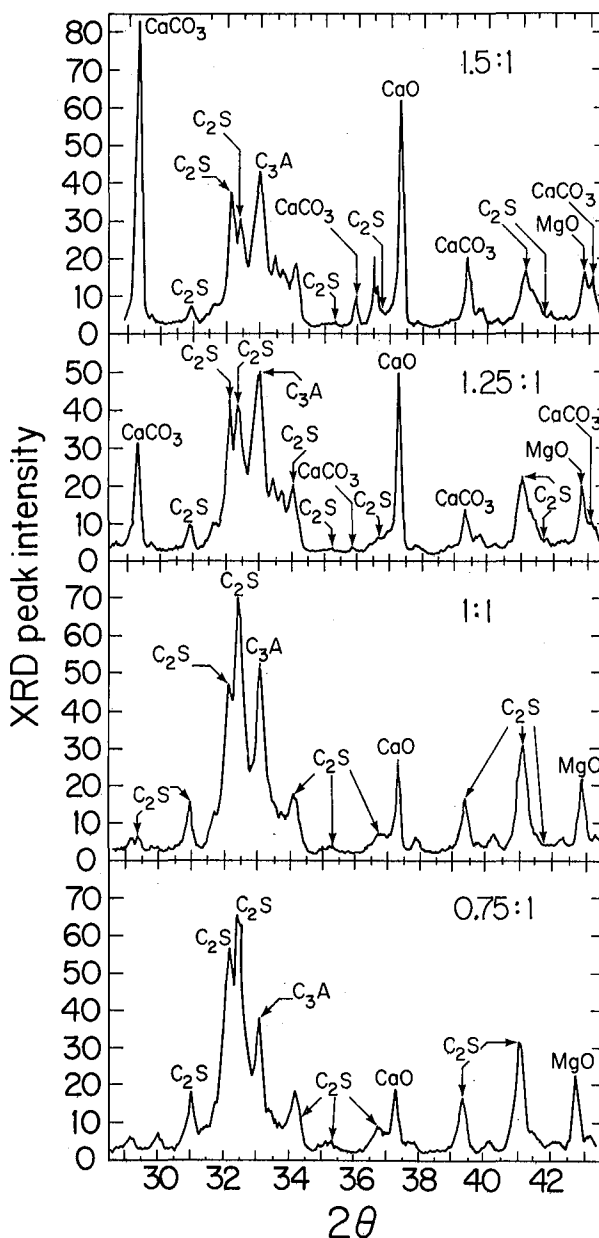


Fig. 1. X-ray diffraction analysis of cements produced by heating  $\text{CaCO}_3$ -Lurgi spent shale mixtures ranging in weight ratio from 0.75:1 to 1.5:1, at  $1000^\circ\text{C}$  for one hour. (XBL 7910-4719)

Table 4. Effect of water-cement ratio and gypsum addition on the cement made from 1:1  $\text{CaCO}_3$ -spent shale mixture.

Water/cement ratio	0.625	0.52	0.52
Gypsum addition to cement	None	None	5%
Compressive strength, psi			
7 days	670	970	1510
28 days	2600	3150	3750

resource recovery. A groundwater flow model will be used to determine the permeability of grouted retorts needed to minimize leaching of spent shale by groundwater.

Specimens simulating cores from grouted retorts will be prepared and tested against these requirements. Mixtures of various spent shale cements and untreated spent shale will be used as the grout in these specimens to deter-

mine the minimum cost of grout that can be used.

#### FOOTNOTES

\*This program is jointly funded by the Department of Energy's Division of Environmental Control Technology and Division of Oil, Gas, and Shale Technology.

†University of California, Berkeley, CA.

## WATER QUALITY EFFECTS OF LEACHATES FROM AN IN-SITU OIL SHALE INDUSTRY\*

J. P. Fox

### INTRODUCTION

Oil shale is a marlstone that contains about 20 percent organic material; oil can be extracted from it by mining and pyrolysis in a surface retort or by direct pyrolysis in the ground (following rubbling). The latter approach, referred to as "in-situ" retorting, is presently under study by industry and the Department of Energy as a cost-effective alternative to surface retorting.

Since most of the oil shale deposits are located in or adjacent to aquifers, in-situ processing may result in groundwater disruption. The purpose of this program is to evaluate the magnitude and significance of in-situ leachate discharge from an oil shale industry so that environmental control requirements can be identified. This article focuses on a hypothetical modified in-situ facility located on lease tracts C-a and C-b (Fig. 1).

### ACCOMPLISHMENTS DURING 1979

The potential effect of leachates from an in-situ oil shale industry was assessed by compiling available literature on leachate quality and local hydrologic conditions and using this data to compute hydraulic and chemical transport parameters in the vicinity of an in-situ industry. This analysis indicated that local groundwaters and surface waters may be significantly degraded by a large-scale in-situ oil shale industry if measures are not taken to prevent leaching of abandoned in-situ retorts. The results of this analysis are summarized here.

### Geohydrology of Leachate Formation

In-situ leachates are produced by the interaction of local groundwater with in-place spent

shales and other retorting products, including gases, waters, oils, and tars. They originate when groundwater flows through an abandoned in-situ retort and from gas leakage during retorting.

Modified in-situ retorting requires partial mining and fracturing of the retort block to create adequate porosity for effective retorting. This introduces permeability into an otherwise largely impermeable strata. The stratigraphy described in Fig. 2 is typical of that found in the Piceance Creek Basin where the richer oil shale deposits occur.

The lower aquifer is normally confined and the upper aquifer acts as an unconfined aquifer although confined conditions exist. A head difference of 10 feet to 55 feet exists in most parts of the basin. Thus, permeability produced by partial mining, fracturing, and retorting could create the possibility of groundwater migrating into an abandoned in-situ retort after completion of retorting.

### Factors Affecting Leachate Quality

Water migrating through abandoned in-situ retorts under a pressure gradient may leach soluble organic and inorganic constituents from the spent shale and dissimilar waters may be mixed, modifying their quality. The leaching of inorganic and organic materials from in-situ spent shale will be influenced by (1) chemical-mineralogical characteristics of raw oil shale; (2) retorting conditions; (3) particle size distribution of the spent shale; (4) quality and temperature of groundwater; and (5) the flow regime of groundwater migrating through an abandoned retort. The first two, mineralogy of oil shales and retorting conditions, are believed to be the most significant.

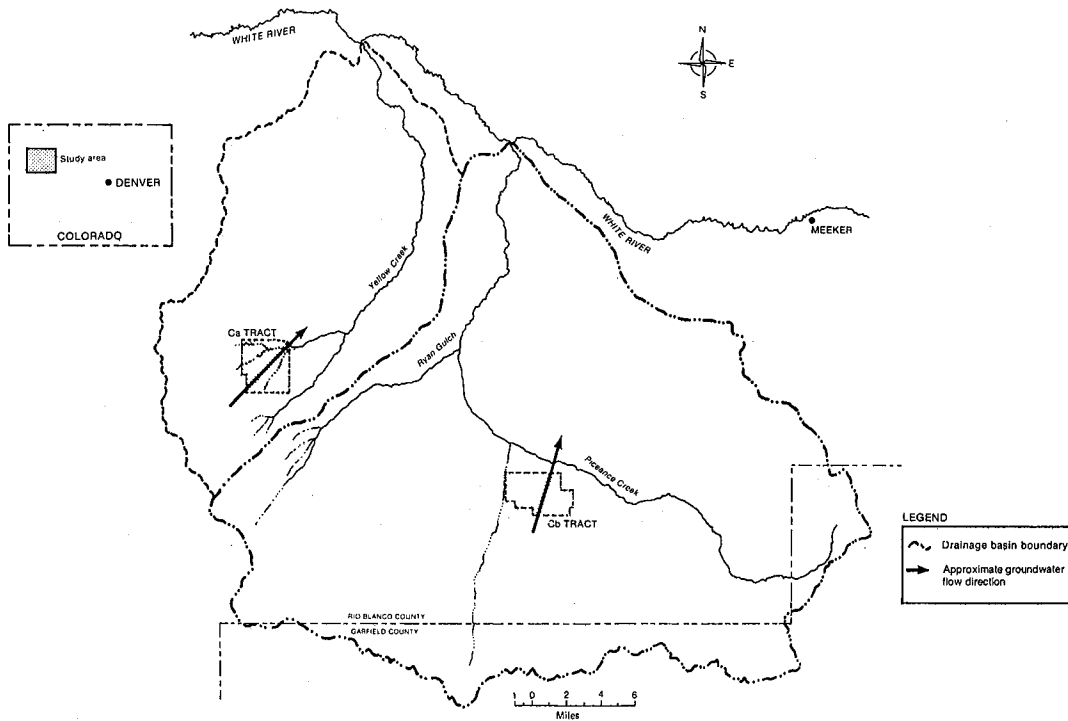


Fig. 1. Piceance Creek Basin, Colorado showing location of federal lease tracts C-a and C-b. (XBL 791-182)

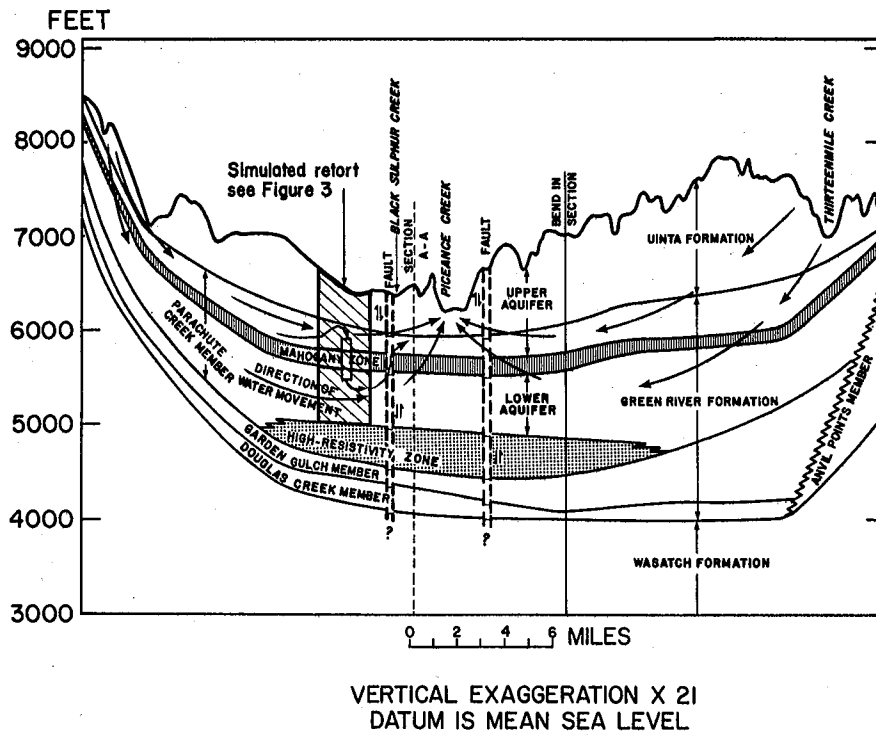


Fig. 2. Geohydrologic section through the Piceance Creek Basin. (XBL 7811-12780)

In addition to these factors, which are recognized and quantifiable, there are two other factors unique to field retorts about which little is known. In field retorts, material at the bottom of the retort may be incompletely retorted, wet with oil, and have accumulated condensed metal species, such as mercury. The effect of this bottom plug on leachate quality is unknown and research on it is needed. In addition, gases produced during retorting may migrate out of the burn area and into ground-water aquifers. The magnitude of this would depend, among other things, on the fracture system present and on gas holdup. This is poorly understood and laboratory and theoretical investigations are required.

#### Leachate Composition

A large number of experiments have been conducted to determine the composition of leachates from simulated in-situ spent shales. In most of this work, a weighed quantity of spent shale from a laboratory-scale retort is contacted with a specific volume of distilled water for times up to several months. The leachate is then collected and analyzed for various major, minor, and trace elements. Some investigators have used column leaching experiments to obtain similar information. The results of these investigations show that the major constituents in these leachates are Ca, Cl, CO<sub>3</sub>, F, HCO<sub>3</sub>, K, Na, and SO<sub>4</sub>. The salinity and pH are characteristically high and environmentally significant concentrations of certain toxic and carcinogenic materials, such as phenols and Pb, occur in some of the leachates.

These data may be used to estimate the composition of leachate produced by a field in-situ retort. These calculations require information on the composition of groundwaters that are used for leaching, estimates of void volume in the retort, and certain assumptions about chemical equilibrium in the retort. If it is assumed that the void space in the retort is 20 percent, that the majority of the leachable material is removed in the first two to six pore volumes of water, and that the mass of leachable material per 100 grams of shale is at equilibrium, then the concentration C of a given element i in the leachate exiting an abandoned retort is given by

$$C_i = \frac{10M_i m + (C_g)_i nV}{nV}$$

where  $M_i$  = mass in milligrams of ith constituent per 100 grams spent shale (experimental values from literature<sup>1</sup>)  
 $m$  = mass of spent shale in a single retort = (1.1 x 10<sup>9</sup> kg for tract C-a and 7.5 x 10<sup>8</sup> kg for tract C-b)  
 $(C_g)_i$  = concentration of ith constituent in groundwater in milligrams per liter  
 $V$  = volume of water within a single retort (5.0 x 10<sup>8</sup> liters for tract C-a and 2.0

$x 10^8$  liters for tract C-b)  
 $C_i$  = average concentration of ith constituent exiting the retort  
 $n$  = number of pore volumes (two to six) required to remove most of leachables.

This equation was used to estimate the average composition of leachate from abandoned in-situ retorts located on lease tracts C-a and C-b. The results of these calculations are shown in Table 1. This compilation indicates that the average concentration in the leachate for tabulated constituents may greatly exceed levels in native groundwater.

These comparisons illustrate the effect of two separate impacts on water quality, leaching and mixing. Both may either increase or decrease the concentration of various constituents. In-situ retorts located in the Mahogany Zone form a permeable zone or a conduit which may transport water from one aquifer to the other. Thus, water quality may be affected by the mixing of two dissimilar waters. If flow is from a better quality aquifer, such as the upper aquifer, to the lesser quality aquifer, the lower aquifer in this case, the quality of the latter aquifer will be improved by mixing with higher quality water. Thus, many constituents may actually be lowered, in the absence of significant leaching, when flow is downward in the Piceance Creek Basin system. On the other hand, if flow is from the lesser quality aquifer to the better quality aquifer, the latter will be degraded as a consequence of mixing with a poorer quality water. Thus, when flow is upward in the Piceance Creek Basin, the upper aquifer will be degraded due to mixing with a lower quality water. In addition to mixing, flow through abandoned retorts may remove soluble constituents from the contained spent shale. This material will be transported into the receiving aquifer where it will usually increase the concentration of various constituents. In certain cases, some of the leached constituents may react chemically with compounds present in the groundwaters and thereby remove them. An example of this would be the precipitation of CaCO<sub>3</sub> and Mg(OH)<sub>2</sub>.

The consequences of leaching on tract C-a may not be as significant as on tract C-b if predevelopment flow conditions are re-established on site abandonment. On tract C-a, leachate is discharged into the lower aquifer which does not directly recharge surface streams and is not used locally due to its poorer quality and the significant pumping heads that would be required to raise it. However, significant changes in the quality of the lower aquifer would eventually occur, over millenia, leading to the degradation of the upper aquifer by slow leakage through vertical cracks in the Mahogany Zone. The significance of these long time periods in evaluating environmental impacts is unknown and should be considered in other studies. The water quality impacts on tract C-b would be more immediate because the leachate discharges into the upper aquifer which recharges local surface streams and is used for stock watering and irrigation.

Table 1. Estimated composition of leachate exiting an in-situ retort located on lease tracts C-a and C-b.

Constituent	Predevelopment Groundwater Quality, mg/l				Estimated Leachate Composition, mg/l	
	Tract C-a		Tract C-b		Tract C-a	Tract C-b
	Upper aquifer	Lower aquifer	Upper aquifer	Lower aquifer		
Al	0.14	0.24	0.3	0.3	0.49 - 31	0.89 - 53
B	0.33	0.84	1.4	36	0.33 - 1.9	36 - 39
Ca	35	8.8	32	14	35 - 2350	14 - 3950
Cl	12	22	26	1200	32 - 73	1234 - 1300
CO <sub>3</sub>	0.88	69	21	220	110 - 2400	408 - 4250
Cr	0.01	0.01	0.002-0.3	0.009	0.02 - 20	0.01 - 34
F	0.41	15	10	21	4.8 - 47	29 - 100
Fe	5.0	0.78	0.5	0.8	5.0 - 5.5	0.8 - 1.6
HCO <sub>3</sub>	482	842	790	4000	560 - 920	4140 - 4750
K	2.2	2.6	2.2	21	2.5 - 200	21 - 360
Li	0.13	0.13	3.1	10	0.20 - 4.8	10 - 18
Mg	52	20	42	11	52 - 140	11 - 160
Na	212	397	330	2500	212 - 2800	2500 - 6900
NO <sub>3</sub>	0.93	0.4	0.41	0.46	1.7 - 30	1.7 - 49
Pb	0.17	0.21	0.01	0.03	0.22 - 0.36	0.12 - 0.35
Si	12	4.7	17	13	100 - 980	170 - 1660
SO <sub>4</sub>	325	112	220	63	326 - 1800	65 - 2500
Zn	0.26	0.24	0.2	0.2	0.26 - 0.54	0.2 - 0.7
TDS	905	1075	1100	6190	905 - 31,700	6190 - 58,700
TOC	8.5	11	3	10	12 - 430	16 - 720
Phenols	0.003	0.002	-	-	0.04 - 0.44	0.06 - 0.8

### Leachate Transport

Leachate will be transported in aquifers of the oil shale region for centuries and eventually be discharged to springs and streams or withdrawn in wells. The Darcy flow equations and simple hydraulic calculations were used to estimate the time required to leach an in-situ retort and for leachate discharged from tracts C-a and C-b to reach surface streams. These calculations and pertinent assumptions are summarized in Table 2.

After a retort block is abandoned, the dewatering wells will be turned off and groundwater will slowly refill the abandoned retorts. The rate at which groundwater passes through the retorts will be governed by the permeability of the surrounding aquifers and by the head difference between the aquifers. Residence time of groundwater in the retorts (Table 2) indicates that leachate may be released from abandoned retorts over very long periods of time. This means that the retorts would act as sources of contamination for long periods. Additionally,

the contact time between the leach water and the spent shale is of the order of years. These times are considerably higher than contact times used in laboratory leaching studies and may enhance or inhibit certain chemical reactions relative to laboratory results.

Once the leachate has emerged from the abandoned retort, it will be transported in either the lower or upper aquifer and eventually be discharged in a local surface stream. If it is assumed that the aquifers are isotropic and that the hydraulic parameters summarized in Table 2 are reasonable, flow velocities and leachate transit times from tracts C-a and C-b will be similar to those shown in Table 2. This table shows that it will take centuries for the leachate to reach the nearest surface streams.

### Effects on Groundwater Quality

Groundwater degradation is a key concern because it is typically irreversible and may have long-term consequences. Since groundwater flow velocities are low, it will take centuries

for contaminated water to degrade large areas. However, if these waters are withdrawn at some point during these centuries, they may still have significant effects. There is no guarantee that during these centuries a farm or home or even a city will not be built at the retorting site and that groundwaters will not be withdrawn for use.

Analyses suggest that the composition of groundwaters in the vicinity of an in-situ facility will approach that of in-situ leachate (Table 1). The significance of this degradation may be determined by examining the present and future uses of groundwater and by comparing the requisite quality to sustain these uses with estimated quality of the groundwater following leaching of in-situ spent shale. The water-quality criteria recommended by the EPA to sustain the uses of domestic water supply, stock watering, and irrigation have been compared to pre-development and post-development groundwater quality. This comparison indicates that predevelopment groundwaters are acceptable for irrigation of some salt-resistant crops but would require limited treatment on a case-by-case basis for use as a domestic supply or for stock watering. If these waters were further degraded by in-situ spent shale leachate, the level of treatment required to render them

suitable for domestic supply or stock watering would be greater and the cost to supply the water accordingly higher. Since the area is sparsely settled and because most users are individuals or single farms or ranches, it is unlikely that treatment would be affordable or that knowledge of its requirement would be available. Because some constituents in post-development groundwaters may be toxic or carcinogenic, especially among the organics and trace metals, the use of these waters by unsuspecting parties may result in local or regional public health problems. In the long term, these waters may become largely unavailable for use unless large-scale development of the area were to occur.

#### Effect on Surface Water Quality

In-situ spent shale leachate will travel through aquifers of the Piceance Creek Basin for centuries. Eventually, assuming no change in the hydrologic system, it will discharge into either Piceance Creek or Yellow Creek. These creeks drain into the Colorado River System and, thus, changes in their quality will affect downstream reaches.

The potential effect of the discharge of in-situ leachate from a single line source of

Table 2. Aquifer characteristics and leachate transport in the vicinity of lease tracts C-a and C-b.

	Tract C-a		Tract C-b	
	Upper	Lower	Upper	Lower
<b>Aquifer characteristics</b>				
Transmissibility (T), ft <sup>2</sup> /day	330	940	200	53
Aquifer thickness (b), ft	220	220	250-400	200-500
Permeability (k), ft/day	1.5	4.3	0.5-0.8	0.1-0.3
Hydraulic gradient (dh/dL)	0.01	0.01	0.01	0.01
Effective porosity (φ)	0.1	0.1	0.1	0.1
<b>Groundwater transport</b>				
Groundwater velocity (v), ft/yr	55	160	20-30	4-10
Shortest distance from tract to closest discharging stream (d), mi		4		1
Time for leachate to reach stream (t), yr		130-380		180-1450
<b>Retort transport</b>				
Head difference between aquifers (dh), ft		25		25
Direction of groundwater flow in retort		Down		Up
Controlling permeability (k), ft/day		1.5		0.1-0.3
Hydraulic gradient in retort (dh/dl)		0.083		0.083
Groundwater velocity in retort (v <sub>R</sub> ), ft/yr		680		45-140
Residence time in retort (R), yr		1		3-10

retorts into surface streams is summarized in Table 3. This table presents the average annual discharge and estimated maximum possible increase in total dissolved salts (TDS), sodium (Na), and total organic carbon (TOC) at four points in the Upper Colorado River Basin due to the discharge of groundwater-borne, in-situ spent shale leachate into surface waters. If pulses from several line sources of retorts arrived at the streams simultaneously, the increases would be correspondingly larger.

#### PLANNED ACTIVITIES FOR 1980

The present investigation has been completed and described in a technical task report. In 1980, existing numerical models will be adapted to the Piceance Creek Basin and used to make

detailed investigations of the flow field in the vicinity of in-situ oil shale retorts. Parametric studies will be conducted to evaluate pressure transient effects associated with large-scale dewatering, and the rates and time scales involved in dewatering will be explored. Unsaturated flow will be studied, and post-abandonment infiltration will be investigated.

#### FOOTNOTE AND REFERENCES

\*This program is funded by the Department of Energy's Division of Environmental Control Technology and the Office of Technology Impacts.

1. J. P. Fox, "Water-Related Impacts of In-Situ Oil Shale Processing," Lawrence Berkeley Laboratory Report, LBL-6300 (1980).

Table 3. Estimated increase in TDS, Na, and TOC in surface waters of the Upper Colorado River Basin due to the discharge of in-situ leachates from tracts C-a and C-b into Piceance Creek and Yellow Creek as base flow.

	Average annual discharge acre-ft/yr	Maximum possible increase, mg/l		
		Na	TDS	TOC
	(1)	(2)	(3)	(4)
Piceance Creek at White River <sup>a</sup>	14,500	1740 - 5260	4100 - 46,100	10 - 570
Yellow Creek at White River <sup>a</sup>	1,150	0 - 2100	0 - 24,600	3 - 340
White River near Watson, Utah	532,000	50 - 150	110 - 1310	0.3 - 16
Green River near Green River, Utah	4,427,000	6 - 18	13 - 160	0.03 - 2
Colorado River at Lees Ferry, Arizona	12,426,000	2 - 6	5 - 56	0.01 - 0.7

<sup>a</sup>It is assumed that the leachate from tract C-a discharges into Yellow Creek and from tract C-b into Piceance Creek.

## A MATHEMATICAL MODEL FOR LEACHING OF ORGANIC CARBON FROM IN-SITU RETORTED OIL SHALE\*

W. G. Hall, R. E. Selleck,<sup>†</sup> and J. F. Thomas<sup>†</sup>

### INTRODUCTION

The rich oil shale deposits in Colorado's Piceance Creek Basin are being considered for early commercialization by vertical modified in-situ retorting. In this process, large underground chambers of oil shale, several hundred feet in cross section and up to 700 feet high, are pyrolyzed in place. This type of processing may result in several environmental problems, including leaching of retorted shale, subsidence, and low resource recovery. These problems are described elsewhere in this report.<sup>1</sup>

One of the major environmental concerns is leaching of the retorted shale. Most of the rich oil shale deposits in the Piceance Creek Basin are laced with groundwater aquifers. During in-situ retort preparation and retorting, groundwater levels adjacent to the development site are lowered below the retorts by pumping. After oil recovery is complete, the returning groundwater may pass through the spent underground chambers and leach out soluble organic and inorganic materials. These materials may be transported in surrounding aquifers where they may be withdrawn from wells or discharged to local springs and streams.

A number of methods have been proposed to solve these problems.<sup>1</sup> These include grouting, intentional leaching, and various hydrologic modifications. The purpose of this program, initiated in June 1978, is to investigate selective leaching as a means to minimize the impact of abandoned in-situ retorts on local water quality. In this approach, water would be injected into the retort, collected, and treated in a surface facility. This appears feasible because previous experimental work revealed that most of the leachable material is readily removed with a few pore volumes of water.

The approach we are using is to first define the kinetics of leaching of inorganic and organic compounds from spent shale by using data collected from batch and column leaching experiments. The kinetic data are then incorporated into a mathematical model of the leaching and transport processes. This model may then be used to predict the movement of leached organic and inorganic compounds through the in-situ retort and into the surrounding aquifers. The resulting model will be used to predict the number of pore volumes that must be treated to produce a leachate with a sufficiently low concentration of organics and inorganics.

### ACCOMPLISHMENTS DURING 1979

This year we selected and tested a mass transport equation and conducted a number of batch and continuous-flow column leaching experiments to develop kinetic constants for use in the model. This work is summarized here.

#### Mass Transport Equation

Water passing through a bed of spent shale leaches out soluble material and transports it through the pores of the bed. The solute is a complex mixture of organic and inorganic compounds. Since the modeling of multi-component mass transfer and diffusion is beyond the scope of this study, it is assumed that the organic portion of the solute can be characterized by total organic carbon (TOC) and the inorganic portion by electrical conductivity (EC). Both of these parameters are easily measured.

The leaching and transport of the solute, EC and TOC, can be modeled by a mass transport rate equation:

$$\frac{\partial C}{\partial t} = -\mu_{\text{pore}} \frac{\partial C}{\partial z} + D \frac{\partial^2 C}{\partial z^2} + r_r - \frac{\partial q}{\partial t} \frac{P_B}{E} \quad (1)$$

in which:

C	=	concentration of solute in the liquid phase
t	=	time
$\mu_{\text{pore}}$	=	velocity of the liquid phase in pores of the media
z	=	distance along column
D	=	dispersion coefficient
$r_r$	=	rate of chemical reaction
q	=	concentration of solute in the solid phase
$P_B$	=	bulk density
E	=	porosity of shale bed.

The terms on the right side of the equation are the contributions to the net change of the solute concentration with time due to convection, dispersion, chemical reaction, and mass transfer. The chemical reaction term is neglected since it is assumed that TOC and EC are conservative. The mass-transfer term is coupled with an equation describing the transfer of solute between the solid and liquid phases as follows:

$$\frac{\partial q}{\partial t} = K_a F(C, q) \quad (2)$$

in which:

$a$  = interfacial area between phases  
 $K$  = mass transfer coefficient  
 $F(C, q)$  = driving force expressed as a difference between equilibrium and actual solute concentrations in solid or liquid phases.

In the application of Eq. (2) we are following the approach of Amy.<sup>2</sup> Mass transfer between phases may be represented by a series of equations similar to Eq. (2), each one in the series applicable to the movement of solute in a particular domain. These domains include the solid shale, pores within the solid boundaries, and interfaces between solid and liquid phases. It is likely that the overall mass transfer will be dominated by transfer within a single domain, such as movement through the solid phase. Investigations are directed toward the determination of the dominant domain and the development of an overall mass transfer coefficient applicable to the total movement of solute from the solid to liquid phase. An isotherm relating equilibrium concentrations of TOC in the solid and liquid phases was developed from batch studies of solid shale and water mixtures for use in Eq. (2).

#### Leaching Experiments

Batch and column leaching experiments were performed on spent shale produced in the Laramie Energy Technology Center 10-ton retort in Wyoming. The raw shale was mined at Anvil Points, Colorado, and had an oil content of 26 gallons per ton. The maximum temperature reached in the retort was 1200°F and the retorting rate was 1.53 in/hr under a 67 percent/33 percent air/steam atmosphere.

Column leaching experiments are being conducted in lucite columns, 11.4 cm in diameter by 1.3 m long (Fig. 1). At the completion of the small column studies additional runs will be made in steel columns, one foot in diameter by

ten feet long. Several runs of the small column have been completed. Distilled water from a glass reservoir is pumped through an activated carbon filter to a column containing a bed of packed spent shale. Taps are located at 15-cm intervals along the bed centerline so that leachate samples can be withdrawn. Pools of water are provided at the top and bottom of the bed to assure uniform entry and exit across the entire cross section. Flow may be established in either direction, up or down.

Typical results from a small column experiment are shown in Fig. 2. This particular column was packed with 1/2- to 1/8-inch spent shale having a porosity of 66 percent. The pore velocity of the leachate was 150 cm per day. A marked decrease in TOC is demonstrated in the figure. Concentrations greater than 30 ppm at one hour decreased in an exponential manner to 6 ppm or less after 69 hours. The significance of this is that much of the organics leached from shale are removed in the first few pore volumes of water passing through the bed. Withdrawal of this leachate to the surface for treatment and reinjection may be a feasible control strategy.

In the first few column experiments, the leaching flow through the column was in the upward direction. During filling of the shale voids with water from the bottom prior to establishing upward flow, leaching occurs only under saturated conditions and the volume of water below the wetted front has a net upward velocity. Alternatively, when the column is filled from the top prior to establishing downward flow, leaching takes place in both saturated and unsaturated flow zones. In addition, a pool of relatively stagnant water is formed in the lower regions of the bed until the column is filled and downward flow is established. Modeling of flow in the three-phase unsaturated region and the quiescent pool is beyond the scope of this investigation.

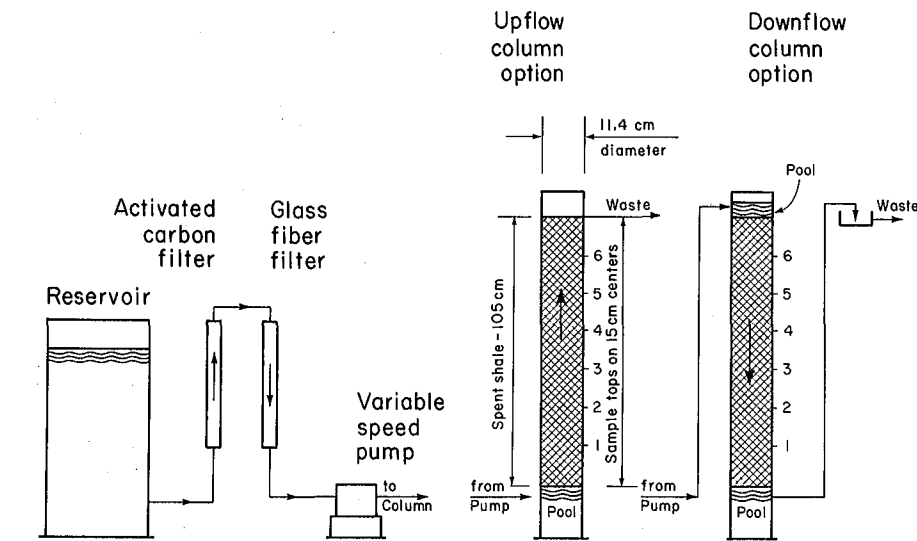


Fig. 1. Experimental setup for small column leaching studies.  
(XBL 802-6795)

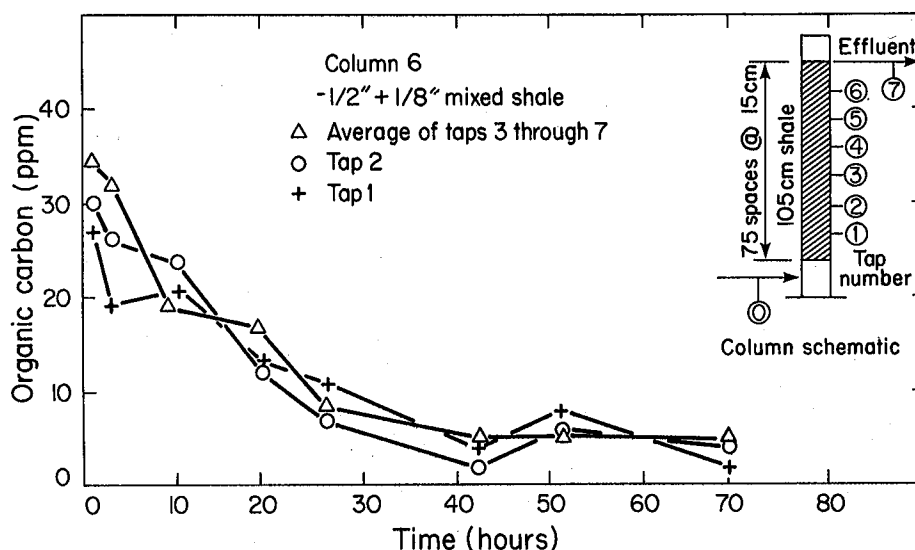


Fig. 2. Results of typical column leaching experiment.

(XBL 798-2582)

At first, it was deemed simpler to model the leaching process under upflow conditions. After several runs it was observed that density currents within the shale bed were obscuring the results. As the distilled water rose in the bed, it picked up salts from the shale. A portion of leachate, more dense because of greater dissolved salt content, fell back to the pool at the bottom. This pattern, repeated throughout the bed, has two adverse effects which complicate the analysis of the column studies. First, although net flow is upward, there are downward velocity components which violate the assumption of uniform flow implicit in the derivation of the mass transport equation. Secondly, the concentration of TOC in the fluid entering the bed is continually changing as dense leachate falls from the bed above and, therefore, entry conditions to the shale bed cannot be well defined.

A small column containing 1/2- to 1-inch shale, run under downflow conditions starting with shale voids full of water, showed a significant improvement in internal flow patterns. Leachate density, due to dissolved salt pickup, increased in the direction of flow. This creates a density gradient favorable to the formation of uniform flow in the downward direction. As might be expected, TOC data also showed a similar increasing gradient in the direction of flow. Consequently, all remaining column investigations in this study will be conducted under downflow conditions.

The presence of density currents in small-scale columns indicates that similar

density currents are likely to form in actual in-situ retorts during the passage of groundwater through the interstices in the shale. Density differences in leachates due to differential dissolved salt concentrations of 20,000 mg/l or greater are possible. These differences can create significant driving forces counter to the direction of net flow and must be accounted for in the modeling effort.

#### PLANNED ACTIVITIES FOR 1980

Work planned for the next calendar year includes the completion of the small and large column studies and the incorporation of kinetic data into the transport model.

#### FOOTNOTE AND REFERENCES

\*This program is funded by the Department of Energy's Division of Environmental Control Technology and Division of Oil, Gas, and Shale Technology.

†University of California, Berkeley, CA.

1. P. Persoff and J. P. Fox, "Control Strategies for Abandoned In-Situ Oil Shale Retorts," Energy and Environment Division Annual Report 1979, Lawrence Berkeley Laboratory Report, LBL-10486 (1980).
2. Gary L. Amy, Contamination of Groundwater by Organic Pollutants Leached from In-Situ Spent Shale, Ph.D. Dissertation, University of California, Berkeley (1978).

# PENETRATION OF NON-NEWTONIAN GROUTS THROUGH RUBBLE\*

P. Persoff

## INTRODUCTION

Adverse environmental effects of oil shale development by modified in-situ retorting include groundwater degradation due to leaching of in-situ spent shale, subsidence of retort overburden, and low resource recovery because of the need to leave large pillars of intact raw shale in place to support overburden. These problems and potential solutions are discussed in another report in this volume.<sup>1</sup> One possible solution to all three of these problems is backfilling abandoned retorts with a grout containing a large proportion of surface retorted shale. Development of a hydraulic cement based on surface-retorted shale is described elsewhere in this volume.<sup>2</sup>

The distribution of such a grout into an abandoned retort is one of the most technically difficult and potentially costly aspects of retort abandonment. The abandoned retort consists of a packed chamber of retorted shale with a complex void distribution. Voids include spaces between pieces of rubble which may range from fines to boulders, fractures along the bedding plane in individual pieces of shale, and micropores created by the pyrolysis of kerogen. The introduced grout must uniformly penetrate a majority of these voids to achieve low permeabilities. This may be achieved if a sufficiently large number of closely spaced drill holes are used or if the viscosity of the grout is sufficiently low. An economic tradeoff exists between the number of drill holes and grout viscosity. Since retorts are deep, one to two thousand feet below the surface, drilling grout injection holes will be costly. On the other hand, use of slurry fluidizers to reduce the grout viscosity will also be costly.

The purpose of this program, initiated in June 1978, is to develop a mathematical model of the flow of a Bingham fluid through a packed bed of rubble and to develop rheological data on candidate grouts. Laboratory and mathematical investigations will be conducted to develop relationships between grout penetration, distance, injection pressure, and grout viscosity. The resulting model will be used to determine grout properties required to penetrate rubble in abandoned retorts.

## ACCOMPLISHMENTS DURING 1979

The yield stress of non-Newtonian fluids was tentatively identified as the controlling factor limiting the penetration of slurries of spent shale through rubble. Rheological data were obtained for several candidate grouts, which showed that they are best described by the Casson model.<sup>3</sup>

## Flow of Non-Newtonian Fluids

Slurries of spent shale (more generally, suspensions of solid particles in a Newtonian fluid) are not Newtonian, but follow the Bingham or Casson model. Figure 1 shows schematically the difference between these types of fluids. Newtonian fluids will flow when subjected to any shear stress, no matter how small. Non-Newtonian fluids described by the Bingham or Casson model will not. They are characterized by a finite yield stress,  $\tau_0$ , which is the minimum shear stress that must be imposed upon such a fluid before it will flow. The yield stress is the intercept in Fig. 1. A non-Newtonian fluid with yield stress  $\tau_0$  will not flow through a cylindrical pore of radius  $r$  unless the applied pressure gradient is greater than  $\frac{2\tau_0}{r}$ .

Figure 2 shows the velocity profiles for a Newtonian and a Bingham or Casson fluid flowing through cylindrical pores in laminar flow. The Newtonian fluid flows with a paraboloidal velocity profile. The Bingham and Casson fluids flow as a central plug, not in shear, which is carried along by an annular cylinder of fluid in shear. As the pressure gradient decreases, approaching  $\frac{2\tau_0}{r}$  from above, the central plug becomes wider until it fills the pore. At this point the velocity is zero everywhere in the

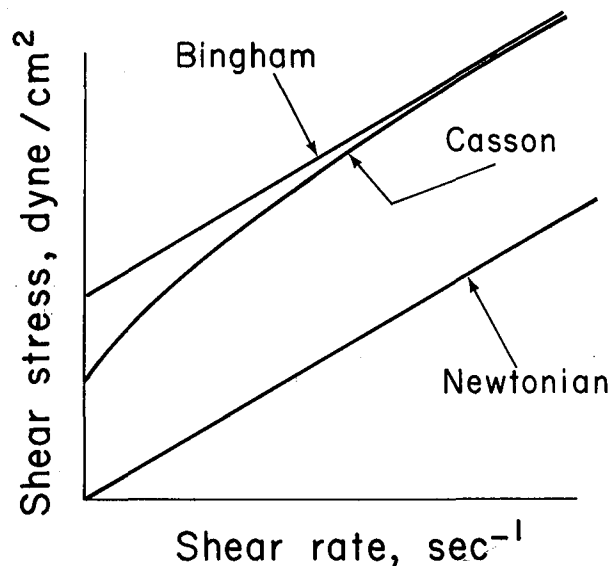


Fig. 1. Schematic representation of rheological behavior of Newtonian and non-Newtonian fluids. (XBL 802-167)

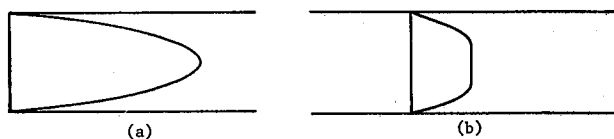


Fig. 2. Velocity profiles for laminar flow cylinder of (a) Newtonian fluid and (b) Bingham or Casson fluid. (XBL 793-706)

pore and the flow stops. This decrease in pressure gradient to a limiting value is exactly what happens as grout moves away from the point of injection. Note also that the minimum pressure gradient for flow is inversely proportional to pore radius. This means that as grout penetrates further from the point of injection, the flow will stop first in fine pores while it continues through larger ones.

The yield stress value of the grout is a function of the water-solids ratio (wsr). This is of interest because while a high water-solids ratio would give a low yield value, and thus favor complete grout penetration, it also results in greater permeability of the grout and lower strength, and promotes bleeding of water from the grout, or it may prevent the grout from setting. Complicating the situation is the fact that in-situ spent shale rapidly absorbs water, up to 4 gallons/ft<sup>3</sup>.<sup>4</sup> This means that pre-wetting of the in-situ spent shale will be needed to prevent dehydration (and flow stoppage) of the grout during injection.

#### Experimental

Rheological measurements were made on slurries of Lurgi spent shale in water. Slurries were prepared with water-solids ratios ranging from 0.8 to 1.8. The material used is described in the article on hydraulic cement production by Mehta and Persoff referred to earlier.<sup>2</sup> Viscosity measurements were made using a Contraves viscometer, model 15-T. Bleeding was measured by letting a volume of the slurry stand for four hours in a graduated cylinder. If any clear fluid separated to the top of the slurry, this volume was expressed as a percentage of the total volume.

#### Results and Discussion

The shear stress-shear rate relationships for slurries of Lurgi spent shale are shown in Fig. 3. This figure indicates that the data are in good agreement with the Casson model:<sup>3</sup>

$$F^{1/2} = a + bD^{1/2}$$

where  $F$  = shear stress, dyne/cm<sup>2</sup>

$$a = \tau_0^{1/2}, (\text{dyne/cm}^2)^{1/2}$$

$$b = \text{constant } (\text{g/cm-sec})^{1/2}$$

$$D = \text{shear rate, sec}^{-1}.$$

Table 1. Yield stress and percent bleeding for various water-solid ratios.

Bleeding for slurries of Lurgi spent shale.		
Water-solid ratio	Yield stress, dyne/cm <sup>2</sup>	Bleeding, percent
0.8	167	0
1.0	96	0
1.2	25	11
1.5	6	21
1.8	4	31

The yield stress (the square of the intercept in Fig. 3) is shown in Table 1. Note that the yield stress increases very rapidly as the wsr decreases below 1.2.

Table 1 also shows the percent bleeding of the slurries. Bleeding is the settling of solid grout particles from suspension leaving a clear supernatant. The volume of this supernatant (expressed as a percentage of the total) becomes an

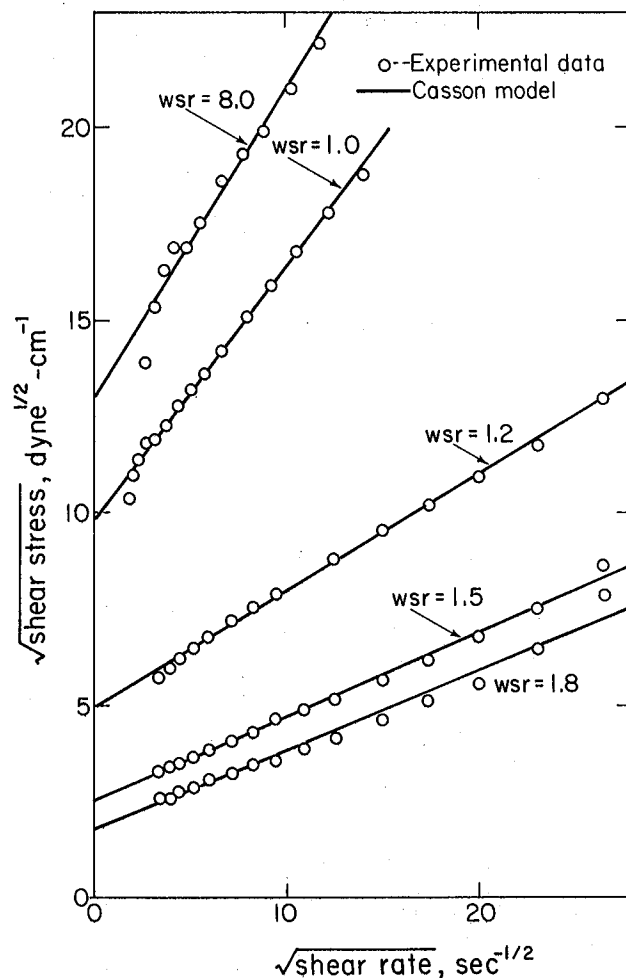


Fig. 3. Square root of shear stress versus shear rate showing fit of slurries of Lurgi spent shale to the Casson model. (XBL 805-1109)

ungrouted void, leading to increased permeability and decreased strength. As expected, bleeding increases rapidly above a wsr of 1.0. The significance of this is that if a non-bleeding grout is required, a high yield stress must be accepted.

The measured yield stresses may be used in a mathematical model of flow of non-Newtonian fluid through rubble to predict grout penetration. If classical theory is used to make these predictions, the penetration radius is about 20 meters. However, preliminary laboratory experiments in which grouts are pumped into simulated packed columns of rubble indicate that the penetration radius may be as much as an order of magnitude smaller than the calculated value. Thus, classical theory appears not to apply to grout penetration in in-situ retorts and theoretical and physical modeling studies have been initiated to develop predictive techniques and reliable penetration distances.

#### PLANNED ACTIVITIES FOR 1980

Theoretical and physical modeling will be conducted to develop a relationship that describes the penetration of spent-shale grouts as a function of yield stress, injection pressure, and void distribution.

#### FOOTNOTE AND REFERENCES

\*This program is jointly funded by the Department of Energy's Division of Environmental Control Technology and Division of Oil, Gas, and Shale Technology.

1. P. Persoff and P. Fox, "Control Strategies for Abandoned In-Situ Oil Shale Retorts," Energy and Environment Division Annual Report 1979, Lawrence Berkeley Laboratory Report, LBL-10486 (1980).
2. P. K. Mehta and P. Persoff, "Hydraulic Cement Production from Lurgi Spent Shale," Energy and Environment Division Annual Report 1979, Lawrence Berkeley Laboratory Report, LBL-10486 (1980).
3. N. Casson, "A Flow Equation for Pigment-Oil Suspensions of the Printing Ink Type," in C.C. Mill, ed., Rheology of Disperse Systems, Pergamon Press, N.Y. (1959).
4. T. D. Nevens, C. H. Habenicht, and W. J. Culbertson, "Disposal of Spent Ash in In Situ Retorted Caverns," Progress Report, Denver Research Institute (1977).

## WASTEWATER TREATMENT STUDIES

### TREATMENT OF WASTEWATER FROM IN-SITU RETORTING OF OIL SHALE\*

*R. H. Sakaji, J. P. Fox, R. E. Selleck,† D. Jenkins,† and C. G. Daughton†*

#### INTRODUCTION

Two unique types of water are produced during in-situ oil shale retorting from combustion, mineral dehydration, input steam, and groundwater. These are referred to as retort water and gas condensate. They are produced in rather large volumes, from about 0.5 to 22 barrels of water per barrel of oil, and have proven to be very difficult to treat. If this water could be successfully renovated, it would represent a valuable resource for the arid oil shale region.

These waters are produced within an in-situ retort system as a vapor that is condensed with the oil and separated from it by decantation, heat treatment, or condensation. The water that condenses in the retort and collects in an underground sump at the bottom of the retort is referred to as retort water while the water removed from the gas stream in the above-ground condenser train is referred to as gas condensate.

The relative proportions and composition of each type of water depend on the exit gas temperature and product collection system design and operation. The retort water travels down the packed bed of shale in an emulsion with the oil, and thus may leach constituents from the shale matrix and from the oil itself. Therefore, this water is expected to contain high concentrations of certain elements by virtue of its intimate contact with the oil and shale. Retort waters are characteristically brown to yellow, they have a pH that ranges from 8 to 9, and they contain high levels of many inorganic and organic constituents, including  $\text{NH}_3$ ,  $\text{NH}_4$ ,  $\text{HCO}_3$ ,  $\text{SO}_4$ , carboxylic acids, and various organo-nitrogen compounds. The gas condensate which leaves the retort as steam contains lower concentrations of most organics and inorganics than retort water and higher concentrations of dissolved gases, such as  $\text{NH}_3$  and  $\text{CO}_2$ . Because of these different compositions, retort water and gas condensate will be collected and treated separately in a commercial in-situ operation.

The purpose of this program, initiated in June 1978, is to develop treatment systems capable of upgrading retort waters and gas condensates for on-site reuse or for discharge to the environment. These systems of necessity will include novel processes, such as spent shale adsorption.<sup>1</sup>

#### ACCOMPLISHMENTS DURING 1979

This year we initiated work to develop a treatment system for retort water. We acquired a range of samples, characterized them, and assessed their treatability based on their characteristics. We encountered a number of problems when we attempted to use standard analytical methods to measure water quality parameters and thus, we initiated work to develop new methods.

We also conducted bench-scale treatability studies on oil and grease removal, air stripping, and biological treatment.

The composition of in-situ retort waters is summarized in Table 1. This table indicates that the concentrations of ammonia, carbonates, oil and grease, organic carbon, and dissolved salts are too great to permit direct reuse or discharge. Other presently unknown constituents may also have to be removed.

A retort water treatment system that we believe is viable for most uses of this water includes oil and grease removal, stripping to remove NH<sub>3</sub> and other volatiles, biological treatment to reduce organics, and a salinity reduction step. (See Fig. 7b, Ref. 1).

Table 1. Chemical composition of various oil shale process waters (mg/l).

Parameter	Range		Average <sup>a</sup>
Alkalinity, total (mg/l CaCO <sub>3</sub> )	18,200	110,900	
Aluminum	0.041	16.6	
Arsenic	0.46	10	1.8
Barium	0.002	0.47	0.07
Beryllium	<0.001	<0.001	
Bicarbonate mg/l HCO <sub>3</sub> <sup>-</sup>	4,200	73,640	
Biochemical oxygen demand, 5-day	350 <sup>d</sup>	5,500 <sup>d</sup>	
Bromine	<0.001	1.94	0.082
Cadmium	<0.001	0.005	
Calcium	0.0	94	7.6
Carbon, inorganic mg-C/l	1960	19,200	7,500
Carbon, organic, mg-C/l	2,200	19,000	4,700
Carbonate, mg-CO <sub>3</sub> <sup>2-</sup> /l	0.0	15,210 <sup>d</sup>	
Chemical oxygen demand	8,500 <sup>d</sup>	43,000 <sup>d</sup>	18,500 <sup>d</sup>
Chlorine	0.007 <sup>b</sup>	1910 <sup>d</sup>	
Chromium	0.009	0.08	0.015
Cobalt	0.002	0.65	0.12
Conductivity, μmhos/cm	15,100	193,000	31,000
Copper	0.003	160	0.019
Fluoride	0.1 <sup>b</sup>	270 <sup>b</sup>	
Hardness	20	1,500	88
Iodine	<0.001	1.3	
Iron	0.091	77	7.6
Lead	0.002	0.83	
Lithium	<0.001	7.1	0.70
Magnesium	3.2	350	22
Manganese	0.001	0.39	0.099
Mercury	<0.001	0.39 <sup>d</sup>	
Molybdenum	0.033	1.2	
Nickel	0.014	2.6	
Nitrogen, ammonia, mg-NH <sub>3</sub> -N/l	1,700	13,200	7,000
Nitrogen, ammonium, mg-NH <sub>4</sub> <sup>+</sup> -N/l	930	24,450	10,000
Nitrogen, nitrate, mg-NO <sub>3</sub> <sup>-</sup> -N/l	1.4	8.7	
Nitrogen, nitrite, mg-NO <sub>2</sub> <sup>-</sup> -N/l	<1.0		
Nitrogen, organic, mg-N/l	73.3 <sup>c</sup>	1510 <sup>c</sup>	
Nitrogen, Kjeldahl, mg-N/l	6,600	19,500	
Oil and grease	3,800	3,800	
pH	8.1	9.4	8.7
Phenols	2.2 <sup>d</sup>	169 <sup>d</sup>	
Phosphorus	0.23 <sup>d</sup>	19.0 <sup>d</sup>	1.25 <sup>d</sup>
Potassium	8	120	37
Selenium	<0.001	1.7	
Silica, mg-SiO <sub>2</sub> /l	4 <sup>b</sup>	128 <sup>b</sup>	17
Silver	<0.001	0.23	
Sodium	45 <sup>b</sup>	1600 <sup>b</sup>	320
Solids, dissolved	1,750 <sup>d</sup>	24,500 <sup>d</sup>	6,800 <sup>d</sup>
Solids, total	6,350 <sup>d</sup>	121,000 <sup>d</sup>	
Solids, volatile	2,070	119,300	
Sulfur, sulfate, mg-SO <sub>4</sub> <sup>2-</sup> /l	42	2,200	1,400
Sulfur, sulfide, mg-S <sup>2-</sup> /l	0.0	156 <sup>d</sup>	
Sulfur, total, mg-S/l	14	2320	
Uranium	0.018	93	
Vanadium	0.004	>190	0.27
Volatile acids	807	1481	
Zinc	0.020	15.1	0.28

<sup>a</sup>An average is reported only if more than 15 waters were available. Most values are based on 18 waters.

<sup>b</sup>Significant discrepancies noted in reported values determined with alternate analytical methods. Values shown are for spark source mass spectrometry.

<sup>c</sup>Based on two values only.

<sup>d</sup>Significant chemical interferences suspected.

We have initiated laboratory investigations on oil and grease removal, biological treatment, and ammonia stripping. The following section describes the results of the oil and grease removal work. The other investigations are still in preliminary stages and will be reported in the next Annual Report.

#### Oil and Grease Removal

When we started this work, it was assumed that retort water contained a significant fraction of emulsified oil and grease. This was a widely held opinion among oil shale researchers and was based on experimental measurements. We initiated studies on the removal of oil and grease from retort waters because emulsified oil and grease can interfere with treatment processes, as well as reuses such as cooling tower waters. The process studied was coagulation followed by dissolved air flotation. This method is conventionally used to treat refinery effluents and is economical because it allows reclamation of the oil.

However, we subsequently discovered, that only a small fraction of the "measured" oil and grease was emulsified. The balance of the "measured" oil and grease is dissolved organic material with a high molecular weight, such as carboxylic acids. This necessitated the development of a reliable oil and grease analytical method which is reported elsewhere.<sup>2</sup> Work is now in progress to characterize the dissolved fractions to determine whether or not they should be removed from retort water.

This section reports the results of experimental work to select a suitable coagulant for oil and grease removal from retort waters. Zeta potentials of retort water were measured and tests performed to screen several chemical coagulants and polymers on two retort waters. This work indicated that the surface charge of the suspended particles in retort water is negative and that several cationic polymers produce floc at dosages in excess of 100 ppm. Oil and grease removal at these high dosages was poor. These results are partially attributed to the fact that only a fraction of the measured oil and grease is suspended and thus amenable to coagulation. Because of the low oil and grease removals and high dosages of polymer, coagulation may not be effective for oil and grease removal from retort waters.

#### Coagulation and Flocculation.

Large particles in a wastewater are conventionally removed by gravity sedimentation. However, very small particles and colloids such as suspended and emulsified oil and grease are too small to remove in this way because of their very slow settling velocities. These smaller particles are removed from water by coalescing them into larger particles and then using conventional removal mechanisms, such as sedimentation or flotation. Coagulation refers to the addition of chemicals to induce particle aggregation while flocculation is the process of forming large particles from small ones by

aggregation; sedimentation is the removal of the aggregated particles.

Colloidal particles remain in suspension because of the high surface charge that they carry. Oil droplets tend to acquire a negative charge by preferential adsorption of anions, particularly hydroxyl ions. This surface charge must be reduced to bring about particle aggregation or flocculation. This may be done by the addition of electrolytes, polymers, or chemicals that form hydrolyzed metal ions, i.e., alum and ferric sulfate.

#### Zeta Potential.

Zeta potential measurements are commonly used to estimate the surface potential of suspended particles. The measurement can be used to assess the type and doses of a coagulant that are required for floc formation. Zeta potential,  $\zeta$ , is defined by the equation

$$\zeta = 4\pi\delta q/D$$

in which  $q$  is the surface charge on the particle (or the charge difference between the particle and the body of the solution),  $\delta$  is the thickness of the layer around the particle through which the charge difference is effective, and  $D$  is the dielectric constant of the solution. Thus, the zeta potential is a measure of both the charge on the colloidal particle and the distance over which the charge is effective.

Zeta potential analysis of retort water demonstrated a decrease in the negative mobility of the particles with decreasing dilutions. This results from the influx of positive counter ions into the diffuse double layer of charge around the oil droplets. A plateau of electrophoretic mobility at approximately  $-1.35 \mu\text{m}/\text{sec}$  per volt/cm was attained at a dilution of about 20 percent (v/v). The zeta potential of the particles in L-3 retort water was thus about  $-17.4 \text{ mV}$ .

The negative charge on the droplets indicates that they can be coagulated with a cationic polymer or a metal salt. On the one hand, the high ionic strength of the retort waters tends to suppress the diffuse double layer around the oil droplets. This should enhance coagulation. However, the high ionic strength also tends to inhibit the coagulative potential of the polymers. The net result is generally an increase in the dose of coagulant required to achieve good flocculation.

#### Coagulant Performance by Jar Testing.

A variety of metal salts and polymers was first visually screened for floc formation using water L-2. The more successful of these polymers was then evaluated using standard jar testing methods on L-3 and 150-ton retort waters. Coagulant performance was evaluated by measuring residual turbidity and suspended oil and grease.

In the screening tests, alum, ferric chloride, ferric sulfate, and a total of 36 com-

mercial anionic, nonionic, and cationic polymers were tested for their ability to produce a visible floc. This was accomplished by dosing a 50-ml sample of retort water with a given concentration of polymer. The sample was stirred for 30 sec with a magnetic stirrer and was checked for visible signs of floc formation. Table 2 summarizes the results of these screening tests. This table indicates that Tretolite and Nalco are the most promising polymers tested.

The second screening procedure involved dosing a 50-ml sample of retort water with a known concentration of polymer. After 30 sec of rapid stirring, the sample was allowed to settle for 60 min. An aliquot of the supernatant was drawn off and residual turbidity was measured. This procedure was repeated for a range of polymer doses to determine the dose that produced minimum residual turbidity in the wastewater. This value is commonly referred to as the optimum coagulant dose. The results of the jar tests for the six most promising coagulants, in terms of turbidity removal, are shown in Fig. 1. Table 3 lists the optimum coagulant dose and corresponding turbidity reduction.

All of the successful polymers were cationic, which is consistent with the zeta potential measurements. Table 3 indicates that polymer doses of 40 to 160 ppm are required to achieve turbidity reductions of 12 to 64 percent. These results are not encouraging because of high dosages required.

The six polymers that showed promise in producing floc in the L-3 retort water were tested on 150-ton retort water. The above approach to testing the polymers was found inadequate for 150-ton retort water because of low concentration of materials and low turbidities. The residual turbidity of 150-ton water following coagulation and settling remained constant or increased. Tretolite 398 was the only polymer that reduced turbidity in 150-ton retort water. Consequently this polymer was selected for further testing in a series of jar tests employing oil and grease removal as a means of evaluating process performance.

Varying doses of Tretolite 398 were added to jars containing 250 ml of 150-ton retort water. The samples were rapidly mixed at 150 rpm with a standard jar test apparatus for 60 sec. This was followed by slow stirring for 15 min at 40 rpm. The samples were then centrifuged for 15 min at 2500 rpm. Portions of the supernatant were withdrawn from beneath the liquid surface and analyzed for oil and grease by the standard method described by Sakaji et al.<sup>2</sup> The results are summarized in Fig. 2 which show residual oil and grease as a function of polymer dose. The polymer was not effective in removing suspended oil and grease.

Additional work is required to develop and refine analytical methods to characterize the nature of the oil and grease in retort waters and to screen each retort water with all potentially viable polymers.

Table 2. Results of screening tests on L-3 retort water.

Name of Polymer	Chemical Class	Floc Formation +/-
Magnifloc	Polyamide	
1561C		-
1839A		-
1906N		-
521GH		-
581C		-
507C		+
587C		-
Tretolite		
J-189	Quaternary	+
TFL-300	Polyamines	+
TFL-362		+
TFL-383		+
TFL-391		+
TFL-398		+
Calgon		
WT 3000		
CAT FLOC	PDADMA	+
WT 2575	PDADMA	-
WT 2640	PDADMA	-
Garret-Callahan		
LDOW		
766N		
764N		
Dark Amber	Polyamine	+
720 CL		-
721 CL		
Herco Floc		
863 (Dry)		-
Nalco		
603		-
7103		+
7105		+
7107		+
7132		+
7134		+
7123		+
7730		+
7731		+
7734		-
8101		+
8102		+
8104		+
8106		+
Alum		+
FeCl <sub>3</sub>		+
Fe <sub>2</sub> (SO <sub>4</sub> ) <sub>3</sub>		+

#### PLANNED ACTIVITIES FOR 1980

Retort water treatability studies will be conducted on additional methods of oil and grease removal, on air and steam stripping, and on various biological processes including trickling filters and activated sludge. These results will be used to design a larger scale, continuous-flow system that includes several unit processes. This treatment system will be interfaced with packed columns of spent shale,<sup>1</sup> and overall removal efficiencies for TDS, NH<sub>3</sub>, alkalinity, and organic carbon will be determined. Work will be initiated on the treatability of gas condensates.

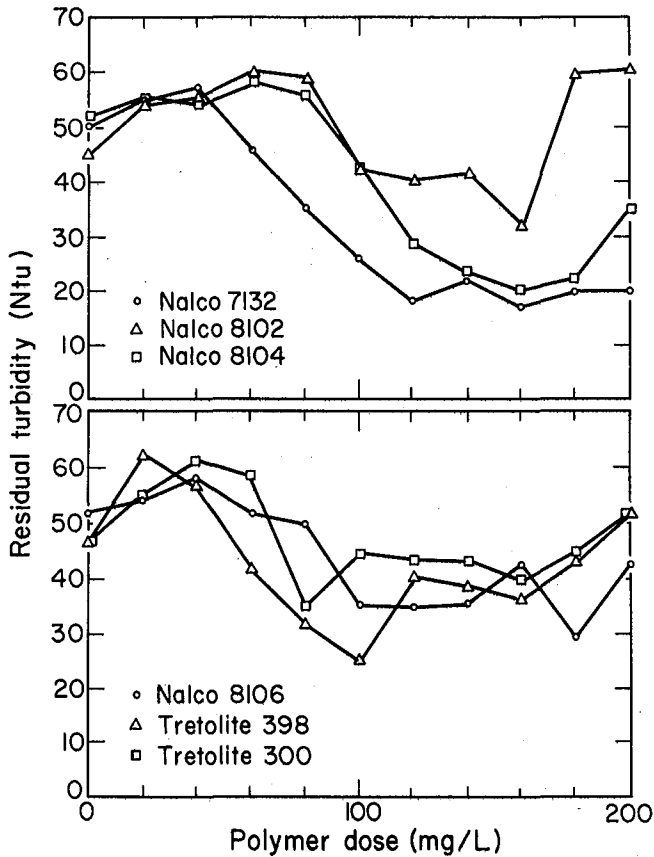


Fig. 1. The effect of six polymers on the residual turbidity of L-3 retort water. (XBL 807-1379)

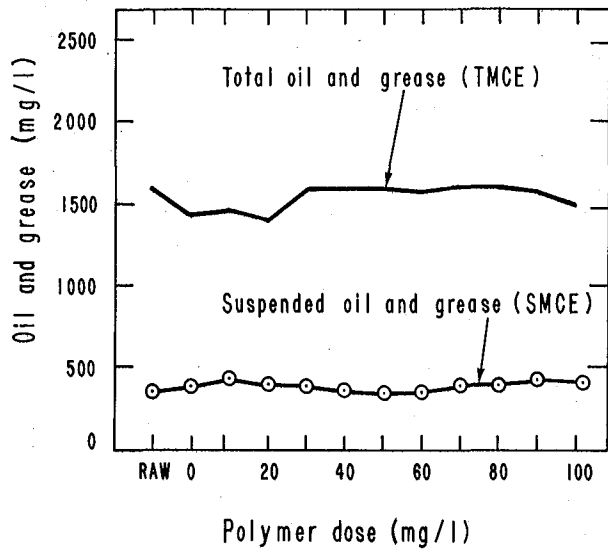


Fig. 2. The effect of Tretolite 398 polymer on oil and grease in 150-ton retort water. (XBL 805-1049)

FOOTNOTES AND REFERENCES

\*This program is funded by the Department of Energy's Division of Environmental Control Technology.

†University of California, Berkeley, CA.

1. J. P. Fox and D. E. Jackson, "Spent Shale as a Control Technology for Oil Shale Retort Waters," Energy and Environment Division Annual Report 1979, Lawrence Berkeley Laboratory Report, LBL-10486 (1980).
2. R. H. Sakaji, S. Onysko, J. P. Fox, C. G. Daughton, D. Jenkins, and R. E. Selleck, "The Analysis of Oil and Grease in Oil Shale Retort Waters," Energy and Environment Division Annual Report 1979, Lawrence Berkeley Laboratory, LBL-10486 (1980).

Table 3. The effect of Tretolite and Nalco polymers on residual turbidity of two oil shale retort waters.

Coagulant	Retort Water	Dosage <sup>a</sup> ppm	Percent Turbidity Reduction
NALCO 7132	L-3	120	64
NALCO 8102	L-3	160	29
NALCO 8104	L-3	160	62
NALCO 8106	L-3	100	49
TRETOLITE 398	L-3	100	47
TRETOLITE 300	L-3	80	28
NALCO 7132	150-TON	---	Increased turbidity
NALCO 8102	150-TON	---	Increased turbidity
NALCO 8106	150-TON	---	Increased turbidity
TRETOLITE 398	150-TON	40	12
TRETOLITE 300	150-TON	---	Increased turbidity

<sup>a</sup>Dosage required to produce minimum turbidity following jar testing.

## THE ANALYSIS OF OIL AND GREASE IN OIL SHALE RETORT WATERS\*

R. H. Sakaji, S. Onysko, J. P. Fox, C. G. Daughton,† D. Jenkins,†  
and R. E. Selleck†

### INTRODUCTION

Retort waters are coproduced with shale oil and separated from it by heat treatment and decantation. Because of the intimate contact between these two phases, some oil and grease, about 0.1 to 1 weight percent, may remain associated with the water phase. A knowledge of the quantity of this material is helpful in overcoming operational difficulties in treatment plants, for assessing environmental impacts of waste discharges, and for assessing the potential of recovering oil and grease. Oil and grease may coat adsorption media and stripping column packings and interfere with anaerobic digestion of sludges. If wastewaters containing oil and grease are discharged to receiving waters, surface film and shoreline deposits may result, and federal and state laws require their removal. If sufficient oil and grease is present in waters, it may be possible to reclaim it.

The purpose of this study, begun in June 1979, is to develop reliable methods to measure oil and grease in retort waters.

### ACCOMPLISHMENTS DURING 1979

We investigated the partition-gravimetric method<sup>1</sup> and Soxhlet extraction procedure<sup>2</sup> for the measurement of dissolved and suspended oil and grease in retort waters. Analytical problems were encountered with these methods including emulsion formation and sample loss during drying. Thus, work was initiated to develop a new method of analysis. This method depends on selective partitioning of hydrophobic materials onto a reverse-phase chromatographic column followed by elution with a small quantity of organic solvent. The eluate is further fractionated by passing it through a normal-phase column to remove polar material, and the eluate is weighed.

### Standard Analytical Methods

Oil and grease was initially determined by the partition-gravimetric analysis outlined in Standard Methods<sup>1</sup>. This method was modified due to analytical problems. The standard method involves acidification of the sample to pH 2, extraction in a separatory funnel with Freon, collection and evaporation of the solvent to dryness, and weighing the residue. Analytical problems encountered included the formation of a precipitate during acidification and severe emulsion formation during Freon extraction. The precipitate has been observed by others<sup>3</sup> and is hypothesized to be elemental sulfur and organic acids. At this point we realized that there were major flaws in the analysis.

Occluded water associated with the emulsion would add to the oil and grease determined gravimetrically. Variables affecting the formation of the emulsion were not understood and therefore could not be adequately controlled.

Studies were conducted in order to develop a method to eliminate emulsion formation. A variety of other organic solvents was tried, with and without acidification. We found that the use of methylene chloride without acidification produced the least emulsion. The organic phase could be separated from the water and the small quantity of emulsion. This extraction procedure was used in combination with other separation techniques to measure various fractions of the oil and grease.

Suspended oil and grease in retort waters was determined by the filtration technique described by Luthy.<sup>2</sup> The suspended oil is important because it represents the fraction of the oil and grease that can be removed from water by coagulation and flotation or other means. The dissolved fraction, on the other hand, is not affected by these techniques and can only be removed by more expensive solvent-extraction methods.

The sample in Luthy's method is passed through Whatman 40 filter paper coated with 100 ml of a 10-gm/l Celite filter aid solution. The filter paper is supported on a Büchner funnel by a muslin cloth. The material collected by the filter paper is dried with  $MgSO_4$  and the residue is Soxhlet-extracted for 4 hours with methylene chloride. The solvent is collected, evaporated, and the residue is dried and weighed to give suspended methylene chloride extractables (SMCE). This fraction, which includes the suspended and emulsified oil, can be removed by coagulation and flotation.

The filtrate from the Celite filtration is extracted by the partition-gravimetric method using methylene chloride. The organic phases, after five extractions, are pooled and taken to dryness. The residue is dried and weighed to give the dissolved methylene chloride extractables (DMCE). Total methylene chloride extractables (TMCE) are determined by adding DMCE and SMCE or:

$$TMCE = DMCE + SMCE.$$

We encountered considerable difficulty in the drying procedure for the organic extracts of the various fractions of oil and grease. The residues continually lost weight with drying time. The drying procedure was standardized by selecting a drying temperature and time (80°C, 15 min).

Table 1. Oil and grease determination on 150-ton and Occidental retort water using the partition-gravimetric and Soxhlet extraction method with methylene chloride and no pH adjustment (mg/l). (Drying temperature was 80°C for 15 min.)

	150-ton Retort Water	Occidental Retort Water <sup>a</sup>
Suspended methylene chloride extractables (Soxhlet Extraction)	354	285 ± 14
Dissolved methylene chloride extractables (Partition-Gravimetric)	1254	467 ± 42
Total methylene chloride extractables (By Addition)	1608	752 ± 77

<sup>a</sup>Average of three replicates.

The results of these studies, summarized in Table 1, indicate that the partition-gravimetric and Soxhlet extraction methods are reproducible when the samples are fractionated by Celite filtration. Table 1 presents the results of suspended and dissolved oil and grease measurements on Occidental and 150-ton retort waters. These are the first such measurements ever reported, and they show that suspended oil and grease represents less than half of the total oil and grease in these two retort waters. This is a significant finding because it suggests that oil and grease removal by coagulation and dissolved air flotation or other similar methods may not be effective in removing oil and grease from retort waters. It also indicates that oil and grease in retort waters is very different from that in conventional wastewaters for which the standard method of oil and grease was developed. Retort waters have high concentrations of carboxylic acids<sup>3</sup> which are extracted during the oil and grease test. These organic acids have different properties than oil and grease, are much less significant environmentally, and may not create a fouling problem in downstream treatment units. Therefore, the significance of the standard oil and grease test and the rationality of environmental regulations based on it must be questioned. This issue should be investigated in other studies.

#### Reverse-Phase Chromatographic Method of Oil and Grease Analysis

Development of an alternate method of oil and grease analysis is in progress. This new method is being developed to circumvent some of the problems noted with standard methods and to accelerate the analytical procedure. In the new method, oil and grease is determined by passing a known quantity of sample through a reverse-phase C-18 column (C-18 Sep Pak; Waters and Associates, Milford, Mass.). This column removes the nonpolar fraction (neutral hydrocarbons or the oil and grease fraction) and passes most of the polar fraction which is discarded. The

column is eluted with methylene chloride after mobile phase switch-over with methanol, and the eluate is dried, dissolved in a nonpolar solvent and further fractionated by passing it through a normal-phase Si column (Si Sep Pak). The Si column removes any residual polar material from the C-18 eluate and passes the nonpolar fraction which is collected, dried, and weighed. We have used this method to measure oil and grease in 150-ton retort water and have studied the elution efficiency, breakthrough characteristics, and suitable solvents for the Si column.

The aqueous sample can be filtered through Celite, and the Celite filtrate processed through the C-18 and Si columns. The result is an estimate of dissolved hydrophobic material (DHM). Total hydrophobic material (THM) is determined on unfiltered water. An estimate of suspended hydrophobic material, SHM, is obtained as

$$\text{SHM} = \text{THM} - \text{DHM}.$$

One advantage of this approach is that it saves time. The process of separatory funnel extraction, Soxhlet extractions, and sample drying requires about 60 hours for 20 samples. The values for THM would be analogous to those for TMCE, and similar relationships would apply to DMCE and DHM, and to SMCE and SHM.

Table 2 summarizes the results of oil and grease analyses by reverse-phase column separation only. The results indicate that the C-18 columns may give a facile indication of methylene chloride extractables. The value of THM and DHM bracket those for TMCE and DMCE (Table 1), respectively. The samples for DHM and THM analyses were dried at 60°C and 100°C. The results also demonstrate the influence of drying temperatures on the recovery of oil and grease.

A study of the efficiency of methylene chloride for eluting oil from the Si column was conducted. A 30-mg sample of Occidental shale

Table 2. Oil and grease determination on 150-ton retort water using reverse-phase column separation (C-18 Sep-Pak) and methylene chloride elution with no pH adjustment (mg/l).

Drying Temperature	Dissolved Hydrophobic Material	Total Hydrophobic Material	Suspended Hydrophobic Material (By Subtraction)
60°C	2000	2780	780
100°C	560	1300	720

oil was dissolved in 10 ml of methylene chloride and the solvent was passed through the Si column and collected. The column was then eluted with three fresh 10-ml aliquots of methylene chloride and each eluate was collected separately in a tared pan. The solvent was evaporated from the samples and the residue was weighed. The data show that a single elution with 10 ml of methylene chloride is sufficient to recover 97 percent of the total mass that could be eluted.

Breakthrough studies were performed to determine the sorptive capacity of the Si column for polar material in the Occidental shale oil. Oil samples of various weights were dissolved in methylene chloride and passed through the Si column. The organic effluent and the eluate from one rinsing with 10 ml of methylene chloride were combined and evaporated to dryness. The data indicate that 71 percent of the oil was recovered in the nonpolar fraction, i.e., the fraction that is passed by the Si Sep-Pak. Up to 130 mg of oil was applied to the column with no evidence of polar compound breakthrough.

The effect of an eluotropic series of organic solvents on the recovery of oil and grease from the Si column was investigated. As expected, the partitioning between polar and nonpolar fractions was dependent on the organic solvent used. The fraction of hydrophobic material recovered from the oil decreased with decreasing solvent polarity, i.e., methylene chloride, benzene, Freon, hexane, and petroleum ether.

The initial results of these studies indicate that liquid chromatographic columns can be

used in sample preparation for oil and grease analysis.

#### PLANNED ACTIVITIES FOR 1980

Work will continue on the development and application of the reverse-phase chromatographic method of oil and grease analysis. Alternatives to gravimetric determination, including high performance liquid chromatography with infrared detection, will be evaluated. The new method will be used to analyze oil and grease in several retort waters.

#### FOOTNOTES AND REFERENCES

\*This program is funded by the Department of Energy's Division of Environmental Control Technology.

†University of California, Berkeley, CA.

1. Standard Methods for the Examination of Water and Wastewater, Am. Pub. Health Ass., Am. Water Works Assoc., Water Poll. Control Fed., 14th Ed (1975).
2. R. G. Luthy, Air Flotation of Oil Wastewater with Organic Coagulants, Ph.D. Dissertation, University of California, Berkeley, (1976).
3. J. P. Fox, D. S. Farrier, and R. E. Poulson, "Chemical Characterization and Analytical Considerations for an In Situ Oil Shale Process Water," Laramie Energy Technology Center Report of Investigation, LETC/RI-78/7 (Nov 1978).

## SPENT SHALE AS A CONTROL TECHNOLOGY FOR OIL SHALE RETORT WATER\*

*J. P. Fox, D. E. Jackson, and R. H. Sakaji*

### INTRODUCTION

Production of synthetic crude from oil shale generates from 0.10 to 22 barrels of water and 25 to 100 pounds of solid waste per barrel of oil, depending on the specific process used. The water, referred to as retort water, originates from combustion, mineral dehydration, input steam, and from groundwater intrusion (in-situ processes only). The organic content of retort water may reach three percent while inorganic concentrations of as much as five percent are typical. The principal organic constituents are carboxylic acids and nitrogen-containing organic compounds, and the principal inorganic components are ammonium, sodium, and bicarbonate, with lesser but significant amounts of thio-sulfate, chloride, sulfate, and carbonate. The solid waste, referred to as spent shale, is a porous material that contains weight percent concentrations of sodium, calcium, magnesium, iron, potassium, and inorganic carbon. The spent shale and retort water pose a significant disposal problem for the oil shale industry.

The retort water would be a valuable resource for the arid regions in which oil shale deposits are located if effective and economical treatment methods can be found. However, past attempts to adapt conventional treatment technologies, such as anaerobic fermentation, activated sludge, and carbon adsorption to remove

organics and inorganics from retort waters indicate that these methods have serious technical and/or economic limitations. However, an observation made at LBL during the course of other work suggests that spent shale might be used to economically reduce some organic and inorganic components of retort water.

The purpose of this program, initiated in June 1978, is to determine whether spent shale can be effectively used in the treatment of in-situ retort waters. In-situ oil shale retorting processes produce large volumes of water compared to surface processes, and they leave large cavities of spent shale underground. In modified in-situ processing, which is currently under development by industry and by the Department of Energy, 20 to 40 percent of the in-place shale is mined and processed in surface retorts.

This program is investigating two potential uses of spent shale for treatment of in-situ retort waters (Fig. 1). In the first application, the abandoned in-situ retort would be directly used in a treatment system. Water generated in one retort would be circulated through an adjacent spent retort to reduce contaminants in the water and to cool the in-situ spent retort in preparation for grouting. In the second application, spent shale produced in surface retorts would be used in packed columns similar to granular activated carbon.

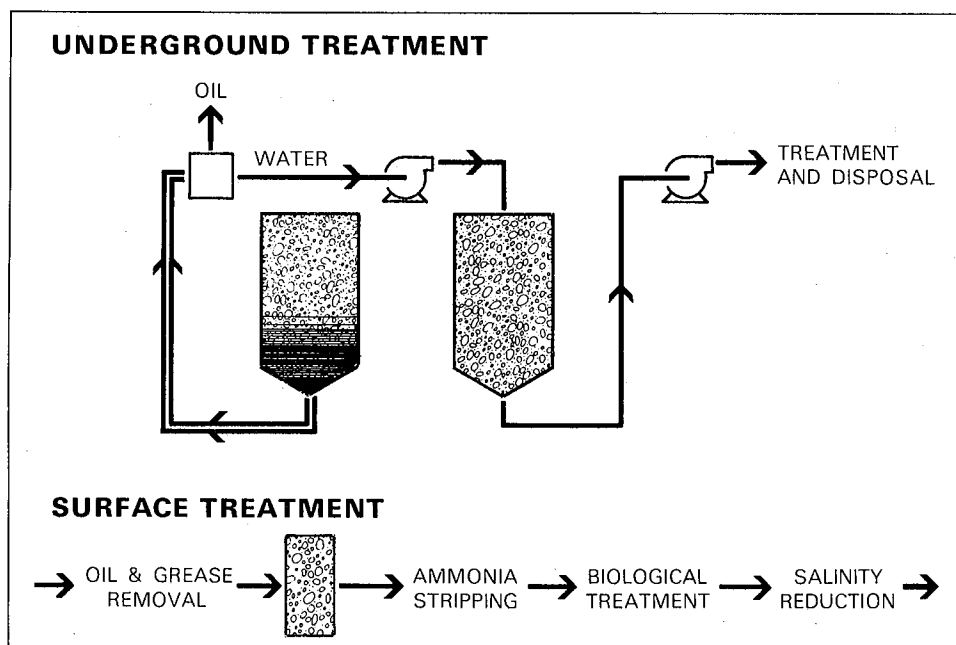


Fig. 1. Potential uses of spent shale in the treatment of retort waters.

(XBL 805-1080)

The exhausted spent shale would be disposed with other solid wastes in an on-site solid waste disposal facility.

The effect of spent shale treatment on organic carbon, inorganic carbon, electrical conductivity, and pH is being investigated in batch and column studies. The results of these studies will be used to design a complete treatment system that includes spent shale treatment.

Batch studies will be conducted to determine the adsorptive characteristics of various spent shale/retort water combinations. Equilibrium conditions will be determined for all combinations, and adsorption isotherms will be developed for the most favorable combinations. Continuous-flow column studies will be used to determine optimum operating conditions for favorable spent shale/retort water combinations. When the spent shale columns are optimized, they will be interfaced with a system that includes oil and grease removal, ammonia stripping, and biological treatment.<sup>1</sup>

#### ACCOMPLISHMENTS DURING 1979

We completed equilibrium batch studies of a number of retort water/spent shale combinations. A gas chromatography fingerprinting technique was developed and used to determine the organic components removed by the spent shale. Surface areas and chemical compositions were determined for several spent shales. Column studies are in progress to investigate breakthrough characteristics and to obtain design parameters. This work indicates that spent shales are effective in removing color, odor, inorganic carbon, and certain classes of organic compounds and in elevating the pH of retort waters. Spent shale treatment removes the methylene chloride extractable components at pH 2 and 11.

#### Surface Area of Spent Shales

The surface area of spent shales is important in assessing their adsorptive properties. Residual carbon and internal pores contribute to the surface area of spent shales. When kerogen is removed by pyrolysis, it leaves behind a network of pores. Additionally, the pyrolysis of kerogen produces not only oil and gas, but also a char or residual carbon which is left on the surface of the spent shale. Some processes burn this char for process heat while others leave it on the spent shale (TOSCO II, Lurgi).

The surface area of six spent shales were measured using a BET apparatus. These values, which ranged from 2.1 (L-1) to 10.2 (TOSCO II)  $m^2/gm$  for 60 to 230 mesh particles, were an order of magnitude higher than those calculated for perfectly round spheres of equivalent diameter. This means that interstitial pores contribute to the surface area. The effect of retorting temperature on surface area is shown in Fig. 2 which indicates that surface area decreases as the retorting temperature increases. This trend is probably due to residual carbon. The majority of the residual carbon was burned

off of all of these spent shales except TOSCO II and Lurgi. The L-1, S-14, S-55, and Paraho spent shales were produced by combustion retorting, and residual carbon was burned to supply process heat. The decrease in surface area at higher temperatures may also be partly due to high-temperature mineral reactions that fuse some of the kerogen pores.

#### Batch Studies

The effect of spent shale treatment on dissolved organic and inorganic carbon, electrical conductivity, and pH in several retort waters was evaluated in equilibrium batch experiments. The results of these experiments are summarized in Table 1. The specific adsorption ranged from 0.07 to 1.6 mg organic carbon per g of shale. TOSCO II is the best adsorbent for organic carbon in the retort waters investigated, followed by Paraho spent shale. The remaining four shales, Lurgi, L-1, S-14, and S-55, are as much as an order of magnitude poorer in organic adsorptive capacity than the TOSCO II and Paraho samples. The percent reduction in organic carbon ranged from near zero to 66 percent for TOSCO II shale and was found to decrease for spent shales retorted at high temperatures (Fig. 3). This effect is due to the decrease in surface area of spent shales at higher temperatures (Fig. 2). There was a positive correlation between surface area and adsorption for all spent shales except Paraho. Paraho spent shale, with a relatively small specific surface area, is one of the best organic adsorbents. This suggests that the chemical nature of the spent shale surfaces varies significantly.

Spent shale may also remove up to 98 percent of the dissolved inorganic carbon from retort

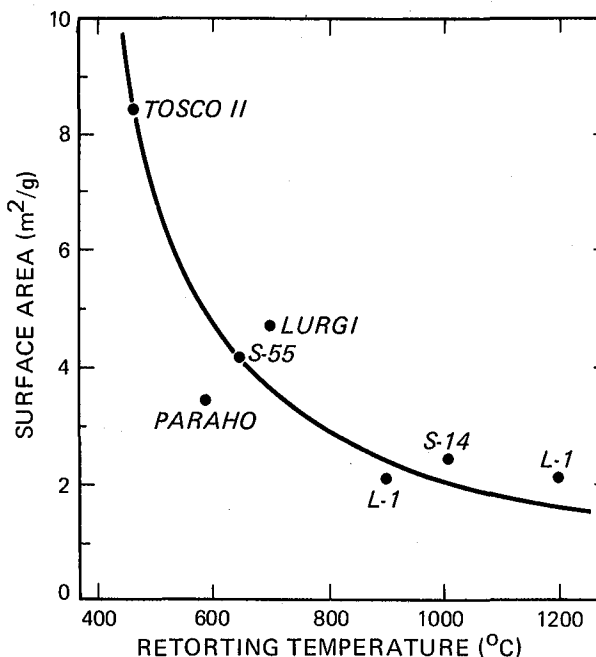


Fig. 2. The effect of retorting temperature on surface area of spent shales. (XBL 801-7734)

Table 1. Percent change in organic carbon, inorganic carbon, electric conductivity, and pH of retort water after 120 hours of contact with spent shale in batch experiments using 50 g shale and 50 ml retort water.

Parameters Measured in Retort Water	P E R C E N T C H A N G E <sup>a</sup>						
	Surface Spent Shales			In-Situ Spent Shales			
	Paraho	Lurgi	TOSCO II	L-1	S-14	S-55	
Omega-9	Organic Carbon	-49	NS <sup>b</sup>	---	-18	NS	-12
	Inorganic Carbon	-91	-98	---	-98	-98	-98
	Electrical Conductivity	-28	-6	---	-20	---	-31
	pH	+116	+119	---	+131	---	+136
150-ton	Organic Carbon	-24	NS	-48	NS	NS	-7
	Inorganic Carbon	-89	-97	-60	-98	-97	-98
	Electrical Conductivity	-40	---	NS	-36	---	-54
	pH	+111	+110	NS	+116	---	+119
L-2 Retort Water	Organic Carbon	-51	-17	-66	-13	NS	-18
	Inorganic Carbon	-89	-96	-47	-97	-98	-98
	Electrical Conductivity	-54	---	---	-60	---	-60
	pH	+117	+109	---	+126	---	+123
L-2 Gas Condensate	Organic Carbon	-45	-21	-27	-11	NS	NS
	Inorganic Carbon	-91	-93	-65	-97	-99	-97
	Electrical Conductivity	-49	---	---	-54	---	-75
	pH	+111	+113	---	+121	---	+127

<sup>a</sup>A negative value indicates that the concentration was reduced by the indicated amount while a positive value indicates an increase in the retort water.

<sup>b</sup>No statistically significant change.

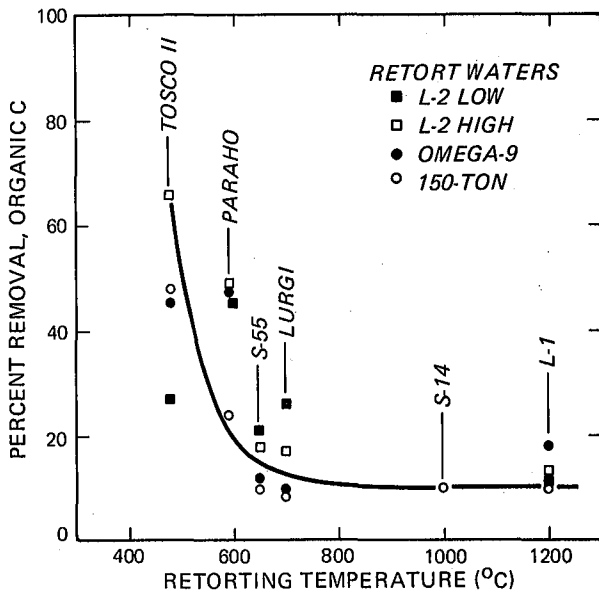


Fig. 3. The effect of retorting temperature on the percent removal of organic carbon from retort waters. (XBL 801-7731)

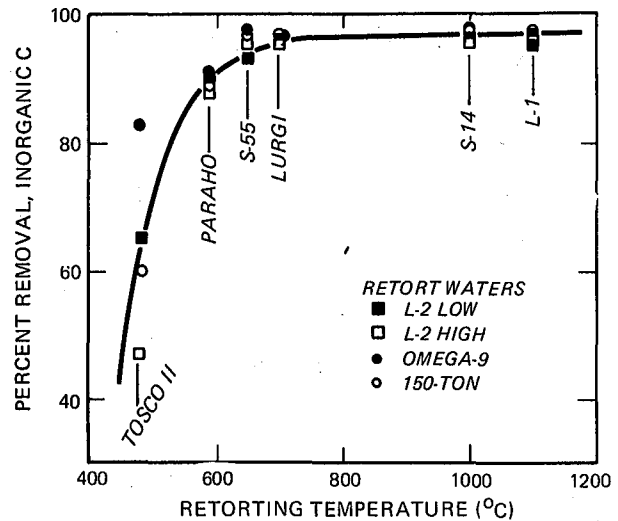
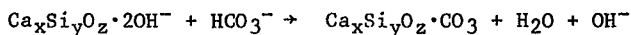
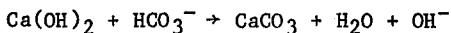


Fig. 4. The effect of retorting temperature on the percent removal of inorganic carbon from retort waters. (XBL 801-7732)

water samples. The percent reduction increases approximately linearly up to 700°C and levels off at higher temperatures at 98 percent (Fig. 4). Spent shales with the highest organic adsorptive capacity appear to be least effective in removing inorganic carbon. Thus, Paraho and TOSCO II spent shales effect the least inorganic carbon reduction and the remaining spent shales, Lurgi, L-1, S-14, and S-55, are the most effective in this respect. The reason for this inverse relationship is unknown but is probably related to different removal mechanisms. Inorganic carbon may be removed by an ion exchange process, while organic removal may be more dependent on the lipophilic character and organic content of the spent shale.

The reduction in carbonate levels is accompanied by a decrease in electrical conductivity and an elevation in pH. The decrease in conductivity results from the removal of dissolved inorganic carbon (i.e.,  $\text{CO}_3$ ,  $\text{HCO}_3$ ) from the water.

Contact of retort water with spent shale elevates the pH from initial levels of 8 to 9 to final values of 10 to 11. The simultaneous decrease in dissolved inorganic carbon and increase in pH is hypothesized to result from chemical reactions between the carbonate species in the retort water and hydroxides formed from the hydration of  $\text{CaO}$  and other metal oxides present in the spent shale. This type of reaction can be summarized by the following equations:



#### Column Studies

A single column study was conducted using Paraho spent shale and Geokinetics retort water. The column influent and effluent were characterized spectrophotometrically and by gas chromatography.

The characteristic color and odor of retort water was almost completely removed by the spent shale column. This may be related to the removal of organic components responsible for the color and odor of these waters.

This study indicated that spent shale adsorption may not be effective for removing gross organics (dissolved organic carbon) because column breakthrough occurs before two pore volumes can be treated. This means that operation and maintenance costs of a spent shale column may be excessive. However, spent shale columns may be useful for removing specific organic compounds or classes of organic compounds or for reducing color and odor.

The nature of the specific organic compounds removed by columns of spent shale was investigated spectrophotometrically and by gas chromatography. The methylene chloride extractable components in retort water are reduced during spent shale treatment. Figure 5 shows the complete removal of basic extractables while Fig. 6 shows only one major peak remaining in the acid extract. This not only demonstrates the effectiveness of spent shale as an adsorbent for at least some of the organic contaminants in retort water, but also indicates that the organic carbon that is not adsorbed is the most polar and soluble fraction. This is predictable since non-specific adsorption is inversely related to solubility. Thus, we expect that those compounds which are least soluble in water will be removed

most easily from aqueous solution by adsorption onto spent shale.

#### Application to Treatment of Retort Waters

These studies indicate that spent shale may be used to reduce the organic and inorganic carbon, electrical conductivity, color, and odor, and to elevate the pH of retort waters. These characteristics have important and immediate applications to the treatment of retort water. Conventionally, retort water would be treated using a system similar to that shown in Fig. 7a. Oil and grease removal would be followed by steam stripping to remove ammonia, biological treatment to reduce soluble organics, and a desalination step to remove dissolved salts. The results of this work suggest that a system similar to that shown in Fig. 7b is feasible. A packed bed of spent shale could be placed ahead of the ammonia removal step. The increase in pH achieved in the spent shale column would convert ammonium to ammonia which could be removed from the water by air stripping instead of steam stripping, resulting in a cost saving. Air stripping may be cheaper than steam stripping due to reduced energy requirements. The simultaneous reduction of electrical con-

ductivity and dissolved organic and inorganic carbon through the spent shale column would decrease the load of these constituents on subsequent treatment steps, allowing the use of smaller units. The removal of toxic organic components may improve the operation of the biological treatment system. These features of spent shale columns could result in considerable cost savings over conventional treatment systems. Additional work, however, is required to study breakthrough characteristics of spent shale columns and to develop design parameters.

#### PLANNED ACTIVITIES FOR 1980

Batch studies will be conducted on additional spent shale/retort water combinations, and column studies will be conducted using the most promising spent shales. Other unit processes, including oil and grease removal, ammonia stripping, and a biological treatment process will be selected for use with spent shale columns. Batch and continuous-flow studies will be conducted on these other processes and on a complete treatment system.

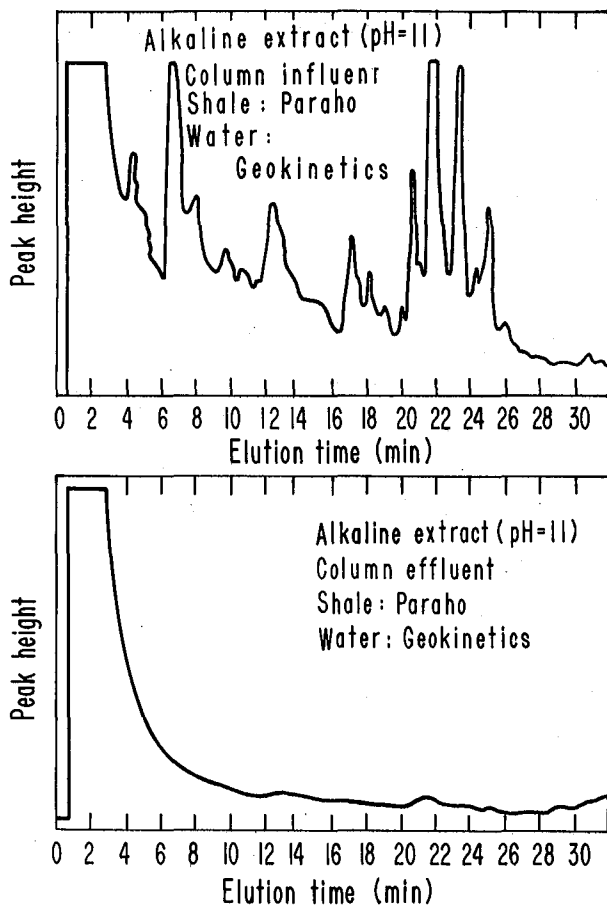


Fig. 5. Gas chromatography fingerprints of alkaline extracts of Paraho/Geokinetics column influent and effluent. (XBL 805-1046)

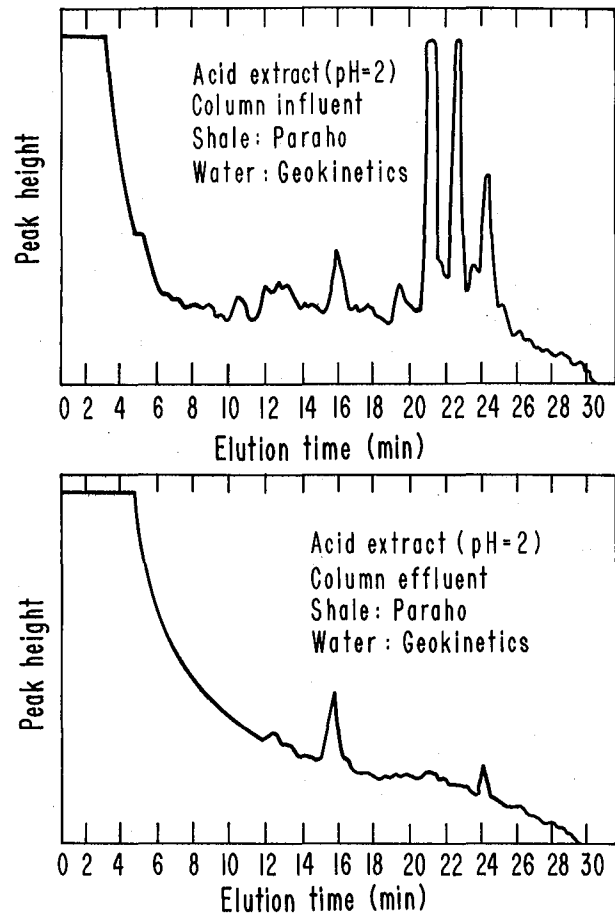


Fig. 6. Gas chromatography fingerprints of acid extracts of Paraho/Geokinetics column influent and effluent. (XBL 805-1045)

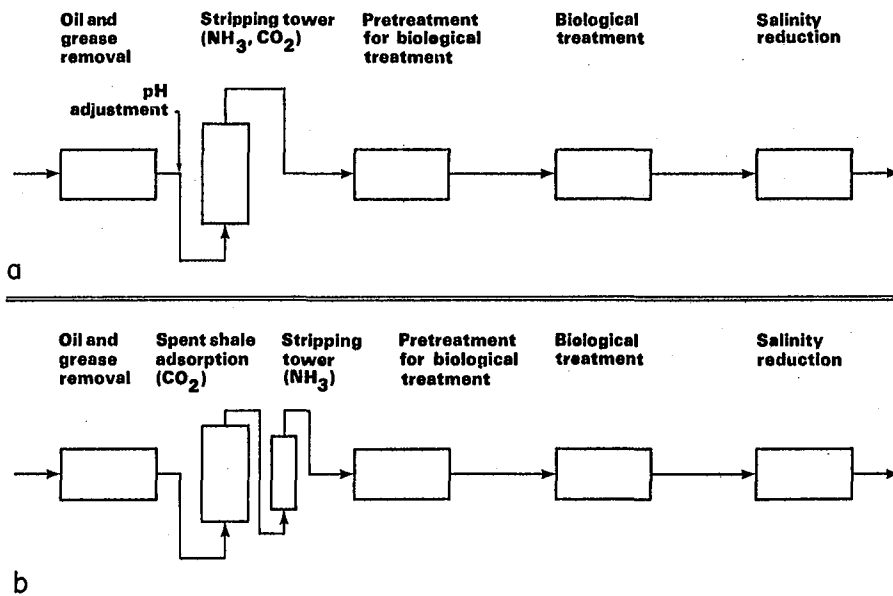
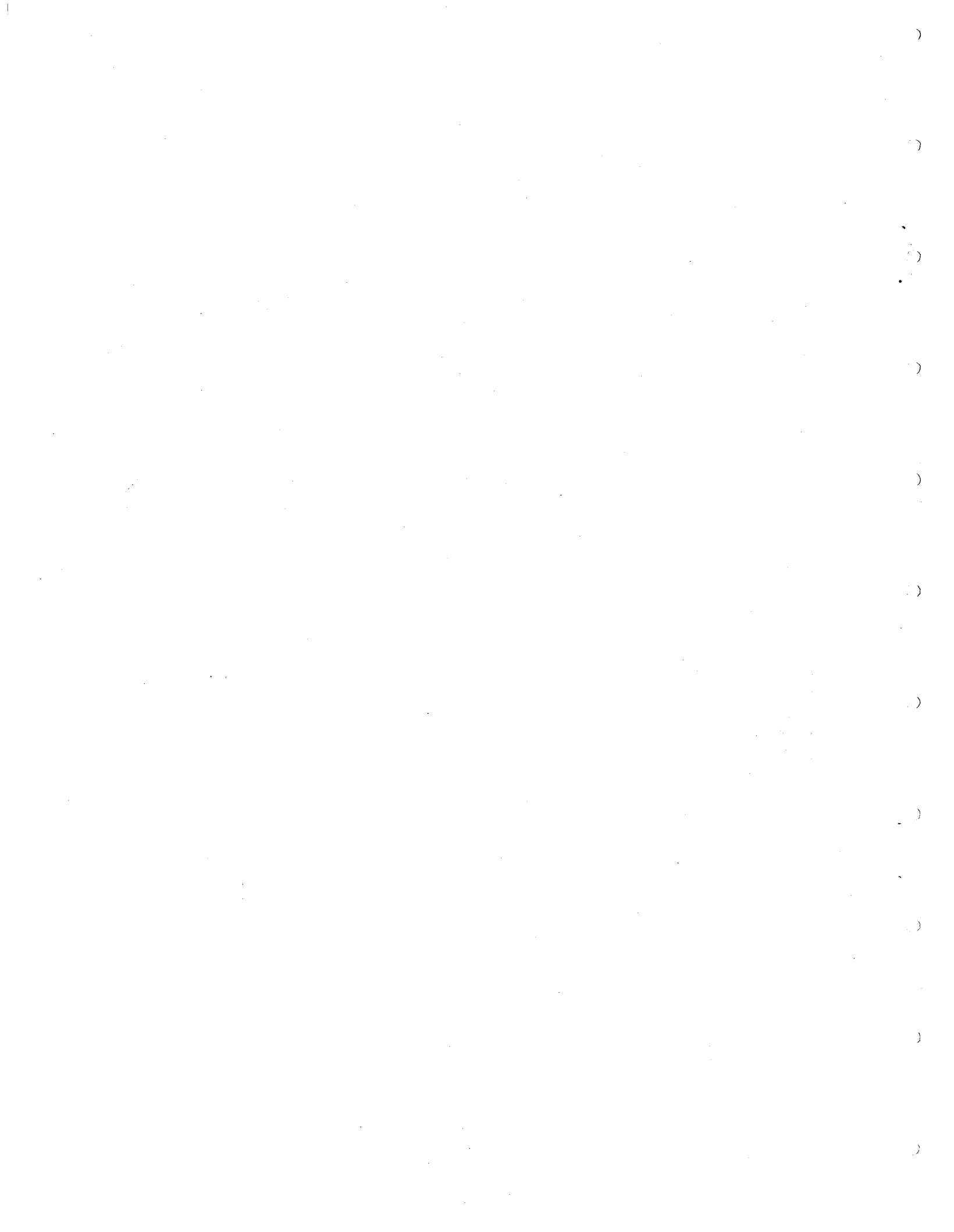


Fig. 7. Proposed treatment system for upgrading retort water (a) using conventional technology; (b) using columns of spent shale. (XBL 796-1762)

#### FOOTNOTE AND REFERENCES

\*This program is funded by the Department of Energy's Division of Environmental Control Technology.

1. R. H. Sakaji, S. Onysko, J. P. Fox, D. Jenkins, R. E. Selleck, and C. G. Daughton, "Treatment of Wastewaters from In-Situ Retorting of Oil Shale," Energy and Environment Division Annual Report 1979. Lawrence Berkeley Laboratory Report, LBL-10463 (1980).



# COMBUSTION RESEARCH

## INTRODUCTION

Approximately 95% of the energy consumed in the United States is released through combustion processes. While this fraction will decrease with the continued development of nuclear, solar, and other technologies, combustion processes will dominate energy utilization for the remainder of this century and probably well into the next. The art of combustion has been highly developed during the past hundred years. A variety of combustion devices that convert chemical energy into thermal and mechanical energy efficiently and economically have evolved through trial-and-error and empirical design. Gasoline engines, diesel engines, gas turbines, and large steam turbine generators for electric power production are the primary examples.

The desire to employ new fuels, particularly those derived from coal, heavy crude oil, shale, and biomass in these devices poses a dilemma. Much of the scientific understanding of combustion processes required for predictive analysis and design is lacking. Urgency for the introduction of these fuels prevents a repetition of the hundred-year empirical development approach. The problem is compounded by the need to constrain the emission of noxious substances.

Combustion research at the Lawrence Berkeley Laboratory focuses on the study of chemical and physical processes which are important in utilizing new fuels while limiting pollutant formation. A second component of the combustion research is concerned with reduction of fire hazards associated with energy generation and conservation technologies.

Principal program areas include the interaction of fluid-mechanical turbulence and combustion, pollutant formation and destruction processes, physical and chemical diagnostic techniques for combustion research, theoretical and computational modeling of combustion processes, combustion processes in engines, flame propagation, and fire safety.

The research team is composed of research scientists at the Lawrence Berkeley Laboratory, faculty and students of the Departments of Mechanical and Civil Engineering at the University of California, visitors from throughout the United States and the world, and a supporting technical, clerical, and administrative staff.

A major component of the research program is the training of combustion scientists and engineers at all levels. Laboratory facilities are located at the Lawrence Berkeley Laboratory, on the campus of the University of California, and at the Richmond Field Station. The research was sponsored by the Department of Energy through the Divisions of Energy Technology, Environment, and the Office of Energy Research; also by the National Science Foundation, the National Aeronautics and Space Administration, the Office of Army Research, the Air Force Office of Scientific Research, the National Bureau of Standards, the California Air Resources Board, and Sandia Laboratory.

## ENGINE COMBUSTION AND IGNITION STUDIES

### ADVANCED OPTICAL MEASUREMENTS IN AUTOMOBILE ENGINES\*

*J. W. Daily, D. S. Pechter, and J. T. Metcalf*

To understand the processes that occur in a piston engine, the flow characteristics within the cylinder must be known. This flow information is best obtained with devices which do not physically intrude into the gas flow. Optical methods can be used to this end if access is possible. The square piston engine, developed in our laboratory, provides optical access to the entire cylinder. In addition to conventional flow visualization methods, we are developing a Laser Doppler Anemometer (LDA) system to measure velocity, and a laser absorption system to measure methane concentrations in the engine.

The LDA system is of the conventional two-beam real fringe interferometer design. The fringe system is given a velocity bias by frequency shifting. Light is collected in the forward scattering direction and processed by counter electronics.

The laser absorption system was built based on the resonant methane absorption of the HeNe 3.39 micron laser line. Using a high-speed infra-

red photodetector, the system has a time resolution of better than 100 nanoseconds. Methane detectability should be below one percent. Applied to the square piston machine, this *in situ* measurement system promises spatial and temporal resolution of cylinder methane concentration that is beyond the capability of a gas chromatograph.

The experimental arrangement includes a HeNe laser with an output of approximately 13 mW at 3.39 microns. A dichroic mirror is used to isolate 3.39 microns from the companion laser line at 1.15 microns. The filtered beam is then reflected through quartz sidewalls on the square piston machine and onto the photodetector. Photographing oscilloscopes are presently used for data collection. Direct computer data collection is planned. Calibration studies are in progress.

In addition to the experimental work, computer studies modeled the temperature dependence of the methane absorption coefficient. For temperatures up to 1500K, the decrease of absorptivity with temperature can be accounted for by depopulation of the absorbing rotational state. At higher temperatures a "hot" band absorption becomes important. This absorptivity temperature was modeled in the low temperature range.

---

\*This work was supported by the Energy Technology Division of the U.S. Department of Energy.

### HEAT TRANSFER WITH COMBUSTION\*

*R. Greif, H. Heperkan, J. Naccache, D. Huang, and W. Leung*

#### INTRODUCTION

The research has focused on the determination of the unsteady heat transfer during variable gas temperatures and pressures. In respect to internal combustion engines, the transient, variable volume (moving surface), variable pressure aspects of compression-expansion processes result in complex phenomena that have proven to be difficult to appraise and predict. One particular objective of this program has been the experimental determination of the wall heat flux and comparison of the data with theoretical predictions. Another consideration is the utilization of the results to elucidate fundamental aspects of combustion phenomena. Previously, measurements were carried out in a single-pulse, compression-expansion apparatus that was built by Oppenheim et al.<sup>1</sup> This system was built in order to study reciprocating engine processes under well-controlled laboratory conditions which simulate the operation of a spark-ignition engine. Completed studies in the apparatus have included the experimental and theoretical determination of the unsteady wall heat transfer in nonreacting gases during piston compression.<sup>2,3</sup> The present effort has extended the work to include heat transfer to reacting gases.

ACCOMPLISHMENTS DURING 1979

Measurements were carried out to determine the heat transfer during combustion. In view of the complex nature of piston compression process as noted above, it was decided to first carry out measurements during combustion in a shock tube in the end-wall region behind the reflected shock wave. This is desirable because during the pre-ignition period the free steam temperature and

pressure are constant, and resulting phenomena during this period are well understood. When ignition occurs, the effects of combustion are then clearly displayed and this provides a useful basis for appraising the phenomena.

Tests were carried out in a 1-1/2 x 1-3/4 inch cross-section tube where a mixture of  $2H_2 + O_2 + 27A$  was subjected to a shock wave which propagated at a Mach number of 2.39 and reflected off the end wall. The temperature of the end wall of the shock tube was measured as a function of time by using a thin-film resistance thermometer. The resistance thermometer consisted of a thin platinum film on an insulated backing and was mounted flush with the wall to avoid disturbing the flow; it was connected as the active element in a dc bridge. The increase in wall temperature (due to shock wave heating) then caused a change in resistance of the platinum film which caused an unbalance in the bridge. The determination of the resistance versus time variation then yielded the desired wall temperature variation.

Based on the above measurements, the temporal variation of the wall heat flux was obtained. Specifically, the result was based on a solution of the conduction equation in the solid wall (insulated backing) subject to a variable surface temperature, and the heat flux was expressed as a Duhamel integral in terms of the variable surface temperature and the wall properties. These results for the heat flux,  $q_{w,s}$ , are shown in Fig. 1 and are designated as the experimental results.

An alternative and independent approach for the determination of the wall heat flux is based on a solution of the conservation equations in the gas behind the reflected shock wave as applied to the thin boundary layer near the wall. Neglecting viscous dissipation and taking the pressure to be uniform but time dependent yields the appropriate equations of continuity and energy. These equations have been solved numerically to obtain a heat flux based on the gas properties,  $q_{w,g}$ , designated as the calculated results in Fig. 1. For completeness, it is noted that the temporal variation of the pressure and the temperature were calculated based on the strong ignition condition (cf. Oppenheim et al.<sup>4</sup>, Cohen<sup>5</sup>).

From Fig. 1 it is seen that the wall heat flux continues to decrease during the pre-ignition period which is consistent with the constant "free stream" temperature and the increasing thermal penetration depth. When combustion is initiated, the gas temperature increases and this results in an increase in the wall heat flux. The location and propagation of the combustion zone towards the cold end wall is, however, unknown. Therefore, to calculate the heat flux,  $q_{w,g}$ , during combustion, the location of this zone must be specified. One preliminary specification of the combustion zone being ignited at 20  $\mu\text{sec}$  and then moving linearly with time towards the end wall and then halting (at a location 0.006 cm away from the wall) resulted in the calculated heat flux  $q_{w,g}$ , shown in Fig. 1. The agreement between the two heat fluxes is good.

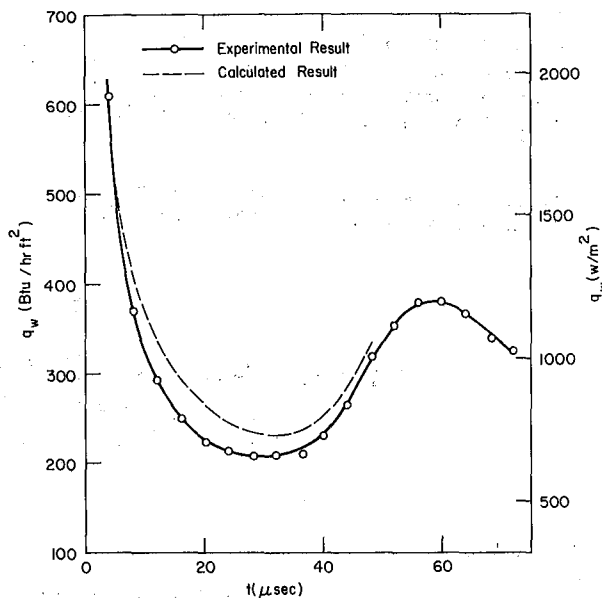


Fig. 1. Heat flux variation (calculated result is based on ignition at 20  $\mu\text{sec}$ ).

(XBL 801-106)

#### PLANNED ACTIVITIES FOR 1980

A more complete formulation and solution of the basic conservation equations will be made which will include the effects of combustion. Theoretical results will be obtained from both numerical and integral methods. Detailed attention will be given to the propagation of the combustion zone. Additional measurements will be made in the shock tube to validate the results. It is also planned to carry out experiments and theoretical studies in a constant volume combustion chamber as a prelude to studying the more general phenomena relative to combustion in the single-pulse engine.

#### FOOTNOTE AND REFERENCES

\*This work was supported by the Energy Technology Division of the U.S. Department of Energy.

1. A. K. Oppenheim, R. K. Cheng, K. Teichman, O. I. Smith, R. F. Sawyer, K. Hom, and H. E. Stewart, "A cinematographic study of combustion in an enclosure fitted with a reciprocating piston," in Stratified Charge Engines, Institution of Mechanical Engineers Conference Publications 1976-11, ISBN 0 85298 355 7, 127-135, 1976.
2. M. Nikanjam and R. Greif, "Heat transfer during piston compression," Transactions of the ASME, J. of Heat Transfer, 100, 527, 1978 and Lawrence Berkeley Laboratory Report #LBL-7338.

3. R. Greif, R. Namba, and M. Nikanjam, "Heat transfer during piston compression including side wall and convection effects," International J. of Heat and Mass Transfer, 22, 901-908, 1979.
4. A. K. Oppenheim, L. M. Cohen, J. M. Short, R. K. Cheng and K. Hom, "Dynamics of the exothermic process in combustion," Fifteenth Symposium (International) on Combustion, 1503-1515, 1974.
5. L. M. Cohen, personal communication.

## EXPERIMENTAL FACILITY FOR ENGINE COMBUSTION STUDIES\*

*R. F. Sawyer, A. K. Oppenheim, and H. Stewart*

### INTRODUCTION

Studies of lean combustion processes important to engine combustion have been conducted in a single-pulse compression-expansion apparatus. This unique facility, which incorporates a square piston and two glass walls, permits unobstructed observation of the entire chamber where combustion takes place under conditions similar to those existing in reciprocating piston engines. This apparatus has been successfully used for the investigation of piston-induced flow fields, valve-generated turbulence, ignition processes, flame structure and propagation, bulk and wall quenching, and time-resolved heat transfer phenomena. In the initial version of the apparatus, the piston is pneumatically driven and hydraulically controlled. The piston trajectory does not fully reproduce that of a reciprocating engine, especially with regards to piston dwell

at top dead center. To extend the capability of this experimental facility, an improved version has been designed and constructed.

### ACCOMPLISHMENTS DURING 1979

On the basis of experience gained with the first version, an improved version of the machine has been designed and constructed. Among the improvements and advantages are that: 1) the piston is driven by a crank-shaft and its motion is controlled by a fast-acting clutch-brake mechanism permitting 1, 2, 3, or 4 stroke operation (Fig. 1), 2) the cross-section of the combustion chamber is larger (85 x 85 mm), which corresponds in area to the standard CFR single cylinder laboratory test engine, and 3) the head is fitted with conventionally operated overhead intake and exhaust valves (Fig. 2). The heavier construction of the new machine allows

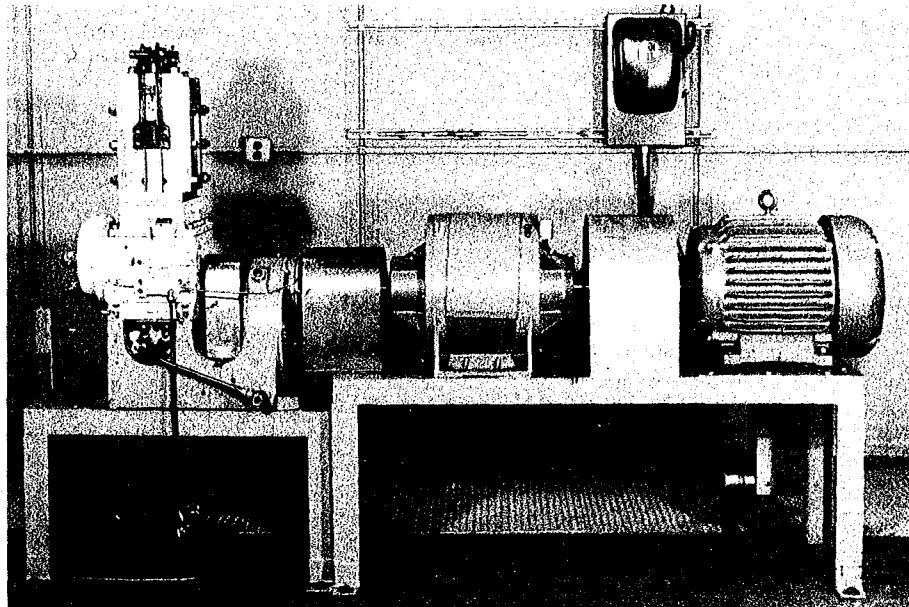


Fig. 1. Mark II version of the compression-expansion apparatus for the study of engine combustion processes--from right to left: drive motor, fly wheel, fast-acting clutch-brake, reciprocating drive mechanism and test section.

(XBB 790-16306)

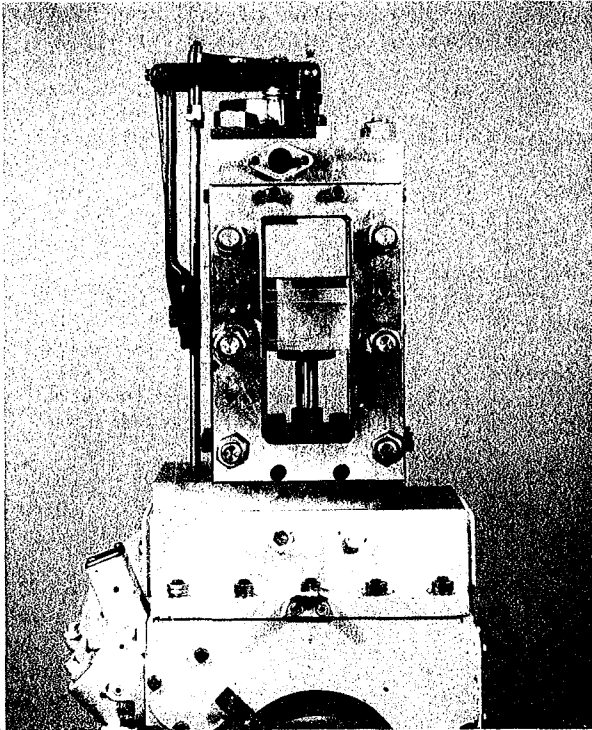


Fig. 2. Square piston test section showing piston, optical side wall access and overhead valves. (XBB 790-16307)

studies such as compression ratios typical of diesel engine combustion. Uncertainties in funding allowed construction of the mechanical apparatus and test section only.

#### PLANNED ACTIVITIES FOR 1980

The second version of the compression-expansion machine will be completed during 1980, following fabrication of the automatic controller for the apparatus. An initial instrumentation package will be designed and, depending upon funding availability, procurement will be initiated.

#### FOOTNOTE:

\*This work was supported by the Energy Technology Division of the U.S. Department of Energy.

## IGNITION STUDIES\*

*A. K. Oppenheim, F. C. Hurlbut, and F. Robben*

### INTRODUCTION

This project is an outgrowth of our investigations of lean combustion in engines conducted in our laboratory by the use of the single pulse machine.<sup>1</sup> Preliminary results we obtained were reported last year. It was demonstrated then that jets of plasma have many properties in common with those generated by combustion, and experimental evidence was provided for the two prime advantages offered by jet ignition, namely:

1. As a consequence of their inherent penetration depth, plasma jets are capable of initiating combustion in the middle of the charge, away from the walls, thus eliminating all the adverse effects due to their proximity--a significant factor in the enhancement of ignition.

2. In contrast to the initially very low burning rate of a typically laminar flame kernel initiated by a conventional spark discharge, plasma jets generate a turbulent cloud where after a certain induction time, multi-point ignition takes place and combustion proceeds at a relatively high rate--a consequence of the relatively large surface area of the convoluted flame front thus created.

It then became clear that:

a) since clean and efficient engines must operate at spatially uniform temperature,

their realization depends crucially on the availability of well-distributed multi-point ignition sources which can be best provided by jet ignition, and

b) since jet ignition depends on the exploitation of free radicals, their generation and the role they play must be established by a fundamental study of ignition in gaseous hydrocarbon-air mixtures.

Accordingly our program of research was channeled into four phases of study:

1. Performance Evaluation
2. Diagnostics
3. Thermochemistry
4. Fluid Mechanics

The first is concerned primarily with experimental and analytical studies of actual igniters. The second is concerned with the achievement of a capability to measure local state and composition in the jet prior to and throughout the process of ignition. The third deals with the development of a comprehensive theory of ignition to provide a rational basis for our study. The fourth deals with the investigation of the fluid-mechanic properties of turbulent jets and their mixing in the presence of exothermic reactions typifying the operation of jet igniters.

Progress on each of these phases is reported in the next section.

#### ACCOMPLISHMENTS DURING 1979

##### Performance Evaluation

Rational basis has been established for the evaluation of the prominent fluid mechanical features of jet ignition. The methodology thus developed was applied to test a set of simple plasma jet igniters, that is those devoid of any means to modify the plasma medium or its energy content.<sup>1</sup>

Experimental tests of the igniters were performed in a cylindrical, stainless steel bomb, fit-

ted with optical glass windows of schlieren quality, providing an unobstructed view of the cylindrical cavity. The total volume of the bomb was 530.6 cm<sup>3</sup>, and the port diameter was 8.58 cm. On the sides, the bomb was equipped with four instrument plugs. One provided a fitting for the igniter, two were used for filling and purging, and the fourth served as holder for a pressure transducer. The transducer signal, processed through a charge amplifier, was displayed on the screen of a storage oscilloscope. Concurrently with pressure records, schlieren movies were obtained at a speed of 5500 frames per second. The experiments were monitored electronically so that when the camera was brought up to speed it provided a signal for triggering the discharge in the plasma cavity. At the same time, the oscilloscope sweep was triggered and

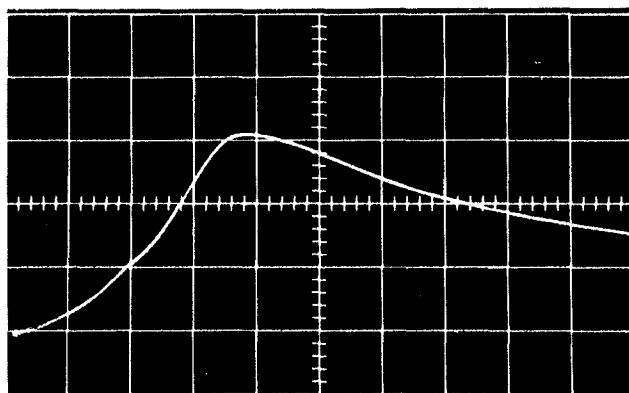
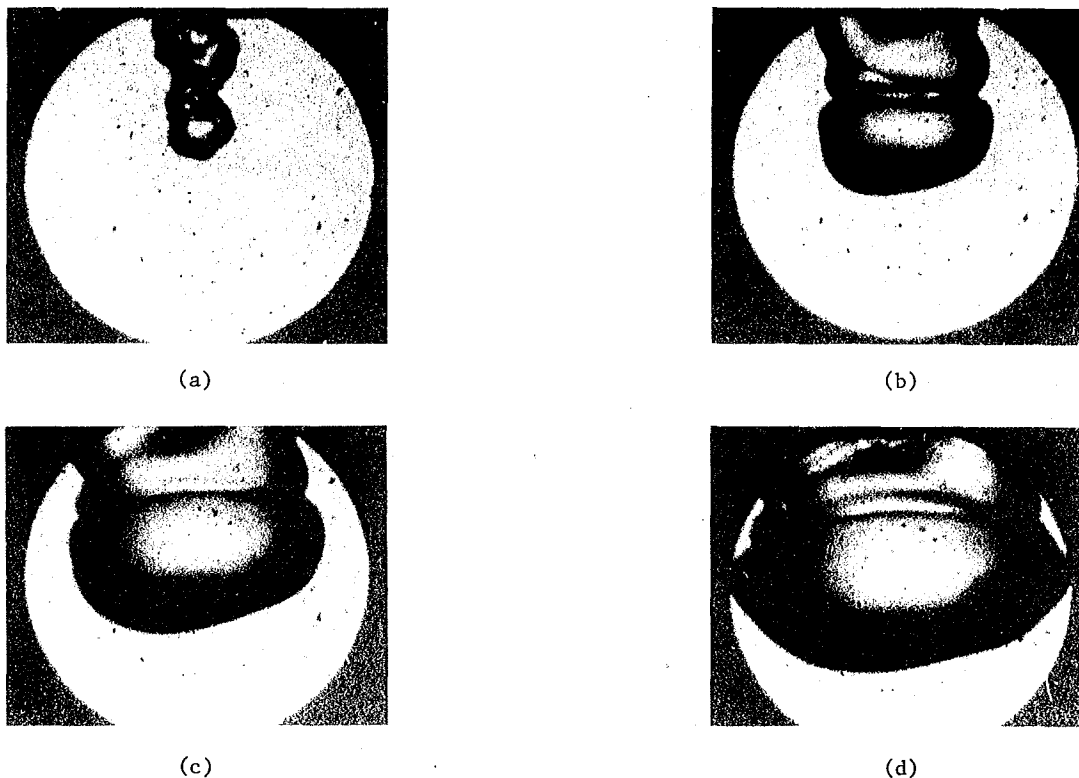


Fig. 1. Schlieren photographs and pressure record of combustion process in a methane/air mixture at  $\phi = 0.6$  ignited by plasma jet igniter with  $L^* = 1.675$  cm.

Schlieren photographs: (a) 1 msec; (b) 10 msec; (c) 20 msec; (d) 30 msec. Pressure record: pressure, 10 psi/div; time, 20 msec/div; time, 20 msec/div. (XBB 7911-15808)

a time mark was flashed upon the edge of the film. Schlieren cinematography was thus synchronized with pressure measurement.

As an example of experimental results, a representative set is presented in Fig. 1. It was obtained with a plasma jet igniter whose characteristic length (ratio of cavity volume to orifice area) was 1.675 cm while the volume of the cavity was  $10 \text{ mm}^3$ , fed with 2.5 J of electrical energy and igniting a methane/air mixture at an equivalence ratio of 0.6, initially at atmospheric pressure and room temperature. The set consists of four schlieren photographs reproduced from cinematographic frames at 1, 10, 20, and 30 msec after the electrical discharge and the concomitant pressure transducer record.

Schlieren photographs provide information on the flame area and burned volume. Pressure records furnish data on the rate of burning. By combining the two, one can evaluate burning velocities. As an example, Fig. 2 presents the evolution of "turbulent" burning velocity deduced from tests performed with the use of three igniters. Figure 3 displays the ratios of turbulent to laminar velocities. As apparent, the effect of the convolutions of the flame front is sustained throughout the whole process of combustion in the bomb at a uniform level corresponding to a three-fold augmentation of the effective burning velocity. This implies that the smoothing and enlarging of the convolutions maintains the factor by which the flame area is increased approximately constant. The important conclusion which emerges from this is that whereas chemical effects due to active radicals in the plasma may die out quickly, the fluid mechanical effects persist over an appreciable amount of time.

#### Diagnostics

In order to acquire a capability to measure local concentration of radicals at high time resolution, a molecular beam sampling apparatus based on the use of a quadrupole mass spectrometer has been designed and is now under construction.

Figure 4 shows the assembly of the apparatus, depicting its general features centered around the vacuum pumping system. Figure 5 provides the cross-

sectional view of the molecular beam processing elements: the nozzle, skimmer, chopper, and the sensing gap of the mass spectrometer.

It is hoped that the apparatus will be ready for preliminary calibration tests before the end of fiscal 1980. The particular combustion systems to be used for such tests include a practically homogeneous photochemical ignition and a flat flame.

#### Thermochemistry

In order to provide a rational basis for the investigation of the role played by radicals as temperature substitutes in the ignition of hydrocarbon-air mixtures, we became engaged in a theoretical study of the process of ignition. Methane was adopted as the representative fuel because of the complete data available on the elementary chemical kinetic steps governing its oxidation mechanism. By restricting the scope of the analysis to the case of constant pressure, the problem could be defined in terms of  $(N + 1)$  ordinary differential equations expressing the conservation of  $N$  chemical species and energy, including the effects of heat losses. The complete set was solved numerically using an appropriate technique for "stiff" ordinary differential equations. The results brought out the key role played in the early stages of ignition by the methyl and hydroxyl radicals and the hydrogen atom. To examine global properties of the solution, the kinetic scheme was expressed in terms of a two reaction mechanism and the problem reduced thereby to a three-dimensional phase-space, namely one consisting of temperature, fuel, and relative radical concentration as the coordinates. Using this formulation, a systematic study was carried out exploring the effects of the initial temperature and radical concentration, subject to energy dissipation effects due to heat losses expressed in terms of a thermal relaxation time. This yielded an explicit definition for ignition temperature. The results revealed the existence of a locus of critical radical concentrations delineating the minimal amount that is required to produce a distinct reduction in this temperature.

As an example of the results we obtained, Fig. 6 presents the conventional plot of time profiles of the temperature and the concentration of

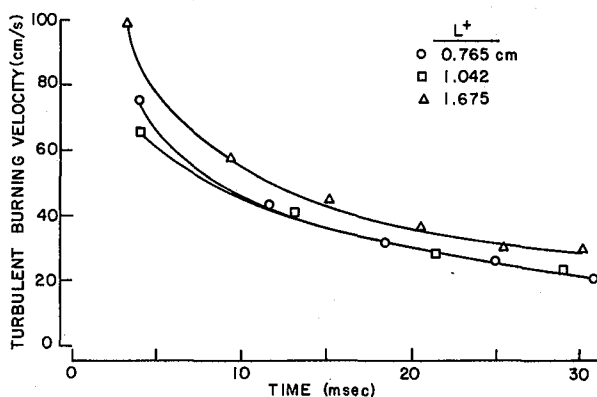


Fig. 2. "Turbulent" burning velocities in plasma jet ignited methane-air mixtures at an equivalence ratio of 0.6 initially at NTP. (XBL 798-6780A)

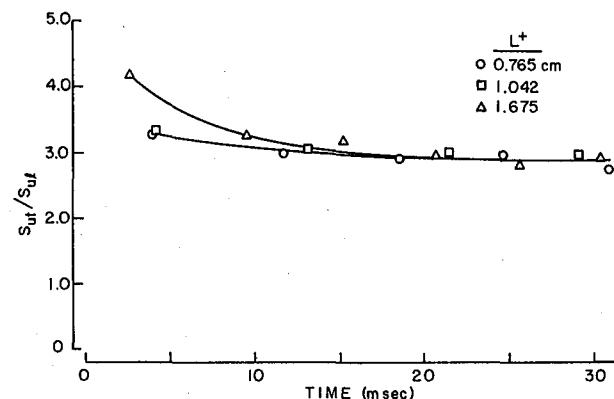


Fig. 3. Ratio of "turbulent" to "laminar" burning velocities in plasma jet ignited methane-air mixtures at an equivalence ratio of 0.6 initially at NTP. (XBL 798-6773)

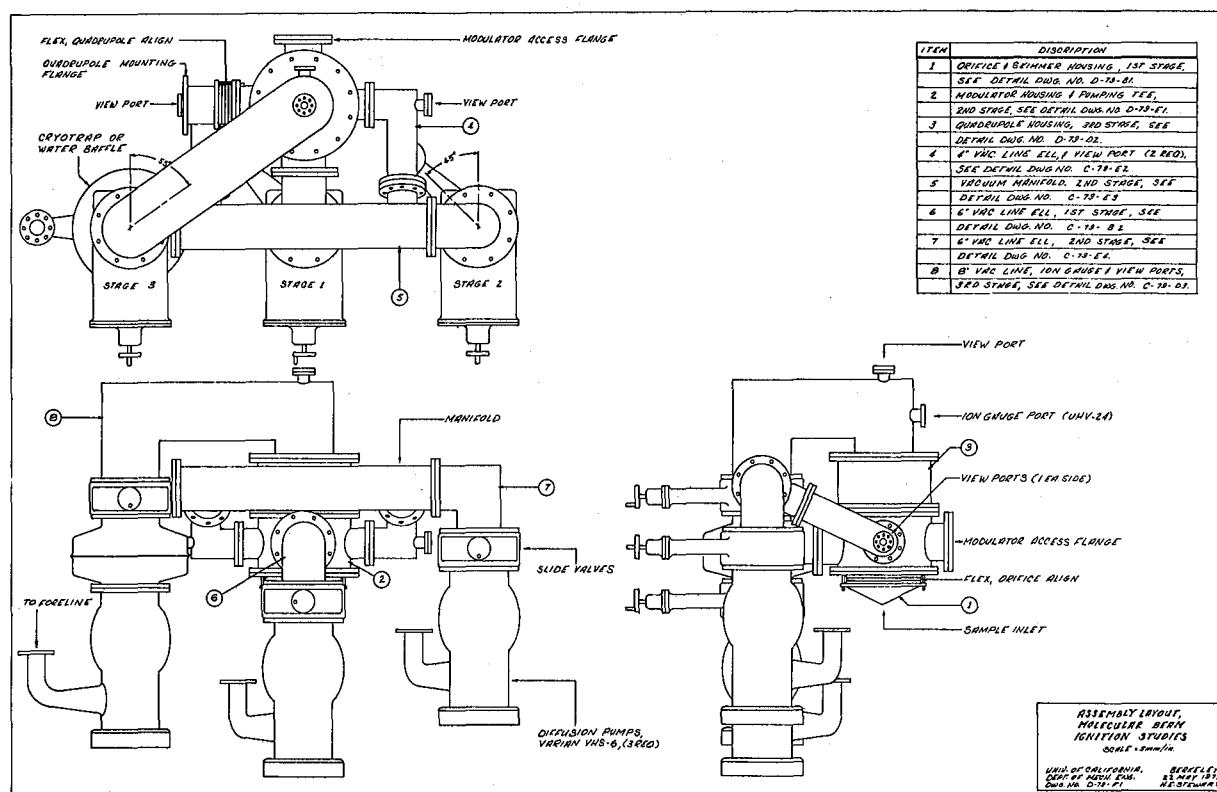


Fig. 4. Assembly of molecular beam sampling mass spectrometer.  
(XBL 7912-13715)

the main radical species,  $\text{CH}_3$ ,  $\text{H}$ , and  $\text{OH}$  using the detailed kinetics scheme for a methane-air mixture at equivalence ratio  $\phi = 0.5$  and the thermal relaxation time  $\tau_h = 10^{-2}$  sec, while  $T_a = 300\text{K}$ . There are four cases:

- Ignition following thermal initiation<sup>†</sup>
- Extinction following thermal initiation<sup>†</sup>
- Ignition following initiation involving radical input<sup>‡</sup>
- Extinction following initiation involving radical input<sup>‡</sup>

In the first two cases, after the initial exponential evolution of radicals--the classical property of the induction process<sup>2,3</sup>--their growth rate is visibly slowed down. In the case of ignition, this is followed by an extremely fast increase in radical concentration accompanied by an equally fast rise in temperature after a slight decrease manifesting the influence of endothermic reactions. This is followed by a rapid decay, first in the concentration of  $\text{CH}_3$  and then in that of  $\text{H}$ ,  $\text{OH}$  and temperature--the characteristic features of the so-called "thermal explosions".<sup>4,5</sup> In the case of extinction, there is only a continuous decay in the temperature while the radicals, after reaching maximum concentrations, disappear quite rapidly.

<sup>†</sup>temperature jump only

<sup>‡</sup> initial concentrations specified in the figures.

The latter two cases are representative of processes involving an appreciable initial concentration of radicals. Instead of the initial exponential evolution, the radicals at first recombine, giving rise to an exothermic process manifested by temperature increase, thereupon reaching a temporary state of equilibrium followed by a rapid growth or decay, as in the case of thermal initiation.

The salient feature of the set of ordinary differential equations of ignition is that they are autonomous. Their solutions are therefore best described in terms of integral curves in the phase space of the dependent variables: the species concentrations and the temperature. Each integral curve is fixed by the parameters of state at  $t = 0$ --the coordinates of its initial point. In order to visualize the integral curves, it is sufficient for our purpose to consider their projection on the plane of the temperature and methyl radical, the latter being singled out in view of the prominent role it plays in methane ignition.<sup>6</sup>

Depicted in Fig. 7 are families of such curves obtained for the detailed kinetic scheme (upper row), as well as for the two reaction model (lower row), in methane-air mixtures at equivalence ratios of  $\phi = 0.5$  and  $\phi = 1$ , while the thermal relaxation time  $\tau_h = 10^{-2}$  sec for with  $T_a = 300\text{K}$ . Numbers in circles denote the four general cases of Fig. 6.

Figure 8 displays clearly the existence of a separatrix surface between solutions for ignition

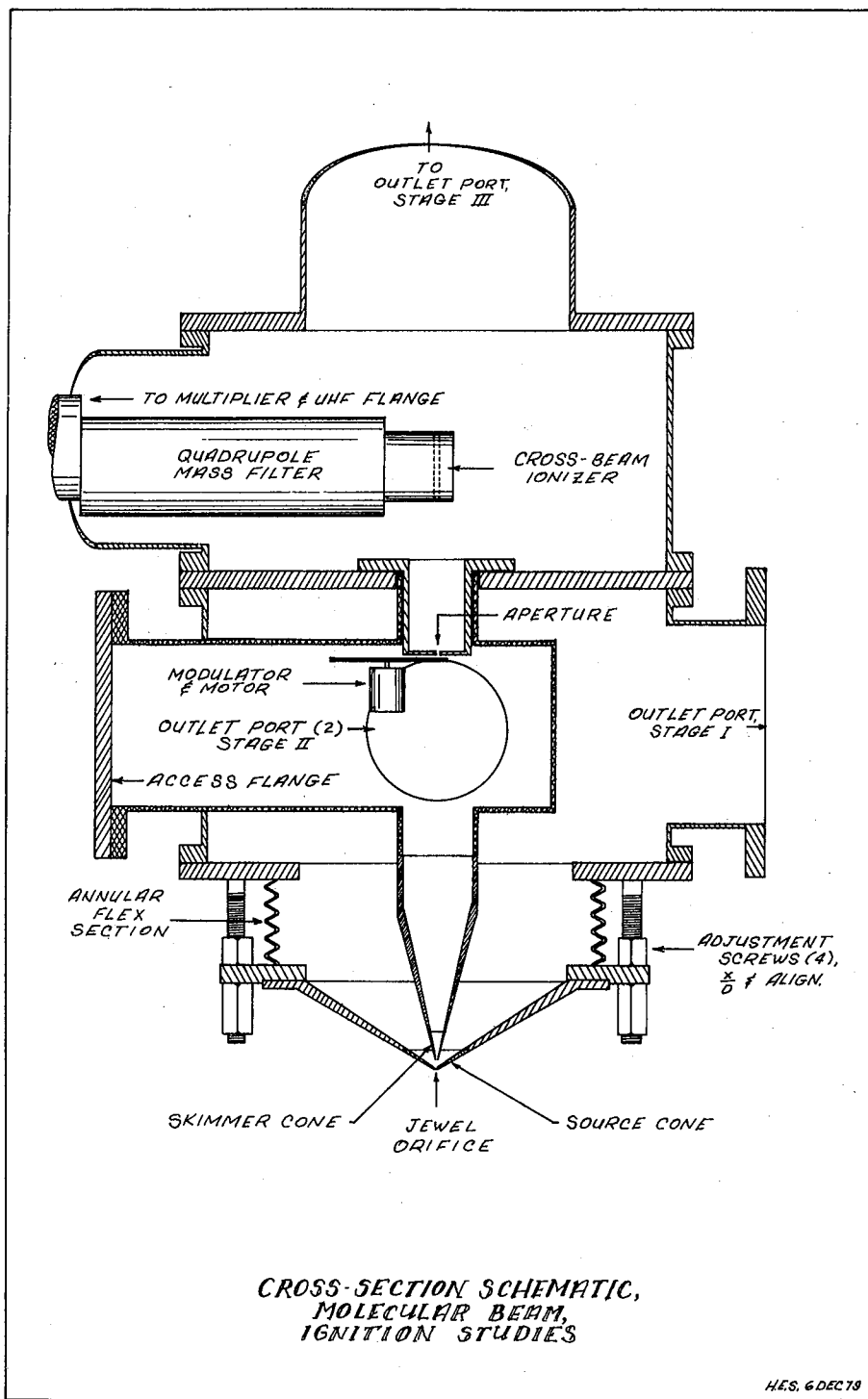


Fig. 5. Cross-section of molecular beam sampling mass spectrometer.  
(XBL 7912-13716)

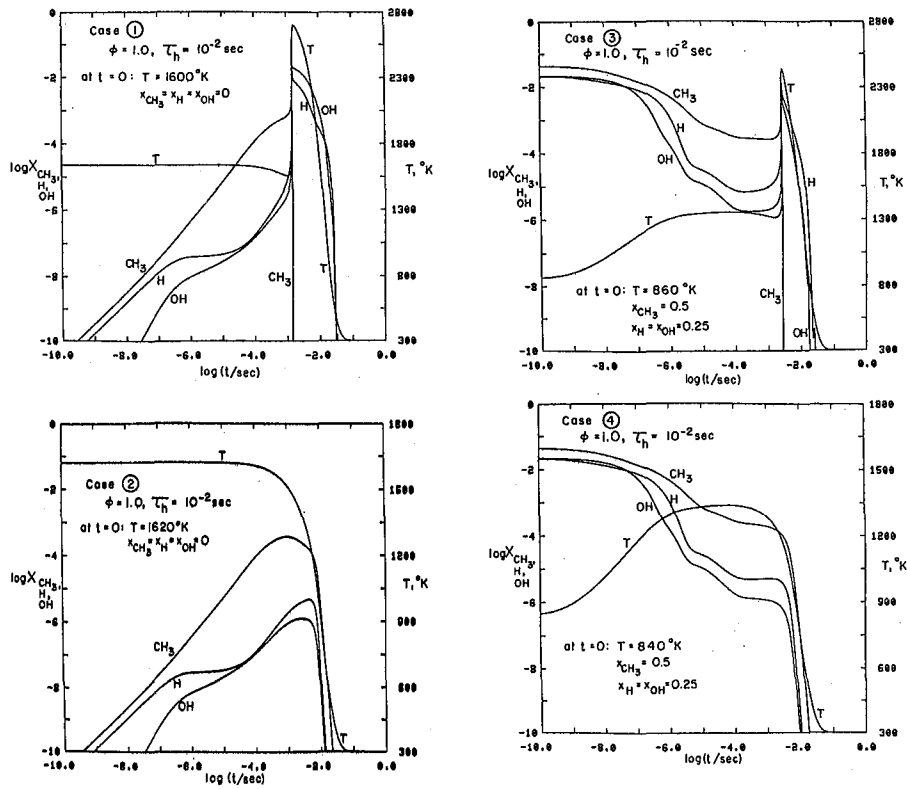


Fig. 6. Time profiles of temperature and major radicals concentration. Detailed kinetics for stoichiometric methane-air mixtures. Thermal relaxation time: 0.01 sec. (XBL 7910-12572)

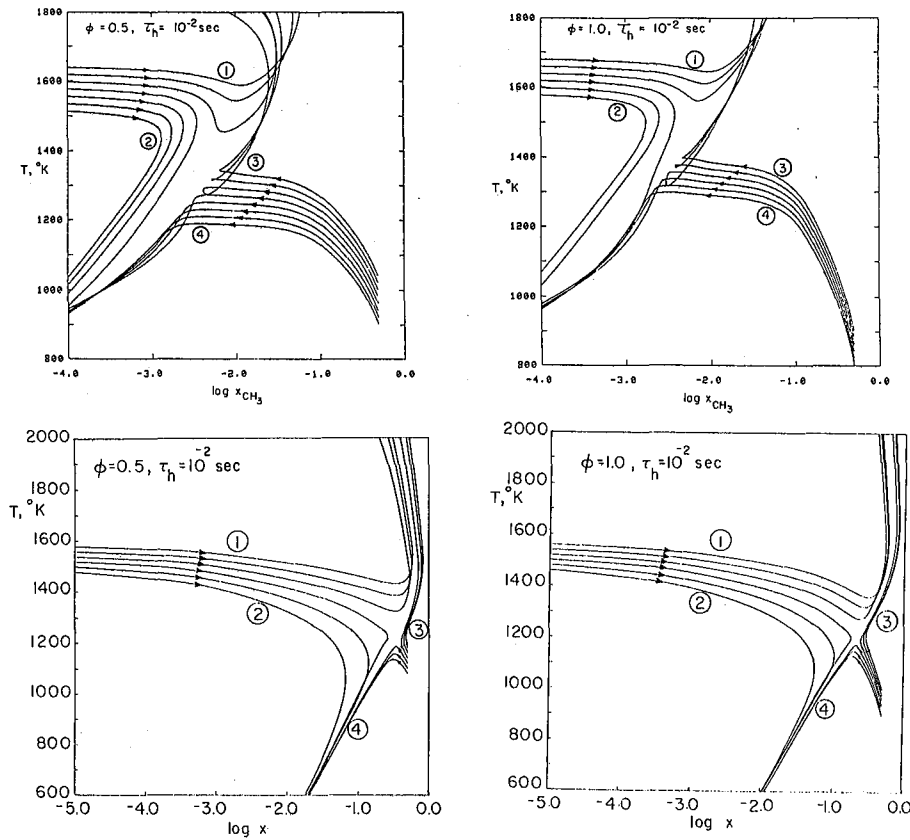


Fig. 7. Integral curves on the plane of temperature and methyl radical concentration. Upper row: detailed kinetics  
Lower row: two-reaction model  
Methane-air mixtures at equivalence ratios of 0.5 and 1  
with thermal relaxation time: 0.01 sec.  
Arrows denote direction of increasing time. (XBL 7910-12574)

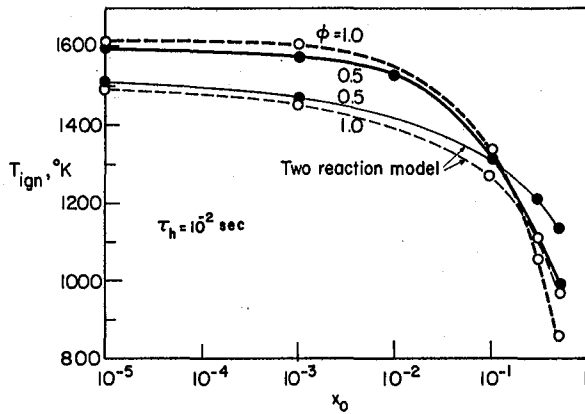


Fig. 8. Influence of initial radical concentration on ignition temperature. Radical concentration is expressed in terms of its ratio to the initial concentration of fuel. (XBL 797-6663A)

and extinction. This surface marks the threshold for ignition and provides a distinct definition of the ignition temperature—a quantity which, as it becomes apparent from the graph, is, for a given chemical system, a function of the thermal relaxation time and the initial concentration of radicals.

The integral curves displayed in Fig. 7 tend towards the envelope surface of the solutions for thermally initiated processes, rendering it an important property as a locus of critical concentrations. If the initial concentration of a radical is below its critical level delineated by this surface, it will increase in the course of the process, irrespective of whether this leads to ignition or to extinction. If, on the other hand, the initial concentration of a radical is above its critical level, as was in fact the case for the solutions corresponding to finite initial concentrations of radicals presented in Fig. 6 and 7, it will at first decrease. As illustrated in Fig. 7, this trend may be subsequently reversed as a consequence of the shape of the surface of critical concentrations in the phase space.

The solutions presented in Fig. 6 correspond to the integral curves which in Fig. 7 are closest to those separatrices, thus bracketing the ignition temperature. Concomitantly, the integral curves for finite initial radical concentrations shown in Fig. 7 correspond to the same values of concentrations as those of the solutions presented in Fig. 6.

The significant practical results of our study are displayed by the plot of the ignition temperature as a function of the initial radical concentration, Fig. 8. Major conclusions one can reach on this basis are as follows:

1. The dependence of the ignition temperature on the initial radical concentration evaluated by the use of the two-reaction model is in agreement with that determined for the detailed kinetics scheme within a band of about 100K—as good as one may expect.

2. The effect of the initial concentration of radicals in diminishing the ignition temperature becomes noticeable when it reaches the level of about 1% of the initial concentration of fuel. This is in close agreement with the coordinate of the surface of critical concentrations. Thus, in order to be of practical significance, the initial radical concentration should be supercritical.

Preliminary results of this study were presented at the Seventh International Colloquium on Gasdynamics of Explosions and Reactive Systems in Göttingen, August, 1979.<sup>7</sup>

#### Fluid Mechanics

The salient feature of our method of approach is the realization that in a gaseous medium the process of ignition is significantly influenced by the fluid mechanical phenomena. However, the driving mechanism is derived from chemical reactions. Thus in spite of the fact that the fluid mechanical aspects can be of crucial importance, especially under the significant limit conditions, they are per force secondary in nature.

Nonetheless, they are prominently included in our studies, as exemplified by the methodology we developed for performance tests described here earlier, and we have developed a plan of attack based on the random vortex technique described in the section on "Numerical Modeling of Turbulent Combustion."

The eventual aim of our study is the determination of the relative influence of fluid mechanical phenomena and chemical kinetic processes on ignition in gaseous media, with particular relevance to future evolution of internal combustion engines.

#### PLANNED ACTIVITIES FOR 1980

With reference to the four phases of this program of research, our plans for 1980 consist of the following tasks:

1. carry out performance tests of combustion-generated jet ignition systems and expand the investigation of plasma jet igniters to include the effects of modifying the plasma medium and energy;
2. complete the construction of the molecular beam and perform preliminary calibration tests;
3. expand the thermochemical analysis to the non-homogeneous process of flame generation, i.e. to the domain of partial differential equations including the effects of diffusion;
4. apply the modeling technique based on the Random Vortex Method to jets and jet ignition, the latter simulated by the action of volume sources in the turbulent regime created by the jet; for this purpose the technique will have to be extended to cover the "slightly compressible" effects of confinement on the increase in bulk density of the medium.

## FOOTNOTE AND REFERENCES

\*This work was supported by the Engineering, Mathematical, Geosciences Division and the Energy Research Office of the U.S. Department of Energy.

1. B. Cetegen, K. Y. Teichman, F. J., Weinberg, and A. K. Oppenheim, "Performance of a plasma jet igniter," to be presented at the SAE 1980 International Automobile Engineering Congress, Warren, Michigan (1980).
2. J. N. Bradley, "Induction times and exponential growth rates in branching-chain reactions," Trans. Faraday Soc., **63**, 2945-2954 (1967).
3. R. S. Brokaw, "Analytic solutions to the ignition kinetics of the hydrogen-oxygen reaction," Proceedings of the Tenth Symposium (International) on Combustion, The Combustion Institute, Pittsburgh, 269-278 (1965).
4. D. A. Frank-Kamenetskii, Diffusion and Heat Exchange in Chemical Kinetics (1947). Translation by N. Thon, Princeton University Press, Princeton (1955).
5. N. N. Semenov, Some Problems in Chemical Kinetics and Reactivity (1954). Translation by M. Boudart, Princeton University Press, Princeton, Vol. 1 (1958), Vol. 2 (1959).
6. J. R. Creighton, "A two reaction model of methane combustion for rapid numerical calculations", Lawrence Livermore Laboratory Preprint UCRL-79669, Rev. 1 (1977).
7. R. H. Guirguis, I. Karasalo, J. R. Creighton, and A. K. Oppenheim, "On the thermochemistry of methane ignition," Proceedings of the Seventh International Colloquium on Gasdynamics of Explosions and Reactive Systems, in press.

## NUMERICAL ANALYSIS OF A HYPOTHETICAL EXPLOSION\*

*J. Kurylo and A. K. Oppenheim*

### INTRODUCTION

At approximately 4:00 A.M., March 28, 1979, the Three Mile Island Nuclear Plant Unit 2 in Harrisburg, Pennsylvania, while operating at approximately 97% of full power, experienced a loss of feed water.<sup>1,2</sup> Unlike previous incidents,<sup>3</sup> a series of events took place resulting in the formation of a potentially explosive gas bubble within the reactor pressure vessel. While field monitors recorded releases of radioactive gases, Nuclear Regulatory Commission, General Public Utilities, and Industry Advisory Group personnel struggled to gain control over the growing gas bubble. Estimates of the bubble's size were as large as 2000 ft<sup>3</sup> at a pressure of 68.03 atm and a temperature of at least 422K. Chemical analysis indicated the gas bubble's composition to be a rich mixture of hydrogen, oxygen, and water vapor.

Questions concerning the explosibility and flammability of the gas bubble arose. The immediate and primary concern was to assess the vulnerability of the reactor pressure vessel to the most serious of possible future events—accidental explosion of the gas bubble. Failure of the vessel to contain the explosion could have led to the venting and subsequent dispersion of highly toxic radioactive material into the atmosphere. A potentially serious threat to the public existed.

We were asked by the Nuclear Regulatory Agency to evaluate the effects of a hypothetical explosion. In response, we determined by numerical analysis the evolution of pressure and impulse loadings on the walls of the hemispherical dome of a reactor pressure vessel arising from a centrally ignited gaseous detonation. Included in the investigation were the effects of richness of the

hydrogen-oxygen gas mixtures, as well as effects due to inclusion of water vapor.

### ACCOMPLISHMENTS

#### Analysis

It was assumed that initial conditions at the instant the gas bubble is consumed are given by the self-similar solution of a Chapman-Jouguet detonation front headed by a blast wave. The evaluation of such an event was described by Oppenheim et al.<sup>4</sup> The analysis was performed using a numerical technique, the CLOUD CODE<sup>5</sup> developed and modified by Oppenheim et al.<sup>6</sup> This technique is set in Lagrangian coordinates and incorporates the smoothing action of artificial viscosity.<sup>7,8</sup>

Since the accuracy of the wave interaction processes, especially those occurring between the blast wave front and reactor wall, was of particular interest, special attention had to be paid to the spatial resolution of the gas bubble. Over 400 grid points were used for this purpose.

#### Results

For the same thermodynamic properties of the reacting medium, we analyzed the following three cases:

- (1) Constant volume combustion (EV)
- (2) Chapman-Jouguet detonation (CJ)
- (3) Chapman-Jouguet detonation including the von Neumann spike (VN)

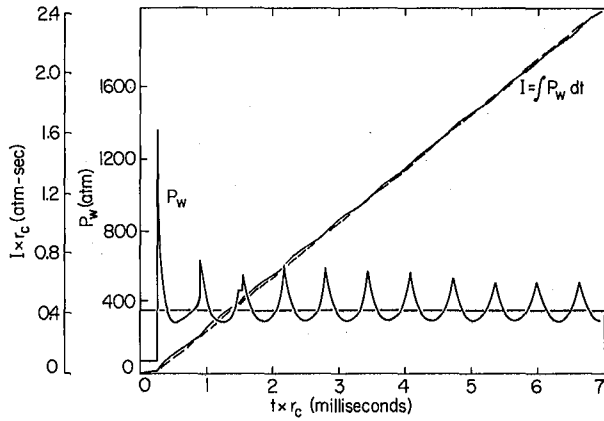


Fig. 1. Static wall pressure and impulse loading histories. (Continuous line refers to the Chapman-Jouguet detonation; dashed line refers to constant volume combustion; while  $r_c$  denotes radius of hemispherical gas bubble in meter). (XBL 798-2468)

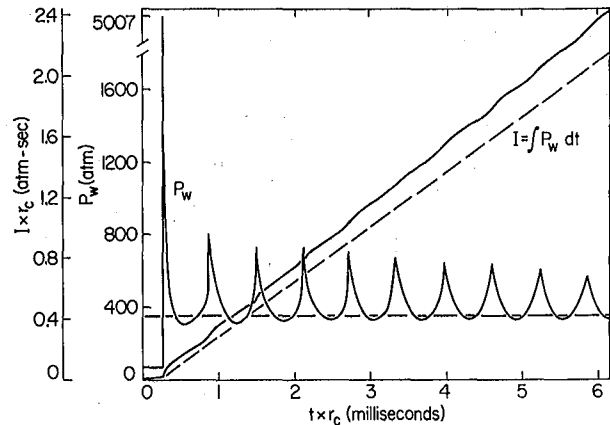


Fig. 2. Static wall pressure and impulse loading histories. (Continuous line refers to the Chapman-Jouguet detonation including von Neumann spike; dash line refers to the constant volume combustion; while  $r_c$  denotes radius of hemispherical gas bubble in meter). (XBL 798-2469)

The medium considered was one consisting of two components, unburned and burned, each behaving essentially as a perfect gas with constant but different specific heats.

As an example of the results we obtained, Figs. 1 and 2 present the static pressure and static impulse loading histories on the reactor vessel wall, assumed to be perfectly rigid for cases (2) and (3) respectively. Initially the gas bubble consisted of 90% hydrogen and 10% oxygen (in volumetric fractions). The dashed line corresponds to case (1), the constant volume combustion. Prominently displayed is the rapid decay of the peak static pressure and the subsequent ringing of the blast front—a characteristic feature of confined explosions. After the first reflection, the static pressure peaks are slowly reduced, except for the third peak which is always lower than the second and fourth. If it is assumed that the detonation front reaches the von Neumann spike, the amplitude of ringing pressures is about 30% higher, while the frequency remains practically the same. The pressure patterns are quite similar, except for the plateau prior to third reflection which occurs only in case (2).

#### CONCLUSIONS

The conclusions derived from our results are as follows:

1. Maximum peak pressure is attained by the initial reflection of the detonation front from the wall of the reactor vessel. Its value can be estimated within about 15% accuracy by calculating the pressure due to planar reflection of the detonation front.
2. Pressure peaks of the ensuing ringing process are much weaker than that of the first peak, but they are, nonetheless, quite significant.

3. Impulse loadings are essentially the same as those attained by constant volume combustion.
4. Increasing the richness of the gas bubble mixture and introducing water vapor lessens the potential danger due to detonation.
5. The ringing frequency is virtually independent of the initial composition of the mixture, ranging from 1300 to 1600 cps for the various cases we analyzed.

#### FOOTNOTE AND REFERENCES

\*This work was supported by the Energy Research Office of the U.S. Department of Energy and the LBL Director's Office Fund, Lawrence Berkeley Laboratory.

1. NSAC-1 "Analysis of Three Mile Island - Unit 2 Accident," Nuclear Safety Analysis Centre, Electric Power Research Institute, Palo Alto, CA (July 1979).
2. NUREG-0560 "Staff report on the generic assessment of feedwater transients in pressurized water reactors designed by the Babcock and Wilcox Company," Office of Nuclear Reactor Regulation, United States Nuclear Regulatory Commission, Washington, D. C. (May 1979).
3. NUREG-75/014 WASH-1400, "An assessment of accident risks in U.S. commercial nuclear power plants," Reactor Safety Study, United States Nuclear Regulatory Commission, Washington D.C. (Oct 1975).
4. A. K. Oppenheim, A. L. Kuhl, and M. M. Kamel, "On self-similar waves headed by the Chapman-Jouguet detonation," *J. Fluid Mechanics* **55**, 2, 257-270 (1972).

5. L. M. Cohen, J. M. Short, and A. K. Oppenheim, "A computational technique for the evaluation of dynamic effects of exothermic reactions," Combustion and Flame 24, 3, 319-334 (1975).
6. A. K. Oppenheim, J. Kurylo, L. M. Cohen, and M. M. Kamel, "Blast waves generated by exploding clouds," Eleventh International Symposium on Shock Tubes and Waves, University of Washington, 465-473 (1977).
7. J. von Neumann and R. D. Richtmyer, "A method for the numerical calculation of hydrodynamic shocks," J. Applied Physics 21, 3, 232-237 (1950).
8. M. L. Wilkins, "Calculation of elastic-plastic flow," Lawrence Livermore Report UCRL-7322, Rev. 1, Livermore, CA (1969).

## COMBUSTION CHEMISTRY AND POLLUTANT FORMATION

### COMPARATIVE STUDIES OF COMBUSTION INHIBITION\*

*R. W. Schefer and N. J. Brown*

#### INTRODUCTION

There are incidents of unwanted fire where it is undesirable to use water as an extinguishing agent. In many of these cases, low molecular weight halogenated hydrocarbons of the methane type (where halogen atoms are substituted for hydrogen) are used as inhibiting and extinguishing agents. In order to choose the optimum inhibitor for a give set of combustion conditions, it is important to understand the detailed mechanism of inhibition and extinguishment. A research program has been sponsored at Lawrence Berkeley Laboratory by the National Bureau of Standards to conduct a modeling study of combustion inhibitors to improve our understanding of inhibitors. The following parameters were considered in the study: 1) combustion configuration; 2) fuel type; 3) inhibitor type; 4) inhibitor concentration, and 5) pressure.

Flame inhibitors are broadly classified as being either of the physical or chemical type. The former type is believed to act simply as a physical diluent while the latter is thought to participate directly in the reaction mechanism important to flame propagation. Although no general consensus exists regarding the mechanism(s) of chemical inhibition, it is recognized that certain molecules have been observed to retard flame propagation out of proportion to their thermal influence. This leads to the supposition that this type of inhibition is directly linked to chemical reactivity.

Although a large body of literature associated with flame inhibition studies exists, it has not been possible to formulate a generalized inhibition mechanism which can explain the various results over the wide variety of conditions which have been employed in these studies. This is largely due to (1) uncertainties in the inhibition kinetic mechanism and (2) the complex interaction between thermal dilution and chemical effects discussed above. The objective of the present investigation was to undertake a set of modeling studies in which the influence of the various processes involved

in flame inhibition could be ascertained, and, from these results, develop a more detailed understanding of the overall combustion inhibition mechanism.

During the previous year modeling calculations were carried out in which the effect of inhibitor addition on the combustion characteristics of H<sub>2</sub>/O<sub>2</sub>/Ar mixtures in an idealized perfectly stirred reactor was determined.<sup>1</sup> Two physical inhibitors, N<sub>2</sub> and Ar, and one chemical inhibitor, HBr, were investigated. The physical inhibitors acted as diluents and the chemical inhibitors were found to decrease the total radical pool concentration.

#### ACCOMPLISHMENTS DURING 1979

The inhibition of H<sub>2</sub>/O<sub>2</sub> mixture by HCl and HBr reacting in both a perfectly stirred reactor and in plug flow was investigated. In addition, perfectly stirred reactor calculations were also performed on inhibited moist carbon monoxide mixtures.

Calculations were completed for HCl addition to the perfectly stirred reactor,<sup>2</sup> and the variables considered in the study were pressure, equivalence ratio, and inhibitor concentration. The effectiveness of HCl as a flame inhibitor was characterized by a tradeoff between reaction exothermicity and radical scavenging ability. At low concentrations HCl promoted the combustion process rather than inhibiting it due to the large heat release associated with recombination reaction:  $(H + Cl + M \rightleftharpoons HCl + M)$  where M is any third body. This resulted in a substantial reduction in reactor residence at blowout which is indicative of the promotion of combustion. As the HCl concentration was increased, radical removal via the reactions  $H + HCl \rightleftharpoons H_2 + Cl + M \rightarrow HCl + M$  became competitive with radical production reactions, and HCl exhibited a behavior more characteristic of a flame inhibitor in which reactor residence time at blowout increased with increasing HCl addition. HBr exhibited a similar tradeoff between reaction exothermicity and radical scavenging ability. However, due to the relatively lower heat

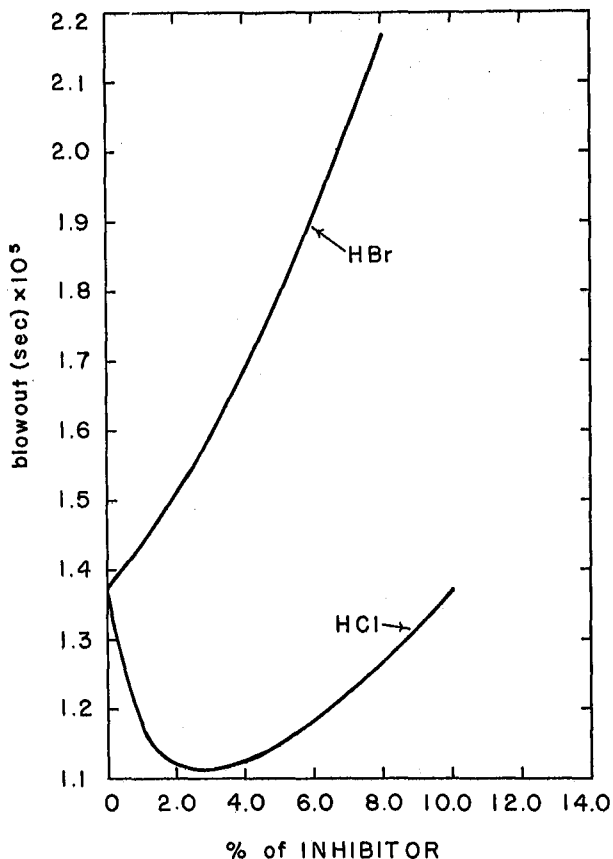


Fig. 1. Reactor residence times vs inhibitor mole fraction for HCl and HBr for stoichiometric H<sub>2</sub>/O<sub>2</sub>/ Ar mixtures at 1 atmosphere pressure. (XBL 802-7991)

release rates associated with HBr recombination, radical removal was the predominant effect and, over the range of conditions investigated, HBr was effective as a flame inhibitor. A comparison of the effect of HCl and HBr addition on the blowout characteristics of a perfectly stirred reactor is shown in Fig. 1.

Calculations performed on inhibited moist CO mixtures in a perfectly stirred reactor showed that both HBr and HCl acted effectively as inhibitors over the range of conditions investigated. Although heat release due to HCl recombination contributed significantly to the total heat release, radical removal reactions involving HCl were more competitive with radical production reactions involving H, OH, and H<sub>2</sub> due to the lower concentrations of the latter species in the moist CO mixtures.

In the plug flow reactor utilizing hydrogen/oxygen/argon mixtures HBr was significantly more effective as an inhibitor than HCl. HBr effectiveness was directly attributable to radical removal via the reaction  $\text{HBr} + \text{H} \rightarrow \text{H}_2 + \text{Br}$ . Because of the lower rate coefficient associated with the corresponding HCl reaction ( $\text{HCl} + \text{H} \rightarrow \text{H}_2 + \text{Cl}$ ) radical removal rates were not competitive with radical production rates and HCl was relatively less effective as an inhibitor. In both the HCl and HBr case, three body HCl and HBr recombination reactions made negligible contributions to radical removal and heat release.

#### PLANNED ACTIVITIES FOR 1980

The research objectives of this study were completed during FY 1979, and two manuscripts will be submitted for publication during FY 1980.

#### FOOTNOTE AND REFERENCES

\*This work was supported by the Center for Fire Research, National Bureau of Standards.

1. N. J. Brown and R. W. Schefer, "A computational study of physical and chemical flame inhibition," Paper No. 78-43, Western States Section/Combustion Institute, Spring Meeting, Boulder, Colorado, 1978. Lawrence Berkeley Laboratory report, LBL-6899.
2. R. W. Schefer, N. J. Brown, and M. Chan, "Comparative study of HBr and HCl inhibition," to be submitted for publication.

## MEASUREMENTS OF NITROGENOUS POLLUTANTS IN COMBUSTION ENVIRONMENTS\*

N. J. Brown, E. Cuellar, T. S. Eitzen, A. S. Newton, R. W. Schefer and T. Hadeishi

Combustion sources utilizing alternative and fossil fuels pose a substantially more serious threat to air quality than natural gas and distillate oils since they contain nitrogen and sulfur chemically bound to the fuel. The importance of the potentially serious fuel nitrogen pollution problem associated with increased alternative and fossil fuel utilization has not been assessed since all the nitrogen-containing combustion products have been neither identified nor quantified. Thus it becomes increasingly important to develop and characterize analytical techniques which are suitable for quantitatively measuring nitrogenous compounds in the post combustion environment. This is a crucial step in the determination of source emissions and the assessment of the health and environmental effects of pollutant species.

Research emphasis has been placed upon measuring the concentrations of NO and NH<sub>3</sub> in combustion mixtures. A flat-flame burner system has been set up and characterized to ascertain that the flame is one dimensional. Concentrations of NO are determined via two methods and compared. The first method involves extracting a gas sample from the flame with a quartz aerodynamic quenching probe and analyzing the sample with a chemiluminescent analyzer. The second method is a spectroscopic technique which is extremely sensitive to concentrations in the ppm range. The particular type of spectroscopy to be used is Zeeman Atomic Absorption Spectroscopy (ZAA) which was developed at Lawrence Berkeley Laboratory for the quantitative determination of atoms and small molecules.<sup>1</sup> The technique is non-intrusive, *in situ* and of the differential absorption type.

Concentrations of NH<sub>3</sub> were determined in the post-combustion environment of a prototype alternative fuel. Samples were extracted via a quartz aerodynamic quenching probe and then passed through a sampling cell filled with spherical glass beads which were coated with a weak H<sub>3</sub>PO<sub>4</sub> solution. After collecting a known volume of sample, the sampling tube was removed and the NH<sub>3</sub> was transferred to an aqueous solution via washing. The quantitative measurement of the dissolved NH<sub>3</sub> was then determined colorimetrically by the sodium phenolate method. Briefly, the dissolved NH<sub>3</sub> is chlorinated and then reacted with sodium phenolate to form an indophenol dye of unknown structure. The optical density of this dye is measured using a Beckmann Model DK Spectrophotometer at a wavelength of 632 nm. Figure 1 shows the optical density as a function of the amount of NH<sub>3</sub> in 10 mL water.

### ACCOMPLISHMENTS DURING 1979

Ammonia was measured over a range of concentration and combustion conditions. It is important to collect the sample for an appropriate period of time so that the optical density is linear with concentration. The great difficulty in measuring NH<sub>3</sub> in

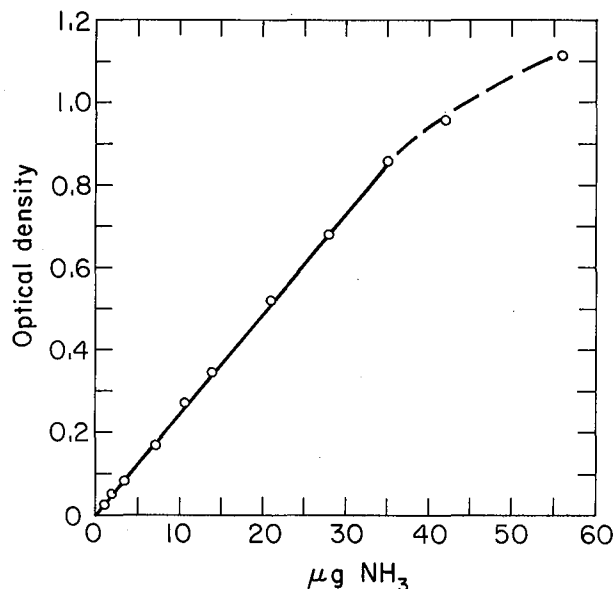


Fig. 1. Optical density as a function of the amount of NH<sub>3</sub> in 10 ml water by the hypochlorous acid-sodium phenolate method. (XBL 803-181)

product combustion gas mixtures is in sample collection. Ammonia tends to condense on the walls of the sample manifold and is difficult to transfer quantitatively from the acid treated glass beads used in the collection system. Several techniques for improving sample collection have been attempted, but none have been found which give good reproducibility.

A chemiluminescent analyzer was constructed and tested for the suitability of measuring NO and NO<sub>2</sub> concentrations in the ppm range. A series of experiments was performed on premixed methane/air flames of varying equivalence ratios to which known concentrations of NO were added. Survival of NO through the flame front was then determined by measuring NO concentrations with the *in situ* spectroscopic technique and via the probe/chemiluminescent method. Thermal NO could then be determined by extrapolating the results of the doping experiments to zero doping levels. Figure 2 is a plot of NO concentration measured via probing and chemiluminescent analysis versus NO added to the flames.

### PLANNED ACTIVITIES FOR 1980

Two new techniques will be investigated to improve the sampling of NH<sub>3</sub>. One of these will utilize cryogenic trapping to collect the NH<sub>3</sub>. It is anticipated that errors in the NH<sub>3</sub> quantification can be reduced to less than 20 percent. The work

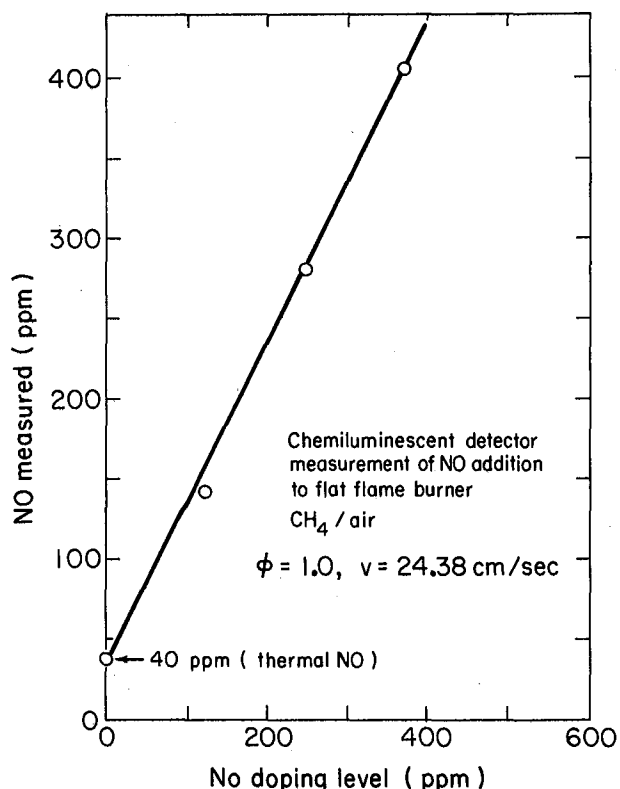


Fig. 2. The survival of NO in an atmospheric, stoichiometric premixed methane/air flame of velocity 28.4 cm/sec. The ordinate represents the concentration of NO that was measured in the post flame region with a chemiluminescent analyzer, and the abscissa represents the concentration of NO added to the flame. (XBL 803-182)

describing the quantification of  $\text{NH}_3$  in combustion product mixtures will be described in a paper<sup>2</sup> which will be submitted for publication.

An analytical technique for measuring HCN in combustion environments utilizing gas chromatography is under development. A sampling system is also being constructed for the GC/MS so that samples collected from combustion experiments can be analyzed and nitrogen- and sulfur-containing species can be identified.

The comparative study of NO quantification in combustion environments will be completed. The survival of  $\text{NO}_2$  throughout the flame front will be determined and  $\text{NO} \rightleftharpoons \text{NO}_2$  probe conversions will be investigated. A paper<sup>3</sup> describing this study will be written and submitted for publication.

#### FOOTNOTE AND REFERENCES

\*This work was supported by the Environment Division of the U.S. Department of Energy.

1. H. Koizumi, T. Hadeishi, and R. D. McLaughlin, *Appl. Phys. Lett.* **34**, 279 (1979).
2. A. S. Newton, T. S. Eitzen and N. J. Brown, "The quantification of  $\text{NH}_3$  in combustion environments." In preparation.
3. E. Cuellar, R. W. Schefer, T. Hadeishi and N. J. Brown, "Comparison between probe and *in situ* measurements of NO in premixed methane/air flames." In preparation.

## THE SELECTIVE REDUCTION OF NO BY $\text{NH}_3$ \*

N. J. Brown, T. S. Eitzen, and R. F. Sawyer

### INTRODUCTION

Combustion, both of the mobile and stationary types, is the primary source of the nitrogen oxides, NO and  $\text{NO}_2$ . Control of nitrogen oxides emissions is essential since these compounds result in atmospheric nitrogen dioxide, photochemical smog formation, formation of nitrate and perhaps other compounds whose role in air pollution is less well understood.

This research is concerned with characterization of a new NO control technology, described by Lyon and Longwell,<sup>1</sup> which selectively removes NO from combustion effluent gases through homogeneous reactions with ammonia and oxygen. The process differs from conventional NO abatement techniques since it does not prevent or limit NO formation but rather removes the NO through reaction in the post-combustion gases.

The selective reduction of NO by  $\text{NH}_3$  is being investigated in a laboratory-scale combustion tunnel which supports steady-state, reproducible combustion under a variety of experimental conditions. Figure 1 is a schematic diagram which illustrates the five component parts of the experimental system. The first part is the gas metering and mixing section for fuel, oxidizer, and prototype fuel nitrogen compound. The fuel used throughout the study was propane and the fuel nitrogen compound was NO. The second segment of the tunnel where combustion occurs consists of a flame holder, igniter and quartz flame tube. The desired combustion-product temperature,  $T^*$ , for the selective reduction reaction is achieved in the third portion of the tunnel where secondary  $\text{N}_2$  is injected into the flow from four stainless steel injectors. The  $\text{NH}_3$  injection system is the fourth component of the tunnel, and here mixtures of  $\text{NH}_3$  and  $\text{N}_2$  are injected into the products of combustion through four quartz injectors.

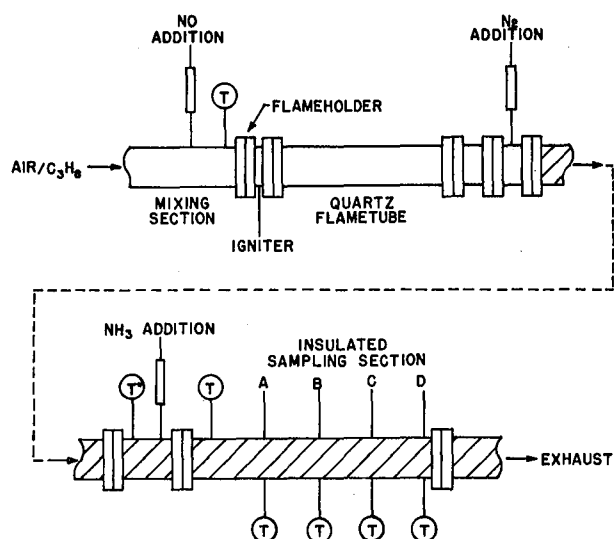


Fig. 1. Schematic diagram of the laboratory-scale combustion tunnel. (XBL 802-7968)

Composition and temperature measurements are performed in the final portion of the tunnel which is a test section where five probe-access ports are located. The entire tunnel is approximately 3.5 m in length and has an inside diameter of 5 cm. Experimental variables considered in our study are: (1) equivalence ratio, (2) concentration of NO prior to  $\text{NH}_3$  addition, (3) temperatures of the combustion products prior to  $\text{NH}_3$  addition, and (4) the concentration of  $\text{NH}_3$  added to the product gases. Temperatures and concentrations of CO, NO,  $\text{CO}_2$  and  $\text{NH}_3$  are measured in the test section. Samples are extracted with quartz aerodynamic quenching probes and analyzed with continuous gas analyzers or wet chemical techniques. Results are analyzed in terms of NO survival yields and concentrations of  $\text{NH}_3$  present at the final probe station, after reduction has occurred.

#### ACCOMPLISHMENTS DURING 1979

Nitric oxide reduction via  $\text{NH}_3$  addition to the post-combustion gases have been investigated at three equivalence ratios and three addition temperatures for four  $\text{NH}_3$  concentrations and a concentration of 500 ppm NO in the test section. Figure 2 is a plot of NO survival as a function of  $\beta$  for a lean mixture. The quantity  $\beta$  is the ratio of the number of moles of  $\text{NH}_3$  added through the injectors to the number of moles of NO present prior to addition. The temperature of the combustion products at  $\text{NH}_3$  injection is designated  $T^*$ . As seen from the figure, the survival of NO decreases with increasing  $\beta$ , and survival is least (optimum reduction) at 1170K. The results of several experiments are summarized in two papers<sup>2,3</sup> and are briefly described in the paragraphs below.

At excess air operating conditions the observed behavior of the ammonia injection process for nitric oxide control was consistent with previous investigations.<sup>4</sup> An optimum temperature and ammonia addition level for maximum nitric oxide

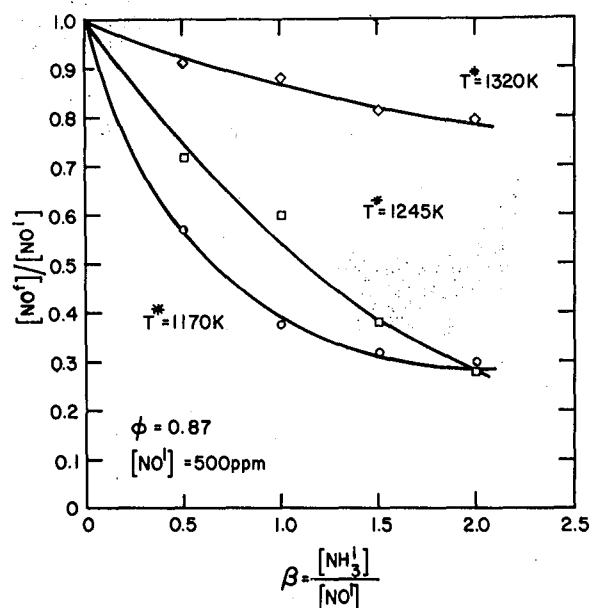


Fig. 2. The NO survival,  $[\text{NO}^f]/[\text{NO}^i]$ , as a function of  $\beta$  for three values of  $T^*$ . The initial concentration of NO is 500 ppm and the equivalence ratio  $\phi = 0.87$ .  $[\text{NO}^f]$  and  $[\text{NO}^i]$  signify the final and initial NO concentrations respectively. (XBL-802-7969)

removal were observed. Nitric oxide survival was somewhat greater than had been obtained by other investigators.<sup>4</sup> This difference is probably attributable to differences in experimental configuration.

The effectiveness of nitric oxide removal improves as the stoichiometric mixture is approached from the lean side but is very sensitive to the mixture ratio under near-stoichiometric conditions. Once the stoichiometric condition is reached and (apparently) there is no excess oxygen available, the effectiveness of nitric oxide removal drops rapidly. Under fuel-rich conditions ammonia addition is ineffective for nitric oxide removal.

Ammonia breakthrough was not determined to be a problem for operating conditions close to those at which the ammonia injection process is intended to be used. Ammonia breakthrough occurs under conditions of excess fuel (absence of excess oxygen), low temperature at the point of injection, and high ammonia to nitric oxide ratios.

The optimization of the process in practical applications may prove difficult because of expected variations in space and time of parameters to which process effectiveness is sensitive (temperature, excess oxygen, and nitric oxide level). Trade-offs exist between nitric oxide removal and ammonia breakthrough which suggest that optimization also must involve an assessment of the relative importance of nitric oxide and ammonia emissions. For a large-scale application, the desirability of monitoring temperature, nitric oxide level, and excess oxygen as a means of selecting the amounts

and possibly location of ammonia injection should be investigated. Because of the sensitivity of the process to system parameters, monitoring of exhaust nitric oxide and ammonia would appear advisable (particularly in large scale applications).

#### PLANNED ACTIVITIES FOR 1980

Current work is concerned with the identification of nitrogeneous species which may also be produced in competition with the selective reduction reactions. Near-stoichiometric and rich mixtures will be investigated under a variety of experimental conditions for the purpose of identifying other nitrogeneous compounds.

The selective reduction of NO via NH<sub>3</sub> addition will be investigated in the product gases of light fuel oil combustion as a function of several experimental parameters. A newly-designed combustion section and fuel delivery system suitable for the combustion of light oils are under construction. The concentration of fuel sulfur and fuel nitrogen will be controlled by doping light oils with known amounts of thiopene and pyridene. Possible synergistic effects between sulfur compounds present in the product gases and the selective reduction will be investigated.

#### FOOTNOTE AND REFERENCES

\* This work was supported by the California Air Resources Board through the U.S. Department of Energy.

1. R. K. Lyon and J. P. Longwell, "Selective non-catalytic reduction of NO<sub>x</sub> with NH<sub>3</sub>," EPRI NO<sub>x</sub> Control Technology Seminar, San Francisco, California, 1976.
2. T. S. Eitzen, N. J. Brown, A. S. Newton, A. K. Gordon, and K. S. Basden, "Characterization of NO<sub>x</sub> removal through ammonia addition," Western States Section, The Combustion Institute Paper No. 79-22 (1979). Also Lawrence Berkeley Laboratory report, LBL-8849.
3. N. J. Brown, R. F. Sawyer, and T. S. Eitzen, "Characterization studies of the selective reduction of NO by NH<sub>3</sub>." Final report submitted to the State of California Air Resources Board. Lawrence Berkeley Laboratory report, LBL-10254.
4. L. J. Muzio, J. K. Arrand, and D. P. Teixeira, "Gas phase decomposition of nitric oxide in combustion products," Sixteenth Symposium (International) on Combustion, The Combustion Institute, Pittsburgh, 199-208 (1977).

## UNIMOLECULAR DISSOCIATION AND RECOMBINATION REACTIONS\*

*N. J. Brown and A. H. Abdel-Hafez*

#### INTRODUCTION

A detailed understanding of combustion involves full comprehension of its chemistry, fluid mechanics, and the interaction of these two. Multistep reaction mechanisms prevail during combustion so that single reactions are difficult to isolate for study. The complex mechanisms and the difficulties inherent in working in the high-temperature environments of combustion complicate the study of combustion chemistry. Relative to the considerable experimental effort, the success in applying recent theories of chemical kinetics to gain a more complete knowledge of combustion chemistry has been quite minimal.

This research is concerned with formally extending and applying unimolecular reaction rate theory to important combustion reactions. Three types of reactions successfully treated with unimolecular rate theory are dissociation, recombination and isomerization reactions. One or more of these reaction types plays a crucial role in ignition, fuel pyrolysis, radical quenching, and pollutant-formation and destruction mechanisms. Unimolecular reactions are governed by a competition between collisional energy transfer and intramolecular energy redistribution. The kinetics are of the second order type at low pressure where collisional intermolecular energy transfer is rate controlling and first order in the high pressure regime which is rate-limited by intramolecular

energy transfer. Currently, research is being directed toward achieving an improved description of bond fission reactions occurring at or near the high pressure limit. Rate coefficients will then be calculated for dissociation reactions which are important to combustion processes.

#### ACCOMPLISHMENTS DURING 1979

During FY 1979 work associated with the remaining two parts of a four part study of the H<sub>2</sub> + D<sub>2</sub> biomolecular exchange reactions was completed. Two papers<sup>1,2</sup> summarize the results of these studies. The adiabatic channel model description of bond fission reactions has been examined in detail and the channel energy expression has been modified to better describe the transition from a reactant vibration to a hindered rotation and finally to the free rotation of the two fragments relative to one another. A computer program has been written to determine the density and total number of vibration states via a direct counting procedure.

#### PLANNED ACTIVITIES FOR 1980

Revised adiabatic channel model calculations will be performed to determine microcanonical and canonical rate coefficients for H<sub>2</sub>O and NO<sub>2</sub> dissociations. These will be compared with minimum density of states, and with minimum number of states

calculations. Near threshold behavior will be examined in detail.

#### FOOTNOTE AND REFERENCES

\*This work was supported by the Energy Research Office of the U.S. Department of Energy.

1. N. J. Brown and D. M. Silver, "Comparison of reactive and inelastic scattering of  $H_2 + D_2$

using four semiempirical potential energy surfaces," Lawrence Berkeley Laboratory report, LBL-8847 (1979). To be published in J. Chem. Physics, 72 (1980).

2. D. M. Silver and N. J. Brown, "Valence bond model potential energy surface for  $H_4$ ," Lawrence Berkeley Laboratory report, LBL-8846 (1979). To be published in J. Chem. Physics, 72 (1980).

## COMBUSTION CHARACTERISTICS OF COAL AND COAL RELATED FUELS\*

R. F. Sawyer and W. K. Chin

### INTRODUCTION

The renewed importance of coal as a primary energy source has motivated our study of the fundamental combustion characteristics of coal and coal-derived fuels. The opposed-flow diffusion-flame configuration has been employed to provide a well-controlled laboratory environment for the comparative study of the combustion of several fuels under steady-state conditions. The heating rates which are known to be important to the pyrolysis and combustion of coal are considerably less than those for pulverized coal combustion, but they match those of the fluidized bed or stoker fed combustion of coal. In previously completed work, the experimental program has demonstrated

the suitability of the opposed flow diffusion flame technique to the burning of pressed pulverized coal and solvent refined coal.

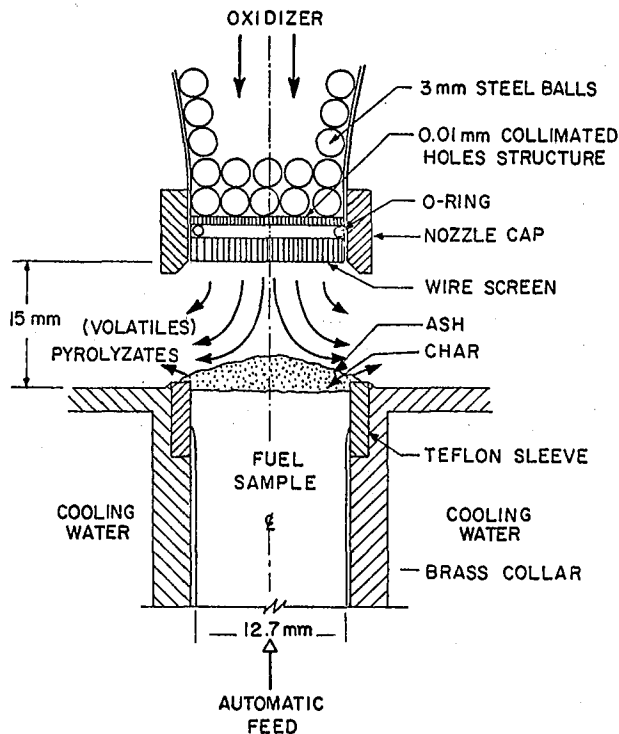


Fig. 1. Opposed flow diffusion flame apparatus for the study of the combustion of coal and coal related fuels. (XBL 798-6829)

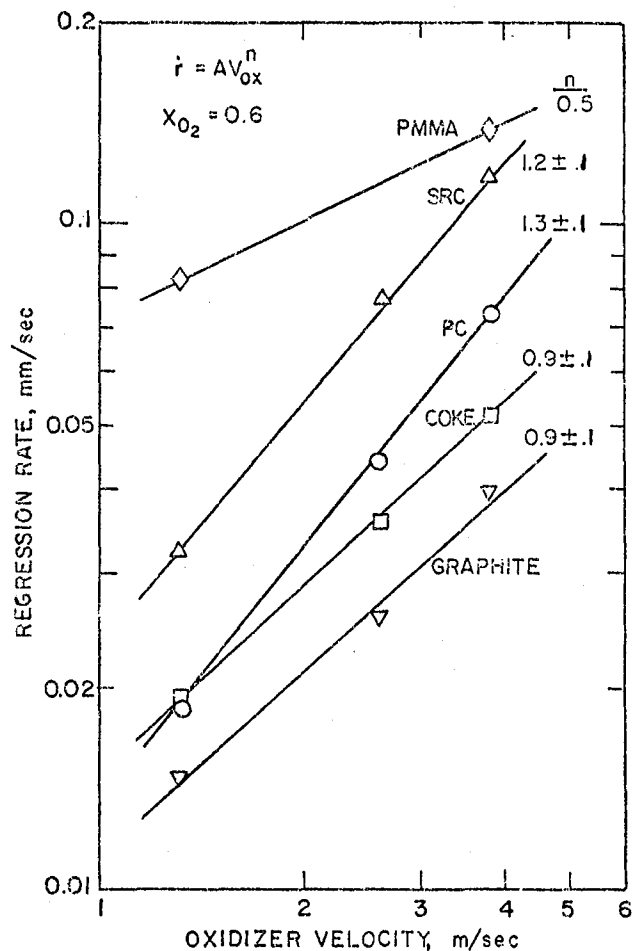


Fig. 2. Experimental burning rates for several fuels in a mixture of nitrogen and oxygen. (XBL 798-6852)

## ACCOMPLISHMENTS DURING 1979

The opposed flow diffusion flame apparatus, Fig. 1, was used to measure the combustion characteristics of coke, pressed pulverized graphite, and polymethylmethacrylate (PMMA) thereby completing the comparative study of these fuels. These fuels span the range of volatility from a fuel which completely volatilizes before combustion (PMMA) to one which produces essentially no volatilizations before combustion (pressed pulverized graphite). The effects of oxygen concentration in the gaseous flow were investigated and an approximately first order dependence was observed for all fuels. The effect of blowing velocity was investigated, and the results are summarized in Fig. 2. Unlike PMMA, which exhibits the expected square root dependence of burning rate on blowing velocity, the surface burning fuels show an approximately first order dependence on blowing velocity. This same figure shows that the relative burning rates of the fuels are ordered in the manner expected from the relative volatilities of the fuels.

Additional investigations were made of the gas phase combustion products, thermal diffusivity of the fuels under burning conditions, and effective

mass transfer numbers for the fuels under burning conditions. Attempts to resolve the relative importance of surface oxidation by oxygen and by carbon dioxide were not successful because of the confounding effects of surface radiation. Further work on this important problem is suggested which would require control of the surface heat flux (and thereby surface temperature) through irradiation from an external source.

## PLANNED ACTIVITIES FOR 1980

The present studies have been completed and no continuing research is planned for 1980.

## FOOTNOTE AND REFERENCES

\*This work was supported by LBL Director's Office Fund, Lawrence Berkeley Laboratory, Berkeley, California.

1. W. K. Chin, "The combustion of carbon, coal and coal related fuels in an opposed flow diffusion flame burner," Ph.D. thesis, College of Engineering, University of California, Berkeley (1979).

## OPTICAL MEASUREMENTS OF COMBUSTION PRODUCTS BY ZEEMAN ATOMIC ABSORPTION SPECTROSCOPY\*

*E. Cuellar and T. Hadeishi*

## INTRODUCTION

The characterization of emissions produced in the combustion of fossil and alternative fuels is of recognized importance in the search for new energy sources. Nitrogen- and sulfur-containing combustion products are particularly important as potential pollutants, since alternative and fossil fuels contain both of these species chemically bound to aromatic rings and hydrocarbon chains. With this in mind, we have initiated a research project aimed at the detection and measurement of small molecules containing nitrogen and sulfur by a non-intrusive, *in situ* optical technique called Zeeman Atomic Absorption (ZAA) Spectroscopy.

ZAA Spectroscopy was developed at Lawrence Berkeley Laboratory for the quantitative determination of atomic species with high specificity and high selectivity.<sup>1</sup> This technique was recently extended to the detection of small molecules which exhibit a sharp rotational structure when undergoing electronic transitions.<sup>2,3</sup> In the presence of an external magnetic field, the atomic energy levels may be split into Zeeman components whose separation is proportional to the strength of the magnetic field. Each new energy level can be described by a magnetic quantum number  $M_J$ , and transitions between these new states are given by the selection rule  $\Delta M_J = 0, \pm 1$ . The  $\Delta M_J = 0$  components are called  $\pi$  components and are normally not shifted or shifted very little from the zero-

field transition, whereas the  $\Delta M_J = \pm 1$  components, called  $\sigma$  components, are shifted symmetrically to shorter and longer wavelengths. The  $\pi$  and  $\sigma$  components can also be differentiated by virtue of their polarization. The  $\pi$  components have their electric vectors linearly polarized parallel to the magnetic field, while the  $\sigma$  components are linearly polarized perpendicular to the field.

The splitting of spectral lines produced by the magnetic field as well as the polarization of these lines form the basis for the background correction by the Zeeman effect. One of the Zeeman components of the emission line is tuned (by varying the strength of the magnetic field) into exact coincidence with a sharp vibrational-rotational transition in the electronic spectrum of the molecule to be detected. This matching component will indicate the extent of absorption by the molecule of interest plus any background absorption due to other species present. The unmatched Zeeman components indicate background absorption only. A differential measurement of the absorption of the matched and unmatched components provides a quantitative measurement of the molecule to be detected. Since both components of the light which is used to make the differential absorption measurement originate from the same source, any fluctuations in spatial and temporal intensity distributions are identical for both components and hence cancel out.

## ACCOMPLISHMENTS DURING 1979

We have applied the technique of Zeeman Atomic Absorption Spectroscopy to the detection of  $S_2$  in a reactive gas mixture.<sup>4</sup> The corrosive nature of  $S_2$  makes this species important in the combustion of coal, and it could be a significant component in a coal gasifier atmosphere. A block diagram of the experimental system is shown in Fig. 1. The light source is a magnetically confined arc lamp which is placed between the poles of a permanent magnet. The cathode is made of stainless steel on which a strip of nickel-chrome sheet is spot welded, and the anode is constructed from an automobile spark plug which is modified to minimize the likelihood of discharge to the chamber wall. Direct current power is supplied to the light source at a current between 30 and 100 MA. Discharge to the cathode results in intense Cr (I) atomic emission at 3017.57Å. In the presence of the magnetic field the atomic emission is split into its Zeeman components. The Zeeman splitting pattern for this transition is complex, resulting in seven closely spaced  $\pi$  and fourteen  $\sigma$  components, grouped symmetrically to shorter and longer wavelengths about the  $\pi$  components. One (or more) of the  $\pi$  components matches a discrete vibrational-rotational transition in the  $X^3\Sigma_g^- + B^3\Sigma_u^-$  electronic system of  $S_2$ . Ro-vibronic transitions for  $S_2$  have been calculated from the spectroscopic constants of these two electronic states,<sup>5</sup> and the  $S_2$  transitions involved can be assigned to either  $v'', J'' = 7, 13 \rightarrow v', J' = 2, 14$  or  $v'', J'' = 9, 31 \rightarrow v', J' = 3, 32$ .<sup>6</sup>

The Cr (I) emission is collimated and passed through a quartz cell containing a flowing mixture of  $H_2S$  and  $H_2$  (2.1%, 7.5% or 10%  $H_2S$ ). The gas mixture enters the cell through a 56 cm-long quartz side arm which can be heated to 1000°C. The cell itself is 24 cm long and is also heated to the same temperature. The variable phase retardation plate shown in Fig. 1 consists of a block of fused quartz mounted in a magnetic clamp. The applied stress produces a retardation of the phase of the light, and it alternately switches the matched and unmatched Zeeman components. The output of the photomultiplier tube is processed electronically and displayed on a strip chart recorder.

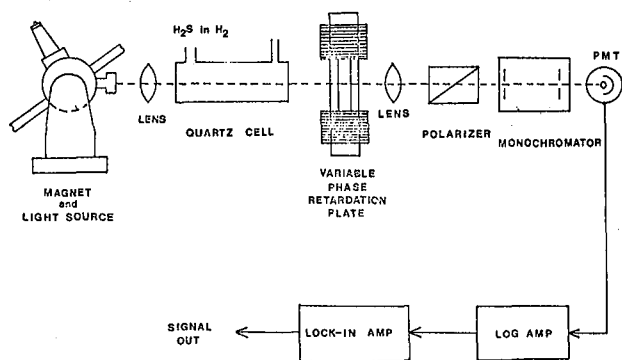


Fig. 1. Block diagram of the experimental apparatus. (XBL 802-8005)

$S_2$  is formed by the thermal decomposition of  $H_2S$  according to the reaction

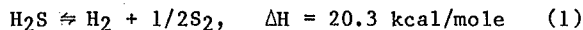


Fig. 2 shows the signal due to  $S_2$  obtained when a 10%  $H_2S$  in  $H_2$  mixture flowed through the cell at 760°C. As the gas temperature increases and  $H_2S$  decomposition increases, the intensity of the  $S_2$  signal increases. The main drawback of this flow measurement, however, is the difficulty in heating up the gas mixture. This is demonstrated by the dramatic increase in signal intensity when the gas flow is terminated. Figure 3 shows a similar result on a different scale. The lower trace records the gradual increase in  $S_2$  when the gas flow is terminated, followed by eventual decay as the  $S_2$  disappears from the optical path by reaction or diffusion out of the open cell. The upper trace records the signal output of the photomultiplier tube, and is in effect a measure of the absorption by all species present in the heated cell. The absorption level remains high even after the  $S_2$  has disappeared, indicating the presence of other species in the cell. A uv absorption spectrum revealed a vibrational progression characteristic of  $SO_2$ . The  $SO_2$  is probably formed by reaction with atmospheric oxygen backstreaming through the open end of the cell when flow was terminated. The presence of  $SO_2$ , however, does not interfere with the detection of  $S_2$ , although it may complicate the chemistry.

In order to quantify the results obtained on  $S_2$ , an evacuated cell was made containing a small amount of solid sulfur in a side arm. The side arm is immersed in a heated oil bath whose temperature determines the vapor pressure of sulfur.<sup>7</sup> The body of the cell is heated to about 750°C. At this temperature sulfur vapor exists mainly as  $S_2$ , with negligible amounts of  $S_4$ ,  $S_6$  and  $S_8$  present.<sup>8</sup> In this manner, an absolute calibration can be obtained. An additional correction for line-broadening needs to be considered, however, since the calibration cell is at low pressure while

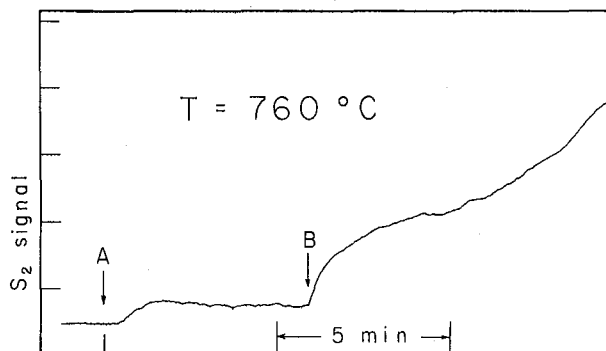


Fig. 2. Signal due to  $S_2$  formed by the thermal decomposition of  $H_2S$ .  $t = 0$  is the time at which the  $H_2S/H_2$  flow was started. The external temperature of the cell was 760°C. (XBL-802-8006)

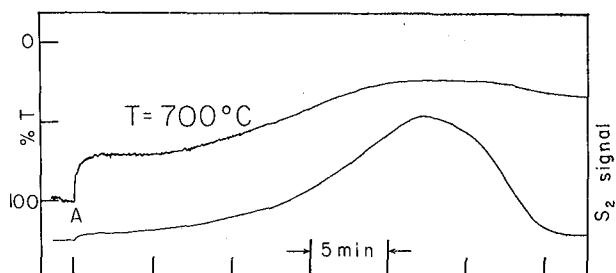


Fig. 3. The lower trace records the growth of the signal due to  $S_2$  when the gas flow is terminated. The upper trace records the presence of an additional absorbing species which was identified as  $SO_2$  (see text). (XBL 802-8007)

the flow cell measurement is near atmospheric pressure. We have not yet measured the broadened correction for  $S_2$ , but as a first approximation, we can assume it is the same as that for  $NO$ .<sup>9</sup> With this assumption, the signal shown in Fig. 2 is found to correspond to  $4.5 \times 10^{-5}$  atm of  $S_2$ .

A second estimate of the concentration of  $S_2$  can be made assuming thermodynamic equilibrium for reaction (1). At equilibrium, the  $S_2$  concentration is only a function of gas temperature. Assuming the gas temperature to be  $750^\circ C$ , then the predicted  $S_2$  concentration is  $5.6 \times 10^{-8}$  atm, three orders of magnitude lower than that obtained using the calibration with the evacuated cell containing sulfur.

#### PLANNED ACTIVITIES FOR 1980

We plan to continue our investigation on the detection and measurement of  $S_2$ . As indicated above, more work is needed on the problem of the calibration of the  $S_2$  signals. Furthermore, the broadening of the  $S_2$  absorption needs to be investigated. Two Mg atomic lines at 2928 and 2937Å can also be used for the detection of  $S_2$ . The Zeeman splitting pattern for Mg is much simpler than that for Cr, so these lines can be used to obtain the line shape of the absorbing transition of  $S_2$ .

Another area which we plan to explore is the detection and measurement of NO produced in a flat flame  $CH_4$ /air burner. The flat frame burner has been characterized, and the thermal NO produced can be compared with the results obtained using a conventional chemiluminescent analyzer. The Zeeman Atomic Absorption technique promises to be at least an order of magnitude more sensitive than the recent measurement by Hanson and co-workers<sup>10</sup> using a tunable diode laser.

A third area which we plan to investigate is the detection of  $NH_3$  by ZAA Spectroscopy. The first question to be answered is whether the electronic spectrum of  $NH_3$  has any sharp features

which can be Zeeman-tuned to an atomic emission line.  $NH_3$  is of considerable importance in combustion since the selective reduction of NO through  $NH_3$  addition to the post combustion gases<sup>11</sup> is under consideration as a potential control strategy to reduce  $NO_x$  emissions from stationary combustion sources. No satisfactory method to measure  $NH_3$  in the effluent gases has yet been developed.

#### FOOTNOTE AND REFERENCES

\*This work was supported by the Environment Division of the U.S. Department of Energy.

1. T. Hadeishi and R. McLaughlin, "Zeeman atomic absorption spectrometry," Lawrence Berkeley Laboratory report LBL-8031 (1978).
2. H. Koizumi, T. Hadeishi, and R. D. McLaughlin, Appl. Phys. Lett. **34**, 279 (1979).
3. H. Koizumi, T. Hadeishi, and R. D. McLaughlin, Appl. Phys. Lett. **34**, 382 (1979).
4. T. Hadeishi, A. V. Levy, D. P. Whittle, and E. Cuellar, "Determination of  $S_2$  in reactive gas mixtures by tunable atomic line molecular spectroscopy," presented at the 1979 Symposium on Instrumentation and Control for Fossil Energy Processes, Denver, Colorado, Aug. 20-22, 1979. Lawrence Berkeley Laboratory report LBL-9678 (1979).
5. K. P. Huber and G. Herzberg, Molecular Spectra and Molecular Structure IV. Constants of Diatomic Molecules, Van Nostrand-Reinhold Co., New York (1979).
6. A more accurate measurement requires inclusion of the spin fine structure of the rotational levels of  $S_2$ .
7. W. A. West and A. W. C. Menzies, J. Phys. Chem. **33**, 1880 (1929).
8. H. Braune, S. Peter, and V. Neveling, Z Naturforsch., **6a**, 32 (1951).
9. H. Koizumi, T. Hadeishi, and R. D. McLaughlin, "Nitric oxide determination utilizing a Zeeman-tuned, frequency modulated atomic line source," Lawrence Berkeley Laboratory report LBL-8188 (1979). To be published in Anal. Chem.
10. P. K. Falcone, R. K. Hanson, and C. H. Kruger, "Measurement of nitric oxide in combustion gases using a tunable diode laser," paper 79-53, presented at the meeting of the Western States Section of the Combustion Institute (October, 1979).
11. R. K. Lyan and J. P. Langwell, "Selective non-catalytic reduction of  $NO_x$  with  $NH_3$ ," EPRI  $NO_x$  Control Technology Seminar, San Francisco, California (1976).

# COMBUSTION SOURCES OF NITROGENOUS COMPOUNDS\*

R. D. Mathews<sup>†</sup> and R. F. Sawyer

## INTRODUCTION

Nitric oxide has been recognized as one of the more important combustion-generated air pollutants. It plays an important role in the formation of photochemical smog and can be transformed in the atmosphere to noxious substances such as nitrogen dioxide, nitrates, and perhaps other compounds. Approximately 95% of nitric oxide emissions are attributable to combustion sources. It has been traditionally held that nitric oxide is the only significant nitrogen-containing air pollutant emitted from combustion systems.

Other nitrogenous species have recently been identified in combustion products from a variety of combustion systems. Production of these other nitrogenous species is a cause for concern because molecular nitrogen, N<sub>2</sub>, is the only clearly innocuous N-species. Other members of the family of gas-phase nitrogenous species are odorants or lacrymators at low concentrations; affect visibility; play a role in the formation of photochemical smog; take part in atmospheric reactions which affect the ozone layer; are capable of shifting the energy balance of the earth; are toxic at low levels; are precursors of carcinogens; or are directly carcinogenic.

## ACCOMPLISHMENTS DURING 1979

A review of investigations reporting the measurement of nitrogenous compounds from combustion

systems was conducted. The matrix of species and combustion systems for which they have been identified are summarized in Table 1. The measurement of these compounds at low concentrations in combustion products is difficult and the quantitative results are often uncertain. Contrary to commonly accepted dogma, the oxides of nitrogen from some combustion devices at particular operating conditions can be dominated by nitrogen dioxide rather than nitric oxide. For example, both gas-turbine and diesel engines at idle or low-load operation have been observed to produce oxides of nitrogen which are more than 50% (in some cases up to 100%) nitrogen dioxide. Other nitrogenous compounds produced include nitrous oxide, N<sub>2</sub>O, ammonia and other amines, hydrogen cyanide and other nitriles. Catalytic devices used to reduce pollutant levels commonly lead to the formation of nitrogen compounds other than the desired N<sub>2</sub>. An estimate based on existing data, in some cases limited, indicates that the total combustion emission of gaseous nitrogenous species other than N<sub>2</sub> is apportioned as follows:

NO	76.3%
NO <sub>2</sub>	8.1%
N <sub>2</sub> O	15.5%
NH <sub>3</sub> , other amines	0.1%
HCN, other nitriles	0.03%
other	0.02%

Table 1. Combustion sources of nitrogenous compounds.

COMBUSTION SYSTEMS	GAS PHASE NITROGENOUS SPECIES DETECTED																															
	AMINES	AMMONIA	CYANOGEN	CYANO - ARENES	DIMETHYLAMINE	ETHYL CYANIDE	HYDROGEN CYANIDE	GLYCOLONITRILE	IMIDAZOLE	METHYL CYANIDE	MONOMETHYLAMINE	NITRIC OXIDE	NITROETHANE	NITROGEN DIOXIDE	NITROMETHANE	NITRO - OLEFINS	NITROSAMINES	NITROUS OXIDE	n - VALERONITRILE	PHENYL CYANIDE	PYRAZOLE	VINYL CYANIDE	I-NITRO-2-METHYL-1-PROPENE	I-NITRO-2-METHYL-2-PROPENE	2-METHYL-2-NITROPROPANE	2,4-DIMETHYL INIDAZOLINE	3-NITRO-2-METHYL-2-BUTENE	3-NITRO-3-HEXENE	3,6-DIPROPYL-1,2,4,5-TETRAZINE	β-KETO-1-NITROOCTANE		
Diesel Engines	•					•					•		•				▲															
Fires	•					•				•			•							•												
Gas Turbines							•	•	•	•			•	•	•				•		▲					•	•					
Laboratory Syst.	•	•	•	•		•					▲		•	•	•							▲										
Power Plants	•	•				•							•	•																		
Spark Ign. Engs.	•	•	•		•	•				•	•	•	•	•	•	•	•	•		•		•	•	•		•	•					

- Positively Identified
- ▲ Tentatively Identified

## PLANNED ACTIVITIES FOR 1980

This review has been completed.

## FOOTNOTES AND REFERENCE

\*This work was supported by the Environment Division of the U.S. Department of Energy.

†Department of Mechanical Engineering, University of Texas.

1. R. D. Matthews and R. F. Sawyer, "Combustion sources of unregulated gas phase nitrogenous species," Lawrence Berkeley Laboratory report LBL-10280 (Jan. 1980).

## PARAMETRIC STUDY OF SUBMICRON PARTICULATES FROM PULVERIZED COAL COMBUSTION\*

*J. Pennucci, R. Greif, F. Robben, and P. Sherman*

## INTRODUCTION

Recent studies have shown that very fine particles (50-1000 Å) represent a significant portion of the fly ash produced during the combustion of pulverized coal. While these particles represent only a small fraction of the mass of ash, they are extremely numerous.<sup>1</sup> A number of factors contribute to the health hazard of these particulates. Their small size allows them to be inhaled deeply into the lung and makes them difficult to remove from the stack gasses. Indications are that they may be enriched in certain toxic trace elements.<sup>1,2</sup> Because the noncombustible material in the coal is necessarily converted to ash, it should be in the form that is least hazardous and most easily cleaned, i.e., large particles.

A parametric study is currently being carried out to determine the effect of combustion and heat-transfer variables on the production of submicron particulates and to see if this provides a feasible method of controlling their production. This work was initiated in 1977 and an experimental system was built in 1978. A small amount of pulverized coal is entrained in a methane : air : oxygen mixture which is burned in a bunsen-type burner. Following combustion, a sample of fly ash is collected and prepared for examination in an electron microscope. The sampler design and electron microscope technique were described in detail in last year's annual report.

## ACCOMPLISHMENTS DURING 1979

The work during most of 1979 has focused on refining the system to provide the control of the combustion and heat-transfer parameters necessary to make a study of their effect on the particulate size distribution. The original bunsen burner has been abandoned and an enclosed burner was built. The reactants enter at the bottom of a 3/8 in. mixing tube 12 in. long. At the exit of the mixing tube, the flame is stabilized with a ceramic flameholder. The initial flame burns the methane and provides a stream of hot gasses in which the pulverized coal burns.

The coal combustion takes place in a sealed 2 in. ceramic chimney. The chimney prevents

ambient air from mixing with the flame and, by varying the wall temperature, provides a means of controlling the cooling rate. The cooling rate is reduced by adding insulation. As a means of increasing the cooling rate, water cooling was found to be relatively ineffective compared to the uninsulated ceramic. The uninsulated chimney cools a 1700K flame to 1000K over its 14 in. length; with insulation the exit temperature is 1350K. These arrangements correspond to cooling rates of 3000K/sec and 1500K/sec, respectively. Downstream of the chimney, dilution air is added to cool the gases for sampling.

By using small coal flow rates, the effect of the coal on the combustion temperature is minimized and the combustion parameters can be controlled with the gaseous components. To vary the flame temperature, the flow of methane is changed; a proportionate change in the oxygen concentration must be made to provide the same amount of oxygen for the coal. A total flow of 30 L/min has been selected; 8 to 12% of this is methane. By concurrently increasing the oxygen concentration from 26% to 37%, a flow of 2.5 L/min of oxygen is maintained for coal combustion. A coal flow rate of 0.5 g/min will consume 1 L/min of the oxygen. As a separate trial, the flow of excess oxygen is varied from 1.5 - 4.5 L/min.

Additional work performed this year includes construction of the thermocouples used to obtain the temperature profiles in the chimney and the development of a new coal hopper that produces a flow of 0.5 g/min. The hopper uses a jet of air to entrain coal particles from the surface of a fluidized bed. The coal flow rate is controlled by adjusting the air flow but is also affected by the coal level and particle size. If the runs are kept short, the variation in the flow rate is small and does not affect the overall combustion significantly.

## PLANNED ACTIVITIES FOR 1980

Samples have been collected over the range of conditions that can be achieved with the burner and they are currently being analyzed. The matrix of combustion conditions varies the initial temperature, oxygen concentration and cooling rate. The

dependence of the particle size distribution on these parameters will be analyzed in terms of the possibilities for control, and for the existence of condensation as the dominant formation mechanism of the small particulates.

#### FOOTNOTES AND REFERENCES

\*Supported by the Basic Energy Sciences Division of the Department of Energy.

†Aerospace Engineering Department, University of Michigan, Ann Arbor.

1. J. A. Campbell, J. C. Laul, K. K. Nielsen, R. D. Smith, "Separation and chemical charac-

terization of finely-sized fly-ash particles," Anal. Chem. 1032 (July 1978).

2. R. L. Davison, F. S. Natush, J. R. Wallace, "Trace elements in fly-ash dependence of concentration on particle size," Envir. Sci. and Tech. (Dec. 1974).
3. P. M. Sherman, A. F. M. Akhtaruzzaman, F. Robben, R. Grief, "Submicron particulates generated by combustion of pulverized coal," Lawrence Berkeley Laboratory report UCID-8044 (Aug. 1978).

## SURFACE CATALYZED COMBUSTION\*

*R. Schefer and F. Robben*

### INTRODUCTION

Catalyzed combustion has been proposed as a method for promoting efficient burning of a variety of conventional and future alternative fuels with a minimum of pollutant formation.<sup>1</sup> While preliminary tests have been quite promising, a number of aspects of catalyzed combustion are either not well understood or the necessary data are lacking. Necessary steps for the development of an optimum catalyst design will be (1) to develop a greater understanding of the role of the catalyst in the combustion process, and (2) to determine high-temperature catalytic surface reaction mechanisms and reaction rates. It is the goal of the present study to provide some of the necessary understanding and data for catalytic combustor design.

Previous work has provided a detailed study of the combustion characteristics of lean H<sub>2</sub>/air mixtures flowing over a platinum catalytic surface.<sup>2</sup> Some regions were identified in which only surface reaction was present and others, at higher equivalence ratios and surface temperatures, in which both surface reaction and stable gas phase boundary layer combustion occurred simultaneously. Surface energy release rates were measured for H<sub>2</sub>/air mixtures on a platinum surface and from these measurements a model was developed for the high temperature surface oxidation of H<sub>2</sub>.<sup>3</sup> Based on this model and known gas-phase kinetic data for H<sub>2</sub>/air reactions, a numerical computational scheme was developed for modeling H<sub>2</sub>/air combustion in the presence of a catalytic surface and the effect of catalytic surface reactions on gas-phase combustion was investigated.<sup>4</sup>

### ACCOMPLISHMENTS DURING 1979

Planned activities during 1979 included an extension of the above study to typical hydrocarbon fuels flowing over catalytic surfaces. Surface reaction rate data obtained for these fuels, and models were developed for surface and gas phase

reactions. Measurements over a noncatalytic surface were planned to further aid in developing an understanding of the role of the catalyst surface.

During FY 1979 the combustion of lean propane/air mixtures flowing over a platinum catalytic surface and a quartz (SiO<sub>2</sub>) noncatalytic surface was studied using differential interferometry for gas phase temperature field visualization. The range of equivalence ratios and surface temperatures was determined under which gas phase and surface reaction were present. A typical interferogram for the platinum surface is shown in Fig. 1 for a plate temperature of 1250°C and an equivalence ratio of 0.8. The displacement of the interference fringes from their undisturbed position (at a 45° angle to the plate surface) is proportional to the local temperature gradient. It can be seen that the combustion process typically consists of an induction period during which little increase in thermal boundary layer thickness occurs, followed by a downstream region where gas-phase heat release (thermal ignition) results in a significant increase in thermal boundary layer thickness. The point at which thermal ignition occurs moves upstream toward the plate leading edge as the equivalence ratio or plate temperature is increased. With a noncatalytic surface, no such induction period was observed, and thermal ignition occurred very near the plate leading edge. These results strongly support the results of previous numerical calculations for H<sub>2</sub>/air mixtures over a platinum surface which showed a delay in the onset of gas-phase combustion due to the depletion of fuel and radical species near the catalyst surface. Gas-phase combustion with an SiO<sub>2</sub> surface was also observed at surface temperatures up to 100°C lower under comparable conditions than with the platinum surface.

Extensive Rayleigh scattering measurements of gas density were taken for lean H<sub>2</sub>/air mixtures flowing over an SiO<sub>2</sub> noncatalytic surface. A comparison with similar data taken over a platinum surface again provided experimental verification

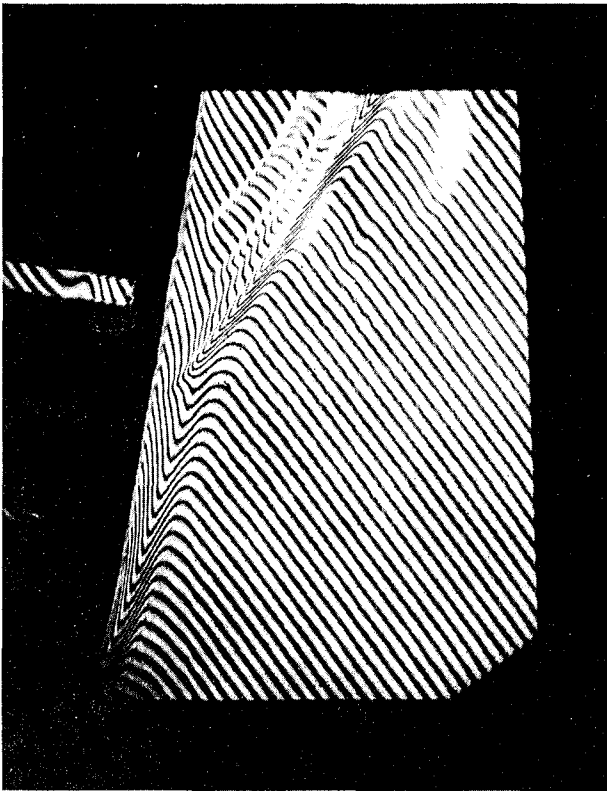


Fig. 1. Interferogram of the flat plate boundary layer for propane/air combustion on a platinum surface.  $\phi = 0.8$ ,  $T_s = 1250$  K,  $U_\infty = 1.5$  m/s. (XBB 790-16549)

of the quenching effect of the catalyst surface on gas-phase reaction due to the depletion of fuel and radical species near the plate surface. This can be seen from Fig. 2 where experimentally measured thermal boundary layer thicknesses are shown as a function of distance from the plate leading edge for platinum and  $\text{SiO}_2$  surfaces at the same temperature. For comparison, the corresponding numerical results for the case of no combustion are also shown. The agreement between experimental results with the platinum surface and the numerical results for no combustion heat release indicates very little gas-phase heat release. In the case of the relatively noncatalytic  $\text{SiO}_2$  surface, the presence of heat release due to gas-phase combustion results in a significant thickening of the thermal boundary layer. This effect is in agreement with that predicted previously by the numerical calculations.

The numerical computational scheme was modified to include multicomponent diffusion coefficients and thermodiffusion of gas species. These modifications represent a more realistic approximation to species transport and should improve agreement with the experimental results. The kinetic scheme was also modified to include reactions involving  $\text{H}_2\text{O}_2$ .  $\text{H}_2\text{O}_2$  should be important in lower temperature regions, away from the surface where it effectively acts as a radical scavenger and, it appears, could reduce the high predicted heat-release rates.

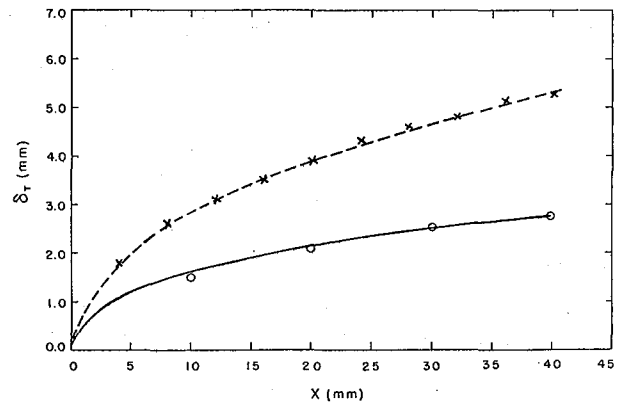


Fig. 2. Thermal boundary layer thickness as a function of distance from the plate leading edge for  $\text{H}_2/\text{air}$  combustion.  $\phi = 0.2$ ,  $T_s = 1070$  K,  $U_\infty = 1.5$  m/s; x -  $\text{SiO}_2$  surface; o - platinum surface. Solid line indicates numerical results for the case of no combustion. (XBL 802-8008)

#### PLANNED ACTIVITIES FOR 1980

During FY 1980, work will continue on determining gas phase and surface ignition characteristics of conventional hydrocarbon and future alternative fuel/air mixtures flowing over a catalytic surface. From this additional data, it will be possible to determine with greater certainty the precise role of the catalyst and to determine both reaction mechanisms and kinetic constants for surface and gas-phase reactions. Catalyst operation under fuel-rich conditions will also be investigated with the emphasis on soot-formation characteristics in the presence of a high-temperature catalyst.

#### FOOTNOTE AND REFERENCES

\*This work was supported by the Division of Fossil Fuel Utilization of the U.S. Department of Energy.

1. W. C. Pfefferle, "The catalytic combustor: an approach to cleaner combustion," *J. Energy* 2, 3, 142 (1978).
2. R. W. Schefer, F. Robben, and R. K. Cheng, "Catalyzed combustion of  $\text{H}_2/\text{air}$  mixtures in a flat plate boundary layer: I. Experimental results." To be published in *Combustion and Flame* (1980).
3. R. W. Schefer, R. Cheng, F. Robben, and N. Brown, "Catalyzed combustion of  $\text{H}_2/\text{air}$  mixtures on a heated platinum plate." Western States Section/The Combustion Institute, Boulder, CO (1978).
4. R. W. Schefer, "Catalyzed combustion of  $\text{H}_2/\text{air}$  mixtures in a flat plate boundary layer. II. Numerical results." Western States Section/The Combustion Institute, Stanford, CA (1977).

## COMBUSTION CHARACTERISTICS OF SPOUTED BEDS\*

R. F. Sawyer, H. A. Arbib<sup>†</sup> and F. J. Weinberg<sup>†</sup>

### INTRODUCTION

Spouted beds have found their primary application in the drying of grain and other agricultural products, coating application, and the mixing of solids. Khoshnoodi and Weinberg<sup>1</sup> were apparently the first to report on the use of a spouted bed as a combustor. Their interest focused on the spouted bed as a heat recirculation device, and the resulting possibility of extending the lean flammability limit of premixed gaseous reactants. Others are studying the use of spouted beds as exothermic chemical reactors for the gasification of coal.<sup>2,3</sup>

A cooperative research effort with the Combustion Research Group of the Department of Chemical Engineering and Chemical Technology at Imperial College, London was established. This activity includes cooperative research efforts on other combustion topics which have been conducted through an exchange of personnel.

The present work focuses on the interaction of combustion with the spouted bed fluid mechanics. Particular attention is paid to those processes which control the lean flammability limit and to assessing the effectiveness of the simple spouted bed as a heat recirculation device. Cylindrical geometry with a high velocity reactant injection at the apex of an inverted cone was used in all cases. If one broadens the concept of a spouted bed to include all granular beds in which the solid phase is transported by a gaseous reactant feed, then other geometries can be conceived which provide better control of the relative motions of the gaseous and solid phases. The optimization of such combustors in terms of increasing power densities, widening stability limits, increasing combustion efficiency, reducing pollutant emissions, and improving heat transfer characteristics will depend upon an improved understanding of the controlling physics and chemistry of combustion in these spouted bed devices. The objective of our work is to expand this understanding.

### ACCOMPLISHMENTS DURING 1979

The combustion characteristics of a spouted bed were studied to determine the interaction between bed fluid mechanics and the combustion process. A cylindrical geometry, particles 500 to 1000  $\mu\text{m}$  diameter, and methane/air reactants were

employed. Combustion reduces the entrance jet velocity at which a spout can be maintained, increases particle circulation rates, and increases spout height in comparison with operation at identical conditions without combustion.

Measurement of bed temperatures revealed that the particle temperature remains approximately constant. Particle-gas contact times are inadequate to allow these two phases to approach thermal equilibrium. Accordingly, the minimum lean flammability limit which could be obtained was approximately 75% of ordinary flammability limit, higher than the 50% predicted if the particle temperature were to reach the exit gas temperature.

### PLANNED ACTIVITIES FOR 1980

Based on the work conducted at Imperial College, a spouted bed facility will be assembled, fabricated, and characterized in the combustion laboratories at Berkeley. A rectangular two-dimensional geometry with a slotted spout will provide better access for the studying of fluid and particle motions. Mapping of the temperature, gas and particle velocities, and local composition is sought to fully characterize the interactions between combustion and bed fluid mechanics.

### FOOTNOTES AND REFERENCES

\*Professor Sawyer's participation in this research while at Imperial College was sponsored by the University of California, Department of Mechanical Engineering, through sabbatical leave support.

<sup>†</sup>Department of Chemical Engineering and Chemical Technology, Imperial College of Science and Technology, London.

1. M. Khoshnoodi and F. J. Weinberg, "Combustion in spouted beds," Combustion and Flame **33**, 11-21 (1978).
2. National Coal Board, Personal communication, Coal Research Establishment, Stoke Orchard, Cheltenham, England (May 1979).
3. J. F. Davidson, Personal communication, University of Cambridge, Chemical Engineering Department (May 1979).

## COMBUSTION FLUID MECHANICS

### FLAME PROPAGATION IN GRID INDUCED TURBULENCE\*

R. G. Bill, Jr., I. Namer, R. K. Cheng, F. Robben, and L. Talbot

#### INTRODUCTION

The importance of the effect of fluid mechanical turbulence on combustion is well known (see, for example, the recent review of Andrews et al.<sup>1</sup> in which flame speed is correlated with turbulent intensity and scale). Precise measurements of these effects in well characterized flows, however, have been notably lacking due to the inherent difficulty of measurements in flows with combustion. The present study, begun in FY 1979, seeks to quantify the effect of grid-generated turbulence on a rod-stabilized, V-shaped, premixed,  $C_2H_4$ -air flame.

The initial objectives of the study are to correlate measurements of the turbulent flame speed with turbulent parameters, such as scale and intensity, and to study the evolution of length scales and turbulent kinetic energy through the flame front. The long-term objective of the study is to characterize the statistical nature of the turbulent combustion process sufficiently enough to provide a means of testing and improving the assumptions of numerical models of turbulent combustion, such as that of Bray and Libby.<sup>2</sup> In this regard, our study is one of several ongoing experiments which have been undertaken due to the abundance of background data available from noncombustion studies and the experiment's amenability to numerical modeling. These experiments include an experimental study of  $H_2$ -air combustion in a turbulent boundary layer, and the interaction of a vortex street with a plane flame front. Since these flows have been well characterized without combustion, the effect of combustion may be readily determined.

#### ACCOMPLISHMENTS DURING 1979

During this period, Laser Doppler Velocimetry (LDV) measurements of the streamwise velocity component were obtained upstream and through a V-shaped, premixed,  $C_2H_4$ -air flame stabilized on a rod downstream of a turbulence-generating grid. The measurements were obtained using the combustor and computerized data-acquisition system described in the previous LBL annual report (FY 1978). The LDV system used is of the intersecting dual-beam type with real fringes. An equal path-length beam splitter with a fixed separation of 5 cm is used and the two laser beams are focused by a 250 mm focal length lens to form the scattering volume. Seed particles of  $Al_2O_3$  are introduced into the air supply prior to the stagnation chamber. Scattering bursts from the particles are collected 90° from the forward scattering direction by a lens, filter and photomultiplier tube assembly. The frequency of the bursts are obtained using a TSI 1090 frequency tracker.

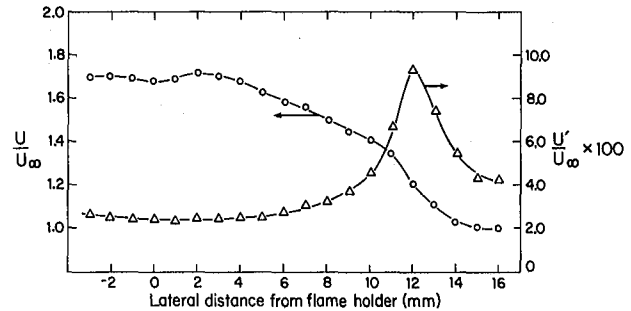


Fig. 1. Mean and rms velocity in grid induced turbulence. (XBL 801-159)

In Fig. 1, typical LDV measurements of the mean and rms levels of the streamwise velocity component are shown at a location 8 cm downstream of a grid with a mesh size of 5 mm. The y coordinate is normal to the free stream. The grid Reynolds number of 700 is slightly above the lower limit reported by Batchelor and Townsend<sup>3</sup> for grid turbulence. The particle arrival rate was approximately 8000/sec and the sampling rate was 2000 samples/sec. The position of the flame holder corresponds to  $y = 0$ ; while the position,  $y = 16$ , corresponds to a point upstream of the flame front. As the flame front is approached, the gas density drops, and the flow is accelerated. A sharp rise in the fluctuation level occurs at the flame front. Beyond the reaction zone, the fluctuation level drops sharply with the turbulence intensity dropping below the level induced by the grid. We note that theoretical predictions of Bray and Libby<sup>2</sup> indicate net turbulent kinetic energy may be either produced or destroyed by the flame front depending upon competing production terms related to mean shear and loss terms related to mean flow dilation.

In addition to these time-averaged measurements, computer programs have been completed which will allow the time series data to be interpreted in terms of the autocorrelation functions, the power spectra, and the probability density function. The data have been recorded on 7-track digital magnetic tape and is currently being analyzed on the CDC 7600 computer.

#### PLANNED ACTIVITIES FOR 1980

During FY 1980, velocity measurements obtained using LDV will be analyzed to provide information concerning the evolution of length scales through the flame front. Density measurements will then be

made under the same flow condition using Rayleigh scattering. Since the flame front is more precisely defined by density measurements than by velocity measurements, profiles of mean and rms density will be important in the interpretation of velocity data.

In order to measure the flame propagation speed, measurements of the normal velocity component will be obtained with LDV. These measurements, along with the previously measured streamwise component, will allow us to produce a map of the mean flow streamlines, hence the flame propagation velocity. Finally, in order to obtain further comparisons of our experiment with numerical models, cross correlation of density and velocity will be obtained using Rayleigh scattering and LDV. This will be necessary since models such as that of Bray and Libby<sup>2</sup> use density-weighted time averaging.

## COMBUSTION IN A TURBULENT BOUNDARY LAYER\*

R. K. Cheng, R. G. Bill, Jr., T. T. Ng, F. Robben, and L. Talbot

### INTRODUCTION

The goal of this program is to study the interaction of turbulence with combustion in a heated turbulent boundary layer where premixed combustion can occur. The experimental results are to be compared with numerical modeling results in order to assist in the formulation of suitable approximations for turbulent combustion as well as to critically evaluate numerical modeling approximations.

The turbulent boundary layer is a classical fluid mechanics problem; experimental and theoretical studies on the subject have been quite extensive. The nature of the turbulence in the boundary layer is relatively well understood, making it possible to investigate the change in the scale and intensity of turbulence as a result of combustion. The heated boundary layer is quite suitable for combustion studies as it can support combustion under a wide range of equivalence ratios from rich to very lean. The combustion heat release can be adjusted to occur throughout the boundary layer, permitting detailed study of the interaction of the exothermic combustion process with the turbulent flow field.

### ACCOMPLISHMENTS DURING 1979

An experimental study of lean H<sub>2</sub>-air combustion supported by the turbulent boundary layer over a heated surface has been completed. It was carried out in the 2.5 cm square channel 7.5 cm in length, shown schematically in Fig. 1. The heated wall was lined with five heating strips made of Kanthal, a high-temperature, iron-base heating alloy. This arrangement provided surface temperatures approaching 1500K. The premixed air and fuel was supplied by a cylindrical stagnation chamber, and the assembly was mounted on a three-axis, computer-controlled, stepping-motor-driven traverse mechanism.

### FOOTNOTE AND REFERENCES

\*This work was supported by the Air Force Office of Scientific Research through the University of California, Berkeley, Campus Research Office.

1. G. E. Andrews, D. Bradley, and S. B. Lwakabamba, "Turbulence and turbulent flame propagation—a critical appraisal," *Combustion and Flame*, **24**, 285-304 (1975).
2. K. H. C. Bray and P. A. Libby, "Interaction effects in turbulent premixed flames," *Phys. of Fluids*, **19**, 1687-1701 (1976).
3. G. K. Batchelor and A. A. Townsend, "Decay of isotropic turbulence in the initial period," *Proc. Roy. Soc. A*, **193**, 539-558 (1948).

Three well-developed laser diagnostic techniques have been used. Differential interferometry provided a convenient means to display and study the density gradient pattern, the intensity of Rayleigh scattering gave the local time resolved gas density, and the Laser Doppler Velocimetry (LDV) gave the local velocity. The Rayleigh and LDV systems were interfaced with the PDP 11/10 computer controlled data acquisition system,<sup>1</sup> and the Fortran

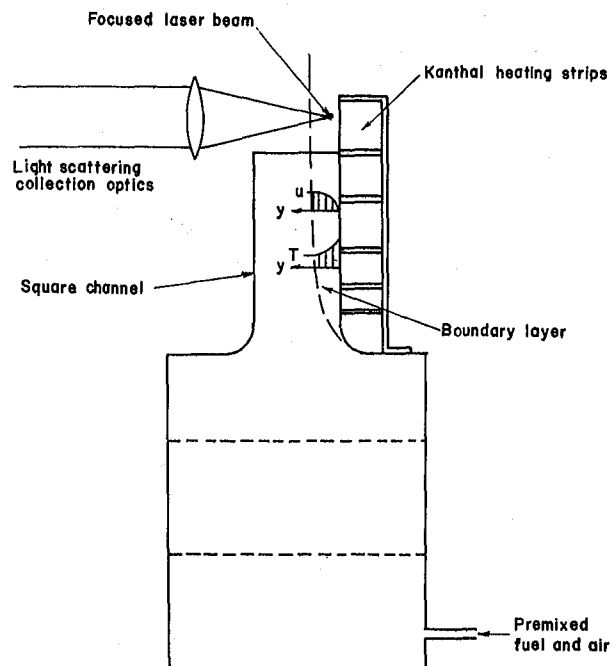


Fig. 1. Schematic of the 2-5 cm square channel. (XBL 796-10211)

software was developed for data processing. Mean and root-mean-square (rms) values of density and velocity and their probability density functions (pdf) have been calculated using the PDP 11/10 computer. Further statistical analyses to obtain the auto-correlation and spectral density functions have been carried out using the CDC 7600 computer at LBL.

The maximum free-stream velocity obtained was about 20 m/sec, giving a Reynolds number at the measurement point of  $3 \times 10^5$ , about the minimum necessary to sustain a transition regime turbulent boundary layer. The velocity fluctuation level in the nonheated boundary layer was about 6% of the free stream velocity,  $U_\infty$ , somewhat higher than expected. The high fluctuation level is attributed to the relatively uneven surface provided by the heating strips which induces unsteady motion in the boundary layer. Comparison of mean velocity profiles with empirical velocity-defect laws for a fully developed turbulent boundary layer<sup>2</sup> is shown in Fig. 2. It can be seen that the data is quite good. Also, the distribution of fluctuation intensity in the boundary layer is found to be in good agreement with observations of fully developed turbulent boundary layers. Nevertheless, due to the low Reynolds number, the boundary layer here cannot be regarded as typical for a fully developed turbulent boundary layer.

The use of LDV in a heated boundary layer is seriously handicapped by the movement of seed particles due to thermophoretic force.<sup>3</sup> However, data, obtained in the outer region of the boundary layer where the particle count rate was adequate, indicates that the mean velocities in the boundary layer are decreased by wall heating and combustion, while the fluctuation level is increased by wall heating, but decreased when combustion occurs. The apparent turbulence damping effect of combustion may be associated with induced cross-stream motion of the flow by the combustion heat release.

Examples of mean and rms density profiles are shown in Fig. 3. The change in the shape of the mean profiles indicates heating due to combustion. At an equivalence ratio,  $\phi$ , of 0.1, heat release

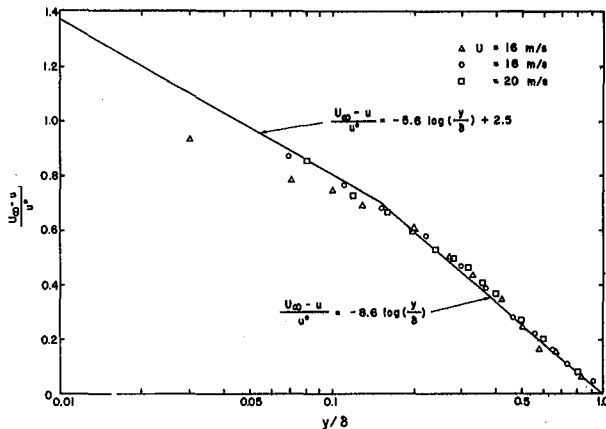


Fig. 2. Comparison of velocity profiles in the non-heated turbulent boundary layer with the empirical velocity defect laws. (XBL 796-10218)

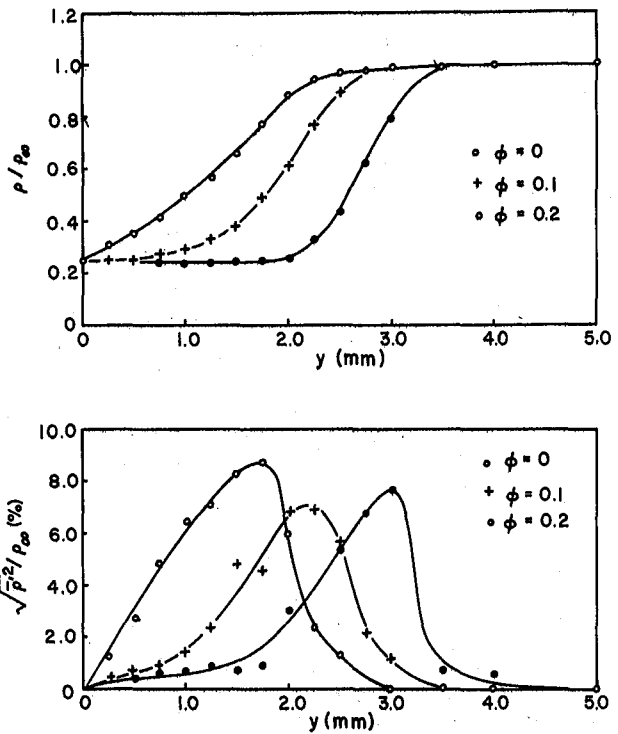


Fig. 3. Density  $\rho$  and rms fluctuation  $\rho'^2$  profiles in a heated boundary layer with and without combustion.  $T_W = 1120K$ ,  $U_\infty = 20.0$  m/s. (XBL 796-10215)

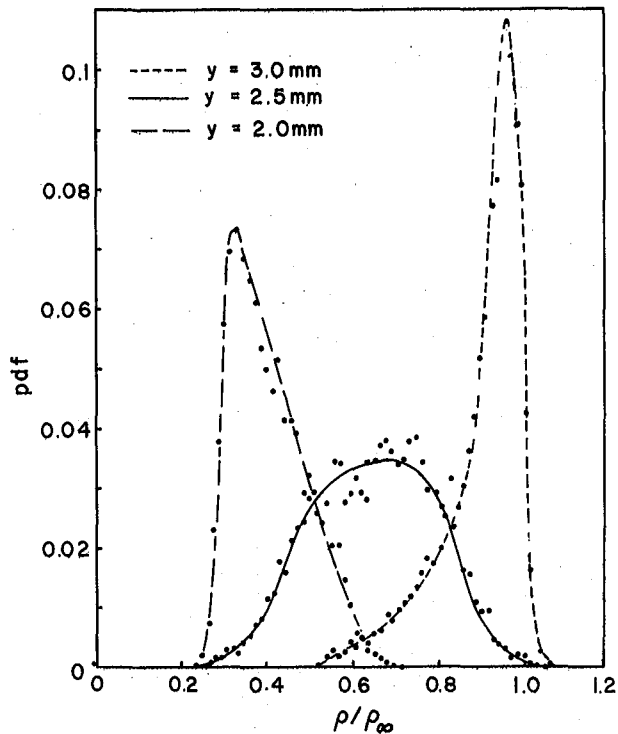


Fig. 4. Density probability density function at three positions in a heated boundary with combustion,  $T_W = 1120K$ ,  $U_\infty = 10.0$  m/s. (XBL 796-10217)

takes place throughout the boundary layer. At  $\phi = 0.2$ , the heat release zone, characterized by the S-shaped density distribution, moves away from the wall and forms a flame-like structure. The maximum fluctuation intensity for all cases occurs near the point of maximum density gradient and does not appear to be strongly dependent on the thermodynamic or combustion parameter.

The density pdf's for three points along the flame-like structure are shown in Fig. 4 where  $y = 2.5$  corresponds to the peak fluctuation point and  $y = 2.0$  and  $3.0$  corresponds to the edges of the hot and cold regions. The pdf for  $y = 2.5$  mm is quite symmetrical and extends almost from the cold to the hot levels, while the ones for  $y = 2.0$  and  $3.0$  are skewed. The high probability for cold and hot gas to penetrate into  $y = 2.5$  mm seems to indicate cross-stream oscillation of the reaction zone.

The spectral density distribution for the  $y = 2.5$  mm point of Fig. 4 is shown in Fig. 5. The peak centered at about 450 Hz is quite apparent. Discrete peaks at other frequencies are found in most of the spectral density distributions for cases involving combustion; they are most pronounced at the highest fluctuation points. These fluctuation frequencies do not correlate with any thermodynamic or combustion parameter and are too low to be associated with the characteristic acoustic frequencies of the channel. The most likely origin of these fluctuation frequencies could be associated with the geometry of the heated Kanthal surface where ignition occurs. These results were presented at the 2nd Symposium on Turbulent Shear Flow;<sup>4</sup> a more detailed publication is under preparation.

Construction of a larger experimental system based on a horizontal wind-tunnel with a 10 cm square channel test section has been completed. The wind tunnel is driven by a centrifugal pump and is mounted on a 3-axis stepping-motor-controlled traverse mechanism. The channel is 1 m long with the last 30 cm of the lower wall lined with 9 Kanthal strips stretched over a ceramic block. The length of the channel enables the boundary layer to more nearly approach fully developed turbulence. Preliminary surveys of the flow field have been carried out by hot-wire anemometry. Typical boundary layer thickness at  $U_\infty = 20$  m is about 10 mm with about 6% rms fluctuation level. The mean profiles compare quite well with those of a fully developed turbulent boundary layer. Density measurements in the heated boundary layer without combustion are currently being undertaken.

#### PLANNED ACTIVITIES FOR 1980

Studies of lean combustion in the heated boundary layer of the 10 cm channel will be carried out. Density and the streamwise and cross-stream components of the velocity will be measured. Particular attention will be paid to the initiation of combustion reactions in a well-developed turbulent boundary layer by having the heated surface section begin

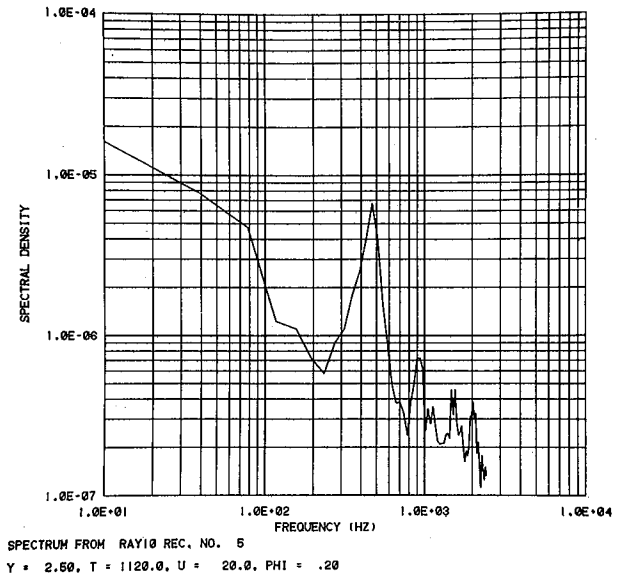


Fig. 5. Energy spectrum of density fluctuations at the maximum intensity point in a heated boundary layer. (XBL 7912-5216)

only after a cold turbulent boundary layer has been formed. The experimental results will be processed to obtain the statistical functions, and the dependence of these functions on combustion will be obtained. For further analysis of the results, simple statistical modeling of the flow will be undertaken, and the modeling parameters will be varied in an effort to obtain agreement with the experiment. Presumably, this will lead to a phenomenological characterization of the experimental results and to further insight into turbulent combustion processes.

#### FOOTNOTE AND REFERENCES

\*This work was supported by the Basic Energy Sciences Division of the Department of Energy.

1. R. G. Bill, Jr. I. Namer, R. K. Cheng, F. Rodden, and L. Talbot, "Flame propagation in grid induced turbulent flow," Article 11, this report.
2. H. Schlichting, *Boundary Layer Theory*, McGraw-Hill, New York (1968).
3. L. Talbot, R. K. Cheng, R. Schefer and D. R. Willis, "Thermophoresis of particles in a heated boundary layer," Article 21, this report.
4. R. K. Cheng, R. G. Bill, Jr., F. Robben, R. W. Schefer, and L. Talbot, "Experimental study of combustion in a turbulent boundary layer," Proceedings of the 2nd Symposium on Turbulent Shear Flows, Imperial College, London (July 2-4, 1979). Also Lawrence Berkeley Laboratory report LBL-8946 (1979).

# CHEMICALLY REACTING TURBULENT FREE SHEAR LAYERS\*

J. W. Daily, J. D. Keller, and R. W. Pitz

## INTRODUCTION

Most flames of industrial interest burn in turbulent free-shear flows. These flames are of 2 types: diffusion flames and premixed flames. Diffusion flames are characterized by fuel on one side of the shear layer and oxidizer on the other side. The reaction rate is controlled by molecular diffusion; hence the name "diffusion flame." Premixed flames consist of a premixed fuel and oxidizer flow on one side of the layer and hot products on the other side. This flame is stabilized by the diffusion of heat which raises the reactants to the ignition temperature. There is a strong interest in lean premixed combustion since it shows promise in solving the  $\text{NO}_x$  pollution problem. Recent research in turbulent-free shear layers has given a new direction to understanding reacting flows.<sup>1</sup> The existence of large-scale structures which have a very distinct behavior has opened up a new approach to the problem of turbulence. The existence of these structures leads to a deterministic approach to turbulence and turbulent combustion rather than a statistical one.

## ACCOMPLISHMENTS DURING 1979

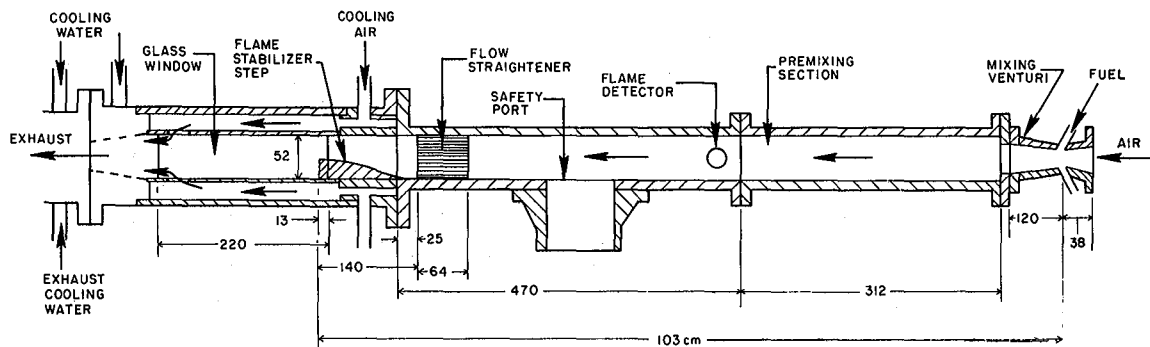
Our test facility is a turbulent combustion tunnel with flow over a rearward facing step. The tunnel is equipped with quartz side windows which allow optical access (Fig. 1). This facility is capable of making the following types of flow measurements:

1. Hotwire anemometry and LDV measurements of the mean flow and turbulent quantities.
2. Rayleigh scattering total number density measurements.
3. Laser schlieren power spectra.
4. Schlieren movies of the flow.

The hotwire, Rayleigh, LDV and schlieren systems are of the standard type. Our laser is mounted on top of a milling table equipped with a stepping motor for the vertical scanning direction. This has the capability of being interfaced with an 11/34 PDP computer. Software has been developed to handle the data taking and perform on-line data manipulations. This software gives us the ability to evaluate the validity of the data as well as to immediately plot the data in final form.

We have conducted a study of premixed combustion on the 2-D shear layer. In characterizing the entrance flow, we found the power spectra remarkably similar to that found at the exit of gas turbine compressors (Fig. 2). The power spectrum was smoothed substantially by packing the mixing section of the test facility with steel wool and employing turbulence damping screens. The power spectra and autocorrelation functions are now typical of grid turbulence. Experiments were then performed studying the effects of combustion on the layer. The results show relatively little effect on the structure due to combustion. It can be seen from schlieren and LDV measurements that the main effect is a shifting of the layer downward toward the hot side (Fig. 3).

The shear layer may be divided into 2 distinct processes. First, entrainment is the engulfment of irrotational fluid into the shear layer; and second, mixing is the microscopic molecular mixing within the large-scale structures. Konrad and Breidenthal have shown that the mixing process is separate from the entrainment process.<sup>2,4</sup> The mixing process is a strong function of the Reynolds number; however, the 2-D large scale structure is not.<sup>3</sup> This raises the question, which of the two processes is the governing process in combustor flows? By examining the schlieren movies of the flow, and by calculating the characteristic times in the flow, one can show that this combustion process is entrainment limited.<sup>5</sup>



EXPERIMENTAL APPARATUS

Fig. 1. Two-dimensional combustor test section (dimensions in mm). (XBL 794-9131)

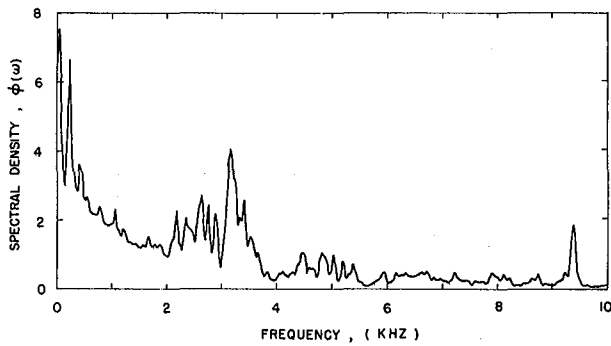


Fig. 2. The power spectrum of the axial velocity measured by hot wire ( $U_0 = 13.2$  m/s,  $x = 0$  mm,  $y = 12.5$  mm,  $R_h = 2.2 \times 10^4$ ). (XBL 802-8229)

#### PLANNED ACTIVITIES FOR 1980

We are actively installing a new 2 stream test facility (Fig. 4). With this facility we will continue our studies of combustion on the free shear layer. This facility will enable us to examine many more flow configurations than is now possible. The facility has the capability of varying the pressure gradient along the flow axes. Hence the influence of the apparatus can be reduced. We also have visual access in both the horizontal and vertical planes which will allow studies of the three dimensionality of this flow.

#### FOOTNOTE AND REFERENCES

\*This work was supported by the National Science Foundation through the Engineering Office of Research Services, University of California, Berkeley.

1. G. Brown and A. Roshko, *J. of Fluid Mech.*, 64, 775 (1974).
2. R. E. Breidenthal, Ph.D. thesis, Calif. Inst. of Technology (1978).

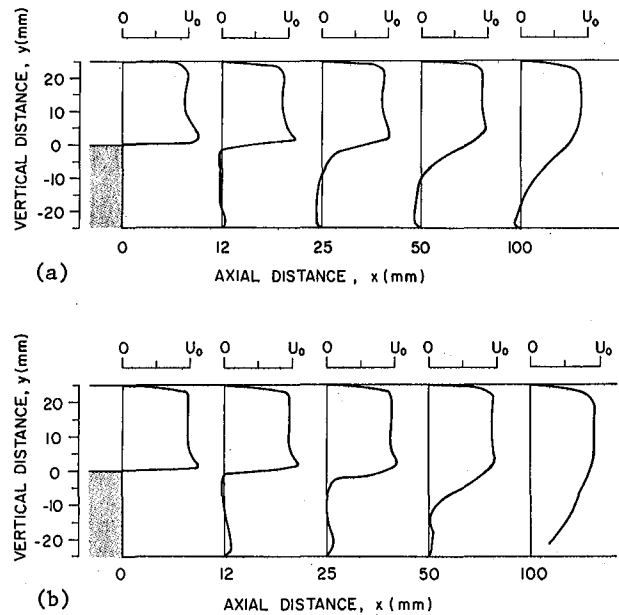


Fig. 3. Laser anemometry profiles of the mean velocity.

- (a) Non-reacting flow ( $U_0 = 13.7$  m/s,  $R_h = 2.3 \times 10^4$ ). (XBL 802-8230)
- (b) Reacting flow ( $U_0 = 14.0$  m/s,  $\phi = .61$ ,  $R_h = 2.3 \times 10^4$ ). (XBL 802-8231)

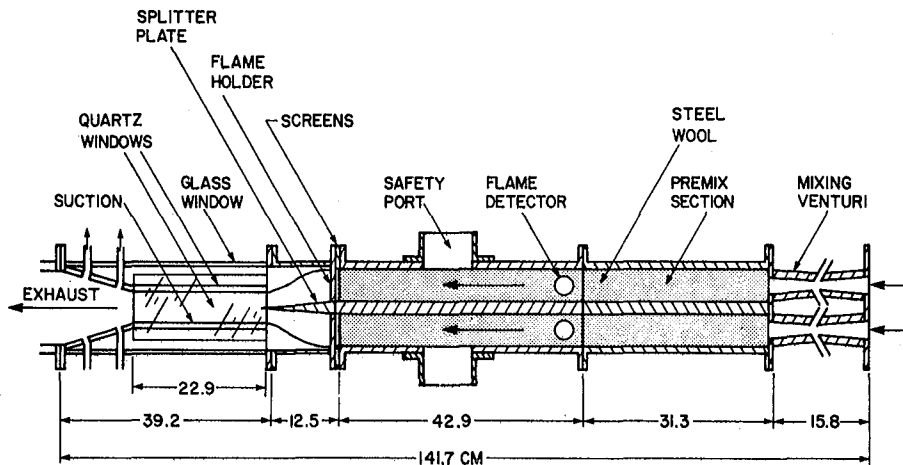


Fig. 4. Two-stream two-dimensional combustor test section (dimensions in mm). (XBL 802-8232)

3. G. M. Corcos and F. Sherman, *J. of Fluid Mech.*, 73, 241 (1976).
4. J. H. Konrad, SQUID Report CIT-8-PU (1976).
5. R. W. Pitz and J. W. Daily, "Experimental studies of combustion in a two-dimensional free shear layer," presented at the Second Symposium on Turbulent Shear Flows, Imperial College, London, July 2-4, 1979.

## LASER INDUCED FLUORESCENCE STUDIES OF TURBULENT REACTING FLOWS\*

*J. W. Daily, N. A. Al-Shamma, C. Chan, and M. Azzazy*

### INTRODUCTION

The problem of turbulent flows involving chemical reactions is important from both the theoretical and applied aspects. Turbulent motion is often responsible for bringing reactants together so that a reaction can occur within a finite time, and it is also responsible for dispersing the products of reaction. Of prime interest for statistical theories are the first and second statistical moments of the different variables (velocity, temperature, species, concentrations, etc.). A probability distribution function (pdf) of products' mass fraction can be introduced as a tool for obtaining the different statistical moments. Using the pdf of product concentration is more general than time or space averaging which can be used only in the case of stationary or homogeneous turbulence. The shape of this pdf in a turbulent premixed flame is affected by the degree of turbulence, i.e., turbulence intensity and Kolmogorov length scale. Also in premixed flames the pdf will serve as a closure assumption for the mean reaction rate.

### ACCOMPLISHMENTS DURING 1979

We have been studying the limit of the thin combustion zone in large-scale structure and the same order of turbulence intensity and laminar flame speed. We are using the Laser Induced Fluorescence Spectroscopy (LIFS) techniques for measuring the pdf of product concentration. The method of LIFS is a promising diagnostic technique for turbulent flow measurements because of its high-frequency

response. It is several orders of magnitude faster than all turbulence time scales, and it does not interfere with the flow pattern.

Preliminary results of pdf measurements in turbulent flames stabilized on a rod above a flat flame burner have already been reported by Daily and Chan. A new burner system has been designed specifically to study turbulent flows. The flame is stabilized on a rod at 3.5 cm above the nozzle rim, and turbulence is created by a turbulent screen placed at the nozzle rim. All the previous measurements of the pdf were based on measuring the pdf of temperature through a series of thermocouples and assuming the flow to be adiabatic and to have unity Lewis number.

### PLANNED ACTIVITIES FOR 1980

The effort in the next year will be directed towards obtaining reliable data for the shape of the pdf of product concentration at different points normal to the flame front using the LIFS technique. A model equation for the pdf of product concentration will be derived. This model equation will be solved simultaneously with the governing equations.

### FOOTNOTE

\*This work was supported by the Air Force Office of Scientific Research through the Engineering Office of Research Services, University of California, Berkeley.

## TWO LINE LASER FLUORESCENCE TEMPERATURE MEASUREMENTS IN TURBULENT FLOWS\*

*J. W. Daily and R. G. Joklik*

In the study of combustion in a turbulent-free shear layer, it is of interest to measure the temperature distribution in the flow as well as its variation with time. This requires a temperature-measurement technique that has spatial and temporal resolution on the order of the size and time duration of the structures found in the shear layer, and in addition, one that does not disturb the flow. The Two-Line Fluorescence (TLF) temperature measurement technique is ideal for use with combustor flows in that it is capable of attaining the necessary spatial resolution and sampling frequency, and since it is an optical technique, it is non-disturbing.

TLF temperature measurement involves seeding the flow to be studied with metal atoms whose second excited state is at a substantially higher energy level than the ground and first excited states. The seed is then pumped sequentially at the two wavelengths required to excite transitions from the lower two levels to the higher one. At the same time, the nonresonant fluorescence is measured. The ratio of the two fluorescent signals so obtained can be used to calculate the temperature.

The advantage of TLF over other optical techniques is that it eliminates the effect of quenching on the measured temperature. Since the extent of

quenching is difficult to determine in combustion, this becomes an important characteristic of TLF. In addition, the measured signal is at a wavelength different from the pumping wavelength, thus eliminating interference effects caused by scattering of the incident light.

## FOOTNOTE

\*This work was supported by the National Aeronautics and Space Administration through the Engineering Office of Research Services, University of California, Berkeley.

## COMBUSTION IN A VORTEX DOMINATED TWO DIMENSIONAL FLOW\*

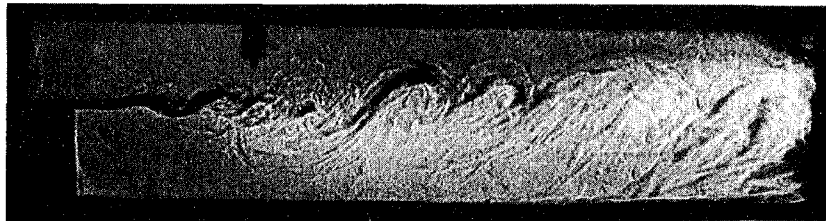
A. R. Ganji, R. F. Sawyer, and L. J. Parker<sup>†</sup>

### INTRODUCTION

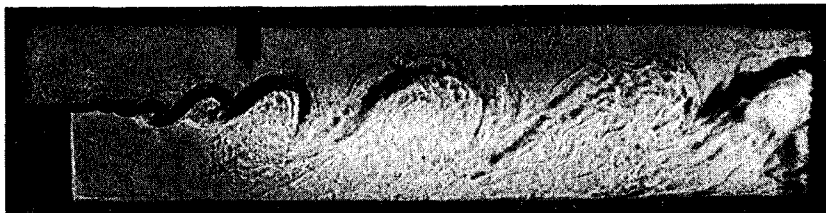
Lean premixed prevaporized combustion in aircraft gas turbine engines is one possible approach to the reduction of oxides of nitrogen and particulate emissions at higher power and cruise modes of operation, and the reduction of unburned hydrocarbons and carbon monoxide emissions at the idle mode of operation. Lower emission levels of oxides of nitrogen are due to a lower peak combustion temperature compared to the peak temperature in the nearly stoichiometric primary zones of present gas turbine combustors. Reduction of particulates, carbon monoxide, and hydrocarbons is due to the prevaporization

of the fuel, premixing of the fuel and air, and the more uniform combustion in the primary zone of the combustion chamber. These gains are unlikely to be obtained without the introduction of new or increased problems of stability, flashback and auto-ignition.

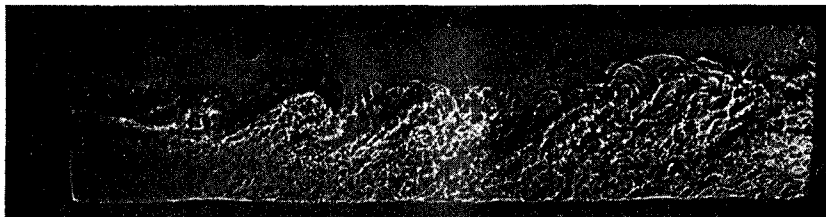
Research was undertaken for the Lewis Research Center of the National Aeronautics and Space Administration to study the combustion characteristics of a two-dimensional flow of premixed propane/air. The part of the work described here was focused on optical flow visualization with emphasis on the nature of the vortices which dominate the shear zone behind



a. Velocity 9.1 m/sec,  $N_{Re} = 5900 \text{ cm}^{-1}$ ,  $\phi = 0.60$



b. Velocity 13.3 m/sec,  $N_{Re} = 8600 \text{ cm}^{-1}$ ,  $\phi = 0.60$ .



c. Velocity 22.2 m/sec,  $N_{Re} = 14400 \text{ cm}^{-1}$ ,  $\phi = 0.58$ .

Fig. 1. Spark shadowgraphs of the flame behind the step for different velocities.

(XBB 801-764)

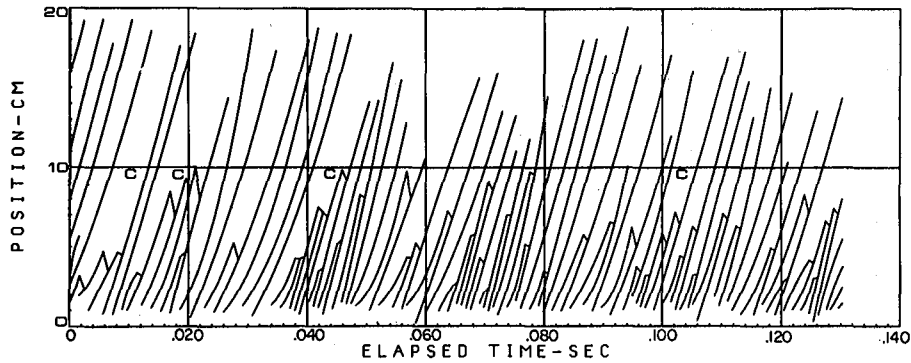


Fig. 2. Eddy trajectories for a flame stabilized behind a step.  $V_0 = 13.6$  m/sec,  $N_{Re} = 8800$   $cm^{-1}$ ,  $\phi = 0.57$ ,  $T_0 = 295K$ . (XBL 802-8016)

a rearward facing step, determination of the stability limits for combustion, and mapping of the time-average temperature, velocity, and composition in the reaction zone.

#### ACCOMPLISHMENTS DURING 1979

This work was concluded during 1979 with the following major results. Spark shadowgraphs, Fig. 1, showed that for a range of entrance velocities of 7.5 to 22.5 m/sec and equivalence ratios of 0.4 to 0.7, the mixing layer is dominated by Brown-Roshko type large coherent structures in both reacting and non-reacting flows. High-speed schlieren movies showed that these eddies were convected downstream and increased their size and spacing through combustion and coalescence with neighboring eddies. Tracing individual eddies in the reacting shear layer revealed that, on the average, eddies accelerate as they move downstream with the highest acceleration close to the origin of the shear layer (Fig. 2).

Schlieren movies of the flame in the transition to flashback show a gradual lift of the flame from the edge of the stabilizer, and propagation of the flame into the region upstream of the step. In the flashback mode, the flame front is periodically lifted from the edge of the holder and propagates into the premixing section. Stability limits for both blowout and flashback are shown in Fig. 3.

Space-resolved (time-averaged) composition measurements of CO, CO<sub>2</sub>, NO, NO<sub>x</sub>, and total hydrocarbons inside the combustor showed that CO, NO<sub>2</sub>, and NO were nearly constant in the recirculation zone and that the combustion efficiency was greater than 99% in this same region. The oxides of nitrogen in the recirculation zone were almost entirely NO while those in the cooler regions of the mixing layer were up to 80% NO<sub>2</sub>.

A modified laser schlieren and fast Fourier transform analysis system was developed and applied to the study of vortex frequencies in this combustor.

This system was sensitive to the passage of vortex structures and provided a convenient method of collecting power spectra which are characteristic of the processes triggering the vortex shedding, Fig. 4.

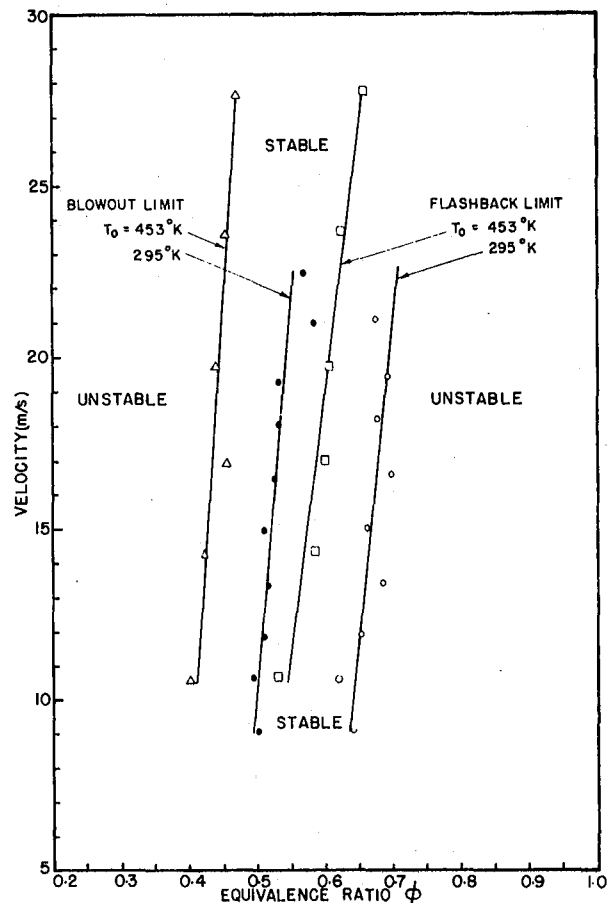


Fig. 3. Effect of temperature on stability limits. (XBL 802-8010)

## PLANNED ACTIVITIES FOR 1980

This research has been concluded.

## FOOTNOTES AND REFERENCES

\*This work was supported by the National Aeronautics and Space Administration through the University of California, College of Engineering, Office of Research Services.

†Sandia Laboratories, Livermore, California.

1. L. J. Parker, R. F. Sawyer, and A. R. Ganji, "Measurement of vortex frequencies in a lean, premixed prevaporized combustor," *Combustion Science and Technology*, **20**, 235-241 (1979).
2. A. R. Ganji, "Combustion and stability of characteristics of a premixed vortex dominated two dimensional flow," Ph.D. thesis, University of California, Berkeley, College of Engineering.
3. A. R. Ganji and R. F. Sawyer, "Turbulence, combustion, pollutant, and stability characterization of a premixed, step combustor," to be published as a NASA Contractor's Report.

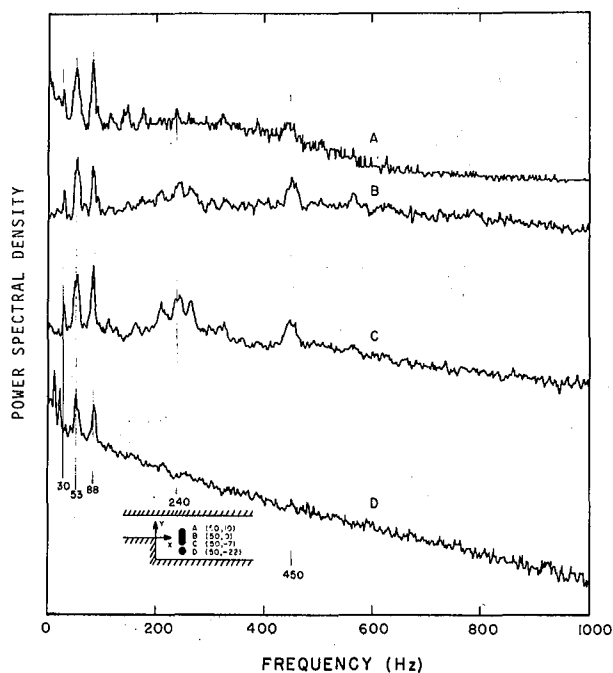


Fig. 4. Comparison of frequency spectra at different vertical locations, reacting flow,  $\phi = 0.60$ ,  $V = 13$  m/s,  $T_0 = 290$ K,  $n = 256$ . (XBL 802-8009)

## NUMERICAL MODELING OF TURBULENT COMBUSTION\*

A. Ghoniem, A. J. Chorin,<sup>†</sup> and A. K. Oppenheim

### INTRODUCTION

Traditionally, turbulent flow has been treated as a stochastic process. Recently significant progress has been made in the development of a deterministic theory of turbulence, as revealed in the famous Hugh Dryden Lecture by Roshko.<sup>1</sup> The experimental insight into large-scale flow structure, the so-called "coherent" turbulence, has been accompanied by advances in numerical modeling, in particular the random vortex method,<sup>2</sup> capable of providing rational interpretation for these phenomena.

Our current work is concerned with the application of this novel method of approach to turbulent combustion. For this purpose, the vortex technique had to be augmented by an interface advection algorithm which keeps track of the flame front trajectory<sup>3</sup> and of a volume source algorithm to incorporate the fluid mechanic effects of energy deposition due to the heat of combustion.

The problem we adopted for our study pertains to the essential means used in most practical systems for the stabilization of turbulent combustion, the recirculation zone behind a bluff body. To elucidate the phenomenological features of such systems, a combustion tunnel specially designed

for this purpose has been built in our laboratory. Some of the experimental results obtained thereby have been reported last year.<sup>4,5</sup>

The basic feature of bluff-body stabilization is realized in the experimental apparatus by the turbulent flow behind a step. A sequence of cinematographic schlieren records of the flow field in a recirculation zone created behind the step is reproduced here as Fig. 1. The large-scale vortex structure of the flow field, referred to in the literature as 'coherent turbulence' is clearly visible on the photograph, while the flame front is recorded by dark streaks, the loci of maximum gradient in refractive index reflecting the rapid change in density and temperature due to combustion.

### ACCOMPLISHMENTS DURING 1979

The numerical analysis we developed is based on the following idealizations:

1. the flow is two-dimensional, i.e. strictly planar;
2. the flowing substance consists only of two incompressible media;
3. the flame is treated as an interface between the two media, propagating locally

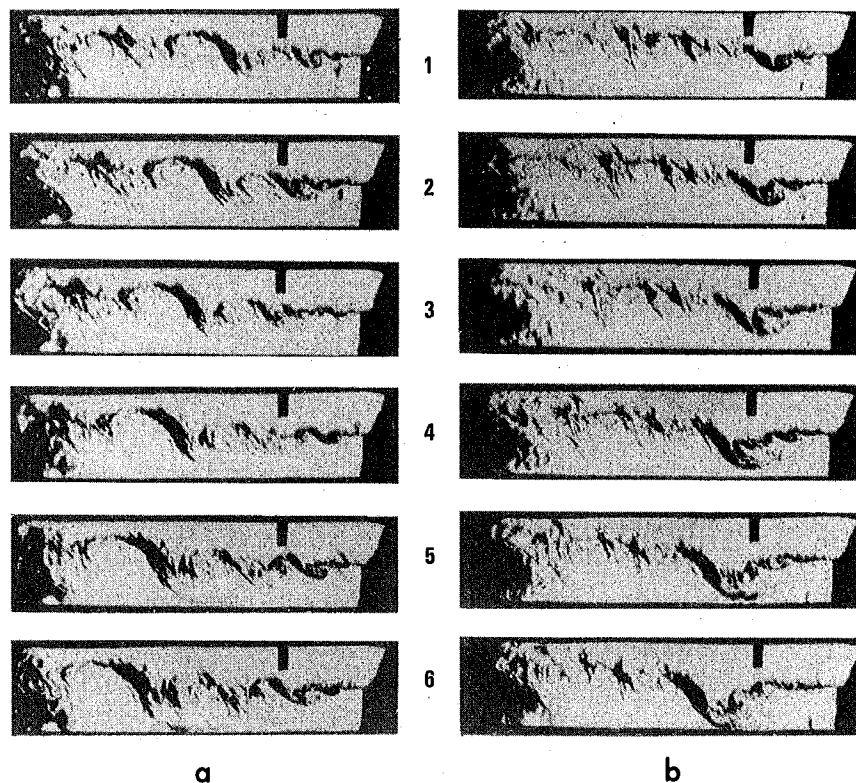


Fig. 1. Two sequential series of high-speed schlieren movie of a flame stabilized behind the step.  $V_0 = 13.6$  m/sec,  $Re = 8800$  cm<sup>-1</sup>,  $\phi = .57$ ,  $T_0 = 295$ K. (a) Normal formation and development of eddies in the mixing layer. Time interval between the frames is 1.16 msec. (b) Coalescence of a sequence of eddies and process of intrusion into the recirculation zone. Time interval between the frames is 1.22 msec. (Flow from right to left). (XBB 7912-16303)

4. at a prescribed "laminar" velocity; the heat release due to combustion is manifested solely by an increase in specific volume associated with the transformation of one component medium into the other and taken into account by an appropriate array of potential volume sources to satisfy the continuity equation.

Thus completely neglected are, respectively, the following physical phenomena:

1. three-dimensional effects, in particular vortex stretching;
2. compressibility effects, in particular acoustic wave interactions;
3. chemical kinetic effects, in particular the flame structure as well as the influence of the state and composition of reactants on its propagation velocity;
4. thermal effects, in particular heat transfer.

The numerical analysis is founded upon the kinematics of the velocity field. At each time step the velocity vector at any point is calculated as a sum of three components:

1. that of the potential velocity field which assures the boundary conditions due to

2. walls and solid bodies are satisfied; that produced by the vorticity field governed by the vortex transport equation and satisfying the no-slip boundary conditions at the walls;
3. that generated by the volumetric expansion satisfying the law of conservation of mass.

By virtue of the random walk sampling procedure incorporated into the computational technique as its most prominent feature, the results satisfy the Navier-Stokes equations.

Our study should elucidate the essential fluid mechanic features of turbulent combustion, such as the effect of velocity fluctuations on viscous stresses and on the structure shear layers when significant changes in specific volume due to heat release take place. We hope that with this technique we will be able to clarify the exact mechanism whereby the heat release due to combustion exerts an influence on the flow of the reacting fluid, and vice versa.

As an example of the results we have obtained in the course of our preliminary effort, Fig. 2 shows a sequence of computer graphs depicting the generation of the turbulent flow field behind a step in the absence of combustion. Each graph displays the flow velocity vector field at a given

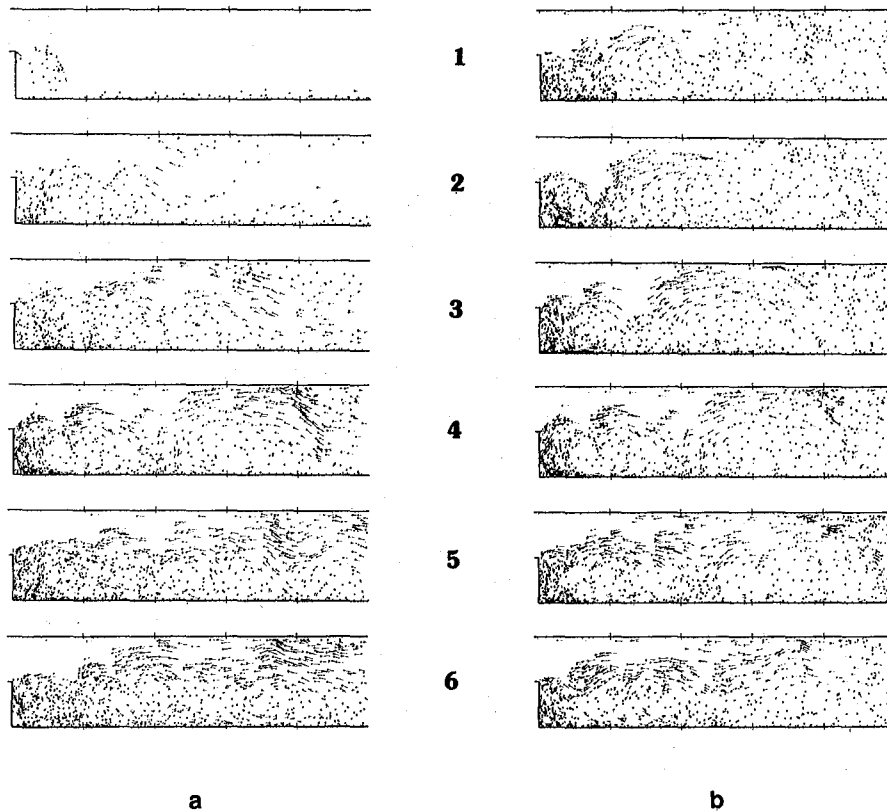


Fig. 2. Two sequential series of computer graphs displaying vortex velocity fields in turbulent flow behind a step at inlet  $Re = 10^4$ . (a) Development of the flow field at time intervals  $\tau \equiv U_0 t/H = 5$  where  $U_0$  is the flow velocity at inlet and  $H$  is the width of the inlet channel (equal to the height of the step). (b) Growth of a large scale eddy at time intervals  $\tau = 1$ ; frame 4 is the same in both sequences. (Flow from left to right) (XBL 7912-13714)

time step, tracing the motion of vector "blobs," the elementary components of the flow field employed in the analysis. A velocity vector is usually represented as a line segment, providing information on its magnitude and direction; however, instead of being provided with the conventional arrowhead, it is attached to a small circle, denoting the location of the vortex "blob" to which it pertains.

The model of the nonreactive flow we have thus obtained displays similar features of large scale structure as those of turbulent combustion presented in Fig. 1.

#### PLANNED ACTIVITIES FOR 1980

Our studies have just begun and the results are most promising. We hope that we will be able to develop our technique further and apply it to a variety of practical combustion problems. Among our objectives are the following:

1. analyze the flow behind the step in the presence of combustion;
2. develop proper methodology to display the results and extract from them information on stochastic properties of turbulent flow associated with combustion;

3. expand the scope to other geometrical configurations, in particular planar jets and flows past a cylinder and across a grid;
4. perform a parametric study for each geometrical configuration leading to the establishment of its optimum operating conditions;
5. include transport processes, in particular convective heat transfer.

#### FOOTNOTES AND REFERENCES

\*This work was supported by the National Aeronautics and Space Administration through the Engineering Office of Research Services, University of California, Berkeley, and by the Engineering, Mathematical, and Geosciences Division of the U.S. Department of Energy.

†Division of Physics, Computer Science and Mathematics.

1. A. Roshko, "Structure of turbulent shear flows: A new look," *AIAA Journal*, 14, 10, 1349-1357 (1976).

2. A. J. Chorin, "Numerical study of slightly viscous flow," *J. of Fluid Mech.*, **57**, 785-796 (1973).
3. A. J. Chorin, "Flame advection and propagation algorithms," *J. of Comp. Phys.*, in press (1979).
4. "Energy and Environment Division Annual Report-1978," Lawrence Berkeley Laboratory report LBL-8619, pp. 308-310 (1978).
5. A. R. Ganji and R. F. Sawyer, "An experimental study of the flow field and pollutant formation in a two-dimensional pre-mixed, turbulent flame," paper 79-0017, presented at the 17th AIAA Aerospace Sciences Meeting (January 1979).

## INTERACTION OF A FLAME WITH A KÁRMÁN VORTEX STREET\*

*I. Namer, R. G. Bill, Jr., F. Robben, and L. Talbot*

### INTRODUCTION

One of the major shortcomings of models of turbulent flame propagation using the wrinkled laminar flame model of turbulent flames is the need to make assumptions about the geometry of the wrinkling. The importance of this assumption is noted by Karlovitz,<sup>1</sup> Scurlock and Grover,<sup>2</sup> and Peterson and Emmons.<sup>3</sup> Calvin and Williams<sup>4</sup> point out the importance of this assumption and propose a theory for the kinematics of the wrinkling. However, they only consider the case of unity density ratio across the flame.

We are presently studying the flow field of a flame in a Kármán vortex street. This study began in 1977. The regularity of the vortex street enables us to use phase-locked signal averaging. The velocity field is measured using laser Doppler anemometry (LDA) and the density field by Rayleigh scattering. The phase angle is determined by a reference hot wire fixed to the cylinder shedding the vortex street. These measurements will provide the data base from which the wrinkling of the flame can be modeled. Furthermore, turbulent flame speed correlations with scale and intensity as reported by Andrews et al.<sup>5</sup> may be appraised under more ideal conditions, i.e., flow with one length scale.

### ACCOMPLISHMENTS DURING 1979

Data acquisition programs for a PDP 11/10 computer have been completed. The programs involve automatically positioning the test section with computer-controlled stepping motors and acquiring 1000 measurements at one millisecond intervals from the reference hot wire voltage and either the LDA tracker output voltage or the Rayleigh scattering intensity. These are acquired simultaneously on 2 channels of a 12 bit A/D converter. The data are stored on disks and later transferred onto 7-track magnetic tape. Programs to calculate the mean and rms of the fluctuations as well as to perform the ensemble averaging on the PDP 11/10 have also been written. Page plots of the reduced data can be produced on line with the PDP 11/10. Programs to read the 7-track tape on the LBL CDC 7600 have also been written.

The optical system for the LDA and Rayleigh scattering are described by Namer et al.<sup>6</sup> and

Schefer et al.<sup>7</sup> The flow system was described in the previous annual report.

Measurements of the streamwise velocity component were made in the wake of a 2.0 mm and 3.0 mm diameter wake generator. Profiles through a C<sub>2</sub>H<sub>4</sub>-air flame in the wake of a 2.0 mm diameter rod were also acquired. Preliminary analysis of this data on the PDP 11/10 indicate that the algorithms for ensemble averaging are capable of reproducing the complete flow field as a function of time. Figure 1 shows a velocity profile across the flame in a vortex street.

When making preliminary LDA measurements we found that the most efficient procedure was to have a particle rate greater than 5000/sec in order to treat the LDA tracker output as a continuous signal. Thus the individual particle arrival times do not have to be monitored. We found that since arrival times were Poisson-distributed, there were significantly long periods of time in which no particles were recorded at particle rates less than 5000/sec. This is illustrated in Fig. 2.

### PLANNED ACTIVITIES FOR 1980

The velocity data already taken will be analyzed on the Lawrence Berkeley Laboratory CDC 7600 computer. The ensemble averaged results will be

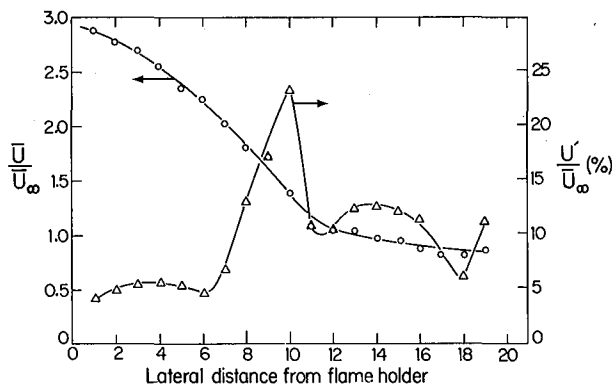
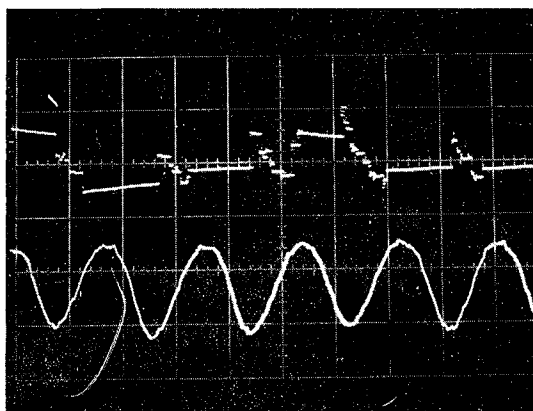
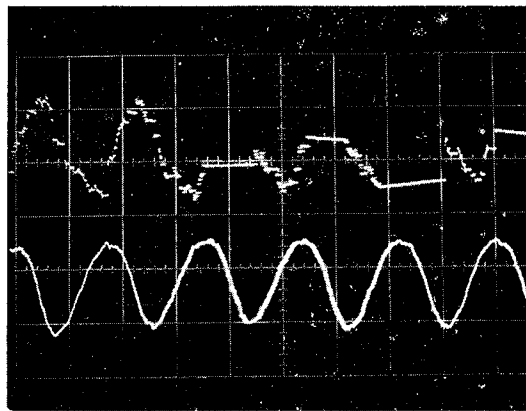


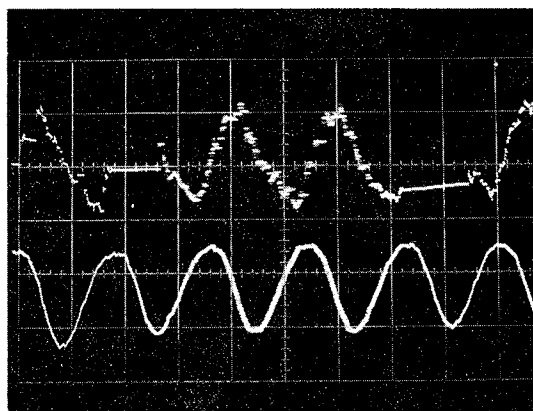
Fig. 1. Velocity profile across the flame in a vortex street. (XBL 802-8011)



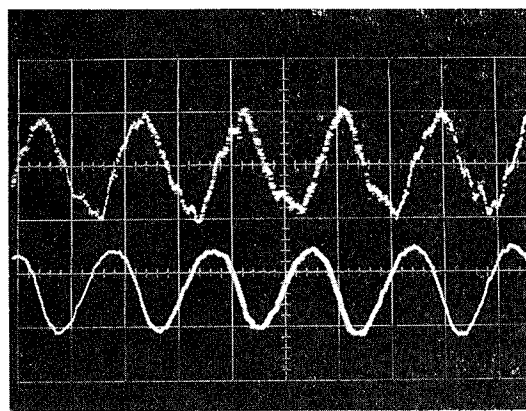
500 PARTICLES/SEC.



2000 PARTICLES/SEC.



5000 PARTICLES/SEC.



10,000 PARTICLES/SEC.

Fig. 2. Comparison of LDV output (upper trace) with hot wire (lower trace) at four particle rates, in the wake of a rod.  $D = 3$  MM.,  $X = 20.0$  MM,  $Y/D = 1.0$ , Sweep = 50 msec/div. (XBB 801-765)

used to construct contour plots of velocity at a given phase angle. Phase-locked Rayleigh scattering measurement will be made through the flame. Contours of constant density will show the geometry of flame wrinkling. Measurements of the cross-stream velocity component will enable us to construct the streamlines as a function of time. Furthermore, we will be working closely with Dr. A. Chorin and Dr. I. Karasalo who will attempt to model this experiment as an inviscid flow. Their model represents the flame as a line source of specific volume to account for the decrease in density across the flame. A further modification of Chorin<sup>8</sup> is the use of the Markstein parameter to modify the local laminar flame speed in order to account for the two dimensional heat and mass transfer in a wrinkled flame.

#### FOOTNOTE AND REFERENCES

\*This work was supported by the Air Force Office of Scientific Research through the University of California, Berkeley, Campus Research Office.

1. B. Karlovitz, Selected Combustion Problems, Butterworths, London, 248 (1954).

2. A. C. Scurlock and J. H. Grover, 4th Symp. (Int) on Combustion, 645 (1953).
3. R. E. Petersen and H. W. Emmons, Phys. of Fluids, 4, 456 (1961).
4. P. Calvin and F. A. Williams, JFM, 90, 3, 589 (1979).
5. G. E. Andrews, D. Bradley, S. B. Lwakabamba, Combustion and Flame, 24, 285 (1975).
6. I. Namer, Y. Agrawal, R. K. Cheng, F. Robben, R. Schefer, and L. Talbot, "Interaction of a plane flame front with the wake of a cylinder," UCB Report FM-77-3 (1977).
7. R. W. Schefer, F. Robben, and R. K. Cheng, "Catalyzed combustion of  $H_2$ /air mixtures in a flat plate boundary layer," to be published in Combustion and Flame (1980).
8. A. J. Chorin, "Flame advection and propagation algorithms," to be published in J. Comp. Phys. (1980).

## THERMOPHORESIS OF PARTICLES IN A HEATED BOUNDARY LAYER\*

L. Talbot, R. K. Cheng, R. W. Schefer, and F. Robben

The use of laser Doppler velocimetry (LDV) for the measurement of mean and fluctuating velocity components in reacting turbulent flows requires the introduction of "seed" particles to act as light scatterers. In accurate LDV measurements, the seed particles must follow the fluid motion faithfully. Among the many forces which might act on a small particle and cause its motion to depart from that of the fluid is the thermophoretic force, which arises when a temperature gradient exists in the gas, and which causes motion of the particle in the direction negative to the direction of  $\nabla T$ . It is a rarefaction effect, which depends on the Knudsen number,  $\lambda/R$ , where  $\lambda$  is the mean free path and  $R$ , the particle radius. A common example of the phenomenon is the blackening of the glass globe of a kerosene lantern; the temperature gradient established between the flame and the globe drives the soot particles produced in the combustion process towards the globe, where they deposit.

We encountered the thermophoresis phenomenon in connection with the measurement of the velocity distribution within a boundary layer adjacent to a heated plate, where catalytically supported combustion was being investigated. It was observed that when the plate was heated, the seed particles introduced for the LDV measurements were driven away from the wall, and the inner half of the boundary layer was essentially particle-free. Although this limited the region within the boundary layer where velocity measurements could be made, it at the same time provided an opportunity for estimating the magnitude of the thermophoretic force, and for assessing the accuracy of the different theories which have been developed to predict this force.

A computer program was developed to calculate the trajectories of particles entering the boundary

layer, using the various theoretical expressions for the thermophoretic force. It was found that for low values of the Knudsen number,  $\lambda/R \lesssim 0.1$ , the boundary of the particle-free region agreed best with the particle trajectory calculated according to the Brock<sup>1</sup> analysis, when revised to incorporate the most accurate values currently available for the thermal slip, momentum transfer and temperature-jump surface interaction coefficients.

The existing theories are applicable only for the two limiting conditions  $\lambda/R \lesssim 0.1$  and  $\lambda/R \rightarrow \infty$ . To find an expression for the thermophoretic force that would be applicable over the entire range  $0 \leq \lambda/R \leq \infty$ , the experimental data available in the literature were examined, and a fitting formula was devised which is in satisfactory agreement with most of these data and which coincides with theoretical predictions in the two limits  $\lambda/R \rightarrow 0$  and  $\lambda/R \rightarrow \infty$ .

The details of this investigation are given in Ref. 2.

### FOOTNOTE AND REFERENCES

\*This work was supported by the Division of Basic Energy Sciences of the Department of Energy.

1. J. R. Brock, J. Colloid Sci. **17**, 768 (1962).
2. L. Talbot, et al., "Thermophoresis of particles in a heated boundary layer," Lawrence Berkeley Laboratory report 10113 (December 1979). Submitted for publication to J. Fluid Mech.

## FIRE RESEARCH

## POLYMER COMBUSTION\*

W. J. Pitz, R. F. Sawyer, and N. J. Brown

## INTRODUCTION

The use of polymeric materials is increasing, in part, because of their energy conservation potential. These savings result from weight reduction (primarily in transportation applications) or enhanced thermal insulation properties (primarily in building applications). Unfortunately, these savings are sometimes accompanied by an increased fire risk. Research has been conducted to assess the flammability of polymers and to understand the physical and chemical characteristics which control flammability. Both experimental and theoretical studies have been undertaken which focus on an opposed-flow diffusion flame in which the quasi-steady combustion of polymers has been examined.

Earlier studies upon the steady-state combustion of polymers yielded data on burning rates, mass transfer numbers, and thermophysical polymer properties under burning conditions. More recent studies of combustion near and at the extinction limits have been conducted to yield information on flame inhibition. This work involves the determination of the chemical structure of the flame, extinction parameters (primarily oxidizer composition and flow rate at extinction), and the effect of chemical inhibitors upon the structure and extinction parameters.

## ACCOMPLISHMENTS DURING 1979

Techniques were developed for measurement of composition profiles under burning conditions near extinction. Samples were extracted by a quartz microprobe and analyzed by gas chromatography.

A typical composition profile is shown in Fig. 1. The luminous flame zone coincides approximately with the peak in carbon dioxide and water concentration, as expected. The thickness of the reaction zone is not consistent with the normally applied assumption of a "collapsed flame zone" which is often used to model laminar diffusion flames. Oxygen penetration of the flame zone is also observed, but estimates of the flux of oxygen reaching the polymer surface suggest that energy release through surface oxidation is not a major contributor to fuel pyrolysis.

Similarity of the composition profiles in the radial direction is predicted for stagnation point flow. Composition measurements at different radial locations verified that this was indeed the case for this experimental configuration. As extinction conditions are approached through the reduction of the oxygen concentration, the flame expands in the axial direction and flame stand-off distance increases. This is consistent with the requirement

that the pyrolyzed polymer must diffuse further into the oxidizer flow before sufficient oxygen is encountered for complete reaction.

## PLANNED ACTIVITIES FOR 1980

Extinction measurements will be completed for high-purity polyethylene, polyethylene doped with inhibitor, and oxidizer doped with inhibitor. Computation studies of the opposed flow configuration with finite reaction rates will be completed to provide a qualitative comparison of experimental and model flame structure and extinction characteristics. Final reporting of the research will be accomplished and this research will then be concluded.

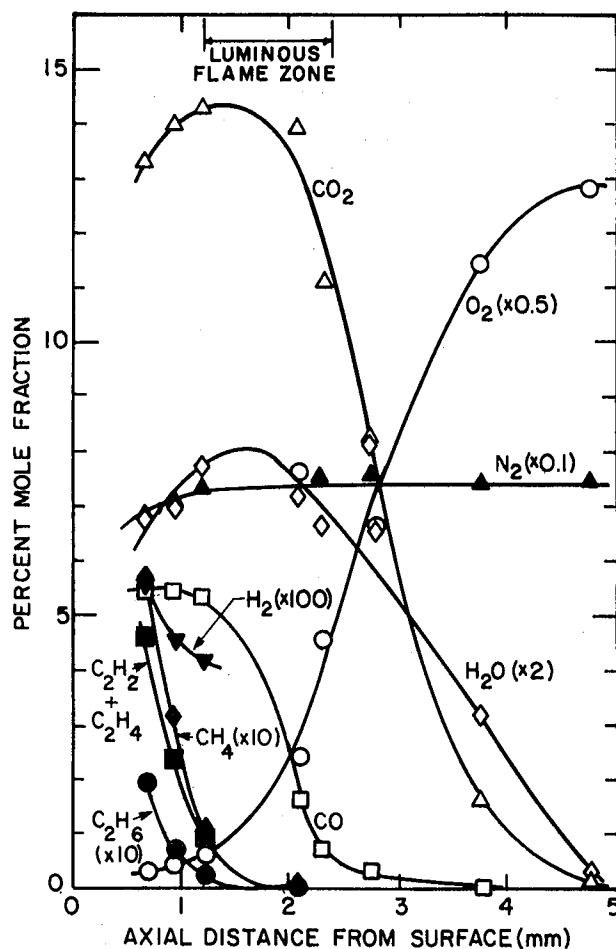


Fig. 1. Composition profiles for a high oxygen concentration in the oxidizer flow ( $X_{O_2} = 0.253$ ,  $r^* = 0.31$ ). (XBL 798-6731)

## FOOTNOTE AND REFERENCE

\*This work was supported by the Center for Fire Research, National Bureau of Standards.

1. W. J. Pitz, N. J. Brown, and R. F. Sawyer, "Flame structure measurement of polymer diffusion flames," Western States Section/The Combustion Institute Paper No. 79-47 and Lawrence Berkeley Laboratory report LBL-9567.

## PARTICULATE VOLUME FRACTIONS IN DIFFUSION FLAMES\*

*P. J. Pagni and S. Bard*

### INTRODUCTION

Flame radiation, the dominant heat-transfer mechanism in full-scale fires, is in turn controlled primarily by the fraction of the flame volume occupied by solid carbon.<sup>1-3</sup> Particulate volume fractions,  $f_v$ , are measured *in situ* in small scale, 0(10 cm), buoyant diffusion flame pool fires supported in air by solid polystyrene, PMMA and POM, cellular polystyrene; two cellular polyurethanes and liquid isooctane, acetone and alcohol. Two measurement techniques, based on attenuation of known monochromatic laser radiation by the flame, are described. In the small-particle absorption limit, valid in the visible for POM, acetone and alcohol, transmittance at a single wavelength suffices to determine  $f_v$ . For the remaining fuels, scattering becomes significant and multiwavelength transmittance measurements are used to determine an approximate two-parameter particle radii distribution,  $N(r) = N_o (27r^3/2r_{max}^4) \exp(-3r/r_{max})$  where

$r_{max}$  is the most probable radius and  $N_o$  is the particle concentration. The resulting  $f_v = 18.6$

$N_o r_{max}^3$  may be used to calculate the infrared

emission from solid carbon in the flames considered. Volume fractions rank in the expected order of flame luminosity and smokiness from polystyrene,  $f_v \sim 5 \times 10^{-6}$ , to alcohol,  $f_v \sim 10^{-7}$ . Within the approximations of flame homogeneity, spherical particles, known optical properties<sup>4-7</sup> and assumed form for the size distribution, the  $f_v$  data are from  $\pm 5\%$  to  $\pm 15\%$  accurate. Good agreement exists with  $f_v$  of solid polystyrene and PMMA derived independently from infrared flame transmittance and radiance data<sup>8</sup> and between experimental mass pyrolysing rates and calculated rates obtained using these results in a radiation model.<sup>9</sup>

### ACCOMPLISHMENTS DURING 1979

Some of this work has been published.<sup>1</sup> During the current period, reducing uncertainties in the  $f_v$  and size data and in the soot optical properties consumed the major effort. The apparatus was modified so that the two laser wavelengths in the soot size distribution determining technique occupy the same physical path. This has two advantages with regard to uncertainties: (1) the most probable particle size may be found without measuring the distance traversed by the laser beams through the

flame; and (2) the variation of  $f_v$  along the beam path and with location within the flame became unimportant. In addition, an on-line computer has been incorporated in the apparatus for data storage and reduction and a video-tape system has replaced 8 mm cinematography to record flame size and shape. These improvements are now being utilized to obtain additional data on a wide variety of fuels.

The soot optical properties of Dalzell and Sarofim<sup>4</sup> were previously used to obtain soot volume fractions from extinction data. However, recent work<sup>5-7</sup> suggests that those values may have underestimated the index of refraction for flame soot due primarily to voids within compressed soot samples. The average value in the visible,  $m = 1.56-0.57i$  used in Ref. 1, based on Ref. 4, has now been replaced with  $m = 1.93-0.53i$ , based on Refs. 5-7. Table 1 lists soot volume fractions and size distributions obtained from extinction measurements using these new optical properties.

### PLANNED ACTIVITIES FOR 1980

Measurements of the soot volume fraction variation with location in a given flame and with the size of the fuel sample supporting these buoyant pool fire diffusion flames will be made. Most of the effort aimed at measuring  $f_v$  fields will be redirected to buoyant and forced flow boundary layer flames. Flames in boundary layers are much better defined than pool fires and have received considerable analytic attention in the recent literature.<sup>10</sup> The necessary apparatus to conduct these studies under a variety of flow rates and ambient oxygen concentrations already exists in the UCB Fire Research Laboratory. In addition, analyses of radiating-combusting boundary layers are now under development here to complement the experiments and utilize the soot volume fraction spatial distribution data as soon as it is available. It will be of special interest to determine the differences between the boundary layer diffusion flame soot volume fraction and the pool fire soot volume fraction for the same fuel and ambience.

### FOOTNOTE AND REFERENCES

\*This work was supported by the Center of Fire Research, National Bureau of Standards.

1. P. J. Pagni and S. Bard, "Particulate volume fractions in diffusion flames," Seventeenth

Table 1. Experimental flame soot volume fractions and size distributions

	Absorption Limit $\sim f_v \times 10^6$	$r_{\max}$ ( $\mu\text{m}$ )	$N_0 \times 10^{-9}$ ( $\text{cm}^{-3}$ )	$f_v \times 10^6$
<i>Solids</i>				
Polystyrene ( $\text{C}_8\text{H}_8$ ) <sub>n</sub>	7.3	0.047	1.7	3.3
Polypropylene ( $\text{C}_3\text{H}_6$ ) <sub>n</sub>	0.44	-	-	0.44
Polymethylmethacrylate ( $\text{C}_5\text{H}_8\text{O}_2$ ) <sub>n</sub> , PMMA	0.49	0.045	0.13	0.22
<i>Foams</i>				
Polystyrene, GM-48 ( $\text{C}_8\text{H}_8$ ) <sub>n</sub>	7.5	0.066	0.75	4.0
Polyurethane, Mattress ( $\text{C}_{3.2}\text{H}_{5.3}\text{ON}_{0.23}$ ) <sub>n</sub>	1.2	0.052	0.21	0.56
<i>Liquids</i>				
Iso Octane ( $\text{C}_8\text{H}_{18}$ )	1.0	0.047	0.24	0.46
Acetone ( $\text{C}_3\text{H}_6\text{O}$ )	0.23	-	-	0.23
Alcohol ( $\text{C}_2\text{H}_6\text{O}$ )	0.14	-	-	0.14

- Symposium (International) on Combustion, 1017-1028, The Combustion Institute (1978).
- J. De Ris, "Fire radiation - a review," Seventeenth Symposium (International) on Combustion, 1003-1016, The Combustion Institute (1978).
  - H. G. Wagner, "Soot formation in flames, a review," Seventeenth Symposium (International) on Combustion, The Combustion Institute (1978).
  - W. H. Dalzell and A. F. Sarofim, "Optical constants of soot and their application to heat-flux calculations," J. Heat Transfer, 91, 100-105 (1969).
  - S. C. Graham, "The refractive indices of isolated and of aggregated soot particles," Comb. Sci. and Tech. 9, 159-163 (1974).
  - S. Chippett and W. A. Gray, "The size and optical properties of soot particles," Comb. and Flame 31, 149-159 (1978).
  - C. L. Tien and D. Lee, "Flame soot optical properties," in preparation.
  - R. O. Buckius, and C. L. Tien, "Infrared flame radiation," Int. J. Heat Mass Transfer, 20 93-106 (1977).
  - S. Bard, K. H. Clow, and P. J. Pagni, "Combustion of cellular urethane," Comb. Sci. and Tech. 19, 141-150 (1979).
  - C. M. Kinoshita and P. J. Pagni, "Laminar wake flame heights," J. Heat Transfer, in press (1980).

# LAMINAR WAKE FLAME HEIGHTS\*

C. M. Kinoshita and P. J. Pagni

## INTRODUCTION

One important measure of material fire hazard is the flame height a given polymer produces upon burning in a specified ambience.<sup>1,2</sup> Six systems are considered here—two fuel geometries: wall-mounted and free standing; and three flow fields: forced, free, and mixed-mode.<sup>3</sup> In each case, the extent of the combusting gas downstream of a pyrolyzing slab is obtained as a function of the fuel's thermochemical properties. The flow is modeled as a steady, laminar, two-dimensional, nonradiative boundary layer. The combustion is described by a single Shvab-Zeldovich energy-species equation assuming unit Lewis number and a fast one-step overall gas-phase reaction. Numerical methods are employed due to the abrupt change in boundary conditions at the end of the pyrolyzing slab. However, an approximate similarity solution is found for forced flow which yields explicit flame heights. Based on these results, explicit functional fits to numerical flame heights are obtained for free and mixed-mode flows. Comparisons between theory and experiment indicate quantitative agreement.

## ACCOMPLISHMENTS DURING 1979

Subject to the restrictive assumptions listed above, the following set of explicit expressions summarizes the flame height modeling results. The notation is defined below.

### Forced Flow:

$$X_{fl \text{ wall-wake}}^* \approx 0.14 \left[ \frac{(1+r)}{r} \frac{(1+B)}{B^{1.15}} \ln(1+B) \right]^2 \quad (1)$$

$$X_{fl \text{ wake}}^* / X_{fl \text{ wall-wake}}^* \approx 0.72 Pr^{-0.2}$$

within 20% of numerical results for  $0.5 \leq Pr \leq 2.0$ ,  $0.5 \leq B \leq 5.0$  and  $0.1 \leq r \leq 0.5$ .

### Free Flow:

$$X_{fl \text{ wall-plume}}^* \approx 0.24 \left[ \frac{(1+r)}{r^{1.16}} \frac{(1+B)}{B^{1.06}} \frac{\ln(1+B)}{D_c^{0.03}} \right]^{1.33} \quad (2)$$

$$X_{fl \text{ plume}}^* / X_{fl \text{ wall-plume}}^* \approx 0.9$$

within 20% of numerical results for  $Pr = 0.73$ ,  $0.5 \leq B \leq 5.0$ ,  $0.1 \leq r \leq 0.5$  and  $2.0 \leq D_c \leq 60$ .

### Mixed Flow:

$$\frac{X_{fl}^*}{X_{fl \text{ free}}^*} \approx (1 - \xi_\ell^{0.2}) \frac{X_{fl \text{ forced}}^*}{X_{fl \text{ free}}^*} + \xi_\ell^{0.2}, \quad \xi_\ell \leq 1.0 \quad (3)$$

$$\frac{X_{fl}^*}{X_{fl \text{ free}}^*} \approx 1.0, \quad \xi_\ell = Gr_\ell / Re_\ell^2 \geq 1.0$$

within 20% of numerical results for both wall and free-standing geometries with  $Pr = 0.73$ ,  $0.5 \leq B \leq 5.0$ ,  $0.1 \leq r \leq 1.0$  and  $2.0 \leq D_c \leq 60$ . Equations (1) and (2) give the following flame heights for Products Research Committee Sample Bank Materials using property data from Tewarson.

From these detailed combusting boundary layer analyses of six systems (wall-wake, wake, wall-plume, plume, mixed-mode wall-wake and mixed-mode wake), emphasizing the constancy of the flux of the Shvab-Zeldovich energy-species variable  $J$  in the extended flame region, the following conclusions are drawn:

1. For forced flow,  $X_{fl}^*(r, B, Pr)$  and is independent of  $Re_\ell$ . Explicit expressions are presented which quantify the strong increase in  $X_{fl}^*$  as  $r$  decreases and the moderate increase in  $X_{fl}^*$  as  $B$  increases. The  $Pr$  dependence is very weak. Good agreement with experiment is obtained.

2. For free flow,  $X_{fl}^*(r, B, Pr, D_c)$  and is independent of  $Gr_\ell$ . Explicit fits to numerical results are given which quantify the  $r$  and  $B$  dependence as in forced flow. The dependence on  $D_c$  and  $Pr$  is weak. Free flow flames are generally shorter than forced flow flames for the same fuel and ambience. Reasonable agreement with experiment is obtained.

3. For mixed-mode flow,  $X_{fl}^*(r, B, Pr, D_c, \xi_\ell)$  with the forced and free limits approached at  $\xi_\ell \leq 10^{-2}$  and  $\xi_\ell \geq 1$  respectively. The mixed-mode case appears to be a simple superposition of forced and free flow.

4. Wall-mounted flames are longer than free-standing flames for the same fuel and ambience. This difference depends on flow type and  $Pr$ , i.e., wall-wake flames are ~30 percent longer than wake flames; wall-plume flames are ~10 percent longer than plume flames.

More experimental results for comparison would be valuable. We hope that flame-height measurement

Table 1. Predicted flame heights based on ideal material properties.

Material (a) (Type)	Formula (b)	s	$\Delta H_c$ (b,c) (kJ/gm)	$Q_p$ (kJ/gm $O_2$ )	$T_w$ (c) (°K)	L (c) (kJ/gm)	B	$Y_{FW}$	r	$D_c$	$X_{f1}^*$ wall plume	$X_{f1}^*$ wall wake
Polystyrene (Foam, GM-49)	$C_8 H_{8.4} O_{0.03}$	0.33	38	12	750	1.3	1.7	0.6	0.12	4.8	11	24
Polystyrene (Foam, GM-53)	$C_8 H_{8.4} O_{0.10}$	0.33	38	12	780	1.3	1.7	0.6	0.13	4.5	11	23
Polystyrene (Foam, GM-51)	$C_8 H_{8.1} O_{0.17}$	0.34	36	12	760	1.4	1.5	0.6	0.13	4.6	10	21
Polypropylene (Granular)	$C_3 H_6$	0.29	43	13	770	2.0	1.1	0.5	0.13	4.7	9.4	19
Polystyrene (Granular)	$C_8 H_8$	0.33	39	13	850	1.7	1.3	0.5	0.14	4.1	9.3	18
Polystyrene (Foam, GM-47)	$C_8 H_{8.1}$	0.32	38	12	830	1.9	1.1	0.5	0.15	4.1	7.9	15
Polyurethane (Foam, GM-25)	$C_{3.1} H_{5.4} ON_{0.22}$	0.46	25	11	850	1.2	1.5	0.6	0.19	3.6	6.5	11
Polymethyl- methacrylate (Granular)	$C_5 H_8 O_2$	0.52	25	13	750	1.6	1.5	0.6	0.22	5.1	5.2	8.9
Polyurethane (Foam, GM-21)	$C_{3.9} H_{6.1} ON_{0.18}$	0.44	26	12	730	2.0	1.1	0.5	0.22	4.7	4.9	8.4
Polyurethane (Foam, GM-27)	$C_{3.3} H_{5.7} ON_{0.26}$	0.45	23	11	850	1.9	0.9	0.4	0.25	3.4	4.0	6.6
Polyurethane (Foam, GM-23)	$C_{2.8} H_{5.0} ON_{0.16}$	0.48	27	13	790	2.7	0.9	0.4	0.27	4.7	3.5	5.7
Polyurethane (Foam, GM-29)	$C_{4.4} H_{5.1} ON_{0.42}$	0.45	26	12	770	3.1	0.7	0.3	0.31	4.3	2.9	4.6
Polyurethane (Foam, GM-31)	$C_{4.6} H_{5.4} ON_{0.44}$	0.44	25	11	830	3.1	0.6	0.3	0.33	3.7	2.6	4.1
Polyurethane (Foam, GM-37)	$C_{5.1} H_{6.4} ON_{0.41}$	0.42	28	12	840	4.5	0.5	0.2	0.40	3.8	2.0	3.0
Polyisocyanurate (Foam, GM-41)	$C_{5.3} H_{5.2} ON_{0.57}$	0.43	26	11	800	4.5	0.4	0.2	0.43	4.0	1.8	2.8
Polyoxymethylene (Granular)	$C H_2 O$	0.94	15	14	740	2.4	1.1	0.4	0.50	5.8	1.8	2.4
Polyisocyanurate (Foam, GM-43)	$C_{5.0} H_{4.7} ON_{0.54}$	0.44	22	10	800	4.5	0.4	0.2	0.55	3.5	1.4	2.0
Cellulose (Whatman Filter Paper)	$C_6 H_{10} O_5$	0.84	17	14	650	3.5	0.8	0.3	0.60	6.9	1.4	1.8

<sup>a</sup>Here  $Y_{Ox\infty} = 0.23$ ,  $T_\infty = 293K$ ,  $c_p = 1.3$  J/gmK,  $s = v_{FW} / v_{Ox} W_{Ox}$  (assuming complete combustion of the specified formula),  $Q_p = \Delta H_c s$ ,  $h_w = c_p (T_w - T_\infty)$ ,  $B = (Q_p Y_{Ox\infty} - h_w) / L$ ,  $Y_{FW} = (B Y_{ft} - s Y_{Ox\infty}) / (1 + B)$ ,  $r = s Y_{Ox\infty} / Y_{FW}$ , and  $D_c = Q_p Y_{Ox\infty} / h_w$ . The GM designation refers to the Products Research Committee Material Sample Bank available through the National Bureau of Standards. Materials are listed in order of increasing r and therefore of decreasing flame height.

<sup>b</sup>A. Tewarson, and R. F. Pion, "A laboratory-scale test method for the measurement of flammability parameters", Technical Report 22524, FMRC, Norwood, MA. (October 1977).

<sup>c</sup>A. Tewarson, "Experimental evaluation of flammability parameters of polymeric materials", Technical Report 22524, RC79-T9, FMRC, Norwood, MA. (February 1979).

under controlled conditions will become one of the standard procedures for assessing material fire hazard.

#### PLANNED ACTIVITIES for 1980

To maximize future utility, these studies need to include flame radiation, external radiation, vitiated ambience, compartment geometry effects, and turbulence. The first step toward describing flame heights within compartments has been taken by considering the effects of nonsoffited ceiling

on free and forced flames.<sup>4</sup> Substantial increase in flame extension is predicted. Radiation due to combustion products and soot will be described in simple geometries during this grant period.<sup>5,6</sup> The full incorporation of the Equation of Transfer in combustng boundary-layer analyses will also be a major effort. In addition, we plan to examine externally imposed radiation and varying  $Y_{Ox\infty}$  as would be found in a soffited compartment. Turbulence is the most difficult aspect of compartment fire modeling and as such will be delayed until the next grant period. Dr. Phillip Thomas from

the Fire Research Station, Borehamwood, England will join us for one quarter in January 1980 as a Russell Severance Springer Visiting Professor of Mechanical Engineering to collaborate in this research and offer a short course on Compartment Fire Behavior.

## NOMENCLATURE

B	mass transfer number
$c_p$	specific heat
D	species diffusivity
$D_c$	dimensionless heat of combustion, $Q_p Y_{O_{x\infty}}/h_w$
$Gr_x$	Grashof number, $g(T_w - T_\infty)x^3/\nu_\infty^2 T_\infty$
g	acceleration of gravity
h	specific enthalpy
L	effective latent heat of pyrolysis
$\ell$	fuel slab length
$M_i$	molecular weight of specie i
Pr	Prandtl number
$Q_p$	energy released by combustion per gram of $O_2$ consumed
$Re_x$	Reynolds number, $u_\infty x/\nu_\infty$
r	mass consumption number, $Y_{O_{x\infty}} s/Y_{fw}$
s	$\nu_f M_f/\nu_{ox} M_{ox}$
T	temperature
u	streamwise velocity
v	transverse velocity
$X,$	dimensionless streamwise coordinate, $x/\ell$
x	streamwise coordinate
$Y_i$	mass fraction of specie i
$\Delta H_c$	heat of combustion per gram of fuel consumed

$\nu$	kinematic viscosity or stoichiometric coefficient
$\xi$	mixed convection number, $Gr_x/Re_x^2$

## SUBSCRIPTS

f	fuel
f $\ell$	flame
ox	oxidizer
t	transferred gas
w	fuel surface
$\infty$	ambient

## SUPERSCRIPTS

*	measured from the downstream edge of the fuel slab
---	--

## FOOTNOTE AND REFERENCES

\*This work was supported by Center for Fire Research, National Bureau of Standards.

1. C. M. Kinoshita and P. J. Pagni, "Laminar wake flame heights," J. Heat Transfer, in press (1980).
2. P. J. Pagni and T. M. Shih, "Excess pyrolyzate," Sixteenth Symposium (International) on Combustion, 1329-1342, The Combustion Institute (1976).
3. T. M. Shih and P. J. Pagni, "Laminar mixed-mode, forced and free, diffusion flames," J. Heat Transfer, 100, 253-259 (1978).
4. C. M. Kinoshita and P. J. Pagni, "Turning wake flames," in preparation.
5. C. M. Kinoshita and P. J. Pagni, "Stagnant film combustion in an absorbing-emitting gas," in preparation.
6. C. M. Kinoshita and P. J. Pagni, "Incorporation of radiation in opposed flow diffusion flame analyses," in preparation.

## FLAME RADIATION\*

C. L. Tien and S. C. Lee

### INTRODUCTION

Thermal radiation of luminous flames is becoming widely recognized as a critical factor in many physical and transport phenomena in fires. In flames as well as smoke, both gaseous and particulate matters emit, absorb and scatter thermal radiation in a significant fashion. In a broad sense, thermal radiation of flames and smoke constitutes an essential element in all practical fire problems such as fire detection, ignition, spread, plume convection and modeling. It assumes an even more prominent role in enclosure fires such as in urban housing because of the restricted high-temperature field and the interactions of flames and smoke with ceilings, floors and side walls.

During the past few years, a research program on flame radiation has been carried out at the University of California at Berkeley and the Lawrence Berkeley Laboratory as one specific task in an interdisciplinary project of fire research. The overall goal of the flame radiation research is to establish a simple physical framework for complex fire and smoke radiation calculations. The basic research approach is based on developing approximate formulations by systematically experimenting and analyzing the fundamental aspects of the problem.

Major research progress achieved in the past was concerned primarily with the physical and analytical basis of infrared radiation from flames. Specific findings include the developed methods of calculation for overlapping band radiation, non-homogeneous temperature and composition effect, continuum radiation of soot clouds, interaction between band and soot radiation, flame radiation to surrounding surface elements, effect of anisotropic scattering of particles on radiative transfer, and measurements of soot volumetric fraction for various flames.

### ACCOMPLISHMENTS DURING 1979

Research during the past year was focused on the following three topics: 1) soot radiation and optical constants, 2) radiation analysis for absorbing and scattering media, and 3) computation of enclosure convection and radiation. Research accomplishments made during the year are described below.

#### Soot Radiation and Optical Constants

The infrared radiation apparatus used previously by Buckius and Tien<sup>1</sup> for flame radiation study has been extended and modified to allow more comprehensive and accurate measurements. Major modifications include a large test chamber (3' x 3.5' W x 5' H nominal), additions of a visible-laser system, controlled ventilation, controlled oxidizer content of feed-in gas, and computerization of the data system. The new system is capable of providing data on emission, transmission and scattering character-

istics of various kinds of flames under controlled environmental conditions.

On the analytical side, a dispersion model for optical constants of soot in hydrocarbon flames has been developed in a more rigorous manner.<sup>2</sup> The deduced dispersion constants are based on in situ flame transmission data in the visible and infrared ranges, thus truly representing actual soot conditions in flames. It is shown that the soot optical properties are rather insensitive to temperature in the range of 1000 - 1600K, and relatively independent of the fuel H/C ratio.

#### Radiation Analysis for Absorbing and Scattering Media

Radiative heat transfer in flames and smokes can be modeled on the basis of dispersed particles acting as independent absorbers and scatterers in the gaseous medium. Simple, convenient representation of the absorption field has recently been successfully made.<sup>3,4</sup> The scattering field is given by the Mie solution and the phase function for each scatterer is often expressed in a series of Legendre polynomials, with the first few terms of the series characterizing isotropic scattering, linear anisotropic scattering, and Rayleigh scattering. The mean beam length formulation for Rayleigh and linear anisotropic scattering in planar geometry has been established, and extensions to cylindrical and spherical geometries is being conducted at present. Resistance network representation of an absorbing-scattering system has also been developed on the basis of the two-flux model, and the linear anisotropic scattering model.<sup>5</sup> Current effort is directed to further improvement in the modeling of anisotropic scattering and in the realistic computation of flame and smoke radiation.

#### Computation of Enclosure Convection and Radiation

Different computation schemes for enclosure convection (elliptic-type) have been examined carefully with their respective strengths and limitations.<sup>6</sup> Proposed refinements include more effective ways of handling boundary conditions<sup>7</sup> and the formulation of higher-order differencing schemes.<sup>8</sup> Progress has also been made in achieving simple approximate solution for radiation heat transfer in one-dimensional, non-planar geometries<sup>9</sup> and multi-dimensional geometries.<sup>10</sup> Interaction between enclosure convection and radiation is currently being pursued.

### FOOTNOTE AND REFERENCES

\*This work was supported by the Center for Fire Research, National Bureau of Standards.

1. R. O. Buckius and C. L. Tien, "Infrared flame radiation," International Journal of Heat and Mass Transfer, 20, 93-106 (1977).

2. S. C. Lee and C. L. Tien, "Optical constants of soot in hydrocarbon flames," submitted for publication.
3. W. W. Yuen and C. L. Tien, "A simple calculation scheme for the luminous-flame emissivity," Proceedings of the 16th International Combustion Symposium, 1481-1487 (1977).
4. G. L. Hubbard and C. L. Tien, "Infrared mean absorption coefficients for luminous flames and smoke," Journal of Heat Transfer, 100, 235-239 (1978).
5. T. W. Tong and C. L. Tien, "Network representation of radiative heat transfer with particulate scattering," Paper No. 79-42, Western States Section/The Combustion Institute, Fall Meeting (1979).
6. L. C. Chow and C. L. Tien, "An examination of four differencing schemes for some elliptic-type convection equations," Numerical Heat Transfer, 1, 87-100 (1978).
7. L. C. Chow, Y. K. Cheung, and C. L. Tien, "A new finite-difference representation for the vorticity at a wall with suction," Numerical Heat Transfer, 1, 417-423 (1978).
8. L. C. Chow, Y. K. Cheung, and C. L. Tien, "A higher-order difference scheme for convective-diffusive equations," AIAA Paper No. 79-1466 (1979).
9. W. W. Yuen and C. L. Tien, "Approximate solutions of radiative transfer in one-dimensional non-planar systems," Journal of Quantitative Spectroscopy and Radiative Transfer, 19, 533-549 (1978).
10. W. W. Yuen and C. L. Tien, "A successive approximation approach to problems in radiative transfer with a differential formulation," Journal of Heat Transfer, 102 (1980).

## FIRE GROWTH EXPERIMENTS — TOWARD A STANDARD ROOM FIRE TEST\*

*R. B. Williamson and F. L. Fisher*

### INTRODUCTION

The object of this fire research project is to develop experimental methods which can be utilized for a standard room fire test. There is a growing trend to use full-scale room fire experiments for evaluation of the fire growth characteristics of materials and building systems. Yet, in spite of this, there is still no standard version of a room fire test. The exact details of a standard room fire test are presently being debated by working groups within the American Society of Testing and Materials (ASTM). Their place of departure is the ASTM E603-77 Guide for Room Fire Experiments<sup>1</sup> which discusses the choices available for such parameters as compartment design, ignition source, instrumentation, test procedure, analysis of data and reporting of results.

The purpose of a large-scale standard test would be to evaluate the fire performance of materials under actual in-use situations. Tests at the Forest Products Laboratory<sup>2</sup> to relate the 8-foot tunnel furnace to realistic fire situations, and more recently, Lee and Parker's research<sup>3</sup> on the contribution of furnishing and lining materials to fire growth, have found that compartment or room-like experiments were necessary to predict realistically the behavior of a specimen when subjected to a pre-flashover fire environment.

The two principal small-scale, or laboratory scale fire test methods for fire growth in the United States, ASTM E84 and E162, have simplistic

data reduction schemes masking much of the true test specimen performance. In addition, many plastic specimens give little indication of how they will behave under end-use conditions. Presently, a series of small-scale tests are being developed, but there is a need for full-scale test data to support the validity of these tests.

It is the researchers' view that a standard room fire test could be used as both a development tool and as a performance evaluation method until the series of smaller, less expensive tests have been verified. Even then, new materials and systems would continue to require full scale testing to prove applicability of the small-scale tests.

The experiments conducted in connection with this research have been directed toward answering the following questions:

1. Can a room fire test be expected to be a repeatable, scientific experiment and supply information on which to base a prediction of the contribution of materials to fire growth?
2. What details have to be fixed to insure a meaningful standard test and what values should be chosen for such important parameters as the ignition source?
3. What is the contribution of a thin cellulosic material to fire growth under the standard test conditions?

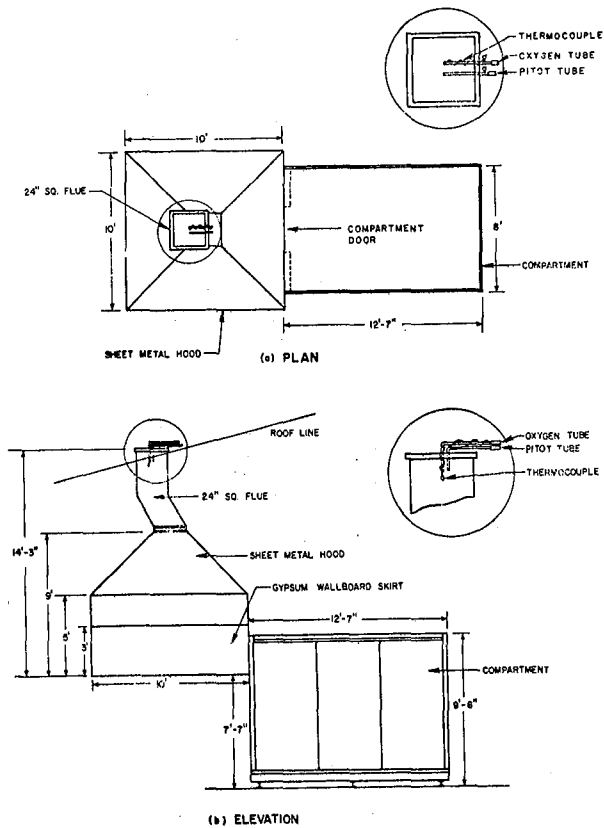


Fig. 1. The experimental compartment and vent system as shown in plan (a) and elevation (b). (XBL 802-8012)

Eleven room fire experiments were conducted in a 2.44 m x 3.66 m x 2.44 m (8' x 12' x 8') test compartment shown in Fig. 1. The experiments had a variety of materials on all walls and ceilings:

Test No.	Wall	Ceiling
C-162	Glass Fiber Insulation	Glass Fiber Insulation
C-162,171,172	Gypsum Wallboard	Gypsum Wallboard
C-164	Plywood	Gypsum Wallboard
C-169	Plywood	Glass Fiber Insulation
C-165 - 168	Glass Fiber Insulation	Plywood
C-170	Plywood	Plywood

The experimental conditions were chosen to be consistent with an earlier version of the standard room test method under consideration by ASTM in which a gas flow of 0.117 m<sup>3</sup>/min (419 ft<sup>3</sup>/min) of CH<sub>4</sub> was specified. This is 50% of that in the current draft standard. Measurements were made of 1) the oxygen depletion in the exhaust gases leaving the room, 2) the air temperature at a number of locations, 3) the air flow and temperature at the doorway, and 4) heat fluxes at several locations.

## ACCOMPLISHMENTS DURING 1979

The eleven separate experiments are summarized in Table 1. They fall into the following categories:

1. Experiments C-162, 163, 171, and 172 are essentially calibration experiments in which the ignition source released the only significant energy within the compartment.
2. Experiments C-164 and 169 are duplicate experiments; both had plywood on the walls. These two experiments are particularly interesting since they took approximately the same time to flashover (within 15 seconds) and thereby illustrate the repeatability of such experiments.
3. Experiments C-165, 166, 167, and 168 prove that the plywood ceiling was not ignited unless the flame from the ignition source played directly on its surface. In experiment C-168, the ignition source was raised to enable the flames to reach the ceiling and the compartment reached flashover in 6 minutes, 13 seconds. Typical measurements of air temperature 1" below the ceiling and heat flux as a function of time are shown for C-168 in Figs. 2 and 3 respectively.
4. Experiment C-170 with plywood on both walls and ceilings proved to be the fastest and most intense fire.

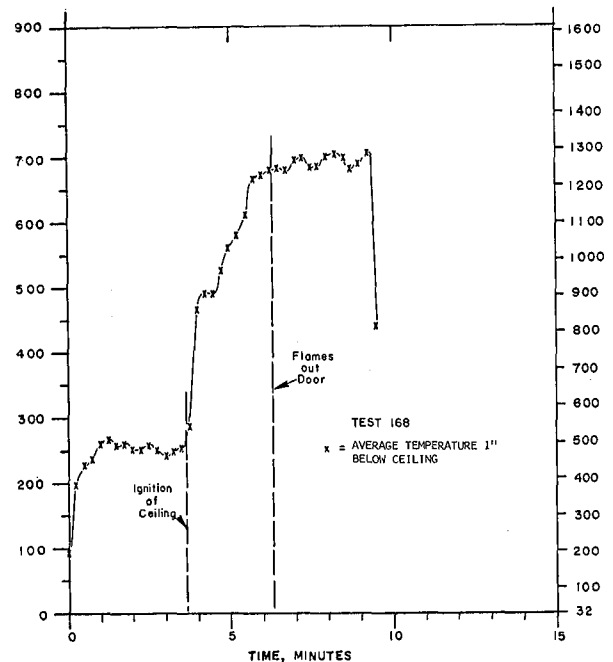


Fig. 2. Average temperature 1" below ceiling for experiment C-168 which had exposed glass fiber insulation on the walls (except in the ignition corner which was covered with gypsum wallboard) and 6.4 mm (1/4") unfinished A-D plywood on ceiling. (XBL 802-8013)

Table 1. Summary of fire test.

TEST NUMBER	MATERIAL		DURATION OF STATES			TIME TO FLASHOVER	EXTINGUISH TIME	NOTES
	WALL	CEILING	J	K	L			
C-162	Glass Fiber Insulation	Glass Fiber Insulation	-	-	-	-	15:00	A
C-163	Gypsum Wallboard	Gypsum Wallboard	0:33	-	-	-	15:00	A
C-164	Plywood	Gypsum Wallboard	0:45	0:51	2:09	3:45	4:42	B, MC = 6.16%
C-165	Glass Fiber Insulation	Plywood	-	-	-	-	10:00	B, D
C-166	Glass Fiber* Insulation	Plywood	-	-	-	-	1:00	B, D
C-167	Glass Fiber* Insulation	Plywood	-	-	-	-	10:00	A, D
C-168	Glass Fiber* Insulation	Plywood	-	3:42**	2:31	6:13	9:20	C.
C-169	Plywood	Glass Fiber Insulation	0:30	0:50	2:40	4:00	5:13	A, MC = 8.13%
C-170	Plywood	Plywood	0:16	0:39	1:56	2:51	4:10	A, MC = 10.71%
C-171-2	Gypsum Wallboard	Gypsum Wallboard	-	-	-	-	15:00	A,E

## NOTES

A - Surface of burner is 12" above the floor, against the wall  
 B - Surface of burner is 12" above the floor, 1" away from the wall  
 C - Surface of burner is 34" above floor, against the wall  
 D - No ignition of the plywood occurred  
 MC - Moisture content of plywood at time of test

E - Calibration tests done with Gypsum Wallboard on the corner walls and ceiling. The remaining inside surface area of the compartment consisted of exposed glass fiber insulation.

\* - Gypsum Wallboard in corner on both walls behind ignition source

\*\* - Ignition of ceiling

The results of these experiments have led the researchers to believe that it is indeed possible to evolve a standard room fire test which is a repeatable, scientific experiment able to supply the information allowing a prediction of the contribution of materials to fire growth.

The observations reported by these eleven experiments should be considered in establishing the many details which have to be fixed in order to prevent undesirable scatter in the results of a standard test. Other items, such as criteria for and size of the ignition source, are more than mere details; they are major components of a standard test method. These experiments also contributed to a better understanding of this major test method parameter.

The ignition source used in this research proved to be a reliable, repeatable device, yet there are some problems in utilizing it in a standard room fire test. It is the researchers' opinion that the flames should reach the ceiling from its standard location without the walls contributing to the flame spread. This is necessary if ceilings and walls are to be evaluated separately.

As mentioned above, the gas flow in these experiments was less than the draft standard currently under consideration by ASTM. Preliminary experiments show that if the gas flow is increased to the burner to achieve 42 Kcal/sec ( $10^4$  Btu/min), the value under current consideration, the flames reach the ceiling. This is true for either methane or propane. The current ASTM draft standard specifies propane because it has higher radiation which more closely approximates some actual ignition sources. Measurements of the oxygen depletion of the fire in the compartment lead to the determination of the heat release rate shown in Fig. 4, which makes it apparent that the proposed increase in heat release rate of the ignition source would not have been excessive. Figure 4 shows that the specimen contribution increased from approximately 50 Kcal/sec to approximately 200 Kcal/sec in the one minute following 6:13 when the flames emerged from the door. Because of the time delay in the measurement system, this increase probably occurred prior to the flames emerging from the door, and it illustrates that the increased heat release rate from the proposed ignition source is well below the heat release rate required for flashover.

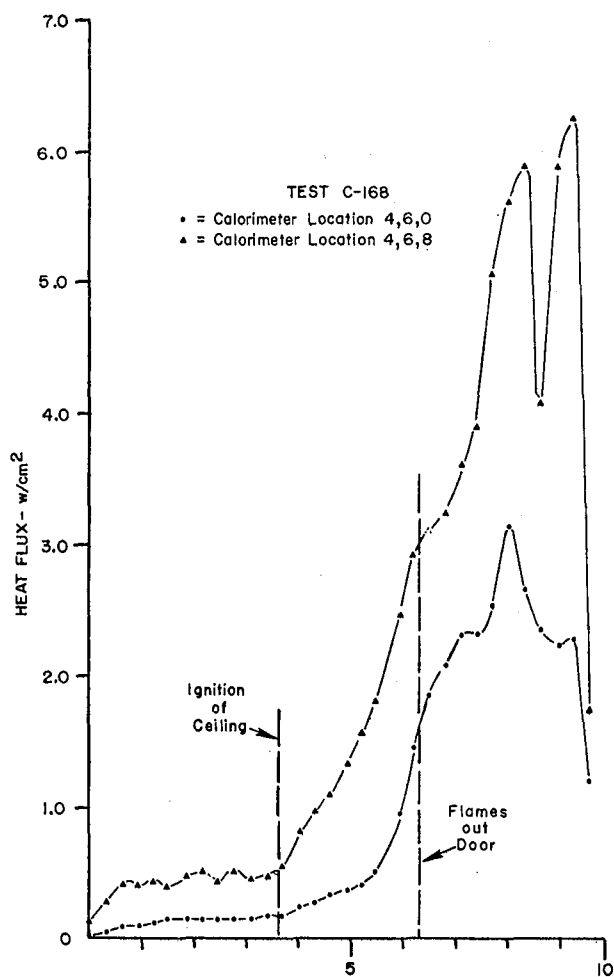


Fig. 3. Total heat flux to the center of the floor (location 4,6,0) and to the center of the ceiling (location 4,6,8) for experiment C-168. (XBL 802-8014)

The results of these eleven tests provide data on the contribution of a thin cellulosic material to fire growth under standard test conditions. This information will enable all parties involved in the consensus standard process to put the proposed test methods into perspective. Furthermore, it is also the researchers' view that the proposed standard room fire test will be utilized on materials contributing considerably less to fire growth than the thin cellulosic material used here, and that these 11 experiments will become a benchmark for comparison with other materials. For this purpose, a pass/fail criteria might be imposed based on the average ceiling temperature, time-to-flashover, heat flux at the floor, heat release rate or other data from the tests. But considerable research, particularly with regards to a precise definition of flashover, needs to be undertaken before establishing such criteria.

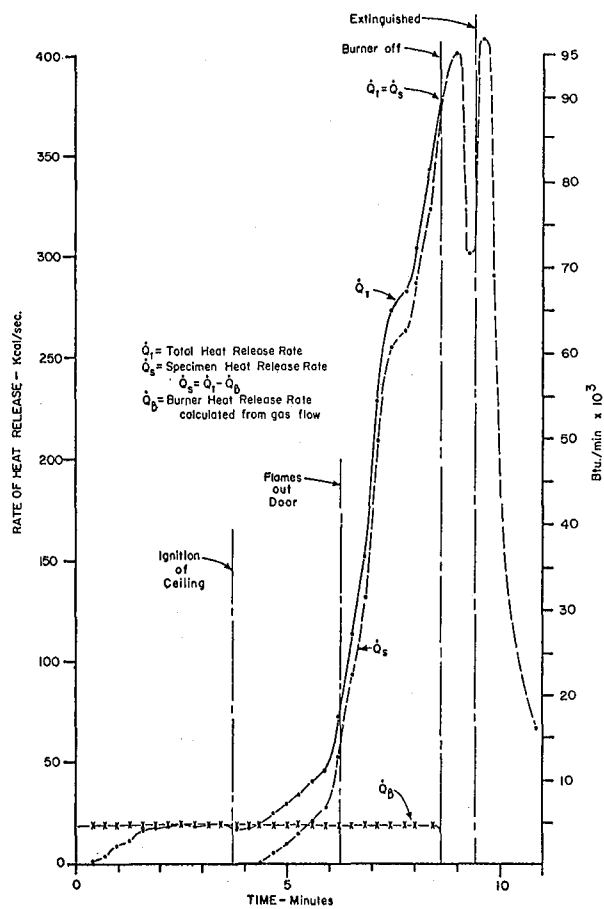


Fig. 4. The heat release rate for experiment C-168 is shown here as a function of time. (XBL 802-8015)

#### PLANNED ACTIVITIES FOR 1980

Further research in this area is now being proposed to NBS. The emphasis will be on conducting experimental fire tests which conform exactly to the current standard room fire test. A series of test specimens will be fabricated which are characterized by a range of flame spread classifications (FSC) as measured by ASTM E-84 and E-162. The emphasis in this research will be to provide a rational and scientific basis for the standard room fire test. Youden<sup>4</sup> and Wernimont<sup>5</sup> have written extensively about the procedures for developing new test methods. They discuss removing the effects of assignable causes, searching for systematic causes of variation, optimizing measurement-property relationships and evaluating ruggedness. All of these procedures and the documentation of the sensitivity of the test method will be part of the proposed research program.

## FOOTNOTE AND REFERENCES

\*This work was supported by the Center of Fire Research, National Bureau of Standards.

1. Annual Book of ASTM Standards. American Society for Testing and Materials, 1916 Race St., Philadelphia, PA.
2. Anonymous, "Surface flammability as determined by the FPL 8-foot tunnel method," U.S.D.A. Forest Products Laboratory Report 2257 (1962).
3. R. B. Williamson, "Fire performance under full-scale test conditions - A state transition model," 16th Symposium (International) on Combustion, The Combustion Institute, 1357-1372 (1976).
4. W. J. Youden, "Experimental design and ASTM Committees," Materials Research and Standards, 1, 862-867 (November 1961).
5. G. Wernimont, "Development and evaluation of standard test methods, the role of statistical design of experiments," Materials Research and Standards, 9, 8-21 (Sept. 1969).

## TESTS AND CRITERIA FOR FIRE PROTECTION OF CABLE PENETRATIONS\*

*R. B. Williamson and F. L. Fisher*

### INTRODUCTION

The spread of fire in nuclear reactors depends critically on the barrier qualities of the cable penetrations of fire resistant walls and floor/ceiling assemblies. The ASTM E-119 Fire Endurance Test Method has been used to qualify the unpenetrated walls and floor/ceiling assemblies, but if such assemblies contain cable penetrations special attention is required. This is the focus of this report.

The actual fire conditions represented by the E-119 test method are termed "post-flashover" conditions in which fire fully involves a compartment. Post-flashover fires are characterized by a positive pressure differential between the upper half of the fire compartment and the unexposed face of the wall and floor/ceiling assemblies which make up its boundaries. The initial portion of this post-flashover period is also characterized by excess amounts of fuel which have been pyrolyzed by the fire within the compartment. The positive pressure and excess pyrolyzate are clearly proven by the flames which commonly are observed to emerge from the doors and windows of both actual and laboratory post-flashover building fires.

The ASTM E-119 Standard does not specify either the pressure differential or the presence of excess fuel at the surface of the test assembly. One of the objectives of this project in the first year has been to establish the effects of varying furnace pressure on cable penetrations performance in the ASTM E-119 fire test. Another objective has been

to investigate the modes of failure for these cable penetrations and to explore the possibility of new pass/fail criteria.

### ACCOMPLISHMENTS DURING 1979

Twelve cable penetrations have been tested in two separate E-119 fire tests, and the effects of positive pressure and excess pyrolyzates have been clearly shown to play a vital role in fire spread of the cable penetration openings. If there is a path through the penetration opening, flames always appear on the unexposed face when there is a positive pressure differential and there are excess pyrolyzates in the furnace. A report is now (January 1980) being prepared which focuses on the nature of post-flashover fires and its implications on fire testing of cable penetrations.

### PLANNED ACTIVITIES FOR 1980

A draft fire test standard for cable penetrations will be written and circulated to both the fire protection and nuclear engineering communities. Fire tests will be conducted pursuant to the draft standard, and their results will be utilized to improve the standard.

### FOOTNOTE

\*This research was supported by the U.S. Nuclear Regulatory Commission through Sandia Laboratories, Albuquerque, New Mexico.

)

)

.

)

.

)

)

)

)

)

.

)

)

)

# EFFECTS OF POLLUTANTS ON BIOLOGICAL SYSTEMS

## INTRODUCTION

D. LEVY

Planning a rational energy future requires anticipating the environmental consequences of various technologies. This is difficult to do with precision as the effects of pollutants are often determined by interactions between and among complex physical (abiotic) and biological (biotic) systems. A given pollutant may affect human beings through direct exposure or indirectly through inducing changes to biological systems which humans need to utilize. The concentration of a toxin in the food chain or the destruction of organisms necessary for the maintenance of high quality water are examples of indirect effects. Pollutants can be transformed and/or degraded as they establish residence in various components of an ecosystem. Anticipation and amelioration of pollutant effects involves the integration of a vast range of data. This data includes:

- physical and chemical characterization of the pollutant as it enters the environment,
- determining effects on the various components (biotic and abiotic) within the context of the functioning ecosystem of interest,

- transformation in movements and/or degradation of the pollutant within that ecosystem and within specific organisms and physical components, and
- determining a detailed biochemical and biological picture of the interactions of pollutants with particular organisms and/or their cellular components judged salient for various processes.

The major programs described below are designed to answer parts of the above fundamental questions relevant to pollutants generated by energy related technologies. Their emphasis is on anticipating consequences to the biological components of various ecosystems. The work ranges from studies involving parts of a single cell (the membranes) to studies involving the whole ecosystem (in the pelagic zone of a lake). The programs take advantage of expertise and technical abilities present at LBL.

Two small exploratory projects which were of brief duration and not related to anticipating biological effects of pollutants are included in this section. They concern geothermal technology and its improvement using techniques based on organic and physical properties of certain materials.

## PAREP: POPULATIONS AT RISK TO ENVIRONMENTAL POLLUTION\*

*D. Merrill, B. Levine, S. Sacks, S. Selvin, and C. Hollowell*

### INTRODUCTION

The project PAREP (Populations at Risk to Environmental Pollution) supersedes an earlier project PARAP (Populations at Risk to Air Pollution). An integrated data base assembled by the LBL Computer Science and Applied Mathematics Department<sup>1</sup> is being analyzed by the LBL Energy and Environment Division in collaboration with the School of Public Health of the University of California.

The PAREP data base covers the United States and territories at the county level, with subcounty detail for some data elements. The data base consists of socioeconomic and demographic data, mortality data, and air-quality data. Approximately 3,000 data items are available for each county.

### Air Quality Data

Previous nationwide analyses have averaged air-quality measurements from the monitoring stations within each county. Such a method is unsatisfactory because (1) many counties have no active monitoring stations, and (2) many people live closer to stations outside their county than to those within their county of residence.

Accordingly, in its task of creating a nationwide directory of air-quality data by county, the

PAREP group first determined reliable latitudinal and longitudinal coordinates for each active monitoring station, corrected numerous errors in the existing EPA monitoring station directory file, and combined these data with related files from several independent sources. Discrepancies were resolved by computer, when possible, and by consulting maps.

Yearly summaries of air-quality data for 1974-1976, covering nine pollutants, were obtained from the EPA SAROAD (Storage and Retrieval of Aerometric Data) data bank and merged with corrected coordinates.

Figure 1 displays the three-year geometric mean value of total suspended particulate concentration at monitoring stations in California. As is evident from the figure, air quality is poorest in the Los Angeles area. Air quality was then estimated at the population center of each county as a weighted average of measurements from all nearby stations, whether in the county or not.

### Mortality Data

The PAREP data base contains county-level age-adjusted mortality rates<sup>2</sup> by sex and race from two sources: (1) 1968 to 1972 mortality statistics for 53 causes of death, from the University of Missouri; (2) 1950 to 1969 mortality statistics

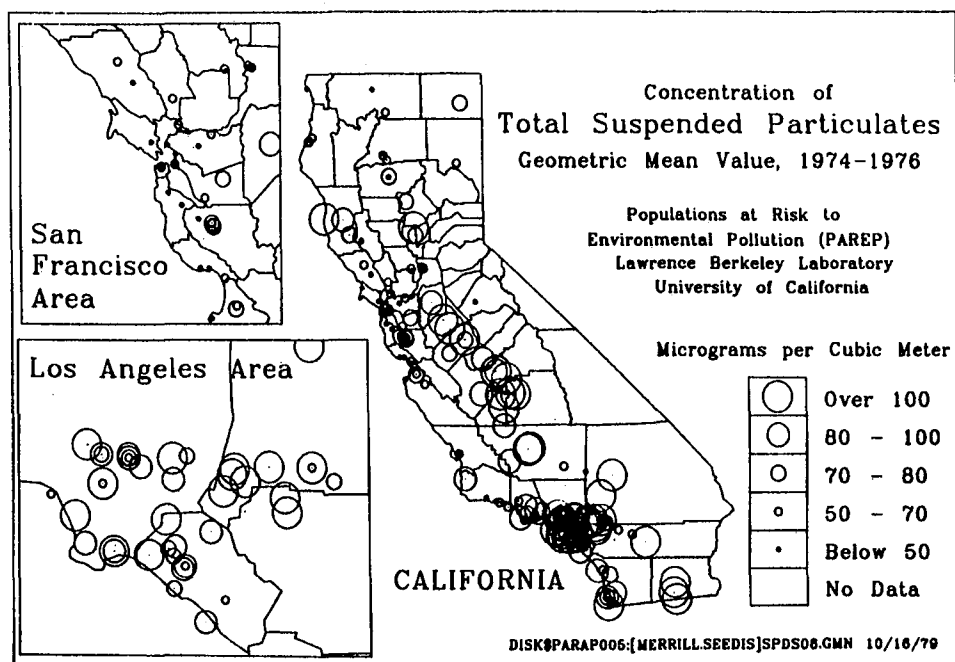


Fig. 1. Three-year geometric mean value of total suspended particulate concentration is plotted as a circle at the station's location. The size of each circle indicates the relative pollutant concentration.

for 35 cancer sites, from the National Cancer Institute.

Standard scores were calculated as  $(\text{county rate} - \text{U.S. rate})/(\text{error})$  where "error" is the absolute statistical error of the county rate, estimated as the county rate divided by the square root of the number of deaths (or the expected number of deaths, if no deaths occurred).

Table 1 illustrates the incidence of stomach cancer among white males in Arizona for 1968-1972 using this standard score. Although the rate in Maricopa county (around Phoenix) is not as low as in four other counties, its deviation below the U.S. mean is statistically the most significant.

Figure 2 presents similar data for California and Hawaii in map form. Significant deviations above the U.S. mean are observed around Los Angeles, San Francisco, Sacramento, and Hononulu. By plotting standard scores rather than rates, random fluctuations in small counties do not obscure statistically significant trends in large cities.

#### Socio-economic and Other Data

Indicators of socio-economic status (SES) (income, education, employment by industry and occupation, etc.) were obtained from the 1970 U.S. Census. In addition, the PAREP data base includes corrected 1970 population counts by age, sex, race, and marital status (for the purpose of normalizing mortality or morbidity rates), the Census Bureau's best available 1970 county population estimates, and related files providing subcounty detail on the geographic distribution of the U.S. population.

Most of the PAREP data base is being converted to a format suitable for use in the SYSTEM 2000 Data Base Management System. The same data and

Table 1. Stomach cancer in white males, State of Arizona U.S. rate = 10.20.

	1970 Population	1968-72	
		Annual Rate per 100,000	Standard Score
AN PINAL	29983	15.02	1.43
AN YAVAPAI	17982	15.26	1.16
AZ YUMA	28938	12.24	0.65
AZ APACHE	3913	0.00	-0.00
AZ SANTA CRUZ	6429	10.11	-0.02
AZ GRAHAM	7381	9.68	-0.10
AZ GILA	12066	9.75	-0.12
AS PIMA	160936	10.10	-0.12
AZ GREENLEE	5038	9.00	-0.20
AS MOHAVE	12588	8.36	-0.49
AZ NAVAJO	11683	4.13	-2.18
AZ COCONINO	17359	3.99	-2.77
AZ COCHISE	30222	4.81	-2.89
AZ MARICOPA	448324	7.97	-3.61

associated files are installed in LBL SEEDIS (Socio-economic Environmental Demographic Information System), an interactive information system operating in a network of DEC VAX computers. SEEDIS permits the PAREP data to be used in combination with files from other sources. Selected data, as well as data entered by the user, can be easily combined and displayed in tabular or graphic form, including maps.

#### ANALYSIS

Analysis of the PAREP data base is in progress in the following areas.

#### Estimation of Air Quality

This analysis considers the problems involved in geographic interpolation of annual average air-quality measurements. Statistical and graphic techniques are used to determine the validity of the averaging procedures described above. The basic criterion is that the model must accurately predict air quality at the position of a monitoring station as a function of measurements from nearby stations. The study will attempt to determine (1) the best value of the scaling parameter  $d_0$  (described above) and (2) realistic standard deviation errors associated with county air-quality estimates.

#### Ecologic Patterns of Disease in the United States

The PAREP data base is an ecological data base, i.e., the basic unit is a group of individuals whose characteristics are known only on the average. In other words, analysis of PAREP data will not identify cause-and-effect relationships between air pollution and lung cancer, for example. The data on which the PAREP must rely does not permit such inferences to be drawn. On the other hand, PAREP can provide, at low cost, a quantitative description of the relationships among a large number of variables. Any strong correlations that emerge and cannot be explained would become candidates for intensive study. We are using the straightforward analysis technique of multiple regression, with mortality as the dependent variable and other variables (income, education, air quality, etc.) as independent variables. Patterns of disease are analyzed after removal or partial removal of the hypothesized linear influences of SES and air-quality variables. Such an analysis was performed earlier<sup>3,4</sup> on a preliminary data base containing California data. Statistical limitations prevented any firm conclusions from being drawn. A similar analysis is being repeated for the entire United States.

As part of the PAREP project, we are also analyzing data from the Third National Cancer Survey, which recorded all incidences of cancer between 1969 and 1971 in nine areas of the United States. Individual case records, coded by census tract, have been merged with tract-level SES data from the 1970 census, and tract-level air quality estimates calculated as described above. Multiple regression and other techniques are being used to describe relationships among air quality, socio-economic status, and the incidence of certain histologic cancer types.

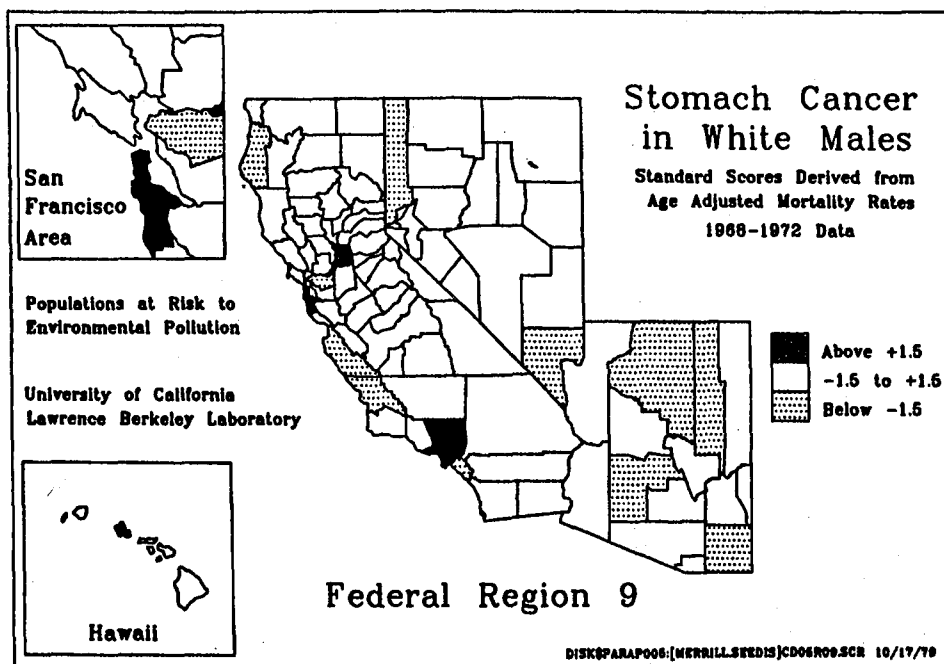


Fig. 2. Typical of maps used to display geographic correlations in mortality statistics.

#### PLANNED ACTIVITIES FOR 1980

The following projects, to be described in terms of data, general analytic strategy, and potential future direction, are proposed for 1980.

1. Ecologic patterns of disease in the United States.
  2. Air quality, socio-economic status and cancer incidence in the San Francisco Bay Area.
  3. Consequences of ecologic regression.
  4. The association of socio-demographic measurements and histologic cancer type for nine sites.
  5. Standardization of age-adjusted mortality rates for county-level data.
1. S. T. Sacks, S. Selvin, and D. W. Merrill, Building a United States County Data Base: Populations at Risk to Environmental Pollution, presented at the National Institute of Aging, Bethesda, Md., June 26, 1979; Lawrence Berkeley Laboratory Report, LBL-9636 (September 1979).
  2. S. Selvin, S. T. Sacks, and D. W. Merrill, "Standardization of age-adjusted mortality rates," Lawrence Berkeley Laboratory Report, LBL-10323 (February 1980).
  3. D. W. Merrill, S. T. Sacks, S. Selvin, C. D. Hollowell, and W. Winkelstein, Jr., "Populations at Risk to Air Pollution (PAREP). Data base description and prototype analysis," Lawrence Berkeley Laboratory Report, UCID-8039 (August 1978).
  4. C. D. Hollowell, S. T. Sacks, S. Selvin, B. S. Levine, D. W. Merrill, and W. Winkelstein, Jr., "PAREP: Populations at Risk to Environmental Pollution- Data base description and prototype analysis," in Energy and Environment Division Annual Report 1978, pp. 152-155; Lawrence Berkeley Laboratory Report, LBL-8619 and UC-13 (1979).

#### FOOTNOTE AND REFERENCES

\* The work described in this report was funded by the Office of Health and Environmental Research, Assistant Secretary for Environment of the U.S. Department of Energy under Contract No. W-7405-ENG-48.

## MEMBRANE OXIDATIVE DAMAGE\*

L. Packer, A. Quintanilha, E. Kellogg III, R. Mehlforn,  
M. Nova, L. Cheng, and J. Maguire

### INTRODUCTION

We are pursuing studies on the effects of environmental and polluting factors on mammalian cellular membranes. Our previous reports<sup>1,2</sup> showed how sensitive isolated mitochondria, whole cells (Hepatocytes), and model membranes are to the damaging species of oxygen.

We have assumed that ozone and various reactive species of oxygen, some of which could be generated by several cellular photosensitizers in the presence of visible light, will react with enzymes and other protein and lipid constituents of membranes thereby altering their activity and structure.<sup>3</sup> Our studies have been extended to *in vivo* and *in vitro* studies of light sensitivity of catalase, a crucial enzyme involved in the protection against oxidative damage. Since catalase is a key enzyme in  $H_2O_2$  metabolism, the importance of its inactivation to the overall metabolic protective capacity of cells is at present being carefully characterized to identify its significance in the time sequence of cellular damaging events. Superoxide involvement in the elusive bactericidal effects of negative air ions has also been investigated. Spin trapping techniques have been used to assay for different types of radicals, and model systems have been perfected to monitor membrane protein and lipid-protein interactions to allow us to localize and characterize the mechanisms of oxidative damage.

### CATALASE STUDIES

Catalase, an enzyme consisting of four heme containing subunits, decomposes  $H_2O_2$  and may be one of the main defenses against oxidative toxicity in the cell. Figure 1 shows the main physiological

pathway in which catalase is involved. We have described the inactivation of catalase *in vivo*, in intact isolated hepatocytes exposed to visible light.<sup>4</sup> Photoinactivation of catalase with visible light ( $>400$  nm) was also done in peroxisomal catalase in the mitochondrial fraction of rat liver, and in purified bovine liver catalase.<sup>5</sup>

The action spectrum (Fig. 2) indicates that light with a wavelength corresponding to that of maximal absorbance of the heme moiety acted most effectively in the photoinactivation of catalase. The  $O_2$  dependence of catalase photoinactivation shows that high concentrations of  $O_2$  stimulate inhibition, while anaerobic samples are not inactivated. Scavengers of  $\cdot OH$  (0.25 M sucrose),  $^1O_2$  (1 mM histidine) and  $O_2^-$  (10  $\mu g/ml$  SOD, superoxide dismutase) did not prevent the inactivation process, while catalase substrates (100  $\mu M$  formic acid, methanol or ethanol) afforded complete protection.

Peroxisomal catalase in the mitochondrial fraction is far more susceptible to photoinactivation than purified catalase; much lower light intensities are required for inactivation in the mitochondrial system, but superoxide dismutase does afford partial protection. Our results indicate that despite the strict dependence upon  $O_2$ , no protective effect of scavengers of  $\cdot OH$  and  $^1O_2$  could be detected. This lack of protective effect may result from the inaccessibility of these scavengers to the active site. The complete protective effect of substrates may involve their scavenging of  $\cdot OH$  at the active site itself. The fact that in the case of the substrate formic acid, only 0.1% of the hemes are ligated at any time, suggests that the protective effect of substrates

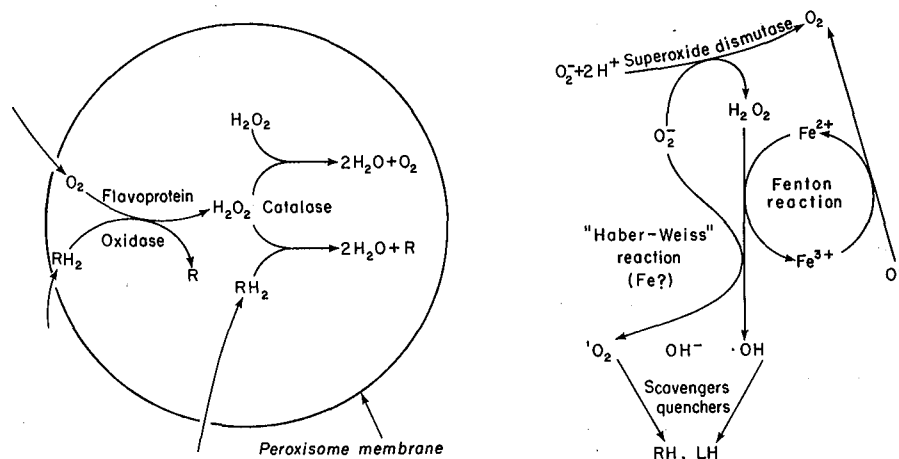


Fig. 1. Chemical and biochemical reactions for the formation and removal of peroxides. (XBL 809-1920)

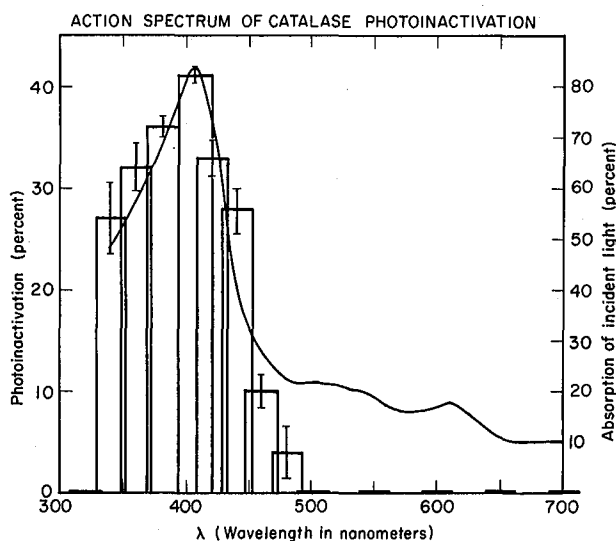


Fig. 2. Action spectrum of catalase photoinactivation. (XBL 793-3330)

results from their conversion of catalase from Compound I to the Ferricatalase form<sup>6</sup> and a marked photosensitivity of Compound I alone.

The protection of catalase of the mitochondrial fractions by superoxide dismutase suggests that  $O_2^-$  and  $H_2O_2$  may be produced by the mitochondria or the peroxisomes during illumination. The physiological importance of the photoinactivation of catalase may be particularly important in "Acatalasemic" individuals exposed to short term light stress. Catalase inactivation would result in large increases in  $H_2O_2$ , thereby promoting the formation of  $\cdot OH$ , a dangerous oxygen radical. Recent work<sup>7,8</sup> has shown that the wavelength responsible for chromosomal damage peaked at 405 nm, the wavelength that corresponds to the maximal absorbance and inactivation of catalase in our studies. These results, and the fact that externally added catalase eliminated the light induced chromosomal damage, suggest that the light damage seen in their systems may result mainly from catalase inactivation.

#### SUPEROXIDE EFFECTS ON BACTERIA

The underlying biochemical changes of the biological effects of small air ions have only been detected in a few instances.<sup>9</sup> Many studies have demonstrated the bacterial effects of  $O_2^-$ . Since the mysterious physiological and psychological effects of negative air ions have attracted the interest of many investigators, we decided to test for the involvement of  $O_2^-$  in this phenomenon by evaluating the protective effect of SOD.<sup>10</sup>

We found that exposure of bacteria to negative air ions caused total loss in viability. The addition of 10  $\mu g/ml$  SOD protected bacteria completely while catalase or denatured SOD had no significant protective effect. A possible mechanism of the observed effect might involve  $O_2^-$  acting as a

nucleophile on the phospholipid bilayer, causing a de-esterification of fatty acids. This could lead to an increase in surface charge and a weakening of the membrane, which under hypotonic conditions might lead to cell lysis and death. These results support the concept that the negative air ions responsible for bacterial death must either be hydrated superoxide anions or must generate  $O_2^-$  in the suspension medium.

#### MODEL STUDIES

Spin trapping techniques have been used to study the effects of both biological chelators (such as transferrin and ferritin) and synthetic chelators (such as ethylenediamine tetra acetate, EDTA and diethylenetriamine penta acetate, DETPA) on the Fenton reaction (Fig. 1), where iron reacts with hydrogen peroxide to produce hydroxyl radicals (probably the most potent biological toxicant found *in vivo*). Our results show that biologically bound iron in ferritin has no significant pro-oxidative effect, while iron bound to EDTA has a somewhat enhanced pro-oxidative effect compared to free iron. Other studies involving iron catalysis of epinephrine (a neuro transmitter) autooxidation show a similar pattern of enhancement or suppression of pro-oxidant catalysis by various forms of bound iron. Since iron has been shown to be a powerful oxidant and  $\alpha$ -Tocopherol (Vitamin E) is a well known antioxidant, a series of studies is in progress on the protective or damaging effects of different levels of Fe and Vitamin E in controlled diets fed to rats. We have found that iron deficiency decreases the total amount of Fe-S centers in mitochondria and that Vitamin E deficiency increases lipid peroxidation in isolated cells (hepatocytes) and cellular organelles. The effect of Vitamin E deficiency on mitochondrial membranes seems to indicate an increase in their overall negative surface charge which may be related to the presence of greater levels of lipid peroxides found in these membranes. Sucrose (a known  $\cdot OH$  radical scavenger) in the incubation medium, decreases the effects of Vitamin E deficiency on the photooxidative damage to lipids and enzymes of mitochondria. The photo-destruction of spin labels has been used successfully to monitor the release of flavins from biological membranes. Our results indicate that a possible mechanism for mitochondrial photooxidative damage may be the release of important flavin co-factors in some of the dehydrogenase complexes found in these membranes. Several techniques (spin labeling and cross-linking) have been perfected in our laboratory for studying the importance of peptide mobility on enzymatic activity and electron transport in mitochondria and for determining the orientation of intrinsic membrane components.<sup>11-15</sup>

#### PLANNED ACTIVITIES FOR 1980

Future studies will concentrate on four major areas:

- 1) To arrive at an understanding of photo-sensitive mechanisms of oxidative damage in cells and to determine the specific oxygen species responsible for such damage. Other metabolic pathways that involve hemes and flavins (both believed

to be important photosensitizers) such as the drug-metabolizing mixed-function cytochrome P-450 oxidase and other amino oxidases will be studied.

2) To use spin-trapping and spin-destruction techniques to identify the radicals and radical generating species in *in vitro* membrane systems that are responsible for the damage observed.

3) To continue the use of controlled diet studies in rats to modify the composition of the biological membranes under study and to help us in determining the components that enhance or reduce photooxidative damage. Dietary iron and Vitamin E levels will be controlled in those studies.

4) To continue spin-labeling and other EPR techniques which play a major role in the study of such parameters as membrane permeability and fluidity and which will be used to measure membrane surface charge, peptide mobility and the concentration of free radical intermediates in many of the membrane associated enzymatic reactions.

#### FOOTNOTE AND REFERENCES

\*This work was supported by the Department of Energy, Secretary of Environment.

1. Energy and Environment Division Annual Report-1977, Lawrence Berkeley Laboratory report, LBL-6877, pp. 142-146 (1977).
2. Energy and Environment Division Annual Report-1978, Lawrence Berkeley Laboratory report, LBL-8619, pp. 166-170 (1978).
3. L. Packer and E. W. Kellogg III, "Photooxidative damage to mammalian cells and proteins by visible light" in ACS Symposium Series 123, Chemical Deterioration of Proteins (J. R. Whitaker and M. Fujimaki eds.) pp. 83-93, 1980, Lawrence Berkeley Laboratory report, LBL-9672 (1979).
4. L. Y. L. Cheng, and L. Packer. "Photodamage to hepatocytes by visible light," FEBS Lett. 97, 124-178 (1979).
5. L. Y. L. Cheng, E. W. Kellogg III and L. Packer. "Photoinactivation of catalase by visible light," submitted to Photochem. Photobiol., Lawrence Berkeley Laboratory report, LBL-9743 (1979).
6. G. R. Schonbaum and B. Chance, The Enzymes, Vol. XIII, pp. 363-408 (1976).
7. R. Parshad, K. K. Sanford, G. M. Jones, and R. E. Tarone, Proc. Natl. Acad. Sci. USA, 75, 1830-1833 (1978).
8. R. Parshad, K. K. Sanford, G. Taylor, R. E. Tarone, G. M. Jones, and A. E. Baeck. Photochem. Photobiol. 29, 971-975 (1979).
9. A. P. Krueger, and E. J. Reed. Science 193, 1209-1213 (1976).
10. E. W. Kellogg III, M. G. Yost, N. Barthakur and A. P. Krueger. "Superoxide involvement in the bactericidal effects of negative air ions on staphylococcus albus," Nature 281, 400-401 (1979).
11. M. Swanson, and L. Packer. "Effect of cross-linking on mitochondrial cytochrome c oxidase," submitted to Arch. Biochem. Biophys. (1979).
12. R. Mehlhorn, and L. Packer. "Membrane surface potential measurements with amphiphilic spin labels," Methods in Enzymology, Vol. LVI, Part G, pp. 515-526 (1979).
13. A. T. Quintanilha, M. S. Swanson and D. D. Thomas. "Rotational mobility of soluble and reconstituted cytochrome oxidase," Biophys. J. 25, 170a (1979).
14. M. Swanson, R. Mehlhorn, L. Packer, and P. Smith, "An imidoester spin-label probe of cytochrome c-cytochrome oxidase interactions," submitted to Arch. of Biochem. Biophys. (1979).
15. M. Swanson, A. T. Quintanilha, and D. D. Thomas. "Protein rotational mobility and lipid fluidity of purified and reconstituted cytochrome c oxidase," J. Biol. Chem. 255, 7494-7502 (1980), Lawrence Berkeley Laboratory report LBL-9661 (1979).

# LAKE ECOTOXICOLOGY: METHODS AND APPLICATIONS\*

*J. Harte and D. Levy*

## INTRODUCTION

The complexity of ecological processes and the wide range of potentially toxic substances that can be released into the environment from energy-related activities presents the ecotoxicologist with an enormous task. The purpose of this research is to develop and apply improved methods for predicting ecological effects of toxic substances in freshwater lakes. Part of our research is aimed at understanding the behavior of laboratory microcosms and improving their design and operation to make them more useful, while a second part focuses on applications of laboratory microcosms to selected problems in ecotoxicology.

In an ecological context, a laboratory microcosm is simply a collection of chemicals and organisms within well-defined spatial boundaries, usually under controlled physical conditions, in a volume convenient for laboratory study. The ease with which aquatic microcosms can be perturbed or manipulated, and the opportunity they provide for replication and control of systems with considerably more diversity than single organism cultures, suggests that they may be a useful tool for work in ecotoxicology. However, a number of drawbacks are implicit in their small size and artificial environment, and these drawbacks may drastically limit the range of assessment studies that can be performed reliably. Results obtained from microcosm studies may in some, or perhaps most, cases bear little relation to what would be observed in the natural systems that the microcosms were designed to describe. Even when microcosms are initiated from nearly identical conditions, their replication may not be faithful. Moreover, surface effects may complicate the analysis of nutrient budgets and pollution pathways. Over the past four years we have undertaken a series of studies on microcosm design and operation in order to understand these limitations, and at the same time to improve the effectiveness of microcosms as assessment tools in ecotoxicology.<sup>1-3</sup> These studies utilized microcosms ranging in size from 2 to 700 liters and containing a diverse assemblage of biota initially obtained from local lakes.

One of the most serious problems in using microcosms is the excessive growth of algae on the inner walls of the containers. Because the surface-to-volume ratio of a microcosm is considerably larger than that of a natural lake, surface growth of algae and bacteria can exert a disproportionate, or unnatural, influence on water-column nutrient concentrations and pelagic communities. In addition to the distorting influence of this effect, reliable sampling of the sides and bottom is very difficult to perform. Thus, if the most frequent and reliable measurements are in the water column, then much of the activity in the microcosm is missed during periods of heavy side growth and efforts to balance nutrient budgets will be futile. In FY 78, we demonstrated that surface growth could be eliminated

successfully from our systems by the simple expedient of transferring the contents of each system to a clean vessel at weekly intervals. This process of periodic transfer introduces periodic mixing in the microcosms, which could affect biological or chemical phenomena and, potentially, result in a loss of replicability. In an ongoing series of experiments, possible side-effects of this surface-growth-control strategy are being investigated. We have also concentrated on determining how well lake microcosms behave like, or "track", the natural lakes that supply the microcosm water. The goal of this phase of our research is to learn how to design and operate the microcosms so as to increase the resemblance between them and their "parent" lake, with the proviso that the systems developed are not prohibitively complex or expensive. To this end, we have closely integrated our laboratory studies with field investigations of the parent lakes.

As our understanding of microcosm behavior and our ability to enhance microcosm design and operation have progressed, we have initiated experiments relevant to current ecotoxicological problems. One such problem is the alteration of decomposition processes in aquatic ecosystems; such alteration can have a great effect on nutrient cycles and therefore on primary productivity. An ongoing application of our microcosms is the investigation of effects of pollutants on the ability of microorganisms to decompose and mineralize organic detritus. A new research program was organized this year to investigate the impact of acid precipitation on aquatic ecosystems in the Sierra Nevada. It includes two phases: 1) background water quality measurements of selected watersheds on the western slope of the Sierra Nevada, and 2) microcosm research simulating ecosystem response to additions of acid precipitation. Emphasis is placed on acid-metal interactions as the possible mechanism for toxic effects on biota.

## ACCOMPLISHMENTS DURING 1979

Two experiments comparing in detail a particular lake's behavior over several months with the microcosms derived from it were carried out.<sup>4</sup> Each experiment utilized a different lake. Field sampling was accomplished using a 14 foot boat equipped with a non-polluting electric motor and standard field sampling equipment. The variables measured in both lakes and microcosm systems on a weekly basis were pH, illumination levels, fluorescence, inorganic nutrients, and phytoplankton and zooplankton species (volume and numbers). Our microcosms are housed in a temperature-controlled room, illuminated by banks of high-output fluorescent lights on a 12h:12h light:dark cycle. The light irradiance at the surface of the water is now set at 7.0 watts/cm<sup>2</sup> (PAR). Cylindrical containers are used for the microcosms, with the larger containers made of nalgene or fiberglass and the smaller systems made of glass.

In the first experiment, a small reservoir (Lafayette, CA) was compared with replicates of 4 liter and 200 liter microcosms. The reservoir is well used for boating and fishing, and receives substantial run-off after rains. The tracking of this reservoir by the microcosms was very poor. The dominant phytoplankton in the lake throughout the run were diatoms whereas in the microcosms the diatoms disappeared within the first two weeks. Subsequently, flagellates and filamentous greens become the dominant phytoplankton in the 200 liter microcosms. The 4 liter microcosms did not support any significant phytoplankton populations after the first two weeks. Total zooplankton volumes in the microcosms were higher than in the lake. During and subsequent to rain fall, high levels of  $\text{NH}_4^+$  (probably due to run off) were found in the lake as compared to the microcosms.

In the second experiment, a considerably larger reservoir (Briones) was compared with replicate -- 15, 50, and 150 liter microcosms. This reservoir is a deep (200 ft) lake which receives little run-off. Its water comes, via aqueduct, from the Mokelumne River of California. One set of the 50-liter microcosms received a weekly 1-liter inoculation of water from the reservoir (gathered on sampling days) while the other 50 liter set did not. During the first 6-7 weeks, tracking of the lake by all the microcosms was excellent, with diatoms, Phacus, and other flagellates the dominant phytoplankton. In addition zooplankton and inorganic nutrients in the microcosms tracked the lake well. After 7 weeks, diatoms in both the lake and microcosms disappeared. After this period, the dominant phytoplankton in the lake were dinoflagellates and blue-green algae, while in the 50 and 150 liter microcosms an attached filamentous green (Ulotrix) dominated. In the small 15 liter systems, a green algae (Gloeocystis) dominated after 7 weeks. Similar behavior was observed within replicate microcosms.

From the results of these experiments and other tracking studies currently in progress, we will extract implications for microcosm users. Preliminary analysis of the data from the completed experiments suggests that tracking may be inadequate in lakes that are not sufficiently large to reduce the relative effects of the surrounding watershed on their behavior, and it may also be inadequate in microcosms that are too small. Tracking difficulties also can arise when diatom populations are important in the natural lake, for these populations do not do well under microcosm conditions. Under suitable conditions, excellent tracking is attainable over periods of 6-7 weeks. The importance of careful taxonomic data collection, as well as water chemistry measurements, is underscored by these studies. If care is taken in the initiation process, replication of results among systems set up under nearly identical conditions is attainable. All of these tentative conclusions are subject to the proviso that they apply to the planktonic, or water-column, studies undertaken to date. Their extension to microcosms with benthic communities remains to be shown, and that is a major aspect of our planned work in FY 1980.

In the acid-precipitation research project<sup>5</sup> progress was made in both field studies and labora-

tory microcosm work. Field investigation included collection and characterization of 14 western slope lake samples in terms of pH and ambient levels of total and dissolved metals in the water column. These measurements allow for the identification of those lake basins particularly sensitive to acid inputs. Such data will be made available for consideration in energy facility siting decisions in California.

Using both 4-liter and 50-liter microcosms, simulated Bay Area (Briones) and Sierra (Dark Lake) lake systems, with and without sediment, have been established and then disturbed by the addition of synthetic acid rain. Changes in zooplankton and phytoplankton species and numbers have been tracked following these perturbations. Changes in metals levels (Al, Cd, Cu, Fe, Mn, Pb, Zn) in the water column of these microcosms have been measured using graphite-furnace atomic absorption spectrometry techniques. Fluctuations in levels of Al, Cu, Pb, and Fe are particularly significant in the systems with sediment, with 10-100 fold increases in dissolved metals levels being observed following acid additions.

Progress has been made in designing and applying small microcosms useful for studying detailed patterns of succession in simple planktonic systems in which the species and numbers of plankton, and the nutrient concentrations, are all adjusted at the outset.<sup>6</sup> These systems are designed to have precisely similar light levels, and are constructed so as to minimize inhomogeneities and other complications arising from mixing patterns and surface growth.

A description of earlier work on the analysis of a practical measure of ecological stability was published in a theoretical paper.<sup>7</sup> It contained proof of a rigorous relation between the value of this measure and the distribution of eigenvalues of the community matrix. Other theoretical studies in progress include an extension of the fluctuation-dissipation theorem from classical mechanics to an ecological context, and development and analysis of models of the interactions of microbes with detritus leading to an understanding of the results of experiments on decomposition that we have carried out.

The fluctuation-dissipation theorem relates the correlations in time of the fluctuations of a stochastic system to the recovery rate from a disturbance of such a system. One of us has shown that currently favored ecological models of population fluctuations in a stochastic environment predict behavior in accordance with the fluctuation-dissipation theorem, despite the fact that the assumptions needed for a rigorous justification of the theorem are not satisfied by these models.<sup>8</sup> Phenomena observed by us in a series of decomposition experiments,<sup>9</sup> which studied the response of lake water samples to detritus additions, are in conflict with models traditionally used to describe the kinetics of microbe-detritus interactions. Using mathematical models, we have shown that the phenomena can be accounted for by assuming the existence of a density-dependent, carrying capacity limitation on the ability of microbes to immobilize mineralized nutrients for their growth.<sup>10</sup> The

importance of this coupled experimental and theoretical development is that it may lead to a relatively simple, reliable method for measuring density-dependence effects in microbial populations. These effects are believed to provide an indicator of robustness of ecological nutrient cycles.

Finally, several reviews and assessments of the ecological impacts of energy activities, with an emphasis on water-related damages, were prepared. A paper<sup>16</sup> sponsored by the University of California's Water Resources Center on water resource constraints on energy development in California was published in 1979. Another paper,<sup>12</sup> presented at an international conference on resources at IIASA, Vienna, described a framework for analysis of ecological risks of water-intensive energy technologies.

#### PLANNED ACTIVITIES FOR 1980

In order to improve the realism of microcosms and their effectiveness as tools for ecotoxicology, study of two microcosm design features will be initiated in FY 80: (1) the establishment of proper mixing rates in the microcosms, and (2) the inclusion of benthic sediments.

Effects of mixing have been studied in detail for estuarine microcosms by other groups,<sup>13,14</sup> who find that microcosm behavior can be quite sensitive to the degree of water-mixing, with unmixed systems often bearing little resemblance to the natural parent system. In a series of tracking experiments involving Briones Reservoir, we will investigate the degree to which tracking depends upon the rate of water mixing in our microcosms. Mixing rates in the lake and the microcosms will be compared using gypsum dissolution measurements. A simple motor-driven paddle wheel assembly will be used to create mixing in the microcosms.

The benthic zone plays an important role with respect to nutrient recycling in most fresh-water lakes. It can also function as a temporary sink for many contaminants which initially find their way into the water column. In shallow non-stratified lakes, such exchanges occur more rapidly than in stratified deeper lakes where turnover times on the order of a year are common. Inclusion of a benthic compartment in a shallow lake-like microcosm is difficult. If the benthic sediments cover the entire bottom, the ratio of benthic surface area to overlying water volume (BS/WV) is often at least an order of magnitude greater than that of most natural systems and so the benthic compartment in this case would exert much too large an effect on the overlying water. Even if the benthic compartment's surface area is reduced so that the ratio (BS/WV) is realistic when compared to a particular lake, mimicking realistic aeration, mixing and dilution may be difficult, particularly when examining models of stratified lakes. Benthic compartments scaled approximately to the size of microcosm containers will be filled with benthic materials from the study lakes. Two variables characterizing the benthic compartment will be studied--the benthic surface area and the rate of water flow across the benthic surface, taking advantage of design features similar to those used

by Perez et al.<sup>13</sup> The degree to which water-column chemical concentrations and population levels track those in the parent lake will be monitored.

In order to investigate effects of toxic substances on lake decomposition rates using a method developed by our group,<sup>9</sup> large quantities of highly concentrated dissolved and particulate lake-water detritus are needed. We will develop suitable methods for preparing and concentrating detrital materials of various characteristic size spectra and chemical constituency.<sup>15</sup>

Changes in decomposition activity induced by toxic substances can alter the spectrum of molecular sizes in the detritus pool and cause the fractions of the pool with various degrees of lability to change. To investigate the extent to which altered decomposition activity can affect the constituents of the detritus pool, we will explore the possibility of obtaining a characteristic "fingerprint" of detritus, adapting a method developed in the atmospheric aerosol research group at the Lawrence Berkeley Laboratory for studying the components of materials trapped on air filters. Our approach will consist of measuring separately CO<sub>2</sub> and NO<sub>x</sub> evolution from detritus samples that are subjected to increasing temperatures, ranging from ambient to about 800°C. The fingerprint consists of the curve of gas evolution as a function of temperature. A wide range of water samples from California lakes will be fingerprinted. This technique will also be used in the benthic sediment studies described above to characterize changes in the organic constituents of benthic sediments that have remained in laboratory microcosms for various lengths of time. Comparisons with sediment fingerprints from the parent lake will be made.

Both field and laboratory studies on the ecological impact of acid precipitation will be continued. Further characterization of lakes located on the western slope of the Sierra and downwind of major population centers will be pursued through the analysis of sediment and watershed soil samples for metals content. These measurements will aid in the selection of those lakes considered to be most susceptible to damage due to metals resuspension. Additional lake water samples will be collected in the Spring, with emphasis on collection during the period of peak snowmelt when an acid "pulse" may be detected.

Laboratory microcosms will be set up at the Aquatic Microcosm Facility at LBL using water and sediment collected from additional Sierra lakes and will be subjected to successive lowering of pH. Metals levels in the water column and changes in zooplankton and phytoplankton species and numbers will be tracked to determine the biological consequences of acid inputs to simulated aquatic systems.

Theoretical investigations of models for microbial-detritus interactions will continue, with the main emphasis on developing methods of determining basal decomposition rates from measurements of enhanced decomposition activity as stimulated by additions of detritus. Further exploration of the fluctuation-dissipation theorem in an ecological context will also be pursued, with stress on trying to understand the extent of, and the reasons for,

its apparent applicability to ecosystem models. An effort will be made to design a suitable experimental test of the theorem in laboratory microcosms.

In order to extrapolate results on ecological impacts of toxic substances from laboratory microcosms to a field situation, it is necessary to consider the fact that lake microcosms are inherently different from natural lakes. The types of variables that the public are generally most concerned with in real lakes, such as the health of sport fish populations, odor, and water clarity (which we call macrovariables), do not lend themselves to direct investigation in the laboratory. Nevertheless, the types of ecosystem components most amenable to laboratory study, such as phytoplankton, zooplankton, and water chemistry (which we call microvariables) often exert a great influence on the macrovariables. In a review article prepared for a National Academy of Sciences study, we will describe the limitations and opportunities in current ability to extract results about macrovariables from information obtained about microvariables from microcosms.<sup>16</sup>

#### FOOTNOTE AND REFERENCES

\*This work was supported by Electric Power Research Institute and the California Policy Seminar.

1. A. Jassby, M. Dudzik, J. Rees, E. Lapan, D. Levy, and J. Harte, "Production cycles in aquatic microcosms," Environmental Protection Agency, Office of Research and Development Research Report EPA-600/7-77-097, National Technical Information Service, Springfield, VA, 51 (1977).
2. M. Dudzik, J. Harte, A. Jassby, E. Lapan, D. Levy, and J. Rees, "Some considerations in the design of aquatic microcosms for plankton studies," Intern. J. Environmental Studies, 13, 125-130 (1979).
3. J. Harte, D. Levy, J. Rees, and E. Saegbarth, "Making microcosms an effective assessment tool," Proceedings from the symposium on microcosms in ecological research, John Giesy ed., (to be published) (1979).
4. This work was carried out by J. Harte, D. Levy, J. Rees, and E. Saegbarth.
5. This work was carried out primarily by K. Tonnessen, a graduate student in the Energy and Resources Program, with assistance by J. Oldfather and G. Lockett.
6. M. Dudzik, a graduate student in biophysics, has been carrying out this effort.
7. J. Harte, "Ecosystem stability and the distribution of community matrix eigenvalues," in Theoretical Systems Ecology, E. Halfon, ed., pp. 453-465, Academic Press (1979).
8. This work was carried out by J. Harte.
9. J. Harte and D. Levy, "Investigation of the responses of lake waters to detritus additions," Lawrence Berkeley Laboratory report, LBL-9314, to be submitted for publication (1979).
10. This work was carried out by J. Harte, D. Levy, and E. Saegbarth.
11. J. Harte, "Water resource constraints on energy development" in California Water Planning and Policy, E. Englebert, ed., pp. 65-87, University of California, Water Resources Center, Davis, CA (1979).
12. J. Harte, "Water constraints on energy development: A framework for analysis," presented at the IIASA-RSI Conference on Systems Aspects of Energy and Mineral Resources, Laxenburg, Austria, July 1979.
13. K. T. Perez, G. M. Morrison, N. F. Lockie, C. A. Oviatt, S. W. Nixon, B. A. Buckley, and J. F. Heltsche, "The importance of physical and biotic sealing to the experimental simulation of a coastal marine ecosystem," Helgolander wiss, Meereunters, 30, 144-162 (1977).
14. M. E. Pilson, G. A. Vargo, and C. A. Oviatt, "Nutrient cycles in MERL microcosms," Proceedings from the symposium on microcosms in ecological research, John Giesy, ed., to be published (1979).
15. D. Schneider, a graduate student in the Energy and Resources Program, will carry out this work.
16. P. Gleick, a graduate student in the Energy and Resources Program, will carry out this study.

# TREATMENT METHODS FOR REMOVAL OF BORON FROM BRINES\*

W. Garrison and S. L. Phillips

## INTRODUCTION

The presence of boron in geothermal brines at concentrations ranging up to several hundred ppm<sup>1</sup> represents a potential hazard to plants and crops. Boron in the form of boric acid and its water soluble salts is an essential trace element in the normal growth of all higher green plants.<sup>2</sup> However, as is the case with most trace-element nutrients, excessive amounts become toxic and lead to plant death. Some boron-sensitive plants and crops show toxic effects when irrigated with water containing boron concentrations as low as 1 ppm.<sup>3</sup> The project has as its objective a study of the mobility and sorption of boron through soils. The goals are: (1) to analyze soil samples for their boron content, (2) to study the sorption of boron by soils from waters such as geothermal brines, and (3) to assess treatment methods for boron removal.

## ACCOMPLISHMENTS DURING 1979

A survey was completed of the available data for treatment methods to remove boron from geothermal brines.

The development of economically feasible methods for removal of boron at the ppm level from waste waters--industrial, agricultural and geothermal--is still in progress.<sup>1,3,4,5</sup> Various approaches have been employed with varying degrees of success as outlined below.

Adsorption of boric acid onto hydrated aluminum oxide and iron oxide sites in clays and clay-components of soils could provide an effective method for boron removal. Unfortunately, the adsorptive capacities of clays and related materials are low (0.1 mg/gm) even under optimum conditions. From the plant engineering standpoint, prohibitively large amounts of adsorbate would be required in most cases. However, adsorption processes are an important consideration in the removal of boron by soils in situ following a spill or other accidental contamination.

Precipitation methods commonly used in the water treatment industry, e.g., lime-magnesium, require 13 mol mg/mol B and are costly because of the large quantities of chemicals required. In addition, the conventional sedimentation and biological treatment processes employed in sewage treatment plants have little or no effect on boron levels.

Reverse osmosis (through cellulose acetate) would appear to have limited application in the removal of boric acid from waste waters. At an operating pressure of 500 psi, only 20-30 percent of the boron in sea water is rejected as compared to over 95 percent of the sodium chloride.

Of the waste water treatment processes, those involving ion-exchange resins appear to be the most promising. It is recognized, of course, that the complete de-ionization of water by strongly basic ion-exchange resins such as Amberlite IRA-400 and Dowex 2, does not represent an economical approach for removal of boron from waters containing appreciable concentrations of other exchangeable anions such as chloride ion. However, the strongly basic resins might be employed economically in the removal of boron from geothermal steam condensates which are relatively low in total salinity. Similarly, the Amberlite IRA-400 and Dowex 2 resins could be used in the removal of boron from brackish waters previously treated by one or more reverse-osmosis cycles.

However, it appears that the most direct and economical method for removal of boron from geothermal brines may be the use of the recently developed boron-specific resin, Amberlite XE-243. This is a crosslinked microreticular gel-type polymer derived from the amination of chloro methylated styrene-divinyl benzene with N-methylglucamine. The resin exhibits equilibrium boron capacities in the range 5 mgB/gm with good hydrodynamic properties and chemical stability. The boron selectivity of Amberlite XE-243 is not affected by high concentrations of various other salts including sodium chloride. It has been estimated that total costs for the lowering of boron concentrations from 10 ppm to 1 ppm in irrigation waters would be below \$0.03 per thousand gallons. One estimate for removal of both boron and arsenic from geothermal brines using XE-243 is \$2,884,000 for 1976 dollar values.<sup>5</sup> Alternative methods such as adsorption onto activated carbon, bauxite and alumina should be studied.<sup>1</sup>

## FOOTNOTE AND REFERENCES

\*This work was supported by the Lawrence Berkeley Laboratory Director's Funds.

1. W.-W. Choi and K. Y. Chen, "Evaluation of boron removal by adsorption on solids," *Env. Sci. Technol.*, **13** (2), p. 189-196 (1979).
2. J. E. Bonner and J. E. Varner, *Plant Biochemistry*, Academic Press, New York, NY (1976).
3. F. T. Bingham, "Boron in cultivated soils and irrigation waters," *Adv. Chem. Ser.*, **123**, p. 130 (1973).
4. *Chemical Technology and Economics in Environmental Perspectives, Task II - Removal of Boron from Wastewater*, EPA-560/1-76-007, Environmental Protection Agency, Office of Toxic Substances, Washington, D.C. 20460, April 1976.

5. D. C. Christiansen and J. A. McNeese, "Removal of arsenic and boron from geothermal brines,"

Proceedings of 32nd Annual Purdue Industrial Waste Conference, May 10-12, 1977 (Battelle Northwest Laboratories, Richland, WA 1977).

## ORGANIC COMPOUNDS IN COAL SLURRY PIPELINE WATERS\*

A. S. Newton, J. P. Fox, and R. Raval

### INTRODUCTION

In order to meet the expected increase in use of coal, especially low-sulfur western coals, a large increase in transport capacity will be necessary. Much of this increased capacity will be met by the construction of coal slurry pipelines. At present only one coal slurry pipeline is in operation but several others are expected to be constructed soon.

The transport of coal by slurry pipeline involves the grinding of coal with water in a rodmill to a fineness such that the resulting slurry remains suspended during pipeline transport. A slurry of about 50 percent can be transported by pipeline. The coal user recovers the coal by centrifugation and/or filtration and the recovered moist coal can be burned directly in a power plant. The recovered water must be disposed of in some manner if it is not used as make-up in the power plant. In the Black Mesa pipeline system and Mohave power plant, the moist coal from the centrifuge is burned directly. The water from the centrifuges is further filtered and used as make-up cooling water. Washings from the filters are evaporated in watertight ponds, and no water is released to the aquatic environment.

Because the disposal of pipeline water in a closed system may not be possible in all situations, it is important to have information on what contaminants might be present in the recovered water if proper treatment is to be made before disposal into the aquatic environment. A bibliography of coal-water interactions has been compiled. Several studies of coal-water interactions have been made, either in glass laboratory shaker bottles,<sup>1,2</sup> or in a closed pipeline test loop.<sup>3</sup> These studies have been principally concerned with the leaching into the water of inorganic species such as compounds of the elements As, Pb, Cr, Cd, Mn, Zn and Hg, and the ions nitrate, sulfate and carbonate. Little work has involved the study of the organics in the water. Godwin and Manaham<sup>3</sup> found that leaching of lignites and sub-bituminous coals release humic acids into water and were concerned about possible complexing of metals by the humic acids. Humic acids were estimated to be equal to the chemical oxygen demand (COD) of water. Other studies on the drainage water from coal mines, water from washing coal, and drainage from open coal piles are related but are not exactly equivalent since in these cases the overall system is oxidizing because of the presence of air. In wet grinding coal in a steel rodmill, hydrogen gas is

produced and the system rapidly becomes reducing. Possible interactions of nascent hydrogen can result in the fragmentation of organic groups from the surface of the coal to produce organic compounds which may remain in the water. Because of the structure of coal, polynuclear aromatic hydrocarbons and phenolic compounds are expected of this interaction.

Expected concentrations of organic compounds in slurry water is limited to the respective solubility of each compound in water. For phenolic compounds this may be quite high, but for hydrocarbons such as phenanthrene, pyrene, etc., the solubility in water has been shown to vary from 2,700 ppb to less than 1 ppb (micrograms/liter) as shown in Table 1.<sup>4</sup> It is possible that the concentrations can exceed these solubility values if organic compounds are absorbed onto colloidal material or very fine particulates in the water. It is also possible that the coal itself can act as an absorbent for these organic compounds and that the concentrations in pipeline water may be well below the solubilities.

Table 1. Solubilities of some polynuclear aromatic hydrocarbons in water.

Compound	Solubility in micrograms/liter
(anthracene)	89 (@ 20°)
(phenanthrene)	2700 (@ 20°)
anthracene	75
phenanthrene	1600 (1650)
naphthalene	1.0
chrysene	1.5
5-Me chrysene	62
6-Me chrysene	25
1,2 - Benzanthracene	11
Triphenylene	38
Pyrene	165
Perylene	0.5
Picene	2.5
3,4 Benzpyrene	9.0 (4.0)

## EXPERIMENTAL

An industrial rodmill for the preparation of coal slurries is some 4 meters in diameter and 5.5 meters long. The average residence time of coal in a continuous mill is only a few minutes. A laboratory batch mill cannot exactly duplicate all of these plant conditions, but a laboratory mill which does duplicate some of them is shown in Figs. 1 and 2. It is made from a 9 inch long piece of 8 inch O.D. seamless steel pipe. Inside are welded 1/2 x 1/2 inch steel bars to carry the rods and provide a good grinding action. Five one inch diameter steel rods are adequate. The cover is sealed with an "O" ring, and it also contains a flush valve through which gas samples can be removed from the rodmill. The net volume of the mill for coal, water and gas space is 5278 ml. The mill is driven on a jar mill drive, Fisher Scientific Co., Model 753 RM. The drive was modified to reduce the speed by adding an additional 4:1 reduction pulley system. With the modified drive the rodmill is rotated at 28 RPM.

The coals to be investigated are Black Mesa coal and Illinois No. 6 coal obtained from the Peabody Coal Company, and Wyodak Roland Seam Coal obtained from Wyodak Resources.

The procedure in the first preliminary experiments has been to add the coal to water and contact with agitation for 16 - 18 hours. The slurry was centrifuged in glass bottles. The water was further filtered. The filtered water was extracted with nano-grade hexane and the hexane extract concentrated to a 1 - 2 ml volume in a vacuum evaporator. The sample volume was further reduced to a few microliters by evaporation with a stream of nitrogen gas.

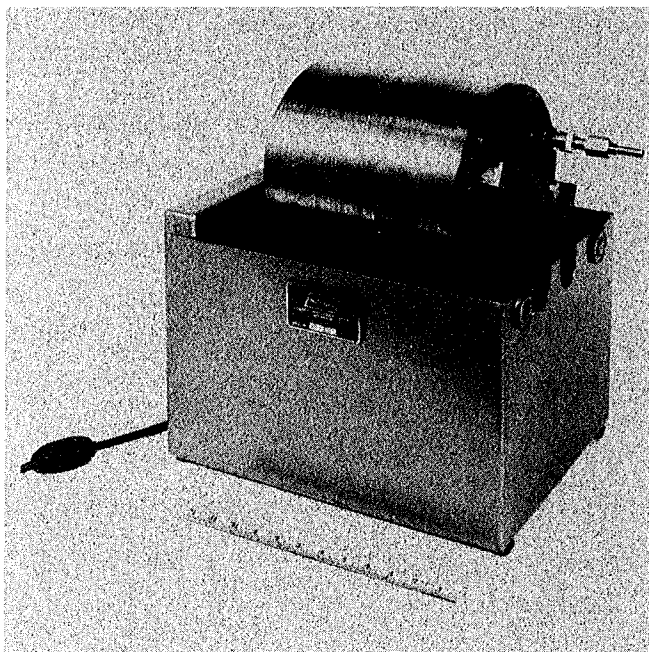


Fig. 1. Photograph of laboratory rodmill and its drive for the preparation of coal slurries. (XBB 790-15385)

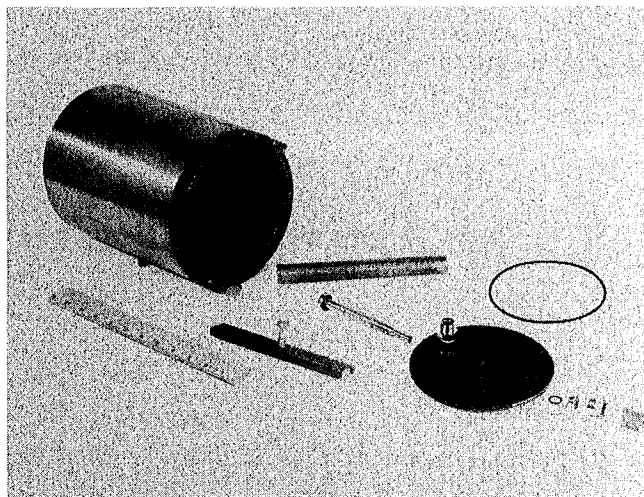


Fig. 2. Photograph of laboratory rodmill in exploded view showing positioning of rods, cover and valving system. (XBB 790-15386)

The concentrated sample was studied using a Finnigan Model 4023 GC/MS. A 30 meter OV-101 capillary GC column was used with Grob injection. This system and method gives excellent identification of many components, but only an approximate quantitative result can be cited. At the present stage of the investigation, the citation of only approximate concentrations is justified.

## RESULTS AND DISCUSSION

Three preliminary experiments, the results of which are shown in Table 2, have been performed. Samples Coal A and Coal C were made up with Wyodak coal and laboratory de-ionized water. The results show gross contamination with phthalate esters and squalene. As shown in Table 3, the phthalate esters are traceable to the de-ionized water which is in contact with polyvinyl chloride pipes. The squalene probably arises from fingerprints. These results illustrate the extreme care that must be taken in obtaining and analyzing samples.

The sample Rodmill-1 (Table 2) shows much less contamination than did the earlier samples made with de-ionized water. The low concentrations of hydrocarbons observed in sample Rodmill-1 may be residual contamination from traces of oil which were not removed in cleaning the rodmill but which should gradually be eliminated with use of the rodmill. Water must, however, be distilled from alkaline permanganate to eliminate all organic compounds from that source. No impurities were observed in the hexane.

In Table 4 the gases present in sample Rodmill-1 are shown. Hydrogen, some CO<sub>2</sub>, and the oxygen depleted air initially present in the sample were found. In this sample some gas was lost because of excessive pressure build-up. No methane was detected.

Table 2. Organic compounds found in coal slurry water.

Compound	Concentration in p.p.b. in water		
	Coal A <sup>1</sup>	Coal C <sup>2</sup>	Rodmill-1 <sup>3</sup>
Diethyl Phthalate	5.0	0.15	≤0.005
Dibutyl Phthalate	15	2.8	0.15
Hexanedioic acid ester unidentified (not a phthalate)	--	--	0.15
Di-iso-Octyl Phthalate	3.0	0.25	0.05
Squalene	0.3	0.007	0.10
Hydrocarbons C <sub>15</sub> -C <sub>30</sub> (each)	≤0.1	<0.015	<0.005

<sup>1</sup>Coal A sample was 250 gms Wyodak Coal (<100 mesh) shaken with laboratory de-ionized water in a 500 ml glass bottle. Hexane extract of water analyzed.

<sup>2</sup>Coal C sample was like Coal A except 500 gms lump coal used with 500 ml water and 100 gms 1 cm steel ball bearings added. Hexane extract of water analyzed.

<sup>3</sup>Rodmill-1 sample was 2300 gms of Wyodak coal ground with 2500 cc LBL tap water (EBMUD water) for 16 hours. Hexane extract of water analyzed.

Table 3. Blank determinations of water and hexane used.

Compound	P.P.B. Impurities In:			
	Deionized water		Tap water	Hexane
	A	B		
Diethyl phthalate	--	--	--	--
Dibutyl phthalate	0.1	0.6	0.001	<0.001*
Hexanedioic acid ester	--	1.6	--	--
Di-iso-Octyl phthalate	14	12	0.004	<0.001*
Squalene	0.3	10	--	<0.001*
Hydrocarbons	--	--	--	--

\* No contamination observed at this sensitivity level.

Table 4. Analysis of gases from sample rodmill - 1.

Compound	% Compound	Amount of Gas, Millimoles
H <sub>2</sub>	78.9	97
N <sub>2</sub>	19.3	24
O <sub>2</sub>	0.0	(-6) <sup>a</sup>
Ar	0.24	0.3
CO <sub>2</sub>	1.51	1.8

<sup>a</sup>This amount of O<sub>2</sub> was depleted from the air initially present.

The results presented here show that water from a slurry with Wyodak sub-bituminous coal contains no hexane-extractable contaminants attributable to the coal in amounts larger than about 0.1 ppb. In the present experiments phenols and other polar compounds were not determined and volatile compounds such as benzene and toluene

would have been lost in the hexane concentration step.

#### FOOTNOTE AND REFERENCES

\*This work was supported by the Fossil Fuel section of the Department of Energy.

1. J. W. Moore, "Water quality aspects of coal transportation by slurry pipeline," Proc. 4th Int. Tech. Conf. on Slurry Transportation, Las Vegas, Nevada, March 28-30, 1979.
2. O. L. Anderson, M. B. Rogozen, W. L. Margler, P. Mankiewicz, and M. H. Axelrod, "Water pollution control for coal slurry pipelines," Institute of Geophysics, UCLA and Science Applications, Inc. Report SA 1-068-79-516, June 30, 1978.
3. J. Godwin and S. E. Manahan, "Interchange of metals and organic matter between water and sub-bituminous coal or lignite under simulated coal slurry pipeline conditions," Environmental Science and Technology, **13**, 1100 (1979).
4. H. Seidell and W. F. Linke, "Solubilities of Inorganic and Organic Compounds," p. 758, supp. to 3rd Ed. D. Van Nostrand Co., NY (1952).

## PROTECTION OF GEOTHERMAL BRINE PIPING USING ELECTRODEPOSITED ORGANIC LININGS\*

*S. L. Phillips, R. G. Clem, and S. G. Chang*

### INTRODUCTION

It is basic to progress in utilization of geothermal energy that adequate and economic materials be available for commercial use. This is true in all aspects of the problem: piping to transport the corrosive hot brine and steam; heat exchangers to transfer heat for driving turbines and for heating structures; drilling of exploratory injection and production wells; measuring flow rates, temperatures and pressures; and establishing material specifications and standards. The present state of the art is far from satisfactory, however, with unprotected or expensive metals being widely used for handling hot brine and steam. Corrosion and scale encrustations are encountered in all geothermal plants; their presence adversely affects plant lifetimes and power output. The problem is sufficiently serious that the use of expensive materials such as type 316 stainless steel and titanium base alloys may be required to insure long term operation of power plants and direct utilization facilities. However, a real economic gain will be realized if the less expensive materials such as carbon steel, which has been used as the primary material of construction in piping and heat exchangers, can be used to handle hot brine and other aerated geothermal fluid.<sup>3,4,5</sup>

A commonly used technique to control corrosion and to increase the resistance of carbon steel piping to erosion, corrosion, and scaling is to use protective coating. These coatings are applied to the metals in a number of ways; the films may be organic or metallic. A more recent approach to this problem, which has found acceptance by industrial manufacturers for a variety of applications, is the electrodeposition of organic films.

The electrodeposition of organic coatings from aqueous systems is widely used, for example, to paint automobiles for corrosion protection. The advantages of this method include ease of automation; uniformity of film thickness; penetration of the film into cracks, flaws and other not easily accessible places; high utilization of both resin and pigment (greater than 95 percent); and the short time needed between film deposition and rinsing. Besides these, it is possible to electrodeposit resins such as fluorocarbons (e.g., Teflon) which are included among those coatings with superior resistance to chemicals, abrasion, high temperature, and friction.<sup>1,2,6,7</sup>

Because of these considerations, work was initiated in September, 1979, to evaluate electrodeposition procedures for coating and lining the

inside of piping with Teflon for geothermal energy applications.<sup>8</sup>

#### ACCOMPLISHMENTS DURING 1979

During the one month of funding, laboratory work was centered mainly on assembling equipment, obtaining commercially available resin dispersions, and proving the concept of lining the interior of metal piping with an electrodeposited organic film. For reasons stated, Teflon was selected as the initial resin for the pipe lining. It is impossible to deposit Teflon onto metals such as copper with satisfactory adhesion; Hycar (acrylonitrile/butadiene) is co-deposited thereby providing a marked improvement in adhesion.<sup>1</sup>

#### Experimental

The electrodeposition was carried out under conditions of constant applied voltage using a Power Designs Inc. Model 2050 power supply. For coating the interior of copper pipes, collars were machined from bulk Teflon to fit over each end and to contain the aqueous coating bath. The copper piping was 2.5 cm (1 inch) diameter, 15 cm (6 inch) long, hard drawn seamless, ESR NC No. 234. A 1.3 cm (0.5 inch) diameter copper rod was inserted through the center of the Teflon collars to serve as the cathode during electrodeposition. Copper coupons for deposition studies were cut from 0.025 cm thick OFHC cold rolled, half-hard copper sheeting, CDA alloy 110, ESR 120; typical dimensions of the coupons were 2 cm x 2 cm. A 0.5 cm x 2 cm long tab was left on each coupon to provide electrical contact via an alligator clip with a moving anode bar. The anode bar was moved back and forth about 2.5 cm (1 inch) at a rate of six cycles per minute using a synchronous motor. This moving bar provided agitation and reduced concentration polarization effects traceable to the dispersed material during deposition. A 1000 ml stainless steel beaker served simultaneously to contain the coating bath and as the cathode for deposition onto the coupons.

Both dispersions were proprietary and were used as received. The polytetrafluoroethylene was E. I. DuPont Teflon 30; the acrylonitrile/butadiene copolymer was B. F. Goodrich Hycar 1561. Table 1 lists selected properties of the dispersions; Table 2 consists of selected properties of bulk Teflon. Electrocoating baths were prepared by mixing known weights or volumes of each dispersion.

Table 2. Selected properties of bulk Teflon.

Resin	Thermal conductivity, W/m.K	Rockwell Hardness	Specific gravity
Teflon	2510	D50 to D60	2.1 to 2.3

#### Electrocoated Coupons

Copper coupons were cleaned by scrubbing with a proprietary powder cleaner, followed by washing, etching for 10-15 minutes in ammonium persulfate solution (160 g/l), and rinsing with distilled water. The presence of a continuous water film on the resulting salmon-colored copper was taken as the criterion for a cleaned surface. After electrocoating, the coupons were rinsed with distilled water, dried 1-2 hours at ambient temperature, heated to 75-80°C for 4-5 hours; then placed in a muffle furnace at 300°C for 15-20 minutes. (Blisters developed on coupons which were placed in the muffle furnace directly after coating.)

The Teflon/Hycar film was bluish-green in color after deposition; the color was unchanged on heating to 150°C. However, heating to 300°C resulted in a black, smooth film. Bending a coated coupon 180° caused white cracks to appear in the coating, but the film was not readily dislodged from the copper by picking with a sharp knife. This indicated good adhesion. Table 3 shows the variation in film thickness,  $\ell$ , with time,  $t$ , for a series of coated coupons. The constancy of the ratio  $\ell/t^{1/2}$  indicates diffusion-controlled film buildup.

#### Electrocoated Piping

The inside of the copper pipe was cleaned by scrubbing with a powder cleaner using a bristle brush, followed by water rinsing. The rinsed tube was then filled with about 55 ml of ammonium persulfate solution and allowed to sit for 10-15 minutes. After this time, the persulfate was decanted, the pipe rinsed with distilled water, and the Teflon/Hycar resin dispersion added. After 2-3 minutes, the two leads to the power supply were connected and 10 volts applied for 2 minutes. Gas evolution was evidenced by foaming at the top

Table 1. Selected properties of water-based Teflon 30 and Hycar 1561 dispersions from manufacturer's literature.

Resin	Solids, %w	Particle size, micron	pH	Wetting agent, %w	Viscosity, centipose	Specific gravity
Teflon 30	60	0.05 to 0.5	10	8	20	1.50
Hycar 1561	41	--	10	--	27	1.00

Table 3. Effect of deposition time on coating thickness using moving anode bar and copper coupons. Deposition voltage was 40 volts; dispersion was composed of 600 ml of Teflon 30 mixed with 325 ml of Hycar 1561.

Coating time sec. (t)	$t^{1/2}$	*Coating thickness, cm. (l)	$1/t^{1/2}$
10	3.16	0.010	0.0032
30	5.48	0.0178	0.0032
60	7.75	0.0229	0.0030
120	10.9	0.0305	0.0028
180	13.4	0.0381	0.0028
300	17.3	0.0457	0.0026

\*Coating thickness measured with a micrometer; copper coupon was 0.025 cm thick.

of the pipe. Following deposition, the aqueous dispersion was decanted, the tube thoroughly washed with distilled water, and allowed to dry at ambient temperature for several hours. The tube was then heated to 300°C for 15-20 minutes, after which time a smooth and adherent black lining was formed.

The plating current was monitored during deposition; see Table 4.

Table 4. Variation in current with time for electrolined copper piping. Applied potential, 10 volts.

Time, sec.	5	30	60	90	120
Current, amp.	1.8	1.4	0.8	0.5	0.4

The results of this work show that copper piping can be lined with an organic film comprised of Teflon and Hycar using electrodeposition procedures.

#### PLANNED ACTIVITIES FOR 1980

Proposals will be submitted to request funding for a project centered on developing both materials and processes for lining steel piping with organic resins using electrodeposition methods.<sup>9</sup> The result of this proposed work will consist not only of lined steel piping, but also of test data on the corrosion, erosion and scaling protection afforded to the piping in contact with geothermal hot brines and vapor systems. Methods for joining shorter lengths of piping and for coating angular bends (e.g., elbow joints) will form part of the proposed work. Both materials and deposition processes will be characterized using modern instrumental methods.

#### FOOTNOTE AND REFERENCES

\*This work was supported for one month by the Earth Science Division of Lawrence Berkeley Laboratory, and by the DOE Division of Geothermal Energy.

1. S. L. Phillips and E. P. Damm, "Electrophoretic deposition of resins at soluble metal anodes," *J. Electrochem. Soc.*, **118**(2), 1916-1919 (1971).
2. F. Beck, "Fundamental aspects of electrodeposition of paint," in *Progress in Organic Coatings*, **4**, 1-60 (1976).
3. Alternate Materials of Construction for Geothermal Applications, BNL 50979, October - December 1978, Progress Report No. 17, Brookhaven National Laboratory, Upton, NY 11973.
4. American Society for Testing and Materials Task group on Geothermal Seals, Proceedings of Technical Seminar, CONF-7806141, April 1979, Boston, MA, June 27, 1978.
5. Materials Selection Guidelines for Geothermal Power Systems, ALO-3904-1, D. W. DeBerry, P. F. Ellis and C. C. Thomas, Radian Corp., Austin, TX 78766, September 1978.
6. E. B. Ewan, "Coatings that can really take it," *Materials Engineering* **89**, 38-42 (1979).
7. A. G. Roberts, Organic Coatings, Building Science Series 7, National Bureau of Standards, Washington, DC (1968).
8. D. R. Sherwood and D. J. Whistance, The Piping Guide, Part 1 (1973).
9. Proposal submitted to DOE Division of Geothermal Energy, January 30, 1980.

# ATMOSPHERIC AEROSOL RESEARCH

## INTRODUCTION

*T. Novakov*

The complex set of questions concerning the origin and the chemical and physical characterization of carbonaceous particulates and their role in atmospheric chemistry has been central to the program of the Atmospheric Aerosol Research group since the group's beginning in 1972. As a result of this research, our group advanced the hypothesis that much of the carbonaceous material in urban environments is soot, i.e., primary particulate material. These preliminary results on the origin and nature of carbonaceous particles were first reported at the First Annual NSF Trace Contaminants Conference at Oak Ridge National Laboratory in August 1973, just one year after the start of our research, which was at that time entirely sponsored by the National Science Foundation.

Carbonaceous particles, together with sulfur and nitrogen compounds, account for most of the submicron particulate mass. Of the above species, particulate carbon is often the most abundant material found in urban environments (e.g., Los Angeles, Denver, New York). According to the view prevailing at the time our research was initiated, it was postulated that most of the particulate material was produced by certain atmospheric photochemical reactions from gaseous hydrocarbons. The products of these reactions were believed to be certain highly oxygenated high molecular weight hydrocarbons which condense into carbonaceous particles. More specifically, reactions of ozone with olefinic hydrocarbon vapors were assumed to be the

principal mechanism for such gas-to-particle conversion processes. The principal ingredient necessary for these reactions is ozone, which--according to some investigations--has to exist in concentrations exceeding about 0.2 ppm.

In contrast, the view emerging from our work has suggested that most of the particulate carbon is either directly of primary origin or contains, in addition, secondary carbonaceous material produced in nonphotochemical reactions--for example, surface reactions that involve primary particles. It is clear that the control technology and strategy for the abatement of carbonaceous particulates will depend on the relative importance of these two alternative pathways for the formation of carbonaceous species.

Primary soot particles are not only a major constituent of ambient particles but also are a catalytically and surface chemically active material that could be responsible for the formation of sulfates resulting from fossil fuel combustion. Following is a review of recent work performed by the Atmospheric Aerosol Research group, which further stresses the importance of primary particles in the atmosphere.

Funding for this work is from the Department of Energy--Division of Biomedical and Environmental Research, the National Science Foundation, and the Environmental Protection Agency.

# CARBON-CATALYZED REACTIONS IN AQUEOUS SUSPENSIONS: OXIDATION OF SO<sub>2</sub> AT LOW CONCENTRATIONS\*

R. Brodzinsky, et al.

## INTRODUCTION

Activated carbon, because of its adsorptive properties, has long been used as a scrubber for gases and organic molecules. It is also used as a catalyst in industry for the control of gaseous emissions from smoke stacks. The catalytic oxidation of SO<sub>2</sub> on activated carbons has been shown to occur<sup>1</sup> and has been used in certain industrial scrubber processes.<sup>2</sup> Novakov et al.<sup>3,4</sup> have shown by photoelectron spectroscopy that SO<sub>2</sub> oxidation can be catalyzed by combustion-generated soot particles. These studies indicated that the soot-catalyzed reaction is more efficient in prehumidified air than in dry air, but the specific role of water was not clear from their experiments.

Environmentally, this soot-catalyzed reaction may be extremely important as soot particles are a major constituent of the ambient particulate burden.<sup>3</sup> The effects of liquid water on the reaction are important because the water may condense on soot particles in plumes as the particles pass through clouds and fog.

We have extended the research on the role of soot particles as catalysts for SO<sub>2</sub> oxidation by studying the effect of liquid water on the carbon-catalyzed reaction.<sup>5</sup> In that paper we studied the roles of the activated carbon surface, oxygen, temperature, and pH. The results of that study are summarized as follows:

1. The reaction rate is first order and 0.69<sup>th</sup> order with respect to the concentration of carbon and dissolved oxygen respectively.
2. The reaction rate is effectively pH independent (pH < 7.6).
3. The activation energy of the reaction is 11.7 kcal/mole.
4. There is a mass balance between the consumption of sulfurous acid and the production of sulfuric acid.

The dependence of the reaction rate on the concentration of sulfurous acid was not seen since only a narrow concentration range (10<sup>-4</sup> - 10<sup>-3</sup> M) was used. In this range, the reaction rate is independent of sulfurous acid concentration.

In this paper we present the results of the effects that the concentration of S(IV) species have on the reaction rate, a reaction rate law, and a proposed reaction mechanism for the catalytic oxidation of SO<sub>2</sub> on carbon particles in an aqueous suspension. (Note: Because, in solution, SO<sub>2</sub> can form the three species SO<sub>2</sub>·H<sub>2</sub>O, HSO<sub>3</sub><sup>-</sup> (bisulfite), and SO<sub>3</sub><sup>2-</sup> (sulfite), the terms "sulfurous acid" and "H<sub>2</sub>SO<sub>3</sub>" have been used to signify all of the S(IV) species in solution.)

## EXPERIMENTAL METHODS AND RESULTS

As in the previous studies, an activated carbon (Nuchar C-190, a trademark of West Virginia Pulp and Paper Co.) was used as a model system since it is difficult to prepare soot suspensions reproducibly. A Dionex Model 14 anion chromatography system was used for sulfurous acid and sulfate concentrations of less than 10<sup>-4</sup> M. An eluent of 0.002 M NaOH/ 0.0035 M Na<sub>2</sub>CO<sub>3</sub> at a flow rate of 138 ml/hr and pressure of 600 psi, through a system consisting of a 3 x 50 mm concentrator, 3 x 150 mm precolumn, 3 x 500 mm separator, and 6 x 250 mm suppressor columns was used. The sulfite peak eluted at 10 minutes with sulfate following at 15. Iodometric titrations were used to determine sulfurous acid concentrations above 10<sup>-4</sup> M, as in the previous experiments. The pH of the solution was varied in the range of 4.0 to 7.5 for the experiments done on the ion chromatograph.

Figure 1 shows the effective rate of reaction (normalized carbon concentration, room temperature (20°C), and air) versus the sulfurous acid concentration. The data points are the instantaneous rates based on three-point averages from the various experiments. The rate of reaction is second order with respect to H<sub>2</sub>SO<sub>3</sub> below 10<sup>-7</sup> M, moves through a first order reaction around 5 x 10<sup>-6</sup> M, and becomes independent of H<sub>2</sub>SO<sub>3</sub> concentrations above 10<sup>-4</sup> M.

This behavior may be summarized and added to our previous four results as:

5. The reaction rate has a complex dependence on the concentration of H<sub>2</sub>SO<sub>3</sub>, ranging between a second and zeroth order reaction.

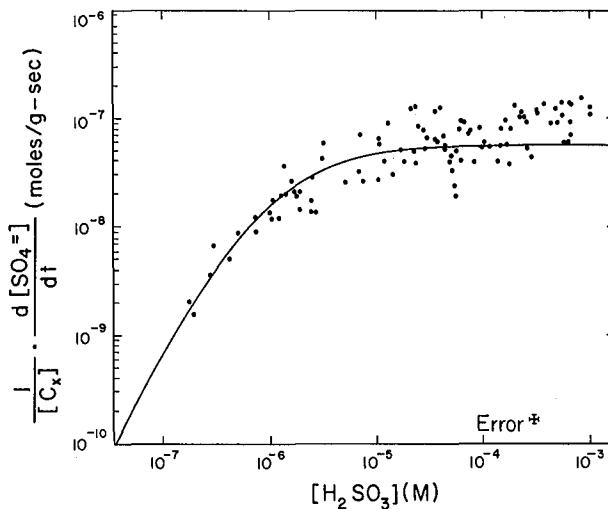
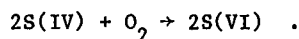


Fig. 1. Effective rate of reaction vs [H<sub>2</sub>SO<sub>3</sub>]. Curve is least squares fit to proposed rate expression. (XBL 7911-13280)

## DISCUSSION

The oxidation of S(IV) to S(VI) can be expressed simply by the symbolic net reaction,



(For this and following reactions, let  $C_x$  = carbon surface; S(IV) =  $H_2O \cdot SO_2$ ,  $HSO_3^-$ , and  $SO_3^-$ ; S(VI) =  $HSO_4^-$ , and  $SO_4^{2-}$ .)

The experimental results yield the following empirical rate law for this reaction:

$$\frac{d[S(VI)]}{dt} = k[C_x][O_2]^{0.69} \frac{\alpha[S(IV)]^2}{1 + \beta[S(IV)] + \alpha[S(IV)]^2} \quad (I)$$

where  $k = 1.69 \times 10^{-5}$  moles $^{.31} \cdot l^{.69} / g \cdot sec$

$$\alpha = 1.50 \times 10^{12} l^2 / mole^2$$

$$\beta = 3.06 \times 10^6 \text{ l/mole}$$

$$[C_x] = \text{grams of Nuchar C-190/l,}$$

$$[O_2] = \text{moles of dissolved oxygen/l, and}$$

$$[S(IV)] = \text{total moles of S(IV)/l.}$$

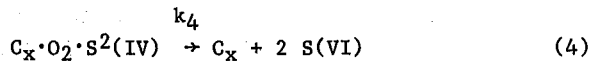
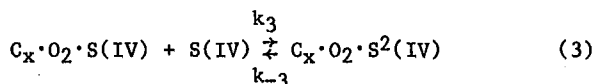
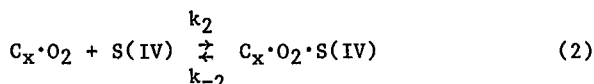
Using the Arrhenius equation, the rate constant may be expressed as

$$k = A e^{-E_a/RT}$$

where  $E_a = 11.7$  kcal/mole

and  $A = 9.04 \times 10^3$  moles $^{.31} \cdot l^{.69} / g \cdot sec$

The reaction rate being first order with respect to the activated carbon catalyst is representative of a surface catalysis. The reaction will then proceed via the adsorption of the reaction species onto a catalytically active site. A series of adsorption steps can explain the fractional and varying order of reaction with respect to  $O_2$  and S(IV) and are proposed here in the following four-step reaction:



With the Langmuir adsorption equation, the following is arrived at for the rate expression:

$$\frac{d[S(VI)]}{dt} = 2k_4[C_x] \left[ \frac{K_1[O_2]}{1+K_1[O_2]} \right] \left[ \frac{K_2 S(IV)}{1+K_2 S(IV)} \right] \left[ \frac{K_3 S(IV)}{1+K_3 S(IV)} \right]$$

where  $K_1 = k_1/k_{-1}$ ,  $K_2 = k_2/k_{-2}$ ,  $K_3 = k_3/k_{-3}$ .

Equation II can be changed simply to Equation I. A fractional order adsorption reaction is achieved by substituting the Freundlich isotherm

$$\theta = k[X]^n,$$

where  $\theta$  is the fraction of the surface covered by adsorbed species X, for the Langmuir isotherm<sup>6</sup>

$$\theta = \frac{K[X]}{1 + K[X]}$$

Multiplication of the S(IV) terms yields the experimentally seen expression, where  $K_2 K_3 = \alpha$  and  $K_2 + K_3 = \beta$ .

Preliminary experiments with other activated carbons, as well as laboratory-generated combustion soots, have shown the same rate law behavior, while the actual numerical constants are different. This behavior has also been reproduced using coal fly ash samples, which have a low percentage of carbon. An activated surface-catalyzed reaction can be very important in the plumes of coal-fired plants, even in the absence of carbonaceous soot.

We have done comparisons of this reaction with the rates of the other atmospherically important  $SO_2$  oxidation reactions.<sup>7</sup> It is clear that the carbon-catalyzed reaction can be a major contributor to the formation of aerosol sulfates.

## FOOTNOTE AND REFERENCES

\* Condensed from Lawrence Berkeley Laboratory Report, LBL-10488 (1980) (Submitted to Journal of Physical Chemistry.)

1. J. Siedlewski, "The mechanism of catalytic oxidation on activated carbon: The influence of free carbon radicals on the adsorption of  $SO_2$ ," Int. Chem. Eng. 5, 297 (1965).
2. M. Hartman and R. W. Coughlin, "Oxidation of  $SO_2$  in a trickle-bed reactor packed with carbon," Chem. Eng. Sci. 27, 867 (1972).

3. T. Novakov, S. G. Chang, and A. B. Harker, "Sulfates as pollution particulates: Catalytic formation on carbon (soot) particles," *Science* **186**, 259 (1974).
4. T. Novakov, S. G. Chang, R. L. Dod, "Application of ESCA to the analysis of atmospheric particulates," in *Contemporary Topics in Analytical and Clinical Chemistry - Vol. I*, D. M. Hercules, G. M. Hieftje, L. R. Snyder, and M. A. Evenson, eds. (New York, Plenum, 1977), p. 249.
5. R. Brodzinsky, S. G. Chang, S. S. Markowitz, and T. Novakov, "Kinetics and mechanism for the catalytic oxidation of SO<sub>2</sub> on carbon in aqueous suspensions," in *Atmospheric Aerosol Research Annual Report, 1977-78*, Lawrence Berkeley Laboratory Report LBL-8696 (1978).
6. S. W. Benson, *The Foundations of Chemical Kinetics* (New York, McGraw-Hill, 1960), p. 624.
7. S. G. Chang, R. Brodzinsky, R. Toossi, S. S. Markowitz, and T. Novakov, "Catalytic oxidation of SO<sub>2</sub> on carbon in aqueous suspensions," in *Proceedings of the Conference on Carbonaceous Particles in the Atmosphere*, Lawrence Berkeley Laboratory Report LBL-9037, p. 122 (1979).

## REDUCTION OF NO<sub>x</sub> BY SO<sub>2</sub> IN AQUEOUS SOLUTION\*

S. Oblath, et al.

### INTRODUCTION

The oxides of both sulfur and nitrogen are abundant and well-studied atmospheric pollutants. The interaction of the two has been previously studied only in the gas phase.<sup>1-3</sup> Although liquid water is present in clouds, fogs, plumes, and the human respiratory system, atmospheric chemists have not yet investigated reactions of SO<sub>2</sub> and NO<sub>x</sub> after dissolution into water. In addition, these aqueous reactions need investigation because deliquescent salts such as NH<sub>4</sub>HSO<sub>4</sub> can pick up liquid water at a low relative humidity.<sup>4</sup>

Previous investigations of the reactions of NO<sub>x</sub> with SO<sub>2</sub> in aqueous solutions revealed many competing reactions.<sup>5,6</sup> Nitric, nitrous and sulfurous acids are the immediate products upon dissolution of the gases. Nitric acid reacts with sulfurous acid to form nitrosylsulfuric acid.<sup>6</sup> Nitrous acid can be reduced by sulfurous acid to produce nitrogen species such as N<sub>2</sub>O, N<sub>2</sub>, NH<sub>3</sub>, hydroxylamine sulfonates and amine sulfonates while sulfurous acid is oxidized to sulfuric acid. A summary of the reactions and products formed is shown in Fig. 1. The kinetics and mechanisms of these reactions have not been well characterized. Nevertheless, it has been demonstrated that the products of the reaction depend on the concentrations of reactants, temperature, and acidity of the solution.

Because the formation of hydroxylamine disulfonate (HADS) is the first step to any of the products when nitrous acid reacts with sulfurous acid under most atmospheric conditions, investigating the kinetics of HADS is essential to any attempt at assessing the importance of this system as a sink of NO<sub>x</sub> and as a source of sulfate and reduced nitrogen species.

Previous work determined the order of reaction with respect to nitrite, bisulfite, and hydrogen ion. The results showed reactions first order in nitrite at all pH's, first order in bisulfite at

pH of 4.5 and 5.5, and second order in bisulfite at pH of 7.<sup>7</sup> Experiments have been carried out this year to determine the pH, temperature, and ionic strength dependencies of the reaction and a mass balance for nitrogen species. A reaction rate law has been obtained and a mechanism is proposed.

### EXPERIMENTAL METHODS AND RESULTS

The study has been carried out by reacting NO<sub>2</sub> and HSO<sub>3</sub><sup>-</sup> in various buffers to have a well-characterized system. The reaction is monitored by spectrophotometric determination of NO<sub>2</sub><sup>-</sup>. Sulfur (IV) species were monitored by standard iodometric techniques. Concentrations were varied between 5-30 millimolar in NO<sub>2</sub><sup>-</sup>, 20-200 millimolar in HSO<sub>3</sub><sup>-</sup>, and 10<sup>-7</sup> to 10<sup>-4</sup> molar in H<sup>+</sup>.

Experiments have been made to determine pH dependence on the reaction. The process first order in bisulfite shows a first order H<sup>+</sup> ion dependence.<sup>7</sup> The second order portion, which is predominant at pH of 7, is independent of hydrogen ion and sulfite concentrations. The results are shown in Table 1.

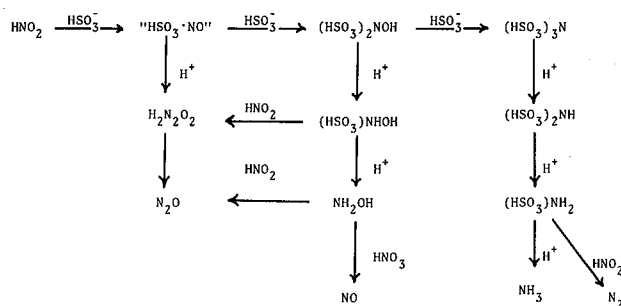


Fig. 1. Reaction scheme for the reduction of nitrite with bisulfite. Species in quotes has been postulated but not yet observed.

Table 1. Typical runs to determine pH dependence at  $\mu = 1.2$  for second order process.

Run #	$[\text{NO}_2^-]^a$	$[\text{HSO}_3^-]^a$	$[\text{SO}_3^{=}]^a$	pH	$\frac{d \ln[\text{NO}_2^-]^b}{dt}$		
					Total	1st order	2nd order
1	0.010	0.10	0.10	6.53	0.0136	0.0074	0.0062
2	0.010	0.10	0.20	6.85	0.0102	0.0035	0.0067
3	0.015	0.10	0.15	6.73	0.0114	0.0047	0.0067
4	0.015	0.10	0.15	6.71	0.0112	0.0049	0.0063
5	0.015	0.20	0.10	6.30	0.0492	0.0251	0.0241
6	0.015	0.20	0.20	6.58	0.0364	0.0132	0.0232
7	0.015	0.20	0.15	6.46	0.0395	0.0173	0.0222
8	0.015	0.25	0.10	6.25	0.0680	0.0351	0.0329
9	0.015	0.25	0.20	6.52	0.0569	0.0189	0.0380
10	0.015	0.25	0.15	6.38	0.0601	0.0261	0.0340

<sup>a</sup> concentrations in moles/liter

<sup>b</sup> rates in  $\text{min.}^{-1}$

The temperature dependence of the reaction was investigated by varying the temperature by means of a water bath. The rest of the experimental conditions were not varied. For the runs at low pH (4.5), the reaction was found to vary with temperature, as can be seen by the results in Fig. 2. The activation energy from this study is 12.1 kcal/mole, in good agreement with the literature.<sup>8</sup> A similar set of runs for the second order process reveals that it is nearly independent of temperature.

Further experiments were done to find the ionic strength ( $\mu$ ) dependence of the reaction. This was accomplished by varying ionic strength upon addition of  $\text{NaNO}_3$  and  $\text{Na}_2\text{SO}_4$ . The first order process shows no dependence on ionic strength. The second order process shows a marked dependence, which is presented in Fig. 3.

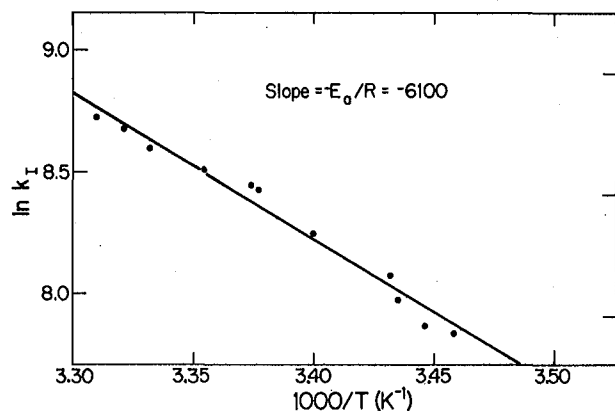


Fig. 2. Arrhenius plot showing temperature dependence of the rate constant for the process first order in bisulfite. (XBL 7911-13319)

Final experiments were carried out to determine a mass balance for nitrogen species. HADS was measured spectrophotometrically after oxidation to nitrosodisulfonate.<sup>9</sup> Results are shown in Fig. 4, indicating that HADS is the major product in the reaction. Hydrolysis and sulfonation reactions caused the apparent loss of nitrogen species.

#### DISCUSSION

The data indicate that there are two concurrent processes for the formation of HADS. This can be stated in the experimental rate law.

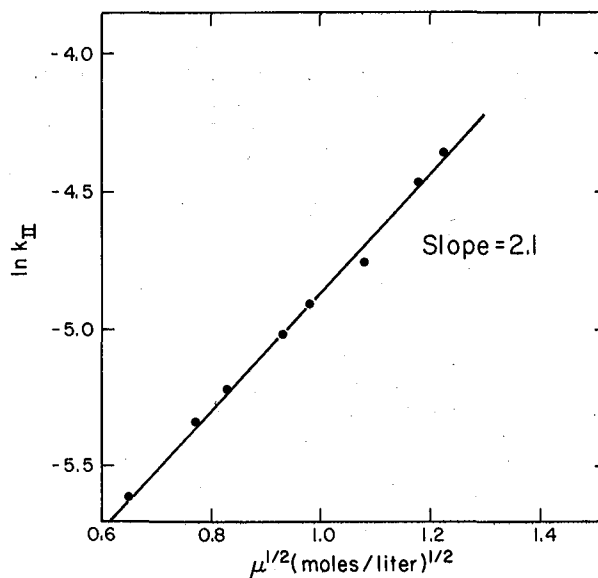


Fig. 3. Dependence of the rate constant for the process second order in bisulfite on the ionic strength. (XBL 7911-13320)

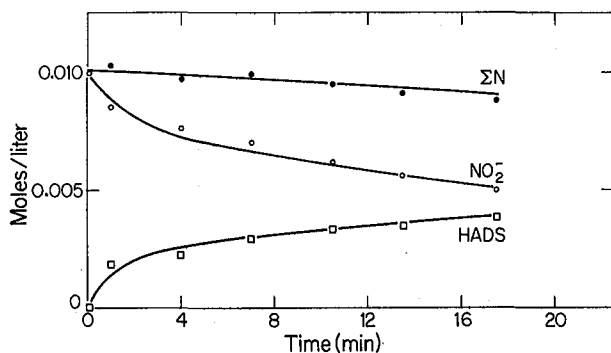


Fig. 4. Mass balance for nitrogen species.  $\Sigma N$  represents the sum of nitrite and HADS. (XBL 7911-13321)

$$\text{Rate} = k_1 (\text{H}^+) (\text{NO}_2^-) (\text{HSO}_3^-) + k_2 (\text{HSO}_3^-)^2 (\text{NO}_2^-) ,$$

$$\text{where } k_1 = (2.2 \times 10^{14}) e^{-6100/T} \frac{\text{liter}^2}{\text{mole}^2 \text{min}}$$

$$\text{and } k_2 = (5.4 \times 10^{-2}) e^{2.2 \sqrt{\mu}} \frac{\text{liter}^2}{\text{mole}^2 \text{min}}$$

Since there are a limited number of sulfur species present and the restriction that the two processes cannot have the same intermediate, we propose the following mechanism:

- 1)  $\text{H}^+ + \text{NO}_2^- = \text{HNO}_2$  fast equilibrium
- 2)  $\text{NO}_2^- + \text{S}_2\text{O}_5^{2-} = \text{NO}(\text{SO}_3)_2^{-3}$
- 3)  $\text{HNO}_2 + \text{HSO}_3^- = \text{NOSO}_3^- + \text{H}_2\text{O}$
- 4)  $\text{NOSO}_3^- + \text{HSO}_3^- = \text{NOH}(\text{SO}_3)_2^{-2}$

Since  $\text{NOSO}_3^-$  has never been detected, we can assume it is in a small steady state concentration. Using this steady state assumption, and looking only at the rate expression for the initial reaction times, we get the following rate expression,

$$\text{Rate} = k_A (\text{HONO}) (\text{HSO}_3^-) + k_B (\text{NO}_2^-) (\text{HSO}_3^-)^2 ,$$

which is identical in form to the observed rate law.

The ionic strength data for this mechanism fit exactly as expected from Debye-Huckel Theory. However, because of the breakdown of the theory at these higher ionic strengths, these are tentative conclusions. The fact that the second order process does not correlate to either  $\text{H}^+$  or  $\text{SO}_3^{2-}$  concentration but only to  $\text{HSO}_3^-$  lends credence to  $\text{S}_2\text{O}_5^{2-}$  as the reacting species. The first order process correlates equally well with sulfur (IV) and  $\text{HSO}_3^-$ , as would be expected since  $\text{HSO}_3^-$  is the major species.

The significance of this reaction in terms of atmospheric aerosol production is the formation of

sulfate and reduced nitrogen-containing sulfonates. The sulfate comes from each of the hydrolysis steps in the scheme in Fig. 1. In addition, gaseous species such as  $\text{NO}$ ,  $\text{N}_2\text{O}$ ,  $\text{N}_2$ , or  $\text{NH}_3$  could form as a result of the interaction between nitrous acid and sulfurous acid. The extent to which these gaseous species are produced depends on the condition of the reaction. One of the major obstacles to evaluating this reaction is that there are limited data on the nitrous acid concentration in water under atmospheric or plume conditions. There are indications, however, that under these conditions, a considerable amount of nitrite is found,<sup>10</sup> which clearly indicates a need for an understanding of these reactions.

#### FOOTNOTE AND REFERENCES

\* Condensed from Lawrence Berkeley Laboratory Report, LBL-10504 (1980). (Submitted to Journal of Physical Chemistry.)

1. R. P. Urone, H. Lutsep, C. M. Noyes, and J. F. Parcher, "Static studies of sulfur dioxide reactions in air," *Environ. Sci. Technol.* **2**, 611 (1968).
2. A. P. Altshuller and J. Bufalini, "Photochemical aspects of air pollution: A review," *Environ. Sci. Tech.* **5**, 39 (1971).
3. J. G. Calvert, F. Su, J. W. Bottenheim, and O. P. Strausz, "Mechanism of the homogeneous oxidation of sulfur dioxide in the troposphere," *Atmos. Environ.* **12**, 197 (1978).
4. R. J. Charlson, D. S. Covert, T. V. Larson, and A. P. Waggoner, "Chemical properties of tropospheric sulfur aerosols," *Atmos. Environ.* **12**, 39 (1978).
5. F. Raschig, *Schwefel und Stickstoffstudien* (Verlag Chemie, Berlin, 1924).
6. W. Latimer and J. Hildebrand, *Reference Book of Inorganic Chemistry* (New York, MacMillan, 1951), p. 208.
7. S. B. Oblath, S. S. Markowitz, T. Novakov, and S. G. Chang, "Kinetics and mechanism of the reactions of  $\text{NO}_x$  with  $\text{SO}_2$  in aqueous solutions," in *Atmospheric Aerosol Research Annual Report, 1977-78*, Lawrence Berkeley Laboratory Report LBL-8696 (1978).
8. S. Yamamoto and T. Kaneda, "Kinetics of formation of hydroxylaminedisulfonate and nitrilosulfonate by Raschig's hydroxylamine process," *Nippon Kagaku Zasshi* **80**, 1098 (1959).
9. V. F. Seel and E. Degener, "Kinetik und Chemismus der Raschigschen Hydroxylamin-Synthese," *Z. Anorg. Allg. Chem.* **284**, 100 (1956).
10. H. J. Crecelius and W. Forwerg, "Untersuchungen zum 'Saltzman-Faktor'," *Staub-Reinhalt Luft* **30**, 294 (1970).

## SULFATE FORMATION BY COMBUSTION PARTICLES IN A LABORATORY FOG CHAMBER

W. Benner, et al.

### INTRODUCTION

Particulate sulfate can compose a significant fraction of the total suspended particulate material in urban air and has been implicated in visibility reduction and as the cause of the characteristic low pH observed in acid rain.<sup>1</sup> Inhaled sulfate can also pose a health hazard, but the severity of the health threat is not clear. The description of the chemical and physical processes which introduce sulfate into the atmosphere is being revised constantly. Recent attention has been directed towards sulfate formation pathways which involve liquid water. The work reported here focuses on a pathway in which SO<sub>2</sub> is oxidized by dispersed water droplets such as those found in plumes, clouds, and fogs.

Work in our laboratory plus recent literature suggests that liquid water is an important component in the mechanism by which SO<sub>2</sub> is oxidized in the ambient air. Penkett et al.<sup>2</sup> calculated that the oxidation of SO<sub>2</sub> by O<sub>3</sub> and/or H<sub>2</sub>O<sub>2</sub> in cloud droplets can lead to sulfate formation. Wolff et al.<sup>3</sup> present ambient sampling data suggesting that particulate sulfate is formed by two mechanisms: one involving photochemical oxidation, the other proceeded by an O<sub>3</sub>-fog droplet route. Enger and Hogstrom<sup>4</sup> found that the rate of SO<sub>2</sub> oxidation in a power plant plume increases when the plume relative humidity (RH) is high. Johnstone and Mall<sup>5</sup> studied SO<sub>2</sub> oxidation in a laboratory fog chamber and found that SO<sub>2</sub> is oxidized rapidly when the droplets contain Mn<sup>2+</sup>. Dittenhoefer and de Pena<sup>6</sup> report that after a relatively dry power plant plume merged with a nearly saturated cooling tower plume, sulfate formed on the power plant plume particles. Work in our laboratory has shown that aqueous suspensions of soot particles can oxidize SO<sub>2</sub> rapidly.<sup>7</sup> Earlier fog chamber studies in our laboratory indicated that dispersed water droplets which contain soot nuclei can also oxidize SO<sub>2</sub>.<sup>8</sup>

It is hypothesized that under certain meteorological conditions, soot particles in the ambient air can become sites for SO<sub>2</sub> oxidation; this reaction pathway needs additional investigation. The work reported here is a continuation of our laboratory investigation concerning oxidation of SO<sub>2</sub> by water encapsulated soot particles. This year's work was conducted in an improved experimental system in which a new fog chamber and a new gas burner and associated sampling devices could be operated under conditions more properly controlled than previously possible in earlier fog chamber studies.<sup>8</sup>

### EXPERIMENTAL

Figure 1 shows a diagram of the experimental system. The fog chamber is 15 cm i.d. x 2.4 m tall and was constructed from stainless steel pipe with plexiglass end-caps. A 1-mW He-Ne laser beam is directed downward through the top plexiglass end-cap and is used to visually judge the fog density.

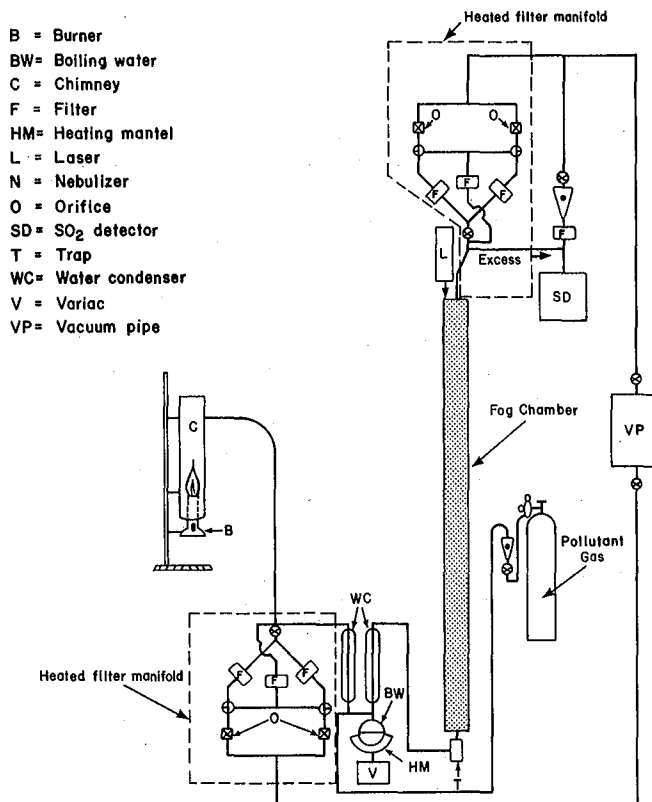


Fig. 1. Fog chambers and associated equipment used to study the oxidation of SO<sub>2</sub> by fog droplets which contain combustion nuclei. The filters were heated to ~45°C. (XBL 804-4123)

Pipeline natural gas is burned (~2 L/min) in a Fisher-type Bunsen burner. A diffusion flame is produced by covering the air holes at the burner base, and a premixed flame results when the air holes are open. The premixed flames produce many combustion particles which nucleate water, but these particles are not sooty and do not produce a gray deposit when collected on filters. The diffusion flames produce many black soot particles which nucleate water. The combustion gases from the burner are directed into an 8 cm i.d. x 40 cm tall stainless steel chimney. A portion of the combustion gases is withdrawn from the chimney and then drawn through the fog generator (humidifier and condensers) and finally through the vertical fog chamber. The flow rate of gases and particles through the chamber was held constant, and thus the time during which the droplets could react with SO<sub>2</sub> was the same for all runs. The reaction time or droplet residence time in the fog chamber was ~15 min. SO<sub>2</sub> (205 ppm SO<sub>2</sub> in N<sub>2</sub>) can be introduced into the air stream before water is condensed onto the soot particles.

Filter samples of fresh soot particles, i.e., particles before exposure to fog and SO<sub>2</sub>, and fog droplets withdrawn from the top of the chamber can be collected simultaneously. Samples are collected on 0.5- $\mu$ m pore Fluoropore filters and prefired quartz fiber filters. The filter holders are heated to  $\sim$ 45°C to prevent liquid water from collecting on the filters. This precaution precludes the possibility of chemical reactions involving liquid water occurring on the filter media. An SO<sub>2</sub> specific detector (Thermo Electron Corp.) is used to continuously monitor the SO<sub>2</sub> concentrations in the chamber. A 12-stage impactor can be used in place of the filters to collect samples of either fresh soot particles or fog droplets from the top of the chamber. Prefired quartz filters are used as the impaction surfaces and the after-filter in the impactor.

Pieces of the particle-laden quartz filters were analyzed for total carbon by a combustion technique which converted the carbon on the filter to CO<sub>2</sub>, and the resultant CO<sub>2</sub> was quantitated by infrared spectroscopy. Separate pieces of the quartz filters were extracted by sonication in water, and the extract was then filtered through a pre-extracted 0.22- $\mu$ m pore Millipore filter. The filtered extract was analyzed by ion chromatography. To correct for artifact formation, i.e., the conversion of SO<sub>2</sub> to sulfate by the dry quartz filters, two back-to-back quartz filters were used during sample collection, and thereby the concentrations of anions on the backup filter could be subtracted from those concentrations found on the front (particle-laden) filter. We eventually switched to Fluoropore filters instead of quartz filters because background concentrations and artifact formation were negligible on the Fluoropore filters. Extracts of the Fluoropore filters were obtained by placing pieces of the filter, along with some water, in a capped test tube and vigorously shaking the tube on a motor-driven shaker. This extract was subsequently filtered through a pre-extracted 0.22- $\mu$ m pore Millipore filter and then analyzed by ion chromatography.

An ion chromatograph (Dionex Corp., Sunnyvale, California) was used to quantitate the concentrations of NO<sub>2</sub>, NO<sub>3</sub>, SO<sub>3</sub>, and SO<sub>4</sub> in the filter extracts. Several mL of filter extract were injected onto an anion concentrator column. A flow of  $\sim$ 140 mL/min (30% flow) of 0.002 M NaOH + 0.0035 M Na<sub>2</sub>CO<sub>3</sub> was then directed through the concentrator column, and the displaced anions were separated on a 3 x 500 mm separator column; a 6 x 250 mm suppressor column was used to lower the conductivity of the eluent so that the separated anions could be detected by conductimetry. Various dilutions of a mixed standard solution of NO<sub>2</sub>, NO<sub>3</sub>, SO<sub>3</sub>, and SO<sub>4</sub> were injected separately and a graph of signal (peak height in micromhos) vs. weight was plotted for each anion. The concentration of an anion in a sample was obtained by comparing its peak height to the proper standard curve.

## RESULTS AND DISCUSSION

The collection of particles in the cascade impactor revealed that  $\sim$ 20% of the soot particles on a weight basis were covered with water. This

finding is shown in Fig. 2. The curve labeled Soot in Fig. 2 is the mass size distribution for fresh soot particles and shows that few particles are larger than  $\sim$ 2  $\mu$ m diameter. The curve labeled Fog in Fig. 2 shows the mass size distribution of the wet soot particles. The fog caused some of the soot particles to shift to a larger size range. This size shift is due to at least two processes. First, the soot particles served as centers onto which liquid water condenses and second, Brownian diffusion causes some of the soot particles to collide with fog droplets and become incorporated into the droplets. The stages on the impactor which collected fog droplets, i.e., 2- to 10- $\mu$ m diameter size range, became wet and gray, indicating the concurrence of soot particles and fog droplets. The ratio for the carbon in the 2- to 10- $\mu$ m diameter range (fog droplets) to the total carbon for curve F is 0.2. This ratio indicates that for conditions used, not enough water was available to cover all the soot particles with an equal amount of liquid water. The Kelvin effect, which states that the vapor pressure above a curved surface increases as the curvature increases, is an influencing factor which determines which particles become condensation nuclei. This effect would cause the larger soot particles to become condensation nuclei preferentially over smaller soot particles because the larger ones have less curvature and can thus condense water at a lower supersaturation ratio than that ratio required by smaller particles. The surface properties of the particles can also influence condensation. We have hypothesized that the wet soot particles are the ones which oxidize SO<sub>2</sub> to sulfate, but definitive experimental data are not available. If only the wet soot particles cause sulfate formation, then the fraction of soot particles which are wet is an important consideration in those experimental runs. On-going experiments are, in part, directed towards answering this question.

Chemical analysis of filter samples collected from the fog chamber showed that SO<sub>2</sub> was easily oxidized by wet soot particles. The results of the filter analysis are presented in Fig. 3. Net sulfate produced equals [SO<sub>4</sub><sup>-</sup>] fog - [SO<sub>4</sub><sup>-</sup>] fresh

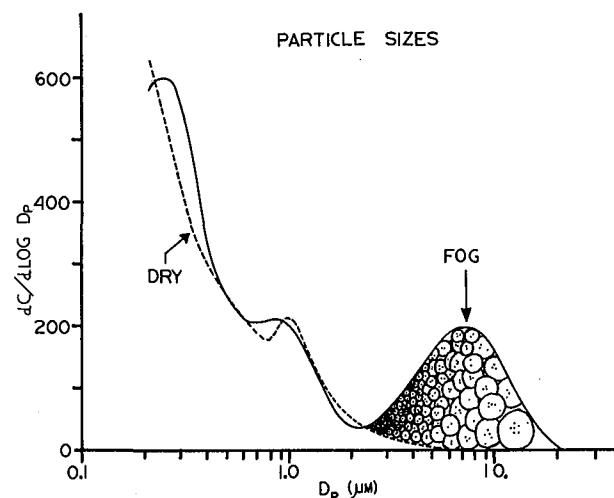


Fig. 2. Particle size distributions of fog chamber particles. (XBL 799-11295)

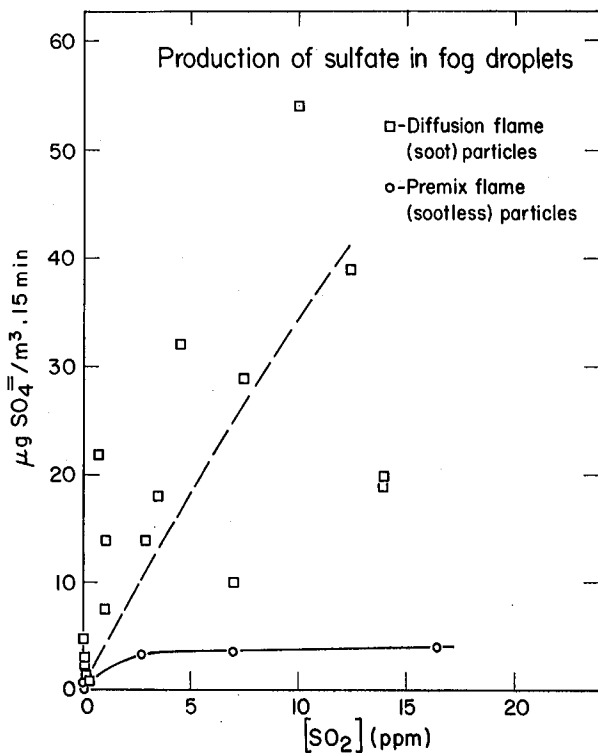


Fig. 3. Net sulfate produced by wet combustion particles exposed to SO<sub>2</sub>. The sulfate values correspond to a droplet reaction time of 15 min. (XBL 804-4122)

soot. The data for diffusion flames in Fig. 3 show, in general, that the [SO<sub>4</sub>]<sub>fog</sub> increased as the [SO<sub>2</sub>] was increased above [SO<sub>2</sub>]<sub>BKGD</sub>. [SO<sub>2</sub>]<sub>BKGD</sub> is the [SO<sub>2</sub>] that was present in the system due to combustion of sulfur in the fuel. [SO<sub>2</sub>]<sub>BKGD</sub> was always less than 0.05 ppm.

A large amount of scatter is associated with the diffusion flame data points in Fig. 3. It was thought that much of the scatter was due to variable soot particle concentrations that occurred from run to run because of irreproducible flame conditions. Normalization of [SO<sub>4</sub>] to [C] did not significantly reduce the scatter. Other uncontrolled factors could have caused the scatter. Since wet soot particles readily oxidized SO<sub>2</sub> to sulfate, while wet premixed flame particles showed decreased ability to oxidize SO<sub>2</sub>, the importance of soot in the droplets was realized. It is not known at this time whether or not a constant fraction of particles becomes covered with water in the condensation process. Visual observations using the laser beam indicated that fogs formed in air streams having soot number concentrations of ~300,000/cm<sup>3</sup> are about as optically dense as fogs formed in air streams having 30,000/cm<sup>2</sup>. This suggests that the fraction of the soot particles which becomes wet is variable. It is also not known if the absolute number of droplets which is formed remains constant for a given set of fog generator conditions, regardless of the number of soot particles present. If the number concentration of fog droplets were nearly constant from run to run, more soot particles would be incorporated

into fog droplets where the soot concentration is high. This is because the coagulation of soot particles with fog droplets increases as the soot particle concentration increases.

Figure 3 also presents results from experimental runs in which combustion particles from premixed flames were used to nucleate fog droplets. The curve labeled "premixed" in Fig. 3 shows that the [SO<sub>2</sub>] does not have a large effect on the amount of sulfate produced and, for a fixed [SO<sub>2</sub>], fog droplets which contain premixed flame particles produce little sulfate compared to fog droplets which contain soot particles. The data for the premixed flame curve show little scatter, which tends to confirm the lack of reactivity of wet premixed flame particles.

The particulate carbon concentration for the premixed flame data points was considerably less (as much as a factor of 10) than the runs using soot particles because the premix flames burn much cleaner. The total number concentration of particles produced by the diffusion or premixed flames was not measured routinely but several samples showed that the number concentrations were similar in each. Two L/min of gas was burned in all experimental runs regardless of the flame type, so in terms of sulfate formed per Btu of fuel, the wet soot particles produced the most sulfate.

At this time not enough data are available to determine the shape of the curve for diffusion flame data points in Fig. 3. It is not known whether the [SO<sub>4</sub>] increases linearly with [SO<sub>2</sub>] or whether the curve will gradually level off at high SO<sub>2</sub> concentrations. Evidence from other investigations in our laboratory shows that the rate of sulfite to sulfate oxidation in aqueous soot suspensions, for a constant [soot], increases as the [SO<sub>2</sub>] increases over several decades of concentration to ~10<sup>-5</sup> M SO<sub>3</sub> and above 10<sup>-5</sup> M SO<sub>3</sub> the rate remains nearly constant.<sup>9</sup> More data need to be collected before we can determine a rate expression for the fog chamber data.

Rough conversion rate estimates can be calculated from the data in Fig. 3. Such estimates are risky because of the scatter associated with the data. The influence of the soot particle concentration is not taken into account in these estimates because of the difficulty in estimating the "wet" soot particle concentration. For wet soot particles exposed to 10 ppm SO<sub>2</sub>, Fig. 3 indicates that approximately 40 μg SO<sub>4</sub>/m<sup>3</sup> can be expected to form in 15 min. This corresponds to a conversion rate of ~0.8%/hr. At an SO<sub>2</sub> concentration of 0.5 ppm, a value of 15 μg SO<sub>4</sub>/m<sup>3</sup> · 15 min was chosen from Fig. 3. This corresponds to a conversion of ~5%/hr which is quite competitive with other mechanisms suggested for sulfate formation in the atmosphere.

#### CONCLUSIONS

The preliminary results presented here indicate that water can condense onto soot particles and encapsulate them with a liquid layer. Depending on conditions, it is possible that not all the soot particles become encapsulated with water. The

presence of soot in the soot-fog-SO<sub>2</sub> system is important for sulfate formation because experiments conducted with sootless flames produced little sulfate. In general, the amount of sulfate which formed in fog-soot-SO<sub>2</sub> reactions was dependent upon [SO<sub>2</sub>] because more sulfate formed at higher SO<sub>2</sub> concentrations.

#### REFERENCES

1. G. E. Likens, R. F. Wright, J. N. Galloway, and T. J. Butler, "Acid rain," *Scientific American* 241 (1979).
2. S. A. Penkett, B. M. R. Jones, K. A. Brice, and A. E. J. Eggleton, "The importance of atmospheric ozone and hydrogen peroxide in oxidizing sulphur dioxide in cloud rainwater," *Atmos. Environ.* 13, p. 123 (1979).
3. G. T. Wolff, P. R. Monson, and M. A. Ferman, "On the nature of the diurnal variation of sulfates at rural sites in the eastern United States," *Environ. Sci. and Technol.* 13, p. 1271 (1979).
4. L. Enger and U. Hogstrom, "Dispersion and wet deposition of sulfur from a power plant plume," *Atmos. Environ.* 13, p. 797 (1979).
5. H. F. Johnstone and A. J. Moll, "Formation of sulfuric acid in fogs," *Ind. and Eng. Chem.* 52, p. 861 (1960).
6. A. C. Dittenhoefer and R. G. de Pena, "A study of production and growth of sulfate particles in plumes from a coal-fired power plant," *Atmos. Environ.* 12, p. 297 (1978).
7. R. Brodzinsky, S. G. Chang, S. S. Markowitz, and T. Novakov, "Kinetics and mechanism for catalytic oxidation of SO<sub>2</sub> on carbon in aqueous formation," in *Atmospheric Aerosol Research Annual Report, 1977-78*, Lawrence Berkeley Laboratory Report LBL-8696 (1978).
8. W. H. Benner, H. Rosen, and T. Novakov, "SO<sub>2</sub> oxidation by water droplets containing combustion nuclei," in *Atmospheric Aerosol Research Annual Report, 1977-78*, Lawrence Berkeley Laboratory Report LBL-8696 (1978).
9. R. Brodzinsky, this year's annual report.

## LIFETIME OF LIQUID WATER DROPLETS: AN EXPERIMENTAL STUDY OF THE ROLE OF SURFACTANTS

*R. Toossi, et al.*

#### INTRODUCTION

Chemical reactions of air pollutants in liquid water have been extensively studied in the laboratory. These wet processes are suggested to be important in the formation of atmospheric sulfate and nitrate particulates, and thus presumably contribute to the increase in the acidity of rain. The assessment of the impact of wet chemical processes, however, has been largely based on the chemical reaction rates. The effect of the diffusion rate and the lifetime of water droplets has been largely ignored or based on theoretical considerations at best. The experimental measurement of these effects with actual atmospheric water droplets has not been carried out to the best of our knowledge.

Recent studies of atmospheric liquid water droplets<sup>1-3</sup> indicate the presence of various soluble and insoluble impurities. These impurities can drastically affect the evaporation rate of the droplets either by reducing the vapor pressure due to a solution effect or by increasing the surface resistance due to a film of surfactants. For example, a reduction of four orders of magnitude has been observed with a film of certain surfactants.<sup>4</sup> A recent mathematical model<sup>5</sup> shows that the resistance due to surface film can be rate controlling for small droplets ( $r \ll 10 \mu\text{m}$ ) and small accommodation coefficient ( $\alpha < 10^{-4}$ ). For this reason the

accommodation coefficient is an important parameter in studies of water droplet stability.

In this article, we report experimental measurements of the lifetime of water droplets in the presence of various realistic organic impurities which are generated from combustion sources. These results are compared to laboratory-generated fog samples and rain samples. From these measurements, the accommodation coefficients of the various samples are calculated. The measurements will be extended to atmospheric fog and cloud samples in the near future.

#### EXPERIMENTAL METHODS

Solution droplets were suspended from a quartz fiber located in a quartz spring microbalance. The quartz fiber was coated with a layer of paraffin wax to prevent the droplet from being wetted. Deflections of .001 cm could be measured using a horizontal microscope (magnification of 50x) with an ocular scale. A spring sensitivity of 1 mg/cm allowed the measurement of droplet weight loss with an accuracy of .001 mg. The system was sealed, except for a small leak to equilibrate pressure. The relative humidity in the chamber was maintained with a known concentration of a NaCl solution. A dewpoint hygrometer directly measured humidity in the chamber. This assembly was placed in a thermostatted room where temperature never changed

by more than .2°C during each experiment. A high-intensity lamp was used to illuminate the droplet during each measurement. The lamp was on only for a few seconds during the measurement, and therefore heating of the droplet was not expected. To verify this, measurements were repeated without the light source. No change was observed. Enough time was allowed for the system to reach equilibrium before any measurement was made; then droplet size was measured directly by the microscope and calculated from weight measurements. Referring to Fig. 1, the diameter of the droplet can be calculated from the following formula:

$$m = \frac{1}{6} \pi d^3 - \frac{1}{4} \pi d \cdot d'^2 \quad (1)$$

The two methods for determining the diameter of the droplet agreed to within 5%. No attempt was made to measure droplet temperature. Evaporation measurements were made for as long as the droplet remained spherical, usually at one-fifth its original diameter. Experiments have been carried out on a number of laboratory and field samples.

Sample extracts were made by extracting the particulates collected on quartz filters from various combustion-dominated sources such as a tunnel and a parking garage and from ambient samples. Particulates were washed off by sonicating the sample filters in water and then filtering the emulsion to remove large particles. The concentrations of contaminants are normalized by their carbon content determined by a combustion technique. Laboratory fog was collected from a fog chamber which is described in this report (see Benner et al.). The procedure for collection involved impaction on a porous surface and suction by capillary action.

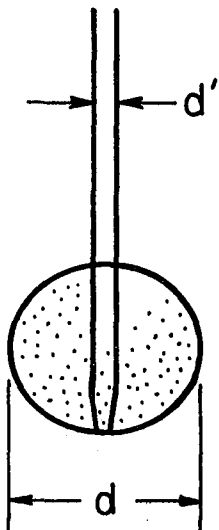


Fig. 1. Schematic drawing of a droplet on a fiber support.  $d'$  is the fiber diameter and  $d$  is the droplet diameter. (XBL 807-3460)

## RESULTS AND DISCUSSION

The equation for the rate of evaporation has been derived as follows:<sup>5</sup>

$$\frac{dr}{dt} = \frac{\rho_{eq}(\infty)}{\rho_l} \frac{S - (1 - X_s) \exp(2\sigma\rho_{eq}(\infty)/r\rho_l)}{R_i + R_m + R_T}$$

where  $R_i = \frac{1}{\alpha v}$ , the resistance at the interface;

$R_m$  is the resistance to mass diffusion;

$R_T$  is the resistance to heat diffusion;

$\alpha$  = the accommodation coefficient;

$v = \frac{\bar{v}}{4}$ , and  $\bar{v}$  is the velocity of the

evaporating molecule calculated from the kinetic theory of gases.

$\rho_{eq}(\infty)$  is the equilibrium vapor density at large distances from the droplet,  $\rho_l$  is the density of the liquid phase,  $S$  is the relative humidity,  $\sigma$  is surface tension, and  $X_s$  is mole fraction of solute in the solution droplet. For droplets of 1.0  $\mu$ m in diameter at 90% relative humidity, only 1% error is introduced when the curvature effect is neglected. With a larger droplet or at a lower humidity, the effect is still smaller. Calculations indicate that the solution effects can be neglected for relative humidities below 70%. The specific rate of evaporation of large droplets of salt solutions ( $X_s = .01$ ) is only 3.4% lower than those of pure water at  $S = .70$ .

The surface degradation rate ( $-dA/dt$ ) as a function of the accommodation coefficient has been calculated and is plotted in Fig. 2 at different relative humidities. These plots can be used to evaluate the accommodation coefficient of the contaminated droplets if the surface degradation rate is measured experimentally. For pure water, evaporation is controlled by the rate of diffusion, and

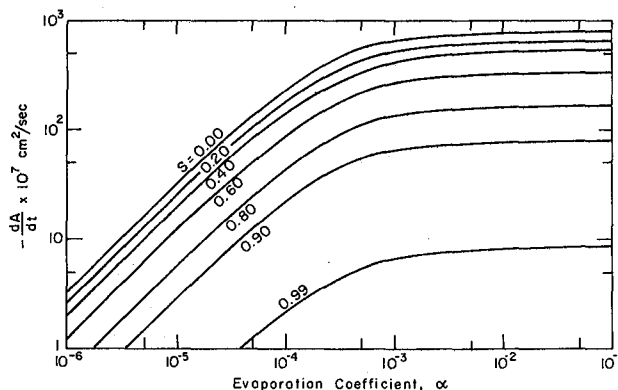


Fig. 2. Surface degradation rate of aerosol droplets. (XBL 801-4500)

the surface degradation rate becomes independent of the accommodation coefficients. Therefore the values of  $\alpha$  for pure water cannot be accurately measured by this method. Table 1 gives the measured values of  $dA/dt$  for pure water at different relative humidities.

Table 1. Surface degradation rates for pure water.

Relative Humidity	$-\frac{dA}{dt} \times 10^6 \text{ cm}^2 \cdot \text{sec}^{-1}$
91	0.320
75	0.766
42	1.710

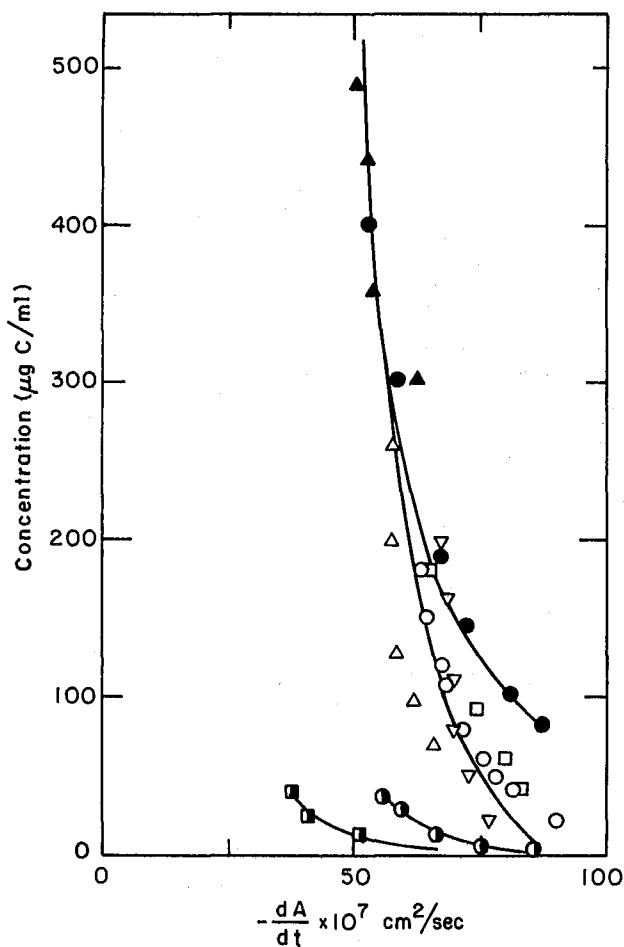


Fig. 3. Surface degradation rate of water extracts of ambient Berkeley and Berkeley rain samples.

- △ □ ○ Ambient Berkeley, 3-4 October 1978
- ▲ ● Ambient Berkeley, 2-3 May 1978
- Berkeley rain, 24-27 March 1978
- Berkeley rain, 6 April 1978

Different symbols on the same graph represent results for different samples prepared at different initial contaminant concentrations from the same extract. (XBL 801-4505)

However, for sufficiently contaminated drops the evaporation coefficient can be found from the surface degradation rate curves. Figures 3 and 4 show such graphs for rain and water extract of ambient Berkeley particulate aerosol samples. Results from tunnel samples, parking garage samples, and laboratory fog are shown in Fig. 5. These figures show that there exists a critical concentration of contaminants, above which evaporation is greatly retarded. At this concentration a monolayer of surfactant presumably covers the entire droplet surface. All molecules of water vapor have to cross this barrier before evaporating into gaseous media. At lower concentrations all the sites are not filled, and water molecules can bypass this resistance. Therefore evaporation is controlled by diffusion and proceeds like pure water until the solution becomes concentrated enough for the solution effect to become important.

A summary of these results is given in Table 2. The lifetimes of droplets of 10  $\mu\text{m}$  in diameter are estimated at relative humidities of 60% and 90% where the surfactant concentration is greater than the critical concentration. A comparison of these results with those of pure water, which is also shown in the table, indicates that surfactants if present in sufficient quantities can have a large effect on the lifetime of liquid water drops in the atmosphere.

#### REFERENCES

1. D. Winkler and C. Junge, "The growth of atmospheric aerosol particles as a function of the relative humidity. Part II. An improved concept of mixed nuclei," *Aerosol Sci.* **4**, 373 (1973).

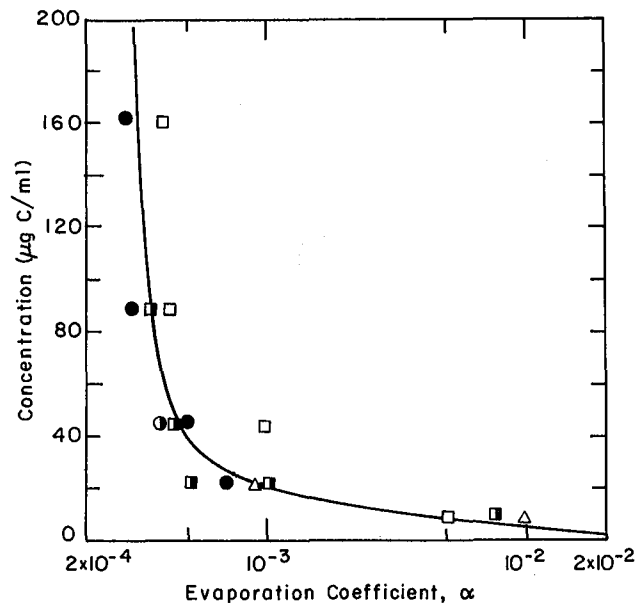


Fig. 4. Evaporation coefficient for water extract of an ambient Berkeley sample as a function of the carbon content. (XBL 801-4504)

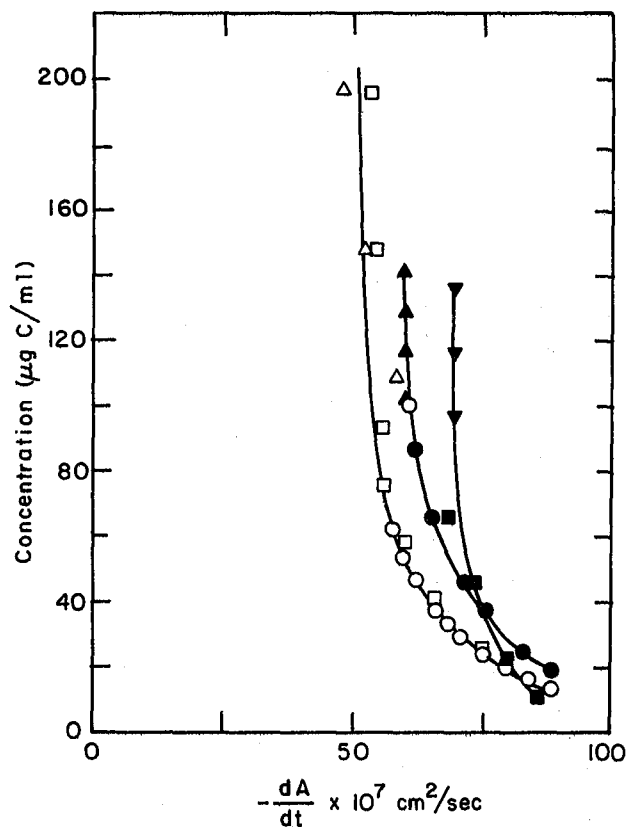


Fig. 5. Evaporation coefficient for water extract of an ambient Berkeley sample as a function of the carbon content. (XBL 801-4503)

Table 2. Evaporation coefficients and associated lifetimes of different aerosol samples.

Sample	Date collected	$\alpha$	Lifetime (minutes)	
			$r_0 = 5 \mu\text{m}$ $S = .60$	$S = .90$
Ambient Berkeley	10/3-4/78	$7 \times 10^{-5}$	1.5	10
	5/2-3/78	$7 \times 10^{-5}$	1.5	10
Tunnel	3/30/78	$7 \times 10^{-5}$	1.5	10
	3/30/78	$10^{-4}$	0.7	4
Parking garage	4/14/78	$6 \times 10^{-5}$	2.0	12
	4/15/78	$6 \times 10^{-5}$	2.0	12
Laboratory fog	11/1/79	$1.4 \times 10^{-4}$	0.4	2
Pure water	--	$4 \times 10^{-2}^a$	$<10^{-2}$	$10^{-2}$

<sup>a</sup>Ref. 6.

- D. S. Covert, "A study of the relationship of chemical composition and humidity to light scattering by aerosols," *J. Appl. Meteorol.* **11**, 968 (1972).
- Yu. S. Georgievskiy and G. V. Rosenberg, "Humidity as a factor in aerosol variability," *Izv. Atmos. Oceanic Phys.* **9**, 66 (1973).
- R. S. Bradley, "The rate of evaporation of micro-drops in the presence of insoluble monolayers," *J. Coll. Sci.* **10**, 751 (1955).
- R. Toossi, S. G. Chang, and T. Novakov, "Lifetime of liquid water drops in ambient air: Consideration of the effects of surfactants and chemical reactions," in *Atmospheric Aerosol Research Annual Report, 1977-78*, Lawrence Berkeley Laboratory Report LBL-8696 (1978).
- N. A. Fuchs, *Evaporation and Droplet Growth in Gaseous Media* (English translation), New York, Pergamon (1959).

# A PHOTOACOUSTIC INVESTIGATION OF URBAN AEROSOL PARTICLES\*

Z. Yasa, et al.

## INTRODUCTION

The nature of the absorbing species in atmospheric aerosol particles has recently attracted considerable attention among atmospheric and environmental scientists. Recent studies using Raman spectroscopy and an optical attenuation technique<sup>1</sup> indicate that the absorbing species in urban particulates is "graphitic" carbon. We report here on the results of a photoacoustic investigation which gives an independent verification of this hypothesis.

Unlike conventional optical absorption techniques, photoacoustic spectroscopy measures the energy deposited in a sample due to absorption. Since questions have been raised whether the optical attenuation technique exclusively measures the absorbing rather than the scattering component of the aerosol, a comparison between photoacoustic and optical attenuation measurements made on the same aerosol sample should help resolve this ambiguity.

## EXPERIMENTAL METHOD AND RESULTS

The photoacoustic measurements were made in an acoustically nonresonant detector with cylindrical geometry (Fig. 1). A Knowles microphone (Model BT-1759) was used, and the cell dimensions were 2.1 cm in diameter and 0.3 cm in length. The gas in the detector cell was air at atmospheric pressure. A He-Ne laser operating at 632.8 nm with 0.5 mW of power was used as the light source, and the experiments were performed at a modulation frequency of 20 Hz. The aerosol particles, collected on 1.2- $\mu$  Millipore filter substrates, were mounted on a 1.5-mm-thick Pyrex backing with the particles facing the incident light beam. Experiments were also performed with the laser beam first incident on the filter substrate.

In the limit of low frequency light modulation ( $\leq 100$  Hz), it can be shown<sup>2,3</sup> that the photoacoustic signal is given by:

$$V(\omega) = \frac{\eta \gamma P W \mu_g \mu_{sb} G(\omega)}{2\sqrt{2} b T V K_{sb}} 1 - \exp(-\alpha \ell) \quad (1)$$

where  $\eta$  - heat conversion efficiency  
 $\gamma$  - specific heat ratio for air ( $C_p/C_v$ )  
 $P$  - cell pressure  
 $W$  - input power  
 $\mu_g$  - thermal diffusion length in air  
 $\mu_{sb}$  - thermal diffusion length in substrate

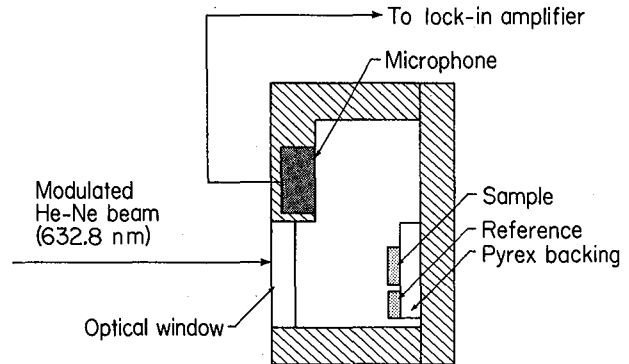


Fig. 1. Experimental arrangement. (XBL 794-1230)

$G(\omega)$  - microphone response

$b$  - dimensionless parameter taking into account the diffusion of heat from the sample to the Pyrex backing

$T$  - temperature

$V$  - cell volume

$K_{sb}$  - thermal conductivity of substrate

$\alpha$  - adsorption coefficient

$\ell$  - effective path length

From Eq. (1) it follows that the photoacoustic signal saturates exponentially with increasing absorption to a value of

$$V_{\text{sat}}(\omega) = \frac{PW_g \mu_{sb} G(\omega)}{2\sqrt{2} b T V K_{sb}} \quad (2)$$

Hence the ratio of the signal from a given sample to a reference sample for which the signal is saturated yields

$$S_{\text{ph}} = V/V_{\text{sat}} = 1 - \exp(-\alpha \ell) \quad (3)$$

This saturable behavior was observed for highly absorbing samples, and the sample which yielded the largest photoacoustic signal was used as the reference,  $V_{\text{sat}}$ . Note that such samples yield values of  $\alpha \ell \geq 3$ , as deduced from the optical attenuation measurements; hence the highest signal obtained from available samples is close to the actual saturation value.

The experimental setup for the optical attenuation measurements is described elsewhere.<sup>1</sup> In this technique the signal  $S_{op}$  is defined as  $1 - \exp(-x)$ .  $x$  is the optical attenuation of the sample and is given by  $-\ln I/I_0$ , where  $I$  is the transmitted intensity of a loaded filter, and  $I_0$  is the transmitted intensity of a blank filter.

In Fig. 2 we present a plot of the normalized photoacoustic signal  $S_{ph}$  vs.  $S_{op}$  for a wide range of ambient samples and samples collected directly from combustion sources. The samples include urban particulates collected over a 24-hr period in Fremont and Anaheim, California; Denver, Colorado; and New York, New York; particles collected in a highway tunnel and from an acetylene torch. The least squares fit of the experimental points yields a correlation coefficient  $r$  of 0.98 and a slope of 1.03, which would be expected if both techniques measure the same optical property of the aerosol particles. Since the photoacoustic signal is proportional to the heat generated by absorption, we conclude that the optical attenuation method measures the light absorbing component of the aerosol particles.

From a theoretical point of view, this result is somewhat surprising since aerosol particles have a large scattering coefficient, which would be expected to contribute to the optical attenuation measurement and not to the photoacoustic signal. However, careful examination of the experimental arrangement shows that the incident light interacts

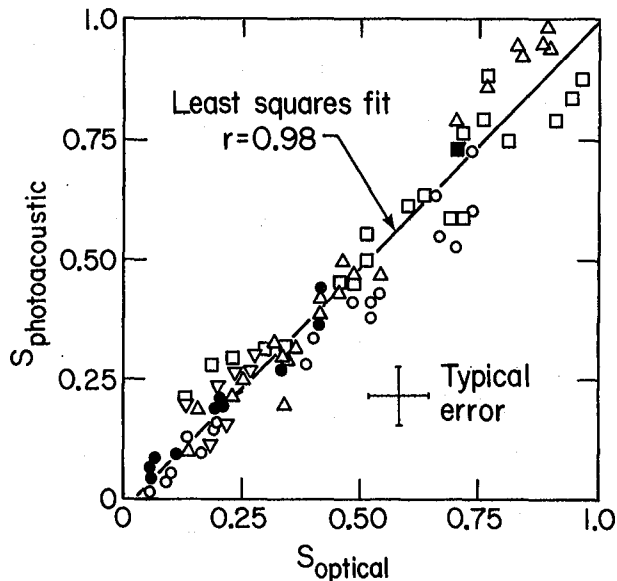


Fig. 2. Plot of  $S_{ph}$  vs.  $S_{op}$  for various samples:  $\nabla$  - Fremont;  $\square$  - Anaheim;  $\circ$  - Denver;  $\triangle$  - New York City;  $\blacksquare$  - highway tunnel;  $\bullet$  - acetylene torch. The solid line is a least squares fit of the data. (XBL 794-1229)

not only with the aerosol particles but also with the filter medium, which is almost a perfect diffuse reflector. In this circumstance, it is possible to show<sup>4</sup> that because of multiple reflections between the particles and the filter substrate, the optical attenuation measurement is insensitive to the scattering properties of the aerosol.

#### CONCLUSION

In conclusion, the results presented here, when combined with Raman scattering data<sup>1</sup> and thermal analysis<sup>5</sup> and solvent extraction results,<sup>6</sup> indicate that the optically absorbing component of urban aerosol particles is "graphitic" carbon. Extensions of this work are presently being carried out in our laboratories.

#### FOOTNOTE AND REFERENCES

\*Collaborative work between Applied Laser Spectroscopy group and Atmospheric Aerosol Research group. (Published in *Applied Optics* **18**, 2528 (1979).

1. H. Rosen, A. D. A. Hansen, L. Gundel, and T. Novakov, "Identification of the optically absorbing component in urban aerosols," *Appl. Opt.* **17**, 3859 (1978).
2. Over a frequency range of 5-100 Hz, the photoacoustic signal showed no variation, indicating that the sample was thermally thin. In this case Eq. (1) follows from Eq. (21) of Ref. 3 in the limit of  $\omega \rightarrow 0$  and after modification of their parameters to take into account an additional boundary layer introduced by the Millipore filter.
3. A. Rosenzwaig and A. Gersho, "Theory of photoacoustic effect with solids," *J. Appl. Phys.* **47**, 64 (1976).
4. H. Rosen and T. Novakov, "Optical attenuation: a measurement of the absorbing properties of aerosol particles," in *Atmospheric Aerosol Research Annual Report 1977-78*, Lawrence Berkeley Laboratory Report LBL-8696, p. 54.
5. H. Rosen, A. D. A. Hansen, L. Gundel, and T. Novakov, "Identification of the graphitic carbon component of source and ambient particulates by Raman spectroscopy and an optical attenuation technique," *Proceedings of Conference on Carbonaceous Particles in the Atmosphere*, Lawrence Berkeley Laboratory Report LBL-9037 (1979).
6. R. E. Weiss, A. P. Waggoner, R. J. Charlson, D. L. Thorsell, J. S. Hall, and L. A. Riley, "Studies of the optical, physical, and chemical properties of light absorbing aerosols," *Proceedings of Conference on Carbonaceous Particles in the Atmosphere*, Lawrence Berkeley Laboratory Report LBL-9037 (1979).

# THE USE OF AN OPTICAL ATTENUATION TECHNIQUE TO ESTIMATE THE CARBONACEOUS COMPONENT OF URBAN AEROSOLS

A. Hansen, et al.

## INTRODUCTION

Carbon-, sulfur-, and nitrogen-containing particles account for most of the anthropogenically generated particulate burden in urban areas. The carbonaceous aerosol is often the single most important contributor to the submicron aerosol mass and is expected to have a substantial impact on visibility and health.<sup>1</sup> It was also postulated as early as 1974<sup>2</sup> that the surface of these particles might be an effective catalyst for the heterogeneous conversion of SO<sub>2</sub> to sulfate in the presence of moisture--a process that has subsequently been confirmed both theoretically<sup>3</sup> and under laboratory conditions.<sup>4,5</sup> These carbonaceous particles consist of two major components--graphitic or black carbon (sometimes referred to as elemental or free carbon) and organic material. The latter can either be directly emitted from sources (primary organics) or produced by atmospheric reactions from gaseous precursors (secondary organics). We define "soot" as the total primary carbonaceous material, i.e., the sum of graphitic carbon and primary organics. There has been considerable uncertainty and debate over the relative importance of primary and secondary carbonaceous material in urban air.<sup>1</sup> It is important to resolve this issue since it is obvious that a control strategy and technology for particulate carbon pollution abatement will depend on which of these alternatives prevails. In this paper we present data from a large-scale sampling program and results showing that a measurement of the optical absorption of the particles may be used to quantitate the black

carbon component and to estimate the total carbon loading.

## SAMPLING AND EXPERIMENTAL METHODS

Because relatively few consistent studies of ambient carbonaceous particles had been conducted, we established in 1977 an ongoing routine sampling program at numerous sites. The data consist of information obtained from 24-hour samples (collected every morning Monday through Friday) and multi-day samples collected over weekends. For the purpose of data analysis, these two data sets can be separated. Table 1 lists the routine sampling sites with the beginning date of sampling.

The samples are collected in parallel on pre-fired quartz fiber and Millipore filter membranes. The flow rates employed are in the range of 0.6-2.2 cubic meters of air per square centimeter of active filter area per 24-hour sampling period. The Millipore filter is used for x-ray fluorescence (XRF) elemental analysis and an optical attenuation technique developed in this laboratory.<sup>6</sup> The latter technique gives a measurement that is proportional to the amount of light-absorbing (black) carbon present on the filter.<sup>7</sup> It is based on a principle similar to that of the opal glass method used by Weiss et al.<sup>8</sup> and measures the absorbing rather than the scattering properties of the aerosol. For fixed optical constants, a quantitative relationship between the optical attenuation and the black carbon content can be written as:

Table 1. Aerosol sampling sites.

Site	Location	Date of first sample
Lawrence Berkeley Laboratory	Berkeley, Calif.	1 June 1977
BAAQMD monitoring station	Fremont, Calif.	15 July 1977
SCAQMD monitoring station	Anaheim, Calif.	19 August 1977
Argonne National Laboratory	Argonne, Ill.	22 January 1979
DOE Environmental Measurements Laboratory	Manhattan, New York	22 November 1978
National Bureau of Standards	Gaithersburg, Maryland	23 January 1979
Denver Research Institute	Denver, Colorado	15 November 1978
Naval Arctic Research Station	Barrow, Alaska	1 October 1979
Oregon Graduate Center	Beaverton, Oregon	22 April 1979
University of Arizona	Tucson, Arizona	8 March 1979
University of Washington	Seattle, Washington	14 February 1979
C.S.I.R.O.	Sydney, Australia	11 September 1978
B. Kidric Institute	Belgrade, Yugoslavia	1 October 1979
National Center for Atmospheric Research	Boulder, Colorado	4 January 1980

The latter six samplers have been operated on an intermittent basis. In addition to the above locations, samplers are currently being shipped to the following locations:

Cheng Kung University, Taiwan, Republic of China  
Washington University, St. Louis, Missouri

$$[C_{\text{black}}] = (1/K) \times \text{ATN} \quad (1)$$

where  $\text{ATN} = -100 \ln(I/I_0)$ .  $I$  and  $I_0$  are the transmitted light intensities for the loaded filter and for the filter blank.

Besides the black carbon, particulate material also contains organic material which is not strongly optically absorbing. The total amount of particulate carbon is then:

$$[C_{\text{tot}}] = [C_{\text{black}}] + [C_{\text{org}}] \quad (2)$$

A fundamental characterization of a particulate sample can be given by its attenuation per unit mass of total carbon, i.e., its specific attenuation,  $\sigma$ :

$$\sigma \equiv \frac{\text{ATN}}{[C_{\text{tot}}]} = K \times [C_{\text{black}}]/[C_{\text{tot}}] \quad (3)$$

The determination of specific attenuation therefore gives an estimate of black carbon as a fraction of total carbon.

Carbon-specific analyses are performed on the quartz fiber filter, since the carbon loading of a blank is typically 30 to 100 times less than the loading after exposure. These analyses include total combustible carbon determination,<sup>9</sup> successive solvent extraction<sup>10</sup> to separate nonextractable and "organic" carbonaceous material, and a progressive combustion-optical attenuation technique<sup>11</sup> that yields both chemical and physical information. The information recorded in the data base includes the above particulate analyses as well as meteorological and gaseous pollutant data and may be used in many ways to study seasonal effects and inter-correlation of pollutants. In this report we concentrate on studies of the concentration of "total" and "black" carbon in the ambient aerosol.

#### Total Carbon Loadings

From analysis of the quartz fiber filters, we may determine the average loading of particulate carbonaceous material during the sampling period. Overall average carbon concentrations are shown in Table 2. In Fig. 1 we show the variations of total

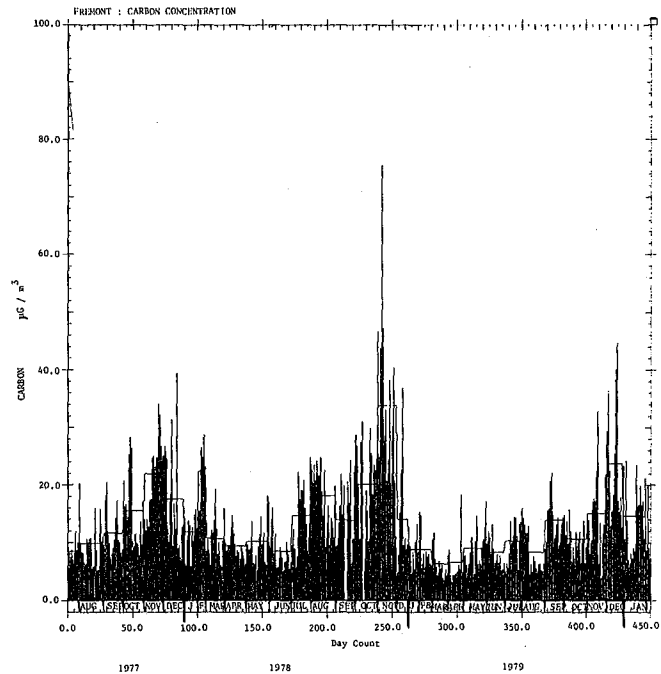


Fig. 1. Total carbon loading of 24-hour samples taken at the Fremont site. (XBL 806-10534)

carbon at the Fremont site for 24-hour samples (i.e., weekends excluded), with the monthly averages superimposed. It is evident that there are large day-to-day variations, but that the averages peak during the late fall season. A similar pattern is observed at other California locations, supporting the hypothesis that the loadings at these receptor sites are largely controlled by ventilation. In contrast, results from the New York site (Fig. 2) show much less variation on both a daily and monthly scale. This is consistent with the location of the site above a heavily traveled street canyon, resulting in an aerosol dominated by direct source emissions.

From XRF analysis of the Millipore filter we obtain the loadings of silicon and heavier elements. We may apply a simple model of the chemical form of these elements to calculate an "accountable mass" from this data. The algorithm used is necessarily crude and overlooks important contributions of oxygen and nitrogen. Reported figures for the mass contribution of water to the accumulation

Table 2. Carbon concentrations ( $\mu\text{g}/\text{m}^3$ )

Site	Dates on file	# samples	Average	Highest	Lowest
New York	Nov. 78 - Apr. 80	439	15.2	53.1	3.4
Argonne	Jan. 79 - Mar. 80	438	8.1	25.1	3.1
Gaithersburg	Jan. 79 - Mar. 80	381	6.1	17.6	2.3
Denver	Nov. 78 - May 79	141	9.8	30.8	4.1
Anaheim	Aug. 77 - Jan. 80	852	16.6	112.9	3.1
Fremont	July 77 - Mar. 80	924	12.0	75.6	3.4
Berkeley	June 77 - Apr. 80	998	6.7	31.7	3.0

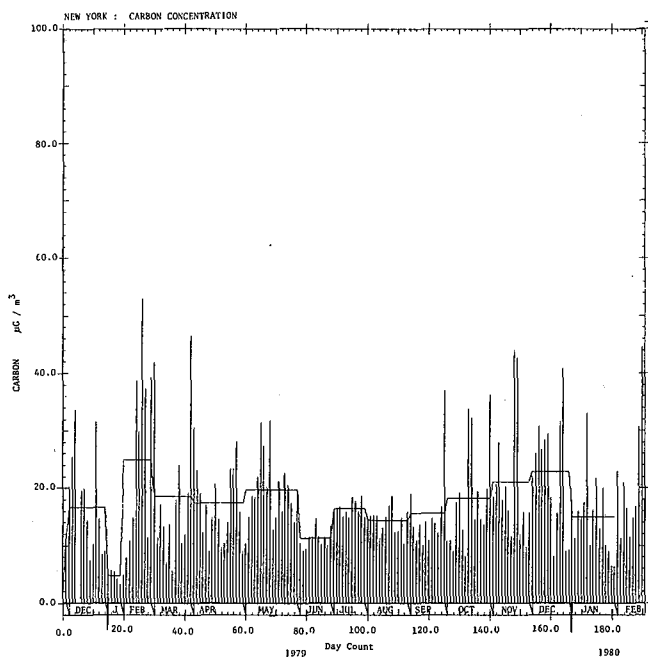


Fig. 2. Total carbon loading of 24-hour samples taken at the New York City site. (XBL 806-10535)

mode of ambient aerosols range up to 20%,<sup>12</sup> and loadings of up to 30  $\mu\text{g}/\text{m}^3$  of nitrate are not uncommon.<sup>13</sup> The conventional nitrate determination method has been subject to question on the basis of artifact formation,<sup>14</sup> but may still be indicative of substantial quantities.

Despite these obvious sources of underestimation, we find a good correlation ( $r > 0.8$  in all cases) between particulate carbon and accountable mass at all locations, with a proportionality, representing the percentage contribution of carbon, that varies widely as shown in Table 3.

At present the best interpretation of these results is that the Denver aerosol probably consists mainly of carbon, oxygen, nitrogen, and hydrogen, while the Washington aerosol contains a large contribution of other elements, notably sulfur and silicon. Note that the two most polluted locations, Anaheim and New York, both have a 40-50% contribution of particulate carbon to the accountable mass.

Data on actual total suspended particulate mass are available at some sites for a fraction of

Table 3. Average percentage of carbon in calculated accountable mass.

Berkeley	55%	Chicago	37%
Fremont	48%	New York	49%
Anaheim	41%	Washington	28%
Denver	83%		

the number of days sampled. We find a good correlation at the Fremont and Anaheim locations between TSP measurements and our calculated "accountable mass," with similar proportionality at the two sites and similarity between heavily loaded and clean days. These facts suggest a roughly constant aerosol composition.

### "Black" Carbon

The carbonaceous fraction of the aerosol is a complex mixture of many forms and compounds of carbon. Solvent extraction is capable of characterizing this material into the categories of "polar extractable," "nonpolar extractable," and "nonextractable." Generally we find about 35% ( $\pm 10\%$ ) of the carbonaceous material to be nonextractable for California ambient samples, rising to about 55% ( $\pm 10\%$ ) for samples from New York. In nearly all cases we find that the optical attenuation of a filter is affected very little by solvent extraction, as shown in Fig. 3. This suggests that the material responsible for the optical absorption is nonextractable carbon that may have a "graphitic"-like form. This form of carbon would be expected to be relatively stable in oxygen at elevated temperatures, a hypothesis that is validated by the progressive thermal analysis method. From this latter method we generally find that the optical attenuation remains until temperatures of around 450°C, at which the rate of removal of optical attenuation is often closely followed by the rate of CO<sub>2</sub> detection (see Fig. 4). A comparison of the room-temperature optical attenuation measurement with the amount of carbon represented by the area under the high-temperature peak in the CO<sub>2</sub> evolution curve is shown in Fig. 5. In Fig. 6 we show the optical attenuation versus the amount of nonextractable carbon; both these figures contain data from a variety of ambient samples as well as source emission samples. In each figure a line is drawn representing a specific attenuation of 20. We see that many of the thermogram points lie a little above this line, a feature that would be accentuated by incomplete recovery of the carbon as CO<sub>2</sub> after combustion. On the other hand, the extraction data often lie below the line,

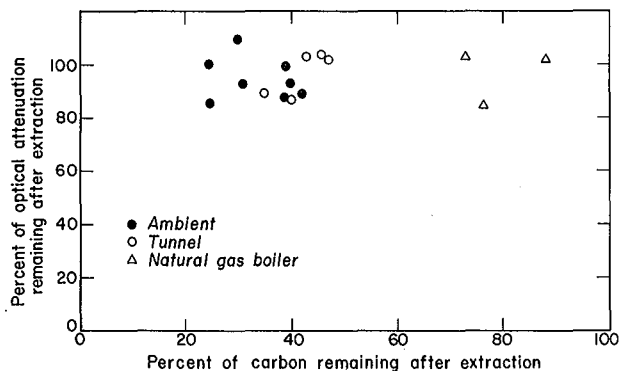


Fig. 3. Plot of the percent of the optical attenuation remaining after successive Soxhlet extraction in benzene and a methanol-chloroform mixture as a function of the carbon remaining after extraction for various ambient and source particulate samples. (XBL 783-344)

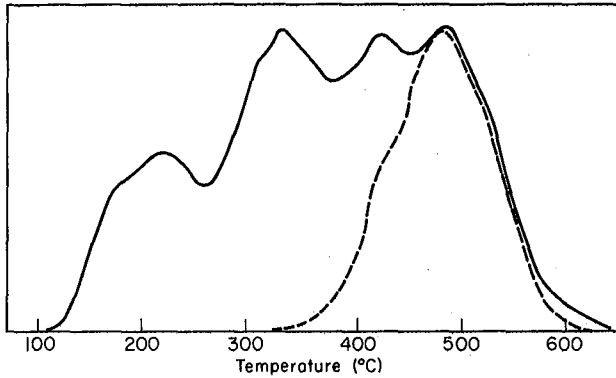


Fig. 4. Progressive thermal analysis result on ambient sample from Sydney, Australia. Solid curve - rate of  $\text{CO}_2$  detection. Dashed curve - rate of change of optical attenuation. (Arbitrary units, scaled to match). (XBL 807-3461)

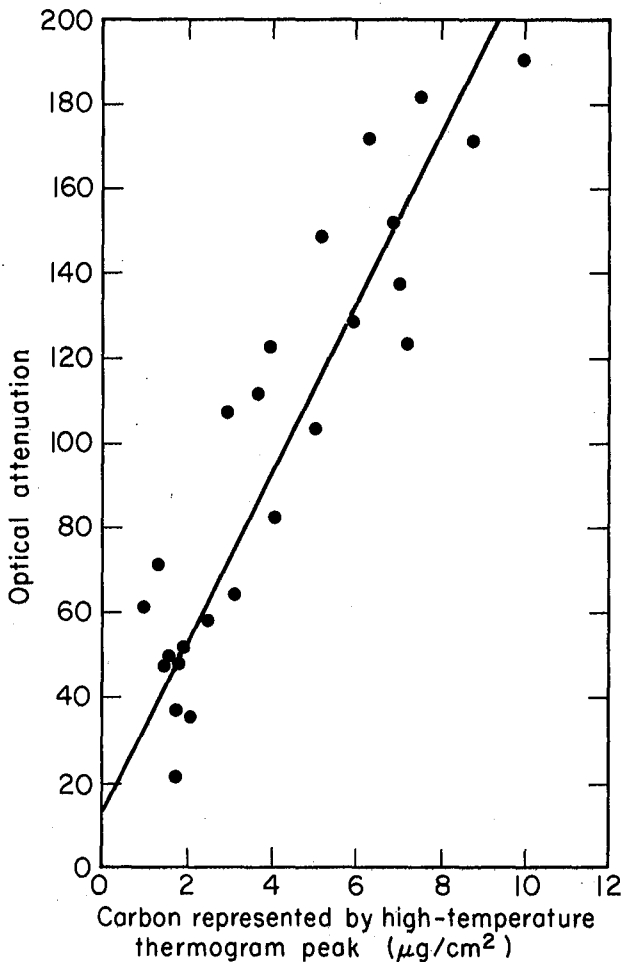


Fig. 5. Graph of optical attenuation versus carbon represented by high-temperature thermogram peak. Line is best fit to points. (XBL 807-3462)

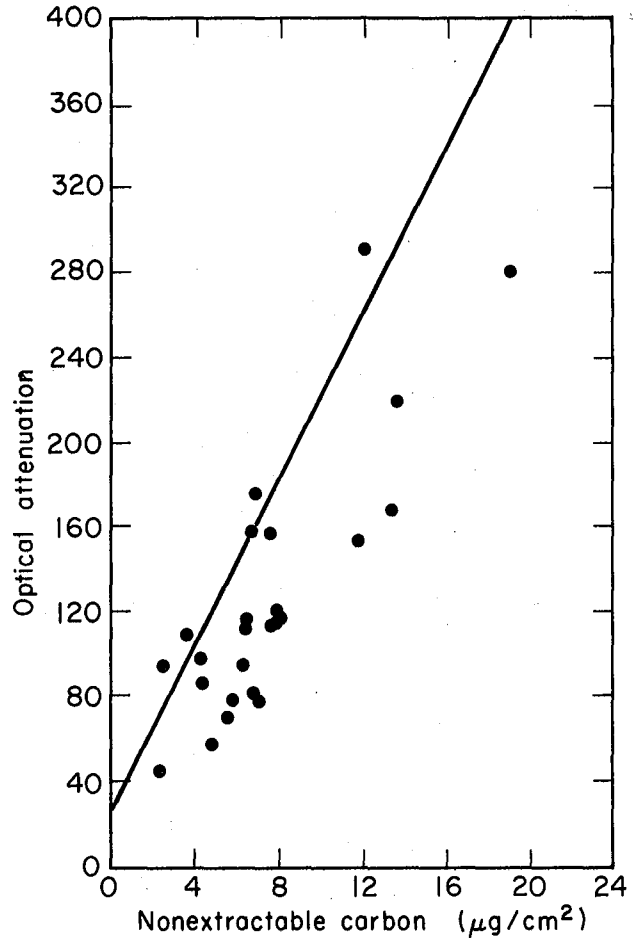


Fig. 6. Graph of optical attenuation versus nonextractable carbon. Line is best fit to Fig. 5. (XBL 807-3463)

possibly characteristic of incomplete extraction. The line  $\sigma = 20$  is the basis of our operational definition of "black" carbon. Black carbon is that fraction of the carbonaceous aerosol, responsible for optical absorption, that yields a transmission attenuation measurement in our apparatus of 20 units (optical density 0.2 at 6328 Å) when deposited on a Millipore filter with a surface density of  $1 \mu\text{g}/\text{cm}^2$ . It is nonextractable and stable in oxygen for moderate lengths of time at temperatures of up to about  $400^\circ\text{C}$ .

#### Correlations Between Total Carbon and ATN

Statistical analysis of the data shows that there is a strong correlation ( $r > 0.85$ ) between optical attenuation and total particulate carbon at every site studied.<sup>14</sup> Furthermore, a study of a number of source samples shows that there is also a strong correlation between optical attenuation and total carbon for these samples. The correlations between optical attenuation and total carbon for ambient samples and source samples are discussed in the following paper.

Results obtained from ambient samples imply that the fraction of graphitic soot to total particulate carbon is approximately constant under

the wide range of conditions occurring at a given site. On specific days, however, there can be large variations in the ratio, reflecting the variations in the relative amounts of organic and black carbon. The least squares fit of the data shows regional differences which are related to the fraction of black carbon due to primary emissions. These differences would suggest an increase in the relative importance of the primary component for samples collected respectively at Berkeley, Fremont, Anaheim, Argonne, and New York.

Black Carbon in Ambient Aerosols

Figure 7 displays the optical attenuation of 24-hour samples from the Fremont site. The pattern is very similar to that of Fig. 1, representing the total carbon content of those samples. This suggests a roughly constant aerosol composition in terms of the ratio of black to total carbon. Figure 8 shows this ratio, expressed as the specific attenuation [attenuation]/[total carbon]. We may use the value of 20 for the specific attenuation of black carbon to convert the specific attenuation of an ambient sample into a measure of its black carbon content:

$$[BC]/[C] = \sigma_{\text{ambient}}/20 \quad (4)$$

The compositional variations represented in Fig. 8 are much less pronounced than the absolute loadings (Figs. 1,7) and show no clear seasonal pattern. Similar features of total C, ATN, and ATN/C are also observed at the Berkeley and Anaheim sites. At the New York, Gaithersburg, and Argonne sites, daily and monthly variations of total C and

ATN are much less pronounced than at the three West Coast sites. The black carbon fractions (ATN/C values) at these sites also do not show any systematic seasonal trends.

Concentrations of Black Carbon

Determination of specific attenuation,  $\sigma \equiv \text{ATN}/\text{C}$ , enables a straightforward estimation of black carbon. From relation (4) one can calculate black carbon as a percentage of total carbon, and the concentration of black carbon in  $\mu\text{g}/\text{m}^3$ . Table 4 lists the average specific attenuation ( $\sigma$ ) and black carbon (BC) percentages for all samples (including multi-day samples) analyzed to date. In addition to the average values, the highest and lowest values are given. Based on this estimate, on the average 20% of the total carbon is black carbon. This fraction can on occasion be as high as 56% or as low as 6%. The latter occurs as a rule when total carbon concentrations are low.

CONCLUSIONS

We may summarize the results presented in the previous sections as follows:

1. There are substantial quantities of carbon present in the ambient aerosol at every sampling site studied so far.
2. This carbon contains a black component that may be rapidly quantitated by the optical attenuation measurement.
3. The fact that the black carbon accounts for an approximately constant fraction of the carbonaceous aerosol at all locations

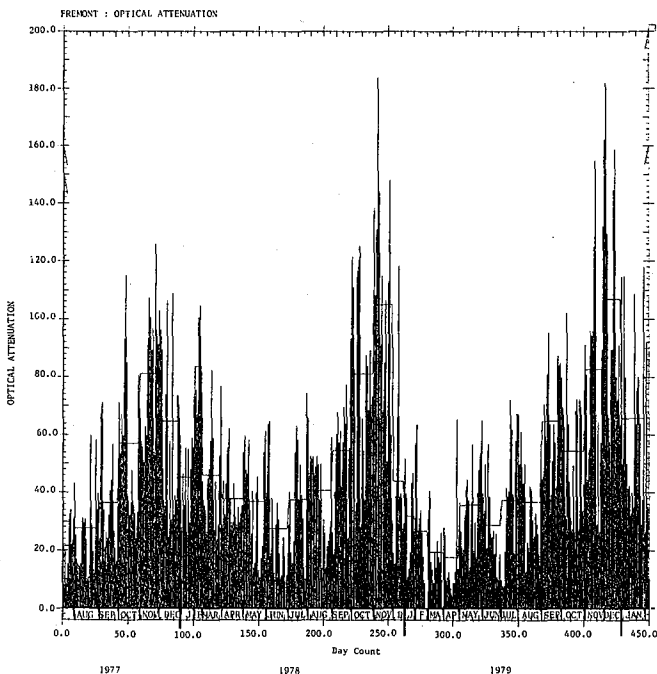


Fig. 7. Optical attenuation of 24-hour samples taken at the Fremont site. (XBL 806-10536)

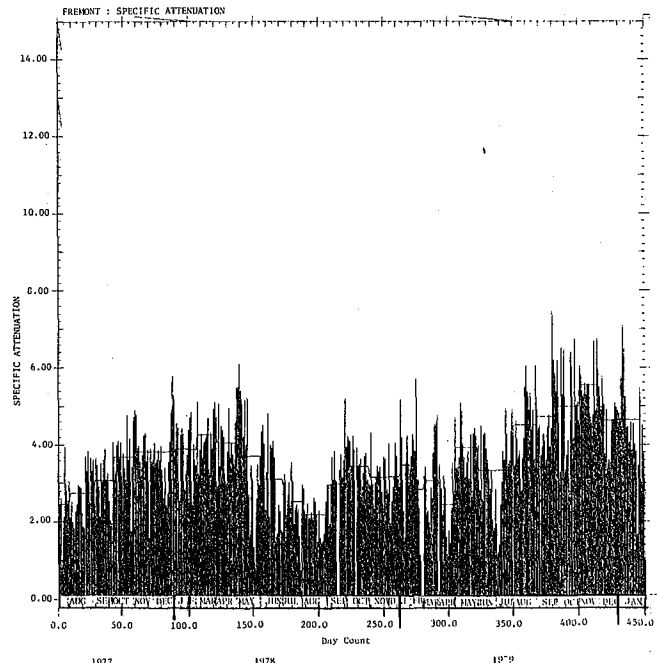


Fig. 8. Specific attenuation of 24-hour samples taken at the Fremont site. (XBL 806-10537)

Table 4. Specific attenuation ( $\sigma$ ) and black carbon (BC) (% of total C) from ambient samples.

Site	Average		Highest		Lowest	
	$\sigma$	%BC	$\sigma$	%BC	$\sigma$	%BC
New York	5.44	27%	11.1	56%	2.8	14%
Argonne	4.30	22%	9.1	46%	1.1	6%
Gaithersburg	4.33	22%	8.0	40%	1.8	9%
Denver	3.23	16%	5.7	29%	1.4	7%
Anaheim	3.70	19%	9.6	48%	0.8	4%
Fremont	3.55	18%	8.3	42%	1.6	8%
Berkeley	4.09	20%	9.2	46%	1.2	6%

implies that the optical attenuation measurement may be used to estimate the total carbon content of an ambient sample.

## REFERENCES

1. Proceedings, Conference on Carbonaceous Particles in the Atmosphere, T. Novakov, ed., Lawrence Berkeley Laboratory Report LBL-9037 (1979).
2. T. Novakov, S. G. Chang, A. B. Harker, "Sulfates as pollution particulates: Catalytic formation on carbon (soot) particles," Science **186**, 259 (1974).
3. R. Toossi, T. Novakov, and S. G. Chang, "Relative importance of various sulfate production mechanisms in aqueous droplets," in Atmospheric Aerosol Research Annual Report, 1977-78, Lawrence Berkeley Laboratory Report LBL-8696 (1978), p. 132.
4. W. H. Benner, H. Rosen, and T. Novakov, "SO<sub>2</sub> oxidation by water droplets containing combustion nuclei," in Atmospheric Aerosol Research Annual Report, 1977-78, Lawrence Berkeley Laboratory Report LBL-8696 (1978), p. 88.
5. R. Brodzinsky, S. G. Chang, S. S. Markowitz, and T. Novakov, "Kinetics and mechanism for the catalytic oxidation of SO<sub>2</sub> on carbon in aqueous suspensions," in Atmospheric Aerosol Research Annual Report, 1977-78, Lawrence Berkeley Laboratory Report LBL-8696 (1978), p. 110.
6. A. D. A. Hansen, H. Rosen, R. L. Dod, and T. Novakov, "Optical characterization of ambient and source particulates," in Proceedings, Conference on Carbonaceous Particles in the Atmosphere, T. Novakov, ed., Lawrence Berkeley Laboratory Report LBL-9037 (1979), p. 116.
7. H. Rosen and T. Novakov, "Optical attenuation: A measurement of the absorbing properties of aerosol particles," in Atmospheric Aerosol Research Annual Report, 1977-78, Lawrence Berkeley Laboratory Report LBL-8696 (1978), p. 54.
8. R. E. Weiss, A. P. Waggoner, R. J. Charlson, D. L. Thorsell, J. S. Hall, and L. A. Riley, in Proceedings, Conference on Carbonaceous Particles in the Atmosphere, Lawrence Berkeley Laboratory Report LBL-9037 (1979).
9. P. K. Mueller, R. W. Mosley, and L. B. Pierce, "Carbonate and noncarbonate carbon in atmospheric particulates," in Proceedings, Second International Clean Air Congress (New York, Academic, 1971).
10. L. A. Gundel, G. E. Mason, and T. Novakov, "Characterization of source and ambient particulate samples by solvent extraction," in Atmospheric Aerosol Research Annual Report, 1977-78, Lawrence Berkeley Laboratory Report LBL-8696 (1978), p. 68, and references therein.
11. R. L. Dod, H. Rosen, and T. Novakov, "Optico-thermal analysis of the carbonaceous fraction of aerosol particles," in Atmospheric Aerosol Research Annual Report, 1977-78, Lawrence Berkeley Laboratory Report LBL-8696 (1978), p. 2.
12. H. Puxbaum, "Die Charakterisierung von Kohlenstoff, Schwefel und Stickstoffverbindungen in luftgetragenen Staeben durch kombinierte thermische und gasanalytische Methoden," submitted to Fresenius Zeit. f. Anal. Chemie.
13. Monitoring data from South Coast Air Quality Management District and Bay Area Air Quality Management District.
14. C. W. Spicer and P. M. Schumacher, "Particulate nitrate: Laboratory and field studies of major sampling interferences," Atmos. Environ. **13**, 543 (1979).

## IDENTIFICATION OF SOOT IN URBAN ATMOSPHERES BY AN OPTICAL ABSORPTION TECHNIQUE\*

*H. Rosen, et al.*

### INTRODUCTION

Particulate carbon is a major fraction of the respirable particulate burden in urban atmospheres, yet the chemical composition and origin of this component are poorly understood. The major cause of these particles is fossil fuel combustion, which produces both primary particulate carbonaceous emissions (soot) and gaseous hydrocarbons, which can be transformed in the atmosphere by gas-to-particle conversion processes to secondary organic material.<sup>1</sup> For an effective control strategy, it is necessary to establish the relative importance of each of these components. In this paper we describe the application of a new method of analysis which uses the unique optical properties of "graphitic"<sup>2</sup> soot to trace the primary component of the carbonaceous particulates under widely different atmospheric conditions over a wide geographical area. The results of our work are consistent with the earlier work of Novakov et al.<sup>3</sup> and indicate that primary soot emissions compose a major fraction of the urban carbonaceous aerosol.

Soot consists of a "graphitic" component and an organic component. The "graphitic" component can be conveniently monitored because of its large and uniform optical absorptivity, which has recently been shown to be responsible for the gray or black appearance of ambient and source particulate samples collected on various filter media.<sup>4-6</sup> The "graphitic" content of the aerosol can be measured by an optical attenuation method developed in our laboratory.<sup>4</sup> In addition to the attenuation, we have also determined total particulate carbon, which enables us to study the correlation between the "graphitic" and the total carbon content of the aerosol.<sup>7</sup> The correlation or lack of it should depend on the relative amounts of primary and secondary material.

### EXPERIMENTAL METHODS AND RESULTS

Measurements have been obtained of the optical attenuation and the total carbon content of over 1000 ambient samples collected in two California air basins and in the Chicago area. These samples have been collected daily from 1 June 1977 at Lawrence Berkeley Laboratory, Berkeley, California; from 15 July 1977 at the Bay Area Air Quality Management District monitoring station, Fremont, California; and from 19 August 1977 at the South Coast Air Quality Management District monitoring station, Anaheim, California. Samples were also taken from 23 March 1978 to 9 April 1978 and then continued from 19 February 1979 at Argonne, Illinois. All these samples were taken in parallel on 47-mm diameter Millipore filter membranes (1.2- $\mu$ m nominal pore size, type RATF), which were used for the optical attenuation measurements, and pre-fired quartz fiber filters (Pallflex type 2500 QA0), which were used for the carbon determinations. The monitored flow rates varied between 1.0 and 2.6 m<sup>3</sup>/cm<sup>2</sup>-day (i.e., 0.24 to 0.62 CFM for the

total exposed filter area of 9.6 cm<sup>2</sup>), corresponding to face velocities of 11.6 to 30.1 cm/sec. The samples were not size segregated. A number of representative source particulates have also been sampled and analyzed. These include particles collected 1) in a freeway tunnel, 2) in an underground parking garage, 3) from a small 2-stroke engine, and 4) from a 4-stroke diesel engine. The optical attenuation is defined as

$$ATN = -100 \ln (I/I_0)$$

where  $I_0$  is the intensity of the light ( $\lambda = .63 \mu$ ) transmitted through a blank Millipore filter and  $I$  is the intensity through a loaded filter. If we assume fixed optical constants, this quantity should be proportional to the "graphitic" content of the aerosol. The carbon loading on the quartz fiber filters was determined by a total combustion/ $CO_2$  evaluation method.<sup>8</sup> The quartz filters were pre-fired overnight at 800°C to remove all combustible carbon before sample collection. Periodic analysis of blanks typically yielded about 0.5  $\mu$ g C/cm<sup>2</sup>, compared with loadings after exposure in the range 20-100  $\mu$ g C/cm<sup>2</sup>.

Photochemical gas-to-particle conversion reactions should be most pronounced in the summer in the Los Angeles air basin, while in the winter in Argonne or Berkeley, these reactions should play a much smaller role and the primary component should be much more important. These different photochemical conditions should manifest themselves in the ratio of the "graphitic" soot to total carbon content of the particles. That is, under highly photochemical conditions one would expect this ratio to be significantly smaller than under conditions obviously heavily influenced by sources. In view of the above, the graphs of optical attenuation versus carbon loading shown in Fig. 1 for samples collected at Berkeley, Fremont, and Anaheim, California, and Argonne, Illinois, as well as various combustion sources, are unexpected. Analyses of the data show that:

1. There is a strong correlation ( $r > 0.85$ ) between optical attenuation and total suspended particulate carbon at every site.
2. The least squares fit of the data shows relatively small regional differences with a trend toward increasing slope (enrichment in primary carbonaceous matter) for samples collected respectively at Berkeley, Fremont, Anaheim, and Argonne.
3. There is a strong correlation between the optical attenuation and the carbon loading for the source samples, and the slope of the least squares fit is comparable to that found in the ambient samples.

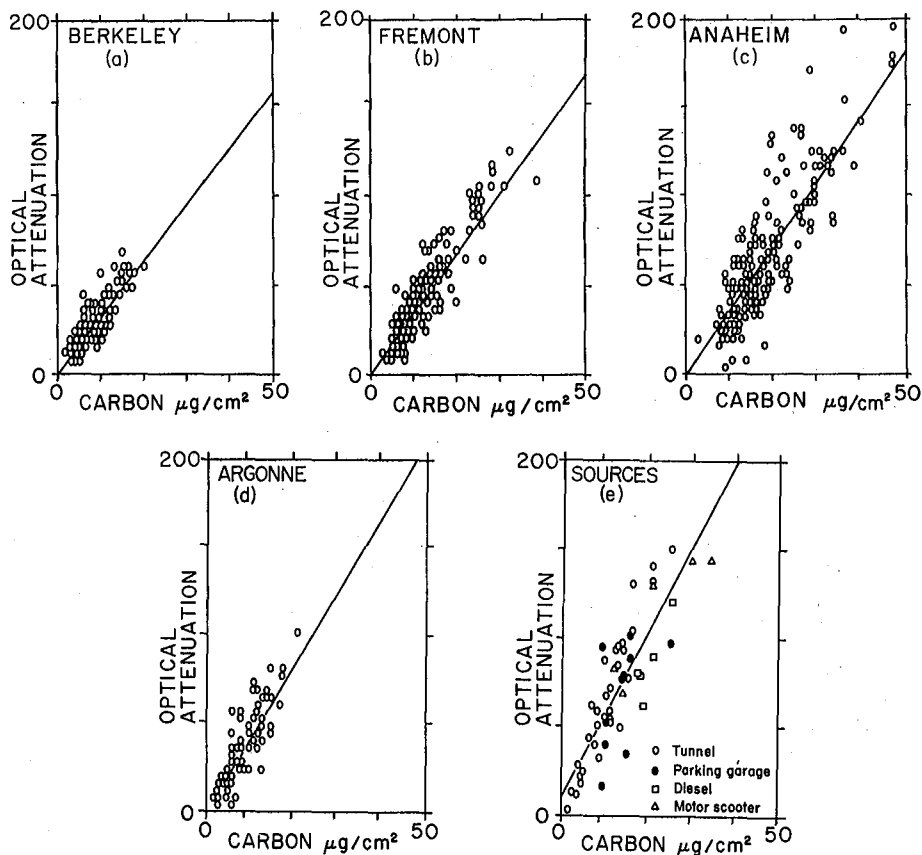


Fig. 1. Plots of optical attenuation versus carbon loading in  $\mu\text{g}/\text{cm}^2$  for particulate samples collected at Berkeley, Fremont, Anaheim, and Argonne, and from various combustion sources. The solid line represents the least squares fit of the data points. (XBL 796-1920A)

Result 1 shows that it is possible to predict the total amount of particulate carbon with an RMS deviation of 30% by means of a simple measurement of optical attenuation. This implies that the fraction of "graphitic" soot to total particulate carbon is approximately constant under the wide range of conditions occurring at a given site. On specific days there can be large variations in the ratio, but no large systematic differences are found as a function of the ozone concentration, which has been viewed as a monitor of the photochemical activity. This is graphically demonstrated in Fig. 2, which shows the distribution of the ratios of the optical attenuation to total carbon content for ambient samples from all the California sites taken together, subdivided according to peak hour ozone concentration. Clearly there is no trend for high-ozone days to be characterized by aerosols which have a significantly reduced "graphitic" fraction. This places a rather low limit on the maximum importance of secondary organic particulates formed in correlation with the ozone concentration.

As seen in Fig. 1e, a strong correlation is also observed between the optical attenuation and the carbon content of the source samples. The slope of the least squares fit of the source data

is somewhat larger than that found for the ambient samples, but there is still considerable overlap between the two data sets. This similarity in the absorbing properties of the ambient and source samples strongly suggests that a large component of the carbonaceous aerosol studied is of primary origin. However, due to the spread in both the ambient and the source data, these results do not exclude the possibility of significant secondary species produced in nonozone-related reactions. Indeed the results of Grosjean,<sup>9</sup> Gundel et al.,<sup>10</sup> and others<sup>11</sup> suggest that the polar component of the carbonaceous aerosol cannot be accounted for directly from primary emissions. The trend of the sources to have higher optical attenuation per unit carbon than that found in urban air may also be indicative of a secondary component. An analysis based on comparing the least squares fit of the source and ambient data at all sites is consistent with a secondary component, which ranges between 15 and 35% of the carbonaceous mass. The data presented here were taken in two California air basins and in the Chicago area. The generality of these results to other areas across the United States and in some areas of Europe is presently being tested. Preliminary data obtained on samples from New York City, Denver, Seattle, Portland, and Washington, D.C. are in agreement with the findings outlined in this paper.

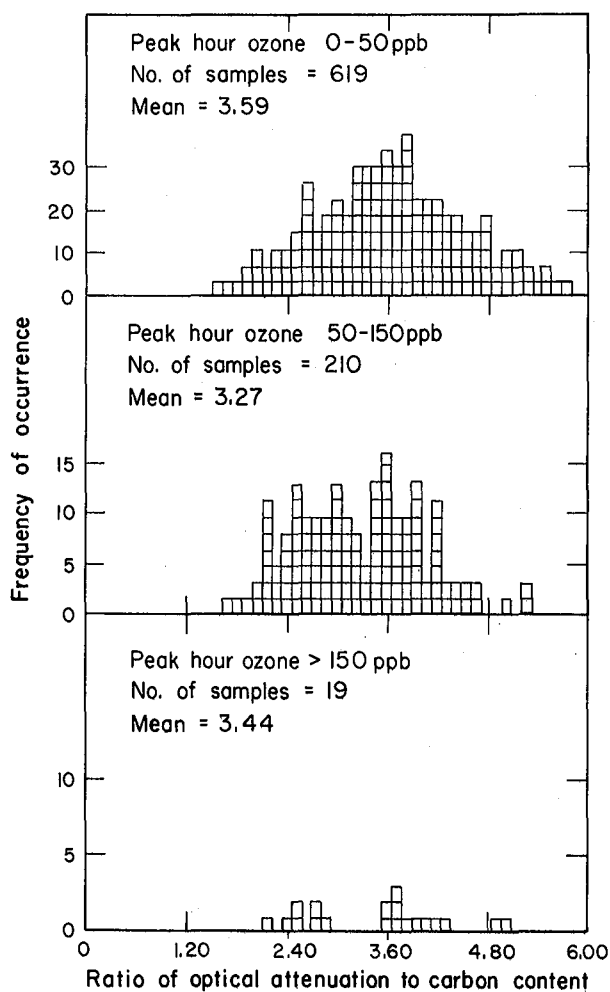


Fig. 2. Distribution of the ratios of optical attenuation to total carbon content in  $\mu\text{g}/\text{cm}^2$  subdivided according to the peak ozone concentration. Note that the means of the distributions are only marginally smaller at larger ozone concentrations, which puts a rather low limit on secondary organics produced in correlation with ozone. (XBL 798-2704)

#### FOOTNOTE AND REFERENCES

\*Published in *Science* **208**, 741 (1980).

1. For a review of chemical mechanisms for secondary organic formation, see D. Grosjean, in *Proceedings, Conference on Carbonaceous Particles in the Atmosphere*, Lawrence Berkeley Laboratory Report LBL-9037, p. 107 (1979). (available from NTIS).

2. The use of the term "graphitic" is not meant to imply the three-dimensional structure of graphite, but only to indicate a structure similar to that of carbon black. This structure can be viewed to a first approximation as made up of small layered crystallites which have the hexagonal graphitic structure within aromatic planes but a random orientation of the planes about the C axis of the crystallites.
3. The hypothesis that much of the carbonaceous material in urban environments is soot was first advanced by T. Novakov, A. B. Harker, and W. Siekhaus, in *Proceedings, First Annual NSF Trace Contaminants Conference* (Oak Ridge National Laboratory Report CONF-730802, p. 354-379, 1974, available from NTIS). Additional results strengthening this hypothesis are in (a) T. Novakov, *Proceedings, Second Joint Conference on Sensing of Environmental Pollutants* (Pittsburgh, Instrument Society of America, 1973), pg. 197; (b) T. Novakov, S. G. Chang, and A. B. Harker, *Science* **186**, 259 (1974); (c) S. G. Chang and T. Novakov, *Atmos. Environ.* **9**, 495 (1975).
4. H. Rosen, A. D. A. Hansen, L. Gundel, and T. Novakov, *Applied Optics* **17**, 3859 (1978).
5. H. Rosen, A. D. A. Hansen, L. Gundel, and T. Novakov, in *Proceedings, Conference on Carbonaceous Particles in the Atmosphere* (Lawrence Berkeley Laboratory Report LBL-9037, p. 49, 1979, available from NTIS).
6. Z. Yasa, N. M. Amer, H. Rosen, A. D. A. Hansen, and T. Novakov, *Applied Optics* **18**, 2528 (1979).
7. Preliminary evidence for the correlation between optical attenuation and total particulate carbon were presented by H. Rosen, A. D. A. Hansen, R. L. Dod, and T. Novakov, in *Proceedings, Fourth Joint Conference on Sensing of Environmental Pollutants* (Washington, American Chemical Society, p. 640, 1978); and by A. D. A. Hansen, H. Rosen, R. L. Dod, and T. Novakov in *Proceedings, Conference on Carbonaceous Particles in the Atmosphere* (Lawrence Berkeley Laboratory Report LBL-9037, p. 116, 1979, available from NTIS).
8. A similar system is described by P. K. Mueller, R. W. Mosley, and L. B. Pierce, in *Proceedings, Second International Clean Air Congress* (New York, Academic Press, 1971), p. 532.
9. D. Grosjean, *Anal. Chem.* **47**, 797 (1975).
10. L. Gundel, G. E. Mason, and T. Novakov, in *Atmospheric Aerosol Research Annual Report 1977-78* (Lawrence Berkeley Laboratory Report LBL-8686, p. 68, 1979).
11. See, for example, B. R. Appel, E. M. Hoffer, E. L. Kothny, S. M. Wall, M. Haik, and R. L. Knights, *Environ. Sci. Technol.* **13**, 98 (1979).

## APPLICATION OF THERMAL ANALYSIS TO THE CHARACTERIZATION OF NITROGENOUS AEROSOL SPECIES

R. Dod, et al.

In a previous report we described a combined optical attenuation-thermal analysis apparatus for the characterization of particulate carbonaceous aerosol material.<sup>1</sup> We have extended the use of this apparatus to include the simultaneous characterization of nitrogenous species.

A schematic representation of the apparatus used in our analysis of carbonaceous material is shown in Fig. 1. The particulate sample, collected on a pre-fired quartz filter, is placed in the quartz combustion tube so that its surface is perpendicular to the tube axis. The tube is supplied with purified oxygen, excess oxygen escaping through an axial opening at the end of the tube. The remainder of the oxygen (together with gases produced during analysis) passes through a nondispersive infrared analyzer (MSA LIRA 202S) at a constant rate. Sample carbon may be evolved through volatilization, pyrolysis, oxidation, or decomposition. To ensure complete conversion of this carbon to CO<sub>2</sub>, a section of the quartz tube immediately outside the programmed furnace is filled with CuO catalyst, which is kept at a constant 900°C by a second furnace. This is especially necessary at relatively low temperatures when volatilization and incomplete combustion are the dominant processes occurring.

The actual measurement consists of monitoring the CO<sub>2</sub> concentration as a function of the sample temperature. The result is a "thermogram," i.e., a plot of the CO<sub>2</sub> concentration vs temperature, with the area under the thermogram proportional to the carbon content of the sample. The carbon content is quantitated by calibration with a calibration gas (CO<sub>2</sub> in oxygen) and by measuring the flow rate through the system. This calibration is cross-checked by analyzing samples of known carbon content.

The thermograms of ambient and source aerosol samples reveal distinct features in the form of peaks or groups of peaks. One important component of the carbonaceous aerosol is the "graphitic" carbon, which is known to cause the black or gray coloration of ambient and source particulate samples.<sup>2</sup> To determine which of the thermogram peaks corresponds to this "graphitic" carbon, we monitor the intensity of a He-Ne laser beam which passes through the filter. This provides simultaneous measurement of sample absorptivity and CO<sub>2</sub> evolution. The light penetrating the filter is collected by a quartz light guide and filtered by a narrow band interference filter to minimize the effect of the glow of the furnaces. An examination of the CO<sub>2</sub> and light intensity traces enables the assignment of the peak or peaks in the thermograms corresponding to the black carbon because they appear concurrently with the decrease in sample absorptivity.

The potential of this method (in the CO<sub>2</sub> mode) is illustrated in Fig. 2, where the complete thermogram of an ambient sample is shown. The lower trace represents the CO<sub>2</sub> concentration, while the

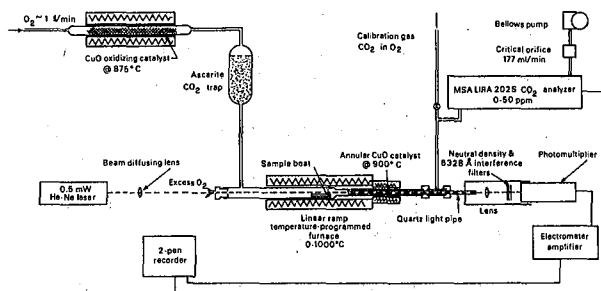


Fig. 1. Optico-thermal analysis apparatus. (XBL 791-167)

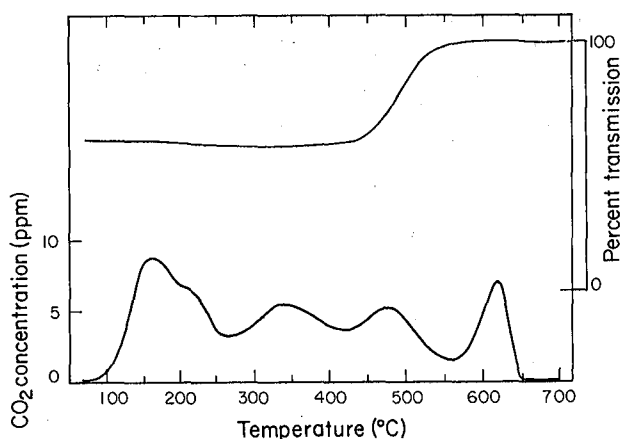


Fig. 2. CO<sub>2</sub> thermogram of Berkeley ambient aerosol particles (5/31/79). (XBL 807-1696)

upper curve corresponds to the light intensity of the laser light beam that reaches the detector during the temperature scan. Inspection of the thermogram shows that a sudden change in the light intensity occurs concomitantly with the evolution of the CO<sub>2</sub> peak at about 470°C. The light intensity  $I_0$ , after the 470°C peak has evolved, corresponds to that of a blank filter. This demonstrates that the light-absorbing species in the sample are combustible and carbonaceous, the "graphitic" carbon referred to above. The carbonate peak evolves at about 600°C; and as carbonate is not light absorbing, it does not change the optical attenuation of the sample. In addition to black carbon and carbonate, the thermogram in Fig. 2 also shows several distinct groups of peaks at temperatures below ~400°C that correspond to various organics.

We have expanded the capabilities of the thermal analysis method to nitrogenous species by connecting the outlet of the passive CO<sub>2</sub> analyzer through an orifice to a chemiluminescent NO<sub>x</sub> analyzer (Thermo-Electron, Model 14D). No modifications were made to the combustion section of the

system or to the oxidation catalyst. The modified thermal analysis system was tested by analyzing known amounts of nitrogen-containing compounds. Examples of inorganic and organic standards are shown in Figs. 3-5.

Ammonium nitrate produces a sharp, single  $\text{NO}_x$  thermogram peak centered at about  $160^\circ\text{C}$  (Fig. 3). Ammonium sulfate results in a double peak located at about  $210^\circ$  and  $270^\circ\text{C}$  (Fig. 4). The fact that  $(\text{NH}_4)_2\text{SO}_4$  produces a double peak suggests that this compound decomposes initially into ammonia and ammonium bisulfate ( $\text{NH}_4\text{HSO}_4$ ). The  $\text{NO}_x$  peak for melamine is, as expected, coincident with the  $\text{CO}_2$  peak at about  $275^\circ\text{C}$  (Fig. 5).

At present this method is in the developmental stage and therefore is not yet completely quantitative. We have nevertheless applied the method to analyze several ambient particulate samples. The principal reason for analyzing ambient samples was to see whether non-nitrate and non-ammonium nitrogenous species can be detected. Such species were identified in ambient particles by x-ray photoelectron spectroscopy (ESCA) but have not been clearly demonstrated by other techniques.

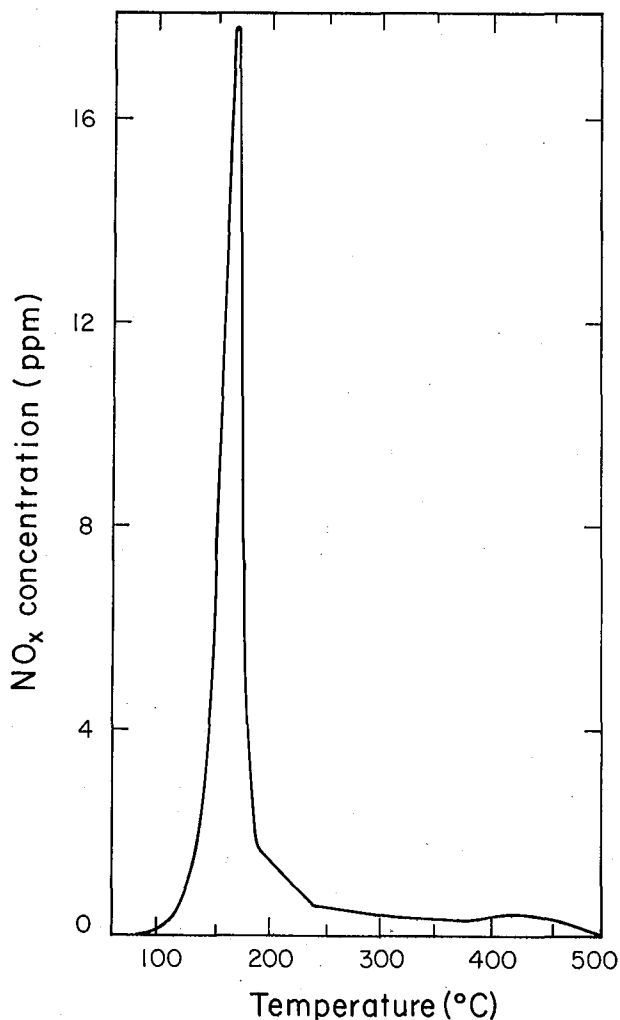


Fig. 3.  $\text{NO}_x$  thermogram of  $\text{NH}_4\text{NO}_3$ . (XBL 807-1693)

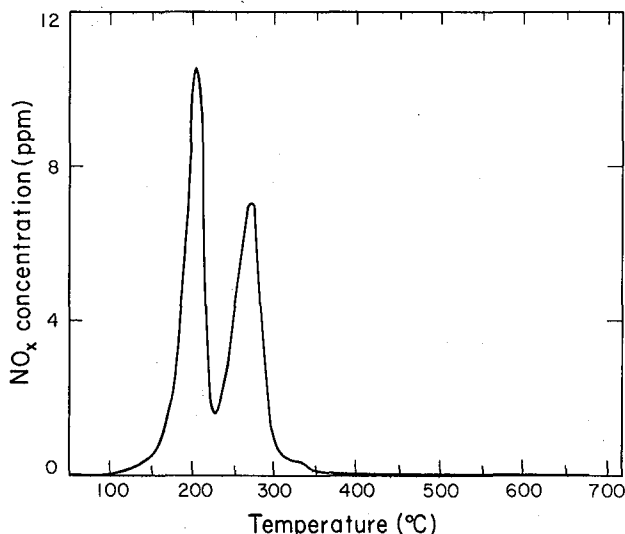


Fig. 4.  $\text{NO}_x$  thermogram of  $(\text{NH}_4)_2\text{SO}_4$ . (XBL 807-1694)

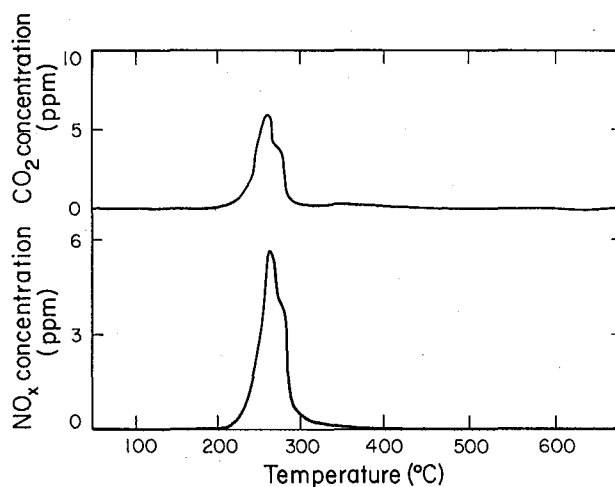


Fig. 5.  $\text{NO}_x$  thermogram of melamine. (XBL 807-1695)

Two examples of ambient sample  $\text{NO}_x$ ,  $\text{CO}_2$  thermograms are shown in Figs. 6 and 7. The thermogram of the sample collected on 4/26/79 at the NBS facility near Washington, D.C., shows that the principal nitrogen species is ammonium nitrate with a relatively small amount of ammonium sulfate. No other nitrogenous species were detected in this sample. The other sample (Fig. 7) shows that the ammonium sulfate and/or bisulfate are the principal nitrogen-containing species. Here, however, a broad peak in the  $\text{NO}_x$  thermogram is seen between  $400^\circ$  and  $500^\circ\text{C}$ , which can be attributed to a non-nitrate, non-ammonia, probably organic nitrogenous species. Similar broad peaks have been seen in thermograms of ambient species from other sites.

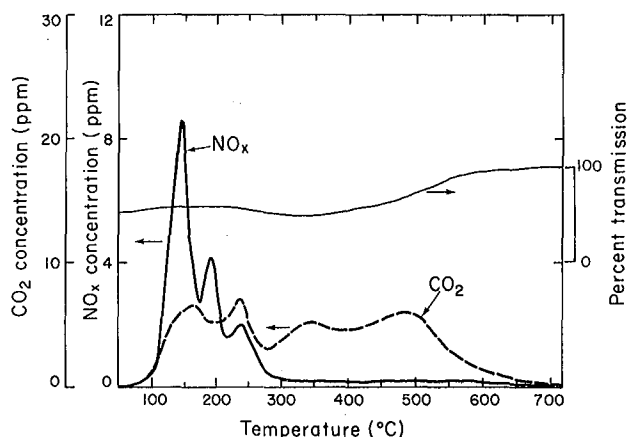


Fig. 6.  $\text{CO}_2/\text{NO}_x$  thermogram of Washington, D.C., ambient aerosol particles (4/26/79) ( $4.6 \mu\text{g}$  sulfur in sample). (XBL 807-1692)

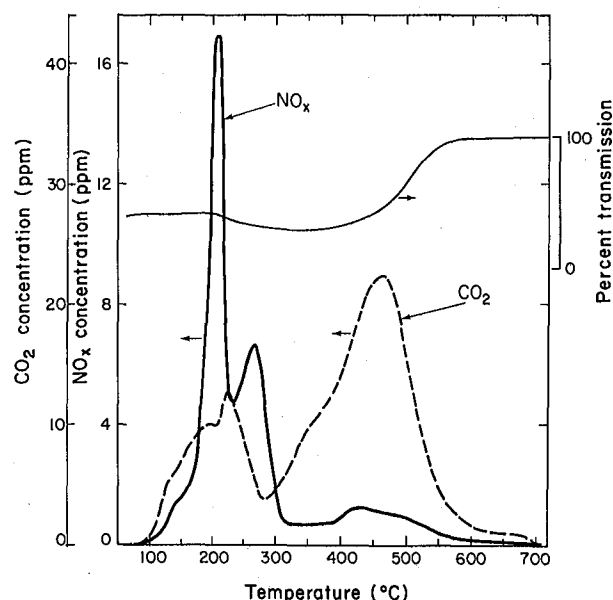


Fig. 7.  $\text{CO}_2/\text{NO}_x$  thermogram of Washington, D.C., ambient aerosol particles (4/24/79) ( $22.6 \mu\text{g}$  sulfur in sample). (XBL 806-1143)

#### REFERENCES

1. R. L. Dod, H. Rosen, and T. Novakov, "Optico-thermal analysis of the carbonaceous fraction of aerosol particles," Lawrence Berkeley Laboratory Report LBL-8698 (1978).
2. H. Rosen, A. D. A. Hansen, L. Gundel, and T. Novakov, "Identification of the optically absorbing component in urban aerosols," *Appl. Opt.* **17**, 3859 (1978).
3. T. Novakov, P. K. Mueller, A. E. Alcocer, and J. W. Otvos, "Chemical composition of Pasadena aerosol by particle size and time of day. III. Chemical states of nitrogen and sulfur by photoelectron spectroscopy," *J. Coll. Interface Sci.* **39**, 225 (1972).

## APPLICATION OF SELECTIVE SOLVENT EXTRACTION AND THERMAL ANALYSIS TO AMBIENT AND SOURCE-ENRICHED AEROSOLS

*L. Gundel, et al.*

#### INTRODUCTION

Selective solvent extraction (SSE) has been used to characterize carbonaceous aerosol particles by estimating the fractions of "primary," "secondary," and "elemental" carbon in ambient and source aerosols.<sup>1-5</sup> This laboratory has recently developed a thermal analysis (TA) technique<sup>6-7</sup> which allows simultaneous measurement of light transmission through a filter and evolved  $\text{CO}_2$  during its temperature-programmed combustion. In this study we use these techniques in a complementary manner by performing TA on particulate samples which have been subjected to SSE. The samples chosen for this study were collected during the same sampling periods at two locations in Berkeley, California—one close to a freeway and the other closer to our laboratory. The aims of this work include:

1. Comparison of average secondary:primary:elementary (S:P:E) ratios for these two sites to each other and to ratios obtained previously<sup>5</sup> for source and ambient particulate matter.
2. Comparison of thermal analysis results for the two sites.
3. Observation of the effects of SSE on thermogram "fingerprint" features to enable solubility characterization of the typical "volatile," "high molecular weight," and "high temperature" peaks.
4. Characterization of "primary" and "secondary" carbon by construction of difference thermograms.
5. Comparison of "elemental" carbon as defined by SSE to optically absorbing or "black" carbon.

## EXPERIMENTAL DETAILS

High volume samplers were operated simultaneously for 24-hour periods at 40 SCFM at a freeway sampling site located about 200 feet east of the Bayshore Freeway and at LBL, about 700 feet above sea level, 4 miles east of the freeway sampling site. Usually the prevailing winds were from the west toward the LBL site. The filter samples were collected on pre-fired quartz during September, 1979. During the sampling period, 17-20 September 1979, there were night and morning low clouds which cleared by midmorning. Maximum and minimum temperatures averaged 73° and 62°F respectively. Average ozone level was 20 ppb during this week.

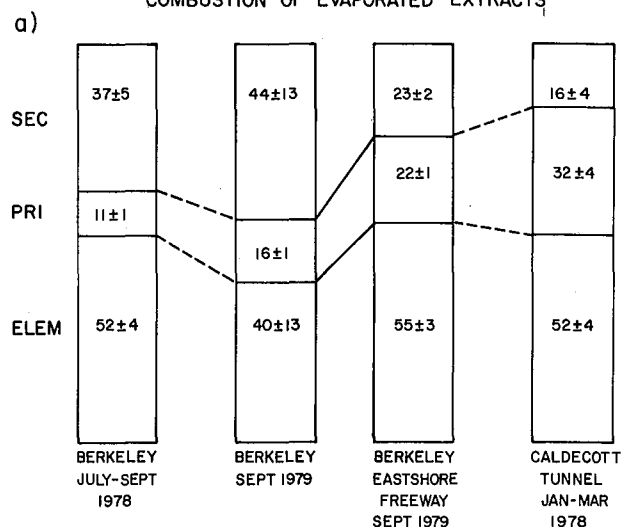
Selective solvent extraction was performed on the three pairs of samples. The soxhlet extraction technique has been described previously.<sup>3-5</sup> Cyclohexane was used to extract a piece of filter 50 cm<sup>2</sup> in area; another section of filter of the same area was sequentially extracted in benzene and in a methanol-chloroform (1:2 v:v) mixture. All solvents were spectral grade and residue free. Fractions of "primary," "secondary," and "elemental" carbon were determined according to a procedure described by Appel et al.<sup>3,5</sup>; "primary" carbon is cyclohexane-extracted carbon; "secondary" carbon is the difference between the total carbon extracted by the benzene, methanol-chloroform sequence and the cyclohexane-extracted carbon. "Elemental" carbon is the difference between total carbon and carbon extracted by the benzene, methanol-chloroform sequence. "Primary," "secondary," and "elemental" carbon fractions of the total carbon were determined using both the evaporated extracts and the extracted filters so that two sets of numbers were computed for each filter. Thermal analysis was performed on 1.69 cm<sup>2</sup> sections of the extracted and unextracted filters.

## RESULTS

Figure 1 contains the SSE results for the three pairs of filter samples, along with results obtained earlier<sup>5</sup> for particulate matter collected at the LBL site and in the Caldecott Tunnel. Figure 1a represents the results based on combustion of evaporated extracts; Fig. 1b displays the results based on combustion of the extracted filters. Losses of volatile carbon during extraction<sup>5</sup> and esterification of some organic components<sup>5</sup> may make the "primary" carbon percentage low and the "secondary" component high when evaporated extract results are compared to results based on combustion of the extracted filters.

Comparison of the newer SSE results for the LBL sampling site with results obtained in the summer of 1978 shows that the same patterns exist in S:P:E ratios, but the recently collected particulate samples contain somewhat less "elemental" and more "secondary" than the earlier samples do, based on combustion of extracted filters. Particulates collected near the freeway contain less "secondary," more "primary" and more "elemental" carbon than do particulates collected at the LBL site. S:P:E ratios are 22:23:55 compared to 40:26:34, respectively, based on combustion of extracted filters. Ratios based on evaporated

## PERCENTAGE OF TOTAL CARBON AS MEASURED BY COMBUSTION OF EVAPORATED EXTRACTS



## PERCENTAGE OF TOTAL CARBON AS MEASURED BY COMBUSTION OF EXTRACTED FILTERS

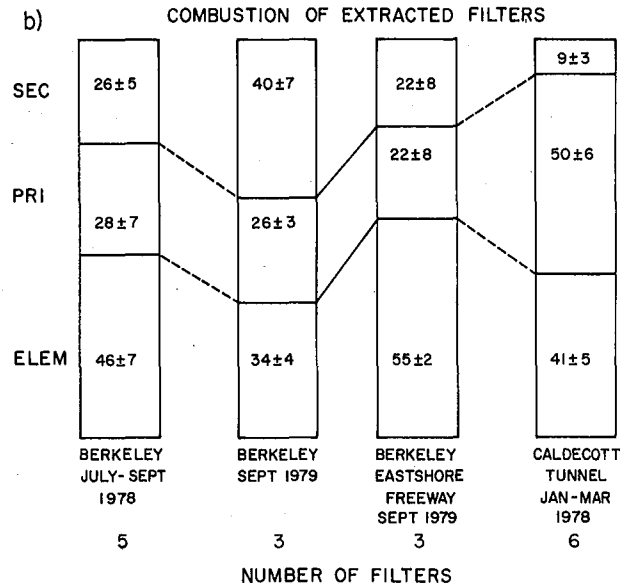


Fig. 1. Selective solvent extraction results expressed as a percentage of total original carbon. "ELEM" = "elementary" carbon = carbon insoluble after successive extraction with benzene followed by a methanol-chloroform mixture; "PRI" = "primary" = cyclohexane-soluble carbon; "SEC" = "secondary" = difference between total soluble carbon and cyclohexane-soluble carbon. (XBL 801-109)

extracts show the same trend. The average total carbon at the freeway is 2.1 times that at LBL. Particulates collected near the freeway contain more "secondary," less "primary," and more "elemental" carbon than do particulates collected in the Caldecott Tunnel during 1978, based on combustion of extracted filters: S:P:E ratios are 22:23:55 and 9:50:41 respectively.

Thermograms of one pair of particulate loaded filters are presented in Fig. 2. Figure 2a shows

thermograms for the LBL sampling site. Figure 2b contains difference thermograms for the same filter. The "primary" carbon difference thermogram was obtained by subtraction of the cyclohexane-extracted filter thermogram from the thermogram for the unextracted filter. The "secondary" carbon difference thermogram was obtained by subtracting the benzene, methanol-chloroform-extracted filter thermogram from the cyclohexane-extracted filter thermogram. The "elemental" carbon thermogram is the benzene, methanol-chloroform-extracted filter thermogram. The temperature midpoint in optical transmission change is indicated on each part of the figure. The same information is provided for the corresponding freeway particulate sample in parts c and d of Fig. 2. Thermograms for the other two pairs of filters show the same effects as those discussed below. The following observations can be made from study of these thermograms:

1. For particulate samples from both sites, cyclohexane extraction removes most of the low temperature or "volatile" carbon, part of the "higher molecular weight" carbon, and little of the "black" carbon, since the optical transmission is not affected by cyclohexane extraction. The "primary" carbon difference thermograms contain most of the structural features of the original thermograms. The CO<sub>2</sub> maxima in the "primary" carbon thermograms correspond to the "volatile" carbon peak of the unextracted filters.

2. For particulate samples from both sites, sequential benzene and methanol-chloroform extraction removes the low temperature or "volatile" carbon, as well as part of the "high molecular weight" carbon. The optical transmission is not affected by sequential benzene and methanol-chloroform extraction. The "secondary" carbon difference thermograms show maxima between 300 and 450°C.

3. Nonextractable or "elemental" carbon from both sites contains organic material which does not absorb light, with combustion temperature peaks at about 325°C, in addition to "black" or "graphitic" carbon with combustion peaks at about 480°C. This means that nonextractable carbon cannot be equated with elemental or "graphitic" carbon.

4. Since the high-temperature peak from both sites contains some extractable carbon in addition to "black" carbon, "high temperature" carbon cannot be equated with "black" carbon.

5. The complementary use of SSE and TA makes it possible to determine the fraction of "black" carbon in these particulate samples. For the LBL site and the freeway site, the fractions of "black" carbon are 0.235 and 0.383 respectively.

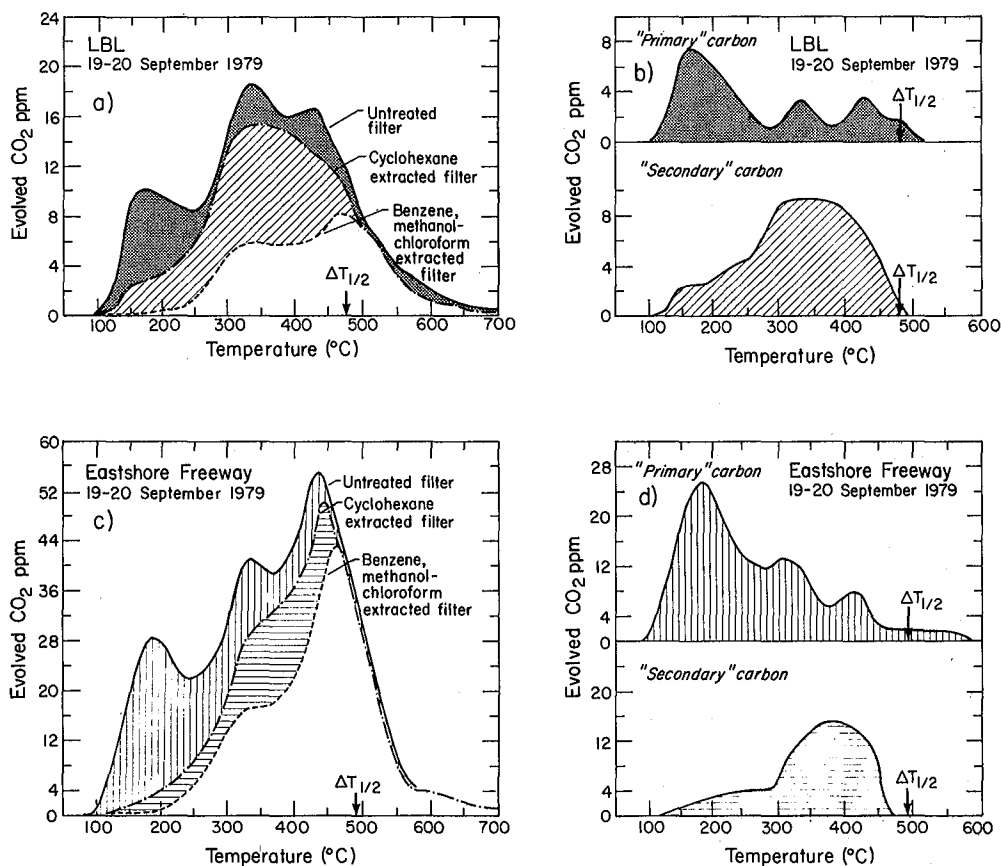


Fig. 2. Thermal analysis results for particulate matter collected at LBL and at a site near the Eastshore Freeway. The temperature midpoint in the optical transmission change is indicated as  $\Delta T_{1/2}$ . (XBL 801-110)

## DISCUSSION AND CONCLUSION

Thermal analysis of extracted filters provides further characterization of carbonaceous particulates than can be achieved with either TA or SSE alone. It is now possible to determine the amounts of "black" carbon in particulate matter using combined selective solvent extraction and thermal analysis. We plan to extend these preliminary measurements to study particulates collected by low-volume samplers in several urban areas throughout the United States.

## REFERENCES

1. D. Grosjean, "Solvent extraction and organic carbon determination in atmospheric particulate matter: The organic extraction-organic carbon analyzer (OE-OCA) technique," *Anal. Chem.* **47**, 797 (1975).
2. B. R. Appel, P. Colodny, and J. J. Wesolowski, "Analysis of carbonaceous materials in southern California atmospheric aerosols," *Environ. Sci. Technol.* **10**, 359 (1976).
3. B. R. Appel, E. M. Hoffer, M. Haik, S. M. Wall, E. L. Kothny, R. L. Knights, and J. J. Wesolowski, Characterization of Organic Particulate Matter, Final Report to California Air Resources Board, Contract No. ARB 5-682 (1977).
4. B. R. Appel, E. M. Hoffer, E. L. Kothny, S. M. Wall, M. Haik, and R. L. Knights, "Analysis of carbonaceous material in southern California atmospheric aerosols," *Environ. Sci. Technol.* **13**, 98 (1979).
5. L. A. Gundel, G. E. Mason, and T. Novakov, "Characterization of source and ambient particulate samples by solvent extraction," in Atmospheric Aerosol Research Annual Report 1977-78, LBL-8696 (1979), p. 63.
6. R. L. Dod, H. Rosen, and T. Novakov, "Optico-thermal analysis of the carbonaceous fraction of aerosol particles," in Atmospheric Aerosol Research Annual Report 1977-78, LBL-8696 (1979), p. 2.
7. R. S. Dod, this report, previous article.

## DETERMINATION OF CARBON IN ATMOSPHERIC AEROSOLS BY DEUTERON-INDUCED NUCLEAR REACTIONS

*M. Clemenson, et al.*

## INTRODUCTION

Carbon has been found to be a major constituent of urban particulate pollution.<sup>1,2</sup> The determination of the origin of the carbon in terms of primary and secondary components is a difficult problem to which a solution is necessary if meaningful control strategies are to be implemented. Some work has been done, but much more work is required.<sup>3,5</sup> Of important analytical concern is the nondestructive determination of the total carbon content of atmospheric aerosol samples. The common method of carbon determination in atmospheric aerosol samples is by combustion analysis. This method, however, is destructive of the sample and thus does not allow other analyses to be performed on the same sample. A new method for the nondestructive determination of carbon and other low-Z elements in atmospheric aerosols has been developed by Macias and coworkers.<sup>6</sup> Their method involves the in-beam measurement of  $\gamma$  rays from the inelastic scattering of 7-MeV protons accelerated in a cyclotron. This type of analysis requires lengthy use of accelerator time. Another method for the nondestructive determination of carbon has been developed by Gordon and coworkers.<sup>7</sup> This involves the measurement of prompt  $\gamma$  rays following neutron capture; they use an external beam port of the National Bureau of Standards (NBS) research reactor as the neutron source. Relatively large samples ( $\sim 1$  g), however, and long irradiation periods ( $\sim 20$  hr) are required. A new activation-

analysis method for the determination of carbon in atmospheric aerosols using only a short amount of beam time (2 min) will be described here. This method has already been used to determine nitrogen in aerosols and future work will center on the development of a method for the determination of oxygen in aerosols.<sup>8</sup>

Other nondestructive methods can be used for the determination of elemental concentrations in atmospheric aerosols. The most commonly used methods are x-ray fluorescence analysis and neutron activation analysis; neither is suitable for the determination of low-Z elements. The x-ray fluorescence method is of great importance for the sensitive and nondestructive determination of elements as light as sulfur, but for elements lighter than sulfur two effects limit its usefulness: (a) the fluorescence yield drops to the range of a few percent for these elements and (b) there are large x-ray absorptive effects because of the very low energy of the x rays ( $< 0.5$  keV). Neutron activation analysis for low-Z elements is limited by unfavorable nuclear properties of the important nuclides in this area. The thermal-neutron absorption cross sections are very small for the important reactions. The induced radioactivities are also unsuitable for counting because of very long or very short half lives.

The deuteron activation analysis takes advantage of favorable nuclear properties and

cross sections. Carbon is detected by the use of deuterons to induce the  $^{12}\text{C}(\text{d},\text{n})^{13}\text{N}$  reaction. The decay of the 10.0-min  $^{13}\text{N}$  is followed by its 0.511-MeV annihilation radiation using  $\gamma$ -ray spectrometry. The use of activation analysis for elemental determinations has reached into almost every field where sensitive and nondestructive analyses are required. The general principles of charged-particle activation analysis have been discussed by Markowitz and Mahony.<sup>9</sup> New advances in the field of activation analysis have been reviewed in a recent article by Lyon and Ross.<sup>10</sup>

## EXPERIMENTAL

### Targets

The targets used to determine the  $^{12}\text{C}(\text{d},\text{n})^{13}\text{N}$  excitation function were 2 mg/cm<sup>2</sup> polystyrene foils,  $(\text{C}_8\text{H}_8)_n$ . The targets were 2.2-cm diameter and the deuteron beam was collimated into a 1.3-cm diameter central spot. Polystyrene was selected for its purity and high carbon content of 92.3% C.

### Irradiations

The Lawrence Berkeley Laboratory 88-inch cyclotron facility was used for the irradiations. Aluminum foils were used to degrade the beam from the initial energy to the desired energy. The range-energy tables of Williamson, Boujot, and Picard were used to calculate the required aluminum thickness.<sup>11</sup> The targets were irradiated at different energies by the stacked-foil technique. The targets were typically irradiated for 2 minutes at an average beam intensity of 0.5  $\mu\text{A}$ . The total charge received by the Faraday cup was measured by an integrating electrometer.

### Counting

The irradiated samples were analyzed by detecting the 0.511-MeV positron-annihilation radiation of  $^{13}\text{N}$ . The counting system consisted of a high-resolution Ge(Li) detector and fast electronics coupled to a 4096-channel computer-controlled analyzer. The data were recorded on magnetic tape for later analysis. The Ge(Li) detector used for this work has an active volume of 60 cm<sup>3</sup>. The resolution of the detector is 2.0 keV (full-width at half-maximum) at the 1.3325 MeV  $\gamma$ -ray of  $^{60}\text{Co}$ . The use of this system allowed the collection of  $\gamma$ -ray information up to 2.0 MeV with excellent resolution. The information obtained permitted a more complete identification of other radionuclides produced during the irradiation and also protected against  $\gamma$ -ray interferences that might not be detected with a low-resolution system such as a NaI spectrometer (6-7% resolution). In routine use a simple counting system consisting of a NaI detector and a single-channel analyzer could be used after the high-resolution system has demonstrated that there are no  $\gamma$ -ray interferences with the 0.511-MeV annihilation radiation.

The decay of the 0.511-MeV annihilation-radiation activity of an activated ( $E_d = 8.6$  MeV) polystyrene target is shown in Fig. 1. The decay is a single component with a half life of 10.0 min corresponding to the decay of  $^{13}\text{N}$  in the target.

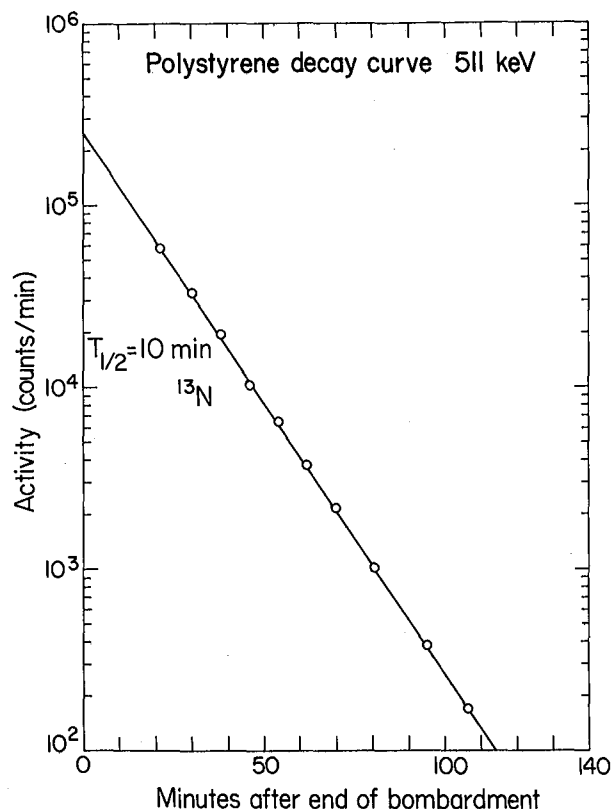


Fig. 1. Decay of the 0.511-MeV annihilation radiation activity following deuteron irradiation of a polystyrene foil. (XBL 797-2330)

The samples were counted approximately 5 cm from the face of the Ge(Li) crystal. In this geometry, the 0.511-MeV  $\gamma$ -ray overall detection coefficient (ODC) was 0.97%.  $\text{ODC} \equiv (\text{c/m})$  in the photopeak/(d/m) from the standard source. It was determined with a  $^{22}\text{Na}$  calibrated standard, obtained from the International Atomic Energy Authority, Vienna. The decay curves were analyzed with the CLSQ computer code.<sup>12</sup>

## RESULTS

### Excitation Function

The absolute cross sections at several energies were determined for the  $^{12}\text{C}(\text{d},\text{n})^{13}\text{N}$  reaction with the polystyrene foils (Fig. 2). The excitation function measured in 1959 by Brill and Sumin<sup>13</sup> agrees well with our result. The estimated accuracy of the excitation function is approximately 5%. The production of  $^{13}\text{N}$  from  $^{13}\text{C}$  (1.11% abundance) was neglected. The uncertainties in the measurement include: (a) statistical fluctuations in the counting rates, (b) decay-curve component resolution, (c) determination of the integrated charge, (d) measurement of the weight of the polystyrene foils, and (e) the determination of the overall detection coefficient.

### Interferences

Two types of interferences that must be considered in charged-particle activation analysis

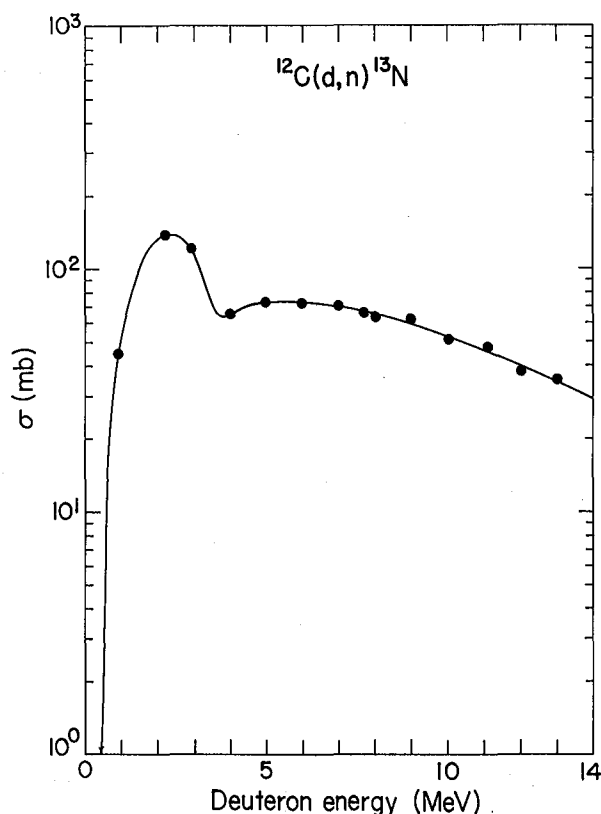


Fig. 2. Excitation function for the  $^{12}\text{C}(\text{d},\text{n})^{13}\text{N}$  reaction. (XBL 797-2331)

using  $\gamma$ -ray spectroscopy to detect the 0.511-MeV annihilation radiation are: (a) the production of positron-emitting activities of similar half life to the activity of interest, and (b) the production of the activity of interest from elements other than the one under analysis. Because the annihilation radiation is only characteristic of a positron decay event, all positron-emitting nuclides will contribute to the 0.511-MeV radiation. The activities must be separated by their half lives in a decay curve analysis. The possible interfering radionuclides must be identified and their importance carefully investigated. The production of positron-emitting activities of similar half life to  $^{13}\text{N}$  ( $t_{1/2} = 10.0$  min) is not a serious problem with the carbon determination because the  $^{13}\text{N}$  activity is by far the dominant positron-emitting activity, and it is easily resolved in the decay-curve analysis.

Interfering reactions can sometimes be avoided by selection of the incident particle energy to be below the reaction threshold. The possible interfering reactions of importance are listed in Table 1. The reaction used for the determination of carbon is listed first. If the sample is irradiated with deuterons of energy less than 8 MeV, the  $^{14}\text{N}(\text{d},\text{dn})^{13}\text{N}$  and  $^{16}\text{O}(\text{d},\alpha\text{n})^{13}\text{N}$  interfering reactions will be energetically forbidden. The  $^{14}\text{N}(\text{d},\text{t})^{13}\text{N}$  reaction cross section was measured (with GaN as target) at a deuteron energy of 7.6 MeV and found to be 1.3 mb. This cross section

is much smaller than the  $^{12}\text{C}(\text{d},\text{n})^{13}\text{N}$  cross section at this energy ( $\sigma = 70$  mb). Furthermore, typical atmospheric aerosols contain 4 to 8 times as much carbon as nitrogen. Nitrogen, therefore, does not constitute an interference. The aerosol samples were irradiated at a deuteron energy of 7.6 MeV.

Table 1. Nuclear reaction thresholds for the reaction of interest and the principal interfering reactions.

Reaction	Threshold, MeV
$^{12}\text{C}(\text{d},\text{n})^{13}\text{N}$	0.33
$^{14}\text{N}(\text{d},\text{t})^{13}\text{N}$	4.91
$^{14}\text{N}(\text{d},\text{dn})^{13}\text{N}$	12.06
$^{16}\text{O}(\text{d},\alpha\text{n})^{13}\text{N}$	8.37

#### Aerosol Sample Analyses

The atmospheric aerosol was collected on a silver-membrane filter with the use of a vacuum pump. Silver filters are the best commercially available filter for the analysis of aerosol samples using deuteron activation analysis. Because silver has a high atomic number, the Coulomb barrier can be used to minimize deuteron reactions on the filter material. The relatively massive filter (40 mg  $\text{Ag}/\text{cm}^2$ ) is only slightly activated. This permits the most sensitive detection of the  $\gamma$  radiation from the activation of the aerosol itself. The deuteron energy of 7.6 MeV that was used for the irradiation of the filter sample is below the Coulomb barrier of 8.4 MeV for deuterons plus silver.

The typical loading of particulates on the silver filter was approximately 250  $\mu\text{g}/\text{cm}^2$ . A stacked-foil arrangement was used for the irradiations. In the stack was a polystyrene foil used as the carbon standard, a filter sample, and aluminum foils. The aluminum foils were used to degrade the beam energy to the desired value. The polystyrene standard was irradiated at a deuteron energy of 8.6 MeV. The filter sample was irradiated at a deuteron energy of 7.6 MeV. The stack was typically irradiated for 2 minutes at a beam intensity of 0.5  $\mu\text{A}$ .

The decay of the 0.511-MeV annihilation radiation was followed for 2 to 3 hours. A typical gamma-ray spectrum of an aerosol sample is shown in two parts in Figs. 3 and 4. Figure 3 shows the region between 0 and 1 MeV. Besides the annihilation radiation, several  $\gamma$  rays are present. Most of these  $\gamma$  rays are a result of the activation of the silver filter. The  $\gamma$ -ray at 844 keV, however, is due to the production of  $^{27}\text{Mg}$  by the  $^{27}\text{Al}(\text{d},2\text{p})^{27}\text{Al}$  reaction. The  $^{27}\text{Mg}$  activity is a result of deuteron reactions involving the aluminum in the particulate matter and in the aluminum foil used to degrade the beam energy. The reaction products from the aluminum foil recoil into the filter sample and are stopped. Figure 4 shows the region

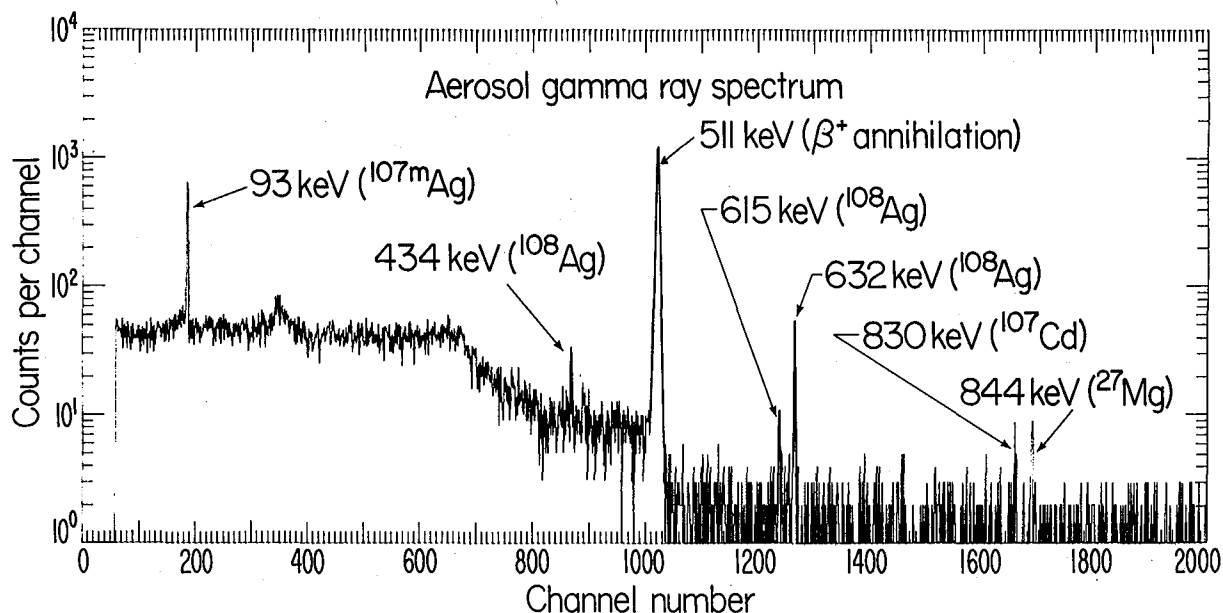


Fig. 3. The region from 0 to 1 MeV in the gamma ray spectrum of an aerosol sample following deuteron irradiation. (XBL 797-2335)

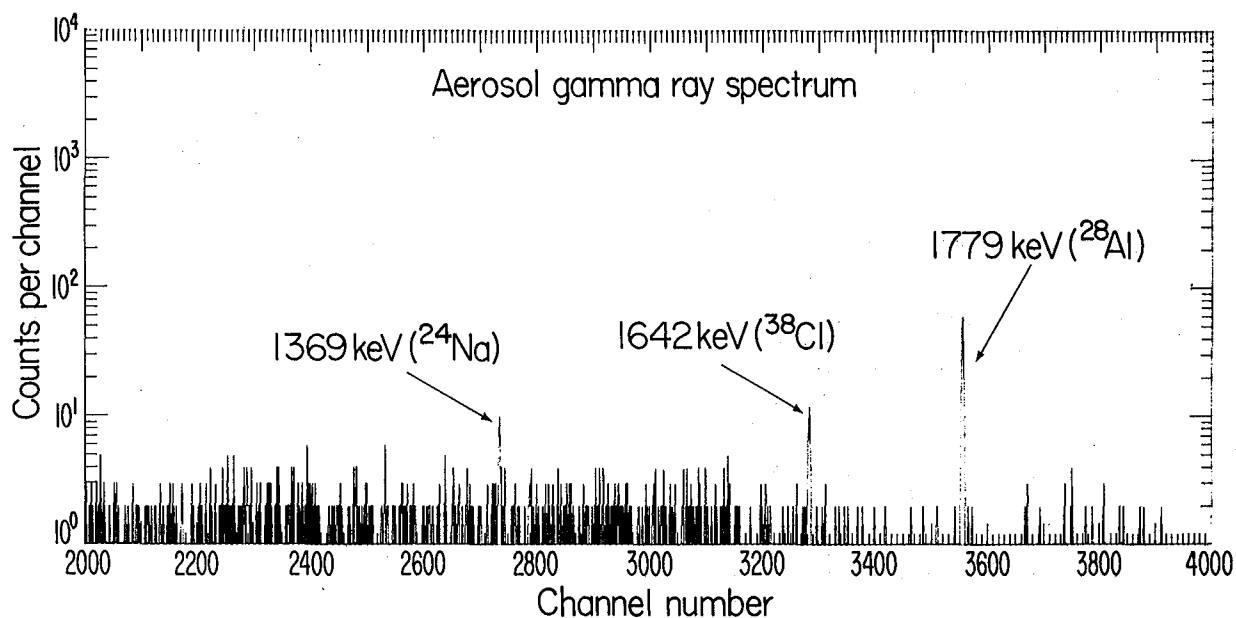


Fig. 4. The region from 1 to 2 MeV in the gamma ray spectrum of an aerosol sample following deuteron activation. (XBL 797-2336)

of the  $\gamma$ -ray spectrum between 1 and 2 MeV. Three  $\gamma$ -rays are observed in this region. The  $\gamma$ -ray at 1779 keV is from deuteron reactions involving aluminum. The  $^{28}\text{Al}$  activity is produced by the  $^{27}\text{Al}(d,p)^{28}\text{Al}$  reaction. The  $\gamma$ -ray at 1642 keV is from the production of  $^{38}\text{Cl}$  in the aerosol by the  $^{37}\text{Cl}(d,p)^{38}\text{Cl}$  reaction. The  $\gamma$ -ray at 1369 keV is due to  $^{24}\text{Na}$  produced by deuteron reactions involving aluminum.

A typical decay curve for the integrated 0.511-MeV peak of an aerosol sample following deuteron irradiation is shown in Fig. 5. The end-of-bombardment counting rate,  $A_0$ , for the  $^{13}\text{N}$  component in the aerosol was compared to the  $A_0$  value for the  $^{13}\text{N}$  component in the carbon standard. The carbon content of the aerosol was calculated relative to the carbon content of the standard. A carbon blank of approximately  $0.5 \mu\text{g}/\text{cm}^2$  was

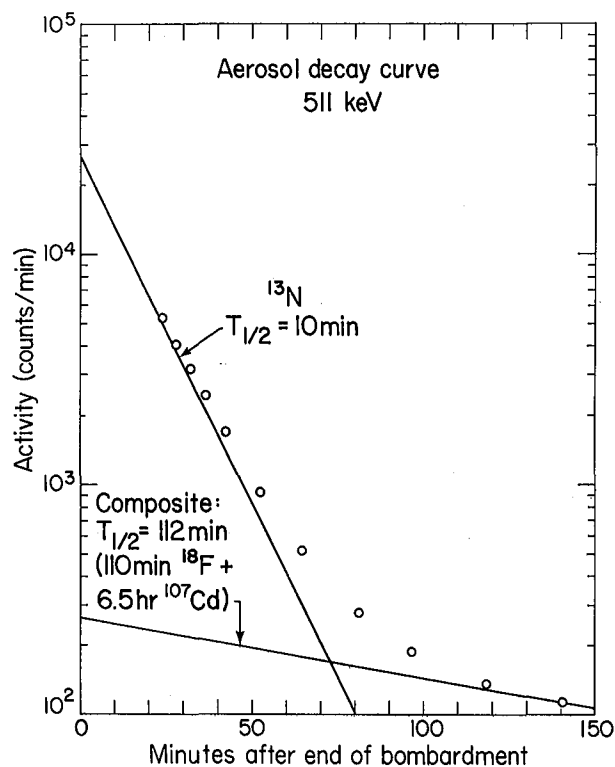


Fig. 5. Decay of the 0.511-MeV annihilation radiation activity following deuteron irradiation of an atmospheric aerosol sample. (XBL 797-2332)

found after the filters had been heated to 300°C for 24 hours; unheated Ag has a C content of approximately 5  $\mu\text{g}/\text{cm}^2$ .

The deuteron activation method was used to analyze nondestructively samples containing varying amounts of carbon. The samples were subsequently analyzed for carbon in two separate laboratories using destructive combustion methods. The results of these analyses are summarized in Table 2. The samples can be divided into two groups. One group was prepared in the laboratory by depositing pure ammonium oxalate,  $(\text{NH}_4)_2\text{C}_2\text{O}_4$ , on a silver-membrane filter. These samples correspond to the first five listed in Table 2. The second group of ten samples are ambient aerosols collected in the San Francisco Bay Area.

Comparison of the carbon found by deuteron activation analysis and that found by the independent combustion methods shows a standard deviation of 10% for the 15 samples that were analyzed, i.e.,  $R$ , the ratio of C found by activation to C found by combustion, =  $1.01 \pm 0.10$ . The agreement holds over a wide range of carbon contents from 0.6 to 268  $\mu\text{g C}/\text{cm}^2$ . The agreement is good for both the laboratory-prepared samples and the ambient aerosol samples.

The detection limit is estimated from a reasonable set of irradiation and counting conditions. The irradiation is carried out for three minutes

at a deuteron beam intensity of 0.5  $\mu\text{A}$ . The filter sample is irradiated at a deuteron energy of 7.6 MeV at which the  $^{12}\text{C}(\text{d},\text{n})^{13}\text{N}$  reaction cross section is 70 mb. The overall detection coefficient for the annihilation radiation of  $^{13}\text{N}$  is approximately 2%. The minimum activity that can be detected easily with reasonable precision is approximately 1000 counts/minute of  $^{13}\text{N}$  at the end of bombardment. The minimum  $A_0$  value takes into account the contribution of the other positron-emitting nuclides that are always present. Under these conditions the carbon detection limit is approximately 0.5  $\mu\text{g}/\text{cm}^2$ ; for an aerosol loading of 250  $\mu\text{g}/\text{cm}^2$ , this corresponds to a C concentration of 0.2%.

#### REFERENCES

1. Proceedings of the Conference on Carbonaceous Particles in the Atmosphere, T. Novakov, Ed., Lawrence Berkeley Laboratory Report LBL-9037 (1979).
2. "Atmospheric Aerosol Research Annual Report, 1977-78," H. Rosen, ed., Lawrence Berkeley Laboratory Report LBL-8696 (1978).
3. H. Rosen, A. D. A. Hansen, R. L. Dod, and T. Novakov, "Soot in urban atmospheres: determination by an optical absorption technique," *Science* **208**, 741 (1980).
4. D. Grosjean, in Proceedings of the Conference on Carbonaceous Particles in the Atmosphere, T. Novakov, ed., Lawrence Berkeley Laboratory Report, LBL-9037, 107 (1979).
5. R. L. Dod, H. Rosen, and T. Novakov, Lawrence Berkeley Laboratory Report LBL-8696, 2 (1978).
6. E. S. Macias, C. D. Radcliffe, C. W. Lewis, and C. R. Sawicki, *Anal. Chem.* **50**, 1120 (1978).
7. M. P. Failey, D. L. Anderson, W. H. Zoller, G. E. Gordon, and R. M. Lindstrom, *Anal. Chem.* **51**, 2209 (1979).
8. M. Clemenson, T. Novakov, and S. S. Markowitz, *Anal. Chem.* **51**, 572 (1979).
9. S. S. Markowitz and J. D. Mahony, *Anal. Chem.* **50**, 80R (1978).
10. W. S. Lyon and H. H. Ross, *Anal. Chem.* **50**, 80R (1978).
11. C. F. Williamson, J. P. Boujot and J. Picard, Centre d'Etudes Nucleaires de Saclay, France, Report CEA-R 3042 (1966).
12. J. B. Cumming, in "Applications of Computers to Nuclear and Radiochemistry," G. D. Kelley, Ed., National Academy of Science-National Research Council, Nucl. Sci. Ser., NAS-NS 3107, 25 (1963).
13. O. D. Brill and L. V. Sumin, *Atomnaya Energiya* **7**, 377 (1959).

Table 2. Comparison of methods for carbon determination in atmospheric aerosols.

Sample	Material	C found, $\mu\text{g}/\text{cm}^2$		Ratio (actv./comb.)
		Deuteron activation	Combustion	
AO-1	ammonium oxalate	218	210	1.04
AO-2	ammonium oxalate	268	224	1.20
AO-3	ammonium oxalate	131	122	1.07
AO-4	ammonium oxalate	74	62	1.19
AO-5	ammonium oxalate	109	113	0.96
AA-1	aerosol	84	85	0.99
AA-2	aerosol	100	99	1.01
AA-3	aerosol	106	111	0.95
AA-4	aerosol	76	76	1.00
AA-5	aerosol	103	100	1.03
AA-6	aerosol	93	93	1.00
AA-7	aerosol	5.2	4.8	1.08
AA-8	aerosol	0.6	0.7	0.86
AA-9	aerosol	57	62	0.92
AA-10	aerosol	28	32	0.88
				$\bar{R} = 1.01 \pm 0.10$

## INVESTIGATION OF SAMPLING ARTIFACTS IN FILTRATION COLLECTION OF CARBONACEOUS AEROSOL PARTICLES

*R. Dod, et al.*

### INTRODUCTION

Carbon is a major fraction of the ambient atmospheric aerosol and is usually sampled by collecting particles on a filter. Questions have been raised as to how well the particles collected on a filter represent those actually present in the air.<sup>(1-4)</sup> Speculations regarding sampling artifacts have included adsorption and desorption of carbonaceous compounds from the collected particles and filter material as well as chemical transformations which would affect the volatility of some compounds. We have applied optico-thermal combustion analysis as well as total carbon combustion analysis to samples collected on pre-fired quartz fiber filters in an effort to elucidate the magnitude of some of these effects.

### EXPERIMENTAL METHODS

The experimental configuration initially used was a filter stack of two quartz fiber filters inserted into a single 47-mm low-volume filter holder. Because of questions regarding the potential physical transfer of liquid aerosol from the first to the second filter, a series filter configuration was adopted consisting of an open-face 47-mm filter holder followed by an in-line 47-mm filter holder with a separation between the two of 5 cm. The filter medium in all cases was Pallflex 2500 QAO quartz fiber filters, which had been fired at 800°C for 2-6 hours to remove all combustible carbon. The face velocity for sampling was chosen to be approximately 0.18 m/sec to correspond to that typically used in our continuing ambient aerosol

sampling program. Tests were made at face velocities up to 0.40 m/sec, which approximates the face velocity in an 8" x 10" hi-volume sampler operating at 40 cfm. In order that sufficient sample could be collected for the analytical procedures used, the minimum sampling time was approximately 24 hours, with maximum sampling time of 7 days. Total carbon combustion analysis was done using a technique derived from that of Mueller<sup>5</sup> and the optico-thermal combustion analysis was done as described elsewhere.<sup>6</sup>

As a further check on the compatibility of this low-volume sampling technique with the standard hi-volume sampler, parallel samples at comparable face velocities showed no difference, either in total carbon or in type of carbon as determined by optico-thermal analysis.

As shown in Fig. 1. the carbon particulate loading in the air at our Berkeley sampling site has not changed greatly over a four-month period through the fall of 1979. However, the amount of carbon present on the second (in-line) filter has changed by about a factor of two over the same period from approximately 15% of the open-face loading to only about 8%. This relative change may be indicative of some type of annual variation in vapor phase or volatile carbon composition. The mean fraction of carbon found on the second filter shows no variation with sampling time (Table 1), indicating that if a saturation effect is operative, it was not reached in the sampling times investigated.

While the open-faced filter had in all cases a grey or black deposit, the second filter was in each case unsoiled, indicating that very few if any of the solid particles penetrated the first filter. The carbon present on the second filter must therefore be adsorbed hydrocarbon, either adsorbed from the ambient air or from material desorbed or vaporized from the first filter. Optico-thermal analysis shows that the material present on the second filter is primarily detected below ~250°C (Fig. 2), which from previous experiments indicates that it is due to small volatilizable organic compounds. Based on these results

and from the apparent lack of saturation, it would seem reasonable to attribute the carbon on the second filter to vapor phase compounds adsorbed from the ambient air onto the quartz filter medium, with the adsorption being of sufficient strength not to be reversed under most ambient conditions. As a check of this, portions of one of the second filters were analyzed and the remainder of the filter was placed in a drying oven in air for 24 hours at 40-45°C; approximately 55% of the carbon was lost in this heating process.

The information gained to date is as conflicting as that which is already in the literature. Effects which have been observed could be due either

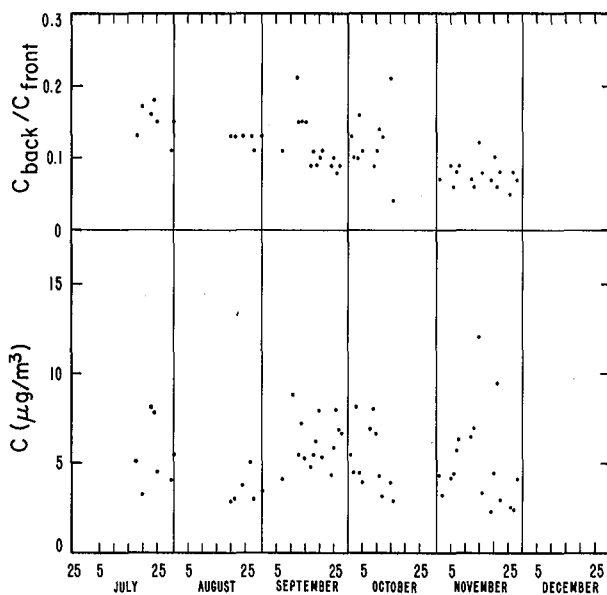


Fig. 1. a) Carbon on second filter as a fraction of carbon on open face filter.  
b) Ambient carbon loadings from total carbon analysis of open face filter.

(XBL 806-1144)

Table 1. Carbon determined on second filters as a fraction of open-face filters.

Sampling time (days)	Number of samples	Carbon on second filter Carbon on open-face filter
1	26	0.12 ± 0.04
2	2	0.14 ± 0.01
3	7	0.13 ± 0.02
4	1	0.11
5	1	0.15
7	1	0.13

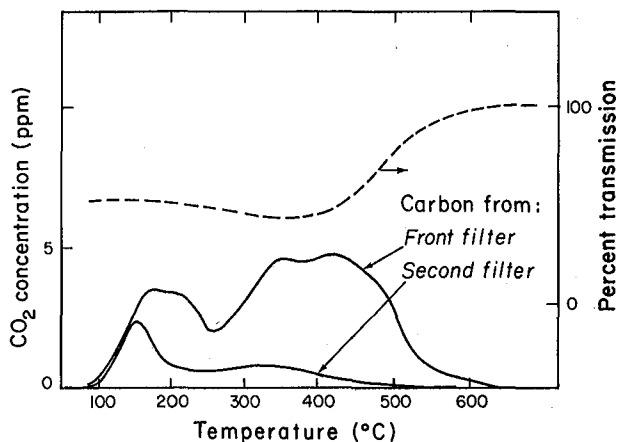


Fig. 2. Optico-thermal analysis of a typical Berkeley ambient series filter pair. (XBL 806-1146)

to gain or loss of "particulate carbon" on the filter. It is planned to continue this examination for a longer period of time to discover whether or not an annual cycle exists as well as to investigate the adsorptive/desorptive behavior of the collected organics.

The results shown here are consistent with results from preliminary experiments in both Berkeley and Anaheim using the filter pack technique, indicating that over a period of several days, the physical transfer of carbonaceous aerosol by liquid flow is not significant.

#### REFERENCES

1. W. Gautreels and K. Van Cauwenberghe, *Atmos. Environ.*, **12**, 1133 (1978).
2. P. W. Jones, R. D. Giammar, P. E. Strup and T. B. Stanford, *Environ. Sci. Technol.*, **10**, 806 (1976).
3. L. Van Vaeck and K. Van Cauwenberghe, *Atmos. Environ.*, **12**, 2229 (1978).
4. H. Della Fiorentina, F. De Wiest and J. De Graeve, *Atmos. Environ.*, **9**, 517 (1975).
5. P. K. Mueller, R. W. Mosley, and L. B. Pierce, "Carbonate and non-carbonate carbon in atmospheric particles," *Proceedings of the 2nd International Clean Air Congress*. New York, Academic Press (1970).
6. R. L. Dod, H. Rosen and T. Novakov, Lawrence Berkeley Laboratory Report, LBL-8696 (1979).

## SURFACE CHARACTERIZATION OF FLYASH

*S. Cohen, et al.*

### INTRODUCTION

Electron spectroscopy for chemical analysis (ESCA) can be used as a nondestructive surface-speciation technique. Not only can different elements be identified using ESCA, but information regarding chemical state--e.g., Fe(II) versus Fe(III)--is provided. Sample preparation is relatively simple, and only a small amount of sample--enough to dust over a piece of double-backed Scotch tape--is required. Provided that the signal can be distinguished from noise, ESCA therefore seems an ideal technique for characterizing a complex surface such as coal flyash. Two main difficulties of the technique are:

1. Matrix effects can be serious so that even comparison with model compounds will not give unambiguous assignment of ESCA peaks. In addition, a single element in flyash may exist in several chemical states and/or crystalline forms, thereby making peaks broad and diffuse and speciation difficult.

2. Of ultimate interest in flyash studies are the compounds released to the environment by leaching in waterways and the ease with which toxic substances in flyash are released in the respiratory tract at physiological pH. This is not strictly related to what species are initially on the flyash

surface. The presence of pores, for instance, could enhance dissolution of species deep inside the flyash particle.

Solvent leaching studies should aid in these two problems and may even provide depth profiling information if the leachate is analyzed as a function of time. Unfortunately, complex equilibria in the extract probably mix the original salts and may cause precipitation where resulting mixtures are insoluble. For instance,  $\text{BaCl}_2 + \text{CaSO}_4 \rightarrow \text{BaSO}_4 \downarrow + \text{CaCl}_2$ . Thus  $\text{Ba}^{2+}$  leached from the flyash in initially soluble form could precipitate and not be found in the leachate. Nevertheless, because solvent leaching when run in conjunction with ESCA studies may provide important surface information, and because solvent leaching may become an important technique in labs where ESCA is unavailable, the correlative study has been pursued.

D. F. S. Natusch has used "time resolved solvent leaching" to study flyash surfaces.<sup>1</sup> The method entails continuous leaching of the sample by a solvent, the leachate being analyzed as a function of time. The problems described above due to complex equilibria limited the study. The work described below is an attempt to develop the method proposed by Natusch.

## EXPERIMENTAL

All ESCA work was done on an AEI spectrometer using the Al  $K_{\alpha}$  (1486.6 eV) exciting line. Flyash samples were dusted onto a piece of double-backed Scotch tape. Scans were made over a 20-50 eV region (B.E. step = 0.2 to 0.5 eV for 100 channels) for times ranging from 10 seconds/channel for strong signals to 375 seconds/channel for very weak signals. Peaks were referenced to spectrometer hydrocarbon contamination with  $C(1s) = 284.6$  eV.

Solvent extractions were done in acid-washed glassware by 15 minutes of ultrasonic treatment. In all cases, Barnstead deionized water was used to make up extracting solutions. Leachates were stored in acid-washed linear polyethylene containers, after filtering through an 0.2- $\mu$  pore-size Millipore filter.

Ion chromatography was done on a Dionex Model 14 ion chromatograph at a sensitivity of 10  $\mu$ mo full scale. Atomic absorption work was performed on a Perkin-Elmer Model 360 atomic absorption instrument.

## RESULTS AND DISCUSSION

Initial studies in this laboratory consisted of ESCA analysis of unleached flyash. Elements most strongly detected are listed in Table 1. Some information on chemical state was obtained, as can be seen by inspection of Figs. 1 and 2. Sulfur appears to be in the S(VI) form, in agreement with the work of Small.<sup>2</sup> Arsenic closely resembles the model compound  $As_2O_3$ ; however, the similarity of  $As_2O_3$  and  $As_2O_5$  ESCA peaks will necessitate further work to confirm this hypothesis. Satellite structure, which yields information on both oxidation state and ligand environment, was faintly present for both Cu (Fig. 3) and Fe, but no assignments have yet been made.

The flyash was then leached by ultrasonic treatment. Compounds found in the leachate were compared with changes found on the flyash surface using ESCA. Because a flyash solution in water yields a basic pH (due to dissolution of CaO), both deionized water and dilute  $HNO_3$  were used to vary extracting conditions. Leachate analyses are displayed in Table 2.

Although most of the initial leachate analyses were qualitative, some quantitative information was obtained.  $Ba^{2+}$  was detected at a concentration equal to the solubility limit of  $BaSO_4$  in the  $H_2O$

leachate. This is precisely the result expected if the sparingly soluble salt  $BaSO_4$  precipitates out of the wash. In every case examined, the nitric acid was found to be a better extractant than  $H_2O$ .

Inspection of flyash surfaces after sonication provided good correlation for some species; Figure 4 shows the effect of  $H_2O$  and acid washes on the flyash surface. Because ESCA is a relative, and not an absolute, technique, in order to compare peak intensities from separate samples it is advisable to normalize to a flyash constituent unaffected by the washes. Since even the matrix elements Fe, Si, and Al are found in the  $HNO_3$  leachate, no reliable reference could be selected. Hence the intensities are listed in Fig. 4 as simply counts/sec/channel (unnormalized). The trends observed are nevertheless considered significant since: 1) the extent of the differences is too large to be caused by sample orientation in the spectrometer or thoroughness of coverage of the Scotch tape,

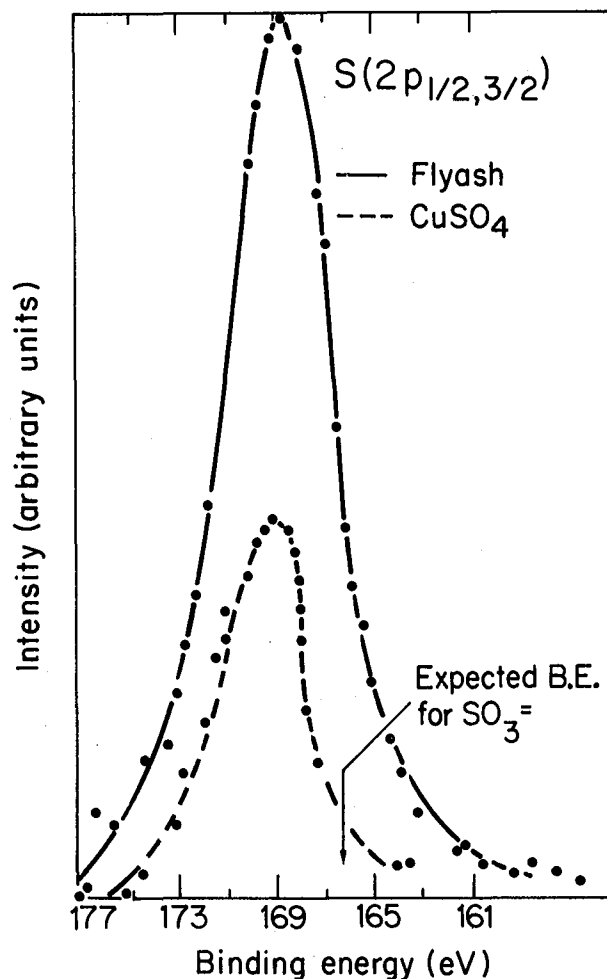


Table 1. Elements detected on untreated flyash surfaces by ESCA.

Transition metals	Cu, Cr, Fe
Alkaline and alkaline earth	Ba, Ca, Na
Other	Al, As, C, Cl, O, P, S, Si

Fig. 1. Comparison of a flyash ESCA spectrum in the sulfur  $2P_{1/2, 3/2}$  region to that of reagent-grade  $CuSO_4$ . If  $S^{+4}$  species were present, a shoulder should be observed in the position indicated. Binding energies in this and all ESCA spectra shown are referenced to spectrometer hydrocarbon contamination at 284.6 eV.

(XBL 801-43)

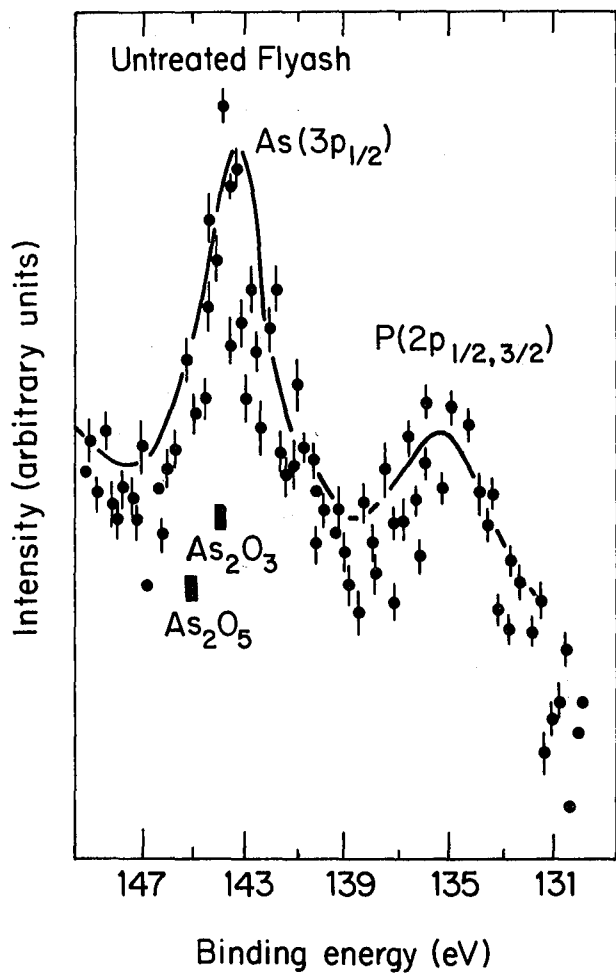


Fig. 2. ESCA spectrum of untreated flyash in the As  $3P_{1/2}$  region. Positions of this peak for  $As_2O_3$  and  $As_2O_5$  are indicated. The peak at  $\sim 135$  eV is due to phosphate ( $2P_{1/2,3/2}$ ). It was removed by both water and acid wash.

(XBL 801-44)

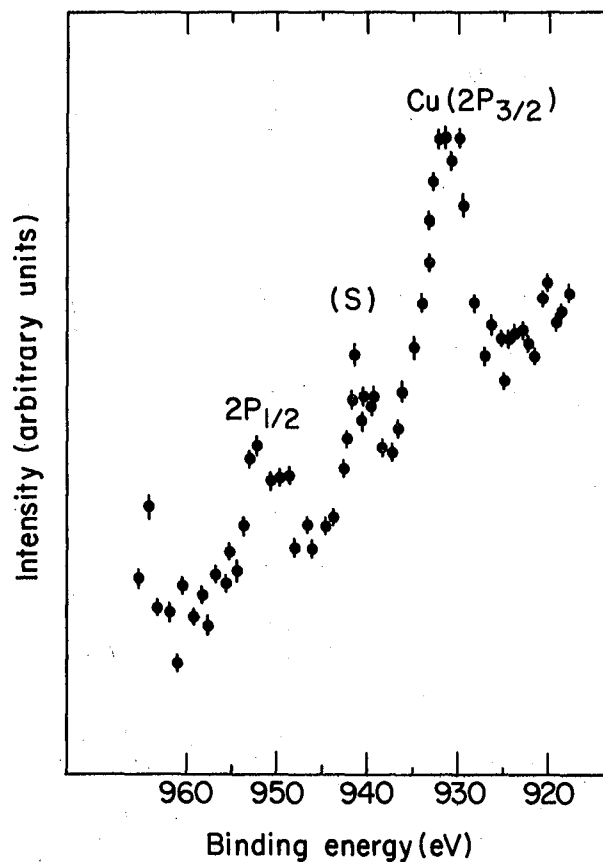


Fig. 3. Cu  $2P_{1/2}$ ,  $2P_{3/2}$  peaks and satellite structure (s) as indicated. (XBL 801-45)

Table 2. Species found in leachate from flyash.

	H <sub>2</sub> O wash	Acid wash
Anions	$SO_4^{2-}$	$SO_4^{2-}$ , $F^-$ , $Cl^-$
Cations (Fe, Ba, Cu, Al, Si) <sup>a</sup>	$Ca^{2+}$ , $Na^+$ , $K^+$	$Ba^{2+}$ , $Ca^{2+}$ , $Na^+$ , $K^+$ , $Mg^{2+}$

<sup>a</sup>These elements were determined using AA; all other entries in the table provided by I.C.

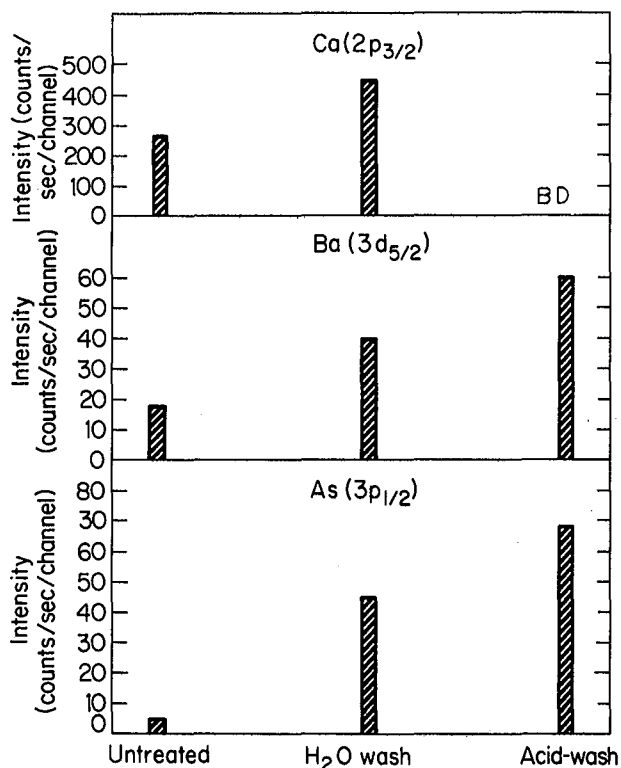


Fig. 4. Bar graphs showing the effect of water and acid wash on the (a) Ca (b) Ba and (c) As surface concentrations on flyash. The peak monitored is as indicated. The calcium peak was below detection for the acid-washed sample.

(XBL 801-46)

and 2) the trends shown in Fig. 4 were found to be reproducible.

As expected from the large amount of Ca<sup>2+</sup> found in the nitric acid leachate, the acid wash completely removes Ca<sup>2+</sup> from the surface. The surface enhancement of Ca<sup>2+</sup> by the water-wash is rather unexpected, since the leachate results (Table 2) indicate the flyash has been depleted of Ca<sup>2+</sup>. Keeping in mind that ESCA is a surface,

not a bulk technique, we may be observing a novel surface adsorption of the Ca species onto the flyash surface as leaching from the interior proceeds. Enhancement of As and Ba on the flyash surface is effected by acid and water washes (Fig. 4). Presumably formation of insoluble compounds BaSO<sub>4</sub> and FeAsO<sub>4</sub>, which precipitate onto the surface, explains this enhancement.

#### CONCLUSION

The investigation of flyash surfaces by combining ESCA and solvent leaching may prove to be a valuable analytical tool. The example of barium provides an indication of the strength of the method. Whereas detection of Ba<sup>2+</sup> in the H<sub>2</sub>O leachate at the concentration limit of BaSO<sub>4</sub> does not by itself provide conclusive evidence of BaSO<sub>4</sub> formation, enhancement of Ba in the ESCA spectrum supports such a conclusion. The latter observation also indicates that BaSO<sub>4</sub> is not initially present but is formed during the wash. In transition metals, changes in satellite structure could similarly be used to monitor transformation among various metal salts.

Future work will examine the hypothesis of time-resolved solvent leaching for both surface and matrix elements. Fe, Al, and Si are known to be distributed throughout the flyash matrix;<sup>3</sup> hence they would be expected to show constant concentration vs time profiles. In addition, surface concentrations of these species should not vary significantly with time. As, Cu, and Cr, however, which show surface enrichment, should yield observable changes in both the leachate profiles and surface studies.

#### REFERENCES

1. D. S. Natusch and M. Tomkins, private communication, July, 1979.
2. J. A. Small, An Elemental and Morphological Characterization of the Emissions from the Dickerson and Chalk Point Coal-fired Power Plants, Ph.D. thesis, University of Maryland (Chemistry) 1976.
3. R. L. Davidson, D. F. S. Natusch, J. R. Wallace, and C. A. Evans, "Trace elements in flyash dependence of concentration on particle size," *Environ. Sci. Technol.* **3**, 1107 (1974).

# APPLIED RESEARCH IN LASER SPECTROSCOPY AND ANALYTICAL TECHNIQUES

## APPLIED PHYSICS AND LASER SPECTROSCOPY RESEARCH\*

N. Amer,<sup>†</sup> N. Bergstrom, J. Costello, R. Gerlach, W. Jackson, R. Johnson,  
S. Kohn, C. Rosenblatt, D. Wake, and Z. Yasa

### OVERVIEW

The research philosophy of our group is to apply advanced laser spectroscopy and condensed matter physics to energy and environmental problems. With the narrow linewidth and the tunability of lasers, unsurpassed sensitivity and specificity can be achieved in detecting trace contaminants of the atmosphere. The advanced state of condensed matter physics enables us to apply such knowledge to energy production processes and to test novel methods for energy conversion, such as photovoltaic devices, superionic electrical energy storage devices, and the extraction of oil from oil shales with lyotropic liquid crystal emulsifiers.

### LASER PHOTOACOUSTIC MEASUREMENTS & CHARACTERIZATION

Laser photoacoustic spectroscopy provides a very powerful tool for the detection of trace contaminants in air and water as well as a means for investigating the fundamental properties of gaseous, liquid, or solid phases of matter. One of our goals is to develop ultrasensitive multiparameter elemental and molecular detectors for the characterization of pollutants released in the process of energy production and utilization. Another aim is to maintain a state-of-the-art capability in photoacoustic detection by fully understanding the physics of this technique. Concurrent with these efforts, we are active in developing new or modified laser systems compatible with our particular needs. Below we report on some of our results.

### A Resonant Spectrophone for Intracavity Use\*\*

As acoustically resonant spectrophones began to be used in conjunction with lasers for trace gas analysis, it was quickly realized that their already high sensitivity to weak optical absorption could be further enhanced by use of a multipass geometry to increase the amount of absorbed power.<sup>1,2</sup> A comparable increase in absorbed power could be achieved by placing the spectrophone inside the cavity of a laser, where the increase is due not to an increased path length but to a higher beam power available for absorption.

A principal obstacle to intracavity operation is that for conventional resonant spectrophone designs, in which the beam passes through the windows at normal incidence, the window reflection losses impair operation of the laser. A further problem, not unique to intracavity spectrophones, is that if the beam enters and leaves the cell at points of high pressure amplitude for the mode being excited, as is the case when the beam passes

directly down the center of a cylindrical cell and a radial mode is excited, any window absorption can give rise to a spurious background signal resulting from window heating. The first problem can be alleviated by antireflection coating the windows, but single-layer AR coatings are usable over only a limited range of wavelengths. It would be more desirable to have the beam enter and leave at Brewster's angle, since for many commonly used optical materials, such as fused silica and sodium chloride, Brewster's angle is nearly constant over a wide range of wavelengths, and tolerance to small variations is large since reflectivity varies quadratically with small deviations from Brewster's angle. Window heating can be alleviated by placing the windows at nodes of the mode being excited. Somewhere inside the cell, however, the beam must pass through a region where the mode has a high amplitude in order to excite that mode efficiently.

For a spectrophone to be used for monitoring ambient air, it would be desirable to eliminate the windows altogether.<sup>3</sup> This would permit continuous sampling by inducing a slow flow of air through the cell. Absence of windows certainly solves the optical insertion loss problem, yet it can greatly degrade the quality factor (Q) of the acoustical cavity resonance. Again, the solution is to let the beam enter and leave the cell at pressure nodes, where the holes will constitute a minimal perturbation.

Our spectrophone design, based on the above considerations, is shown in Fig. 1. As for all cylindrical acoustical resonant cells, the pressure amplitude for the first radial mode is a maximum

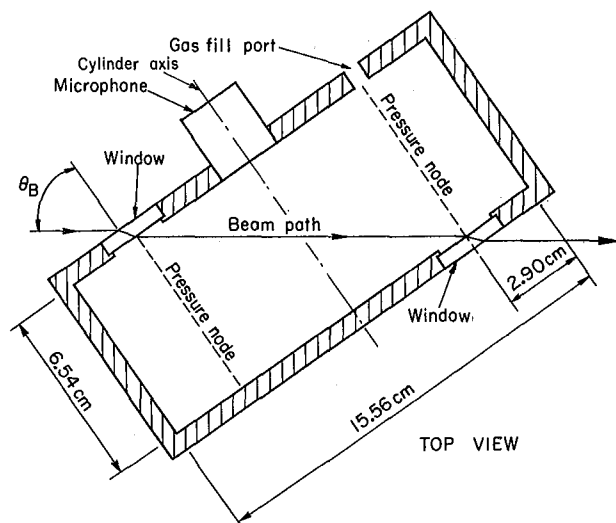


Fig. 1. Brewster Window Spectrophone (top view).  
(XBL 803-3125)

<sup>†</sup>Group Leader

along the center axis of the cylinder, passes through zero about 2/3 of the way out to the wall, and reaches a negative extremum at the wall. The beam enters our cell through a window mounted virtually flush with a flat end wall, passes diagonally through the center of the cell, and exits through a window on the other flat wall. The entry and exit points are chosen to lie on a node of the first radial mode. For the beam to pass through the windows at Brewster's angle, the ratio of cell radius to length must be 0.7967 times the refractive index of the window material; thus for  $n=1.5$ ,  $R/L=1.19$ .

The microphone is centered directly on the cell axis. This has two advantages. First, the flat microphone face mounts approximately flush with the flat end wall of the cylinder and does not perturb the cell geometry as it would on a cylindrical wall. Second, the microphone is now at the absolute maximum of the first radial mode, where the pressure amplitude is 2-1/2 times larger than at the cylindrical wall, the usual microphone location.

The same design is applicable to windowless operation. However, there is no longer a constraint on the ratio  $R/L$ , and it is therefore desirable to make the ratio smaller. Smaller beam entrance holes can be used without aperturing the beam, the importance of viscous losses on the flat end walls is reduced, and the first radial resonant frequency is moved farther from the relatively broad first longitudinal resonance, which is strongly excited by ambient room noise.

We have investigated the performance of the spectrophone using a calibration mixture of 54 ppm of ethylene in nitrogen and using pure nitrogen to determine background signal levels. The light source for these experiments was a current-modulated CO<sub>2</sub> laser tuned to the P(14) line in the 10.6  $\mu\text{m}$  band, for which the absorption coefficient of ethylene is known to be about  $31 \text{ atm}^{-1} \text{ cm}^{-1}$ . The  $R/L$  ratio for our design was appropriate for NaCl Brewster windows, but we also tried operating the cell without any windows. Our investigations established the following:

- The Q of the first radial resonance at 2700 Hz is 560 when the cell is operated with windows. Removing the windows only decreases the Q to 509.
- The calibration of the cell was 26.5 volts per watt per cm of absorbed power, or in terms of pressure units, 241 Pa per watt per cm.
- The calibration does not depend very sensitively on the precise alignment of the beam through the cell, so misalignments can be tolerated as far as calibration is concerned.
- The coherent background signal due to window heating and to scattered or reflected light heating the cell walls is indeed minimized by the geometry chosen. As the beam deviates from its intended path through the cell, background signal increases, but shows a sufficiently broad minimum as a

function of the various pertinent geometrical variables so that, again, alignment of the beam is not ultracritical. Also, variations of the beam polarization from the plane of incidence by a few degrees can be tolerated. The background is equivalent to an absorption coefficient of  $2.1 \times 10^{-7} \text{ cm}^{-1}$ , or an ethylene concentration of 6.6 parts per billion.

- The random noise level when the spectrophone is operated with windows is equivalent to an absorption coefficient which can be found by multiplying  $3.8 \times 10^{-8} \text{ W cm}^{-1} \text{ Hz}^{-1/2}$  times the square root of the bandwidth divided by the laser power. For intracavity operation with a 1 Hz bandwidth this could be made very small,  $7.5 \times 10^{-10} \text{ cm}^{-1}$ , equivalent to 25 parts per trillion of ethylene. In this case, however, sensitivity would be limited by the coherent background signal.
- Windowless operation is limited in sensitivity by ambient room noise. For the cell dimensions used, the first radial mode lies close to the first longitudinal mode, which has a low Q and is strongly excited by room noise.

In conclusion, our new spectrophone design offers low insertion loss making possible intracavity operation, high sensitivity, and low background signal. These features should make it attractive for a wide variety of gas analysis and spectrophone investigations, especially where broadly tunable lasers are used.

#### FOOTNOTE AND REFERENCES

\*\*Complete version accepted for publication in Applied Physics (1980).

1. C. F. Dewey, R. D. Kamm and C. E. Hackett, Appl. Phys. Lett. 23, 633 (1973).
2. E. Max and L. G. Rosengren, Opt. Commun. 11, 422 (1974).
3. Another design for a windowless resonant spectrophone, differing drastically from ours, was presented by S. Shtrikman and M. Slatkine, Appl. Phys. Lett. 31, 830 (1977).

#### Piezoelectric Photoacoustic Detection: Theory and Experiment\*

##### Introduction

When an intensity modulated light beam is absorbed by a medium, part of all of the excitation energy is converted to thermal energy. In "conventional" photoacoustic spectroscopy, the generated heat is coupled to an optically nonabsorbing gas and the time-dependent pressure fluctuation is detected with a microphone. The universal applicability of this approach to gases,<sup>1-6</sup> liquids,<sup>7-9</sup> solids,<sup>10-14</sup> and aerosols<sup>15,16</sup> makes it a versatile detector scheme. Nevertheless, this approach suffers from certain crucial limitations, particularly in

the case of condensed matter samples. Perhaps the most serious restrictions are the narrow bandwidth of the microphone response, the relatively complex nature of the heat transfer process from the sample to the gas, and the inability to perform experiments at low pressures. Furthermore, saturation problems limit the usefulness of this technique in the case of strong optical absorption.

An alternative photoacoustic detection scheme is to attach a piezoelectric transducer (PZT) directly to the sample. The absorption-induced heating causes the sample to develop thermal stresses and strains which are transmitted to the sample surface. The attached PZT converts these stresses and strains to a measurable voltage.

This approach has several advantages over gas cell photoacoustics. PZTs have a wide frequency response range from a few Hz to many MHz, and they can be used over a broad range of temperatures and pressures. Since the sample-PZT configuration is compact and rugged, it is useful in space-limited experiments (e.g., inside a low temperature optical dewar). Because the PZT responds to absorption of radiation by the entire sample, not merely within a thin thermal length, the complicated solid-gas coupling is eliminated. Furthermore, as we shall demonstrate, piezoelectric-photoacoustic spectroscopy (PZT-PAS) is a very sensitive means for measuring absorption coefficients as low as  $10^{-5} \text{ cm}^{-1}$  for a 1 W laser, and does not show saturation for  $\alpha l$  as high as 10.

Below, we develop a computationally tractable thermoelastic theory for piezoelectric photoacoustic detection at low modulation frequencies. This theory was tested experimentally with samples whose thermal and optical properties cover a wide range. We find that our theoretical treatment quantitatively accounts for the observed magnitude and phase of the signal, and describes its functional dependence on modulation frequency, absorption coefficients, and thermal properties of the sample.

### Theory

An outline of the steps of the theory of PZT-PAS is shown in Fig. 2. The signal is generated when a beam of light is incident on an absorbing solid. The temperature of the illuminated volume increases, leading to the expansion of that region and the outflow of heat (Fig. 3a). The expansion of the central region causes displacement of the sample surface by two separate mechanisms. First, the enlargement of the central region causes the expansion of both surfaces of the sample (Fig. 3a). Second, in the case of strongly absorbing samples, the heat in the illuminated region decays spatially through the thickness of the sample (Fig. 3b). Consequently, the front portion of the sample expands more than the rear, resulting in a bending of the sample. Such bending compresses the rear surface of the solid and opposes the general expansion shown in Fig. 3a. The bending also causes expansion of the front surface, thus adding to the expansion described in Fig. 3a. This displacement of the sample surface is then sensed by the transducer (Fig. 4a) causing a voltage to develop in the  $z$ -direction between the two surfaces of the PZT.

### CALCULATION FLOW CHART

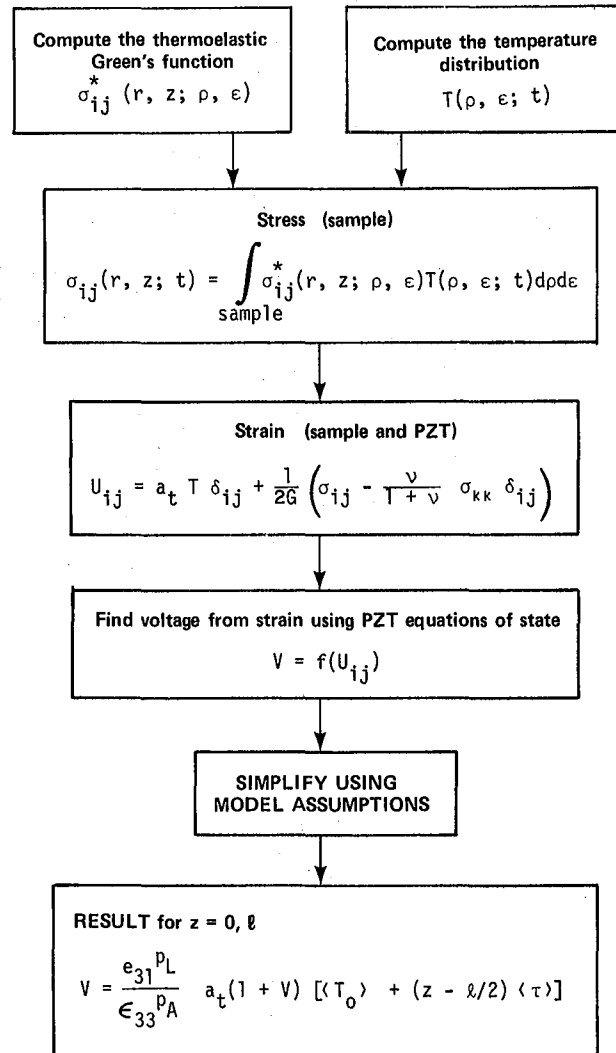


Fig. 2. Flowchart showing steps in the calculation. The symbols are defined in the text.

(XBL 797-2310)

**Detector Geometry.** Consider the geometry shown in Figs. 4a and 4b. We treat two cases: (1) optically thick samples, where the light beam is not transmitted and the PZT is a slab covering the entire back surface of the solid (Fig. 4b), and (2) optically thin samples, where the PZT is an annulus and is located on either side of the solid (Fig. 4a). As will be shown, the nature of the generating strain in the latter case is dependent upon the side on which the transducer is located.

**Assumptions of the Theory.** To simplify the problem, we assume the solid to be an isotropic, infinite, elastic layer. This approximation is reasonable since a focused light beam is typically much smaller than the sample dimensions. We also assume that the sample responds as if its boundaries

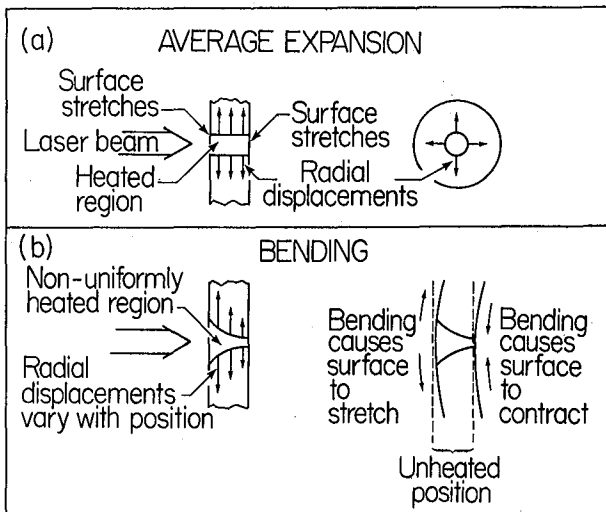


Fig. 3. Sources of surface strain. Transducer may be attached to either side of the sample. (XBL 797-2315)

were free from stress. This is plausible since the transducer is much thinner than the sample. In fact, for a transparent solid (Fig. 4a) the sample is free in its central region.

**Predictions of the Theory.** By calculating the temperature distribution in the sample and the corresponding induced strain, we were able to calculate the potential difference  $V$  generated by the PZT as a result of stress induced in the sample itself from the absorption of the electromagnetic radiation. We show that such a potential difference  $V$  is given by

$$V \approx \frac{e_{31}^P L a_t}{\epsilon_{33}^P A} (1+\nu) \left[ \langle T_0 \rangle + (z-l/2) \langle \tau \rangle \right]_{z=0,l} \quad (1)$$

where  $e_{31}^P$  and  $\epsilon_{33}^P$  are the piezoelectric and dielectric constants of the PZT,  $L$  is its thickness, and  $A$  is its area.  $a_t$  is the expansion coefficient of the sample,  $\nu$  is Poisson's ratio,  $\langle T_0 \rangle$  is the in-plate displacement due to the average temperature  $T_0$ . The second term represents the sample buckling due to the average temperature gradient  $\tau$ . When the transducer is on the laser side of the sample, the average term and the buckling term add since  $\langle \tau \rangle < 0$ . When the transducer is away from the laser, the terms subtract.

**Implications of the Theory.** Physically, the implications of Eq. (1) are more apparent if one considers specific cases. In the following cases,  $l_t = (2\lambda/\omega)^{1/2}$  is the thermal length,  $l_o (=1/\alpha)$  is the optical length of the sample, and, for simplicity, we have neglected surface conduction from the sample to the ambient air.

**Case 1:** For thermally and optically thick samples with the transducer located at  $z=l$ , we have with  $l \gg l_t$  and  $l \gg l_o$

$$V \approx - \frac{2M P a_t}{i\omega l (\rho C)_{\text{sample}}} \quad (2)$$

where

$$M = \frac{e_{31}^P L}{\epsilon_{33}^P A} \frac{2(1+\nu)}{\pi}$$

**Case 2:** For thermally thin but optically thick samples ( $l_t \gg l \gg l_o$ ), we have

$$V \approx \frac{M P a_t}{i\omega l (\rho C)_{\text{sample}}} \quad (3)$$

again when the transducer is located at  $z=l$ .

**Case 3:** For thermally thick but optically thin samples ( $l_o \gg l \gg l_t$ ), we have

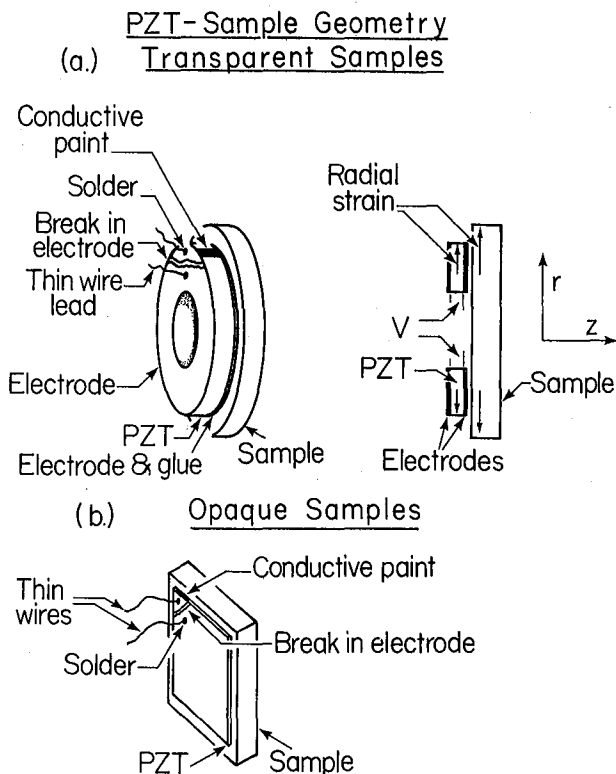


Fig. 4. Transducer-sample geometry. 4a) Configuration used for transparent samples. 4b) Configuration for opaque samples. (XBL 797-2316)

$$V \approx \frac{M a_t P}{i\omega\ell(\rho C)_{\text{sample}}} \quad (4)$$

$$\left\{ 1 - e^{-\alpha\ell} \pm \frac{6}{\lambda\alpha} \left[ \left( 1 - \frac{\lambda\alpha}{2} - e^{-\alpha\ell} \left( 1 + \frac{\lambda\alpha}{2} \right) \right) \right] \right\}$$

where the negative sign applies for ( $z=\ell$ ) the case when the transducer is away from the laser beam, and the positive sign is applicable when the transducer is towards the laser ( $z=0$ ).

From the above cases we find the general form of the signal is

$$V \propto M a_t \frac{1}{\rho C} \frac{P}{\omega}$$

$P/\omega$  is the energy deposited per cycle,  $1/\rho C$  converts the energy to a temperature,  $a_t$  transforms the temperature rise to a strain, and  $M$  is a voltage for a given strain.

Based on this theory, the following predictions are made.

- 1) The signal amplitude is proportional to the reflection-corrected incident power.
- 2) The signal amplitude is related to the material parameters through the quantity  $a_t(1-R)/(\rho C)_{\text{sample}}$ . Note that the signal does not depend on Young's modulus or on the conductivity  $\kappa$  directly. The conductivity affects the signal as a result of its effect on the thermal length.
- 3) The signal amplitude has a  $1/\ell$  dependence; hence thin samples tend to yield higher signals.
- 4) The signal has approximately  $1/\omega$  dependence. The exact theory shows that the frequency dependence closely approximates a  $1/\omega^{0.9}$  dependence for thick metal samples.
- 5) The phase for metal data undergoes a  $180^\circ$  phase shift as the thermal length becomes smaller than the sample thickness.

6) For small values of  $\alpha$ , the photoacoustic signal is directly proportional to  $\alpha$ . For high values  $\alpha$ , the position of the PZT with respect to the direction of the incoming beam ( $z=0$  or  $z=\ell$ ) yields significantly different results. When the transducer is away from the laser beam ( $z=\ell$ ), as  $\alpha$  increases, the signal should decrease, eventually passing through zero and changing signs at higher values of  $\alpha$ . On the other hand, when the transducer is attached to the sample surface towards the laser beam ( $z=0$ ), it is predicted that the signal will show little saturation until  $\alpha$  reaches very high values.

#### Experimental Verification of the Theory

The predictions of our theory were tested experimentally for solids with a wide range of

optical and thermal properties. The samples used were tungsten, tantalum, copper, glass coated with black paint, and didymium glass. The piezoelectric transducers (type 5502 lead zirconium titanate alloy) were obtained from Channel Industries and electrodes were attached to them with low temperature solder. For opaque samples (Fig. 4b), a  $0.01 \times 0.8 \times 0.8$  cm PZT slab was used; for optically thin samples (Fig. 4a), PZT annuli were employed to minimize the scattering of the exciting light on the transducer itself. After testing several types of adhesive, we chose to employ Eastman 910<sup>17</sup> and a low viscosity epoxy<sup>18</sup> for the work reported below. Our experimental apparatus is shown in Fig. 5.

Verification of  $1/\omega$  Dependence. Equation (2) predicts that the amplitude of the photoacoustic signal is approximately inversely proportional to the modulation frequency of the exciting light. By varying the chopping frequency using a computer, we found this to be the case for all of our samples over the modulation range tested (5-2000 Hz) as shown in Fig. 6.

Power Dependence of the Signal. The power dependence of the observed signal was verified by attenuating the intensity of the laser beam with calibrated filters. For various samples we found the signal to depend linearly on the power for over six orders of magnitude. The minimum power we could detect was  $0.1 \mu\text{W}$  for a signal to noise ratio of one. This is in agreement with our predictions. By using a copper sample and continuously varying the wavelength of a dye laser, we verified the prediction that the signal is a linear function of the incident power when corrected for the reflectivity of the sample.

Signal Dependence on the Optical Absorption Coefficient. The absorption bands of the didymium glass around the 5800 Å region were used to test the theoretical prediction of the signal dependence on the absorption coefficient. The sample absorption was measured simultaneously by transmission and by photoacoustics on two identical samples (Fig. 5). The experiments were performed for the transducer away and towards the laser beam. The agreement between the theory and the experimental results is good, as can be seen in Figs. 7-8. When the transducer is away from the beam ( $z=\ell$ ), the

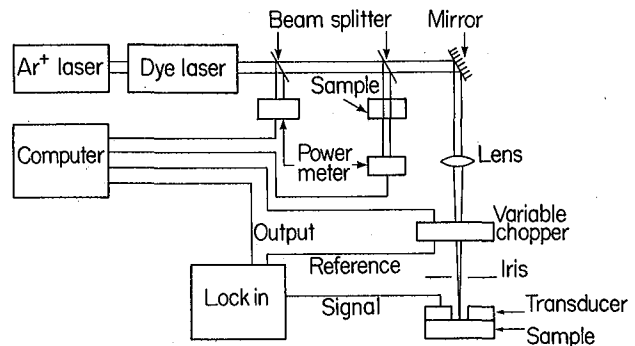


Fig. 5. Experimental apparatus. The two samples are identical. (XBL 797-2317)

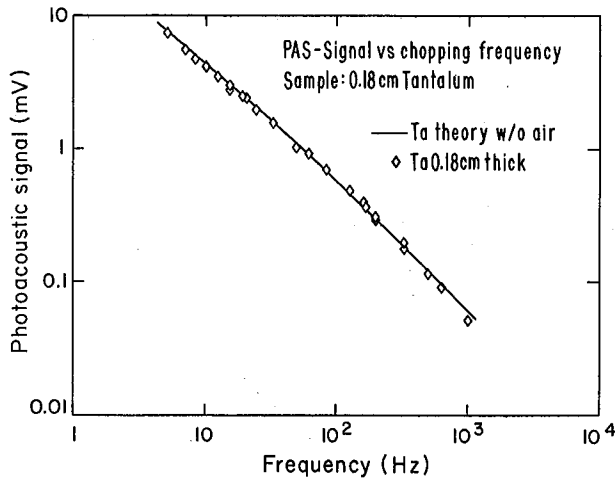


Fig. 6. PAS signal vs. modulation frequency. Both full theory (no thermal or optical length approximations are made) and experiment show slightly less than a  $1/\omega$  dependence ( $1/\omega+0.9$ ). (XBL 797-2312)

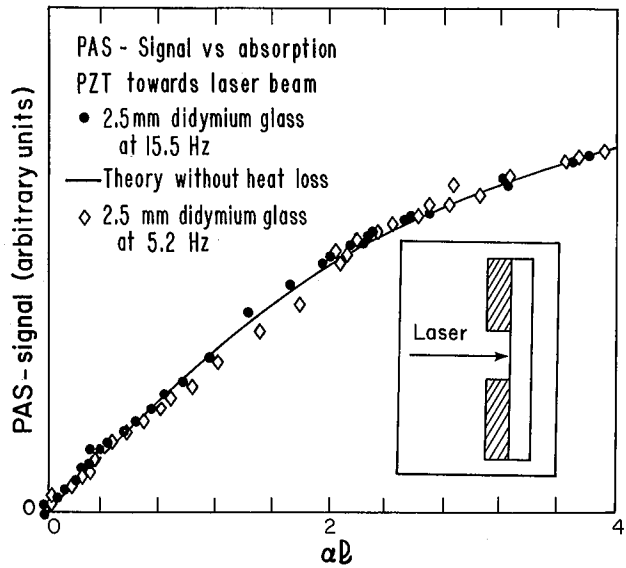


Fig. 8. PAS signal vs.  $\alpha\ell$ . (XBL 797-2308)

relationship between the photoacoustic signal and optical absorption is highly nonlinear. The signal goes to zero at  $\alpha\ell = 2$ , where the compression due to the bending equals the expansion due to the heating. In Fig. 7 we show the abrupt  $180^\circ$  phase shift by a negative amplitude. When the transducer is towards the laser beam ( $z=0$ ) (Fig. 8), the bending and expansion terms add, increasing the observed signal. There is no saturation until high values of absorption.

The Dependence of Signal on Sample Thickness. To test the  $1/\ell$  (Eq. 2) dependence, we varied the thickness by using varying lengths of black coated glass rods. We found that the signal exhibits approximately a  $1/\ell$  dependence.

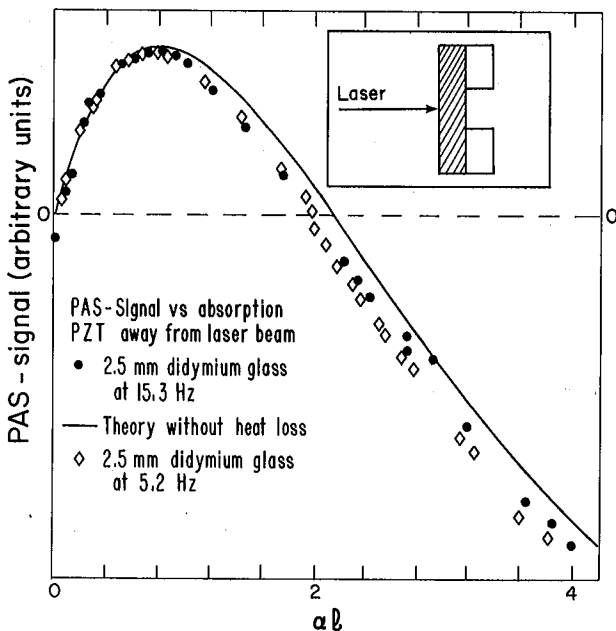


Fig. 7. PAS signal vs.  $\alpha\ell$ . Inset shows direction of incident light in relation to the transducer. At  $\alpha\ell \sim 2$ , the phase undergoes a  $180^\circ$  phase shift which is indicated by making the signal amplitude negative. (XBL 797-2309)

Signal Dependence on the Thermal Properties of the Sample. We have compared the relative magnitudes of the photoacoustic signal obtained from aluminum, tantalum, and copper samples of identical thickness. Although the results are complicated by uncertainties concerning the reflectivity of the samples, the relative values are in agreement with the predictions. The experimental ratio of tungsten (which has a high  $E$ ) to tantalum is smaller than predicted. However, the experimentally obtained tungsten signal is smaller than that obtained for tantalum, as is qualitatively predicted by our theory.

The phase of the metal samples shows the predicted  $180^\circ$  phase shift at the predicted frequencies. When the thermal diffusion length is on the order of the sample thickness, the phase shifts. Consequently, because copper has a longer thermal diffusion length, the phase shifts at a higher frequency than tungsten.

We also point out that the absolute theoretical magnitudes of the signal are within a factor of 2 of experimental values. Part of the discrepancy is due to greater absorption than was assumed in the theory. The greater absorption results from surface irregularities and contaminants. Finally, we verified that to within 5% the signal does not depend on the beam radius.

Having tested the theory on a variety of samples with a wide range of thermal and optical properties, we have found good agreement. Consequently, we believe that the theory is useful for quantitative calculations of the expected signal.

### Noise Analysis and Noise Equivalent Power

We next analyze the sources of noise and estimate a total noise equivalent power (NEP) for our detector. This discussion identifies factors which limit the sensitivity and serves as a guide for designing an optimized PAS-PZT detector. The noise factors we have considered are electronic noise, material dielectric loss noise, DC leakage noise, Brownian motion of the detector, and thermal noise. The first two are the most important, although DC leakage noise can become significant if the detector is improperly constructed.

**Electronic Noise.** Since the PZT is a high impedance device, the preamp should contain an FET front end. Consequently, we follow the approach of Van der Ziel<sup>19</sup> and Byer<sup>20</sup> for constructing a noise equivalent circuit including an FET. One can neglect  $R_{dc}$ ,  $R_{ac}$  (providing no low resistance path shunts the transducer), and  $C_a$  as far as their effect on the impedance of the network. Furthermore, since one is typically operating at a frequency such that  $1/\omega C \ll R_{inp}$ , the total impedance of the network is  $Z = 1/i\omega C$ . The rms noise voltage due to the amplifier is given by:

- 1)  $V_I = i_n |Z| \Delta f^{1/2}$  from the current noise
- 2)  $V_V = e_n \Delta f^{1/2}$  from the voltage noise

where

$$i_n^2 = 2eI_g$$

$$e_n^2 = (8k_B T / 3g_m) (1 + f_o/f) + (4k_B T) / R_L \text{ gm}^2$$

$I_g$  - gate leakage noise

$g_m$  - FET transconductance

$f_o$  - 1/f noise corner frequency

$R_L$  - load resistor

$T$  - amplifier temperature

$\Delta f$  - lock-in bandwidth.

Since the signal for all cases has the form

$$V = J P |Z| / \ell$$

where

$$J = e_{31}^P a_t (1+\nu) / (C\rho)_{\text{sample}}; \quad Z = 1/\omega C = L/\omega \epsilon_{33}^P A$$

we get the contributions to the NEP,

$$(NEP)_I = i_n \ell / J \quad (5)$$

$$(NEP)_V = e_n \ell \epsilon_{33}^P A / J L \quad (6)$$

At low frequencies since  $e_n \sim 1/\omega^{1/2}$ . Then  $(NEP)_V \propto \omega^{1/2}$ .

**PZT Material Noise Sources.** The dielectric loss and leakage noise contributions are

$$(NEP)_D = \ell / J \left( \frac{4k_B T \omega \epsilon_{33}^P A \tan \delta}{L} \right)^{1/2} \quad (7)$$

and

$$(NEP)_{DC} = \ell / J \left( \frac{4k_B T \sigma A}{L} \right)^{1/2} \quad (8)$$

where  $\tan \delta$  is the dielectric loss tangent and  $\sigma$  is the volume resistivity.

**Fundamental Noise Sources.** The NEP due to fluctuations of the temperature of the transducer is

$$(NEP)_{\text{thermal}} = \frac{(4k_B g_H)^{1/2} T_P \ell}{(\rho C)_{\text{PZT}} L J} \quad (9)$$

and the NEP due to Brownian motion is approximately

$$(NEP)_{\text{Brownian}} = \left( \frac{4k_B T A \ell \omega \epsilon_{31}^P}{L^3 Q \rho_{\text{PZT}} \omega_o^3 J} \right)^{1/2} \quad (10)$$

where  $g_H$  is the thermal conductance with the surroundings,  $\rho$  is the pyroelectric coefficient for the transducer,  $Q$  is the  $Q$  of the transducer, and  $\omega_o$  is the first resonance of the PZT.

**Numerical Results.** We consider a numerical example. For our PZT,  $C = 1.2 \times 10^{-8}$  F,  $A = 1 \times 10^{-5}$  m<sup>2</sup>,  $\tan \delta = 0.01$ ,  $L = 1.78 \times 10^{-4}$  m,  $\sigma = 10^{-11}$   $\Omega^{-1}$  cm<sup>-1</sup>,  $g_H = 7.019 \times 10^2$  J/sec/°C,  $\rho = 0.1 \times 10$  coul/cm<sup>2</sup>/°C,  $\rho = 5.2$  g/cm<sup>3</sup>,  $C_V = 0.4$  J/g/°C,  $Q = 75$ ,  $\omega_o = 2\pi(5 \times 10^5)$ . Using the noise figures for our lock-in amplifier we get the noise shown in Table 1. The measured system noise was 17 nV/Hz<sup>1/2</sup> at 16.6 Hz for a totally isolated detector. The agreement between the theoretical and measured noise is fortuitous since many factors such as  $\tan \delta$  are estimates. However, these values are useful for assessing the relative contributions of the different noise sources.

The measured voltage responsivity was giving an  $NEP_V = 5 \times 10^{-8}$  W at 16.6 Hz. If the dielectric loss tangent does not become significantly large at lower frequencies, operation at 5 Hz can improve this figure somewhat. In our experiments, we achieved an NEP of  $1 \times 10^{-7}$  W for thin metals and  $6 \times 10^{-7}$  W for transparent samples.

### Discussion

Despite the complex nature of the problem, we have shown that our three-dimensional treatment

Table 1. Noise contributions (nV/ $\sqrt{\text{Hz}}$ ).

Source	Magnitude (nV/Hz <sup>1/2</sup> )
Electronic	12.9
Dielectric loss	11.42
DC leakage	0.61
Brownian motion	1.37
Thermal	1.67
Total rms	17.4

yields a simple expression (Eq. 1) which quantitatively describes the experimentally observed PZT photoacoustic signal.

We show that the PZT measures the temperature distribution within the sample. There is no complication due to the delay or propagation of a thermally induced sound wave. For thermally non-conductive samples, the temperature distribution is proportional to the heat deposited per volume.

It is important to point out that our theory is not a linearized theory, and it does not assume that the sample is thin, although in thin sample cases one can derive an identical expression using thin plate theory. Our theory is applicable for  $\alpha l$  as high as 10 for thermally non-conductive media. The applicability of this theory may be readily extended beyond the limitations of our assumptions and without appreciably altering our findings.

Several simplifications of the theory which cannot easily be eliminated should be noted. The first one involves neglecting the interaction between the sample and the PZT. If the sample is thick compared to the PZT and the PZT is relatively compliant, the transducer measures the strain of the sample as assumed by the theory. If, however, the transducer thickness is comparable to or larger than that of the sample, the theory may be expected to break down for three reasons. First, the transducer will measure the stress in the sample rather than the strain. Second, the expansion of the sample will be altered. Finally, the neutral surface (the surface of zero displacement) for the transducer-sample combination is located within the transducer. This causes a reduction in the signal since the piezoelectric material on one side of the neutral surface expands while it compresses on the other sides. These two contributions tend to cancel out, reducing the net signal. Consequently, although the signal to noise ratio improves as the transducer gets thicker, the theory may no longer be valid.

A second limitation concerns the contribution of the pyroelectric effect. If significant amounts of heat are transmitted to the transducer, the transducer would develop thermal stresses of its own and produce a voltage due to the pyroelectric

effect. This would become significant only in the case of very low chopping frequencies, high thermal conductivities of the sample, and thermally conductive adhesive.

Finally, the transducer restricts large bending motions even if it is relatively compliant or thin compared to the sample. Hence, one expects that at high absorptions and low diffusivities the bending contribution may be somewhat less than that theoretically predicted.

From an experimental viewpoint, the main factor limiting the detector performance is the background signal which results from the scattering of light on the PZT. This background signal is wavelength dependent and can be minimized, for example, by depositing a layer of highly reflecting material on the PZT before coupling it to the sample.

#### Considerations for Detector Optimization and Final Remarks

Equations 5-10 do not yield an absolute value for the NEP. However, they do give the relative dependence of the NEP on various important parameters and can be used for the purpose of optimizing the PZT-PAS detector. In Table 2, we give a set of rules of thumb for an optimized detector.

In conclusion, we have presented and experimentally verified a theoretical model which quantitatively accounts for the PZT photoacoustic signal. This should enhance the utility of PZT-PAS as a useful spectroscopic tool. We have also shown that the PZT directly detects heat-induced strain caused by the absorption of electromagnetic radiation.

#### FOOTNOTE AND REFERENCES

\*The complete version of this work was published in J. of Appl. Phys. 51, 3343 (1980).

1. L. B. Kreuzer, J. of Appl. Phys. 42, 2934 (1971).
2. J. G. Parker and J. Ritke, J. Chem. Phys. 59, 3713 (1973).
3. R. D. Kamm, J. App. Phys. 47, 3550 (1976).
4. R. Gerlach and N. M. Amer, App. Phys. Lett. 32, 228 (1978).
5. L. J. Thomas, M. Kelly, and N. M. Amer, App. Phys. Letters 32, 736 (1978).
6. D. Wake and N. M. Amer, Appl. Phys. Lett. 34, 379 (1979).
7. J. F. McClelland and R. N. Kniseley, Appl. Phys. Lett. 28, 467 (1976).
8. G. C. Wetsel, Jr. and F. A. McDonald, J. Acoust. Soc. Am. 60, 852 (1976).
9. C. K. N. Patel and A. C. Tam, Appl. Phys. Lett. 34, 760 (1979).
10. A. Rosencwaig and A. Gersho, J. Appl. Phys. 47, 64 (1976).

Table 2. Recommendations for signal to noise optimization.

Category	Quantity	Recommendation
Electronic	$g_m$	large
	1/f noise	small
	$I_g$	small
	PZT Area	small
	PZT Thickness	large <sup>a</sup>
	Sample Thickness	large <sup>a</sup>
PZT Properties	$\epsilon_{31}^p$	large
	$\tan \delta$	small
	$\epsilon_{33}^p$	small
	$\sigma$	small
	$\rho$	small
Sample Properties	$a_t$	large
	$(\rho C)_{\text{sample}}$	small
	$T_{\text{PZT}}$	low
Modulation Frequency	$\omega$	low <sup>b</sup>

<sup>a</sup>The sample should not be much thinner than the PZT, otherwise the neutral surface of the PZT-sample configuration will occur within the PZT leading to a reduction of the signal.

<sup>b</sup>The amplifier voltage NEP goes down as the frequency until the amplifier current noise NEP dominates. Further reduction will not improve the signal to noise ratio because of the difficulty in isolation low frequency vibrations.

11. L. C. Amodt, J. C. Murphy and J. G. Parker, J. Appl. Phys. 48, 927 (1977).
12. H. S. Bennett and R. A. Forman, Appl. Optics 15, 1313 (1976).
13. H. S. Bennett and R. A. Forman, J. App. Phys. 48, 1432 (1977).
14. J. G. Parker, Appl. Optics 12, 2974 (1973).
15. S. A. Schleusener, J. D. Lindberg, K. O. White, and R. L. Johnson, Appl. Opt. 15, 2546 (1976).
16. Z. Yasa, N. M. Amer, H. Rosen, A. D. Hanson, and T. Novakov, Appl. Optics 18, 2528 (1979).
17. Eastman 910 is a cyanoacrylate adhesive manufactured by Eastman Company.
18. TRA-CON 2113 low viscosity epoxy manufactured by TRA-CON.
19. A. Van der Ziel, Noise in Measurements (John Wiley and Sons, New York, 1976).
20. C. B. Roundy and R. I. Byer, J. Appl. Phys. 44, 929 (1973).

### A New Method for the Determination of Absolute Absorption Coefficients by Photoacoustic Spectroscopy

It has been well recognized that photoacoustic spectroscopy provides a sensitive means for measuring absorption coefficients ( $\alpha$ ) of various substances. One method for the determination of  $\alpha$  is a least square fit of the data as a function of frequency using the general expression for the photoacoustic signal.<sup>1</sup> Another approach is to obtain a reference signal from a medium with identical thermal properties to that of the sample of interest but with a different yet known absorption coefficient.<sup>2</sup> By taking the ratio of the two signals, unknown constants other than the absorption coefficients cancel and  $\alpha$  is thus determined. However, for many substances (particularly solids) such a reference is not readily available.

We describe here a novel approach which uses the sample itself to yield the reference signal (Fig. 9). We show that for high frequency modulation at which the sample is thermally thick, the ratio of signals  $S_2$  and  $S_1$  (obtained when the light is incident on  $W_2$  and  $W_1$ , respectively) yields a measure of  $\alpha$  as given by  $S_2/S_1 = k \exp(-\alpha \ell)$  where  $k$  is a correction factor for reflection at the boundaries.

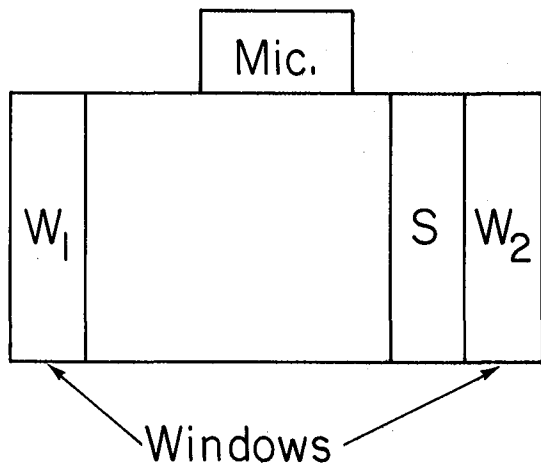


Fig. 9. Experimental apparatus. (XBL 8010-4443)

#### REFERENCES

1. G. C. Wetsel, Jr. and F. A. McDonald, *Appl. Phys. Letters* **30**, 252 (1977).
2. A. C. Tam, C. K. N. Patel, and R. J. Kerl, *Opt. Letters* **4**, 81 (1979).

### A Novel Approach to Photoacoustic Determination of the Thermal Diffusivity of Condensed Matter

We report on a new method for determining the thermal diffusivity of liquids and solids.

Consider the experimental geometry shown in Fig. 10. For a highly absorbing sample M, the ratio of the magnitudes of the signal ( $S_2$ ) obtained when the beam is incident from the sample side to that obtained when it is incident on the window side ( $S_1$ ) gives a measure of the thermal diffusivity as shown below:

$$S_2/S_1 = \left\{ \cosh^2 (\pi f/\beta)^{1/2} \ell - \sin^2 (\pi f/\beta)^{1/2} \ell \right\}^{-1/2}$$

where  $\beta$  is the thermal diffusivity,  $f$  is the modulation frequency, and  $\ell$  is the sample thickness.

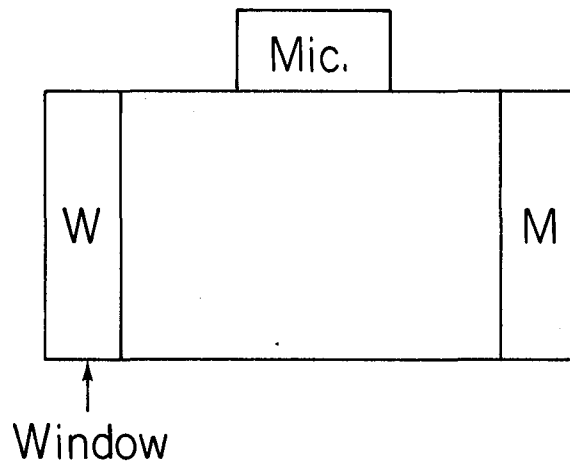


Fig. 10. Experimental apparatus. (XBL 8010-4442)

### A Photoacoustic Investigation of Urban Aerosol Particles\*

The nature of the absorbing species in atmospheric aerosol particles has recently attracted considerable attention among atmospheric and environmental scientists. Recent studies using Raman spectroscopy and an optical attenuation technique<sup>1</sup> indicate that the absorbing species in urban particulates is "graphitic" carbon. We report here on the results of a photoacoustic investigation which gives an independent verification of the hypothesis.

Unlike conventional optical absorption techniques, photoacoustic spectroscopy measures the energy deposited in a sample due to absorption.

Since questions have been raised whether the optical attenuation technique exclusively measures the absorbing rather than the scattering component of the aerosol, a comparison between photoacoustic and optical attenuation measurements made on the same aerosol sample should help resolve this ambiguity.

The photoacoustic measurements were made in an acoustically nonresonant detector with cylindrical geometry (Fig. 11). A Knowles microphone (Model BT-1759) was used, and the cell dimensions were 2.1 cm in diameter and 0.3 cm in length. The gas in the detector cell was air at atmospheric pressure. A He-Ne laser operating at 632.8 nm with 0.5 mW of power was used as the light source, and the experiments were performed at a modulation frequency of 20 Hz. The aerosol particles, collected on 1.2- $\mu$  Millipore filter substrates, were mounted on a 1.5-mm-thick Pyrex backing with the particles facing the incident light beam. Experiments were also performed with the laser beam first incident on the filter substrate.

In the limit of low frequency light modulation ( $\leq 100$  Hz), it can be shown<sup>2,3</sup> that the photoacoustic signal is given by:

$$V(\omega) = \frac{\eta\gamma PW\mu_g\mu_{sb}G(\omega)}{2\sqrt{2bkTVK_{sb}}} [1 - \exp(-\alpha l)] \quad (1)$$

where

- $\eta$  - heat conversion efficiency
- $\gamma$  - specific heat ratio for air ( $C_p/C_v$ )
- $P$  - cell pressure
- $W$  - input power
- $\mu_g$  - thermal diffusion length in air
- $\mu_{sb}$  - thermal diffusion length in substrate
- $G(\omega)$  - microphone response

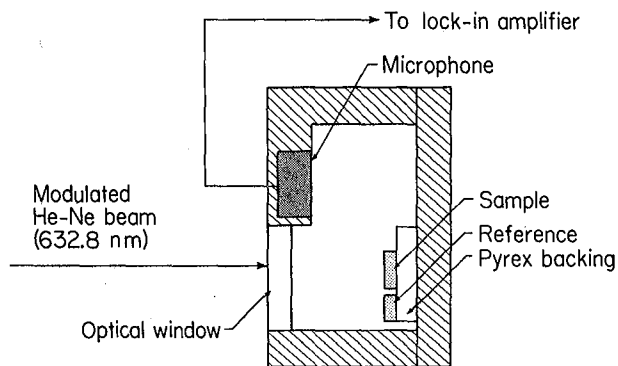


Fig. 11. Experimental arrangement. (XBL 794-1230)

$b$  - dimensionless parameter taking into account the diffusion of heat from the sample to the Pyrex backing

$T$  - temperature

$V$  - cell volume

$K_{sb}$  - thermal conductivity of substrate

$\alpha$  - absorption coefficient

$l$  - effective path length.

From Eq. (1) it follows that the photoacoustic signal saturates exponentially with increasing absorption to a value of

$$V_{sat}(\omega) = \frac{\eta\gamma PW\mu_g\mu_{sb}G(\omega)}{2\sqrt{2bkTVK_{sb}}} \quad (2)$$

Hence the ratio of the signal from a given sample to a reference sample for which the signal is saturated yields

$$S_{ph} = V/V_{sat} = 1 - \exp(-\alpha l) \quad (3)$$

This saturable behavior was observed for highly absorbing samples, and the sample which yielded the largest photoacoustic signal was used as the reference,  $V_{sat}$ . Note that such samples yield values of  $\alpha l \geq 3$ , as deduced from the optical attenuation measurements; hence the highest signal obtained from available samples is close to the actual saturation value.

The experimental setup for the optical attenuation measurements is described elsewhere.<sup>1</sup> In this technique the signal  $S_{op}$  is defined as  $1 - \exp(-x)$ .  $x$  is the optical attenuation of the sample and is given by  $-\ln I/I_0$ , where  $I$  is the transmitted intensity of a loaded filter, and  $I_0$  is the transmitted intensity of a blank filter.

In Fig. 12 we present a plot of the normalized photoacoustic signal  $S_{ph}$  vs.  $S_{op}$  for a wide range of ambient samples and samples collected directly from combustion sources. The samples include urban particulates collected over a 24 hour period in Fremont and Anaheim, California; Denver, Colorado; and New York, New York; and particles collected in a highway tunnel and from an acetylene torch. The least squares fit of the experimental points yields a correlation coefficient  $r$  of 0.98 and a slope of 1.03, which would be expected if both techniques measure the same optical property of the aerosol particles. Since the photoacoustic signal is proportional to the heat generated by absorption, we conclude that the optical attenuation method measures the light absorbing component of the aerosol particles.

From a theoretical point of view, this result is somewhat surprising since aerosol particles have a large scattering coefficient, which would be expected to contribute to the optical attenuation measurement and not to the photoacoustic signal.

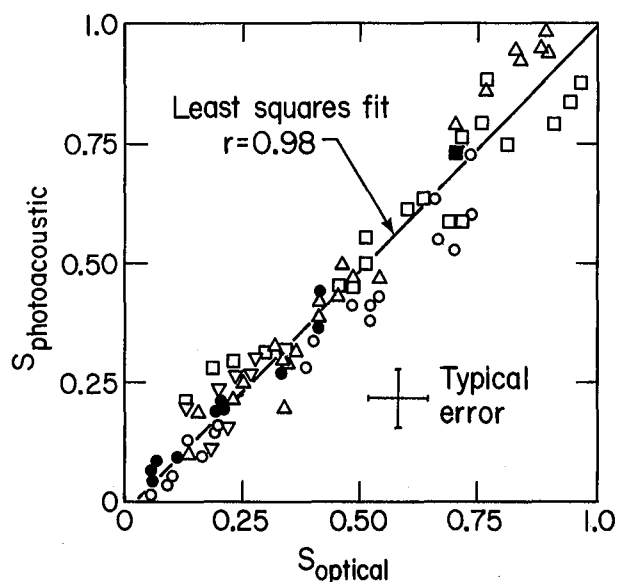


Fig. 12. Plot of  $S_{ph}$  vs.  $S_{op}$  for various samples:  
 ▽ - Fremont; □ - Anaheim; ○ - Denver  
 ▲ - New York City; ■ - highway tunnel;  
 ● - acetylene torch.  
 The solid line is a least squares fit of the  
 data. (XBL 794-1229)

However, careful examination of the experimental arrangement shows that the incident light interacts not only with the aerosol particles but also with the filter medium, which is almost a perfect diffuse reflector. In this circumstance, it is possible to show<sup>4</sup> that because of multiple reflections between the particles and the filter substrate, the optical attenuation measurement is insensitive to the scattering properties of the aerosol.

In conclusion, the results presented here, when combined with Raman scattering data<sup>1</sup> and thermal analysis<sup>5</sup> and solvent extraction results,<sup>6</sup> indicate that the optically absorbing component of urban aerosol particles is "graphitic" carbon.

#### FOOTNOTES AND REFERENCES

\*Appeared in *Applied Optics*, **18**, 2528 (1979).

†In collaboration with H. Rosen, A. D. A. Hansen and T. Novakov of the Atmospheric Aerosol Research Group at LBL.

1. H. Rosen, A. D. A. Hansen, L. Gundel, and T. Novakov, "Identification of the optically absorbing component in urban aerosols," *Appl. Opt.* **17**, 3859 (1978).
2. Over a frequency range of 5-100 Hz, the photoacoustic signal showed no variation, indicating that the sample was thermally thin. In this case, Eq. (1) follows from Eq. (21) of Ref. 3 in the limit of  $\omega \rightarrow 0$  and after modification of their parameter  $b$  to take into account an additional boundary layer introduced by the Millipore filter.

3. A. Rosencwaig and A. Gersho, "Theory of photoacoustic effect with solids," *J. Appl. Phys.* **47**, 64 (1976).
4. H. Rosen and T. Novakov, "Optical attenuation: a measurement of the absorbing properties of aerosol particles," in *Atmospheric Aerosol Research Annual Report 1977-78*, Lawrence Berkeley Laboratory Report LBL-8696, p. 54.
5. H. Rosen, A. D. A. Hansen, L. Gundel, and T. Novakov, "Identification of the graphitic carbon component of source and ambient particulates by Raman spectroscopy and an optical attenuation technique," *Proceedings, Conference on Carbonaceous Particles in the Atmosphere*, Lawrence Berkeley Laboratory, 1978 (in press).
6. R. E. Weiss, A. P. Waggoner, R. J. Charlson, D. L. Thorsell, J. S. Hall, and L. A. Riley, "Studies of the optical, physical, and chemical properties of light absorbing aerosols," *Proceedings, Conference on Carbonaceous Particles in the Atmosphere*, Lawrence Berkeley Laboratory, 1978 (in press).

#### Photoacoustic Characterization of the Optical Properties of Hydrogenated Amorphous Silicon

Recently, there has been strong interest in amorphous silicon and hydrogenated amorphous silicon because of their potential photovoltaic applications and their unique properties as amorphous materials.

The amorphous silicon hydrogen films (a-Si:H) are produced either by r.f. decomposition of silane ( $\text{SiH}_4$ ) or sputtering silicon targets in a hydrogen environment. The resulting films can contain up to 50 atomic percent hydrogen which gives the films their interesting properties. The films have an optical band gap which varies with hydrogen content from 1.2 eV to 2 eV and, unlike other amorphous materials, can be both n and p-type doped. The latter property allows one to construct solar cells from a-Si:H films which could be manufactured for much lower cost than current crystalline solar cells.

The role of hydrogen in determining the density of states in the gap, defect traps, recombination centers, and doping mechanisms are poorly understood at present. The usual method of studying such problems is to measure the absorption of the sample using radiation of energy less than the band gap. Since the thin films have weak absorption and scatter significantly, conventional absorption measurements yield inaccurate or misleading results.

We have developed a sensitive photoacoustic technique which solves these problems. Since the technique only measures the power absorbed, we find that it is very sensitive to small absorption and is insensitive to scattering.

Using a dye laser, we have obtained spectra over limited regions of the visible which are quite similar to traditional absorption measurements.

We are extending our measurements to  $1\mu$  (1.2 eV) by using appropriate dyes.

Due to the greater tuning range of pulsed laser sources in the 1-2.2  $\mu\text{m}$  region, we are currently investigating the pulsed response of our photoacoustic signal. The integral of the peak response of the detector over short time periods after the laser pulse arteries can be related to the absorption of the sample. Consequently, we should be able to extend absorption measurements throughout the region below the band gap of 1.5 eV.

Having demonstrated the feasibility and power of our photoacoustic technique, we plan to make systematic measurements of the gap absorption as a function of film quality, hydrogen content, defect, and impurity concentration, and doping levels. Such measurements enable us to understand those factors which determine the ultimate conversion efficiency of amorphous photovoltaic devices, and will shed light on some aspects of the physics of amorphous semiconductors.

#### APPLICATIONS OF LIQUID CRYSTALS

The liquid-crystalline state of matter is characterized by a spontaneous anisotropic order and by fluidity. The anisotropic order leads to anisotropy in the physical properties of the medium, and the fluidity makes it easily susceptible to external perturbations. Such perturbations can be in the form of electric or magnetic fields, pressure or temperature. In addition, we have demonstrated that certain gaseous organic pollutants change the liquid-crystalline structure. This change, which is readily detectable, is the basis for an inexpensive and sensitive ( $10^6$ ) personal dosimeter for some organic pollutants. Two other applications of liquid crystals are described below.

##### Liquid Crystal Magnetometer

The purpose of this program is to develop a sensitive (fraction of a gauss) and simple dosimetry technique for occupational exposures to magnetic fields in fusion plants. Our approach will involve the use of ferro-nematic and ferro-cholesteric liquid crystals.

The physics behind the proposed device is that incorporating non-spherical magnetic grains into the liquid crystal matrix allows the nematic and cholesteric molecular orientation to be coupled to a very weak external magnetic field. The coupling, which is mechanical in nature, is due to the elastic properties of the liquid-crystalline phase. This coupling is what we proposed to exploit as the basis for our magnetic dosimeter.

Specifically, the orienting effect of the "host" liquid-crystalline matrix upon the "guest" magnetic grains results in a net magnetization in the absence of an applied field, and this remnant magnetization provides the mechanism for coupling to the external magnetic field. At zero external field, the ferro-liquid crystal exhibits certain optical properties. In the case of ferro-cholesterics, a specific wavelength of light is

selectively reflected. For ferro-nematics, a given light intensity is transmitted through the birefringent sample.

Upon the application of an external magnetic field (as weak as one gauss), the coupling of the spontaneous magnetization to the field induces the disruption of the liquid-crystalline order causing the optical properties of the matrix to change: (1) in the case of ferro-cholesterics the wavelength of the selectively reflected light will vary as a function of the applied field, and at a critical field strength, complete disruption of the cholesteric order will occur; (2) in the case of ferro-nematics, as the external field increases, the matrix birefringence will change and the intensity of light transmitted through crossed polarizers will vary. As in the case of ferro-cholesterics, at a certain critical external field, total disorder of the nematic phase sets in.

Typical preliminary results are shown in Fig. 13 depicting the change in induced birefringence as a function of applied magnetic field.



Fig. 13. The change in induced birefringence as a function of applied external magnetic field.  
(XBB 793-3173)

To prevent the magnetic grains ( $\text{Fe}_2\text{O}_3$ ) from flocculating, the following procedure was adopted. The magnetic grains are ellipsoidal in shape and are approximately  $0.5 \mu$  long; the aspect ratio is approximately 7:1. In addition, the particles carry a magnetic dipole moment, averaging  $2 \times 10^{-12}$  gauss-cm<sup>3</sup>.

The earliest attempts to disperse the particles involved placing them directly in the liquid crystal (MBBA) at room temperature ( $T_r$ ) and sonicating. It was observed that dispersion is difficult, particularly in light of the large energy associated with adjacent magnetic dipoles ( $\sim 10^5 k_B T_r$ ). Furthermore, once the particles were dispersed, there appeared to be a strong tendency to recluster, the result of strong magnetic interactions as well as Van der Waal attractions.

To overcome these difficulties, a multistep procedure has been implemented. The magnetic particles are first placed into an approximately 10 percent (by weight) solution of hexadecyl-trimethylammonium-bromide (HTAB) in chloroform. The entire mixture is placed in a bottle, along with a dozen small steel balls, and agitated in a vortex mixer for several minutes. The turbulent motion is sufficient to overcome the large dipolar energy, and the particles are readily separated. During this time, the non-polar ends of the HTAB molecules attach themselves to the magnetized particles, while the polar heads protrude into the highly polar chloroform.

The mixture is allowed to sit for about 30 minutes, during which time the largest non-dispersed aggregates settle out. A sample from the fine suspension (top) is removed and slowly centrifuged until nearly all the particles have settled out. The remaining suspension, composed of chloroform, HTAB, and well-dispersed HTAB-coated particles, is removed and again centrifuged this time at high speeds, forcing all the remaining particles to settle. The chloroform and HTAB solution on top is then poured off, and new chloroform is added. In this way the excess HTAB is disposed of.

The system of chloroform and HTAB-coated magnetic particles is again shaken in the vortex mixer to redisperse the particles. Since the head groups of the HTAB are sufficiently polar, they tend to prevent the particles from recluster. (At this point it may be necessary to repeat the procedure, beginning with rapid centrifugation, to further dispose of any remaining excess HTAB.)

A sample of chloroform and well-dispersed HTAB-coated particles is then mixed in equal amounts with MBBA. By heating the system and simultaneously vacuum pumping, it is possible to purge nearly all the chloroform, leaving a mixture of HTAB-coated particles in a matrix of MBBA which provide the matrix for our dosimeter.

#### Novel Applications of Amphiphilic Liquid Crystals for Energy Production

The polymorphism of amphiphilic liquid crystals can be exploited for the recovery of oil from oil shale and for cleaning oil spills. However, the nature of such polymorphism is not well charac-

terized. One of the goals of our research is to gain a better understanding of the behavior of these amphiphilics and to devise the optimum parameters for their utilization as a means of oil extraction.

The molecules being studied contain both polar and non-polar regions (amphiphilic molecules) and it is this property that gives the substance its interesting behavior. For example, bulk solutions containing a few percent of water exhibit a complex liquid crystalline behavior. Bilayers of such molecules have been studied as models for the cell's membrane. One can also form monomolecular films using amphiphilics and this is where our interest lies. In particular, we form a layer at the interface between water and a non-polar hydrocarbon solvent. This layer ranges in surface density from zero up to a maximum molecular density before the 2-d monolayer collapses into a more thermodynamically stable 3-d system. Within this density range, for various temperatures, we are able to measure the 2-d equivalent pressure and thus generate phase diagrams and possibly also study some nonequilibrium properties. In our recent work, we have observed phases that perhaps correspond to the 2-d equivalent of a solid, liquid, and liquid crystalline phases. Our earlier work investigated the phase transitions of these monolayers at the air/water interface using the non-perturbing technique of light scattering to probe the physics of the monolayer. We are now trying to clarify some of the many unanswered questions concerning films at the water/oil interface. These questions include the nature of the phases, whether the transitions are first or second order, the local symmetry of the "solid" region and the importance of possible three dimensional effects.

Our experimental method is to study the light scattered from thermally excited interfacial ripples or "ripples". Thermal fluctuations of the system near room temperature spontaneously produce surface waves of a few angstroms mean amplitude. (By comparison, the lipid molecules we are studying, L- $\alpha$ -DPPC, are about 25 angstroms long and can be compressed to a maximum surface density of 30 square angstroms per molecule.) These ripples move with a velocity which varies with the monolayer concentration and have a lifetime dependent on surface as well as bulk viscosities. Thus if we choose to measure only ripples of a precise  $q$ , by scattering into a lens/pinhole system at  $\approx 1^\circ$ , we can extract physical information by analyzing the doppler shifted laser frequency and the lifetime determined linewidth. Since frequency shifts due to ripplon-photon scattering are on the order of tens of kilohertz, we use light beating spectroscopy. The scattered, frequency-shifted beam is mixed with unshifted laser light and the two beat together on the photocathode of a PMT. Using photon counting techniques, this signal is fed to a digital autocorrelator and the resulting time domain spectrum is then fit by an in-lab computer. Thus if we know the ripplon  $q$ , we are able to extract the frequencies and damping coefficient of the ripplon. Then, using hydrodynamics we extract the 2-d pressure (surface tension) and viscosity. Since we already know temperature and density (we vary density with an all glass, specially coated compression piston) we have all variables required

to study the phases of the system, thus obtaining the equilibrium thermodynamic properties of this 2-d system.

Other parameters can also be varied such as length of the molecule, type of polar and non-polar region, chain length of the hydrocarbon solvent, etc. In addition, one must be very careful about surface absorbing impurities. This puts very stringent purity requirements on all components of the system. Room vibration effects must also be minimized and a precision, actively leveled, air piston isolated optical table has been set up. Temperature control is also critical since the laser beam is totally internally reflected from the oil/water interface and convection currents tend to grossly defocus the laser beam.

Some of these experimental difficulties were overcome during the early work of H. Birecki and N. M. Amer investigating films at air/water interfaces.<sup>1</sup> We have subsequently developed the light scattering technique for oil/water systems and are now setting up a new experimental cell designed to eliminate problems we encountered earlier and to deal with new difficulties peculiar to liquid/liquid systems. During initial oil/water monolayer experiments, we were able to perfect the injection technique used to apply the molecules to the liquid interface. We also observed the expected change in surface density due to the oils' solvation of the lipid's tails. The elimination of what may have been a 2-d liquid-gas coexistence region in the earlier air/water interface experiments was also seen. Mutual attraction of the DPPC molecules' tails would presumably have provided the mechanism for this transition. This attraction is greatly reduced by the hydrocarbon solvent. In addition, we have paid close attention to items such as impurities, monolayer leaks, temperature gradients, and  $g$  calibration in the new cell. We anticipate clean data from this set up with the emphasis on carefully measuring the phase transitions in this 2-dimensional system. Once this is achieved, work on vesicle formation and emulsification in this amphiphilic system will be initiated.

\*This work supported by DOE/EV, Office of Pollutant Characterization and Measurement.

#### REFERENCES

1. H. Birecki and N. Amer, Journal de Physique 40, C3-433 (1979).
2. H. Birecki and N. Amer, Bull. Am. Phys. Soc. 24, 251, A09 (1979).

#### FUTURE DIRECTIONS

Laser photoacoustic detection work will continue in the direction of developing ultra-sensitive multiparameter molecular detectors for the characterization of gaseous trace contaminants, particularly those associated with synfuels. We plan to extend photoacoustic detection to water pollutants, with specific emphasis on nitrates, sulphates and organic contaminants. Efforts will be given to the elemental detection and analysis by a tunable laser photoacoustic spectrometer. Our collaboration with the Atmospheric Aerosol Research Group at LBL will continue investigating optical properties of carbonaceous particulates.

Research on the optical characterization of amorphous silicon will continue to study the optical nature of the "gap states". De-excitation mechanisms of the photoexcited amorphous films will be investigated, and photoacoustic spectra of hydrofluorinated amorphous silicon will be obtained. Our prime motivation is to explore optically the means of achieving higher conversion efficiencies from these devices.

Various applications of liquid crystals will continue to be explored. Optimization and comparison of ferro-nematic and ferro-cholesteric dose-integrating magnetometers will be made, and prototypes will be constructed; the actual field tests will be conducted in magnetic fusion experimental areas. Work on gaseous organic detectors will aim at investigating the fundamental mechanism responsible for the observed effect, and sensitizers will be incorporated in the liquid crystal detector to adjust the concentration threshold. Finally, in the case of lyotropic monolayers, work will continue on the oil-water interface, and the investigation of emulsification and vesicle formation will be carried out.

## OPERATION OF A GAS CHROMATOGRAPH/MASS SPECTROMETER FOR THE IDENTIFICATION OF COMPONENTS IN FOSSIL ENERGY AND ENVIRONMENTAL SAMPLES\*

*A. S. Newton and W. Walker*

The Finnigan Model 4023 gas chromatograph/mass spectrometer/data system has operated with few problems other than routine maintenance during the year. The system has been operated almost exclusively with a 30 meter, OV-101 capillary column. This column gives excellent results with most samples,

and mixtures too complex to be resolved on this column are unlikely to be better resolved on a different type column. In some cases, however, major components in a mixture will elute at identical times even with capillary column separation ability (~100,000 theoretical plates). For iden-

tification, if the compounds are of unrelated types, it is often possible to determine that an obvious mixture exists and to identify each component present. A case of this type was observed in the reconstructed ion chromatogram (RIC) of a mixture of fatty acid methyl esters contaminated in the methylation step by methylated cyclo siloxanes. The heptanoic acid methyl ester and octamethyl cyclo tetrasiloxane each eluted at 744 seconds. Each compound was identifiable in the mixture owing to the very different mass spectra of the two materials. A different type chromatographic column would have separated the two compounds.

Attempts to use the Finnigan GC/MS in the chemical ionization mode have not been successful, and work needs to be done in improving the operation in the CI mode.

During the past year the system has been used for the investigation of approximately 400 samples, including several test mixtures. Each research group submitting samples for the instrument has different type samples and the problems of investigating the samples differ. Most samples received have been complex, containing more than 20 components each. A few have hundreds of components and the reconstructed ion chromatogram is a manifold of largely unresolved gas chromatographic peaks.

It is not possible to identify every component in a complex mixture. However, for those components with well resolved chromatographic peaks and mass spectra of good quality, information on molecular weight and composition can be obtained from good parent ion intensity information. From the occurrence or non-occurrence of mass peaks at key mass numbers, it is frequently possible to identify the component as a compound type without identification of the specific isomer present. This is particularly true of compounds containing long alkyl groups. The number of isomers possible in 8 or 9 carbon alkyl or alkenyl groups is formidable. A separate analysis of each mass spectrum by a knowledgeable chemist may lead to the identification of the compound from which the spectrum was derived. This is, however, too time-consuming to be used as a general procedure unless the specific identification is of prime importance.

A very interesting series of samples resulting from the catalytic polymerization of the low molecular weight alkenes ( $C_2H_4$ ,  $C_3H_6$ , and  $i-C_4H_8$ ) were studied. The polymerization products were higher alkenes in the  $C_8$  to  $C_{20}$  carbon number range. While the mass spectral libraries have the mass spectra of only a few isomers of alkenes in this molecular weight range, the interaction of the mass spectroscopist with the experimenter resulted in the identification of many specific branched alkenes from the fragmentation patterns of each chromatographic peak with some knowledge of the polymerization mechanism.

Air samples taken in Tenax sampling tubes have been studied for the identification of organic

compounds in air. As the GC/MS has not yet been adapted for directly accepting the gaseous products desorbed from the Tenax collectors, the air impurities were desorbed into a small drop of pentane. The pentane solution was then investigated by GC/MS. This method has been successfully applied for the identification of many of the pollutants present in various air samples. If was found, however, that the relative amounts of each specific component in the pentane solution was highly dependent on the conditions of storage of the pentane solution before injection into the GC/MS. The ampoule cap materials were found to be selective adsorbents for trace impurities in the pentane, and even overnight storage in a refrigerator or freezer made a drastic change in the RIC of the samples. Some lighter components were completely missing after overnight storage of the sample.

Samples from the methylation of waste waters from various oil shale retorting processes have resulted in the identification of fatty acids and di-acids as significant organic contaminants of those waters. Acids from 5 to 14 carbons were identified. Branched chain fatty acids and unsaturated acids were present in lesser amounts than were the straight chain acids. A direct extract of the oil shale water shows a complicated chromatograph with some heterocyclic nitrogen bases such as the pyridines and quinolines as prominent components.

Samples of several metal-organic compounds have been investigated for their behavior in a GC/MS analysis scheme. Samples of Ni and Hg diketone complexes were not successfully chromatographed, whereas the Zn and Cu compounds were chromatographed. Much work remains to be done on various types of metal-organics before their gas chromatographic behavior can be successfully predicted and dependable identifications and analyses made by this method.

The GC/MS system has proved to be useful in many ways to other research and supporting groups at LBL. One example is the identification of chlorinated biphenyls in various transformers being replaced at LBL. This is an important problem in the disposal of these transformers.

A series of samples were studied in regard to the composition of vapors emitted from various construction materials in a vacuum. This information is of prime importance in the construction of particle detectors.

GC/MS characterization of samples derived from the extraction of sea water and of organisms living in sea water was continued. The extreme complexity of most such samples makes identification of more than a few specific components impossible. By searching the mass chromatograms of specific ions, e.g.,  $M = 256$ , the possible occurrence of specific compounds can be documented, and an upper limit on the amount of such compounds present can be set within fairly wide probable error limits.

\* This work was supported in part by the Assistant Secretaries of Environment and Fossil Energy, DOE.

## DEVELOPMENT AND APPLICATION OF X-RAY FLUORESCENCE ANALYTICAL METHODS\*

R. D. Giauque

### INTRODUCTION

The development and application of trace multi-element x-ray fluorescence (XRF) analytical methods are used to support a variety of research programs. Using XRF analytical techniques, oil shale, shale oils, oil shale retort waters, liquid and solid industrial wastes, atmospheric aerosols, coal fly-ash, geological specimens, salts, foods, and alloys have been analyzed during the past year.

### ACCOMPLISHMENTS DURING 1979

Members of the Instrument Techniques Group completed modifications to one of our x-ray systems. A pulsed x-ray tube was installed and the automatic sample handling system was redesigned. Subsequently, we developed computer programs applicable for analysis of both liquid and solid samples using this x-ray system. Additionally, a straight-forward procedure was established for the determination of 42 elements (Ti → La, Hg, Pb, Bi, Th, and U) in aqueous samples. Seven 4 λ drop-lets are placed in a reproducible geometrical array over a 1 cm<sup>2</sup> area on 1/4 mil polypropylene film and dried overnight in a desiccator. These samples are treated as infinitely thin specimens with no significant x-ray absorption for the elements determined. Using three different x-ray excitation conditions for each sample, and a total analysis time of approximately twenty minutes, typical sensitivities realized are in the 0.5 to 5 ppm range. Table 1 lists results determined for two industrial waste liquids. These results illustrate the capability of the method.

Additionally, a method for the direct determination of trace elements in light element matrices has been published.<sup>1</sup> This method was briefly described in the 1979 Energy and Environment Division Annual Report, pg. 288.

### PLANNED ACTIVITIES FOR 1980

X-ray fluorescence analytical methods will be applied to support oil shale, geochemical, industrial waste management, and atmospheric aerosol research programs. A method for the determination of 42 elements in small quantities (25 mg) of geochemical samples is being developed. Additionally, a procedure for the determination of the elements Mo → Ba in oil samples will be established.

Table 1. Elemental concentrations in two industrial waste liquid samples ( $\mu\text{g/g} \pm 2\sigma$ ).

Element	HML-614	HML-615
Ti	<6	<12
V	<4	<8
Cr	88.9 ± 8.8	80.5 ± 8.0
Mn	3.2 ± 2.4	48.6 ± 5.4
Fe	379 ± 37	3920 ± 390
Co	<9	<14
Ni	1.9 ± 0.6	7.2 ± 1.4
Cu	2.8 ± 0.8	25.3 ± 2.5
Zn	48.9 ± 4.8	224 ± 22
Ga	<2	<2
Ge	<1	<1
As	<5	<5
Se	<1	<0.6
Br	<0.6	0.8 ± 0.4
Rb	<0.6	2.1 ± 0.4
Sr	2.4 ± 0.4	11.0 ± 1.0
Y	<2	2.5 ± 1.0
Zr	<0.6	9.6 ± 1.0
Nb	<0.6	<0.6
Mo	13.2 ± 1.3	1.8 ± 0.6
Ru	<2	<2
Rh	<2	<2
Pd	<2	<2
Ag	<2	<2
Cd	<2	4.8 ± 1.8
In	<2	<2
Sn	26.3 ± 2.6	86.8 ± 8.6
Sb	<3	<3
Te	<3	<3
I	<4	<5
Cs	<5	<5
Ba	36.9 ± 4.8	293 ± 29
La	<8	<8
Hf	<12	<15
Ta	<15	<22
W	<8	<15
Hg	<6	<6
Pb	312 ± 31	238 ± 23
Bi	<4	<4
Th	<3	<6
U	<5	<4

### REFERENCE

1. R. D. Giauque, R. B. Garrett, and L. Y. Goda, *Anal. Chem.* **51**, 511 (1979).

\*This work supported by DOE, Basic Energy Science.

## THE SURVEY OF INSTRUMENTATION FOR ENVIRONMENTAL MONITORING\*

*M. S. Quinby-Hunt, Y. C. Agrawal, C. R. Chen, R. D. McLaughlin,  
G. Morton, D. L. Murphy, and A. V. Nero*

### INTRODUCTION

The survey of Instrumentation for Environmental Monitoring began at LBL in 1971 and has continued to the present.<sup>1</sup> It has become an important resource for those involved in monitoring our environment and with controlling the emission of pollutants in various industrial processes. An analysis of the 4000 purchasers of the survey indicates that the majority of them are responsible directly or indirectly for the monitoring or control of pollutant emissions. This is an area of growing concern so that interest in the survey can be expected to increase.

The survey volumes describe the various substances, both conventional and radioactive, which may pollute the air and water surrounding us, giving their characteristics, sources and effects.<sup>2</sup> The methods for detecting and analyzing each pollutant are also described and compared. And finally, detailed specifications for instruments which are commercially available for carrying out the more common techniques used in each field are given in complete sets of Instrument Notes. The contents of the volumes are given in Fig. 1.

Volume 1 AIR		Volume 2 & 2A WATER	Volume 3 RADIATION	Volume 4 BIOMEDICAL
Parts 1 & 1A	Part 2			
Gases	Particulates	Calibration	Type of	Gases
Calibration	Systems	Metals	radiation	CO
SO <sub>2</sub>	Mass	Nitrogen	Alpha	SO <sub>2</sub>
NO and NO <sub>2</sub>	Size	Phosphorus	radiation	Organics
Oxidants	Opacity	Sulfur	Beta radiation	Particulates
CO	Composition	Biochemical	X and gamma	Asbestos
Hydrocarbons	Mercury	oxygen	radiation	Metals
	Asbestos	demand	Neutron	Arsenic
	Beryllium	Chemical	Spectroscopy	Beryllium
	Lead	oxygen	Personnel	Cadmium
	Noise	demand	dosimetry	Lead
		Dissolved oxygen	Radionuclides	Mercury
		Total organic	Tritium	Nickel
		carbon	Krypton-85	Radiation
		Pesticides	Strontium-	
		Phenolics	89,90	
		Petrochemicals	Iodine-129,131	
		Oil and grease	Radon-222 &	
		pH	daughters	
		Turbidity	Radium	
		Temperature	Plutonium	
		Radiation	Sources	
			Nuclear	
			reactors	
			Mining &	
			milling	
			Natural	
			radiation	
			Fallout	
INSTRUMENT COMPARISONS are contained in appropriate sections				

Fig. 1. Contents of the volumes comprising the Survey of Instrumentation for Environmental Monitoring.

\*This work supported by DOE/EV, Office of Health & Environmental Research.

### ACCOMPLISHMENTS DURING 1979

In 1979, a number of major updates were completed. Several other updates and revisions were started. The completed updates include:

1. The Introduction for the WATER volume was revised to include an extensive discussion of Federal water regulations (including P.L. 92-500 and current changes in it).
2. The section on Metals in Water in the same volume was revised and expanded to include instrument notes on plasma emission spectrometers and discussions on atomic spectroscopy, ultraviolet spectrometry, x-ray fluorescence and neutron activation analysis.
3. Several new sections on metals were added to the BIO volume.
4. The BIO volume was expanded to include a section on Gaseous Organic Pollutants.

### PLANNED ACTIVITIES FOR 1980

In 1980, several major revisions are planned. By mid-1980, the work now underway on the complete revision of the RADIATION volume will be finished. This work will include sections on Radiation Types, Monitoring by Radiation Type, and Monitoring by Radionuclide. There will be new sections on nuclear reactors, fuel processing and reprocessing. The discussion of biological effects of radiation will be brought up to date and expanded.

Further updating of the WATER volume will include sections on the halogens and cyanide, suspended and dissolved solids, asbestos and coliform bacteria.

Updates of the AIR volume, part 2, will discuss sampling and calibration, and will contain updated instrument notes on Mass and Size. Particle composition will be examined next. Some of the analytical techniques described in this section will include expanded sections on x-ray fluorescence, and new sections on techniques such as ESCA, SSMS and others.

In carrying out these revisions and updates, material is included in response to reader-expressed interest and in response to the need for consideration of pollutants associated with developing energy technologies. Much of the material in the survey has a direct bearing on the pollution problems associated with energy generation and interest in the survey can be expected to grow as the demand for new energy sources within a safe environment becomes more urgent.

## REFERENCES

1. Environmental Instrumentation Survey Group, Instrumentation for Environmental Monitoring, Lawrence Berkeley Laboratory Report, LBL-1 (1971-present).
2. The report is divided into four volumes, currently in seven looseleaf binders: AIR, Part 1, Gases (2 binders) and Part 2, Particulates; WATER (2 binders); RADIATION; BIOMEDICAL.

## EXTRATERRESTRIAL CAUSE FOR THE CRETACEOUS-TERTIARY EXTINCTION: EXPERIMENT AND THEORY

L. W. Alvarez,\*† W. Alvarez,†† F. Asaro,\* and H. V. Michel\*

### INTRODUCTION

Abundant fossil remains provide a record of organic evolution for the last 570 million years of Earth history. During this time there have been six great biological crises, during which many groups of organisms died out. Numerous crises of less severity are also recorded.

The most recent of the great extinctions is used to define the boundary between the Cretaceous and Tertiary Periods, about 65 million years ago. At this time, the marine reptiles, the flying reptiles, and both orders of dinosaurs died out.<sup>1</sup> Extinctions occurred at various taxonomic levels among the marine invertebrates, for example, the ammonoid and belemnoid cephalopods and various groups of gastropods, pelecypods, brachiopods, and echinoderms. Dramatic extinctions occurred among the microscopic floating animals and plants; both the calcareous planktonic foraminifera and the calcareous nannoplankton were nearly exterminated, with only a few species surviving the crisis. On the other hand, some groups were little affected, including the land plants, crocodiles, snakes, birds, mammals, and many kinds of invertebrates.

Many hypotheses have been proposed to explain the Cretaceous-Tertiary extinctions,<sup>2</sup> and two recent meetings on the topic<sup>3,4</sup> produced no sign of a consensus. Suggested causes include gradual or rapid changes in oceanographic, atmospheric, or climatic conditions<sup>5</sup> resulting either from a random<sup>6</sup> or a cyclical<sup>7</sup> coincidence of causative factors, the effect of a magnetic reversal<sup>8</sup> or a nearby supernova.<sup>9</sup> Various mechanisms specific to a single group, such as disease or destruction of dinosaur eggs by mammals, are incapable of explaining why the extinctions affected many groups.

A major obstacle to determining the cause of the extinction is that virtually all available information on events at the time of the crisis deals with biological changes seen in the paleontological record, and is thus inherently indirect. Little physical evidence is available, and it, also, is indirect. This includes variations in stable oxygen and carbon isotopic ratios across the boundary in pelagic sediments, which may reflect changes in temperature, salinity, oxygenation, and organic productivity of the ocean water, and these variations are not easy to interpret.<sup>10</sup> These isotopic

changes are not particularly striking, and taken by themselves they would not suggest a dramatic crisis. Changes in minor and trace element levels at the Cretaceous-Tertiary boundary have been noted from limestone sections in Denmark and Italy,<sup>11</sup> but these data also present interpretational difficulties. It is noteworthy that in pelagic marine sequences, where nearly continuous deposition is to be expected, the Cretaceous-Tertiary boundary is almost invariably marked by a hiatus.<sup>12</sup> Because of the lack of clear evidence outside the field of paleontology, it is still possible to argue that the various extinctions were not exactly synchronous, that they were produced by a fortuitous combination of ordinary environmental stresses, and that there really was no Cretaceous-Tertiary boundary crisis.<sup>6</sup>

### ACCOMPLISHMENTS DURING 1979

In this work direct physical evidence was found for an unusual event at exactly the time of the extinctions in the planktonic realm. None of the current hypotheses adequately accounts for this evidence, but we have developed a new hypothesis that appears to offer a satisfactory explanation for nearly all the available paleontological and physical evidence.

Anomalous concentrations of platinum-group elements in deep-sea sediments are used as indicators of influxes of extraterrestrial material; the technique is based on the extreme depletion of these elements in the earth's crust. We have made measurements by neutron activation analysis of many elements including the platinum-group element iridium (Ir) in Upper Cretaceous-Lower Tertiary marine limestones from two areas. The first area is in the Umbrian Apennines of Italy, where recent paleomagnetic studies have established the timing of the planktonic extinction in the sequence of geomagnetic polarity reversals.<sup>13</sup> Analysis of the acid-insoluble clay fraction of the limestone shows iridium levels of about 0.3 ppb in the uppermost Cretaceous. The Cretaceous-Tertiary boundary is marked by a 1 cm clay layer in which iridium suddenly jumps to about an average of 6 ppb in the acid-insoluble residue, then gradually decreases to the previous background level in less than 1 m above the boundary as shown in Fig. 1. To test whether this is a local phenomenon, we have

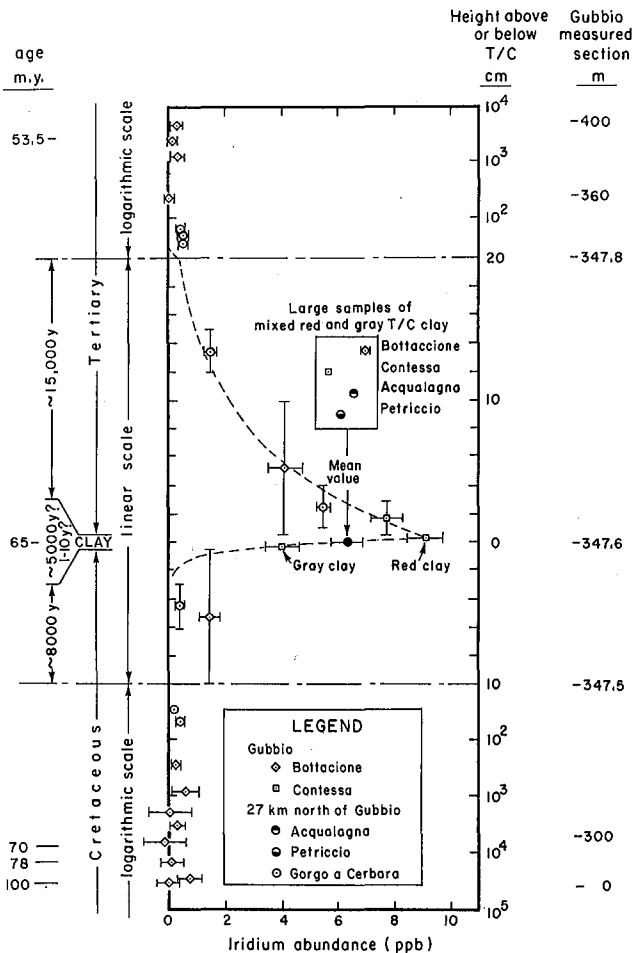


Fig. 1. Stratigraphic section at Gubbio (6,7).  
 (a) Meter levels. (b) Systems. (c) Stages.  
 (d) Magnetic polarity zones (black is normal, white is reversed polarity; letters give Gubbio polarity zonation, numbers are equivalent marine magnetic anomalies). (e) Lithology. (f) Samples used in first neutron activation analysis study (samples I, J, L are from equivalent positions in the Contessa section, 2 km to the northwest). (g) Formation names. (XBL 7911-13250)

analyzed samples from a classic exposure of the Cretaceous-Tertiary boundary near Copenhagen and found iridium levels nearly ten times higher than are seen in the Italian sections, with an increase from the background levels by about a factor of 160. Figure 2 shows the elemental abundances in twelve samples from Gubbio, Italy.

Discussion of these results leads to the conclusion that the anomalous iridium was probably introduced into the Earth's atmosphere as part of an abnormal influx of extraterrestrial material at the time of the extinctions. One possible extraterrestrial cause of the extinctions, a nearby supernova, has been debated for some time. Three lines of evidence are used for rejecting the supernova hypothesis:

- $^{244}\text{Pu}$  (80 x  $10^6$  yr half life) should be detectable along with Ir in the boundary

clay if a supernova is responsible for the Ir anomaly, but if present,  $^{244}\text{Pu}$  is at least a factor of 10 below predicted levels. This fact alone is not conclusive, as oceanic chemistry could alter the Ir/Pu ratio.

- The ratio  $^{191}\text{Ir}/^{193}\text{Ir}$  might well be significantly different in supernova material at the boundary and in normal terrestrial material, but no difference was found.
- To account for the Ir seen in the boundary clay, a hypothetical supernova would have to be so close that the probability of such an event becomes vanishingly small.

We conclude that the extraterrestrial material introduced at the time of the extinctions came from a solar system source and not a galactic source (including a supernova).

After consideration and rejection of a number of possible explanations for the extraterrestrial material and the extinctions, we have developed the following hypothesis, which seems to account for most or all of the relevant observations: A number of asteroids have orbits with perihelions inside the Earth's orbit; these are called "Apollo Objects." Collisions of Apollo objects with the Earth are inevitable, and the many known meteor craters are the result. We suggest that the impact of a large Apollo object was the cause of the Cretaceous-Tertiary extinctions. Four independent calculations indicate that the impacting Apollo object had a diameter of approximately 10 km. Such an impact would produce a crater approximately 175 km in diameter. The material expelled from the crater would weigh about 100 times as much as the asteroid, and much of the combined mass would stay aloft for several years as dust in the stratosphere. Comparisons of this effect with the much smaller explosion of Krakatoa in 1883 indicate that the atmosphere would become opaque to visible light until the dust settled, although enough heat would reach the surface to prevent a major drop in temperature.

The resulting suppression of photosynthesis appears to be capable of explaining the major features of the extinctions. The marine phytoplankton would die out through loss of light with which to carry on photosynthesis. This would cause the collapse of the food chain supporting the planktonic foraminifera and the large open marine fauna, including ammonites, belemnites, and marine reptiles. Terrestrial plants would cease to grow, but would not die out because their seeds could lie dormant until the dust settled and light returned. Small terrestrial animals including the mammals, as well as the birds, would survive on a food chain based on seeds and nuts. The herbivorous dinosaurs and the carnivorous dinosaurs that preyed on them depended on a food chain based on growing vegetation; this chain would have collapsed. The survival of many marine invertebrates and aquatic animals such as crocodiles may be due to their ability to utilize food chains based on nutrients derived from decaying land plants carried by rivers to the shallow seas.

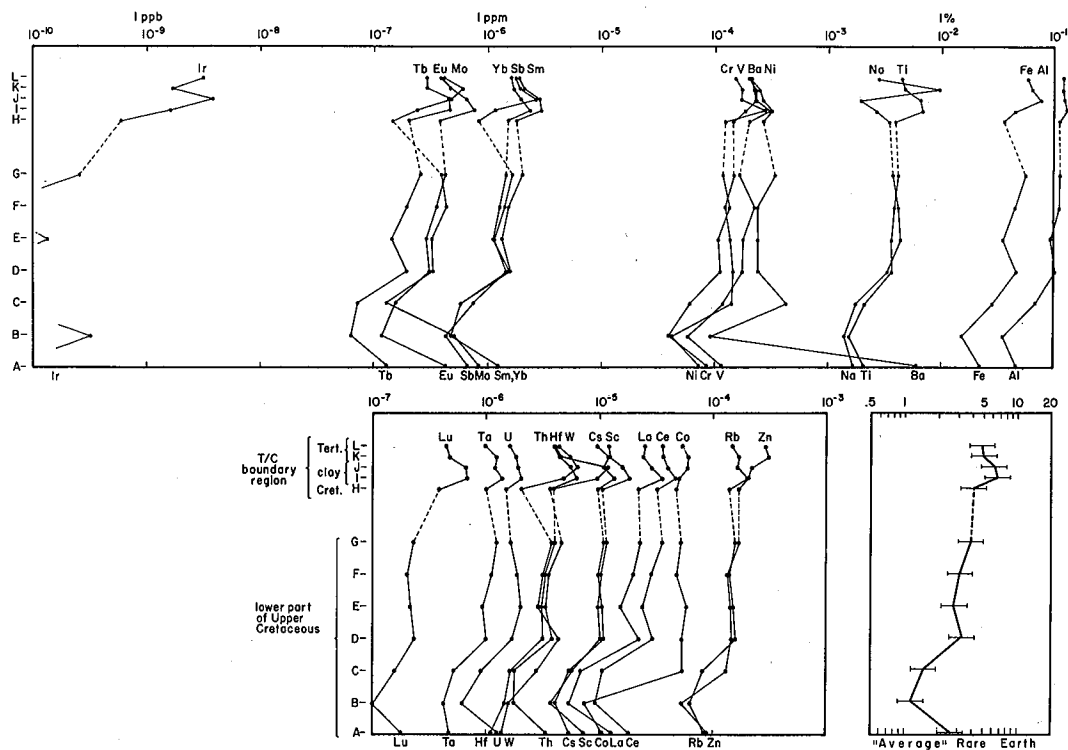


Fig. 2. Abundance variations of 28 elements in 12 samples from two Gubbio sections. (XBL 795-9861)

Thus it appears that a highly probable sequence of events could produce the observed extinctions, and independent physical evidence for this mechanism has now been found.

#### IDENTIFICATION OF EXTRA-TERRESTRIAL PLATINUM METALS IN DEEP-SEA SEDIMENTS

This study began with the realization that platinum group metals and some related elements (Pt, Ir, Os, Rh) are  $10^3 - 10^4$  times more abundant in chondritic meteorites than they are in the earth's crust and upper mantle.<sup>14</sup> Carbonaceous chondrites are thought to come from undifferentiated bodies giving a close approximation to average solar system elemental abundance. Depletion of the platinum group metals in the earth's crust and upper mantle is probably the result of concentration of these elements in the earth's core.

Platinum elements are apparently below detection levels in most sedimentary rocks, judging from the few published data.<sup>15</sup> This is reasonable because in addition to their scarcity in rocks from which sediments are derived, they are also extremely insoluble and should be present only at very low levels in river and sea water (again, data are not available).

These considerations suggested to us that much of the iridium to be found in sedimentary rocks comes from ablated meteoritic dust, deposited at a

roughly constant rate. We suspected that measurement of platinum metals might shed light on the time interval represented by the 1 cm thick clay layer that marks the Cretaceous-Tertiary boundary in the Umbrian Apennines. We therefore undertook an investigation of the abundance of iridium, which can easily be determined at low limits by neutron activation analysis (NAA) because of its large capture cross section for slow neutrons, and because the gamma rays given off during de-excitation of the decay product are not masked by other gamma rays. The other platinum group elements are more difficult to determine by NAA.

After we had begun our work, we learned that this method of identifying extraterrestrial material had been suggested in the early 1950's by Pettersson and Rotschi and by Goldschmidt<sup>16</sup> and actually carried out in the 1960's by Barker and Anders.<sup>17</sup> Subsequently the method was used by Ganapathy et al.<sup>14</sup> to demonstrate an extraterrestrial origin for silicate spherules in deep-sea sediments. Sarna-Wojcicki et al.<sup>18</sup> suggested that meteoritic dust accumulation in soil layers might enhance the abundance of iridium sufficiently to permit its use as a dating tool.

We have found that iridium does show anomalously high abundances at exactly the stratigraphic position of the Cretaceous-Tertiary boundary in two areas, Italy and Denmark, where marine limestones preserve a complete or nearly complete record of this time interval.

## ACKNOWLEDGMENTS

It will be obvious to anyone reading this paper that we have benefited enormously from our conversations and correspondence with many friends and colleagues throughout the scientific community. We would particularly like to acknowledge the help we have received from James R. Arnold, Andrew Buffington, I. S. E. Carmichael, Garniss Curtis, Philippe Eberhard, Earl K. Hyde, Christopher McKee, Maynard C. Michel (who was responsible for the mass spectrometric measurements), John Neil, Bernard M. Oliver, Charles Orth, Barrie Pardoe, and Andrew M. Sessler. One of us (W. A.) thanks the U.S. National Science Foundation for support, the other three authors thank the U.S. Department of Energy for support, and one of us (L.W.A.) thanks NASA for support. The XRF measurements of trace elements, Fe and Ti by Robert D. Giaouque and the XRF measurements of major elements by Steve Flexer and Marian Sturz were most appreciated. We appreciate the assistance of Dan Jackson and Cecilia Nguyen in the sample preparation procedures. We are grateful to Tek Lim and the staff of the Berkeley Research Reactor for many neutron irradiations used in this work. We also appreciate the efforts of Gordon Pefley and the staff of the Livermore Pool Type Reactor for the irradiations used for the Ir isotopic ratio measurements.

## FOOTNOTES AND REFERENCES

\*Lawrence Berkeley Laboratory, University of California, Berkeley.

\*†Space Sciences Laboratory, University of California, Berkeley.

††Department of Geology and Geophysics, University of California, Berkeley.

1. D. W. Russell, Geol. Assoc. Canada Sp Rep 13, 119 (1975).
2. M. B. Cita and I. Premoli Silva, Riv. Ital. Pal. Strat. Mem. 14, 193 (1974). D. A. Russell, Ann. Rev. Earth Planet. Sci. 7, 163 (1979).
3. K-TEC group. Proceedings of the Workshop held in Ottawa, Canada. 16-17, Nov. 1976. Syllogus No. 12. Cretaceous-Tertiary Extinctions and Possible Terrestrial and Extraterrestrial Causes. Nat. Mus. of Natural Sciences.
4. T. Birkelund and R. G. Bromley, ed. Cretaceous-Tertiary Boundary Events. Symposium, Univ. of Copenhagen 1979. I. The Maastrichtian and Danian of Denmark. W. K. Christiansen and T. Birkelund ed., Symposium Univ. of Copenhagen 1979. II. Proceedings.
5. H. Tappan, Paleogeography, Palaeoclimatology, Palaeoecology 4, 187 (1968); T. R. Worsley, Nature (London) 230, 318 (1971); W. T. Holser, ibid. 267, 403 (1977); D. M. McLean, Science 200, 1060 (1978); D. M. McLean, ibid. 201, 401 (1978); S. Gartner and J. Keany, Geology 6, 708 (1978).
6. E. G. Kauffman, Ref. 4, Vol. II, p. 29 (1979).
7. A. G. Fischer, Ref. 4, Vol. II, p. 11 (1979); A. G. Fischer and M. A. Arthur, Soc. of Economic Paleontologists and Mineralogists, Sp. Pub. 25, 19 (1977).
8. J. F. Simpson, Geol. Soc. Am. Bull. 77, 197 (1966); C. G. A. Harrison and J. M. Prospero, Nature (London) 250, 563 (1974); J. D. Hays, Geol. Soc. Am. Bull. 82, 2433 (1971).
9. O. H. Schindewolf, Nenes Jahrb. Geol. Paleontol. Monatsh. 1954, 451 (1954); ibid. 1953, 270 (1958); A. R. Leoblich, Jr., and H. Tappan, Geol. Soc. Am. Bull. 75, 367 (1964); V. I. Krascvski and I. S. Shklovsky, Dokl. Adad. Nauk SSR 116, 197-199 (1957); K. D. Terry and W. H. Tucker, Science 159, 421 (1968); H. Laster, ibid. 160, 1138 (1968); W. H. Tucker and K. D. Terry, ibid. 160, 1138 (1968); D. Russell and W. H. Tucker, Nature (London) 229, 553 (1971); M. A. Ruderman, Science 184, 1079 (1974); R. C. Whitten, J. Cuzzi, W. J. Borucki, J. H. Wolfe, Nature (London) 263, 398 (1976).
10. A. Boersma and N. Schackleton, Ref. 4, Vol. II, p. 50 (1979); B. Buchardt and N. O. Jorgensen, Ref. 4, Vol. II, p. 54 (1979). L. Christensen, S. Fregerslev, A. Simonsen and J. Thiede, Bull. Geol. Soc. Denmark 22, 193 (1973).
11. N. O. Jorgensen, Ref. 4, Vol. I, p. 33 (1979). N. O. Jorgensen, Ref. 4, Vol. II, p. 62 (1979). M. Renard, Ref. 4, Vol. II, p. 70 (1979).
12. H. P. Luterbacher and I. Premoli Silva, Riv. Ital. Paleont. 70, 67 (1964); M. B. Cita and I. Premoli Silva, Riv. Ital. Paleont. Strat., Mem., 14 193 (1974).
13. M. A. Arthur and A. G. Fischer, Geol. Soc. Bull. 88, 367 (1977); I. Premoli Silva, ibid. 88, 371 (1977); W. Lowrie and W. Alvarez, ibid. 88, 374 (1977); W. M. Roggenthen and G. Napoleone, ibid. 88, 378 (1977); W. Alvarez, M. A. Arthur, A. G. Fischer, W. Lowrie, G., Napoleone, I. Premoli Silva, W. M. Roggenthen, ibid. 88, 383 (1977); W. Lowrie and W. Alvarez, Geophys. Jour. Roy. Astr. Soc. 51, 561 (1977); W. Alvarez and W. Lowrie, ibid. 55, 1 (1973).
14. R. Ganapathy, D. E. Brownlee and P. W. Hodge, Science 201, 1119 (1978).
15. J. R. DeVoe and P. D. Lafleur, Modern Trends in Activation Analysis, U.S. Government Printing Office, June 1969. J. H. Crocket in "Activation Analysis in Geochemistry and Cosmochemistry," Proc. of the NATO Advanced Study Inst., p. 339-351, Norway (1970), Universitetsforlaget 1971 OSLO.
16. H. Pettersson and H. Rotschi, Geochim. Cosmochim. Acta 2, 81 (1952); V. M. Goldschmidt, Geochemistry, Oxford Univ. Press. (1954).

17. J. L. Barker, Jr., and E. Anders, *Geochimica et Cosmochimica Acta* 32, 627 (1968).

18. A. M. Sarna-Wojcicki, H. R. Bowman, D. Marchand and E. Helley, private communication to F. Asaro (1975).

## PRECISE ANALYSIS FOR BETTER UNDERSTANDING OF GUATEMALAN OBSIDIAN\*

*F. Stross, F. Asaro, and H. V. Michel*

### INTRODUCTION

The use of sophisticated instrument techniques has proven fruitful in the field of archaeology. Both x-ray fluorescence (XRF) and neutron activation analysis (NAA) have been applied to categorize the compositions of obsidian. During the past fifteen years, the study of the composition patterns of obsidians has been useful in establishing the course of supply routes and trade networks in Mesoamerica. A prime requirement in this work has been to provide a detailed, accurate data bank of the compositions of the regional sources of obsidian. This paper presents information on the extensive source area designated Rio Pixcayá, Department of Chimaltenango, and on recently collected material from a nearby source area, San Bartolomé Milpas Altas, Department of Sacatepequez, the existence of which had been questioned.<sup>1</sup> A map of these areas is shown in Fig. 1.

### RIO PIXCAYÁ

The Rio Pixcayá, Chimaltenango, source area represents a complex series of deposits. Some of the outcrops are difficult to reach, and the samples available for analysis were collected by different individuals at different times, in different geographical contexts. The region from which samples were made available lies within the triangle formed by the villages or towns of Chimaltenango, Choatalum ("Aldea Chatalun"<sup>2</sup>), and Comalapa, all in the Department of Chimaltenango (Fig. 1). Neutron activation analyses of samples of some of these outcrops have been recorded in an earlier report.<sup>3</sup> This paper presents additional information obtained by XRF as well as by NAA. The XRF results, shown in Table 1, include the ratios Rb/Zr and Sr/Zr separately, since the ratios eliminate some systematic errors of measurement. This source area is of particular interest because it was used

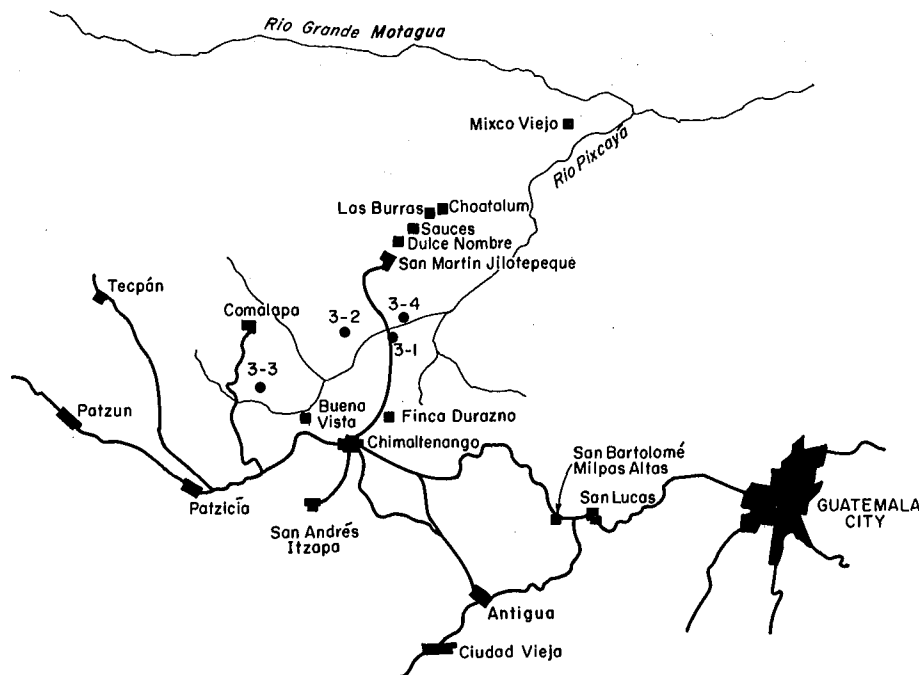


Fig. 1. Map of obsidian sources near Chimaltenango, Guatemala.

nearly 12,000 years ago,<sup>4</sup> although in later times it appears to have played a smaller role than the great deposits of El Chayal and Ixtepeque.

The obsidian collected from the Finca Durazno in the south<sup>3,5</sup> near Chimaltenango, to "Dulce Nombre" in the north, form a coherent group which probably also includes obsidian from the village Chatalun or Choatalun, somewhat further to the north. The measurements on Aldea Chatalun obsidian were made by others and cannot be directly compared with our work. Formulas were developed for comparing the different sets of data, however, and the recalibrated values for Aldea Chatalun obsidian are shown in Table 1. These are roughly consistent with the main group just discussed. Obsidian collected at "Sauces" and "Las Burras", which are reportedly located between Choatalun and San Martin Jilotepeque, are different in composition and readily distinguishable by XRF methods, as seen in Table 1.

The measurements by Zeitlin and Heimbuch<sup>6</sup> on "Jilotepeque" obsidian (San Martin Jilotepeque) agree most closely with the Las Burras group. The source of the "Jilotepeque" obsidian could not be ascertained from their publication.

In addition to the exploratory XRF measurements, NAA runs also were made, and they are recorded in Table 2. The samples collected in the Rio Pixcayá itself near San Martin Jilotepeque, from the Finca Durazno, and from Outcrop 3-1<sup>1</sup> formed a homogeneous group and are combined into a single group designated "representative Rio Pixcayá". The measurements by Hurtado de Mendoza and Jester<sup>7</sup> on San Martin Jilotepeque obsidian agree most closely with the Sauces group as shown in Table 2.

In summary then, nearly all source obsidian labelled Rio Pixcayá or Pixcayá appears to be of the same composition regardless of who collected or measured the obsidian. This composition pattern was found at Dulce Nombre (north of S. M. J.) as well as close to the city of Chimaltenango (Buena

Vista and the Finca Durazno). Most artifacts from distant areas which have been assigned a provenience of S. M. J. or Pixcayá have this composition profile. One "source" sample collected from the Rio Pixcayá by Payson Sheets had a different profile as shown in Tables 1 and 2, and its exact geologic source is not known. Obsidian collected from S. M. J. and the region north and northeast exhibited at least two other composition patterns besides that of the Rio Pixcayá. These are shown in Tables 1 and 2 as the Sauces and Las Burras compositions.

#### SAN BARTOLOMÉ MILPAS ATLAS

The source area of San Bartolomé Milpas Atlas, Sacatepequez, is even less well understood than the Rio Pixcayá source. Recently, several kilograms of obsidian were collected on the Finca Nimachay (in the immediate vicinity of San Bartolomé Milpas Atlas) by the owner, Tomasa Martinez, and forwarded to us by Sr. Enrique Ruiz. Table 3 gives the detailed analyses of a sample from the Finca Nimachay.

Measurements of source material from San Bartolomé Milpas Atlas have been reported.<sup>2,6-8</sup> The data of Cobean and Zeitlin and Heimbuch were intercalibrated with the LBL data and agree as well as could be expected as shown in Table 3. The data of Stross et al. on many elements (not Zr) were intercalibrated with LBL data and agree as well as could be expected except for Zr. Thus, the Zr discrepancy may be a calibration problem. Intercalibration between two laboratories or sets of data does not imply one is more correct than the other, but only serves to make the data interchangeable.

The various measurements by different laboratories and techniques of obsidian from near San Bartolomé Milpas Atlas give similar abundances when intercalibrated. Thus, the source undoubtedly exists. The abundances shown for Finca Nimachay in Table 3 may be taken as representative of the San Bartolomé Milpas Atlas composition group with the qualification that the Sr and Zr values can have calibration uncertainties of ~15-20 percent.

Table 1.

## Chimaltenango - Obsidian Abundances Measured by X-ray Fluorescence

Location:	Other Composition Groups							Other Workers		
	Rio Pixcayá Riverbed	Dulce Nombre	Buena Vista	Representative Rio Pixcayá	Sauces	Las Burras	Odd Sample From Rio Pixcayá Riverbed	Aldea Z & H <sup>(a)</sup> (Revised)	Chatalun Cobean <sup>(b)</sup> (Revised)	Jilotepeque <sup>(c)</sup> Z & H <sup>(a)</sup> (Revised)
No. of samples	4	5	5	14	2	5	1			
<u>Element</u>										
Rb	118 ± 6	115 ± 7	116 ± 6	116 ± 6	120 ± 7	106 ± 6	123 ± 6	127 ± 8	112	118 ± 11
Sr	189 ± 4	192 ± 9	188 ± 6	190 ± 6	191 ± 5	225 ± 11	93 ± 3	186 ± 15	190	202 ± 8
Zr	113 ± 3	117 ± 3	114 ± 3	115 ± 3	137 ± 3	183 ± 8	152 ± 3	111 ± 14	116	180 ± 14
Rb/Zr	1.04 ± .06	.98 ± .07	1.02 ± .04	1.01 ± .05	.88 ± .06	.58 ± .04	.81 ± .04	1.14 ± .16	~ .97	.66 ± .08
Sr/Zr	1.67 ± .06	1.64 ± .08	1.65 ± .06	1.65 ± .06	1.39 ± .05	1.23 ± .08	.61 ± .02	1.68 ± .25	~1.64	1.12 ± .10

- a) In order to compare the data of Zeitlin and Heimbuch with LBL measurements, the Z & H data were modified as follows:  
 $Rb = (Z \& H \text{ value}) * 1.01 - 25$ ,  $Sr = (Z \& H \text{ value}) * 1.12 - 25$ ,  $Zr = (Z \& H \text{ value}) * 1.43 - 25$ . In addition, 15% of the Sr was removed from the Zr value. The errors are the maximum of the square root of the pooled sources variance given by Z & H or the root-mean-square direction in the calibration coefficient used to intercalibrate the two laboratories. These latter are 5%, 4% and 8% for Rb, Sr and Zr respectively.
- b) In order to compare the data of Cobean with LBL measurements, the Cobean data were modified as follows:  
 $Rb = (\text{Cobean mean Rb}) * .9$ ,  $Zr = (\text{Cobean mean Zr}) * 1.23 - .15 * (\text{Cobean mean Sr})$ .  
 Cobean's lower Sr limits were taken as 5 rather than 30 ppm.
- c) "Jilotepeque" obsidian as measured by Z & H cannot be distinguished from Las Burras obsidian as measured in the present work.

Table 2.

Chimaltenango Obsidian Abundances<sup>(a)</sup> Measured by Neutron Activation Analysis

No. of Samples	Representative <sup>(b)</sup> Rio Pixcayá	Las Burras	Sauces	Odd Sample From Rio Pixcayá Riverbed	Other Workers		
					Hurtado de Mendoza et al <sup>(d)</sup>		Jack <sup>(d)</sup>
					San Martin Jilotepeque	Pixcayá	Rio Pixcayá
	8	1	1	1	4	4	1
Al%	7.03 ± 0.20						
Ba	1105 ± 32	1096 ± 17	1042 ± 21	1074 ± 31			1000
Ce	47.5 ± 0.3	51.5 ± .7	47.2 ± .6		47	48	~40
Co	0.38 ± 0.6	0.57 ± .05	.63 ± .05				
Cs	3.37 ± 0.12	2.24 ± .06	3.70 ± .08		4.2	3.8	
Dy	2.03 ± 0.10	2.49 ± .12	2.42 ± .15	3.35 ± .09			
Eu	0.543 ± 0.10	.708 ± .009	.594 ± .010				
Fe%	0.655 ± 0.018	.899 ± .011	.758 ± .010		.78	.65	.65
Hf	3.21 ± 0.10	4.71 ± .07	3.65 ± .06				
K%	3.54 ± 0.25	3.26 ± .35	3.18 ± .34	3.24 ± .31			3.4
La	26.3 ± 0.5	27.1 ± .5	25.8 ± .5				~25
Mn <sup>(c)</sup>	521 ± 10	626 ± 6	589 ± 6	554 ± 6			
Na%	2.94 ± 0.05	3.33 ± .03	3.15 ± .03	3.42 ± .03			
Rb	122 ± 6	118 ± 5	118 ± 4		120	115	129
Sb	0.37 ± 0.05	.31 ± .04	.46 ± .06				
Sc	1.99 ± 0.03	2.031 ± .020	2.112 ± .021		2.12	1.99	
Sm	2.69 ± 0.03	3.170 ± .032	2.839 ± .028				
Ta	0.757 ± 0.008	.683 ± .007	.751 ± .008				
Th	9.24 ± 0.12	7.33 ± .07	9.21 ± .09		9.6	9.4	~5
U	2.81 ± 0.05	2.264 ± .028	2.971 ± .033				
Yb	1.403 ± 0.025	1.759 ± .029	1.676 ± .025				

## Comment:

(a) The errors are the larger of the counting error or (if more than one sample) the root-mean-square deviation.

(b) This group includes 2 samples from the riverbed, 4 from Finca Durazno and 2 from a road cut (outcrop 3-1 as designated by Sidrys).

(c) Recalibrated Z & H Mn values for Aldea Chatalun and Jilotepeque are 496 ± 50 and 561 ± 56 respectively. The recalibration formula was Mn = (Z & H value) \* (.82 ± .08).

(d) Hurtado de Mendoza and Jester's gamma ray counting rate data were changed to ppm or % by multiplying their Ce, Cs, Fe, Rb, Sc (1121 Kev) and Th values by 1.79, .45, .229, 61, .165 and .45 respectively. This calibration is crude and assumes these Cerro Chayal obsidian group is like our El Chayal Village - La Joya obsidian group.

(e) These are XRF measurements by R. N. Jack. They are included in a summary by Stross et al, 1976.

Like Sauces

Like Representative  
Rio PixcayáLike Representative  
Rio Pixcayá

Table 3.

## Element Abundances of Obsidian from San Bartolomé Milpas Altas in Sacatepequez

	<u>Finca Nimachay (this work)</u>	<u>Stross et al - 1976 (see reference e Table 2)</u>	<u>Zeitlin &amp; Heimbuch (Revised) (c)</u>	<u>Cobean (Revised) (d)</u>	<u>Finco Matilandia Hurtado de Mendoza &amp; Jester (Revised) (e)</u>
Al (%)	6.71 ± .10 <sup>(a)</sup>				
Ba	1116 ± 14	1100			44
Ce	42.4 ± .6	~40			
Co	.62 ± .05				
Cs	3.43 ± .07				3.7
Dy	2.15 ± .08				
Eu	.523 ± .009				
Fe (%)	.828 ± .011	.84			.78
Hf	4.09 ± .06				
K (%)	3.48 ± .23	3.3			
La	21.4 ± .5	~20			
Mn	497 ± 10	535	493 ± 40	~465	
Na (%)	3.15 ± .06				
Rb	139 ± 5	115	132 ± 11	~128	131
Sb	.25 ± .04				
Sc	2.258 ± .023				2.20
Sm	2.525 ± .025				
Sr	128 ± 4 <sup>(b)</sup>	115	132 ± 8	~125	
Ta	.593 ± .006				
Tb	9.77 ± .10	~15			10.3
U	3.21 ± .04				
Yb	1.649 ± .024				
Zr	149 ± 4 <sup>(b)</sup>	125	153 ± 12	~144	

(a) Abundances are expressed in ppm or, if indicated after the chemical symbol, in %. The indicated errors in the Finca Nemachay measurements are counting errors.

(b) Measured semi-quantitatively by XRF. These are calibration uncertainties besides the counting errors.

(c) See footnote a of Table 1.

(d) See footnote b of Table 1.

(e) See footnote d of Table 2.

## ACKNOWLEDGMENTS

We thank Professor Payson Sheets of the University of Colorado at Boulder for contributing most of the obsidian sources from Chimaltenango analyzed in this work. More detailed discussions of these samples are appearing in the reports on the excavations in which he has participated under the auspices of the University of Pennsylvania Museum.

## FOOTNOTE AND REFERENCES

\*Work on Mesoamerican obsidian has been funded by the University of Colorado at Boulder, the University of Texas at San Antonio, the University of Pennsylvania, and the U.S. Department of Energy.

1. R. Sidrys, J. Andresen, and D. Marcucci, "Obsidian Sources in the Maya Area," *J. New World Archaeology* 1 (5):1-13 (1976).
2. R. H. Cobean, M. D. Coe, E. A. Perry, Jr., K. K. Turekian, and D. P. Kharkar, "Obsidian Trade at San Lorenzo Tenochtitlan, Mexico," *Science* 174:666-671 (1971).
3. F. Asaro, H. V. Michel, R. Sidrys, and F. H. Stross, "A High-Precision Chemical Characterization of Major Obsidian Sources in Guatemala," *Am. Antiquity* 43:436-443 (1978).
4. F. H. Stross, F. Asaro, H. V. Michel, and R. Gruhn, "Sources of Some Obsidian Flakes from a Paleo-indian Site," *Am. Antiquity* 42:114-118 (1977).
5. F. Asaro, F. H. Stross, R. Sidrys, and H. V. Michel, Energy and Environment Division Annual Report 1978, Lawrence Berkeley Laboratory report, LBL-8619, p. 291-293.
6. R. N. Zeitlin, and R. C. Heimbuch, "Trace Element Analysis and the Archaeological Study of Obsidian Procurement in Precolumbian Mesoamerica," Lithics and Subsistence -- The Analysis of Stone Tool Use in Prehistoric Economics, (D. Davis, ed.) Vanderbilt University, Publications in Archaeology #20 (1978).
7. L. Hurtado de Mendoza and W. A. Jester, "Obsidian Sources in Guatemala: A Regional Approach," *Am. Antiquity* 43:424-435 (1978).
8. F. H. Stross, T. R. Hester, R. F. Heizer, and R. N. Jack, "Chemical and Archaeological Studies of Mesoamerican Obsidian," Advances in Obsidian Glass Studies, (R. E. Taylor, ed.), Noyes Press (1976).

This report was done with support from the Department of Energy. Any conclusions or opinions expressed in this report represent solely those of the author(s) and not necessarily those of The Regents of the University of California, the Lawrence Berkeley Laboratory or the Department of Energy.

Reference to a company or product name does not imply approval or recommendation of the product by the University of California or the U.S. Department of Energy to the exclusion of others that may be suitable.

TECHNICAL INFORMATION DEPARTMENT  
LAWRENCE BERKELEY LABORATORY  
UNIVERSITY OF CALIFORNIA  
BERKELEY, CALIFORNIA 94720